



*TWENTY-EIGHTH
INTERNATIONAL
CONGRESS
ON LARGE DAMS*

*VINGT-HUITIÈME
CONGRÈS
INTERNATIONAL DES
GRANDS BARRAGES*

*16th May–23rd May 2025
CHENGDU – CHINA*

AVERTISSEMENT – EXONERATION DE RESPONSABILITE:

Tous droits réservés. Aucune partie de la présente publication ou des informations contenues dans les présentes ne peut être reproduite, stockée dans un système de récupération, ni transmise sous quelque forme ou par quelque moyen que ce soit, électronique, mécanique, par photocopie, enregistrement ou autre, sans l'autorisation préalable écrite de la CIGB.

Les informations, analyses et conclusions auxquelles cet ouvrage renvoie sont sous la seule responsabilité de leur(s) auteur(s) respectif(s) cité(s).

Les informations, analyses et conclusions contenues dans cet ouvrage n'ont pas force de Loi et ne doivent pas être considérées comme un substitut aux réglementations officielles imposées par la Loi. Elles sont uniquement destinées à un public de Professionnels Avertis, seuls aptes à en apprécier et à en déterminer la valeur et la portée et à en appliquer avec précision les recommandations à chaque cas particulier.

Malgré tout le soin apporté à la rédaction de cet ouvrage, compte tenu de l'évolution des techniques et de la science, nous ne pouvons en garantir l'exhaustivité.

Nous déclinons expressément toute responsabilité quant à l'interprétation et l'application éventuelles (y compris les dommages éventuels en résultant ou liés) du contenu de cet ouvrage.

En poursuivant la lecture de cet ouvrage, vous acceptez de façon expresse cette condition.

NOTICE – DISCLAIMER:

All rights reserved. No part of this publication or the information contained herein may be reproduced, stored in a retrieval system, or transmitted in any form or by any means, electronic, mechanical, by photocopying, recording or otherwise, without written prior permission from ICOLD.

The information, analyses and conclusions referred to herein are the sole responsibility of the author(s) thereof.

The information, analyses and conclusions in this document have no legal force and must not be considered as substituting for legally enforceable official regulations. They are intended for the use of experienced professionals who are alone equipped to judge their pertinence and applicability and to apply accurately the recommendations to any case.

This document has been drafted with the greatest care but, in view of the pace of change in science and technology, we cannot guarantee that it covers all aspects of the topics discussed.

We decline all responsibility whatsoever for how the information herein is interpreted and used and will accept no liability for any loss or damage arising therefrom.

Do not read on unless you accept this disclaimer without reservation.

QUESTION 109

QUESTION 109

QUESTION 109

DAMS AND LEVEES FIT FOR THE FUTURE

1. Management of an aging portfolio of dams in terms of operation, maintenance, and rehabilitation, including risk-based approaches
2. Safety during construction and rehabilitation
3. Special case for small dams and levees
4. Impact of contracting practices on dam safety (e.g., private sector involvement, EPC contracts)
5. Increasingly difficult sites and their new challenges
6. Need for global capacity building

DES BARRAGES ET DES DIGUES PRETS POUR L'AVENIR

1. Gestion d'un parc vieillissant de barrages en termes d'exploitation, de maintenance et de réhabilitation, y compris avec des approches basées sur les risques
2. Sécurité durant les travaux de construction et de réhabilitation
3. Particularités des petits barrages et des digues
4. Impact des pratiques contractuelles sur la sécurité des barrages (participation accrue du secteur privé, contrats EPC ...)
5. Sites de plus en plus difficiles à aménager : barrages et nouveaux défis
6. Besoin de renforcement des compétences à l'échelle mondiale

QUESTION 109

TABLE OF CONTENTS OF PAPERS

TABLE DES MATIÈRES DES RAPPORTS

R. 1	JUAN MATA, CARLOS SERRA, JOSÉ MURALHA, ANTÓNIO LOPES BATISTA, LUÍS LAMAS (<i>Portugal</i>) Safety control during the Alto Tâmega dam construction.	1
R. 2	MARIA BARTSCH, ANNA ENGSTRÖM MEYER (<i>Sweden</i>) Dam safety in Sweden in times of energy transition and climate change	17
R. 3	ERIK NORDSTRÖM, JAMES YANG, ERIC LILLBERG, KRISTIAN ANGELE (<i>Sweden</i>) Stilling basin damages at low heads – experimental investigation	33
R. 4	PIERRE-LOUIS LIGIER, LISA CARLSSON, MAJA RYLANDER, JOHANNA SIPOLA ÄIJÄ (<i>Sweden</i>) Optimal riverbank protection design by combining hydraulic modelling with turbulence-based design methods	48
R. 5	DAINIUS TIRUNAS, HELMUT STAHL, THOMAS MICHAEL WEBER (<i>Switzerland</i>) Moglice dam, Albania – design, construction, and monitoring of dam grouting gallery under complex geological conditions	67
R. 6	STEPHAN MARTIN, KENNETH ROSS, MATTHIAS GOLTZ, GABRIEL ESCOBAR (<i>Switzerland</i>) Nam Theun 1 RCC dam – flood management during construction	87
R. 7	MARCO CONRAD, MATTHIAS GEHRI, LEONHARD KLEMM (<i>Switzerland</i>) The Mühleberg HPP in Switzerland – concrete condition assessment for the re-concession and investment planning of a 100-year-old hydropower plant	103
R. 8	MOHAN ACHARYA, C. RICHARD DONNELLY, TONY BENNETT (<i>Canada</i>) Examining the factors impacting transboundary projects	121

R. 9	PURIA ASIABAN, ALLEN VEENLAND, BABAK ALINEJAD, MOHAMMAD AL-MAMUN, MOHAN ACHARYA, C. RICHARD DONNELLY (<i>Canada</i>) Application of risk assessment approaches to enhance the understanding of dam safety risks at the Waterton dam.	142
R. 10	NOÉMIE ROUSSEL, JEAN-ROBERT COURIVAUD, GUILLAUME VEYLON, CLAUDIO CARVAJAL, CAPUCINE MASSON, FRÉDÉRIC ANDRIAN, EDOUARD BUCHOUD, BRUNO DAUMAS, SIMON RAUDE, MICHAIL KORRES (<i>France</i>) Advanced analytics to detect anomalies through monitoring	164
R. 11	HUI LU, SOPHIE MESSERKLINGER, JAN ATLE ROTI (<i>Norway</i>) Application of shear strength reduction method to analyze stability of a massive dam structure on soil foundation with excessive pore pressures and reduced effective stresses due to internal erosion.	191
R. 12	NARIO YASUDA, ZENGYAN CAO, NARIO YASUDA, TADASHI NISHIMURA, MASA-AKI SATO (<i>Japan</i>) Investigation of construction optimization of a heightened concrete gravity dam.	205
R. 13	KAZUKI TOKUNAGA, EIJI WADA, KAZUYOSHI YUKIMURA, YOSHIHIRO SUZUKI (<i>Japan</i>) Large-scale reservoir dam management aimed at mitigation of long-term turbidity in the Hitotsuse river.	219
R. 14	MASAYUKI KASHIWAYANAGI, SHOTA NOSAKI (<i>Japan</i>) Long-term in-situ monitoring on dynamic modulus of elasticity of dam concrete and its verification by the analysis of dynamic behavior of the dam	239
R. 15	NICOLA BRIZZO, GABRIELLA VASCHETTI, MARCO SCARELLA, EZIO BALDOVIN (<i>Italy</i>) Ceresole Reale dam rehabilitation: more than 30 years later	259
R. 16	GRÉGORY COUBARD, FRANÇOIS MOREL (<i>France</i>) Reinforcement of existing dams with passive anchors: thoughts and proposals from a French working group	275
R. 17	REMY TOURMENT, LUC DEROO, CHLOE CHANCEL, SEBASTIEN PATOUILLARD (<i>France</i>) Petits barrages et digues : leçons partagées.	293

R. 18	F.P.W. VAN DEN BERG, B.C. NOYONS, M.A. VAN (<i>Netherlands</i>) Safety assessment with an agent-based model for levees with beaver burrowing during high-water events	317
R. 19	M.P.M. SANDERS, A.G. WIGGERS, W. DE FIJTER (<i>Netherlands</i>) Designing a fit-for-the-future levee along the Dutch Meuse River	335
R. 20	GUIREC PREVOT, FRÉDÉRIC LAUGIER, LAURENT PEYRAS, ERIC FOUILLARD ET EMMANUEL CONSIGNY (<i>France</i>) Lessons learnt from dam safety review risk assessment (Sarrazin) in France	351
R. 21	LUC DEROO, STÉPHANE BONELLI, JEAN-JACQUES FRY (<i>France</i>) L'évaluation des risques d'érosion pour les barrages et les digues en remblai – réflexions et pratiques françaises.	371
R. 22	ALAN BROWN (<i>United Kingdom</i>) The legacy of Puddle Clay dams	398
R. 23	RUDOLF SJ VAN WYK, KWEKU KWAKU WIAFE, BENJAMIN NII-TAWIAH ADJEI, ALAN G CHEMALY, REGINALD BARRY (<i>South Africa</i>) Planning the refurbishment of the Kpong dam spillway	412
R. 24	MICHELLE BLAESER (<i>South Africa</i>) Faultless foundations drying up.	430
R. 25	DAVID CAMERON-ELLIS, DANIEL PUIATTI, MICHEL LINO, MARTIN CHIZALEMA (<i>New Zealand</i>) Development of a cemented soils coffer dam - an application of cemented soils technology at Kapichira dam (Malawi).	448
R. 26	CĂTĂLIN POPESCU, PETRUTA ISOFAÇHE, ISABELA BALAN (<i>Romania</i>) Future-proofing dams: strategies for sustainable water management, technological retrofit, and climate resilience in the context of dam refurbishment	473
R. 27	FLORIAN LANDSTORFER (<i>Austria</i>) Rosswiese reservoir – refurbishment of a 65-year-old drainage system for the next 65 year	497

R. 28	LAKSHMIN BACHU (<i>Canada</i>) Empowering large dams for the future by using generative artificial intelligence	510
R. 29	DONGMING ZHANG, CHAOFENG ZHANG, AIGUO WANG (<i>China</i>) Construction technology of 300m-level gravel soil core wall rockfill dam for Lianghekou hydropower station	527
R. 30	PENG CHAO, LIU CHAOJIAN, LUO JINGSONG, LIU MINGWAN, XIE SIXIANG (<i>China</i>) Research on design and construction technology of large silos for sand and stone systems in high altitude areas.	549
R. 31	LI XIAOMING, KONG LINGXUE, YU SHUIYANG (<i>China</i>) Research on high-joint technology of composite dam in Zungeru hydroelectric power project	570
R. 32	GUOYUAN LAN, QI SUN (<i>China</i>) Intelligent management and control system of concrete dam construction	579
R. 33	DONGMING LI, YANG CHAO (<i>China</i>) Data augmentation scheme for predictive maintenance of dams: a case study of an arch dam.	588
R. 34	LIU CHAOJIAN, DENG BING (<i>China</i>) Study on the rapid construction technology of a large sand and gravel processing and concrete production system in a high-altitude canyon area	607
R. 35	GUO GUANGWEN, TAN KAIYAN, ZHU SHENGMIN, BO MINYUE (<i>China</i>) Research on dynamic mix proportion design method of cemented gravel	622
R. 36	ZHOU HOUGUI, TAN KAIYAN (<i>China</i>) Three dimensions of breakthroughs in China's hydraulic concrete construction	633
R. 37	CHENFANG JIANG, HENG CHENG (<i>China</i>) Analysis and evaluation of 3k safety factors of extra high arch dams under valley deformation effects.	652
R. 38	XINGXING ZHANG, JIANZHENG SONG, XUEDONG ZHANG, RUI WANG (<i>China</i>) Experiences in determining the physical and mechanical parameters of soft soil dam foundation	667

R. 39	ZHENGXING WANG, LINTAO MA, ZIQIANG YANG, JUTAO HAO, SHIFA XIA, XIAOGANG WANG (<i>China</i>) Effect research of anti-stripping additives to water susceptibility of hydraulic asphalt concrete.	677
R. 40	WENWEI LI, HUAMEI YANG, SHUGUANG LI, HUI TE WU (<i>China</i>) Coupled hydration and calcium leaching deterioration models for medium/low heat cement concrete in dam structures	698
R. 41	BIFENG WANG, FANGCAI XU, MINGHUA ZHAO, YUSHU TANG (<i>China</i>) Experiences and lessons from grouting of deep overburden dam foundation under high water head.	705
R. 42	YUAN LI, LIU QIANKUN, WANG FEI, LI TONGCHUN, LI JIANGUO (<i>China</i>) A refined analysis method for the operational behavior of Nyabarongo II dam on a vibro-replacement stone column composite foundation	723
R. 43	ZHENG HUIFENG, LIU QIANKUN, LI JIANGUO, ZHENG SHUO (<i>China</i>) Study and design on vibro-replacement stone column treatment for deep ultra-soft dam foundation	742
R. 44	JIANFAN ZHOU, KUNMING LU, GAO FENG ZHANG (<i>China</i>) Safety challenges and operational considerations for cascade reservoir dams.	757
R. 45	ZHANG HANGNING, LI YUANKE, HUANG FEIYA, LIN YISHU (<i>China</i>) Design of foundation treatment for Batang Toru HEPP.	768
R. 46	YANG GUANG, ZHANG SHUAI, LUO MINGQING (<i>China</i>) Research on the safety monitoring indicators Nam Ngum 5 hydropower station dam in Laos	784
R. 47	HE ZHANGUO, YAN JIANG PING, JIAO KAI, HUANG CHENGJIA, ZHAI HAIFENG, LIN HANWEN, PAN HAIJING (<i>China</i>) The research and application of key technologies for the construction of smart sites in large hydropower stations.	797

R. 48	KRZYSZTOF RADZICKI, MACIEJ SIEINSKI, TOMISŁAW GOŁĘBIEWSKI, DAGMARA ZELAYA-WZIĄTEK, ZBIGNIEW DMITRUK (<i>Poland</i>) Condition of dams and levees in Poland - issues, statistics, and challenges	807
R. 49	HAOHAN XIAO, SIYANG CHEN, LONG JIANG (<i>China</i>) Identifying potential fractured rock masses in drilling data using DBSCAN method.	825
R. 50	PAVEL SVATOŠ, JIŘÍ KREMSA, TOMÁŠ KLEMŠA (<i>Czech Republic</i>) Harcov dam - experience of the operator and technical safety supervisors from the ongoing reconstruction	835
R. 51	J. CHANDRASHEKHAR IYER (<i>India</i>) Challenges in the safety management of large portfolio of aging dams in the Indian context	847
	General Report / <i>Rapport Général</i> Q. 109 SHUGUANG LI (<i>China</i>) General Reporter / <i>Rapporteur Général</i>	863

PAPERS ON QUESTION 109

RAPPORTS SUR LA QUESTION 109



Taylor & Francis

Taylor & Francis Group

<http://taylorandfrancis.com>

COMMISSION INTERNATIONALE DES
GRANDS BARRAGES

VINGT-HUITIEME CONGRES DES
GRANDS BARRAGES
CHENGDU, MAI 2025

SAFETY CONTROL DURING THE ALTO TÂMÉGA DAM CONSTRUCTION (*)

Juan MATA, Carlos SERRA, José MURALHA, António Lopes BATISTA &
Luís LAMAS
Concrete Dams Department, LABORATÓRIO NACIONAL DE ENGENHARIA CIVIL

PORTUGAL

SUMMARY

During the excavations stage of Alto Tâmega dam construction, a landslide occurred on the right bank slope, immediately downstream of the dam's insertion surface, involving a rock mass volume of about 23,000 m³.

This paper presents a brief description of the events that led to the slope failure, the countermeasures that were implemented to ensure the safety of the dam (resurfacing of the insertion surface of four blocks of the dam; construction of a new concrete structure to partially restore the geometry and the loading conditions of the rock mass existing before the landslide; extension of the rock gallery under the affected zone, to survey the rock mass foundation in depth and promote water-proofing and drainage of the rock mass; updating of the monitoring plan, including the definition of additional instrumentation to install in the new concrete structure, as well as adjustments to monitor the foundation area on the right bank; and moving the location of the dam's bottom discharge to the left bank) and some results of the monitoring during construction and the first filling of the reservoir that showed the adequate behaviour of the dam.

**Mise en sécurité pendant la construction du barrage de Alto Tâmega*

RÉSUMÉ

Au cours de la phase d'excavation de la construction du barrage d'Alto Tâmega, un glissement de masse rocheuse s'est produit sur la pente de la rive droite, immédiatement en aval du barrage, impliquant un volume de massif rocheux d'environ 23 000 m³.

Cet article présente une brève description des événements qui ont conduit à la rupture de la pente, les contre-mesures qui ont été mises en œuvre pour assurer la sécurité du barrage : la définition de la nouvelle surface d'appui de quatre plots du barrage; construction d'une nouvelle structure en béton pour restaurer partiellement la géométrie et les conditions de charge du massif rocheux existant avant le glissement; extension de la galerie rocheuse sous la zone affectée pour permettre la reconnaissance du massif rocheux de fondation en profondeur et permettre l'imperméabilisation et le drainage de la masse rocheuse, la mise à jour du plan de surveillance, y compris la mise en place d'un réseau de drainage; la mise à jour du plan de surveillance, y compris la définition d'instruments supplémentaires à installer dans la nouvelle structure en béton, ainsi que des ajustements pour surveiller la zone de fondation sur la rive droite; et le changement de l'emplacement de la vidange de fond du barrage sur la rive gauche. Il présente certains résultats de la surveillance pendant la construction et le premier remplissage du réservoir qui ont montré le comportement adéquat du barrage.

1. INTRODUCTION

Alto Tâmega dam, located on the Tâmega River, a right-bank tributary of the Douro River, in the North of Portugal, is part of the Tâmega Electrical Production System (SET), which is owned by Iberdrola Generación.

The Alto Tâmega dam consists of a double-curvature concrete arch, founded on a metamorphic rock mass mainly composed of micaschists, with a powerhouse located at the downstream toe (Fig. 1).

The final design of the dam was done by Granell Ingenieros Consultores [1]. LNEC supported the owner in the design, construction, first filling of the reservoir and operation stages, with studies and activities within the scope of safety control, namely in rock engineering, hydraulics and structures. For the construction phase, LNEC helped in the definition of the monitoring plan [2,3] and in the installation of the monitoring instrumentation.

The dam has a maximum height of 104.50 m between the crest, at elevation 318.00 m, and the lower average surface of the insertion on the rock mass

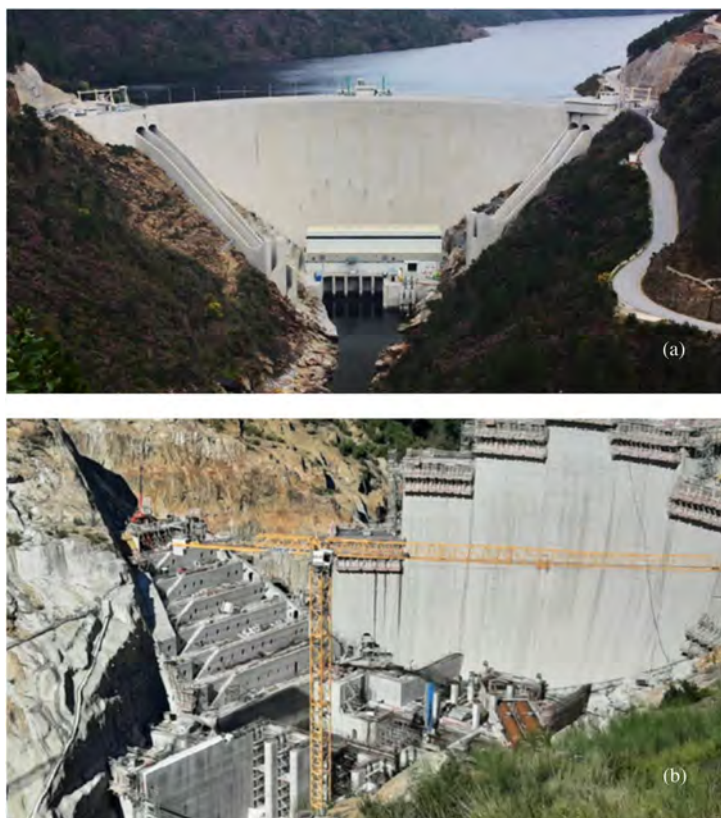


Fig. 1

(a) Downstream view of the Alto Tâmega dam after completion. (b) Downstream view of the Alto Tâmega dam during construction, in October 2021.

(a) Vue en aval du barrage de Alto Tâmega après son achèvement. (b) Vue en aval du barrage de Alto Tâmega pendant la construction, en Octobre 2021.

foundation, at elevation 213.50 m. The geometric definition of the arch is based on parabolic arches, with increasing thicknesses towards the banks, established from the central cantilever and the reference surface. The total crest length, including the abutments, is 332 m, and the chord between abutments is 210 m, leading to a chord/height ratio of 2.01. The dam thickness is 5.00 m at the crest, 17.46 m at the foundation of the central cantilever, with a maximum of 22.61 m at the mid-height of the dam where stresses are highest. The average excavation depth in the bottom of the valley and in the slopes was 12 m and 16 m, respectively. The concrete volume of the dam is about 223,000 m³.

The dam has 21 blocks, the blocks on the right bank are numbered evenly from B2 to B22 and the blocks on the left bank are designated by odd numbers from B1 to B19. The end blocks, blocks B17 and B19 on the left bank and blocks B18, B20, and B22 on the right bank, are gravity profile abutments, where the intake structures for the spillway channels are inserted (Fig. 2). The contraction joints are perpendicular to the upstream face and foundation, so they are arched surfaces. In the lower section, these joints have a curvature defined by parabolic functions in the profile developed by the reference cylinder.

There is a set of galleries inside the dam's body. The perimeter gallery, GP, which follows the dam insertion on the upstream side, serves as a drainage gallery. The horizontal galleries (GO0 to GO4) are inspection galleries, located near the mid-thickness of the arch, at elevations 313.70 m, 303.50 m, 283.30 m, 260.10 m and 238.17 m, respectively. They intersect all blocks until reaching the perimeter gallery and extend through galleries into the rock mass foundation (GO2, GRB, GRA and GRMD). On the left bank, galleries GO2, GRB and GRA reach the elevator shaft, located vertically below block B19. On the right bank, only gallery GO4 extends inside the rock mass foundation (GRMD).

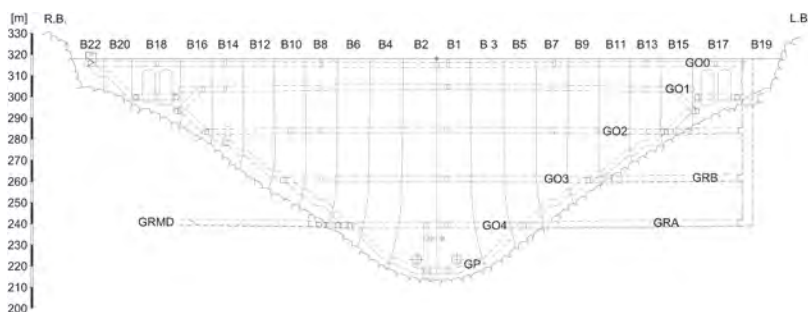


Fig. 2

Alto Tâmega dam. Planned downstream elevation.
Barrage de Alto Tâmega. Élévation prévue en aval.

Excavations on the right bank, in the zone of the powerhouse, began in September 2018. In March 2019, during the final stages of these excavations, movements of rock blocks were observed at the foot of the right bank slope. Works were suspended and the evolution of the displacements on the slope were closely monitored. They showed no signs of stabilization and more significant increases were recorded during rainy periods. On May 2, a major landslide occurred on the right bank slope, immediately downstream of the dam's insertion surface, involving a rock volume of about 23,000 m³.

This work presents a brief description of the events that led to the slope failure, the countermeasures that were implemented to ensure the safety of the dam and some results of the monitoring during the construction and the first filling of the reservoir that showed the adequate behaviour of the dam.

2. DESCRIPTION OF THE RIGHT BANK SLOPE FAILURE

The dam was built in a nearly straight 500 m long stretch of the Tâmega River with an approximate orientation of N 35°E. The valley bed, with a width between 10 and 30 m, is at an elevation 225.0 m. In this section, the valley is practically symmetric; the right bank slope has an average inclination of 34°, while the left bank slope has an average inclination of 44° from the valley bed up to an elevation of 247.0 m and of 34° above that elevation.

In January 2018, at the beginning of the excavations on the right bank slope for the dam foundation, the powerhouse and the spillway channels, three relevant geological structures were recognized immediately downstream from the dam insertion (Fig. 3 [4,5]): i) fault F33 with orientation 66°/078° (dip/dip direction), which had been already mapped in the geotechnical surveys for the design phase; and ii) probable faults FP36 and FP13, which correspond to persistent discontinuities detected only during the excavations, with orientations approximately parallel to joint set D5 (average orientation in the right bank 24°/149°).



Fig. 3

Right bank slope view with reference to the relevant discontinuities [5].

Vue du versant de la rive droite avec les discontinuités pertinentes.

In December 2018, at an early stage of the excavations, surface mapping of the discontinuities revealed that fault FP36 appeared at the powerhouse excavation slope. As a result, the rock mass support defined in the design, consisting of shotcrete and rock bolts, was reinforced with 23 Gewi/Dywidag type anchors with 50 mm diameter and 12 m long threaded bars. Additionally, the slope monitoring was revised, with the installation of additional prismatic targets for geodetic monitoring (Fig. 4) and load cells in some of the anchors, as well as visual inspections on a daily basis.

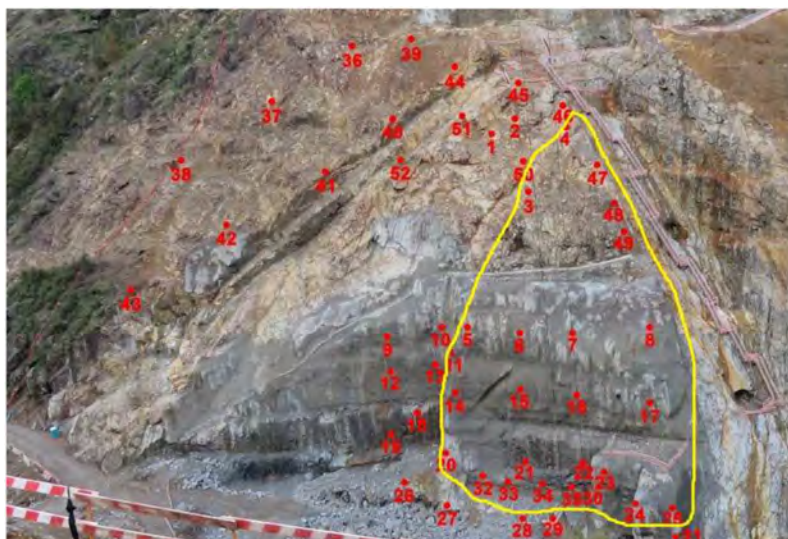


Fig. 4

Location of the slope zone with larger displacements and of the geodetic prism on the slope surface [5].

Localisation de la zone de la pente avec des déplacements plus importants et des prismes géodésiques sur la surface de la pente [5].

At the end of January 2019, with the downwards progress of the powerhouse slope excavation works, a significant variation in the orientation of fault FP36 was detected towards an unfavourable inclination, which led to the execution of more anchors adding to a total of 41.

In March 2019, with excavations at elevation 226 m, a discontinuity was detected on the excavation faces, which later, as excavations progressed, was found to be fault FP13, but with an important change in its orientation. Although the orientation of FP13 fault, mapped until then along the excavation of the downstream slope of the dam insertion, indicated its extension to elevations below the bottom of the riverbed, this this in orientation led to its daylighting on the powerhouse excavation slopes. Additionally, on the exposed surfaces at lower elevations, fault FP13 presented fillings of crushed materials and the emergence of water, therefore, it became designated as fault F13.

On March 21, significant displacements, exceeding 10 mm, were detected in the prismatic targets, along with substantial increases in the forces measured by the load cells installed in the anchors. Additionally, widespread cracking was observed in the shotcrete close to fault F33 and there was subsidence in the shotcrete around the anchoring plates. Works on the right bank were suspended and the monitoring of the slope displacements was intensified. This included the installation of a robotic station with four readings per hour frequency, an increase in the reading frequency of the conventional geodetic stations, and the placement of more prismatic targets above and below fault FP36. Plaster tell-tales were placed on the fault traces and cracks in the shotcrete, and the area of visual inspection was expanded, using escalation means.

It was concluded that the mechanism causing the recorded movements on the slope involved fault F13. Actions were discussed to more accurately define the mechanism that caused the slope movement, the geometry of the faults and the rock mass volume involved. These actions included: i) representing the displacements measured in the targets installed on the slope in a three-dimensional AutoCAD geometric model and in a stereographic projection to identify the discontinuities involved in the mechanism; ii) conducting back-analysis calculations; and iii) performing tests to characterize the filling material of fault F13 to define the necessary rock mass support.

In the following days, the monitoring results showed some stabilization of the movements and confirmed that the displacements were limited to a rock mass volume bounded by faults F13 and F33 (Fig. 5), with more pronounced movements in the downstream area than in the area near the dam insertion.



Fig. 5

Three-dimensional representation of the failure mechanism, with faults F13 in red, F33 in blue, and FP36 in green [4].

Représentation tridimensionnelle du mécanisme de rupture, avec les failles F13 en rouge, F33 en bleu et FP36 en vert.

In the early hours of May 2, 2019, sliding of a rock mass volume of about 23,000 m³ happened, forcing the interruption of all works for around a year and a half. The analysis of the available information and the inspections carried out after the failure, identified a rock mass wedge mechanism involving faults F13, F33 and FP3, which was mainly due to the change of the orientation, mainly the dip, of fault F13. The rock material that slide was removed in the following days and works to stabilize the slope were carried out.

3. SAFETY CONTROL DURING DAM CONSTRUCTION

In October 2020, works resumed after the design adaptation to the new conditions. Measures were defined [4,5] to stabilize the downstream slope and ensure safety conditions during dam construction, first filling and operation. The main measures adopted were the following: i) construction of a concrete structure anchored to the rock mass, to replace the volume of rock mass that was affected by the slope failure (Fig. 6); ii) adjustment of the insertion surface by deepening and widening the excavation of blocks B10, B12 and B14 (Fig. 7); iii) extension of the gallery in the foundation at elevation 237.5 m to monitor faults F13 and F20, and to increase the drainage of the rock mass; and iv) relocating, symmetrically, the dam's bottom discharge from the right side of the river bed to its left side.

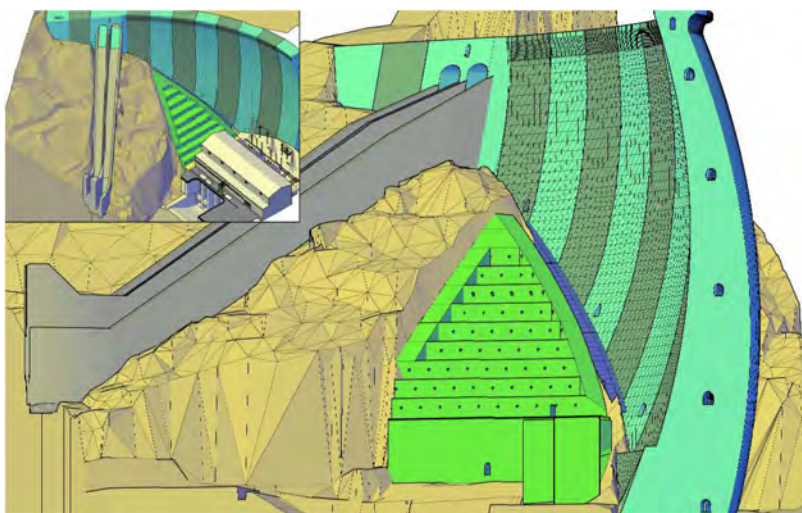


Fig. 6

Schematic view of the new concrete structure on the right bank slope [4].

Vue schématique de la structure en béton sur le versant de la rive droite.

In accordance with the adaptations introduced to the design, the monitoring plan of the right bank was enhanced by installing the following equipment: i) prismatic targets for geodetic observation of displacements of the new concrete structure; ii) piezometers for measuring water pressure in the rock mass, in the area under the new concrete structure; iii) weirs for measuring flows due to seepage and leakage in the new concrete structure; iv) load cells in the anchors of the new

concrete structure; v) rod extensometers and inclinometers for measuring displacements in the rock mass; vi) three-dimensional jointmeters for measuring relative displacements in faults traces (inside the rock mass foundation gallery GRMD); vii) thermometers to control the temperature in the new concrete structure during its construction. The location of the rod extensometers located in the dam body and, on the right side, immediately downstream of the dam body, are presented in Fig. 8.

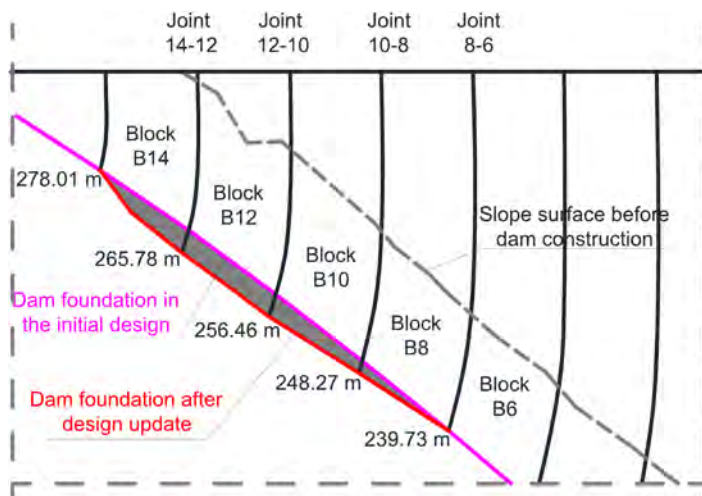


Fig. 7

Schematic view of the deepening of the dam insertion surface, adapted from [4].
Vue schématique de l'approfondissement de la surface d'insertion du barrage.

The results of the numerical model for the structural calculations of the dam, considering the new geometry of the insertion surface, showed that the changes in the stress fields in the dam body were marginal. Therefore, it was concluded that the consequences of the slope failure for the dam safety, considering the new geometry of the right bank downstream of the dam foundation and, consequently, the new risk scenarios that arise, were those involving: i) the possibility that rock mass blocks on the downstream slope of the dam foundation detach and fail due to the dam loads; ii) the global failure due to discontinuities in the dam foundation; and iii) modification of the dam thrust on the right bank foundation.

Several studies were carried out by the designer, reviewed by the owner with the support of the LNEC, which allowed to conclude that the general safety requirements continued to be met.



Localisation de extensomètres à tige du plan de surveillance mis à jour.

11

guaranteeing adequate safety conditions for the work execution and, mainly, to ensure that the project adaptations yielded the intended effects concerning adequate dam and foundations behaviours. In this context, the following construction procedures were implemented: i) the construction of a dam block on the right bank should only start after the new concrete structure is executed up to an elevation higher than the block's foundation (this essential measure is quite important so that the blocks are concreted on a foundation with adequate confinement conditions); ii) the installation and start of operation of the monitoring equipment considered essential for the observation of the right bank during dam construction should be concluded before concreting of block B6; iii) given that various activities carried out involving drilling the rock mass on the foundation of the right bank (namely for consolidation of the rock mass, installation of rock bolts and anchors on the surface of fault F13, waterproofing and drainage curtains and installation of observation equipment), intense monitoring was performed; iv) the results of the observation were immediately made available on a digital platform accessible to all entities involved in the safety control; v) the interpretation of the monitoring results through the use of a numerical model representing the dam-foundation system, including the downstream concrete structure and its connection conditions to the rock mass foundation, was done; vi) contingency plans were drawn up defining the actions to be taken and the responsibilities of the different entities involved, to ensure an effective monitoring of the work, especially in the event of anomalous behaviour; and vii) appropriate planning for the first filling of the reservoir was considered to guarantee a slow and gradual filling of the reservoir and, if required, to implement the corresponding contingency measures.

The evolution of displacements in the foundation, during the construction of the dam are presented in Fig. 9. The construction works took place without any events worth mentioning.

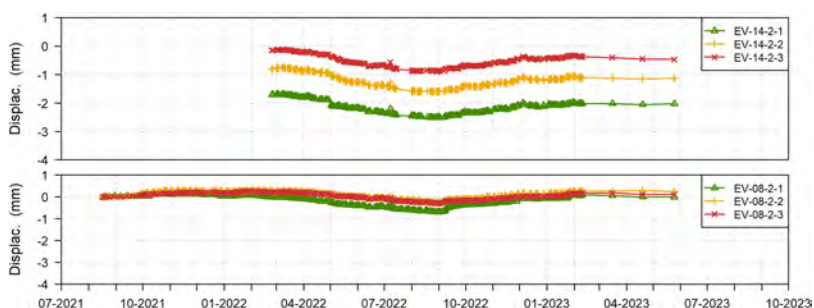


Fig. 9

Displacements measured during the dam construction in rod extensometers located downstream of the dam, close to the new concrete structure, on the right bank.
Déplacements mesurés lors de la construction du barrage dans des extensomètres à tige situés en aval du barrage, à proximité du nouvel ouvrage en béton, en rive droite.

4. STRUCTURAL SAFETY CONTROL ACTIVITIES DURING THE RESERVOIR FIRST FILLING

The behaviour of the reservoir-dam-foundation system was carefully monitored during the first filling of the reservoir. It started in June 2023 and ended in February 2024. The main water level rise started in October 2023. The temporary stop stages of the first filling at the levels defined in the reservoir's first filling plan were generally met.

Based on the analysis of the observed behaviour during this period, some aspects considered relevant are mentioned: i) the first filling of the dam reservoir, with a total duration of around eight months, was started in a hot season and was completed in a cold season; ii) the dam contraction joints showed reduced movements, compatible with the variation of the main loads, according to the measurements performed in embedded jointmeters and in three-dimensional jointmeters; iii) the radial and tangential displacements observed in pendulums (Fig. 10) and the vertical displacements observed in rod extensometers (Fig. 11) were compatible

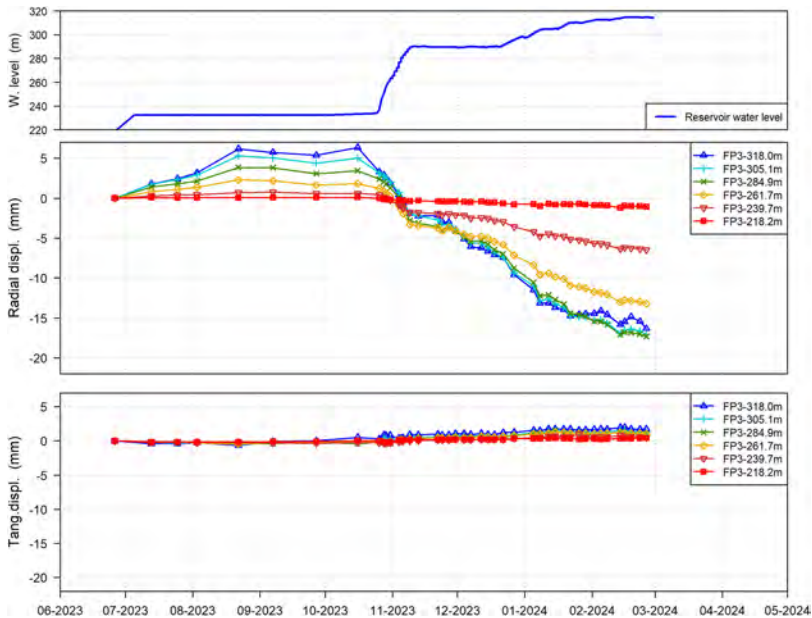


Fig. 10

Horizontal displacements measured in the pendulum FP3 since the first filling of the reservoir, in the cantilever block of the dam.

Déplacements horizontaux mesurés dans le pendule FP3, dans le bloc cantilever du barrage.

with the structural type and size of the dam, and the measurements were compared with results obtained by numerical finite element models developed, independently, by Iberdrola and by LNEC; iv) the seepage and leakage measured through the drainage system were, in general, reduced or null (only the seepage measured in drains D-01-1 and D-01-2, in the central cantilever, showed relevant values in the retention water level (RWL), around 27 l/min and 64 l/min, respectively); v) resurgences were observed in the rock gallery on the left bank (GRA), detected in January 2023, which were duly routed, and no new resurgences were observed; vi) the uplift pressures measured in piezometers showed reduced values, except for piezometers P-01 (block B1), P-05 (block B5) and P-02 (block B2), which reached uplift pressures up to 70%, 80% and 60% of the hydraulic load, respectively; vii) the measurements of the weirs and piezometers of the monitoring system of the new concrete structure had null or reduced values; viii) the measurements in the anchorage load cells have generally remained constant; and ix) no anomalies were detected during the visual inspections carried out during the reservoir's first filling.

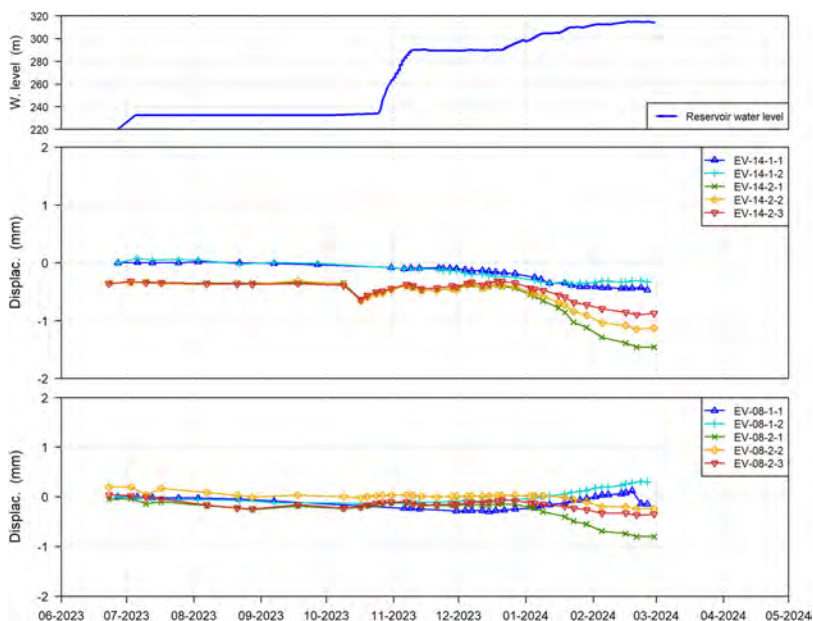


Fig. 11

Displacements measured in rod extensometers located in the perimeter gallery and downstream of the dam, close to the new concrete structure, on the right bank.

Déplacements mesurés dans des extensomètres à tiges situés dans la galerie périphérique et en aval du barrage, à proximité du nouvel ouvrage en béton, en rive droite.

5. CONCLUDING REMARKS

The adaptations introduced in the dam's design, to face the consequences of the landslide that occurred on the slope of the right bank, considered five main components: i) the resurfacing of the insertion surface of blocks B8, B10, B12 and B14 to ensure better conditions for supporting and transmitting stress to the foundation; ii) the construction of a new concrete structure, to partially restore the geometry and the loading conditions of the rock mass existing before the landslide; iii) the extension of the rock gallery at elevation 237.5 m, to survey the rock mass foundation in depth and promote waterproofing and drainage of the rock mass under the affected area; iv) the updating of the monitoring plan, including the definition of additional instrumentation to be installed in the new concrete structure, as well as adjustments to monitor the foundation area on the right bank; and v) moving the location of the dam's bottom discharge to the left bank.

The adaptations were implemented on site without major difficulties. Construction works took place normally, following well-defined planning and strict safety control. The first filling of the reservoir occurred as planned. The dam has been in operation since February 2023, with very good performance.

ACKNOWLEDGEMENTS

The authors acknowledge Iberdrola, that provided the data and information for this work.

REFERENCES

- [1] Granell Ingenieros Consultores, 2017a – H.E. Alto Tâmega. Execution project. Dam (in Portuguese). Ref. 1862/11/121001, rev0, February 2017.
- [2] LNEC, 2011 – Alto Tâmega dam. Monitoring plan and specific monitoring plan during the first filling of the reservoir (in Portuguese). Report 52/2011, February 2011.
- [3] LNEC, 2017 – Alto Tâmega dam. Adaptation of the monitoring plan to the dam to be built (second geometry definition) (in Portuguese). Report 346/2017, October 2017.

- [4] Granell Ingenieros Consultores, 2020 – H.E. Alto Tâmega. Integrative memory of the Alto Tâmega project review (in Portuguese). Ref. 1862-INFT-00072, rev0, February 2020.
- [5] LNEC, 2020 - Alto Tâmega dam. Opinion on the design adaptation, due to the landslide in the right bank slope (in Portuguese). Report 143/2020. April 2020.

COMMISSION INTERNATIONALE DES
GRANDS BARRAGES

VINGT-HUITIEME CONGRES DES
GRANDS BARRAGES
CHENGDU, MAI 2025

DAM SAFETY IN SWEDEN IN TIMES OF ENERGY TRANSITION AND CLIMATE CHANGE (*)

Maria BARTSCH

Dr. Eng. (Civ. Eng.), Dam Safety Specialist, Svenska kraftnät

Anna ENGSTRÖM MEYER

M. Sc. (Civ. Eng.), Senior Advisor Dam Safety, Swedenergy

SWEDEN

SUMMARY

A government assignment on the impact of climate change on dam safety in Sweden was completed in 2023. The purpose of the assignment was to map the influence of climate change and the energy transition on dam safety and to provide guidance on how to address climate change and apply the guiding principles in Sweden's national strategy for climate adaptation to dams. The intention was to strengthen the development of discharge safety and the adaptation of existing dams to a changing climate. The overall goal was to make current and relevant information available to dam owners and concerned authorities, in order to lay the foundation for strategic climate adaptation work regarding dams.

The assignment resulted in extensive compilation of knowledge and a number of conclusions and recommendations. Dams are essential for the adaptation to climate change and an enabler for the energy transition. A changing climate poses potential hazards to dam safety. Climate change can affect dams in various ways, directly on the facilities and their functions and indirectly through changes in the

**La sûreté des barrages en Suède à l'époque de transition énergétique et de changement climatique*

environment. These climate-related risks are primarily already known risks that can be changed and exacerbated by climate change. Simultaneously, uncertainty in the operation of the hydropower system is increasing. Continued work is necessary to better monitor and pro-actively take account of operational changes in dam safety management and vice versa. Care is needed to ensure that currently known dam safety risks do not become more likely, and that new combinations of risks are identified and managed.

The responsibility for safety management of dams including adaptation to climate change primarily resides with the dam owners. The Swedish regulation of dam safety, with associated guidelines, is deemed to be in line with the guiding principles in the national strategy for climate adaptation. Authorities and industry organizations are recommended to collaborate to consider climate change explicitly in their guidelines to facilitate that it is integrated as well as possible into the dam owners' regular dam safety work. They should continue to monitor climate change and work together to make use of the knowledge base from the assignment, develop specific climate indicators and produce supplementary documentation relevant to dam safety.

While it is important to focus on the present and solve today's problems, known risks may be exacerbated by climate change and related operational changes within the lifetime of the dam facility. Dam owners are recommended to analyze potential risks posed by climate change within their ordinary risk management procedures. Risk assessments should be carried out periodically. A need for gradual escalation of adaptation measures over time is foreseen. From increased monitoring, preventive or corrective maintenance, to rebuilding and change of use, or finally possibly decommissioning.

New technologies for forecast predictions and modelling, more accurate and detailed knowledge bases, as well as new possibilities to use and regulate reservoirs entails an even closer future collaboration between dam owners and societal actors. Coordination and collaboration between actors is vital in the long-term climate adaptation of the whole society.

RÉSUMÉ

Une mission gouvernementale concernant l'impact du changement climatique sur la sécurité des barrages en Suède a été achevée en 2023. L'objectif de la mission était de décrire l'influence du changement climatique et de la transition énergétique sur la sécurité des barrages. Il s'agissait également de fournir des conseils sur la manière de gérer les conséquences du changement climatique sur les barrages et d'appliquer les principes directeurs de la stratégie nationale suédoise d'adaptation au climat aux barrages. L'intention était de renforcer le

développement de la sécurité des débits et l'adaptation des barrages existants au changement climatique. L'objectif global était de mettre à la disposition aux propriétaires de barrages et aux autorités concernées des informations actuelles et pertinentes afin de rendre possible un travail stratégique liée à l'adaptation au climat concernant les barrages.

La mission a résulté à une compilation approfondie de connaissances et à des conclusions et recommandations. Les barrages ont une fonction essentielle pour l'adaptation au changement climatique et constituent un catalyseur pour la transition énergétique. Le changement climatique implique des dangers potentiels pour la sécurité des barrages. Le changement climatique peut affecter les barrages de diverses façons, directement sur les installations et leurs fonctions et indirectement par des changements de l'environnement. Ces risques liés au climat sont principalement des risques déjà connus qui peuvent être modifiés ou accentués par le changement climatique. En outre, l'incertitude du fonctionnement du système hydroélectrique augmente. Ceci devra être étudié plus profondément afin de mieux surveiller et de prendre en compte les changements opérationnels dans la gestion de la sécurité des barrages et vice versa de manière proactive. Il reste à suivre que la probabilité des risques actuellement connus pour la sécurité des barrages n'augmentent pas et que de nouvelles combinaisons de risques soient identifiées et gérées.

La responsabilité de la gestion de la sécurité des barrages, y compris l'adaptation au changement climatique, est principalement la responsabilité des propriétaires de barrages. La réglementation suédoise sur la sécurité des barrages, avec les directives associées, est considérée comme conforme aux principes directeurs de la stratégie nationale d'adaptation au climat. Les autorités et les organisations dans le domaine de l'industrie devraient collaborer pour tenir explicitement compte du changement climatique dans leurs lignes directrices afin de faciliter son intégration dans le travail régulier des propriétaires de barrages en matière de sécurité. Ils devraient continuer à surveiller le changement climatique et travailler ensemble pour utiliser les connaissances actuelles, développer des indicateurs climatiques spécifiques et produire une documentation supplémentaire pertinente pour la sécurité des barrages.

Bien qu'il soit important de se concentrer sur le présent et de résoudre les problèmes d'aujourd'hui, les risques connus peuvent devenir plus accentués par le changement climatique et les changements opérationnels connexes pendant la durée de vie de l'installation du barrage. Les propriétaires de barrages doivent prendre en compte et analyser les risques potentiels posés par le changement climatique dans le cadre de leurs procédures ordinaires de gestion des risques. Des évaluations des risques doivent être effectuées périodiquement. Il est prévu d'intensifier progressivement les mesures d'adaptation au fil du temps. De la surveillance accrue, de la maintenance préventive ou corrective, à la reconstruction et au changement d'usage, ou enfin éventuellement au démantèlement.

Les nouvelles technologies de prévision et de modélisation, les bases de connaissances plus précises et plus détaillées, ainsi que les nouvelles possibilités d'utilisation et de régulation des réservoirs impliquent une collaboration future encore plus étroite entre les propriétaires de barrages et les acteurs sociétaux. La coordination et la collaboration entre les acteurs sont essentielles pour l'adaptation de l'ensemble de la société au climat à long terme.

1. INTRODUCTION

Dams and dam engineering have been instrumental in the development of hydropower in Sweden. During the 20th century, the expansion of hydropower for electricity production was one of the cornerstones of wealth development. The first large hydropower dams in Sweden were built in the early 1900s, and the development culminated in the 1950s-1970s. Today there are more than 2000 hydropower facilities, 200 of them with an installed capacity of 10 MW or more. In total, there are about 200 large dams in the country, 15 m or higher, most of which are hydropower dams while some are tailings dams. Very few large hydropower dams have been built after the 1980s.

Dams constitute important infrastructure in society through their importance for the storage and regulation of water and mixtures of water and other material for e.g. hydropower production and mining operations. Secure fossil-free electricity supply is one of the cornerstones for sustainable social development. Hydropower supplies many important benefits to the power system and thereby has a decisive role as an enabler in Sweden's climate and energy transition. In addition, access to minerals and metals is central to the mitigation of climate change, and Sweden is one of Europe's most important mining nations. In this context tailings storage facilities with embankment dams enable both storage of mining waste and residual products of tailings and handling of water. Climate adaptation of existing dams, through the activities they enable, thus contributes to the overall societal climate adaptation and the reduction of climate impact.

Dams can also bring risks as a dam failure - with the release of retained water and mixtures and water and other material - can cause flooding with serious consequences as well as loss of essential services to the society. Maintaining satisfactory dam safety is therefore a basic prerequisite for continued operations. The ongoing changes in climate may entail the need for adaptation measures during the technical lifetime of existing dams. Changes in operating patterns and environmental factors related to climate change and/or the energy transition may also lead to the need for adaptation measures. Mapping of the overall effects of already occurred, as well as foreseeable future changes, in climatic and operational conditions are therefore relevant from a dam safety perspective, with safe management of floods in particular focus.

This paper reports from a recently completed government assignment on the effects on dam safety in Sweden of the ongoing changes in climate and hydropower operation. The assignment was performed in 2022-2023 under the lead of the authors of this paper, both working at Svenska kraftnät at that time, in cooperation with a group of experts representing authorities, hydropower and mining industry organizations and dam owners.

2. A NATIONAL STRATEGY FOR CLIMATE ADAPTATION AND ITS RELEVANCE FOR DAMS

In 2018, the Swedish Parliament adopted a national strategy for climate adaptation [1]. The strategy includes a package of policies, legal changes, national boards of experts, authority networks and priorities to address climate mitigation and adaptation. The overall purpose of the strategy is to strengthen the long-term climate adaptation work in Sweden and the national coordination of climate adaptation. It should be used as a basis for climate adaptation for the whole society. It thereby constitutes a basis also for dam owners for their future management, development and operation of dams, hydropower and tailings facilities.

A key to achieve Sweden's climate goals and enable the green transition is to succeed in the electrification of the transport sector and industry (e.g. fossil-free steel production). To enable this the national need for electricity is expected to increase sharply in the coming two decades. In the past 100 years the production of hydropower has played a central role in Sweden's electricity supply as a source of energy and regulating power. During the last few years, installation of new wind power has gone from producing an insignificant part of Sweden's electricity to about 20 percent of our use, and this development is expected to continue. In line with this, the need for regulating capacity has increased and already today, changes in the hydropower operation are evident. Hydropower's ability to quickly adapt to variations in need and maintain the power balance in the electricity system, both by delivering frequency-based support services and through the flexibility to production, which storage in water reservoirs enables, will be crucial for Sweden to meet its climate goals and implement electrification.

The national strategy includes the following ten principles for the work on climate adaptation:

- Sustainable development – the interests of existing and future generations are taken into account.
- Mutually supportive – measures for climate adaptation and reduced climate impact support each other.
- Scientific basis – actions are based on scientific basis incl. knowledge from the IPCC.

- Precautionary principle – potential demonstrated risks are managed even if available scientific knowledge is insufficient for a firm conclusion.
- Integration of measures – all societal actors integrate measures into existing strategies and plans where possible.
- Flexibility – measures are designed to be flexible and robust to different courses of action in the future.
- Uncertainty management – measures are analyzed based on several possible outcomes of emission scenarios.
- Risk management – likely risks with serious consequences are addressed.
- Time perspective – measures are adapted the service life of current facilities.
- Transparency –uncertainties, choice of scenarios, risks and time perspectives are presented.

In 2022 the Government assigned Svenska kraftnät to analyze the impact of climate change on dam safety, with focus on extreme floods and existing high consequence dams. The purpose was to map the influence on dam safety of climate change and the energy transition and provide guidance on how to address climate change and apply the guiding principles, to strengthen the development of discharge safety and the adaptation of existing dams to a changing climate. The overall goal was to make current and relevant information available to dam owners and concerned authorities, to lay the foundation for strategic climate adaptation work regarding dams. The assignment included the following:

- To compile current knowledge on climate change with influence of dam safety.
- To investigate changes in the operation of the hydropower system and the interdependence between operation and dam safety.
- To investigate how the national strategy for climate adaptation and its guiding principles should be applied in the field of dam safety.

Svenska kraftnät performed the assignment in close cooperation with experts from the hydropower and mining industries, the Swedish Meteorological and Hydrological Institute (SMHI) and other concerned authorities. Svenska kraftnät reported the assignment to the Government in December 2023 [2]. The main findings are presented in the following sections.

3. HOW IS THE CLIMATE CHANGING?

For a long time the established picture is that Sweden is heading towards a warmer and wetter climate. Increasing temperatures, more precipitation with more torrential rains and higher winter inflows are examples of this. Information about how and why the climate is changing is primarily made available on SMHI's website in its role as an expert authority for knowledge, research and services in climatology and climate adaptation. With climate indicators variations and trends over time of for example mean temperature, sea levels and days with snow are followed. Based on

SMHI's observations and modelling of future changes (conditions towards the end of this century in comparison with a reference period at the end of last century) the current knowledge on climate change in Sweden with particular relevance for dam safety was compiled as a base for the further assessment [3].

In Summary Sweden's climate is characterized by high variability on time scales from single days, via months and years, to several decades. Climate scenarios indicate that there will be a continued time shift of seasons, gradually increasing temperatures and generally more precipitation, which to an ever lesser extent will fall as snow. Climate change is also about changes in extremes, with more intense heat waves and less frequent cold snaps that won't be as cold as before. Changes are expected to lead to more extreme weather events with increased occurrence of high flows and floods, landslides, forest fires and storm-felled forests, but also some increased risk of drought in the south in precipitation-poor years.

In a future climate, hydrological extremes may be of other characters and unfavorable conditions may coincide or come in a sequence that does not occur today. If hydropower's role in the energy system changes, historical operating patterns may also change, which adds additional factors to consider.

The value of measuring meteorological and hydrological parameters is expected to increase in the future. SMHI has recently taken the initiative to develop additional indicators that are specific to extreme flows. However, there is a need for further knowledge about changes in extreme rain and snow events, extreme inflows and seasonal changes.

4. HOW CAN DAM SAFETY BE AFFECTED BY CLIMATE CHANGE?

Climate change can affect dam facilities in various ways, directly on the facilities and their functions and indirectly through changes in the environment. These are primarily already known risks that can be changed and exacerbated by climate change.

Within the assignment, an R&D project including an overall analysis of climate change that may lead to risks to dam safety was carried out [4]. The project started with a literature review on methodology for analysis of and adaptation to climate change, and climate indicators that can be used to identify changes that may affect dam safety. Initiatives taken at national and international level, as well as in various institutes and industry organizations related to hydropower activities, mining activities and dam safety were identified. Using the results of the literature review, a systematic analysis including a workshop on climate change indicators and impact chains that may have an impact on dam safety were performed. The approach was qualitative and broad to cover changes that could affect various aspects of dam

safety but did not relate to any particular facility or activity. In total about seventy impact chains were established and described.

In many cases, the requirements in the field of dam safety are governed by unusual or extreme climatic conditions and events. Normally occurring relatively large seasonal and inter-annual variations can be handled within the normal operation of the dam facilities. Dependencies on the surrounding environment, physical planning and design of infrastructure in general exist in that weather events and loads – which are expected to increase in a changing climate – may affect access roads and can make access to facilities more difficult. The same changes can lead to, for example, more power outages, which in turn can affect power supply and the production capacity of hydropower facilities.

The ability to handle floods is central to dam safety. Dam facilities are designed to, or have been upgraded to, be able to withstand and pass extreme flow. Since 2007 the Swedish guidelines on design floods for dams include recommendations on how to address climate change and related uncertainties [5]. The methods on how to analyze and describe the impacts of climate scenarios have been further developed since then and are now widely implemented. The current guidelines include guidance on the use of climate change scenarios [6,7]. In recent years, renewed design calculations are being carried out, or are underway, in major hydropower rivers to consider additional flow and climate data and by using more modern calculation models. The calculations also include sensitivity analyses using climate scenarios. For some dam facilities, the need for additional upgrading measures have been identified under current conditions. In such cases, the dam owner can benefit from the knowledge base regarding changes in future floods when evaluating alternative upgrading measures and decision making for sustainable actions.

High and extreme inflows are expected to be increasing in large parts of the country during the current century, indicating an increasing risk of flooding. In the longer term, towards the end of the century, this means that further adaptation measures may be necessary at some dam facilities in the major hydro power rivers. For smaller dam facilities, where the design flood guidelines have not previously been applied the need for overall review and actions in the short perspective are deemed to be greater. Mainly small companies or municipalities, e.g. actors outside the hydropower industry, own these facilities.

5. HOW CAN DAM SAFETY BE AFFECTED IN THE FUTURE HYDROPOWER SYSTEM?

Continued efficient use of hydropower will be decisive for Sweden to achieve its climate goals and enable the green transition through increased electrification. The need for regulating capacity will increase in line with increased production of

wind and solar power. To meet this need, several companies are analyzing the conditions for increasing the output of existing hydropower plants and changes in water regulation are already evident.

For hydropower facilities and their operation, a number of factors that change over time affect the water regulation. Current examples, in addition to climate change, are the ongoing change in hydropower's role in the energy system – with comparatively rapid changes in the electricity market, production mix and geography – and the environmental adaptation of permits for dams and hydropower facilities. For larger hydropower rivers, general tendencies include changes over time in the overall supply of water, winter inflows and water levels in regulating reservoirs. The changes are partly of importance to dam safety and vigilance is needed to ensure that actual reservoir regulation does not conflict with assumptions about reservoir level, spillage and regulations strategies applied in design flood calculations.

One of the strengths of hydropower is that it is good at handling large variations in inflow and demand of electricity both during the day, year and between years. In the future, hydropower's flexibility with short-term regulation is expected to become increasingly important. Annual regulation is expected to become less important. At the same time, the climate is expected to become more variable and different events may coincide suddenly and in an unfavorable way for which it is difficult to make forecasts. More events will need to be handled. Operating and maintenance conditions will change. Changes are already seen in the form of, among other things, more spillage in winter for power balance purposes. Increased variations in hydropower production with more frequent starts and stops of turbines and regulation of spillway gates also affect the need for maintenance.

All in all, uncertainty in the operation of the hydropower system is increasing. Care is needed to ensure that currently known dam safety risks do not become more likely, and that new combinations of risks are identified and managed. Continued work is necessary to better monitor and pro-actively take account of operational changes in dam safety work and vice versa. Dam owners' measures continue to include appropriate design of dam systems with their components and functions, better measurements and forecasts, adaptation of maintenance and operational readiness, collaboration and exchange of information with authorities, and adaptation of water regulation rules.

6. HOW CAN RISKS RESULTING FROM A CHANGING CLIMATE BE MANAGED IN THE FIELD OF DAM SAFETY?

Internationally, several different initiatives relating to methodology for analysis and adaptation to climate change have been taken over the past ten years. There is a consensus that risks resulting from climate change can be integrated into existing

risk management processes for dam owners and others. The focus of current adaptation measures in many cases involves a gradual escalation over time with increased monitoring, preventive or corrective maintenance, to rebuilding and change of use, or finally possible decommissioning.

The responsibility for dam safety lies with the owner/operator of the dam. This includes managing risks that may arise because of climate change. The dam owner must be able to demonstrate that they comply with the obligations under the legal framework. In Sweden several general statutes are applicable to dams and dam safety issues. The most important regulations are found in the Environmental Code and the Civil Protection Act. Dams where a failure could have serious consequences from a societal point of view must be classified and comply with special requirements for dam safety work and dam safety. Closer guidance and supporting documents based on the dam safety regulation is provided by industry organizations and authorities [8–11]. Swedenergy published their first technical guidelines for dam safety, RIDAS, in 1997. The 2022 edition is aligned with the legal requirements and relevant standards and collects about 25 guidelines.

Today climate change is mentioned in industry guidelines, but except for a reference to the guidelines on design flood determination not specific guidance is given regarding how to assess or handle climate risk. As already mentioned, the Swedish guidelines for determining design flow for dam facilities already contain guidance for application in a changing climate, such as recommendations of a review of calculation assumptions every ten years and instructions for sensitivity analysis using climate scenarios. Correspondingly, the government assignment recommends that the existing dam safety guidelines are elaborated to address other aspects of climate-related risks explicitly.

7. HOW CAN THE NATIONAL STRATEGY FOR CLIMATE ADAPTATION BE APPLIED FOR DAMS?

In Sweden, the responsibility for dam safety and adaptation to a changing climate resides with the dam owners. In the assignment, it was investigated how the guiding principles of the national strategy agree with the legal framework and how they could be applied in dam safety work. The main finding from the assignment is that the Swedish regulation of dam safety, with associated guidelines, is in line with the guiding principles in the national strategy for climate adaptation. However, the existing dam safety guidelines could highlight and clarify the principles in a clearer way. To address climate adaptation of dams should be an integral part of the dam owners' regular risk management and management of their facilities.

The assignment report states that dam owners should consider and evaluate both internal and external conditions and hazards when developing routines for risk

management. Climate-related factors are recommended to be an integral part of the regular risk management work. At an overall level, the principles of climate change adaptation are proposed to be established as prerequisites and safety criteria against which risks are evaluated. Dam owners could also use the principles when evaluating alternative risk management measures. In this way potential measures can be verified in terms of whether they are sustainable in relation to the climate adaptation principles.

In the assignment report the following initial interpretation of the ten guiding principles were proposed, with focus on dam owners' application for dams and dam safety in hydropower and mining operations. To concretize how these principles can be applied, the assignment report recommended that research and development initiatives are taken. The aim would be to concretize how the principles can be applied as safety criteria within a framework for risk management in dam safety, and to propose an appropriate scope and approach. The results from such initiatives were recommended to be incorporated into the current guidelines for dam safety.

7.1. SUSTAINABLE DEVELOPMENT AND MUTUAL SUPPORT

Dam owners should strive for measures that strengthen dam safety today and at the same time support long-term sustainability and society's climate transition. Dam safety work should be based on the principle of long-term sustainability, which means that decision-making, planning and implementation of measures must consider interests in both the short and very long term. When choosing adaptation measures, measures that are fruitful regardless of the degree of climate change and other changes should be taken into account.

7.2. INTEGRATION OF ADAPTATION MEASURES

All societal actors should integrate measures into existing strategies and plans where possible. Dam owners are responsible for analyzing, planning and conducting their operations with regard to both short-term and long-term risks and opportunities that may arise because of climate change or in the event of changes in operations. It is the dam owner's responsibility to take adaptation measures within the operation. Where possible and appropriate, adaptation strategies and measures should be integrated into existing risk management efforts, strategies and plans by dam owners. Existing guidelines and guidelines from authorities and industry organizations that guide and support dam safety work in the country should also be further developed to take into account and include the consequences of and adaptation to a changing climate.

7.3. SCIENTIFIC BASIS

Analysis and adaptation measures should be based on the best available technology and the latest available knowledge. Dam safety work, as well as adaptation measures, must be based on science and be based on an analysis of risks and consequences based on the best technology and the latest available knowledge. SMHI, an expert authority in climatology, and Sweden's contact point for the IPCC, has a central role in climate adaptation work in Sweden, producing and making available knowledge base for society's general needs regarding climate development up to today and for various future scenarios.

7.4. THE PRECAUTIONARY PRINCIPLE, MANAGEMENT OF RISK AND UNCERTAINTY

Uncertainties and lack of knowledge about a demonstrated risk must not be used as a reason for not taking protective measures or necessary dam safety measures. For potential high-risk events, preventive measures should be implemented and preparedness planned.

The precautionary principle means that the operator is obliged to carry out the protective measures, comply with the restrictions and take the precautions in general that are necessary to prevent or counteract the activity or measures that may cause damage or inconvenience to human health and the environment. Dams are designed for extreme loads and conditions, which in itself means significant uncertainties. Caution is applied in relation to the degree of uncertainty. Lack of complete knowledge of a demonstrated potential risk should not be used as a reason to postpone or refrain from cost-effective protective measures.

The extent of the consequences of a dam failure determines the requirements for dam safety. A dam must at any given time have the degree of safety against dam failure that is reasonable with regard to the cost of achieving this degree of safety. This principle of dam safety (risk management) thus involves a balance of plausibility between the degree of safety and the cost of achieving that level of safety. The balance means that the more serious the consequences of a dam failure, the less consideration is given to the costs of maintaining dam safety. In the case of high risk, i.e. when the balance between the probability of an event and the negative consequences that may result from the event can be described as high, it is generally the case that preventive measures should be taken, preparedness should be designed and responsibilities and cooperation clarified.

For classified dams, and especially those in a high class, both the design and the dam safety work in general take into account events with a very low probability of occurring. Designing dams to be able to handle very extreme flows, determined by "method I" in the Swedish guidelines on design floods, is an example of this. If

adaptation measures are needed, robust measures that work under a range of possible future scenarios should be prioritized.

Risk assessment and planning of adaptation measures are analyzed based on various possible future developments. Several possible outcomes from these should be considered. With regard to future climate, the analysis should include several different emission scenarios and climate models, i.e. an ensemble of scenarios, which is now the practice at SMHI. The uncertainties caused by climate change and the climate transition must not lead to the postponement of dam safety measures that are necessary under current conditions.

7.5. FLEXIBILITY AND TIME PERSPECTIVE

Dam owners should strive for robust measures that take into account the lifespan of the dam and favor gradual adaptation with a variety of future policy options. The time perspective for climate adaptation measures should be based on the lifespan of the specific dam or structural part. Adaptation measures should be designed as far as possible with the aim of allowing for flexibility and robustness in a way that favors gradual adaptation with a variety of options for the future. Lock-in effects should be avoided.

The focus of current adaptation measures in many cases involves an expansion over time of monitoring and maintenance, adaptation of operations and finally physical reinforcement or rebuilding measures. In the choice of solutions for increased discharge capacity and/or increased temporary storage capacity through raising of dams, solutions should be sought that facilitate any further measures in the future. At the same time, in many cases it may be appropriate and cost-effective to implement measures with a margin, in order to avoid having to return to a facility for the implementation of a new project in the near future. In addition, margins provide additional safety already for today's climate.

7.6. TRANSPARENCY

Dam owners should be transparent regarding their management of uncertainties, risks, time perspectives, choice of climate scenarios, including the implementation of adaptation measures. This applies both internally and in communication with the relevant authorities and the public, taking information security into account

Dam owners have an obligation to document their self-monitoring and report annually on dam safety to the supervisory authority. At least once every ten years,

an overall assessment of dam safety must be carried out, documented and reported to the supervisory authority. Rehabilitation and upgrading measures and changes in water management regulations are normally subject to a permit issued by the Environmental Court. Information on safety and justification for the chosen action, as compared to alternative options, must be included in the court application.

8. CONCLUSIONS

The main conclusions from the government assignment are summarized below.

- **Benefits of dams:** Dams constitute important infrastructure in society. Climate adaptation of existing dams, through the activities they enable, contributes to the overall societal climate adaptation and the reduction of climate impact. Hydropower supplies important benefits to the power system and thereby has a decisive role as an enabler in Sweden's climate and energy transition.
- **Potential impact:** Climate change can affect dams in various ways, directly against the dam and its function, but also indirectly by changing the operating environment. In a dam safety perspective, the occurrence and safe handling of floods and new combinations of risks should be a particular focus.
- **Legal framework:** The adaptation to climate changes is an obligation for dam owners and can be carried out within the current legal framework for dam safety. Legal changes are not deemed to be necessary to date.
- **Knowledge base:** Authorities, research and industry organizations should continue to monitor climate change and work together to make use of the produced knowledge base from the assignment, develop specific climate indicators and produce supplementary documentation relevant to dam safety. Collaboration between actors is vital.
- **Guidelines:** Authorities and industry organizations should take climate change into account in their guidelines to facilitate that it is integrated as well as possible into the dam owners' regular dam safety work. Current guidelines can be further developed to explicitly include climate change and interrelated operational changes as factors to consider in risk assessments and projects to enhance dam safety. Checklists can facilitate for dam owners not to overlook potential risks.
- **Risk management:** Dam owners should take into account and analyze the risks posed by climate change within their ordinary risk management procedures. It is important to focus on known risks, that may be exacerbated by climate change and related operational changes, but also to identify potential future risks within the lifetime of the dam facility. Risk assessments should be carried out periodically.

- **Operational changes:** Uncertainty in the operation of the hydropower system is increasing. Care is needed to ensure that currently known dam safety risks do not become more likely, and that new combinations of risks are identified and managed. Continued work is necessary to better monitor and pro-actively take account of operational changes in dam safety work and vice versa.
- **Adaptation measures:** A need for gradual escalation of actions over time is foreseen. From increased monitoring, preventive or corrective maintenance, to rebuilding and change of use, or finally possibly decommissioning. For some dam facilities, dam owners have already identified the need for adaptation and implementation of upgrading measures. In such cases, it may be appropriate for the dam owner to take the knowledge base regarding future changes during the lifetime of the component or the dam into account when evaluating alternative upgrading measures and taking decisions for cost-effective and sustainable actions.
- **Future possibilities:** New technology can improve long-term weather forecasting, which can lead to opportunities to act in advance by adapting the reservoir regulation. Existing dams built for special purposes may transition to be used as multipurpose dams as a result of climate change, which may include adaptation of reservoir regulation to reduce the risk of flooding and to ensure a long-term supply of water for various purposes.

ACKNOWLEDGEMENT

Acknowledgements are given to our fellow members in the "Committee on climate change and dam safety", the group of experts that collaborated with Svenska kraftnät during the work with the government assignment.

REFERENCES

- [1] KLIMAT OCH NÄRINGS- OCH FÖRTÄRNINGSDEPARTEMENTET (2018). Nationell strategi för klimatanpassning, prop. 2017/18:163. regeringen.se/contentassets/d16e55bcada44149a8c9b8e6a7caa867/uppdrag-att-kartlagga-och-analysera-klimatforandringarnas-paverkan-pa-dammsakerheten/
- [2] SVENSKA KRAFTNÄT (2023). Klimatförändringars påverkan på dammsäkerhet. Avrapportering av uppdrag I2022/00621 att kartlägga och analysera klimatförändringarnas påverkan på dammsäkerheten. Klimatförändringars påverkan på dammsäkerhet (svk.se)

- [3] SVENSKA KRAFTNÄT (2023). Regionala klimatförändringar. En kunskapssammanställning om observerade och framtida klimatförändringar med relevans för dammsäkerhet. Regionala klimatförändringar (svk.se)
- [4] ENERGIFORSK (2023). Brandesten, C.-O. Impact of climate change on dam safety - Literature review and initial analysis. Report no. 2023:947. 2023-947-impact-of-climate-change-on-dam-safety.pdf (energiforsk.se)
- [5] SVENSKA KRAFTNÄT, SWEDENERGY AND SVEMIN (2007). Swedish Guidelines for Design Flood Determination for Dams – 2007 edition.
- [6] SVENSKA KRAFTNÄT, SWEDENERGY AND SVEMIN (2022). Swedish Guidelines for Design Flood Determination for Dams – 2022 edition. design-flood-guidelines_2022.pdf (svk.se)
- [7] BARTSCH, M., ENGSTRÖM MEYER, A. (2023). Climate change, floods and dam safety in Sweden. Symposium “Management for Safe Dams” - 91st Annual ICOLD Meeting – Gothenburg 13-14 June 2023 ICOLD2023 | SwedCOLD
- [8] SVENSKA KRAFTNÄT (2024). Dam safety - Legislation, guidance and supporting documents. <https://www.svk.se/siteassets/english/dam-safety/dam-safety—legislation-guidance-and-supporting-documents.pdf>
- [9] SWEDENERGY (2022). RIDAS – Swedenergy's dam safety guidelines. ridas_hd_eng_apr_2022_signerad.pdf (energiforetagen.se)
- [10] SVEMIN (2021). GruvRIDAS 2021 – Gruvbranschens riktlinjer för dammsäkerhet. [10] svemin-gruvridas21-dp.pdf (triggerfish.cloud)
- [11] ENGSTRÖM MEYER, A., BARTSCH, M. (2023). Dam safety regulation in Sweden – implementation process and current status, Symposium “Management for Safe Dams” - 91st Annual ICOLD Meeting – Gothenburg 13-14 June 2023 ICOLD2023 | SwedCOLD

COMMISSION INTERNATIONALE DES
GRANDS BARRAGES

VINGT-HUITIEME CONGRES DES
GRANDS BARRAGES
CHENGDU, MAI 2025

STILLING BASIN DAMAGES AT LOW HEADS – EXPERIMENTAL INVESTIGATION (*)

Erik NORDSTRÖM

Adj. Prof. (Civ. Eng.)

Vattenfall Research & Development, Älvkarleby

KTH Royal Institute of Technology, Stockholm

James YANG

Ph. D. (Civ. Eng.)

Vattenfall Research & Development, Älvkarleby

KTH Royal Institute of Technology, Stockholm

Eric LILLBERG

M.Sc. (Fluid Mechanics)

Vattenfall Research & Development, Älvkarleby

Kristian ANGELE

Ph. D. (Eng. Mechanics)

Vattenfall Research & Development, Älvkarleby

SWEDEN

SUMMARY

Structural integrity for energy dissipation of spillways is essential to maintain a high dam safety level. In some Swedish low-head facilities (< 15 m), damages appear also where flow velocities are expected to be too low to cause cavitation. To better understand the reason for damages a study including desktop survey,

**Dommages de bassin de dissipation sous faibles chutes - étude expérimentale*

hydraulic scale model tests and numerical modelling with CFD has been initiated at Vattenfall R&D.

Most common damages found in an inventory were erosion of bedrock in stilling basins, often in or adjacent to weak zones (clay filled cracks or crushed rock). Sometimes the damages progressed under concrete structures. A flow velocity above 15 m/s at the end of the crest or at the intersection with the downstream water level seems to be a limit for when damages occur in the studied spillways.

Scale model tests (1:17.5) of a case with damages has been performed to study the energy dissipation and potential causes for initiation of the damages. A CFD-model (OpenFOAM) of the same case, in model scale, has been set up to make a comparison. Measurements of flow velocities give that the tested scenario could cause flow velocities above 15 m/s in prototype scale. The pressures given by the CFD-model where in line with the ones from the model tests. From the model test the pressures, near the transition from the crest to the stilling basin, were low but not sub-atmospheric. In the CFD-model the indicated risk for cavitation was high and in the same area as the real damages. Excluded from both model tests and CFD-model is the fact that cracks where visible in the real structure. Therefore, it cannot be ruled out that the initiation of damages also was stagnation pressure in the cracks. The study will continue with further tests with more pressure gauges and simulations. and the validation of the numerical model and conclusions presented are therefore preliminary.

RÉSUMÉ

Maintenir l'intégrité structurelle lors de la dissipation de l'énergie des déversoirs est essentiel pour garantir un niveau élevé de sécurité des barrages. Dans certaines installations suédoises à faible chute (< 15 m), des dommages apparaissent là où les vitesses d'écoulement devraient être trop faibles pour provoquer une cavitation. Pour mieux comprendre la raison de ces dommages, une étude comprenant des simulations numériques, des essais sur modèle hydraulique et une modélisation numérique avec CFD a été effectuée au département R&D de Vattenfall.

Le dommage le plus couramment observé est l'érosion du substrat rocheux dans les bassins de stabilisation, souvent dans ou à proximité de zones de faiblesses (fissures remplies d'argile ou roche concassée). Dans certains cas, les dégâts se sont propagés sous les structures en béton. Une vitesse d'écoulement supérieure à 15 m/s en extrémité de crête ou à l'intersection avec le niveau d'eau aval semble être une limite lors de l'apparition de dommages dans les déversoirs étudiés.

Des tests sur modèle réduit (1:17,5) d'un cas présentant des dommages ont été effectués pour étudier la dissipation d'énergie et les causes potentielles de

l'initiation des dommages. Un modèle CFD (OpenFOAM) du même cas, à l'échelle du modèle, a été développé pour effectuer une comparaison. Les mesures des vitesses d'écoulement indiquent que le scénario testé pourrait provoquer des vitesses d'écoulement supérieures à 15 m/s à l'échelle du prototype. Les pressions données par le modèle CFD se sont révélées conformes à celles des essais sur modèle. D'après les essais sur modèle, les pressions, près de la transition de la crête au bassin de stabilisation, étaient faibles mais pas sub-atmosphériques. Dans le modèle CFD, le risque de cavitation était élevé et se situait dans la même zone que les dommages réels. Le fait que des fissures étaient visibles dans la structure réelle est exclu des essais sur modèle et du modèle CFD. On ne peut donc pas exclure que le déclenchement des dommages soit également dû à une pression stagnante dans les fissures. L'étude se poursuivra avec d'autres essais avec davantage de manomètres et de simulations. La validation du modèle numérique et les conclusions constituent donc une étape préliminaire.

1. INTRODUCTION

Structural integrity for energy dissipation of spillways is, during a flood event, essential to maintain a high level of dam safety. Most of the Swedish dams and spillways were constructed more than five decades ago. Over the years, various types of discharge events have occurred. Both routine and conditioning tests of the spillway gates and flood events at different levels have been the causes for discharge and thereby use of energy dissipating structures. In assessment of stilling basins and other structures, normally submerged, damages sometimes are observed. In some low-head facilities (< 15 m), damages appear even if the flow velocities are expected to be too low to cause cavitation. Eroded concrete, rock and concrete scouring to sizable depths, removed or demolished reinforcement, backwards erosion under guide walls or thresholds, etc. are damages often found.

To better understand the reason for damages and to get a better theoretical basis for design of remedial measures, a series of projects have been initiated at Vattenfall Research & Development (R&D). Some of the ongoing activities are presented below with their current status including desktop study, experimental scale model tests and numerical modelling with CFD. The experimental series is ongoing, and the validation of the numerical model and conclusions are therefore preliminary.

2. SPILLWAY INVENTORY ALONG A RIVER REACH

Quantitative data regarding spillways commonly only contain information on discharge capacity, water levels and drawings. To create knowledge about parameter parameters that cause damages in stilling basins, even at relatively low

heads, an inventory of 31 Swedish dam spillways was done. The systematic review of the spillways consisted of parameters like:

- Type of spillway
- Geometrical data (threshold level, spillway width, shape of overflow crest, energy dissipation structure, etc.)
- Hydrological parameters (floods of different return periods, design flood, reservoir and downstream water levels, etc.)
- Hydraulic parameters (spillway discharge capacity, flow regimes, flow velocity, etc.)
- Preferred sequence for gate operation and potential restrictions
- Historical activities (changes and repairs)
- Identified changes

In summary, the most identified damages for the examined facilities were erosion of bedrock in stilling basins, often in or adjacent to weak zones (clay filled cracks or crushed rock). Sometimes the damages were initiated in the weak zone and then progressed as backwards erosion under concrete structures close to the weak zone (e.g. crest, guide walls). Varying degree of erosion of concrete surfaces was identified both along the spillway chute above the downstream water level, in the submerged parts of the spillway or further downstream in the stilling basin.

Several facilities have been refurbished or re-designed. To make comparisons or follow the development of a damage is more challenging since the prerequisites have changed. Most repairs downstream of the spillway and down into the stilling basin have been repaired with underwater concrete anchored with a large amount of un-tensioned anchors grouted into the bedrock (spacing 1-2 meters). Damaged spillway crests are often repaired with patching or hydro demolishing, followed by applying conventional concrete with slipform or shotcrete.

To investigate any systematic correlation or pin-point parameters of importance for why damages has occurred in the spillway or stilling basin some simple comparisons were made. In Fig. 1, the spillways along the investigated river stretch are highlighted in a graph with flow velocities at the sill/gate position (free flow) on the x-axis and the calculated flow velocity at the end of the crest or in the position where the water intersects with the downstream water level at the y-axis. The relation between flow velocities and damages for the structures, not being redesigned or more recently constructed, seems relatively good. Flow velocity above 15 m/s at the end of the crest or at the intersection with the downstream water level seems to be a limit for when damages occur in the studied spillways.

Apart from the above used data there are several other parameters that could influence the risk for damages. The roughness of surfaces, offsets due to poor construction quality and presence of cracks are seldom compiled. In addition, a poor design can be a problem from a hydraulic perspective.



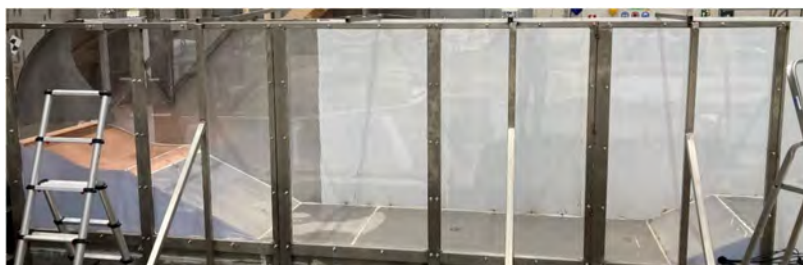


Fig. 2
 Overview photo of energy dissipation rig
Photo d'ensemble de l'installation de dissipation d'énergie

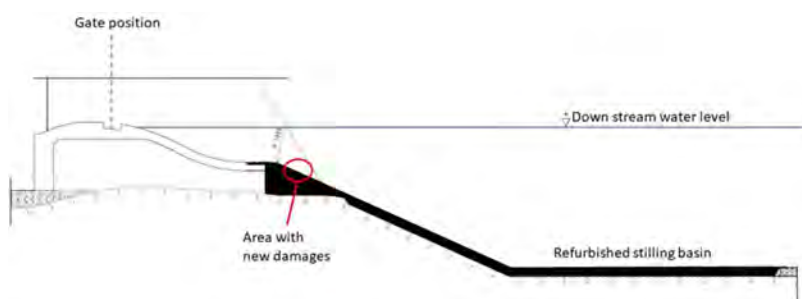


Fig. 3
 Schematic layout of spillway for the studied case
Aménagement du déversoir pour le cas étudié

The case studied was inaugurated in the 1960s and the head of the facility is only 12 m. The discharge capacity of the studied spillway is $\sim 820 \text{ m}^3/\text{s}$ at full retention level. Early in the 21st century, extensive concrete damages in the stilling basin floor were repaired; the transition between the crest and the stilling basin was redesigned to prevent new damages. During a follow-up with a remotely operated vehicle under water in 2022, it was noted that the area where the previous damages occurred remained unchanged. Instead, new damages were identified very close to the connection between the crest and the refurbished basin. Local, but partially several decimetres deep, damages were identified along the slope down into the stilling basin. During the time after rehabilitation, no extreme flood events with long duration has occurred. Ordinary seasonal variations with higher discharge during snow melt periods in the spring, spillage due to interruption in power production or operation of gate during inspections caused spillage.

The question is under what type of conditions the damages did occur and which the paramount mechanisms and loads where that caused it. During ordinary operation at the facility the downstream water level will be at normal average when the gate is opened, and during inspection the gate sometimes is fully opened with full discharge and free outflow to test all mechanical equipment and functions in connection to this. That scenario will give one level of flow velocities, position of the hydraulic jump and following energy dissipation in the stilling basin. In a flooding situation or at design flood, the downstream water level will be much higher than average and with another position for the hydraulic jump and much better energy dissipation in the stilling basin due to this.

In the energy dissipation rig, a series of potential scenarios for tests was set up. One scenario is the sudden interruption of the power production, with a $308 \text{ m}^3/\text{s}$ discharge in the prototype, corresponding to 240 l/s in the scale model. To capture what happens in the damaged area, several pressure gauges were installed to measure the pressure fluctuations and any signs of sub-atmospheric pressure (Fig. 4).

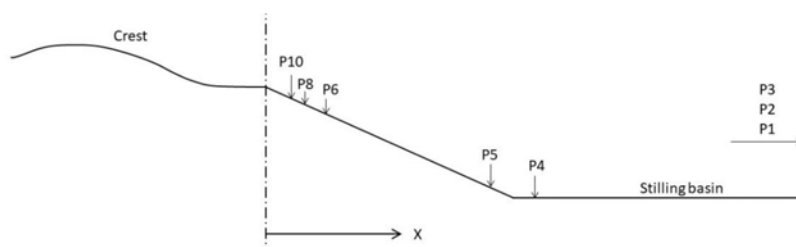


Fig. 4

Positioning of pressure gauges in the upstream part of the model
Positionnement des manomètres en partie amont du modèle

Firstly, the quality of experimental set-up was tested by checking if stationary conditions with constant flow velocities and downstream water level could be kept. Repeated tests gave that repeatability was within the measurement uncertainty of the sensors. In the following tests a higher discharge pushes the hydraulic jump and the streamwise position for large water-level variations further downstream. The amplitude of the water-level variations increases with an increasing discharge, and the covered area becomes larger. In Fig. 5 photos from a test with 240 l/s is shown.

The pressures measured in the area close to the transition between crest and slope down into the stilling basin are very low, but not sub-atmospheric. A presentation of the measured pressures in relation to the numerical model can be seen in Fig. 12. In addition to the pressure measurements the water-depth was measured at the transition ($x = 0 \text{ m}$) during a discharge of 240 l/s and thereby the average flow



Fig. 5
Model tests in energy dissipation rig at 240 l/s
Essais sur modèle de dissipation d'énergie avec 240 l/s

velocity was calculated as 3.7 m/s. In the prototype scale this would correspond to a velocity of 15.4 m/s.

4. NUMERICAL MODELLING

To further investigate the reasons for development of damages in the studied case, CFD modelling was done. The first attempt was to compare with the experiments and validate the CFD setup.

The simulations were performed using the open-source toolbox OpenFOAM version 2306 [1]. The equations solved are the Navier-Stokes equations for turbulent, two-phase, incompressible flow with gravity. The two phases, water and air, are non-miscible and the convection of both phases is done using a common velocity field and a volume fraction scalar, referred to as a Volume of Fluid (VOF) approach [2].

Since the pressure fluctuations resulting from the large-scale mixing in the stilling basin are important, Detached Eddy Simulation (DES) was used for the turbulence modelling. The kOmegaSSTDES [3] model was used which limits the requirements on mesh resolution in the boundary layer region compared to standard Large Eddy Simulation (LES) models [4].

The experiment simulated numerically was $Q_m = 240$ l/s ($Q_p = 308$ m³/s), with a 1.0 m differential head up- and downstream. The geometry was the same as in the test rig. The spillway crest and the stilling basin were assigned no-slip walls while remaining surfaces given a slip boundary condition. Shown in Fig. 6, the light blue surface was the inlet with the hydrostatic pressure in the upstream reservoir. At the outlet, a constant water level was set up as in the experiment.

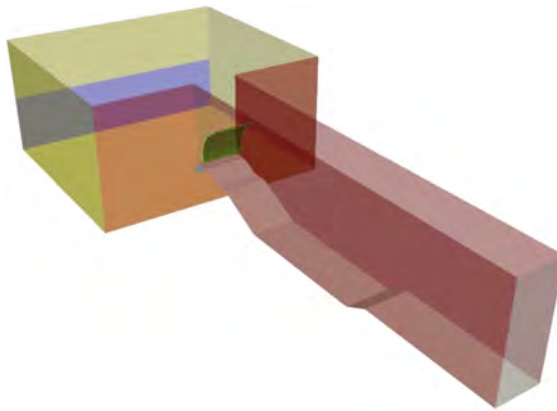


Fig. 6
Computational domain with boundary conditions
Domaine de calcul avec conditions aux limites

The mesh was generated using the OpenFOAM native tool snappyHexMesh which automatically generates a hex dominated polyhedral mesh. The mesh is coarse with a 0.0125 m spacing in the mixing region using a refinement box which contains the entire mixing region and the free surface interface, as seen in Fig. 7. A wall normal distance of 0.0005 m was used giving a $max\ 30 < y+ < 300$ and the total number of cells were 3 895 230.

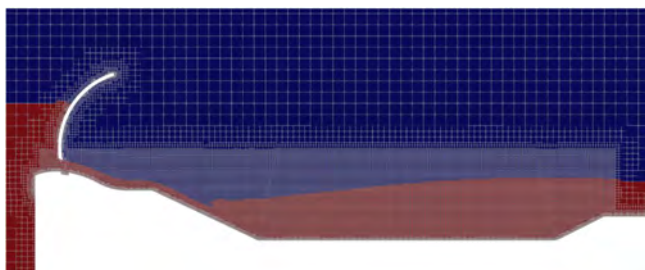


Fig. 7

Computational mesh with mean two-phase distribution as reference
Maillage de calcul avec distribution diphasique moyenne comme référence

In Fig. 8 the instantaneous velocity magnitude is shown 0.005 m above the bottom surface and on a cut-plane which is clipped at the free water surface. Here the high velocity flow under the gate is seen and the formation of the hydraulic jump halfway down on the upstream slope of the stilling basin. As the flow accelerates under the gate, the sill geometry slows down the velocity before the horizontal part just before the slope. Over the edge to the slope the velocity increases again and reaches a maximum at the 25° corner before the slope down into the basin below. The streamwise vortices which rolls up at the entrance by the acceleration of the water into the flow channel gets stretched under the gate and creates a striped velocity pattern on the sill and the slope.

In Fig. 9 the free surface is added together with the bottom surface and the cut-plane colored with velocity magnitude. Here the violent mixing region is clearly seen and the ridges building up on the free surface as the flow exits under the gate and interacts with the streamwise vortices.

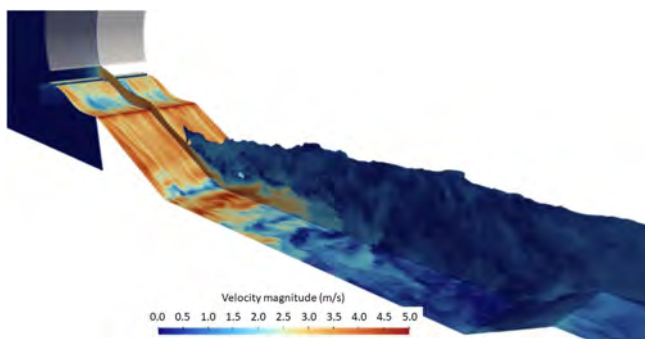


Fig. 8

Velocity magnitudes, cut plane at 0.005 m above bottom and at free water surface.
Champs de vitesses, coupe à 0,005 m au-dessus du fond et à la surface libre

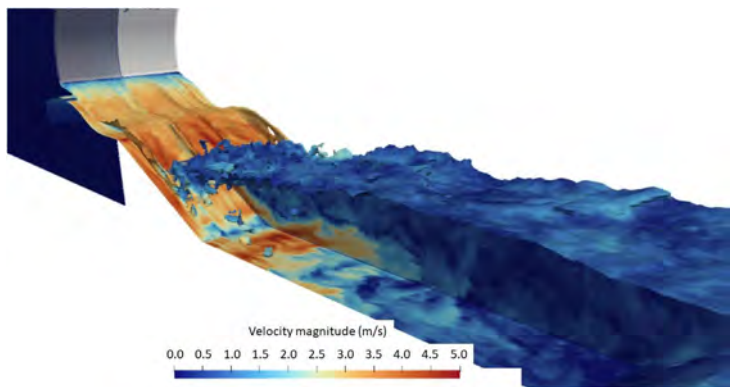


Fig. 9

Velocity magnitudes, cut plane at 0.005 m above bottom and at free water surface and the free water surface

Champs de vitesses, plan de coupe à 0,005 m au-dessus du fond et à la surface libre et aperçu de la surface libre

The high velocity creates large mean pressure changes and pressure fluctuations along the flow path. In Fig. 10 the mean gauge pressure is shown as contours on the bottom surface. Noticeable is the high pressure at the bottom of the stilling basin as the water jet hits the corner and the very low pressure over the crest before the slope into the basin. The pressure predicted by the simulations is in fact so low that it would result in cavitation in the prototype.

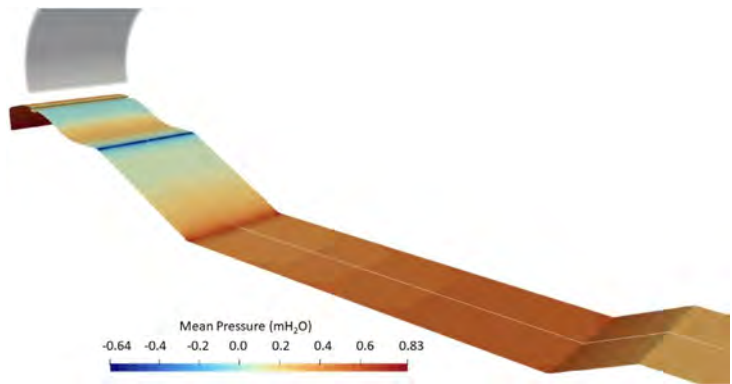


Fig. 10

Mean pressure shown as contours on the bottom

Pression moyenne représentée sous forme de contours sur le fond

For the root mean square (RMS) of the pressure fluctuations the highest values are in the region after the hydraulic jump and where the high velocity flow hits the bottom of the basin, but also on the crest before the slope. In Fig. 11 RMS of the pressure fluctuations is shown along the bottom surface.

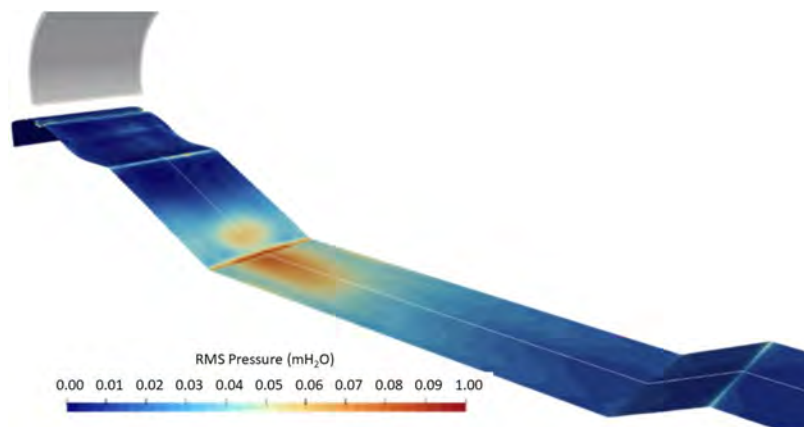


Fig. 11
RMS pressure along the bottom surface
Pression RMS le long du fond

The CFD results are compared to the experimental data along the centerline from the upstream slope of the stilling basin to the outlet, as shown by the white line in Fig. 10 and Fig. 11. The computational model domain is somewhat shorter than the experimental rig; therefore, the far downstream measurement point is not exactly covered by the simulation. Compared to the measurement data the mean pressure is captured well by the simulations at the points where it was measured (Fig. 12). The low gauge pressure seen at the crest was not measured in the experiment and the pressure predicted in the CFD is very sensitive to mesh resolution and treatment of the turbulent boundary layer, hence it's difficult to say what the actual pressure is without real measurements. By e.g. adding some wall roughness, the boundary layer thickens, and the pressure increases in the region which makes the indicated risk of cavitation in the prototype decrease or vanish completely. It was observed experimentally that there is in fact a low-pressure region but it remains to verify the actual pressure level.

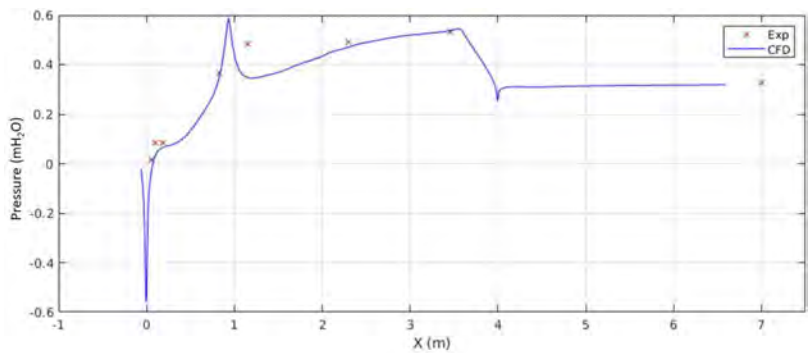


Fig. 12

Mean pressure along centerline (physical & CFD model)

Pression moyenne le long de la ligne médiane (modèle physique et CFD)

Similarly, the RMS of the pressure fluctuations is compared to the measurements in Fig. 13. Here the RMS levels at the first peak is quite well captured but the two points just after the first peak, directly downstream of the crest, are under-predicted by the simulation. Further downstream the agreement is good considering that there are just a few measurement points and that very small changes in the strength and position of the mixing region will lead to large changes in the position of the peaks. In the downstream mixing region, the decay of the turbulent flow structures is well captured, although the mesh is very coarse.

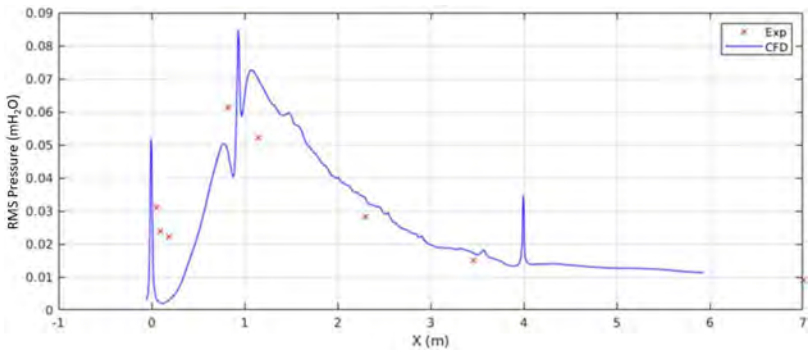


Fig. 13

RMS of pressure fluctuations at the bottom along the center line

RMS des variations de pression au fond le long de la ligne médiane

In the region of low gauge pressure there is an apparent risk of cavitation in the prototype. Calculating the cavitation number, *Sigma*, from local pressures and velocities scaled to prototype and visualizing it together with a drawing of the damages to scale (see Fig. 14), it is clearly seen that the region of low values of *Sigma* overlaps the region where the damages has been detected in the prototype and where potential cavitation bubbles could implode.

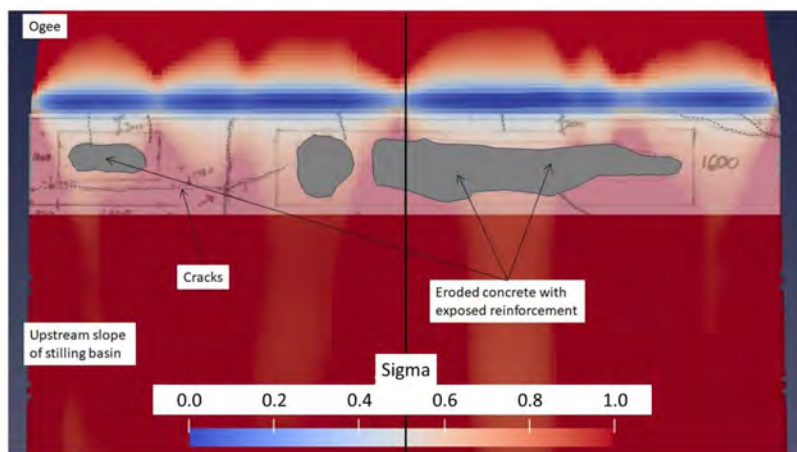


Fig. 14

Cavitation number from CFD overlayed with damages in stilling basin slope
Numéro de cavitation du modèle CFD superposé aux dommages dans la pente du bassin de tranquillisation

5. CONCLUSIONS

Damages in the stilling basin are found in several low head facilities after several decades of normal operation without being exposed to design flood or extreme flooding events. Physical scale model tests together with numerical modelling on a specific case have been used to investigate the pressure situation in the stilling basin. The CFD-model of the physical scale model tests gave that cavitation might be caused with the current geometry and for the tested case. At partial discharge (of the maximum capacity) the CFD-model show very low cavitation numbers that indicate risk for sub-atmospheric pressures due to high flow velocities. Measurements in the scale model tests also show that flow velocities above 15 m/s at the position for the transition from the crest to the stilling basin could occur at the same discharge.

The fact that cracks are found in prototype, in the concrete along the upstream slope of the stilling basin, give the possibility that also dynamic pressure fluctuations or stagnation pressure in the cracks could be a possible explanation to the initiation of damages in the real structure.

After initiation of concrete damages, pressure fluctuations in general, potentially together with cavitation could make damages progress by causing vibrations on the rebars. This would further crack the surrounding concrete and extend the area of damages.

Additional tests in the energy dissipation rig at Vattenfall R&D with increased number of pressure gauges at more positions together with further CFD-modelling are planned. The continued investigation will further shed light on the phenomena regarding energy dissipation in low head facilities with damages.

ACKNOWLEDGEMENTS

The physical model studies discussed herein were carried out at Vattenfall R&D's hydraulic laboratory, Älvkarleby, Sweden. The authors are grateful for financial support from Vattenfall, BU Hydro that has made the study possible. Sharing of detailed info from several cases is also of utmost importance for the project. Thanks also to all staff from Vattenfall R&D workshops and Anna Helgesson for performing the scale model tests.

REFERENCES

- [1] <https://www.openfoam.com>. Version 2306
- [2] HIRT, C.W.; NICHOLS, B.D. (1981). "Volume of fluid (VOF) method for the dynamics of free boundaries". *Journal of Computational Physics*. 39 (1):201–225. doi:10.1016/0021-9991(81)90145-5.
- [3] GRITSKEVICH, M. S., GARBARUK, A. V., SCHÜTZE, J., & MENTER, F. R. (2012) "Development of DDES and IDDES formulations for the $k-\omega$ shear stress transport model." *Flow, turbulence and combustion*, 88(3), 431–449. DOI:10.1007/s10494-011-9378-4
- [4] POPE, S. B. (2000) "*Turbulent Flows*", Cambridge University Press. ISBN:9780521598866

COMMISSION INTERNATIONALE DES
GRANDS BARRAGES

VINGT-HUITIEME CONGRES DES
GRANDS BARRAGES
CHENGDU, MAI 2025

**OPTIMAL RIVER BANK PROTECTION DESIGN BY COMBINING HYDRAULIC
MODELLING WITH TURBULENCE-BASED DESIGN METHODS (*)**

Pierre-Louis LIGIER, Lisa CARLSSON & Maja RYLANDER
Hydropower and Dams Division, Sweco

Johanna SIPOLA ÄIJÄ
Vattenfall Vattenkraft AB

SWEDEN

SUMMARY

Damages of the bank protection on the right side of the tailrace and spillway discharge channel have been identified downstream of one of Vattenfall's hydropower plant located in Northern Sweden. The bank protection on the right side of the discharge channel, downstream the stilling basin, are made of armourstone material in three different zones: $D_{50} = 1.14$ m along 90 m downstream of the stilling basin, $D_{50} = 0.87$ m along 45 m further downstream and finally $D_{50} = 0.30$ m along 180 m. The affected area is located more than 120 m downstream the spillway's stilling basin, in which the bank protection is composed of the smallest armourstone size. In order to identify appropriate remediation measures, a hydraulic assessment has been performed in order to investigate the flow conditions in this region. A two-dimensional hydraulic model has been developed using high resolution bathymetry from multibeam echo-soundings and LiDAR topography. The model covers approximately 700 m of the discharge channel. As high turbulence levels are expected during high flows, turbulence was modelled using the two-equation,

**Optimisation de la conception des protections de berge en enrochements en combinant modélisation hydraulique et méthodes de dimensionnement basées sur la turbulence*

depth-averaged k-epsilon model. Results showed that if the velocities in the region where damages occurred were not extremely high, they also showed an increased turbulence level compared with the center of the channel, with the highest turbulence level occurring in the vicinity of the affected area. Turbulence-based design methods, to prevent damages caused by erosion, showed that rock sizes of D_{50} between 0.60 and 0.90 m are required along the right bank in order to withstand local turbulence levels. The method used earlier for the design of the existing bank protection was relying on cross-section-averaged velocities and schematic description of expected flow conditions. Comparison of the two methods showed that multi-dimensional hydraulic and turbulence modelling combined with turbulence-based design methods can contribute to a better understanding of erosion phenomena and to optimal bank protection design.

RÉSUMÉ

Des dommages au niveau de la protection de berge en rive droite du canal de fuite collectant le débit de la centrale et de l'évacuateur de crue ont été identifiés en aval d'un des barrages hydroélectriques de Vattenfall située dans le nord de la Suède. La protection des berges du côté droit du canal de fuite, en aval du bassin de dissipation, est constituée de blocs dans trois zones différentes : $D_{50} = 1,14$ m sur 90 m en aval du bassin de dissipation, $D_{50} = 0,87$ m sur 45 m plus en aval, et enfin $D_{50} = 0,30$ m sur 180 m. La zone touchée est située à plus de 120 m en aval du bassin de dissipation, où la protection des berges est composée de la fraction la plus fine. Afin de déterminer les mesures correctives appropriées, une étude hydraulique a été réalisée pour caractériser les conditions d'écoulement dans cette région. Un modèle hydraulique bidimensionnel a été mis en œuvre à l'aide d'une bathymétrie à haute résolution au sondeur multifaisceaux et d'une topographie LiDAR. Le modèle couvre environ 700 m du canal de fuite en aval du barrage. Étant donné que des niveaux élevés de turbulence sont attendus dans le canal en cas de fonctionnement de l'évacuateur, la turbulence a été modélisée à l'aide du modèle k-epsilon. Les résultats ont montré que si les vitesses dans la région où les dommages se sont produits n'étaient pas extrêmement élevées, ils indiquent que le niveau de turbulence y est plus important qu'au centre du canal. Ils indiquent également que les niveaux de turbulence les plus élevés se produisent à proximité de la zone touchée. Les méthodes de dimensionnement de protection de berge en enrochements basées sur la turbulence ont montré que des tailles de roches de D_{50} comprises entre 0,60 et 0,90 m sont nécessaires le long de la rive droite pour résister aux niveaux de turbulence locaux. La méthode utilisée antérieurement lors la conception de la protection des berges existante reposait sur des vitesses moyennes de section transversale et une description schématique des conditions d'écoulement attendues. La comparaison des deux types de méthodes a montré qu'une modélisation multidimensionnelle hydraulique associée avec un modèle de turbulence approprié, combinés avec des méthodes de dimensionnement basées

sur la turbulence, peuvent contribuer à une meilleure compréhension des phénomènes d'érosion ainsi qu'à une optimisation de la conception de la protection de berge en enrochements.

1. INTRODUCTION

1.1. PRESENTATION OF THE HYDROPOWER SCHEME

The hydropower plant and dam highlighted in this article are located in Northern Sweden and are owned by Vattenfall. The facility is composed of two embankment dams separated by a central concrete dam hosting the powerplant and the spillway. The hydropower plant was commissioned in the early 1960s.

The spillway has three radial gates discharging in three parallel chutes exiting in a stilling basin located just next to the powerplant outlet. The discharge from the powerplant and the spillway is conveyed downstream in a tailrace channel. A site plan is presented in Fig. 1.



Fig. 1

*Site plan. © Swedish Land Survey authority (Lantmäteriet)
Plan de situation. © Swedish Land Survey authority (Lantmäteriet)

1.2. HISTORY OF RIVER BANK PROTECTION DESIGN AND DAMAGES

In 2006, reinforcement of erosion protection on both sides of the tailrace channel was done. The new bank protection was designed so that the tailrace channel could withstand a 100-year flood event without damages, while some minor damages with no consequences for dam safety could be tolerated for the facility's design flood (class I flood, which is a hydrological event that can be considered having a return period of over 10 000 years). The banks are characterized by a slope of 2H:1V.

Flow velocities and water depths determined from physical model tests were used to design the material sizes to be used in the bank protection based on the HEC-11 Design of Riprap revetment method [1]. In the following, only bank protection characteristics along the right side of the tailrace channel are considered. Three different zones have been defined, from the downstream end of the stilling basin and covering approximatively 300 m of the right bank in the downstream direction. The zones delineation and corresponding armourstone material size defined by means of the median diameter D_{50} are (see Fig. 1):

- Zone 1 – 0+130 to 0+210: $D_{50} = 1.14 \text{ m}$
- Zone 2 – 0+210 to 0+255: $D_{50} = 0.87 \text{ m}$
- Zone 3 – 0+255 to 0+435: $D_{50} = 0.30 \text{ m}$

In the upstream part of Zone 1, the lower part of the bank is protected by an anchored concrete retaining wall. Only the upper part of the bank, approximatively from the normal water level, is protected by armourstone material. In the rest of the right bank, the protection is composed of two layers of armourstone material covering the whole slope and the toe.

In 2007, a discharge test was conducted for a total discharge corresponding to the 100-year flood. Damages to the newly installed bank protection were observed on both sides of the tailrace channel. The damages on the right bank occurred at the beginning of Zone 3 where the median armourstone diameter is $D_{50} = 0.30 \text{ m}$, where maintenance repair operations were performed after the event.

Since 2007, damages to bank protection in Zone 3 have been regularly observed after the use of the spillway during spring flood, which required regular maintenance operations. Overall, bank protection damages have been observed along approximately 80 m between sections 0+250 and 0+330. The observed damages in this zone are not considered as a potential dam safety risk.

In 2022, a bathymetrical survey performed with multibeam echo-soundings revealed the presence of slumped material at the right bank toe in the upstream part of Zone 3 (between sections 0+250 and 0+300), where earlier damages were observed. Observations made during a site inspection in 2023 revealed that the

material used in the bank protection in this region have a smaller size compared with the downstream part of Zone 3 (between sections 0+330 and 0+435) where no damages were observed.

No damages have been observed in Zones 1 and 2 since 2006.

2. PURPOSE OF THE STUDY

In 2023, Vattenfall initiated a project aiming at defining remediation measures for the bank protection on the right bank of the tailrace channel. The steps involved in this project were as follows:

- Detailed hydraulic assessment in order to investigate flow conditions in the tailrace channel focused on the right bank.
- Definition of remediation measures based on the findings from the hydraulic assessment. The design criteria chosen was a 100-year flood event.

The focus of the study was put on the analysis of bank protection design in Zone 3. The rest of this article focuses on presenting the methodology and results from the detailed hydraulic assessment as well as the lessons learned regarding bank protection design.

3. HYDRAULIC ASSESSMENT

3.1. PRELIMINARY ANALYSIS AND CHOICE OF MODELLING APPROACH

The analysis of historical damages along the tailrace channel's right bank showed that bank protection damages start at the limit between Zones 2 and 3, located approximately 120 m downstream of the stilling basin and where the median diameter D_{50} of the armourstone material changes from 0.87 m down to 0.30 m (decrease by almost factor 3). This region also coincides with the beginning of a left bend of the tailrace channel. Analysis of aerial photographs showed that during spillway operation, turbulence patterns are visible in the flow all along the three bank protection zones, hinting at relatively high turbulence levels propagating downstream of the stilling basin (see Fig. 1). Hence, turbulence was identified as a key factor to be accounted for in the hydraulic assessment.

Based on data available (geometry, bathymetry) for the project, it was decided to use a two-dimensional hydraulic model (2D, depth-averaged). A 2D hydraulic model was deemed the most suitable approach being given the channel geometry that is not complex enough to require 3D or CFD modelling, while still being able to

perform high-resolution calculations using the multibeam echo-sounding survey with a low computational cost. The lack of 3D CAD model for the spillway construction was also an inconvenient for performing a throughout CFD analysis from upstream of the dam down to the tailrace channel.

3.2. INPUT DATA AND HYDRAULIC MODEL FEATURES

The main input data to the 2D hydraulic model is a Digital Elevation Model (DEM). The DEM was created by combining the high-resolution multibeam echo-sounding survey performed in 2022 with LiDAR data for the topography above the water surface from the Swedish Land Survey authority (Lantmäteriet). Special care was given to handle the transition between LiDAR and multibeam echo-soundings in order to retain a good interpolation across the water surface in shallow areas. The DEM covers approximately 700 m of the tailrace channel including the stilling basin and has a spatial resolution of 0.5 m. The region immediately downstream of the powerplant outlet could not be surveyed but bottom levels were recreated based on information from drawings.

The 2D hydraulic model used was TELEMAC-2D (version 8.3.0) from the open-source suite openTELEMAC-MASCARET [2]. TELEMAC-2D solves the Shallow Water Equations on an unstructured triangular mesh using the Finite Element Method with a large choice of turbulence models [3].

The 2D model developed has the same extent as the DEM. The computational mesh is composed of approximately 250 000 triangular cells with an edge length of 1 m in the whole domain. The model domain and the bottom elevations as well as the location of the bank protection damages and slumped material identified in Zone 3 are illustrated in Fig. 2.

The model has four boundaries: the three spillway chutes (boundaries are located inside the stilling basin) where the total inflow corresponding to a 100-year flood event is prescribed, as well as the downstream boundary located approximately 700 m downstream of the stilling basin where the stationary water level corresponding to the same flood event is set as boundary condition (+46.15 m.a.s.l.). It was considered that all the 100-year flood was discharged through the spillway with no turbine flow through the powerplant.

Turbulence was modelled using the depth-averaged k-epsilon turbulence model in order to use the computed turbulent kinetic energy as input to bank protection design. The depth-averaged k-epsilon turbulence model belongs to the family of Reynolds-averaged Navier Stokes (RANS) based turbulence models [3] [4].

As the length of the model is limited in the streamwise direction (approximately 700 m), no significant friction losses develop between the upstream and downstream ends, making calibration in terms of bottom friction coefficient not

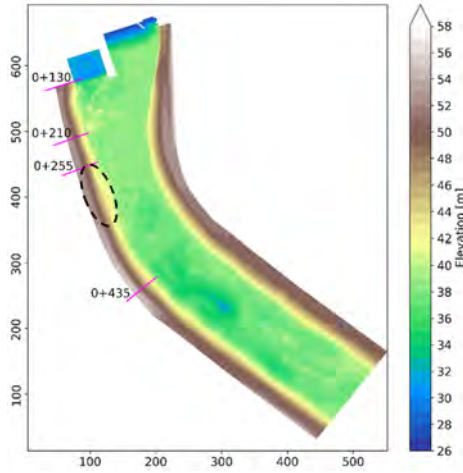


Fig. 2

Model domain and bottom elevations. Dashed ellipse: location of bank protection damages and visible slumping at bank toe

Emprise du modèle numérique et bathymétrie. Ellipse : emplacement des dommages et de l'éboulement identifié en pied de berge

relevant. Bottom friction was modelled using a Strickler coefficient of $K_s = 30 \text{ m}^{1/3}/\text{s}$, which corresponds to a Manning coefficient $n = 0.0333 \text{ s/m}^{1/3}$. A sensitivity analysis on this parameter has been performed in order to estimate its influence on flow conditions. No significant influence was identified, hence all the simulations were performed with the aforementioned values.

3.3. TURBULENCE-BASED EROSION PROTECTION DESIGN METHODS

Erosion protection design methods are usually based on the incipient motion concept defined by the Shields equation. The Shields equation states that the load required to set particles into motion (called the critical bed shear stress τ_c [N/m^2]) is proportional to the strength of the bed material defined as $(\rho_s - \rho)gD_{50}$, with the proportionality factor being called the critical Shields parameter Ψ_c [-]:

$$\tau_c = \Psi_c (\rho_s - \rho)gD_{50} \quad (1)$$

With ρ_s the material specific density [kg/m^3], ρ the water density [kg/m^3], g the acceleration of gravity [m/s^2] and D_{50} the median particle diameter [m]. The value of

the critical Shields parameter Ψ_c varies in function of material type and particle Reynolds number. For natural materials (sediments to stones), Ψ_c typically varies between 0.02 and 0.06 [5].

One of the main challenges in applying incipient motion methods based on the Shields equation is the estimation of the bed shear stress. The bed shear stress is often estimated assuming steady-state flow conditions. If this assumption is usually acceptable for uniform flow conditions, it can become uncertain in non-uniform flow conditions in which the dynamic bed-pressures variations, arising from flow turbulence, can significantly affect the onset of material erosion.

The concept of turbulence-based erosion protection design methods is to explicitly account for flow turbulence in the load term used in the Shields equation. The turbulence parameter used is called the relative turbulence intensity r_0 [-] defined as [5]:

$$r_0 = \frac{\sqrt{k_0}}{U_0} \quad (2)$$

With k_0 the depth-averaged turbulent kinetic energy [m^2/s^2] and U_0 the depth-averaged flow velocity [m/s]. By combining the Shields equation (Eq. [1]) with the definition of bed shear stress τ_0 [N/m^2]:

$$\tau_0 = \rho u_*^2 \quad (3)$$

and with the relationship between the depth-averaged turbulent kinetic energy k_0 and the friction velocity u_* [m/s]:

$$\sqrt{k_0} = \alpha_0 u_* \quad (4)$$

Hoffmans proposed the following design equation [5]:

$$D_{50} = 0.7 \frac{(r_0 U_0)^2}{\Delta g \Psi_c} \quad (5)$$

With Δ the relative material density defined as $(\rho_s - \rho)/\rho$ and using a numerical value of 1.2 for the coefficient α_0 as suggested in [5].

The equation is valid for bed material in both uniform and non-uniform flow conditions [5]. In uniform flow conditions, differences between this method and the classic methods based on bed shear stress are small as flow turbulence is generated by bottom friction. On the other hand, in non-uniform flow conditions, differences between the two types of methods might arise due to the direct influence of local flow turbulence on shear stress at near the bed. Typical values for relative turbulence intensity are presented in Table 1.

Table 1
Relative turbulence intensity typical values [5]
Valeurs indicatives pour l'intensité turbulente relative [5]

r_0	Turbulence level	Remarks
0	No turbulence	Laminar flow
< 0.08	Small turbulence	-
0.08 – 0.15	Normal turbulence	Channel, river flow
0.15 – 0.20	High turbulence	Downstream of structures (bridges, piers, etc.)
0.20 – 0.30	Very high turbulence	Downstream hydraulic jumps, sharp bends, etc.
0.30 – 0.60	Extreme turbulence	-

The design equation proposed by Hoffmans (Eq. [5]) can easily be combined with 2D hydraulic models in which the k-epsilon turbulence model is used as U_0 and k_0 are variables given directly by the numerical model.

For erosion protection design, the critical Shields parameter can be used as a design criterion for permissible damage. A typical value for riprap revetments used in bank protection is $\Psi_c = 0.03$ while a value of $\Psi_c = 0.02$ represents a more conservative criterion for permissible damage [5].

For bank protection design, D_{50} calculated with Eq. [5] should be divided by the bank slope factor K_{sl} [-]:

$$K_{sl} = \sqrt{1 - \left(\frac{\sin \theta}{\sin \Phi} \right)^2} \quad (6)$$

With θ the bank slope angle and Φ the material friction angle which is usually 40° for bank protection material (armourstone made of blasted rock). For this study, $\theta = 26.6^\circ$ yielding $K_{sl} = 0.72$ are used. The results regarding calculated D_{50} values presented in the following section are based on Eq. [5] which has been applied for both $\Psi_c = 0.03$ and $\Psi_c = 0.02$. For bank protection design, D_{50} should be calculated with $\Psi_c = 0.03$ and then been divided by K_{sl} . As $0.02/0.03 \approx 0.72$, the results obtained with Eq. [5] and $\Psi_c = 0.02$ were used as input for the bank protection design.

3.4. RESULTS

Flow conditions in the tailrace channel for the 100-year flood event and for the current bathymetry (with the slumped material left in place at the upstream end of

Zone 3) are illustrated in terms of water depth, depth-averaged flow velocity, depth-averaged turbulent kinetic energy and relative turbulence intensity in Fig. 3.

Water depth along the right bank toe varies from approximately 6 m in Zone 1 to 7-8 m along Zone 2 and progressively increases along Zone 3 from 7-8 m to locally approximately 10 m. Water depth in the center of the channel follows the same pattern with a gradual increase from approximately 6-7 m in front of Zone 1 to 10-12 m in Zone 3. Water depth in the region where damages were observed (upstream part of Zone 3) is varying between 7-8 m.

Analysis of flow velocities shows that they follow an inverse pattern compared with water depth in the central part of the channel, with the highest velocities (approximately 4 m/s) occurring in front of Zone 1 and decreasing progressively to 3-3.5 m/s along Zone 3 before decreasing even further downstream where water depth increases. Along the channel banks, two regions with circulation zones (eddies) are observed, one along the right bank in Zone 3 starting approximately from the location of the observed damages and one along the left bank in front of the downstream end of Zone 3. In these eddies, the steady-state velocity is lower than 1 m/s. Finally, a large eddy is also occurring in the region immediately downstream of the powerplant outlet. The presence of this eddy is linked to the assumption that no flow is conveyed through the powerplant.

Analysis of the turbulent kinetic energy and relative turbulence intensity shows that a very high turbulence level occurs in the three regions affected by eddies. The turbulent kinetic energy is high along the right bank in the downstream part of Zone 3. In the center part of the channel, the relative turbulence intensity varies from approximately 0.5 in the stilling basin (which corresponds to the value assumed and set as boundary condition at each spillway chute), progressively decreasing to 0.2 at the limit between Zones 2 and 3 and then further decreasing towards 0.15 in the remaining part of the channel, which corresponds to an expected turbulence level (normal to high) in such a channel geometry for the flood event under consideration (see Table 1).

Overall, results show that flow conditions along Zone 3 are challenging with an eddy inducing high turbulence levels along the bank and with flow velocities larger than 3 m/s in the central part of the channel outside the eddy.

A computation made for a configuration with the slumped material removed showed only minor differences on flow conditions. The size of the eddy located along Zone 3 is slightly smaller, which implies that the flow velocities near the bank slope toe are slightly increased. The turbulence level inside the eddy remains high.

Finally, computed flow velocities and relative turbulence intensities were used in order to produce maps of corresponding median armourstone diameter based on Eq. [5] proposed by Hoffmans and for the two critical Shields parameters considered ($\Psi_c = 0.03$ and $\Psi_c = 0.02$), see section 3.3.

The two maps presented in Fig. 4 correspond to the current geometry and to the geometry in which the slumped material at the upstream end of Zone 3 has been removed. Results have also been extracted along a profile located approximately at the toe of the bank slope. Values for velocity, relative turbulence intensity and calculated D_{50} based on the equation proposed by Hoffmans and for $\Psi_c = 0.02$

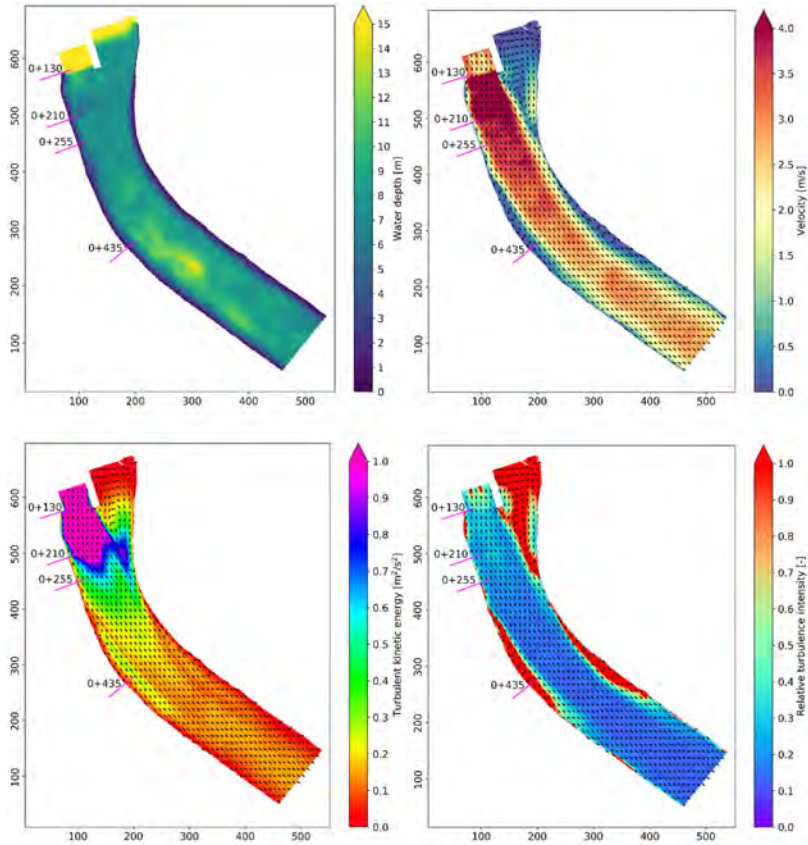


Fig. 3

Flow conditions for the 100-year flood. Top left to bottom right: water depth, depth-averaged velocity, depth-averaged turbulent kinetic energy and relative turbulence intensity with velocity vectors.

Résultats pour le débit centennial. De gauche à droite et de haut en bas : profondeur, vitesse moyenne sur la verticale, énergie turbulente et intensité turbulente relative. Les vecteurs matérialisent le champ des vitesses.

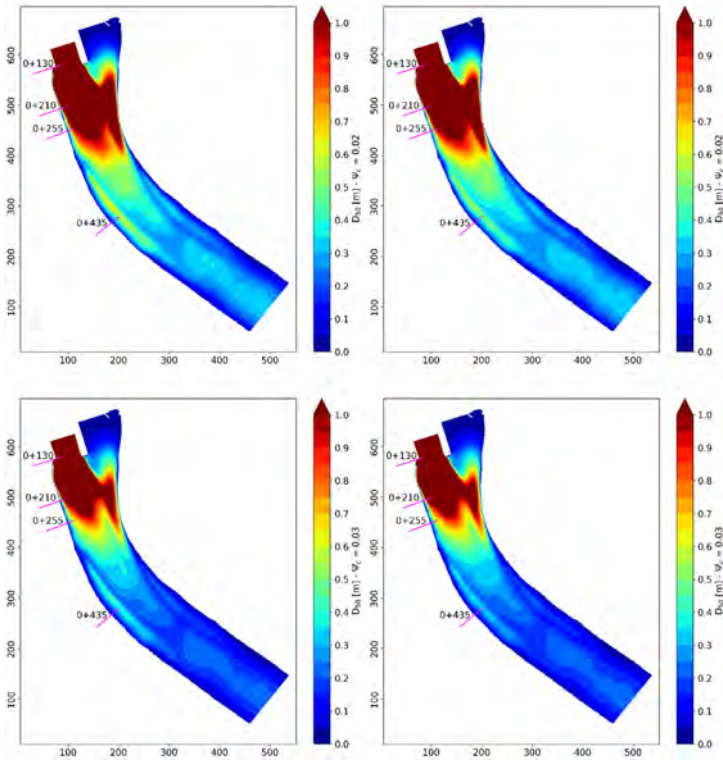


Fig. 4

Calculated D_{50} for the 100-year flood. Images on left side: current geometry with slumped material in place (between sections 0+250 and 0+300). Images of right side: geometry with slumped material removed. Upper images: $\Psi_c = 0.02$. Lower images: $\Psi_c = 0.03$

D_{50} calculé pour le débit centennal. Images de gauche : bathymétrie actuelle avec éboulement en place (entre sections 0+250 et 0+300). Images de gauche : bathymétrie sans éboulement. Images du haut : $\Psi_c = 0.02$. Images du bas : $\Psi_c = 0.03$

(value chosen for bank protection design, see section 3.3) are presented in Fig. 5 for the current geometry and for the geometry in which the slumped material at the upstream end of Zone 3 has been removed.

The flow velocity along the right bank oscillates between approximately 4 and 5 m/s in Zone 1 and then progressively decreases to reach approximately 3 m/s at the downstream end of Zone 2. The relative turbulence intensity in this part of the channel oscillates between approximately 0.2 and 0.3. In Zone 3, both velocity

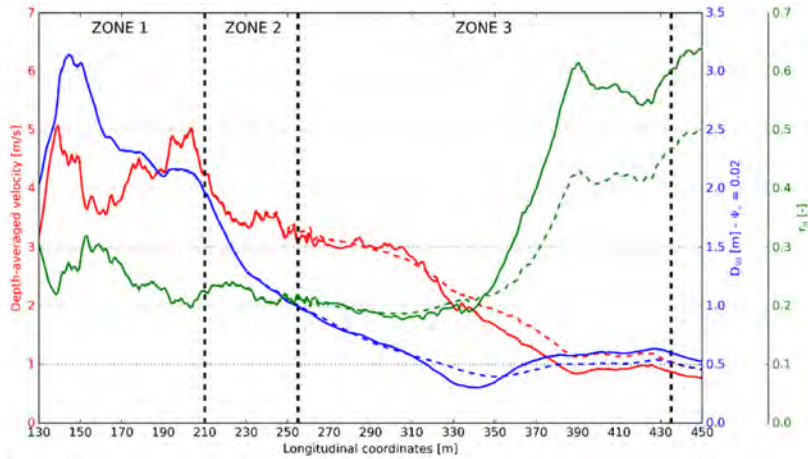


Fig. 5

Longitudinal profile along right bank extracted at bank slope's toe with depth-averaged velocity, relative turbulence intensity and calculated D_{50} for the 100-year flood. Solid lines: current geometry with slumped material in place Dashed lines: geometry with slumped material removed.

Profile en long de la rive droite en pied de berge avec vitesse moyenne sur la hauteur, intensité turbulente relative et D_{50} calculé pour le débit centennal. Lignes pleines : bathymétrie actuelle. Lignes en pointillés : bathymétrie sans éboulement.

and relative turbulence intensity remains approximately constant (3 m/s and 0.2, respectively) until the section 0+310 that materializes the downstream part of the observed bank protection damages. Downstream of this point, flow velocity decreases progressively down to approximately 1 m/s around section 0+390 while the relative turbulence intensity increases up to 0.4-0.6. This region corresponds to the outer part of the eddy occurring along the right bank. The comparison between results for the current geometry and for the geometry in which the slumped material at the upstream end of Zone 3 has been removed shows that velocity downstream of section 0+310 are up to 20% higher with the latter geometry while the relative turbulence intensity decreases by approximately 50% from 0.6 down to 0.4. Although the size of the eddy and its turbulence level is larger in the presence of slumped material at the bank slope's toe, the removal of the slumped material does not allow a significant diminution of the turbulence level in this region. Hence, it is likely that the natural high turbulence level in this region contributed to the apparition of bank protection damages during the discharge test performed in 2007.

The calculated D_{50} in each zone (interval between minimum and maximum values) based on $\Psi_c = 0.02$ (value chosen for bank protection design, see

section 3.3) are summarized in Table 2, together with the D_{50} of the existing bank protection.

Table 2

Summary of calculated D_{50} in each zone (minimum and maximum values) for the geometry with slumped material removed for the 100-year flood and comparison with existing D_{50}

Synthèse des valeurs de D_{50} calculées dans chaque zone (minimum et maximum) dans la configuration sans éboulement et comparaison avec les D_{50} existants. Débit centennal

	Zone 1	Zone 2	Zone 3
D_{50} ($\Psi_c = 0.02$) [m]	2.0-3.1	1.0-2.0	0.4-1.0
Existing D_{50} [m]	1.14	0.87	0.30

Comparison shows that the calculated D_{50} is always larger than the values for the existing bank protection. The analysis of the longitudinal profile shows that the calculated D_{50} varies strongly along each zone, with the highest value always located at the upstream end of each zone (excepted for Zone 1 where the maximum values is reached after 15 m).

The comparison between the calculated and the existing D_{50} in Zones 1 and 2 should be interpreted with care. The upstream part of Zone 1 features a different design with anchored retaining wall for the lower part of the bank, thus increasing the overall protection against erosion. Furthermore, the fact that no damages have historically been observed in this region might indicate that the design method used to calculate D_{50} is potentially yielding conservative results. Finally, as this region is located near the upstream boundaries of the 2D hydraulic model and immediately downstream of the stilling basin, it is likely that the results from the model contain significant uncertainties. Further analysis with more sophisticated methods or observations is required in order to draw final conclusions regarding suitability of armourstone size in these two zones.

The analysis of the results along Zone 3, which was the focus of the study, shows that the armourstone size of the existing bank protection ($D_{50} = 0.30$ m) is inferior to the calculated D_{50} . At the beginning of the zone, the calculated D_{50} is approximately three times larger than the existing D_{50} . In the second half of the zone, the calculated D_{50} is approximately 0.50 m, which is 67% larger than the existing armourstone ($D_{50} = 0.30$ m).

As a conclusion, the hydraulic assessment performed in the tailrace channel in combination with a turbulence-based bank protection design method has shown that the existing armourstone size in the upstream part of Zone 3 (right bank), where flow conditions are characterized by a high turbulence level, does not fulfill design

requirements for the design flood (100-year return period). These findings are in agreement with the observation of damages that has regularly occurred in this region for discharges lower than the design flood.

3.5. COMPARISON WITH OTHER BANK PROTECTION DESIGN METHODS

It is interesting to compare the calculated D_{50} obtained from the combination of 2D hydraulic modelling and the design method proposed by Hoffmans (see section 3.3) with other classical bank protection design methods. A collection of bank protection design methods is available in the Rock Manual handbook [6], and the following methods have been used: Pilarczyk, Escameia & May as well as Maynard. Additionally, the classic Isbash method [7] as well as the HEC-11 method [1] used in the original design from 2006 were also used. Among these methods, three of them use turbulence characteristics as an explicit input parameter (relative turbulence intensity for Hoffmans and Escameia & May and a turbulence factor for Pilarczyk). In the other three methods (Maynard, Isbash and HEC-11), coefficients are used to account for expected flow conditions, type of construction, river sinuosity, but no explicit guidance is given to account for flow turbulence.

The methods have been applied for the flow and geometrical characteristics corresponding to the upstream part of Zone 3 along the right bank (see Fig. 5): flow depth of 7.5 m, velocity of 3.0 m/s, relative turbulence intensity of 0.2, bank slope of 2H:1V ($\approx 26.6^\circ$) and material friction angle of 40° . As the main part of the methods considered are based on a design Shields parameter of $\Psi_c \approx 0.03$, only this value has been used for the Hoffmans method in which the bank slope factor K_{st} was applied (see section 3.3, Eq. [6]). For the Pilarczyk method, a turbulence factor $k_T^2 = 2.0$, corresponding to “non-uniform flow, sharp outer bends”, was chosen. The HEC-11 method was applied with a flow velocity of 3.3 m/s (average velocity in the channel) and a material friction angle of 32° , which correspond to the parameters used in the original design from 2006. The results are presented in Table 3.

The comparison of the results reveals that the three methods that use turbulence characteristics as an explicit input parameter (Hoffmans, Pilarczyk and Escameia & May) yield the largest D_{50} values of the set, with a relatively large spread between 0.50 and 0.87 m. The Pilarczyk method gives D_{50} values of 0.55 and 0.87 m for a fully developed and for a not fully developed velocity profile, respectively. The Hoffmans method lies in between those two values, with $D_{50} = 0.72$ m.

The three other methods (Maynard, Isbash and HEC-11), when used with the standard assumptions, yield D_{50} values significantly lower than the three methods mentioned above, between 0.19 and 0.30 m. However, the Isbash method applied in outer bends for a bend angle of 30° similar to the left bend in the tailrace channel,

Table 3
Calculated D_{50} with different bank protection design methods
Valeurs de D_{50} calculées avec différentes méthodes de dimensionnement

Design method	Remarks	D_{50} [m]
Hoffmans (Eq. [5])	$\Psi_c = 0.03$, bank slope factor applied (Eq. [6])	0.72
Pilarczyk	Fully developed velocity profile	0.55
	Not fully developed velocity profile	0.87
Escameia & May	-	0.50
Maynard	Straight channels, inner bends	0.19
	Downstream of concrete structures / end of dikes	0.25
	Outer bends	0.23
Isbash	Straight channels	0.22
	Outer bends (30°)	0.50
HEC-11	SF = 1.6 (original design, 2006)	0.30
	SF = 2.0	0.42

yields a D_{50} value of 0.50 m. In the original design from 2006, the HEC-11 method was used with a so-called stability factor $SF = 1.6$ corresponding to the upper range of flow conditions characterized by gradually varying flow and moderate bend curvature. Using $SF = 2.0$, corresponding to the upper range of flow conditions characterized by rapidly varying flow, sharp bend curvature, turbulently mixing flow at bridge abutments and uncertain design parameters, yields a D_{50} value of 0.42 m.

Changing the turbulence characteristics used in the Hoffmans, Pilarczyk and Escameia & May methods to match normal turbulence levels during floods (relative turbulence intensity of 0.10-0.15, turbulence factor $k_t^2 = 1.0$) yields D_{50} values in the same range as the non-explicitly turbulence-based methods with standard assumptions (≈ 0.2 -0.3 m), unless for Pilarczyk with a not fully developed velocity profile that gives a slightly larger estimate (0.35 m).

The comparison presented in this section shows that turbulence-based bank protection design methods lead to larger armourstone dimensions than other design methods where flow turbulence is high. The findings from this specific study, based on observations of historical bank protection damages, suggest that turbulence-based bank protection design methods should be used when high flow turbulence is expected. This conclusion is in agreement with a similar comparison reviewed in [5].

4. DEFINITION OF REMEDIATION MEASURES

Based on the results from the hydraulic assessment, it has been decided to undertake remediation measures in order to reinforce the bank protection in Zone 3. The new bank protection is characterized as follows (see Fig. 6):

- Section 0+255 to 0+315: $D_{50} = 0.90$ m, which effectively corresponds to a prolongation of Zone 2 60 m inside Zone 3. Two layers of armourstone material (thickness 1.7 m) and two additional filter layers underneath.
- Section 0+315 to 0+435: $D_{50} = 0.60$ m. Two layers of armourstone material (thickness 1.2 m) and two additional filter layers underneath.

No remediation measures were defined downstream of Zone 3 as any possible damage in this region is not expected to affect dam safety.

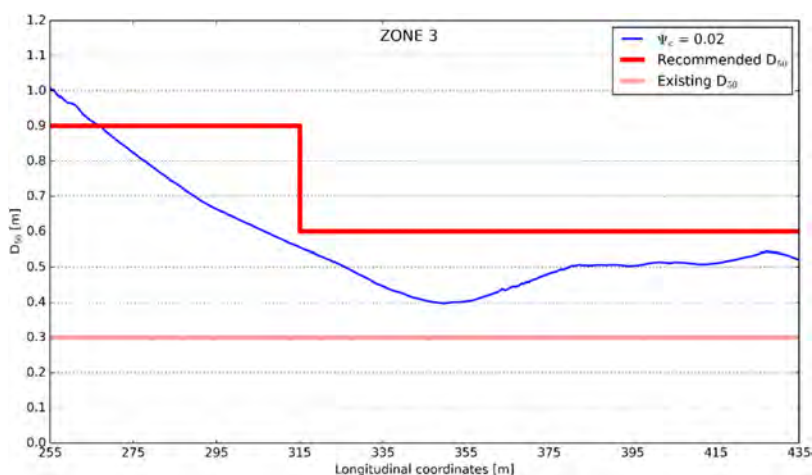


Fig. 6

Longitudinal profile along Zone 3 with existing and recommended D_{50} values. The blue line corresponds to the calculated D_{50} with $\Psi_c = 0.02$ (value chosen for bank protection design, see section 3.3) for the geometry with slumped material removed for the 100-year flood.

Profil en long de la Zone 3 avec D_{50} existant et valeurs recommandées. La courbe bleue matérialise le D_{50} calculé avec $\Psi_c = 0.02$ (valeur retenue pour le dimensionnement de la protection de berge, voir section 3.3) pour la configuration sans éboulement. Débit centennal.

5. CONCLUSIONS

In this article, a hydraulic assessment of flow conditions in a tailrace channel affected by bank protection damages has been presented. The hydraulic assessment has been performed with 2D hydraulic modelling combined with a turbulence-based bank protection design method in order to investigate the required armourstone size in the area affected by damages. Results from the 2D hydraulic model showed that high turbulence in the affected zone is likely to have facilitated the occurrence of damages. The armourstone size used in the existing bank protection does not fulfill the requirements from turbulence-based design methods.

Comparison between turbulence-based bank protection design methods and methods in which flow turbulence is not an explicit input parameter has shown that the latter yield potentially unconservative design values when high flow turbulence is expected. As a result, remediations measures have been defined in order to reinforce the bank protection in the region affected by damages (Zone 3). The new bank protection in this zone is characterized by armourstone material with median diameters D_{50} 0.90 m (section 0+255 to 0+315) and 0.60 m (section 0+315 to 0+435). It represents a significant upgrade compared with the existing armourstone material characterized by a median diameter D_{50} of 0.30 m.

The combination of multi-dimensional hydraulic and turbulence modelling combined with turbulence-based design methods can contribute to a better understanding of erosion phenomena and to optimal bank protection design.

REFERENCES

- [1] BROWN S.A., CLYDE E.S. Design of Riprap Revetment. *Hydraulic Engineering Circular No. 11 (HEC-11), Report FHWA-IP-89-016*. Federal Highway Administration, Washington, D.C., 1989.
- [2] EDF R&D. TELEMATAC-2D, User manual. Version v8p3, 2021. www.open-telemac.org
- [3] HERVOUET J-M. Hydrodynamics of free surface flows. *John Wiley & Sons*, 2007.
- [4] RODI W. Turbulence Models and Their Application in Hydraulics. A state-of-the-art review. Third edition. *A.A. Balkema*, 1993.

- [5] HOFFMANS G. The influence of turbulence on soil erosion. *Eburon Delft*, 2012.
- [6] CIRIA, CUR, CETMEF. The use of rock in hydraulic engineering (2nd edition). *The Rock Manual*. London: C683, CIRIA, 2007.
- [7] COMITE FRANÇAIS DES BARRAGES ET RESERVOIRS (CFBR). Recommandations pour la justification de la stabilité des barrages et des digues en remblai. 2010.

COMMISSION INTERNATIONALE DES
GRANDS BARRAGES

VINGT-HUITIEME CONGRES DES
GRANDS BARRAGES
CHENGDU, MAI 2025

MOGLICE DAM, ALBANIA – DESIGN, CONSTRUCTION, AND MONITORING OF DAM GROUTING GALLERY UNDER COMPLEX GEOLOGICAL CONDITIONS (*)

Dainius TIRUNAS

Principal Engineer / Project Manager, AFRY Switzerland Ltd.

Helmut STAHL

Principal Engineer, AFRY Switzerland Ltd.

Thomas Michael WEBER

Managing Director, Studer Engineering GmbH

SWITZERLAND

SUMMARY

Construction of the Moglicë dam and its engineering design began in 2014 and spanned a period of five years. A critical structure from the point of view of operational safety was the injection gallery, located along the main axis. The gallery's functions include monitoring the dam's behavior and providing access for mortar injections into the foundation during the operational phase if required. The rock mass beneath the dam gallery required injections to significantly reduce the in situ permeability of the rock mass.

During construction, the detailed design of the gallery underwent several revisions due to new geological revelations along the central and lower left abutment, necessitating a transition from a structure initially resting on the lateral rock

**Barrage de Moglicë, Albanie – Conception, construction et auscultation – Galerie d'injection avec des conditions géologiques complexes*

abutment to a gravity-type structure capable of handling hydrostatic pressure through friction. However, the main challenge lay in the design and construction of the gallery in the Upper Left Abutment (ULA) area of the dam, characterized by unfavorable geology with a rocky roof plunging up to 65 meters below the planned gallery. This unfavorable geology became apparent during excavation of the ULA area. The challenge of achieving a uniformly treated foundation was evident in the execution of the initially planned jet-grouting wall and the mix/pressure adjustments for the mortar injections. Core sampling revealed voids and insufficient grout penetration at various depths, posing a risk of erosion induced by leakage after impoundment.

In the search for an alternative solution, it was vital to reconcile three main criteria: constructability under complex in situ conditions, impermeability of the ULA window above the rock roof, and resistance to settlement. Given the depth of the bedrock up to 65 metres, meeting all these criteria was a difficult task. This led to the adaptation of the gallery design with a bored pile wall foundation support.

Nevertheless, the design team, in constant exchange with the technical coordination teams from the developer's and contractor's organizations, succeeded in adapting the initially validated design while continually making the necessary improvements. Optimizations to the technical design were conditioned by discoveries made during the construction excavation process. The refined design and its implementation were recently verified by three and a half years of performance monitoring data in collaboration with the dam operator.

RÉSUMÉ

La construction du barrage de Moglicë et sa conception technique ont commencé en 2014 et se sont étendues sur une période de cinq ans. Une structure critique du point de vue de la sécurité opérationnelle fut la galerie d'injection, située au long de l'axe principal. Les fonctions de la galerie comprennent la surveillance du comportement du barrage et l'accès pour des injections de mortier dans la fondation pendant la phase d'exploitation le cas échéant. La masse rocheuse sous la galerie du barrage a nécessité des travaux d'injections afin de réduire considérablement la perméabilité *in situ* de la masse rocheuse.

Pendant la construction, la conception détaillée de la galerie a subi plusieurs révisions en raison de nouvelles révélations géologiques le long de l'appui central et inférieur gauche, nécessitant une transition d'une structure initialement reposant sur l'appui rocheux latéral à une structure de type gravitaire capable de gérer la pression hydrostatique par friction. Cependant, le principal défi résidait dans la conception et la construction de la galerie dans la zone de l'appui supérieur gauche (ULA – Upper Left Abutment) du barrage, caractérisée par une géologie défavorable

avec un toit rocheux plongeant jusqu'à 65 mètres en-dessous de la galerie prévue. Cette géologie défavorable est apparue lors de l'excavation de la zone de l'ULA. Le défi de réaliser une fondation traitée de manière uniforme fut évident dans l'exécution du mur de jet-grouting initialement prévu et les ajustements des mélanges/pressions pour les injections de mortier. Des carottages ont révélé des vides et une pénétration insuffisante de coulis à diverses profondeurs, posant un risque d'érosion induite par des fuites après la mise en eau.

En recherchant une solution alternative, il était primordial de concilier trois critères principaux : constructibilité dans des conditions *in situ* complexes, imperméabilité de la fenêtre ULA au-dessus du toit rocheux et résistance aux tassements. Compte tenu de la profondeur du toit rocheux jusqu'à 65 mètres, satisfaire tous ces critères fut une tâche difficile. Cela a conduit à l'adaptation de la conception de la galerie avec un support de fondation en mur de pieux forés.

Néanmoins, l'équipe de projection, en constant échange avec les équipes de coordination technique des organisations du développeur et de l'entrepreneur, a réussi à adapter la conception initialement validée tout en apportant continuellement les améliorations nécessaires. Les optimisations de la conception technique ont été conditionnées par les découvertes au cours du processus d'excavation de la construction. La conception affinée et sa mise en œuvre ont été récemment vérifiées par trois ans et demi de données de surveillance de la performance en collaboration avec l'exploitant du barrage.

1. INTRODUCTION

Moglice Hydropower Project is located about 100 km southeast of the Albanian capital Tirana and forms the Devoll river cascade together with the lower Banja HPP dam. Moglice dam is an asphalt core rockfill dam with a height of around 170 m, what makes it one of the highest of its type (Fig. 1). One of the key structures integrated into the dam embankment is its grouting gallery going along the main axis and foreseen as interface between asphalt core and the foundation. The main purpose of the gallery is to monitor dam behaviour and to provide necessary access for grout injections into the foundation during the operation phase in case such a need arises. The rock mass below the dam gallery itself was foreseen for grouting works with the emphasis of a defined reduction of the in-situ rock mass permeability.

During the construction process, several revisions of the gallery detail design were necessary due to new geological findings along the central and lower left abutment. Therefore, the gallery was re-designed from the structure which was supposed to rely on lateral rock support while dealing with hydrostatic pressure after impounding to the solid gravity structure which deals with referred horizontal forces by means of its own mass.



Fig. 1
Moglice Dam

However, the main challenge in gallery design and construction was the Upper Left Abutment (ULA) zone of the Dam. The present paper deals with design, construction, and post-construction monitoring of gallery behaviour in the referred ULA section, which is characterized by an unfavourable in-situ material matrix with diving bedrock line up to 65 meters below the designed gallery bottom. In this case study, the authors analyse the soundness of design solutions applied at complex foundation conditions and discuss the “lessons learnt”. The concluding analysis is verified in the context of a solid 3,5 years post-construction period time series of dam instrumentations data.

2. PROJECT OVERVIEW

The construction of Moglice HPP began in 2014 and was commissioned in 2019 (Fig. 2). The project is the biggest hydropower plant of the Devoll Hydropower Project cascade and located approx. 50 km upstream of its downstream counterpart project Banja HPP. With a gross head of 300 m and two vertical Francis units, it's total installed capacity amounts to 184.3 MW which on average produces 448 GWh of electricity per year. The key feature of the project is a 170 m high embankment dam made of rockfill with an impervious asphalt core. This feature places Moglice dam among the highest of its type in the world. The dam impounds a reservoir with a total capacity of 378 million m³ of which 157 million m³ is the live storage. The dam appurtenant structures consist of a three-bay-spillway with radial gates, a steep chute with three aerators and a flip bucket (Fig. 1), as well as low- and medium-level outlet tunnels with underground gate chambers.

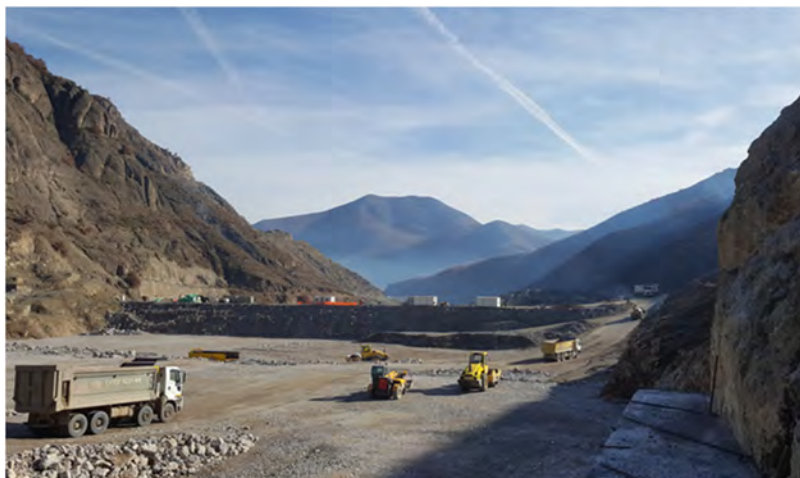


Fig. 2
Construction of the dam embankment

The power scheme of Moglice HPP comprises the main power intake diverting water into the 10.8 km long headrace tunnel which delivers a maximum discharge of $65 \text{ m}^3/\text{s}$ to the underground powerhouse cavern. Here, the flow is discharged back to the river via a 0.9 km long tailrace tunnel. The environmental flow of $1 \text{ m}^3/\text{s}$ is released into the river stretch between the Dam and the tailrace of the main powerhouse through a small, 1.2 MW power station (producing about 10 GWh/year) which is located at the downstream dam toe.

The reservoir impounding started in June 2019 by closing two stop gates at the inlet of the low-level outlet tunnel, which in the initial phase served as the diversion tunnel. The reservoir Full Supply Level (650 m.a.s.l.) was reached in April 2020.

3. INITIAL DESIGN

During the design phase, a stability analysis of Moglice dam was performed by means of GeoStudio 2012 as the main software. The validation of the calculations was achieved with the help of Plaxis 2D 2015 program while using the same model dimensions and material parameters as for GeoStudio. Due to in-situ conditions explained above, a main focus of the analysis was the cut-off system, including the asphalt core with the gallery and grout curtain below it, at the Upper Left Abutment (ULA) of the Dam (Fig. 3).

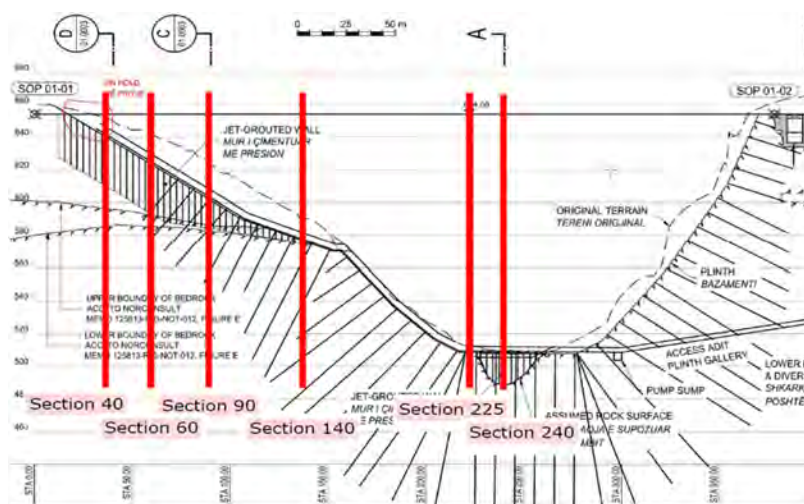


Fig. 3

Longitudinal section of the embankment with representative cross sections (STA)

As a result of the mentioned analysis, characteristic shear strength values were indicated, which were used with selected safety margin to support the design solutions. The cut-off solution initially applied for ULA consisted of a massif jet grouted wall which was supposed to ensure impermeability as well as vertical stability of the gallery (Fig. 4).

In the engineering analysis process, the top of the jet grout wall has been replaced by a wedge-shaped concrete cone for a smoother transition of gallery stresses to the top of the jet grout wall. In the original design the depth of the jet-grouting wall has been varied, from considering no jet-grouting wall at all, over a depth of 20 m, a depth of 30 m and a full depth down to the underlying rock. It was expected that a depth of 20 m will be providing a substantial reduction in seepage water, gallery settlements and differential settlements at reasonable cost.

The gallery itself was designed as self-sustaining gravity structure casted on site out of 10 m long segments, with the joints containing water stops and shear keys. It was planned that in case the measurement of the tilting indicate that a gap would be forming between the gallery foundation and the jet-grouting wall, the gap should be sealed by means of injections from inside the gallery. Besides, since the surrounding material has a high fines content, it was expected that a self-healing effect is triggered to seal the gap. Calculations with lower bound soil parameters resulted in even larger horizontal deformation of up to 19 cm due to impounding and up to 18 cm in vertical direction due to dam construction. For this reason, the gallery

was designed with 8 m long elements connected to each other with open joints to allow horizontal and vertical movements. The joints are fitted with shear keys to avoid differential displacement between the elements and joint filler and waterstops to avoid leakage through the joints. To avoid opening of a gap between the gallery foundation and the bored pile wall, the connection is made by a trapezoidal foundation cone, as well as supporting piles are added on the upstream and downstream side to reduce tilting

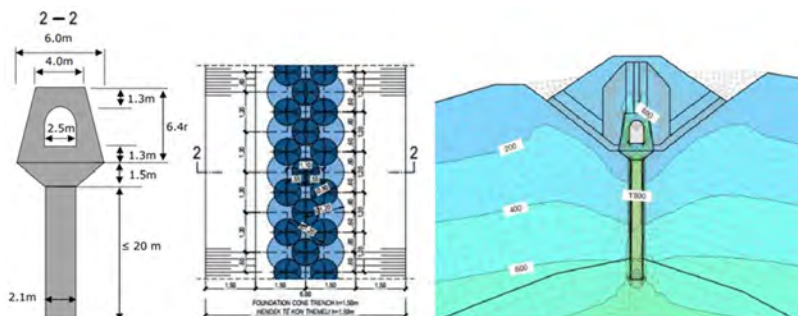


Fig. 4
Jet-grout wall section – Design and FEM analysis

4. CONSTRUCTION PHASE

4.1 CHALLENGES AND ADAPTATION OF DESIGN SOLUTIONS

However, later during the construction phase, while excavating the ULA area, a complex geological matrix material was discovered (Fig. 5). While executing the jet grouting wall and adjusting the mixes/pressure for grout injections, a challenge to achieve a uniformly treated foundation was evident. The core drillings inside the first sections of the jet grout wall indicated remaining voids and poor grout penetration at various depths. The risk of having remaining voids and non-fully treated material would have created a risk of leakage triggering internal erosion after impounding, i.e. when the wall would start to operate under full hydrostatic pressure. Hence, the need for an alternative solution appeared obvious.

While searching for an alternative solution, there was a need to reconcile three main criteria: 1. *Constructability* under given complex in-situ conditions within a steep slope, 2. *Impermeability* of the ULA window above the rock bed and 3. *Resistance to vertical settlements*. Having in mind the depth above the rock bed line of up to 65 m, meeting and reconciling all referred criteria was considered a challenging task. In case of a standard diaphragm wall, which should ensure both

vertical stability and sufficient impermeability, constructability criteria would have not been met due to such depths and due to cost/time. On the other hand, an alternative of applying some “weak” mix injections, which would ensure impermeability and crack resistance, was not an option from the vertical stability point of view. Besides, drilling a deep secant pile system, which afterwards is filled with a strong mix concrete, would overload the wall laterally at the post impoundment phase and could induce extra cracks/leakages to the downstream area. In that way, the search and analysis of a feasible hybrid solution were performed.



Fig. 5
Construction of the Dam Gallery

Therefore, to ensure that all mentioned criteria demands are fulfilled, it was decided to stabilize and treat the gallery foundation with a complex system of secant piling cut off and bored concrete piles. It was expected that a secant pile system along the gallery central line will allow to drill down substantially deep and can be filled with the “weak” mix, in that way fulfilling criteria No 1 and 2. In parallel to that, the gallery foundation was supposed to be supported from below by 2 rows of reinforced concrete piles on the upstream and downstream side, which by means of friction forces would ensure the vertical as well as lateral stability of the gallery (Fig. 6). As a result, the jet grout wall solution was applied only in the section from STA 0 to 56. From STA 56 down to the end of the ULA at STA 140 the new solution of Secant-support pile system was applied.

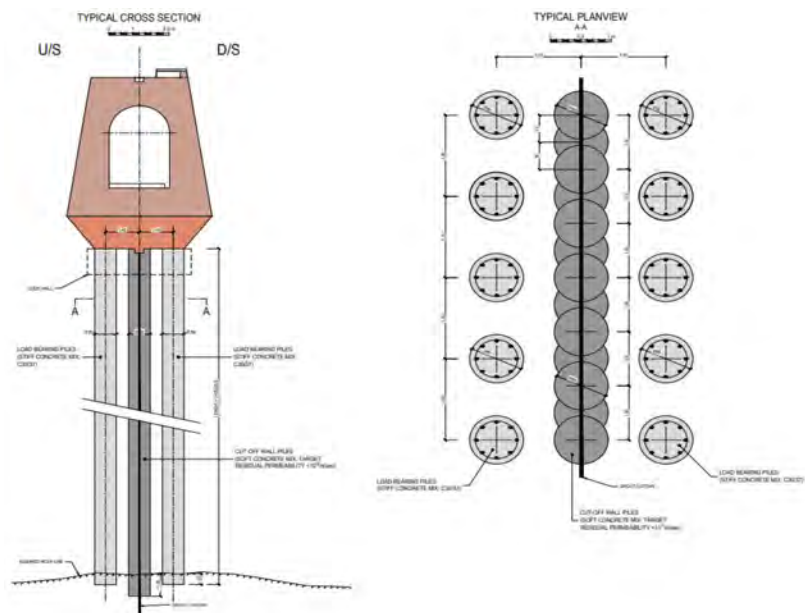


Fig. 6
Secant-support pile system – Vertical Cross Section and plan view

4.2 NUMERICAL ANALYSIS OF GALLERY FOUNDATION DESIGN

A numerical analysis of the left abutment has been performed to support the decision-making process during the design phase of the gallery configuration in the ULA. The software GeoStudio 2012 was primarily used to perform numerical analyses in all design phases. GeoStudio allows for a 2-D plain strain analysis of the geotechnical structures. Hence, several cross sections of the left abutment as shown in Fig. 3 with STA 40, 60, 90 and 140 were assessed with their various geometrical boundary conditions to evaluate the behaviour of the deep foundation and the gallery. The presentation of the numerical results in this paper focuses on the two main cross sections STA 60 and STA 90.

A comprehensive variability study had been performed. Beside the variability of soil properties for median, lower, and upper bound soil properties, also different bored pile wall layouts had been investigated for optimisation. The key focus of the numerical analysis was the assessment of the gallery deformation for the verification of serviceability and the assessment of stresses for possible crack development in the interface between the gallery and the bored pile wall. For a correct stress path

modelling, stage construction had been performed with the modelling of the initial conditions, excavation, construction of bored pile wall and gallery, stage construction of dam body and impounding.

Various bored pile wall design alternatives were studied during the optimisation process. The bored pile wall layout was varied starting from a single secant bored pile wall leading to the final design of three rows of bored piles with one secant bored pile wall in the centre and two separated bored pile walls for enhanced gallery support with one row on the upstream and one row on the downstream side (Fig. 6). The stiffness parameters of a separated bored pile wall needed to be adjusted due to the 2-D plain strain conditions in the numerical model. The bore pile diameter is taken as trench width. The normal stiffness needs to be adjusted for an equivalent E-modulus considering unit area of soil and unit area of concrete pile normalised by unit area of the trench.

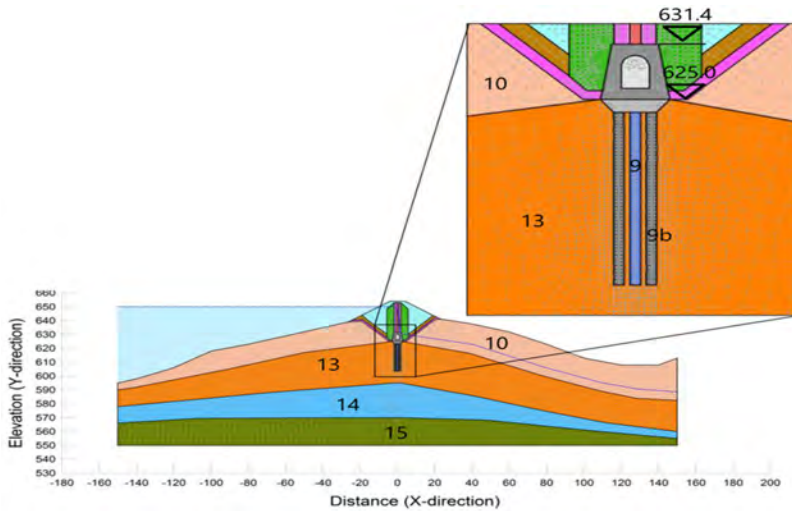


Fig. 7
STA 60 - numerical model with secant-support pile wall

The numerical model of STA 60 is shown in Fig. 7. The model materials are as follows: 9 - Secant bored pile wall; 9b - Separated bored support pile wall; 10 - Soil surface layer; 13 - Weathered conglomerate (soil-like); 14 - Stiff clay; 15 - Massive conglomerate (bed rock). Since the soil layers are thick, the bored pile wall is constructed with floating piles of 20 m length. Calculation results of section STA 60 with the assumption of best guess material stiffness parameters are given in the subsequent figures. Based on the numerical results, the gallery will experience

approximately 13 mm heave due to impounding. Fig. 8 and Fig. 9 show the horizontal displacements of the asphalt core and of the gallery and the deformed mesh around the gallery after impounding, respectively. The figures show approximately 72 mm downstream galley movement and practically no gallery tilt (0.1 mm/m).

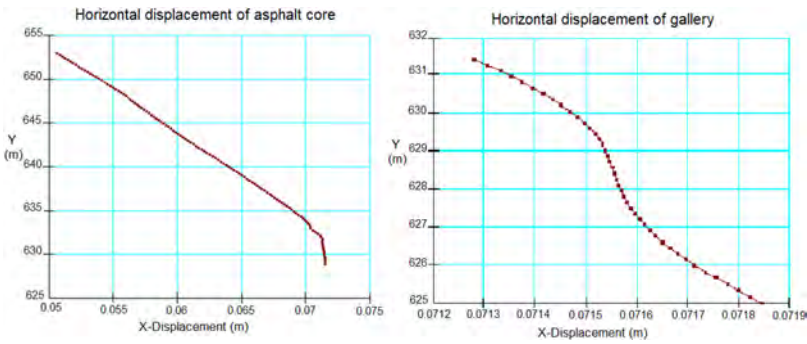


Fig. 8
STA 60 - horizontal displacements of asphalt core and of the gallery after impounding

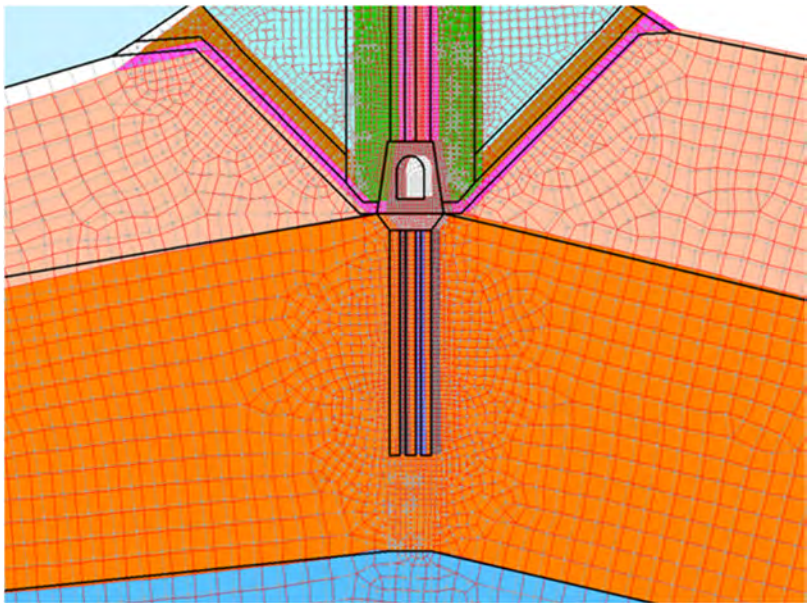


Fig. 9
STA 60 - deformed finite-element-mesh around gallery after impounding, deformation 10 times magnified

The identical numerical analysis process was performed for section STA 90. The modelling results indicate that horizontal displacements of the asphalt core, the gallery and the deformed mesh around the gallery after impounding generates 182 mm downstream gallery movement and a gallery tilt of 3.1 mm/m. These deformations at STA 90 are larger than at STA 60 due to higher hydrostatic pressure. The gallery and their ductile element connections are designed to accommodate these deformations. There are practically no vertical deformations expected due to impounding: settlements and heave are 0 mm at the centre of the gallery.

The numerical assessment supported the decision making for the gallery foundation design and showed that the bored pile wall design performs robust in respect to settlement reduction and improvement of seepage reduction and sealing behaviour. The bored pile wall design has limited influence on the horizontal dam deformation due to impounding. Gallery settlements are primarily reduced in the segment of end bearing piles, but overall gallery deformations are homogenised with limited differential and bending deformation of the gallery for better performance.

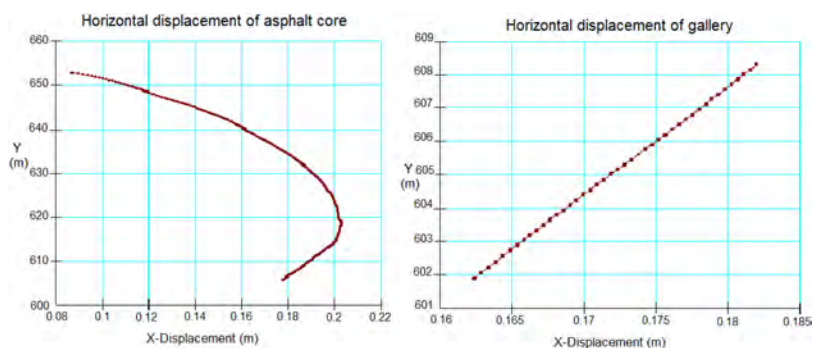


Fig. 10

STA 90 - horizontal displacements of asphalt core and gallery after impounding

5. POST-CONSTRUCTION MONITORING AND VERIFICATION OF DESIGN DECISIONS

5.1 OBSERVATIONS OF THE PERFORMANCE

Monitoring of the Moglice dam behaviour with difficult geological setting in the ULA and in high seismicity region, with a peak ground acceleration of 0.47 g, was considered a key measure while managing any potential performance risks during construction and especial during the operation phase. Therefore, a

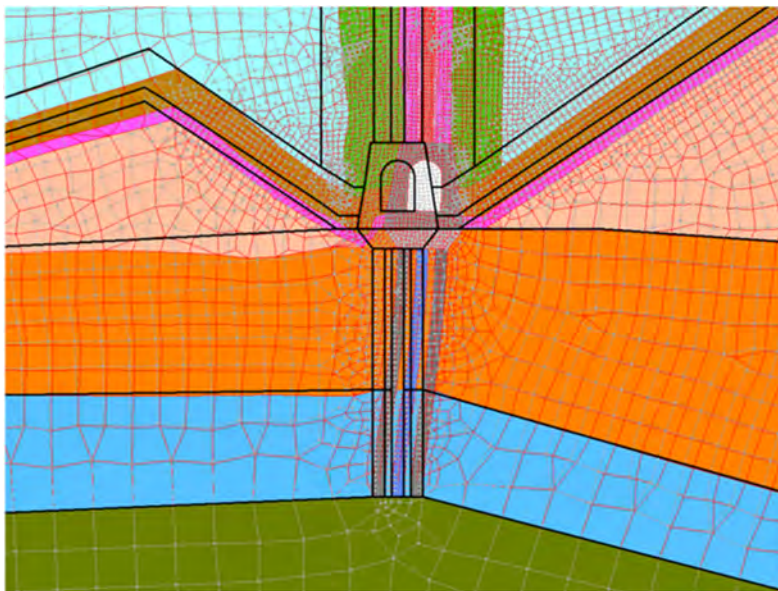


Fig. 11
STA 90 - deformed finite-element-mesh around gallery after impounding,
deformation 10 times magnified

substantial dam instrumentation campaign was carried out on the Moglice dam. The monitoring system of the dam body includes a geodetic network with measuring points at the dam's surface, internal settlement cells, an inclinometer to monitor the deflection of the asphalt core in the main section, temperature sensing cables to monitor seepage within the dam body as well as roof drains in the gallery (Fig. 12). Deformation measurement of the ULA gallery consists of geodetic measuring points for horizontal and vertical movements and tiltmeters. The monitoring system of the dam is completed with foundation and abutment piezometers and accelerometers.

Figure 12 indicates the overall instrumentation system of Moglice dam with the locations of the instrumented cross-sections. The ULA zone contains two instrumentation sections at STA60 and STA90, respectively.

The monitoring instruments were installed, and first readings were taken during the construction process. The behaviour during dam construction is therefore not completely documented. For this reason, the evaluation of the behaviour and comparison to the precalculated values is concentrating on the impounding and post-impounding stages.

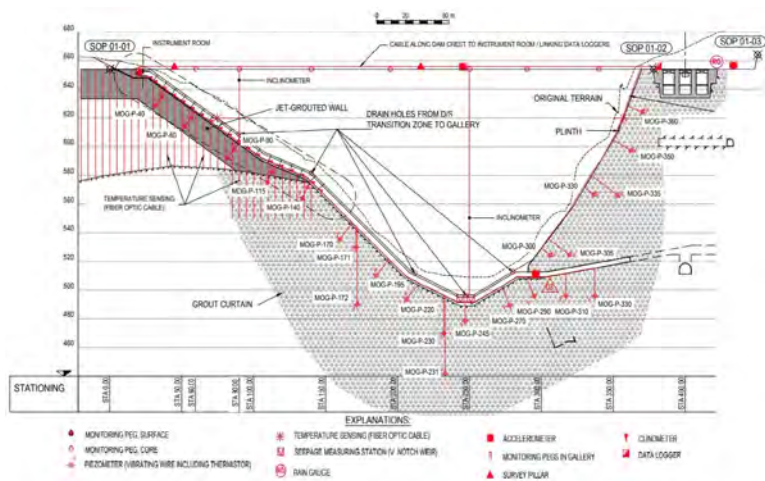


Fig. 12
Instrumentation system along longitudinal dam axis

5.2 DAM CORE DEFORMATIONS IN THE UPPER LEFT ABUTMENT

The dam surface settlements and horizontal deformations are measured by geodetic means. The distribution of the monitoring pegs along the longitudinal dam axis is as indicated in Figure 12. The pegs referred to are also located on the upstream dam face, along the crest in rock-fill and in the asphalt core, and on the downstream face.

Some horizontal deflection is expected towards the downstream side due to impounding. The expected horizontal displacement of the asphalt core after full impounding has been calculated during the design process. The expected horizontal displacement for the asphalt core pegs is indicated in Figures 8 and 10 and in Table 1 below. The table contains both the expected as well as the observed horizontal displacement between June 2019 at the start of impounding and May 2020 just after first full impounding and March 2023.

Table 1
Horizontal displacement of the crest asphalt core pegs after full impounding -
expected vs. observed

Crest Asphalt Core Peg	Expected at full im- pounding	Observed May 2020 just after first full impounding	Observed March 2023
STA 60	51 mm	45 mm (88%)	78 mm (153%)
STA 90	85 mm	128 mm (151%)	165 mm (194%)

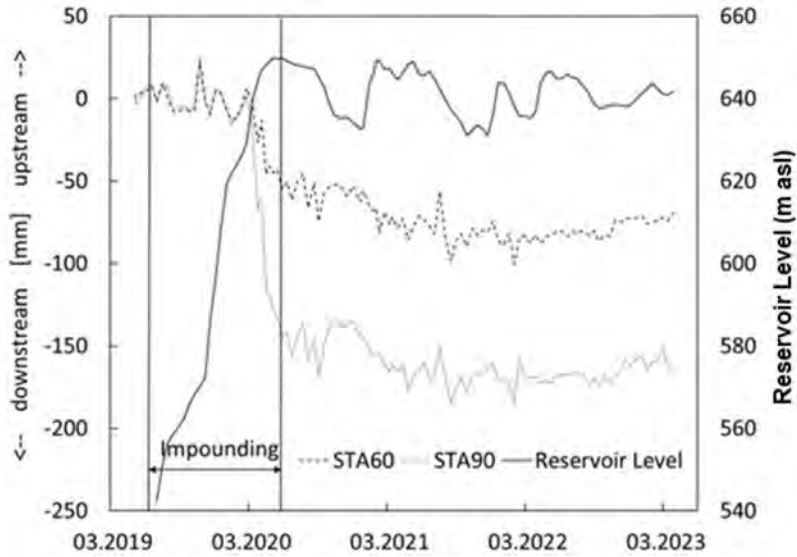


Fig. 13

Measured horizontal displacement of the asphalt core in STA60 and STA90

The post-construction time series indicate that a horizontal displacement observed through the impounding period is in the order or moderately larger than it was predicted in the design stage analysis. On the longer term, within 3 years of post-impoundment period, the cumulative horizontal displacement of the core in both STA60 and STA90 sections has increased further beyond the values reached at the end of the impounding period. Nevertheless, the horizontal displacement values over three years of operation indicate a clear stabilization. The monitoring series obviously presents that major horizontal displacement took place during the last three months of the impounding period which clearly correlates with the reservoir water level reaching the elevation of ULA beyond the bedrock line above 620.0 m asl.

At the same time, the observed horizontal displacement of the core along the crest and the stress distribution inside the core were found to be uniform, which is considered as a favourable performance indicator. The displacement of the core along the dam axis was found to be as expected, i.e. the observation pegs both on the left and right abutment moved towards the valley centre.

The vertical settlement of the monitoring points in STA60 and STA90 at the dam surface amounts to maximum 0.6% of the dam height at the end of impounding. After three years of operation the settlement increased to 0.8%,

except on the upstream face where the total settlement reached around 0.6%. As it will be shown in the subsequent chapter, the vertical displacement measured at the surface must fully be attributed to the settlement of the dam body itself and not the vertical movement of the foundation material. The measured dam settlement is in the upper range of the settlement expected according to literature. However, with absolute values of a few decimetres, the settlements remain well below critical values.

5.3 PERFORMANCE OF THE GALLERY ABOVE THE PILING SYSTEM

The deformation of the gallery in the ULA area was measured with the geodetic measuring points inside the gallery for horizontal and vertical movement as well as tiltmeters.

The following tables give a comparison of the predicted and measured gallery deformation at STA 60, where the gallery is supported by the floating bored and secant pile wall system, and at STA 90, where the gallery is supported by the same pile system reaching the bedrock level.

Table 2
STA 60 - Deformations of the gallery (expected vs observed)

STA 60	Predicted after full impounding (median soil properties)	Measured after full impounding	Measured after 3 years of operation
Gallery vertical displacement	+13 mm	+10 mm	+12 mm
Downstream movement	−72 mm	−25 mm	−20 mm
Tilting	0.1 mm/m	3.2 mm/m	4 mm/m

Table 3
STA 90 - Deformations of the gallery (expected vs observed)

STA 90	Predicted after full impounding (median soil properties)	Measured after full impounding	Measured after 3 years of operation
Gallery vertical displacement	0 mm	+ 15 mm	+ 21 mm
Downstream movement	−182 mm	−50 mm	−32 mm
Tilting	3.1 mm/m	5.5 mm/m	6 mm/m

After first full impounding in April 2020 the reservoir water level remained at a high-level fluctuating between the maximum operation level and 20 m below this level (Figure 13).

In line with the numerical model, almost all geodetic measuring points along the gallery indicate a slight heave during impounding. In STA 60 and 90 it amounts to 10 and 15 mm, respectively. The heave has further developed between first full impounding in April 2020 until late 2020. Since then, constant vertical displacements are observed in the two sections amounting to some 12 and 21 mm, respectively.

In the horizontal direction the gallery moved downstream during impounding. The movement started in February 2020 and reached 25 and 50 mm after first full impounding, respectively. In September 2020 several points moved slightly back towards upstream. The geodetic points near STA 60 and 90 remain around 20 mm and 32 mm downstream since then.

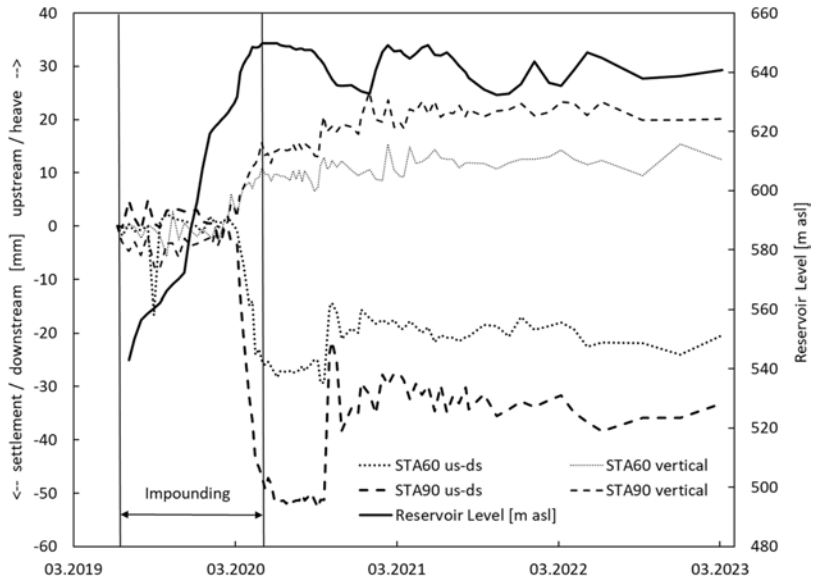


Fig. 14

Horizontal and vertical movement of the gallery due to impounding in STA 60 and STA 90

Tilting due to impounding in STA 60 started in March 2020 when the reservoir level passed 635 m asl with the level of the instrument at 628 m asl, and reached 2.7 mm/m towards downstream at first full impounding at the end of April 2020

(Fig. 15). Mid-May 2020, an inclination of 3.2 mm/m towards downstream was reached. Since then, the additional tilting is only small and amounts to some 4 mm/m since March 2020. Greater tilting than predicted in the model can be caused by local inhomogeneity in the foundation soil or in the compaction of the embankment.

Tilting due to impounding around STA 90 started in January 2020 when the reservoir level passed 617 m asl with the level of the instrument at 600 m asl. It then increased parallel to the rising of the reservoir water level and reached 4.5 mm/m towards downstream at first full impounding end of April 2020. The inclination then slowed down and reached some 5.5 mm/m in July 2020. Since then, the additional tilting is only small and amounts to 6 mm/m since January 2020.

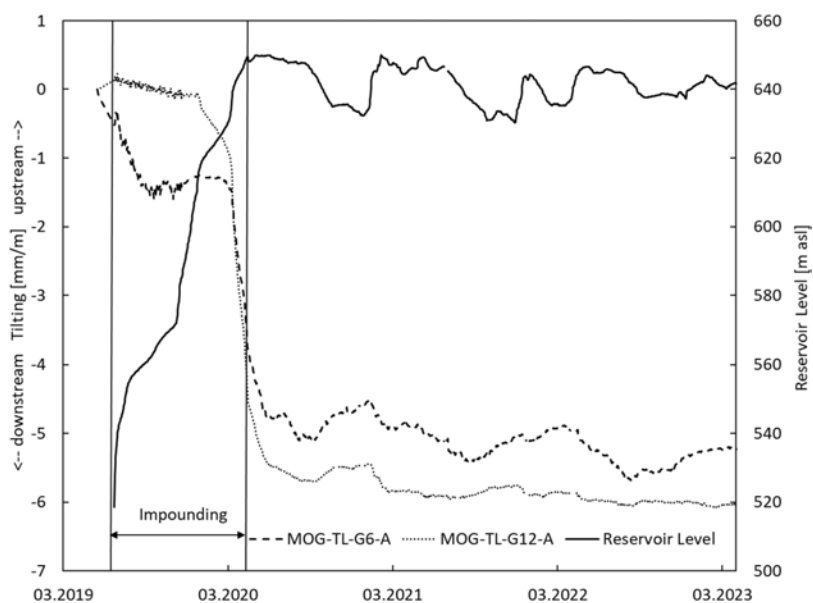


Fig. 15
Tilting due to impounding in STA 60 and STA 90

The measured displacements in horizontal direction are smaller than predicted. On the other hand, the gallery tilted more than anticipated. The observed heave in STA 60 is close to the predicted vertical displacement, whereas in STA 90 it is greater. The observed greater tilting towards downstream can at least partly explain the heave of the geodetic point in STA 90, which is located on the upstream side of the gallery.

5.4 MEASURED WATER SEEPAGE AT THE UPPER LEFT ABUTMENT GALLERY

With the rising water level during impounding, some minor seepage and damp spots on the gallery walls have been observed. However, the extend of seepage has been considered to be normal. Still, the most important seepages were treated with chemical grouting. Therefore, only few damp spots at the upstream wall close to the bottom as well as humid sinterings on the upstream wall and from the bottom are observed. The general state of the gallery is dry and the comprehensive sealing measures have proven their functionality.

Seepage through the interface between the gallery roof and the asphalt core is collected through roof drains at STA 90 and STA 140. The roof drain at STA 90 was dry during impounding and remained dry ever since. The drain at STA 140 had a small discharge of maximum 0.2 l/min before impounding, probably related to water from the left abutment. During impounding no increase of the discharge related to the reservoir water level was observed and since mid-2020 the seepage flow has stopped.

6. CONCLUSIONS

The lessons learned from the present case study gives insights into the design and construction including the design adjustments process which is be validated by means of long-term deformation monitoring data. Summarizing the experience gained from the engineering process and monitoring data interpretation at an extreme complex area like the Upper Left Abutment of Moglice dam, the following conclusions can be drawn:

- The high embankment dam with a complex foundation situation and grouting galleries protruding deep along the main dam axis is to be regarded as a high-risk structure from the engineering design point of view. The complexity of the underground concrete structure system with hardly parametrizable in-situ foundation material matrix and deep diving rock bed lines, which cannot be reached by conventional construction applications, requires a non-standard design approach with a proper balance between risk and cost.
- In this situation, a flexible gallery design to adapt to vertical and horizontal displacements of up to several decimetres is a prudent approach. This was implemented with 10 m long elements, connected to each other with shear keys, joint filler and flexible waterstops as well as a trapezoidal foundation cone to connect to the bored pile wall.
- Calculation with various parameter sets and various design layouts helped to evaluate the possible future gallery behavior.

- The numerical assessment supported the decision-making process for the gallery foundation design. Parametric studies showed the influence of individual parameters on gallery performance and allowed for robust foundation design. Even with the assumptions of conservative unfavourable soil parameters, the design criteria with respect to settlement reduction and foundation sealing could be met. The initially best guess numerical model shows good agreement with measured gallery and embankment dam deformation data. This agreement confirms the confidence in the numerical assessment.

ACKNOWLEDGEMENTS

The authors express their profound gratitude to the Statkraft AS (Devoll Hydropower S.A.) operation team for their valuable contribution of monitoring data, which was crucial for the analyses presented in this paper. The data provided by the operator enabled a comprehensive examination of early hypotheses, verification of design solutions, and enriched the findings. We are thankful for their continuous support and cooperation throughout the duration of this work. Their responsiveness and willingness to collaborate have played a pivotal role in achieving the goals set out for this project.

COMMISSION INTERNATIONALE DES
GRANDS BARRAGES

VINGT-HUITIEME CONGRES DES
GRANDS BARRAGES
CHENGDU, MAI 2025

NAM THEUN 1 RCC DAM – FLOOD MANAGEMENT DURING CONSTRUCTION (*)

Stephan MARTIN

Technical Manager/Deputy Project Manager, AFRY Switzerland Ltd.

Kenneth ROSS

Resident Senior Project Manager, AFRY Switzerland Ltd.

Matthias GOLTZ

Principal Engineer, AFRY Switzerland Ltd.

Gabriel ESCOBAR

Resident Dam Engineer, AFRY Thailand Ltd., Thailand

SWITZERLAND

SUMMARY

The characteristics of the Nam Theun 1 RCC dam and the ancillary structures constructed to manage the dry season flows in the Nam Kading River, and to safely control the floods through the construction site during four rainy seasons, have been presented in this Paper. In addition, the thorough hydraulic model tests carried out, and the careful planning of the RCC placement sequence to create open channels across the dam at various elevations on the right side, have been described. In the 2018, 2019, 2020 and 2021 rainy seasons the diversion tunnel reached its capacity and the cofferdams, and the main dam (excluding the 2018 rainy season) were overtopped and the floods passed safely through the construction site without causing unexpected damage to the right abutment consisting of interbedded layers

*Barrage en BCR de Nam Theun 1 – Gestion des crues pendant la construction

of erodible mudstone and stronger sandstone, the RCC dam or any other part of the civil works.

RÉSUMÉ

Les caractéristiques du barrage en BCR de Nam Theun 1 et des structures auxiliaires construites pour gérer les crues de la rivière Nam Kading de la saison sèche, et pour contrôler en toute sécurité les crues à travers le site de construction pendant les quatre saisons des pluies, ont été présentées dans cet article. En outre, les tests approfondis effectués sur le modèle hydraulique et la planification minutieuse de la séquence de construction du barrage BCR dans le but de créer des déversoirs temporaires sous forme de canaux à travers le barrage à différentes élévations en rive droite, ont été décrits. Au cours des saisons des pluies 2018, 2019, 2020 et 2021, la galerie de dérivation provisoire a atteint sa capacité, les batardeaux et le barrage principal (à l'exception de la saison des pluies 2018) ont été débordés et les crues ont traversé le chantier en toute sécurité sans causer de dommages significatifs en rive droite constituée de couches intercalées de latérite érodable et de grès plus résistant, au barrage en BCR ou à toute autre partie des travaux de génie civil.

1. INTRODUCTION

The Nam Theun 1 Hydropower Project (NT1 HPP) constructed on a Build-Operate-Transfer (BOT) basis and commissioned in 2022 is located around 33 km upstream of the confluence of the Nam Kading River with the Mekong River at the downstream end of the 13,856 km² Nam Theun – Nam Kading basin in central Lao PDR. The 650 MW storage plant for hydro-peaking, with an active reservoir storage volume of roughly 2,020 MCM currently provides 80% of the generated energy (2,063 GWh/year) to Electricity Generating Authority of Thailand (EGAT) with power evacuated via a new 500 kV (154 km) transmission line. A new 115 kV transmission line has been provided to supply the residual 20 % of the generated energy to Electricity du Laos (EdL) for domestic consumption. AFRY (Pöyry) was appointed as the Owner's Engineer to carry out the various duties assigned to him including those required for the completion of the Project under the FIDIC Red Book (Civil and Hydromechanical works) and two FIDIC Yellow Books (Electromechanical and Transmission Lines works).

The main feature of the project is a curved gravity RCC dam with a maximum height of 187 m and a crest length of 772 m (see Fig. 1). The total RCC volume is circa 4.14 million m³.



Fig. 1
Nam Theun 1 RCC Dam

Construction of the Nam Theun 1 RCC dam began on 15 January 2019 and the reservoir was fully impounded on 09 July 2022. One of the key challenges encountered during the construction of the dam was the diversion and management of the Nam Kading River during the annual rainy seasons. During the dry season, the Nam Kading River was diverted through a 11 m inner diameter, 932 m long concrete-lined diversion tunnel. This tunnel was capable of diverting the 50-year dry-season flood of around 1,300 m³/s without overflowing the upstream cofferdam. During the rainy seasons, the analysis of historical data showed peak flows were considerably higher, with mean annual and 20-year floods reaching 5,600 m³/s and 10,400 m³/s respectively. The upstream and downstream RCC cofferdams were therefore overtopped during each rainy season, and the partially completed main RCC dam had to be designed in such a way that the excess flow could be conveyed over the dam and safely through the construction site. This required careful planning and the development of a tailored RCC dam construction sequence.

The RCC placement sequence had to enable continuous progress to be made on the critical path of the dam construction throughout the entire year, including the rainy season, together with giving due consideration to the overall construction programme of the Nam Theun 1 Hydropower Project. This meant that the dam progress had to be fast enough to allow the main civil (including hydromechanical) and electromechanical contractors to meet their respective contractual milestones. This essentially required that impounding start as soon as possible, while ensuring

safe passage of floods without causing damage to the project structures or endangering the population downstream of the construction site.

This paper presents the actual RCC construction sequence, including the achieved placement rates and the geometry of the opening created in the dam before the start of each rainy season, to safely pass the design construction floods. The design concept included mitigation measures that were later implemented to prevent erosion and block stability problems, and to avoid damage to the dam during overtopping. Hydraulic model tests were also performed for the large openings formed in the RCC dam for each rainy season, and these will also be described in this paper.

2. CHARACTERISTICS OF THE RCC DAM

A summary of the RCC dam characteristics is given in Table 1.

Table 1
RCC Dam Characteristics

Description	Characteristic
Type	Curved Gravity RCC Dam
Crest Elevation	297.0 masl
Maximum Height	187.0 m
Deepest Foundation Elevation	110.0 masl
Crest Length	771.0 m
Crest Width	8.0 m
Excavation Volume	1,840,000 m ³
RCC Volume	4,141,213 m ³
Structural Concrete Volume	272,500 m ³
Upstream Slope	1.0V/0.2H
Downstream Slope	1.0V/0.75H
Spillway Capacity (PMF)	30,200 m ³
Spillway Radial Gate Dimension	20.0 m x 17.3 m (6 no.)

The dam incorporates a gated ogee crested spillway located on the Nam Kading River axis and has a centrally located bottom outlet. To form the curved RCC dam, 31 blocks with a width of 25 m have been constructed, with the spillway occupying the 7 central blocks. The spillway occupies a significant length of the dam

and had to be curved to enable the discharge from the flip buckets to safely land in the plunge pool excavated below the existing riverbed. A radius of 500 m was selected as the most appropriate curvature for the central part of the dam after considering the hydraulics of the spillway. In addition to the influence the spillway has on the longitudinal profile of the dam, its crest layout also had to be considered when the cross-sectional geometry of a stable dam in this location was determined. If the width of the dam had been narrowed in the spillway location, a large upstream crest cantilever would have been required to accommodate the geometry of the ogee weir crest including the required radial gates, and the weir transition into the spillway chute, which would have proven to be challenging from a structural and constructability perspective.

To complete the design of a stable dam, its profile between the spillway and the abutments continued the curvature of the dam on both sides of the spillway with a radius of 700 m after giving due attention to the abutment topography.

The curved gravity dam section which satisfies the required design criteria (with the necessary height of 187 m) has an upstream slope from the crest to the heel of 1.0:0.2 (V:H) and a downstream slope (measured from the upstream face at full supply level) of 1.0:0.75 (V:H). Such a curved gravity design also has the added benefit of minimising risks that may relate to any less than ideal foundation conditions. Fig. 2 (left) shows a typical cross section through the spillway section. The cross section of the non-overflow sections is indicated by the dashed line. The geometric definition of the dam axis is shown in Fig. 2 (right).

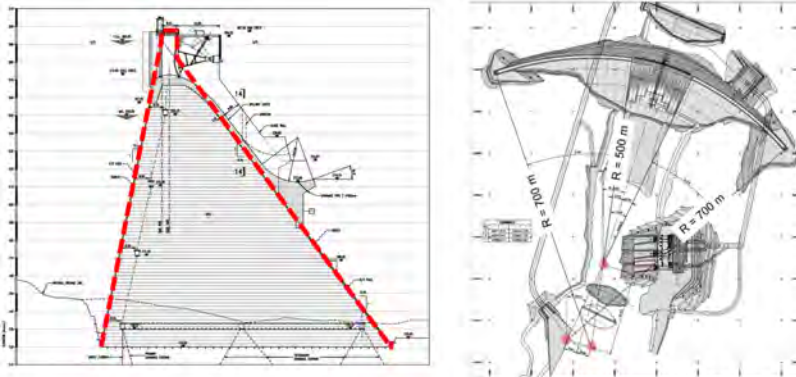


Fig. 2
Geometry of Nam Theun 1 RCC Dam

3. RIVER DIVERSION SCHEME AND DAM CONSTRUCTION SEQUENCE

3.1 OVERVIEW AND DEFINITION

The dam construction sequencing and hydraulic design of the flood management during construction were intertwined. Considering the hydrological conditions of the project with pronounced dry seasons (low flow seasons) from November to June and rainy seasons (high flow seasons) from July to October the dam construction sequence was divided into a number of distinct stages. Each stage had to be completed within a single rainy season or dry season. In general, the construction stages carried out during the dry seasons were protected against the 50-year dry season flood by the diversion tunnel and the upstream and downstream RCC cofferdams but were designed to provide a flood corridor for the following rainy season. The construction sequence of the RCC dam had to manage four rainy seasons.

The adopted construction sequence is shown in Fig. 3 in terms of construction stages to be completed during a rainy or dry season:

- Rainy season 2018: only excavation of the dam foundation above the water level between the upstream and downstream RCC cofferdams.
- Dry season 2018/2019: River diversion and final excavation of the dam foundation and placement of Stage I.
- Rainy season 2019: Placement of Stage II and erection of the bottom outlet.
- Dry season 2019/2020: Placement of Stage III and completion of the bottom outlet.
- Rainy season 2020: Placement of Stage IV and concreting of spillway chutes and flip buckets
- Dry season 2020/2021: Placement of Stage V and concreting of spillway chutes and flip buckets
- Rainy season 2021: Placement of Stage VI and completion of ogee crest and spillway concrete piers
- Dry season 2021/2022: Placement of Stage VII and erection of all six spillway radial gates.

3.2 DIVERSION CHANNEL FOR THE 2019 RAINY SEASON – RCC STAGE I

Initially, the construction schedule required placement of RCC (Stage I) during the 2018/2019 dry season in Blocks B14 to B21 from foundation level up to 135.3 masl. (25.3 m above foundation level), and then raising the left bank Blocks B17 to B23 to reach 162.3 masl as early as possible. The RCC site installations were positioned on the left bank to give the Contractor early access to a flood safe platform for the erection of the bottom outlet, while inflows in excess of the diversion tunnel capacity were diverted through the dam site. This plan led to the requirement to place approximately

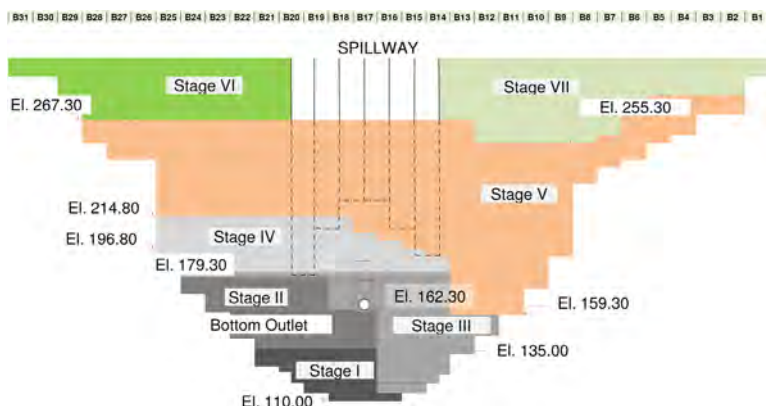


Fig. 3
Construction Sequence of Nam Theun 1 RCC Dam

636,000 m³ of RCC from 15 January 2019 to May 2019, with a required average placement rate of 4,700 m³/day. However, after the first few weeks of RCC placement, when it became obvious that the given targets could not be achieved, Stage I was adjusted assuming a lower placement rate. Based on the results of the numerical simulations which were confirmed by the hydraulic model tests, it was concluded that flood safety during the 2019 rainy season would be ensured by covering the foundation of dam Block B16 with a minimum 3.6 m of RCC and raising Blocks B17 to B22 to El. 162.3 masl as fast as possible. In the period 15 January 2019 to 31 May 2019 the Contractor placed around 269,000 m³. At the end of the dry season 2018/2019 the left bank Blocks B17 to B21 were raised to approximately El. 139.30 masl.

Under close monitoring of the flood forecasting system designed and installed by AFRY, RCC placement in Blocks B17 to B23 continued during the 2019 rainy season. The targeted platform at El. 162.30 masl was finally reached on 18 August 2019.

During the 2019 rainy season (Stage II) from 1 June 2019 to 30 October 2019, 529,000 m³ of RCC was placed at the left abutment (Blocks B19 to B24) up to approximately El. 175.20 masl.

3.3 DIVERSION CHANNEL FOR THE 2020 RAINY SEASON – RCC STAGE III

During the initial part of the 2019/2020 dry season from 1 November 2019 to 20 November 2019 approximately 54,000 m³ of RCC were placed in Block 19 to Block 24.

From 24 December 2019, still within the 2019/2020 dry season, Stage III was completed by Sinohydro Corporation (Bureau No. 3) by raising Blocks B12 and B13 to El. 159.30 masl and raising Blocks B14 to B24 to El 181.30 masl. This created a 75 m wide channel at El. 159.30 masl at the right bank for safe passing of the floods during the 2020 rainy season. To achieve this milestone 710,000 m³ of RCC in total have been placed from November 2019 to June 2020 with an average placement rate of 3,400 m³/day.

During the 2020 rainy season (Stage IV), RCC was placed at the left abutment in Blocks B18 to B25 up to El. 214.80 masl and in Blocks B14 to B17 with a variable height which were all well above the water level. For this stage, around 600,000 m³ of RCC in total had been placed from July 2020 to October 2020 with an average placement rate of 4,900 m³/day.

3.4 DIVERSION CHANNEL FOR THE 2021 RAINY SEASON – RCC STAGE V

The construction of the ogee crest and spillway piers were among the most time-consuming aspects of the construction of the dam, and furthermore formed part of the critical path of the dam's construction schedule. Thus, it was crucial that access for the construction of these structures was given as soon as possible. To achieve this goal, the construction schedule required the placement of 1,700,000 m³ of RCC during Stage V from November 2020 to June 2021 at an average daily placement rate of almost 7,100 m³. Balancing construction requirements and hydraulic requirements for passing the 2020 rainy season flood, it was finally concluded that a 125 m wide opening at El. 255.30 masl in Blocks B8 to B12, all located well outside of the spillway section, was the optimum solution.

From a hydraulic point of view, the invert elevation of this channel is best positioned as low as possible to minimize the energy to be dissipated downstream of the dam and the potential for erosion of the downstream toe of Blocks B6 to B13. The invert elevation was however subject to two additional constraints, namely the maximum allowable elevation difference between adjacent blocks (taken to 60 m to ensure dam stability in case of seismic loading) and the quantity balance between construction stages (achievable production rates and construction scheduling).

The resulting invert elevation of the opening (El 255.30 masl) was 135 m above the foundation level of the downstream toe of the dam. The main task of the hydraulic design was to size the stepped chute following the downstream toe of the dam, again protecting the right abutment with RCC, and to provide means for the controlled discharge of flood flows into the existing plunge pool. Downstream

perimeter guide walls were constructed to contain the flow within the stepped channel. This channel, like the dam body itself, was constructed in discrete RCC lifts, which had the advantage of increasing the energy dissipation along the downstream face with the formation of the steps.

Research of literature has shown that this stepped spillway (channel) is the highest structure of its type for temporary use ever constructed (it has a height of 123.30 m).

During the 2021 rainy season (Stage VI), RCC has been placed at the left abutment outside of the spillway section up to the dam crest elevation. For this stage, 130,000 m³ of RCC in total were placed from July 2021 to October 2021 with an average placement rate of 1,100 m³/day.

The placement of the remaining 150,000 m³ of RCC (Stage VII) and the completion of spillway were achieved in the 2021/2022 dry season from November 2021 to May 2022.

4. HYDRAULIC MODEL TESTING FOR FLOOD MANAGEMENT DURING CONSTRUCTION

4.1 OVERVIEW OF HYDRAULIC MODEL TESTING

Different scenarios of rainy season floods overtopping the RCC cofferdams and dam were tested at the Asian Institute of Technology (AIT) in Bangkok. The actual elevations of the RCC on the right side of the dam, where it was left low during each rainy season to carry the floods, were modelled. Three construction stages of the dam were required to be simulated in the hydraulic model, representing conditions during the 2019, 2020 and 2021 rainy seasons with 2, 5, 10, 20 and 50-year return period floods.

Erosion of the abutment especially when consisting of soft and erodible mudstone, as well as erosion of the downstream toe of the right abutment RCC Blocks (final rainy season), were of key focus.

The hydraulic model of the river diversion through the construction site covers the river reach between the upstream and downstream RCC cofferdams in the final stages. It consists of the following main components.

- Site topography (fixed bed) within the boundary area up to El. 290 masl.
- Fully constructed upstream RCC cofferdam.

- Main dam in various construction stages.
- Pre-excavated plunge pool.
- Fully constructed downstream RCC cofferdam.
- Tail water level of the Nam Kading River downstream of the downstream RCC cofferdam.

The hydraulic model was constructed at an undistorted geometric scale of 1/100 and was tested according to Froude Number similarity. The general layout of the hydraulic model is shown in Fig. 4.

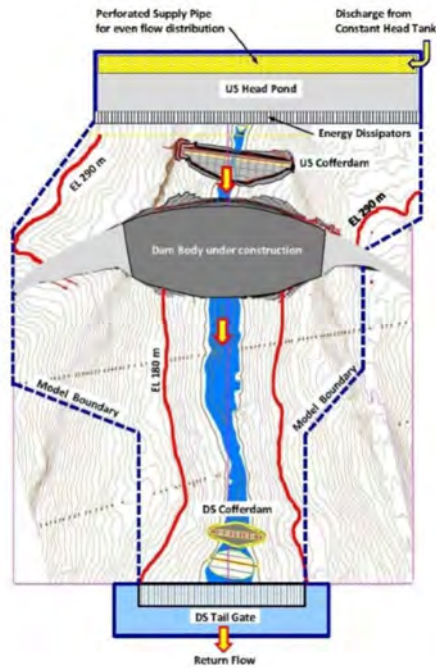


Fig. 4
General Layout of Hydraulic Model for Flood Management During Construction of NT1 RCC Dam

Of particular relevance was the hydraulic model testing for the river diversion through the dam site in the 2021 rainy season, which is described in more detail in the following paragraphs.

4.2 RIVER DIVERSION THROUGH THE DAM SITE IN THE 2021 RAINY SEASON

The geometry of the main dam corresponding to the construction stage in the 2021 rainy season is defined in Table 2. The downstream face of the main dam and the overflow release channel (temporary stepped spillway) were constructed in RCC in steps of 1 m to 3 m in height. The lifts were designed to contribute to the energy dissipation of the dam crest overflow.

Table 2
Dam Block Elevations in 2021 Rainy Season

Blocks	Construction Progress
Block 2 to 4	Constructed to El. 282.3 masl
Block 5	Constructed to El. 279.3 masl
Block 6	Constructed to El. 273.3 masl
Block 7	Constructed to El. 259.8 masl
Blocks 8 to 12	Constructed to El. 255.3 masl
Blocks 13 to 29	Constructed to El. 267.3 masl

The complete model is shown in Fig. 5.



Fig. 5
Hydraulic Model for River Diversion Through the Dam Site in the 2021 Rainy Season

For the hydraulic model tests, 5 determinant discharge scenarios were investigated, as shown in Table 3. The peak discharges were determined considering flood routing calculations.

Table 3
Overflow Discharge and Corresponding Water Levels in 2021 Rainy Season

Flood Event	Peak Inflow [m ³ /s]	Peak Discharge for Model (routed) [m ³ /s]	Peak Discharge for Tailwater Level (routed) [m ³ /s]	Tailwater Level [masl]
2	5,600	4,200	4,750	153.2
5	7,600	6,050	6,600	155.1
10	9,300	7,650	8,200	156.6
20	10,400	8,600	9,150	157.4
50	14,000	11,900	12,450	159.9

The hydraulic conditions at the dam crest overflow section and release channel, as well as at the toe of the exit channel and at the opposite left bank abutment, were determined. In addition, the discharge capacity curve of the dam crest overflow section was established. The model tests were carried out with discharges ranging from the 2-year flood ($Q_2=4,200 \text{ m}^3/\text{s}$) up to the maximum design flow with a return period of 50-years ($Q_{50}=11,900 \text{ m}^3/\text{s}$). The water levels at the main dam overflow section were measured at 4 different sections along the crest labelled L1 up to L4. For each section, three different measurements (1, 2 and 3) were taken as shown in Fig. 6.

From the five different flood return periods considered in the model, the Q_{20} ($8,600 \text{ m}^3/\text{s}$) flood is chosen for the purposes of this publication to highlight the procedure undertaken and the characteristics that were measured. Under this operating scenario, the following main observations were measured and recorded:

- Stable flow conditions at the crest of the overflow section. The maximum flow velocities at the crest range from 15.21 m/s on the left section L1 to 4.74 m/s on the right section L4.
- Increased nappe detachment from the stepped downstream face, thus reducing the overall aeration and energy dissipation effectiveness of the steps.
- Along the stepped release channel, minor flow overtopping was noted at the mid-section. The maximum flow velocities at the release channel ranged from 17.78 m/s at the upper section to 30.43 m/s at the lower section.
- At the release channel toe, a maximum velocity of 30.83 m/s was noted. At the dam abutment, recirculating currents with a maximum velocity at 25.98 m/s were recorded.

- At the left abutment, directly opposite to the release channel exit, a maximum velocity of 12.95 m/s was detected. The stability of the left abutment was ensured to avoid the risk of erosion.

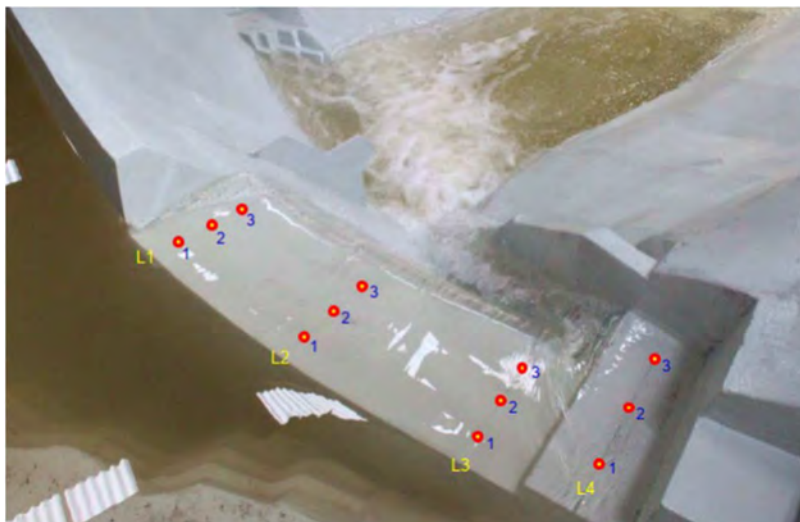


Fig. 6
Water Level Measuring Points at the Dam Crest Overflow Section

5. OVERTOPPING OF RCC DAM

Overtopping of the RCC in the main dam occurred for short periods during three rainy seasons (2019, 2020 and 2021) and with floods which were far less severe than the 50-yr design flood with the elevation of the RCC in the dam at various levels. Discharges from the upstream Theun Hinboun Hydropower Project (from the overflow spillway, weir, and gates) occasionally added to the flows reaching the Nam Theun 1 Project Site.

It is noted that no significant scouring below the design foundation level could be observed after overtopping and the integrity of the excavation and placed RCC was maintained, despite initial concerns especially for exposed mudstone layers.

In the 2019 rainy season, overtopping commenced on 16 August 2019 and lasted until 18 August 2019, resulting in the expected stoppage of RCC placement in Blocks 17 and 18 (see Fig. 7).



Fig. 7.
Overtopping of Upstream RCC Cofferdam and Main Dam on 16 August 2019

In the 2020 rainy season, overtopping of the upstream RCC cofferdam and the main dam occurred from 02 to 04 August 2020, 05 to 07 August 2020 and 16 to 18 August 2020 (see Fig. 8). The RCC in the main dam was kept at El 159.30 masl to manage overtopping without flooding the ongoing RCC placement on the left side. The maximum discharge over the RCC dam was approximately $750 \text{ m}^3/\text{s}$ (with $1,360 \text{ m}^3/\text{s}$ passing through the diversion tunnel).

Final overtopping of the RCC dam occurred during the 2021 rainy season (see Fig. 9), with flood water passing over a flood gap provided on the right hand side of the RCC dam at El. 255.30 masl and passing down the temporary overflow stepped spillway constructed on the right side along the dam toe (as modelled by AIT). The flood gap had a length of 125 m (5 dam blocks), and the height of the temporary stepped spillway was 123.30 m. Overtopping occurred from 11 to 21 August 2021 and from 24 to 25 August 2021, with a discharge of $1,600 \text{ m}^3/\text{s}$ passing through the diversion tunnel, $573 \text{ m}^3/\text{s}$ through the open bottom outlet, and $1,705 \text{ m}^3/\text{s}$ passing through the flood gap and down the temporary stepped spillway. The maximum reservoir level during the rainy season reached El. 259.30 masl (4 m depth through the flood gap).



Fig. 8
Overtopping of RCC Dam on 02 August 2020 ($Q_{in} = 2,110 \text{ m}^3/\text{s}$)



Fig. 9
Overtopping of RCC dam on 11 August 2021 ($Q_{in} = 3,878 \text{ m}^3/\text{s}$, Annual Flood)

6. CONCLUSIONS

One of the key challenges encountered during the construction of the Nam Theun 1 RCC dam was the diversion and management of the Nam Kading River during the construction period. The upstream and downstream RCC cofferdams were overtopped during each rainy season, and the partially completed main RCC dam had to be designed in such a way that the flow could be conveyed safely through the construction site. Beside of careful planning and the development of a tailored RCC dam construction sequence, of most significance in successfully managing the floods, especially during the rainy season 2021, was the 123.30 m high temporary stepped overflow spillway provided along the downstream toe the dam on the right side, which controlled a discharge of $1,705 \text{ m}^3/\text{s}$ in the 2021 rainy season and safely guided it into the existing plunge pool on the Nam Kading River axis below the bottom outlet and the main dam spillway. Due to this temporary spillway being constructed using RCC, simultaneously with the adjacent RCC, it was fast and easy to build, and the formed steps created concurrently with the downstream step of the dam provided a simple energy dissipation element which limited the velocities of the flow at the downstream discharge point. Floods with return periods up to 50 years during each rainy season could have been safely managed with the systems designed and the performance of the structures realised all expectations of a successful (and unique) flood management approach.

COMMISSION INTERNATIONALE DES
GRANDS BARRAGES

VINGT-HUITIEME CONGRES DES
GRANDS BARRAGES
CHENGDU, Mai 2025

**THE MÜHLEBERG HPP IN SWITZERLAND – CONCRETE CONDITION
ASSESSMENT FOR THE RE-CONCESSION AND INVESTMENT PLANNING OF
A 100-YEAR-OLD HYDROPOWER PLANT (*)**

Marco CONRAD
AFRY Switzerland Ltd., Zurich

Matthias GEHRI
BKW Energie AG, Berne

Leonhard KLEMM
TFB AG, Wildegg

SWITZERLAND

SUMMARY

The Mühleberg Hydropower Plant (HPP) in Switzerland was constructed between 1917 and 1920. The works made use of the poured concrete of high-slump consistency instead of the rather expected tamped concrete that was the more typical concrete construction methodology in the 1920's. As the original concession ended in 2017, the owner sought an 80-year re-concession, prompting an in-depth condition assessment of the plant's nearly 100-year-old concrete structures. This assessment aimed to identify ageing and damaging processes, evaluate the current condition, predict remaining service life, and recommend repair measures. The assessment was conducted in two phases: a preliminary qualitative assessment and a detailed condition assessment involving comprehensive testing. This allowed

**La centrale hydroélectrique de Mühleberg en Suisse – Évaluation de l'état du béton pour la re-concession et la planification des investissements d'une centrale hydroélectrique centenaire*

to define a comprehensive set of properties of the 100-year-old mass concrete for the benefit of future analyses, designs and assessments.

A condition assessment with tests on drilled concrete core samples was carried out in 1980 and showed that the condition of the concrete was almost unchanged compared to the assessment in 2015. The available testing results from the 1980 and 2015 concrete condition assessment campaigns allowed an evaluation of the condition development deliberated by individual concrete structures. This allowed the anticipation of the concrete condition development into the future and the planning for required remedial works interventions.

It was demonstrated that the application of poured mass concrete was certainly beneficial for the long-term performance of the concrete water retaining structures. There was no indication of ongoing deleterious and degrading chemical reactions in the interior of the concrete structures. However, it was found that an introduction of supplemental alkalis as part of refurbishment and retrofit works could set off a dormant AAR. Possible concrete strength reduction as a result of continuing or increasing water percolation in certain areas was indicated as the major ageing process in the long-term.

RÉSUMÉ

La centrale hydroélectrique de Mühleberg, en Suisse, a été construite entre 1917 et 1920. Les travaux ont fait appel à du béton coulé de consistance à fort affaissement plutôt qu'à du béton damé, qui était la méthode de construction en béton la plus courante dans les années 1920. La concession initiale ayant pris fin en 2017, le propriétaire a demandé une nouvelle concession de 80 ans, ce qui a donné lieu à une évaluation approfondie de l'état des structures en béton de l'usine, vieilles de près de 100 ans. Cette évaluation visait à identifier les processus de vieillissement et d'endommagement, à évaluer l'état actuel, à prévoir la durée de vie restante et à recommander des mesures de réparation. L'évaluation a été menée en deux phases : une évaluation qualitative préliminaire et une évaluation détaillée de l'état impliquant des tests complets. Cela a permis de définir un ensemble complet de propriétés du béton de masse vieux de 100 ans pour les analyses, les conceptions et les évaluations futures.

Une évaluation de l'état avec des tests sur des carottes de béton foré a été réalisée en 1980 et a montré que l'état du béton était pratiquement inchangé par rapport à l'évaluation de 2015. Les résultats disponibles des campagnes d'évaluation de l'état du béton de 1980 et 2015 ont permis d'évaluer l'évolution de l'état de structures individuelles en béton. Cela a permis d'anticiper l'évolution de l'état du béton dans le futur et de planifier les interventions nécessaires pour remédier à la situation.

Il a été démontré que l'application du béton de masse coulé était certainement bénéfique pour la performance à long terme des structures de rétention d'eau en béton. Il n'y avait aucune indication de réactions chimiques délétères et dégradantes en cours à l'intérieur des structures en béton. Cependant, il a été constaté que l'introduction d'alcalins supplémentaires dans le cadre de travaux de rénovation et de modernisation pouvait déclencher un AAR dormant. La réduction possible de la résistance du béton en raison de la poursuite ou de l'augmentation de la percolation de l'eau dans certaines zones a été indiquée comme le principal processus de vieillissement à long terme.

1. INTRODUCTION

The Mühleberg Hydropower Plant, owned and operated by BKW Energy (Berne, Switzerland), was constructed during the politically and economically difficult times between 1917 and 1920 [1]. It was designed by Gabriel Narutowicz (Professor of Hydraulic Engineering at the ETH Zurich 1907-1919 and President of Poland 1922). At the time, Mühleberg HPP was one of the largest medium-head and most modern storage power plants in Europe. The hydropower plant utilises the river Aare and impounds the Lake Wohlen near Berne. The water retaining structure comprises a 82 m long and about 20 m high concrete gravity structure at the orographic right, and the 170 m long powerhouse at the orographic left bank (Fig. 1). A 61 m wide flap-gated spillway is situated on top of the gravity structure next to the powerhouse.

The concrete components of the Mühleberg HPP remained essentially unchanged since its construction some 100 years ago. Apart from limited reprofiling and other minor measures that did not address the internal condition of the concrete, only the original spillway was replaced entirely with new piers, new bridge and modern flap gates between 2004 and 2006. The bottom outlet was rehabilitated and retrofitted between 1997 and 1998. In 2014, 72 large foundation piles were bored to reinforce the underlying sandstone-marl in case of extreme earthquakes. The powerhouse superstructure in structural and architectural concrete is still in its original state of 1920. A limited condition assessment with tests on core specimens was carried out in 1980.

As the original concession for the Mühleberg HPP terminated in 2017, the Owner implemented procedures to obtain the re-concession for plant operation of a further 80 years. In the context of assessing the existing structural condition and its serviceability, estimating service life, but also for the evaluation of envisaged retrofit and possibly required remedial works during the re-concession period, an in-depth concrete structure condition assessment was devised. The Owner considered a retrofit of the generating units according to two possible scenarios, an early retrofit

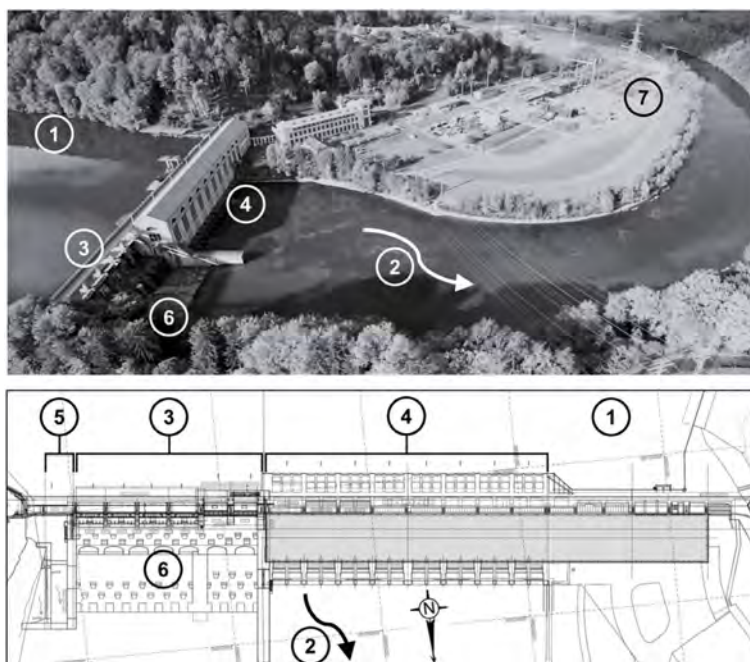


Fig. 1.

Aerial view and plan of Mühleberg HPP

Vue aérienne et plan de la centrale hydroélectrique de Mühleberg

- | | |
|---|---|
| 1. Lake Wohlen, FSL 480.95 m asl | 1. Lac de Wohlen, RN 480.95 alt. msl |
| 2. River Aare | 2. Rivière de l'Aar |
| 3. Gravity dam & spillway with 6 No. gates flap | 3. Barrage-poids & évacuateur avec 6 n° vannes à clapet |
| 4. Powerhouse (intake section) | 4. Centrale électrique (section des prises de l'eau) |
| 5. Boat lift | 5. Ascenseur à bateaux |
| 6. Upper and lower level energy dissipator | 6. Dissipateur d'énergie de niveau supérieur et inférieur |
| 7. Switchyard | 7. L'appareillage pour l'extérieur |

commencing just after the award of the re-concession or some 10 years later (around 2028). These scenarios were considered in relation to the assessed concrete conditions, taking into account an economically reasonable combination of possibly required concrete rehabilitation and retrofit works.

The concrete condition had to be assessed for the entire water retaining structure and for the relevant structural components of the powerhouse substructure and waterways. The rehabilitated bottom outlet and the renewed spillway structures were not part of the condition assessment scope.

2. MASS CONCRETE CONSTRUCTION AROUND 1920 AND THE CONCRETE OF THE MÜHLEBERG HPP

2.1. CONSIDERATIONS ON MASS CONCRETE CONSTRUCTION AROUND 1920 [2] [3]

The general understanding of the concrete construction methodology and the concrete mix design approach applied in the construction of early mass concrete structures, such as the Mühleberg HPP, assists fundamentally in the appraisal of the structure's target state at the time of project implementation as baseline for assessing concrete performance, durability and progress of key ageing processes. This understanding supports framing a practical approach to the concrete condition investigation programme and specifying its detailed scope.

The early mass concrete hydraulic structures were mostly built from an earth-moist and low cement content concrete called 'tamped (or rammed) concrete'. This concrete was placed and compacted in 15 to 30 cm thick layers, using hand-tampers with a mass of about 15 kg, until a 1.5 m high block was completed. Before initial set of the concrete, the horizontal lift joint surface had to be prepared to an uneven and rough finish. The lift joint surface had to be cleaned from loose material, dampened and covered by a bedding mortar prior to receiving the subsequent concrete lift.

In addition to tamped concrete, poured concrete was often used in the construction of hydroelectric power stations, especially for reinforced structures. The poured concrete had to contain enough paste and the aggregate had to contain enough fine particles to fill all the aggregate voids to create a fluid mass that completely embedded the reinforcement. Suitable equipment was required to ensure adequate distribution of the poured concrete against the formwork and across the lift. The fresh poured concrete was not particularly consolidated (comparable to immersion vibration applied today). Compared to the tamped concrete methodology, the poured concrete could be placed in significantly thicker lifts, minimizing number of lift joints, and allowing much better control over the crucial minimization of fresh concrete segregation. Lift joints had to be prepared in the same manner as in the tamped concrete methodology. The poured concrete methodology was primarily applied in the construction of the Mühleberg HPP.

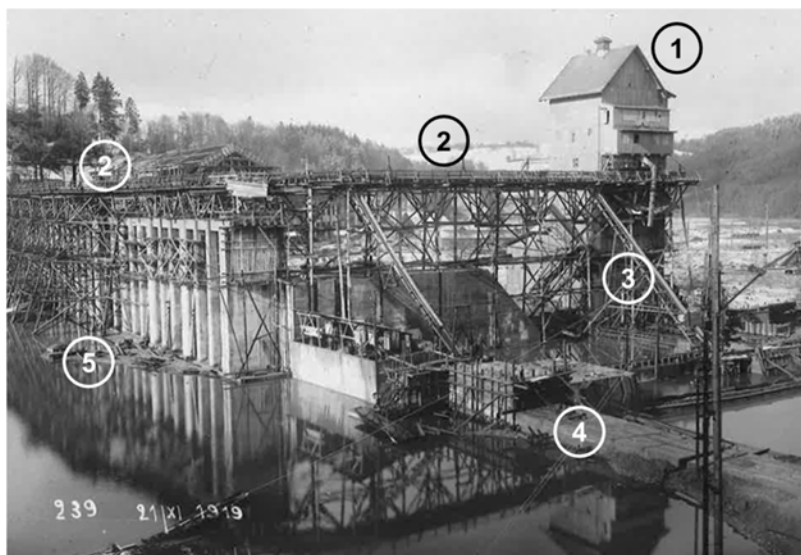


Fig. 2

View of the concrete distribution system (from upstream right)
Vue du système de distribution du béton (depuis l'amont de rive droite)

- | | |
|------------------------------|-----------------------------------|
| 1. Concrete batching plant | 1. Centrale à béton |
| 2. Concrete trolley platform | 2. Plateforme de chariot en béton |
| 3. Concrete chutes | 3. Goulottes à béton |
| 4. Gravity dam section | 4. Section de barrage-poids |
| 5. Powerhouse section | 5. Section de centrale électrique |

Dressed stone as a protection against flowing water was typically used as formwork. Other projects from this period, including the Mühleberg HPP, used a relatively high cement content plaster ('Bockhaut' or 'buckskin') on the external surfaces exposed to flowing water instead of natural stone. The guidelines effective at the time required a cement content of around 700 kg/m³ and a very low water-cement ratio.

Standard aggregate gradations were not provided before 1930. The natural or crushed aggregate was recommended to be as mixed-grained as possible to produce a dense concrete with maximized unit weight. The maximum particle size was defined to allow the concrete passing between rebars and fit between rebars and formwork.

In most cases, normal or slow hardening Portland cement was used. The standards effective from 1916 onwards stipulated a minimum cement content of 300 kg/m^3 in reinforced building structures, whereas cement contents of around 160 kg/m^3 were typical for mass concrete (e.g. foundations and buttresses). The added water for a plastic to mushy consistency was proposed as about 7-10%, and that for a fluid consistency as about 10-13.5% by weight of the air-dry mix. Typical concrete mix designs were specified in proportions by volume of cement (C), sand (S) and coarse aggregates (A), whereas mass concrete mixes used proportions between C:S:A of 1:3:6 to 1:4:8. The typical nominal density of the hardened concrete was assumed around 2.2 to 2.3 t/m^3 . According to the reinforced concrete construction guidelines effective at the time, cube compressive strengths of min. 15 MPa after 28 days had to be achieved (poured concrete 10-13 MPa), whereas the actual compressive stress in the structure was limited to around 20-25% of the compressive strength. The concrete structures were usually designed without consideration of tensile strength, thus, the dimensions of the hydraulic structures from this period are large (in the case of Mühleberg HPP the main water retaining structural members are unreinforced and a minimum 2.0 m thick). When considered, direct tensile strength was assumed approx. 1.2 MPa after 45 days, with a factor of about 2.0 between the flexural and direct tensile strength.

The above indicate the deficits inherent to the concrete construction technology around 1920. In addition to rather random aggregate gradations and particle sizes and an unspecified cement content used in the mass concrete mixes, a major issue was the inadequate compaction technology. This often resulted in mass concrete hydraulic structures that can be characterised by dense and impermeable areas on the one hand, and by horizontally layered porous layers with inadequate compaction and large aggregate pore volume on the other [4]. Therefore, in the absence of deleterious chemical reactions (e.g. ASR), the predominant concrete ageing process in these old structures is related to seepage through open pore volume and related dissolution and leaching over many years.

2.2. CONCRETE OF THE MÜHLEBERG HPP

The gravity dam and the water retaining and substructure parts of the powerhouse consist of poured concrete of high-slump consistency instead of the rather expected tamped concrete. The mass concrete mix contains 180 kg/m^3 Portland cement and $1\,200 \text{ l/m}^3$ sand and gravel (volume w.r.t. loose bulk density, corresponds to approx. $2\,000 \text{ kg/m}^3$) [1]. The water content is not reported but might have amounted to about 160 kg/m^3 , resulting in an apparent density of $2\,340 \text{ kg/m}^3$. The aggregate was extracted from the river in direct vicinity to the construction site. It was separated into sizes 0-10 mm (sand), 10-30 mm (gravel) and 30-45 mm

(gravel). Larger particles were crushed and screened into the separate fractions. It was suspected during the concrete condition assessment discussed in this article that the cement content likely exceeded the 180 kg/m^3 reported in [1] and rather was in the order of 200 kg/m^3 or more, indicated by the lack of aggregate fines and yet the very dense concrete matrix. A test on a single sample from a dense drill core showed a cement content above 300 kg/m^3 that was taken with caution. Considering test sensitivities, this generally indicated that at least in some cases significantly more cement was used in the concrete than reported in [1].

The concrete technology used for the Mühleberg HPP represents the state-of-the-art at the time the plant was constructed. Due to the reduced segregation tendency of the poured concrete and the more uniform consolidation compared to the compaction of tamped concrete, a more homogenous and more impermeable concrete structure was achieved as the precondition for the structure's long-term durability through the past 100 years.

3. CONCRETE CONDITION ASSESSMENT OF THE MÜHLEBERG HPP

3.1. OBJECTIVES, APPROACH AND SCOPE OF THE INVESTIGATION PROGRAMME

The condition assessment was carried out in two phases, starting with a preliminary qualitative assessment including data and information acquisition, followed by a detailed condition assessment comprising a comprehensive testing campaign. The primary objectives of the condition assessment were:

- Identification of the governing ageing and damaging processes in the concrete as well as their progression (comparison with investigations done in 1980).
- Assessment of the concrete structure's actual condition, including lift joints.
- Establishment of the concrete condition target state during construction time and actual condition to assess the progression of concrete ageing.
- Prognosis of a remaining service life.
- Recommendation of possible repair measures and of when they possibly require implementation, informing investment planning.
- Establishment of baseline concrete properties to compare with assumptions made in recent structural analyses, to substantiate the re-concession application procedures, and to support future analyses and works.

The first investigation phase focussed on the general assessment of the concrete condition baseline, concrete deterioration phenomena, and on the general structure condition for identification of short-term rehabilitation needs. Apart from considerations on the concrete construction of the 1920s, the Owner's annual monitoring and surveillance reports were reviewed, as well as a dedicated visual

inspection conducted to identify the structure-specific ageing processes and their development.

The second investigation phase comprised the analysis of further available project documentation incl. construction photos, and the detailed condition assessment combining detailed visual inspection, extraction of different length drill cores from relevant structural elements, non-destructive and destructive testing. The detailed investigation aimed at the quantitative appraisal of the actual internal and external concrete condition of the water retaining structure.

For the actual specification of the test programme scope and for the analysis and presentation of the test results, the various concrete structure elements first were systematised and their specific investigation was then defined based on their functions for plant operation, on their relevance for reservoir retaining structure safety, and age (e.g. new spillway piers and bridge constructed in 2006 were not part of the assessment scope). The distribution of the sampling points for core samples (47 cores, total length approx. 100 m) and the number of physical and mechanical tests permitted conclusions representative for the entire structure.

Table 1
Executed investigations on concrete structures and tests on concrete cores

SUBJECT OF INVESTIGATION	SCOPE OF INVESTIGATION
Concrete structure elements	<ul style="list-style-type: none"> • Visual assessment • Drilled core extraction • Concrete cover (at reinforced elements) • Reinforcement sondage (corrosion condition)
Visual assessment	<ul style="list-style-type: none"> • Cracks • Honeycombs and lift joints • Seepage, pressurized water, efflorescence • Miscellaneous (visible rebars, corrosion, weathering / freeze-thaw, signs of remedial works, etc.)
Concrete cores	<ul style="list-style-type: none"> • Density, total and apparent (open) porosity • Compressive strength • Elastic modulus in compression and dynamic modulus • Split tensile strength • Direct tensile strength (parent concrete, lift joints, adhesive strength) • Direct shear strength • Carbonation depth • Thin section microscopy

3.2. RESULTS AND FINDINGS

3.2.1. *Exterior concrete condition*

In connection with the regular dam surveillance activities, the assessment of the external condition serves to determine changes in comparison to the previous condition assessments and their possible influence on stability and serviceability of the dam.

Crack seals from 1994 and earlier demonstrated that the accessible cracks observed have been known since at least that time. Many of the crack seals were still intact or had only very fine cracks of approx. 0.2 mm, i.e. these cracks have been stable for more than 20 years. The network-like cracks observed have also not changed in recent times. However, they have a different cause and therefore require a more in-depth analysis of the internal condition of the corresponding structural components. Distinctive honeycombs were primarily visible on steeply inclined surfaces where compaction was not possible without problems and the concrete segregated at the formwork or along construction joints. However, these honeycombs were local and were of a much smaller extent compared to similar hydro-power plants from the same period. Pressurised water through construction joints and/or honeycombs and other inhomogeneities were also a local phenomenon. In some places in the structure, older seepage paths have sealed themselves off through calcification. Seepage could be observed only in a few places, mainly at construction joints.

The visual condition survey did not indicate any structurally distressing condition of the concrete. Honeycombs and seepage as observed are typical of the concrete construction methodologies applied at the time. The cracks recorded did also not indicate distress, but these should be observed with regard to their changes over time. The visual condition assessment of the Mühleberg HPP is intended to serve as the basis for the subsequent regular annual or 5-yearly dam surveillances in order to identify possible future changes in the exterior condition. It can be assumed that the exterior condition summarised here, in particular the cracks and calcification phenomena, represents the condition after approx. 95 to 100 years without any significant remedial measures.

3.2.2. *Interior concrete condition*

As a result of the concrete technology and construction methods used at the time of construction, the mass concrete of that time needs to be assumed as essentially heterogeneous and variable in its composition. In the context of systematisation and interpretation of test results, the following concrete categories, which also reflect the mass concrete macro-porosity, were introduced (Fig. 3):

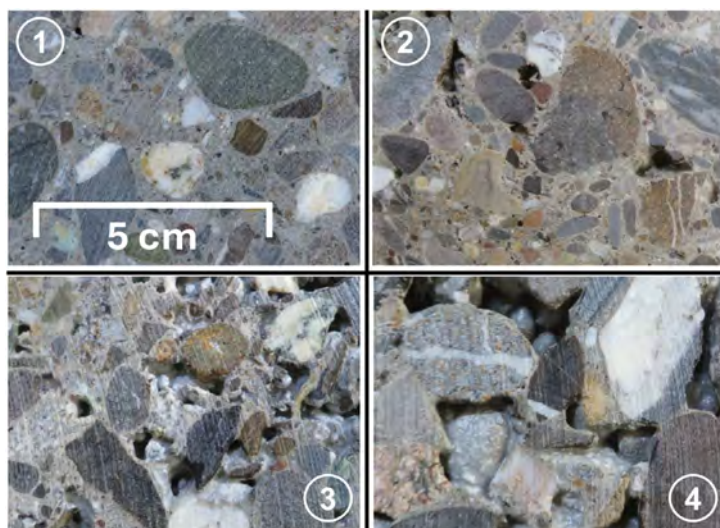


Fig. 3.

Concrete categories distinguished in concrete cores [7]

Catégories de béton distinguées dans les carottes de forage de béton

1. Concrete category K0
2. Concrete category K1
3. Concrete category K2
4. Concrete category K3

1. Catégorie de béton K0
2. Catégorie de béton K1
3. Catégorie de béton K2
4. Catégorie de béton K3

- K0 – Generally well compacted concrete.
- K1 – Concrete with many large compaction (entrapped) pores.
- K2 – Concrete with many interconnected compaction (entrapped) pores.
- K3 – Honeycomb with moderately cemented, almost exclusively coarse aggregate particles. Can be assumed groutable with cementitious grouts.
- K4 – Honeycomb without appreciable bonding between aggregate particles (unverifiable in the concrete drilled core; assumption of no compressive and tensile strength). Can be assumed groutable with cementitious grouts.

The variability of the concrete qualities was confirmed from the logging of the concrete cores extracted at the Mühleberg HPP. However, it was seen that the concrete categories K0 and K1 predominated with around 90% of the total core lengths and the concrete categories K3 and K4 accounted for only 1.7% of the total core lengths.

The logging of adjacent concrete cores allowed an interesting observation regarding the workmanship of concrete lift joints at the time of construction of the

Mühleberg HPP. The concrete lift joints were not executed as horizontal features throughout, but rather inclined in areas or even alternating in elevation and interlocking. This could also be interpreted from construction time photographs.

In summary, it was concluded from the concrete core logging that the concrete components did not exhibit any serious defects that compromised the stability of the water retaining structures. Systematic concrete lift joints were revealed, but these featured systematic interlocking and favourable inclinations. Considering the constraints in the concrete and construction technology of the time, however, the internal condition of the concrete was assessed as quite good. Due to the number and arrangement of the concrete drill cores, the conclusions from the core logging were considered representative of the condition of the entire concrete elements of the water retaining structures.

The concrete porosity affects the mechanical and elastic properties of the concrete. Due to the rather high w/c ratio of the poured concrete, a higher overall porosity was expected. The open pore volume (interconnected pore space) depends primarily on batching and placing the fresh concrete, as well as on any dissolution processes in the event of continuous seepage and cracks. Knowledge of the open pore volume is particularly important for determining possible future rehabilitation options by mass concrete grouting [4].

The average overall total porosity for all concrete structures investigated was in the range of 14 to 18%. The results indicated that the concrete mix composition varied within comparatively narrow ranges and was relatively uniform. The open, entrapped pore volume showed a clearer correlation with the concrete category, respectively the macro-porosity. A maximum value of 3.4% was seen for concrete category K0 and approx. 11% for K1. For concrete categories K2 and K3 there was only one value each, 16.3% and 21%. In this context it is noted that cementitious grouting as a possible rehabilitation methodology for aged mass concrete will only succeed with open pore volumes typically exceeding 12% [4]. However, at a total volume of the concrete categories K2 to K4 of less than 10% (sum of the total of all drilled concrete cores), an improvement of the concrete mass after some 100 years in service did not appear necessary from the point of view of stability and serviceability.

The results from testing the concrete core specimen densities suggested a direct correlation between concrete category, respectively macro-porosity, and concrete bulk density. The mean value of the bulk density for concrete categories K0 and K1 with a dense matrix is $2\,350\text{ kg/m}^3$ with a standard deviation of around 65 kg/m^3 (represents 90% of the total drill core length and is representative of the entire concrete structure). This value fits very well with the estimated bulk density of $2\,340\text{ kg/m}^3$ based on the concrete mix design for the Mühleberg HPP.

Compressive strength tests were carried out on core specimens with a diameter of approximately 110 mm and a height-to-diameter ratio of 1.0. The results from these compressive strength tests correspond to a cube compressive strength on a cube with side length 150 mm. In general, the concrete compressive strength

depended on its macro-porosity, i.e. on the concrete category. A decrease in compressive strength with increasing macro-porosity was observed, as well as a significant strength variability within the same concrete category that could be related to the characteristics of the concrete aggregate gradation and, thus, related to the mass concrete heterogeneity due to the concrete and construction technology available at the time. As expected, the compressive strengths decreased with decreasing bulk densities (Fig. 4). The regression lines for the individual concrete components are comparatively close to each other and are very similar to the regression across the entire sample population and the values from the different structures are in the same range. The compressive strengths therefore were not analysed separately for each concrete structure, but for the different concrete categories. The average for concrete categories K0 and K1 (representative of the concrete structure) was 41.2 MPa with a standard deviation of 12.8 MPa (coefficient of variation 31%), equating with a concrete class C16/20 to C20/25. Concrete category K2 equates with a C12/15 and K3 with a C8/10.

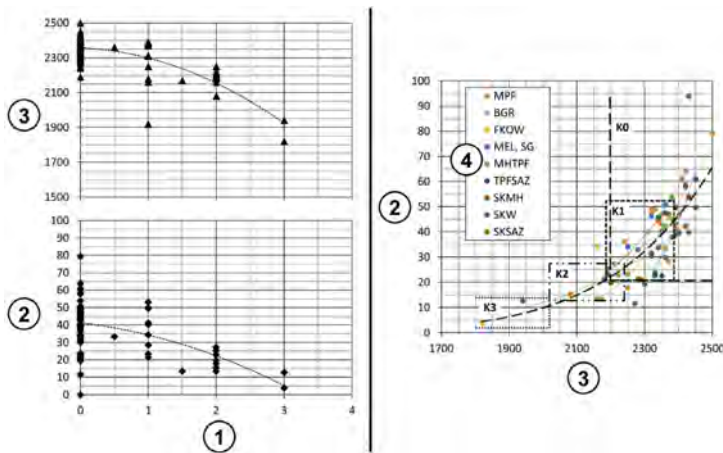


Fig. 4

Correlations between concrete categories, concrete density and core compressive strength

Corrélations entre les catégories de béton, la densité du béton et la résistance à la compression de la carotte

- | | |
|---|--|
| 1. Concrete categories K0-K3 | 1. Catégories de béton K0-K3 |
| 2. Compressive strength of core
Ø100mm H/D=1.0 [MPa] | 2. Résistance à la compression de la carotte
Ø100mm H/D=1.0 [MPa] |
| 3. Concrete density [kg/m³] | 3. Densité du béton |
| 4. Individual concrete structures | 4. Structures individuelles en béton |

The core testing revealed a split tensile strength of 6.4% of the core compressive strength. The mean value across all specimens tested was 3.4 MPa, whereas a mean value of 4.2 MPa (standard deviation 0.6 MPa) resulted for concrete category K0. The mean value for concrete category K1 (including a very low value of 1.9 MPa from an outlier with low density) was 2.3 MPa. The direct tensile strength across construction (lift) joints averaged 1.48 MPa (standard deviation 0.26 MPa). This value corresponded to the expectations based on the Mühleberg HPP concrete mix design and the concrete technology.

The scatter of the modulus of elasticity values obtained from concrete core testing was very large with respect to the different concrete categories, so that no clear correlation could be established. On the other hand, as expected, there was a more significant correlation with the concrete bulk density. The results of the modulus of elasticity tests could be analysed at aggregate level, resulting in a mean elastic modulus value of 38 610 MPa (standard deviation 5 720 MPa). The concrete dynamic modulus of elasticity resulted in an average value of 42 040 MPa across all samples (standard deviation 6 000 MPa), and in a ratio between the dynamic and static modulus of elasticity of 1.09. These values were essentially expected of the subject mass concrete, suggesting that no deleterious reactions were taking place in the interior of the concrete water retaining structures.

Microscopic examinations of thin sections revealed indications of two ageing phenomena in the concrete of the Mühleberg HPP, Alkali Aggregate Reaction (AAR) and dissolution of cement matrix. A high degree of cement hydration was found in all thin sections. Even though a historical AAR could clearly be detected across the entire concrete water retaining structure based on the thin section, no significant structural damage due to an AAR was found. In most cases, the AAR was found close to the exterior surface. Web-like crack patterns were present locally in areas of the gravity dam section and the boat lift. They presumably were associated with reshaping the surface in the past using mortar or shotcrete. The cracks observed in the crack seals (see 3.2.1.) were exclusively single, long and straight cracks and not the web-like pattern of cracks typically caused by AAR. It was more likely that the cracks recognisable in the crack seals were the result of geometric constraint, which suggested that no new crack formation associable to AAR took place in the period from 1985 onwards. It could thus be assumed that the traceable historical AAR was a slow reaction in the past, which abated after a certain time. The geodetic monitoring data from the 15 years prior to the subject condition assessment indicated a hypothetical expansion rate of 0.001 mm/m per year. This value suggested that no significant AAR in the interior concrete mass took place over the preceding 15 years. It is very important to note that an abated AAR can be reactivated at any time, provided that sufficient alkalis (e.g. from newly applied reprofiling mortar or cement grouting of the mass concrete) are made available. The thin sections showed that the concrete aggregate is reactive and, in the past, together with the alkalis from the cement, has led to limited AAR. This aspect in connection with

durability must be considered for possible rehabilitation and retrofit measures in the future.

3.3. UPDATED PROPERTIES OF THE 100-YEAR-OLD CONCRETE & CONDITION DEVELOPMENT

3.3.1. *Updated properties of the 100-year-old concrete of the Mühleberg HPP*

In the 2015 condition survey, it was found that concrete categories K0 and K1 predominated with around 90% of the total concrete core lengths and that concrete grades K3 and K4 only accounted for 1.7% of the total core lengths. Areas of poorer concrete quality were only found locally in the concrete structures and did not extend over their entire dimensions.

The characteristic values were analysed with reference to the different concrete categories or, where appropriate, to the entirety of the test results. The following Table 2 summarises the concrete properties from the 2015 testing campaign, when the concrete age in some structures had reached almost 100 years. As the concrete categories K3 and K4 are underrepresented compared to the concrete categories K0, K1 and K2 and their occurrence was local and not in the sense of discontinuities, the investigated concrete properties are given for the concrete classes K0, K1 and K2.

Table 2
Updated concrete properties of the Mühleberg HPP as of 2015

CONCRETE CATEGORY K	K0	K1	K2	LIFT JOINT
OPEN POROSITY	1%	4%	16%	/
DENSITY [kg/m3]	2 360 ± 60	2 310 ± 80	2 190 ± 50	/
CYLINDER COMPRESSIVE STRENGTH (Ø110mm, h/d=1.0) [MPa]	42 ± 17	38 ± 14	21 ± 6	/
DIRECT TENSILE STRENGTH [MPa]	1.80 ± 0.7	1.30 ± 0.6	0.80 ± 0.2	1.48 ± 0.33
SPLIT TENSILE STRENGTH [MPa]	4.20 ± 0.8	2.30 (2 values)	2.30 (2 values)	/
MODULUS OF ELASTICITY [MPa]	Static: 38 600 ± 5 700			/
	Dynamic: 42 000 ± 6 000			
SHEAR PARAMETERS	/			$\varphi = 35^{\circ}\text{c} = 0.1 \text{ MPa}$

3.3.2. Condition development in comparison with the 1980 test campaign

The 2015 condition assessment was compared with the results from the drill core testing campaign carried out in 1980. At that time, various scenarios were defined for the test evaluation; optimistic, pessimistic and realistic. In Table 3, the 2015 mean value was compared with the 1980 optimistic scenario, the 2015 characteristic strength with a 10% non-exceedance probability is compared with the 1980 pessimistic scenario. As the evaluation at that time related to structures and not to concrete categories, the 2015 data was related to the same structures.

Table 3
Comparison of the Mühleberg HPP concrete properties of 2015 and 1980

STRUCTURE		GRAVITY DAM		WATER RETAINING STRUCTURE POWERHOUSE		ENTIRETY OF WATER RETAINING STRUCTURES	
SCENARIO		Opti.	Pessi.	Opti.	Pessi.	Opti.	Pessi.
DENSITY [kg/m ³]	1980	2 460	2 130	2 480	2 260	2 520	2 130
	2015	2 450	2 190	2 500	2 080	2 500	2 080
CYLINDER COMPRESSIVE STRENGTH (Ø110mm, h/d=1.0) [MPa]	1980	26.4 ± 6.2	16.1 ± 4.0	35.5 ± 8.7	24.6 ± 8.1	35.6 ± 12.9	22.8 ± 9.9
	2015	31.8 ± 12.2	16.2	42.1 ± 14.8	23.2	37.5 ± 14.8	18.6
DIRECT TENSILE STRENGTH [MPa]	1980	1.57 ± 0.62	0.98 ± 0.24	1.68 ± 0.63	1.11 ± 0.36	1.75 ± 0.71	1.22 ± 0.45
	2015	1.52 ± 0.47	0.92	1.47 ± 0.50	0.83	1.52 ± 0.48	0.90
MODULUS OF ELASTICITY [MPa]	1980	37 500	24 000	50 000	22 200	50 000	48 500
	2015	48 500	23 700	45 800	27 000	19 800	23 700

The densities remained almost unchanged over the 35 years. The concrete structure had therefore not changed over this time. Identified seepage in the concrete was localised. The mean values of the cylinder compressive strengths (equivalent to 150 mm side length cube strengths) were significantly higher in 2015 compared to 1980, but the standard deviations were also significantly higher. This could be related to the fact that the more recent data contained a wider range of concrete categories compared to 1980. In the pessimistic scenario, there was hardly any change in compressive strength over the 35 years between the campaigns. The 2015 mean values of the direct tensile strength in the optimistic scenario were slightly lower than the 1980 results, although the values of the gravity dam body were almost identical. In connection with the factors influencing the direct tensile strength test, the small deviations could be described as almost insignificant. On this basis, the condition of the concrete between 1980 and 2015 could also be described as unchanged and good. In the pessimistic scenario, the characteristic direct tensile strengths from the 2015 campaign were at the lower end of the 1980 tensile strength range. There were no recognisable indications of deleterious reactions that would

have reduced the tensile strengths within the observed range. The direct tensile strengths in the pessimistic scenario were within the range of typical parameter assumptions for a concrete such as applied in the Mühleberg HPP. Unfortunately, no split tensile strengths were tested in 1980. In connection with deleterious ageing reactions in concrete, the modulus of elasticity is a very strong indicator. A considerable decrease in the modulus of elasticity over time would indicate a possible increasing degree of damage of the concrete. The ranges shown in Table 3 were unchanged over the years and it could be assumed that no deleterious reaction had been in progress for a long period of time. The historical AAR ascertained was considered to have subsided.

4. PROJECTION OF THE CONDITION DEVELOPMENT (CONCLUSION)

The present condition of the Mühleberg HPP concrete dam and water retaining structure is the result of approx. 100 years of operation without any significant refurbishments or repair, apart from some reprofiling and measures that did not, however, affect the internal condition of the concrete. A condition assessment with tests on drilled concrete core samples was carried out in 1980 and showed that the condition of the concrete was almost unchanged compared to the assessment in 2015. This is due to the poured concrete technology used for the Mühleberg HPP at that time and the good concrete compaction, which minimised seepage and thus also prevented leaching of the concrete structure. The available testing results from the 1980 and 2015 concrete condition assessment campaigns allowed an evaluation of the condition development deliberated by individual concrete structures. This allowed the anticipation of the concrete condition development into the future and the planning for required remedial works interventions.

The results from the microscopy demonstrated that the concrete aggregate used is AAR-reactive. However, due to the relatively low cement content in the concrete and possibly a lower alkali content in the cement, this reaction did not progress and subsided after a certain time. It was therefore concluded that the potential for this reaction must be taken into account in any future refurbishment and retrofit measures.

The condition development into the future will greatly depend on the watertightness of the water retaining structures, respectively the watertightness of the coating mortar ('buckskin'), as well as on the control of the potential re-emergence of AAR. The condition of the structures not exposed to water will not change over a long period of time during the new concession period, as no triggering processes for deleterious reactions take place inside these structures. Structures exposed to flowing water are provided with a coating mortar, that is already leached out to a few millimetres on the surface in some areas and that is weakened. The leaching will progress and significant loss in mortar strength could be expected over the first 20

years of the new concession period. In places where the coating mortar has already spalled, consequences for the durability of the underlying concrete could also be expected over a certain subsequent period, around 10 years, due to an increase in water circulation.

In summary, it was concluded from the recent study, i.e. from the concrete condition assessment (actual condition) and the development of the condition, that the concrete water retaining structures of the Mühleberg HPP, over the period of the new 80-year concession period, could be maintained by localised measures. Based on the findings from the concrete condition assessment, initial measures were recommended, ongoing measures were discussed (especially the surveillance and monitoring as part of the Swiss dam safety practices), and possible future mitigation in the short- middle- and long-term during the new concession period were outlined.

REFERENCES

- [1] Wasserkraftanlagen der Bernischen Kraftwerke AG in Bern, V. Das Elektrizitätswerk Mühleberg. Special Print by the Schweizer Bauzeitung (SBZ), Volume 87, May/June 1926. In German.
- [2] Taschenbuch für Bauingenieure. Editor: Foerster, M.. 4th Edition, Springer Verlag, Berlin, 1925. In German.
- [3] Ageing of Concrete Dams. International Commission on Large Dams (ICOLD). Bulletin No.198, Pre-print Version, Paris, February 2023.
- [4] Injektion von porösem Massenbeton mit hydraulischen Bindemitteln. Wildner, H.. Doctoral Thesis, Reports by the Institute of Hydraulic Engineering and Water Resources, No. 92, Technical University Munich, Munich, 2002. In German.
- [5] Wasserkraftwerk Mühleberg – Gutachten über den Betonzustand. AF-Consult Switzerland Ltd (AFRY), Baden, Switzerland. Report for BKW Energie AG, 2012. In German, unpublished.
- [6] WKW Mühleberg - Betonzustandsbeurteilung und Massnahmenempfehlung. AF-Consult Switzerland Ltd (AFRY), Baden, Switzerland. Report for BKW Energie AG, 2015. In German, unpublished.
- [7] Materialtechnologische Untersuchungen am Beton des WKW Mühleberg. TFB AG, Wildegg, Switzerland. Report for BKW Energie AG, 2015. In German, unpublished.

COMMISSION INTERNATIONALE DES
GRANDS BARRAGES

VINGT-HUITIEME CONGRES DES
GRANDS BARRAGES
CHENGDU, MAI 2025

EXAMINING THE FACTORS IMPACTING TRANSBOUNDARY PROJECTS (*)

Mohan ACHARYA

*Senior Dam Safety Engineer and Team Lead, AGI, Government of Alberta,
Edmonton, AB*

C. Richard DONNELLY

*Global Independent Consultant. C. Richard Donnelly Consulting, Niagara on the
Lake, ON*

Tony BENNETT

Director Dam Safety and Water Resources, OPG, Niagara-on-the-Lake, ON

CANADA

SUMMARY

Some seven years ago the World Economic Forum [66] identified water crises as one of key risks of the 21st century. Given the realities and uncertainties of climate change, population growth and human induced stresses on water the potential for serious conflicts over water looms larger than ever and can only be expected to increase. However, there are tools that can be used to predict the potential for conflict so as to take the actions needed to avoid it.

Organizations such as the International Commission on Large Dams ICOLD and the world Bank Group as well as National Dam Safety Committees and regulatory authorities (local and national) need to play a role in the development and implementation of best practice guidance specifically tailored to the unique needs of transboundary dams including due recognition of the importance of dam safety and

*Examen des facteurs ayant une incidence sur les projets transfrontaliers

emergency management as well as clear and transparent communication with the public to enhance the perception of the benefits, and the management of the hazards that dams present.

RÉSUMÉ

Il y a environ sept ans, le Forum économique mondial [65] a identifié les crises de l'eau comme l'un des principaux risques du XXI^e siècle. Compte tenu des réalités et des incertitudes du changement climatique, de la croissance démographique et des pressions anthropiques sur l'eau, le risque de graves conflits liés à l'eau est plus important que jamais et ne peut qu'augmenter. Cependant, il existe des outils qui peuvent être utilisés pour prédire le potentiel de conflit afin de prendre les mesures nécessaires pour l'éviter.

Des organisations telles que la Commission internationale des grands barrages CIGB et le Groupe de la Banque mondiale, ainsi que les comités nationaux de sécurité des barrages et les autorités de réglementation (locales et nationales), doivent jouer un rôle dans l'élaboration et la mise en œuvre de directives sur les meilleures pratiques spécifiquement adaptées aux besoins uniques des barrages transfrontaliers, y compris la reconnaissance de l'importance de la sécurité des barrages transfrontaliers et de la gestion des urgences, ainsi qu'une communication claire et transparente avec le public, afin d'améliorer la perception des avantages et la gestion des dangers que présentent les barrages.

1. INTRODUCTION

Because borders often correspond with major rivers, transboundary dams are relatively common. The reservoirs created by such dams can provide significant benefits crucial for human health and economic stability. However, water use and governance between neighboring countries can also lead to regional instability and civil unrest. There are at least 2,924 large transboundary dams located in 40 percent of the world's 310 transboundary river basins [1] and an estimated 1,416 large dams planned or under construction in at least 57 transboundary river basins worldwide (Figure 1).

This paper builds on the work performed by CDA Emergency Management Transboundary Subcommittee, Acharya et al. [2] and the research performed by Perdikaris [3], examining the factors that affect the likelihood and intensity of water-related conflicts between riparian nations. It explores the development and implementation of joint best practices that include equitable resource distribution within transboundary river basins. Recommendations are provided with respect to dam

safety and emergency management best practices for transboundary dams, which should be considered in the development of the next generation of dam safety guidelines and regulations, and for the modernization of transboundary treaties.

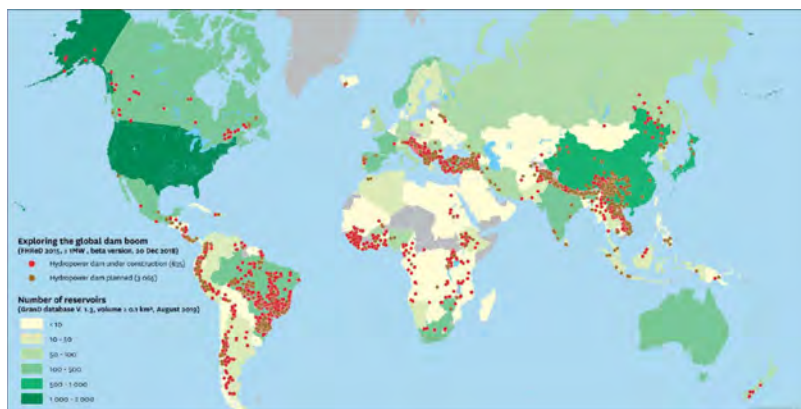


Fig. 1

A Global Boom in Dam construction [4]

Un boom mondial dans la construction de barrages

2. WATER RELATED CONFLICTS – A BRIEF HISTORY

Conflicts related to transboundary dams dates to 3000 BC [5] often with water used as a weapon. In the 6th century BC, one of the first cases of biological warfare occurred when the Assyrians poisoned the water wells of their enemies with rye ergot [6]. Water being used as a weapon can be often attributed to the reallocation or appropriation of water due development projects such as transboundary dams. For example, during the second world war the British devised a unique scheme that successfully destroyed two German dams to disrupt the German steel making industry. In 1965, one of the first of many attacks against Israel's national water carrier, the Palestinian National Liberation Movement attempted to sabotage the diversion pumps of the Israeli national water carrier [7], [8].

River channels, dams, and reservoirs are particularly vulnerable to attacks because of their location in open spaces and ease of access by the public. In July 1999, an improvised explosive device was discovered at a water reservoir near Pretoria, South Africa [9]. If the device had exploded, it would have destabilized a nearby military base and hydrologic research facility. In 2002, the Revolutionary Armed Forces of Colombia (FARC) damaged a gate valve inside the Chingaza Dam, which supplies most of Bogotá's drinking water [10]. In recent times, several

terrorist attacks against water resources and water infrastructure in the Middle East have confirmed the appeal of water as a target for terrorists [11]. In June 2023, a transboundary dam was used as a weapon of war between Ukraine and Russia. The breached Nova Kakhovka dam unleashed heavy flooding across southern Ukraine creating the largest human-made disaster in Europe in decades. Several dozens were killed and tens of thousands displaced.

3. CONFLICTS/COOPERATION BETWEEN TRANSBOUNDARY STATES

The potential for conflict or cooperation among riparian stakeholders is a function of factors such as geopolitics, the exclusion of ethnic groups, water allocation, water availability, failing economies, and climate change. Although many of these disputes can, and are, settled non-violently through cooperation and diplomacy, conflict conflicts between neighboring states continues to occur [12] which is further compounded by the fact that sources of freshwater supplies are increasingly being degraded by both human-induced and natural stresses [13], sedimentation [14], [15] and climate change with water management issues often serving as a significant contributing factor. The dichotomy between conflict and cooperation is especially true for in the case of transboundary dam construction. While the public may perceive a dam as providing significant benefits, it can also be perceived as a significant hazard and a potential threat to water supplies for downstream riparian countries [16], ICOLD [17] showed that a key reason why dams fail is a result of either inadequate design, construction or maintenance. One way to enhance the public's perception of dam safety is to adopt modern dam safety management practices that substantially lower the risk of incidents. Complementing these practices with effective public consultation and education can further mitigate potential consequence of these incidents and build greater confidence in dam safety.

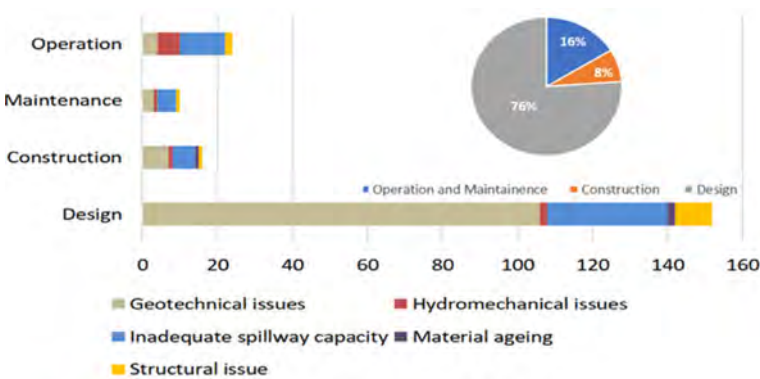


Fig. 2
The causes of dam failure (modified from [17])
Les causes de la rupture du barrage (modifié à partir de [17])

While it is well understood that increased stresses and competition can lead to conflict. It is less understood why the different factors influencing water demand and availability can result in different outcomes. Improvements in this understanding could guide riparian states in mitigating risk and enhancing resiliency to disasters. The capability to foresee whether a transboundary river basin is prone to future water disputes enables stakeholders to alleviate political and economic tensions before they intensify. Understanding the major influencing factors for conflict and cooperation is therefore essential for the development and effective implementation of modern dam safety management practices.

3.1. FACTORS LEADING TO CONFLICT OR COOPERATION

Water conflicts are the product of a number of interrelated factors [18], [19] that include freshwater availability combined with socio-economic, cultural, and topographic characteristics [20]. In this respect, water management issues, such as the construction of a transboundary dam, can result in either increased conflict or increased cooperation [19], [21], [22]. For example, the current Columbia River Treaty allows the USA to override Canadian sovereignty in dam safety situations. Similarly, the Koshi Barrage Treaty gives India full control over a barrage located in Nepal. These examples highlight the need to revisit and modernize existing treaties to reduce the potential for conflict. In this regard, transboundary dam owners and regulators alike need to mandate modern dam safety management practices, understand the interests and needs of all stakeholders while assessing the environmental, economic, and social risks to foster an inclusive approach that both reduces the potential for conflict and improves safety.

3.1.1. *Political factors*

Political tensions between riparian states have historically been the basis for conflicts over water resources. When tensions are high between riparian states, the likelihood of a transboundary dam of causing conflict is also high. Other factors may include the inequitable allocation and appropriation of water due to water infrastructure development projects and their overall vulnerability as a target of opportunity [23]. Even in situations where conflicts have not yet developed, the very existence of these factors serve as an indicator that water conflicts could occur.

3.1.2. *Socio-economic factors*

The impact of water-related conflicts h are often aggravated because of environmental and societal implications [24]. Socio-economic factors, combined with institutional capacity, legal frameworks, and cultural background tend to

influence the diplomatic interactions between states sharing water resources [18], [19], [25]. If other factors, such as the biophysical environment, climate, and topography are considered, it may be possible to anticipate if a transboundary dam may cause water-related conflicts. For example, an indicator of the potential for conflict is low socio-economic status in one or both transboundary states [26]. Poverty is rooted in a lack of access or entitlement to resources, opportunities, and political power, making it difficult to prepare, respond, and recover to water related or other disasters which can certainly lead to conflict even if the disaster does not occur [27]. A country's economic dependency on water, the presence of water infrastructure within the basin, institutional capacity, governance, national capabilities, cultural background, and previous collaborations between riparian states through the establishment of bi-and multi-lateral treaties. Are all factors that need to be considered to reduce the potential for conflict.

Many communities in transboundary river basins suffer from both poverty and harsh environments without appropriate protection and rights and inherently lack political voices [28]. Their specific geopolitical location influences their safety and quality of life. Such location-based vulnerability [29] ultimately results in epistemic injustice [30]. Proper governance and management of water resources, including the implementation of institutional frameworks and modern dam safety management practices can circumvent many transboundary river basin conflicts [31], [32], although there is no guarantee that such arrangements will lead to cooperation [33]. What is important to reduce the potential for conflict is investing in dam safety management and public consultation and education [32].

3.2. THE IMPACT OF WATER ALLOCATION

Violent conflicts have often occurred because of disputes about the allocation of water resources. Many of these conflicts can be attributed to the availability of freshwater. Droughts, low water availability and declining reservoir levels. However, there is a lack of evidence to suggest a correlation between climate data and water-related conflicts [34]. Buhaug [35] determined that the disputes were the by-products of geopolitics, the exclusion of certain ethnic groups, and failing economies. On the other hand, other authors found a strong correlation between conflicts and temperature and rainfall variability on a global scale. This points to a data gap within the literature whether a correlation exists between water-related disputes and climate data. Therefore, there is a need to develop a method for relating climate information to water-related conflicts. According to Kalbhenn [36] water interactions between transboundary states are essentially water management issues. A water management issue can lead to either conflictive or cooperative behaviour depending on the riparian's socio-economic, institutional, cultural, and political conditions. The literature suggests that there is an inverse U-shaped relationship between water scarcity and cooperation among

riparian states, with collaboration being highest when there is a moderate amount of water scarcity as opposed to extreme levels of water scarcity. Such extremes can prevent riparian states from cooperating over water-related issues, including cooperative strategies such as water sharing. De Stefano et al. [18] state that the two most controversial water management issues in transboundary state relations continue to be infrastructure development, such as the construction of transboundary dams and water availability which, somewhat paradoxically, can often be mitigated by the construction of a transboundary dam. Schilling et al. [37] explain that it is not the freshwater supply that leads to conflict but how water is governed and managed. Schilling further argues that power imbalance and inefficiency or lack of diplomacy among states within transboundary river basins drive water-related conflicts. Many of these discourses derive from water nationalism which attempts to justify and legitimize, a state's water policy that can often be challenged domestically and internationally. This requires effective hydro diplomacy and regionally integrated hazard assessment approach to achieve the cooperation needed between riparian states.

4. TREATIES AND AGREEMENTS – CONFLICT MITIGATION

The term water crisis is often associated with the inequities of supply and demands over freshwater or the depletion of a limited resource. According to De Stefano et al. [19], supply-demand basin management and unilateral water infrastructure development without the benefit of transboundary river basin arrangements and unfavourable socio-economic and environmental conditions can lead to transboundary water conflicts. However, more riparian states cooperate over sharing freshwater resources than those embroiled in conflict [38] including regions such as the Middle East and North Africa, which have limited access to fresh water and are plagued by droughts, sedimentation and the threat of violence [39]. Weaker states make use of the resources of third parties, such as donor countries and multi-lateral development banks, to increase their leverage within the water-sharing sphere to promote cooperation. However, such hardline strategies typically have the opposite effect since they fail to achieve the needed cooperation between riparian stakeholders. Strategies that balance economic wealth with legitimate governance are more successful in promoting cooperation.

4.1. FACTORS IMPACTING THE POTENTIAL FOR COOPERATION

Farinosi et al. [40] reported that the chances of riparian states cooperating over the sharing of freshwater resources and adhering to a water agreement are influenced by; time-varying and time-invariant factors. Time-varying factors include

climate data, population data, water availability, socioeconomic issues. Time-invariant factors involve geographical and topographical matters. A combination of time-varying factors such as climate data and socio-economic indicators and time-invariant factors such as cultural, geographic and topographic characteristics, influence the likelihood of reaching an agreement between riparian stakeholders. Increasingly, the effects of climate change impact the physical environment, human health, and relations between transboundary states. Cooley and Gleick explain that global climate change has the propensity to alter the water quantity, quality, and system operations and levy new challenges on freshwater resources. According to Sadoff and Grey [41], for each transboundary river basin, the potential for cooperation between riparian stakeholders is also dependent on an understanding of the hydrologic characteristics of the basin, past collaborations, each riparian's financial investments and cost-sharing. Importantly, a bi-or multi-lateral agreement will only be successful if it can adapt to new challenges. The adaptive strategies that are needed can be attained by creating legislation and institutions addressing issues over sharing freshwater [41].

4.2. BARRIERS TO COOPERATIVE BEHAVIOUR

Marcus et al. [42] note that non-cooperative and competitive behaviour among riparian states and subnational jurisdictions in transboundary basins will typically result in less-than-optimal development outcomes and increase dam safety risks. There are several barriers that can accentuate the challenges of ensuring the safety of transboundary dams and the benefits that they can provide. These include the asymmetric information availability among the riparian states or subnational jurisdictions, technical uncertainties, conflicting individual versus collective interests, political and sovereign rationality, asymmetric characteristics among riparians, and a disconnect between the interests of those upstream of a dam and those downstream. This is particularly true if one country places unilateral demands on available water resources while ignoring the costs and risks imposed on other riparian states or subnational jurisdictions that depend on those resources. The unilateral construction of a transboundary dam, for example, can represent one of the most significant factors that leads to non-cooperation and conflict. In contrast, cooperation around the development and management of transboundary waters and dam safety can substantially increase long-term development gains, providing sustainable benefits to both parties, and enhance the safety of the dam. The transition from conflict to cooperation is a gradual process influenced by various factors related to water policy, water-sharing agreements and treaties, hydro diplomacy, dam safety management practice, climate change, colonial legacy, and the nature of vulnerable communities. In this respect, transboundary agreements need to have a framework with both technical and social/environmental elements which requires an interdisciplinary approach.

4.3. RESOLVING WATER-RELATED CONFLICTS

According to De Stefano et al. [19], water-related conflicts can often be resolved with formal or informal agreements between riparian stakeholders that provide some degree of satisfaction between all parties. In examining water-related issues, the literature indicates that certain degrees of conflict and cooperation coexist for the same water-related issue [43]. For this reason, some authors have claimed that it is better to analyze the water interaction for both conflict and cooperation for the same water event between riparian states as opposed to focusing on a specific conflict or cooperative water-related issue, [44]. Doing so requires focusing on historical water interactions instead of a specific water-related conflict.

Clearly, effective water-sharing agreements and governance structures are important tools to prevent water conflicts. Strategies to account for the dynamic behaviour of future climate conditions in water-sharing agreements can enhance adaptive capacity, improve dam safety, reduce the potential for conflicts, and help minimize the undesirable consequences of future climate change. International river basin organizations, such as IJC, can play a crucial role in hydro diplomacy, fostering cooperation among riparian states by evaluating water supply sustainability, improving water management plans, mandating dam safety management practices, assessing the degree of equivalence among the different dam safety obligations and standards of care, and enhancing water allocation systems to achieve collaboration that minimizes tensions in transboundary river basins. Integrated regional dam safety initiatives might be appropriate in some regions where capacity constraints and consistency in practice are lacking. Such regional initiatives should facilitate the joint development of tools and a resource pool that contributes to improved operation and safety of transboundary dams, such as undertaking joint studies, including integrated hazard assessment, undertaking cross border dam breach and flood-mapping simulations, developing collaborative emergency action plans, implementing mechanisms for data sharing and conflict resolution, ensuring public consultation and education is performed, developing a consistent framework to coordinate and manage the potential impact of cascade operations and/or failure, and developing and implementing a joint community resilience plan in case of dam failure, mis-operation, or special operation (e.g., the scenario where the dam may not be at risk of failure but the downstream community may be impacted by releases from the dam that cause flooding).

4.4. TRANSBOUNDARY DAMS AND DAM SAFETY MANAGEMENT

Unfortunately, transboundary water management treaties rarely address dam safety management issues, focusing instead on bi-lateral agreements for using the transboundary waters. In addition, in most agreements, the legal, socio-economic, and political aspects of shared water use are not fully dealt with and, in some cases,

not at all. This is, perhaps, because dam safety and public safety issues were typically seen as a much lower priority when the agreements were formulated. In many cases, issues associated with flooding, drought, public safety, climate change, and other impacts are not well addressed or, in some cases, not considered. In this context, Acharya et al. [45] emphasized the need for developing and implementing modern dam safety management systems that address the specific requirements of transboundary dams. Considerations should include the legal and institutional framework, a regional collaborative approach for integrated river basin management and hazard assessments, consideration of societal perspectives on risk tolerance, risk-informed decision making and improved risk communication throughout a project's life cycle. The transboundary considerations for dam safety and emergency management are discussed further in Acharya et al. [45].

4.5. HYDRO DIPLOMACY

Hydro diplomacy is the application of diplomatic tools to resolve transboundary disagreements and conflicts over shared water resources and mitigate those issues to achieve cooperation, regional stability, and peace [46]. International River Basin Organizations (IRBOs) are institutions that support hydro diplomacy in transboundary river basins [47]. These IRBOs are using science to help hydro diplomacy by balancing capacity, ownership, and politics [47]. Adaptive governance indicators such as social learning, sustained relationships, flexible governance mechanisms, and state/non-state networks are critical components of hydro diplomacy. For effective hydro diplomacy, freshwater supplies must be carefully evaluated with respect to their sustainability under the impacts of climate change and increased water demands to achieve cooperation between states located in transboundary river basins. According to Amorima et al. [48] and Abedzadeh et al. [49], water management plans are critical for evaluating freshwater resources' sustainability. The river basin's social, economic, and environmental conditions should also be considered when formulating water resource development plans. Wang et al. [50] explain that improving water allocation systems and establishing a water cooperation network among transboundary states may lead to the elimination of conflicts. Using sound science and hydro diplomacy, can reduce or even eliminated conflict.

5. SUSTAINABLE TRANSBOUNDARY ASSESSMENT PRACTICES

Various water conflict risk assessment approaches exist, including qualitative, quantitative, and semi-quantitative methods, each offering a unique means to evaluate and predict the potential for both water-related conflicts and cooperation. Mathematical models and analytical tools like game theory have been used to

define water conflict risks and factors influencing cooperation between riparian states. This research has explored geospatial analysis, socio-economic data, and mathematical modelling to assess the impacts of reservoir operations and management decisions on water conflicts. The role of treaties and agreements in preventing conflicts have also been studied using various analytical approaches.

Acharya et al. [45] noted that transboundary dam projects river basins are subjected to uncertain climatic conditions and evolving patterns of human settlement which increases the potential for water related conflicts. In this context, many countries have implemented integrated risk assessment and management initiatives to deal with the additional risk associated with transboundary dams. Marcus et al. [42] provides several examples of such initiatives, including the transboundary emergency preparedness initiative between France and Italy and the transboundary dam safety management efforts between Spain and Portugal. Similarly, the Eastern Nile Technical Regional Office of the Nile Basin Initiative works with Eastern Nile countries to build technical capacity and establish national and regional safety norms. Likewise, the Zambezi River Basin includes eight riparian states that have established a joint operations technical committee in 2014 as an intergovernmental organization under a 2004 basin-wide agreement with the aim of promoting equitable and reasonable utilization, as well as the efficient management and sustainable development of the basin's water resources. In addition, dam operators in the basin have established a Joint Operations Technical Committee to facilitate the exchange of hydro-meteorological and dam-related information as a contribution to improving and informing the management of the water resources in the basin.. The Columbia River Treaty represents a significant international agreement between the United States and Canada. Signed in 1961, it coordinates the responsibilities of the two countries for flood risk management and hydroelectric energy production. Modernization of this treaty, that is currently underway, needs to consider the issues discussed in this paper from an integrated dam safety and emergency management perspective.

5.1. ASSESSING THE POTENTIAL FOR CONFLICT AND COOPERATION

In the context of evolving societal values and norms, it is necessary to understand the underlying issues of the water-related conflicts and the interests of stakeholders sharing the transboundary river basins to develop sustainable solutions for eliminating conflict and implementing modern dam safety and reservoir management practices that meet the needs of the riparian states.

5.1.1. *Qualitative risk assessments*

Qualitative methods primarily focus on the occurrence and consequences of water-related conflicts and cooperation and are dependent upon the experience of

experts in hydro diplomacy [19]. [51] The Basins at Risk (BAR) project was the first study to examine the causes of water conflict on a global scale. Using a qualitative approach, the study identified 29 transboundary river basins at risk of conflict [51]. According to De Stefano et al. [19], qualitative risk assessment methods for transboundary basins have typically been limited to case studies concerning conflict and cooperation at the local or basin level. De Stefano et al. [19] further explains that quantitative methods are more appropriate for global-scale analyses, although basins that require closer examination may do so using qualitative methods.

5.1.2. *Semi-quantitative risk assessments*

Semi-quantitative approaches use expert knowledge, mathematics, statistics, and analytical tools such as game theory, fault tree analysis, and event tree analysis to define the potential for water-related conflicts to develop [52]. Some studies have focused on the interactions of riparian states involving a combination of conflict and cooperation [38] [18]. Other studies have focused on the likelihood of transboundary states agreeing to share water resources [53] and studies that used the existence of treaties and International River Basin Organizations (IRBOs) as resiliency measures to prevent water-related conflicts [18], [19]. While important, these treaties often do not address the important aspects of dam safety and emergency management issues. Unfortunately, in some cases, projects do not align well with disaster and emergency management because this requires comprehensive risk assessment involving environmental risk and benefit analysis, which can be costly and time-consuming. In addition, in some cases, such assessments can cause delays and interfere with their project aims and goals, creating a reluctance to accept when the costs to mitigate identified risks are significant. As a result, dam safety and disaster, emergency management and public safety around transboundary dams are often not adequately addressed except. Mechanisms are needed for compliance with these matters to avoid both undesirable consequences and conflict.

5.1.3. *Quantitative risk assessments*

Quantitative approaches use mathematical modelling and statistics to quantify dimensions and indicators of water-related conflicts [54] that can involve the use of mathematical models which can be either linear, non-linear, or a combination of both. For example, Rai et al. [55] used a combination of fuzzy logic methodologies to assess the potential for water-related conflicts in transboundary river basins to develop. The Analytical Hierarchy Process (AHP) was used to develop the framework for the model parameters, including development parameters and hegemony parameters. According to Rai et al. [55], development parameters include population, agricultural activities, industrial activities and hydropower generation. Hegemonic parameters include political, military, and economic power. Rai et al. [55] further explained that the approach can be refined by incorporating expert knowledge into the risk assessment process. Maiolo and Pantuso, 2018 used a

similar approach to develop an infrastructure vulnerability index for drinking water systems and computed the indices' weights for the different indicators. Unlike the study by Rai et al. [55], the authors incorporated expert knowledge as part of their assessment for establishing a vulnerability index. Giriagama et al., [56] {83} noted that the application of machine learning tools is useful in informing local and regional specific water management activities, including potential causes for conflicts and cooperations.

Studies have combined socio-economic data with hydrologic modelling to assess the effects of reservoir operations and management decision-making on hydro-political interactions. For example, Ghoreishi et al. [57] developed a large-scale socio-hydrologic model of the Eastern Nile Basin to represent the evolution of the cooperation pathways. The model was used to evaluate the effects of dam operations and management decisions which provided a predictable explanation that could help identify the willingness to cooperate and to guide future decision support. Geospatial statistics are statistical methods that directly use space and spatial relationships data such as distance, height, area, and volume, in their mathematical computations [58]. For example, Veilleux and Dinar [59] developed a resiliency tool using geostatistical analysis to determine whether a nation was susceptible to instability due to water conflicts. The study concluded that countries with the least access to freshwater resources have the lowest water-related resiliency.

5.2. RANKING THE POTENTIAL FOR CONFLICT

In the Transboundary Waters Assessment Project, institutional resilience was defined as a function of the number of institutions used to manage water resources and the number of treaties present. The approach used a combination of geospatial statistics and modelling to determine institutional resilience making use of regression analysis to establish a relationship between the institutional resiliency of the transboundary river basins, their drainage areas, the number of treaties present, and the number of water management agencies present to represent a component of the overall governance indicator [13]. The study also examined the hydro-political tension indicator, part of the governance thematic group. Hydro-political tension was obtained by calculating the institutional resilience of each transboundary basin. Institutional stability was based on at least one water treaty, one treaty with an allocation mechanism, one with a flow variability management mechanism, one with a conflict resolution mechanism, and the presence of a river basin organization. The scores were then grouped, ranked, and assigned a vulnerability level between 1 and 5 using the methodology described in [38]. A hydro-political tension score was then established based on information derived from the water treaties database[†] [18]. De

[†]*Transboundary Freshwater Dispute Database from the College of Earth, Ocean, and Atmospheric Sciences at Oregon State University*

Stefano et al. [19] further developed this approach by calculating institutional resilience as a function of the number of existing treaties and the presence of river basin management organizations.

De Stefano et al. [19] employed regression analysis and geospatial mapping to examine the relationship between the potential for water-related conflicts and a comprehensive set of variables (climatic, geographic, political, and economic) to test hypotheses concerning the impact of a water treaty's development plan on the collaboration between transboundary states over time. The authors then applied multi-criteria analysis to determine the potential for water-related conflicts by considering the rate of developmental change within the basin and the ability of the governing institutions to understand that change. Thirty-six basins were evaluated in the study, with the potential for future conflict categorized as very high or high that demonstrated that the construction of new dams does impact potential for conflict and cooperation. In another study, Garrick et al. [60] applied an institutional analysis and development (IAD) framework to examine the decision-making process for adopting drought adaptation strategies in transboundary river basins. Using risk management in the IAD framework, the authors could characterize droughts from a natural and human perspective. Using global analyses methods, the authors identified regions where severe droughts had occurred, and the governing institutions were fragmented concluding that a coordinated adaptation approach between riparian states would be necessary to minimize conflicts over shared freshwater resources.

With increasing climate-related disasters and growing geopolitical tensions, the potential for future conflicts also increases significantly. Dam owners and regulators need to understand the complex and intricate factors and implement robust policies that consider dam safety and disaster and emergency plans for transboundary dams.

6. TRANSBOUNDARY DAM ISSUES AND CLIMATE CHANGE

Tian et al. [61] demonstrated that climate change and increasing water demands have increased the frequency and intensity of transboundary water conflicts. This, and another study by Schilling et al. explain how climate change can indirectly drive social instability because of the increase in frequency and intensification of flooding. Therefore, improving climate change resilience (such as described by the [62] IHA) is necessary to minimize the future potential for conflicts and potential failures.

The challenge for many transboundary states is incorporating uncertain future climate conditions into their transboundary river basin agreements to increase their adaptive capacity. To resolve this challenge, Cooley and Gleick [63] recommend developing water-sharing contracts that can be adjusted over time to account for

climate-driven water variability, thereby increasing the basin's climate change resiliency. According to Zeitoun et al. [64], transboundary river basins should be managed by means of an adaptive and multilateral approach. Bakker and Duncan [65] argued that, without the necessary institutional provisions to counter the effects of climate change and rising water demands, transboundary river basins may experience an elevated potential for conflict.

7. CONCLUDING REMARKS

Collaborative resolution of disputes through treaties and agreements is essential to minimize the potential for conflicts over transboundary projects. Unfortunately, most existing treaties governing transboundary water management often prioritize equitable water use allocation over dam safety and indigenous, socio-economic, and public safety considerations. Part of what is missing in existing agreements is mechanisms to ensure that modern dam safety and emergency management practices and procedures are adhered to thereby enhancing the owners' social licence to operate, helping to reduce the potential for conflict. This also requires effective communication with relevant stakeholders regarding safety and emergency management and the exploration of ways to enhance community resiliency and readiness throughout the life cycle of a transboundary dam. Conflict reduction also requires proactive diplomatic communication, the developing and implementing joint adaptive measures for the potential impacts of climate change, establishing societal risk tolerance, instituting a risk-informed decision-making framework and incorporating the rights of tribal and indigenous Nations.

In developing new ways to reduce the potential for conflict best practices must cover items such as dam safety and emergency management, regionally integrated risk, hazard, and vulnerability assessments that factor into the impacts on communities, infrastructure, property. The assessment of environmental and cultural heritage assets, joint emergency management coordination, stakeholder engagement, and emergency exercise practices should be integral to these best practices. Strengthening dam safety, enhancing emergency management measures and improving cooperation between neighboring countries are crucial steps in addressing conflicts linked to transboundary dams, where different legal, socioeconomic, cultural and institutional framework for dam safety need to coexist.

ACKNOWLEDGEMENTS

This work represents the initial outcome of the Canadian Dam Association Emergency Management Transboundary Subcommittee, published with the aim of

sharing knowledge with the broader global dam safety community. The authors wish to acknowledge the help and guidance of Professors J. Perdikaris, E. Yasui, and B. Gharabaghi. Special thanks are extended to Dr. Perdikaris for sharing valuable information from his research on the factors affecting the likelihood and intensity of water-related conflicts between riparian nations, as part of his Doctorate in Strategic Security.

REFERENCES

- [1] *World Economic Forum*, «Annual Meeting: Responsive and Responsible Leadership. https://www3.weforum.org/docs/WEF_AM17_Report.pdf,» 2017.
- [2] M. MCCracken ET A. T. WOLF, «Updating the register of international river basins of the world,» *International Journal of Water Resources Development*, vol. 35, n °15, pp. 732–782., 2019.
- [3] M. ACHARYA, J. PERDIKARIS, J. GHARABAGHI, E. YASUI, C. R. DONNELLY ET T. BENNETT, «Dam safety risk assessment for transboundary river basins – examining conflict stressors and cooperation opportunities,» *chez The 2024 annual Canadian Dam Association*, Niagara Falls, 2024.
- [4] PERDIKARIS, JOHN, «*An Innovative Approach to Assessing Water-Related Conflicts : Dissertation presented in partial fulfillment of the requirements for the Doctorate in Strategic Security, Henley-Putnam School of Strategic Security, National American University*, August 2023.
- [5] Geneva Water Hub, «The Role of Large Dams in Transboundary Water Negotiations. https://www.genevawaterhub.org/sites/default/files/atoms/files/roundtablelargedams_20191002.pdf,» 2019. [En ligne].
- [6] H. HATAMI ET P. H. GLEICK, «Chronology of Conflict over Water in the Legends, Myths, and History of the Ancient Middle East,» *Environment: Science and Policy for Sustainable Development*, <https://doi.org/10.1080/00139157.1994.9929156>, vol. 36, n °13, 1994.
- [7] E. M. EITZEN ET E. T. TAKAFUJI, «Medical Aspects of Chemical and Biological Warfare.,» Office of the Surgeon General, Department of the Army, USA., 1997.
- [8] T. NAFF ET R. C. (Matson, *Water in the Middle East: Conflict or cooperation?*, Westview Press., 1984.
- [9] M. DOLATYAR, «Water diplomacy in the Middle East.,» *In E. Watson (Ed.), The Middle Eastern Environment*, pp. 256–257, 1995.

- [10] Pretoria Dispatch Online, «dam bomb may be 'aimed at farmers. <http://www.dispatch.co.za/1999/07/21/southafrica/RESEVOIR.HTM>.», 21 JULY 1999. [En ligne].
- [11] Waterweek, «Water facility attacked in Colombia,» *American Water Works Association*. <http://www.awwa.org/advocacy/news/020602.cfm>, January 2002.
- [12] P. H. GLEICK, «Water as a weapon and casualty of conflict,» : *Freshwater and international humanitarian law. Water Resources Management*, vol. 33, pp. 1737–1751, 2019.
- [13] A. T. WOLF, « A long-term view of water and international security,» *Journal of Contemporary Water Resources Education* <https://doi.org/10.1111/j.1936-704X.2009.00056.x>, vol. 142, pp. 67–75, 2009.
- [14] UNEP-DHI and UNEP, « *Transboundary river basins: Status and trends*,» *United Nations Environment Programme (UNEP)*, Nairobi, 2016.
- [15] G. SCHELLENBERG, C. R. DONNELLY ET C. HOLDER, «Dealing with Sediments: Effects on Hydropower and Dams.,» *Hydro Review World*, vol. 6, n° 113, 2017.
- [16] G. W. ANNANDALE, G. I. MORRIS ET P. KARKI, Extending the Life of Reservoirs Sustainable Sediment Management for dams and Run-of-River Hydropower. *Directions in Development*. doi: 10.1596/978-1-4648-0838-8., Washington, DC : World Bank., 2016.
- [17] Y. M. TARAKY, E. MCBEAN, Y. LIU ET P. DAGGUPATI, « Flood risk management with transboundary conflict and cooperation dynamics in the Kabul River basin <https://doi.org/10.3390/w13111513>,» *Water*, vol. 13, 2021.
- [18] ICOLD, Bulletin 188:: Statistical Analysis of Dam Failures, 2019.
- [19] L. DE STEFANO, J. DUNCAN, S. DINAR , K. STAHL , K. M. STRZEPEK ET A. T. WOLF, «Climate change and the institutional resilience of international river basins. <https://doi.org/10.1177/0022343311427416>,» *Journal Peace Research*, vol. 49, pp. 193–209, 2012.
- [20] L. DE STEFANO, J. D. PETERSEN-PERLMAN, E. A. SPROLES, J. EYNARD, ET A. T. WOLF, « Assessment of transboundary river basins for potential hydro-political tensions,» *Global Environmental Change*, vol. 45, pp. 35–46, 2017.
- [21] H. MUNIA, J. H. GUILLAUME, N. MIRUMACHI, M. PORKKA, Y. WADA ET M. KUMMU, «Water stress in global transboundary river basins: significance of upstream water use on downstream stress.,» *Environmental Research Letters*, 14002. <https://doi.org/10.1088/1748-9322/11/11/114002>, vol. 11, n° 11, 2016.

- [22] A. KALBHENN ET T. BERNAUER, «International Water cooperation and conflict: A new event dataset.,» *SSRN Electronic Journal* <https://doi.org/10.2139/ssrn.2176609>, 2012.
- [23] Y. M. TARAKY, E. MCBEAN, Y. LIU, P. DAGGUPATI, N. K. SHRESTHA, A. JIANG ET B. GHARABAGHI, «Flood risk management with transboundary conflict and cooperation dynamics in the Kabul River basin,» *Water* <https://doi.org/10.3390/w1311151>, vol. 13, 2021.
- [24] F. FARINOSI, C. GIUPPONI, A. REYNAUD, G. CECCHERINI, C. CARMONA-MORENO, A. DE ROO ET G. BIDOGLIO, «An innovative approach to the assessment of hydro-political risk: A spatially explicit, data driven indicator of hydro-political issues.,» *Global Environmental Change*, vol. 52, pp. 286–313.
- [25] L. SEGATO, W. MATTIOLI, N. CAPELLO ET G. MIGLIORIN, «Environmental crimes in the water sector,» *Water Utility Journal*, vol. 20, pp. 13–27, 2018.
- [26] T. BERNAUER, T. BÖHMELT, H. BUHAUG, N. P. GLEDITSCH, T. TRIBALDOS, E. B. WEIBUST ET G. WISCHNATH, «Water-related intrastate conflict and cooperation (WARICC): A new event dataset. International Interactions. <https://doi.org/10.10>,» *International Interactions*, vol. 38, pp. 529–545, 2012.
- [27] B. WISNER, P. M. BLAIEKIE, T. CANNON ET I. DAVIS, *At risk: natural hazards, people's vulnerability and disasters (Second edition.)*, 2004.
- [28] K. HEWITT, *Regions of risk: a geographical introduction to disasters*, Harlow, Essex, England: Longman., 1997.
- [29] C. J. CARR, Ch 4. Transboundary Survival Systems: A Profile of Vulnerability. In *River Basin Development and Human Rights in Eastern Africa — A Policy Crossroads*. DOI 10.1007/978-3-319-50469-8_4, CDA (Canadian Dam Association) Technical Bulletin, 2021.
- [30] E. KLINENBERG, *Heat Wave: A Social Autopsy of Disaster in Chicago (2nd ed.)*, Chicago: The University of Chicago Press., 2015.
- [31] M. FRICKER, *Epistemic Injustice: Power & The Ethics of Knowing*, Oxford: Oxford University Press, 2007.
- [32] T. S. ABEDZADEH, A. ROOZBAHAN ET A. HEIDARI, «Risk assessment of water resources development plans using fuzzy fault tree analysis.,» *Water Resources Management* <https://doi.org/10.1007/s11269-020-02578-5>, vol. 34, pp. 2549–2569, 2020.
- [33] *World Bank Group, Pathways for Peace: Inclusive approaches to preventing violent conflict.*, Washington, DC. , 2018.

- [34] I. A. ESPÍNDOLA ET W. C. RIBEIRO, «Transboundary waters, conflicts, and international cooperation - examples of the La Plata basin,» *ater International* <https://doi.org/10.1080/02508060.2020.1734756>, vol. 45, n° %14, pp. 329–346, 2020.
- [35] M. ZEITOUN ET N. MIRUMACHI, «Transboundary water interaction I: Reconsidering conflict and cooperation. International Environmental Agreements:», *Politics, Law and Economics*. <https://doi.org/10.1007/s10784-008-9083-5>, vol. 8, pp. 297–316, 2008.
- [36] H. BUHAUG, «Climate not to blame for African civil wars.,» *Proceedings of the National Academy of Sciences*, <https://doi.org/10.1073/pnas.1005739107>, vol. 107, pp. 16477–16482, 2010.
- [37] A. KALBHENN ET T. BERNAUER, «International Water cooperation and conflict: A new event dataset. S,» *SRN Electronic Journal*. <https://doi.org/10.2139/ssrn.2176609>, 2012.
- [38] J. SCHILLING, S. HERTIG, Y. TRAMBLAY ET J. SCHEFFRAN, «Climate change vulnerability, water resources and social implications in North Africa. *Regional Environmental Change*, 20(15), 1–12. <https://doi.org/10.1007/s10113-020-01597-7>,» 2020.
- [39] L. DE STEFANO, «(2010). Facing the water framework directive challenges: A baseline of stakeholder participation in the European Union.,» *Journal of Environmental Management*, <https://doi.org/10.1016/j.jenvman.2010.02.014>, vol. 9, n° %16, pp. 1332–1340, 2010.
- [40] A. DEZFULI, S. RAZAVI ET B. F. ZAITCHIK, «Compound effects of climate change on future transboundary water issues in the Middle East.,» *Earth's Future*, vol. 10, n° %14, 2022.
- [41] F. FARINOSI, C. GIUPPONI, A. REYNAUD, G. CECCHERINI, C. CARMONA-MORENO, A. DE ROO ET G. BIDOGLIO, « An innovative approach to the assessment of hydro-political risk: A spatially explicit, data driven indicator of hydro-political issues,» 2018.
- [42] C. W. SADOFF ET D. GREY, «Cooperation on international rivers: A continuum for securing and sharing benefits,» *Water International*, vol. 30, n° % 14, pp. 420–427, 2005.
- [43] J. W. MARCUS, U. SATORU, J. D. PISANIELLO, J. L. TINGEY-HOLYOAK, K. N. LYON ET E. B. Garcl'a, aying the foundation, A Global Analysis of Regulatory Frameworks for the Safety of Dams and Downstream Communities, The World Bank Group, 2020.
- [44] D. KATZ, «Hydro-Political Hyperbole: Examining Incentives for Overemphasizing the Risks of Water Wars.,» *Global Environmental*

- Politics*. https://doi.org/10.1162/GLEP_a_00041, vol. 11, n° %11, pp. 12–35, 2016.
- [45] M. YIMER, « The Nile hydro politics; A historic power shift,» *ternational Journal of political science and development*, vol. 3, n° %12, pp. 101–107, 2015.
- [46] M. ACHARYA, C. R. DONNELLY ET P. A. ZIELINSKI, «Evolution of Dam safety Management Practice for Transboundary Dams – A Global Perspective with a Nepalese context.,» *chez 27th International Congress on Large Dams*, Marseille - France., May 27-June 3rd.
- [47] S. SCHMEIER ET Z. SHUBBER, «Anchoring water diplomacy – The legal nature of international river basin organizations.,» *Journal of Hydrology (Amsterdam)*. <https://doi.org/10.1016/j.jhydrol.2018.09.054>, vol. 567, pp. 114–120, 2018.
- [48] A. MILMAN ET A. K. GERLAK, «International river basin organizations, science, and hydrodiplomacy,» *Environmental Science & Policy*, vol. 107, pp. 137–149, 2020.
- [49] W. S. AMORIMA, I. B. VALDUGAB ET J. M., «The nexus between water, energy, and food in the context of the global risks: An analysis of the interactions between food, and food in the context of the global risks: An analysis of the interactions between food, water, and energy security.,» *Environmental Impact Assessment Review*, vol. 72, pp. 1–11, 2018.
- [50] S. ABEDZADEH, A. ROOZBAHANI ET A. HEIDARI, «Risk assessment of water resources development plans using fuzzy fault tree analysis.,» *Water Resources Management*. <https://doi.org/10.1007/s11269-020-02578-5>, vol. 34, pp. 2549–2569, 2020.
- [51] X. WANG, Y. CHEN, Z. LI, X. WANG, Y. CHEN, Z. LI, G. FANG, F. WANG ET H. HAO, «Water resources management and dynamic changes in water politics in the transboundary river basins of Central Asia.,» *Hydrology and Earth System Sciences*, vol. 25, n° %16, pp. 3281–3299, 2021.
- [52] A. T. WOLF, S. B. YOFFE ET M. A. GIORDANO, «International waters: identifying basins at risk.,» *Water Policy*, vol. 5, n° %11, pp. 29–60, 2003.
- [53] R. ZHU, X. HU, X. LI, H. YE ET N. JIA, «Modeling and risk analysis of chemical terrorist attacks: A Bayesian network method.,» *International Journal of Environmental Research and Public Health*, Article 2051. <https://doi.org/10.339>, vol. 17, n° %16, 2020.
- [54] N. A. ZAWAHRI ET S. M. MITCHELL, «Fragmented governance of international rivers: Negotiating bilateral versus multilateral treaties.,» *International Studies Quarterly*. <https://doi.org/10.1111/j.1468-2478.2011.00673.x>, vol. 55, pp. 835–858, 2011.

- [55] M. LI ET R. ZHANG, «Evolving a weighted Bayesian network for consequence assessment of terrorist attack,» *IEEE Access*, vol. 8, pp. 88282–88293., 2020.
- [56] S. P. RAI, N. SHARMA ET A. K. LOHANI, «Risk assessment for trans-boundary rivers using fuzzy synthetic evaluation technique.,» *Journal of Hydrology*, vol. 519, pp. 1551–1559, 2014.
- [57] L. GIRIHAGAMA, K. NAVEED, P. LAMONTAGNE ET PERDIK, «Streamflow modelling and forecasting for Canadian watersheds using LSTM networks with attention mechanism.,» *Neural Computing and Applications*, vol. 1, n° %121, 2022.
- [58] M. GHOREISHI, A. ELSHORBAGY, S. RAZAVI, G. BLÖSCHL, M. SIVAPALAN ET A. ABDELKADER, «Cooperation in a Transboundary River Basin: a Large-Scale Socio-hydrological Model of the Eastern Nile. Hydrology and Earth System Sciences Discussions, 1-24.,» *Hydrology and Earth System Sciences Discussions*, vol. 1, n° %124, 2022.
- [59] T. WADE ET S. SOMMER, *A to Z GIS, An illustrated dictionary of geographic information systems.*, Esri Press., 2006.
- [60] J. VEILLEUX ET S. DINAR, «A geospatial analysis of water-related risk to international security: an assessment of five countries,» *GeoJournal*, 86, vol. 861, n° %11, pp. 185–238, 2019.
- [61] D. E. GARRICK, E. SCHLAGER, L. DE STEFANO ET S. VILLAMAYER-TOMAS, «Managing the cascading risks of droughts: Institutional adaptation in transboundary river basins.,» *Earth's Future* , vol. 6, n° %16, pp. 809–827., 2018.
- [62] G. TIAN, J. LIU, X. LI, Y. LI ET H. YIN, «Water rights trading: A new approach to dealing with transboundary water conflicts in river basins,» *Water Policy*. <https://doi.org/10.2166/wp.2020.180>, vol. 3, p. 22, 133–152.
- [63] IHA, «Hydropower status report: Sector trends and insights. :https://hydropower-assets.s3.eu-west-2.amazonaws.com/publications-docs/2019_hydropower_status_report_0.pdf, 2019.
- [64] H. COOLEY ET P. H. GLEICK, «Climate-proofing transboundary water agreements,» *Hydrological Sciences Journal* , vol. 56, pp. 711–718, (2011).
- [65] M. ZEITOUN, M. GOULDEN ET D. TICKNER, «Current and future challenges facing transboundary river basin management,» *Wiley Interdisciplinary Reviews: Climate Change*, vol. 4, n° %15, pp. 331–349, 2013.
- [66] M. H. BAKKER ET J. A. DUNCAN, «Future bottlenecks in international river basins: Where transboundary institutions, population growth and hydrological variability intersect.,» *Water international*, vol. 42, n° %14, pp. 400–424, 2017.

COMMISSION INTERNATIONALE DES
GRANDS BARRAGES

VINGT-HUITIEME CONGRES DES
GRANDS BARRAGES
CHENGDU, MAI 2025

**APPLICATION OF RISK ASSESSMENT APPROACHES TO ENHANCE THE
UNDERSTANDING OF DAM SAFETY RISKS AT THE WATERTON DAM (*)**

Puria ASIABAN

Hydrotechnical Engineer, Tetra Tech Canada Inc., Canada

Allen VEENLAND

Senior Geotechnical Engineer, Tetra Tech Canada Inc., Canada

Babak ALINEJAD

Senior Hydrotechnical Engineer, Tetra Tech Canada Inc., Canada

Mohammad AL-MAMUN

Director and Principal Consultant – Dam Practice, Tetra Tech Canada Inc., Canada

Mohan ACHARYA

Alberta Agriculture and Irrigation, Canada

C. Richard DONNELLY

Independent consultant, C. Richard Donnelly Consulting, Canada

CANADA

SUMMARY

Many large dam owners and regulators around the world have recognized that risk-informed decision-making methodologies are an important part of best practices in dam safety management. Alberta Agriculture and Irrigation (AGI), as the major

**Application des approches d'analyse des risques pour améliorer la compréhension des risques au barrage de Waterton*

dam owner in the province of Alberta, Canada, makes use of a semi-quantitative Potential Failure Modes and Effects Analysis (PFMEA) methodology for the identification and prioritization of dam safety risks [5]. For selected key failure modes, AEP supplements the risk informed assessments with Quantitative Risk Assessment (QRA). These two approaches provide the basis for AGI's risk-informed decision making for dam safety.

The results of this case study demonstrated the value that a QRA can bring in providing a more in depth understanding of key potential failure modes allowing for the proactive development of contingency intervention measures and informing instrumentation design and monitoring measures enhancing the safety of the dam. However, the QRA process can be expensive, time consuming and costly. A tradeoff is often required considering the costs of obtaining the information needed to better assess likelihood and consequence and the use of engineering judgement. In the end, the decision should be based on the estimated risks that the dam presents and if the implementation of barriers on either the right- or left-hand side of the bow-tie model can effectively mitigate the risks at a lower cost.

RÉSUMÉ

De nombreux grands propriétaires de barrages et régulateurs du monde entier ont reconnu que les méthodologies de prise de décision fondées sur les risques constituent une des meilleures pratiques en matière de gestion de la sécurité des barrages. Alberta Agriculture and Irrigation (AGI), principal propriétaire de barrages dans la province de l'Alberta, au Canada, utilise une méthodologie semi quantitative d'analyse des modes de défaillance potentiels et de leurs effets (PFMEA) pour l'identification et la hiérarchisation des risques liés à la sécurité des barrages [5]. Pour certains modes de défaillance clés, une AEP complète les évaluations fondées sur les risques par une évaluation quantitative des risques (QRA). Ces deux approches constituent la base de la prise de décision d'AGI en matière de sécurité des barrages.

Les résultats de cette étude de cas ont démontré la valeur qu'une évaluation quantitative des risques peut apporter en fournissant une compréhension plus approfondie des principaux modes de défaillance potentiels, permettant le développement proactif de mesures d'intervention d'urgence et informant la conception de l'instrumentation et les mesures de surveillance améliorant la sécurité du barrage. Cependant, le processus d'évaluation peut être coûteux et long. Un compromis est souvent nécessaire entre les coûts d'obtention des informations nécessaires pour mieux évaluer la probabilité et les conséquences et l'utilisation du jugement des ingénieurs. En fin de compte, la décision doit être basée sur les risques estimés que le barrage présente et sur la question de savoir si la mise en œuvre de barrières sur le côté droit ou gauche du modèle de nœud papillon peut atténuer efficacement les risques à un moindre coût.

1. INTRODUCTION

Dam safety has traditionally been achieved following a Standards-Based Assessment methodology that assesses the current condition of the dam and makes recommendations to maintain the structure or improve it to satisfy the criteria of the applicable standard. In general, the dam industry has been well served through the use of these traditional approaches, coupled with evolving dam safety management practices. For example, ICOLD [1] reported that there has been a steady decrease in the ratio of dam failures to the number of dams built over the years (Fig. 1). Currently, the accepted average annual likelihood of failure rate for dams of all types has leveled out at about 4×10^{-4} failures per dam year. While UK guidelines indicate that this may be a broadly acceptable individual risk, perceptions on acceptable risk are evolving, leading to a desire to continually lower risks of all kinds, including risks associated with dams. This has led to risk-informed approaches gaining increasing popularity worldwide. These methods are intended to reduce the level of conservatism of the traditional, standards-based approaches and address hazards that are not covered in standards-based assessments allowing for a more focused deployment of finite resources to deal with dam safety issues on a priority basis [2].

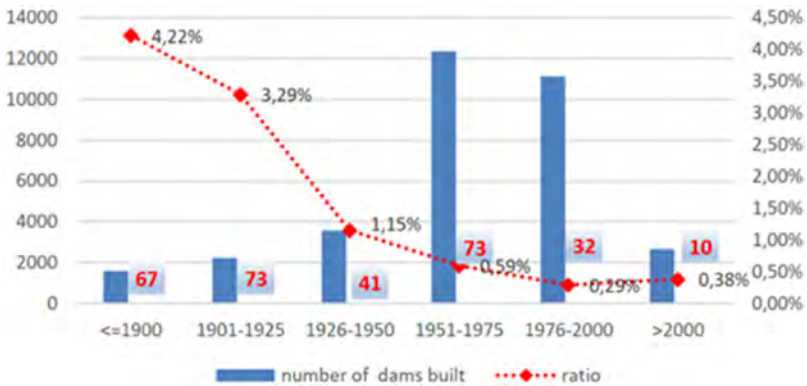


Fig. 1
Percentage failures of dams versus their year of construction
Défaillances des barrages en fonction de leur année de construction

There are a range of tools (Fig. 2) that can be implemented within a “risk-informed” framework, from screening level indexing approaches [3] to qualitative,

experienced-based estimates such as the FERC’s Level 2 risk assessment methodology (SQRA) [4] and the potential failure modes and effects assessment methodology (PFMEA) [5] to full probabilistic multi-parameter modelling of the likelihood of hazards progressing to failure and associated consequences [6]. Each method builds on the previous assessment.

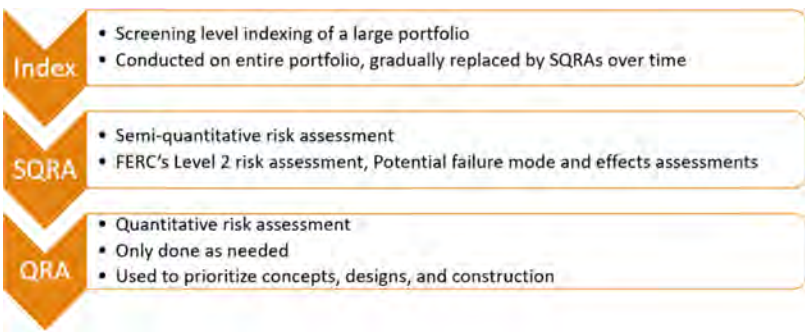


Fig. 2
Percentage failures of dams versus their year of construction
Défaillances des barrages en fonction de leur année de construction

The Quantitative Risk Assessment (QRA) methodology represents the highest level of risk analysis for dam safety. Unlike the SQRA or PFMEA methodologies, a QRA (1) makes use of engineering models and methods instead of qualitative estimates that are largely based on subjective judgements of experts to develop inputs to the risk analysis; and (2) employ structured interaction among experts to achieve a well-documented risk analysis that captures the range of technically defensible interpretations of data, models, and methods used in the risk analysis [7]. This paper presents the results of a QRA completed for a Potential Failure Mode (PFM) of concern at Waterton Dam located in southern Alberta, Canada.

2. THE EVOLUTION OF RISK INFORMED DECISION MAKING

An appreciation of the risks that a dam can impose is not new. In fact, it dates back to prehistoric times where the penalties for improper dam safety management could be severe.

"If somebody is too lazy to maintain his dam in adequate conditions and does not do it and the dam fails so the fields become flooded, then that who caused the failure shall be sold for money, and the collected money shall replace the wheat that was ruined because of him". King Hammurabi Code Section 53 – 1800 BC

The beginnings of structured risk analysis as a project management tool started in the late 1940s when the US Armed Forces introduced the Failure Modes and Effects Analysis (FMEA) methodology as a proactive tool to identify, evaluate, and prevent product or process failures (MIL-P-1629). In the 1960s, the Apollo Space Program adopted the FMEA process incorporating it into its Hazard Analysis and Critical Control Point program, crediting it as a significant contributing factor in the successful moon landing in 1969. Since that time, other industries that demand the highest levels of reliability, including the dam safety industry, have implemented risk assessment processes. As discussed by Zielinski [3], the complexity and costs associated with comprehensive risk assessments as well as the uncertainties associated with the estimation of both consequence and likelihood, led the dam industry to develop practicable turned to practicable methodologies such as the Failure Modes and Effects Analysis (FMEA) or the more simplified Potential Failure Modes Analysis. Both methodologies have advantages and disadvantages [8], [9]. Alberta Agricultural and Irrigation (AGI) developed a risk-informed decision-making approach as a means to combine the best elements of both approaches and developed a Potential Failure Modes and Effects Analysis (PFMEA). The methodology process is explained in a previous article [5].

3. THE WATERTON DAM

The Waterton Dam is located 25 km southeast of the town of Pincher Creek, Alberta, Canada. It is a zoned earthfill embankment with a clay core and granular shells. The dam crest is 850 m long, and the maximum height of the dam is 56 m. The discharge facilities at the dam include a gated service spillway, a low-level outlet, and an irrigation outlet structure. The dam was designed by the Prairie Farm Rehabilitation Administration or the Government of Canada and was constructed between 1956 and 1964. The primary intention of the dam was water diversion, but it also provides water supply for municipal and agricultural use. Waterton Dam is now being operated and maintained by AGI and has an "Extreme" consequence classification rating based on Canadian Dam Association Dam Safety Guidelines (2019).

Fig. 3 shows the location, the layout plan, and an aerial view of the Waterton Dam and the reservoir.

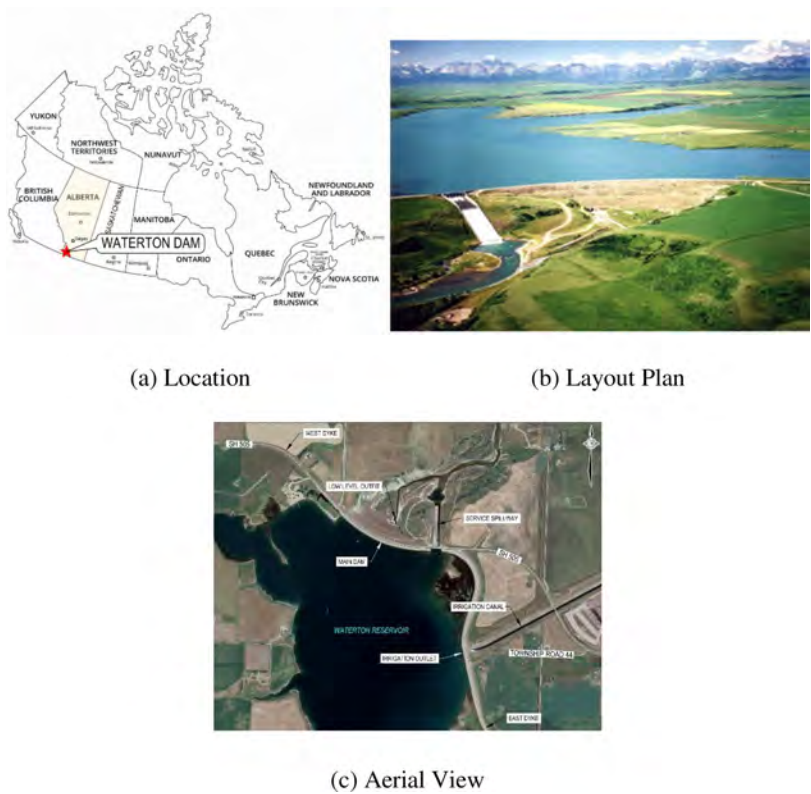


Fig.3
Location (a), layout (b), and aerial photograph (c) of Waterton Dam
Emplacement (a), tracé (b) et photographie aérienne (c) du barrage Waterton

4. DEFINING THE POTENTIAL FAILURE MODES

In 2024, Tetra Tech completed a PFMEA for Waterton Dam. The process commenced with the development of a hazard and failure mode matrix that provided a top-down assessment of relevant external hazards (e.g., meteorological, seismic, reservoir environment, vandalism) and internal hazards (design, construction, maintenance, operation) that could lead to overtopping or collapse of the dam and either an uncontrolled release of the reservoir or the loss of function of the project. This was followed by the development of a functional diagram for the structure and a site visit. The next step involved a three-day PFMEA workshop that was held with

the owner's (AGI) and consultant's (Tetra Tech) engineering teams, including multidisciplinary subject matter experts (SMEs) and operational staff.

The purpose of the workshop was to identify and analyze potential failure modes (PFMs). This included discussion of such factors as failure triggers, failure mechanisms, relevant facts/conditions, adverse factors, positive factors, and risk mitigation measures were discussed. The team collaborated to assign a likelihood category (among five options namely: remote, low, moderate, high, very high) and consequence category (among five options namely: low, significant, high, very high, extreme) to each PFM in accordance with the methodology outlined by Donnelly [5]. The results of the assessments led to the identification of 35 relevant PFMs for the Main Dam spillway, low-level outlet, irrigation outlet, and saddle dyke. The PFMs were then plotted on a 5x5 likelihood-consequence matrix (Fig. 4) as part of a semi-quantitative risk assessment (SQRA). PFMs that were located in the relatively higher priority zone of the SQRA matrix were considered for more detailed QRA.

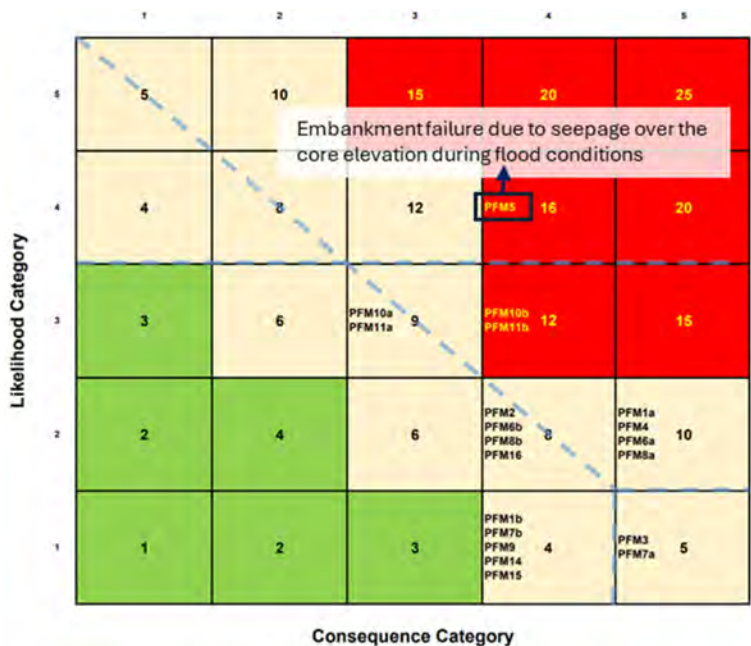


Fig. 4
Results of the PFMEA performed for the Waterton dam
Résultats de l'PFMEA réalisée pour le barrage de Waterton

Two PFM's were found to pose relatively higher risks for the Main Dam; (1) failure of spillway due to failure of the underdrain system and (2) embankment failure due to seepage over the top of the core (core overtopping) during flood conditions.

5. QUANTITATIVE RISK ASSESSMENT FOR WATERTON DAM

In Fig. 5, a typical cross-section of the Waterton Main Dam is shown. At the time of the original construction, the low permeability clay core of the Main Dam was extended to the level of the design flood established at that time. Changes to the design flood to meet current standards, and settlement during and following construction was postulated to have potentially lowered the top of core below the elevation required to satisfy current design standards. To confirm this potential deficiency, AGI undertook a drilling program that found that the top of the core was, in fact, generally lower than the original design level and that the granular fill placed above the core was highly permeable.

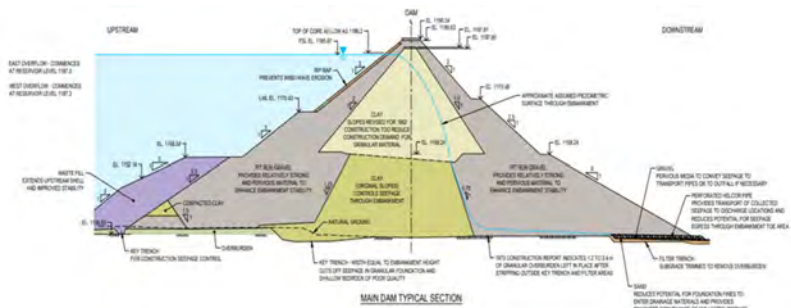


Fig.5
Schematic profile of the Waterton Main Dam
Profil schématique du barrage principal Waterton

During passage of the design flood (the probable maximum flood (PMF)) it was postulated the reservoir water level could exceed the top of the impervious core. In that case, the failure mechanism would involve through the highly pervious granular fill that had been placed above the core and into the downstream shell of the dam. The seepage flows would then emerge on the downstream slope potentially resulting in a progressive sloughing of the embankment fill which could lead to rapid embankment erosion resulting in dam failure and loss of containment of the reservoir. Given over 60 years of safe operation in which the reservoir has never

risen above the top of the core, the question was, is this risk of core overtopping tolerable? The QRA was used to help to answer this question.

5.1. METHODOLOGY

In its simplest form, risk is defined as the product of probability and consequence. For the Waterton dam QRA, consequences had been previously established based on detailed dam classification studies that established incremental losses including potential incremental loss of life (ILOL) as well as environmental, economic, and social/cultural losses. ILOL was selected as the consequence portion of the risk equation. Therefore, the major task for quantifying the risk is the numerical estimation of probability of the failure.

5.2. ESTIMATING PROBABILITY

The probability of failure was estimated using an event tree approach. This is a forward, logical modelling technique for failure that explores the impacts of a single initiating event and lays a path for assessing probabilities of the outcomes and overall system analysis [10]. For the embankment failure due to core overtopping, the chain of events that was utilized to develop the event tree is shown on Fig. 6. The PFM is broken down to eight (8) consecutive events (levels) and these events are discussed in the following sections.

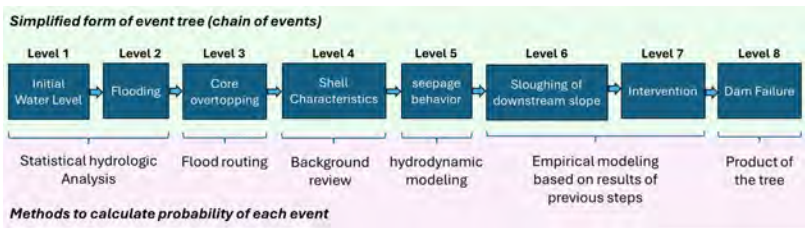


Fig. 6

Chain of events for core overtopping failure mode
Chaîne d'événements pour le mode de défaillance de dépassement du noyau

5.2.1. Initial water level (Level 1 of the event tree)

The initial water level refers to static water level in the reservoir prior to the flood. Depending on initial water level, floods of different magnitudes can raise the

water level to incipient core overtopping. Initial water levels for risk analysis were chosen based on historical daily water levels recorded in the Waterton Reservoir from 1965 to 2022. Fig. 7 shows the level-duration curve for water levels in the reservoir. The reservoir levels were divided into three (3) bins to approximate representative initial water levels. For Bins 1 and 2, the median levels of approximately 1175 m and 1180 m were selected to represent those bins. For Bin 3, 1185 m was chosen as the representative value, which is at the higher end of the data set to consider a near full supply level (FSL) initial condition. Therefore, for development of the event tree, initial water levels were chosen to be 1175 m, 1180 m, and 1185 m, with corresponding probabilities of 0.3, 0.4, and 0.3, respectively.

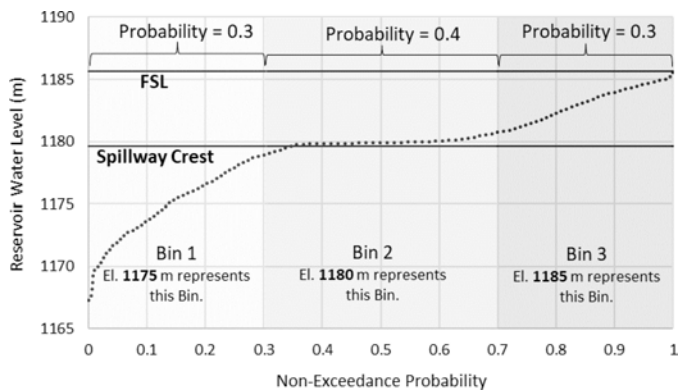


Fig.7
Level-duration curve for daily water levels at Waterton Reservoir (1965-2022)
*Courbe niveau-durée des niveaux d'eau quotidiens au réservoir Waterton
(1965-2022)*

5.2.2. Flooding and core breaching (Level 2 and 3 of the event tree)

Level-pool flood routing was performed for each of the selected representative initial water levels for floods of different return periods (different severity). The graph of Fig. 8 shows flood return period versus the maximum reservoir level that occurs during the passage of the flood. Adding the top of the core elevation on the same plot shows that for initial water levels 1175 m, 1180 m, and 1185 m, floods with return periods equal to or larger than 650-year, 550-year, and 400-year, respectively, cause core breaching. The probability of occurrence of these floods is equal to inverse of their return period. If the reservoir is initially at 1175 m, a flood with a 650-year return period or larger is required to cause core breaching, and the probability of occurrence of such a flood is equal to $1/650 = 0.15$.

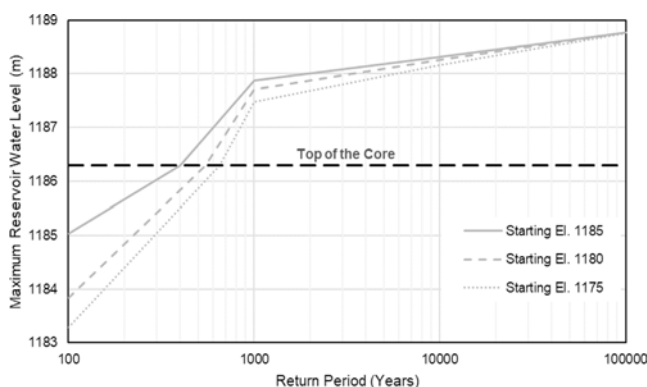


Fig. 8

Flood routing results and incipient core overtopping

Résultats du routage par inondation et début du débordement du noyau

5.3. BEHAVIOUR (LEVEL 4 AND 5 OF THE EVENT TREE)

Another product of level-pool routing is the stage hydrograph of reservoir water levels during the flood. The stage hydrograph shows that, regardless of the flood magnitude, the duration of flow passing over core is about 50 hours. This relatively short duration does not allow development of a new equilibrium state (steady state) seepage flow in the embankment. The seepage flow is time-dependent and the extent of the saturated zone, and the shape of the phreatic surface changes with time during core overflow. For seepage passing over the core to potentially cause sloughing, seepage egress on the downstream slope is necessary because the limit equilibrium assessment of slope stability that was carried out indicated that the downstream slope remained at least marginally stable under the conditions anticipated. For this reason, unsteady hydrodynamic simulation of the seepage flow in the embankment was performed to determine under what conditions seepage egress from the downstream slope occurred or if the seepage drained through the shell into the drainage layer at the foundation level without emerging on the slope. The results of this hydrodynamic simulation also helped in the understanding of the nature of the process in order to establish the associated probability of occurrence.

The characteristics of the shell materials are governed by their gradation and method of placement and compaction. The granular fill for the shell of the dam was spread and compacted by bulldozers in horizontal lifts approximately 0.5 m thick [11]. Given the nature fill placement, the hydraulic conductivity of the shell is expected to be variable. It is impacted by its placement in horizontal lifts, variable competition and by the inherent variability of the fill gradation in the lifts as borrow

source was exploited. The granular fill placed above the top of the core was sourced from the same borrow pit. As such it would be expected to be similar to the fill placed in the shell of the dam. However, the hydraulic conductivity of the granular fill placed above the core was found to be about 1×10^{-1} m/s in 2007 [12] while the average gradational characteristics of the fill making up the body of the dam would indicate a hydraulic conductivity of about 1×10^{-3} m/s. The hydraulic conductivity of the compacted fill is expected to be generally isotropic but variability in the fill that would have developed because of segregation that typically occurs when granular materials are bulldozed into place would tend to cause a lateral flow direction component toward the dam's downstream slope.

To assess these assumptions the SEEP/W module of Geo-studio was used for simulation of the porous media flow. SEEP/W is a powerful finite element numerical solver that can conduct saturated/unsaturated transient analyses with atmospheric coupling at the ground surface, which makes it suitable for modelling infiltration into dry soil. The transient formulation and sophisticated boundary condition options allow SEEP/W to analyze flood events, rapid drawdown, and the effect of severe climate events on the performance of dams and levees. A numerical model was built in SEEP/W, using geometry as shown on Fig. 9 and the reservoir stage-hydrograph as a boundary condition. Different assumptions regarding hydraulic conductivity and isotropy of the shell material were made to support a rudimentary understanding of core overflow seepage flow behaviour. Fig. 9 shows the phreatic surface on a dam profile prior to flood occurrence and at the flood peak with isotropic hydraulic conductivity in the granular fill. The whole rise and fall of the reservoir level takes approximately 50 hours and at the end the reservoir level recedes to FSL.

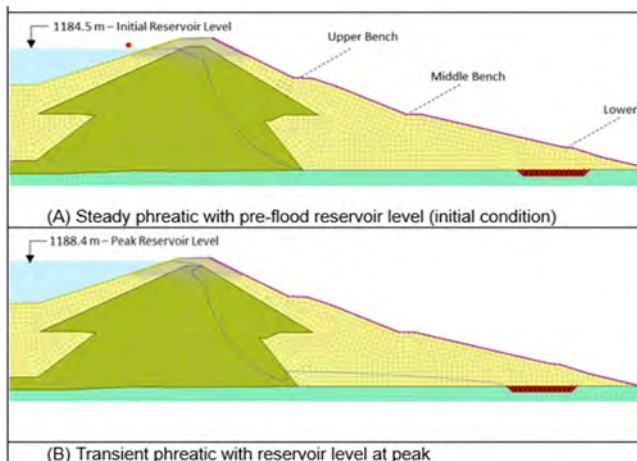


Fig. 9

Rise and fall of the reservoir level in a homogenous shell and the impact on phreatic surface $K_{shell} = 1 \times 10^{-1}$ m/s, $(K_v/K_h)_{shell} = 1$

Montée et descente du niveau du réservoir dans une recharge homogène et impact sur la surface phréatique $K_{shell} = 1 \times 10^{-1}$ m/s, $(K_v/K_h)_{shell} = 1$

The numerical analysis described above was repeated for various shell hydraulic conductivity scenarios, including $k=1 \times 10^{-1}$ m/s and $k=1 \times 10^{-2}$ m/s, and a comparison between an isotropic shell ($k_v/k_h = 1.0$) and an anisotropic shell ($k_v/k_h = 0.1$). The results showed that in a homogenous shell, regardless of the conductivity, the seepage would run along the top of core until it reaches the transition point to the lower part of the core (the Christmas tree shape of the core). Then the seepage percolates as unsaturated flow below the transition point. Note that is the shell materials are perfectly homogenous, the seepage does not egress on the downstream face. In fact, seepage passed over the top of the core would likely saturate only a very small area on top of the core, not the downstream part of the shell. Fig. 10 shows velocity vectors to visualize the core overflow process.

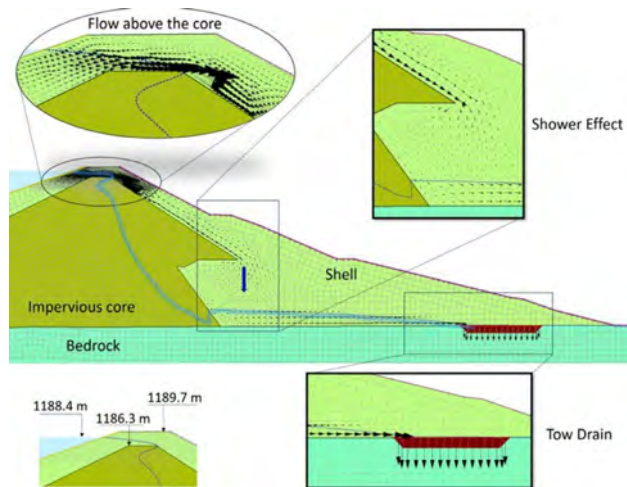


Fig. 10

Velocity vectors of core overtopped flow in a homogenous shell and toe drain
Vecteurs de vitesse de l'écoulement du noyau dans une recharge homogène et un drain de pied

The key characteristic of the downstream shell in the event of core overflow will be the variability of its hydraulic conductivity. If the shell fill were perfectly homogenous, the seepage would be readily drained as shown on Fig. 10. While information regarding the variability of the fill materials making up the downstream shell was not available, it is logical to assume that the shell fill could have layers consisting of relatively finer and courser materials given the nature of the placement and compaction activities. Based on elicitation of the core team's best judgement and review of the literature [11], it was judged that a 1 m thick layer (two lifts as per construction records)

with a hydraulic conductivity of 1×10^{-3} m/s could exist above the upper bench in the downstream shell fill with a probability of 0.9. The remainder of the shell was considered to have a hydraulic conductivity similar to that which was measured in the fill over the top of the core. Although the actual hydraulic conductivity would vary; it was assumed the variation would not be continuous over the body of the dam. On this basis, seepage analysis with a horizontal layer in the shell having a hydraulic conductivity two orders of magnitude than the rest of the fill materials would create a perched saturated area that could potentially reach the downstream face of the dam. The results of analyses performed assuming a nominal 1 m thick layer of reduced hydraulic conductivity with the same k_s/k_h ratio as the remainder of the dam fill showed that the seepage would only emerge from the downstream slope when the relatively less permeable layer was located at or above the upper bench (within the 2H:1V slope segment). The results on Fig. 11 show that if the less pervious layer be placed in the lower (and wider) parts of the shell, a perched saturated zone large enough to reach the downstream slope would not develop.

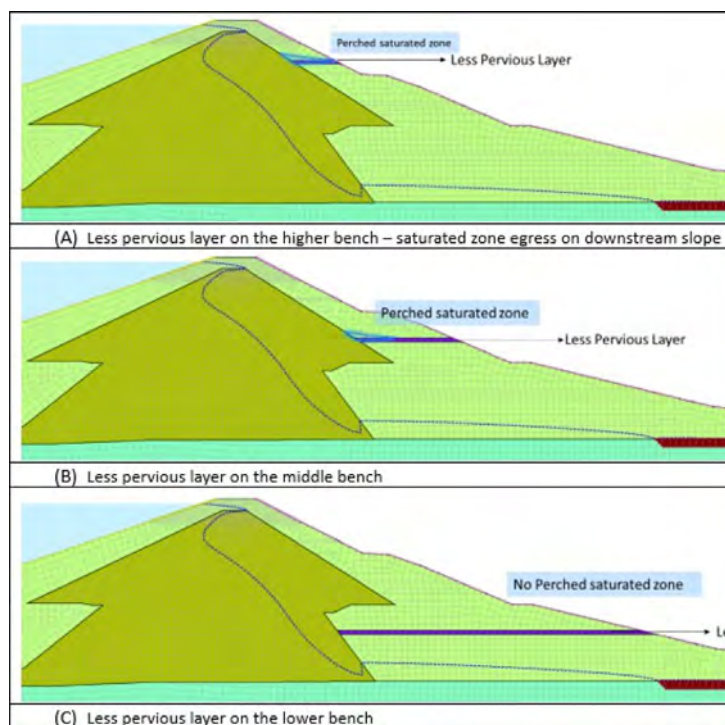


Fig. 11

Hydraulic behaviour of core overtopping in a stratified shell
Comportement hydraulique du débordement du noyau dans une recharge stratifiée

Using these assumptions a transient seepage model was developed to analyze the potential for seepage egress at downstream slope. The results of the analysis that assumed a hydraulic conductivity of two orders of magnitude smaller for the less pervious 1 m thick layer compared to the shell are shown on Fig. 12.

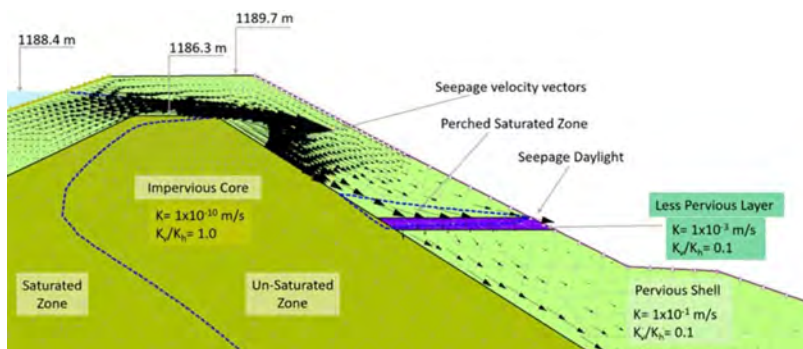


Fig. 12

Hypothetical shell stratification, perched water table, and seepage egress
Stratification hypothétique de la recharge, nappe phréatique perchée et sortie d'infiltration

In previous steps, the probability of occurrence a flood that could cause core overflow was estimated. However, even with the presence of the less pervious layer in the upper part of the downstream shell, a shallow depth of core overflow will not result in seepage emergence on the downstream slope. The flood loading was implemented to the transient seepage analysis with stage-hydrographs that have various peak reservoir levels. During this iterative process, the minimum peak flood level needed to cause seepage egress at the downstream slope was determined. Fig. 13 shows both reservoir elevations and return periods for inception of core overflow and inception of seepage egress at downstream slope plotted with the results of level-pool routing. When the initial water level is at FSL (~ 1185 m), although floods larger than 1 in 400 years can cause core overflow, only floods larger than 1 in 3,000 years could cause seepage daylighting at the slope. As such probability of this event was calculated to be 0.13.

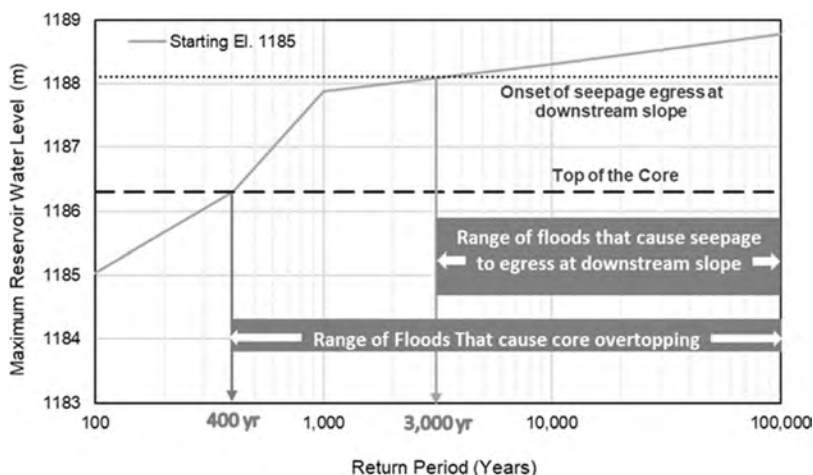


Fig.13

Incipient core overflow and onset of seepage egress at downstream slope for an initial reservoir level equal to 1185 m

Débordement amorçant du tronc central et début de la sortie d'infiltration au niveau aval pour un niveau initial du réservoir égal à 1185 m

5.4. SLOUGHING OF DOWNSTREAM SLOPE AND INTERVENTION (LEVEL 6 AND 7 OF THE EVENT TREE)

The breach mechanism that could potentially develop due to seepage flow over the core of the Waterton Main Dam under flood conditions is sloughing, (sometimes referred to as unravelling in the case of a rockfill dam). Sloughing is distinct from a slope instability failure as it involves a progressive loss or displacement of soil from an embankment dam. This breach mechanism is conditional on the development of seepage flow from the downstream slope of the dam. In the case of the Waterton Main Dam, the analyses indicated that the vulnerable segment of the downstream slope is the steep (2H:1V) upper portion of the slope – above the upper bench.

The probability of breach development at the Waterton Main Dam in the event that seepage egress on the upper segment of the dam's slope occurs was estimated using the United States Army Corps of Engineers (USACE) Internal Erosion Toolbox [13]. Key inputs to the estimate of the probability of dam breach development by sloughing were as follows:

- Material in the downstream shell: Sandy gravel with <20% fines.
- Freeboard at the time of the incident: 1.3 m to 1.6 m.
- Downstream embankment slope: 2H:1V.

Following this approach the estimated probability of breach development by sloughing was estimated to be 0.72. However, If the breach mechanism developed, it could be arrested and failure prevented by successful intervention. The probability of an unsuccessful intervention was estimated using the relevant procedure set out in USACE Internal Erosion Toolbox [13]. Section 12.2 of that reference states in part, "Sloughing is a slowly developing breach mode which should take days or weeks to lead to breach." Other key inputs to the estimate of the probability of unsuccessful intervention to prevent failure due to development of a breach by sloughing were as follows:

- The seepage emanating from the downstream slope is presumed to be observable.
- It is assumed that there would daily observations if the incident developed given the proximity of the dam to the public.

The resulting estimated probability of an unsuccessful intervention that would allow the breach to develop to dam failure was estimated as 0.145.

5.5. DAM FAILURE (LEVEL 8 OF THE EVENT TREE)

The event tree shown on Fig. 14 compiles all the probabilities estimated in levels 1 to 7 to come up with an overall probability for the dam failure. Each node in an event tree is associated with an uncertain event (e.g., reservoir water level, flood magnitude, presence of a less pervious layer in the shell, etc.). Branches originating from a node represent each of the possible events or states of nature that can occur; thus, the sum of them must be equal to one, implying that all potential possibilities have been considered. Once the event tree is completed, probabilities are estimated for each branch to represent the likelihood for each sequence of events that causes dam failure. These probabilities are conditional on the occurrence of the preceding events in the tree. This represents inductive reasoning for the event, in which a bottom-up approach is followed. The conditional structure of the event tree allows the probability for any sequence of events to be computed by multiplying the probabilities for each branch along a pathway, in accordance with the multiplication rule of probability theory. The branching structure of the event tree allows the probability for any combination of event sequences (e.g., total failure probability for a PFM) to be computed by summing branch probabilities across multiple pathways. The computed probability is annualized in the event tree by using annual probabilities to characterize time dependent events such as flood occurrence, whereas other events such as presence of a less pervious layer in the shell is time neutral.

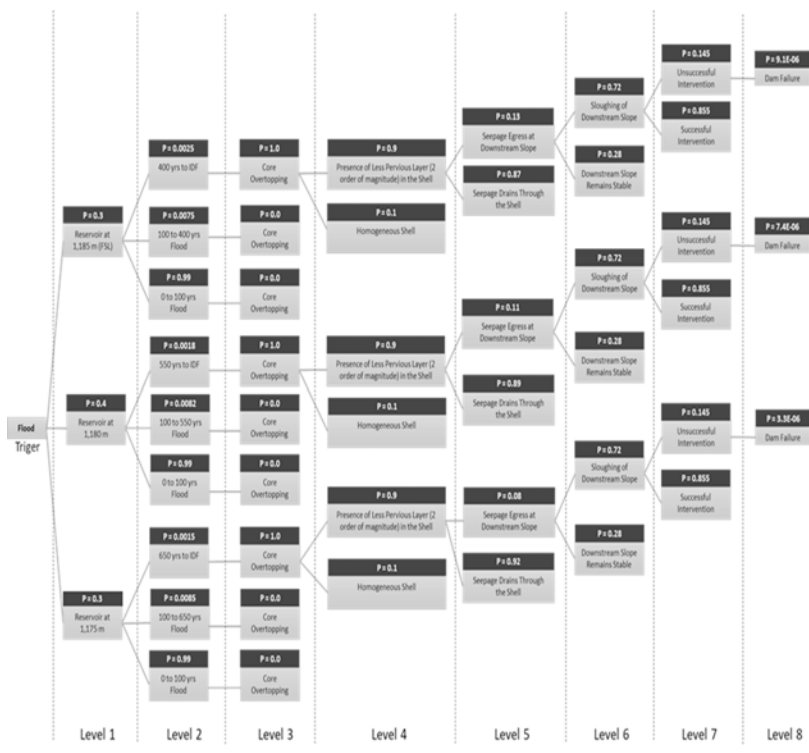


Fig. 14
Event tree for core overtopping failure mechanism for the Waterton Dam
Arbre d'événements pour le mécanisme de défaillance du débordement du noyau du barrage Waterton

Table 1 presents results shown on the event tree in a tabular manner and the shows the sum of the probabilities from the different branches of the event tree. The annual probability of dam failure due to the core overtopping PFM is estimated at 1.98E-05.

Table 1
Tabular Presentation of the Event Tree and Annual Probability of Failure

Branch #	Level 1	Level 2	Level 3	Level 4	Level 5	Level 6	Level 7	Level 8
	Probability: Initial Water Level in Reservoir Being on a Specific Value	Probability: Occurrence of a Flood Causes Core Overtopping	Probability: Core overtopping	Probability: Presence of Less Pervious Layer at Upper Bench	Probability: Seepage to Daylight at Downstream Slope	Probability: Sloughing of Downstream Slope	Probability: Unsuccessful Intervention	Probability: Dam Breach
1	0.3	0.0025	1.0	0.9	0.13	0.72	0.145	9.1E-06
2	0.4	0.0018	1.0	0.9	0.11	0.72	0.145	7.4E-06
3	0.3	0.0015	1.0	0.9	0.08	0.72	0.145	3.3E-06
Annual Probability of Failure								1.98E-05

Note: Level 8 = Level 1 x Level 2 x Level 3 x Level 4 x Level 5 x Level 6 x Level 7

6. ESTIMATE OF RISK

The consequence of failure of the Waterton Dam were estimated by Northwest Hydraulic Consultants [14]. The results of this study showed that the estimated Incremental ILL determined on the basis if the Brown-Graham Method [15] is 145 for sunny-day failure and 74 in the event of PMF. In this study it was determined that the minimum flood that could result in overtopping of the core was 1:3000-yr AEP event. Therefore, this failure mechanism cannot develop under non-flood (sunny day) conditions. Accordingly, an incremental ILOL of 74 was selected as the incremental consequence that could result from failure of the Waterton Main Dam failure. Combining this with the estimated probability of failure an f-n chart was developed which indicates that the estimated risk associated with this failure mechanism is higher than the CDA's [16] guidelines for broadly acceptable risk.

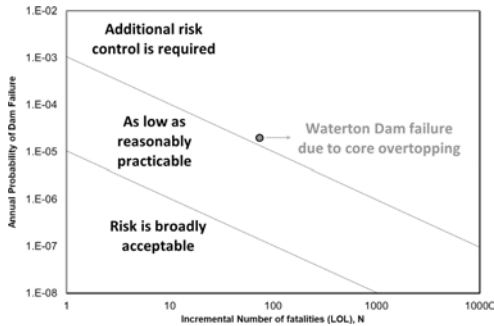


Fig. 15

Risk of Waterton Main Dam failure due to core overtopping and risk tolerability levels
Risque de défaillance du barrage principal Waterton en raison du débordement du noyau et niveaux de tolérance au risque

7. CONCLUSIONS

This paper described the QRA process used in the assessment of the Waterton Dam for a particular key PFM identified during the PFMEA process. The details of process indicated that QRA results can rely heavily on engineering judgement as exact values for all of the variables needed may not be readily available and may require extensive, costly and time-consuming investigations to obtain better estimates. Another source of uncertainty in the QRA is binning of continuum variables. For example, the initial water level in the reservoir can have infinite values whereas only three representative values were considered to represent all the probabilistic space herein. The lessons learned from this case example demonstrated that numerical modelling of the physical process governing the failure mechanism and sensitivity analysis is vital to obtain a correct understanding of the PFM and quantifying probability ranges. For example, seepage modelling showed that for seepage to emerge at downstream slope, the presence of a less pervious layer is required and that overtopping of the core can only occur under certain flood events. Time-dependency of hydrologic factors related to the PFM is an important consideration. High water levels associated with flood events do not last long enough to establish a steady state seepage condition. This time-dependency must be factored into modelling and analysis. Notwithstanding the uncertainties, QRA showed that, although Waterton Dam has rendered satisfactory performance during the last six decades, the risk associated with the top of core level below the crest of the dam does have elevates risk levels which should be addressed.

The value of this QRA is that the location of the potential problem has been established allowing for focused instrumentation design and surveillance to be performed as well as the development of relatively simple contingency intervention measures should the issue be observed. However, a QRA requires a considerable amount of effort and should only be undertaken when a PFM requires additional insight and a thorough evaluation of the factors affecting the PFM is found to be value added either for decision making purposes (capital investment) or there is a lack of consensus on the level of risk for that PFM or potential remedial solutions are either not feasible or prohibitively expensive.

REFERENCES

- [1] ICOLD, "Bulletin 188: Incident database Bulletin 99 update - Statistical analysis of dam failures,," 2019.

- [2] C. R. DONNELLY, "Safe and secure – risk-based techniques for dam safety," *International Waterpower and Dam Construction*, 2006.
- [3] P. A. ZIELINSKI , P. NARAYAN, C. R. DONNELLY, E. HALPIN, J. QUEBBEMAN, H. M. QADDUMI, C. R. SINGH , S. UEDA AND M. WISHART, "The development of a risk screening indexing tool for prioritizing dam safety remedial works," in *ICOLD*, @021.
- [4] FERC, Engineering Guidelines for the Evaluation of Hydropower Projects: Chapter 18 – Level 2 Risk Analysis, Washington DC, 2021.
- [5] C. R. DONNELLY, M. ACHARYA, J. RUTHERFORD, J. GROENEVELD AND C. WOODS, "Alberta Environment and Parks PFMEA Tool for Risk-Informed Dam Safety Prioritization," *CDA Bulletin*, Spring 2022.
- [6] V. FRÉCHETTE AND S. LACASSE , *Risk- Informed Approach For The Safety Assessment Of Dams A Toolkit For The Dam Owner*, 2022.
- [7] M. MCCANN AND G. A. RIX, "framework for quantitative risk analysis of dams,," in *ASCE Proceedings; Geo-Risk 2023*. <https://doi.org/10.1061/9780784484982.032>, 2023.
- [8] S. RIGBEY, H. HAMPTON, D. HARTFORD, S. BOHRN., D. DANIELSON, R. DONNELLY, L. PHILIP, M. RICHARDSON AND A. SMALL, "A. Functions, Failure Modes and Failure Mechanisms," *Canadian Dam Association Bulletin*, 2021.
- [9] C. R. DONNELLY AND M. A. ACHARYA, "Discussion on the Evolution and Application of Quantitative Risk Informed Dam Safety Decision Making," in *MYCOLD International Symposium on Dam Safety and Engineering*, 2019.
- [10] P. I. CLEMENS AND R. J. SIMMONS., System Safety and Risk Management. NIOSH Instructional Module, A Guide for Engineering Educators, Cincinnati, OH: *National Institute for Occupational Safety and Health: IX-3–IX-7.* , March 1998.
- [11] S. CHRUMKA AND K. LAMB, "St. Mary Project Soil Mechanics and Materials Report,," Canada Department of Regional and Economic Expansion – Prairie Farm Rehabilitation Administration, Saskatoon, 1973.
- [12] M. LUNGAL AND W. MACMILLAN, "Waterton Dam – Characterization of Materials above the dam core," UMA|AECOM, 2007.
- [13] J. SCHAEFER, N. VROMAN AND T. O'LEARY, "Internal Erosion Toolbox – A method for estimating probabilities of failure of embankment dams due to internal erosion. Best practice guidance document,," US Army Corps of Engineers, 2009.

- [14] C. ZHAO, "Waterton Dam Breach Inundation Study – Final Report," Northwest hydraulic consultants (NHC), 2012.
- [15] C. BROWN AND W. GRAHAM, "Assessing the threat to life from dam failure.," *Journal of the American Water Resources Association.* , p. Paper No. 88044 of the water resources bulletin., 1988.
- [16] CANADIAN DAM ASSOCIATION, DAM SAFETY GUIDELINES, 2007 (2013 REV).

COMMISSION INTERNATIONALE DES
GRANDS BARRAGES

VINGT-HUITIEME CONGRES DES
GRANDS BARRAGES
CHENGDU, MAI 2025

ADVANCED ANALYTICS TO DETECT ANOMALIES THROUGH MONITORING (*)

Noémie ROUSSEL
PhD student, INRAE & Artelia

Jean-Robert COURIVAUD
EDF Hydro Engineering Centre

Guillaume VEYLON & Claudio CARVAJAL
INRAE

Capucine MASSON & Frédéric ANDRIAN
ARTELIA

Edouard BUCHOUD
EDF DTG

Bruno DAUMAS
EDF Hydro Engineering Centre

Simon RAUDE & Michail KORRES
EDF Lab Saclay

FRANCE

SUMMARY

Analysis of monitoring data is an important part of dam safety assessment. As part of the management of aging dams, it is essential to have efficient tools to help

**Méthodes avancées pour la détection des anomalies par l'auscultation*

detecting behavioural anomalies and pathologies. This report presents two advanced analysis methods for detecting anomalies through monitoring data, both methods aiming to improve their interpretation.

As part of the management of aging dams, the promising methods of Machine Learning are performed on the displacement data of a French concrete gravity dam to analyze monitoring data and detect abnormal behaviors. Regression with the HBRT algorithm allowed to predict displacements and to determine the isolated influence of each external input variable on the data. Thanks to these results, a change in the displacement behavior was observed. Novelty Detection with the Local Outlier Factor algorithm allowed the detection of anomalous values that evolved over time, and were consistent with the Regression results. These combined methods constitute a useful tool for the analysis of dam monitoring data and thus help in their management.

Numerical modeling associated with distributed optical fiber deformation measurements located under the invert of a hydroelectric canal based on deformable materials made it possible to extend the interpretation of these measurements, by translating them into settlements. This type of approach highlights the interest in instrumenting the foundations of structures subject to deformation or cavities with optical fiber deformation measurements.

RÉSUMÉ

L'analyse des données de surveillance constitue un élément crucial de l'évaluation de la sécurité des barrages. Dans le cadre de la gestion des barrages vieillissants, il est essentiel de disposer d'outils efficaces d'aide à la détection des anomalies comportementales et des pathologies. Ce rapport présente deux méthodes d'analyse avancées pour détecter les anomalies grâce aux données de surveillance, les deux méthodes visant à améliorer leur interprétation.

Dans le cadre de la gestion des barrages vieillissants, les méthodes d'Apprentissage Automatique sont appliquées aux données de déplacement d'un barrage-poids béton afin d'analyser les données de surveillance et de détecter d'éventuels comportements anormaux. La Régression avec l'algorithme HBRT a permis de prédire ces déplacements et déterminer l'influence de chaque variable d'entrée sur les données. Grâce à ces résultats, un changement dans le comportement dans déplacements a été observé. La Détection de Nouveauté avec l'algorithme Local Outlier Factor a permis de détecter des valeurs anormales évoluant dans le temps, cohérentes avec les résultats de Régression. La combinaison de ces deux méthodes constitue un outil utile pour l'analyse des données de surveillance des barrages et contribuent ainsi à leur gestion.

La modélisation numérique associée aux mesures réparties de déformation par fibre optique localisées sous le radier d'un canal hydroélectrique fondé sur des matériaux déformables a permis d'étendre l'interprétation de ces mesures, en les traduisant en tassements. Ce type d'approche met en évidence l'intérêt d'instrumenter en mesures de déformation par fibre optique les fondations d'ouvrages sujettes aux déformations ou aux cavités.

1. INTRODUCTION

Analysis of monitoring data is an important part of dam safety assessment. As part of the management of aging dams, it is essential to have efficient tools to help detecting behavioural anomalies and pathologies. This report presents two advanced analysis methods for detecting anomalies through monitoring data, both methods aiming to improve their interpretation.

In its first part, this report presents the contribution of methods based on machine learning. Classical monitoring data analysis methods are based on monitoring data recorded throughout the dam life. Typically, reservoir elevations, pore pressures below the dam, displacements on the dam body and leakage flows are measured. The most widely used method for analysing these data is the HST method (and its derivatives HST-T, HST-P). This statistical method is used to extract the reversible influence of hydrostatic loads, seasons, temperatures or precipitation from the raw data. In this way, any irreversible behavior or drift can be identified. However, this method has several limitations. Input variables are considered independent, which means that coupling and interdependence effects are ignored. Threshold effects and strong nonlinearities are not handled by this method. Finally, the input components of the behavior assumed in advance. As a result, this method is quickly limited by the complexity of the phenomena involved.

Machine-learning methods can overcome these limitations for the monitoring data analysis. This branch of artificial intelligence is based on a computer's ability to learn from data and improve its performance through iterations. This technique has several advantages in the field of data monitoring. It can detect patterns and deal with complex behavior in a high-dimensional space as the one of the monitoring variables and make predictions based on these patterns. According to Salazar, Neural Networks and Boosted Regression Trees were found to be the best choice of algorithms for dam monitoring (Salazar *et al.*, 2015, 2017) and have been tried by several authors (Salazar *et al.* 2016; Tayfur, 2005; Mata, 2011) with promising performance. If Regression tasks are the most commonly used technique (prediction of discrete values), Salazar also proposed a model based on Classification, to detect a normal among several abnormal classes (Salazar, 2021). This is a supervised learning technique which means that all the predictors must be labelled to their target. The data is therefore generated from a numerical Finite Element Model (FEM). In real data sets,

behaviors cannot always be identified as normal or abnormal, and data labeling can be complex. Therefore, the use of unsupervised learning methods (Novelty Detection in this research) can be more effective. The goal of our work is to apply these innovative approaches to the case study of a large gravity dam.

In its second part, this report presents the contribution of numerical modelling in the interpretation of distributed strain fibre optic measurements. The opportunity of renovating the waterproofing and drainage of an EDF hydroelectric canal in 2011 was seized to install a strain monitoring system under the canal invert, in contact with the foundation. This strain monitoring has been working perfectly since the beginning of 2012 and has highlighted, at some locations along the fibre optic cable, sinkholes signatures evolving with slow kinetics. But the final parameter sought being settlement and not strain, it was necessary to use numerical modelling to estimate these settlements. The approach chosen to numerically model this problem, the main input parameters and the results of the sensitivity calculations on these input parameters including the modelled settlements are presented in this report.

2. MACHINE LEARNING APPROACHES

2.1. PRESENTATION OF THE CASE STUDY

The dam considered is a concrete gravity dam of 31 m high above the foundation, with a reservoir level of 24 Mm³. Its crest is 150 m long. The slopes of the upstream and downstream faces are 1V/0.125H and 1V/0.85H respectively. It was built almost a century ago, but the monitoring system was installed only 43 years ago. In addition to equipment for measuring piezometry and leakage rates, the dam is equipped with two inverted pendulums that measure radial and tangential displacements of the dam near its highest cross section. The PL1 pendulum measures the displacement between the top of the dam and the top of the foundation, and the PL2 pendulum measures displacements between the top of the dam and a point approximately 15 m below the dam-foundation interface (Fig. 1).

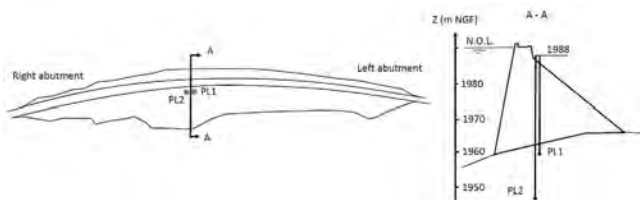


Fig. 1
Plan view and cross-section of the dam

In total, the database contains approximately 2,300 measurements for each instrument.

The behavior of this dam is complex. Unlike most dams, the upstream face of the dam is dewatered for several months of the year, which affects the under-pressure, displacements and seepage rates. Standard statistical methods such as HST are too limited to analyze its behavior. Machine learning methods are used to detect and understand the abnormal behavior of the dam using regression methods, and to uncover potential underlying issues or pathologies within the monitoring data using an unsupervised machine learning technique called Novelty Detection. This article focuses on the measurement of radial displacements of pendulum 1 ("Pendule1_rad"). Looking at its record (on the Fig. 2 below), a lot of variations are observed and could possibly be witnessing an anomaly.

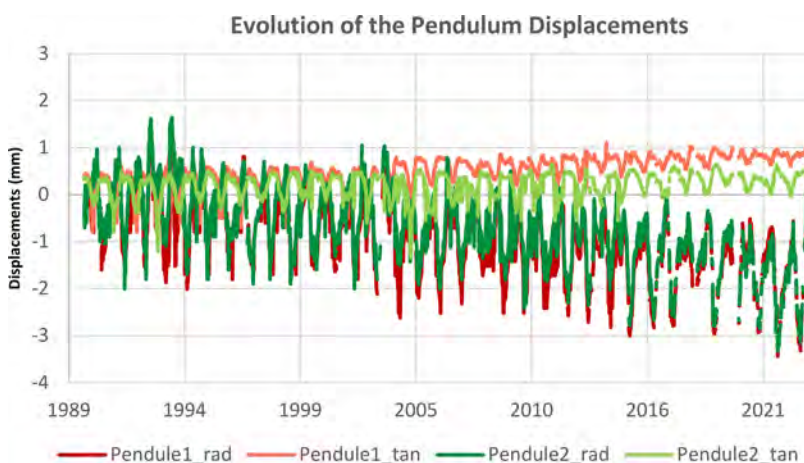


Fig. 2
Pendulum's raw data since the beginning of monitoring

2.2. METHODS

Preliminary analysis showed that classical statistical methods such as HST were too limited to make accurate predictions. Machine learning methods are used to overcome these limitations. To detect the abnormal behavior, two approaches will be tested: i) a supervised anomaly detection algorithm using the Histogram Gradient Boosting Trees (HBRT) regression model and ii) an unsupervised anomaly detection algorithm using Novelty Detection with Local Outlier Factor (LOF). The Scikit-learn library developed by INRIA in the Python language is used (Pedregosa *et al.*, 2011).

2.2.1. Supervised anomaly detection (Regression)

In supervised machine-learning, the training is based on labelled data. Each input data point is associated with a corresponding output. In this study, supervised machine learning is used for a regression task. Several external variables were used to predict the instrument values. The aim is to determine which ones are the most explanatory. They are the presented on Table 1 as follow:

Table 1
Predictors and target used in the regression task

Type	Predictors
Time	Number of days since the first available monitoring data Sinusoid angle of the day in the year
Hydrostatic	Reservoir level
Weather	Daily minimum and maximum and median temperature Daily measure of the temperature at 8am
	Mean minimum and maximum temperatures of the last 7, 30, 60, 70 and 183 days
	Daily rainfall
	Cumulated rainfall over the last 2, 3, 10, 30, 50, 70, 90 days

Various regression algorithms were tested, such as artificial neural network and ensemble models based on Decision Trees, including voting, bagging, stacking and boosting algorithms. It was observed that most methods offered similar a performance, but the Histogram Boosted Regression Tree (HBRT) was found to be the best algorithm to use, which is coherent with Salazar, 2015. It is ten times faster, and also deals with missing values within the predictor's data. The HBRT is a variant of boosting that speeds up the training by grouping each variable's data into groups, like in a histogram. Boosting (and specifically Gradient Boosting) trains a simple model (in this case a DT) sequentially, with each new model being trained to correct the errors made by the previous ones in order to reduce bias, using the Gradient Descent function. Therefore, the following results were computed using this algorithm.

First, the data is randomly divided into a training set and a test set (typically 25% of the data is allocated for testing). This process is repeated 10 times, using different subsets of the data each time. For each iteration, predictions are made for each subset using the remaining data for training. This allows us to make a prediction on the entire dataset, where the prediction is made on data that was not seen during training.

Two metrics are used to characterize the performance of the model. The Mean Absolute Error (MAE), which can be interpreted as the average absolute error between predicted and actual values. It has the same unit as the initial data and thus indicates the accuracy of the model. The R-squared or coefficient of determination

(R^2) measures the proportion of variance between the predicted target and the actual target values. $R^2=1$ indicates that the target is perfectly predicted by the model. R^2 close to zero or negative indicates that the model does not explain the variability of the target.

The HBRT model is tuned in order to find its best performance. This was first done using a Random Search where all the hyperparameters are randomly selected from a given range. This method is very efficient when tuning a large number of parameters. The hyperparameters that has a significant impact on the model performances are selected to perform a Grid Search Cross-validation. Discrete values are given to the model, trying each combination of hyperparameters. The set of hyperparameters that gives the best model using the R-squared metrics are kept for the final results. This has to be done for each target respectively.

When the model is finally tuned and its performance is known for a given period of time, a prediction is computed based on subsequent data in time. The model will predict what the values of the instrument should be, given the past behavior of the dam. A change in behavior can be detected if the predicted values are very different from the actual values. This methodology is illustrated on the Fig. 3 below.

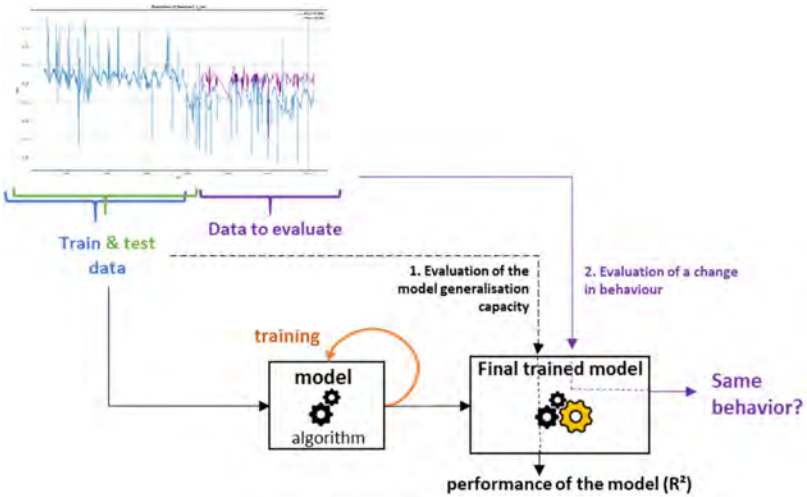


Fig. 3
Method of training and evaluation applied to the monitoring data

To get a more physical interpretation of the prediction results, Partial Dependence Plots (PDP) are constructed. The input variables are fixed at a mean value (or any other combination of inputs) except for one that varies. The variation of

the model predictions is then observed. The variation of the target is plotted against the variation of that input to visualize the effect of **each** predictor on the target variable. Thus, input variables can be selected for the training of a new model. Irrelevant predictors in the model can indeed reduce its performance.

2.2.2. *Unsupervised anomaly detection*

In unsupervised machine learning, the model is trained on unlabeled data. There are no metrics to evaluate the model. Its reliability is tested by cross-validating the results with other methods, such as regression, as seen above.

The Novelty detection method is used in this study, using the Local Outlier Factor (LOF) algorithm. It is given a first set of data corresponding to a first monitoring period. Then, new values are given to the model, and their local density is compared to the ones of their k nearest neighbors. Depending on how much lower this density is, the point is considered an outlier with a score corresponding to its distance to the neighbors. If several abnormal values follow one another in time, it could be considered as a change in behavior.

The location of the datapoints with respect to their neighbors can be visualized in two dimensions by reducing the number of variables using a linear Principal Component Analysis (PCA). It reduces the dimensionality of the data by transforming the original features into a new set of orthogonal components that capture the maximum variance in the data. For further interpretation, the histogram of the scores is plotted, as well as the evolution of the score over time.

Tuning the parameters of this method consists of setting the number of neighbors to consider, as well as the minimum distance to consider a point as an outlier. It is usually set to 1.5. The number of neighbors is visually tuned by looking at the shape of the decision boundary function around the training data points, and was set to 50.

The four pendulum measurements are taken as inputs, in order to see if an abnormal behavior is detected among this set of data. These are the radial and tangential displacements of pendulums 1 and 2.

2.3. RESULTS

2.3.1. *Supervised anomaly detection*

The cross-validated predictions of the radial displacements of pendulum 1 ("Pendule1_rad") is displayed on Fig. 4 below, along with the prediction error graph. The R^2 is equal to 0.903 ± 0.010 and the MAE is $0.155 \text{ mm} \pm 0.006$.

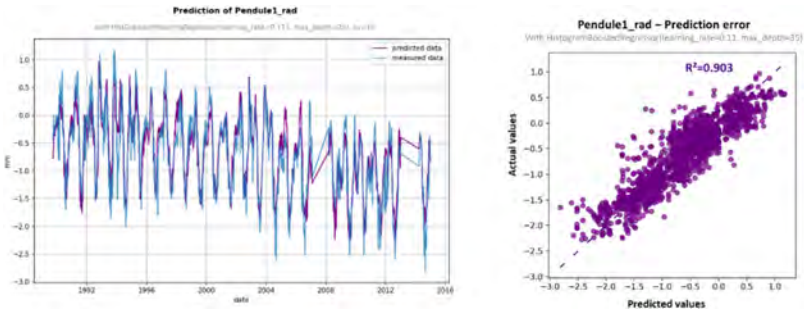


Fig. 4
Cross-validated prediction of the radial displacement of pendulum1 and its prediction error

The influence of all the predictors on the target are displays through PDP. Some of them are illustrated on Fig. 5. It is noted that the day of the year (“DayOfYearSin”) and the minimum temperature do not seem to explain the pendulum variations. However, the 30-days average minimum temperature (“T_min_30d”) and the reservoir level above 1980 mNGF are much more explanatory. The number of days since the first available monitoring data (“DaySinceDayOne”) is responsible for a downward trend in the displacements, which accelerated around 7500 to 8000 days. This corresponds to the year 2004.

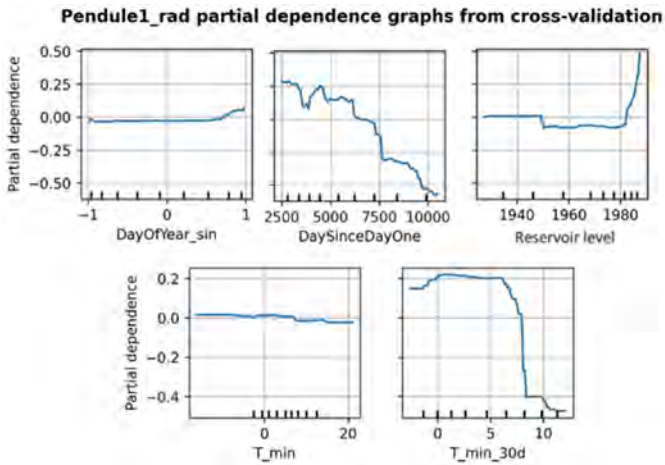


Fig. 5
Partial Dependence Plots for some of the predictors

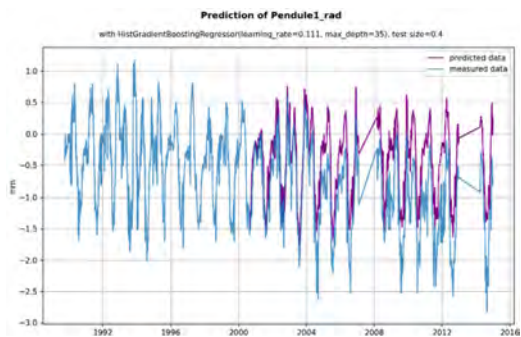


Fig. 6
Simple prediction on the data after 2000

The data is split before and after 2000. On one hand, the cross-validated prediction of the data before 2000 gives a R^2 of 0.754, as shown on the prediction error graph in Fig. 7. A visual boundary is plotted around this first set of data, corresponding to 3.5 times the MAE of this prediction. On the other hand, a simple prediction is made on the data after 2000, using the previous data for training. The result is plotted over time in Fig. 7 below. The predictions match the actual data before 2004, but move further away from it after that. This can be seen on the prediction error graph, where the predicted values are on average 0.5 mm above the $x=y$ axis, and moving away from it over time, outside of the boundary. The R^2 of this prediction has dropped to 0.174. This means that the behavior learned by the model before this date cannot explain the variations after 2004.

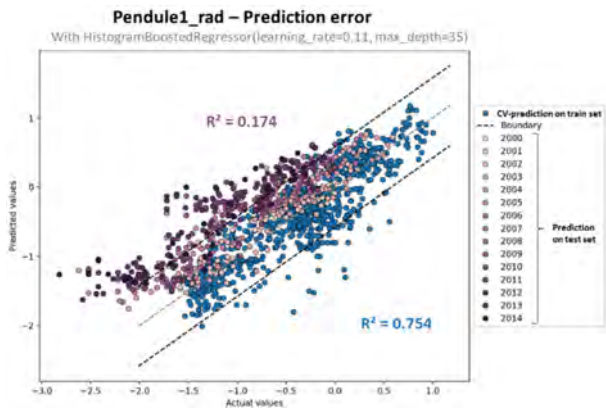


Fig. 7
Errors in cross-validated prediction on data training data before 2000 (in blue) and in the prediction of the displacements after 2000 (in purple)

The plotted boundary around the training data can be seen as a criterion, delimiting a behaviour explained by the training data “as before”, and abnormal data. The prediction error of the test set is plotted over time on Fig. 8. The data outside of this boundary are colored in red. The prediction error is clearly increasing over time, and really appear on 2004.

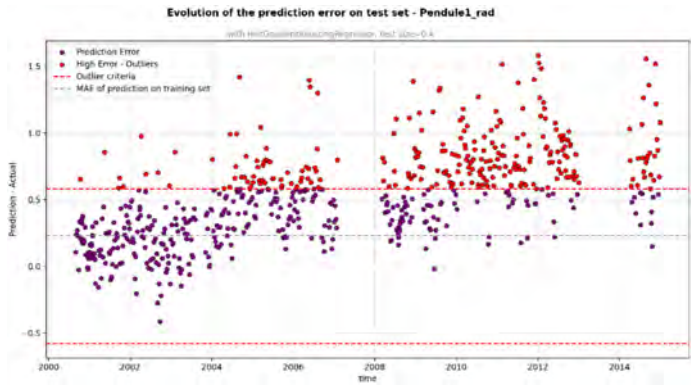


Fig. 8
Evolution of the prediction error over time

2.3.2. *Unsupervised anomaly detection*

The novelty detection results of pendulum 1 are plotted on the graph of its radial displacements against time (Fig. 9). The date for the separation between the training and the validation data was chosen just before the observed drop on the monitoring data, to see if this drop could be detected as a whole outlier.

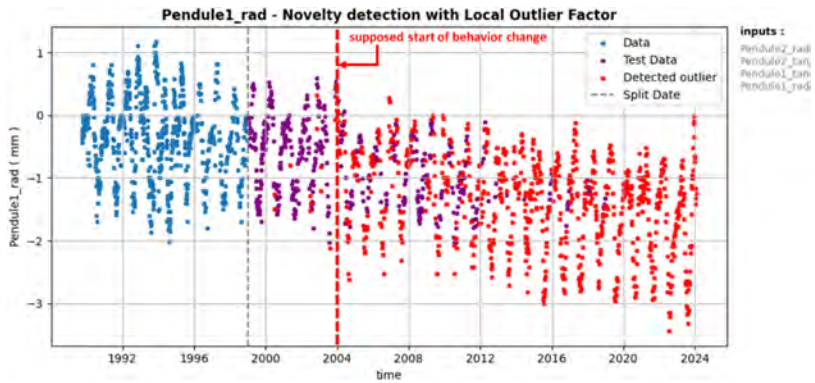


Fig. 9
Results of Novelty detection on the pendulum displacements over time

To visualize the separation between inliers and outliers, the four features are plotted into two principal components using linear PCA, with the decision boundary function on the Fig. 10 below. The inliers are located near the training data, while the outliers form a group that moves away from the main data.

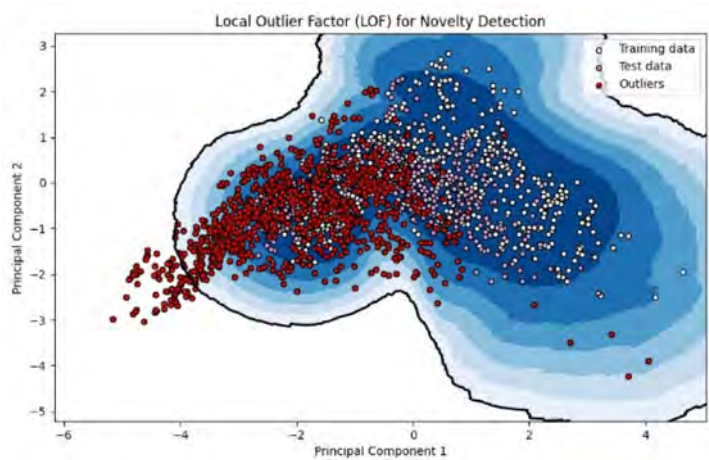


Fig. 10
Visualization with linear PCA of the decision boundary function on the data set

The histogram of all the outlier scores (the distance between the points and their nearest groups) is also plotted, with the red dotted line separating the inliers from the outliers. It is typically set to 1.50. (Pedregosa *et al.*, 2011). The evolution of the scores over time is also plotted on the Fig. 11 below.

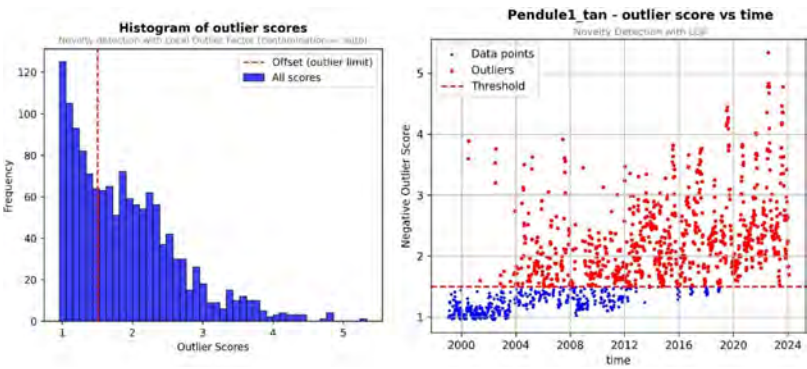


Fig. 11
Histogram of outlier scores and their evolution over time

Both figures show that the distance of the data points between their nearest group decreases progressively. The evolution of the scores over time shows a first jump of the scores in January 2004 with the appearance of many outliers. Other jumps and drops seem to have occurred in 2008, 2013 and 2020. The one of 2008 can be seen on the PDP of “DaySinceDayOne” in Fig. 5. The following cannot be checked as the PDP of the regression method can be applied only up until 2013, where the temperature data is not missing as a predictor.

2.4. DISCUSSIONS

The Histogram Boosted Regression Tree, which shows high performance for low computational time, to predict the radial displacements of pendulum 1. HBRT’s parameters are easily set with a grid or random search, making it very easy to use. It also natively handles missing data within the predictor’s, which the other algorithms do not. This allows a prediction to be made even during periods of incomplete data, although it does not increase the performance of the model. This is often the case in monitoring.

The regression task provides a prediction based on past data that can be visually compared to the real data. A change in behavior can be observed this way, as shown in Fig. 7. By setting a criterion around the prediction of the training data, abnormal data can be highlighted and observed over time.

The Partial Dependence Plots provide an interpretation of the dam’s behavior and help understand the variations recorded by the instruments. These may be explained by external variables or may appear on the PDP of the number of days since the start of monitoring, revealing an irreversible behavior of the instrument. Looking at each instrument in the monitoring system gives a good insight into the complexity of the dam’s behavior.

The Novelty Detection technique could be a useful method to detect abnormal data points. By leveraging a combination of features, it effectively separates out-of-scope data from the expected patterns. A succession of abnormal points can then be treated as an anomaly for further investigation. It detected successfully several changes in the pendulum radial displacements, as seen with the Regression method. This method is applied on a longer timescale because less inputs were used, which means less datapoints were deleted during the cleaning process of the database.

The histogram of the outlier scores is also a useful tool that enables to see whether the points gradually deviate from the norm, or if some points are highly isolated from the rest. It provides an insight on the nature of the anomalies, whether they represent gradual changes over time or sudden, distinct outliers.

3. ELEVEN YEARS OF FIBRE-OPTIC STRAIN MEASUREMENTS AT THE INVERT-FOUNDATION CONTACT OF A HYDROELECTRIC CANAL EMBANKMENT AND NUMERICAL MODELLING OF ASSOCIATED SETTLEMENTS

3.1. GENERAL DESCRIPTION OF THE CANAL EMBANKMENT

The canal embankment is 5.250 km long and forms part of the Durance hydroelectric system in south-east France. This canal was commissioned between 1966 and 1969. It carries a maximum flow of 220 m³/s and contains a volume of water of 1 Mm³. The maximum height of its embankments above the natural ground is 25 m, canal invert width is 9 m and its crest-to-crest width varies between 43 and 50 m. The water level varies between 7.8 and 9.3 m. Its watertightness is ensured by means of an upstream asphalt concrete mask. The embankments are made up of a homogeneous body of alluvial material, mainly sand and silt. This structure is partly founded directly on gypsum. At the time of its construction, two sinkholes 10m in diameter had formed under the embankments, which led the designer to modify its layout and widen the crest of the embankment on the right bank (the left bank being mostly in excavation): 4m wide in the upstream section, the crest had been widened to 13m from MP 3350 to MP 4350 (MP 0 at the upstream end of the canal) and to 30m from MP 4350 to the downstream end of the canal.



Fig. 12
Aerial view of the canal embankment

The slopes and the channel bed were initially lined with one or two layers of 5 cm thick asphalt concrete waterproofing, which over time developed multiple cracks in the above-water section and began to extend into the tidal zone.

Drainage and evacuation of seepage water originally consisted of a layer of draining asphalt concrete placed on the underside of the waterproof mask, connected to two longitudinal drainage trenches located at the foot of each canal slope, each equipped with a perforated drainage collector at the top (diameter 25 to 40 cm). This system collected and drained leakage water to three outlets equipped with leakage measurement and alarm devices. The draining asphalt concrete layer was laid on top of a layer of semi-permeable silty materials ($K = 10^{-7}$ m/s), which was designed to facilitate the collection of leakage water in the event of problems with the main waterproofing and to avoid sending aggressive water towards the gypsum foundation of the canal.

However, after almost 40 years in operation, the main waterproofing, which had been installed in the conventional way at the time, using a two-layer coating, was showing numerous signs of deterioration [ICOLD Report Q95-R17].

Because of the very sensitive foundation and the fear of significant water circulation in the foundation, the operator had imposed a constraint to lower the canal's operating level. As conventional maintenance work could no longer restore the required initial conditions, EDF decided to completely renovate the waterproofing system and drainage system of the canal in 2011, in order to restore normal operating levels under optimum safety conditions.

3.2. WATERPROOFING AND DRAINAGE REHABILITATION WORKS

The waterproofing and drainage rehabilitation work included the following measures [ICOLD Report Q95-R17]:

- Repairing the existing waterproof asphalt concrete covering in the damaged areas;
- Laying a new layer of draining asphalt concrete ($K > 10^{-3}$ m/s) at least 10 cm thick over the entire surface of the canal invert and slopes, on top of the repaired waterproof asphalt concrete;
- On top of this layer of pervious asphalt concrete, apply a new layer of impervious asphalt concrete ($K < 10^{-9}$ m/s) at least 8 cm thick over the entire surface of the canal invert and embankment inner slopes;
- Application of a protective layer in the tidal zones and above the water level of the embankments inner slopes;
- Replacement of the drainage network with a new system for the entire canal, with the installation of 9 outlets and the construction of two new longitudinal drainage trenches under the invert, made of cement concrete and fitted with perforated drainage collectors at the top;
- Installation, in the upper part of each longitudinal drainage trench, of an optical fibre to measure temperatures along the entire length of the canal, making it possible to locate leakage zones very quickly, during the canal impoundment, or in the event of an operating incident;

- Installation, in the central part of the canal most sensitive to potential future deformation of the structure, under the asphalt concrete invert, of an optical fibre for distributed strain measurements, over 2.67 km in the part where the canal is founded above the gypsum.



Fig. 13

Canal emptied, prior to the waterproofing rehabilitation works



Fig. 14

Rehabilitation of the waterproofing mask in 2011

3.3. INSTALLATION OF A SYSTEM FOR MONITORING DEFORMATIONS UNDER THE INVERT USING FIBRE-OPTIC MEASUREMENTS AND MEASUREMENT PRINCIPLE

The fibre-optic cable was placed under the invert, in a trench filled with sand, 20 cm below the old waterproofing (Fig. 15). This cable has both optical fibres for measuring distributed strain using the Brillouin effect, and fibres for measuring temperature using the Raman effect.



Fig. 15

Trench made in the centre of the channel bed in which the fibre optic cable was placed

The principle of distributed fibre optic strain measurement involves using an opto-electronic interrogator connected to the optical fibre, which emits laser pulses lasting a few nanoseconds that propagate along the fibre and interact with the silica molecules of which it is composed. The optical signal backscattered along the light path within the fibre is analysed by the interrogator, which determines its back-scattering spectrum (Fig. 16).

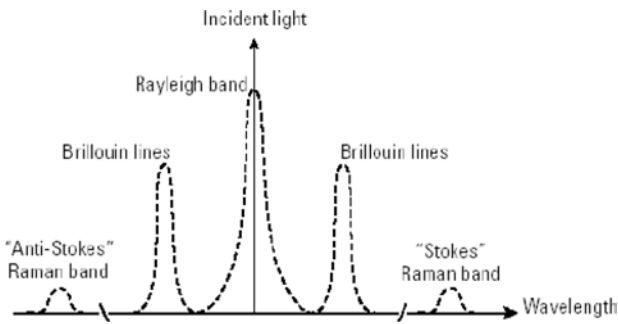


Fig. 16

Silica scattering spectrum

On either side of the main energy band, called the Rayleigh peak, are the Brillouin peaks, each associated with a wavelength. When the optical fibre undergoes

a deformation, the wavelength of the Brillouin peak varies according to the following linear relationship:

$$\Delta\nu_{FO} = C_{\varepsilon FO} \times \varepsilon_{FO} + C_{TFO} \times \Delta T_{FO}$$

With $\Delta\nu_{FO}$: the variation in wavelength of the Brillouin peak generated by the deformation of the optical fibre; $C_{\varepsilon FO}$: a constant specific to the optical fibre; ε_{FO} : the axial strain undergone by the optical fibre (en $\mu\text{m}/\text{m}$) ; C_{TFO} : a constant specific to the optical fibre; ΔT_{FO} : the temperature variation undergone by the optical fibre and determined independently by the Raman effect.

This technology enables deformation measurements to be taken every metre on a fibre up to 30 km long, with an accuracy of 10 to 20 $\mu\text{m}/\text{m}$ (the accuracy depends on the length of the optical fibre).

In the presence of a sinkhole, the classic deformation signals are as follows:

- classic tension/compression/tension signature, as shown in Fig. 17.
- after collapse, a signature with a single tensile peak, as shown in Fig. 18.

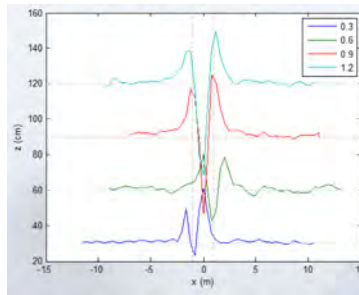


Fig. 17
Tension/compression/tension signature

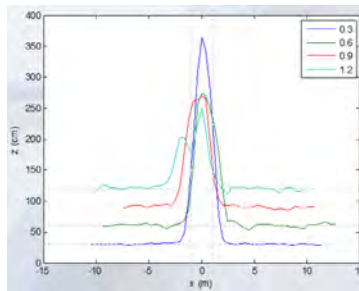


Fig. 18
Tensile peak signature

3.4. RESULTS OF ELEVEN YEARS OF FIBRE OPTIC STRAIN MEASUREMENTS

Following the start-up of this distributed strain measurement facility at the end of 2011, measurements were carried out quarterly for a few months, and then annually.

For each measurement, the data is processed by removing the influence of temperature from independent temperature measurements taken from the same cable, but with different fibres, using Raman technology.

Irreversible changes have been observed over the last 11 years in several sectors of the instrumented canal. Some of these irreversible changes show the signature of a sinkhole, with moderate kinetics (around $400 \mu\text{m/m}$ in 10 years), as shown in Fig. 19, between MP 3151 and 3190.

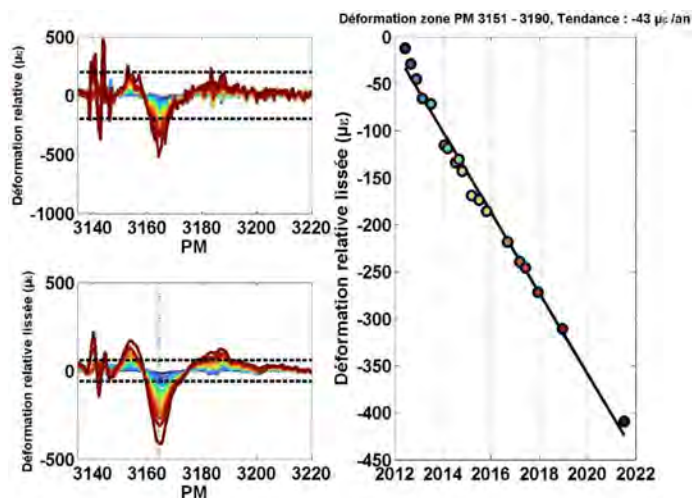


Fig. 19

Deformation measurements with the signature of a sinkhole measure from 2012 to 2022

These measurements show a very regular and constant trend over time, which rules out a measurement artefact or phenomena linked to seasonal variations. They show the typical signature of a sinkhole at a primary stage (small deformations), characterised by a compression peak at the centre of the cavity, surrounded by traction peaks at the cavity boundary. They therefore show that in this 40 m linear

sector, the optical fibre is undergoing settlement, although it is not possible to quantify this settlement directly. In order to better interpret this phenomenon, a mechanical numerical modelling approach was undertaken to estimate this settlement. This is presented in the following paragraph.

3.5. NUMERICAL MODELLING AND SETTLEMENT ASSESSMENT

3.5.1. *Numerical modelling objectives*

The objectives of the numerical mechanical modelling presented below were as follows:

- to propose a modelling framework consistent with the geometry of the section represented, the geological horizons and geotechnical conditions of the site, the hydro-mechanical behaviour of the geomaterials and geotechnical or civil engineering structures (waterproofing) in place and the initial and loading conditions experienced by the structure.
- represent the overall behaviour of the structure as accurately as possible by comparing it with fibre-optic deformation measurements.
- carry out a number of sensitivity studies to demonstrate the influence of the uncertain parameters of the problem in relation to the geometry of the canal, the mechanical properties of the soil, etc.
- establish a link between deformations measured by fibre optics and vertical settlements at the surface, in order to be able to assess and predict surface displacements based on a calibration of deformations calculated using fibre optic measurements.

3.5.2. *General principles of numerical modelling*

The numerical modelling that has been developed represents a vertical section longitudinal to the axis of the canal, which includes the canal and its foundation, in the area of MP 3164, where irreversible deformations have been measured by fibre optics (Fig. 20). The occurrence of a sinkhole is taken into account in the numerical model via the presence of an ovoid cavity explicitly integrated into the gypsum horizon, the dimensions and position of this cavity being the subject of sensitivity studies. The development of this cavity over time is modelled by excavating the material undergoing dissolution, based on the convergence-confinement method commonly used to model tunneling, under the assumption of plane deformations, in rock masses. The modelling is carried out using Code_Aster finite element software, developed by EDF R&D. A purely mechanical approach was considered in this study, taking into account a linear elastic behaviour law for all the materials.

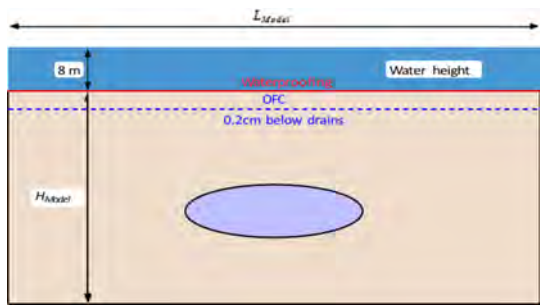


Fig. 20
Geometry of the canal and its foundation modelling

The red line in Fig. 20 represents the watertightness of the channel invert. The blue dotted line represents the fibre optic cable. The blue ovoid shape represents the cavity in the gypsum horizon of the foundation. The parameters H_{model} (height of the foundation, including the gypsum horizon) and L_{model} (length of the model along the longitudinal axis of the canal) are subject to sensitivity calculations.

3.5.3. *Geological model*

Data on the geology of the canal foundation in the area of interest, derived from geophysical and geotechnical surveys, indicate that under the canal invert there is a layer of silty gravel alluvium, around 15 m thick, which overlies the gypsum layer. The depth of the roof of the gypsum horizon is an important input parameter that was the subject of a sensitivity study.

The geological model used is shown in Figure 21.

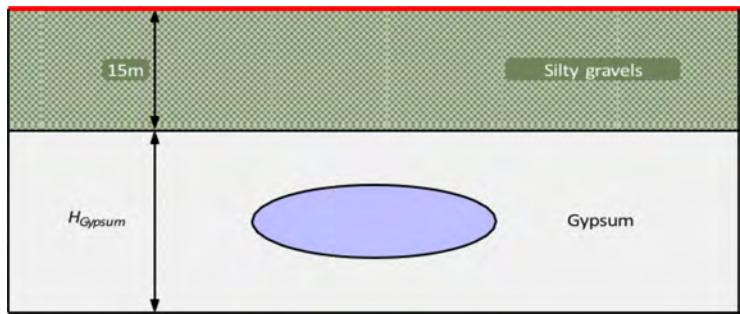


Fig. 21
Foundation geological model

3.5.4. *Geomechanical model*

Three types of materials must be characterised from a geomechanical point of view in the calculation domain:

- the waterproofing of the canal
- the sub-base layer of silty gravel
- the foundation layer of gypsum.

These three types of material are characterised by their unit weight (Y), their Young's modulus (E), their Poisson's ratio (ν), their cohesion (C), their friction angle (φ) and their expansion angle (ψ). The values of these parameters were estimated from typical values published in the literature. They are presented in Table 1 (crosses indicate a lack of information for the properties in question).

Table 2
Materials geomechanical parameters

Material type	Unit weight Y [kN/m ³]	Elastic modulus E [MPa]	Poisson's ratio ν [-]	Cohesion C [kPa]	Friction angle φ [°]	Expansion angle ψ [°]
Asphalt concrete	23	500 - 700	0,3 – 0,35	x	x	x
Silty gravels	21	12-20	0,3 – 0,35	0	35	0 - 35
Gypsum	23	35000 - 42000	0,3 – 0,35	x	x	x

3.5.5. *Sensitivity analysis of input parameters*

Methodology

The sensitivity study on the input parameters is an important stage in the study, the aim of which is to demonstrate the relevance of the numerical model to the physical description of the overall behaviour of the structure, and also to identify the impact of certain input parameters, in order, ultimately, to validate the chosen modelling strategy. In order to find the best compromise between the cost of the numerical calculation and the quality of the solution, the following sensitivity studies were carried out:

- sensitivity to the dimensions of the calculation domain (parameters α and β in Figure 22), in order to limit the influence of the boundary conditions on the results of the study. These dimensions are for a fixed cavity size;
- sensitivity to the geometric properties of the cavity: i) dimensions of the ellipsoid (parameters H_{cav} and L_{cav} in Figure 22), ii) distance between the cavity and the gypsum roof (γ in Figure 22);

- sensitivity of the water head, which acts as an external load, but also influences the stress state of the underlying domain;
- sensitivity of the geomechanical properties of the different soil layers, in particular the elastic moduli of the three layers ($E_{\text{draining asphalt}}$, E_{gravels} , E_{gypsum}).

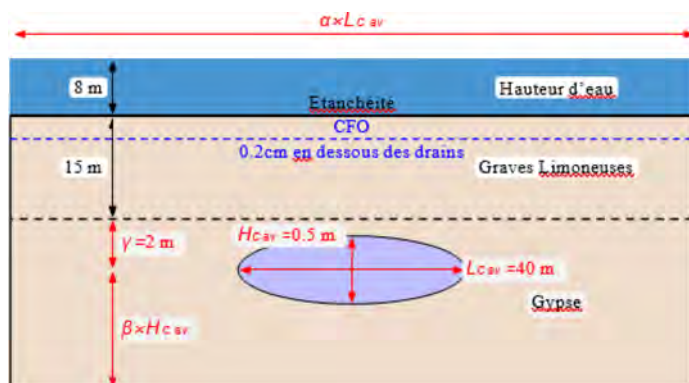


Fig. 22
Geometrical parameters of the calculation domain

Sensitivity to the dimensions of the calculation domain

The coefficients α et β were calculated so as to obtain convergence of the axial deformation in the central part of the cavity and zero deformation at the model boundaries. The following values were used:

$$\alpha = 7,5 \quad \beta = 10.$$

Sensitivity to the cavity geometry

The lateral dimension of the cavity ellipsoid has an important influence on the axial deformation at the location of the fibre optic cable. The width of the cavity also influences the transition point between the tension and compression zones. The height of the cavity, at least in the range of values chosen, seems to have little influence on the response of the model.

The distance between the cavity and the gypsum roof shows, as expected, a strong sensitivity to axial deformation and settlement. A significant part of the overall response of the model is driven by the position of the cavity in space.

Sensitivity to water height

The influence of the water height in the canal on the axial strain at the location of the fibre-optic cable and on the settlement at the same location is significant. As expected, the higher the water height, the greater the axial deformation and settlement.

Sensitivity to the elastic modulus of materials

Extreme values were considered for analysing the sensitivity of the elastic modulus of asphalt concrete to deformation and settlement [100 - 1000 MPa]. While the study showed a high sensitivity to deformation, the sensitivity to settlement was low.

Within the range of variation considered for the elastic modulus of silty gravel [12 - 20 MPa], the study showed a high sensitivity of this parameter to axial deformation, but low sensitivity to settlement.

The sensitivity study on the elastic modulus of gypsum shows that this parameter has a significant influence on both axial deformation and settlement.

3.5.6. *Model calibration based on fibre-optic strain measurements*

The parameters of the numerical model were calibrated to best represent the fibre-optic measurements while maintaining reasonable values for the input parameters.

The model parameters are presented in Table 2 and Figure 22. The width of the cavity, L_{cav} , was set at 30 m, instead of 40 m.

Table 3
Input parameters characterizing the geomechanical properties of materials

Material type	Unit weight γ [kN/m ³]	Elastic modulus E [MPa]	Poisson ratio ν [-]
Asphalt concrete	23	500	0.3
Silty gravel	21	12	0.3
Gypsum	23	35000	0.3

The results of this calibration are shown in Figure 23, where the axial deformation at the location of the optical fibre calculated by the model is compared with the cumulative deformation measurements of the optical fibre from 2012 to 2022. A

good match is observed between the numerical simulation and the fibre optic measurements. However, it should be noted that the set of parameters used to obtain these results is not unique, since a similar response can be obtained by making different assumptions about the input parameters or by modelling non-linear behaviour.

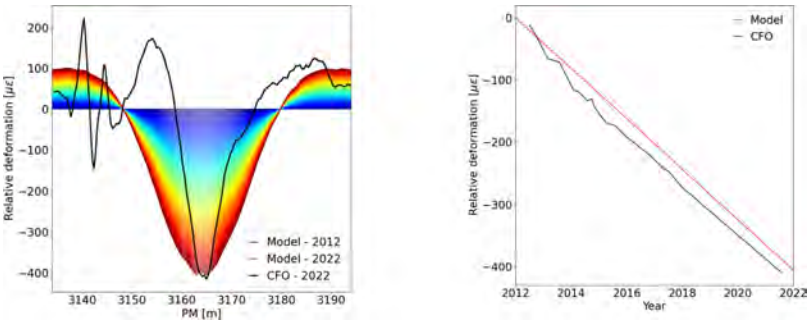


Fig. 23
Comparison between calculations and fibre-optic measurements of strains from 2012 to 2022

The results of the strains and settlements calculated by the numerical model, over the ranges of variation of the various input parameters which were the subject of a sensitivity study, are presented in Table 4 below. These results, which must be considered preliminary, show that settlement after 11 years is around 10 cm in this sector of the canal. The search for greater precision in the most influential input parameters will enable these results to be refined.

Table 4
Deformations and settlements calculated as a function of the value ranges of the most influential input parameters

Input parameters	Strains (µm/m)			Settlements (cm)		
	Min	Max	Variation (Max-Min)/Max	Min	Max	Variation (Max-Min)/Max
L _{cav}	100	1100	9%	1	11	90%
H _{cav}	1000	1100	9%	10	11	9%
γ	100	5000	98%	1	50	98%
H _{water}	900	1100	18%	8	11	27%
E _{draining asphalt}	500	2700	81%	10	11	9%
E _{silty gravel}	1000	1500	33%	10	11	9%
E _{Gypsum}	1000	3000	66%	7	30	90%

4. CONCLUSION

In summary, both advanced analysis methods presented in this report have shown their interest to improve capabilities of interpretation of monitoring data.

The integration of Machine Learning, especially the Regression and the Novelty Detection tasks provides a powerful approach to practical data monitoring. This combines the predictive tool of regression to anticipate trends and the detection capabilities of Novelty Detection to identify outliers. These methods also integrate interpretation tools that increase the efficiency of dam monitoring data analysis and can be developed for a practical application.

The numerical modelling developed to represent strains and settlements below the canal invert enhances the information provided by the fibre optic cable. These results, which should be considered preliminary, will be improved by reducing the uncertainty on the most sensitive input parameters. They highlight the interest of distributed strain measurements by optical fiber for dams and canals founded on deformable materials or above cavities.

REFERENCES

- [1] MATA, J. (2011) 'Interpretation of concrete dam behaviour with artificial neural network and multiple linear regression models', *Engineering Structures - ENG STRUCT*, 33, pp. 903–910. Available at: <https://doi.org/10.1016/j.engstruct.2010.12.011>.
- [2] PEDREGOSA, F. ET AL. (2011) 'Scikit-learn: Machine Learning in Python', *MACHINE LEARNING IN PYTHON [Preprint]*.
- [3] SALAZAR, F. ET AL. (2015) 'An empirical comparison of machine learning techniques for dam behaviour modelling', *Structural Safety*, 56, pp. 9–17. Available at: <https://doi.org/10.1016/j.strusafe.2015.05.001>.
- [4] SALAZAR, F. ET AL. (2016) 'Interpretation of dam deformation and leakage with boosted regression trees', *Engineering Structures*, 119, pp. 230–251. Available at: <https://doi.org/10.1016/j.engstruct.2016.04.012>.
- [5] SALAZAR, F. ET AL. (2017) 'Data-Based Models for the Prediction of Dam Behaviour: A Review and Some Methodological Considerations', *Archives of Comp. Meths. Engng. [Preprint]*. Available at: <https://doi.org/10.1007/s11831-015-9157-9>.

- [6] SALAZAR, F. *ET AL.* (2021) 'Anomaly Detection in Dam Behaviour with Machine Learning Classification Models', *Water*, 13, p. 2387. Available at: <https://doi.org/10.3390/w13172387>.
- [7] TAYFUR, G. *ET AL.* (2005) 'Case Study: Finite Element Method and Artificial Neural Network Models for Flow through Jeziorsko Earthfill Dam in Poland', *Journal of Hydraulic Engineering-asce - J HYDRAUL ENG-ASCE*, 131. Available at: [https://doi.org/10.1061/\(ASCE\)0733-9429\(2005\)131:6\(431\)](https://doi.org/10.1061/(ASCE)0733-9429(2005)131:6(431)).
- [8] Y.L. BECK, J.R. COURIVAUD, S. CRÉNEAU, F. DELORME, « Réhabilitation de revêtement bitumineux et maintenance préventive innovante utilisant des fibres optiques : principes et application au canal de Curbans », *ICOLD, 24th Large Dam Congress*, Kyoto, May 2012, Report Q.95-R.17.

COMMISSION INTERNATIONALE DES
GRANDS BARRAGES

VINGT-HUITIEME CONGRES DES
GRANDS BARRAGES
CHENGDU, MAI 2025

**APPLICATION OF SHEAR STRENGTH REDUCTION METHOD TO ANALYSE
STABILITY OF A MASSIVE DAM STRUCTURE ON SOIL FOUNDATION WITH
EXCESSIVE PORE PRESSURES AND REDUCED EFFECTIVE STRESSES DUE
TO INTERNAL EROSION**

Hui LU
MULTICONSULT, Norway

Sophie MESSERKLINGER
Dr. Sophie Messerklinger, Independent Consulting Engineer, Austria

Jan Atle ROTI
MULTICONSULT, Norway

AUSTRIA

SUMMARY

The stability of a large-scale hydropower dam structure on a soil foundation with excessive pore water pressure and reduced effective stresses due to static liquefaction during construction and later internal erosion is calculated for deep-seated bearing failure mechanisms by an innovative approach. The in-situ effective stress in the foundation soil under the dam structure was investigated by several Cone Penetration Tests (CPTs). By reverse interpretation of these CPTs, reduced effective stresses in the foundation soil in depth are quantified. In the 2D FEM calculation model, the reduced effective stress zones below the dam structure are incorporated with clusters of the size about 5 m x 10 m. They are assigned with different permeabilities and unit weights to calibrate with the measured pore pressures, drainage discharges and CPT reversely interpreted effective stresses. Safety factors are calculated by the Shear Strength Reduction (SSR) method with the

calibrated models. A wide range of sensitivity analyses are also conducted to verify the results and extend the understanding of dam stability.

Keywords: Dam Stability, Dam foundation, Calculation method, Numerical model, Shear Strength Reduction (SSR) method, Internal erosion, Static liquefaction, Artesian pressure.

1. INTRODUCTION

An innovative stability calculation method has been successfully applied to assess the stability of a large-scale existing dam structure in Europe on challenging foundation ground conditions. The massive concrete dam structure forms a dam for a water head of about 40 m. It is composed of two stiff concrete blocks. The soil foundation is composed of low-plastic and low-permeable glacial till, also known as moraine, which fills an over 100 m deep buried valley (Fig. 3). The valley flanks are formed of layers of Dolomites and Sandstones. Some layers of the rock formations are more permeable and form aquifers with artesian water pressures. The aquifers feed artesian pressurised water into the glacial till foundation soil, which leads to an increase of the hydraulic gradients. The bottom of the concrete structure is equipped with horizontal drainages. In addition, vertical drainage piles of approximately 13 m length are also installed in the soil foundation below the bottom of the concrete structure to relieve the excess pore pressures and the upward flow gradients in the foundation soil close to the concrete structure.

2. CONCRETE STRUCTURE

The dam structure is made up of two rigid concrete blocks with a length of ca. 100 m each along the dam axis. The width of the dam structure is around 65 m, and the maximum height is around 57 m. These two rigid concrete blocks are separated by a flexible joint system in the centre of the dam allowing differential displacements of several decimetres. On the left dam abutment, the concrete structure is attached to concrete retaining structures also known as the wing walls for an adjacent embankment dam. On the right dam abutment, the concrete structures are separated by flexible joints to a lightweight service building and attached to concrete retaining structures.

The stability analysis for deep-seated failure mechanisms was performed in sections through the concrete dam structure. The weight of the concrete structure was determined by a 3D-BIM model, and it is applied by line loads shown in Fig. 4.

3. SOIL FOUNDATION

3.1. GENERAL

The foundation soil under the concrete structure has been affected by the high artesian pressure head with a maximum about 35 m from the floor of the concrete structure. The artesian pressure is fed by underground water flows from the bedrock formations. The high groundwater pressure caused problems during the construction period. Despite of installation of many pressure relief wells to lower the groundwater pressures, comprehensive hydraulic ground failure and static liquefaction, occurred. The pressure relief wells, which were installed both for construction purposes and later kept as permanent pressure relief facilities to secure stability, caused also internal erosion and washout of soil particles. During operation period, a collapse of one major pressure relief well resulted in significant out-washing of solids, and it also led to excessive settlements observed for the next 15-20 years.

The stability of the concrete structure for the deep-seated bearing failure mechanism was assessed in the late 1990th. However, due to the limitation of methods 25 years ago, as the Shear Strength Reduction (SSR) [1] [2] method was not available at that time, a reassessment with the state-of-art methods was required.

Moreover, an extensive supplementary ground investigation program was undertaken during 1990th, which gives vital geotechnical information to assess the stability of the concrete structure.

3.2. PORE PRESSURE CONDITION

The pore pressure condition and discharges in the soil foundation of the dam and adjacent structures have been continuously monitored by over 200 piezometers and complex drainage and pressure relief facilities. Fig. 1 gives an overview of the

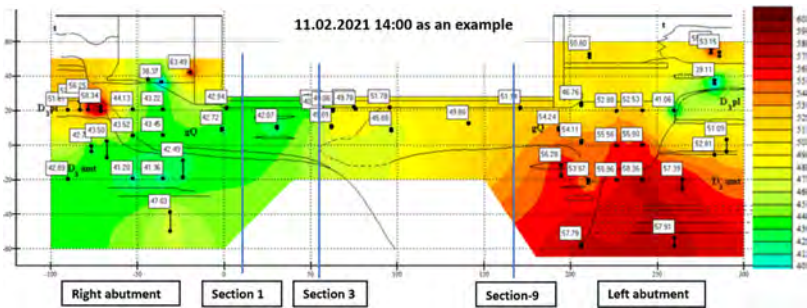


Fig. 1

Longitude section parallel dam axis (view from downstream) shows overall ground water pressure heads including location of the section 1, 3 and 9

pore pressure under the concrete structure and abutments. In general, it shows a comparable lower pressure head under the right abutment than the left abutment, which is due to pressure relief facilities there.

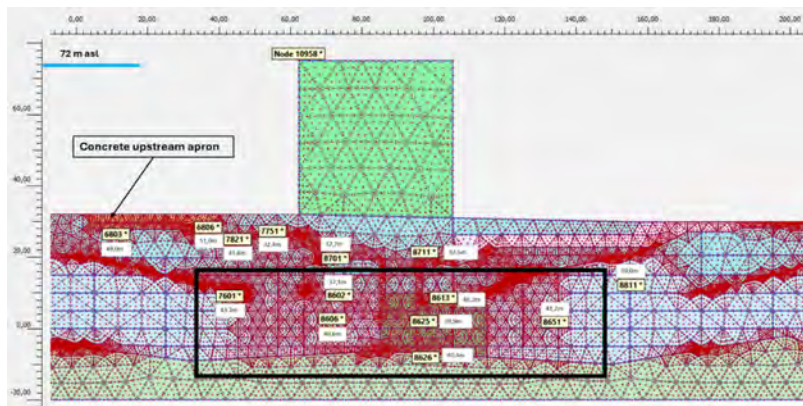


Fig. 2

Model mesh and location of piezometers in foundation soil in depth, section 1 as an example, piezometers inside the black line box are most relevant for the stability calculation

Besides a large number of piezometers right under the concrete structure within the depth of vertical drainage piles, which generally show low and stable pore pressure over time, it is more relevant to study the piezometer measurements installed in the soil foundation in depth. Fig. 2 shows a Plaxis2D model (section 1 as an example) with mesh, it has also mapped out the relevant piezometers in depth, particularly those within the black line box, for the deep-seated foundation stability analysis. With the Automatic Data Acquisition System (ADAS) established in the early 21st century, the highest credible values from these piezometers were selected after reviewing over 20 years of measurements for the stability calculation.

3.3. SOIL PARAMETERS

Based on the supplementary ground investigation conducted in 1990th, the material property of the moraine consists typically of about 10-15 % clay, 30 % silt,

45-50 % sand and 5-10 % gravel. It is well-graded with about only 10 % saturated water content, 0.28 void ratio and 22.7 kN/m^3 Unit weight. The plasticity index is about 9 and permeability is as low as $5\text{E-}10 \text{ m/s}$. $c'=10 \text{ kPa}$, $\phi'=34^\circ$ is obtained as the shear strength for glacial tills.

Extensive triaxial tests were carried out based on both the samples prior to the CPT campaign for the foundation soil in general and the samples taken from the same boreholes as the CPT. They mapped out the undrained shear strength at different vertical effective stress levels highly correlated with CPT. With sufficient number of triaxial tests undertaken at different stress levels, the correlation between vertical effective stresses (σ_{vo}') and undrained shear strength (s_u) is able to be established as $s_u = 150 \text{ kPa} + 0.75 \sigma_{vo}'$.

3.4. EFFECTIVE STRESS IN SOIL FOUNDATION

With the ground investigation conducted in 1990th, 5 CPTs was carried out from the concrete structure to the foundation soil in depth along its axis referred to sections 1, 3, 5, 7 and 9. The location normal to the dam axis is shown in A-A* in Fig. 5 and Fig. 7–9. In addition, CPT-6 was undertaken far away from the concrete structure area but in the same soil condition for reference and calibration purpose.

These CPTs contain important information related to the interpretation of the vertical effective stress in the soil foundation. With measured pore pressures and correlated undrained shear strength in depth, vertical effective stresses can be reversely calculated from the CPT cone resistance measurements, which is referred as the “*CPT-interpreted vertical effective stresses*”. These CPT-interpreted vertical effective stresses can be compared with the theoretical overburden effective stresses to quantify the degree of reduction of the effective stress.

The red bars in Fig. 3 show the location of reduced effective stresses interpreted by this method based on the CPT measurements. Fig. 10 (left), Fig. 11 (right) and Fig. 10 (right) show more detail and comparisons of CPT-interpreted vs. theoretical calculated vertical effective stress with increasing depth at Sections 1, 3 and 9 respectively. The difference between the blue dash line (theoretical vertical effective stress) and orange dash line (CPT-interpreted vertical effective stress) indicates where the vertical effective stresses are reduced due to other reasons than excessive pore pressure, for instance internal erosion. This method was verified with the data from CPT-6 performed at an undisturbed area, and it shows that there is no reduction of effective stresses, which fits well with the reality at CPT-6.

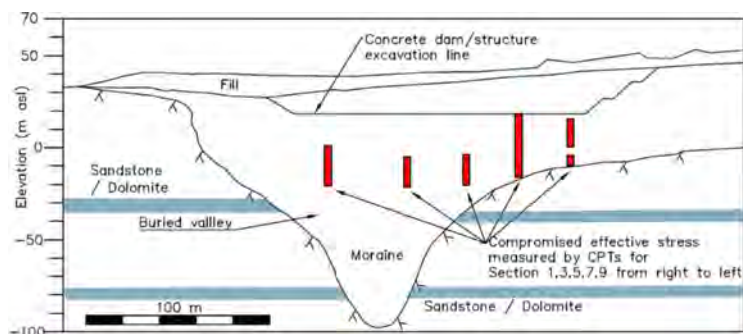


Fig. 3

Red bars in the figure shows the location of the reduced vertical effective stresses due to other reasons than excessive pore pressure, for instance internal erosion, reversely interpreted based on CPT measurements

Besides CPT-6 validation, sensitivity analysis has also been undertaken with different interpretations of N_{kt} and $s_u - \sigma'_{v0}$ correlation. The sensitivity analysis shows that it slightly affects the length and degree of vertical effective stress-reduced zone, but it does not change the overall conclusion. Most importantly, the vertical effective stress reduction zones are well overlapped with mapped areas where the static liquefaction occurred during the construction period and later possible outwash of soil particles (internal erosion). Therefore, it is believed that this method has been validated, and the reduced effective stresses have been quantified with this method.

4. STABILITY ANALYSIS

4.1. ANALYSIS STRATEGY

Plaxis2D modelling is selected. The advantages of 2D FEM model compared to 3D FEM are simplicity and flexibility. Therefore, a large quantity of back-and-forth calculations during the calibration and sensitivity analysis stage are commercially feasible.

As shown in Fig. 4 and Fig. 6, the foundation soil is divided into many clusters with a size about 5 m x 10 m. These clusters are assigned with different material properties to achieve the calibration of measured pore pressures, discharges and the CPT-interpreted vertical effective stresses. Moreover, they also play important roles in the sensitivity analysis.

Section 1, 3 and 9 are chosen for the stability calculation shown in Fig. 1. Taking Section 1 for an example (Fig. 4 to Fig. 7), the analysis is divided into three steps as follows:

Step 1: Calibration-1 stage. By varying and adjusting the permeability of materials to the individual clusters, the model is calibrated to the actual measured pore pressures and drainage discharges. The calibration-1 stage model is shown in Fig. 4. For the seepage analysis result, the total head (equal-potential) distribution is shown in Fig. 5. The total pressure heads in the corresponding locations of piezo-meters (Fig. 2) are calibrated with the measured values with an average accuracy $\pm 0,2$ m and individually up to $\pm 1,5$ m deviation. Total discharge is also calibrated with measured discharge in the drainage system with less than 10 % deviation. Fig. 7 (left), Fig. 8 (left) and Fig. 9 (left) show the vertical effective stress distribution of the calibration-1 stage to compare with the results from the calibration-2 stage.

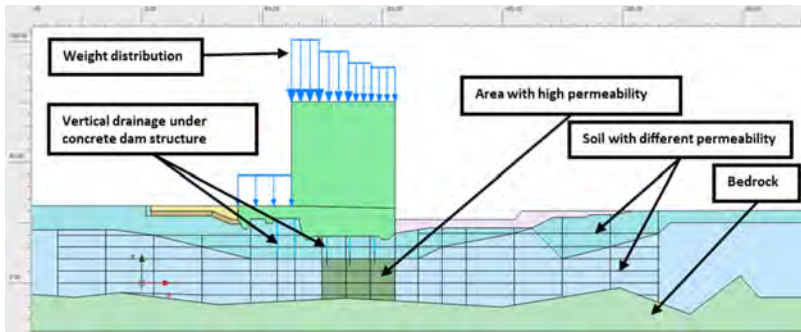


Fig. 4

Section 1 section, Calibration-1 stage model layout including weight distribution and vertical drainages

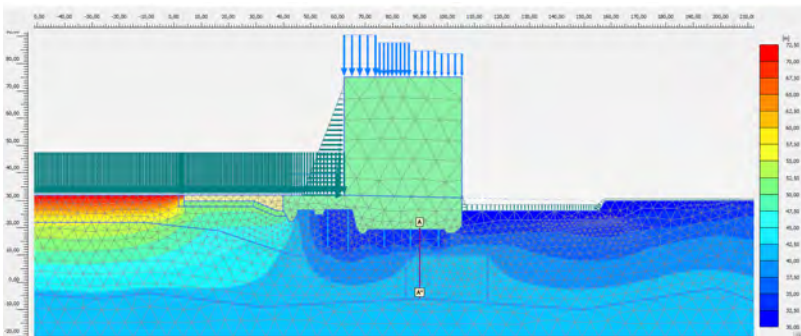


Fig. 5

Total head distribution as the result of Plaxis2D seepage analyses, Section 1

Step 2: Calibration-2 stage. Based on the calibration-1 model, by adjusting unit weights of assigned modelling materials to individual clusters, the model is further calibrated to coincide with CPT-interpreted vertical effective stresses. The secondary calibrated model is called the “reference model”. The “reference model” can be understood as the most representative model with known information, and it is also known as the “anchor points” model for all further sensitivity analyses. Fig. 6 shows a layout of the reference model for the Section 1. Fig. 7 (right) shows the calculated distribution of vertical effective stresses for the section 1, it can be compared with Fig. 7 (left) from the calibration-1 stage analysis, and so as Fig. 8 and Fig. 9 for the section 3 and 9 respectively. The location of CPT is at the line A-A* in Fig. 7, Fig. 8 and Fig. 9. Fig. 10 and Fig. 11 (right) show the vertical effective stresses from the reference model compared with the CPT-interpreted effective stresses for Section 1, 3 and 9.

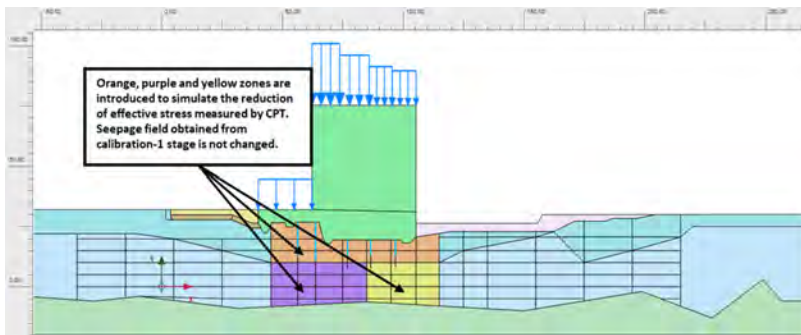


Fig. 6

Section 1, Calibration-2 stage model (also known as reference model) layout

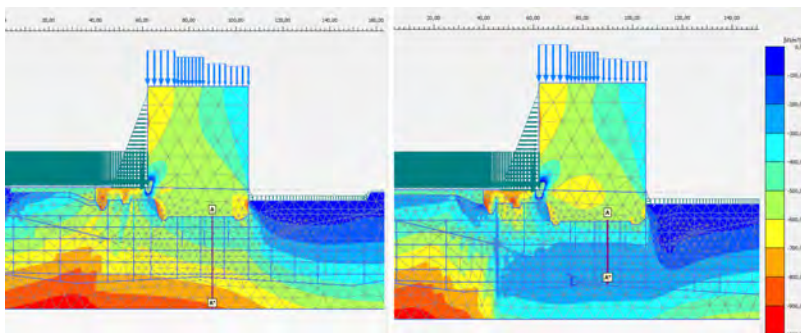


Fig. 7

Section 1 – vertical effective stress distribution in the foundation soil. Figure left (calibration stage 1) shows stresses without reduced effective stress. Figure right (calibration Stage 2) shows stresses with the reduced effective stress. Line A-A* in the figure is where CPT was undertaken, and vertical effective stresses are plotted in Fig. 10 (left)

Step 3: Sensitivity analysis stage. In this stage, variations are applied to the reference model as sensitivity analyses. It is further discussed in the section 4.3.

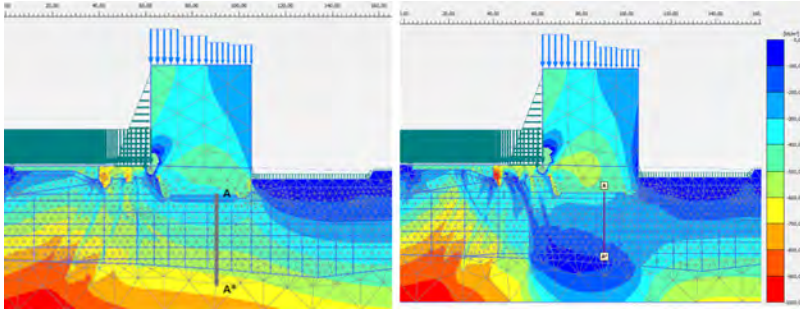


Fig. 8

Section 3 – vertical effective stress distribution in the foundation soil. Figure left (calibration stage 1) shows stresses without reduced effective stress. Figure right (calibration Stage 2) shows stresses with the reduced effective stress. Line A-A* in the figure is where CPT was undertaken, and vertical effective stresses are plotted in Fig. 10 (middle) and updated in Fig.11 (right)

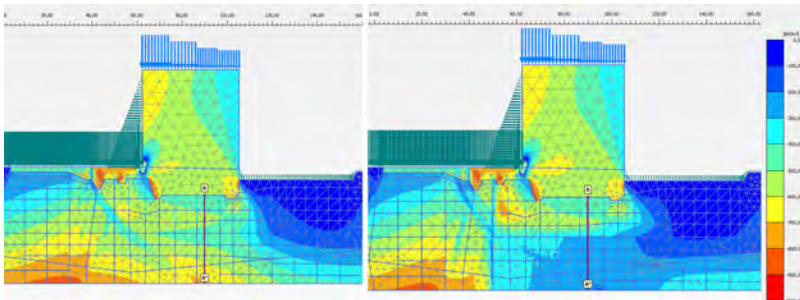


Fig. 9

Section 9 – vertical effective stress distribution in the foundation soil. Figure left (calibration stage 1) shows stresses without reduced effective stress. Figure right (calibration Stage 2) shows stresses with the reduced effective stress. Line A-A* in the figure is where CPT was undertaken, and vertical effective stresses are plotted in Fig. 10 (right)

The calibration-1 and 2 stage analyses for section 3 and section 9 are also shown in Fig. 8 and Fig. 9 respectively. The input parameters including unit weight

and permeability for orange, purple and yellow zones as the results of the two-stage calibration calculation are summarized in Table 1. The values are different for each different section.

Table 1.
Summary of input parameters as the results of the two-stage calibration calculation

Summary of input parameters as the results of the two stage calibration calculation				
Section	Material/ zones	Strength	Unit weight (kN/m ³)	Permeability (m/s)
1	Orange zone	c'=10 kPa, ϕ' =34°	0,1	1E-07
	Purple zone		8	3E-07
	Yellow zone		8	2E-06
3	Orange zone		0,1	4E-08
	Purple zone		6	4E-08
9	Orange zone		0,1	4E-010
	Purple zone		9	3E-08
Other soil materials				22,7

4.2. SECTION 3

Section 3 with the most reduced vertical effective stresses is tricky in the calibration-2 stage analysis. As shown in Fig. 10 (middle), even with unit weight reduced to 0 kN/m^3 , for the clusters right under the concrete structure, the vertical effective stresses from the numerical model are not able to be reduced to the level of the CPT-interpreted vertical effective stresses. It can be compared with Section 1 and 9 (Fig. 10 left and right), which are well calibrated.

The explanation is the bridging/arching effect. Because, for the soil directly under the concrete structure, the vertical effective stresses should be largely decided by the weight of the concrete structure above. It means, that right under Section 3 close to the structure, the CPT-interpreted vertical effective stresses do not correspond to the weight of the concrete structure above. However, the weight does not disappear, and it means that part of the weight from the structure is transferred to somewhere else, possibly to the soils in u/s and d/s direction and neighbouring sections, but there is not sufficient CPT nor accurate enough to be confirmed in practice. The comparable significantly higher stiffness of the concrete structure (two large stiff blocks) than the foundation soil supports this argument.

Therefore, by reducing the weight of the concrete structure by 35 %, the calibration-2 stage analysis is achieved for Section 3 shown in Fig. 11 right. Modelling vertical effective stress is well overlapped with CPT-interpreted vertical effective stresses.

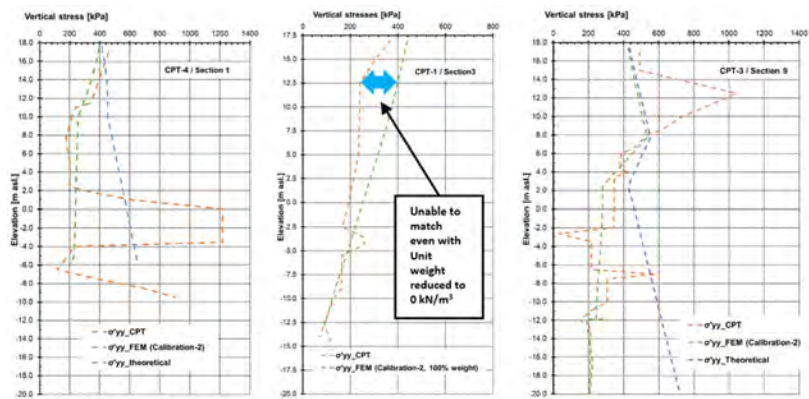


Fig. 10
Comparison of the FEM modelled vertical effective stress with the CPT-interpreted vertical effective stress for Section 1 (left), Section 3 (middle, with 100 % structure weight) and Section 9 (right)

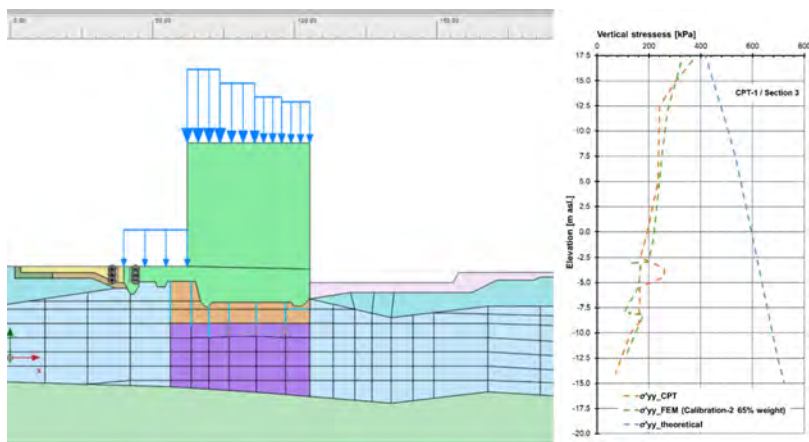


Fig. 11
Re-established reference model for Section 3 (left) with 65 % of concrete structure weight. The FEM modelling vertical effective stress (green dash line) matches well with the CPT-interpreted in-situ effective stress (orange dash line)

4.3. SENSITIVITY ANALYSIS

An extensive sensitivity analysis program has been carried out. Even through the sensitivity analyses are undertaken after the reference model, the reference model can also be understood as the iteration product of sensitivity analysis since it was continuously improved during the process. The most relevant sensitivity analysis is related to the vertical effective stresses described as follows:

- By systematically reducing unit weights of the assigned soil materials under the concrete structure, the reduced factor of safety can be plotted with step-wise decreased vertical effective stresses.
- Extension of unit weight reduced clusters to upstream and downstream direction. The purpose is to verify the best-fit unit-weight reduced clusters. It also helps to understand the most sensitive clusters for possible further investigation and mitigation design.

5. RESULTS

Safety factors are calculated from the reference model by the SSR method. The incremental shear strain plots showing the deep-seated bearing failure mechanism [2] are presented in Fig. 12, Fig. 13 and Fig. 14 for Section 1, 3 and 9 respectively. They all show that slip/failure surfaces are generally under vertical drainage piles, where the vertical effective stresses were reduced.

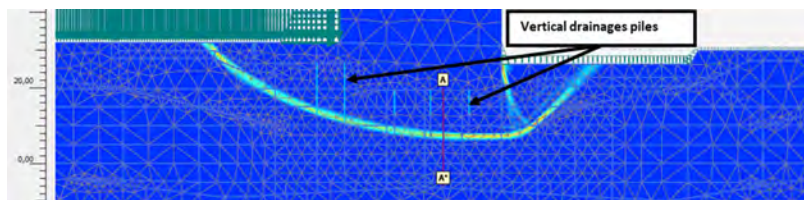


Fig. 12

Incremental shear strain shows deep-seated bearing failure mechanism with SRR calculation for the Section 1

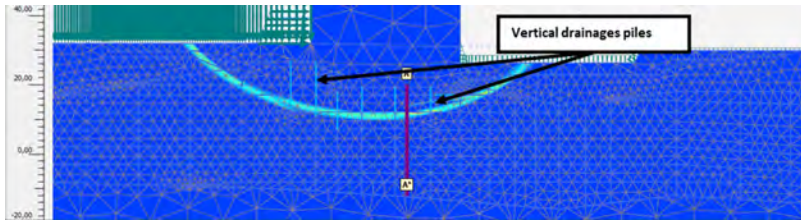


Fig. 13

Incremental shear strain shows deep-seated bearing failure mechanism with SRR calculation for the Section 3-35% reduced weight

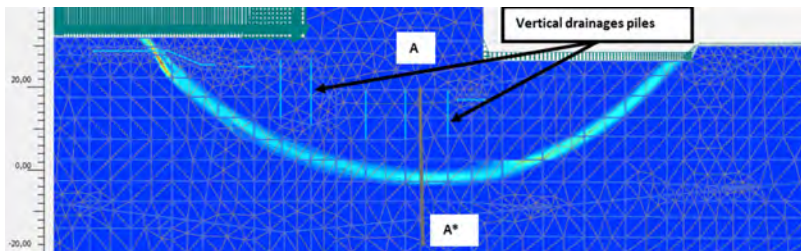


Fig. 14

Incremental shear strain shows deep-seated bearing failure mechanism with SRR calculation for the Section 9

6. CONCLUSION AND DISCUSSION

The factors of safeties of the concrete dam structure for the deep-seated bearing failure mechanism are calculated by the SSR method with the innovative two stages calibration process. The factual measurements such as CPTs including reference CPT-6, discharges & pore pressures as well as other historically documented dam behaviours play important roles in calibrating and validating the numerical models. The failure mechanisms are as expected deep-seated below the vertical drainages. A wide range of sensitivity analysis also contributes to the model validation and extends the understanding of the stability and sensitivity of the concrete structure/dam.

Further discussions are summarised as follows:

- The unit weight reduced clusters is a method to simulate the reduced vertical effective stresses calibrated by the factual measured CPTs. These clusters,

as a numerical modelling method, are not equivalent to where the solid materials are lost in practice. It must not be mixed up for the interpretation.

- Because of reduced vertical effective stresses in the foundation soil, there are bridging effects. The bridging effect is not only parallel to the dam axis, which is discussed in section 4.2, but also in the upstream and downstream directions. Fig. 7 (right), Fig. 8 (right) and Fig. 9 (right) shows the bridging effect normal to the dam axis.
- Sensitivity analyses regarding the extent of unit weight reduced clusters indicate that the vertical effective stress in the foundation soil around the downstream toe of the concrete structure is extremely sensitive to the safety factor. The reason is due to the arching effect described above. New CPTs there could verify this method in practice, and further improve the model and accuracy of FoS calculation.

REFERENCES

- [1] C. BENTLEY, "Safety analysis and displacements (https://bentleysystems.service-now.com/community?id=kb_article_view&sysparm_article=KB0110027)," 2012.
- [2] D. V. GRIFFITHS AND P. A. LANE, "Slope stability analysis by Finite elements," *Géotechnique*, pp. 49:387–403, 1999.
- [3] K. TERZAGHI, *Theoretical Soil Mechanics*, New Yourk: John Wiley and Sons, 1943.

COMMISSION INTERNATIONALE DES
GRANDS BARRAGES

VINGT-HUITIEME CONGRES DES
GRANDS BARRAGES
CHENGDU, MAI 2025

**INVESTIGATION OF CONSTRUCTION OPTIMIZATION OF A HEIGHTENED
CONCRETE GRAVITY DAM (*)**

Nario YASUDA

Head of the Eng. Division 1, JAPAN DAM ENGINEERING CENTER

Zengyan CAO

Senior Advisor, J-POWER BUSINESS SERVICE CORPORATION

Tadashi NISHIMURA

Director of the Ikushyun-betsu River Dam Construction Office, mlit

Masa-aki SATO

Eng. Division 1, JAPAN DAM ENGINEERING CENTER

JAPAN

SUMMARY

Climate change is expected to cause more frequent and severe water-related disasters in the future. Although dams are effective at controlling floods in watersheds, the number of suitable dam sites in Japan is limited. Therefore, there is a growing need to increase the flood control capacity of existing dams; thus, the need for dam rehabilitation is increasing. Among possible measures, dam heightening is an effective means of dam rehabilitation. This study examines the Shin-Katsurazawa Dam, which is a case of coaxial heightening of a concrete gravity dam. (1) The mechanical properties (elastic modulus, unit weight, compressive strength, and tensile strength) of the existing dam concrete, which is 67 years old, were determined based on the results of material tests of core specimens. (2) It was

*Optimisation de la construction d'un barrage-poids surélevé en béton

clarified that concrete placing at relatively high elevations should ideally be planned when the reservoir water level is relatively low if the reservoir is continued to be operated all year round.

RÉSUMÉ

Le changement climatique devrait provoquer à l'avenir des catastrophes liées à l'eau plus fréquentes et plus graves. Bien que les barrages soient efficaces pour contrôler les inondations dans les bassins versants, le nombre de sites de barrages appropriés au Japon est limité. Il existe donc un besoin croissant d'augmenter la capacité de contrôle des crues des barrages existants ; ainsi, le besoin de réhabilitation des barrages augmente. Parmi les mesures possibles, le rehaussement des barrages constitue un moyen efficace de réhabilitation des barrages. Cette étude examine le barrage Shin-Katsurazawa, qui est un cas de surélévation coaxiale d'un barrage-poids en béton. (1) Les propriétés mécaniques (module d'élasticité, poids unitaire, résistance à la compression et résistance à la traction) du béton du barrage existant, vieux de 67 ans, ont été déterminées sur la base des résultats d'essais de matériaux sur des échantillons de carottes. (2) Il a été précisé que la mise en place du béton à des altitudes relativement élevées devrait idéalement être planifiée lorsque le niveau d'eau du réservoir est relativement bas si le réservoir continue à être exploité toute l'année.

1. INTRODUCTION

Recently, large-scale flood disasters have occurred frequently due to increases in abnormally strong rainfall and the size of typhoons. In 2019, the cost of flood damage in Japan reached 2.18 trillion yen [1], and it is expected that climate change will cause more frequent and severe water-related disasters in the future. Although dams are effective at controlling floods in watersheds, suitable dam construction sites are limited. Under these circumstances, there is a growing need to increase the flood control capacity of existing dams, or so-called dam rehabilitation. Among possible measures, dam heightening is effective for dam redevelopment. There are many technical issues involved in the structural design and construction of dam heightening. This study focused on the Shin-Katsurazawa Dam ("Shin" means new in Japanese, distinguish the dam from the existing dam). It is a concrete gravity dam that underwent coaxial heightening, and Table 1 shows the specifications before and after dam heightening. In a previous study [2], the material properties of this dam were investigated through field experiments and analyses of its behavior during earthquakes. In this paper, the following issues were examined:

1. The mechanical properties (elastic modulus, unit weight, compressive strength, and tensile strength) of the existing dam concrete, which is 67 years old, were investigated by material testing of core specimens [3].
2. Assuming the heightening of the dam body during year-round reservoir operations, the effects of the reservoir water level on the stresses generated in the new and existing dam bodies are clarified. Based on the results, a construction plan for suitable heightening a dam body during reservoir operation was proposed.

Table 1
Specifications of the Shin-Katsurazawa Dam before and after heightening

Item	Before heightening	After heightening
Location	Katsurazawa, Mikasa City, Hokkaido	
Type	Concrete gravity dam	
Height	63.6 m	75.5 m
Crest length	334.25 m	397.0 m
Crest width	5.5 m	5.5 m
Crest elevation	EL.188.6 m	EL. 200.5 m
Slope	Upstream side: <EL.153 1:0.10, >EL.153 1:0.08	
	Downstream side: 1:0.77	Downstream side: 1:0.88
Volume	350,000 m ³	646,000 m ³
Basin area	298.7 km ²	298.7 km ²
Water storage	92,700,000 m ³	147,300,000 m ³

2. MECHANICAL PROPERTIES OF THE EXISTING DAM CONCRETE USING CORE SPECIMENS

2.1. OUTLINE OF THE EXISTING KATSURAZAWA DAM AND HEIGHTENING WORK

The Katsurazawa Dam was completed in 1957 as the first multipurpose dam in Hokkaido and has been responsible for flood control, water supply, and hydro-power generation. Fig. 1(a) and (b) show the location and the bird's view shot of the dam. The dam was redeveloped using a coaxial heightening method to enhance its flood control and water supply. The heightening work was completed in March 2023. The standard cross-sections of the dam before and after heightening are shown in Fig. 1(c) and (d). By heightening the dam by 11.9 m, it was possible to increase the water storage capacity by approximately 1.6 times.

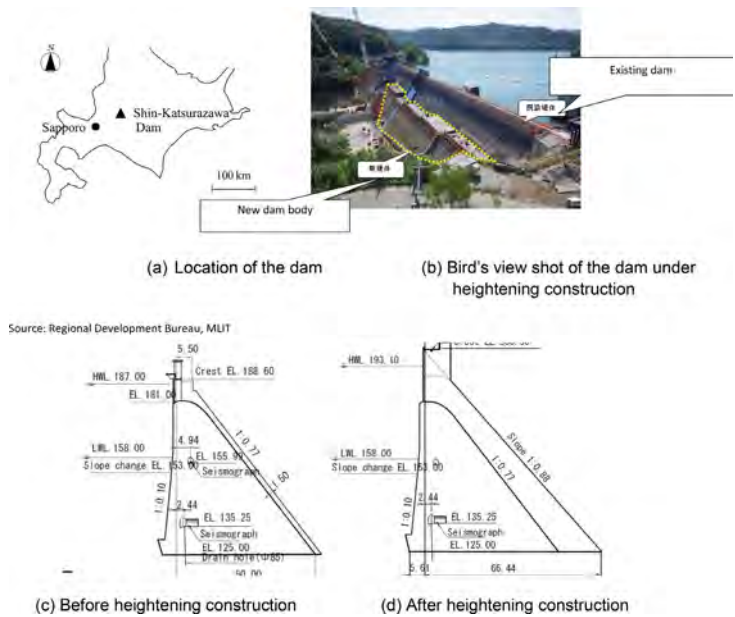


Fig. 1

Dam location and cross-sections before and after the heightening of the dam
*Emplacement du barrage et coupes transversales avant et après la surélévation
rehaussement du barrage*

2.2. INVESTIGATION OF THE MECHANICAL PROPERTIES OF EXISTING DAM
CONCRETE USING CORE SPECIMENS

Sixty-seven years have passed since the completion of the existing Katsurazawa Dam. Investigating the mechanical properties of dam concrete in severe natural environments for many years would be beneficial not only for designing dam heightening but also for planning the maintenance and long-term operation of the dam. Therefore, this paper presents a macroscopic verification of the results of material tests using core specimens from the existing Katsurazawa Dam. Fig. 2 shows the sampling locations of the core specimens. External concrete was collected at upstream locations No. 1 to No. 6 and downstream location B, and external and internal concrete was collected at downstream locations A, C, and D. The test results of the core specimens are reported in this paper.

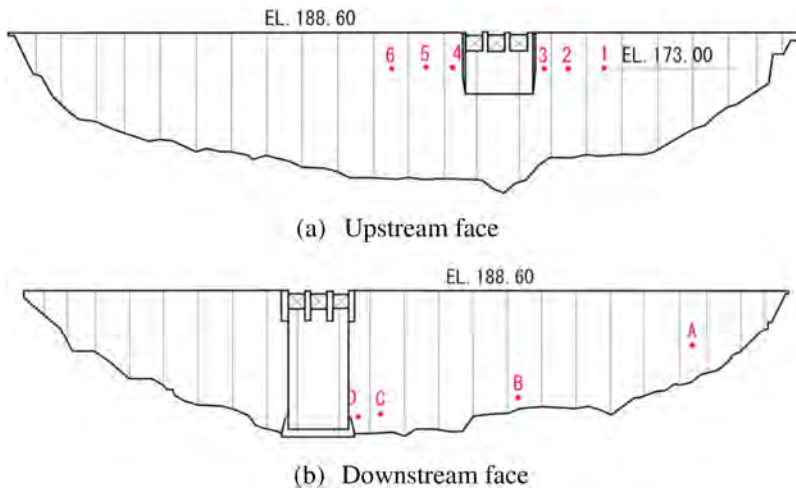


Fig. 2
Locations of the sampled core
Emplacements de la carotte échantillonnée

2.2.1. Compressive and tensile strength of the existing dam concrete

Uniaxial compression tests were performed on the core specimens of each mix and each depth sampled. Fig. 3 shows the relationship between the compressive strength of the existing dam concrete and the unit weight of the concrete. The compressive strength increases as the unit weight of the concrete increases. There is a relatively good correlation, although there is some variation between them. The same figure also shows the results of the quality control test carried out during the construction of the existing dam body (at a material age of 91 days). This comparison shows that the compressive strength of the core specimens is generally equal to or greater than the test results during the construction of the existing dam.

The results of the splitting tensile strength tests of the core specimens are shown in Fig. 4 as a function of unit weight. Although there is more variation than in the compression test results, Fig. 4 generally shows that the tensile strength increases slightly with increasing unit weight. Comparing the approximately linear trend of the splitting tensile strength with that of the compressive strength, the tensile strength is in the range of 1/13 to 1/10 of the compressive strength.

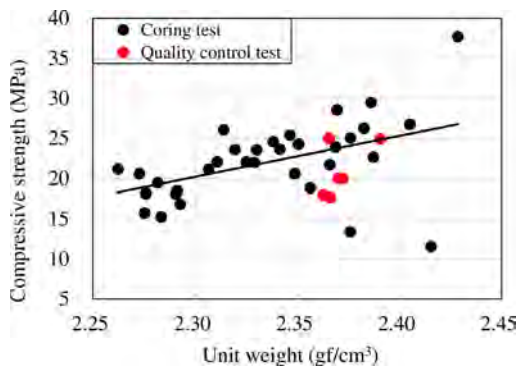


Fig. 3
Relationship between the unit weight and compressive strength
Relation entre le poids unitaire et la résistance à la compression

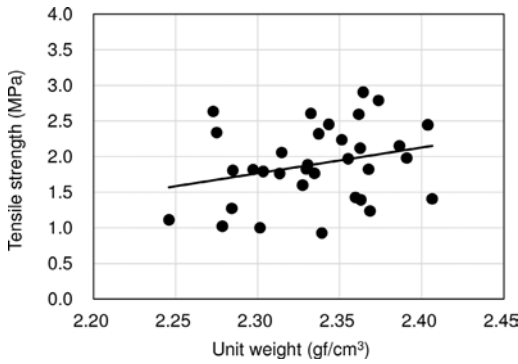


Fig. 4
Relationship between tensile strength and unit weight of concrete specimens
Relation entre la résistance à la traction et le poids unitaire des éprouvettes de béton

2.2.2. Elastic modulus of dam concrete

In the uniaxial compression test of the core specimen described in the previous section, the initial tangential slope of the stress–strain curve is taken as the static elastic modulus of the concrete. The relationship between the static elastic modulus and the compressive strength of the specimen is shown in Fig. 5. The results in this figure are compared with the correlation between the compressive strength and the static elastic modulus from nationwide survey results, as shown in

the Standard Specifications for Concrete Structure (Design) [4]. Although there is variation in the test results of the core specimens, the elastic modulus is maintained at the same level as that of ordinary concrete if the unit weight is 2.3 gf/cm^3 or more. This indicates that the elastic modulus has not deteriorated, even after 67 years. Core specimens with a unit weight of 2.3 gf/cm^3 or less were taken from the internal concrete and were found to have an average static elastic modulus of $15,000 \text{ N/mm}^2$ or greater. Fig. 6 shows the test results of the static and dynamic elastic moduli conducted on core specimens taken from the dam body using the same aggregate as that used in the Katsurazawa Dam. This figure shows that the dynamic elastic modulus is 1.0-1.4 times the static modulus, with an average value of 1.22 times.

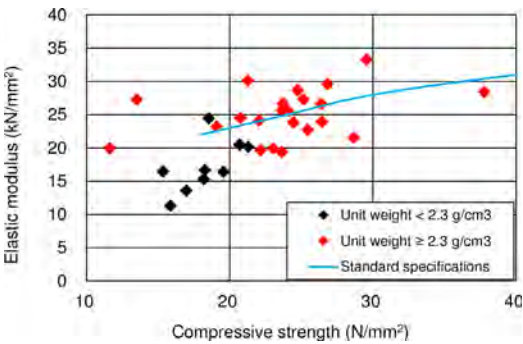


Fig. 5
Relationship between the elastic modulus and compressive strength
Relation entre le module élastique et la résistance à la compression

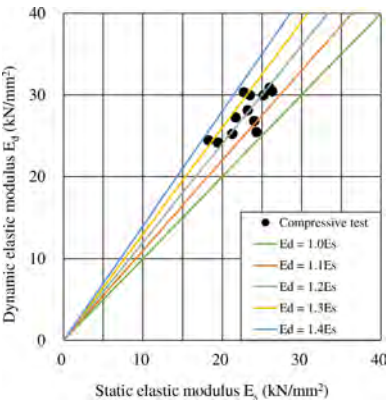


Fig. 6
Relationship between the static and dynamic moduli
Relation entre les modules statiques et dynamiques

The compressive strength, tensile strength, and elastic modulus of the concrete of the Katsurazawa Dam measured 67 years after its completion were clarified by material tests using the above core specimens. The data necessary for evaluating the seismic performance of the dam were thus obtained.

3. OPTIMIZATION OF THE CONSTRUCTION PLAN FOR DAM HEIGHTENING DURING ITS OPERATION

There are several issues to be addressed for coaxial heightening of concrete gravity dams, including coordination with reservoir operations, accounting for the thermal stress of the concrete, and ensuring the seismic resistance of the dam after completion.

It is common to heighten an existing dam while maintaining its functions. The existing dam is deformed by hydrostatic pressure, and stress is generated inside. The concrete for the new dam body is poured in this state. Therefore, a stress discontinuity is generated between the existing and new dam bodies. When the reservoir water level drops after the dam heightening work, the existing dam body is restrained by the new dam body and does not return to its original state. In this chapter, the effects of reservoir water during heightening are examined. For year-round operation of the reservoir, the optimization of the heightening procedure is investigated to prevent excessive stress at the boundary between the existing and new dam bodies and at the bottom of the new dam body. For this purpose, the lowest-water level, the high-water level, and the intermediate water levels (9 levels) for the existing dam are set, and the heightening procedure of the new dam body under each water condition is simulated.

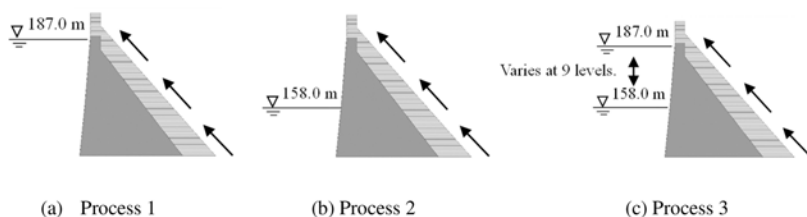


Fig. 7

Heightening processes of different water levels
Processus d'élévation de différents niveaux d'eau

3.1. ANALYSIS CONDITIONS

Fig. 7 shows the assumed heightening processes for different water levels. The newly constructed dam body was assumed to be heightened sequentially in 24 steps. The bottom of the bedrock foundation is fixed, and the lateral boundaries are vertical rollers. Fig. 8 shows the analysis process assuming heightening and reservoir level fluctuations. Process 1 and Process 2 assume that the heightening of the dam body is carried out under the conditions of a high-water level and a lowest-water level for the existing dam, respectively. Process 3 assumes that the heightening is performed under the year-round operation, i.e., fluctuations in the water level. Specifically, four fluctuation patterns of the water level for Process 3 are assumed. In the first and second patterns, the water level monotonically rises and falls, respectively. In the third pattern, the water level falls during the first half and rises during the second half of the heightening work, and the fourth pattern is the reverse of the third one. After the heightening process is completed, stress analyses of the existing and new dam bodies of the new high-water level and the lowest-water level were conducted, and the results were compared.

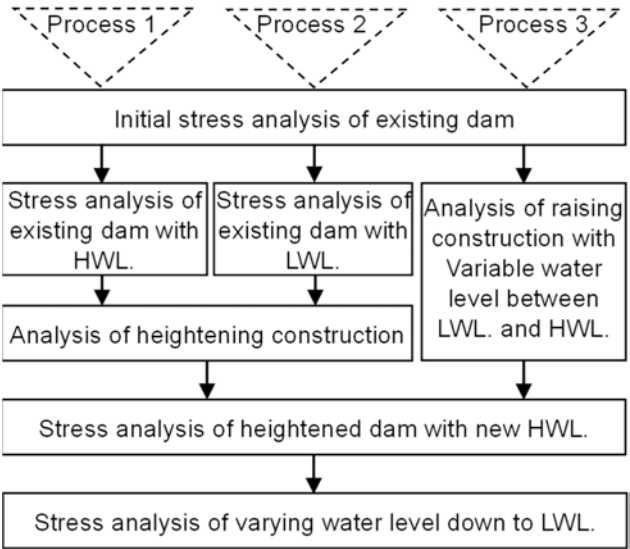


Fig. 8
Process of heightening
Processus de rehaussement

3.1.1. *Reservoir water level during heightening*

The following 3 states were considered:

- The lowest-water level: EL.158.0 m.
- The high-water level for the existing dam: EL.187.0 m.
- The fluctuating water level, with 9 water levels between the lowest-water level and the high-water level.

3.1.2. *Physical properties (linear)*

The physical properties of the concrete for both the existing and the new dam bodies were set based on the test results of the core specimens, while the physical properties of the foundation rock were set based on the rock test results. Table 2 summarizes the physical properties used in the analysis.

Table 2
Material properties used in the analysis

Item	Static elastic modulus (kN/mm ²)	Poisson's ratio	Unit weight (gf/cm ³)
Concrete	23.000 Test of core specimens	0.2	2.3 Test of core specimens
Foundation rock	14.040 In-Situ test	0.3	2.45 Rock test

3.2. ANALYSIS RESULTS

Fig. 9 shows the maximum principal stress (tensile side) that occurs in the dam body when the water level falls to the lowest-water level after the completion of

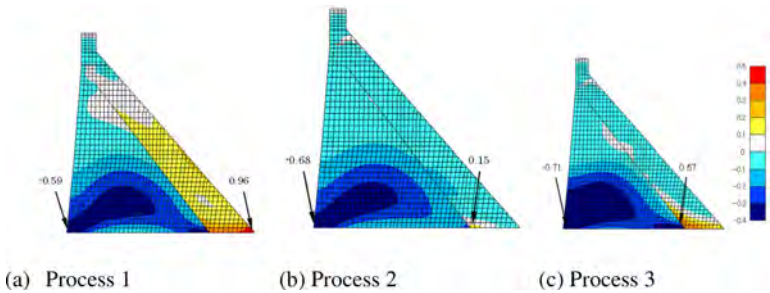


Fig. 9

Maximum principal stress due to drawdown of the water level after the completion of heightening construction

Contrainte principale maximale due à la baisse du niveau d'eau après l'achèvement des travaux de surélévation

the heightening. In Process 1, when the dam is heightened at the high-water level for the existing dam, tensile stress is generated in almost all areas of the newly constructed dam body except near the crest due to the decrease in the reservoir water level. The lower the elevation is, the greater the value of tensile stress, with a maximum of less than 1 MPa at the toe of the dam body. In contrast, in Process 2, when the dam is heightened at the lowest-water level, the stress in the dam body after completion is generally compressive. However, as mentioned earlier, it is not realistic to maintain the reservoir at the lowest-water level because the heightening of a dam body is actually performed under the normal operating conditions of the reservoir. Therefore, the heightening of the dam in a state of fluctuation of the reservoir level (Process 3) was simulated and compared with the analysis results of Processes 1 and 2. The new dam body at higher elevations (from approximately 1/2 of the height to the crest of the existing dam) should be constructed with as low a reservoir water level as possible. On the other hand, the construction of the lower elevation of the new dam body can be performed under any reservoir water level conditions, even if the reservoir water is at a high level. In addition, the stress in the new dam body at a higher elevation above the existing dam crest is not affected by the reservoir water level. If the water level monotonically decreases from the high-water level to the lowest water level during heightening and concrete is successively poured from the bottom to the new crest (in 24 stages), the maximum principal stress of the dam after completion can be predicted, as shown in Fig. 9(c). Although tensile stress occurs at the bottom of the new dam body in Process 3, it is considerably relieved compared to that of Process 1 and is close to the result of Process 2. The difference in the maximum principal stress between Process 1 and Process 3 is shown in Fig. 10. This figure suggests that this degree of tensile stress in the dam body can be avoided if the heightening is planned in accordance with reservoir operations (reservoir level adjustment).

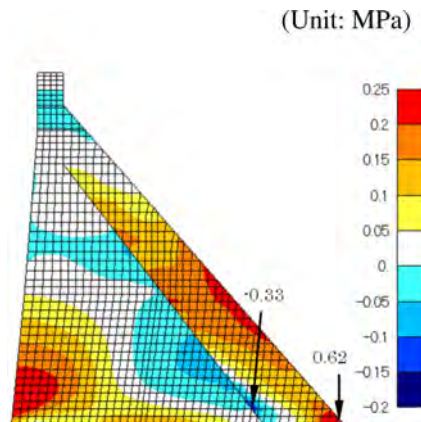


Fig. 10

Difference in the maximum principal stress between Process 1 and Process 3
Différence de contrainte principale maximale entre le processus 1 et le processus 3

Therefore, it is recommended that dam heightening work be performed under the lowest possible water level conditions. When heightening a dam while operating the reservoir year-round, as shown in Fig. 11, the effect of the water level on the stress of the placed concrete at the lower elevation (Zone L: up to approximately 1/2 of the height of the existing dam) is small, even when the water level is high. However, concrete placing at higher elevations (Zone H: from approximately 1/2 of the height of the existing dam to the crest) should be performed when the water level is as low as possible. On the other hand, the stress of the new dam body above the crest of the existing dam (Zone T) will not be significantly affected by any water level. Such a construction plan will reduce the tensile stress inside the heightened dam body after completion due to fluctuations in the water level.

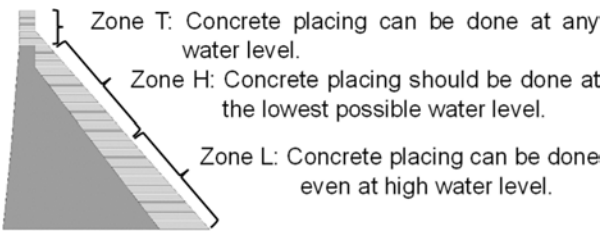


Fig. 11

The proposal of construction plan of heightening
La proposition de plan de construction de surélévation

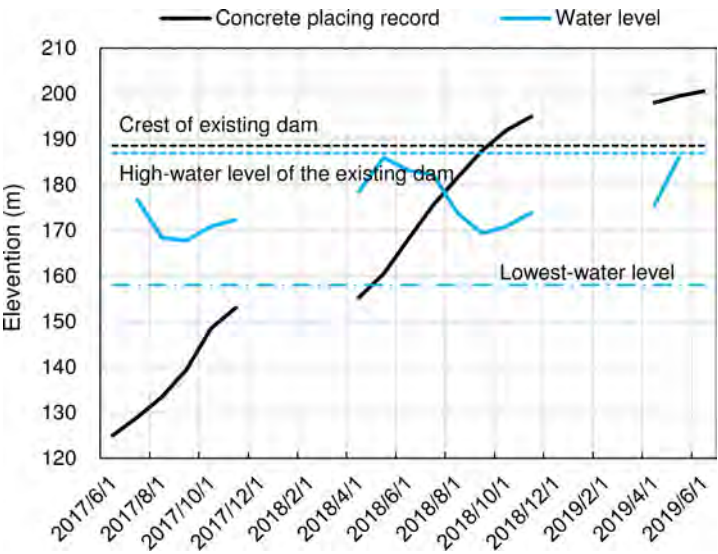


Fig. 12

The relationship between reservoir water level and concrete placing
La relation entre le niveau d'eau du réservoir et la mise en place du béton

3.3. HEIGHTENING RECORDS OF THE SHIN-KATSURAZAWA DAM

Fig. 12 shows the actual construction records of the heightening of the Shin-Katsurazawa Dam and the reservoir water level. The concrete of the new dam body at an elevation between EL.170 m and the crest of the existing dam (EL.188.6 m) was placed during a period when the water level decreased from EL.182 m to EL.170 m. After April 2019, although the water level increased, the concrete placing of the new dam body was at a higher elevation than the crest of the existing dam. Therefore, the new dam body was almost unaffected by the water level.

From the above, it was inferred that the effect of the reservoir water level on the stresses of the dam body during the heightening of the Katsurazawa Dam was limited.

4. CONCLUSIONS

The following conclusions were drawn from this study:

1. The mechanical properties of the original dam concrete in its present condition were clarified by reviewing the results of material tests of core specimens of dam concrete 67 years old. Compared to the data published in the Standard Specifications for Concrete, the elastic modulus of the dam concrete has not decreased 67 years after its completion. The test results also revealed the relationships between the unit weight and compressive strength and between the unit weight and tensile strength. Furthermore, the relationships between the compressive strength and elastic modulus and between the static and dynamic elastic moduli were clarified.
2. When an existing dam is heightened under the condition of a relatively high-water level, stress will remain in the existing dam and new dam body, even when the water level decreases after heightening. Heightening construction at the lowest possible reservoir level is advantageous. In the case of heightening under the year-round operation of reservoirs, it was proposed that concrete at relatively high elevations should be placed when the reservoir level is relatively low.

REFERENCES

- [1] RIVER PLANNING DIVISION, WATER MANAGEMENT AND LAND CONSERVATION BUREAU, MLIT. The amount of damage caused by floods

in 2028, the year of the East Japan typhoon, was the largest since statistics began, -Disclosure of the amount of damage caused by floods in 2028 (confirmed value), *Press Release*, March 31, 2021 (in Japanese).

- [2] NARIO YASUDA, ZENGYAN CAO, TAKAHIRO MANO, TADASHI NISHIMURA. Investigation of the material and vibration properties of a heightened concrete gravity dam, *Symposium "Dams for People, Water and Environment and Development" – 92nd ICOLD Annual Meeting – New Delhi, India 29 Sept. – 03 Oct. 2024*
- [3] KOJI YAMADA, TSUKASA FUJITA, YUICHI YASUDA. Quality of the existing embankment concrete at the time of the Shin-Katsurazawa Dam construction, Concrete elongation capacity test and evaluation, *47th Technical Research Presentation Meeting of Hokkaido Development Bureau*, 2004 (in Japanese)
- [4] JAPAN SOCIETY OF CIVIL ENGINEERS: Standard Specifications for Concrete Structures (Design), *Gihodo shuppan Co., Ltd.*, 1997

COMMISSION INTERNATIONALE DES
GRANDS BARRAGES

VINGT-HUITIEME CONGRES DES
GRANDS BARRAGES
CHENGDU, MAI 2025

LARGE-SCALE RESERVOIR DAM MANAGEMENT AIMED AT MITIGATION OF LONG-TERM TURBIDITY IN THE HITOTSUSE RIVER (*)

Kazuki TOKUNAGA, Eiji WADA, Kazuyoshi YUKIMURA & Katsuma HIGUCHI
Engineers, Miyazaki Branch, KYUSHU ELECTRIC POWER COMPANY

Yoshihiro SUZUKI
*Professor, Department of Civil and Environmental Engineering,
University of Miyazaki*

JAPAN

SUMMARY

Constructed by Kyushu Electric Power Company in 1963, Hitotsuse Dam is a large-scale electric power generating dam with a total reservoir capacity of 260 million m³, located in the midstream of the Hitotsuse River which flows down through the central region of Miyazaki Prefecture, on the island of Kyushu, Japan. Soon after operation of the power station commenced, "long-term turbidity" occurred caused by continued discharge of high-turbidity water from the dam, impacting water use, the fishing industry and riverscape.

With the aim of mitigating long-term turbidity, Kyushu Electric Power Company has studied and implemented a series of turbidity-mitigation methods. Until 2005, by carrying out water intake from the lower section of a selective water intake facility following flood, turbid water was discharged from the dam reservoir. This was the first time for a selective water intake method to be adopted in Japan and was effective in mitigating long-term turbidity.

**Gestion d'un grand barrage-réservoir visant à atténuer la turbidité à long terme dans le fleuve Hitotsuse*

However, when flood on the largest scale ever recorded for the river resulting from Typhoon Nabi in 2005 caused huge inflows of turbid water into the dam reservoir, the effects of turbidity measures were limited. It became clear that with the measures adopted up until 2005, long-term turbidity could not be avoided.

As a result of studies carried out through collaboration between industry, government, academia and private individuals, new measures were created. Under these measures, in times of large-scale flood, large quantities of turbid water are to be promptly discharged from the dam, reducing water level down to the dead water region, then the dam reservoir is to be replenished with clean water thereby diluting the turbid water.

When Typhoon Nanmadol struck Miyazaki Prefecture in September 2022, maximum inflow into Hitotsuse Dam was comparable to the highest maximum ever recorded—that for Typhoon Nabi in 2005. A huge amount of suspended solids flowed into the dam reservoir, and for the first time since their formulation in 2008 the new measures were implemented.

As a result of implementing the new measures, by discharging 70 % of water in the Hitotsuse Dam reservoir, including that in the dead water region, downstream, approximately 93 % of the amount of suspended solids in the reservoir was discharged. Further, the period of turbidity in the downstream was approximately 4 months, that is, 4 months shorter than the maximum period of 8 months for 2005.

From the above, it was confirmed that by using the emergency outlet located in the base of the dam to promptly discharge turbid water and thereby reduce water level to the dead water region, even in the case of large-scale flood, mitigation of long-term turbidity in the downstream could be achieved to a certain extent.

RÉSUMÉ

Construit par Kyushu Electric Power Company en 1963, le barrage de Hitotsuse est un grand barrage hydroélectrique avec un réservoir d'une capacité totale de 260 millions de m³, situé à mi-parcours du fleuve Hitotsuse qui traverse le centre de la préfecture de Miyazaki, sur l'île de Kyushu, au Japon. Peu après le début de l'exploitation de la centrale électrique, un phénomène de « turbidité prolongée » est apparu, qui était causé par le déversement continu d'eau fortement turbide depuis le barrage et qui a eu des conséquences sur l'utilisation de l'eau, l'industrie de la pêche et le paysage fluvial.

Afin de réduire cette turbidité prolongée, Kyushu Electric Power Company a étudié et mis en œuvre une série de méthodes de réduction de la turbidité. Jusqu'en 2005, le prélèvement d'eau s'effectuait après les crues à partir de la section inférieure de l'installation de prise d'eau sélective et l'eau turbide était déversée depuis le

réservoir du barrage. C'était la première fois qu'une méthode de prise sélective était adoptée au Japon et elle s'est avérée efficace pour réduire la turbidité prolongée.

Cependant, en 2005, lors des crues les plus importantes jamais enregistrées, causées par le typhon Nabi, d'énormes quantités d'eau turbide ont afflué dans le réservoir du barrage, limitant l'efficacité des mesures prises contre la turbidité. Il est alors devenu clair que les mesures mises en place jusqu'en 2005 ne pouvaient pas empêcher la turbidité prolongée.

À la suite d'études menées en collaboration avec l'industrie, le gouvernement, des universités et des particuliers, de nouvelles mesures ont été prises, considérant qu'après des crues de grande ampleur, il serait efficace, pour améliorer l'environnement en aval, de décharger rapidement de grandes quantités d'eau turbide du barrage de Hitotsuse, puis de remplir le réservoir du barrage avec de l'eau propre et de diluer ainsi l'eau turbide.

Lorsque le typhon Nanmadol a frappé la préfecture de Miyazaki en septembre 2022, le débit maximal dans le barrage de Hitotsuse était comparable au débit maximal le plus élevé jamais enregistré lors du typhon Nabi en 2005. Une énorme quantité de matières en suspension a donc afflué dans le réservoir du barrage d'Hitotsuse et, pour la première fois, les nouvelles mesures élaborées en 2008, ont été mises en œuvre.

Grâce à la mise en œuvre de ces nouvelles mesures, l'évacuation en aval de 70 % de l'eau contenue dans le réservoir du barrage d'Hitotsuse, y compris celle de la zone d'eau morte, a permis d'éliminer environ 93 % des matières en suspension dans ce réservoir. En outre, la période de turbidité en aval a ainsi été réduite à environ 4 mois, c'est-à-dire 4 mois de moins que la période maximale de 8 mois observée en 2005.

D'après ce qui précède, il a été confirmé qu'en utilisant l'installation de vidange d'urgence situé à la base du barrage pour évacuer rapidement l'eau turbide et abaisser ainsi le niveau de l'eau jusqu'à la zone d'eau morte, il est possible, dans une certaine mesure, de réduire la turbidité prolongée en aval, même en cas de crues de grande envergure.

1. INTRODUCTION

Since ancient times the Japanese people have used river water to irrigate their paddy fields, and thereby came to live with an intimate connection with rivers. This connection with rivers was subsequently expressed in different artforms such as literature and painting, as well as performing arts including *Noh* and *Kabuki*. And further, through this artistic expression, the particular, Japanese view of "rivers being clear and pure, and having scenic beauty" developed. This perspective of rivers

continues today with strong recognition amongst Japanese that river water be transparent and clean, and form beautiful landscape [1].

Constructed by Kyushu Electric Power Company in 1963, Hitotsuse Dam is a large-scale electric power generating dam with a total reservoir capacity of 260 million m³, located in the midstream of the Hitotsuse River which flows down through the central region of Miyazaki Prefecture, on the island of Kyushu, Japan. Since around 1965, highly turbid dam discharge was seen for months at a time in the river downstream of Hitotsuse Dam (hereinafter, long-term turbidity), affecting water utilization, the fishing industry, and scenic beauty of the river. With the aim of mitigating long-term turbidity, Kyushu Electric Power Company has studied and implemented a series of turbidity-mitigation methods [2][3]. This paper summarizes the measures taken against the problem of long-term turbidity that began to occur soon after the Hitotsuse Power Station started operation, and the effects of those measures.

2. OVERVIEW OF THE HITOTSUSE RIVER BASIN

Sourced from Mt. Ichifusa and Mt. Ishinita, located in a mountainous area on the island of Kyushu, Japan, the Hitotsuse River flows in a southeasterly direction down through the central region of Miyazaki Prefecture into the Hyuga Nada Sea. Its mainstream length is approximately 88 km, and the river basin covers about 852 km². The Hitotsuse Power Station (Dam) and the Sugiyasu Power Station (Dam) (Fig. 1, Table 1) are located in the central part of the Hitotsuse River basin.

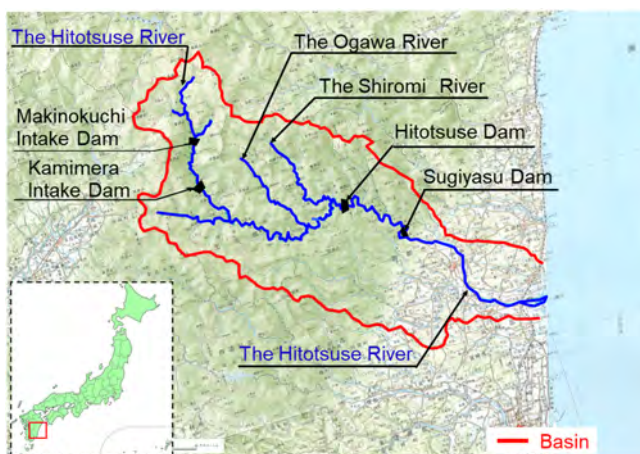


Fig. 1
Map of the Hitotsuse River Basin
Carte du bassin du fleuve Hitotsuse

Table 1
Power Station (Dam) Specifications

Item	Hitotsuse	Sugiyasu
Type	Concrete arch	Concrete arch
Crest length x dam height	415.62 m x 130.00 m	156.00 m x 39.50 m
Design flood flow	4,400 m ³ /s	4,800 m ³ /s
Watershed area	415.00 km ²	485.70 km ²
Total reservoir capacity	261,000,000 m ³	9,000,000 m ³
Available depth	30.00 m	3.50 m
Installed capacity	180,000 kW	11,500 kW
Maximum water usage	137.00 m ³ /s	60.00 m ³ /s
Maximum effective head	151.99 m	22.60 m

3. OVERVIEW OF LONG-TERM TURBIDITY

3.1. DEFINITION OF TURBIDITY IN THE HITOTSUSE RIVER BASIN

In the Hitotsuse River basin, on the premise that sweet fish habitat be unaffected, and as a result of surveying and studying baseline values for qualitative landscape in records and for other water systems, turbid water is defined as water which exceeds a turbidity of 10 ppm. This level has been reached by consensus with river basin stakeholders.

3.2. CONCEPT OF TURBIDITY IN THE HITOTSUSE RIVER BASIN

The turbidity in the Hitotsuse River basin is measured as ppm by an integrating sphere turbidimeter by changing the reading from “degree (kaolin)” to ppm. While the environmental quality standard (Type AA or Type A) generally used for rivers is 25 mg/L or less SS (suspended solids), the Hitotsuse River basin is managed using the additional and unique standard for turbidity of 10 ppm or less.

Both turbidity and SS are measured in the Hitotsuse River and the Hitotsuse Dam reservoir, and it has been confirmed that they have an approximate 1:1 relationship.

3.3. CONCEPT OF NUMBER OF DAYS IN LONG-TERM TURBIDITY

The number of days in long-term turbidity is estimated as the number of days of turbidity at the point of Sugiyasu Bridge, which is downstream of Hitotsuse Dam, minus the number of days in turbidity at an observation point in a village, which is upstream of the Hitotsuse Dam reservoir (Fig. 2).

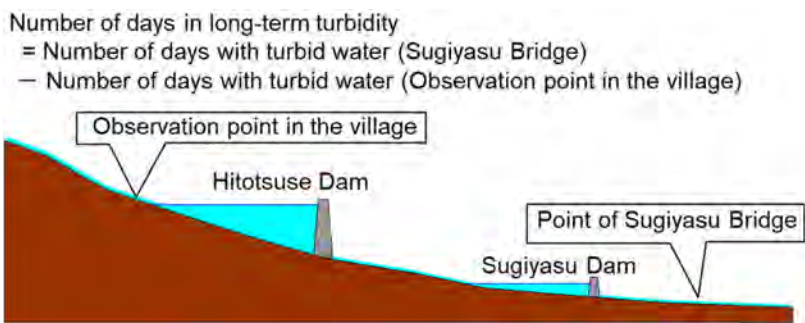


Fig. 2
Concept for estimating number of days in long-term turbidity
Modèle d'estimation du nombre de jours de turbidité à long terme

3.4. CAUSES OF LONG-TERM TURBIDITY

Long-term turbidity has four causes, which can be divided into two: those relating to the area upstream of Hitotsuse Dam, and those relating to the mid- to downstream area (Table 2).

Table 2
Causes of long-term turbidity

Area	Cause
Upstream area (The Hitotsuse Dam reservoir and further upstream)	Slope failure due to forest devastation
	Soil and sand contained in water being highly resistant to settling (suspended solids)
Mid- to downstream area (Downstream of the Hitotsuse Dam reservoir)	Large-scale dam reservoir which accumulates inflows of turbid water
	Mixing throughout the dam reservoir due to winter convection

3.5. MECHANISM OF LONG-TERM TURBIDITY

From around November, due to the decreasing temperature of the surface layer of the dam reservoir, winter convection begins, giving rise to mixing of the entire dam reservoir. With this, suspended solids in the process of settling become re-suspended and the water becomes turbid again. As a result of this, turbidity within the dam reservoir becomes long-term, and due to the effect of discharge from power generation, long-term turbidity also occurs in the downstream (Fig. 3).

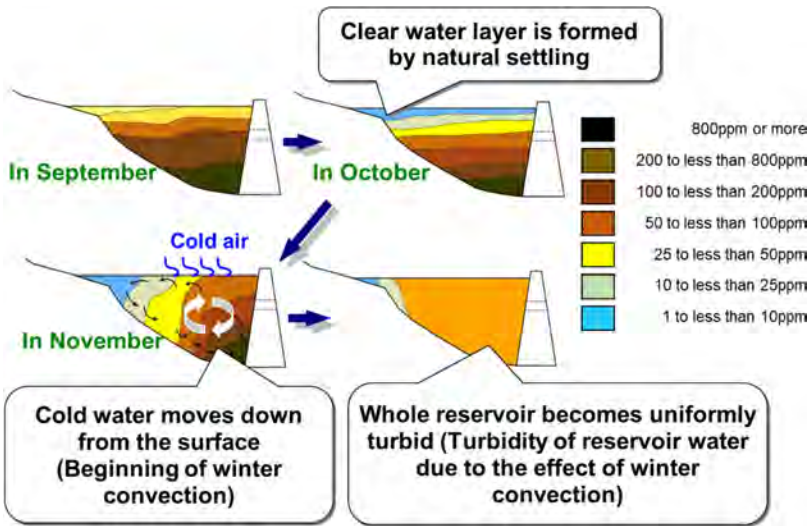


Fig. 3
Winter convection within dam reservoir
Convection hivernale dans le réservoir du barrage

4. OVERVIEW OF TURBIDITY MITIGATION MEASURES UNTIL 2005

4.1. INSTALLATION AND OPERATION OF SELECTIVE WATER INTAKE FACILITY

Having been requested in 1972 by the Miyazaki Prefectural Government to improve the dam's water intake facility, in 1974 Kyushu Electric Power Company installed Japan's first selective water intake facility, with the objective of turbid water removal by selecting water intake from the upper or lower layers following flood (Fig. 4, 5).



Fig. 4
Selective water intake facility
Installation de prise d'eau selective

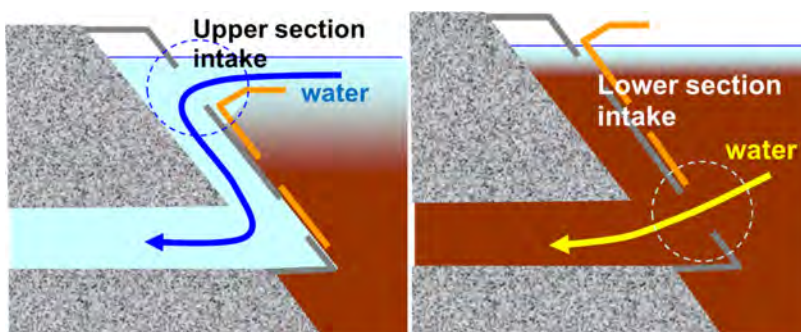


Fig. 5
Image of selective water intake facility operation
Illustration de l'installation de prise d'eau selective

This facility operates as follows: Before flood, the dam reservoir is in a clean condition as shown in Fig. 6[1]. Following flood, turbid water flows into the dam reservoir and the highly concentrated turbid water is drawn from the lower section for power generation and then discharged downstream of the dam, as shown in

Fig. 6[2]. Subsequently, with the formation of a clean surface layer of the dam reservoir, referred to as the clear water layer, selective water intake is switched from the lower section to the upper section as shown in Fig. 6[3]. By using clean water from the surface layer for power generation intake, this clean water is discharged downstream as shown in Fig. 6[4]. In this way, cleansing of water in the downstream is promoted.

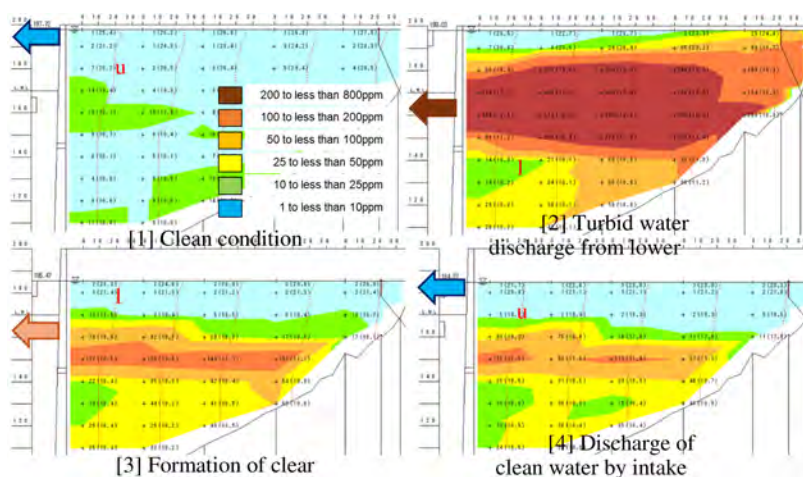


Fig. 6

Selective water intake facility operation method based on actual turbidity distribution diagram

Méthode de gestion d'une installation de prise d'eau sélective basée sur le diagramme d'une distribution réelle de la turbidité

4.2. INSTALLATION OF TURBIDITY CONTROL FENCE

In 1999, with the aim of protecting the reservoir's clean water layer from turbid inflows from the main Hitotsuse River and its tributary Shiromi River, a turbidity control fence, vinyl and impervious to water, was installed. In cases of small-scale flood with flow rates up to $300 \text{ m}^3/\text{s}$, it can be anticipated that turbid water will be diverted under the fence thereby maintaining the clear water layer (Fig. 7).

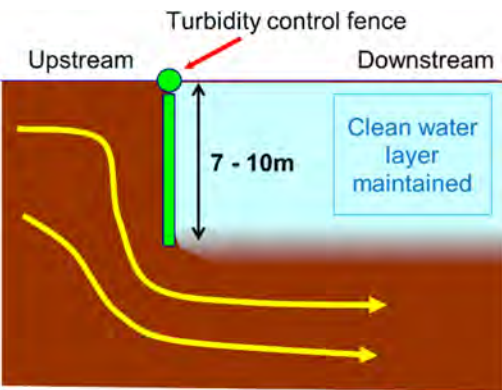


Fig. 7
Image of turbidity control fence
Représentation d'une barrière de contrôle de la turbidité

4.3. INSTALLATION OF SELECTIVE WATER INTAKE FACILITY HOOD

In 2002, hood equipment as shown in Fig. 8 was installed to reduce intake water flow velocity and thereby control the rise of lower layered turbid water. As shown in Fig. 6[4], this can control the rise of turbid water suspended directly below the clear water layer. Up until the present time, the installation of hood equipment has not resulted in an up-flow of turbid water during water intake from the upper section.

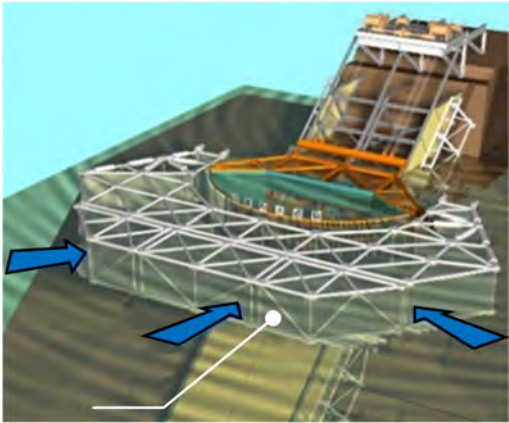


Fig. 8
Schematic view of hood and water flow
Vue schématique de l'auvent et de la circulation de l'eau

5. LONG-TERM TURBIDITY DUE TO TYPHOON NABI IN 2005

5.1. OVERVIEW

During the period from September 4 to 6, 2005, Miyazaki Prefecture was struck by Typhoon Nabi. Maximum hourly rainfall was 31 mm/h and total rainfall amounted to 754 mm, giving rise to flooding in various parts of the Hitotsuse River basin.

The effects on the Hitotsuse Dam reservoir due to Typhoon Nabi were a maximum inflow volume of 4,439 m³/s, the highest ever recorded, together with a 200,000 ton[†] inflow of suspended solids, the largest amount ever (Fig. 9).



Fig. 9
Hitotsuse Dam following Typhoon Nabi in 2005
Barrage de Hitotsuse après le typhon Nabi en 2005

Turbidity in the Hitotsuse River downstream of the dam continued for 8 months, becoming a major social problem in the region around the dam.

5.2. EFFECTS OF LONG-TERM TURBIDITY

There was very considerable impact on the area downstream of Hitotsuse Dam due to long-term turbidity (Table 3).

[†]Amount of suspended solids calculated according to average turbidity within dam reservoir and volume of water stored.

Table 3
Impact on area downstream of Hitotsuse Dam due to long-term turbidity

Item	Impact
Water supply	Major burden on river water purification
Fishery resources	Lack of growth of riverbed moss causes reduced fishery yields
Agricultural produce (rice, tea, vegetables, etc.)	Water spraying contaminates leaf vegetables leading to lower product quality
Riverscape	Fewer people visit river for tourism or aquatic recreation due to worsened riverscape

5.3. LIMITATION OF TURBIDITY MITIGATION MEASURES EMPLOYED UNTIL 2005

From the commencement of turbid water discharge operation in 1991 until 2005, for floods for which suspended solids were less than 50,000 ton, it was possible to limit the period of long-term turbidity to within 2 weeks due mainly to the operation of the selective water intake facility (Fig. 10).

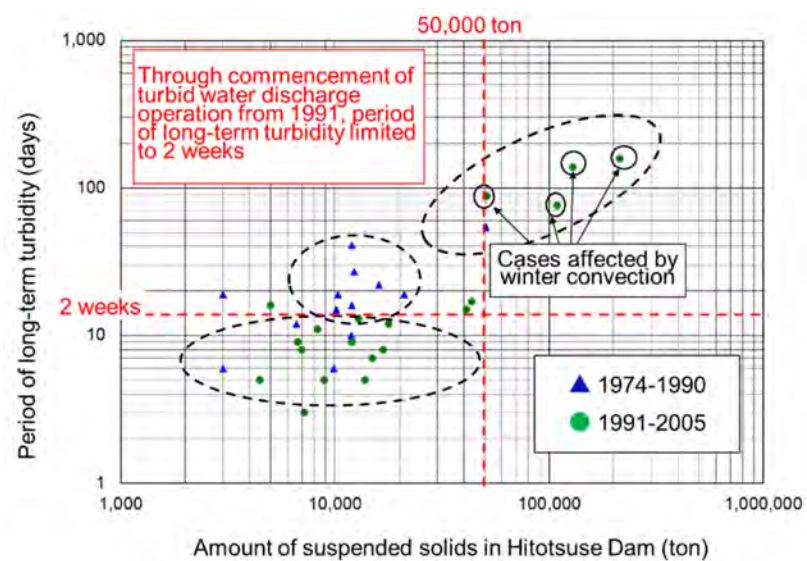


Fig. 10
Relationship between amount of suspended solids and period of long-term turbidity
Relation entre la quantité de matières en suspension et la période prolongée de turbidité

However, with the huge inflow of approximately 200,000 ton of suspended solids due to Typhoon Nabi in 2005, it became clear that the selective water intake facility and other measures implemented have limited effectiveness to avoid long-term turbidity resulting from such typhoons.

6. DEVELOPMENT OF UNIFIED FRAMEWORK FOR ENTIRE RIVER BASIN TO ADDRESS LONG-TERM TURBIDITY

Soon after commencement of operation of the Hitotsuse Power Station in 1963, long-term turbidity became a problem, and up until the present time Kyushu Electric Power Company has responded to various river basin stakeholders on an individual basis. However, there was a gradually growing realization of the need to take a unified approach to long-term turbidity mitigation that would involve stakeholders from the entire river basin. This has been realized, and currently, meetings are held once a year for industry, government, academia and private individual stakeholders (hereinafter Evaluation and Review Committee) to hear explanations on and discuss the yearly implementation status of turbidity measures, and to carry out evaluation and improvement (Fig. 11).



Fig. 11
Evaluation and Review Committee Framework
Structure du Comité d'évaluation et d'examen

7. NEW TURBIDITY MITIGATION MEASURES FORMULATED IN 2008

7.1. NEW MEASURES (MEASURES FOR TURBIDITY MITIGATION THROUGH USE OF EMERGENCY OUTLET AND DISCHARGE FACILITY)

Following Typhoon Nabi which struck in 2005, it became clear that there was a limit to what the turbidity mitigation measures in place then could deal with, so the consideration of new measures was progressed by the Evaluation and Review

Committee. After various studies and analyses, in the case of flood that produced amounts of suspended solids exceeding 50,000 ton, it was considered that it would be effective for downstream environment improvement to promptly discharge large quantities of turbid water from Hitotsuse Dam, then replenish the dam reservoir with clean water thereby diluting the turbid water. The river basin stakeholders' consensus was sought in 2008 regarding the methods ((i) – (iv)) below. Fig. 12 shows a schematic diagram of mitigation measures until 2005, and Fig. 13 new turbidity mitigation measures.

(i) In addition to the existing selective water intake facility used for prompt discharge of turbid water in Hitotsuse Dam, modify the emergency outlet in the base of the dam, and using these facilities, reduce water level to 10 m below the available depth for power generation, which falls within the dead water region, and discharge approximately 70 % of water in the dam reservoir.

(ii) For Sugiyasu Dam located downstream also, install a new discharge facility in the base of the dam, reduce water level to 10.5 m below the available depth for power generation, which falls within the dead water region, and discharge approximately 90 % of water from the dam regulating reservoir.

(iii) Following discharge of turbid water, temporarily reduce amount of compensation discharge, such as for water for agricultural and water supply use to the downstream from Sugiyasu Dam, and promptly replenish the Hitotsuse Dam reservoir with clean water from the upstream to recover the water level in Hitotsuse Dam.

(iv) Following attainment of prescribed target water level in the Hitotsuse Dam reservoir, discharge part of the clean water collected to the downstream.

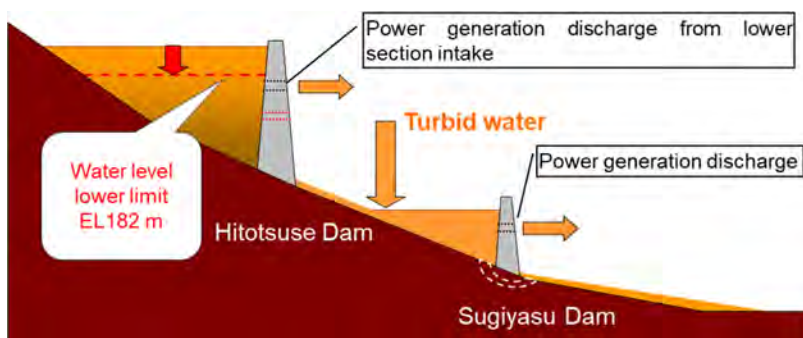


Fig. 12
Turbidity mitigation measures until 2005
Mesures de réduction de la turbidité jusqu'en 2005

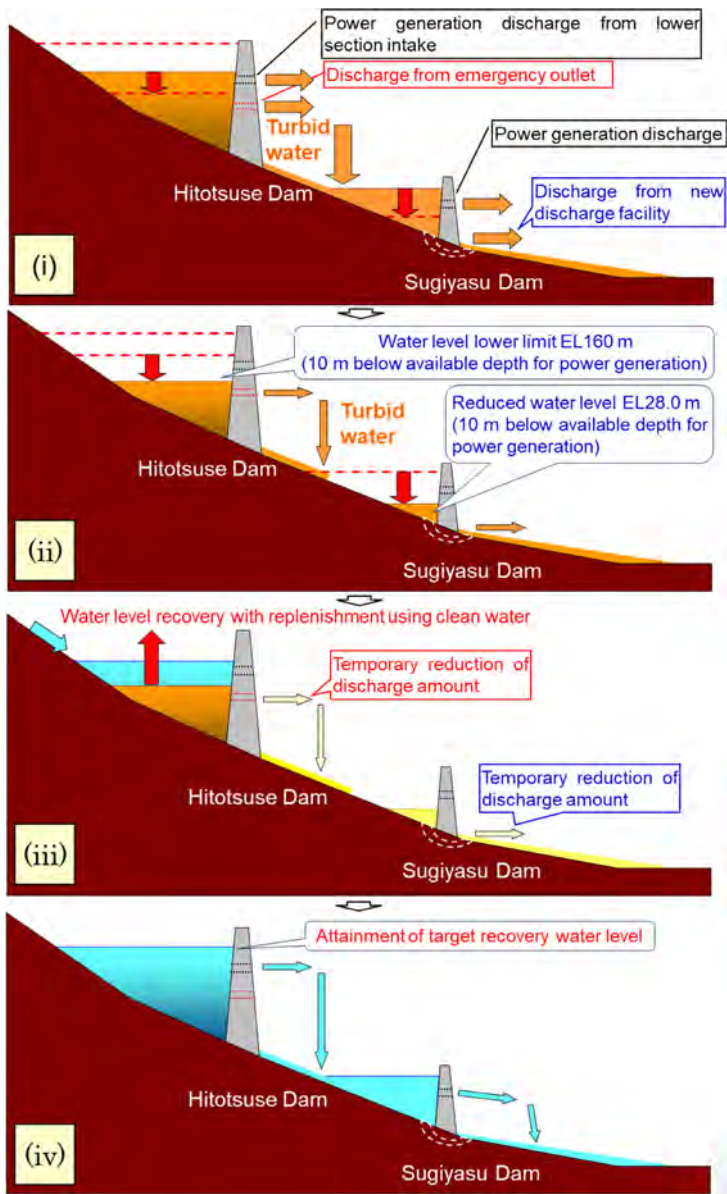


Fig. 13
New turbidity mitigation measures formulated in 2008
Nouvelles mesures de réduction de la turbidité élaborées en 2008

7.2. ENVIRONMENTAL MONITORING SURVEY

As covered in 7.1(iii) above, with the implementation of new measures, the amount of compensation discharge to the downstream from Sugiyasu Dam is temporarily reduced. To understand the environmental effects of this in the downstream, a survey of existing conditions together with analyses and study were conducted. Further, to verify the states of river flow, saltwater intrusion at neap tide, and changes in ground water levels due to reduced discharge amounts, verification testing of reduced discharge amounts was carried out twice in 2007. As a result, it was determined that there was no critical impact due to reduced discharge from which the environment could not recover.

Implementation of environmental monitoring surveys has continued since 2007. The evaluation of results of such surveys are shared and discussed, and improvement promoted at the annual meeting of the Evaluation and Review Committee.

8. FACILITY MODIFICATIONS FROM 2005 TO 2017

8.1. MODIFICATION OF THE EMERGENCY OUTLET IN BASE OF HITOTSUSE DAM [4]

Use of existing selective water intake facility and the emergency outlet can reduce the water level to 10 m below the available depth for power generation, which falls within the dead water region, and enable discharge of approximately 70 % of water in the dam reservoir (Fig. 14).

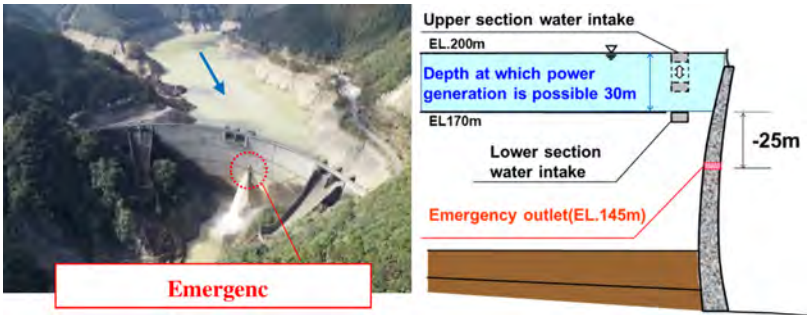


Fig. 14

Emergency outlet of Hitotsuse Dam: Photograph and schematic diagram
*Installation de décharge d'urgence du barrage de Hitotsuse: Photo et schéma
general*

8.2. INSTALLATION OF NEW DISCHARGE FACILITY IN SUGIYASU DAM

The new discharge facility installed at the base of the dam can reduce the water level to 10.5 m below the available depth for power generation, which falls within the dead water region. Therefore, discharge of approximately 90 % of water in the dam reservoir has been made possible (Fig. 15).



Fig. 15

New discharge facility in Sugiyasu Dam: Photograph and schematic diagram
Nouvelle installation de décharge du barrage de Sugiyasu: Photo et schéma général

9. OPERATION AND IMPLEMENTATION OF TURBIDITY MITIGATION MEASURES FORMATULATED IN 2008

9.1. OVERVIEW OF TYPHOON NANMADOL IN 2022

During the period from September 16 to 19, 2022, Miyazaki Prefecture was struck by Typhoon Nanmadol. The section of the river where Hitotsuse Dam is located received maximum hourly rainfall of 47 mm/h and total rainfall amount of 683 mm.

The effect on the dam due to this typhoon was a maximum inflow volume of 4,079 m³/s, comparable that recorded for Typhoon Nabi in 2005, the highest ever recorded.

From the results of a turbidity survey based on on-site measurements following flood, it was judged that the amount of suspended solids in the dam reservoir was at least 50,000 ton. For this reason, for the first time since their formulation in 2008, it was decided to implement and operate the new measures, which utilize the emergency outlet.

9.2. OPERATION AND IMPLEMENTATION OF NEW TURBIDITY MITIGATION MEASURES

From October 15, 2022, reduction of the water level at Hitotsuse Dam was commenced using the emergency outlet. While the speed of reduction was limited to protect reservoir slopes, by November 10, approximately 70 % of the dam reservoir water had been discharged. Following the completion of lowering the water level, with the objective of restoring the water level in the dam, the amount of compensation discharge from the dam, previously agreed at 7 m³/s, was reduced to 6 m³/s.

Downstream of Sugiyasu Dam, leakage in irrigation equipment had occurred making it necessary to continue the discharge of water from the regulating reservoir for irrigation purposes. For this reason, water level reduction was not implemented at Sugiyasu Dam.

9.3. EFFECT OF NEW TURBIDITY MITIGATION MEASURES

As a result of operation and implementation of the new measures, the approximately 60,000 ton of suspended solids in the Hitotsuse Dam reservoir at the end of September was reduced to approximately 4,000 ton by November 11, one day after completing the water level reduction. In other words, discharge had successfully reduced approximately 93 % of the maximum amount of turbid water following flood.

In the downstream of Sugiyasu Dam, following the strike of the typhoon, on September 18 turbidity had exceeded the criterion 10 ppm, and on September 27 the maximum value of 376 ppm was measured. Subsequently, due to the operation and implementation of the new measures, a large amount of turbid water was discharged, and on January 23, 2023, turbidity was reduced to 8ppm, confirming purification of the downstream water.

The period of turbidity downstream of Sugiyasu Dam was about 8 months as a result of Typhoon Nabi in 2005. By comparison, in 2022 due to the new measures, this was cut to around 4 months, a reduction of 4 months (Table 4).

Table 4
Comparison of flood and turbidity mitigation effect in 2005 and 2022

Item	Typhoon Nanmadol 2022	Typhoon Nabi 2005
Period of typhoon	September 16 – 19	September 4 – 6
Amount of rainfall	Total amount 683 mm Maximum hourly 47 mm/h	Total amount 754 mm Maximum hourly 31 mm/h
Maximum inflow amount	4,079 m ³ /s	4,439 m ³ /s
Period of turbidity in downstream	Approx. 4 months	Approx. 8 months

9.4. EFFECTS ON RIVER ENVIRONMENT

The large-scale disruption to the river caused by Typhoon Nanmadol in 2022 and the temporary reduction of compensation discharge, brought about large changes in the following environmental monitoring survey items (survey conducted since 2007): bottom material, fishing industry as well as animals and plants. However, the results of the 2023 monitoring survey showed a definite trend towards recovery. Continued close attention will be given to the process of recovery in the river environment.

10. CONCLUSIONS

The main points made in this paper are as follows:

- Depending on the period and scale of flood, the installation and operation of the selective water intake facility in Hitotsuse Dam can be effective in long-term turbidity mitigation.
- Following large-scale flood which brought an inflow of more than 50,000 ton of suspended solids into Hitotsuse Dam, through use of the emergency outlet at the base of the dam, approximately 70 % of water in the dam reservoir, including the dead water region, was discharged downstream, resulting in successful discharge of 93 % of the amount of suspended solids from the dam reservoir.
- Through operation and implementation of the new measures for turbidity mitigation through use of the emergency outlet, despite Typhoon Nadi in 2005 and Typhoon Nanmadol in 2022 being of similar scale, the period of downstream turbidity resulting from flood for the latter was 4 months shorter than for the former.

Recommendations for future dam projects are as follows:

- The selective water intake facility allows the selective discharge of turbid water from the dam reservoir by switching between the upper layer and the lower layer after flood. Through the installation and operation of this facility, depending on the period and scale of flood, it is possible to effectively mitigate long-term turbidity.
- In case of new large-capacity dam construction in areas where extensive mountainous areas are located in the upstream, long-term turbidity can become a problem. For this reason and for the purpose of prompt removal of turbid water, it is effective to first understand the suspended solid inflow characteristics for the entire river basin and to install a discharge facility in a lower position in the dam body. In addition, by creating a framework for

collaboration between industry, government, academia and private individuals for the resolution of river-basin wide problems, it is possible to mitigate long-term turbidity.

ACKNOWLEDGEMENTS

Through the "Hitotsuse River System Turbidity Measures Evaluation and Study Committee" composed of Miyazaki Prefecture, related cities, towns and villages, universities and Kyushu Electric Power Company, over 10s of years of repeated discussion, study and improvement, turbidity mitigation measures in the Hitotsuse River have been implemented and operated. In connection with implementation of the new measures outlined in this paper, that is, "measures for turbidity mitigation through use of emergency outlet," special gratitude is also due to professor emeritus of the University of Miyazaki, Satoru Sugio, and other people involved for their valuable direction and cooperation.

REFERENCES

- [1] KAWAI M., MIZUNO M. Study on Japanese rivers in view of history and culture – *Japanese and rivers. Report of Riverfront Research Institute*, No. 14 2003, p166–172, (in Japanese).
- [2] TANO J., TASHIRO Y., YATSUGI M. Measures to curb muddy water of Hitotsuse-gawa river (Part 1). *Electric Power Civil Engineering*, No.234, 1991, p46–55, (in Japanese).
- [3] TANO J., TASHIRO Y., YATSUGI M. Measures to curb muddy water of Hitotsuse-gawa river (Part 2). *Electric Power Civil Engineering*, No.237, 1992, p41–51, (in Japanese).
- [4] KAI Y., MURAKAMI T., YOSHITAKE T. Outline of the Hitotsuse Power Station Dam emergency outlet modification work. *Electric Power Civil Engineering*, No. 356, 2011, p26–29, (in Japanese).

COMMISSION INTERNATIONALE DES
GRANDS BARRAGES

VINGT-HUITIEME CONGRES DES
GRANDS BARRAGES
CHENGDU, MAI 2025

**LONG-TERM IN-SITU MONITORING ON DYNAMIC MODULUS OF ELASTICITY
OF DAM CONCRETE AND ITS VERIFICATION BY THE ANALYSIS OF
DAYNAMIC BEHAVIOR OF THE DAM (*)**

Shota NOSAKI & Masayuki KASHIWAYANAGI
*Chigasaki Research Institute, ELECTIRIC POWER DEVELOPMENT
CO., LTD.*

JAPAN

SUMMARY

Japan Commission on Large Dams (JCOLD) has established the technical committee on Research on freeze-thaw impact on dams in 1961. The large scale concrete specimens of 1m cube have been arranged at the six dams sites and been continuously monitored for 60 years since then. J-POWER has participated the research for the Otori dam (VA, 87m high) as well as large scale concrete specimens of the similar mix of the dam.

The dynamic modulus of the elasticity has been perfectly secured in the Otori dam after 60 years passed. The large-scale concrete specimens show different results somewhat according to the mix proportion. These elasticity have been gradually deteriorated to 80 % in minimum. The adverse effect of Fly ash is significant, while the influence of water-cement ratio and AE(Air-Entrained) is not clear. Combined effects can be considered. In addition, it is found that the number of freeze-thaw cycles makes the clear difference in the deterioration of the concrete of the similar mix proportion between the Otori dam and the specimens.

**Surveillance in situ à long terme du module d'élasticité dynamique du béton du barrage et sa vérification par l'analyse du comportement dynamique du barrage*

The current dynamic modulus of the elasticity of the Otori dam is also identified by the reproduction analysis on the Otori dam behavior during the recent earthquake in winter as 40 kN/mm^2 , while a value of 46.9 kN/mm^2 was initially estimated at the surface area of the Otori dam and currently monitored almost as same. Reasons for a certain disagreement in these values between the in-situ measurement and the reproduction analysis are considered as the effect of the zoning of the dam concrete in which the inner concrete is of less cementitious material of 140 kg/m^3 comparing to the outer concrete of 3.5 m thick is of 210 kg/m^3 , and the structural effect due to the transverse joints of the Otori dam which may show less contact pressure in winter. Taking such influences, these values are equivalent. It verifies that both estimation methods for the dynamic modulus of the elasticity of the Otori dam are applicable reasonably.

RÉSUMÉ

JCOLD (Commission japonaise des grands barrages, de l'anglais Japan Commission on Large Dams) a créé en 1961 le comité technique de recherche sur l'impact des cycles gel-dégel sur les barrages. Des échantillons de béton de grande taille (1 mètre cube) ont été disposés sur les sites de six barrages et sont surveillés en continu depuis 60 ans. J-POWER a participé à la recherche pour le barrage d'Otori (VA, 87 m de haut) ainsi que sur des échantillons de béton de grande taille ayant une composition similaire à celle du barrage.

Le module d'élasticité dynamique du barrage s'est parfaitement maintenu après 60 ans. Les échantillons de béton de grande taille présentent des résultats quelque peu différents en fonction de la proportion de la composition du mélange. Leur élasticité s'est progressivement détériorée, jusqu'à atteindre 80 % de la valeur initiale dans le cas le plus défavorable. L'effet négatif des cendres volantes est significatif, tandis que l'influence du rapport eau/ciment et de l'AE (air entraîné) n'est pas claire. Des effets combinés peuvent être envisagés. De plus, il a été constaté que le nombre de cycles gel-dégel est un facteur déterminant dans la détérioration du béton, même pour des proportions de composition de mélanges similaires entre le barrage et les échantillons.

Le module d'élasticité dynamique actuel du barrage a également été identifié par analyse de reproduction du comportement du barrage lors du séisme récent en hiver, à 40 kN/mm^2 , alors qu'une valeur de $46,9 \text{ kN/mm}^2$ a été initialement estimée à la surface du barrage et est actuellement surveillée comme étant presque la même. Les raisons de la légère différence des valeurs pour les mesures in situ et l'analyse de reproduction sont considérées comme provenant de l'effet du zonage du béton du barrage, dans lequel le béton intérieur contient moins de ciment (140 kg/m^3) que

le béton extérieur de 3,5 m d'épaisseur (210 kg/m³), et de l'effet structurel dû aux joints transversaux du barrage qui peuvent présenter une pression de contact moindre en hiver. Compte tenu de ces facteurs, ces valeurs sont équivalentes. Cela confirme que les deux méthodes d'estimation du module d'élasticité dynamique du barrage sont raisonnablement applicables.

1. INTRODUCTION

Cyclic freeze and thaw phenomena of the water contained in concrete cause damages or deterioration on the concrete. It is referred to as freeze-thaw impact. The freeze-thaw impact frequently makes frost damages or deterioration on the concrete structures located in the north area in Japan where snow a lot. Dams located such area could be vulnerable to the freeze-thaw impact. It brings the maintenance issue for the soundness of dams to be verified.

Such as weather, exposure condition, structural dimensions, conditions of embedded steel bars are possible effects on the soundness of dams. It makes the difficulties in the estimation of these effects on the deterioration of real concrete structures by measuring on small-scaled concrete specimen.

Japan Commission on Large Dams (JCOLD) has established the technical committee on Research on freeze-thaw impact on dams (the research committee) in 1961 for the survey on such issue. The large scale concrete specimen of 1 m cube made from the similar mixture of dam concrete have been exposed at the several dam sites including the Kurobe dam (The Kansai Electric Power Co., Inc.), the Midono dam (TEPCO Renewable Power, Inc.) and the Otori dam (Electric Power Development Co., Ltd. (hereinafter referred to as the J-POWER)). The soundness of these specimens has been periodically estimated as well as the degree of the freeze-thaw impact at each dam sites [1] since 1963.

J-POWER have participated the research as a member of the research committee since the beginning. Specimen of the dam concrete have been exposed at two dam sites of the Otori dam and the Senbiri dam. In addition to the concrete specimens, the monitoring on the Otori dam itself has been conducted at the monitoring slot arranged on the upstream surface of the Otori dam. This research has continued over 60 years.

This paper focusses the research at the Otori dam site and presents the monitoring results of the long-term monitoring on the dynamic modulus of elasticity of the specimen and the Otori dam. The freeze-thaw impact is discussed based on the results in terms of the concrete mix proportion. In addition, the dynamic modulus of elasticity of the Otori dam is estimated by the analysis of the dam behavior during

earthquakes for verifying the results. Finally, the soundness of the Otori dam is discussed.

2. LONG-TERM IN-SITU MONITORING ON THE DYNAMIC MODULUS OF ELASTICITY OF DAM CONCRETE

2.1. OUTLINE OF THE MONITORING

The research sites by J-POWER and the view of the Otori dam are shown in Fig. 1. The Otori dam of the thick arch dam (VA) and 83m high has been completed in 1963 for the hydropower and aged over 60years. The reservoir regulates the outflow from the Okutadami hydropower plant by the daily operation with the available water depth of 6 m. The Otori dam is located at the central Japan (Fukushima Pref.) as shown in Fig. 1 where snow a lot and accumulate several meters in winter. These circumstances may cause the concern on the deterioration of the dam due to aging and impact of freeze-thaw cycles. The features of the Otori dam are summarized in Table 1.

To investigate the effects of freeze-thaw action on dam concrete, the dynamic modulus of elasticity, which is relatively easy to measure in situ on dam concrete, was measured. Monitoring slots were placed where the dam is subjected to both water storage and weather effects. This is shown in Fig. 2 and 3.

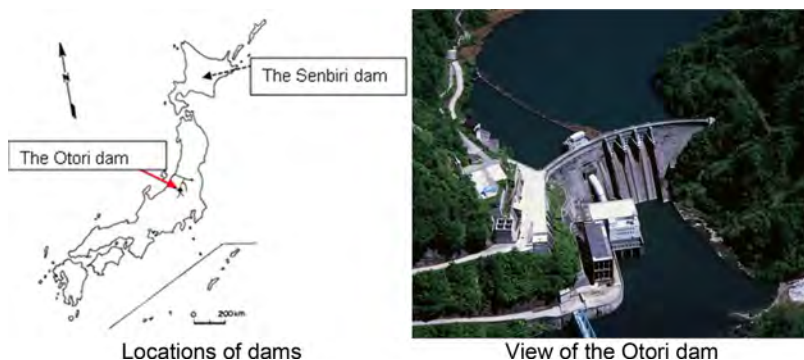


Fig. 1
Locations of monitoring dams
Emplacements des barrages surveillés

Table 1
Characteristics of the Otori dam

Item	Description
Name of dam	Otori
Owner	J-POWER
Completion	1963
Type	Thick arch (VA)
Purpose	Hydropower (182MW)
Dimension	Height: 83 m, Crest Length 188 m
Dam concrete	C+F (30%)Outer 210 kg/m ³ (3.5m thick)Inner 140 kg/m ³

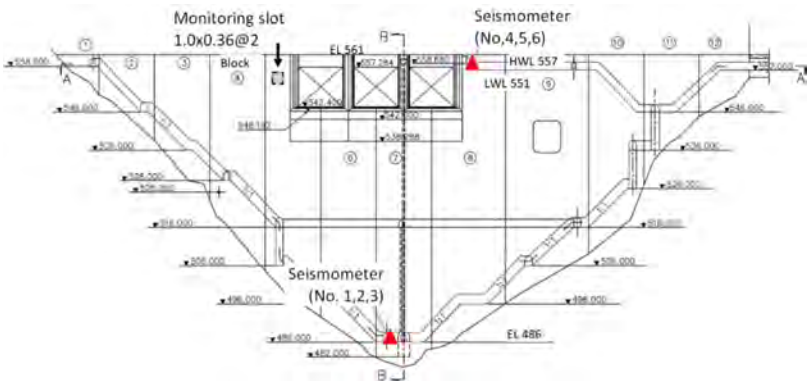
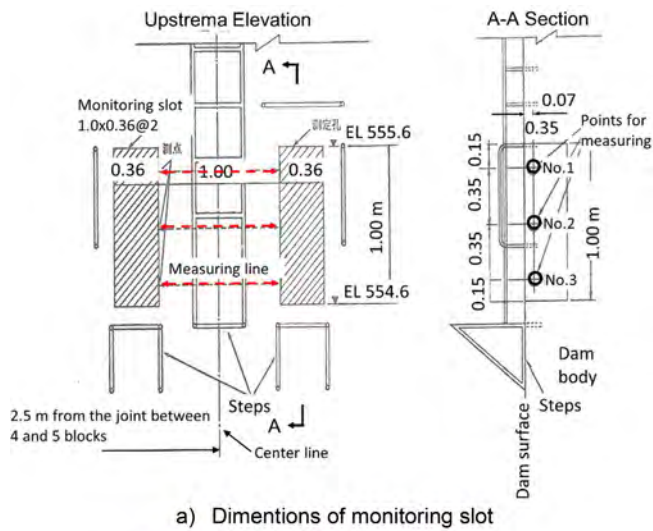


Fig. 2
Locations of monitoring in upstream elevation of the Otori dam
Emplacements de la surveillance en élévation amont du barrage d'Otori

Large-scale concrete specimens (1 m cubic) of the similar mix were prepared using the same batcher plant used for the Otori dam construction, and were exposed at the Otori dam site.

The mix proportion of the Otori dam and specimens are summarized in Table 2. The materials are moderate-heat portland cement, fly ash, crushed stone and sand. The maximum size of coarse aggregate is 150 mm. The Otori dam is made of the same material as the specimen. The specimens are four different mix proportion, identified as A, B, C and D. For example, air content, water-cement ratio, and fly ash replacement ratio are differences. The Otori dam mix proportion is similar to mix proportion A of the specimen. However, the fly ash replacement ratio and unit water volume are different.



Upper: Upstream view of the dam and monitoring slots in the red circle, Lower: Detail of monitoring slots

b) Site of exposure (at the site of the Otori Dam)

Fig. 3
Locations and detail of monitoring
Emplacements et détails de la surveillance

The monitoring results for the Otori dam and specimens are compared. To evaluate of the effects of environmental conditions, such as exposure conditions and water level fluctuations, on the concrete quality. The meteorological data at the Otori dam site are shown in Fig. 4.

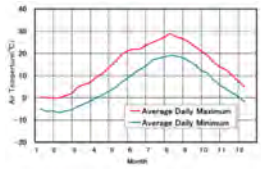
Table 2
Concrete Mix Proportion

Block Specimens					The Otori dam (Outer concrete)
Mix Proportion	A	B	C	D	
Gmax (mm)	150				150
Unit Weight (kg/m ³)	C +F	211			210
	W	93	105	93	99
F/C+F (%)	25			0	30
W/C+F (%)	44	50		44	47
s/a (%)	23	26	24	23	23
Slump (cm) ¹⁾	4.7	7.2	15	1.5	1.5
Air Content (%) ¹⁾	3.3~3.4		0.5	2.9	3.0
air-entraining admixture	with	with	without	with	with
σ_{91} (N/mm ²)	33.1	29	33.5	38.8	37.9
Durability Factor(%) ²⁾	76	87	4	86	83
Remarks	Typical Mix Proportion	W/C increased	W/C increased Non-AE	Non-FA	

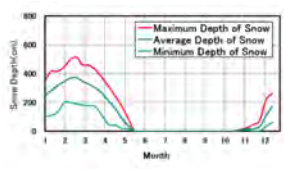
C: Moderate Heat Portland Cement, F: Fly Ash, Aggregate: Crushed Stone and Sand

1) Tested after wet screening

2) Laboratory test (ASTM C292-52T) 300 cycles, after 91-day standard curing



(a) Monthly air temperature



(b) Monthly snow accumulation

Fig. 4
Meteorological data the Otori dam site (2012-2023)
Données météorologiques du site du barrage d'Otori (2012 à 2023)

2.2. METHOD OF MONITORING

The dynamic modulus of elasticity of the Otori dam and the specimens are estimated from ultrasonic propagation velocity. The frequency has been once or twice a year since 1962.

The dynamic modulus of elasticity is obtained from wave characteristics such as vibration period or propagation velocity, and indicator of the change in material properties of concrete [2]. The measuring equipment used by the authors are shown in Table 3. Equipment is replaced in the long-term monitoring period. At the time of replacement, measurements are performed with the old and the new equipment for five years, and the results are corrected.

Eq. [1] estimate the dynamic modulus of elasticity from the ultrasonic propagation velocity[3].

$$E = \rho V^2 / g \times (1 + \nu)(1 - 2\nu) / (1 - \nu) \quad [1]$$


Where E: dynamic modulus of elasticity (kg/cm²), V: ultrasonic propagation velocity (cm/s), ρ : density (g/cm³), ν : Poisson's ratio, g: Acceleration of gravity (980cm/s²)

Eq. [1] has a slightly smaller dynamic modulus of elasticity according to Ogata et al [4]. However, it is reported to have good accuracy. According to Ogata et al., it is important to set the density and Poisson's ratio appropriately to improve the accuracy of the dynamic modulus of elasticity. Therefore, density of 2.4 g/cm³ estimated from mix proportion was adopted. Poisson's ratio is 0.2, which is a typical value for concrete [2].

The monitoring location of the Otori Dam (Refer to Fig. 2 and 3.) is repeatedly subjected to dry and wet conditions. Here, two box cutouts were installed at a distance of 1 m, and the ultrasonic propagation velocity was monitored for three lines after 1964. Ultrasonic propagation velocity was averaged to estimate the dynamic modulus of elasticity. The situation of the monitoring slots is shown in Fig. 3(b).

For each specimen, ultrasonic propagation velocity was monitored at 18 measured lines as a to j and (1) to (9) are shown in Fig. 5. The dynamic modulus of elasticity is estimated by averaging those values. The value at the first year is taken as the initial value, and the ratio of the dynamic modulus of elasticity at the time of monitoring to the initial value (the dynamic modulus percentage) is used to evaluate the soundness of the concrete. The monitoring positions and conditions of specimens are shown in Figs. 5 and 6.

Table 3
Measuring equipment

Equipment	
Type	ELSONIC ESI-10(Toyoko Elmes Co.,Ltd)
Dimensions	W240×H105×D245
Allowable Operating Temperature	0~40°C
Allowable Operating Humidity	80%RH or less
Measuring range	1000mm or less
Repeatability	±0.3μs

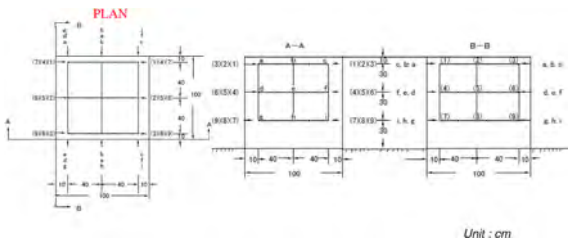


Fig. 5
Monitoring sections of concrete specimen
Sections de surveillance des échantillons de béton



Fig. 6
Situation for monitoring ultrasonic wave propagation
Situation de surveillance de la propagation des ondes ultrasonores

2.3. RESULTS OF MONITORING

(1). Estimation of freeze-thaw times

In this paper, the number of freeze-thaw cycles was defined under the following conditions.

Assuming “freeze” when the temperature remains below 0°C for 3 hours and “thaw” when the temperature remains above 0°C for 3 hours. The number of freeze-thaw cycles is defined as one timing from freeze to thaw.

To determine the number of freeze-thaw cycles at the Otori dam site, a concrete specimen ($\Phi 30$ cm x H30 cm) embedded with the thermometers at 3 cm and 15 cm deep was made in 2008 for measuring the temperature inside of the specimen. It is referred to as the concrete thermometer. The concrete thermometer was placed at the locations of concrete specimens to check the number of freeze-thaw cycles (Fig. 7). The freeze-thaw cycles were measured based on the following conditions.

The number of freeze-thaw cycles for each year is shown in Fig. 8. The maximum number of freeze-thaw cycles is 55 times/year, the minimum is 3 times/year, and the average is 19 times/year at the 3-cm depth. At the 15 cm depth point, the maximum is 26 times/year, the minimum is 3 times/year, and the average is about 11 times/year.

From the above, the number of freeze-thaw cycles is smaller at deeper depths. This indicates that temperature changes are smaller inside the concrete than surface. Although there is increase or decrease in the number of freeze-thaw cycles in each year, no overall increase or decrease trend is observed. In other words, the temperature change during monitoring period is not considered to be significant.

Therefore, the number of freeze-thaw cycles over in 60 years is calculated as 660 and 1,140 times in average values at 3 cm depth and 15 cm depth, respectively.



Fig. 7
Specimen for temperature measurement
Échantillon pour la mesure de la température

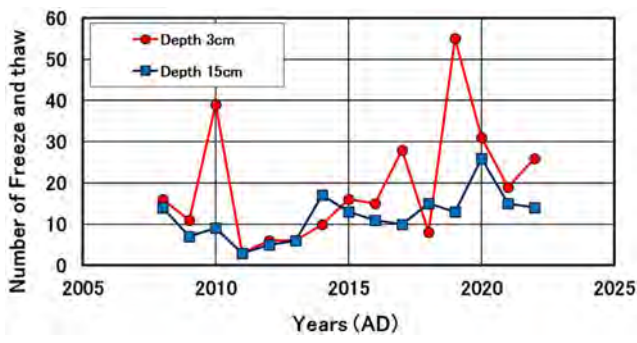


Fig. 8
Changes over time in the number of freeze and thaw
Évolution dans le temps du nombre de gels et de dégels

(2) Trend of the dynamic modulus percentage in 60 years

The dynamic modulus percentage of the Otori dam and specimens in 60 years are shown in Fig. 9. The Otori dam has remained at around 100% after 60 years, maintaining the quality of the dam concrete at the time of construction.

Although ones of specimens have repeatedly increased and decreased, the dynamic modulus percentage has remained at about 85 to 98% after 60 years.

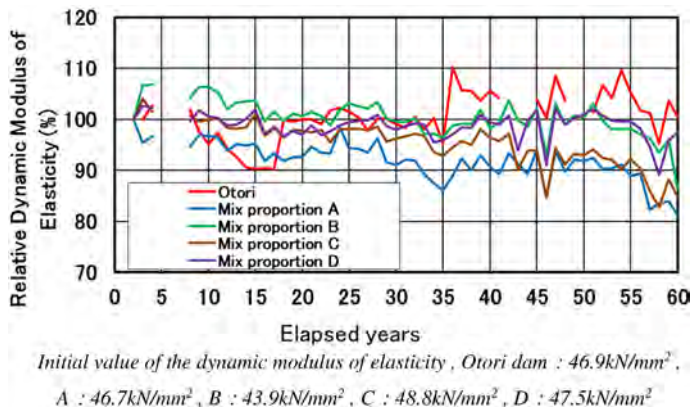


Fig. 9
Changes over Time in the Relative Dynamic Modulus of Elasticity
Évolution dans le temps du module d'élasticité dynamique relatif

(3) Comparison of dynamic modulus percentage of specimens with different mix proportion

The dynamic modulus percentage of specimens is higher than approx. 80 % for all mix proportion. On the other hand, there is some superiority depending on mix proportion. The superiority of the results at the 60 years point is as follows. And possible causes of decrease in the dynamic modulus percentage are frost damage or age-related deterioration. Since the age of the specimens was the same, the adverse effect of aging was excluded. Therefore, in this paper, the decrease in the dynamic modulus percentage is considered to be due to frost damage. () in the following shows the comparison with mix proportion A.

1st place : Mix proportion D (without fly ash)

2nd place: Mix proportion B (higher unit water content and water-cement ratio)

3rd place: Mix proportion C (increased water-cement ratio and without air-entraining admixture)

4th place: Mix proportion A

Factors that affect frost damage resistance include water-cement ratio, AE (Air-Entrained), and fly ash.

First, according to the literature [5], lower water-cement ratio is higher resistance to frost damage. Mix proportion A and D have smaller water-cement ratios than mix proportion B and C. Compared to mix proportion B and C, D has higher resistance to frost damage. But A has lower resistance to frost damage than B and C due to decrease in the dynamic modulus percentage. Therefore, the effect of water-cement ratio is not clear from the results. It is possible that other factors have an effect.

Next, air-entraining admixture is mixed in all mix proportion except C. It is considered B and D are more resistant to frost damage than C. On the other hand, A is less resistant to frost damage than C. From the above, the effect of AE is not clear.

Finally, the adverse effect of the dynamic modulus of elasticity by fly ash is confirmed though mix proportion D and A. Because D has the highest dynamic modulus percentage and D has a greater dynamic modulus percentage than A. It is indicated that D has higher resistance to frost damage than other mix proportion. It has been reported that dam concrete has less resistance to frost damage compared to ordinary concrete [6]. The reason for this is considered that unburned-carbon in fly ash adsorbs AE. Therefore, fly ash is considered to reduce resistance to frost damage. Fly ash is effective in dam concrete construction to reduce heat of hydration and ensure long-term strength and durability. On the other hand, it may make worse frost damage resistance. When frost damage resistance is essential, preliminary studies and mix proportion should be taken into consideration for use of fly ash.

Based on the above, the results suggest that fly ash may have adverse effect on frost damage resistance. However, the effects of water-cement ratio and AE are not clear, and there is high possibility that they have a combined effect. Therefore, we will continue our investigation to clarify the effects of these conditions.

The dynamic modulus percentage of the height (Refer to Fig. 3, measured line at 10 cm, 40 cm, and 70 cm) of specimens, using recent 10 years data are shown in Fig.10. The dynamic modulus percentages at the top(10cm) are lower than those of others(40cm,70cm). The top edge of specimen is horizontal surface, which is prone to accumulation of snow and melting snow water. The closer to the top edge surface, more sensitive influence.

Here, the dynamic modulus percentage estimated at measured lines, excluding the value at the top of the specimen. The result is higher in the dynamic modulus percentage, ranging from 90% to 98% for all mix proportion. The dynamic modulus of elasticity in upper part tends to decrease, this indicate that in upper part are subjected to more freeze-thaw impact (Refer to Fig. 8).

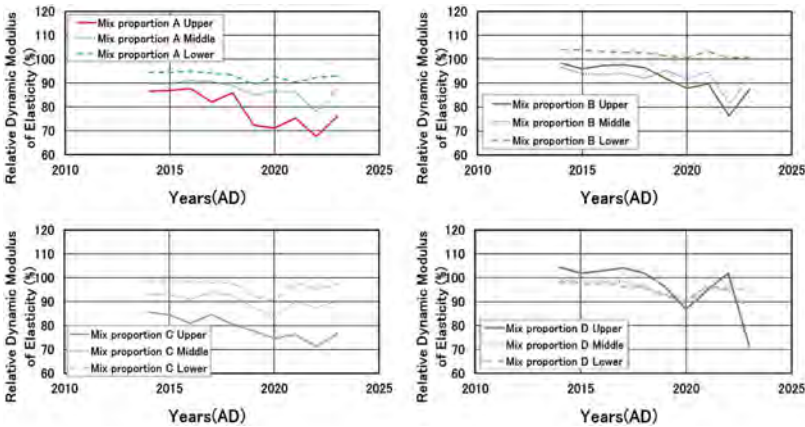


Fig. 10
Changes over Time in the Relative Dynamic Modulus of Elasticity
Évolution dans le temps du module d'élasticité dynamique relatif

- (4) Difference in the dynamic modulus of elasticity between the dam and specimen of mix proportion A

Based on results(Refer to Fig. 9), the Otori dam keep integrity for a long time, this indicates that quality can be maintained for a long time through use of

appropriate materials, mix proportion, and construction. And there is clearly difference in the dynamic modulus percentage between the Otori dam and specimen of mix proportion A. The reason for difference is thought to be number of freeze-thaw cycles. The Otori dam is used as regulating reservoir dam. Water level tends to be relatively lowered during winter season, but water level rises due to operation, and the monitoring point goes underwater. Therefore, the Otori dam is thought to have experienced fewer freeze-thaw cycles than specimen.

3. IDENTIFICATION OF CURRENT PROPERTIES OF DAM CONCRETE BY DYNAMIC BEHAVIOR OF THE OTORI DAM

3.1. OUTLINE

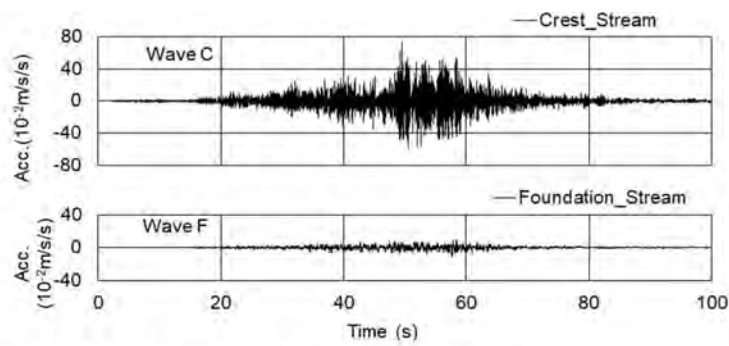
For the verification of the measurement of the dynamic modulus of elasticity by the instruments shown in Table 3, the current dynamic modulus of elasticity of the Otori dam is identified so as to correspond to the dynamic behaviors of the Otori dam during earthquakes by the reproduction analysis. The earthquake monitoring in the Otori dam has been conducted since 2018. The accelerometers have been arranged at the crest and the bottom gallery of the Otori dam as shown in Fig. 2. The 2024 Noto Peninsula Earthquake (referred to as Noto earthquake) caused the acceleration response of $73 \times 10^{-2} \text{m/s}^2$ at the Otori dam crest on 16:10 JST, 1st January 2024, which is the maximum ever. Including this event, thirteen monitored data of the dynamic behavior of the Otori dam during earthquakes have been accumulated so far.

The reproduction analysis of the Otori dam is conducted for the behaviors monitored in a summer season as well as a winter season in which Noto earthquake happened.

3.2. DYNAMIC CHARACTERISTICS OF THE OTORI DAM DURING EARTHQUAKES

A predominant frequency and a damping ratio are estimated as the fundamental dynamic characteristics of the Otori dam for the selection of earthquakes for the reproduction analysis. The acceleration behaviors of the Otori dam monitored at the Otori dam crest and the bottom gallery (Refer to Fig. 2) in the stream direction are shown in the upper figure of Fig.11 as an example. The lower figure of Fig. 11 is a transfer function matrix [7] which identifies the predominant frequency of the Otori dam is 6.3 Hz using the transfer function matrix (TFM) method[7]. The damping ratio from 2.2 % to 4.8 % are identified using damping estimation by TFM (DE/TFM) method [8] which is based on the free vibration of the structure and the logarithmic

decrement method as shown in Fig. 12. These dynamic properties are estimated for the monitored earthquake data in the summer and the winter seasons. The results are summarized in Table 4. The predominant frequencies are clearly identical in both seasons. The reproduction analyses are conducted for the monitored data in both seasons.



These monitored at 16:10 JST, 1st Jan. 2024 are the records perpendicular to the Otori dam axis in direction. The reservoir water elevation was EL 555 m of 2 m below H.W.L of 557 m.

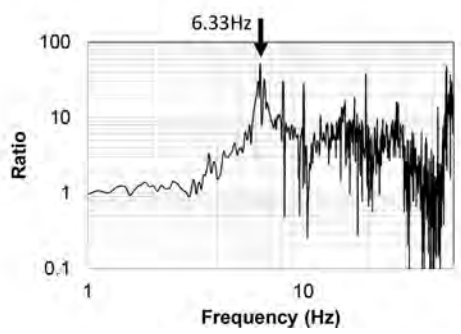
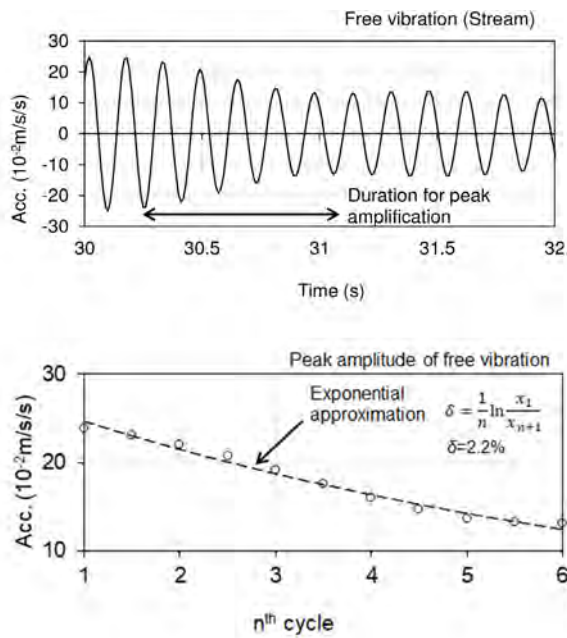


Fig. 11

Acceleration response of the Otori dam to the earthquake of 2024 Noto Peninsula Earthquake, Upper: Acceleration record, Lower: Transfer function matrix
Réponse en accélération du barrage d'Otori au séisme de 2024 dans la péninsule de Noto, en haut : Enregistrement de l'accélération, en bas : Matrice de fonction de transfert



Upper: Extracted free vibration from Wave C. The time is not equivalent to figure in Fig. 10.
Lower: Estimation of damping ratio by the logarithmic decrement

Fig. 12
Estimation of damping ratio by DE/TFM method
Estimation du taux d'amortissement par la méthode DE/TFM

Table 4
Dynamic characteristics of the Otori dam on major earthquakes monitored

Monitored data	Group for TFM method	Max. Acc.		Fp (TFM) (Hz)	Damping ratio (%)
		Foundation	Crest		
Winter					
2024/01/01 16:10:36	GW1	11.6	72.9	6.33	2.2
2024/01/01 18:08:50		0.7	4.2		2.4

(continued)

Table 4
Continued

Monitored data	Group for TFM method	Max. Acc.		Fp (TFM) (Hz)	Damping ratio (%)
		Foundation	Crest		
2024/01/09 17:59:20		3.1	14.3		4.8
2023/04/01 18:41:32	GW2	1.4	5.8	6.32	3.8
2023/05/05 14:42:36		1.6	7.4		2.7
2024/01/01 18:08:50		0.7	4.2		3.7
Summer					
2018/07/29 09:58:48	GS1	2.2	13.9	6.78	3
2019/06/18 22:22:50		4.7	36.1		1.3
2022/10/19 03:35:37		2.5	11.3		1.5
2021/07/18 19:10:56	GS2	2.6	19.8	6.74	1.4
2022/10/19 03:35:37		2.5	11.3		1.7
2023/05/05 21:58:37		1.5	6.7		2.4

The water depths were from approximately 3 to 5 m above EL 551 m.

3.3. REPRODUCTION ANALYSIS

Dam-reservoir-foundation system is represented with a three dimensional (3-D) numerical model as shown in Fig. 13 and UNIVERSE program [9] of a finite element method (FEM) is applied for the reproduction analysis. The dynamic modulus is examined based on the common values to reproduce the Otori dam behavior during earthquakes. The Otori dam body is represented uniformly by ignoring the surface layer of 3.5 m thick of the Otori dam.

Two data of the Otori dam behavior in the summer and the winter seasons are selected for the analysis. These are ones monitored on 1st January 2024, that is the Noto earthquake and on 18th June 2019, which made the maximum acceleration of $73 \times 10^{-2} \text{ m/s}^2$ and $36 \times 10^{-2} \text{ m/s}^2$ at the Otori dam crest. The corresponding water levels are considered. These are referred to as Case A and Case B, respectively.

To make input wave on the bottom of the numerical model, the monitored wave in the bottom gallery is transformed using the transfer function between the bottom gallery and the bottom of the numerical model. Through a few analyses the acceptable coincide has been obtained between the monitored behavior and its simulation at the Otori dam crest. The adjusted dynamic elastic modules of 43 kN/mm^2 for the summer season and 40 kN/mm^2 for the winter season are obtained as shown in Table 5 including other parameters of the analysis. The transfer functions between the bottom and the crest of the Otori dam are shown in Fig. 14, illustrating the coincide of the Otori dam behavior at the crest by the reproduction analysis. The available water depth of the Otori dam for the hydropower generation is only 6 m deep which has few impacts on the Otori dam behavior. It is considered that the difference in the elastic modulus of the Otori dam in summer and winter is attributed to the seasonable temperature fluctuation which make the different structural integrity due to the volume change of the dam concrete.

The dynamic modulus of the elasticity of the Otori dam has been initially estimated at 46.9 kN/mm^2 at the measuring point of the monitoring slot in September 1965 which was the two-year age of the dam concrete. The equivalent value has been confirmed by the in-situ measuring since then described in Chapter 2. The above simulated modulus of the Otori dam is also equivalent to the in-situ measurement, but lower at 9 % in the summer case and 17 % in the winter case to the current value.

Reasons for a certain disagreement in the dynamic modulus of the elasticity of the Otori dam between the in-situ measurement and the structural simulation are considered as the effect of the zoning of the dam concrete in which the inner concrete is of less cementitious material of 140 kg/m^3 comparing to the outer concrete is of 210 kg/m^3 , and the structural effect due to the transverse joints of the Otori dam. The above simulation identifies the dynamic modulus of the elasticity for the whole dam structure from the structural viewpoint.

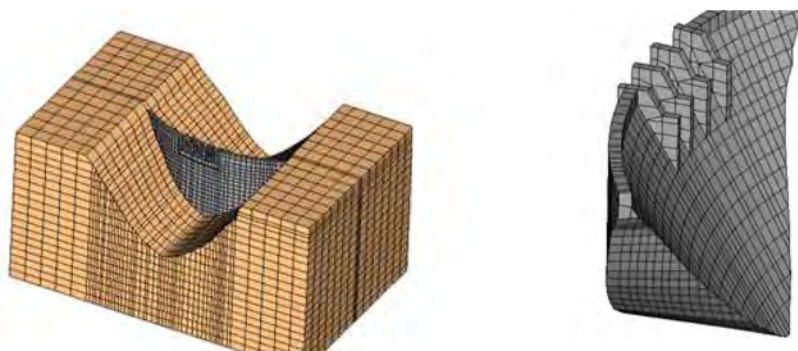


Fig. 13

Numerical model consisting of dam, foundation and reservoir

Modèle numérique comprenant le barrage, les fondations et le réservoir

The analysis on the dynamic behavior of the Otori dam has verified the current dynamic properties of the dam reasonably and concurrently the validity of the in-situ measurement on the dynamic modulus of the elasticity of the dam concrete.

Table 5
Identification of properties by reproduction analysis

Case	Material	Dynamic Elastic modulus (N/mm ²)	Dynamic shear modulus (N/mm ²)	Specific weight (g/cm ³)	Poisson's ratio
A	Dam	40,008	16,670	2.40	0.20
B	Dam	43,008	17,920	2.40	0.20
A & B	Foundation	27,040	10,400	2.60	0.30

Damping ratios of 1.0 % are applied to Dam and Foundation.

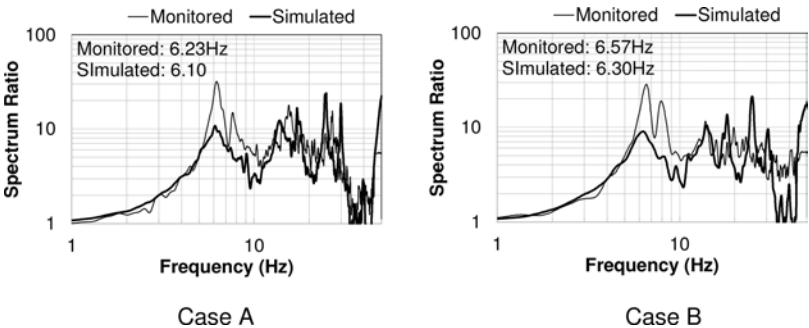


Fig. 14
Ratio of Fourier spectrum of the Otori dam
Rapport du spectre de Fourier du barrage d'Otori

4. CONCLUSIONS

The dynamic modulus of elasticity of the Otori dam and specimens exposed to freezing environment for a long time was estimated from ultrasonic velocity of propagation.

- The dynamic modulus percentage of the Otori dam is maintained perfectly even after 60 years, suggesting that the soundness of dam is secured.
- The specimens also maintained high dynamic modulus percentage. On the other hand, differences were observed depending on mix proportion.
- This reason could be the adverse effect of fly ash, but the effect of water cement ratio and air-entrained is not clear at this time.

- Specimen of mix proportion A showed different deterioration in the dynamic modulus percentage to the Otori dam. This may be due to the number of freeze-thaw cycles.
- The reproduction analysis on the dynamic behavior of the Otori dam during earthquakes identify the dynamic modulus of elasticity of the whole dam structure. It shows reasonable agreement with the in-situ measurement on ones of the dam concrete at the measurement points arranged at the upstream surface of the Otori dam.
- The zoning of the dam concrete in the Otori dam and the structural behavior characterized by the transvers joints of the Otori dam are influential factor to the identification of the dynamic properties of the dam.

REFERENCES

- [1] JCOLD. Durability test of dam concrete with large concrete blocks. *LARGE DAMS* , 1996 , No. 156(in Japanese).
- [2] IKEDA K., SUZUKI T., OHTSU M. A Study on Dynamic Modulus of Elasticity of Deteriorated Concrete in Resonance Method. *Proceedings of the Japan Concrete Institute* , 2004 , Vol.28, No.1(in Japanese).
- [3] ARCHITECTURAL INSTITUTE OF JAPAN. Manual of Nondestructive Testing Methods for Estimating Concrete Strength , 1983(in Japanese).
- [4] OGATA H., HATTORI K., TAKADA R., NONAKA T. Evaluation of Freeze-Thaw Resistance of Concrete by Ultrasonic Method. *Proceedings of the Japan Concrete Institute*, 2002, Vol.24, No.1(in Japanese).
- [5] JAPAN SOCIETY OF CIVIL ENGINEERS. *Standard Specifications for Concrete Structures*, Construction, 2017(in Japanese).
- [6] HASIMOTO M., SAKATA N., HAYASHI D., SUGAMATA T., SAKUE G. Evaluation of Freeze-Thaw Resistance of Concrete by Ultrasonic Method. *Proceedings of the Japan Concrete Institute*, 2002, Vol.24, No.1(in Japanese).
- [7] CAO Z., KASHIWAYANAGI M., YOSHIDA M., ASAKA H. 2018. Application of the transfer function matrix method in dam engineering. *ICOLD 26th Congress, Austria, Vienna*, 2018, C.4
- [8] KASHIWAYANAGI M., CAO Z. Investigation of damping characteristics of dams evaluated by DE/TFM method, *ICOLD 27th Congress, Marseille*, 2022, Q106R3
- [9] WATANABE N., ARIGA Y., CAO Z. Evaluation of dynamic stability of concrete gravity dam by three dimensional dynamic analyses taking non-linearity into account, *Journal of JSCE*, 2002, No.696/I-58 (in Japanese).

COMMISSION INTERNATIONALE DES
GRANDS BARRAGES

VINGT-HUITIEME CONGRES DES
GRANDS BARRAGES
CHENGDU, MAI 2025

**CERESOLE REALE DAM REHABILITATION: MORE THAN 30 YEARS
LATER (*)**

Nicola BRIZZO
IREN ENERGIA

Gabriella VASCHETTI
CARPI

Marco SCARELLA
CARPI

Ezio BALDOVIN
GEOTECNA PROGETTI

ITALY

SUMMARY

Ceresole Reale is a concrete gravity dam built in 1927-1930 in Italy. The progressive deterioration of the original upstream Lévy facing led to increase in leakage. The investigations and the monitoring measures also showed non negligible water infiltration at foundations and increasing considerable uplift pressure at the contact with the foundation in the right part of the dam. In the late 1980s the owner decided to totally renew the water barrier, from crest to deep foundations, and reinforce the upstream face. Works, carried out from 1990 to 1992, consisted in installing a flexible exposed geomembrane system in the upper and middle part of the dam, in a new reinforced concrete block in the lower part of the dam to add

**Réhabilitation du barrage de Ceresole Reale : plus de 30 ans après*

weight at the heel, and of a new grout curtain, injected from the new concrete block, with a new drainage system.

Today, after thirty years of operation of the dam after the rehabilitation works, despite an expected partial decay of the characteristics of the exposed geomembrane (periodically subjected to sampling campaigns and laboratory tests), Ceresole Reale Dam maintains excellent watertightness and structural behaviour and fully guarantees its operation in completely safe conditions.

RÉSUMÉ

Ceresole Reale est un barrage-poids en béton construit en 1927-1930 en Italie. La détérioration progressive du parement amont d'origine de type Lévy a provoqué l'augmentation des infiltrations. Les investigations et les mesures d'auscultation ont montré des infiltrations d'eau non négligeables au niveau des fondations et une sous-pression croissante et considérable au contact avec la fondation dans la partie droite du barrage. À la fin des années 1980, le maître d'ouvrage décide de renouveler totalement le masque, de la crête aux fondations profondes, et de renforcer le parement amont. Les travaux réalisés de 1990 à 1992, consistaient en un système de géomembrane flexible exposée dans la partie supérieure et médiane du barrage, d'un nouveau bloc de béton armé dans la partie inférieure pour ajouter du poids à ce niveau, et d'un nouveau écran d'injection injecté à partir du nouveau bloc de béton, avec un nouveau système de drains.

Aujourd'hui, après trente ans d'exploitation du barrage après les travaux de réhabilitation, malgré une dégradation partielle attendue des caractéristiques de la géomembrane exposée (soumise périodiquement à des campagnes d'échantillonnage et à des tests en laboratoire), le barrage de Ceresole Reale maintient une excellente étanchéité et un excellent comportement structurel et en général et garantit pleinement son fonctionnement dans des conditions de totale sécurité.

1. INTRODUCTION

Ceresole Reale, a successful rehabilitation project where a carefully planned design has allowed to restore to its former functionality a dam that is at present almost a hundred years old, fits very well in the crucial topic of management of an aging portfolio of dams. Many thousands of large dams are more than 50 years old, and many others are approaching 100 years of service. While dam construction has almost ceased in Europe and in USA, dams are needed even more than in the past, as indispensable rescuers in times of excess or scarcity of water, and as reliable sources of clean energy. Many old dams must and can continue to operate safely, if

their conditions are constantly checked, proper maintenance is carried out, and adequate monitoring equipment is provided.

Watertightness and structural consistency are the main aspects to keep under control when dams age. Watertightness concerns the whole water barrier, i.e., the water barrier of the dam itself, which must avoid/minimise water infiltration into the dam body, and the foundations, to avoid uplift pressures increase. Structural consistency involves the renovation and strengthening of any possible deficiency. Ceresole Reale Dam started operation in 1930 and, after 50 years of satisfactory performance, the water barrier experienced increasing leakage at the upstream face and rising uplift pressure especially at the right part of the foundation. The paper presents the story of this ageing dam: its characteristics, the evolution of its behaviour from 1930 to the 1980s, the analysis and repair measures adopted around 1990, and the performance in the more than thirty years that followed, up to the present day. More detailed information on the dam since its construction up to completion of the repair measures can be found in previous literature [1,2].

2. CERESOLE REALE UP TO 1990-1992

Ceresole has been since 1862 called Ceresole Reale, the title of Royal having been bestowed by the king of Italy Vittorio Emanuele II, to whom the municipality had ceded the right to freely hunt chamois and ibex in its area. The dam is situated in the beautiful Gran Paradiso National Park in the western Alps of Italy.

2.1. DAM DATA

The dam, now owned by Iren Energia, is used for hydropower production. Built in the years 1927-1930, it is a concrete gravity dam, 52 m high and 302 m long, at 1574 m elevation, impounding a 34 million cubic metres reservoir. With a design fairly common in those years, when the quality of the concrete was not very good, a facing formed by small concrete arches (Lévy-type facing) was placed over the concrete and being subject to the whole water pressure resulted to be the upstream water barrier. The arches, with a 200 kg/m³ cement content and a 2 m extrados radius, are 0.5 m thick at crest and 1 m thick at foundation; they were continuous along the face of the dam, with a vertical joint every 5 arches. The dam had a longitudinal inspection gallery close to the foundation, a drainage collection and discharge gallery at the foot of the arches, and 4 automatic siphons with a capacity of 520 m³/s, at the right abutment.

Later in 1980s the existing spillway was radically modified with a composite system consisting of a free weir combined with a flap gate, increasing the potentiality

to 650 m³/s, and the downstream face was repaired with a 10 cm thick reinforced concrete lining.

The foundation rock consists of granitic gneiss; the rock mass is divided by a net of more or less close fractures. When the dam was built, a 40 m deep grout curtain was created about 3 m upstream, supplemented by consolidation grouting at foundation, and 40 drainage holes were bored from the inspection gallery.

2.2. EVOLUTION OVER THE YEARS

Ceresole Reale has a continental climate with very cold winters and fresh and formerly rainy summers. Ten years after construction, the upstream Lévy facing, due to thermal stresses and to the action of frequent freeze/thaw, started deteriorating, and over time, regardless of some local repair works, deterioration continued and as early as in 1951 diffused fissures were observed, which caused leakage. It was decided first to fill with concrete the cavities behind the Lévy arches, and after some years to line the arches with cemented hard stones ("bolognini").

For about 15 years these measures were effective, then leakage started increasing again. The most deteriorated parts of the facing appeared to be those affected by the action of big ice blocks in springtime. New cement mortar placed at the hard stones ("bolognini") contacts of the upstream facing at the end of the 1970s, and some underwater repair, did not solve the leakage problems, which at the end of the 1980s cyclically reached, in the fillings of the reservoir, 50-60 l/s. A thorough investigation was carried out at the arches and at the dam. The conditions of concrete appeared acceptable at lower elevations, but unsatisfactory in the upper part of the facing, where evidently the already smaller thickness of the arches had been reduced when the hard stones ("bolognini") facing was installed; on the contrary, the integrity of the dam was in line with what expected in similar dams of similar age. The investigations also showed non negligible water infiltration at foundations. Additional vertical grouting 20 m deep, new 15 m deep vertical foundation drains, and sub-horizontal drains at the right abutment, did not solve the problem. Measurements at the drains showed that water infiltration persisted at the contact rock/concrete, and in the rock foundation, a few metres from it. The residual water flow through the foundation was not high, but had to be addressed because, as indicated by piezometers readings, it caused an increasing considerable uplift pressure at the contact with the foundation in the right part of the dam.

The owner, at that time AEM Torino, then decided to put an end to repeated repairs by a total renewal of the water barrier, from crest to deep foundations, and a reinforcement of the upstream face.

Indeed, after one year for the Detail Design and the approvals, the civil works started in 1990 and were concluded in 1992. Geomembrane waterproofing works

started in June 1992 and were completed in November 1992, for a total of 9,000 m² of new geomembrane facing.

2.3. THE NEW UPSTREAM FACE AND WATER BARRIER

The water barrier (Fig.1) consists of a flexible exposed geomembrane system in the upper and middle part of the dam, from crest down to elevation 1536.50 m, of a new reinforced concrete block from elevation 1536.50 m to the rock surface also to add weight at the heel, and of a new grout curtain with two series of holes, injected from the new concrete block, and reaching 35 m of depth where the dam is higher, and decreasing to 20 m at the abutments, with a new drainage system.

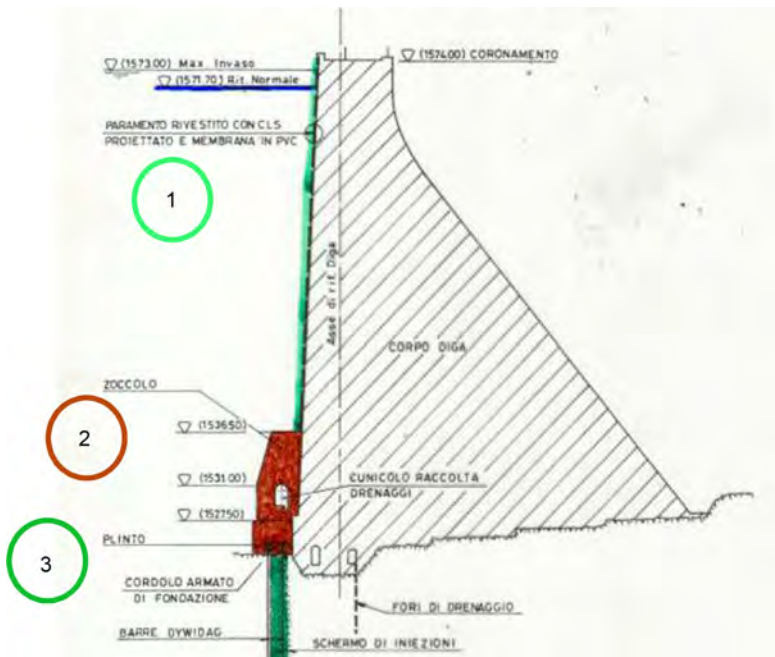


Fig. 1

Vertical cross section of Ceresole Real Dam with the new water barrier

Section verticale du Barrage de Ceresole Reale avec nouveau écran d'étanchéité

- 1 Exposed geomembrane
- 2 New reinforced concrete block
- 3 New grout curtain

- 1 Géomembrane exposée
- 2 Nouveau bloc en béton armé
- 3 Nouveau écran d'injections

2.3.1. *Upstream face: exposed geomembrane system*

Two options were available for a new watertight upstream facing: partial demolition of the Lévy facing (down to the needed elevation), followed by placement of a new, simplified concrete liner against the dam body, or keeping the Lévy facing and installing a new liner over it. The first option was ruled out because, besides being expensive, it would present several issues: major interface problems at the contact between the new concrete liner and the dam body, need to dewater the reservoir for a long period, which, besides being expensive could cause lack of safety during works, in the case of a flash flood hitting the dam when it still lacked the new watertight facing. On the other hand, placing a new concrete liner without demolishing the Lévy facing was not an option because the poor characteristics of the concrete of the arches would not allow applying a rigid concrete facing over them. Instead, the second option, installation of a new thin waterproof liner over the existing facing, was feasible.

Anyway, besides the complicated geometries created by the Lévy arches, the "bolognini" formed a particularly rough subgrade, unstable at several locations, and the concrete under them was of poor quality and thinner than designed. It was then decided to regularise and stabilise the existing facing, after removal of the most weathered stones, by two layers of shotcrete (Fig. 2), each reinforced with a steel mesh, secured to the concrete of the dam body with anchor bars, to fill the macro-porosities of the Lévy arches with local and widespread injections of cement mix, in order to prepare a stable surface to install the thin lining. The 18 cm thickness of the shotcrete was increased to 30 cm at the springing of the arches, to house the anchorage system for the lining.

Among available liners, mortar coating was discarded because of its poor resistance to high hydraulic gradients and its poor weathering properties, resin films were considered unsafe because prone to bubbling and detachment due to lack of drainage behind the film. A prefabricated flexible geomembrane system, following the rehabilitation criteria at that time already adopted on several dams, was selected as the best option.

The selection of the geomembrane was based on the return of experience available at the time. Exposed polyvinylchloride geomembranes had successful precedents on large Italian dams at high altitudes: Lago Miller gravity dam with masonry facing, at 2170 m, lined in 1976, Lago Nero gravity dam, at 2000 m, in 1980, Barbellino gravity dam, at 1872 m, lined in 1987, Cignana gravity dam, at 2173 m, lined in 1988, Publino double arch dam, at 2135 m, lined in 1989. The tensile and weathering properties of such materials under high UV radiations were more adequate for the site conditions than elastomeric liners and bituminous geomembranes (which in any case would not have been suitable for a vertical facing) and were also more convenient from a financial perspective [1]. The selected liner, of the same type adopted at the aforementioned dams, is SIBELON® CNT 3750, a 2.5 mm thick flexible PVC geomembrane thermally bonded at fabrication to a 500 g/m² nonwoven needle punched polyester geotextile. The geomembrane provides watertightness, the geotextile protects the geomembrane against residual irregularities of the subgrade, increases thermal stability and has some drainage capability.

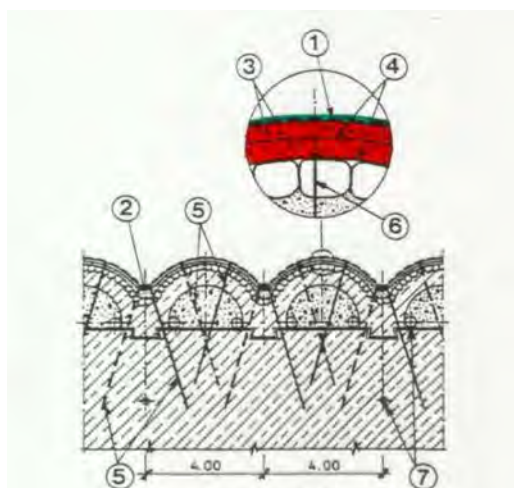


Fig. 2

Horizontal cross section of Ceresole Reale Dam at upper/middle part of the facing
Section horizontale du Barrage de Ceresole Reale en partie supérieure/milieu du parament

- 1 Exposed geomembrane
- 2 Anchorage system
- 3 Shotcrete
- 4 Steel mesh
- 5 Anchor bars
- 6 Fixing nail
- 7 Vertical drains

- 1 Géomembrane exposée
- 2 Système d'ancrage
- 3 Béton projeté
- 4 Maillage en acier
- 5 Barres d'ancrage
- 6 Clou de fixation
- 7 Drains verticaux

The geomembrane liner is secured to the dam by a face anchorage system, by a watertight peripheral seal that avoids water infiltrating behind the liner at submersible boundaries, and by a top seal watertight against rain and snowmelt. The face anchorage is based on a well-known patented tensioning system that was later listed in ICOLD guidelines [3], and that is composed by an assembly of the stainless-steel profiles (Fig. 3), whose geometry is such that when they are tightened over the geomembrane sheets they achieve a slight tensioning effect, avoiding that self-weight weight and loads due to thermal differentials and water level variations can create some slack areas in the geomembrane sheets, where ice or snow ice can potentially cling and stretch down the liner.

The design of the tensioning system is adjusted to the peculiar shape of the facing: the first profile of the assembly is embedded in the 30 cm thick new shotcrete placed at the springing of the arches, the geomembrane liner is placed over it, and

the second profile is secured to the first one. A strip of Sibelon® C 3250 geomembrane, the same material composing the waterproofing liner, but without bonded geotextile, is placed over the profile assembly and watertight sealed upon the underlying geomembrane liner, avoiding water seepage under it. The tensioning assembly also solves another function: the cavity formed by the two profiles constructs a vertical drainage conduit at the springing of the arches, conveying water by gravity to bottom collection and discharge via transverse pipes from the upstream face to the gallery of the new concrete toe block.

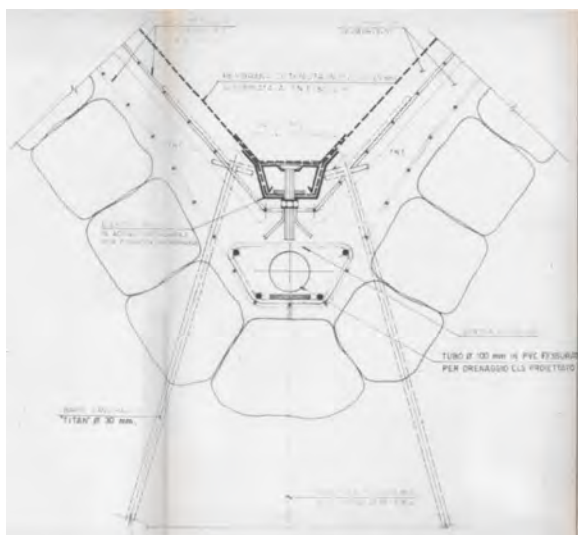


Fig. 3
Tensioning profiles
Profilés de tensionnement

The design of the tensioning system is adjusted to the peculiar shape of the facing: the first profile of the assembly is embedded in the 30 cm thick new shotcrete placed at the springing of the arches, the geomembrane liner is placed over it, and the second profile is secured to the first one. A strip of Sibelon® C 3250 geomembrane, the same material composing the waterproofing liner, but without bonded geotextile, is placed over the profile assembly and watertight sealed upon the underlying geomembrane liner, avoiding water seepage under it. The tensioning assembly also solves another function: the cavity formed by the two profiles

constructs a vertical drainage conduit at the springing of the arches, conveying water by gravity to bottom collection and discharge via transverse pipes from the upstream face to the gallery of the new concrete toe block.

Depending on the geometry of the arches, one or two tensioning profiles were placed at the springing of each arch. Installation of the waterproofing system was divided in horizontal and in vertical sections, following the construction of the new shotcrete and the concurrent embedment of the first tensioning profiles. Mostly in the left part of the dam the geomembrane liner was installed in single sheets, each covering four arches and laid vertically, working from a fixed scaffolding. In other zones, to expedite installation, the liner was prefabricated in larger panels, 5 m wide and 10 m high which were installed horizontally from travelling platforms, each panel spanning two arches. Fig. 4 shows the placement of the new shotcrete layers embedding the first tensioning profiles at the springing of the arches, and placement of the geomembrane liner.

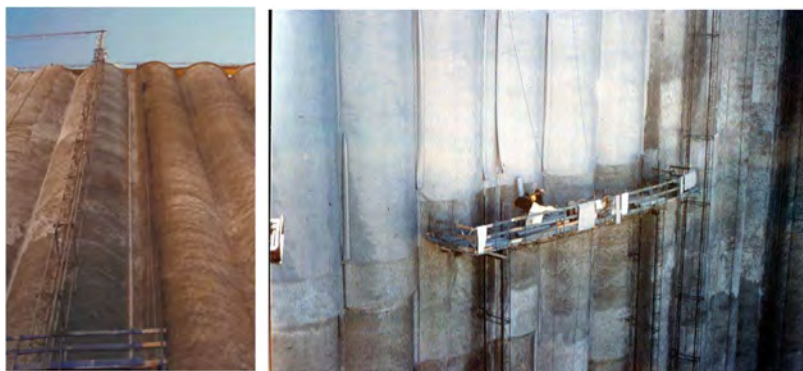


Fig. 4

New shotcrete layer embedding the first tensioning profiles at the springing of the arches (left); the geomembrane sheets and the second tensioning profiles under placement (right)

Nouveau béton projeté et premiers profilés de tensionnement noyés au niveau des ressorts des arcs (à gauche); les lés de géomembrane et les deuxième profils de tensionnement en cours de mise en place (à droite)

After the second tensioning profile is placed on the overlapping panels/sheets, the two profiles are tightly bolted together, providing permanent anchorage of the liner. The geomembrane cover strip over the profiles (Fig. 5) ensures that no water can seep where the bolting devices cross the liner.



Fig. 5

All profiles bolted and waterproofed, waterproofing liner perfectly tensioned
Tous profilés boulonnés et étanchés, géomembrane parfaitement tendue

The bottom submersible seal of the geomembrane was placed on the horizontal surface of the new reinforced concrete block cast from elevation 1536.50 m to the rock foundation (see section 2.3.2), close to the upstream face. A first U-shaped component was embedded into the new concrete, and the second U-shaped component compresses the geomembrane unto the embedded one, achieving watertightness also by an appropriate gasket (Fig. 6).



Fig. 6

Watertight seal on new reinforced concrete block, during works and in 2008
Fixation étanche sur nouveau bloc en béton armé, pendant les travaux et en 2008

A 50 x 4 mm flat profile, waterproofed by a Sibelon® C 3250 geomembrane cover strip, keeps the geomembrane liner taut against the subgrade at the concave corner. The bottom seal connects in a watertight manner the geomembrane liner to the new concrete block, from whose gallery the new grout curtain is injected, thus achieving continuity of the new water barrier from crest to deep foundations.

2.3.2. *Transition area: reinforced concrete block*

From elevation 1536.50 m to the rock surface, which is the most deteriorated area with highest ice aggression during the lowering of the reservoir level occurring at springtime, a new massive reinforced concrete block was placed next and connected to the existing concrete structure in order to transfer weight to the heel of the dam. This block, incorporating a longitudinal gallery and a plinth, has maximum height on foundations of 16 m, and goes up in steps along the abutments. A finite element numerical analyses confirmed that subdividing the block into structurally independent elements could obtain adequate distribution of tensions within the new structure, under the action of the hydrostatic load. The block is composed of three parts (Fig 7). The upper element includes a 1.20 x 2.20 m gallery, to which all the water drained from the geomembrane liner flows. The lower element, 3 m wide and 1.5 m thick, is anchored to the rock by a net of partially tensioned steel bars and acts like a cap for the new grout curtain.

An important interface structure between the Lévy arches and the new block consists of vertical concrete beams filling the cavities between arches, to obtain a planar surface for casting of the new block. The beams and the block are anchored to the dam by steel bars cemented 3 m inside the dam body.

A compressed air bubble system was installed at the bottom of the upper part of the block, to avoid that ice blocks can form in the vicinity of the upstream face of the dam, thus protecting the block and the geomembrane from the impact of ice at springtime. The system consists of 28 injectors that keep the temperature of the water above 0° C near the surface.

2.3.3. *The new grout curtain and foundation drainage*

The new grout curtain is connected to the concrete block, whose width at the base of approximately 4 m allowed the creation of a mesh of punctual injections. Despite the excellent conditions of the rock on the left bank, the curtain was built over the entire extension of the foundation, for a total length of approximately 250 m. It is made up of grouting injections in two rows, 1.5 m apart, with holes arranged in a quincunx with a 5 m pitch and with an axis coinciding with the centre line of the 3.5 m wide intervention strip. Of the two rows, the upstream one has subvertical holes, while the downstream one is made up of laterally inclined holes. The curtain reaches a depth of 35 m in the area of maximum height of the dam, while at the banks it has a minimum of 20 m.

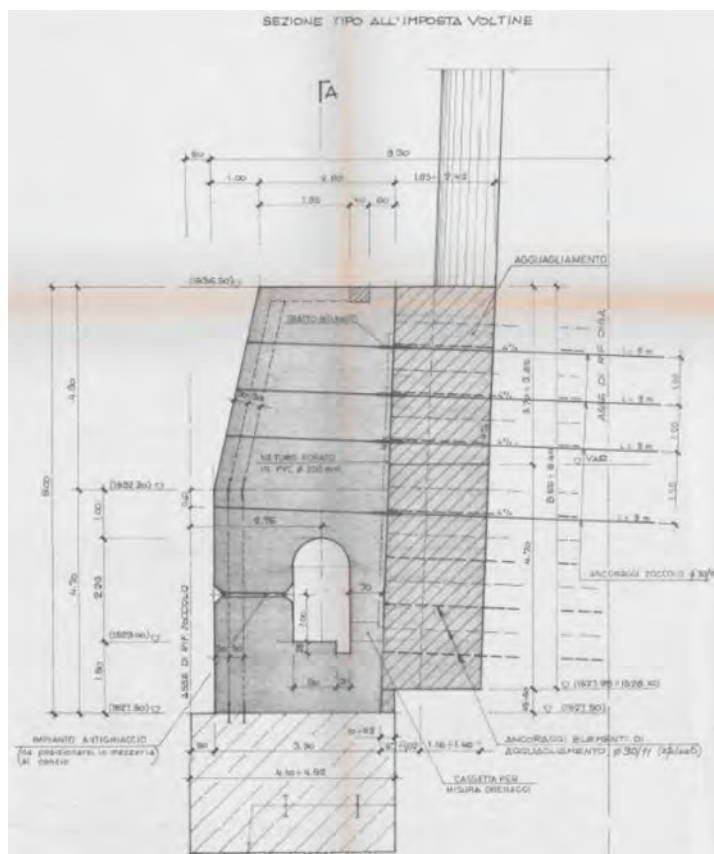


Fig. 7

Typical cross section of the reinforced concrete block
Coupe typique du bloc en béton armé

In each hole, progressively denser cement mixtures were used, in relation to the absorptions recorded (water/cement ratios from 3/1 to 1/1) and with pressures increasing in depth from 5 to 30 bar. Average absorption of 40 kg/m of cement was recorded with maximum peaks in the central area, in correspondence with a fault, of 3300 kg/m and on the right bank, in very localized sections, of 1430 kg/m. The final effectiveness of the intervention was verified through permeability tests carried out in control holes; in the more permeable areas on the right bank the absorptions were reduced, after the injections, from 8 to 0.5 Lugeon. The presence inside the concrete

block of an inspection tunnel of adequate size guarantees the possibility, at least in the central part with the greatest head, to integrate the grout curtain at any time and without interfering with the operation of the reservoir.

After the injections, once the intervention was completed, drainage holes were drilled in the foundation starting from the furthest downstream inspection tunnel with a depth varying between 20 and 8 m, with a diameter of 15 cm. As required by Italian legislation, they have been thickened compared to the pre-existing situation up to a distance between centres of 2.5 m.

3. CERESOLE IN 2024

The now thirty-years of operation of the dam after the rehabilitation works allow to outline a clear analysis of the behaviour of the dam body and of the foundation. Particular attention must obviously be paid to the trend of water leakage, an indicator of the effectiveness and durability of the interventions carried out on the upstream face and foundations, and of the uplift pressures, to be correlated to the completed integration of the waterproofing barrier with the drainage of foundations.

3.1. PERFORMANCE OF THE WATERPROOFING GEOMEMBRANE

The graph of daily leakage over time (Figure 8) highlights the progressive deterioration of the sealing system in the years preceding the rehabilitation, with maximum values exceeding 30 l/s in the decade 1980-1989 (the precise value of approximately 100 l/s was produced by the failure of filling between "bolognini", promptly sealed with resin by divers). After installation of the new waterproofing liner at the upstream face in 1992, total leakage remained always lower than 3 l/s, without showing any tendency to increase during the following years of regular operation. Slight increases in leakage were recorded during some episodes of local deterioration of the liner (2020-2022). During the summer of 2023, a rapid increase in leakage was detected (around 30 l/s) caused by a local damage to the liner located at the connection point between the upstream face and the concrete block. Repair works were carried out in March 2024 when the reservoir level was suitable for executing them in the dry.

In addition to the analysis of the monitoring measures, since the construction of the waterproofing liner, it has also been subjected to sampling campaigns and laboratory tests (1997, 2003, 2007, 2011 and 2022), in order to evaluate its deterioration over time and estimate its remaining useful lifetime.

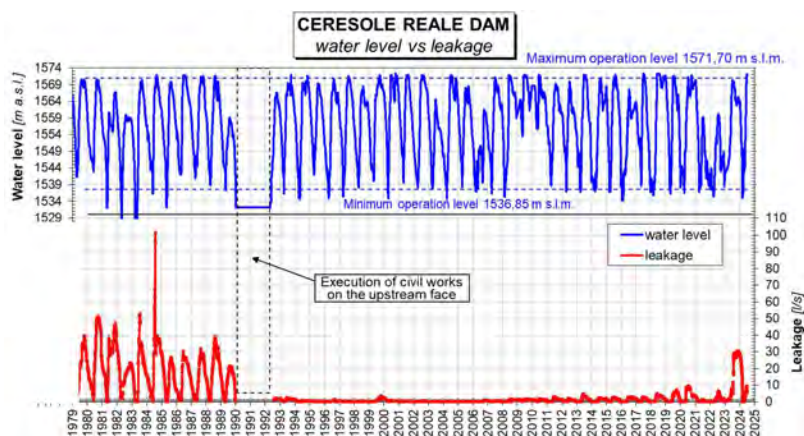


Fig. 8
Leakage versus water level
Infiltrations par rapport au niveau d'eau

The most recent sampling dates back to 2022. Tests relating to the plasticizers content, tensile properties, nominal thickness, density, Shore A hardness, low-temperature flexibility and water vapor permeability were carried out on the geomembrane layer. Transmissivity tests were carried out on the geotextile layer with different static loads and with variable hydraulic gradient. In these analyses, particular reference was made to the plasticizer content and its loss over time compared to the initial value. Based on this parameter it was possible to estimate a remaining useful lifetime of approximately 12-16 years.

3.2. UPLIFT PRESSURES

By analysing the trend of uplift pressures over time, the effectiveness of the grout curtain is evident. As an example, the measurements of piezometer PZ05, on the right shoulder, are shown in the graph in Figure 9. In fact, it is possible to observe the different behaviour following the works and the subsequent achievement of significantly lower piezometric levels.

The same considerations are even more evident in the graph in Figure 10, which represents the trend of the uplift pressure at the same piezometer PZ05, as a function of the reservoir level.

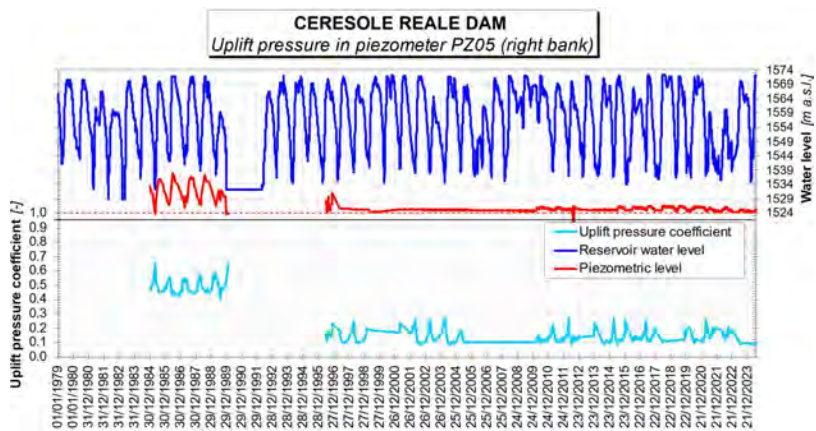


Fig. 9
Uplift pressure at PZ05 versus water level
Sous-pression au PZ05 par rapport au niveau d'eau

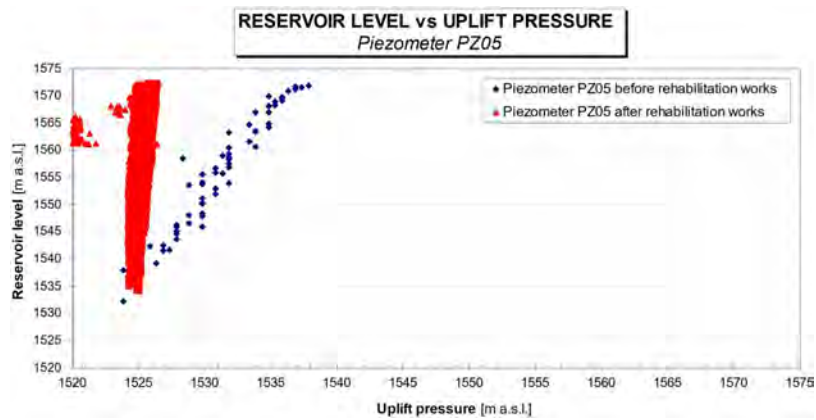


Fig. 10
Uplift pressure at PZ05 versus water level before and after the rehabilitation
Sous-pression au PZ05 par rapport au niveau d'eau avant et après la réhabilitation

Similar direct correlations between uplift pressures and reservoir level can be obtained for the other installed piezometers, which clearly indicate the different behaviour before and after the rehabilitation, and a decidedly lower dependence of the piezometric measurements from the level fluctuations in the reservoir.

4. CONCLUSIONS

In the context of the management of hydropower plants, monitoring and maintenance of an infrastructure asset during its progressive ageing constitutes a fundamental aspect. The case of the Ceresole Reale Dam shows how, following several decades of operation, the execution of significant rehabilitation works may become necessary, in order to guarantee safe and efficient conditions.

The civil works carried out during the 90s were overall aimed at restoring an adequate watertightness, a typical aspect that tends to degrade with the progressive aging of concrete dams, and to improve the structural consistency. They involved both the dam body with the construction of a new water barrier (consisting of an exposed geomembrane system placed on the upper face reinforced with anchored shotcrete and of a reinforced concrete block able to add weight at the heel in the lower part) and the foundation through the realization of a new grout curtain and of new drainage holes.

Today, over 30 years after the execution of the works, despite experiencing an expected partial decay of the characteristics of the exposed geomembrane, the Ceresole Reale Dam maintains excellent watertightness and structural behaviour and in general fully guarantees its operation in completely safe conditions.

REFERENCES

- [1] BALDOVIN G., BALDOVIN E., FIAMBERTI A. Rehabilitation and water-proofing of the upstream facing of Ceresole Reale Dam. Proceedings, 18th ICOLD Congress, 1994.
- [2] BALDOVIN E., BRIZZO N. Riabilitazione della Diga di Ceresole Reale. L'ACQUA – Rivista dell'Associazione Idrotecnica Italiana, 1/2009.
- [3] ICOLD. Bulletin n° 135. *Geomembrane Sealing Systems for Dams – Design principles and review of experience*. 2010.

COMMISSION INTERNATIONALE DES
GRANDS BARRAGES

VINGT-HUITIEME CONGRES DES
GRANDS BARRAGES
CHENGDU, MAI 2025

**REINFORCEMENT OF EXISTING DAMS WITH PASSIVE ANCHORS:
THOUGHTS AND PROPOSALS FROM A FRENCH WORKING GROUP(*)**

Grégory COUBARD & François MOREL
EDF
CFBR working group on passive anchors

FRANCE

SUMMARY

This paper is dedicated to the survey carried out by a French task force mobilized in the aegis of the French Committee on Large Dam and relating to the reinforcement of existing concrete dam with passive anchors. The main objectives of the said working group were: to overview the state of the art regarding the use of passive anchors for concrete dam reinforcement, underground works and rock slope stabilization in France and abroad, to benchmark the calculation methods dedicated to the reinforcement of concrete dams with passive anchors, to draft recommendation relating to concrete dam reinforcement with passive anchors to be used in France.

The main specificity of the use of passive anchors to stabilize existing concrete dams is the irreversible displacement of the structure required to mobilize the said anchors. Allowing such displacement for concrete gravity dam is uncommon.

French, Swiss, Swedish, Norwegian, American and Canadian practices were reviewed. The paper benchmarks these recommendations and apply them to the

**Le confortement par ancrages passifs des barrages existants*

reinforcement of a small overflow dam. The paper proposes an innovative method developed to account for the dilatancy effect at the reinforced interface.

French recommendations regarding the reinforcement of existing concrete dam are currently under drafting. The said recommendation will namely deal with: the methodology and criteria devoted to passive anchor contribution to dam stability, the installation of passive anchors on site (namely corrosion protection), and the surveillance and monitoring of concrete dams reinforced by passive anchors.

A lot of work is still to be performed in this field. The study currently carried out by our working group could be shared with other committees potentially interested, or in the framework of the International Commission On Large Dams.

RÉSUMÉ

Cet article est dédié à l'analyse conduite par un groupe de travail français mobilisé sous l'égide du Comité Français des Grands Barrages pour traiter le renforcement des barrages en béton existants avec des ancrages passifs. Les principaux objectifs de ce groupe de travail étaient : d'effectuer la revue de l'état de l'art dans les domaines du renforcement des barrages en béton par ancrages passifs, des travaux souterrains et de la stabilisation de talus rocheux en France et à l'international, d'intercomparer les méthodes de calcul dédiées au renforcement des barrages en béton avec des ancrages passifs, et de rédiger une version préliminaire des recommandations dédiées au renforcement des barrages en béton par des ancrages passifs, qui entreront en vigueur en France.

La principale spécificité liée à l'utilisation des ancrages passifs pour stabiliser des barrages en béton existants et le déplacement irréversible de la structure qui s'avère nécessaire pour mobiliser lesdits ancrages. Autoriser de tels déplacement est inhabituel dans le domaine des barrages poids en béton.

Les pratiques françaises, suisses, suédoises, norvégiennes, américaines et canadiennes ont fait l'objet d'une revue. Le présent article intercompare ces méthodes et propose un cas d'application théorique relatif au renforcement par ancrages passifs d'un barrage déversant de faible hauteur.

En France, des recommandations dévolues au renforcement par ancrages passifs de barrages en béton existants sont actuellement en cours de rédaction. Lesdites recommandations traiteront notamment : des méthodes et critères régissant la contribution des ancrages passifs à la stabilité des barrages, la mise en œuvre des ancrages passifs sur le site (et notamment la protection contre l'usure par corrosion), la surveillance et l'auscultation des barrages en béton renforcés par ancrages passifs.

Un travail conséquent reste à accomplir dans ce domaine. La réflexion actuellement conduite par notre groupe de travail pourrait être partagée avec d'autres comités potentiellement intéressés, ou dans le cadre de la Commission Internationale des Grands Barrages.

1. INTRODUCTION

In France, passive anchors have been and are still occasionally implemented to reinforce existing gravity dams on rock foundations. Despite being a straightforward and robust solution, passive anchor reinforcement is not fully integrated into specific French guidelines, leading to a lack of consistent national standards. The main challenge comes from the mechanical behavior of this kind of reinforcement, which implies an irreversible displacement of the gravity dam to be efficiently mobilized. This behavior deviates from established practice for stability analyses of gravity dams, as irreversible displacements are not allowed except under extreme loading conditions. Nevertheless, passive anchor solutions seem relevant for moderate height dams without specific pathologies where conventional stability analysis methods fail to meet the criteria. Passive anchors offer a complementary stabilization at a moderate cost without significant structural modifications under normal operating conditions.

A working group was established in 2020 under the aegis of the French Committee on Large Dams and Reservoirs (CFBR) to develop recommendations and guidelines on this topic. The group's work plan involved three main stages: (i) synthesizing the state of the art in concrete dam reinforcement in France and internationally, as well as in underground works and rock stabilization; (ii) benchmarking existing and innovative calculation methods for analyzing concrete gravity dams reinforced with passive anchors; and (iii) drafting French recommendations and guidelines on dam reinforcement with passive anchors.

This paper highlights the thoughts and findings of our French working group, which could be of interest to other committees and the ICOLD community.

The outline of this article follows the three main stages of work plan previously presented:

- Overview of the state of the art in the dam and underground works fields,
- Presentation and comparison (benchmark) of shortlisted methods for considering the stabilization effect of passive anchors,
- First thoughts and highlights concerning the French guidelines currently being drafted, especially in connection with risk management.

2. OVERVIEW OF THE STATE OF THE ART

The literature analysis concerning passive anchoring considered three main domains:

- Past experiences and state of the art relative to French practices in the concrete dam field,
- Guidelines and state of the art at an international level in the concrete gravity dam field,
- Guidelines and state of the art in France in the underground works and rock stabilization fields.

The working group produced three comprehensive documents on these topics (currently available only in French, with an English translation planned), which provide an objective summary and helped short-list potential calculation methods for developing future French guidelines.

2.1. STATE OF THE ART IN FRANCE

Several French dams have been reinforced using passive anchors. Nevertheless, French practices regarding their use for rehabilitation works and their incorporation into stability analyses, are highly variable. Three main approaches were identified:

- Passive anchors are not explicitly considered in the analysis and are viewed as an additional qualitative measure,
- Passive anchors are considered in the stability analysis in the same manner as post-tensioned anchors: as point loads in the axial direction of the passive anchors. The mechanisms and the consequences of an irreversible displacement on the dam's behavior (i.e. dilatancy effects and hydro-mechanical coupling at the reinforced interface) are rarely analyzed in detail,
- Passive anchors are introduced with more accurate methods including the mobilization of axial and transversal forces in the anchors and potential hydro-mechanical coupling.

Relevant renovations using passive anchors in France concern Pinet gravity dam in 1987-1988 and Chancy-Pougny dam in 2014. This paper does not describe these two examples in detail. Some information concerning the Chancy-Pougny rehabilitation is provided by [1]. This dam is located on the border between France and Switzerland, the reinforcement design therefore benefited from Swiss recommendations concerning corrosion protection, with ribbed protective sheathing of the rebars (Fig. 1.).



Fig. 1

Passive anchors protected by ribbed sheathing and installation into the Chancy-Pougny dam piers

Ancrages passifs protégés par une gaine nervurée et mise en œuvre dans les piles du barrage de Chancy-Pougny

2.2. INTERNATIONAL GUIDELINES AND STATE OF THE ART

Typically, international guidelines do not mention passive anchors, and when they do, practices are also highly variable.

The USA advises against the use of passive anchors for dam reinforcement in different guidelines published by USACE, USBR, FERC or FEMA.

Passive anchoring is very commonly used in Scandinavian countries (Sweden and Norway) and is advised in their guidelines, including for initial design and construction of dams. However, significant conservatisms and safety margins are included, coupled with very low allowable stresses in anchors (140 or 180 MPa) and a requirement for stability criteria to be met without anchoring when no safety factor is taken into account. This paper does not enter into detail regarding these recommendations. Useful information can be found in [2] and [3].

In Switzerland, the utilization of passive anchors is formally authorized by a national directive. Comprehensive normative documents provide detailed guidelines on corrosion protection for passive anchors, including the use of ribbed protective sheathing. However, the calculation methods are not detailed, and in practice, the use of passive anchors for concrete gravity dam rehabilitation appears to be infrequent.

In Canada and more precisely in Quebec, discussions are in progress and a calculation method has been developed by Polytechnique Montréal [4] but it has not been yet transposed, as we understand, into guidelines. This method is described in paragraph 3.2 of this paper.

2.3. PRACTICES AND GUIDELINES IN UNDERGROUND WORKS AND ROCK STABILIZATION

Passive anchors are widely used in the underground works and rock stabilization fields, with numerous documents available: academic literature (with research works and experimental data), guidelines concerning design and calculation methods, and technical recommendations relating to their installation. Nevertheless, directly applying these practices to the dam rehabilitation domain is challenging due to some significant differences: (i) in the underground works or rock stabilization field, the estimation of irreversible displacements due to the passive anchor mobilization is not a major issue contrary to concrete dam reinforcement, and (ii) in the underground and rock stabilization fields, passive anchors are generally uniformly distributed over a contact surface, while in the case of dam reinforcement the anchors would generally be installed along a single line. Notable literature includes:

Firstly, the CEREMA French guide [6] that illustrates the behavior of a passive anchor along a sheared interface depending on the stiffness of the surrounding materials (i.e. hard or soft rocks). It highlights the influence of rock stiffness on the irreversible displacements: if the surrounding rock is hard, the irreversible displacements will be lower and the anchor will be sheared with moderate deformations, if the surrounding rock is soft, the irreversible displacements will be higher, the anchor will deform in an S-shape and the break will occur by excessive rotation / bending moment or traction.

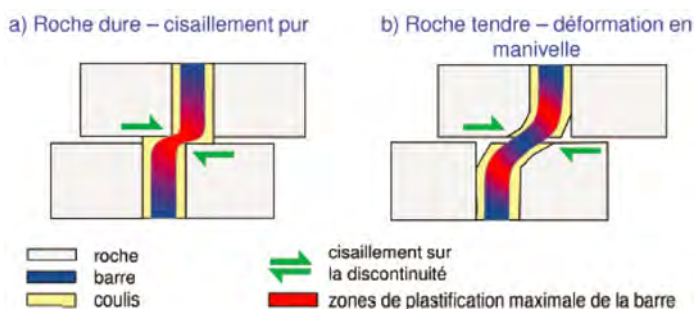


Fig. 2

Illustration of the behavior of a sheared rock discontinuity reinforced by passive anchor, CEREMA French guide

Illustration du comportement d'une discontinuité rocheuse renforcée par ancrage passif, guide CEREMA

Secondly, Pellet's thesis [5] linking irreversible displacement to axial and transversal efforts in the anchors for a sliding mechanism at the reinforced interface. Pellet's method relies on an analytical calculation. The input values are the diameter of the passive anchor, the angle between the reinforced joint and the passive anchor, the uniaxial compressive strength of the surrounding materials, the steel yield limit and the steel deformation at failure. The method gives valuable results that have been confirmed by numerous experimental campaigns with various rock materials (from a sandstone with a uniaxial compressive strength of 10 MPa to a granite of 105 MPa).

This method seems to be the only analytical calculation that allows the estimation of irreversible displacements due to a sliding mechanism. It has been used by our working group to develop a method that is called "the French method" (see. Paragraph 3.4) in this paper.

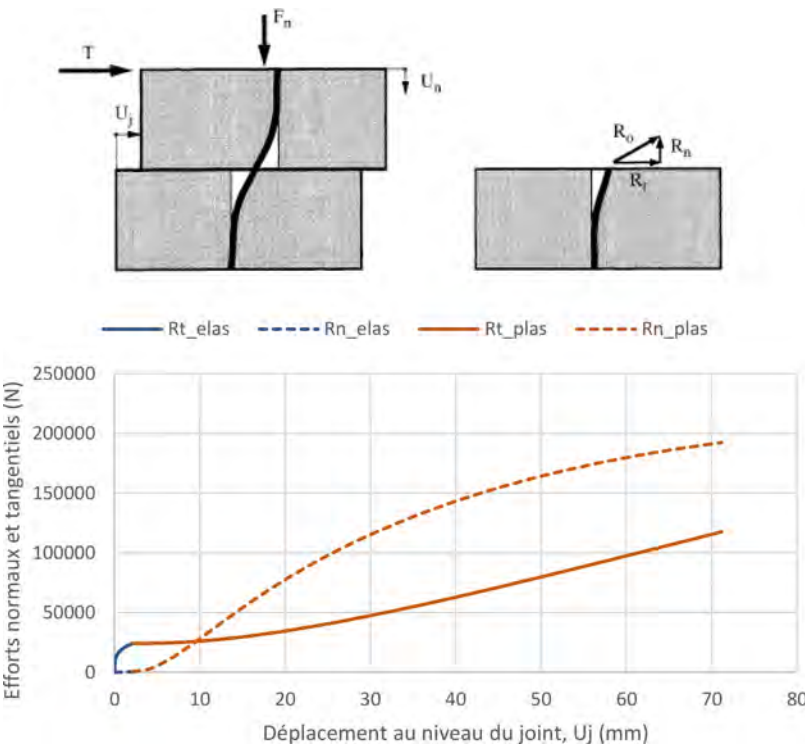


Fig. 3
Illustration of Pellet's numerical method and results
Illustration de la méthode de Pellet

3. COMPARISON (BENCHMARK) OF PASSIVE ANCHOR CALCULATION METHODS

Following the first phase of the working group plan concerning the overview of the state of the art, a second phase was launched to compare existing (and innovative) passive anchor calculation methods. Four analytical methods were short-listed thanks to the first phase:

- Swedish/Norwegian method: Based on a force equilibrium, without estimating the necessary irreversible displacements.
- Canadian method: Analytical equilibrium method for normal and tangential forces, considering interface opening and sliding.
- Rock stabilization (CEREMA) method: Based on maximum work principle, allowing for dilatancy considerations.
- Innovative French method (derived from [5]): estimating irreversible sliding displacements and integrating dilatancy effects.

The benchmark was carried out on a small overflow dam (7 m high) typical of the candidate dams for rehabilitation by passive anchoring. The objective was to determine the spacings for a line of anchors parallel to the dam's face, with different hypotheses concerning the angle of the rebars and the dilatancy of the reinforced concrete-to-rock interface. Since it is difficult to assess the evolution of uplift pressures under the reinforced dam with irreversible opening and sliding, a full uplift pressure all along the interface was considered for this benchmark.

All the calculations were performed without safety factors to easily compare the four methods.

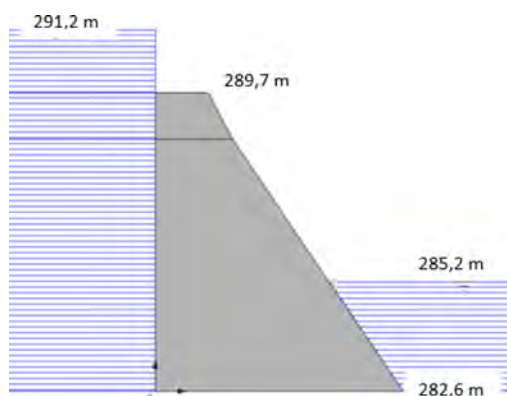


Fig. 4

Geometry of the small overflow dam studied for the benchmark
Géométrie du barrage déversant de faible hauteur étudié dans le cadre de l'analyse comparative

The Canadian method is described in detail in reference [4]. The method is performed in two phases:

- firstly, an analytical equilibrium analysis of the normal force and moment at the reinforced interface, aimed at stabilizing the overturning mechanism (this first step is very similar to a reinforced concrete calculation).
- secondly, an analytical equilibrium analysis of the tangential force at the reinforced interface, aimed at checking against the sliding failure mode, assuming that the anchor can be mobilized up to the shear yield criterion of the rebar.

This Canadian method allows for simultaneous analysis of the opening and the sliding of the reinforced interface. It can incorporate the hydromechanical coupling associated with the interface opening (propagation of uplift pressures). In its current form, the method is not able to consider either the dilatancy or rebars that are not perpendicular to the analysis plane.

3.3. ROCK STABILIZATION (CEREMA) METHOD

The rock stabilization method, as described in the French CEREMA guidelines [6], is based on the principle of maximum work. The mechanism considered is a sliding rock mass stabilized by passive anchors. The principle of maximum work implies that the passive anchors will function as efficiently as possible. The axial and transversal forces in the passive anchors are distributed to achieve maximum stability.

This method allows the dilatancy of the reinforced interface to be considered.

3.4. FRENCH (INNOVATIVE) METHOD

This innovative method, developed by the working group, is based on [5]. The objective of the method is to evaluate the irreversible displacements associated with sliding mechanisms. The principle is straightforward: an irreversible sliding displacement occurs when the sliding safety factor defined below is inferior to one. Some additional explanations can be found in [1] and [7].

The method has been improved to incorporate the dilatancy effect at the reinforced interface.

This method is, to our knowledge, the only analytical method that estimates irreversible sliding displacements.

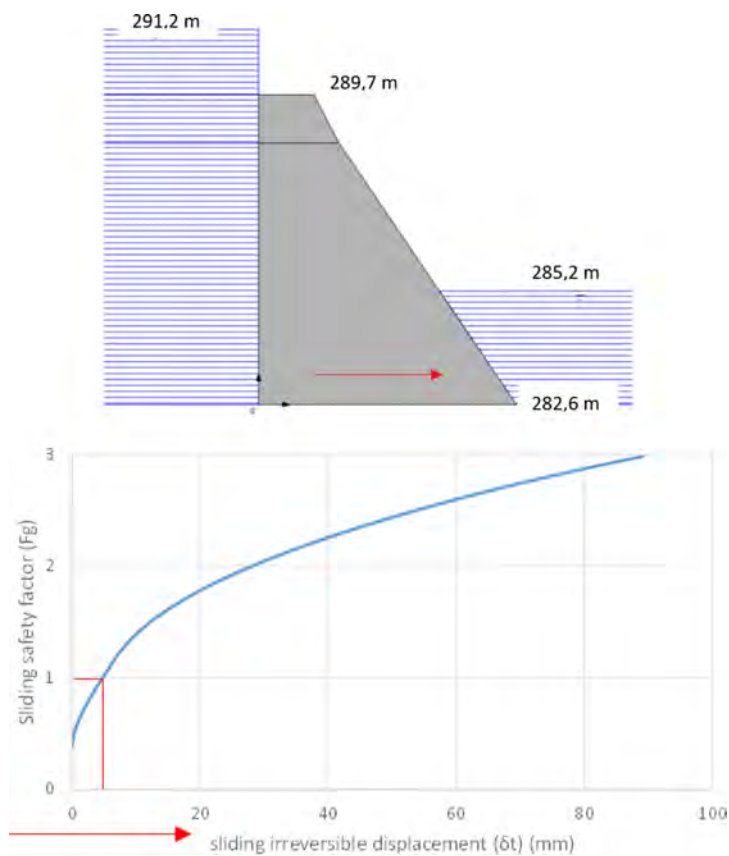


Fig. 6

Résultat de modélisation du facteur de stabilité au glissement en fonction du déplacement

Result of safety sliding factor related to irreversible displacement

3.5. SUMMARY OF BENCHMARK RESULTS

The preliminary results of the benchmark are shown in Figure 7. It is noteworthy that the different methods produce similar results (here passive anchors spacing) when the anchors are inclined (except the Swedish method with a transversal contribution of the anchors) but that when they are vertical (perpendicular to the reinforced interface), the results are quite different. In particular, wider spacings are obtained using the French method. This discrepancy can easily be explained by

the fact that the French method describes the anchor's real behavior more accurately, including its S-shape deformation, which allows it to better withstand the efforts.

Beyond the results (spacing of the passive anchors with the different short-listed methods), the benchmark highlighted the strengths and weakness of each analytical method and their respective domain of application. The analysis showed that no one method is fully satisfactory, but they can be combined to provide a more accurate description of the behavior of interfaces reinforced by passive anchoring. The following table summarizes the main features of each method.

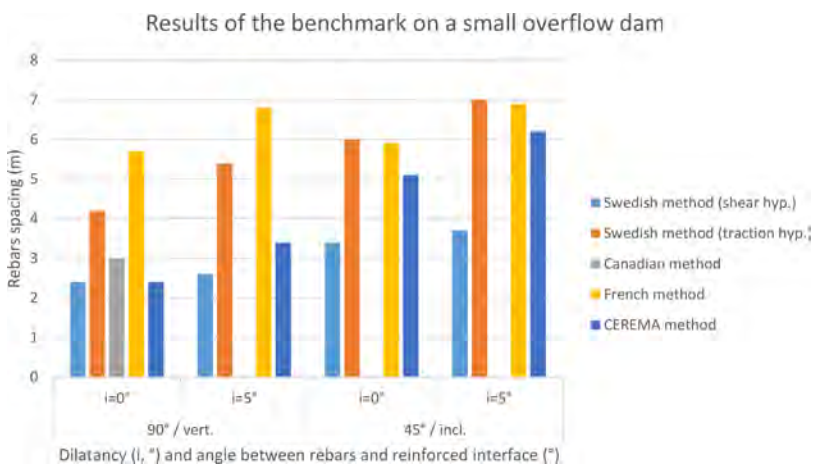


Fig. 7
Benchmark results summary
Résultats synthétiques de l'analyse comparative

Table 1
Strengths and weaknesses of the different analytical methods
Forces et faiblesses des différentes méthodes analytiques

Analytical method	Inclination of the anchors	Dilatancy of the interface	Combined mechanisms: sliding and overturning	Irreversible displacement estimation
Swedish	Yes	Yes	No	No
Canadian	No	No	Yes	No
Rock stabilization	Yes	Yes	No	No
French	Yes	Yes	No	Yes

The table above highlights that only the Canadian method fully accounts for the combined failure mechanisms (i.e. opening and sliding) at the reinforced interface. However, it does not model, in its current form, an inclination of the rebars nor the effect of dilatancy at the interface. This method complements the French method, which is the only method that estimates irreversible displacements and can consider both an inclination of the anchors and dilatancy. However, this method relies on the initial assumption that the mechanism involves only sliding along the interface.

Developments must continue in order to improve these methods. Research work has been launched recently in France, through a thesis, to reach this objective.

4. FRENCH DRAFTGUIDELINES

Our working group is currently drafting French guidelines. Given the required developments mentioned in the previous chapter, these guidelines will be provisional for a preliminary phase (a few years).

The main points covered by the French guidelines on passive anchors will be:

- The methodologies and criteria concerning the contribution of passive anchors to stability analyses,
- Design and installation recommendations including corrosion protection,
- The surveillance, monitoring and operation of dams reinforced by passive anchors.

Remark:

It is important to note that the reinforcement of an existing dam with passive anchors requires the acceptance of structural behavior generally avoided. Specifically, passive anchors require displacements to be mobilized, which represents a significant departure from conventional reinforcement solutions. Dam owners and decision-makers must be fully aware of this difference. For this reason, our recommendations contain the following disclaimer:

Reinforcement by passive anchoring requires, in some loading situations, IRREVERSIBLE displacement of the structure, the PLASTIC deformation of the anchor and LOCAL FAILURE of the grout, the concrete and the rock surrounding the anchors.

Passive anchors are generally used as a long-term solution in potentially aggressive environments. Consequently, the surveillance and monitoring of a

structure reinforced by passive anchors is essential, in order to observe and understand the structure's behavior when it endures an unusual loading case.

Additionally, if the anchor's mobilization leads to damage to the reinforced structure, a reassessment of the dam's safety must be engaged including if necessary, immediate measures to restore its safety (for example, a drawdown of the reservoir).

4.1. ANALYSIS METHODOLOGIES

The guidelines concerning the analysis methodologies are still in the drafting stage. Nevertheless, some main principles are already established:

- The analysis of existing gravity dams reinforced by passive anchoring will be coherent with the current French guidelines for the stability analysis of gravity dams [8]. The limit states proposed in the upcoming guidelines on passive anchoring will include and adapt limit states of the gravity dam guidelines. Additional limit states will be proposed.
- Since no single method allows the analysis of all the input items (see §. 3.5: combined mechanics, inclined anchors, dilatancy at the interface), the designer must first identify the predominant mechanism of potential failure (i.e. sliding or overturning) to apply a suitable analytical method. Table 10 can assist in making this decision. Additionally, we recommend using several methods to compare the results and more particularly the anchor's behavior (i.e. evolution of axial and transversal efforts in the rebars).

Table 2
Suitable analytical methods according to initial failure mechanisms
Méthodes analytiques adaptées en fonction de la cinématique de rupture

Main initial failure mechanisms	Sliding	Overturning	Combined mechanisms
Suitable analytical methods	Swedish method (shear hyp.) CEREMA method Canadian method French method	Swedish method (traction hyp.) Canadian method	Canadian method

Further considerations are being made additional limit states. The resistance of the dam body upstream of the rebars to the efforts exerted by the anchors is being investigated through a new limit state yet to be defined. The associated risk or failure includes cracking and separation of the lower upstream corner of the dam body if the concrete cover over the anchor is insufficient.

4.2. INSTALLATION AND DURABILITY

The 2012 French guidelines for gravity dam stability analysis [8] include initial proposals regarding passive anchor installation and corrosion protection.

Our upcoming recommendations will provide more detailed specifications. Our current position is to impose a double corrosion protection composed of grouting and a plastic ribbed sheath. These recommendations will be globally in accordance with Swiss practice [9].

This chapter will also include some advice concerning installation and detailing provisions.

4.3. SURVEILLANCE, MONITORING AND OPERATION

The surveillance of structures reinforced by passive anchors is a critical aspect. Passive anchoring rehabilitation profoundly changes the behavior of the dam. This type of reinforcement implies that the owner (and by extension, the regulatory authorities) accepts a structure that can face irreversible displacements, damage to the interface between the dam and its foundation and significant leakage when the anchors are mobilized. Before implementing this type of reinforcement, a comprehensive risk analysis must be undertaken, and surveillance and monitoring instructions must be established to clearly define an action plan in case of displacements or damage.

The working group's proposals concerning this chapter have not yet been written but they will probably involve a surveillance and monitoring procedure that considers the predicted behavior of the reinforced structure. An example of potential thresholds and related actions are given in Table 3.

Table 3
Example of surveillance and monitoring procedure related to passive anchoring
Exemple de procédure de surveillance et d'auscultation en lien avec le confortement par ancrages passifs

Loading situation	Forecasted anchor mobilization	Estimated irreversible displacements	Surveillance (visual inspection) action	Monitoring (device measures) action
Normal water level	NO	-	-	-
Q50 (i.e. 50 years return period flood)	YES	< 1 mm	Under two weeks	-
Q100	YES	10 mm	Under a week	Under a week
Q500	YES	40 mm	As soon as possible	As soon as possible

If the actual (and measured) behavior deviates from the predictions (for example, an effective irreversible displacement of 30 mm for a Q100 flood instead of a forecast of 10 mm), then immediate safety actions such as a reservoir drawdown could be considered, with the regulatory authorities being informed.

All these considerations and thoughts are currently under discussion in our working group.

5. CONCLUSION

In this paper dedicated to the reinforcement of concrete dams by passive anchors:

- The state of the art regarding the use of passive anchors for concrete dam reinforcement, in France and abroad, has been reviewed. The survey was extended to include the use of passive anchors in the underground works and rock slope stabilization fields, where the use of such anchors is common.
- French, Swiss, Swedish, Norwegian, American, and Canadian guidelines were analyzed. It appears that the practices are highly variable: USA advises against the use of passive anchors, while Sweden and Norway consider their use to be acceptable, with appropriate conservatism.
- An innovative method that accounts for the dilatancy and confinement effects is proposed.
- Both relevant existing methods and the innovative method were benchmarked on a theoretical case: a small concrete overflow gravity dam. It appears that none of the methods give fully satisfactory results. Methods should be combined to describe, as precisely as possible, the behavior of the interface reinforced by passive anchors.
- The main elements concerning French draft guidelines relating to the use of passive anchors to reinforce existing concrete dams are described, namely: corrosion protection of the anchors, monitoring and surveillance of dams reinforced by passive anchors.

A lot of work is still to be completed to reach our objectives. The study currently underway in our working group could be shared with other potentially interested committees, or within the framework of dedicated ICOLD technical committee.

MEMBERS OF THE CFBR WORKING GROUP ON PASSIVE ANCHORS

Members	Entities
CHAMPIRE Florian	PoNSOH
COUBARD Grégory	EDF
DE BARMON Paul replaced by SAFAR Edgard	Tractebel
FARGIER Yannick	UGE
GUILLEMOT Thibaut	ISL
LANDEL Rémi replaced by LE Thu Nga	CNR
LHERBIER Jean-Rémi	Artélia
MOREL François	EDF
ROYET Paul	CTPBOH
TARDIEU Bernard	CTPBOH
VEYLON Guillaume	INRAE
COUTURIER Bernard	CTPBOH
GUERINET Michel	CTPBOH
LAIGLE François	WSP BG

REFERENCES

- [1] G. COUBARD, F. LAUGIER, L. DEROO, M. FERRIÈRE, Confortement par ancrages passifs : quel comportement ? quel dimensionnement ? Proposition d'une méthode innovante de justification. Dam Strengthening with passive anchors: Innovative approach to design. Colloque CFBR 2019.
- [2] RIDAS, Swedish Hydropower companies guidelines for dam safety, application guideline 7.3 Concrete dams, Svensk energi, Stockholm, 2011.
- [3] Flödeskommittén, Riktlinjer för bestämning av dimensionerande flöden för dammanläggningar, Svensk Energi, Svenska Kraftnät & SveMin, 2007.
- [4] L. STEFAN, P. LÉGER, Cracked section analysis of gravity dams including passive reinforcement and uplift pressures, CDA 2010 Annual conference.
- [5] F. PELLET, Strength and Deformability of Jointed Rock Masses Reinforced by Rock Bolts, Ecole Polytechnique Fédérale de Lausanne, Thesis n°1169, 1994.

- [6] CEREMA, Protection contre les instabilités rocheuses, dimensionnement et exécution des boulons, 2017.
- [7] G. COUBARD, Are passive anchors an interesting solution to stabilize gravity dams? Fourth international dam world conference, Lisbon, 2020.
- [8] CFBR, Recommendations for the justification of the stability of gravity dams, October 2012
- [9] SIA, Tirants d'ancrage passifs (clous) à adhérence totale, SIA 191/1 :2001

COMMISSION INTERNATIONALE DES
GRANDS BARRAGES

VINGT-HUITIEME CONGRES DES
GRANDS BARRAGES
CHENGDU, MAI 2025

PETITS BARRAGES ET DIGUES : LEÇONS PARTAGÉES (*)

Rémy TOURMENT
INRAE

Luc DEROO
ISL

Chloé CHANCEL
ARTELIA

Sébastien PATOILLARD
DREAL CVL

FRANCE

SUMMARY

The design and construction techniques for levees and small dams have developed relatively independently over the past decades and centuries, as have their governance and operation.

These separate approaches have their logic: even if design and construction call on the same disciplines (hydrology, geology, geotechnics, etc.), and even if in both cases the aim is to retain water, there are fundamental differences: in geometry, in the nature of the stresses, in governance, in operating and monitoring conditions. These differences have consequences: engineering practices are not the same. But an analysis of the similarities and differences between the different types of structure will enable progress to be made on both sides.

**Small Dams and Levees: Shared Lessons*

One of the major differences between the design of flood protection levees and that of dams is the location of the structure. In the case of dams, geological considerations contribute to the choice and validation of the location of the structure. Levees, on the other hand, are sited according to the area to be protected, which often requires specific adaptation to the site. When geological conditions are unfavourable, innovations are sometimes needed to overcome these challenges. A very specific example of the raising of the perimeter protection levee at the Blayais nuclear power plant illustrates this point, as well as the general principles presented in the rest of the article. The Blayais site occupies the St-Ciers marsh, a marshy area bordering the right bank of the Gironde estuary for around 20 km. In the area of the levee, the marsh is made up of a significant thickness of 8 to 11 m of highly compressible Flandrian clayey silt, resting on gravel. To guarantee the stability of the structures over a 40-year period and to adapt to the complexity of the site (geology and right-of-way), an original and innovative compromise of a levee made of quicklime-treated materials on rigid inclusions with a cut-off wall in the foundation and protected by a rock armour was designed.

In areas with very limited right-of-way that prevented the construction of a conventional embankment levee, a levee solution consisting of a reinforced embankment retaining wall was implemented (on the central side). These solutions proved to be the best compromise in the face of the different constraints and generated challenges to be met during the studies to demonstrate the robustness of the structure.

RÉSUMÉ

Les techniques de conception et de construction des digues et des petits barrages se sont développées de manière relativement indépendante au cours des décennies et des siècles passés, de même que leur gouvernance et leur exploitation.

Ces approches séparées ont leur logique : même si la conception et la construction font appel aux mêmes disciplines (hydrologie, géologie, géotechniques, ...), et même si dans les deux cas il s'agit de retenir de l'eau, il y a des différences fondamentales : de géométrie, de nature des sollicitations, de gouvernance, de conditions d'exploitation et de surveillance. Elles ont des conséquences : les pratiques d'ingénierie ne sont pas les mêmes. Mais une analyse des similarités et des différences entre les différents types d'ouvrages permet des progrès de part et d'autre.

Une des différences notables pour la conception des digues de protection contre les inondations et celle des barrages réside dans l'emplacement de l'ouvrage. Pour les barrages, les considérations géologiques contribuent au choix et à la validation de l'emplacement de l'ouvrage. En revanche, les digues sont implantées en fonction de la zone à protéger, ce qui exige souvent une adaptation spécifique au site. Lorsque les conditions géologiques sont défavorables, des innovations sont

parfois nécessaires pour surmonter ces défis. Un exemple très particulier de la rehausse de la digue de protection périphérique du Centre Nucléaire de Production d'Electricité (CNPE) du Blayais illustre ce constat ainsi que les principes généraux présentés dans le reste de l'article. En effet, le site de Blayais occupe le marais de St-Ciers, une zone marécageuse bordant la rive droite de la Gironde sur environ 20 km. Au droit de la digue, le marais est constitué d'une épaisseur significative de 8 à 11 m de vases argileuses Flandrienne très compressibles, reposant sur des graves. Pour garantir la stabilité des ouvrages sur une durée de 40 ans et s'adapter à la complexité du site (géologie et emprise) un compromis original et innovant de digue en matériaux traités à la chaux vive sur inclusions rigides avec un écran étanche en fondation et protégée par une carapace en enrochement a été conçu. Dans les zones d'emprises très limitées empêchant la réalisation d'une digue à talus classique, une solution de digue constituée d'un mur de soutènement en remblai renforcé a été mis en place (côté centrale). Ces solutions se sont avérées le meilleur compromis trouvé face aux différentes contraintes et ont générés des défis à relever pendant les études pour démontrer la robustesse de l'ouvrage.

1. INTRODUCTION

Les grands et petits barrages, les digues de protection ou le long des canaux, ainsi que tous les autres ouvrages retenant de l'eau font partie d'une même famille, partageant des similarités mais comportant néanmoins certaines différences notables, en termes d'ingénierie comme de gouvernance. La fonction hydraulique de base de tous ces ouvrages est similaire : retenir et permettre la gestion de l'eau ; leur conception et leur construction font appel aux mêmes disciplines : hydrologie, hydraulique, géologie, géotechnique, génie civil, ... Pour autant, comme on le verra dans les prochains chapitres, il existe des différences fondamentales d'approche. Cet article vise à tirer parti de cet état de fait, en présentant quelques-unes de ces différences, partant des raisons qui y ont conduit, pour tenter d'éclairer ce que les spécialistes des digues, des petits barrages ou des grands barrages peuvent apprendre les uns des autres.

Les grands barrages ont fait depuis longtemps l'objet d'une attention particulière de la part de leurs propriétaires et exploitants, des pouvoirs publics et de la communauté scientifique et technique. En termes réglementaires, en France, le Comité Technique Permanent des Barrages, créé en 1966, et la circulaire du 14 août 1970 réglementaient les barrages "intéressant la sécurité publique", principalement ceux de plus de 20 mètres de hauteur. En termes de communauté professionnelle on remonte plus dans le temps : le Comité Français des Grands Barrages a été créé en 1926 et la Commission Internationale des Grands Barrages peu après, en 1928.

A l'inverse, les petits barrages, et plus encore les digues de protection contre les inondations, n'ont fait que beaucoup plus récemment l'objet de corpus technique

adapté aux enjeux contemporains et d'une réglementation dédiée, que ce soit en France ou dans la plupart des pays. Les standards et réglementations pour les digues et les barrages sont souvent distincts suivant les pays et avec des différences plus ou moins marquées voire fondamentales. En termes techniques, aujourd'hui encore, il y a souvent une tendance à séparer ces trois types d'ouvrages. Jusqu'à très récemment, la plupart des spécialistes des digues travaillaient essentiellement sur les digues, les spécialistes des barrages essentiellement sur les barrages et c'est encore le cas pour nombre d'entre eux, que ce soit en France et encore plus dans certains pays où la limite des compétences est très marquée, voire figée. Les petits barrages ont bénéficié (et parfois subi) l'influence des approches progressivement mises au point pour les grands barrages, les digues de protection ont de leur côté souvent été conçues et réalisées par le passé indépendamment des approches "barrages", avec souvent même des moyens très rustiques. Les deux chapitres suivants de ce rapport illustrent respectivement les différences entre petits et grands barrages et entre digues de protection et barrages, le chapitre qui leur succède illustre le propos avec un cas particulier de digue de protection.

2. LES PETITS BARRAGES

2.1. DEFINITION

Au sens de la CIGB, un petit barrage est un barrage de moins de 15 m de hauteur, qui retient moins de 3 hm³ d'eau. Il ne s'agit pas d'une définition universelle : dans nombre de pays, les réglementations distinguent également les barrages selon des caractéristiques géométriques (hauteur du barrage, volume de la retenue), mais fixent différemment la limite entre les différentes classes de barrage.

Historiquement, dans l'esprit de la communauté des barragistes, un « petit barrage » se distingue d'un « grand barrage » par deux caractéristiques liées :

- une éventuelle rupture d'un « petit barrage » a des conséquences généralement moins grave que la rupture d'un « grand barrage » ;
- les « petits barrages », très nombreux, sont pour la grande majorité des barrages en remblais à vocation agricole, conçus et construits pour des communautés locales, avec des moyens visant à la simplicité et à l'économie.

Pour ces deux raisons, les « petits barrages » sont longtemps restés (et restent encore souvent) une discipline spécifique, distincte des « grands barrages », et pour laquelle des cultures d'ingénieries propres se sont développées :

- ingénierie des petits barrages agricoles en remblai ; le plus souvent des remblais homogènes avec une conduite de prise d'eau sous remblai, et un évacuateur à seuil libre en rive,

- ingénierie des petits barrages en rivière pour la navigation et les prises d'eau usinières ou à usage d'eau potable ; barrages en maçonnerie ou béton, complétés parfois par des ailes en remblai, équipés de sections vannées pour le passage des crues,
- ingénierie des petits barrages pour la production de neige de culture : barrages en remblai le plus souvent grossier avec étanchement par géomembranes,
- ingénierie des petits barrages écrêteurs de crue : barrages de conception variées, comportant souvent un pertuis ouvert.

Les réglementations pour la sécurité des barrages conduisent à une homogénéisation des principes de dimensionnement ou de vérification de la sécurité (tout en admettant des critères différenciés selon les classes de barrages) : crues de projet, évaluation de la sécurité des évacuateurs, vérifications de stabilité, justification vis-à-vis de l'érosion interne. Cependant, ces réglementations ne s'appliquent pas toujours aux « petits barrages », et généralement pas aux plus petits des « petits barrages ». Par exemple, en France, un barrage de 10 m qui retient 1 hm³ d'eau est un barrage de classe C (un « petit barrage », mais suffisamment « grand » pour être réglementé au sens de la sécurité hydraulique) ; un barrage de 10 m qui retient un peu moins de 20 000 m³ d'eau n'est pas concerné par la réglementation. La figure 1 présente les limites des classes des barrages dans la réglementation française.

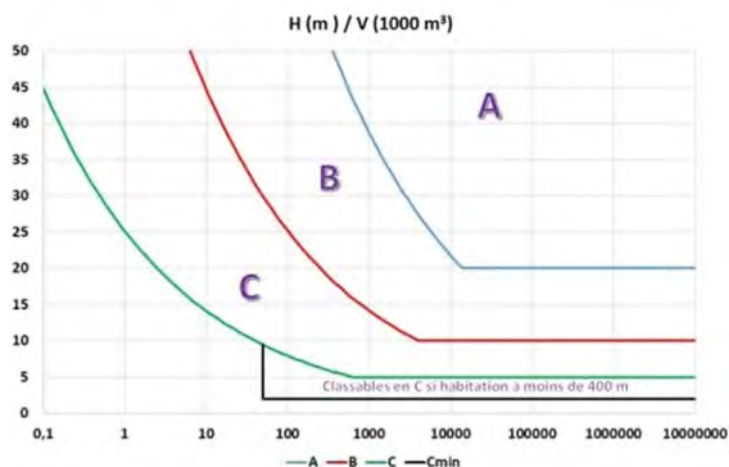


Fig. 1

Les Classes de barrages selon la réglementation française (figure extraite de <https://www.barrages-cfbr.eu/Classes-de-barrages.html>)

Classes of dams under French regulation (figure taken from <https://www.barrages-cfbr.eu/Classes-de-barrages.html>)

Dans la suite de ce rapport, nous nous intéressons plus spécifiquement aux petits barrages en remblai, à vocation essentiellement agricole. Parmi ceux-ci, on trouve les plus grands des « petits barrages » en remblai, dont la conception et la justification tendent à s'aligner sur celle des grands barrages, et les plus petits d'entre eux, pour lesquels cet alignement n'est pas requis par la réglementation française.

2.2. ACCIDENTOLOGIE

L'accidentologie des petits barrages est riche : nombreuses ruptures, nombreux dysfonctionnements. Les informations sur les ruptures de petits barrages [1] indiquent ceci :

- Dans un pays quelconque, lorsque les petits barrages sont inventoriés, il apparaît que leur nombre est important ; il représente typiquement 90% de l'effectif des barrages dans ce pays. Et il est certain que la plupart des plus petits barrages ne sont pas comptabilisés.
- Le pourcentage de petits barrages ayant rompu est également plus élevé que celui des grands barrages : les données sont insuffisantes pour calculer ce pourcentage avec une fiabilité suffisante, mais dans tous les pays inventoriés, des ruptures de petits barrages se produisent chaque année.
- Sauf exception très rare, ces ruptures ne font pas (ou très peu) de victimes, ce qui justifie que les réglementations soient moins exigeantes. Parmi les exceptions : des barrages avec des enjeux situés immédiatement sous l'ouvrage ; et -même si cela est peu documenté- des barrages situés à une altitude élevée par rapport aux enjeux (le long de l'onde de rupture, l'énergie libérée par l'accident est augmentée de la perte d'altitude ; du fort transport solide peut être généré).
- Les causes de rupture sont pour la très grande majorité : les ruptures par érosion interne ; les ruptures par surverse, ce qui est dû à la prépondérance des ouvrages en remblai.

L'inondation aval causée par la rupture du barrage n'est pas le seul événement redouté. Dans les pays en développement, les retenues des petits barrages peuvent représenter un enjeu majeur pour des communautés locales. C'est alors parfois davantage la perte de la retenue, plus que l'onde de rupture, qui est dangereuse.

Les enquêtes [1] font état également d'une autre problématique : de nombreux petits barrages ne remplissent pas le service attendu par défaut de remplissage (hydrologie déficitaire, fuites), envasement très rapide et/ou blocage des organes de prise d'eau.

2.3. LEÇONS PARTAGEES : LES CAUSES DE RUPTURE

Le premier mode de rupture des barrages en remblai est lié à la crue, lorsqu'elle dépasse la capacité de l'évacuateur ou lorsque les structures de l'évacuateur sont emportées par l'écoulement. Cela peut se produire en cas d'événement climatique extrême ou en raison d'une mauvaise appréciation de l'hydrologie des crues, de l'hydraulique des écoulements ou de la résistance des structures à l'érosion.

Le deuxième mode de rupture des barrages en remblai est l'érosion interne, qui se manifeste le plus souvent lors de la première mise en eau : le long de la conduite sous remblai, et aussi parfois en fondation. Mais parfois également au-delà, comme le montre le retour d'expérience des barrages de canaux, une catégorie importante de petit barrage : nombre de ces petits barrages sont construits en matériaux alluvionnaires perméable (sable, de granulométrie plus ou moins fine ; plus ou moins silteux), avec étanchement par une couche d'argile (« corroi ») ; cette conception est peu sûre : la frange d'argile assurant l'étanchéité est aisément percée, par exemple par fissuration de dessiccation, pouvant conduire à des scénarios de rupture par érosion interne.

Le troisième mode de rupture des barrages en remblai est l'instabilité des talus, qui résulte d'une maîtrise insuffisante des pressions interstitielles.

Ces trois modes de rupture peuvent également survenir en raison du vieillissement des ouvrages : altération du revêtement de l'évacuateur, fragilisation des structures de la conduite ou galerie sous remblai, colmatage d'un tapis de drainage, altération de la crête par dessiccation et passage de véhicules ou d'animaux.

Les petits barrages ne peuvent pas aisément bénéficier des barrières de défense mises en œuvre pour les grands barrages : les périodes de retour des crues de projet sont plus faibles, le zonage des remblais et le traitement des fondations sont coûteux.

En revanche, les petits barrages peuvent profiter des recherches en cours, souvent initiées pour les digues, qui, elles non plus, ne peuvent pas être protégées pour des crues aussi rares que les barrages et qui bénéficient assez rarement d'une structure zonée :

- les recherches vers une meilleure caractérisation de la résistance des matériaux à l'érosion interne (notamment : érosion de conduit, érosion régressive) pourront apporter des moyens simples d'évaluation de la sécurité en l'absence de filtre;
- les recherches vers la conception et l'évaluation de matériaux ou dispositifs résistants à la surverse et pouvant être installés sur les remblais peuvent offrir des solutions avantageuses de mise en sécurité des barrages ; pour certains petits barrages neufs, elles peuvent conduire à se passer d'évacuateur de crue;

- l'utilisation des géomatériaux, par exemple en remplacement ou complément des corrois d'argile, des filtres ou encore des drains.

2.4. LEÇONS PARTAGÉES : LES NON-RUPTURES

L'accidentologie recèle un nombre significatif de ruptures, mais surtout un nombre considérable de « non-rupture ». Les leçons de ces « non-ruptures » méritent d'être partagées, et peuvent alimenter la réflexion concernant les digues de protection.

- Les filtres sont des protections très efficaces, à condition de couper tous les chemins d'écoulement. La localisation des filtres et un remblai assurant le confinement du filtre sont des paramètres plus importants que le strict respect de la courbe granulométrique (l'absence de fines plastiques est toutefois nécessaire).
- De la végétation (arbustes, arbres) s'est développée de manière non contrôlée sur le parement aval de nombreux petits barrages. En théorie, les racines des arbres peuvent initier des scénarios de rupture par érosion interne, le long des vides que laissent les racines après qu'elles ont pourri. Pourtant, nous ne connaissons pas de cas de rupture de petit barrage certainement associée à ce mécanisme. Au contraire parfois, les racines des arbres peuvent améliorer les conditions de stabilité des talus, par la résistance à la traction des racines, et par la succion racinaire qui rabat la nappe. Dans l'état actuel des connaissances, il est recommandé de maintenir les talus libres de toute végétation arbustive et arborée, pour les trois raisons suivantes: (1) il n'y a pas encore de certitude sur le fait que les racines ne peuvent pas provoquer de scénario d'érosion interne, (2) la chute des arbres en cas de tempête peut provoquer des dégâts dangereux et (3) le développement de végétation perturbe la surveillance visuelle (détection des terriers de fouisseurs, apparition de zones de suintements). Mais il n'est pas systématiquement recommandé d'enlever (et dessoucher) les arbres qui se sont développés sur les petits barrages à talus argileux raides. Ce retour d'expérience concernant les petits barrages amène plus généralement à repenser la question de la gestion de la végétation sur les talus des digues et barrages en remblai ; les recherches devraient se poursuivre à ce sujet.
- Les petits barrages en remblai argileux homogènes de hauteur limitée (typiquement 5 m) se sont généralement parfaitement comportés, y compris dans des circonstances sévères : fuites localisées à la faveur de fissures de tassement différentiel ou dessiccation ; surverse modérée en crue. Trois paramètres essentiels interviennent : la nature de l'argile & l'intensité du compactage (qui guident : la résistance à l'érosion interne de conduit, et la cohésion), la nature de la fondation (une fondation sableuse génère un risque d'érosion régressive ; une fondation rocheuse fracturée ou caillouteuse génère un risque d'érosion de l'argile vers la fondation). De plus, en cas

d'ouverture de brèche, l'argile compactée limite la vitesse d'élargissement, ce qui limite le débit maximum de l'hydrogramme de rupture. En première approximation, le paramètre d'intérêt est l'indice de plasticité de l'argile (un IP typiquement entre 20 et 35 est souvent associé à une argile résistant à l'érosion) ; cependant il ne s'agit que d'une première approximation, et cela devrait toujours être confirmé par des essais HET.

2.5. LEÇONS PARTAGEES : LES BARRAGES ECRÊTEURS DE CRUE

Les petits barrages écrêteurs de crue, souvent appelés ouvrages de ralentissement dynamique (ORD) sont des petits barrages avec trois spécificités qui les rapprochent des digues de protection contre les crues : (1) leur mise en charge n'est que temporaire et liée à l'occurrence des crues ; cela rend parfois difficile leur mise à l'épreuve contrôlée par une procédure de première mise en eau progressive ; (2) par leur fonction même, ils sont situés à l'amont de zones avec une population importante, qui se trouve dans l'emprise d'une éventuelle onde de rupture et (3), la mise en charge n'est que temporaire, et les remblais en sols fins n'ont généralement pas le temps de se saturer.

Compte-tenu de l'accidentologie des barrages en remblai et des spécificités des barrages écrêteurs de crue, les précautions particulières associées à ces ouvrages sont les suivantes [2] :

- Prévoir des organes d'évacuation des crues « robustes », c'est-à-dire peu sensibles aux incertitudes. Un évacuateur robuste est typiquement un évacuateur à seuil libre de forte capacité sous faible lame déversante, et pouvant supporter une lame d'eau plus forte. Les solutions techniques répondant à ce critère sont nombreuses (seuil libre de grand développement, PKWeirs, remblais rendus résistants à la surverse, ...).
- Faire en sorte que la conception et la construction évitent les défauts dangereux ; notamment défauts de traitement des fondations et défauts à l'interface entre les remblais et les ouvrages traversants. Cela passe par l'identification des risques géologiques en phase conception (certaines fondations présentent un risque élevé, d'autres sont sans danger). Cela passe également par une surveillance attentive des travaux, pour identifier et traiter les points faibles.

Il reste cependant des sujets ouverts, pour lesquels une meilleure compréhension des mécanismes pourrait permettre d'augmenter la sécurité, en préservant l'économie de ces projets ; ces sujets concernent également les digues :

- Comment concevoir efficacement la « clé d'étanchéité » souvent mise en œuvre sous les ouvrages, c'est-à-dire : quel est l'incidence réelle sur les chemins d'érosion de conduit et d'érosion régressive, lorsque cette clé ne traverse pas l'entièreté des horizons érodables de la fondation ?

- Comment mieux prédéterminer les conditions de saturation des remblais, en crue, compte-tenu de la nature des remblais, et aussi compte-tenu de la fissuration susceptible de les traverser.

2.6. GOUVERNANCE

Un petit barrage, avec un propriétaire unique, c'est peu de moyens : peu de moyens pour la conception, peu de moyens pour le suivi des travaux. Ainsi, et paradoxalement, les petits barrages sont souvent plus difficiles à concevoir que des barrages plus grands, car le temps d'ingénierie et les données disponibles sont maigres. C'est ce qui a pu conduire à tant de déboires : des ruptures de barrage, des retenues qui ne se remplissent pas, ou qui s'envasent très vite.

Il est possible d'améliorer ce constat, lorsqu'on peut mutualiser les moyens d'ingénierie à l'échelle d'un territoire, pour un certain nombre de petits barrages. L'intérêt est évident car, localement, les conditions se ressemblent souvent, et il est alors possible de mutualiser les études :

- pour l'évaluation des conditions naturelles : hydrologie des apports, hydrologie des crues, géologie, sédimentation,
- pour les standards de conception, construction : connaissance des matériaux de construction, standardisation de certains choix de conception et méthodes de construction,
- pour l'évaluation des risques, via l'estimation des zones inondées en cas de rupture,
- pour l'acquisition de données en surveillance (par exemple interférométrie radar satellitaire).

3. LES DIGUES DE PROTECTION CONTRE LES INONDATIONS

Les digues de protection contre les inondations sont proches des barrages par de nombreux points, et depuis ces dernières années on constate un rapprochement entre les communautés professionnelles de ces deux types d'ouvrages hydrauliques, particulièrement au sein des bureaux d'études et des comités nationaux de la CIGB, entre autres le CFBR. Malgré cela il existe de nombreuses différences dues principalement aux facteurs suivants :

- une mise en charge occasionnelle, mais avec une forte sollicitation mécanique des digues via les mouvements de la masse d'eau (courants longitudinaux, vagues de houle) et des solides qu'elle transporte,
- leur géométrie : les digues ont généralement des hauteurs faibles de quelques mètres (mais il existe néanmoins dans le monde plusieurs exemples de

- digues de plus de 10 mètres de haut) et à l'inverse de très grandes longueurs (plusieurs kilomètres, parfois dizaines, voire centaines de km),
- leur historique : souvent les digues sont très anciennes, ayant été construites à l'origine par les acteurs locaux sans forcément l'intervention d'une ingénierie compétente et spécialisée comme celle des grands barrages, et elles ont fortement évolué au cours du temps.

Il est à noter qu'il existe parfois du fait de l'histoire des différences de terminologie, aussi bien en français qu'en anglais, ce qui ne facilite pas toujours le dialogue entre spécialistes ; par exemple en français "digue" désigne dans certain cas un barrage en remblai ; des problèmes de traduction ou de simple compréhension au niveau international se posent aussi, entre autres dans les cas où un même mot a deux sens différents dans une langue et un seul dans l'autre.

Dans la suite de ce chapitre on présente successivement les spécificités des digues de protection en ce qui concerne la gouvernance (responsabilité du gestionnaire et réglementation), les approches liées au risque inondation, et les spécificités en termes d'ingénierie.

3.1. GOUVERNANCE EN FRANCE

Nombre d'événements de ces dernières décennies ont mis en évidence le rôle important, voire essentiel, du gestionnaire de digues pour leur efficacité et leur sûreté, cette gestion devant être cohérente à l'échelle du système. Sur le Rhône aval entre autres, les structures de gestion mises en place au XIX^{ème} siècle ont montré leurs limites lors des crues de 1993 et 1994, ce qui a conduit à la création et à l'organisation du gestionnaire actuel, le SYMADREM. Le gestionnaire d'un système donné a en charge la surveillance et l'entretien des ouvrages, y compris en période de crue, afin de garantir leur efficacité et d'éviter la formation de brèches.

En parallèle aux évolutions locales des structures gestionnaires et de leurs pratiques, souvent initiées par des événements de crue majeures et d'inondations résultantes, l'État français a pris conscience de la nécessité de cette bonne gestion à l'échelle nationale. Après avoir engagé depuis 1999 un recensement des ouvrages, de leurs zones protégées et de leurs gestionnaires (bases de données nationales gérées par l'administration), une réglementation concernant les ouvrages de protection contre les inondations a progressivement été développée. Cette réglementation, d'abord purement technique, a depuis précisé les rôles respectifs du gestionnaire et de l'État, elle a enfin clarifié l'attribution de la responsabilité de la gestion des systèmes d'endiguement et autres ouvrages de protection contre les inondations avec la nouvelle compétence GEMAPI. Les digues ne sont pas les seuls ouvrages de protection contre les inondations, les barrages écrêteurs de crue, les bassins de stockage en dérivation du cours d'eau ou encore les canaux de

dérivation sont également utilisés pour diminuer l'aléa inondation naturel sur un territoire. Parfois ces ouvrages fonctionnent de manière très intégrée au sein d'un système mais dans tous les cas sur un même territoire protégé le gestionnaire est identique pour tous les ouvrages de protection.

La réglementation française comme la bonne pratique des gestionnaires conduit à réaliser de manière régulière diagnostics et analyses de risque, ce qui fournit des outils d'aide à la décision pour la définition des programmes de travaux et l'organisation de la surveillance des ouvrages.

3.2. L'APPROCHE "RISQUE"

Les digues de protection sont associées au risque (d'inondations) par leur fonction même ; en conséquence, les approches basées sur le risque sont plus naturelles, courantes et intégrées dans leur conception et leur diagnostic que pour les barrages. Pour les barrages, éviter la rupture a généralement un poids plus important dans le processus de décision que d'analyser les conséquences possibles d'une rupture et les intégrer dans une évaluation des risques. En outre, les ruptures d'un système de digues peuvent se produire de manières très différentes et à des endroits variés, et peuvent entraîner des scénarios d'inondations et de conséquences très différentes. Les digues fonctionnent au sein de systèmes de protection contre les inondations, ce qui représente la bonne échelle pour l'analyse des risques, la conception et la prise de décision en termes d'objectifs fonctionnels et de priorités, tandis que chaque digue ou tronçon présente la bonne échelle d'analyses en termes de conception et d'évaluation géotechnique et structurelle. Les systèmes de digues remplacent un danger naturel d'inondation par une combinaison de ce danger naturel avec un danger technologique (la rupture possible). L'analyse des risques d'un système de digues comprend tous les composants du modèle Source-Pathway-Receptor (SPR) (figure 2) : l'aléa naturel, la performance de protection / le danger de rupture, les conséquences de l'inondation dans la zone protégée.

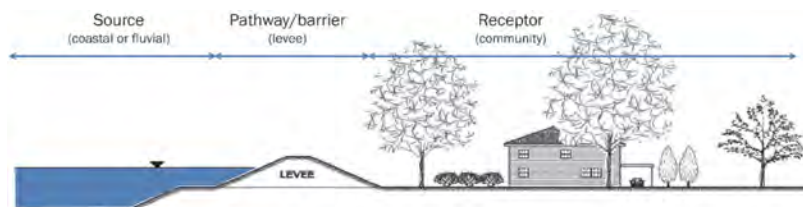


Fig. 2
Le modèle conceptuel SPR et les digues (d'après [3])
SPR conceptual model and levees (from [3])

Une difficulté apparaît néanmoins du fait de la confusion fréquente par le passé entre la protection apportée par les digues, par nature limitée, et une absence complète de risque. Beaucoup de digues en remblai ont un aléa de rupture résiduel, quasi certain pour un niveau d'eau au-delà de leur crête voire, dans certains cas de digues anciennes et insuffisamment entretenues, non négligeable en deçà. Ce constat a conduit la profession à introduire les notions distinctes de "niveau de protection" (NP, absence d'inondation de la zone protégée) et de "niveau de sûreté" (NS, probabilité de rupture négligeable), avec le corollaire que pour une bonne prévention du risque inondation NS doit être significativement supérieur à NP.

Les responsables de la gestion des digues en France sont le plus souvent responsables de leur surveillance et de leur entretien, y compris en période de crue, et ce sont le plus souvent d'autres autorités qui sont responsables de la gestion de crise et de la sécurité des populations. Compte tenu de la faible différence, ou pire de la confusion, entre NP et NS il existe un recouvrement de responsabilité aux alentours de cette limite de performance des ouvrages.

3.3. INGENIERIE

En termes d'ingénierie, les digues ont, par rapport aux barrages réservoirs, de nombreuses particularités que nous résumons ci-dessous.

- Les digues anciennes, du fait de leur historique (grande longueur et constructions avec les matériaux de proximité, réhausses successives, réparations de brèches, maintenance plus ou moins régulière) sont très hétérogènes dans toutes leurs dimensions. Cet état de fait conduit dans le contexte actuel de reprise en main de ce patrimoine à de forts besoins de confortements. Le CFBR a publié en 2021 un recueil de méthodes de confortements associé à une partie guide méthodologique [4].
- Les actions et sollicitations hydrauliques sur les digues sont occasionnelles et leur aspect dynamique est souvent à prendre impérativement en compte, à la différence des barrages où l'on peut considérer un niveau constant pour beaucoup de justifications. Des digues sont présentes dans tous types de milieux : fluvial, maritime, estuarien, lacustre, torrentiel, ce qui conduit à des caractéristiques de sollicitations très variables en termes de vitesse d'écoulement, de variation des niveaux de mise en charge, de vagues et de transport solide et d'érosion.
- Les ruptures de digues sont souvent la conséquence d'enchaînements de mécanismes. Au-delà des mécanismes "classiques" (érosion interne, érosion externe par surverse ou par le courant ou les vagues, instabilités) on commence à envisager d'autres mécanismes tels que la fissuration due à la sécheresse ou encore la liquéfaction statique qui, associés à d'autres, peuvent conduire à une brèche.
- L'absence de mise en charge régulière des digues de protection conduit à une difficulté de suivi de leur comportement. Les méthodes classiques sur les

barrages d'auscultation du comportement hydraulique (piézomètres, mesures de débits de drains) ne sont pas appropriées, d'autant plus que pendant les périodes de mise en charge les gestionnaires de digues sont très occupés par la surveillance visuelle et les éventuelles interventions d'urgence. Un besoin de développement de méthodes d'auscultation spécifiques a fait jour. On peut citer parmi les développements récents l'utilisation de fibre optique ou encore de mesures topographiques et infrarouge à partir de drones.

- Compte tenu de la grande longueur et de l'hétérogénéité des digues, leur diagnostic comprend de nombreuses sources d'incertitudes. Afin d'affiner le recueil de données sur leur composition, l'association de reconnaissances géophysiques à des essais géotechniques, est désormais courante. Des méthodes avancées de traitement utilisant l'ensemble de ces données (fusion, "machine learning") font l'objet de recherches prometteuses.
- Au-delà des disciplines classiques pour l'ingénierie des barrages que sont l'hydrologie, l'hydraulique et la géotechnique, compte tenu de la forte interaction entre les digues et le milieu eau contre lequel elles protègent, il faut insister sur l'importance de considérer dans les diagnostics et dans la conception des ouvrages les évolutions morphologiques et prévoir systématiquement un volet d'étude spécialisé.
- Comme pour les barrages mais à un degré encore plus élevé, les incertitudes sur le changement climatique vont devoir être intégrées dans la conception et la gestion des digues en vue de leur résilience, à la fois vis à vis de l'accroissement des débits, des niveaux et des éventuelles actions des vagues mais aussi vis-à-vis des sécheresses.
- La présence d'ouvrages et réseaux inclus dans les digues, souvent gérés par d'autres entités que le gestionnaire de digues crée des difficultés lors des diagnostics, mais également lors de travaux, que ce soit des travaux de confortement des digues, ou à l'inverse des travaux de création ou de maintenance commandités par le gestionnaire d'un de ces réseaux. Cette problématique engendre un besoin de solutions techniques à la fois en termes de conception, comme de réalisation. Le groupe de travail du CFBR ayant rédigé [4], et dont le mandat a été prolongé pour rédiger de nouvelles fiches descriptives de techniques, a cette problématique parmi ses priorités.
- La surverse ou le franchissement des digues sont fréquemment la cause de leurs ruptures. Historiquement, les digues étaient souvent rehaussées après chaque crue majeure les ayant rompues en les surversant, ce qui ne résolvait pas réellement le problème en l'absence de déversoir de sécurité ... Un des challenges en termes de fiabilisation des systèmes de digues est la mise en place de tels déversoirs ou de tronçons résistants à la surverse, permettant de rendre ces systèmes résilients à ce dépassement de niveau. La France est un des rares pays dans le monde préconisant une telle solution, directement liée à la distinction entre niveau de protection et niveau de sûreté. Depuis quelques années, en France, on peut constater la mise en place de tels déversoirs, qui ont par ailleurs fait l'objet d'un guide [5], comme par exemple le déversoir de Lattes (figure 3) situé sur le Lez en aval de la ville de Montpellier. En solution d'attente, ou en complément voire en alternative à la mise en

place de déversoirs, on peut envisager, par exemple, d'aménager certains tronçons pour la gestion de surverse en adaptant le niveau de crête aux premières entrées d'eau et en améliorant la résistance à la surverse de la crête et du talus côté zone protégée. Des recherches en géomécanique et la mise au point de solutions techniques sont en cours ; ces recherches peuvent bénéficier également aux barrages.



Fig. 3
Le déversoir de Lattes (photo R. Tourment)
The Lattes spillway (photo credit R. Tourment)

On le voit dans l'énumération rapide ci-dessus que les problématiques spécifiques aux digues sont nombreuses. Elles ne sont néanmoins pas sans intérêt pour la communauté "barrages" et le fait que des groupes de travail des comités nationaux regroupent des spécialistes issus des deux communautés montre bien que les analyses et les réflexions sur l'un ou l'autre des types d'ouvrage s'alimentent mutuellement.

4. UN EXEMPLE : LES DIGUES DE PROTECTION DU CNPE DU BLAYAIS

Une différence notable entre les digues de protection contre les inondations et les barrages est l'emplacement de l'ouvrage. Pour les barrages, c'est un choix fortement influencé par la géologie, tandis que pour les digues, l'emplacement est imposé par la zone à protéger et nécessite de s'adapter au site. Il faut parfois innover pour des sites complexes lorsque les conditions géologiques ne sont pas favorables.

Cela a été le cas pour la digue de protection périphérique du Centre Nucléaire de Production d'Electricité (CNPE) du Blayais dont les travaux de rehausse de la digue de protection contre les inondations se sont achevés en 2022 [6].

4.1. CONTEXTE DU PROJET

Le Centre Nucléaire de Production d'Electricité (CNPE) du Blayais est situé en rive droite de l'estuaire de la Gironde sur le territoire de la commune de Braud et Saint-Louis (33), à environ 48 km au nord-ouest de Bordeaux. Le CNPE était protégé de l'inondation externe depuis sa construction par une protection périphérique constituée d'une digue en remblai de 2,4 km de long, arasée à une cote variant entre +5,75 et + 6,20m NGF, soit une hauteur de 2 à 3 m environ.

Suite à la catastrophe qui a affecté la centrale nucléaire de Fukushima-Daiichi en 2011, EDF a réévalué le niveau extrême d'inondations et défini les caractéristiques de la houle et du clapot dans le marais entourant le site. Les niveaux de protections initiaux se sont révélés insuffisants pour couvrir le risque d'inondation de type post-Fukushima, et ont conduit à mettre à niveau la protection inondation externe existante du CNPE du Blayais avec une conception permettant de contrôler les différentes venues d'eau (franchissement, infiltrations, fuites à travers les by-pass) en accord avec les préconisations du guide 13 de l'Autorité de Sureté Nucléaire (ASN) avec une garantie des niveaux de protection à 40 ans.

Les études de conception de la mise à niveau de la digue ont montré qu'une réhausse de 2m en moyenne était nécessaire et ont fait l'objet de multiples réflexions de choix de conception. Il s'agissait de prendre en compte les conditions particulières de ce site liées à la fois au niveau de sécurité élevé requis dans le domaine du nucléaire, la présence de réseaux enterrés sous les digues existantes, les contraintes d'emprises fortes, mais surtout la nature fortement compressible des sols en fondation qui imposerait classiquement des pentes de talus réduites donc de larges emprises non compatibles avec le site.

Dans ce contexte, des solutions classiques de réhausse en remblais courants ou par rideau de palplanches n'étaient pas envisageables. Par conséquent ARTELIA, TERELIAN et MENARD, en groupement, ont conçu un ouvrage pouvant répondre aux objectifs du projet, à savoir un ouvrage étanche dimensionné pour le niveau de crue de projet et les effets de la houle et du clapot et un ouvrage permettant de limiter l'amplitude des tassements, tout en prenant en compte les contraintes de site.

Pour garantir la stabilité des ouvrages sur une durée de 40 ans et s'adapter à la complexité du site (géologie, emprises et réseaux enterrés), un compromis original et innovant de digue a été proposé et conçu. Celle-ci est en effet réalisée en matériaux traités à la chaux vive et repose sur des inclusions rigides. L'ouvrage est composé d'un talus en enrochement côté marais et d'un talus classique ou d'un mur

de soutènement en remblai renforcé côté CNPE dans les zones d'emprises fortement restreintes. Il est également muni d'un écran étanche en fondation.

4.2. SPECIFICITES GEOLOGIQUE ET GEOTECHNIQUE DU SITE

Le site de Blayais occupe le marais de St-Ciers, une zone marécageuse bordant la rive droite de la Gironde sur environ 20 km. Le marais est constitué de vases argileuses Flandrienne, reposant sur des graves.

La succession stratigraphique de haut en bas sous la digue est la suivante :

- Des remblais récents sablo-limoneux (U1) constituant la rehausse du terrain naturel d'une épaisseur variant entre 2 et 5 m d'épaisseur.
- Des Argiles vasardes très compressibles (U2) pouvant présenter des horizons tourbeux (U2bis) d'une épaisseur significative de 7 à 12 m.
- Des alluvions sablo-graveleuses très perméables d'une épaisseur d'environ 14 m.

La digue existante était constituée de remblais argilo-limoneux. La coupe lithologique schématique de la digue existante et sa fondation est présentée ci-dessous dans la Figure 4 :

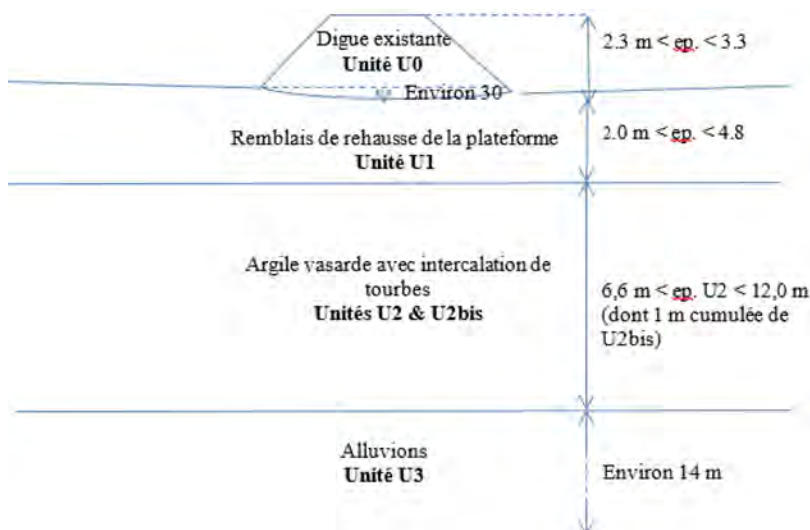


Fig. 4

Coupe lithologique schématique de la digue existante et de sa fondation
Schematic lithological section of the existing levee and its foundation

Les principaux paramètres géotechniques des formations en place sont dans le Tableau 1.

Tableau 1
Paramètres géotechniques caractéristiques des formations en place

Paramètres	U0 Remblais limonoargileux	U1 Remblais limono-sableux	U2 Vases argileuses	U2bis Tourbes au sein des vases	U3 Graves flandriennes
γ_h (kN/m ³)	19	18,8	16	13,2	20,8
c' (kPa)	5	0	2	0	
ϕ' (°)	25	28	23	30	
c_u (kPa)	60	/	$13 < c_u < 25$	/	
k_h (m/s)	$5 \cdot 10^{-7}$	$1 \cdot 10^{-4} < k_h < 5 \cdot 10^{-4}$	$1 \cdot 10^{-9} < k_h < 1 \cdot 10^{-8}$		
k_f/k_v	10	1	10	10	10

4.3. LES SOLLICITATIONS (NIVEAU D'EAU STATIQUE + HOULE)

Les ouvrages de protection inondation externe du CNPE du Blayais ont été dimensionnés pour résister à un phénomène extrême d'inondation et de submersion en considérant les données hydrauliques ci-dessous :

- Le niveau d'eau statique (hors houle et clapot) est de +6,86 m NGF O,
- Le limnigramme de crue,
- Les caractéristiques de la houle et du clapot à prendre en compte selon les orientations de la digue. Les valeurs maximales sont les suivantes à titre informatif :
 - Hauteur significative maximale ($H_s, \max.$) : 1,50 m
 - Période ($T_m-1,0$) au H_s max : 4,80 s

4.4. SOURCES D'ENTREE D'EAU POTENTIELLES SUR LA PLATEFORME

Les trois possibilités d'entrées d'eaux sur la plateforme ont été identifiées :

- V_f : le volume de franchissements au-dessus des ouvrages anti-inondation.
- V_p : le volume de percolation au travers, ou sous les ouvrages anti-inondation et le long des réseaux enterrés.
- V_b : les bypass sources de débit de fuite d'eau.

Elles sont illustrées sur la Figure 5 :



Fig. 5
Illustration des sources d'entrée d'eau à l'intérieur du site.
Sources of water going into the site

4.5. PRESENTATION DE LA CONCEPTION INNOVANTE DES OUVRAGES

4.5.1. Présentation des ouvrages

Au regard du contexte géotechnique du site qui présente une formation très compressible, des conditions de houle et des contraintes de site (faible emprise disponible et présence de réseaux traversants), la solution retenue est une digue en remblai argileux, traité à la chaux vive, sur inclusions rigides et munie d'un écran étanche comme illustré sur la Figure 6.

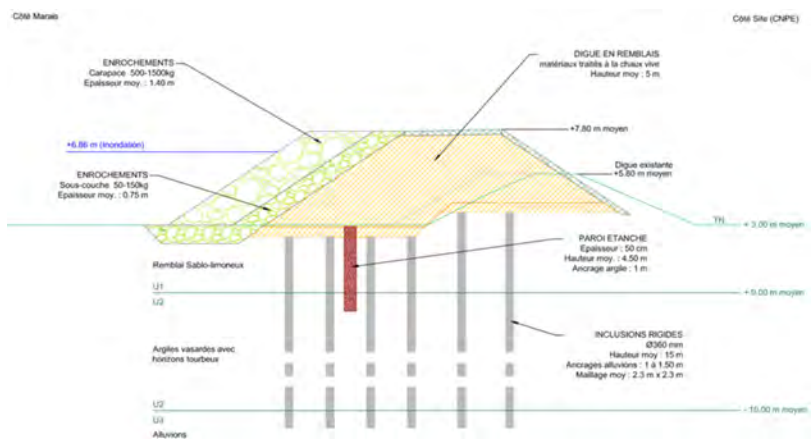


Fig. 6
Digue en remblai traité à la chaux sur inclusions rigides.
Lime-treated embankment levee on rigid inclusions

Les digues sont également protégées des actions de la houle et du clapot par une protection en enrochements dimensionnée selon les formules développées par Van Der Meer. Cette protection est composée de deux couches de matériaux (carapace et sous-couche), posées sur deux épaisseurs chacune.

Pour limiter l'emprise au sol et la quantité de matériaux, les pentes de talus sont de 3H/2V côté marais et côté site (sauf sur les zones d'emprises fortement restreintes, où le parement est vertical côté CNPE).

Une approche différente a été menée dans les zones où les emprises sont très limitées, empêchant la réalisation d'une digue classique. Une solution de digue à talus avec un parement vertical a été retenue comme illustrée sur la Figure 7. Cette solution, Terre Armée®, de type TerraTrel® minéral associe des panneaux de treillis galvanisés à des armatures synthétiques de type EcoStrap® constituées de fibres en alcool polyvinilique ancrées dans le remblai traité.

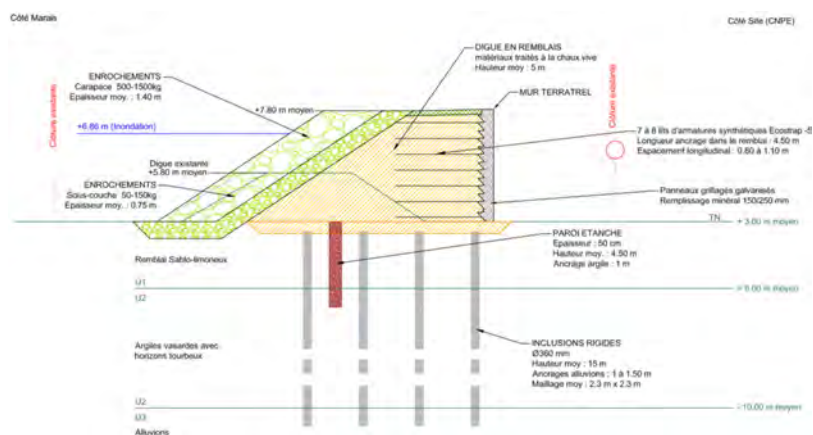


Fig. 7

Digue en remblai traité à la chaux sur inclusions rigides avec mur de soutènement.
Lime-treated embankment levee on rigid inclusions with retaining wall

4.5.2. *Nécessité de limiter les volumes de franchissement et nécessité de garantir la tenue de l'ouvrage et son niveau de protection à 40 ans*

Les calculs de franchissements ont montré que la hauteur de digue initiale (2,5 m en moyenne) devait être quasiment doublée ($H_{max} = 5$ m) et équipée d'une carapace et d'une sous-couche en enrochements augmentant de façon significative les emprises de l'ouvrage ainsi que son poids. La géologie du site, composée notamment d'une épaisseur importante de 8 à 11m d'argiles vasardes très

compressibles, ne permettait pas de supporter le nouvel ouvrage. La fondation de la digue a donc été renforcée par un dispositif d'inclusions rigides ancré dans les alluvions (U3) permettant ainsi de résoudre les problèmes de déformations liées aux tassements de la fondation ainsi que les risques de poinçonnement dans les argiles vasardes.

Le dimensionnement des inclusions rigides a été réalisé aux éléments finis sur Plaxis en tenant compte de l'historique du site par rétrocalage des paramètres de compressibilité à partir des chroniques de tassements depuis la construction de la centrale en 1977. A titre informatif, 60 cm de tassements ont été mesurés jusqu'en 2017 au droit de la digue existante.

L'intégrité des inclusions rigides a été vérifiée pour les différentes situations de calculs et pour différents modes de rupture. Ces vérifications ont été réalisées à l'ELS et l'ELU selon les recommandations ASIRI [1].

Les cotes de crête de la digue doivent être garanties à 40 ans malgré les tassements qui pourraient subvenir. Les inclusions rigides ont été dimensionnées sur Plaxis pour limiter le tassement à moins de 20 cm à 40 ans sans poinçonner le matériau constitutif de la digue. Par conséquent, toutes les digues ont été rehaussées de 20 cm par rapport à la cote admissible calculée pour contenir la crue et limiter les volumes de franchissements sur la plateforme.

Les inclusions rigides ont un diamètre de 360 mm et une hauteur moyenne de 15 m. Elles sont ancrées dans les alluvions (U3) de 1 à 1,5 m. Le maillage est en moyenne de 2,3 x 2,3 m.

4.5.3. *Nécessité de garantir l'étanchéité de l'ouvrage, limiter les volumes d'infiltrations et éliminer les risques d'érosion interne et de liquéfaction statique*

La digue a été réalisée en matériaux sablo-argileux traités à 1% de chaux vive en utilisant des matériaux excédentaires d'un site extérieur préservant ainsi les ressources de matériaux de carrière non renouvelables. Le choix du traitement à la chaux des matériaux du corps de digue est innovant, il apporte au matériau un couple cohésion/angle de frottement favorable à la stabilité de la digue, une perméabilité $\leq 1.10^{-6}$ m/s qui se maintient dans le temps ainsi qu'une grande résistance à l'érosion interne testée avec des essais HET.

La digue est fondée sur un horizon de sable limoneux de 2 à 5 m d'épaisseur. Le risque d'infiltrations et d'érosion interne à travers la fondation a été écarté par la mise en place d'un écran étanche d'une épaisseur de 50 cm et d'une perméabilité minimale de 1.10^{-7} m/s, ancré de 1 m dans les argiles vasardes peu perméables. Cet écran a été réalisé par un mélange du sol avec du ciment avec une trancheuse (soil mixing par voie humide).

4.5.4. *Contraintes d'emprises*

Une zone du chantier n'avait pas les emprises suffisantes pour recevoir la digue à talus. Le talus intérieur d'environ 4.8 m de haut a été remplacé par un mur de soutènement avec un parement minéral construit en remblai renforcé avec les matériaux traités à la chaux vive et des lanières synthétiques de largeur 50 mm et de 4,5 m de long, en nombre de 7 à 8 lits selon la section, avec un espacement longitudinal de 0,80 à 1,10 m. Cette « digue-mur » est aussi fondée sur des inclusions rigides.

4.6. BILAN

Les ouvrages définis par le Groupement sont issus d'une étude globale des protections à prévoir sur la totalité du linéaire de protection de la centrale, intégrant :

- Les contraintes du projet (spatiale, géologique et géotechnique, environnementale ...),
- Les contraintes de construction des ouvrages (franchissement, phasage des travaux, ...),
- Les contraintes d'exploitation et de durabilité des ouvrages (volume admissible dans l'enceinte des ouvrages, tassements, ...).

Au regard de la mauvaise qualité de la fondation, de la situation hydraulique de dimensionnement extrême type Fukushima et des contraintes de projet, la conception des digues a été un véritable challenge nécessitant une étroite collaboration entre EDF et le Groupement.

La solution mise en œuvre a permis de répondre à l'ensemble des contraintes du site, en renforçant le sol d'assise pour limiter les tassements grâce aux inclusions rigides, en renforçant le comportement de la digue face aux inondations grâce aux matériaux traités à la chaux vive dont la résistance à l'érosion interne et leurs performances dans le temps ont pu être démontrées. L'ouvrage comporte également une protection en enrochements vis-à-vis de la houle et du clapot et un écran étanche en fondation afin de réduire les infiltrations sur la plateforme et garantir la tenue de la fondation de la digue à l'érosion interne. Dans les zones d'emprises restreintes, le talus côté zone à protéger est composé d'un mur en terre renforcée.

L'ensemble des défis techniques à surmonter a nécessité une longue phase de conception et d'essais en laboratoire. Ce temps était nécessaire et prévu dans le planning global de l'opération afin de justifier des solutions innovantes dans la constitution de digues de protection contre les risques d'inondations externes.

La conception proposée permet de garantir le niveau de protection à 40 ans, et de démontrer un niveau de robustesse suffisant par rapport au volume d'eau attendu sur la plateforme en cas de crue accidentelle et les marges prises vis-à-vis des différents modes de défaillance.

Cette phase de conception a duré toute l'année 2020 permettant de réaliser en 2021 et 2022 une digue de protection de 2,4 km de long fondée sur un total de 98 km d'inclusions rigides et protégée par 80 000 tonnes d'enrochements.

7. CONCLUSION

Ces dernières années, la communauté des grands barrages a, au niveau français comme dans d'autres pays ainsi qu'au niveau international, porté une attention grandissante aux petits barrages et aux digues. Cette prise de conscience que ces ouvrages plus modestes ont globalement un même ordre de grandeur que les grands barrages au point de vue de leur utilité sociétale comme au point de vue des risques qu'ils engendrent a amené la CIGB et de nombreux comités nationaux dont le CFBR à les inclure de manière visible dans leurs travaux, ce qui s'est entre autres illustré par la Question 103 au congrès de Vienne en 2018 "Petits barrages et digues" [7] et l'inclusion de ces sujets dans plusieurs comités techniques de la CIGB ou groupes de travail de comités nationaux, dont le CFBR. La communauté scientifique et technique a intérêt à s'intéresser en parallèle à tous les types d'ouvrages hydrauliques. L'analyse de leurs similarités comme de leurs différences permet un enrichissement des connaissances et des pratiques parmi les praticiens plus spécialisés dans tel ou tel type d'ouvrage ; elle permet également des recherches plus pertinentes et avec un cadre d'utilisation plus large.

En termes de gouvernance, l'intérêt pour la collectivité au sens large au vu des bénéfices liés aux usages de ces ouvrages et les risques que représentent leur énorme parc, démontrent la nécessité pour les collectivités de se doter d'un cadre organisationnel, pour qu'il n'y ait plus d'ouvrages orphelins ou mal gérés. Les événements d'inondation de ces dernières décennies en France ont conduit le pays à se doter d'un tel cadre pour les digues et barrages de protection contre les inondations [8], qui couvre à la fois leur gouvernance et les exigences techniques.

RÉFÉRENCES

- [1] Petits barrages à faible risque, bulletin CIGB en cours de préparation

- [2] L. DEROO, P. ROYET, C. POULARD. Sûreté et efficacité des barrages écrêteurs de crue. Colloque CFBR " Sûreté des barrages et enjeux ", Nov 2016, Chambéry, France. pp.203-221, 10.24346/fbr_colloque2016_c01. hal-01467467
- [3] CIRIA, Ministère de l'écologie, du développement durable et de l'énergie, United States Army Corps of Engineers (2013). *The International Levee Handbook*. CIRIA, Londres
- [4] CFBR (2021). Recueil de méthodes et de techniques de confortement et réparation des digues de protection en remblai. ISBN 979-10-96371-17-4. CFBR, La Motte Servolex: 156+501p.
- [5] DEGOUTTE, G. *Les déversoirs sur les digues fluviales*, 2012, Editions Quae, 184p.
- [6] CHANCEL, C., AYMARD, N., DUTAILLY N. ET AL., Conception et réalisation de la protection périphérique contre les risques d'inondations externes pour le CNPE du Blayais. *Colloque Digues 2024*. DOI :10.5281/zenodo.10634109
- [7] TOURMENT, R., 2018. *Rapport Général de la Question 103 "Petits barrages et digues". Vingt Sixième Congrès de la Commission Internationale des Grands Barrages 01/07/2018-07/07/2018*, Vienne, AUT. 96 p.
- [8] TOURMENT R. ET AL., 2020. The new French regulation on flood protection structures: consequences on risk management. FLOODrisk2020, Jun 2021, Online conference, Hungary. 10.3311/FLOODRisk2020.14.11 . hal-03268621

COMMISSION INTERNATIONALE DES
GRANDS BARRAGES

VINGT-HUITIEME CONGRES DES
GRANDS BARRAGES
CHENGDU, MAI 2025

**SAFETY ASSESSMENT WITH AN AGENT BASED MODEL FOR LEVEES WITH
BEAVER BURROWING DURING HIGH-WATER EVENTS (*)**

F.P.W. VAN DEN BERG
Sr. Researcher, Deltares

B.C. NOYONS
Researcher, Deltares

M.A. VAN
Sr. Specialist, Deltares

THE NETHERLANDS

SUMMARY

Since the reintroduction of the beaver in the Netherlands in 1988, its population has grown exponentially and poses a safety problem for the levees because: (1) The safety of the levees can be (seriously) endangered by burrowing in the levee, all the more so since beavers tend to dig new burrows when high-water is developing. (2) The beaver burrow is exceedingly difficult to detect, because its entrance is below the water level and then remains submerged to such an extent that it can hardly be discovered with conventional detection methods. (3) The beaver is protected by the EU Habitat Directive and plays a key role in improving biodiversity in flora and fauna. It is not allowed to kill or disturb a beaver, nor is it allowed to deteriorate its habitat.

**Évaluation de la sécurité pendant les crues à l'aide d'un modèle basé sur des agents pour les digues avec terriers de castors*

In this paper an improved model of the behaviour of beavers during high-water is presented with an Agent-Based Model (ABM). The inputs of this model are based on an extensive overview of parameters that influence beaver behaviour, which is based on literature and consultation with beaver experts.

When comparing the model result with field observations, the model appears to be able to predict the locations of the beaver burrows with acceptable accuracy but is not yet very sensitive to hydro-meteorological conditions. The validation data is not very comprehensive, hence a challenge remains in determining the hydro-meteorological conditions at the burrow locations at the time of their construction. A more complete set of data would greatly improve calibration effectiveness and advance the model even more. It is always necessary to run the model several times on the same settings to account for randomness of hydro-meteorological sensitivity, lodge location (beaver's home), and burrow location selection. The more information about the territory is available, such as lodge locations and number of beavers in the river section, the more accurate the prediction will be. Nevertheless, it is important to note that there is still much uncertainty related to beaver behaviour and the extent to which it can be modelled.

The results of this research study will be used to determine the probability of levee failure given animal burrows. This model can also be used to discover patterns of where beavers will possibly dig during a high-water event, so levee inspectors can prioritize those locations.

RÉSUMÉ

Depuis la réintroduction du castor aux Pays-Bas en 1988, sa population a connu une croissance exponentielle et pose un problème de sécurité pour les digues car : (1) La sécurité des digues peut être (gravement) mise en danger par le creusement de terriers dans la digue, d'autant plus que les castors ont tendance à creuser de nouveaux terriers lors des crues. (2) Le terrier de castor est très difficile à détecter, car son entrée se situe sous le niveau de l'eau et reste ensuite tellement immergée qu'elle peut difficilement être découverte avec les méthodes de détection conventionnelles. (3) Le castor est protégé par la directive européenne sur l'habitat et joue un rôle essentiel dans l'amélioration de la biodiversité de la flore et de la faune. Il est interdit de le tuer ou de déranger un castor, ainsi que de détériorer son habitat.

Dans cet article, un modèle amélioré du comportement des castors en période de crues est présenté à l'aide d'un modèle basé sur des agents (ABM). Les données d'entrée de ce modèle sont basées sur une vue d'ensemble des

paramètres qui influencent le comportement des castors, basée sur la littérature et la consultation d'experts du castor.

En comparant les résultats du modèle avec les observations sur le terrain, le modèle semble être capable de prédire les emplacements des terriers de castors avec une précision acceptable, mais n'est pas encore très sensible aux conditions hydrométéorologiques. Les données de validation ne sont pas très complètes, et il reste donc difficile de différencier de déterminer les conditions hydrométéorologiques à l'emplacement des terriers au moment de leur construction. Un ensemble plus complet de données permettrait d'améliorer considérablement l'efficacité de la calibration et de faire progresser le modèle. Il est toujours nécessaire d'exécuter le modèle plusieurs fois avec les mêmes paramètres pour tenir compte du caractère aléatoire de la sensibilité aux conditions météorologiques, de l'emplacement de la hutte (maison du castor) et de la sélection de l'emplacement du terrier. Plus on dispose d'informations sur le territoire, comme l'emplacement des huttes et le nombre de castors dans la section de la rivière, plus la prédiction sera précise. Néanmoins, il est important de noter qu'il y a encore beaucoup d'incertitudes sur le comportement du castor et sur la mesure dans laquelle il peut être modélisé.

Les résultats de cette étude seront utilisés pour déterminer la probabilité d'une rupture de digue en fonction des terriers d'animaux. Ce modèle peut également être utilisé pour découvrir des modèles d'endroits où les castors se rendent lors d'une crue, afin que les inspecteurs des digues puissent donner la priorité à ces endroits.

1. INTRODUCTION

1.1 ANIMAL BURROWS IN LEVEES

Animal burrowing in levees is a phenomenon that has been dealt with for years in The Netherlands and abroad to prevent failure of the levee. This task is being carried out expeditiously by the Water Authorities. Since the reintroduction of the beaver in the Netherlands in 1988, its population has grown exponentially and poses a safety issue for the levees because:

1. The safety against flooding of the levee can be (seriously) endangered by burrowing.
2. During high-water periods beavers will search higher places near the river to dig a burrow, in many cases choosing a levee as a refuge location.
3. The beaver burrow is extremely difficult to detect, because its entrance is below the water level and then remains submerged to such an extent that it can hardly be discovered with conventional detection methods.

4. The beaver is protected by the EU Habitat Directive and plays a key role in improving biodiversity in flora and fauna [1]. It is not allowed to kill or disturb a beaver, nor is it allowed to deteriorate its habitat.

Especially during high-water, beaver burrows in the levee are a major risk because then beavers tend to dig into the levee to create a new burrow, which in many cases has a negative effect on the strength of the levee. Thus, animal burrows in flood defences such as levees can, depending on location, type of animal, and other factors, increase flood risk substantially.

1.2 AIM OF THE STUDY AND APPROACH

In this paper the behaviour of beavers during a high-water period in The Netherlands is simulated with an Agent-Based Model (ABM) to investigate whether and where they dig. The model [2] is derived by extensions in a previous version of the model [3], by adding geographical information and updated parameters. Any area in The Netherlands can be selected from a GIS dataset and then analysed with this new model. The model predicts beaver behaviour in various conditions for a specific part of the river and its surrounding levees. The results are patterns in beaver behaviour during high-water by which management recommendations for water authorities can be given and levee inspectors can be guided to potential danger areas during high-water events. It also provides quantitative input for a risk assessment with a developed safety framework of animal burrows in levees.

2. BEHAVIOUR OF THE BEAVER

After the last beaver was killed in The Netherlands in 1826, the beaver was reintroduced in The Netherlands in 1988. At present, the Eurasian beaver (*Castor Fiber*) populations is not only expanding in The Netherlands but also across Europe [4]. The beavers shape their environment to their needs and are often found in the floodplains of the rivers and can form a serious threat to the safety of the levee [5]. During high-water events the beaver will follow a sequence of behaviour. When the river rises, the beaver will lie on their lodges. When the water rises higher, the beaver will move to alternative (higher) structures (earthen structures, floating tree limbs, sheds etc.). When the water rises even more, the beaver will cross the levee to the dry area land inward and sometimes it will create a burrow in the levee which could lead to a significant effect on the flood safety [6].

Based on expert knowledge of the Dutch Mammal Society (zoogdierenvereniging) and literature [7] and [8] aspects and key parameters have been identified

which play an important role whether beavers make burrows in levees during high-water. These aspects are subsequently given in this section 2 and the key parameters that are included in the model are described in section 3.

Availability of an alternative resting place like high-water refuges: The quality of an alternative resting place is very important. E.g. whether it is high enough, there are other animals in the vicinity, there are alternative places inland or there are waterways inland. Alternative resting places have to be stable for a long period.

Air temperature: This plays an important role for young beavers because their temperature regulation is not yet well developed. The bigger the animal, the less effect the air temperature has on them. When the beaver is in a burrow it will use less energy.

Wind direction/-speed: During high-water, the beaver will look for places in the lee to shelter or to dig. Also, windchill plays a big role (see air temperature).

Precipitation (rain/hail/snow): Precipitation during the winter period can cause the beaver to seek shelter earlier and, if possible, to dig into a levee. There is also a relationship with the temperature and the duration and height of the high-water event.

Duration high-water situation: The longer the high-water situation lasts, the higher the probability that a beaver starts digging a burrow in a levee.

Experience with previous high-water: There seems to be a correlation, but it is difficult to model. There is also an assumed correlation with age.

Steepness of levee slope: In case of a mild outer slope of the levee, the beaver has to dig further to reach a dry place. This could be an important aspect for a high-water refuge design for beavers.

Type of vegetation: The beaver likes to seek protection around the place where he digs. So, the beaver will often dig his burrow on a location where there is a lot of vegetation. This protects him and is also a source of food. Especially vegetation like roots, trees, certain plants and thicket. With little vegetation around, there is less probability of digging.

Availability of driftwood: In the aftermath of the high-water event of December 2023 in the Netherlands, when the river levels dropped, several beaver burrows were found underneath driftwood, see for example Fig.1. As mentioned, this is also gives them a feeling of safety.

Age of beaver: The age of a beaver plays an important role. It is assumed that younger beavers are more likely to seek a hiding place and therefore possibly dig into a levee than older beavers.



Fig. 1

Discovered beaver burrow under driftwood after the high-water recede in December 2023 at Waterschap Rivierenland (source Waterschap Rivierenland)
Découverte d'un terrier de castor sous du bois de grève après la décrue en décembre 2023 à Waterschap Rivierenland (source Waterschap Rivierenland)

Relation to other agents nearby: In this case other agents are beavers. This is one of the factors which can be investigated with earmarked beavers. Scent marks on the slopes play an important role. If the other agents are no family, there will be a very hostile reaction from both sides. Other agents can also be other animals, predators or even boats.

The hierarchy or order of importance of these factors for the decision to dig is assumed to be first windchill, then precipitation, then duration of the high-water. For burrow location selection, first wind cover, then proximity to trees and then proximity to water are assumed to play the largest role.

Also, some additional aspects have been indicated, but at this moment it is uncertain if these aspects play an important role. These additional aspects are: Social status, family size, origin/experience in this territory, moving out of offspring, natural enemies, protected status, sex of the beaver, moment in the season, water depth of the ditch, water temperature, obstructions (i.e. revetment, netting, riprapi, etc..) and material of the levee.

3. METHODS AND MATERIALS

3.1 INTRODUCTION AND DATA

3.1.1 *Introduction*

This research expands on a previous study to model beaver behaviour during high-water using Agent-Based Model (ABM) software NetLogo 6.3.0. An extensive overview on this study and the background of ABM is available in [3]. The version of the model in current research includes an extended set of parameters and expanded sub-models. It also includes Dutch GIS data and is illustrated by two case studies for Dutch river sections.

3.1.2 *Data and preprocessing*

Spatial datasets from the Dutch government are used in the model and they consist of Digital Elevation Models (DEM) and vector files of landscape elements such as levees, trees, shrubs and water bodies, derived from topographical maps. These can be openly accessed and downloaded from the Dutch PDOK platform (PDOK.nl) and processed in QGIS or other GIS software to convert to the necessary file formats for NetLogo.

The water authority 'Waterschap Drents Overijsselse Delta' (WDOD) shared a dataset of 184 beaver burrow observations that were found in their administrative area between January 2020 and May 2024.

3.2 SIMULATION MODEL FOR BEAVER BEHAVIOUR

3.2.1 *Entities, state variables, and scales*

The model is represented by agents and patches. The agents are beavers and their competitors. The patches are grid cells in the world in which the agents can move. Both agents and patches have attributes. The behaviour of agents in the model is determined by the processes (or sub-models) described in the model code and depends on a number of parameters.

3.2.2 *Process overview and scheduling*

The behaviour of the beaver during a high-water event is a chain of processes, based on knowledge and aspects as explained in section 2. In Fig. 2 is shown how

the boundary conditions of the study area, and various processes and parameters determine the modelled behaviour of the beaver.

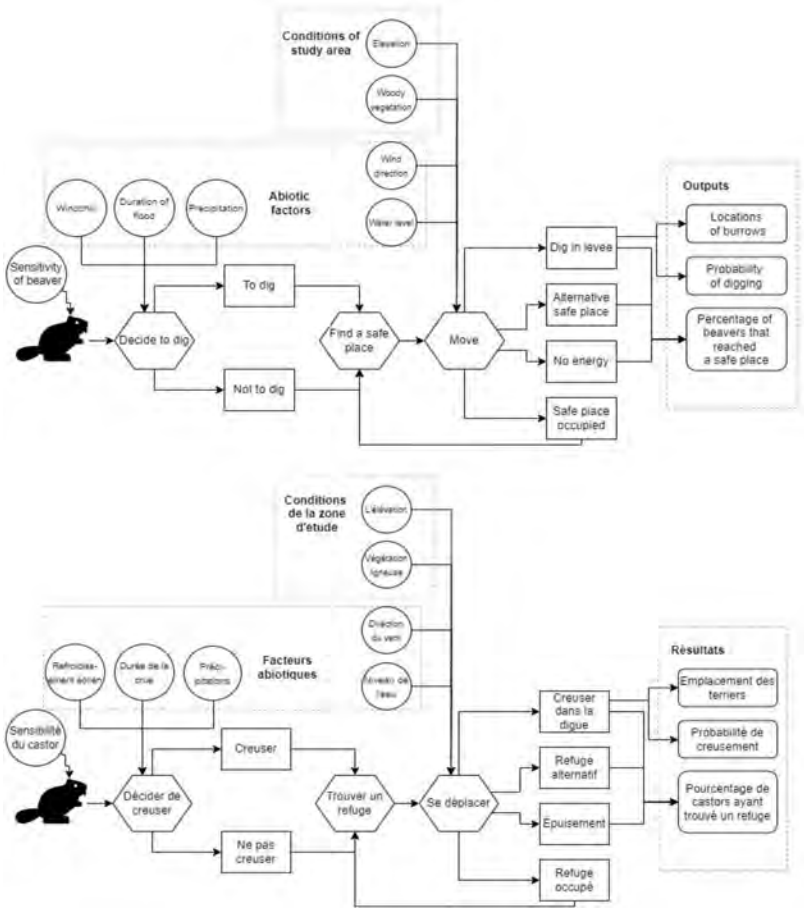


Fig. 2

Conceptual diagram showing the overview of processes and parameters in the model

Diagramme conceptuel montrant l'aperçu des processus et des paramètres du modèle

First, the beaver decides whether it wants to dig, based on the weather conditions and its own sensitivity to these conditions. Then, it will move to a safe place,

which is determined by the conditions of the area, the start location of the beaver, its energy level and the proximity of competitors. The main outputs are the burrow location and its probability.

3.2.3 *Sub-models*

To ensure code readability and execution of processes in the right order, the model is divided into sub-models. These are elaborated below.

The '*Create-flooding*' sub-model creates the high-water event that floods the patches within the floodplains and indicates local inundation depth.

The '*Decide-to-dig*' sub-model weighs the windchill, duration and precipitation parameters against the beaver's sensitivity to those conditions (threshold values) and determines whether the beaver is uncomfortable enough to want to dig.

The '*Find-target-patch*' sub-model determines the ideal patch for the beaver to flee to within a search radius that expands continuously by 10% if none is found nearby. The desirability of patches is predominantly determined by wind cover, proximity to woody vegetation and proximity to water, as well as a slope to dig into. The search runs through several loops in order of importance and is based on the assumptions in section 2 of this paper. The maximum search radius is dependent on the initial energy level which is specified by an input parameter.

The '*Calculate-target-patch*' sub-model calculates the distance between the beaver's start location and its target patch found in the previous process.

The '*Move*' sub-model moves the beaver step-wise towards its target patch and is dependent on the energy level of the beaver and the distance to the target patch.

The '*Avoid-others*' sub-model diverts the beaver moving direction 180 degrees when it meets a competitor or other beaver within a specified radius.

The '*Midway-check*' sub-model finds a new target patch for the beaver if the first one is already occupied by another beaver or competitor.

The '*Energy*' sub-model regulates the energy level of the beaver while it is moving towards his target patch. It is dependent on the patch-type since it costs less energy to swim than to walk on land. The initial energy is specified by the user.

The '*Stop-entirely*' sub-model stops the beaver moving and then shows statistics of the model run when all beavers in the model either reached their destination or ran out of energy.

The '*Find-success-failure*' sub-model compares the destination of the beaver at the end of the model run to the initial decision whether to dig and the patch type. This determines whether the beaver dug into a levee or found an alternative safe place like i.e. a treetop. It is also the input of the export function for the burrow coordinates.

3.2.4 *Sensitivity analysis and calibration*

Due to the lack of observational data on burrows and beaver behaviour and the complexity of the model, calibration of the model is a challenge. For better validation it is necessary to refine the details of the burrow data as collected by levee inspectors.

To validate the model, and whether the model results align with the assumed importance of the parameters in section 2 of this paper, sensitivity analyses were conducted. These analyses were done with different settings of the water level and wind direction parameters, as well as random lodge starting points, as these parameters were expected to have the largest influence on burrow locations. Default settings for model runs for The Netherlands are a south-west wind direction, windchill temperature of 3 degrees Celsius, flood duration of 6 days, initial energy level (so maximum steps) of 1500 moves, 3 beaver families and 3 lodges. The model ran 100 times in case there were 3 beaver families, or 300 times when there is only one beaver family.

In order to run many simulations with different parameters, and prepare for future availability of new data, the model was configured in Python using the library PyNetLogo [9]. This makes it efficient to run a high number of tests, use sampling for multiple parameters, perform statistical tests and create plots. It also improves the user experience if preprocessing the GIS data is done in Python as well.

4. CASE STUDIES

4.1 DODEWAARD

4.1.1 *Area description*

The case study area of Dodewaard is located along the Waal River in the Dutch province of Gelderland as shown in Fig. 3. This location is chosen because it was also part of an earlier research in animal burrowing in levees [10]. The case study area is rich in woody vegetation, such as trees and shrubs and has many ponds and other small water bodies, which are desirable habitat elements for beavers [11].

In setting up the model, lodge locations were selected based on general knowledge of the study area and from previous research.



Fig. 3

Satellite image of the study area near Dodewaard with a reference map of The Netherlands.

Image satellite de la zone d'étude près de Dodewaard avec une carte de référence des Pays-Bas.

4.1.2 Results

Running the model with default settings and with one beaver family resulted in burrow locations as shown in Fig. 4. The input settings of one beaver family and constant variables were selected to assess the accuracy of the model. It is not surprising that burrow locations are often near trees along the levees, as well as near small water bodies. Model results were not sensitive to wind direction nor to water level (once the flood plains were flooded), nor to lodge location (see Fig. 5).

4.2 HARCULO

4.2.1 Area description

Harculo is located along the IJssel river, just south of Zwolle. This case study area was selected because of availability of the burrow data provided by the local

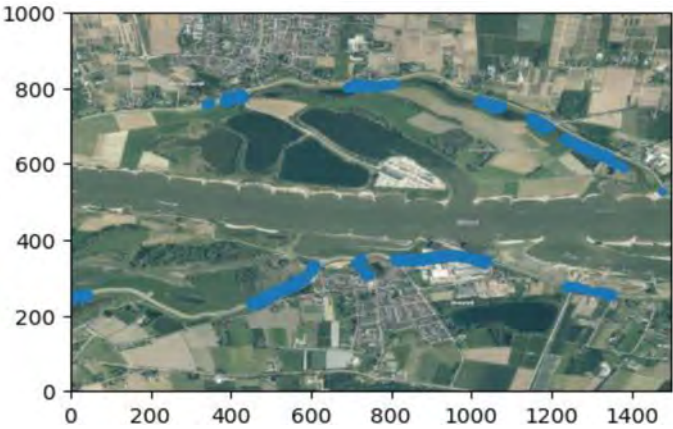


Fig. 4

Burrow locations resulting from running the model on default settings. The numbers on the axes represent the patches in the model environment.
Emplacements des terriers résultant de l'exécution du modèle avec les paramètres par défaut. Les nombres sur les axes représentent les parcelles dans l'environnement du modèle.

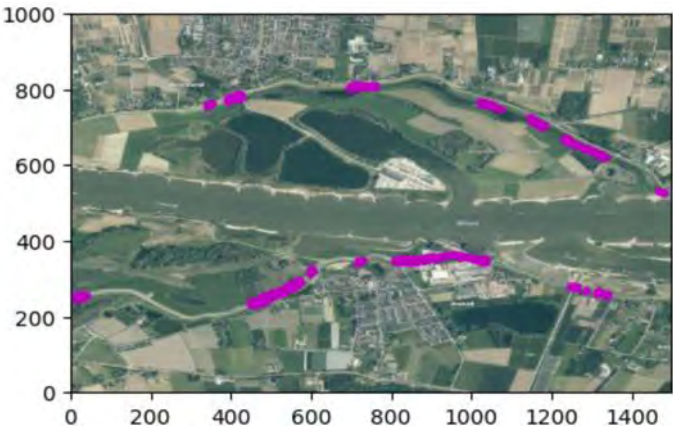


Fig. 5

Burrow locations resulting from running the model on default settings with random lodge locations. The numbers on the axes represent the patches in the model environment.
Emplacements des terriers résultant de l'exécution du modèle avec des paramètres par défaut avec des emplacements des huttes randomisées. Les nombres sur les axes représentent les parcelles dans l'environnement du modèle.

Water Authority WDOD. The landscape elements of the study area are also relevant. The river here has two small harbours around a former power plant, and four ponds. Along the levee on the east side of the IJssel river, some forest patches and other woody vegetation can be found. The burrow observations of recent years are shown in Fig. 6.



Fig. 6

Satellite image of the study area near Harculo with a reference map of The Netherlands with beaver burrow observations from WDOD, near and not near levees, and a known lodge location.

Image satellite de la zone d'étude près de Harculo avec une carte de référence des Pays-Bas avec des observations de terriers de castors du WDOD, près et pas près des digues et un emplacement de hutte connu.

4.2.2 Results

Running the model with one beaver family and default settings resulted in the results in Fig. 7. The results of this run highlight that randomness in burrow location selection is minimal, as clearly four locations are frequently chosen. As mentioned in section 2 of this paper, wind direction was expected to be a parameter with a large impact on burrow location selection. Therefore, experiments were run with varying wind directions to assess the performance of the model in these different weather situations. However, the results of these runs did not show significant differences, meaning that wind direction does not yet have a high impact on the burrow location selection of the beaver family in this case study.

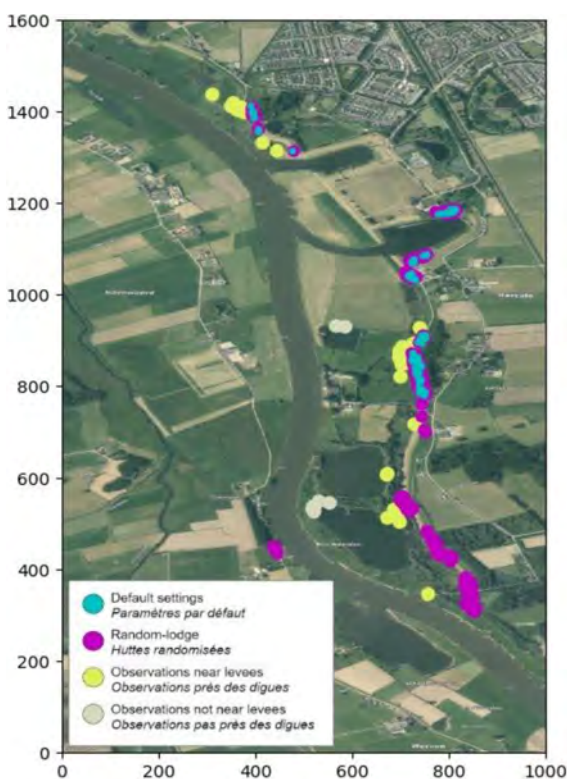


Fig. 7

Burrow locations resulting from running the model on default settings and with random lodge locations. The numbers on the axes represent the patches in the model environment.

Emplacements des terriers résultant de l'exécution du modèle avec des paramètres par défaut et avec des emplacements des huttes randomisées. Les nombres sur les axes représentent les parcelles dans l'environnement du modèle.

A variable with large impact in the model is the lodge location, which is the starting point of the beavers in the model. Default settings only included the single known lodge (see in Fig. 6). Running the model with the random lodge function resulted in burrows extending to the southern part of the study area as well, since in this case lodges will be placed randomly across the floodplains, preferably close to woody vegetation and water bodies. This includes the southern part of the study area even though there is no currently known lodge at that location. Thus, when no lodge locations are known in a study area (which is often the case), the random-lodge function can be used, as it does not seem to decrease accuracy as long as the number of model runs is large enough.

5. SAFETY FRAMEWORK

A safety framework for the impact of animal burrows in levees is currently being developed. This safety framework aims to assess the impact of burrowing on the failure probability of levees. Preventative and mitigating measures by the Water Authorities can also be added into the framework. In the framework, the probability of failure of a levee due to animal burrow ($P_{F,AB}$) is equal to the probability of the presence of an animal burrow (P_{AB}) times the probability of failure given an animal burrow ($P_{F|AB}$). See Eq. [1] and Eq. [2].

$$P_{F,AB} = P_{AB} \cdot P_{F|AB} \quad (1)$$

$$P_{AB} \approx P_{\text{Barrier}} \cdot P_{AB,local} \cdot P_{\text{detection,repair}} \quad (2)$$

The probability of the presence of an animal burrow (P_{AB}) is dependent on three aspects: (1) The probability of a barrier in the levee, like netting or sheet piles (P_{Barrier}), (2) The probability of the presence of an animal burrow ($P_{AB,local}$), which is dependent on various aspects such as mentioned in section 2. (3) The probability of detection and prompt repair of the burrow ($P_{\text{detection,repair}}$).

The probability of digging during high-water is one of the aspects of ($P_{AB,local}$) and is the output of the ABM-model as discussed in this paper.

6. DISCUSSION, CONCLUSIONS AND RECOMMENDATIONS

6.1 DISCUSSION

Based on observational data from the WDO Water Authority for the Harculo case study, a comparison between the model output (Fig. 7) and observed burrow

locations could be made (Fig. 6). Graphically, two out of the four burrowing areas resulting from the model with default settings seem to be in accordance with the observations in the field. Additionally, in the random-lodge model run, the burrows found in the southern part of the area are also in line with the observed burrow locations.

The data from WDOD does not differentiate between normal and high-water situations, which means that the assumption could be made that the burrows close to the normal water level (in the floodplain) can be excluded from the comparison as those would be flooded in high-water situations.

Draft conclusions can be drawn, but it is evident that more and more detailed observational data is needed to perform the calibration of the model. The need for more calibration is illustrated by the lack of differences in model results under different parameter settings, which is not in line with expected results based on expert knowledge. More data, and specifically, more detailed data of the beaver behaviour is needed to improve the model. At this stage, the model does not indicate a major role of wind direction in the burrow location selection of beavers during a high-water situation. However, from consultation with beaver experts, we know that it should play a big role. As calibration with climatological data and burrow observations was not yet possible, the model could not yet be made more accurate in this regard, but this is highly recommended in an update of the model once data becomes available. When this happens, it is also advisable to include or adjust for wind speed in the updated model, since it is not likely that wind direction has a big role if the wind speed is very low.

The random-lodge function seems to give realistic results, which can be used when a field area is not widely researched yet and not a lot is known about the different beaver territories in that area.

6.2 CONCLUSIONS

An Agent-Based Model of the behaviour of beavers during high-water has been built. This model predicts patterns of locations including probabilities where beavers may burrow during high-water. The method can also be used to derive probabilities of burrows that are input for a safety assessment of a levee. In subsequent steps from beaver observations until its behaviour under high-water conditions, the failure probability of a levee in these situations where burrowing may occur may be assessed.

6.3 RECOMMENDATIONS

The agent-based model is running and will give insight into the effect of the behaviour of beavers during high-water on the levees. For further development of the model the following recommendations and proposed extensions are important:

- Including river flow velocity in the model.
- To obtain a better calibration of the model, it is necessary to obtain more and more detailed data and have more insight in beaver behaviour. To facilitate the process of obtaining accurate data for calibration, a detailed questionnaire has to be prepared, and levee inspectors or other observers should be trained for using these questionnaires correctly.
- Comparing observations with model results will further validate the model and help to find the key aspects and parameters that result in sound predictions [12].
- Publishing the model on Netlogo Modelling Commons, an online platform for open-source ABM. In a later stage, after calibration is finished, the model could be integrated into a dashboard, for an easy user experience, since the model was created with the intention to be shared with professionals in the field such as levee inspectors of water authorities.

REFERENCES

- [1] NICA, A., PETREA, M.-S., SIMIONOV, I.-A., ANTACHE, A., & CRISTEA, V. Ecological Impact of European Beaver, *Castor Fiber*. *Animal Science*, 65(1), 2022. <https://www.carpathia.org/ro/castorul->
- [2] VAN DEN BERG, F.P.W., NOYONS, B.C. Beaver digging during highwater with ABM, Case studies in Dutch river sections, Deltares, draft report 11210269-002-GEO-000, august 2024
- [3] VAN DEN BERG F.P.W., NATARAJAN, A. Beaver behaviour during high water regarding burrows in levees. I1000679-001-OA-0002, 2023, Deltares. https://publications.deltares.nl/1000679_001_0002.pdf
- [4] DIJKSTRA, V. Beverpopulatie blijft groeien, 2019 <https://www.zoogdierverseniging.nl/nieuws/2019/beverpopulatie-blijft-groeien> (in Dutch).
- [5] VAN DEN BERG, F. KOELEWIJN, A. Graverij door dieren, Meer praktijk-cases, inspectietechnieken en uitsplitsing invloed op overstromingskans, Deltares, report, 11209262-001-ZWS-0001, 2023, https://publications.deltares.nl/11209262_001_0001.pdf (in Dutch).

- [6] DIJKSTRA, V., POPULIER, T., OVERMAN, W. Bever & Das in het dijkverbeteringstraject Cuijk – Ravenstein, report 2022.07, 2022 (in Dutch).
- [7] NITSCHKE, K.-A. Behaviour of beavers (*Castor fiber albus* Matschie, 1907) during the flood periods. In A. Czech & G. C. H. S. Schwab (Eds.), *Proceedings of the 2nd European Beaver Symposium*, 27-30 September 2000 (pp. 135–139). Carpathian Heritage Society.
- [8] NITSCHKE, V. K. BIBER (*Castor fiber* L.) und Hochwasser: Verhalten, Maßnahmen für den Biberschutz und Hochwasserschutz, 2003 www.biologiezentrum.at.
- [9] JAXA-ROZEN, M. & KWAKKEL, J.H., PyNetLogo: Linking NetLogo with Python, *Journal of Artificial Societies and Social Simulation*, 21 (2) 4, 2018, <http://jasss.soc.surrey.ac.uk/21/2/4.html>, DOI: 10.18564/jasss.3668
- [10] VAN DEN BERG, F.P.W. & KOELEWIJN, A.R. Degradatie van dijken door dieren en droogte, Uitwerking observaties graverijen en scheuren, Deltares, report, 11208034-002-ZWS-0001, 2022, https://publications.deltares.nl/11208034_002_0001.pdf (in Dutch).
- [11] GRAHAM, H. A., PUTTOCK, A., MACFARLANE, W. W., WHEATON, J. M., GILBERT, J. T., CAMPBELL-PALMER, R., ELLIOTT, M., GAYWOOD, M. J., ANDERSON, K., & BRAZIER, R. E. Modelling Eurasian beaver foraging habitat and dam suitability, for predicting the location and number of dams throughout catchments in Great Britain. *European Journal Of Wildlife Research*, 66(3), 2020. <https://doi.org/10.1007/s10344-020-01379-w>
- [12] GRIMM, V., RAILSBACK, S. F. Pattern-oriented modeling: A “multi-scope” for predictive systems ecology. In *Philosophical Transactions of the Royal Society B: Biological Sciences* (Vol. 367, Issue 1586, pp. 298–310). Royal Society, 2012 <https://doi.org/10.1098/rstb.2011.0180>.

COMMISSION INTERNATIONALE DES
GRANDS BARRAGES

VINGT-HUITIEME CONGRES DES
GRANDS BARRAGES
CHENGDU, MAI 2025

DESIGNING A FIT-FOR-THE-FUTURE LEVEE ALONG THE DUTCH MEUSE RIVER (*)

M.P.M. SANDERS

Design leader levees, Royal HaskoningDHV

A.G. WIGGERS

Principal geotechnical engineer, Royal HaskoningDHV

W. DE FIJTER

Technical manager, Water Authority Limburg

THE NETHERLANDS

SUMMARY

During the summer of 2021, catastrophic flooding took place in the Eifel-Ardennes region of Germany and Belgium. At the same time, water levels along the Dutch Meuse reached values close to the Meuse levees design levels, raising awareness that with additional future climate change a similar event could have caused primary levee failures which were avoided in 2021, albeit with a narrow margin in some cases. Foreseen climate scenarios are already included in the Dutch design approaches, but there is still the possibility of unexpected climate effects on river discharges. Moreover, the levees themselves may also be affected by future trends, such as droughts, extreme local rainfall, but also other factors like animal burrowing. To account for all this and for spatial development, an adaptive, fit for future, design approach would be needed. Such an approach is based on resilience, and on a common view of flood-risk managers, local communities, and other

**Un exemple de conception de digue adaptable au futur le long de la Meuse Hollandaise*

stakeholders. The adaptive design approach should focus on reserving space for unforeseen levee modifications, in a way that levee-raising schemes could easily fit into the environment and landscape, and benefit from locally available fill materials. An adaptive approach considers not only the levee itself but also the whole system of riverbed, foreland, levee and hinterland.

Based on this philosophy, the water authority of Limburg decided to design such an adaptable levee, considering the environmental values, use of locally available fill materials, the historical context of the area and the water management in the area. The selected levee in the project area, presented in this paper, was already scheduled for improvement to bring its safety level up to standards. A major part of the project comprises eliminating a discharge bottleneck in the river Meuse by creating a new side channel. Besides these river adjustments, the adaptive approach was applied to the design of the levees as well, enriching conventional design practice by (i) adding adequate robustness, (ii) applying an observational method to support adaptivity and (iii) to postpone large levee reconstruction works whenever justified.

RÉSUMÉ

Au cours de l'été 2021, des inondations catastrophiques ont eu lieu dans la région Eifel-Ardenne en Allemagne et en Belgique. Au même moment, les niveaux d'eau le long de la Meuse néerlandaise ont atteint des valeurs proches des niveaux de conception des digues de la Meuse, ce qui a fait prendre conscience qu'avec un changement climatique supplémentaire dans le futur, un événement similaire aurait pu provoquer des défaillances des digues primaires qui ont été évitées en 2021, bien qu'avec une marge étroite dans certains cas. Les scénarios climatiques prévus sont déjà inclus dans les approches de conception néerlandaises, mais il existe toujours la possibilité d'effets climatiques inattendus sur les débits des cours d'eau. De plus, les digues elles-mêmes peuvent également être affectées par des événements récurrents futurs, telles que les sécheresses, les précipitations locales extrêmes, mais aussi d'autres facteurs tels que les terriers d'animaux. Pour tenir compte de tous ces facteurs et de l'aménagement du territoire, une approche de conception adaptée à l'avenir devrait être adoptée. Une telle approche est basée sur la résilience et sur une vision commune des gestionnaires des risques d'inondation, des communautés locales et des autres parties prenantes. L'approche adaptative de la conception devrait se concentrer sur la réservation d'espace pour des modifications imprévues des digues, afin que les projets d'élévation des digues puissent facilement s'intégrer dans l'environnement et le paysage, et bénéficier des matériaux de remblai disponibles localement. Une approche adaptative tient compte non seulement de la digue elle-même, mais aussi de l'ensemble du système constitué par le lit du fleuve, l'avant-pays, la digue et l'arrière-pays.

Sur la base de cette philosophie, l'autorité de l'eau du Limbourg a décidé de concevoir une telle digue adaptable, en tenant compte des valeurs environnementales, de l'utilisation de matériaux de remblai disponibles localement, du contexte historique de la région et de la gestion de l'eau dans la région. Des travaux d'amélioration avaient déjà été prévus pour la digue sélectionnée dans la zone du projet et présentée dans ce document afin de mettre son niveau de sécurité en conformité avec les normes. Une grande partie du projet consiste à éliminer un goulot d'étranglement dans la Meuse en créant un nouveau canal latéral. Outre ces ajustements fluviaux, l'approche adaptative a également été appliquée à la conception des digues, enrichissant la pratique de conception conventionnelle (i) en ajoutant une robustesse adéquate, (ii) en appliquant une méthode d'observation pour soutenir l'adaptabilité et (iii) en reportant les grands travaux de reconstruction des digues chaque fois que cela est justifié.

1. INTRODUCTION

Dutch levee improvement works are commonly engineered in accordance with a comprehensive system of national levee design guidelines. Dutch flood risk requirements are defined in terms of a maximum allowable probability of flooding. The safety level required by law is derived from flood risk analyses carried out on a national level, accounting for societal and economic risks and the life-loss risk that each individual faces. In most parts of the Netherlands the high-water levels measured so far did not even come close to design conditions due to the high required safety levels. In the Dutch province of Limburg however, the Meuse water levels during the 2021 summer floods were much closer to design conditions.

This paper describes how levee designers have anticipated on future scenarios within a levee reinforcement project in the province of Limburg near the village of Well. The project, in short "Project Well", comprises designing a redevelopment of the entire area including the new flood plain, a modified levee alignment, designing new levees and improving the remaining existing levees. Figure 1 presents the project scope. The village of Well and planned activities are located north of the existing course of the Meuse River. Section 5 of this paper outlines the scope of the Project Well in more detail.

2. DEALING WITH FLOOD RISKS IN THE NETHERLANDS

The upstream part of the Meuse River in the Netherlands, where the Meuse runs through the province of Limburg, has relatively small floodable areas with generally shallow inundation depth due to the shape of the valley. More

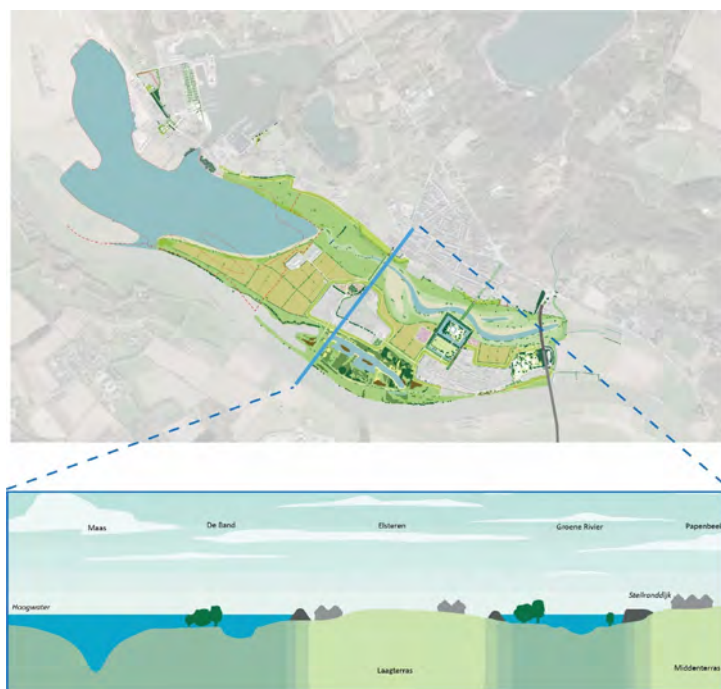


Fig. 1

Plan view and cross-section of redevelopment project Well with new river side channel between village centres [1]

Vue de dessus et coupe transversale du projet de réaménagement Well avec le nouveau chenal au bord de la rivière entre les centres des villages [1]

downstream, in the deltaic region, the flood-risk areas become much wider and inundation depths are generally deeper. As a result of flood-risk studies, including consequences and evacuation scenario's, the maximum allowed flood probability by law is set to 1/100 per year for the Province of Limburg, with some exceptions for larger towns. For the densely populated deltaic regions, where social and economic risks of flooding are generally higher, the maximum allowed probability of failure is below 1/3,000 per year and is generally 1/10,000 or less per year.

Figure 2 presents the safety level required by law (left-hand side map) and a recent estimate of the actual individual life-loss risks per region (map right-hand side). The right-hand map is only presented to illustrate the extent of the area that is susceptible to flooding.

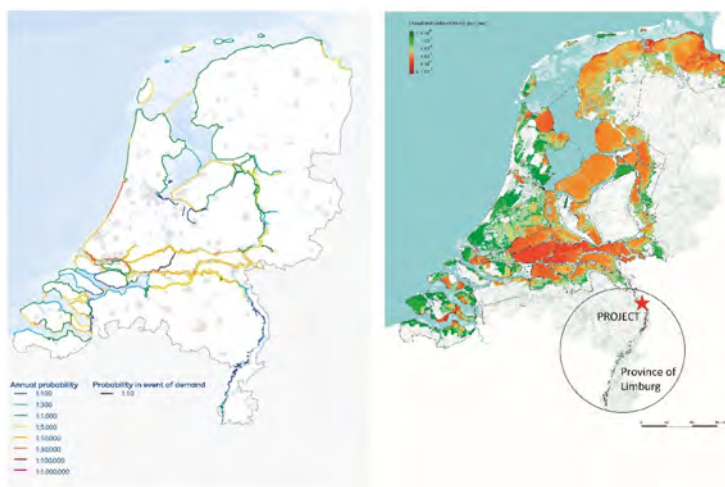


Fig. 2

Left-hand map: maximum allowed annual probability [2] where blue-green denotes 1/100 to 1/1,000 yr, yellow-red 1/3,000 to 1/30,000 yr and brown-purple 1/100,000 yr and less; right-hand map Individual annual risks [3] where red denotes more than 1/10,000 yr and green denotes less than 1/1,000,000 yr

Carte de gauche : Probabilité annuelle maximale autorisée [2] où le bleu-vert désigne 1/100 à 1/1 000 an, le jaune-rouge 1/3 000 à 1/30 000 an et le marron-violet 1/100 000 an et moins; carte de droite: Risques annuels individuels [3] où le rouge désigne plus de 1/10 000 an et le vert moins de 1/1 000 000 an

The safety level required by law directly refers to a breach and subsequent flooding of the hinterland. This implies that damage to the levees is allowed as long as the hinterland is not severely flooded. Dutch levee engineers are trained from the start of their careers to apply probabilistic principles when performing design verifications based on this high-level law-requirement.

3. CHANGING CONDITIONS

During the summer of 2021, a catastrophic flooding took place in the Eifel-Ardenne region of Germany and Belgium. At the same time, water levels along the Dutch Meuse reached values close to the Meuse levees design levels. This raised awareness that with additional future climate change a similar event could have caused primary levee failures which were avoided in 2021, albeit with a narrow margin in some cases. In fact, the water level of the river Meuse in Limburg almost

reached the design conditions and locally even exceeded the design conditions and overtopped the levee. Although no primary levee has failed, the 2021 event made us aware once again that the likelihood of flooding in this region is of a different level than in other regions in the Netherlands. Foreseen climate scenarios are already included in the Dutch design approaches, but there is still the possibility of unexpected climate effects on river discharges. Moreover, the levees themselves may also be affected by future trends, such as droughts, extreme local rainfall, but also other factors like animal burrowing. To account for all this and for spatial development, an adaptive, fit for future, design approach would be needed.

4. WHAT DOES THIS MEAN FOR THE DESIGNER?

4.1 UNDERSTANDING OF INSTITUTIONAL SETTING AND RESPONSIBILITIES

Levee reinforcement works in the Netherlands require thorough consultation of all involved stakeholders. Preferred designs result from careful balancing the needs, costs, and environmental and social impacts. At the end of a design process the Water Authority submits their plan for approval to get the required funding from the State/Minister via the national levee improvement programme. The local Water Authority needs to provide a sound justification of the required investments, including any spatial claims required for the new levee. The availability of space affects the design of the levee improvement, especially in heavily built-up areas. Spatial restrictions and 'short-term' interests of local stakeholders often conflict with the 'long-term' design principles of the levee designer. For instance, the designer might prefer a broad levee using locally available fill material, while landowners may opt for the smallest footprint possible.

Stakeholder management has become an important part of spatial design tasks in the Netherlands. The designer is aware of the institutional setting and the impact of reinforcement measures. The role of the designer focusses more and more on explaining the importance of applying long-term visions accounting for future (climate) changes (adaptive design) and of design that minimizes the impact to our environment (sustainable design). This paper gives examples of how those design principles could be applied in practice, how this differs from traditional designs and how this could be done without conflicts of interest with stakeholders.

4.2 ADAPTIVE DESIGN

Adaptive design requires a change in mind-set and starts with asking fundamental questions, such as: "what is needed to get an optimal river

discharge to sufficiently reduce the river water levels? “Is this the right time for a ‘landscape change’, could this be combined with other regional developments?”; “Can the levees easily be raised in the future in case design flood levels increase?” and “What is the impact on the performance of the levee after periods of drought?”. The designer can deal with these unknowns, for instance by creating more space for the river and the levee or by applying the principles of an observational design approach based on monitoring of the levee’s performance and being prepared for repair work. The circumstances around a reinforcement project near the village of Well were quite suitable for this adaptive design approach: the design of the levees was done in combination with the redevelopment of the entire area; defining a new levee alignment and creating additional flood-plain area were both part of the design. As a result, the discussion with landowners and other stakeholders was open and positive. Moreover, observational designs were feasible because of the relatively lenient safety requirements for this location.

4.3 SUSTAINABLE DESIGN

Recently, the levee improvement programme has provided guidance to Dutch engineers on how to implement sustainability into regional developments and levee improvements, using a ‘roadmap and sustainability framework’ [5]. It is the responsibility of the local Water Authority to anchor the ambitions into their regional plans and monitor the execution of the sustainability and durability ambitions. The anchoring of sustainability ambitions is reached by putting project top goals and design requirements in the design contracts. The roadmap and sustainability framework are both used as a manual. Figure 3 presents the Dutch Sustainability Framework of the national levee improvement programme, which comprises three main categories: Energy & Climate, Circularity and Spatial Quality.

A sustainability consultant is nowadays a common member of the design team who helps by setting goals and defining ambition levels for each theme; helping to monitor whether goals are achieved throughout the project; preventing the team from losing focus on their original ambitions. The set ambition level by the project Well resulted in smart goals for the re-use of materials, the use of locally available materials, for combining functions of the levee and to consider the cultural and historical context of the area to improve the spatial quality, for coverage of ecology and biodiversity and for reduction of emissions during execution of the improvement works. The paper will focus on the circularity (resulting in the use of locally available materials) and improvement of spatial use by combining functions.



Fig. 3
Sustainability Framework of the High-Water Protection Programme of the Ministry of
Public Works (Rijkswaterstaat) [5]
*Cadre de durabilité du programme du ministère Néerlandais des Travaux Publics
(Rijkswaterstaat) de Protection contre les Crues [5]*

5. CASE OF ADAPTIVE FUTURE FIT DESIGN

5.1 PROJECT SCOPE

The Water Authority of Limburg decided to redesign the area around the existing levees of the village of Well, located in the province of Limburg (Figure 1 and 2). The design comprised flood-plain extension as well as a levee design that meets sustainability goals. The flood-plain extension works are part of a national programme and should result in a 17 cm decrease of flood-water level downstream

of the village of Well. This paper will focus on the levee design and will not further address the issues of flood-plain extension works.

The existing levees around the village of Well were already scheduled for improvement because they did not comply with the safety levels required by law. During the 2021 summer flood, the water level nearly reached crest level, figure 4.



Fig. 4

Picture of demountable structure in Well during 2021 flood (Source: Water Authority Limburg)

Photo d'une structure démontable à Well lors de l'inondation de 2021 (Source: Autorité de l'Eau du Limbourg)

5.2 IMPLEMENTATION OF SUSTAINABILITY GOALS AND ADAPTIVE DESIGN

The Water Authority had the ambition to turn this project into one of the most sustainable levee improvements of the country. The design should include adaptivity to be fit for future, without compromising the interests of residents, environmental organisations, and the cultural-historical context of the area. Strong ambitions were set for all three themes of the sustainability framework as far as feasible and applicable in this specific area.

The ambition level resulted in smart goals for circularity, spatial quality and sustainable execution and operation & maintenance as presented in Table 1.

Table 1
Sustainability goals at the start of the project

THEME	GOAL
Circularity	<ul style="list-style-type: none"> • Minimize environmental impact of the design. • Use of locally available fill material as key principle of the design. • Minimize the use of primary and non-recyclable materials.
Spatial quality	<ul style="list-style-type: none"> • Multi-functional levee areas. • Use of natural heights of landscape. • Nature development in new flood plain of green river.
Sustainable execution, and operation & maintenance	<ul style="list-style-type: none"> • Minimize transportation movements within project. • Design on low-maintenance solutions. • Minimize the emissions in executions.

In addition to the sustainability goals, the following adaptive design principles have been applied:

- Add adequate robustness to allow for durability and extension where possible.
- Apply observational method design to failure modes that require learning by performance. This is only applicable if flood risks can be reasonably controlled by frequent monitoring and repair works after a flood event, or by planned flood fight measures.
- Consider postponing drastic levee construction works when those are only a result of predefined standard design lifetime.

The next sections describe the application of the first two approaches within the project of Well. The third approach is applied to a historical structure that initially had to be reinforced to meet standard lifetime requirements. Drastic reinforcement works could be postponed by applying a shorter lifetime. This is not discussed in this paper.

5.3 DEALING WITH CIRCULARITY AND SPATIAL QUALITY

5.3.1 *Optimal use of locally available material requires reverse thinking*

The goals for redevelopment of the area have created opportunities to reconsider the traditional Dutch levee geometry. A typical traditional levee in this

region is presented in Figure 5. Most levees in this region have: a crest height ranging from 2 to 3.5 meters; a crest width ranging from 4 to 5 metres; slopes of approximately 1V:3H; an embankment core of clayey fill covered with fat clay and overlain with a thin layer of lean clay for the development of grass. It is common practice in the Netherlands to apply pre-defined material specifications for cover layers and fill materials to assure sufficient resistance against erosion and sufficient geotechnical stability. In most cases this required material is not locally available and must be hauled from distant borrow areas, sometimes even from abroad.

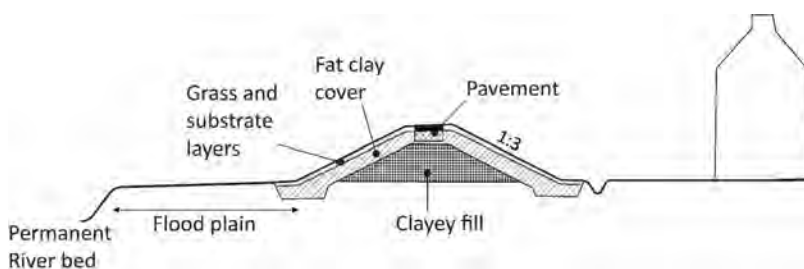


Fig. 5

Traditional levee geometry levee along Meuse River
Géométrie traditionnelle d'une digue le long de la Meuse

For project Well there is a lot of local material available due to the excavation of the new side channel of the river. The available material does not comply with the standard material specifications in levee construction guidelines. Consequently, an alternative design approach is required. The locally available sandy material has less erosion resistance than the fat clay that was traditionally used in cover layers.

In the traditional Dutch design approach, the functional components are defined first. The geometry of those components is based on design calculations, such as stability analysis, erosion requirements and the analysis of backward erosion piping. Those analyses assume that all fill materials meet national standard material and construction specifications. After design approval, the contractor searches for a supplier that can deliver the required fill material. This process is presented in the upper part of Figure 6. Materials that deviate from the standard specifications are not accepted. In areas where fat clays are scarce, such as the region of the Meuse valley, this results in long hauling distances between project site and the supplier. This conflicts with sustainability goals (circular economy).

For the project of Well an alternative approach has been followed. This is presented by the lower path in Figure 6. In this approach, the locally available material and local conditions are leading. Therefore, the properties of locally

available material (excavation of the channel and parts of existing levee) will be determined first. The design of required functional components and their dimensions will be tailored to the fill that consists of this local soil regardless standard specifications. This reverse way of thinking was perfectly applicable for this project and results in a different geometry. Details are given in Section 5.4.

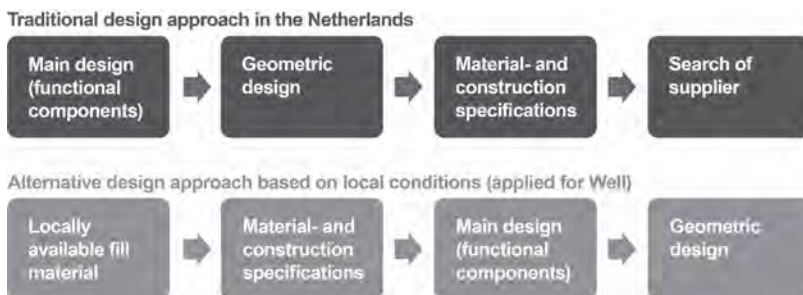


Fig. 6

Main steps of traditional and alternative design approach
Principales étapes de l'approche traditionnelle et alternative de la conception

The alternative approach requires:

- good understanding of the properties of the locally available soil. This starts with understanding the geomorphological setting and the historical land use. For good understanding a proper field reconnaissance is necessary.
- thorough knowledge of levee design and material behaviour: different types of levees, not only focussing on traditional methods; knowledge on functional requirements of levee components and how these components act together; knowledge on how the levee behaves when material is applied that doesn't comply with standard requirements.
- all involved parties to agree and accept the reverse way of designing and its consequences. In some cases, this will not only impact on space but on maintenance and operations as well.

5.3.2 Understanding geotechnical and hydrological setting and properties

Nowadays good software is available for the preparation of three-dimensional ground models presenting the deposited soil layers and properties, provided sufficient boreholes and field test data, such as CPT's are available. In this case project Bentley Leapfrog 3D was used to set up an 3D underground model. Figure 7 gives an impression of a slice of the 3D underground model that was used. The figure shows some superficial soil layers and the levee. The vertical and horizontal dimensions are plotted in different scales for practical reasons.

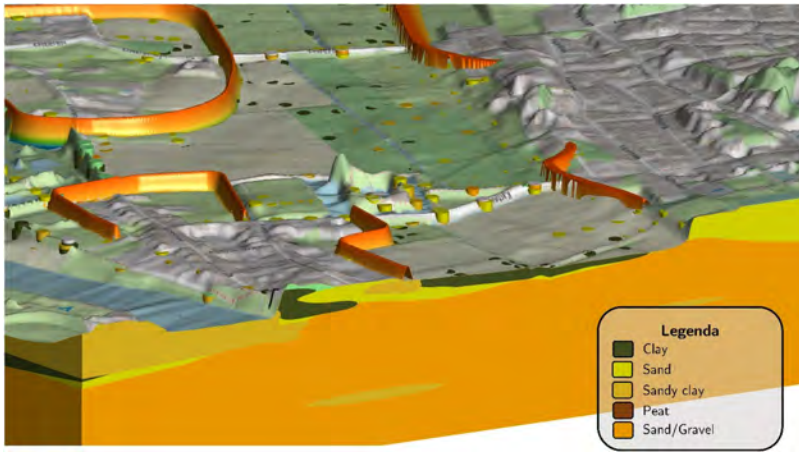


Fig. 7

Leap Frog 3D underground model

Leapfrog modèle 3D stratigraphique des sols présents

The 3D underground model allows one to get a quick overview of the availability of potential fill material for different excavation schemes. The model is very applicable for studying geohydrological impacts of excavations as the model clearly shows the spatial variability and properties of a clay top layer along the riverbed. The variability of this layer was a critical factor to consider for the earth works and for the scope of levee improvement measures to avoid backward erosion piping, as the total length of seepage screens along the levee could be drastically reduced.

5.4 RESULTS

5.4.1 Resulting cross-section of levee using locally available material

For the project Well the application of this alternative approach resulted in acceptance of the use of locally available sandy soil in the core and lean clay on the slopes. This was compensated by a gentler landside slope of all new levees along the new side channel, see figure 8. A gentle slope helps to mitigate failure risk due to macro and micro-instability and is more resistant for overtopping (although the wave heights and overtopping values were very limited at this location along the Meuse). The gentle slope also allows to experiment with different types of grass that are expected to be more suitable in terms of ecology and resistance to drought and climate change.

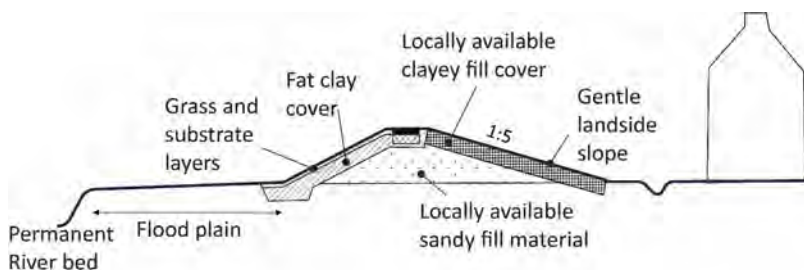


Fig. 8

Gentler landside slope, use of local material
Versant intérieur plus doux, utilisation de matériaux locaux

From an adaptive point of view, a wider footprint of the levee also gives more space for future crest raising.

5.4.2 Resulting cross-section of combining functions and using local material

The landscape around the village of Well has specific characteristics with steep edges along terraces which were farming areas in the past. The goal of the present project was to retain the character of the area and bring it to the required safety level using locally available material. This goal resulted in a so-called landscape levee, see figure 9. This "landscape levee" is comprised of four zones: a landscape zone at the river side; an erosion buffer of clay; a levee core zone; and a zone with combined functions with a very gentle landside slope (1V:10H up to 1V:20H). The core and landside zone contain locally available sandy fill material. At the river side the core is protected by an erosion buffer of material with slightly erosion resistant local material. At the outer slope a landscape zone of local material with natural erosion behaviour is applied. This landscape zone needs to be monitored after floods and needs to be repaired if the rate of erosion turns out to be unacceptable. This design is based on the principles of the observational method where risk and damage are controlled by monitoring the behaviour during flood conditions. This type of landscape levee is recently implemented close by in the area and performed well during the 2021 flood.

The landscape levee has a relatively high cultural historical value in this area as it fits perfectly in the natural terrasses of the river valley. Circularity ambitions were achieved as well since this levee does not require material that is not available in the area. Finally, the gentle landside slope could be used for keeping cattle and gardening.

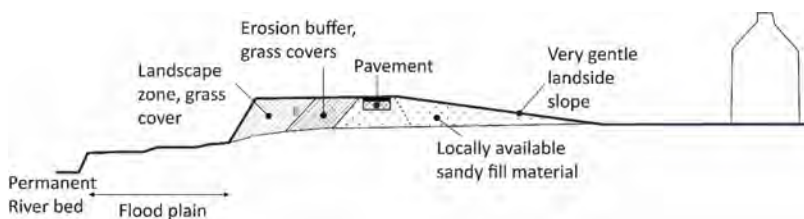


Fig. 9

The landscape levee: combined functions and levee form part of its surrounding landscape

La digue paysagère : fonctions combinées et digue font partie du paysage environnant

6. CONCLUSIONS

A fit-for-the-future concept for levees successfully marries the principles of adaptive and sustainable levee design. It requires a modified design procedure, in which it is no longer a pre-decided levee geometry which dictates the required fill properties, but rather the available fill properties which determine the levee geometry. This comes with the benefit of sustainability or even circularity since hauling distances for the fill can be reduced by order of magnitude, using local fill materials. It also comes with an additional challenge, since the larger levee footprint is likely to require additional efforts in terms of stakeholder involvement. However, the large footprint also offers opportunities in terms of secondary multifunctional uses of the levee.

A good understanding of the institutional setting and responsibilities is required to implement good stakeholder management. Dedicated professionals, such as a stakeholder manager and sustainability specialists are added to the design team to keep focus on communication and consultation with stakeholders and setting and monitoring of sustainability goals.

Also, it is relevant to note that applying adaptive design principles may require courage and time to gain experience and knowledge, especially where it concerns innovative solutions.

ACKNOWLEDGEMENTS

We would like to thank the Water Authority of Limburg to give us the opportunity to present the approach and results from the project Well.

REFERENCES

- [1] WATERSCHAP LIMBURG Ruimtelijk kwaliteitskader deel II, Gebiedsontwikkeling Groene Rivier Well, August 2024
- [2] EXPERTISE NETWERK WATERVEILIGHEID Fundamentals of Flood Protection, 2017.
- [3] RIJKSWATERSTAAT-VNK The National Flood Risk Analysis for the Netherlands, 2015.
- [4] EXPERTISE NETWERK WATERVEILIGHEID Hoogwater 2021, Feiten en Duiding, 2021.
- [5] HOOGWATERBESCHERMINGSPROGRAMMA Programmatische aanpak ondersteuning borging duurzaamheid en ruimtelijke kwaliteit Hoogwater-beschermingsprogramma, March 2020.

COMMISSION INTERNATIONALE DES
GRANDS BARRAGES

VINGT-HUITIEME CONGRES DES
GRANDS BARRAGES
CHENGDU, MAI 2025

LESSONS LEARNT FROM DAM SAFETY REVIEW RISK ASSESSMENT (SARRA) IN FRANCE (*)

Guirec PREVOT
PoNSOH

Frédéric LAUGIER
EDF – CIH

Laurent PEYRAS
INRAE

Eric FOUILLARD Et Emmanuel CONSIGNY
VNF

FRANCE

SUMMARY

French regulations introduced in 2007 the obligation to carry out risk analyses for large dams (around 650 class A and B dams in France) through Safety Review Risk Assessment studies (SaRRA). SaRRA are at the heart of the risk management and prevention system. They identify risks and quantify their occurrence and consequences. With almost 15 years of practical experience leading to the production of around 650 SaRRA in France, the aim of this article is to provide technical and quantitative feedback on the practice of risk analysis and safety assessment, and then to address the contribution of hazard studies through the vision and feedback

**Retour d'expérience des études de dangers de barrages en France*

of the stakeholders in dam safety in France: project owners, design offices and the safety authority.

RÉSUMÉ

La réglementation française a introduit en 2007 l'exigence de réaliser des analyses de risque et des évaluations de sûreté pour les grands barrages (environ 650 barrages en France de classe A et B) à travers les Etudes de Dangers (EDD). Les EDD sont au cœur du système de gestion et de prévention des risques. Elles identifient les risques, quantifient leurs occurrences et conséquences. Avec une expérience de presque 15 années de pratique ayant conduit à la production d'environ 650 EDD en France, l'objectif de l'article est de fournir un retour d'expérience technique et quantitatif sur les pratiques de l'analyse de risques et d'évaluation de la sûreté, puis d'aborder l'apport des études de danger à travers la vision et le retour d'expérience des acteurs de la sécurité des barrages en France : les MOA, les bureaux d'études, et l'Autorité de Sûreté.

1. INTRODUCTION - THE ORIGINS OF RISK ASSESSMENT AND CONTROL IN FRANCE

For several centuries, the growth of industry in France has been accompanied by the constant evolution of regulations aimed at controlling activities of all kinds likely to present risks for people or the environment. Over the decades, these regulations have had to take into account numerous parameters of all kinds:

- diversification of activities, processes or operating methods.
- the increasingly close proximity of housing to industrial sites, a direct consequence of increasingly intensive industrial development, which accelerated in the post-war period. In particular, industrial development intensified along certain rivers (processes, logistics, etc.).
- public awareness and risk culture following accidents that have had disastrous consequences in terms of their impact on environmental, human and economic issues, etc. have progressed.

The development of dam regulations and risk management is also linked to the industrial boom that began in the late 18^e century. It was marked by two major accidents in France: the failure of the Bouzey dam in 1895 and the Malpasset dam in 1959. The latter catastrophic accident led to a marked strengthening of government control over dam safety, with the creation of a group of experts at the disposal

of the State[†] in 1966, which gives its opinion on all projects for the creation or reinforcement of large dams and on draft government regulations relating to dam safety.

Since 2006, French legislation has undergone significant changes, with an overhaul of the regulations governing the safety of hydraulic structures, and the introduction of risk analysis studies in the same way as other high-risk industrial sectors. The Safety Review Risk Assessment (SaRRA) for dams has become a systematic exercise for most important French large dams. Figure 1 shows the evolution of dam regulations in France in relation to these two events.

A decree published in 2007, supplemented in 2015 clarifies the general requirements for dam safety depending on the class and size of the dams. In 2018, two additional regulatory texts were published:

- a first decree [2], sets minimum technical requirements for dams
- a second decree [3], sets out the requirements for dam Safety Review Risk Assessment studies in France.

This report presents the main expectations of a dam SaRRA in France. A few figures will give the main findings in terms of feared events for concerned French large dams and will conclude with the contribution of SaRRA to dam safety from the viewpoint of the various players in the field.



Fig. 1
Regulatory developments in dam safety in France
Évolutions réglementaires sur la sécurité des barrages en France

[†]Permanent Technical Committee for Dams (CTPB)

2. EXPECTATIONS OF A SAFETY REVIEW RISK ASSESSMENT STUDY (SARRA)

2.1 DAMS CONCERNED BY SAFETY REVIEW RISK ASSESSMENT STUDIES

In France, regulations define three classes of dams, based essentially on geometric criteria (dam height and reservoir volume[‡]) and leading to specific frequencies for SaRRRA.

Table 1
French dam classification and SaRRRA requirement

CLASS	CRITERIA	DAM SaRRRA
A	$H > 20 \text{ m}$ and $H^2 \cdot V^{0.5} > 1500$.	Yes – Every 10 years
B	$H > 10 \text{ m}$ and $H^2 \cdot V^{0.5} > 200$	Yes – Every 15 years
C	$H > 5 \text{ m}$ and $H^2 \cdot V^{0.5} > 20^{\S}$	No Dam SaRRRA

SaRRRA concern some 650 dams in France, considered to be the most important for public safety. The frequency of SaRRRA varies between 10 and 15 years, depending on the dam class. SaRRRA is required for a new dam or for important refurbishment project.

2.2 GENERAL PRINCIPLES OF DAM SaRRRA

SaRRRA study follows a plan and content defined by regulations [3]. The level of detail and the methodologies used are left to the choice of the dam owner and his consultant, while respecting the principle of proportionality according to the complexity of the dam and the stakes at risk downstream.

A dam SaRRRA study is carried out by a government-approved an engineering office. The latter must have sufficient references and experience in the field of dams.

SaRRRA comprises 5 main stages:

- (i) Functional analysis
- (ii) Condition and design assessment of structures and equipment

[‡](H: dam height in m, V: reservoir volume in hm^3).

[§]Or smaller dams with downstream housings at a distance of less than 400 m

- (iii) Failure modes analysis
- (iv) Safety assessment
- (v) Improving safety – Risk reduction advise

Determining natural hazards (hydrology as the most important, earthquakes, wind, landslides, rockfalls, lightning, etc.) is of course an essential input to risk analysis. In particular, they feed into stages ii. and iv. of SaRRA.

Dam SaRRA realization involves a number of uncertainties inherent in the non-standard nature of dams (in the sense that each dam is unique, including its components and equipment) and in natural hazards, for which the level of uncertainty remains potentially high. The depth of analysis must therefore remain proportionate and coherent, so as to maintain the overall homogeneity of the analysis.

In view of the uncertainties inherent in the field of dams, the level of uncertainty of a large number of parameters remains high.

- ⇒ The aggregate results provided by SaRRA are orders of magnitude that need to be interpreted with hindsight. However, they enable us to assess risks in a hierarchical manner, as rationally as possible, and to propose risk reduction measures that are themselves hierarchical and proportionate to the issues at stake.

2.3 REALIZATION OF SaRRA

Step 1: Functional analysis

First of all, SaRRA includes a functional analysis of the system under study:

- description of the system under study and its environment
- an external functional analysis of interactions with the dam's environment,
- an internal functional analysis of the system itself.

Step 2: Condition and design assessments of structures and equipment

The second step is to determine the intrinsic reliability of each of the dam's components, and their ability to withstand different loads. This demonstration is based on several steps:

- an exhaustive collection of all existing documents: plans, calculation notes, photographs, organization, operation, monitoring and maintenance data
- examination and investigation of all components and parts of the structure
- an assessment of their operation, behaviour and maintenance
- a review of the structural design.

This last stage also checks the dam's compliance with the minimum safety requirements set out in the regulations [2].

Step 3: Failure mode analysis

The third stage is a failure mode analysis, which studies the causes and effects of failures in the functions performed by the various dam components.

The two main methods used in dam hazard studies in France are:

- the PRA (Preliminary Risk Analysis – 75% of SaRRA) method, which relies on a simple risk analysis based on expertise
- the FMEA method (Failure Modes and Effects Analysis – 25% of SaRRA), a more comprehensive analysis of failure modes

The application of the PRA method relies heavily on expert assessment: the identification of hazards is based on the experience and knowledge of the panel of experts. We note that PRA are generally based on a short internal functional analysis, so they present a first-order analysis highlighting only the major failure modes likely to be encountered on dams. The method is relevant for dams, insofar as the expert's judgment remains very important in determining a certain number of degradations and failures. It should be noted that, in the absence of standardization of the method, PRA practices in SaRRA in France show great variability in the tables used and hence in the analysis produced. As a result, some PRA appear to be very comprehensive in their analysis of failure modes, and are ultimately more similar to FMEAs.

The FMEA method provides a detailed analysis of dam failure modes. Within a standardized framework, its main advantage is the precision and quality of the analysis: the FMEA method provides a complete analysis of the failure modes of dam components, following a high-quality functional analysis. It is therefore well-suited to a full, or even quantitative, risk analysis at a later stage. Expertise comes into play when implementing the FMEA method, in the simplification of unrealistic causes and effects on the dam under study. Its application is conditional on structural and functional knowledge of the dam, and therefore depends on the quality of the functional analysis. Care must be taken to maintain consistency between the functional analysis and the FMEA, otherwise this can lead to a loss of information and the omission of failure modes.

Subsequently, the use of tree-based methods enables us to take into account the succession or simultaneity of failures of several elements, independent or not, leading to an accident, according to a functional sequence until the accident occurs. The main accident scenarios are then highlighted.

In France, almost 90% of dam owners use a bow-tie approach, the fundamental part of which is the fault tree., left part of the figure below, event tree being the right part (Fig. 2)

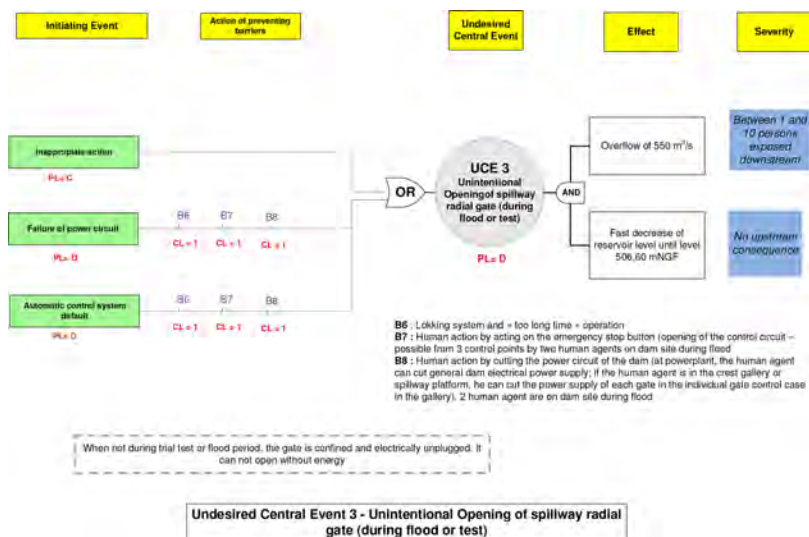


Fig. 2

Example of a bow tie associated with the unintentional opening of a Tainter gate/
radial gate

Exemple d'un noeud-papillon pour une ouverture d'une vanne segment

Step 4: Safety assessment by a multi-disciplinary working group

The fourth stage is a safety assessment. For each failure scenario, the probability of occurrence, the intensity, kinetics and duration of effects (flow rates and volumes released) and the severity of consequences in the concerned area are assessed

Whichever approach is adopted, the risk assessment is produced with the support of a working group comprising a panel of experts and operators, whose role is:

- control and validation of scenario modeling in the form of failure sequences or elementary events.
- assessment of the probabilities of failures of elementary events, in the form of a probability interval or a single probability. The assessment of the probability of occurrence of a scenario is often carried out in a semi-quantitative way, and mainly on the basis of expert opinion.
- checking and validating the assessment of the probability of the scenario as a whole, in particular by inter-comparison with the assessments of the various scenarios, and their ranking in relation to each other.

The working group includes the various engineering and operational components required for these analyses. Typically, expert panels are composed of:

- a panel leader specialized in risk analysis methods
- civil and hydraulic engineer(s) specializing in dams, with a good knowledge of the structure to be evaluated
- engineers specialized in hydromechanics, gate operation and control command systems
- dam operator.

The panel can be enlarged as required, depending on the the complexity of the dam and the technical aspects, to be produced for the scenarios.

- ⇒ The role of the dam operator's representatives is fundamental to the success of the exercise. In practice, it is the operator who has the best practical knowledge of the dam and its equipment, as well as feedback from its operation in the field, including knowledge of how well maintenance and tests have been carried out, and knowledge of incidents and failures that have affected the dam.
- ⇒ When setting up the group, care must be taken to ensure that the dam operator appoints a person or persons with operational knowledge of the dam and its components.

Semi-qualitative occurrence scale

For SaRRA in France, occurrence values are often expressed in terms of frequency classes or levels. Table 2 hereafter is an example of a grid used for semi-quantitative evaluation, proposing 5 classes [A to E]. It comes from the grid used for risk analysis performed in the industrial field in France.

Table 2
Example of a semi-quantitative grid for event evaluation

PROBABILITY SCALE	E	D	C	B	A
Qualitative (if number of installations and feedback are sufficient)	"Possible event. but extremely improbables: <i>is not impossible considering current knowledge, but not experienced worldwide during a large number of installation . years</i>	"very improbables event": <i>already occured in the industry sector. but corrective actions were taken which significantly reduced the probability of occurrence</i>	"improbables event": <i>similar event already occured in the industry sector or in this type or organization worldwide, but no corrective actions were taken which significantly reduced the probability of occurrence</i>	"probables event": <i>already occured or can occur during life duration of the installation</i>	"current event": <i>already occurred or can occur several times during life duration of the installation, in spite of risk reduction measures</i>

(Continued)

Table 2
Continued

PROBABILITY SCALE	E	D	C	B	A
Semiquantitative	This scale is intermediate between qualitative and quantitative scales, and enables to take into account risk reduction measures				
Quantitative (by unit and by year)	10^{-5}	10^{-4}	10^{-3}	10^{-2}	

For equipment, components and materials, the occurrence values of initiating or intermediate events take into account the design, structural analysis, construction and condition of the equipment at the time of analysis, as well as the constraints to which it is subjected (e.g. acidity of the water, which would accentuate the corrosion phenomenon). The rating of these events implicitly includes routine maintenance and monitoring.

It should also be pointed out that certain external initiating events (IE) linked to natural hazards are difficult to grade, and raise methodological and scientific questions (landslides, avalanches, frost, floating debris, etc.).

Aggregation of initiating events

For fault tree construction, initiating events are generally aggregated by simple “AND” / “OR” logic gates.

It is often difficult to take into account possible dependencies between events when using AND logic gate. However, there are conventions that take this difficulty into account to determine the resulting probability.

Assessing the severity of scenarios

The consequences of each failure scenario on human, material, organizational and environmental issues are assessed in order to measure their degrees of severity. The resources deployed here are adapted to the importance of what is at stake for the safety of people and property. The consequences of each potential accident are characterized by the water flow rates and volumes released from the structure, the intensity (water depth and velocity), kinetics and duration of these effects, which then enable us to assess the severity of the consequences for the affected area, particularly with regard to important stakes.

This assessment sometimes distinguishes between counting sedentary people (on houses, premises) and mobile people (walkers, river users, etc.).

The notion of danger water level or danger situation

The danger water level (DWL) is the reservoir level above which the stability of the structure can no longer be guaranteed. It may be reached as a result of extreme flooding or spillway malfunction. The notion of danger water level can be extended to that of danger situation or event (e.g. concomitance of thermal and hydrostatic loading for an arch dam, or different hydrostatic loading situations on a run-off river dam with gates opened or closed).

The notion of danger water level has become an essential indicator of dam safety in the context of SaRRA in France. However, its determination remains an open technical question with uncertainties

Step 5: Improving safety - Reducing risks

Finally, the various accident scenarios are ranked according to their probability of occurrence and severity of consequences, taking into account the impact on human and material assets. The criticality analysis cross-references the assessment of the probability of occurrence with that of the severity of the consequences for each feared event (accident scenario). It is usually produced using criticality grids in France (risk matrix or F-N curve in the USA for example).

Based on this analysis, the project owner, accompanied by its consultant, proposes measures to reduce risks.

3 MAIN RESULTS OF THE FIRST GENERATION OF DAM SARRA

The French government has maintained a database of results for first-generation SaRRA. The database is based on some 500 SaRRA, the results are highly instructive.

3.1 ANALYSIS OF FAILURE SCENARIOS

This database makes it possible to identify the most likely scenarios that could lead to a structure failure. This database is fed solely by the results of the SaRRA, i.e. on the basis of the information and risk analyses provided by dam owners.

Unsurprisingly, the main cause of failure identified by SaRRA (Fig. 3) studies was dam failure due to the danger water level being exceeded (39% of cases studied). These cases (Fig. 4) included not only failures due to the water level being raised by a natural flood (flood alone - 48%), but also the combination of a failure in the flood discharge function and a flood (34% of cases). If we look only at dams with

flood control gates, the combination of flooding and gate failure would be the most likely failure scenario in 40% of cases. This is one major point of interest in the SaRRA studies carried out in France. They enable us to explore the conditions and scenarios of failures whose causes are not solely linked to natural hazards or to the structure itself, but also to integrate other components, as we shall see below.

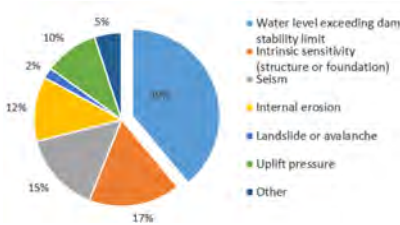


Fig. 3
Causes of dam failure in SaRRA
*Causes des ruptures de barrages
identifiées dans les études de
dangers*

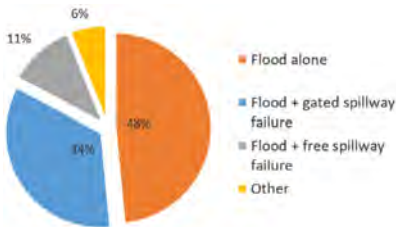


Fig. 4
Causes of water level exceeding dam
stability limit in SaRRA
*Causes de dépassement de la cote de
danger identifiées dans les études de
dangers*

It is therefore interesting to identify the causes of spillway failures (non-opening of gate) when the danger water level is exceeded. The graph below (Fig. 5) shows that about 25% of spillway failures would be due to control failures and 20% to floating debris. The SaRRAs also showed that in about 15% of cases, the operator's organization could lead to spillway unavailability, resulting in failure of the structure. It should also be noted that 10% of cases involved the development of a fire (power demand at the time of operating the equipment). This point has led some dam owners to carry out special thermography tests to monitor overheating in power cabinets.



Fig. 5
Causes of spillway gate unavailability
*Causes d'indisponibilité d'un évacuateur de
crue vannée*

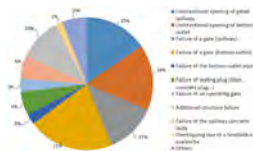


Fig. 6
Most critical feared events identified
in SaRRA after the dam failure
feared event
*Événements redoutés les plus
critiques identifiés dans les
études de dangers après celui de
la rupture de barrage*

Another advantage of the SaRRAs is that it focuses not only on dam failure scenarios, but also on those that could lead to the uncontrolled and dangerous release of impounded water. These failures involve ancillary equipment that is necessary and useful for the safety of the dam and its operation. Two main types of scenarios have been identified as critical after dam failure (Fig. 6): Combining flood evacuation and bottom outlet, these are: “unintentional opening” in 31% of cases, and “gate structural failure” in 37% of cases.

A more detailed analysis of the causes of these failures (see Fig 7) shows that:

- half of the cases of unintentional opening of one or more spillway gates were caused by control-command (Scada) failures, and a third to human error.
- the identified spillway gate failures would be generated mainly by their degraded state (more than half), but also by non-opening of the gate in flood (20%) and impacts from floating debris (20%). It should also be noted that failure of the spillway’s civil engineering piers (following a failure to open the flood gates) is identified (10%) in the most critical feared events.
- these figures can also be interpreted by the fact that flood discharge gates are more carefully maintained than bottom outlet gates. For this reason, the most common cause of failure of bottom outlet gates is their deteriorated condition (90%). Unintentional opening of bottom outlet devices is mainly due to human error (80%). In fact, the operation of these devices is often more basic (less control-command system and simpler kinematic chain), making the operator the most important source of unintentional opening.
- in addition to the rupture and unintentional opening of bottom outlets or spillway engineering structures, sealing devices (concrete plugs in galleries, pipe full back, etc.) account for 6% of the scenarios identified.

On the basis of these lessons, we can see that the work involved in identifying causes, while already rich, can be improved. Indeed, in the first generation of SaRRA, the analysis often stopped at the macroscopic level. Regulations now call for a more in-depth analysis, highlighting the root causes of failure.

3.2 ANALYSIS OF RISK REDUCTION MEASURES

The SaRRA would not be complete if measures to reduce risk were not taken in response to the identified critical failure scenarios according to the risk tolerability criteria’s.

Risk reduction measures involve the implementation of various safety barriers or works on the dam and its equipment to reduce the risk. They can be technical (e.g. adding a mechanical lock to prevent the unintentional opening of a flood gate) or organizational (modifying the operator’s organization and procedures to ensure that a gate is opened on time). These measures can also be more far-reaching,

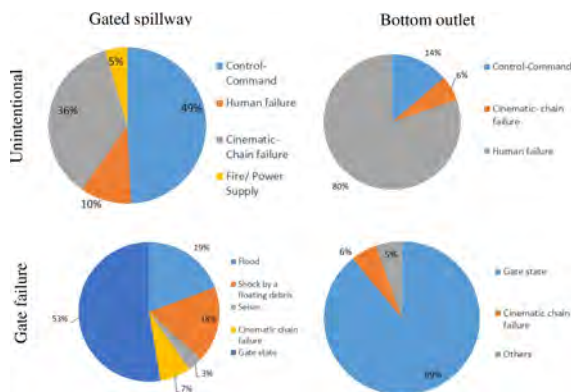


Fig. 7

Summary of the different causes leading to the most critical feared events after dam failure

Résumé des différentes causes conduisant aux événement les plus critiques après la rupture du barrage

involving structural modifications to the structure or its safety components (sealing, drainage, spillway, bottom outlet) in the event of a proven low level of safety. In the latter case, provisional measures are proposed to guarantee an acceptable level of safety before the work is carried out (e.g. lowering the reservoir level, reinforced surveillance, etc.).

The graphs below (Fig. 8 and 9) focus on one French administrative region: Nouvelle-Aquitaine. This region has the advantage of having a large number of dams of all types and ages, and a varied representation of the different types of dam owners (hydropower, drinking water, irrigation, etc.). 111 dams are subject to SaRRA.

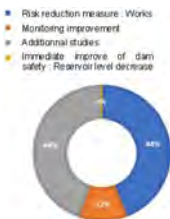


Fig. 8

Measures taken following SaRRA on dams in the Nouvelle Aquitaine region
Mesures prises après les études de dangers sur les barrages de Nouvelle-Aquitaine

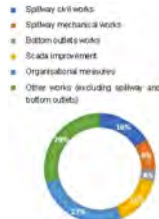


Fig. 9

Work undertaken following SaRRA on dams in New Aquitaine
Travaux réalisés à la suite des études de dangers sur les barrages de Nouvelle Aquitaine

It is interesting to note that the dam SaARRA exercise led to a review of the operator's organization in nearly 30% of the dams in this region, to prevent failure of the dam and its equipment. In the same proportions, work was undertaken on the civil engineering of the structures and on the safety devices.

Électricité de France (EDF) has also carried out a survey of the various measures identified by the company at following of the first generation of SaARRA studies. The graphs below (Fig 10 and 11) show the themes and macro-functions on which risk reduction measures have been implemented.

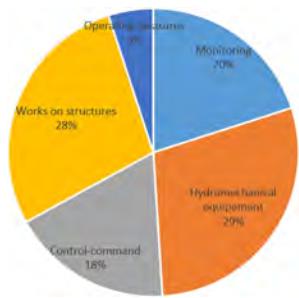


Fig. 10

Topics on which risk reduction measures have been initiated

Sujets sur lesquels des mesures de réduction des risques ont été initiées.

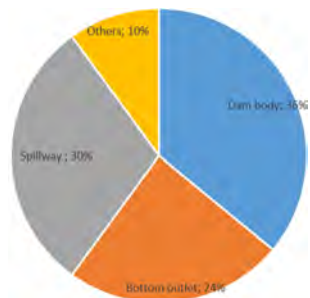


Fig. 11

Macro-functions where risk reduction measures have been initiated

Macro-fonctions sur lesquelles des mesures de réductions des risques ont été initiées

4. THE CONTRIBUTION OF SARRA TO THE SAFETY OF STRUCTURES: THE VISION OF THE VARIOUS STAKEHOLDERS

4.1 RECOGNIZED BENEFITS FOR ALL PLAYERS

The risk analyses carried out through dam SaARRA in France have had, in the opinion of all stakeholders, notable positive impacts on dam safety. Major contributions include:

– **A new multi-field functional approach beyond usual “civil engineering”**

In generic terms, the dam SaARRA have established a new multi-field functional approach, as opposed to the fragmentation that may have existed between each technical field. For a long time, dam safety was examined primarily from a “civil engineering” perspective. The issue of uncontrolled downstream flow releases had also become a major concern in France,

following several incidents in the 1980s and 90s. However, the multi-field functional approach has undoubtedly helped to define a new paradigm in the overall approach to dam safety in their environment (taking into account the hazards of fire, avalanche, landslide, frost, etc.).

– **Better-known dams**

The SaRRA constitutes an excellent documentary and descriptive synthesis of our knowledge of the dam and its components including the systemic functioning. Data contained in SaRRA have been critically reviewed and formally validated. Moreover, the risk analysis has led to a relative exhaustiveness of this knowledge by exploring aspects, which may seem like details, but play an important role in the functional chain. Examples include neglected parts of dam, such as concrete plugs or the full block of old diversion tunnels, very slow kinetic civil engineering pathologies (concrete expansion), or the level switch that plays a role in the dam's warning and information system.

Medium-sized structures (class B under French regulations), which did not always benefit from the history of the largest dams, were less known and documented. As a result, knowledge of these structures has progressed all the more thanks to the SaRRA. The SaRRA were of particular interest for all structures equipped with numerous gates and Scada control devices. The risk analysis highlighted complex scenarios combining hydromechanical or control-command system (Scada) failures, with hydrological scenarios, leading to the dam failure.

– **Identifying and classifying risks: Orders of magnitude**

Risk analysis tools have enabled the emergence of failure scenarios that would not have been easily identifiable without a multi-disciplinary risk analysis methodological approach. Potential flaws that were not necessarily understood by the dam operator were sometimes brought to light. As a result of the risk analysis exercise, operators' attention has considerably broadened in terms of structural safety risks. In addition to the usual focus on civil engineering, mechanical and control-command aspects have also been taken into account.

The quantification of initiating events has enabled to identify major trends. Even if individual quantification of the probability of initiating events needs to be approached with caution, the various methods, notwithstanding their intrinsic qualities, have provided a tool for inter-comparing as objectively as possible and ultimately inter-ranking the main safety risks of the dam.

– **Risk reduction and control measures and preventive posture**

The identification and prioritization of risks carried out in the SaRRA has led to a series of risk reduction or control measures. They are proposed for

implementation over the long or short term, depending on the issues identified. In this way, SaRRA provides the project manager with a roadmap for the improvement of its dam safety. When the risks are deemed too great, the SaRRA can propose measures that can be applied immediately, pending the implementation of risk reduction measures, which may take several years to complete in the case of subjects involving major civil or mechanical engineering studies and works.

– **Internal and external communication**

- *External:* The standard content of SaRRA includes a non-technical summary intended for external communication to a wide audience. Its purpose is to present a summary of the study, and in particular its results. It is intended to be educational, easy to understand and highly concise.
- *Internal:* Internally, it appears that SaRRA provides an excellent opportunity to raise staff awareness of safety issues. People who have been able to take part in the working groups corresponding to the different stages of the risk analysis are in fact aware and have a good understanding of the dam risks and therefore of safety. They contribute to the development of a safety culture among dam owner employees.

4.2 AN OWNER'S VISION

The first essential benefit of SaRRA, already mentioned, is a much better understanding of dams and their associated risks for the dam owner.

For dam owners operating a large portfolio of old dam, the implementation of compliance projects made necessary by technical regulations necessarily raises the question of prioritizing the programming of these projects.

By identifying failure scenarios and the resulting risk reduction measures, dam owners can better understand the transitional risk control measures to be taken while awaiting the implementation of compliance projects and prioritize projects according to the level of risk compared.

SaRRA make it possible to prioritize actions not only on the scale of a single dam, but also and above all on the scale of a portfolio of dams for the owner of a large number of dams.

The involvement of operating teams throughout SaRRA process enables the operator to quickly become aware of certain measures which, at little cost, rapidly and concretely reduce the risk of a failure scenario (e.g. adding an emergency stop button to open a gate or modifying an operating instruction to take account of the risk of freezing). The integration of operator and owner personnel into the panel of multi-

skilled experts enables them to better understand and grasp technical issues that are often poorly understood.

When applying risk reductions measures, the question is raised of their appropriation by dam operator. In this respect, the SaRRA, which also looks at scenarios of uncontrolled and dangerous release of water, assesses the corresponding risks of failure, particularly the level of control by the operator of these new operating modes, both in terms of operation and maintenance. It raises questions about the operator's major-accident prevention policy and safety management system, and forces the operator to adapt its monitoring and, above all, operating procedures, which have sometimes been defined to ensure optimized hydraulic management that is not always perfectly consistent with hydraulic safety issues.

On the whole, participation in SaRRA working group, or its internal communication, contributes significantly to improve the safety culture of both the dam owner and dam operators.

On a broader level, the periodicity of SaRRA imposed by the regulations provides a continuous reassessment of risks that follows the life of the structure and its mode of operation.

On the other hand, the absence of SaRRA for smaller dams, which are therefore not subject to these regulations, means that knowledge of their risk level is lower than for larger dams. However, the stakes for one small dam are generally much lower. On a case-by-case basis, "simplified" approaches of risk analysis make it possible to identify certain potentially critical dams and propose proportionate risk reduction measures.

4.3 A CONSULTANT'S VISION

Introduction of SaRRA in France have led consultant engineers to make their own risk analysis methodologies and systemic functional approaches. After some fifteen years of practice, this field is now well established, and the risk analysis approach can be applied to dams without any major methodological difficulties.

Due to their periodic nature, SaRRA represent a major, long-term workload for engineering firms. They sometimes lead to risk-reduction measures involving major studies and rehabilitation works, which require resources of engineering firms. In this way, the SaRRA have enabled to maintain the skills of a strong French engineering team in the dam sector, while at the same time shifting their technical skills from the construction of new dams to engineering focused on maintenance, risk analysis and reinforcement work on existing dams, with a concern for their integration both in terms of design and in relation to operation, thanks to the multi-field approach of SaRRA. This engineering strength is one of the guarantees of dam safety in France.

When carrying out SaRRA, consultant engineers logically follow a proportionate and graduated approach, starting with simpler and logically conservative methods. Where risks are unacceptable, SaRRA also lead consultant engineers to develop innovative methodologies to better characterize the actual margins of dams and materials (non-linear approaches for dam calculations, with more sophisticated material behavior laws, characterization of the concrete/foundation interface, material ageing, hydrodynamic flows and loads etc . . .). They are also leading to improvements in methodologies in areas that were sometimes little objectified in the past (fire risk, floating bodies, avalanches, block falls, reliability of gate operation, operating organization, etc.). In the field of natural hazard characterization, risk analyses are also leading to improvements in the methodologies used (development of stochastic hydrological methods among others.).

SaRRA are also an opportunity for the consultant to gain exhaustive feedback on all the technical aspects of the studied dam since its commissioning. Prior to SaRRA, consultants, working largely on the design of new structures, had little opportunity to compare theory and practice on a multi-field scale (dam behaviour but also hydromechanical equipment, Scada, operator organization etc..).

In addition, through their contribution to SaRRA working group and the numerous exchanges with the dam operator, SaRRA enable the consultant office experts to gain a better understanding of the operator's "real life" requirements and constraints. All this contributes to improving the safety culture and global vision of the consultants contributing to SaRRA.

Moreover, these methodological advances, this experience feedback, the improvement in safety culture and systemic vision, also constitute resources that design offices can make available to their customers to improve the design and safety of new dams on which they are also working.

For a consultant engineer, SaRRA is sometimes a delicate exercise when the results of a risk analysis highlight sensitive risks. It is important to maintain a balanced dialogue with the dam owner, between the necessary independence of the consultant, the financial interests of the various parties, and the degree of conservatism of the methods and conclusions (for which expert opinion still plays an important role in the dam sector). The way in which SaRRA are contracted out, the quality of follow-up and the involvement of the dam owner in the course of the SaRRA are important levers for maintaining this balance.

4.4 THE CONTROL AUTHORITY'S VISION

Through the systematic introduction of risk analyses in the SaRRA for large dams, the French supervisory authority has sought to ensure that the risks associated with dams are displayed in such a way that they can be reduced and kept at low level.

In the end, nearly 650 SaRRA were carried out. Apart from a few shortcomings inherent in each new process, the supervisory authority noted that, overall, the work carried out was rather pragmatic and operational. This exercise could indeed have remained theoretical, but it is the multi-field approach, the involvement of all the players working on the dam, and the steering of the studies by competent consultants that guarantee the success of the exercise.

Of course, while risk analysis through SaRRA is a highly effective approach to risk management, it is not an absolute weapon against incidents and accidents. All the players involved in dam risk management have an essential role to play in ensuring the safety of dams: the operator in his monitoring, operation and maintenance missions, the consultant engineer who ensure the quality of diagnoses and studies, and the authorities who are in charge of dam safety policy control.

One of the main strengths of the SaRRA is that, through this regulatory exercise, the dam owner becomes aware of the risks associated to its dam cause, and the measures to be explored in order to reduce them.

In France, SaRRA is now an essential document, through which the dam owner demonstrates the safety of its dam in all operating situations. It is a useful document for all parties involved, including the supervisory authority, enabling them to identify the key safety aspects of the dam. And, as the statistical analysis presented in this article shows, it also identifies areas for improvement, on which the entire profession needs to work, to further improve the safety of our dams.

5. CONCLUSION

A key regulatory requirement for all major dams, periodic SaRRA are the documents that dam owners must produce to justify the safety of their structures and identify major risks. They have now been in existence for almost 15 years. This field is now well established in French practice.

The risk analyses carried out through the SaRRA in France have had, in the opinion of all stakeholders, positive and notable impacts on dam safety. Major contributions include:

- A new multi-field functional systemic approach that goes beyond the traditional “civil engineering” approach
- A significant improvement in the general and exhaustive knowledge of dams and equipments
- An identification and classification of failure scenarios and major safety risks
- An interclassification of risks enabling the owner to prioritize the measures to be applied to the dam in a rational manner, starting with the subjects with the highest safety stakes

- The effective reduction of these risks through the implementation of actions undertaken at the end of the SaRRA with the adoption of a preventive posture.

For the second generation of SaRRA, regulations have evolved to improve knowledge of structures, their operation and design. It turns out that this is the most necessary element to guarantee the success of the exercise.

Readers can deepen their knowledge of SaRRA carried out in France by reading the CFBR document, translated into English, which explains the process thanks to many examples [1].

ACKNOWLEDGEMENTS

This paper has been supported by a working group gathering CFBR (French Committee of Large Dams) members: consultant engineers, dam owners, governmental authorities, and research institutes. Under the direction of (alphabetical order) Frederic LAUGIER (EDF CIH), Laurent PEYRAS (INRAE) and of Guirec PREVOT (PoNSOH), the composition of the working group is the following: Thomas ADELINE, Thibault BALOUIN, Catherine CASTEIGTS, Benjamin DELARUELLE, Eric FOULIARD, Thierry GUILLOTEAU, Jean-Charles PALACIOS, Gladys PAVADAY, Michel POUPART, Agnes VALLEE, Eric VUILLERMET.

The paper is based on the document French practices of dam Safety Review and Risk Assessment [1].

REFERENCES

- [1] CFBR, French practices of dam Safety Review and Risk Assessment - June 2020. https://www.barrages-cfbr.eu/IMG/pdf/fr-en_recommandations_cfbr_2021_analyse_de_risques.pdf
- [2] Decree of August 6, 2018 setting technical requirements for dam safety <https://www.legifrance.gouv.fr/download/pdf?id=ybRs0WLloecGX180EOzxjx4itWteOs cszblf1XTI3M4>= Decree explanation notice https://www.ecologie.gouv.fr/sites/default/files/documents/2019_10%20note%20interpretation%20ATB_0.pdf
- [3] Decree of September 3, 2018 defining SaRRA plan https://www.legifrance.gouv.fr/download/pdf?id=mwIYk28StsvqnqjDqwoUdYvKSk5AJ5_K4MfKeTuWgLS== Decree explanation notice https://www.ecologie.gouv.fr/sites/default/files/documents/2020_02_03_AEDDB_note%20d%27interpr%C3%A9tation_vf.pdf

COMMISSION INTERNATIONALE DES
GRANDS BARRAGES

VINGT-HUITIEME CONGRES DES
GRANDS BARRAGES
CHENGDU, MAI 2025

**L'ÉVALUATION DES RISQUES D'ÉROSION POUR LES BARRAGES ET LES
DIGUES EN REMBLAI – RÉFLEXIONS ET PRATIQUES FRANÇAISES (*)**

Luc DEROO
ISL

Stéphane BONELLI
INRAE

Jean-Jacques FRY
Consultant

FRANCE

SUMMARY

The main cause of dam and embankment failure is erosion - internal and external erosion - which accounts for more than 80% of all causes of failure. This phenomenon is not covered by the European standards (Eurocodes) and requires a new approach in order to be considered. In 2024, after 7 years' work involving 26 professionals, the French Committee for Large Dams is presently finalizing a project of recommendations for the assessment of hydraulic structures and their foundations to erosion. This project of recommendations, detailed on over 400 pages, for the first time encompasses internal and external erosion in a common 7-step methodology based on the concept of erosion paths. The proposed recommendations apply to three types of structure: dams, canals and dikes. They develop the

**Dams and levees erosion assessment – French methods and approaches*

use of both deterministic and probabilistic analysis. They propose three levels of analysis for internal erosion and three types of justification for external erosion. They are preliminary in nature, and the scope and novelty of the task mean that feedback will be needed in the coming years to validate the final version.

RÉSUMÉ

La principale cause de rupture des barrages et des digues en remblai est l'érosion - érosion interne et érosion externe - qui représentent plus de 80% des causes de rupture. Ce phénomène n'est pas couvert par les Eurocodes et nécessite une nouvelle approche pour être appréhendé. Le Comité Français des Barrages et Réservoirs au bout de 7 années de travail impliquant 26 professionnels envisage de publier un projet de recommandations pour justifier la résistance des ouvrages hydrauliques en remblai et de leur fondations vis à vis de l'érosion. Ce projet de recommandations, détaillées sur plus de 400 pages, pour la première fois englobent l'érosion interne et l'érosion externe dans une méthodologie commune en 7 étapes à partir du concept de chemins d'érosion. Elles s'appliquent à trois types d'ouvrages: les barrages, les canaux et les digues. Ce projet de recommandations développe aussi bien l'usage d'analyse déterministe que celui d'analyse probabiliste. Elles proposent trois niveaux d'analyse de l'érosion interne et trois types de justification pour l'érosion externe. Elles sont préliminaires, l'étendue et la nouveauté de la tâche obligent à un retour d'expérience dans les années à venir pour valider la version finale.

1. INTRODUCTION

Le CFBR (Comité Français des Barrages et Réservoirs) est en 2024 en cours d'examen et d'approbation d'un projet de Recommandations pour justifier la résistance des ouvrages hydrauliques en remblai et de leur fondations vis à vis de l'érosion. Ce projet de Recommandations englobe l'érosion interne et l'érosion externe dans une méthodologie commune en 7 étapes à partir du concept de chemins d'érosion.

Ce rapport propose un aperçu de ces propositions de Recommandations, au travers de quelques unes des nouveautés qu'elles contiennent. Le chapitre 2 présente le contexte de développement de ce projet de Recommandations. Puis, à défaut de pouvoir exposer l'ensemble du contenu de ce projet, les chapitres 3, 4, 5 et 6 proposent un focus sur quelques thèmes particuliers.

2. CONTEXTE

2.1. RECOMMANDATIONS FRANÇAISES

Le CFBR, Comité Français des Barrages Réservoirs édite des guides et des documents de Recommandations professionnelles, depuis 1997. Les Recommandations couvrent les champs suivants : Justification de la stabilité des barrages-poids (2012), Justification de la stabilité des barrages en remblai (2015), Evacuateurs de crue (2013), Justification de la stabilité des barrages-voûtes (2018), Pratiques de l'analyse des risques (2021).

Ces ouvrages, établis par des groupes de travail ad hoc, font ensuite l'objet d'une validation par la Commission Exécutive du Comité, puis sont utilisés pendant quelques années à titre probatoire, avant d'être transformés en Recommandations définitives. A l'usage, ces ouvrages font référence auprès des différents acteurs pour l'évaluation de sécurité hydraulique des barrages et des digues : maîtres d'ouvrage, bureaux d'études, et autorité de contrôle. Ils sont donc au cœur de l'ingénierie des barrages en France. Le CFBR a décidé d'ajouter un volume supplémentaire à cette collection : des recommandations pour la justification des barrages et des digues vis-à-vis des mécanismes d'érosion, interne et externe. Cette décision est motivée :

- d'une part par le fait que l'érosion représente le mode de rupture prépondérant des barrages et des digues, en France et dans le monde,
- d'autre part par le fait qu'il n'existe pas de corpus de recommandations consolidées applicables à l'ingénierie des ouvrages hydrauliques dans ce domaine, que ce soit en France ou à l'international,
- enfin par le constat que de telles recommandations permettraient des progrès dans la compréhension et la prise en compte de ces phénomènes par l'ensemble de la profession.

2.2. MANDAT ET CONSTITUTION DU GROUPE

Le mandat du groupe de travail (GT) a été délivré en 2017. Il a fixé les principales lignes directrices suivantes :

- poursuivre le travail d'appropriation par la profession des guides (2016-2018) du projet de recherche ERINOH,
- dresser l'état de l'art des connaissances et pratiques en matière d'érosion externe : érosion de surverse et affouillement,
- produire des recommandations professionnelles pour la justification des barrages et digues en remblai vis-à-vis des modes de rupture liés à l'érosion interne,

- produire une synthèse des bonnes pratiques actuelles pour la justification vis-à-vis des modes de rupture liés à l'érosion externe.

L'exécution de ce mandat a conduit à rassembler un groupe de travail au sein duquel les différentes composantes de la profession sont représentées : Maîtres d'Ouvrages de barrages, de barrages latéraux (digues de canaux), et de digues de protection contre les crues ; Bureaux d'étude ; Services d'appui technique aux autorités de contrôle ; Universitaires ; et Experts.

La première phase du travail de ce groupe a été un travail d'inventaire, d'appropriation des acquis récents de la recherche, de mise en cohérence des approches, et de validation de l'approche de Niveau 1 exposée plus loin dans ce rapport.

La deuxième phase du travail consiste à rédiger les Recommandations, et ses deux volumes : le texte principal, qui fixe la démarche de justification recommandée, et le volume des annexes, qui fournit les critères, formules, abaques et exemples. Cette rédaction est un processus par étapes : rédaction par le groupe de travail ; examen par la commission exécutive du CFBR ; publication en version provisoire et intégration des retours des praticiens.

2.3. DOCUMENTATION EXISTANTE

Les Recommandations s'appuient sur un corpus de documentation existant. Sont en particulier valorisés :

- pour l'érosion interne : le Bulletin 164 de la CIGB volume 1 (1976) et volume 2 (2023), les travaux du programme de recherche ERINOH et notamment son Guide Ingénierie (2018), les acquis du colloque d'Aussois de 2005, ainsi que de nombreuses publications scientifiques,
- pour l'érosion externe : les résultats provenant du domaine maritime (Eurotop, Rock Manual), les travaux du BAW et de CIRIA, les acquis du colloque d'Aussois de 2017, ainsi que de nombreuses publications scientifiques.

Le projet de Recommandations valorise également l'interprétation de l'accidentologie publiée, et le retour d'expérience acquis sur les très nombreuses années de service des barrages et digues cumulées en France.

3. QUELQUES POINTS CLÉS

La rédaction d'un projet de Recommandations sur l'érosion interne et externe est à notre connaissance sans précédent dans le monde. Il a donc fallu innover, pour tenter de produire un document qui répondent à plusieurs exigences :

- complétude : il s'agit de couvrir, dans la mesure des connaissances actuelles, la grande variété des processus d'érosion qui peuvent conduire à la rupture,
- rationalité : il s'agit de limiter la part de « jugement d'expert » non étayé par des arguments quantifiables,
- utilité : il s'agit que les méthodes suggérées soient effectivement utilisables et proportionnées aux enjeux.

3.1. MECANISMES, PROCESSUS, CHEMINS ET SCENARIOS D'ÉROSION

3.1.1. Terminologie

Il est apparu utile de distinguer quatre notions différentes.

Un *processus* (par exemple un processus d'érosion) est l'enchaînement d'une série de *mécanismes* élémentaires (par exemple : initiation, puis non-filtration, puis progression, puis ouverture de brèche), provoqué par l'occurrence d'une situation de chargement hydraulique. Un processus d'érosion se développe le long d'un *chemin* particulier, emprunté par l'écoulement. Un chemin d'érosion est initié le long de défauts ou d'hétérogénéités préexistants ou qui ont pu se développer au fil du temps ou par accident et engendrant des écoulements préférentiels. La rupture par érosion se produit à l'occasion d'une *situation* spécifique, qui définit le chargement (typiquement un niveau d'eau pendant une certaine durée) appliqué à l'ouvrage.

Un *scénario* (de brèche, de rupture) est alors un processus particulier dépendant d'un couple (situation, chemin). Un tel scénario peut résulter de processus simples, ou de processus plus complexes, faisant intervenir des mécanismes variés, par exemple débutant par des mécanismes successifs d'érosion, puis se poursuivant par des mécanismes d'instabilité en grand. Des *barrières de défense* contre la rupture sont mises en place par des fonctions principales de conception (étanchéité, résistance, filtration, drainage, protection) et par les procédures d'exploitation (surveillance et intervention). La sécurité de l'ouvrage dépend donc de la capacité de ces barrières de défense à empêcher, stopper ou limiter l'érosion.


3.1.2. Une démarche d'analyse par chemins d'érosion

Le projet de Recommandations considère que la démarche d'analyse ne consiste pas à **examiner les mécanismes** potentiels d'érosion, mais plutôt à **rechercher les chemins** le long desquels l'érosion peut se développer et **imaginer les scénarios** de rupture correspondant, scénarios pouvant faire intervenir un seul ou plusieurs mécanismes.

L'identification des chemins d'érosion devient alors le point de départ de l'analyse. Il s'agit d'abord de faire l'inventaire *exhaustif* des chemins d'érosion à partir de la liste des défauts ou hétérogénéités initiateurs (observés ou suspectés ou pouvant se produire à l'occasion d'une situation de chargement nouvelle). L'accidentologie montre en effet que c'est bien le long de chemins provoqués par ces défauts et hétérogénéités que les scénarios de rupture se sont produits. Les défauts sont des anomalies : géologiques (karst, diacalse, faille, joint) ; géométriques (trou, ouverture au contact de deux matériaux) ; géomécaniques (tassement différentiel, fissure, fracturation, granulométrie défavorable – sensibilité à la suffusion ou à la liquéfaction) ; hydrauliques (grande perméabilité, écoulement préférentiel, chenal, fort gradient hydraulique de sortie sans filtre) ; environnemental (terrier, fissure de dessiccation, trou de racine, gel) ; etc. Les hétérogénéités sont des variations locales de géologie ou de constitution des remblais qui, dans certains cas peuvent faire naître un chemin d'érosion.

Cette liste est ensuite épurée, au cas par cas, pour aboutir à l'inventaire *raisonnable* des chemins, en écartant d'emblée les chemins pour lesquels les barrières de défense correspondent à l'état de l'art (par exemple en raison de la présence d'un filtre efficace) et ceux où le défaut est insuffisant pour déclencher l'érosion.

Tableau 1
Présentation de l'analyse préliminaire d'un chemin d'érosion

Code et Titre : S1-Ch1 - Claquage de la clé d'étanchéité à la mise en eau.	<p align="center">Schéma du chemin d'érosion</p> 
Évènement	Description de la défaillance et de la marge de la barrière
1 Situation	Mise en eau
2 Localisation	Claquage hydraulique dans la tranchée parafouille étroite et sans filtre.
3 Initiation	Erosion de conduit dans le noyau.
4 Filtration	Absence de filtre et de calfatage dans la tranchée. Filtre aval du noyau insuffisamment drainant, écoulement le contournant par le rocher fissuré.
5 Progression	Formation d'un conduit d'érosion à la base du noyau, formation d'une conduite à la base de la recharge aval. Absence de protection aval : déchaussement et érosion régressive de la recharge aval
6 Détection	Détection seulement par inspection visuelle.
7 Intervention	Echec de la tentative de bloquer la résurgence par des enrochements. Elargissement du conduit jusqu'à l'amont et brèche.

3.2. EROSION INTERNE, EROSION EXTERNE

Les phénomènes génériques de l'érosion interne et de l'érosion externe ont été classés de manières différentes.

3.2.1. *Erosion interne*

Il existe 4 mécanismes d'initiation de l'érosion interne (CIGB, 2016).

Erosion de conduit. L'érosion de conduit (d'un sol nécessairement cohésif) se produit tout le long d'un défaut préexistant : un conduit, ou une fissure.

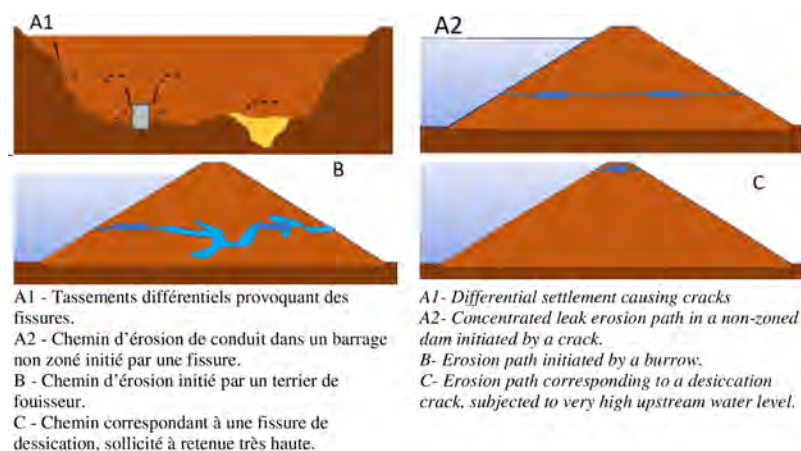


Fig. 1

Chemins d'érosion de conduit
Paths of concentrated leak erosion

Erosion régressive. L'érosion régressive (d'un sol nécessairement granulaire) détache les particules à l'exutoire du chemin qui régresse dans le sol.

Erosion de contact. L'érosion de contact se développe le long de toute interface entre un sol fin (érodable) et un sol grossier ou un terrain fissuré.

Suffusion. La suffusion est l'érosion des particules fines à travers les restrictions des particules grossières dans des matériaux à granulométrie étalée.

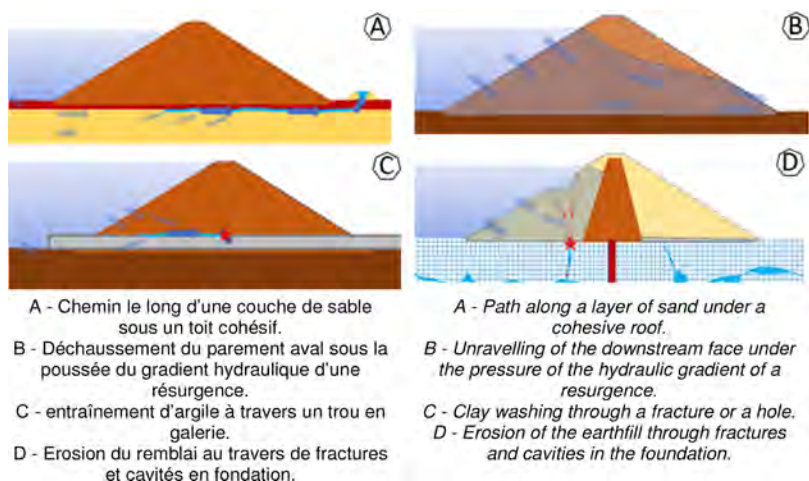


Fig. 2
 Chemins d'érosion régressive
Paths of backward erosion

Le sol grossier ou rocher fissuré joue deux rôles : (1) il contient un écoulement suffisamment rapide pour éroder (2) il évacue les particules de sol fin érodées.

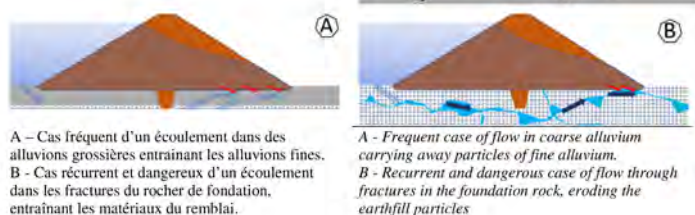


Fig. 3
 Chemins d'érosion de contact
Paths of contact erosion

Claquage hydraulique (annulation de la contrainte principale mineure σ'_3). Ce n'est pas un mécanisme d'érosion, mais il joue un rôle important dans de nombreux scénarios d'érosion. En initiation, c'est le défaut qui provoquera l'érosion de conduit ou l'érosion régressive, en phase de progression, c'est le mécanisme qui ouvrira de nouveaux chemins d'érosion. Son statut particulier, au regard d'autres mécanismes

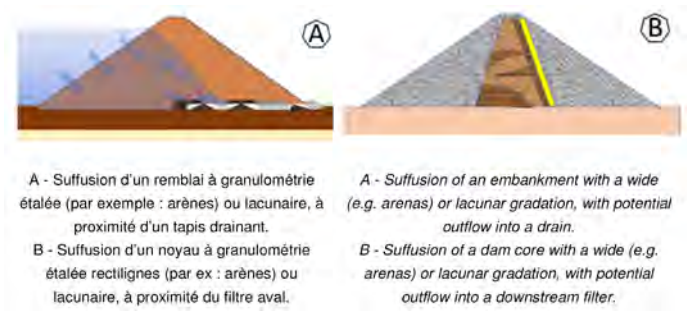


Fig. 4
Chemins de suffusion
Paths of suffusion erosion

initiateurs (tel que le développement d'un terrier de fouisseur ou la perte de l'étanchéité), tient à ce que l'ensemble (claquage + érosion interne) fait partir d'un même processus : claquage puis érosion se développent le long du même chemin, dans la même temporalité, résultant de la même sollicitation initiale.

Ces mécanismes individuels peuvent se combiner, ou se combiner à d'autres mécanismes (érosion interne, saturation des remblais, ...) pour former le

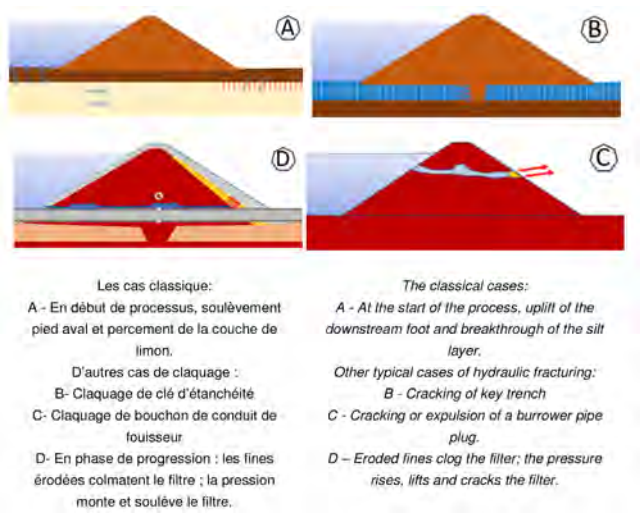


Fig. 5
Cas de claquage hydraulique
Cases of hydraulic fracturing

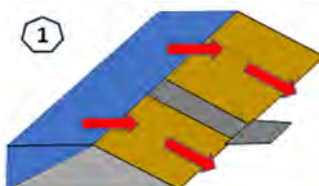
processus redouté. De nombreux accidents passés résultent d'une telle combinaison de mécanismes successifs.

3.2.2. *Erosion externe*

Pour l'érosion externe, une approche différente a été retenue. Plutôt que de distinguer des mécanismes physiques, il a été jugé pertinent de distinguer des catégories de chemins d'érosion (Fig. 6).

La surverse par un écoulement continu.

Continuous overflowing



Le franchissement par les vagues; par les ondes d'intumescences; par les vagues solitaires (glissement ou rejet sismique dans la retenue).

The overtopping by the waves; by waves from intumescence; by solitary waves (impact from landslide or active fault in the reservoir).



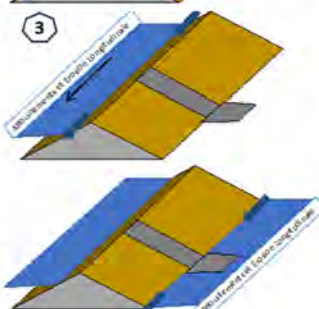
L'affouillement (à la base du talus) et l'érosion (sur le parement du talus) par écoulement longitudinal :

- Côté intérieur
- Côté extérieur

Scouring (at the base of the slope) and erosion (along the slope) by longitudinal flow:

- *Inner side*
- *Outer side*

Nota : les autres types d'affouillement sont traités plus bas dans ce tableau



L'érosion autour de l'évacuateur : débordement par-dessus les bajoyers; érosion sous la structure par défauts d'étanchéité; érosion du revêtement de l'évacuateur; affouillement dans la fosse de dissipation.

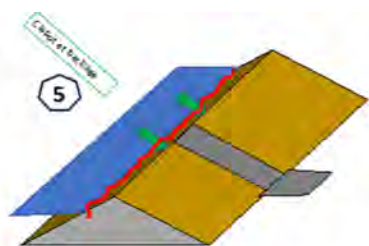
Erosion around the spillway: overflow over the guide walls; erosion under the structure due to leaks; erosion of the spillway lining; scour in the spilling basin.



Fig. 6
Catégories de chemins d'érosion externe
Categories of external erosion paths?

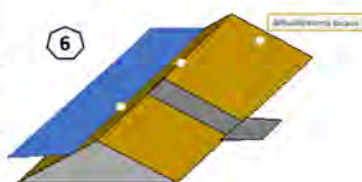
L'érosion du revêtement du parement amont par les vagues périodiques (vent, navigation)

Erosion of the upstream dam or levee protection by periodic waves (wind, navigation)



Les affouillements locaux particuliers, qui recouvrent deux catégories d'érosions locales :
1/ les affouillements par turbulences locales au droit ou à proximité d'ouvrages ou éléments particuliers : piles de ponts, arbres en talus, ...

2/ les érosions locales par la concentration d'un écoulement localisés et à forte vitesse : jets d'hélices, rupture locale de conduites en charge, ...



Specific local scouring, which covers two categories of local erosion:

1/ scour caused by local turbulence at or near structures or special features: bridge piers, trees on embankments, etc.

2/ local erosion caused by the concentration of localized, high-speed flows: propeller jets, local rupture of pipes, etc.

Fig. 6
(Continued)

Dans le cas de l'érosion externe, il est apparu particulièrement utile de distinguer trois approches pour apporter la justification de stabilité.

- Type 1 : Absence de sollicitation : le chemine d'érosion n'est pas sollicité,
- Type 2 : Absence d'érosion : la sollicitation est inférieure à la résistance,
- Type 3 : Erosion acceptable : la sollicitation est supérieure à la résistance, mais les dégradations sont jugées acceptables vis-à-vis de l'aptitude au service de l'ouvrage (et des procédures d'intervention mises en place par l'exploitant pour remédier à temps aux dégradations).

Naturellement, la profondeur des justifications est proportionnée au Type de justification ; il est plus difficile d'apporter la preuve de Type 3 que la preuve de Type 1 ou 2.

3.3. BARRAGES, BARRAGES LATÉRAUX, ET DIGUES DE PROTECTION

Trois catégories d'ouvrages ont été considérés : les barrages « classiques », les barrages latéraux, qui sont les barrages formant les canaux (de navigation,

d'alimentation et de bief d'usines hydro-électriques au fil de l'eau), les digues de protection contre l'érosion.

Les processus élémentaires d'érosion sont les mêmes pour ces trois catégories d'ouvrage, cependant, leurs particularités conduisent à les analyser différemment :

Barrages latéraux

Les barrages latéraux sont soumis à des situations spécifiques, que l'on ne rencontre pas (ou rarement) dans les barrages-réservoirs. Les barrages latéraux ferment des biefs de canaux, soumis à des vitesses d'écoulement longitudinal, dans lesquels peuvent se développer des ondes d'intumescences provoquées par les manœuvres des organes hydromécaniques (vannes, portes) ou par les disjonctions des turbines. Les ondes d'intumescence positives peuvent conduire à des franchissements de la crête des remblais avec des volumes significatifs. Dans le cas des canaux de navigation, il faut également tenir compte des sollicitations de navigation : batillage, effet piston au passage des navires, jets d'hélice, accidents de navigation.

Dans les canaux de navigation, le vent peut soulever des vagues significatives le long de longues sections droites. Les formules habituelles utilisées pour les barrages sont à adapter à l'étroitesse du canal pour le calcul de la hauteur de houle et aux faibles angles d'incidence pour le calcul du run-up dans les courbes en extrémité de ces sections droites.

De plus, des facteurs d'accidentologie leurs sont spécifiques :

- ces barrages sont généralement traversés par des ouvrages sous-remblai, de rétablissement hydraulique, rétablissement routier ou rétablissement de réseau (gaz, eau, ...) ; les tassements différentiels et les écoulements au passage de ces ouvrages ont occasionné des ruptures par érosion interne,
- ces barrages sont sensibles aux écoulements des cours d'eau voisins : érosion externe des talus de remblai, arrivées d'eau dans le canal par débordement pouvant ensuite provoquer une surverse.
- les incidents et accidents de navigation peuvent provoquer des ruptures de l'étanchéité des remblais équipés d'étanchéités minces en parement côté canal.

Digues de protection contre les inondations

Pour des raisons historiques et techniques, la réglementation française en matière de digues de protection diffère de la réglementation barrages. La réglementation acte des probabilités de brèches plus fortes que les probabilités de rupture des barrages. Elle demande que soient caractérisés deux situations :

- la situation de crue pour laquelle la probabilité de brèche est suffisamment faible (5%) ; son niveau définit le niveau de sûreté,
- la situation de crue pour laquelle la probabilité de brèche est suffisamment élevée (au moins 50%) ; son niveau définit le niveau de danger

La justification de sécurité hydraulique est donc conduite de manière différente : il s'agit d'examiner toute une gamme de situations de crues et, pour chaque situation, d'inventorier et probabiliser chacun des scénarios (situation * chemin, avec caractérisation du processus redouté) pouvant conduire à la brèche, puis de les combiner pour en déduire la probabilité de brèche résultante. Des démarches spécifiques sont recommandées pour ces calculs, via l'utilisation de « courbes de fragilité ».

Les facteurs d'accidentologie qui leur sont spécifiques comprennent notamment :

- l'érosion externe en pied de talus intérieur (affouillement), par l'effet du courant,
- l'érosion interne régressive pouvant se développer, lorsque les digues sont fondées sur des alluvions silteuses ou sableuses fines
- les terriers de fousseurs pouvant causer la rupture de digues.

3.4. LA QUALIFICATION *RM*, *BP*, *AN* DES METHODES

En matière d'érosion, les méthodes d'ingénierie disponibles et les critères de justification ne sont pas tous clairement établis :

- Certains mécanismes d'érosion ne sont pas couverts par des formules, équations ou abaques. Par exemple : la résistance à l'érosion de surverse d'un talus de remblais.
- Certains mécanismes d'érosion sont couverts par des formules ou abaques, mais avec un domaine de validité qui ne couvre pas tous les cas. Par exemple: la résistance à l'érosion régressive d'un sol silteux ou sableux sous un toit.
- Lorsque les mécanismes sont couverts par des formules ou abaques, une part significative d'incertitude subsiste généralement, dans la caractérisation de la sollicitation et dans la caractérisation de la résistance. Par exemple, la résistance à l'érosion de conduit a des incertitudes liées à sa forte variabilité et aux dimensions du conduit.

Plus fondamentalement, il subsiste encore des interrogations :

- Les processus d'érosion se produisent à la faveur de défauts et hétérogénéités; comment identifier et caractériser ces défauts et hétérogénéités, avec un effort d'ingénierie raisonnablement proportionné aux dimensions de l'ouvrage et aux enjeux attachés à l'ouvrage ?

- Les scénarios de brèche peuvent comprendre des enchainements de mécanismes difficiles à imaginer ; quelle est la complétude de ces processus complexes ?
- La compréhension scientifique des mécanismes d'érosion et les moyens disponibles pour les caractériser ont progressé ; mais quand sera-t-elle définitivement établie ?

Pour toutes ces raisons, les Recommandations proposent trois catégories de qualification des méthodes:

Recommandations méthodologiques [RM]

Les « recommandations » sont des approches méthodologiques assises sur l'état de l'art et la production scientifique validée. Elles se présentent sous la forme de démarches méthodologiques, mais aussi de formules et approches quantitatives validées, en notant bien que les formules peuvent évoluer avec les progrès de la science.

Bonnes pratiques [BP]

Les « bonnes pratiques » sont des approches qui font l'unanimité du groupe de travail, bien qu'elles ne soient pas encore validées par une longue pratique de la communauté internationale ou par un consensus scientifique. Elles sont jugées suffisamment robustes pour être employées dans l'objectif d'approfondir, compléter ou moduler les « RM ».

Approches nouvelles [AN]

Les « approches nouvelles » sont des approches jugées pertinentes par ceux qui les ont pratiquées, mais qui sont trop récentes pour recueillir le consensus du groupe de travail. Elles peuvent faire progresser la précision de l'analyse et traiter les cas non couverts par les « RM » et « BP ».

3.5. UNE DEMARCHE D'ANALYSE PAR ETAPES

Pour toutes les justifications relatives à l'érosion, les Recommandations prévoient une approche en 7 étapes. Ces 7 Etapes ne sont pas conduites de manière linéaire : il y a nécessairement des aller-retours entre les étapes dans la démarche d'ingénierie. Cependant, il est recommandé que le rapport de justification utilise l'ordre ci-dessous, pour faciliter la lecture ou l'examen par des tiers.

- Étape 1 – Appropriation des données à l'aide d'une enquête documentaire préalable et d'un examen visuel détaillé de l'ouvrage.

- Étape 2 – Identification des chemins potentiels d'érosion :
 - Inventaire des chemins potentiels d'érosion à partir de l'inventaire des défauts (connus, suspectés ou pouvant se développer), puis, par un exercice d'analyse, justification de l'élimination de la plupart d'entre eux pour ne conserver qu'un nombre limité de chemins significatifs qui seront étudiés,
 - Identification des scénarios de brèche les plus probables le long des chemins significatifs.
- Étape 3 – Élaboration des modèles de terrain :
 - Modèle géologique : la nature des terrains, les hétérogénéités,
 - Modèle géométrique : les dimensions des ouvrages, les dimensions des défauts,
 - Modèle géomécanique : la caractérisation de la résistance des terrains et de leurs hétérogénéités,
 - Modèle(s) hydraulique(s) : écoulements hydrauliques interne préférentiels (vitesses, pressions, gradients, charges) ou écoulements hydrauliques provoquant l'érosion externe,
 - Modèle morphodynamique pour les digues de protection,
 - Modèle environnemental : notamment inventaire et caractérisation des agresseurs : climat, fousseurs, végétation, navigation ...
- Étape 4 – Définition des situations de projet :
 - Situations d'exploitation normale (pour les barrages) et Situations de crues caractéristiques,
 - Situations particulières : situation post-sismique, situations de sollicitations accidentelles,
 - Sélection des combinaisons pertinentes de Situations et d'Etat du barrage (défauts potentiels) selon les probabilités respectives d'occurrence des situations et de développement des défauts.
 - Le choix des situations à considérer est proportionné à la gravité des conséquences, et donc enjeux associés à chaque ouvrage (cf. §3.6).
- Étape 5 – Justification des barrières de défense. Cette étape consiste à examiner chacun des mécanismes à l'intérieur des processus étudiés, et à évaluer la « probabilité » que le mécanisme d'érosion puisse être initié, se développer, être détecté et arrêté.
- Étape 6 – Evaluation globale de la sécurité le long de chaque chemin, intégrant la modulation des conclusions par l'analyse comportementale.
- Cette étape consiste à appliquer les résultats de l'Étape 5, pour en déduire une évaluation de la sécurité pour chaque scénario examiné.
- Étape 7 – Synthèse de l'évaluation de la tenue à l'érosion

3.6. PROPORTIONNALITE AUX ENJEUX

Il est légitime de proportionner la profondeur des justifications et les marges de justifications à la complexité des ouvrages et aux enjeux en cas de rupture.

Les Recommandations utilisent trois catégories d'enjeu, issues de la réglementation française (2^{ème} colonne du Tableau 2, la 3^{ème} colonne ne provient pas de la réglementation française, elle permet d'apprécier le niveau des enjeux).

Tableau 2
Les trois catégories d'enjeu

CLASSE D'ENJEU	SELON LA RÉGLEMENTATION FRANÇAISE	EN ORDRE DE GRANDEUR DE LA GRAVITÉ D'UNE RUPTURE POTENTIELLE
Enjeu très faible	Barrages et digues non classés	Probablement pas de victimes
Enjeu limité	Barrages et digues de classe C	Peut causer des victimes
Enjeu significatif	Barrages et digues de classe A ou B	Peut causer un nombre important de victimes

4. FOCUS SUR L'ÉROSION INTERNE POUR LES BARRAGES

4.1. LES TROIS NIVEAUX D'ANALYSE : NIVEAU 1, NIVEAU 2, NIVEAU 3

4.1.1. *Principes*

Pour la justification des barrages vis-à-vis de l'érosion interne, trois niveaux sont présentés dans les Recommandations (Tableau 3).

Tableau 3
Les trois niveaux de l'analyse de l'érosion interne

NIVEAU	APPROCHE	CHAMPS D'APPLICATION
Niveau 1	Approche synthétique globale à l'échelle de l'ouvrage complet (à ce niveau d'analyse les différents chemins ou mécanismes d'érosion sont globalisés).	<i>Ouvrages existants uniquement</i> Expertise simplifiée, lorsque les enjeux sont très faibles ou limités Etude préliminaire d'un ouvrage, avant que le Niveau 2 soit engagé
Niveau 2	Evaluation (quantitative ou experte) de tous les chemins d'érosion significatifs.	<i>Ouvrages neufs et existants</i> Approche complète conforme aux standards actuels par chemin. Peut parfois ne pas suffire
Niveau 3	Evaluation détaillée (quantitative ou experte) des chemins d'érosion sensibles. Mise en œuvre de moyens plus lourds qu'en niveau 2 : détection in situ des chemins d'érosion et mesure des vitesses, simulation numérique détaillée, essais en vraie grandeur.	<i>Ouvrages existants principalement</i> Etude approfondie des chemins d'érosion, par exemple en cas de pathologie ou d'incident ; ou lorsque l'approche de Niveau 2 ne permet pas de conclure positivement.

4.1.2. Description de l'approche de Niveau 1

L'analyse de Niveau 1 est principalement basée sur le jugement d'expert, appuyée autant que possible sur des évaluations quantifiées. Elle consiste à analyser la fiabilité (Fig.7) :

- des 3 barrières de défense principales passives (étanchéité, résistance des sols à l'érosion, filtration) et de la barrière de défense active (détection + intervention)
- le long des trois chemins d'érosion principaux : le remblai, la fondation et les ouvrages traversants.

En complément de l'analyse de la fiabilité des barrières de défense de l'ouvrage, l'analyse de l'historique de l'ouvrage permet de déterminer une Note Comportementale (cf. §4.3).

Une note globale est obtenue. La calibration sur une série de cas significatifs permet de relier la note globale à une classe de probabilité d'accident grave d'érosion interne. Cette note, complétée par un avis sur la robustesse des hypothèses faites, permet à l'utilisateur de décider si le Niveau 1 suffit, ou s'il faut passer à une analyse de Niveau 2.

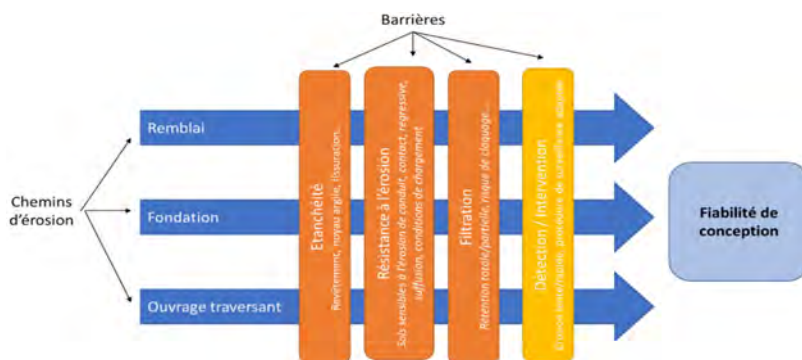


Fig. 7

Diagramme de l'analyse d'érosion interne de Niveau 1
Diagram of Level 1 Internal erosion risk assessment

Un outil spécifique permet d'améliorer la fiabilité de l'analyse de niveau 1, en limitant l'impact des biais de jugement, et en facilitant l'examen de l'analyse par un tiers. Il passe en revue chaque barrière, et aide à leur attribuer une note de fiabilité. La Fig. 8 présente une des 12 pages à renseigner.

Tableau 4
Exemple d'une feuille de l'outil spécifique à l'analyse de niveau 1

ER	TYPE	FIABILITE ELEVEE		FIABILITE MOYENNE		FIABILITE FAIBLE		FIABILITE NULLE	
	Classe	3		2		1		0	
E _{R1}	Pour un barrage a etancheite mince (beton, membrane, palplanche,...) Fragilite etancheite pouvant menacer le remblai	<input type="checkbox"/>	Etancheite et drainage restent efficaces (meme en presence de defect important)	<input type="checkbox"/>	Etancheite sans fragilite (rare!) OU Une rupture partielle de l'etancheite resle efficace; le drainage est dimensionne en consequence.	<input type="checkbox"/>	Etancheite mince pouvant presenter des fragilites, mais les defauts restent de dimensions telles que l'etancheite, meme si elle est affectee, continue a rabattre les pressions.	<input type="checkbox"/>	Etancheite mince pouvant presenter des lacunes importantes. V compris cas particulier: conduite traversant le remblai avec ecoulement en charge.
E _{R2}	Mur longitudinal (parallele a la crete)	<input type="checkbox"/>	Pas de mur OU mur de dimensions tellement modesles que le decollement est sans consequence.	<input type="checkbox"/>	Mur longitudinal. Risque modeste de decollement OU Le decollement est sans grande consequence. (Apprecie selon §5.8.)			<input type="checkbox"/>	Mur longitudinal. Risque important de decollement ET le decollement genere un mecanisme d'instabilite. Apprecie selon §5.8.
E _{R3}	Fouisseurs			<input type="checkbox"/>	Pas d'agresseurs (fouisseurs) OU Protections empechant le developpement OU Ouvrage peu sensible, car de grande largeur en crete (> 10 m), ou car les dimensions des terriers sont trop petites pour poser probleme	<input type="checkbox"/>	Presence d'agresseurs. Les dimensions suspectees des defauts (terriers) laissent penser qu'un comportement hydraulique non desire est possible en cas de montee de la cote du plan d'eau amont.	<input type="checkbox"/>	Presence d'agresseurs. L'etat de l'ouvrage laisse suspecter l'apparition de conduit d'ecoulement concentre traversant directement la digue, en cas de montee de la cote du plan d'eau amont.
E _{R4}	Vegetation			<input type="checkbox"/>	Pas d'agresseurs (arbres) OU Ouvrage peu sensible, car de	<input type="checkbox"/>	Presence d'agresseurs Les dimensions suspectees des defauts (racines)	<input type="checkbox"/>	Presence d'agresseurs L'etat de l'ouvrage laisse suspecter

(Continued)

Tableau 4
Continued

ER	TYPE	FIABILITE ELEVEE		FIABILITE MOYENNE		FIABILITE FAIBLE		FIABILITE NULLE	
	Classe	3		2		1		0	
					grande largeur en crete (> 10 m), ou car les dimensions des racines sont trop petites pour poser probleme.		laissent penser qu'un comportement hydraulique non desire est possible en cas de montee de la cote du plan d'eau amont.		l'apparition de conduit d'ecoulement concentre traversant directement la digue, en cas de montee de la cote du plan d'eau amont.

4.2. ANALYSE DE NIVEAU 2 : PRISE EN COMPTE DES DÉFAUTS

Un point central dans l'analyse est la prise en compte des défauts. Les Recommandations proposent un inventaire des défauts qui peuvent être à l'origine d'un processus d'érosion. Dans la démarche de justification, il s'agit de prendre en compte les défauts *actuels* (constatés sur l'ouvrage, et qui peuvent être stables ou évolutifs), les défauts *cachés* (qu'on ne peut exclure du fait d'incertitudes sur l'état de l'ouvrage), et les défauts *futurs* (qui pourraient apparaître par suite d'agressions extérieures ou résulter du vieillissement). Les défauts cachés et futurs sont classés selon leur probabilité d'occurrence : défaut « fréquent » (exemple : probabilité annuelle $> 10^{-2}$), dont l'occurrence est pratiquement certaine (probabilité $> 0,5$) durant la vie de l'ouvrage, défaut « rare » (exemple : probabilité annuelle $> 10^{-4}$), défaut « extrêmement rare » (exemple : probabilité annuelle $> 10^{-5}$).

4.3. ANALYSE FONCTIONNELLE ET ANALYSE COMPORTEMENTALE

L'évaluation de la sécurité d'un barrage s'appuie d'une part sur l'analyse de la nature et de l'état de ses barrières de défense, appelée analyse fonctionnelle, et d'autre part sur la prise en compte du comportement passé, l'analyse comportementale sur la base des deux grands principes suivants :

1. La première mise en eau est un très bon indicateur de la capacité de résistance à l'érosion interne. Les crues atteignant des cotes supérieures fournissent de nouveaux signes de résistance à l'érosion, en l'absence (1) de symptômes d'érosion à la cote atteinte et (2) de phénomènes de vieillissement.

2. A l'inverse, toute observation d'un symptôme d'érosion interne non stabilisée est un indicateur sérieux de risque d'accident pour la cote de retenue atteinte et encore davantage pour les cotes supérieures.

Une approche nouvelle [AN] intègre l'approche expérimentale dans l'analyse de Niveau 1 (pour les barrages). Elle consiste à noter le comportement du barrage (de Fc : aucun symptôme, à Ac : incident d'érosion qui aurait conduit à la rupture sans intervention volontaire), lors des remplissages passés, en fonction du caractère plus ou moins significatif de l'épreuve de mise en eau : mise en eau complète (épreuve A), mise en eau de durée courte (épreuve B), mise en eau à une cote inférieure (épreuve C). La combinaison de ces deux informations conduit à moduler la note de l'analyse fonctionnelle, en introduisant une modulation α : qui dépend de la nature de l'épreuve et du plus fort symptôme constaté. En ordre de grandeur, une modulation α signifie la multiplication de la probabilité de défaillance par $10^{-\alpha}$.

Tableau 5
Note de modulation de la note de fiabilité de l'analyse de niveau 1

Classe dérosion	Fc	Ec	Dc	Cc	Be	Ac
Information provenant de l'épreuve A	+2.5	+2.5	+1.5	+1	-1	-3
Information provenant de l'épreuve B	+1.5	+1.5	+0.5	-1	-2	-3
Information provenant de l'épreuve C (pour l'érosion de conduit)	+0	+0	+0	-1	-2	-3
Information provenant de l'épreuve C (pour les autres formes d'érosion)	+0.5	+0.5	+0	-1	-1.5	-3

L'analyse comportementale doit prendre en compte deux limitations, qui peuvent en limiter la portée :

1/ La durée de la sollicitation hydraulique est un facteur clé : une sollicitation de courte durée n'a pas nécessairement le temps de développer complètement un mécanisme d'érosion interne.

2/ Le vieillissement change les résistances ou perméabilités des matériaux voire crée de nouveaux défauts. Quatre types d'évolutions contribuent au vieillissement de l'ouvrage : vieillissement des structures (acier, maçonneries, géomembranes ...), vieillissement des filtres et drains par colmatage, agressions de l'environnement : dessication et gel ; fousseurs ou végétation et l'impact des situations accidentelles (séismes, chocs de bateau, etc.).

4.4. FILTRES

En matière de justification des filtres, les Recommandations apportent des compléments à la pratique antérieure.

4.4.1. Justification des filtres

Le focus ne doit pas être sur le seul fuseau granulométrique

La fiabilité, l'intégrité et la durabilité de la filtration sont assurées si toutes les spécifications fonctionnelles sont satisfaites : interception des chemins d'érosion, rétention des particules, drainage, non-fissuration, autofiltration, épaisseur, confinement, non-ségrégation, non-pollution, non-écrasement des grains au compactage, rétention par les matériaux aval, résistance des grains, non-altération chimique, insensibilité au colmatage. Cela fait 14 spécifications, qui ne sont pas toutes d'importance égale.

Le tableau ci-dessous identifie les spécifications qui, lorsqu'elles n'ont pas été remplies, ont conduit à des accidents (!) ou des désordres graves (+), parfois seulement dans une configuration défavorable (>). Ce sont donc également les spécifications qu'il faut, en première approximation, être en mesure d'apprécier systématiquement pour juger de la fiabilité d'un filtre.

Tableau 6
Spécifications dont le non-respect a de graves conséquences

SPÉCIFICATION		COMMENTAIRES
Interception	!	Spécification majeure. On note que les défauts de continuité du filtre se développent parfois nécessairement dans le prolongement des défauts initiant l'érosion interne (raccordement aux ouvrages, tassements importants, ...), par un effet de « mode commun » de défaillance.
Confinement du filtre	!	Spécification majeure. Le filtre doit être placé sous une recharge apportant un poids (une contrainte de confinement) suffisant pour empêcher le claquage hydraulique du filtre, y compris après colmatage éventuel du filtre.
Non fissuration	+	Un filtre non fissurable permet de garantir contre le développement de défauts d'interception tels que ceux mentionnés ci-dessus, dans la ligne « interception ».
Rétention	+	La rétention est la capacité du filtre, par sa granulométrie, à retenir les particules du sol à protéger. Une rétention imparfaite peut limiter l'érosion. Cependant, une rétention imparfaite peut conduire au colmatage.
Drainage & Colmatage	>	Selon les cas, l'insuffisance de capacité de drainage (ou le colmatage) d'un filtre peut être sans conséquence ou conduire à des modifications du réseau d'écoulement, plus ou moins dangereuses.
Épaisseur	>	L'épaisseur permet de garantir la continuité du filtre dans les situations de tassements, tassements différentiels, séismes. Elle limite également les possibilités de colmatage.

4.4.2. Filtres géotextiles

Il est utile de distinguer les filtres critiques et non-critiques. Les filtres « critiques » : leur *perte ou leur absence risquerait de causer la rupture*. Les filtres « non critiques », dont le dysfonctionnement ou la perte ne mène pas directement à la rupture du barrage (il y a le temps de procéder aux réparations qui procèderaient de la perte de la filtration) ; l'enjeu est alors la durabilité ou la disponibilité de l'ouvrage, et pas sa sécurité.

L'accessibilité joue un rôle important dans le choix du filtre : les *filtres non-réparables* sont au cœur du remblai, inaccessibles sans déconstruire l'ensemble du remblai, ou sans mettre durablement hors service l'ouvrage. Les *filtres réparables* sont accessibles après déblaiement de quelques mètres d'épaisseur, et sans affecter trop gravement l'exploitation de l'ouvrage.

Le tableau 7 précise le domaine d'emploi des filtres géotextiles dans les barrages neufs.

Tableau 7
Domaine d'emploi des filtres géotextiles dans les barrages neufs

FILTRES EN GÉOTEXTILE	ENJEUX		
	SIGNIFICATIF	LIMITÉ	TRÈS FAIBLE
Filtre critique non-réparable	Non	Non	Oui
Filtre critique réparable	Oui(*)	Oui	Oui
Filtre non critique	Oui	Oui	Oui

(*) : sous réserve que l'étude de dangers démontre que tout dysfonctionnement est maîtrisé en examinant en particulier : (1) les conséquences du colmatage intégral ; et (2) : les risques de déchirure par tassement ou cisaillement.

Dans tous les cas où l'utilisation d'un filtre géotextile n'apporte pas d'économie ou d'autre avantage substantiel, il est préférable de recourir au filtre granulaire, plus sûr et plus durable.

Les digues de protection, avec une plus petite hauteur (moins de risques de déchirure par tassement, à condition que les sols de fondation ne soient pas trop compressibles), une plus grande accessibilité (quelques mètres de couverture) et des sollicitations plus courtes (moindre propension au colmatage) permettent plus facilement d'envisager l'emploi de géotextiles.

5. FOCUS : EROSION EXTERNE POUR LES BARRAGES LATÉRAUX

Quelques modulations pour les barrages latéraux méritent attention, en particulier vis-à-vis de la justification à l'érosion externe.



Fig. 8

Exemples de barrages latéraux : aménagement type du Rhône (remblais latéraux en rouge) et barrage du projet Canal Seine-Nord Europe (remblais, pont-canal et ouvrage de rétablissement hydraulique sous remblai)

Examples of lateral dams: the Rhone scheme (lateral embankments in red) and the Canal Seine-Nord Europe project (lateral embankments, canal bridge and hydraulic culvert)

5.1. SITUATIONS PARTICULIERES A CONSIDERER

Les situations de justification des barrages latéraux sont similaires à celles des autres barrages. Néanmoins, il apparaît nécessaire de traiter des situations spécifiques supplémentaires. Un inventaire des situations supplémentaires pouvant être pertinentes est donné ci-dessous :

Situations normales d'exploitation : débit dans le canal, sollicitations normales de navigation (batillage, jet d'hélice dans les zones de manœuvre), ondes d'intumescence lors des opérations normales d'exploitation : éclusages, ondes de disjonction.

Situations rares : crue exceptionnelle des rivières longeant ou traversant l'ouvrage : sollicitations par la vitesse de l'eau le long de l'extérieur des remblais, par l'élévation du niveau d'eau à l'extérieur des remblais, par la mise en charge des ouvrages de rétablissement hydraulique ; remontée de nappe exceptionnelle (pouvant menacer la stabilité de l'étanchéité).

Situations accidentelles : selon les résultats des analyses de risques, il peut dans certains cas être nécessaire de tenir compte de situations particulières, telles

que : ouverture ou rupture de vannes / portes vis-à-vis du bief aval ; non ouverture des vannes ; pompage d'alimentation non interrompu ; accidents de navigation ou accidents routiers (incendie dans les passages inférieurs) ; ruptures de conduites traversant l'ouvrage ou passant sous l'ouvrage.

5.2. FRANCHISSEMENT : MODULATIONS AUX RECOMMANDATIONS POUR LES BARRAGES

Des Recommandations spécifiques sont prises en compte pour les barrages latéraux, pour raisons exposées en 3.3.

Vagues dues au vent. La formation, la propagation et le déferlement des vagues dues au vent le long des canaux de navigation sont modifiées par la géométrie particulière de ces ouvrages. Ces canaux ont de longues sections droites, suivies de courbes à grand rayon de courbure. Le « fetch effectif » des formules habituelles est plus petit que la plus grande longueur de la section droite, y compris dans le cas d'un vent dominant soufflant dans cette direction. Un abattement de la longueur de fetch est pris en compte. Dans l'extrados de la courbe qui reçoit la houle, il y a un effet de surélévation du plan d'eau. Il ne s'agit pas d'un simple phénomène de run-up, mais plutôt d'une surélévation due au changement de direction de la houle imposé par la courbe. Des approches par simulations numériques mettent en évidence des sur hauteurs plus faibles que celles calculées par les abaques de run-up.

Intumescences. Dans le cas des vagues dues au vent, la littérature relative aux barrages fournit des indications quant au déferlement tolérable ; il est caractérisé par un certain pourcentage de vagues pour lesquelles on accepte que le run-up franchit la cote de crête. Cette approche ne permet pas de fournir un critère pour les ondes d'intumescences. Pour les barrages latéraux à enjeux significatifs, il est recommandé que les ondes d'intumescence d'exploitation courante ou provoquées par un incident d'exploitation exceptionnel ne puissent pas provoquer de franchissement. Pour les barrages à enjeux limités, un franchissement est toléré dans le cas des incidents d'exploitation, à condition de montrer que cela ne doit pas générer d'érosion dangereuse. Les acquis de l'ingénierie maritime (notamment Eurotop 2018) fournissent des indications de débits et volumes limites, qui fournissent une base de réflexion jugée pertinente.

6. FOCUS : DIAGNOSTIC DES DIGUES DE PROTECTION

Dans le cas des digues de protection, la démarche de justification doit tenir compte : de la variabilité de la constitution de la digue (et de sa fondation) le long de

son tracé ; de l'exigence réglementaire qui oblige à combiner l'ensemble des scénarios de brèche pour aboutir à une probabilité globale de défaillance ; de la nécessité de procéder à cet examen pour un certain nombre de scénarios de crue.

Il s'agit ici de résoudre la difficulté liée au grand nombre de combinaisons : x scénarios de crues (pour couvrir une gamme raisonnable), y profils-type du tronçon, z scénarios de brèche. Il convient de procéder de manière ordonnée, pour éviter les erreurs liées à une mauvaise combinaison des probabilités.

Première étape : découpage en tronçons suffisamment homogènes

Dans les deux cas, le système d'endiguement doit au préalable être découpé en une série de tronçons. Un tronçon doit être suffisamment homogène pour que l'hypothèse de corrélation parfaite entre profils-type du tronçon soit réaliste. Cette hypothèse s'écrit de la manière suivante :

$$\forall S, \quad \forall i, j \quad P(X_i \text{ OU } X_j) = \max(P(X_i); P(X_j)), \text{ c'est-à-dire :}$$

Pour tout scénario de brèche S , et pour deux profils-types X_i et X_j quelconques du tronçon, la probabilité d'une brèche de l'un des deux profils-type est la probabilité de brèche du plus fragile des deux au regard de ce scénario.

Dans la pratique, même si on ne peut pas espérer atteindre l'homogénéité parfaite, l'hypothèse d'homogénéité peut être retenue tant que chacun des scénarios S se développe dans chacun des profils à travers des matériaux de même nature et selon un processus analogue. On peut dédoubler les scénarios pour couvrir par exemple des conditions de fondation différentes sans mettre en péril l'hypothèse d'homogénéité (un scénario $S1$ pour la fondation sur les profils-type courant, un scénario $S2$ pour un profil-type particulier sur un sol différent).

Deuxième étape : définition des profils-type

Le tronçon est représenté par ses différents profils ; les profils-types sont choisis de sorte à représenter l'ensemble des configurations possibles. Ainsi : un tronçon = y profils ; chacun caractérisé par ses particularités (géométrique, géomécanique, ...). Il est possible de simplifier cette étape lorsque le « maillon faible », profil-type de moindre résistance pour un scénario donné, peut-être défini a priori. Alors le tronçon peut-être valablement représenté par ce seul profil « maillon faible ».

Troisième étape : courbes de fragilité par profil et par scénario

Cette étape se fait pour un scénario de brèche donné.

Il s'agit de calculer la probabilité de brèche de chaque profil, pour ce scénario et pour différents niveaux de crue. On construit ainsi la courbe de fragilité de chaque

profil, pour le scénario considéré. Un exemple typique est donné Fig. 9, dans lequel un scénario de brèche par érosion de conduit le long d'un terrier de fousseur est envisagé. Ce scénario comporte plusieurs étapes, chacune faisant l'objet d'une évaluation de probabilité pour différents scénarios de crue.

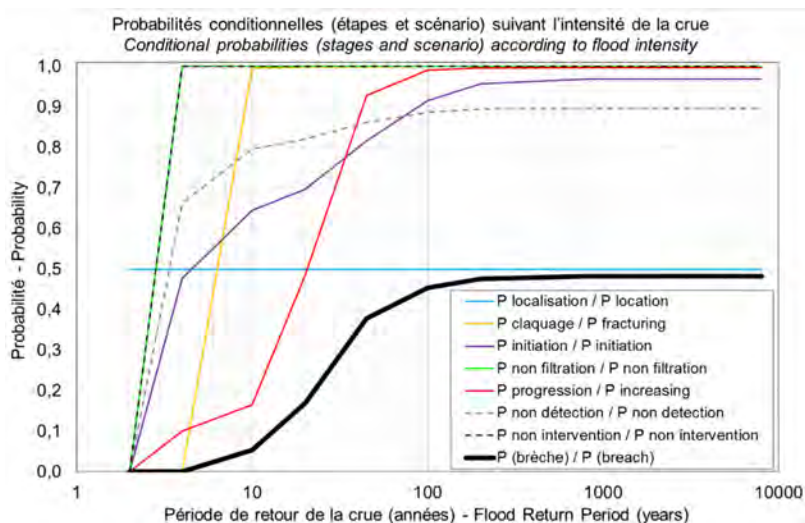


Fig. 9

Exemple de probabilités conditionnelles d'étapes d'un scénario de brèche en fonction de la période de retour de la crue
Example of conditional probabilities of successive steps of a breach scenario with respect to the return period of the flood

Quatrième étape : courbes de fragilité du tronçon, par scénario

L'hypothèse d'homogénéité permet de calculer la courbe de fragilité pour le tronçon : il s'agit simplement du MAX des courbes de fragilité de chacun des profils-type.

Cinquième étape : courbe de fragilité du tronçon

Enfin, pour obtenir la courbe de fragilité du tronçon, tous scénarios confondus, il faut combiner les courbes de fragilité par scénario. Dans les cas usuels, on fait l'hypothèse que les différents scénarios sont indépendants les uns des autres. C'est alors la règle de combinaison de Morgan qui s'applique.

REMERCIEMENTS

Le projet de Recommandations a été réalisé sous l'impulsion de Luc Deroo (Président), Stéphane Bonelli (Vice-Président) et Jean-Jacques Fry (secrétaire), avec les contributions suivantes :

Organismes: Ponsoh, Artelia, Tractebel Engineering, Cerema, Géophyconsult, Inrae, EDF-CIH, ISL, Safege, CNR, CACG, Egis, Symadrem, Dreal Centre - Val de Loire, BRLi, SCSNE, Voies Navigables de France.

Contributeurs : Stéphan Aigouy, Lucie Alazard, Patrice Anthiniac, Dominique Batista, Véronique Berche, Rémi Béguin, Stéphane Bonelli, Olivier Bory, Chloé Chancel, Jean-Robert Courivaud, Luc Deroo, Eric Fouliard, Jean-Jacques Fry, Vincent Jouve, Jean Launay, Zoé Laurent, François Lauvergnier, Benjamin Maclet, Thibaut Mallet, Tarik Oussalah, Sébastien Patouillard, Christophe Picault, Pierre-Louis Regazzoni, Laurent Smadi, Patrick Soulat, Bachir Touileb, Eric Vuillemeret.

RÉFÉRENCES

- [1] CFBR (2023) Recommandations pour la justification de la tenue à l'érosion des barrages et des digues en remblai (publication à venir).
- [2] CIGB (2017, 2023) Bulletin 164, volume 1 et volume 2

COMMISSION INTERNATIONALE DES
GRANDS BARRAGES

VINGT-HUITIEME CONGRES DES
GRANDS BARRAGES
CHENGDU, MAI 2025

THE LEGACY OF PUDDLE CLAY DAMS (*)

Alan BROWN

Global Technology Lead for dams, Jacobs

UNITED KINGDOM

SUMMARY

Prior to the introduction of mechanised plant in the 1960s, the watertight element in UK dams was provided by a puddle clay core, whereby water was added to a clay by "puddling" to produce a clay with an undrained shear strength of around 10kPa.

The paper describes the common features and design development of puddle clay dams, with four phases of design being identified.

As part of periodic dam safety review we need to understand the characteristics and design features of these dams, to allow risk-informed assessment of their safety and any need for improvements. The paper includes a brief description of findings from recent upgrade works.

RÉSUMÉ

Avant l'introduction des installations mécanisées dans les années 1960, l'élément d'étanchéité des barrages britanniques était assuré par un noyau d'argile

*L'héritage des barrages en argile corroyée

corroyée dans lequel de l'eau était ajoutée à une argile pour produire une argile avec une résistance au cisaillement non drainée d'environ 10 kPa.

Le document décrit les caractéristiques communes et le développement de la conception de ces barrages en argile, avec quatre phases de conception identifiées.

Dans le cadre de l'examen périodique de la sécurité des barrages, nous devons comprendre les caractéristiques physiques et les caractéristiques de conception de ces barrages, afin de permettre une évaluation fondée sur les risques de leur sécurité et de tout besoin d'amélioration. Le rapport comprend une brève description des résultats des récents travaux de mise à niveau.

1. INTRODUCTION

Prior to the introduction of mechanized plant in the 1960s, the watertight element in UK dams was provided by a puddle clay core, whereby water was added to a clay by "puddling" to produce a clay with an undrained shear strength of around 10kPa. Approximately 80% of UK dams were constructed prior to 1960, with a large proportion being puddle clay dams, the subject of this paper.

This type of watertight element has generally performed well, although some important improvements in practice were introduced in the period of use from around 1860 to 1960.

Increasing attention is being paid to the characteristics of puddle clay dams to both ensure their continuing safety as they age, and to allow improved assessment of the risk of failure of this dam type.

This paper summarises the key aspects of puddle clay dams, and insights from recent projects to improve dam safety management.

2. DEFINITION OF "PUDDLE CLAY"

Puddle clay is not a description of a particular type of clay but refers to the way that the clay was placed at a high moisture content by puddling. Initially this was done manually; then when steam engines were developed by mechanical methods. The clay that was used depended on the material available in the vicinity of the dam. In some cases, as-dug material was used and in other cases materials were mixed. Puddling is a process which destroys the as-dug structure of the clay by remoulding

and working in extra water to form a very wet clay with an undrained shear strength as low as about 10kPa on placement.

Some examples of specification for puddle clay are given in appendix to the UK Guide to embankment dams [1], with typical requirements in 1940-1950 being:

- Clay ex borrow area to be left exposed in layers of less than 300mm for at least 24 hours, watered as necessary. Then put through a pugmill to produce consistent homogenous mass
- Broken up, spread in layers, watered as directed, allowed to weather (sour, or mellow) for at least a week. Souring governed by natural water content of clay in borrow area. Tsted by forming 25-38mm diameter by 300mm long samples, which should not break when held by one end (tenacity test)
- Place in layes not less than 75mm thick, and not more than 150mm thick
- "Bond" with previous layers by cutting with a suitable blade and thoroughly trodden
- Daywork protection by watering the surface and covering to prevent shrinkage cracking

3. HISTORICAL DEVELEOPMNT OF PUDDLE CLAY

3.1 GENERAL

Early puddle clay was used in canal dams, built from 1770 onwards [2]. By the middle of the 19th century a fairly standard embankment design had been adopted with typical upstream slope of 1 vertical in 3.0 horizontal, a downstream slope of 1 vertical in 2.0 or 2.5 horizontal, as shown in Figure 1. Although most of embankments of this type were less than 15m high, some were built as high as 30m.

As a result of the failures of Bilberry in 1852 and Dale Dyke in 1864 and some serious problems encountered with other embankment dams, important developments in design occurred during the latter half of the 19th century. These developments are considered under the headings below, with changes summarised in Table 1 [3].

Table 1
Phases of puddle clay construction in United Kingdom

PHASE	FROM	TO	CORE	CUT-OFF	SHOULDERS	
					TYPE	COMPACTION
1	1840	1865	Puddled insitu	Puddle in trench	Random fill	None
2	1865	1880			Select fill (Capt. Moody zoning, post Bilberry)	Incidental
3	1880	1945	"Pugged" at steam pugmill			Limited
4	1945	1960		Concrete in trench	Add internal drainage	Controlled

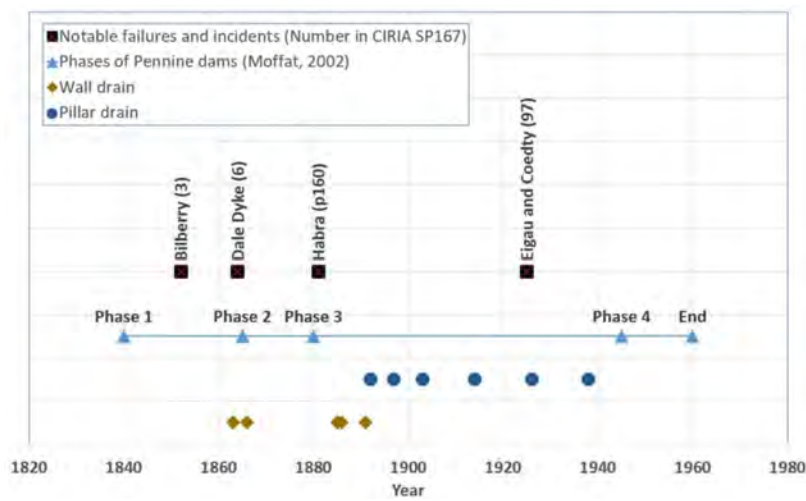


Fig. 1
Timeline of puddle clay dams

3.2 WATERTIGHT ELEMENT WITHIN EMBANKMENT

At some dams the core was excessively narrow, for example on the 29.0m high Dale Dyke dam the top width of the core was a mere 1.2m and with batters of 1:16 (H:V) the maximum width at ground level; was only 4.9m. Following the failure of the original dam the reconstructed dam had a much wider puddle clay core.

The core height to width ratio was around 4:6 for phase 1 of Pennine dam construction, but then reduced to commonly 3:4 for the later phases.

3.3 WATERTIGHT ELEMENT IN FOUNDATION

In the early puddle clay cores, it was usual to extend the puddle clay into a cutoff trench below ground level, this connecting the core to a stratum of low permeability. This trench often continued into the valley sides. Sometimes a very deep trench was dug but it was usually narrow with vertical sides. Later there was a general trend to change from puddle clay to concrete filled cut-off trenches. Grouting of the rock foundation came into place in the late 19th century.

3.4 EMBANKMENT SHOULDERS

The earliest concept of puddle clay dams was that the shoulders merely served to support the core and only needed to be stable and reasonably solid. However, it was realised that it was not prudent to place poorly compacted highly permeable fill next to the puddle core. Selected fill which was generally more cohesive and better compacted than the general fill came to be used either side of the core.

3.5 OUTLET WORKS

Initially the practice was to lay the outlet pipe through the embankment and puddle core. It came to be recognised that it was not good practice to bury such material as cast iron under an embankment which could have a 500 ft (150m) wide base, so that nothing but the destruction of the bank could ever render it accessible for repair (Rawlinson, 1879). Sometimes the pipe was placed in a culvert passing through the embankment, and this was then further improved by locating the outlet works in a tunnel in an abutment on the side of the valley.

Similarly the early practice of controlling the flow of water by a single valve at the downstream toe was superseded to controls upstream, either just upstream of the core in a shaft, or at the upstream toe.

3.6 DEVELOPMENT OF CONSTRUCTION PRACTICE

Available information on how fill was placed and some of the key dates, largely as given in Binnie [4] are summarised in Table 2. This shows both differences in practices between different engineers, and how practice evolved with time.

Wiltshire [5] gives a description of the development of design and construction in the USA from 1902 to 2002, including use of steam rollers to compact fill at Belle Fourche dam built 1905 to 1911, and that "Although vibratory rollers had been developed for compacting cohesionless soils for roads in Europe in the 1930s, they were first used to compact rockfill dam materials at Quoich Dam in Scotland around 1958. In the United States, the use of vibratory rollers for compaction of rockfill materials was first attempted by the Corps at the 445-foot-high Cougar Dam in Oregon, built between 1959 and 1964."

Table 2
Some examples of development of placing and consolidating fills in
puddle clay dams

DATE	DEVELOPMENT	SOURCE [4]
1797	<i>The bank must be laid on solid ground and raised in regular strata throughout its whole length, none of which should exceed 2 feet thick, these strata must be laid . . . so the whole may lean towards the puddle. The puddle must be set on solid ground both in the bottom and sides of the vale that will hold water and must be made of good clay, or clay and gravel mixed in about 2 of the former to 1 of the latter. These materials must be laid in their strata about 8 inches (20cm) thick and covered with water until they are dissolved, after which they must be well chopped and mixed gradually rising with the bank</i>	page 115, quoting specification written by Rennie for Rudyard dam
1847	Specification for two puddle clay embankments required <i>"the clay puddle to be worked in regular and level courses not exceeding 6 inches each course in thickness. Level courses with a limit of 6 inches is also specified for the earthwork in the embankment and "the whole to be rammed solid as the work proceeds"</i>	page 87 quoting specification written by James Simpson
1859	<i>"the railways had introduced a loose way of making embankments which were thrown up with great rapidity but without sufficient attention being placed to their consolidation throughout. Hence failures had arisen from the dams not being watertight. At Leslie's Edinburgh waterworks all waggons were excluded, carts only being allowed and the banks were formed in 6 inch layers, each layer being thoroughly indurated and punned by the constant passage of carts used in spreading the successive layer"</i>	page 101 quoting discussion on Yan Yeian scheme.
1864	Specification for Barrow No 2 reservoir required Contractor to provide <i>"clay mill with rollers and pug mill capable of producing 7.5 tons per hour of clay</i>	page 88 quoting specification written by James Simpson
1867	The company Aveling and Porter was the first to successfully sell steam roller commercially and subsequently became the largest manufacturer in Britain. In 1866 they produced a prototype roller with 3 foot-wide rollers fitted to the rear of a standard 12 nominal horsepower traction engine. In 1867, the steam road roller was patented and the company began production of the first practical steam roller – the new machine's rollers were mounted at the front instead of the back and it weighed in excess of 30 tons. It was tested on the Military Road in Chatham, Star Hill in Rochester and in Hyde Park, London. A New York City chief engineer said of one of these, that "in one day's rolling at a cost of 10 dollars, as much work was accomplished as in two days' rolling with a 7 ton roller drawn by eight horses at a cost of 20 dollars a day." The heavier rollers were found to be hard to handle and the weight of the machines was reduced to around 10 tons. Aveling & Porter refined their product continuously over the following decades, introducing fully steerable front rollers and compound steam engines at the 1881 Royal Agricultural Show. Production ended around 1950	https://en.wikipedia.org/wiki/Steamroller

4. LESSONS FROM RECENT UPGRADE AND REHABILITATION PROJECTS

4.1 GENERAL

Ongoing periodic safety inspections and risk assessments, including intrusive investigations, have both improved our understanding of the construction features of puddle clay dams, and changes that can occur with ageing and this section provides some examples of this.

4.2 INTERNAL DRAINAGE

Recent safety works at Barrowford puddle clay dam built around 1885 involved lowering top water level and the dam crest, to stop leakage along the level of a historic raising of the dam. This identified coarse unfiltered cobble size wall drains running along the downstream shoulder, extending from just below the topsoil to the embankment foundation, and connecting into unfiltered collector drains at the base of the embankment shoulder as shown on Figures 2 to 3.

A desk study of drawings of dams across a variety of dam owners in the UK identified six known examples of dams with wall drains, and a further five dams with "pillar drains, typically being 4 or 5ft square columns of rubble stone at intervals of around 30m centres along the dam, as shown in Figure 4. In addition, some of the drawings included details of the drainage incorporated in the downstream shoulder, which being prior to the invention of plastic and other modern drainage materials, typically comprised stone drains as shown in Figure 5.

This was a surprise as published information [3] suggested that the first internal drainage was incorporated around 1945.

Their purpose is not fully understood, and probably varies between dams but appears to include draining the downstream shoulder and is separate from culverts installed to drain the foundation, typically where springs were encountered during construction [6].

These drains were built prior to a modern understanding of filter rules and seepage analysis, and hence are vulnerable to internal erosion (fines washing into the coarse materials). As long as the drains remain unblocked, they should reduce the phreatic surface in the downstream shoulder, thus improving its stability. However, there is a significant risk that seeing no evidence of leaks can give false confidence that there is nothing much wrong.



Fig. 2
Example of wall drain in downstream shoulder at Barrowford reservoir

4.3 LEAKAGE

Some puddle clay dams have experienced concentrated leakage, although this is often at contacts between the puddle clay and either outlet structures through the dam, or abutments.

Geophysical and temperature sensing methods are often used to identify the location of the leak, and guide selection of the preferred option to seal the leak.



Fig. 3
Close-up of drain on Figure 2

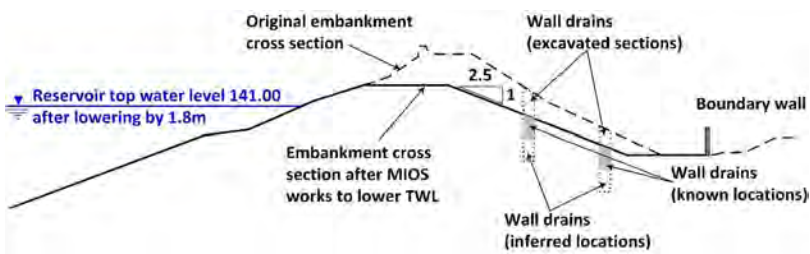


Fig. 4
Cross section on Barrowford reservoir

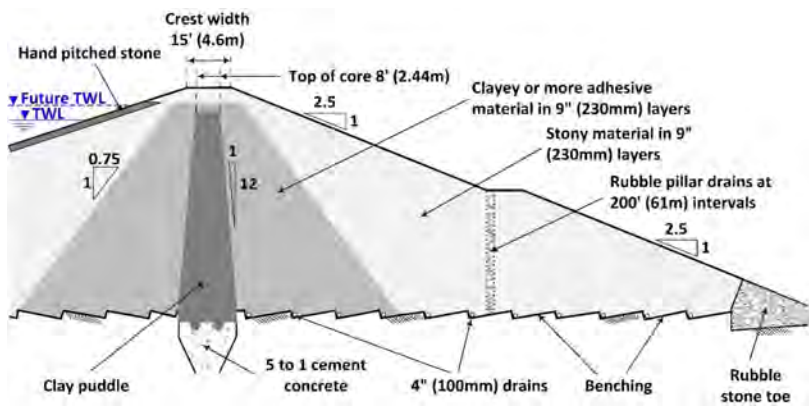


Fig. 5
Example of puddle clay dam with pillar drains in downstream shoulder

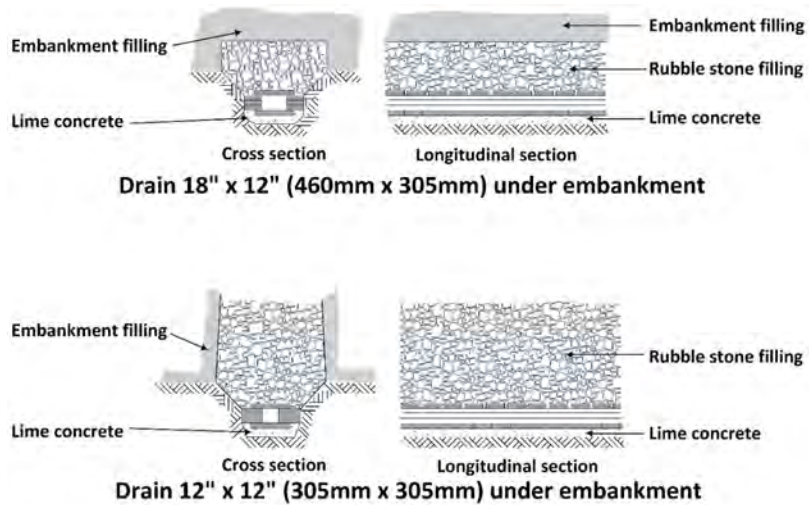


Fig. 6
Example of details of stone collector drains

Charles [7] gives a good overview of instances of hydraulic fracture in cores of UK puddle dams, and techniques used to remediate them, in the 1989 Clay barriers conference following the failure of Carsington dam. Other common problems include leakage

- a) between an original core, and a later raising.
- b) potential leakage between a crest wall and the core, where they were not connected.

5. DISCUSSION

5.1 DEVELOPMENT OF SCIENTIFIC METHODS FOR DAM DESIGN

Terzaghi first developed grain size criteria for granular soils in dam filters in 1922 [8]. These were extended by a test programme at the Soil Conservation Service (now National Resources Conservation Service) with the assistance of James Sherard between 1980 and 1985, published in various papers in ACE in the 1980s and now summarised in the FEMA document "Filters for embankment dams." [9].

Tools to analyse seepage and thus optimize the use of drainage to control internal erosion (piping) was only developed in the 1930s. [10,11] .

The Proctor compaction test to determine at what moisture content soil would achieve its maximum dry density was only developed in 1933 [12], although practical experience and observation had realised that soil needed to be placed in controlled layers and "well rammed" as early as 1797 (Table 2)

Michael Kennard in the Binnie lecture of 1994 summarised development of UK dam engineering in the 40 years from 1955 to 1995, noting that the first Professor of Geotechnical Engineering in UK was Professor Skempton at Imperial College in 1955 [13]. Skempton [14] notes several important advances that were made from 1950 onwards, including

- "In the form of improved testing procedures and stability analyses, systematic piezometer observations and more advanced application of the principle of effective stress" (Skempton, 1989, para 87)
- "Cracking of rolled clay fill due to differential settlement became recognised to an increasing extent in America during the 1950s, but hydraulic fracture was discovered (or more accurately re-discovered) only following failures at Hyttejuvet in Norway in August 1966 and Balderhead in April 1967 (Skempton, 1989, para 109)
- Experimental studies of filters for clay fills subject to possible cracking began around 1964 and received increased attention after the incident at Balderhead, where a filter of conventional design had not prevented

propagation of internal erosion in the rolled clay core dam ((Skempton, 1989, para 110)

It can be seen that puddle clay dams were built prior to development of scientific methods and modern soil mechanics, and so were effectively empirical, based on experience and judgment of the individual engineer.

5.2 RISK ASSESSMENT

Puddle clay dams present some challenges when carrying out risk assessments, including

- a) The age of the dams means that original drawings and records are often not available, or are limited in accuracy, such that surprises such as the presence of unfiltered wall drains described above still occur
- b) Some of the normal tools for assessing internal erosion, such as the seepage and piping toolbox [15] may not be well suited to puddle clay dams, and require adjustment.

UK dam engineers are aware of these challenges and are working to develop tools and standard approaches to risk assessments of this early form of embankment dam. The continuing need for experience-based judgement in engineering is emphasised in the review by Andrew Charles of the impact of soil mechanics on dam construction [16].

These include improving our understanding of typical details of contemporary dams to the dam under assessment, as individual engineers often designed multiple dams. For example, Figure 1.1 of Charles et al [17] suggests that around 25% of British dams were built in this period, or around 10 a year, so there would have been significant activity in design and construction at the time. This is best shown by Figure 9.13 in Binnie [4]) which showed that between 1860 and 1880 Bateman was overseeing between 10 and 15 dams under construction in each year over this period.

6. CONCLUSIONS

Puddle clay dams comprise over 60% of the stock of British reservoirs, where the water retaining element is provided by clay which has had water added to form a puddle with undrained shear strength of around 10kPa.

Although these have generally performed well, they do have some vulnerabilities, and their design has had significant improvements with time as shown in Figure 1 and Table 1. This paper has described both some of the improvements made over time and more recent developments in our understanding of their construction and purpose.

This information is critical for carrying out reliable risk assessments of the safety of these dams, and thus when modifications or upgrades may be warranted.

ACKNOWLEDGEMENTS

This paper has been produced by the current British Dam Society (BDS) representative on the ICOLD embankment dams committee using previously published papers from other members of BDS, and his experience relating to puddle clays. Grateful acknowledgement of these other papers is noted, including those listed in the references.

REFERENCES

- [1] JOHNSTON T A, MILLMORE J P, CHARLES J A and TEDD P (1999). An engineering guide to the safety of embankment dams in the United Kingdom. *Second edition. Building Research Establishment Report BR 363*. 102pp.
- [2] BINNIE G M (1987) *Early dam builders in Britain*. Thomas Telford, London, UK
- [3] MOFFAT A I B (2002). The characteristics of UK puddle clay cores – a review. *Proceedings of 12th British Dam Society Conference*, Dublin, pp 581–601. Thomas Telford, London.
- [4] BINNIE G M (1981) *Early Victorian Water Engineers*. Thomas Telford, London, UK
- [5] WILTSHIRE (2002) 100 Years of Embankment Dam Design and Construction in the U.S. Bureau of Reclamation. In *Proceedings of the Bureau of Reclamation History Symposium at University of Nevada - Las Vegas*, United States Bureau of Reclamation, Washington DC, USA <https://www.usbr.gov/pn/snakeriver/dams/uppersnake/teton/100years.pdf>. Accessed 13 January 2024
- [6] BROWN AJ , BROWN DH, TUDOR S, REYNOLDS (2024) Wall and pillar drains in puddle clay embankment dams. *Dams and reservoirs* 34(1), 26–41

- [7] CHARLES J A (1989). Deterioration of clay barriers: case histories. *Clay Barriers for Embankment Dams. Proceedings of Conference organized by Institution of Civil Engineers*, London, pp 109–129. Thomas Telford, London, 1990.
- [8] TERZAGHI K (1922) “Der Grundguch an Stauwerken und seine Verhütung.” (The failure of dams by piping and its prevention.). *Die Wasserkraft* 17 pp 445–449
- [9] FEMA (2011) *Filters for Embankment Dams. Best Practices for Design and Construction*. Federal Emergency Management Agency, Washington DC, USA. <https://damfailures.org/wp-content/uploads/2015/06/Filters-for-Embankment-Dams.pdf#page=305&zoom=100,0,0> Accessed November 2023.
- [10] Lane E W (1935). Security from under-seepage masonry dams on earth foundations. *In Transactions of the American Society of Civil Engineers* 100 (1) pp 1235–1272.
- [11] Terzaghi K (1939) Soil mechanics – a new chapter in engineering science: 45th James Forrest Lecture. *Journal of Institution of Civil Engineers* 12(7) : 106–141. (Reprinted in A century of soil mechanics, Institution of Civil Engineers, London, UK, 1969, pp. 151–187.).
- [12] Proctor R (1933). Fundamental principles of soil compaction, *Engineering News Record* 111(9) pp 245–248.
- [13] Kennard M G (1995) Four decades of development of British embankment dams (1955-1995). Geoffrey Binnie lecture 1994. *Dams and Reservoirs* 5(2) pp 3–14
- [14] Skempton (1989) Historical development of British embankment dams to 1960. *Keynote address in: Conference on Clay barriers for Embankment Dams*. Thomas Telford, London UK. pp 15–52
- [15] FELL, FOSTER, CYGANIEWICZ, SILLS, VROMAN, DAVIDSON (2008) A Unified Method for Estimating Probabilities of Failure of Embankment Dams by Internal Erosion and Piping” *Draft Guidance Document dated August 21, 2008*.
- [16] CHARLES J A (2024) From Chingford to Carsington: impact of soil mechanics on dam construction, 1937–1987. *Dams and Reservoirs* 34(1): 14–25
- [17] CHARLES J A, TEDD, P, WARREN A L (2014) *Lessons from incidents at dams and reservoirs – an engineering guide - report SP167* . CIRIA, London, UK

COMMISSION INTERNATIONALE DES
GRANDS BARRAGES

VINGT-HUITIEME CONGRES DES
GRANDS BARRAGES
CHENGDU, MAI 2025

PLANNING THE REFURBISHMENT OF THE KPONG DAM SPILLWAY (*)

Rudolf Sj VAN WYK

Technical Director, Zutari, South Africa

Kweku Kwaku WIAFE

Director, Engineering Services Department, Volta River Authority, Ghana

Benjamin Nii-Tawiah ADJEI

Engineer, Engineering Services Department, Volta River Authority, Ghana

Alan G CHEMALY

Dam Engineer, Zutari, South Africa

Reginald BARRY

Technical Director, Zutari, South Africa

GHANA

SUMMARY

The report describes the entire process of rehabilitation of the Kpong Dam spillway built in 1982 on the Volta River in Ghana. All the preliminary phases of investigation and studies that made it possible to define the rehabilitation project are described. The work carried out is discussed both in terms of civil engineering and the structure of the radial gates and the control system.

**Planification de la réhabilitation des déversoirs du barrage de Kpong*

RÉSUMÉ

Le rapport décrit l'ensemble du processus de réhabilitation de l'évacuateur de crues du barrage de Kpong construit en 1982 sur le fleuve Volta au Ghana. Sont notamment décrites l'ensemble des phases préalables d'investigation et d'études ayant permis de définir le projet de remise en état. Les travaux réalisés sont évoqués aussi bien sur le génie civil que sur la structure des vannes segment ou le contrôle commande.

1. INTRODUCTION

The construction of the Kpong powerhouse was completed in 1982 and involved a 148 MW hydropower plant and the Kpong Dam 24 km downstream of the Akosombo Dam on the Volta River in Ghana. The power station and the dam are owned and operated by Volta River Authority (VRA). The dam consists of a 258 m long concrete gravity overflow gated spillway and 6.2 km long zoned earthfill dykes and has a live storage capacity of 15 million m³. The spillway has a maximum discharge capacity of 20,670 m³/s and a deck level of 18.25 m above sea level with a lowest foundation level of 0.00 m i.e. an 18.25 m high composite dam according to the ICOLD definition for the height of a dam.

The gated spillway is still fully operational but due to ageing of equipment, corrosion and the presence of alkali aggregate reaction (AAR) the safety of the dam may become compromised in future. To maintain the spillway's operational effectiveness, a comprehensive rehabilitation of the infrastructure is required. This paper details the multi-faceted approach taken in planning the refurbishment work. The approach involved a site condition assessment of the gates and infrastructure, identifying the requirements of stakeholders, formulating a viable refurbishment plan, outlining the detailed scope of work, establishing an appropriate contracting strategy, and developing an engineer's cost estimate for the refurbishment.

2. KPONG SPILLWAY INFRASTRUCTURE

The spillway has 15 bays, each equipped with a chain driven radial gate (13.5 m wide and 12.6 m high). To enable inspection and maintenance of the gates and bays a 4 section stoplog set and gantry crane are used to close the bay upstream of the radial gates. The deck of the spillway bridge is used as a public thoroughfare to cross the Volta River (see Fig. 1).



Fig. 1

Kpong powerhouse and spillway on the Volta River
Centrale électrique et déversoir de Kpong sur le fleuve Volta

At the time of construction, downstream stoplogs were available for insertion downstream of the gates to close any bay off from the tailwater. Subsequently the downstream stoplogs have been made redundant and the bays cannot be isolated and drained for inspections and maintenance.

The radial gates are anchored to the spillway piers with post-tensioned tendons connected to the trunnion beams. Secondary concrete was cast around the built-in parts of the trunnion beams to make them monolithic with the spillway piers. The post tensioned tendons were grouted after installation and stressing/tensioning. The tendon chamber was filled with concrete to a level above the anchorages (or 'dead' ends) of the tendons at the completion of construction. This has, unfortunately, inhibited access for inspection and condition assessment (see Fig. 2).

Alkali-aggregate reaction (AAR) was detected in 2008 and a follow-up study was done in 2012 [1]. During the AAR investigations a convergence meter system comprising six 12 m long convergence meters were installed in the Kpong powerhouse to enable the monitoring of concrete swelling. A monthly survey of settlement

monuments on the dam and spillway bridge was initiated in 2012 to monitor the impact/ effect of AAR on the spillway.

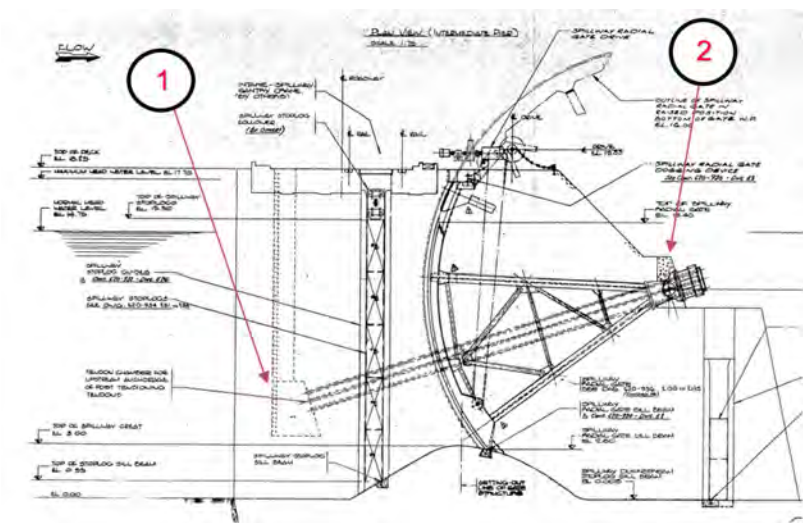


Fig. 2
Scanned copy of original as-built drawings with location of tendon chamber and trunnion girder secondary concrete
Copie numérisée des dessins originaux tels que construits avec emplacement de la chambre de tendon et du béton secondaire des poutres à tourillons

- | | |
|---------------------------------|-----------------------------------|
| 1. Cemented soils coffer dam | 1. Batardeau en sols cimentés |
| 2. Damaged Kapichira embankment | 2. Remblai de Kapichira endommagé |

3. CONDITION ASSESSMENT OF THE SPILLWAY

The planning of the spillway infrastructure rehabilitation required a detailed condition assessment that consisted of a document review, visual and functional inspection, concrete sampling and laboratory analyses of a limited number of drilled cores [2].

3.1. DOCUMENTATION AND HISTORIC DATA REVIEW

A comprehensive set of as built drawings and a construction completion report was available to assess. Unfortunately, the scanned drawings of 1982 were of low

quality and could not be easily replicated using computer aided design tools. However, the construction completion report was comprehensive and provided extensive information on the design intent and the as-constructed status of the spillway and powerhouse.

According to historical maintenance records (from 2009 to date), only minor failure events have been reported for the spillway gates and can be summarised as follows:

- Out of balance synchronising shafts
- Faulty gate position limit switches
- General gearbox failures (damaged seals, broken couplings, water seepage in oil, etc.)
- Inefficient braking causing the gate to drift
- Hoist chain binding
- General corrosion
- Cracking of the spillway gate piers due to AAR (i.e. swelling of concrete)

Acres International Limited was commissioned in 2008 to conduct an AAR study [1] on the spillway and powerhouse. The study included a site inspection, and concrete core sampling that included a laboratory analysis as well as the petro-graphic examination. The study concluded that AAR was present in the gate piers of Kpong Dam spillway and powerhouse. As a result of the study convergence meters were installed in the powerhouse and a monthly survey campaign was initiated to measure the vertical movement of the spillway piers and intake deck.

It is noteworthy that the maintenance logs did not report any of the following:

- Incidents of upstream stoplogs insertion/removal failures or incidents
- Binding of any gates (i.e. gate jammed on the side and thus unable to be raised/ lowered without intervention)

In the Acres report of 2008 binding of gate 1 was reported but the maintenance log does not contain records of any gate binding since 2009. If there had been any excessive swelling of concrete on the spillway piers it would be expected that more incidents of gate binding and problems with respect to stoplog insertion / removal would have been reported.

3.2. VISUAL AND FUNCTIONAL ASSESSMENT OF THE SPILLWAY GATES

The spillway gate was subjected to a visual and functional assessment during February 2024. The assessment consisted of a detailed visual inspection of each component of the radial gates and stoplog set, an underwater survey and functional testing as described in the subsections below.

3.2.1. *Visual inspection*

A thorough visual inspection of each bay was done with the upstream stoplog inserted. Since the downstream stoplogs are not available and the tailwater level is higher than the sill (bottom) seal, the bottom surface of the bays and the bottom part of the gates were submerged during the inspections. A man cage was lowered between the gate and the upstream stoplog using a mobile crane to enable inspection of the side and bottom seal plates and the concrete of each bay. The visual inspection covered the following aspects of each of the bays, the gates and the stoplog:

- All equipment installed on top of the pier and the concrete infrastructure above the water level.
- Trunnion assembly and trunnion girder, trunnion arms and the dry (back) side of the skin plate with the associated steel structure including horizontal support girders and skin plate ribs.
- Concrete infrastructure of each bay.
- Seals, gate wheels, pressure plates and seal lashing strips.
- Upstream stoplog set and grapple.
- Embedded seal plates and associated secondary concrete of the gates and the upstream stoplogs.

No fatal defects were noted during the visual inspection, and the drive systems were fully intact and operational. There is, however, severe corrosion on the skin plates, the trunnion beams and on some of the gate structural elements.

All the gate seals and stoplog seals are worn out and do not provide sufficient sealing. Leaks were noted in the secondary concrete of the upstream stoplog seal plates on some of the bays, as shown in Fig. 4 below.

During the inspection regular overtopping of the gates was noted that exacerbates the corrosion on the gates' structural steel components. As a result of overtopping and insufficient drain holes, debris, grass and vegetation growth accumulates on the gates' structure downstream of the skin plate as shown in Fig. 5. Fig. 6 shows the corrosion induced by insufficient drain holes.

During the visual inspection the end cap of one of the post tensioned tendons at the level of the upper anchor block was removed and no corrosion or ingress of water was visible. As the tendon chamber on the upstream side of the gate piers was not accessible, no additional inspections or assessments of the post tensioned tendons were possible. Seepage/weeping of water along the alignment of the post tensioned tendons (said alignment projected to the face of the gate piers) was noted on some of the piers. This raised a concern that the post tensioned tendons may have been exposed to the ingress of water and thus corrosion.



Fig. 3
Pitting corrosion on the edge of the skinplate
Corrosion par piqûres sur le bord de la tôle d'acier



Fig. 4
Leaks in secondary concrete of upstream stoplog (upstream stoplog installed)
Fuites dans le béton secondaire du sabot d'arrêt en amont (sabot d'arrêt en amont installé)



Fig. 5

Overtopping resulting in vegetation growth and debris on the radial gate
Débordement entraînant une croissance de la végétation et des débris sur la porte radiale



Fig. 6

Corrosion on trunnion arm from water ponding due to no drain holes
Corrosion sur le bras du tourillon en raison de l'accumulation d'eau due à l'absence de trous d'évacuation

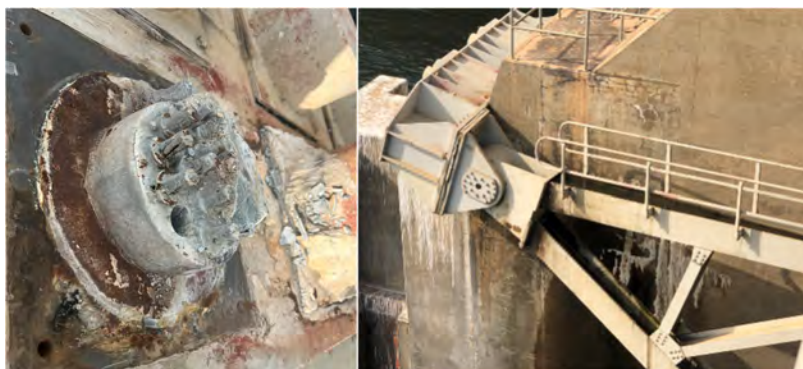


Fig. 7

Post tension cable upper anchor block with steel cap removed (left) and seepage of water from the face of a gate pier (right)

Bloc d'ancrage supérieur d'un câble de post-tension avec capot métallique enlevé (à gauche) et infiltration d'eau de la face d'un pilier de portail (à droite)

Measurements taken of the distance between the gate seal plates on either side of the bay were all within the tolerances of the design reports. It therefore seems that no significant swelling of concrete has occurred in the, or a direction parallel to the centreline of the spillway, bridge deck and the vertical faces of the spillway piers i.e. the y axis.

3.2.2. *Underwater survey*

Due to the remote location and cost associated with commercial divers, an underwater remote operated vehicle (ROV) with a video camera was used to inspect the upstream and downstream stoplog guides, the downstream end of the bay and various underwater seal plates (Fig. 8). The use of the ROV proved to be highly effective from both a time and cost perspective with less safety risks.

3.2.3. *Functional testing*

Each of the gates was cycled from a closed position to a fully open position with the upstream stoplog installed. Only the gate of bay 2 was binding during testing due to uneven tension on the drive chains. Minor vibrations were noted on some of the gates during the functional test and no excessive noise or irregular operation were noted on the drive system. No control system alarms were triggered during the testing and the gate positioning sensing system functioned effectively (currently no redundant gate positioning sensing system is installed)

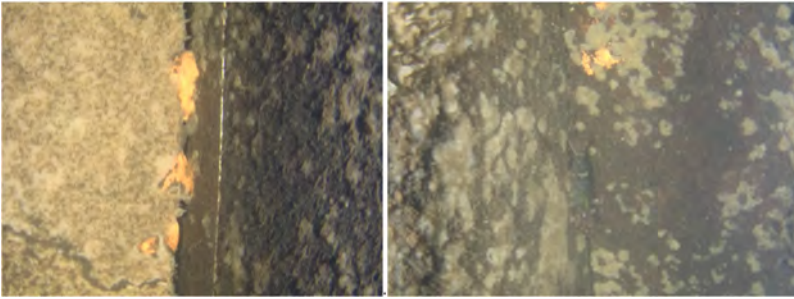


Fig. 8

Underwater inspection of stoplog guides with a ROV

Inspection sous-marine des guides de bûches à l'aide d'un robot télécommandé

During a thunderstorm excessive vibration was noted on the balancing shaft (Fig. 9). Considering the number of thunderstorms the shafts would have been exposed to over 42 years there is a significant risk of fatigue of the shafts.



Fig. 9

Gate drive system and synchronising shaft

Système d'entraînement de la porte et arbre de synchronisation

3.3. SPILLWAY CONCRETE ASSESSMENT

Due to the presence of AAR, it was necessary to carry out a detailed assessment of the spillway concrete. The assessment consisted of the following aspects [3]:

- Visual inspection
- Pier crack mapping
- Analysis of the levels of the twenty-one (21) survey monuments
- Concrete core sampling and laboratory analysis

3.3.1. *Pier crack mapping*

Cracks on the pier sections next to the trunnion beam is of grave concern as this can result in ingress of moisture and water to the post tensioned tendons and induce corrosion. Accordingly, the cracks on this section of all 16 piers were mapped (using a feeler gauge, a vernier and a tape). Cracks with depths of up to 750 mm were measured.



Fig. 10

Horizontal section of piers adjacent to the trunnion beam that cracks were measured
Section horizontale des piliers adjacents à la poutre de tourillon où les fissures ont été mesurées

3.3.2. *Analysis of data from levelling of the survey monuments*

Accurate levelling of the monuments (vertical or z axis) on the crest of the dam and spillway was initiated in 2011 and is done monthly. The survey monuments have not been surveyed in the upstream / downstream direction (x axis) or lateral direction i.e. parallel to the centreline of the spillway and bridge deck (y axis). The distances between vertical surfaces of the piers and movements of the trunnion

beams in the x, y and z axes have also not been surveyed. The results from analysis of the levels of the survey monuments from 2011 to 2024 have indicated that the vertical heights (or levels) of the survey monuments generally decreased and did not increase as would be expected due to the presence of AAR.

Swelling of the concrete of the spillway gate piers in an upstream / downstream direction, or combination thereof, due to AAR can result in failure of the post tensioned tendons due to them being stressed beyond their ultimate limit strength (ULS). This can result in the failure of one or more of the spillway gates depending on the state of stress of any post tensioned tendon or degree of corrosion of any tendon. Therefore, a monthly survey of all the trunnion beams and their adjacent piers in three dimensions (x, y and z axes) has been proposed. It is also recommended that the positions of the gate sealing plates are regularly surveyed i.e. accurate face to face measurements between adjacent piers.

3.3.3. *Concrete core sampling and laboratory analysis*

Laboratory sizes core samples (400 mm deep) were drilled in the upstream gallery of the powerhouse and on the horizontal section of one of the piers just above its trunnion girder and the samples subjected to the following laboratory analysis:

- Visual assessment of cores for AAR
- Compressive strength tests
- Indirect tensile strength tests
- Residual potential expansion of cores i.e. accelerated testing
- Petrographic examination
- Determination of alkali content using the inductively coupled plasma (ICP) spectrometry method

The ICP analysis indicated that there is a high alkali content in the cores. It can therefore be assumed that expansion due to AAR (or “swelling”) will continue on the spillway piers and powerhouse. However, the results from the petrographic laboratory analysis done by a laboratory in Ghana, indicates there is no current alkali-silica reactivity. The residual expansion potential analysis furthermore indicates that the cores contracted rather than expanded, which is unusual. Based on monitoring of AAR affected structures and dams worldwide it has been concluded that AAR never ceases but rather that rate of swelling typically reduces. Therefore, the reduction in levels of the survey monuments and findings from laboratory analyses are contradictory to the known behaviour of AAR.

The only logical deduction from the anomaly noted on the laboratory results is that the samples taken were not representative of the concrete of the spillway piers. The 400 mm long cores were taken from the top (or upper level) of the concrete which is typically high in cement content and not representative of the concrete for a gate pier. It is therefore proposed that on at least three (3) gate piers, longer

concrete samples e.g. 10 m each, are taken to get more representative samples for laboratory testing of the spillway concrete.

3.4. FINDINGS OF CONDITION ASSESSMENT

From the inspection it was found that the spillway equipment has generally been well maintained over the past 42 years of operation. However, signs of deterioration on the equipment were observed. Some aspects of the gates and associated infrastructure exhibit significant deficiencies in condition and functionality, with an increasing vulnerability of risk. Similar conditions were noted across all 15 gates, but some of the gates are in a worse condition than others.

Due to the presence of AAR and water leaks there is a risk that some post-tensioned tendons have been corroded and/or are elongated and this can result in gate failure. Leaks/weeping noted along the vertical faces of the gate piers further exacerbates the risk of corrosion of some post-tensioned tendons. As the tendon chambers of the gates are not accessible it was not possible to determine the state of the cables and therefore the movement of the trunnion beams should be carefully monitored in future. Water ingress to the tendons should also be curtailed as much as practically possible.

4. SCOPE OF REFURBISHMENT WORK

To ensure the ongoing integrity of the spillway, the gates and associated infrastructure will have to be refurbished. This will prevent unexpected failure of the gates and improve reliability, increase equipment efficiency and lifespan, minimise downtime, and enhance safety. The scope of the refurbishment was developed by first determining the client's requirements for the refurbishment work, assessing the various risks and mitigations, assessing options for the refurbishment work and then by finalising the scope of work through consultations and workshops with the client.

4.1. PROJECT OWNER'S REQUIREMENTS

To plan the refurbishment work it is critical to understand the dam owner's objectives and requirements for the work. Key to the understanding this is to assess the risk that the owner is willing to accept for the project as this also informs the type of construction contract. A workshop was held with the owner to discuss the findings of the condition assessment and to help inform and refine the owner's project requirements. Other issues to discuss and agree with the owner are:

- Operational constraints
- Budget constraints
- Required project timeline
- Required life span of equipment and infrastructure
- Operational improvements
- Environmental and regulatory requirements
- Standards and guidelines

4.2. RISK ASSESSMENT

The main risk for the project is dam safety and secondary to this are those for hydropower plant operation and project budget. The safety of the dam during and post construction was a key consideration during the planning of the refurbishment work. The key project risks that were identified are summarised in Table 1.

Table 1
Risk assessment for the refurbishment of the spillway

No	Risk	Risk Description
A. Dam safety risk		
A1	Equipment reliability	To prevent overtopping of the dam the gates should have a high mean time between failure and therefore the equipment should be highly reliable
A2	Flood control during construction	Refurbishment of the gates will require each gate bay is decommissioned for an extended period. Construction planning should ensure that sufficient bays are operable to pass floods
A3	Trunnion girder failure	Due to the unknown state (or degree) of: (a) the percentage of ultimate limit strength (ULS); or (b) corrosion of the post tensioned tendons, there is a risk of the trunnion girders being dislodged from the gate piers and subsequent gate failure
A4	Structural failure due to water leaks	Due to AAR (or the "swelling" of concrete) and the leakage/seepage of water there is a risk that further damage to the dam and spillway piers can occur due to ongoing swelling and cracking of concrete and corrosion of steel reinforcing.
A5	Emergency power supply	There is no emergency power supply available to operate the gates and no manual override. In the event of grid power failure the gates cannot be operated.
B. Construction risks		
B1.	Duration of construction	Due to the number of gates the construction period would likely extend over several years which will result in higher costs and safety risks
B2	Project overspending	Due to the complexity involved with the refurbishment work unexpected project overspending can occur if the scope is ambiguous and not well defined or because of unforeseen rehabilitation that may be required.
B3.	Remote location	The remote location of the site will result in extended delivery time of equipment and material and limited skills and resources near the site.
B4.	Public thoroughfare on the spillway deck	The spillway bridge is a public thoroughfare (pedestrians and vehicles), and a significant risk exists with respect to traffic accidents during construction and injury to the public
B5	Spillway access	Access to the spillway downstream of the gate is limited and requires a long reach from the bridge deck. This complicates installation of the downstream stoplogs and access to the gate for disassembly, removal and any in-situ refurbishment.

4.3. SCOPE OF REFURBISHMENT WORKS

The scope of the refurbishment work was developed based on the owner's project requirements, a risk analysis and evaluation of the various options for the various aspects of the refurbishment work.

4.3.1. *Construction contract*

The refurbishment work is planned to be contracted under FIDIC Plant and Design Build (yellow book) conditions of contract with specific particular conditions. The Contractor will be responsible for the (detailed) design, manufacture, installation, test, commission and defects rectification of the works. A temporary workshop with paint shop would have to be set up near the site for off-site refurbishment work and corrosion protection.

4.3.2. *Corrosion protection*

The corrosion protection of all the equipment is a major aspect of the refurbishment work. Due to limited access within the bays, it is not possible to abrasive blast and paint the gates in situ and therefore the gates will have to be disassembled and transported to workshop with a paint shop near the spillway. It is envisaged that all equipment will be refurbished at the temporary workshop except for the trunnion girders which cannot be removed and will thus have to be refurbished and coated in situ.

To limit the overall construction time two bays will be isolated at a time with stoplogs on either side to enable removal of the gates for refurbishment and corrosion protection. This will result in a total construction period of approximately 48 months for the spillway rehabilitation works. The construction time can potentially be reduced by allowing a third bay to be decommissioned during the dry season.

4.3.3. *Gate enhancements*

To improve the operability and maintainability of the gates the following enhancements will be made to the gates:

- Adjustable side-seals: The current side-seal configuration does not allow for adjustment of the side-seal, thus making seal installation and alignment a very difficult and complicated process.
- Safety rope on trunnion yoke: Currently it is not possible to attach a safety harness at the yoke, thus resulting in unsafe access to the trunnion arms.
- Docking pins sliding surfaces: To improve the operability of the docking pins a sliding surface is to be provided for each of the docking pins.

- Stiffener plates on synchronisation shaft: To avoid excessive vibration during severe weather conditions, the shafts must be stiffened.
- Spring-loaded side-wheel assemblies to allow for minor misalignment of the gates and to help ensure that the side seals remain in contact with the embedded side seal plates.
- Handrails are to be provided on the trunnion assembly, trunnion arms and horizontal girders to allow for safe access during inspections and maintenance.

4.3.4. *Gate refurbishment*

Apart from the general corrosion protection of the gates the following specific refurbishment work will be done on the gates:

- Refurbishment of skin plate: Welding of incomplete welds and replacement of severely corroded sections on the skin plate.
- Replace trunnion bearings: Though no inappropriate vibrations were detected on the trunnion bearings it was decided to refurbish the trunnion assembly with new self-lubricating bearings and thrust rings. This is to ensure ongoing reliable gate operation over the next 25 years of the gate.
- Replace all fasteners: All bolts and nuts on the gates are to be replaced and all fasteners in contact with water will be replaced with stainless steel fasteners.
- Repairs to the gate structure:
 - All unwelded seams on the gates (open seams between two connecting parts) are to be seal welded.
 - Additional weepholes are to be provided where water is being retained on the horizontal girders, trunnion arms and other structural members.
 - Welding of severely corroded parts.
- Replace handrails and cat-ladders: All handrails and cat-ladders are to be replaced

4.3.5. *Drive train*

The entire drive train (gearboxes, brake fans, synchronisation shafts and chains) will be recondition and corrosion protected as required and new motors will be installed.

4.3.6. *Control system (overtopping)*

Due to the 2022 control system upgrade the local gate control system is fully functional, and no changes are required to the system. It was decided not to include a redundant positioning sensing system or an interlock system for the dogging pins.

An early warning system with alarms will be included in the powerhouse central control system to warn operators of potential overtopping of the gates based on the rate of rise of water level of the reservoir.

4.3.7. *Stoplogs*

The existing upstream stoplog set and grapple will be fully refurbished with the following enhancements:

- Step irons: On the downstream side of the stoplog skins to enable personnel to climb down the stoplogs for inspection of the bays. Currently there are no access other than utilising a man cage to inspect the bays when the upstream stoplog set is installed.
- Seal spacers: To be installed between the stoplog panels to prevent damage to the stoplog seals during storage

An additional upstream set of stoplogs will be required to enable temporary decommissioning of two bays simultaneously. Similarly, two downstream stoplog sets will be required for the two bays. As per the original design the downstream stoplogs will be installed and removed with a mobile crane positioned on the spillway deck.

4.3.8. *Concrete repairs*

To restore the concrete all cracks in the primary and secondary concrete must be. These cracks are deemed to be caused primarily by AAR of the concrete. To slow down this process, the cracks in the concrete must be sealed to prevent the ingress of water. Sealing the cracks will also prevent corrosion of the steel reinforcing and spalling. A crack survey of the entire spillway will be conducted with ultrasonic scanner. This scan will provide for more detailed crack mapping and classification in accordance with the proposed crack repairs listed below:

- Delaminated concrete: Remove and recast all delaminated secondary and primary concrete
- Small cracks on and inclined surfaces (<10 mm): The horizontal and inclined surfaces will be coated with a flexible polyurethane sealant impregnated with a durable non-slip particle medium (such as silica sand) and then coated with a polyurea based membrane. This treatment will prevent water ingress into the concrete surface and provide sufficient traction to prevent slipping of personnel.
- Dry vertical cracks (> 5mm): All dry cracks (i.e. no seepage or weeping) on vertical surfaces will be sealed with an ultraviolet (UV) resistant crack filler.
- Wet vertical cracks: All wet cracks i.e. where seepage or weeping is occurring will be sealed with a polyurethane resin using sufficiently sized packers to seal the water leaks.

4.3.9. *Inspection of post tensioned tendons exposed to water leaks*

Due to the importance of preventing any corrosion of the post tensioned tendons exposed to water leaks the concrete at these locations will have to be removed to enable inspection of the tendons. After the inspection of the tendons the water leaks will be arrested by injecting polyurethane into the cracks and recasting the concrete that were removed.

Should the inspection reveal that the tendons are corroded, and that the structural integrity of the trunnion girders might be affected in the future, a design for securing the trunnion girders will have to be developed.

4.3.10. *Spillway and powerhouse surveillance*

To improve monitoring and surveillance of concrete swelling the following systems will be implemented:

- Re-instatement of the convergence meter system in the powerhouse
- Construct geodetic beacons on all gate piers and trunnion beams monthly three-dimensional surveys to be carried out to establish if there is any displacement of the piers and trunnion beams.

5. LESSONS LEARNED

The key lessons learned from this project that apply to planning the refurbishment of gated spillways are as follows:

- The presence of AAR on gated spillways often requires extensive additional repairs and alterations to the spillway and associated equipment to ensure future reliable gate operations.
- Ensure sufficient access to the end points of post tensioned tendons ('dead' ends) to enable effective assessment of tendon integrity.
- The use of underwater drones can be a cost effective and time efficient method for inspection of submerged infrastructure of gated spillways.
- Corrosion protection of large radial gates is a complex and time-consuming process that can be done in-situ or off-site if the gates are disassembled and removed from site.
- Severe wind and weather conditions can induce excessive vibrations on synchronising shafts.
- Radial gates should have adjustable side seal mounting assemblies that allow for adjustments to the side seals.
- Spring-loaded side-wheel mounting systems should be provided to allow for lateral wheel movement.

- Seal lashing strips, fasteners and other steel parts that are in contact with water should be replaced with corrosion resistant steel such as stainless steel.
- Provision should be made in the design of gated spillways for upstream and downstream isolation of gate bays to allow for safe inspection and in-situ refurbishment work.
- Consideration should be provided in the design of gated spillways for access into the bays when stoplogs are installed for maintenance and inspection purposes.
- Spillway gates should have an emergency power supply and ideally also a manual override in the event of total power failure during a flood scenario.
- For at least three of the spillway piers affected by AAR it is recommended that cores up to a length of 10 meters (if possible) are drilled and representative samples subjected to detailed laboratory testing and analysis. The latter should also include residual expansion potential tests carried out over a period of at least two years.
- All AAR affected spillway piers with radial gates should have geodetic monitoring points on the trunnion beams (girders) and the piers, accompanied by an accurate, dedicated and regular survey program to measure displacements in the x, y and z axes over time.
- Ultrasonic pulse velocity (UPV) scanning should be considered for condition assessment of AAR affected spillways, spillways and ancillary civil structures.
- To improve the longevity of gated spillways that are affected by AAR or “swelling concrete”, the cracks on the piers must be regularly inspected and repaired to prevent ingress of water which typically leads to corrosion of reinforcing steel and embedded parts.

ACKNOWLEDGEMENT

The authors thank Volta River Authority for their permission to publish this paper. The opinions and views presented in this paper are, however, those of the authors and do not necessarily reflect those of Volta River Authority.

REFERENCES

- [1] ACRES INTERNATIONAL, *Kpong Generating Station, Akuse, Ghana: AAR Investigations and Inspection of Concrete Structures*, 2008.
- [2] P. ERBISTI, *Design of hydraulic gates*, 2014.
- [3] P. MASON, *Managing the effect of alkali aggregate reaction on the concrete at Dinas Dam, UK. Hydropower and Dams*, May 2018.

COMMISSION INTERNATIONALE DES
GRANDS BARRAGES

VINGT-HUITIEME CONGRES DES
GRANDS BARRAGES
CHENGDU, MAI 2025

FAULTLESS FOUNDATIONS DRYING UP (*)

Michelle BLAESER
Director, ARQ DAMS (PTY) LTD

SOUTH AFRICA

SUMMARY

Identification of appropriate dam sites with acceptable topography, hydrology, materials and foundations generally forms part of the initial scoping study for new dams. However, in the continuously changing dam environment, this is not a luxury that a Dam Engineer cannot presume anymore. Limited available catchments and associated climate change effects (including sedimentation and extreme flooding) restrict the ability to choose a flawless site on which dams can be located. While hydrology and topography are generally the main drivers when deciding on a dam location, available materials and foundations are adapted to ensure constructability and structural integrity of the chosen dam at the particular dam location.

The foundation and available material challenges experienced at two off channel storage dams will be described in this paper. Both dams will be hard-type dams and require competent rockmass foundations, but contrasting difficulties had to be navigated at each site.

Olifantspoort Off Channel Storage Dam (OCSD) will require various closure walls to form a ring structure, requiring competent foundations at various parts of the ring structure. The proposed OCSD is underlain by igneous rock constituting Gabbro, Norite and Anorthosite. These igneous rocks are characteristic of large magmatic bodies of mafic composition, which have intruded into the earth's crust

**Etanchement efficace des fondations de barrage*

and crystallise into large bodies, termed plutons. A characteristic of these plutons is the development of cooling joints, which develop as rock contacts, which subdivided the rockmass into a number of intact rock blocks. At surface, this process forms tors, which comprise a highly permeable jointed rockmass outcropping, and below the surface, the development of boulders suspended in a fine grain soil matrix which may increase differential settlement for foundations. In addition to these cooling joints, a lineation was identified extending through the basin of the OSCD, intersecting two of the closure walls. Both the foundation and OSCD wall configuration (described herewith) had to be adapted to ensure foundation and dam structural integrity and impermeability.

Ntsonyini Dam will be a symmetrical Hardfill dam founded on relatively hard Dolerite. Whereas the design foundation criteria called for minimum values of various parameters, including the rock mass rating (RMR), Uniaxial strength (UCS), weathering, etc., the occurrence of sub-horisonal joint planes was established as the critical failure mode at Ntsonyini Dam. The in-field mapping process, estimation of the shear strength capacity and subsequent remedial measures (in the form of a shear key) are described further herewith.

RÉSUMÉ

L'identification des sites de barrage appropriés avec une topographie, une hydrologie, des matériaux et des fondations acceptables fait généralement partie de l'étude de cadrage initiale pour les nouveaux barrages. Cependant, dans l'environnement des barrages en constante évolution, ce n'est plus un luxe qu'un ingénieur de barrage ne peut plus se permettre. Les bassins versants disponibles limités et les effets associés du changement climatique (y compris la sédimentation et les inondations extrêmes) limitent la capacité de choisir un site parfait sur lequel les barrages peuvent être situés. Alors que l'hydrologie et la topographie sont généralement les principaux facteurs déterminants lors du choix d'un emplacement de barrage, les matériaux et les fondations disponibles sont adaptés pour assurer la constructibilité et l'intégrité structurelle du barrage choisi à l'emplacement particulier du barrage.

Les défis liés aux fondations et aux matériaux disponibles rencontrés sur deux barrages de stockage en dérivation seront décrits dans cet article. Les deux barrages seront des barrages en béton et nécessiteront des fondations en masse rocheuse compétentes, mais des difficultés contrastées doivent être surmontées sur chaque site.

Le barrage de stockage en dérivation d'Olifantspoort (OCSD) nécessitera divers murs de fermeture pour former une structure en anneau, nécessitant des fondations compétentes à différentes parties de la structure en anneau. Le OCSD

proposé repose sur des roches ignées constituées de gabbro, de norite et d'anorthosite. Ces roches ignées sont caractéristiques des grands corps magmatiques de composition mafique, qui ont pénétré dans la croûte terrestre et se cristallisent en grands corps, appelés plutons. Une caractéristique de ces plutons est le développement de joints de refroidissement, qui se développent comme des contacts rocheux, qui ont subdivisé la masse rocheuse en un certain nombre de blocs rocheux intacts. À la surface, ce processus forme des tors, qui comprennent un affleurement de masse rocheuse articulée hautement perméable, et sous la surface, le développement de rochers suspendus dans une matrice de sol à grains fins qui peut augmenter le tassement différentiel pour les fondations. En plus de ces joints de refroidissement, une linéation a été identifiée s'étendant à travers le bassin de l'OSCD, croisant deux des murs de fermeture. La fondation et la configuration des murs de l'OSCD (décrites ci-dessous) ont dû être adaptées pour assurer l'intégrité structurelle et l'imperméabilité des fondations et du barrage.

Le barrage de Ntsonyini sera un barrage symétrique en remblai dur fondé sur une dolérite relativement dure. Alors que les critères de conception des fondations exigeaient des valeurs minimales de divers paramètres, notamment l'indice de masse rocheuse (RMR), la résistance uniaxiale (UCS), l'altération, etc., la présence de plans de joint sous-horizontaux a été établie comme le mode de défaillance critique du barrage de Ntsonyini. Le processus de cartographie sur le terrain, l'estimation de la capacité de résistance au cisaillement et les mesures correctives ultérieures (sous la forme d'une clé de cisaillement) sont décrits en détail.

1. INTRODUCTION

1.1. BACKGROUND

Identification of appropriate dam sites with acceptable topography, hydrology, materials and foundations generally forms part of the initial scoping study for new dams. Limited available catchments and associated climate change effects (including sedimentation and extreme flooding) restrict the ability to choose a flawless site for dams. While hydrology and topography are generally the main drivers when deciding on a dam location, available materials and foundations are adapted to ensure constructability and structural integrity of the chosen dam at the particular dam location.

The foundation and available material challenges experienced at two off-channel storage dams will be described in this paper. Both dams will be hard-type dams and require competent rockmass foundations, but contrasting difficulties had to be navigated at each site.

1.2. DAM SITE 1 – OLIFANTSPOORT OFF CHANNEL STORAGE DAM

Olifantspoort Off Channel Storage Dam (OCSD) will require various closure walls to form a ring structure, requiring competent foundations at various parts of the ring structure. The proposed OCSD is underlain by igneous rock constituting Gabbro, Norite and Anorthosite. These igneous rocks are characteristic of large magmatic bodies of mafic composition, which have intruded into the earth's crust and crystallise into large bodies, termed plutons. A characteristic of these plutons is the development of cooling joints, which develop as rock contacts, which subdivide the rockmass into a number of intact rock blocks. At surface, this process forms tors, which comprise a highly permeable jointed rockmass outcropping, and below the surface, the development of boulders suspended in a fine grain soil matrix which may increase differential settlement for foundations. In addition to these cooling joints, a lineation was identified extending through the basin of the OSCD, intersecting two of the closure walls. Both the foundation and OCSD wall configuration (described herewith) had to be adapted to ensure foundation and dam structural integrity and impermeability.

1.3. DAM SITE 2 – NTSONYINI OFF CHANNEL STORAGE DAM

Ntsonyini Dam will be a symmetrical Hardfill dam founded on relatively hard Dolerite. Whereas the design foundation criteria called for minimum values of various parameters, including the rock mass rating (RMR), Uniaxial strength (UCS), weathering, etc., the occurrence of sub-horizontal joint planes were established as the critical failure mode at Ntsonyini Dam. The in-field mapping process, estimation of the shear strength capacity and subsequent remedial measures (in the form of a shear key) are described further herewith.

2. DAM SITE 1 – OLIFANTSPOORT OFF CHANNEL STORAGE DAM

2.1. PROPOSED DAM

The Olifantspoort OCS Dam has been configured as a ring-type structure with five closure walls to enclose a valley to the west of the existing abstraction weir. The closure walls will be constructed from Rubble Masonry Concrete (RMC) with rock sourced from the immediate surroundings. An inlet structure on/near the southern closure wall will facilitate inflows from the abstraction works, while an off-take structure will be required near the eastern closure wall. The latter will comprise a multi-level off-take structure to facilitate draw-off of the best quality water. The layout of Olifantspoort OCSD is illustrated in Figure 1.

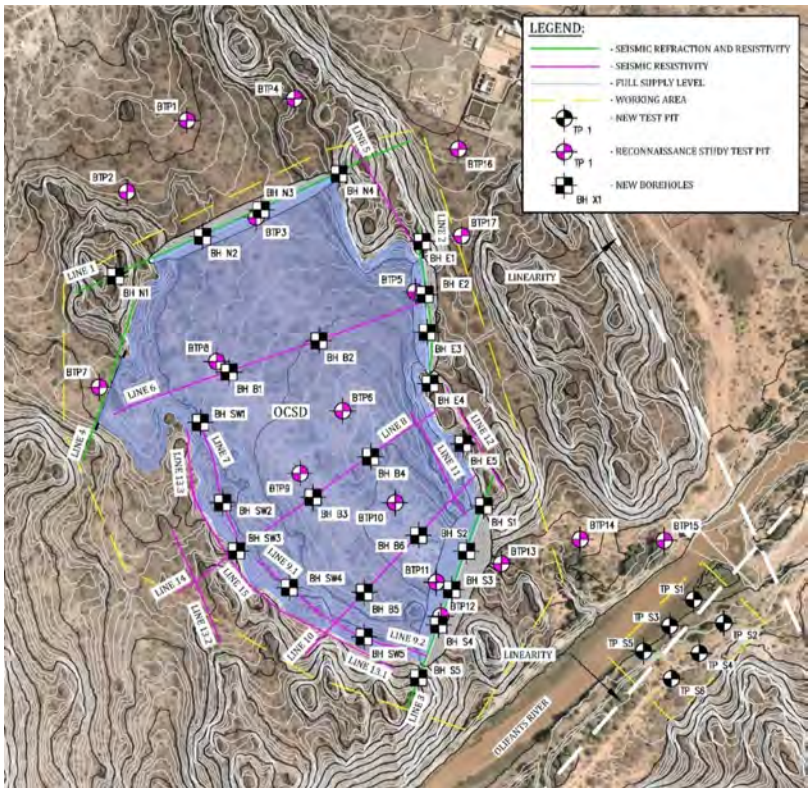


Fig. 1
Plan layout of proposed Olifantspoort OCSD
Plan d'aménagement du projet Olifantspoort OCSD

2.2. PROJECT CHALLENGES

The Olifantspoort OCSD is underlain by Gabbronorite, which is igneous rocks with large magmatic bodies of mafic composition which have intruded into the earth's crust, whereupon the magma crystallises into large igneous bodies, termed plutons. A characteristic to these plutons is the development of cooling joints, which develop as the rock contracts during cooling. These discontinuities are relatively prominent throughout the rock mass and subdivide it into a number of intact rock blocks. Considering the cooling joints and the rock blocks which may appear as a jointed rockmass, permeability of the closure flanks and even basin may be suspicious. A rigorous geotechnical investigation regime had to be undertaken at the design stage to designate the (im)permeability of the basin and closure flanks.

Olifantspoort OCSD is located in the general area where various faults in the Bushveld Complex (BC) were identified, with the Stofpoort fault closest. Sostatic adjustments in response to the BC subsidence resulted in development of large basement domes around the perimeter of the BC, and the Burgersfort dome/bulge was identified in the Olifantspoort OCSD area. While the occurrence of similar dome/bulges was not noted in the conceptual design phase, two lineations (anticipated to be a reappearance of the typical N-S trending lineation of the BC) were identified during the detail design phase investigations. The two lineations (indicated in Figure 2) extend through the north and southern closure walls and adjustments to the closure walls had to be made to ensure the structural integrity of the walls and foundation.

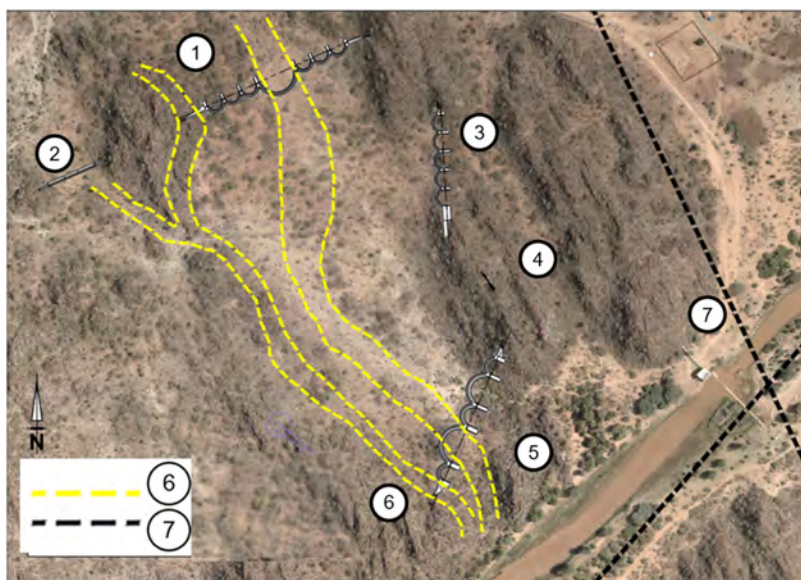


Fig. 2

Estimated location of Lineations in Olifantspoort OCSD
Localisation estimée des linéations à Olifantspoort OCSD

1 Northern Wall	1 Mur Nord
2 Spillway	2 Déversoir
3 Eastern 1 Wall	3 Est 1 Mur
4 Eastern 2 Wall	4 Est 2 Mur
5 Southern Wall	5 Mur sud
6 Probable Lineation	6 Linéation probable
7 Lineation from 1:250 MAP	7 Linéation à partir de 1:250 MAP

2.3. CLOSURE WALL AND BASIN (IM) PERMEABILITY

Lugeon testing was performed in the boreholes drilled at the dam footprint. While most of the results are indicative of fractured and open joints with consequent high Lugeon values at the closure flanks, some areas in the basin seemed near-impermeable. The electrical resistivity undertaken at the south western and eastern ridge (illustrated in Figure 3 and Figure 4) corroborates the Lugeon values where an extensive grouting program will be required to ensure near-impermeable ridges

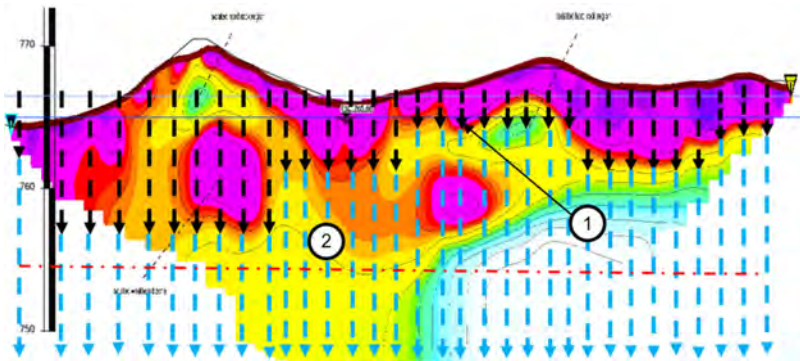


Fig. 3

Long section at South Western Ridge indicating anticipated curtain grouting

Longue section à la crête sud-ouest indiquant l'injection prévue du rideau

1 Grouting curtain on ridge from
NOC level

2 Line at bottom of ridge

1 Rideau de jointoiement sur faitage à partir du
niveau NOC

2 Ligne au bas de la crête

The grouting depth will be the critical depth between the “hydraulic pressure” (blue arrows), as determined by seepage analysis (described below), and the fractured rock (black arrows).

A seepage analysis was undertaken using RS2’s finite element analysis software package. In conjunction with the electrical resistivity results, the Lugeon test results in the various boreholes were utilised to estimate average hydraulic conductivity values for the rock mass as modelled in Figure 5.

While a grout curtain will decrease the permeability of the ridges, the rock-mass will never be completely impermeable. The grout curtain depth was consequently extended to a depth where an insignificant change in anticipated seepage was noted with an increase in grouting depth.

While it is apparent that seepage through the ridges will be decreased with the incorporation of various grout curtains, the viability of the OCSD (in terms of potential water loss through seepage) was tested. The energy (pumping) expended to recover the total volume of water loss through seepage was rated against the energy expended to pump water into the dam from the abstraction works as a comparison mechanism.

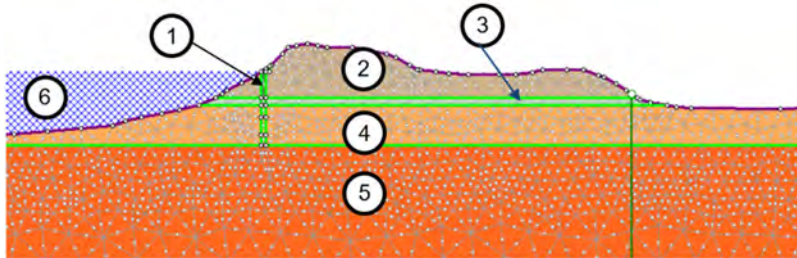


Fig. 4

Seepage Analysis Model of Eastern Ridge

Modèle d'analyse des infiltrations de la crête orientale

1 Grout Curtain	1 Rideau d'injection
2 Fractured rock	2 Roche fracturée
3 Semi Permeable rock	3 Roche semi-perméable
4 Slightly Permeable rock	4 Roche légèrement perméable
5 Near Permeable rock	5 Roche presque perméable
6 FSL RL 765	6 FLS RL 765

Using the results from the boreholes and geophysics traverses at the ridges and along the proposed dam wall centrelines, lengths of anticipated fractured rock (with higher permeability) and less permeable rock were identified. The seepage discharge computed in the steady state seepage analysis was assigned to the fractured rock, while a lower discharge (tested with seepage analyses) was used at the less permeable rock.

The total estimated seepage over the perimeter of the OCSD enumerates to approximately 0.25% of the yearly pump volume (assuming 60% pumping time). The cost associated with this loss of water, when compared to the cost of pumping at the specific time is estimated to be in the order of R4/hour. However, when comparing this to an estimated pump cost of R 2600/h, the cost and consequently the significance of anticipated seepage is deemed insignificant in the broader scheme.

An extensive grouting program will render the basin and ridges at Olifantspoort OCSD near-impermeable and an acceptable storage dam.

2.4. MAJOR IDENTIFIED LINEATIONS

Both seismic refraction and electrical resistivity traverses were undertaken along the proposed centre line of the southern wall in addition to the drilled bore-holes. The traverse indicated areas of low values at certain chainages, anticipated to be an indication of a lineation extending through the dam basin. The identification of this possible lineation had an integral consequence on the final foundation depth and subsequent recommended foundation treatment procedures. A section through the southern wall with seismic refraction superimposed on the section is illustrated in Figure 5.

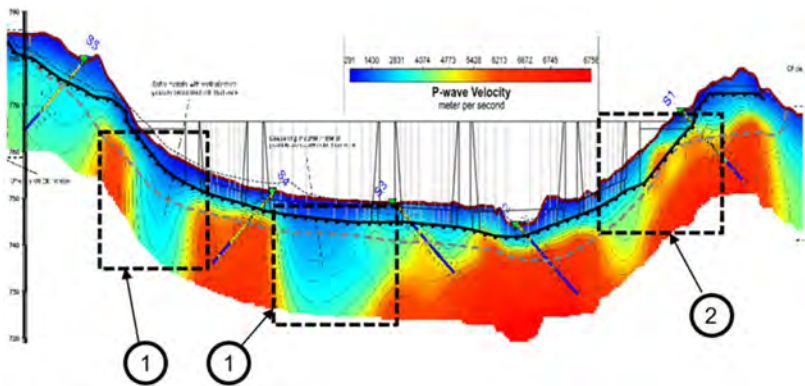


Fig. 5

Long section through Southern wall superimposed on seismic refraction
Longue section à travers le mur sud superposée à une traversée de sismique réfraction

- 1 Consolidation Grouting
- 2 Deeper Foundation

- 1 Jointoiement de consolidation
- 2 Fondation plus profonde

The manifestation of the two areas of thickened fracture rockmass (as noted in Figure 6) initiated foundation modifications to the generally accepted founding criteria specific to this dam type. The buttresses were located on the unfractured rockmass adjacent to the "lineation" zones, allowing the arch to span across the lineation zone. In addition, the excavation of the fractured rock was limited to 5 m, but 8 m deep consolidation grouting is recommended to amalgamate the fractured rock into a competent rockmass. As per logging results, it is deemed that only the RQD is lower than the required criteria in these areas, and the consolidation

grouting is anticipated to bind the fractured rock and consequently increase the RQD. High grout takes are anticipated, and possible thickening to counteract the low RQD.

In order to ensure cross valley stability of the buttress on the left abutment, a gradual slope towards the far-left bank is required, hence the deeper excavations on the left abutment.

Both major lineations extend through both the northern and southern wall founding footprint, and while none of the boreholes was drilled through the lineations, the resistivity and seismic refraction clearly indicated their anticipated extents (as presented in Figure 5). Similarly, to the southern wall, the buttresses at the northern wall were located adjacent to the lineations, allowing the arch to bridge across the fractured rockmass. Additional improvement in the form of consolidation grouting at the low rockmass quality area is recommended.

The structural integrity of both the northern and southern closure walls was proved with a three-dimensional Finite Element (FE) analysis.

3. DAM SITE 2 - NTSONYINI OFF-CHANNEL STORAGE DAM

3.1. PROPOSED DAM

The proposed Ntsonyini Dam will be configured as a symmetrical Hardfill Dam with an upstream concrete face and an intake tower on the left-hand side of the river. The dam will have a straight alignment and will be provided with an integral uncontrolled ogee spillway with a stilling basin. The layout of Ntsonyini Dam is presented in Figure 6.

The dam structure and appurtenant structures at Ntsonyini will comprise the following:

- Hardfill dam (gravity structure), approximately 275 m long and a maximum height above lowest foundation of 35.7 m
- A zoned earthfill embankment on the left flank approximately 55 m in length; and
- An intake tower approximately 36 m in height located on the left flank.

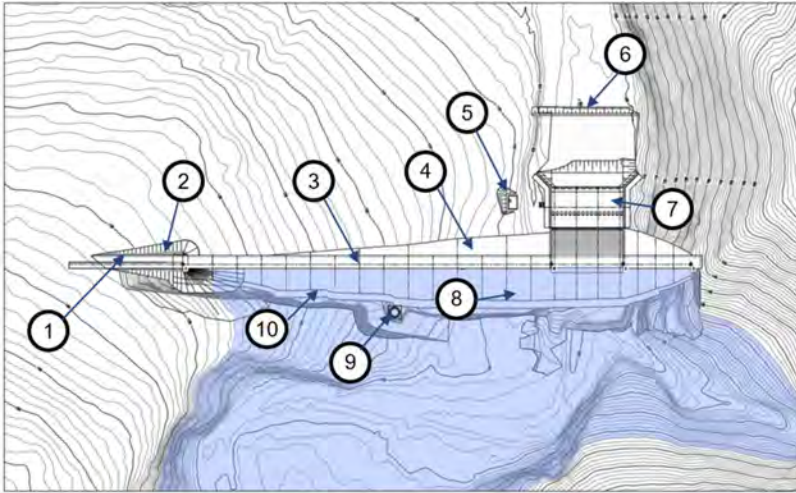


Fig. 6

layout of proposed Ntsonyini Dam

Plan d'aménagement du projet de barrage Ntsonyini

- | | |
|--------------------------------------|---------------------------------------|
| 1 Earth Cut-Off to tie into NGL | 1 Coupure de terre à relier au LGN |
| 2 Earth Cut-Off | 2 Coupure de terre |
| 3 Hardfill Dam with crest RL 136.70 | 3 Barrage en dur avec crête RL 136,70 |
| 4 Backfill to NGL on downstream side | 4 Remblai vers LGN côté aval |
| 5 Valve Chamber | 5 Chambre à 5 soupapes |
| 6 Spillway Sill | 6 Seuil du déversoir |
| 7 Stilling Basin | 7 Bassin de tranquillisation |
| 8 Hardfill Dam | 8 Barrage en dur |
| 9 Intake Tower | 9 Tour d'admission |
| 10 Plinth | 10 Socle |

3.2. PROJECT CHALLENGE

The interpretation of the initial foundation depth during the design stage was based on a limited number of boreholes located some distance downstream of the dam centreline. As coverage of these boreholes did not extend across the entire foundation, various assumptions and extrapolations were used to define the expected foundation depths. Additional geotechnical investigations were performed at the dam centreline prior to foundation excavation, but poor drilling resulted in limited information being derived from this process. Foundation confirmation was deferred to a stage when expected foundation levels were exposed.

A rigorous foundation mapping procedure on the exposed foundation was consequently followed as part of the foundation approval process. This included the estimation of general foundation criteria parameters such as Geological Strength Index (GSI), Deformation modulus (E-Mod), Uniaxial Compressive Strength (UCS), joint spacing and joint condition. As none of the original investigation holes indicated the joint orientation, extensive mapping of specific joint parameters was included in the foundation mapping. The Joint Roughness Coefficient (JRC), Joint Compressive Strength (JCS) and the sub-horizontal joints' continuation were measured to allow for sliding analysis. The results of the mapping presented a challenge which is not generally experienced at competent (and selected) gravity dam foundations. Whereas the integrity of the rockmass at Ntsonyini (rockmass parameters) was suitable, sliding on potential sub-horizontal joint planes in the foundation was established to be the critical failure mode at Ntsonyini's foundation. The typically widely and sub-horizontally jointed areas at the foundation are illustrated in Figure 7.



Fig. 7
Widely jointed areas at Ntsonyini
Zones largement articulées à Ntsonyini

3.3. MEASUREMENT OF POTENTIAL FAILURE PLANES IN ROCKMASS

Determination and selection of appropriate shear strength parameters of the rockmass on potential sliding planes are required to undertake associated sliding stability analyses. Friction of rock joints was used to predict shear strength parameters on the potential sliding planes. In the Barton and Bandis (1990) classification system, this friction is based on three index parameters, namely JRC, JCS and the residual friction angle of the rock. Both JRC and JCS were measured in the field, while residual friction of the specific rock type was estimated from index test results. While the latter is generally constant over a range of effective stresses of at least four orders of magnitude, it was found that both JRC and JCS reduce with increasing joint length. Increasing the length of joints reduces peak shear strength, peak dilation angle and peak shear stiffness. This reduction is generally termed the scale factor.

Shear strength predictions demand that the scale effect on the input variables, such as JRC and JCS, is realistically allowed for. The joint friction shear strength investigations at Ntsonyini accordingly allowed for the scale effect on the input values by using a scale free estimate of the JRC. According to the “critical joint length” concept, as recommended by Bandis (1980), the nearest scale free-estimate of JRC can be measured on samples of minimum length, which is equal to the maximum cross-joint spacing.

The foundation was divided into predetermined blocks (4 m x 4 m blocks) into which the various JRC/JCS values were grouped. The JRC was estimated using the method suggested by Barton and Bandis (1982) in which the measured length and amplitude at a specific profile length provided the JRC value. The use of the Schmidt rebound hammer for estimating joint wall compressive strength proposed by Deere and Miller (1966), was used for the estimation of the JCS on the foundation.

In addition to the JRC and JCS, the normal stress on the foundation at the selected chainage was necessary as part of the input to determine the shear strength at each chosen area. Generally, the normal stress along the foundation varies and is based on the specific loading under the specific load case. The normal stress distribution along the length of the foundation was subsequently divided into 4 m lengths (length of the chosen block) and the average at the block was used as input normal stress value at the specific block for the determination of the shear strength of the foundation at Ntsonyini.

Visual presentations (heat maps) indicating the predicted JCS and JRC are illustrated in Figure 8 and Figure 9. Whereas relatively highly jointed areas were noted at secluded areas, relatively widely jointed areas are interposed in the rock-mass at several areas, as indicated in Figure 8, indicated with low JRC values (areas in red). These widely jointed areas were denoted by sub-horizontal joints with low amplitudes and consequently contributed to the low JRC values. The JCS values were generally greater than the required minimum of 20 MPa, indicating a relatively strong rockmass. Only a few areas were noted where the JCS were lower than the required value and these are generally located at the highly jointed areas on the far left and far right banks.

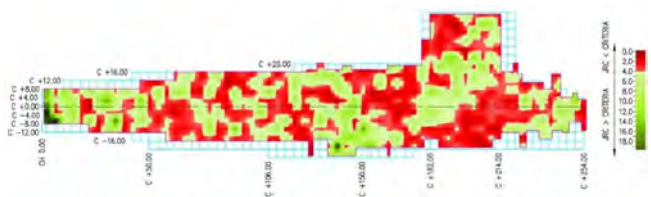


Fig. 8
JRC Heatmap
Carte thermique du JRC

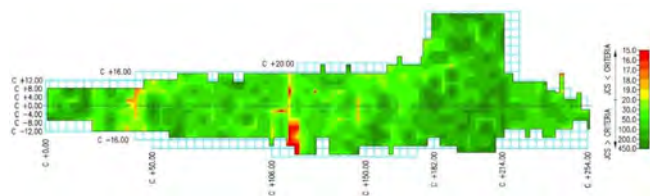


Fig. 9
JRC Heatmap
Carte thermique du JRC

Considering that the design criteria call for a minimum JRC value of 4 and that numerous areas were identified across the foundation where the JRC was lower than the required minimum, additional stability analysis at critical sections had to be undertaken to confirm foundation stability.

3.4. FOUNDATION STABILITY ANALYSES

The shear strength parameters of the foundation at the spillway were estimated using the aforementioned procedures. The estimated values of 38.1° (internal friction angle) and cohesion of 15.1 KPa were lower than the initial design values.

Stability of the dam and rockmass (using the limit equilibrium method) was not achieved under any load case at the spillway. Whereas the resultant normal load can generally be augmented with the inclusion of additional backfilling weight on the dam toe, this was not possible at the spillway area.

As the resistance force against sliding must be increased to ensure stability, the inclusion of a shear key was recommended. With the inclusion of the shear key, a multiple wedge stability analysis was undertaken. The resultant forces acting on these wedges create a multiple wedge system. With the integration of a shear key at the spillway section, resisting wedges downstream of the shear key and dam toe will be developed, which contributes to the horizontal equilibrium along a given sliding plane. For equilibrium to be achieved by using multiple wedges, mobilisation of the wedges and resistance on the sliding plane must be attained. The anticipated system at Ntsonyini is presented in Figure 10.



Fig. 10
Multiple wedge system at Ntsonyini spillway
Système de cales multiples au déversoir de Ntsonyini

The results of the multiple wedge analyses (with the inclusion of a shear key) indicated sufficient resistance against sliding and were considered stable. However, to analyse the structural integrity of the recommended dam configuration with the inclusion of the shear key, and to confirm the sliding stability at various interfaces (dam and foundation, shear key and foundation and foundation layers), a two-dimensional finite element analysis (FEA) using Midas Soilworks were performed.

3.5. STRUCTURAL FUNCTIONING OF RECOMMENDED CONFIGURATION

Static pressure loads were defined according to relevant hydraulic and structural equations and were subsequently modelled in Soilworks. Interface elements with non-linear material properties were created at the anticipated sliding failure planes. Both static non-linear and construction stage analysis were performed in Soilworks. Using the Mohr-Coulomb failure criterion along anticipated sliding plane interface models and the capacity demand ratio in the FE model, compatibility between the multiple wedge analysis and the FEM in terms of Factor of Safety (FOS) achieved along the anticipated sliding plane was confirmed. As with the multiple wedge analysis, the FOS against sliding (with the inclusion of the shear key) was higher than the required criteria at all evaluated load cases, confirming foundation stability with the inclusion of a shear key.

To allow for the mobilisation of the rockmass wedges, the shear key and the dam body material must be able to endure the pressure imposed onto it, and in the case of the dam body, the pressure/force must be transferred into the shear key. A material failure analysis was subsequently undertaken to establish the dam body and shear key structural integrity.

Principal stresses within the hardfill extracted from the Soilworks model at critical locations (and critical loading) where stress concentrations were the highest is illustrated in Figure 11 and Figure 12. Positive stresses denoted computed tensions, while negative stresses denoted computed compressions

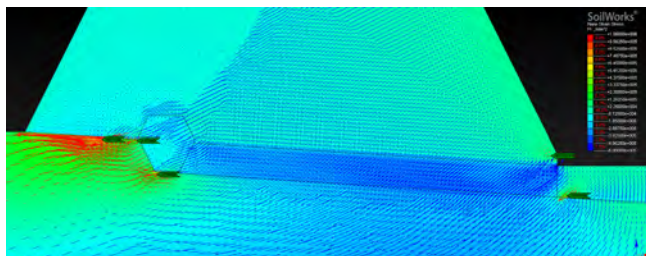


Fig. 11
First principal stresses in Soilwork
Premières contraintes principales en fondation

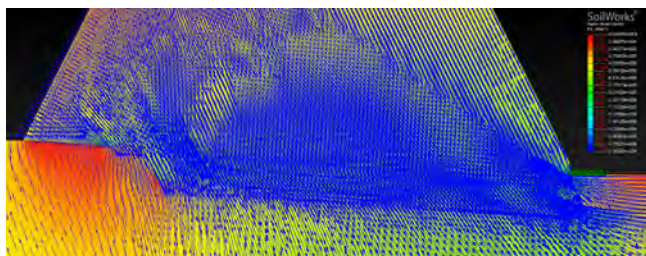


Fig. 12
Third principal stresses in Soilworks
Troisièmes contraintes principales en fondation

While no positive P1 stresses (maximum tensions) occurred within the shear key body, a maximum tensile stress (P1 stress) of 0.9 MPa is anticipated upstream of the shear key in the rock mass (red area in Figure 11) at the critical load case. Using formulations from Hoek (1995) and the average estimated rockmass UCS of approximately 177 MPa (at the spillway), it is clear that an anticipated rockmass tensile strength of 17 MPa will be adequate to resist the critical tensile stress.

A maximum compressive stress of 1.4 MPa was implied at the dam toe at the critical load case, whereas no compressive stress greater than 5 MPa (compressive strength of hardfill) has been identified inside the dam body (Refer to Figure 12).

Referring to the above, the strength of the dam body and shear key material was anticipated to be sufficient to prevent tensile or compressive material failure.

4. CONCLUSIONS

Competent dam foundations without any challenge are a unique occurrence in dam engineering. However, increasingly difficult dam foundations are being encountered in the ever-increasing exploited dam locations. Innovative engineering, as indicated herewith, will be required to adapt dam structures or foundations to ensure the construction of new dams in the future.

ACKNOWLEDGEMENTS

The author wishes to express her gratitude to all members of ARQ who contributed in some way or another to the development of the above-mentioned paper.

The opinions expressed are those of the authors and do not necessarily reflect the views of the Dam Owner. The thank the owners for their permission to publish the paper.

REFERENCES

- [1] ARQ DAMS. 2020. Design Memorandum 1: Dam Storage and Levels. Report No 8865/18063.
- [2] ARQ DAMS. 2022. Olifantspoort Off-Channel Storage Dam. Geotechnical Evaluation Report. Report No 8865/18658.
- [3] ARQ DAMS. 2020. Ntsonyini Dam. Geotechnical Evaluation Report. Report No 8618/17784.
- [4] BIENIAWSKI, Z.T. 1976. Rock mass classification in rock engineering. Exploration for rock engineering, proc. of the symposium, (ed. Z.T. Bieniawski) 1, pp 97-106. Cape Town: Balkema.
- [5] BARTON N. 1976. The shear strength of rock and rock joints. *Int. J. Rock Mech. Min. Sci. & Geomech. Abstr.* 13, 1–24.
- [6] BARTON N. 2002. Some new Q-value correlations to assist in site characterisation and tunnel design. *International Journal of Rock Mechanics and Mining Sciences*.
- [7] BARTON N.R. 1973. Review of a new shear strength criterion for rock joints. *Eng. Geol.* 7, 287–332.
- [8] BARTON, N.R. 1974. A review of the shear strength of filled discontinuities in rock. Norwegian Geotech. Inst. Publ. No. 105. Oslo: Norwegian Geotech. Inst.
- [9] BARTON N.R. 1976. The shear strength of rock and rock joints. *Int. J. Mech. Min. Sci. & Geomech. Abstr.* 13(10), 1–24.
- [10] HOEK E. 1995. Strength of rock and rock masses. Extract from a book entitled "Support of Underground Excavations in Hard Rock" by E Hoek, PK Kaiser and WF Bawden. pp 4-16

COMMISSION INTERNATIONALE DES
GRANDS BARRAGES

VINGT-HUITIEME CONGRES DES
GRANDS BARRAGES
CHENGDU, MAI 2025

**DEVELOPMENT OF A CEMENTED SOILS COFFER DAM - AN
APPLICATION OF CEMENTED SOILS TECHNOLOGY AT KAPICHIRA
DAM (MALAWI) (*)**

David CAMERON-ELLIS
*Technical Director, Damwatch Engineering Limited
New Zealand*

Daniel PUIATTI
Director, DPST Consulting

Michel LINO
*President of ICOLD
France*

Martin CHIZALEMA
*Irrigation Engineer, Shire River Transformation Project
Malawi*

NEW ZEALAND

SUMMARY

The 130 MW Kapichira Hydropower Scheme is located near Kapichira Falls on the Shire River in Malawi, Southern Africa. It is operated by EGENCO (the national generation company). An intake leading to a new irrigation canal was in the process of being constructed on behalf of the Shire Valley Transformation Project (SVTP) in January 2022 when Cyclone Ana passed over Malawi. Heavy rainfall coupled with difficulties experienced with gate control at Kapichira Dam resulted in

**Réalisation d'un batardeau en sol cimenté – une application de la technologie des sols cimentés sur le barrage de Kapichira (Malawi)*

the overtopping of the dam with scour and fusing of the right side of the embankment. A coffer dam made of Cemented Soil (CSD) from soil from a nearby deposit was constructed to allow water level in the dam to be raised to restore power generation, and to protect the damaged portion of the Kapichira Dam embankment.

This paper discusses the development of the coffer dam concept, addressing the challenges in soil investigations and cemented soil mix design, as well as the constraints on design and construction activities in a very limited time. It showcases international cooperation in CSD technology bringing together engineers from, New Zealand, France, Korea, Portugal, South Africa and Malawi to ensure the safe reconstruction of Kapichira Dam.

The conditions for extracting soil, manufacturing and placing cemented soil from within and around the dam basin are presented, addressing the difficult challenges presented by the site. The paper discusses complex interactions between cemented soil design and available construction plant, cement and fuel supply constraints, and how rapid construction in an environmentally sensitive location of a national game park led to the development of specific construction approaches and designs.

In light of lessons learned from this application in a specific context, the paper describes how Cemented Soil Dam technology can be utilised to meet the challenges of dams fit for the future.

RÉSUMÉ

La centrale hydroélectrique de Kapichira, d'une puissance de 130 MW, est située près des chutes de Kapichira sur la rivière Shire au Malawi, en Afrique australe. Elle est exploitée par EGENCO (la société nationale de production). Une prise d'eau menant à un nouveau canal d'irrigation était en cours de construction pour le compte du Shire Valley Transformation Project (SVTP) en janvier 2022 lors du passage du cyclone Ana sur le Malawi. De fortes pluies associées aux difficultés rencontrées avec le contrôle des vannes du barrage de Kapichira ont entraîné la surverse du barrage avec affouillement et rupture du remblai en rive droite. Un batardeau en sol cimenté (CSD) élaboré à partir du sol d'un gisement voisin a été construit pour permettre d'élever le niveau d'eau dans le barrage afin de rétablir la production d'électricité et de protéger la partie endommagée du remblai du Barrage de Kapichira.

Ce rapport présente le développement de la conception du batardeau, en abordant les défis liés aux études de sol et à la formulation du sol cimenté, ainsi que les contraintes sur les activités de conception et de construction dans un temps très limité. Il illustre un exemple de coopération internationale dans le domaine de la

technologie CSD réunissant des ingénieurs de Nouvelle Zélande, de France, de Corée, du Portugal, d'Afrique du Sud, et du Malawi pour assurer la reconstruction en toute sécurité du Barrage de Kapichira.

Les conditions d'extraction du sol, de fabrication et de mise en œuvre du sol cimenté à l'intérieur et autour du bassin du barrage sont présentées en abordant les difficultés propres au site. Le rapport traite aussi des interactions complexes entre la formulation du sol cimenté et l'atelier de construction, des contraintes d'approvisionnement en ciment et en carburant et de la manière dont la réalisation rapide dans un site écologiquement sensible d'une réserve nationale d'animaux a conduit au développement de conceptions et de mode de construction spécifiques.

À la lumière des enseignements tirés de cette application dans un contexte particulier, le rapport illustre comment la technologie des barrages en sol cimenté peut être utilisée pour relever les défis des barrages à l'avenir.

1. INTRODUCTION

The Kapichira Hydropower Scheme is located near Kapichira Falls on the Shire River in southern Malawi. It is operated by Electricity Generation Company (Malawi) Limited (EGENCO). The Power Plant has an installed capacity of 130 MW, a significant proportion of Malawi's energy production.

The Malawi Ministry of Agriculture, Irrigation and Water Development initiated the Shire Valley Transformation Program (SVTP) which aims to increase agricultural productivity and commercial utilisation for targeted households in the Shire River Valley and to improve the sustainable management and utilisation of natural resources. The program includes the construction of a large irrigation canal and offtake from the existing Kapichira Dam to meet its aims.

The irrigation intake was in the process of being constructed in January 2022 when Cyclone Ana passed over Malawi. Heavy rainfall coupled with inadequate gate control at Kapichira Dam resulted in the overtopping of the dam with scour of its embankments. The flooding caused the fusing of the right side of the main embankment, and the destruction of the partially completed intake structure and the first few hundred metres of irrigation canal. See Figure 1 below.



Fig. 1
Overview of Kapichira Dam and Cyclone Damage
Aperçu du Barrage de Kapichira et des dégâts causés par le cyclone

With the aid of the World Bank, EGENCO and SVTP collectively worked to develop a restoration plan to reconstruct both the damaged irrigation intake works as well as the destroyed portions of Kapichira Dam. To achieve this, a coffer dam was conceived to protect the areas designated for restoration from the impounded waters of the dam and the Shire River.



Fig. 2
Plan Layout of Kapichira Dam and the coffer dam
Plan d'aménagement du Barrage de Kapichira et du batardeau

- | | |
|--|---|
| 1 Kapichira Dam embankment | 1 Remblai du Barrage de Kapichira |
| 2 Shire River | 2 Rivière Shire |
| 3 Cofferdam alignment | 3 Tracé du batardeau |
| 4 Irrigation intake (to be rebuilt) | 4 Prise d'eau (à reconstruire) |
| 5 Irrigation canal (to be rebuilt) | 5 Canal d'irrigation (à reconstruire) |
| 6 Damage embankment area (to be rebuilt) | 6 Zone de remblai endommagée (à reconstruire) |

Figure 2 shows the location of the coffer dam, irrigation intake and irrigation canal in the context of the damaged portions of the Kapichira Dam. The coffer dam extends from the right abutment of the Kapichira Lake diagonally across the basin to connect to the undamaged portion of the Kapichira Dam embankment.

Korea Rural Community Corporation (KRCC) were originally appointed by SVTP to undertake the design and construction supervision of the new irrigation intake and canal. To expedite the design and construction processes of the coffer dam, SVTP extended the existing professional services contract with KRCC to include the design of the coffer dam. KRCC also undertook the re-design of the irrigation intake to accommodate the damaged and eroded abutment. Simultaneously, the existing construction contract with Conduril Engenharia of Portugal for the irrigation works was also extended to cater for the construction of the coffer dam, which KRCC oversaw.

SVTP provided technical assistance to both the designer and contractor through a Cemented Soils Expert and Specialist Dam Engineer, the primary co-authors of this paper who were appointed to the project in August 2022.

2. COFFER DAM CONCEPTS

It was considered conceivable that the coffer dam could be overtopped during its expected life of three years while the Kapichira Dam is restored. A dam type capable of resisting overtopping was accordingly desirable. Similarly, since the swift restoration of power generation was crucial for Malawi's economy, a dam type that could be rapidly constructed offered significant benefits. A Cemented Soil Dam (CSD) [1] which utilises locally available materials was accordingly selected. The availability of sediments in the basin of Kapichira Dam meant that this type of dam did not require the opening of new quarries which would have required environmental approvals for exploitation.

The basic concept for the coffer dam was developed from a precedent coffer dam in France, Pannecière Cofferdam which is a zoned CSD with an untreated core [1]. The coffer dam for the Kapichira rehabilitation was initially configured to have a similar arrangement but with a 6 m wide crest and symmetrical upstream and downstream slopes at 1 (H):1.5 (V). The maximum height was 14 m. (Figure 3)

Initially, under tight deadlines to restore power to the Kapichira Hydropower Plant by enabling an interim level of impoundment, the zoned coffer concept was superseded by a staged configuration as indicated in Figure 4 below. This configuration was designed to allow one of the four Kapichira Hydropower Plant turbines to operate while the second stage of the coffer dam was constructed.

At the time of the initial design in mid-2022, it was anticipated that the reduced foundation preparation area and first-stage coffer dam could be constructed rapidly well before the rainy season started in December 2022. Ultimately, however, foundation clearing proved difficult to achieve in the deeper sections of the foundation. The window of opportunity for phased construction closed as construction progressed into the rainy season. The configuration was then changed to a completely homogeneous embankment. This then made it possible to work during the rainy season, with work stoppage only during specifically heavy rainy days as there were no uncemented core soils to contend with.

In order to construct the coffer dam, a pre-coffer dam made of alluvial materials was built to hold back the remaining water in Kapichira Lake, with seepage continuously pumped from the coffer dam foundation area while the lowest portions of the coffer dam were constructed. KRCC oversaw the cleaning and preparation of the foundation of the coffer dam which generally comprised granitic gneiss in varying weathering states. KRCC also undertook in-situ permeability testing to verify foundation suitability. In certain areas, rockfill was placed on the downstream half of the foundation to fill in low spots which would have been difficult to fill with cemented soil materials. The associated upstream portion was infilled with mass concrete.

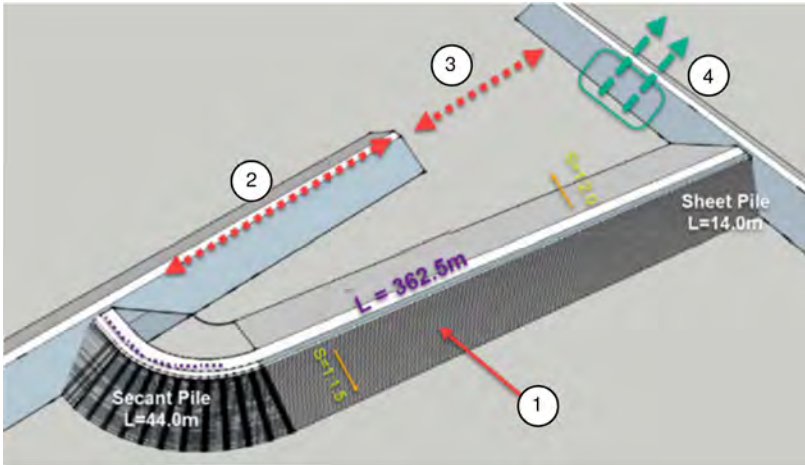


Fig. 3
Schematic of the coffer dam
Vue schématique du batardeau

- | | |
|--------------------------------|----------------------------------|
| 1 Cemented soil coffer dam | 1 Batardeau en sol cimenté |
| 2 Damaged Kapichira embankment | 2 Remblai de Kapichira endommagé |
| 3 Destroyed embankment area | 3 Zone de remblai détruite |
| 4 Irrigation intake | 4 Prise d'eau pour l'irrigation |

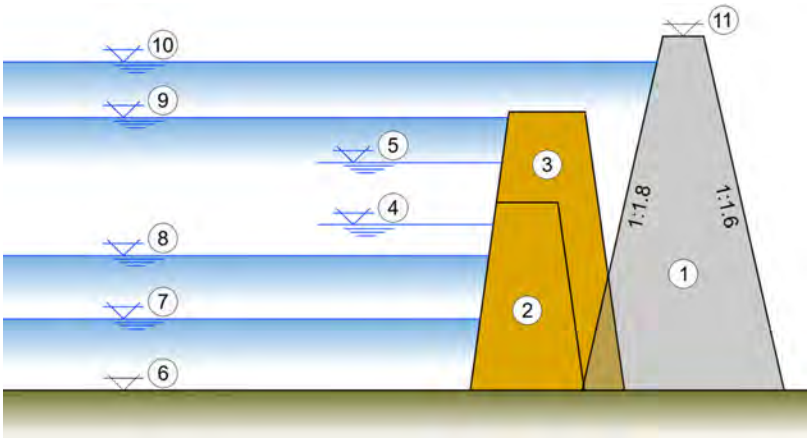


Fig. 4
Coffer Dam Constraints
Contraintes du Batardeau

1 Kapichira Dam embankment	1 Remblai du barrage de Kapichira
2 1 st stage coffer, crest at RL145.5 m	2 Batardeau 1 ^{ère} phase, crête: L 145.5 m
3 2 nd stage coffer, crest at RL 148.0 m	3 Batardeau 2 nd phase, crête: L 148.0 m
4 1 st stage operational level - RL 145.0 m	4 Niveau opérationnel 1 ^{ère} phase - L 145.0 m
5 2 nd stage operational level - RL 147.5 m	5 Niveau opérationnel 2 ^{nde} phase – L 147.5 m
6 Approx. Foundation level	6 134.0 m - Niveau appr. fondation
7 RL 140.0 m - Approx. Sediment level	7 140.0 m - Niveau appr. sédiments
8 RL 144.0 m - Dead storage level	8 144.0 m - Niveau stockage mort
9 RL 148.0 m - Normal power generation level	9 148.0 m - Niveau normal pour la production d'énergie
10 RL 148.5 m - Flood level	10 148.5 m - Niveau de crue
11 RL 149.0 m - Embankment crest level	11 149.0 m - Niveau de la crête du remblai du barrage

Various options for connecting the coffer dam to its abutments were considered. While the placement of the cemented soil onto the surface of the Kapichira Dam embankment was straightforward, a mechanism to limit seepage under the coffer and through the rocky and sandy abutments was necessary. On the right abutment, the in-situ soils comprised silty sands with high permeability and potential

for internal erosion. The left abutment comprised the “dirty rockfill” upstream shoulder of the Kapichira Dam embankment. Excavation into the latter embankment zone was ruled out to preserve the integrity of the remaining portions of the structure. Positive cut-off solutions including sheet piles, diaphragm walls and secant piles were accordingly considered. A secant pile wall constructed from the crest of the completed coffer dam was ultimately selected on the basis of available construction equipment in the region. 1150 mm diameter overlapping auger piles using temporary steel casings were chosen for this solution. A multi-hammer drill bit was required to socket the piles into the bedrock, and where rock in the abutment materials was anticipated. The secant piles were designed to extend from approximately 10 m beyond the toe line of the abutments into the abutment, and in the case of the Kapichira Dam embankment into the clay core. To augment the cut-off provisions, seepage interception systems on the groin of the abutments were specified. These comprised geotextile and gravel filters overlying the abutment materials, which were then ballasted with dump-rock.

3. CEMENTED SOIL CONSTRUCTION MATERIALS

3.1. OVERVIEW OF MATERIAL SELECTION CONSTRAINTS

The presence of significant sandy deposits in the dam basin and riverbed upstream of the Kapichira Dam strongly influenced the decision to construct the coffer dam using cement-treated soil. Consequently, selecting a cementitious binder instead of lime was a natural choice due to the highly sandy nature of the materials. When designing cement-treated soil mixes, it is preferable to use a homogeneous soil source to establish a consistent cement dosage and water content for dam construction. However, if the soil characteristics are inconsistent, two options can be considered. The first option is to design multiple soil mixes to match the variations in soil characteristics. The second option is to carry out soil homogenisation. Additionally, if a particular soil characteristic is unacceptable, corrections can be made e.g. if there is a lack of fine particles, adding fines can address the associated issues.

3.2. SAND FROM THE DAM BASIN

An initial campaign of test pitting was carried out in the sediments in the upstream Shire River and Kapichira Dam basin. It confirmed the general presence of sand but with thick layers of fine plastic soils, rich in organic matter. The sands tested were generally 2 mm in maximum particle size and typically had a practically vertical grading curve. They had the following characteristics:

- Fines content: 4 % < 0,075 mm (See the left curve in Figure 6 below).
- Organic matter which was agglomerated in small pellets (less than 5 mm in diameter).
- A significant proportion of mica particles, which is not favourable to high mechanical performance when treated with lime and/or cement and increases the water demand for cemented mixes.

Alternative sources of material outside the river sediments were then considered.

3.3. NEARBY RESIDUAL SANDS

Following further reconnaissance, a promising source of sandy material was identified on the right bank of the Shire River just downstream, and very close to the site of the coffer dam (Figure 5). While the material was present over a large area, the only accessible portions were a thin strip between the original irrigation canal and the Majete National Game Park. This required careful coordination with the park, as well as adherence to noise and working hour limitations.

The material consisted of in-situ weathered soils derived from the parent granitic gneiss prevalent in the area.



Fig. 5

Left: view of the orange sand cliff on the right bank of the Shire River. Right: view of test pitting in progress

A gauche : vue du massif de sable orange en rive droite de la rivière Shire. A droite : vue d'un sondage en cours

The material proved to be coarser than the basin/river sand with a significantly lower mica content. Soil testing was undertaken to confirm the suitability of this soil for use in a cemented soil coffer dam. The material exhibited the following characteristics:

- Colour: orange at the top, yellow at the bottom
- Particle Size Distribution (PSD): 0/10 mm (See Figure 6)
- Fines content: 5.5 to 7.5 % < 0,075 mm (average 6.5 %)
- Atterberg limits: no plasticity (clean sand, no clay)
- Specific gravity: 2680 kg/m³
- Mica: low mica content
- As this sand comprised in-situ weathered materials, it had limited rounded particles, which was considered promising from a strength perspective.

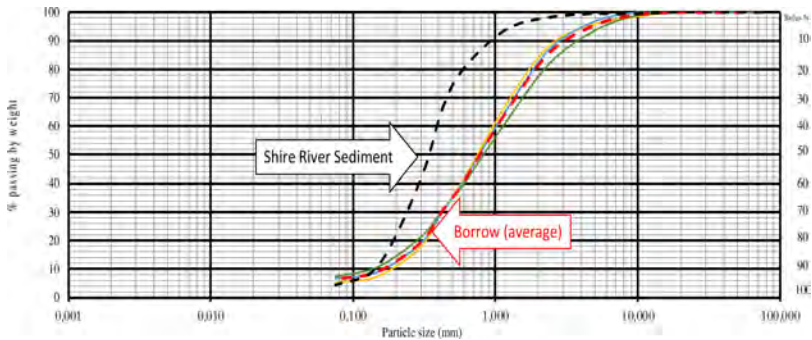


Fig. 6

PSD of orange sand from the borrow pit compared to the sand in dam basin
Courbes granulométriques du sable orange de l'emprunt comparées au sable du bassin du barrage

3.4. SELECTION OF SAND SOURCE

The performance tests showed that the sand from the dam basin was unsuitable for use in a cemented soil coffer dam due to its lack of fines, uniform PSD, and the presence of organic matter and mica. Modification of the PSD by adding fines was not considered to be a viable option for at least three reasons:

- Quality fines (e.g. limestone filler) were not available in the local area and would need to have been imported.
- The addition of a filler would not counteract the effects of the organics and mica, and therefore would not increase the level of performance of the cemented product.
- Replacing a portion of the cement with an imported limestone filler to compensate for the lack of fines was unlikely to reduce the cost of the operation appreciably.

Although not entirely satisfactory, the characteristics of the residual weathered orange soils from the borrow pit presented interesting qualities:

- An acceptable fine particle content.
- A better distributed PSD compared to the sands in the river/dam basin.
- A lower mica content.
- No organic matter.
- Good homogeneity.

Based on the above, it was decided to undertake a series of performance tests on these residual sands without the addition of any fine particles.

3.5. CEMENT

The leading cement supplier in Southern Malawi is Huaxin, a member of the Lafarge-Holcim Group, based in Blantyre. Huaxin generally supplied the cement for the concrete on the SVTP irrigation project as a CEM II 32.5 N (according to the European standard CEN 197-1). This class of cement is also suitable for the treatment of soils provided that the mixing, transportation, placement and compaction of the cemented materials are compatible with the workability period dictated by the cement (estimated at two hours under the local weather conditions). This effectively required optimisation of the anticipated production and placement processes at Kapichira Dam.

The cement plant in Blantyre is a milling plant that uses raw materials from the Huaxin/Lafarge kilns in Zambia. The cement had the following characteristics:

- Composition of the CEM II 32.5 N
 - Clinker: 70 %
 - Pozzolana: 25 %
 - Gypsum: 5 %
- Production capacities
 - Milling in Blantyre: 1200 t/day
 - Burning and milling in Zambia: 4000 t/day
- Storage capacities in Blantyre dedicated to the Kapichira job site
 - 1 300 t silo
 - 1 580 t silo
- Delivery capacity to Kapichira
 - Total capacity 300 t/day (Malawi + Zambia)
 - Mainly in bulk, supplemented by bags depending on availability
 - Possibility of just-in-time delivery

This total daily delivery capacity made it possible to theoretically treat between 1500 to 1800 m³ of material per day at a dosage of 8 % cement. The cement was

brought to the site in tankers and stored in four 60 t silos to provide a total storage capacity of 240 t.

4. CEMENTED SOIL TESTING

4.1. ON-SITE LABORATORY TESTING

Being set up for an irrigation project orientated for significant earthworks, Conduril Engenharia's site laboratory was equipped to carry out essential soil tests as well as concrete strength tests. It also had facilities for curing soil samples in air or immersed in water, both at controlled temperatures. It was therefore decided to make maximum use of the laboratory resources available on site, adapting the testing procedures where necessary.

Density testing was based on the Standard Proctor curve of the material treated with 8 % cement by dry weight:

- Maximum Standard Proctor density of the soil treated with 8 % cement = 2025 kg/m³.
- Optimum Moisture Content (OMC) = 9.2 %.

Unconfined Compressive Strength (UCS) testing of the treated materials, although not directly correlated to their erosion resistance, is generally a good indicator of mechanical performance. It also provides valuable data to evaluate the impact of curing conditions due to its relatively simple test procedures. As a proxy, using available equipment, CBR samples were accordingly prepared with 6 %, 8 % and 10 % cement by dry weight of the soil. The values of 6 % and 8 % were consistent with those used in road construction with similar soils. The dosage of 10 % was retained as an extreme value.

Due to the limited time available for carrying out laboratory treatment testing (less than one month), it was decided to undertake accelerated testing utilising the heated facilities of the site laboratory. Cylinders were cured in air at 40°C for 4 days, followed for some of them by immersion in water at 40°C for 4 days. The laws governing the reactions are complex, but based on French experience, it was considered that this curing regime corresponded with conventional curing between 15 and 30 days at 20°C.

Figure 7 shows the UCS values obtained from some of the adapted accelerated testing after 4 days of curing at 40°C. These values increased by 20 % after an additional 4 days of curing in water at 40°C.

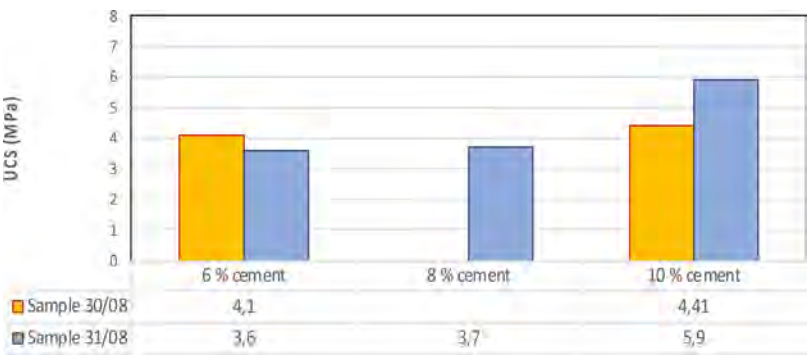


Fig. 7

UCS of the treated soil from borrow pit after 4 days of curing in air at 40°C.
UCS du sol traité de l'emprunt après 4 jours de cure à l'air à 40°C

It is important to note that the slenderness ratio (height/diameter) of the CBR sample is $115/152 = 0.76$, which results in a different outcome compared with standard cylinders with a slenderness ratio of 2.0. Comparative UCS measurements were made on samples of slenderness 2.0 ($D = 50\text{ mm}$; $H = 100\text{ mm}$) kept under same curing conditions as CBR samples. They showed that in the case of the materials studied, the UCS of conventional testing would be approximately half that of the CBR samples tested in the site laboratory i.e. $\text{UCS (slenderness 2.0)} = \frac{1}{2} \text{ UCS (slenderness 0.76)}$. Thus, the values measured after 4 days of curing in air at 40°C, corresponding to approximately fifteen days at 20°C, were, after correction, between 2 MPa (for 6 and 8% cement), and 3 MPa (for 10% cement).

These values are comparable to those obtained in road construction. The accelerated results were considered as minimum values since they will increase over time in accordance with the kinetics of cement hydration.

As a conclusion to the accelerated treatment studies performed on site, the orange weathered soil from the borrow pit presented interesting properties. The fines content, although low to medium, did not prevent high mechanical performance thanks to a lower mica content as well as a better particle size distribution. The latter facilitates higher densities after compaction and therefore higher strengths after cement treatment compared to the sand from the dam basin, even after immersion. This suggested good resistance to erosion. However, erosion tests were carried out to confirm this hypothesis and to determine the appropriate cement dosage.

4.2. SPECIALIST TESTING IN FRANCE

Laboratory erosion tests were carried out in France on both treated and untreated soil samples from the selected borrow area. They were complemented by in situ erosion tests carried out on the field test as discussed in Section 4.4 below. The samples were prepared and cured at the Cerema laboratory near Angers and were tested by the Geophyconsult Laboratory near Montpellier.

For the purpose of these tests, the soil was sieved to 5 mm maximum size. The compaction characteristics of the sample with 8 % cement were:

- Dry density = 95 % of the MDD (2.02 t/m^3) = 1.94 t/m^3
- Water content = 1.1 OMC (10.2 %) = 11.2 %

To simplify the testing processes, these parameters were adopted for all further testing irrespective of the cement content (i.e. 0, 4, 5, 6, 8 and 10 % by dry mass of the soil). The same cement available at Kapichira was used for the tests. The samples were cylindrical with a slenderness ratio of 2.0. Accelerated curing for 8 days in air at 40°C was applied, which in terms of the tests performed at Conduril Engenharia's laboratory on site corresponded with materials cured for 15 to 30 days at 20°C .

Two types of erosion tests were performed by Geophyconsult:

- Jet Erosion Test (JET) to characterise the resistance to surface erosion,
- Hole Erosion Test (HET) to characterise the resistance to internal erosion.

4.2.1. Surface erosion tests (JET)

Despite the high test pressure of the surface erosion tests (approximately 1000 Pa), it was not possible to erode the samples for any of the cement contents used. The critical stress of the treated soil was greater than the capacity of the testing rig, i.e. over 840 Pa. However, it was found that samples treated with 4 and 5 % cement were brittle, while those with 6 % or more cement were not. As expected, the non-treated soil was found not to be resistant at all (Figure 8).



Fig. 8

Samples before and after JET test. Left: untreated: Right: treated with 8 % cement
Eprouvettes avant et après essai JET. A gauche: non traité; à droite: traité à 8 % de ciment

4.2.2. Hole erosion tests (HET)

The hole erosion tests confirmed that the non-treated soil has no erosion resistance (the beginning of collapse occurred a few seconds after the test started – Figure 9). On the other hand, despite high initial test pressures (approximately 2000 Pa), it was not possible to erode the cemented soil samples irrespective of the cement content. The critical stress of the treated soil was over 700 Pa, i.e. higher than the capacity of the device. However, once again, it was found that samples treated with 4 and 5 % cement were brittle during handling compared to samples treated with 6 % cement and more.



Fig. 9

Samples after HET test. Left: untreated; Right: treated with 8 % cement
Eprouvettes après l'essai HET. A gauche: non traité; A droite: traité à 8 % de ciment

Based on the results of the tests, the following dosages were adopted:

- Body of the cofferdam: 7 % by dry weight = 6 % + 1 % to compensate for variations during implementation.
- Foundation (1 m thick) and against abutments and sub-vertical walls: 10 % by dry weight = 7 % + 3 % to compensate for anticipated implementation difficulties, especially during compaction.

4.3. PERMEABILITY TESTS

Two permeability tests were also carried out in France on untreated soil, and soil treated with 7 % cement after 7-day curing in air at 20°C:

- Untreated: $k = 1.18 \times 10^{-6}$ m/s
- Treated: $k < 1 \times 10^{-9}$ m/s

4.4. FULL-SCALE TESTS

Before the start of the prototype construction, a series of full-scale tests were carried out. A 1.20 m high test embankment using soil treated with 7 % cement was constructed to evaluate and calibrate Conduril Engenharia's available construction plant, develop the cemented soils construction methodology, and train site personnel.

One month after the placement of cemented soil on the full-scale embankment, a qualitative surface erosion test was carried out. The objective was to observe the behaviour of the upper layer of the embankment as well as uncompacted slopes. Water was poured into a trench prepared in advance (200 mm wide, 220 mm deep) in 6 stages of 5 minutes each. After 30 minutes of watering (estimated flow: 67 l/min), the trench was not eroded at all whereas the uncompacted slope of the embankment was considerably eroded from the very first attempt. Figure 10 shows the results.



Fig. 10

Left: trench after the sixth erosion testing; Right: view of the non-compacted slope at the end of the erosion test

A gauche : tranchée après le sixième essai d'érosion. A droite : vue du talus non compacté à la fin de l'essai d'érosion

The full-scale test confirmed the following important parameters for the design of the cemented soil production processes:

- Once in place and correctly compacted (> 95 % MDD Standard Proctor), the cemented soil resists surface erosion under the conditions of the test.
- Uncompacted cemented soils are highly erosive.

5. CONSTRUCTION

5.1. GENERAL

Several successive phases of preparation were necessary prior to the construction of the coffer dam, including:

- Assessment of necessary resources and audit of those available.
- Definition of the mixing and placing methodology.
- Development of quality control procedures.

At the beginning of each phase, the SVTP specialists met with all the stakeholders (designer and contractor, as well as SVTP) to brief them on the objectives and the progress, as well as the results obtained. Training in cemented soils processes was also organised for the contractor's personnel.

5.2. AVAILABLE RESOURCES

Having carried out a soil treatment project on a road project in a neighbouring state, Conduril Engenharia already had skills in this area and the necessary specialised construction plant that they were able to transport to the site relatively quickly. In addition to conventional compaction and haulage equipment, this plant included the following:

- A Streumaster SW16 TC powder cement spreader, with a cement storage tank of 16 m³, with volumetric dosing controlled by the forward speed and weight control, and feedback of information to the operator (Figure 121-1). The SVTP advisors assisted with the calibration of the spreader to ensure that the quantity of cement spread was correct.
- A WR2000S Wirtgen recycler with a mixing width of 2000 mm and a maximum mixing depth of 500 mm (Figure 12-2). This recycler was equipped with water injectors in the mixing chamber with flow control allowing the mixing of soil with cement and water in a single operation (a requirement for the type of mixing envisaged for the works at Kapichira). The recycler required some repairs and maintenance, particularly the provision of a new set of teeth on the rotor. The integrated watering function was checked and calibrated.

5.3. CONSTRUCTION METHODOLOGY

The construction methodology for the cemented soils coffer dam was developed in close collaboration with Conduril Engenharia during the initial field tests which were used to train the site personnel and raise their awareness of potential quality issues.

A first field test was undertaken in the borrow pit near the dam site to develop the production methodology. This made it possible to ensure a good match between the water tank and the recycler. The mixing, carried out to a depth of 300 mm, required only one pass to ensure thorough mixing of the cement and water, as well as acceptable grinding. The colour contrast between the treated layer and the untreated in-situ material proved very useful when loading the treated materials into the dumpers. In cases where there was doubt, a comparative test using phenolphthalein made it easy to distinguish whether there was cement present in the soil (Figure 11).



Fig. 11

Phenolphthalein sprayed on the walls of the trench. Red coloration indicates treated soil, no coloration indicates untreated soil.

Phénolphtaléine pulvérisée sur les parois de la tranchée. La coloration rouge indique le sol traité, l'absence de coloration le sol non traité.

A second field test in the form of a 1.2 m thick embankment (Four 300 mm thick compacted layers) was carried out outside the borrow pit and the cofferdam to further develop the methodology for spreading and compacting the layers of cemented soils.

While a small bulldozer with flat grousers was the preferred plant for levelling cemented soil layers, it was not possible to secure an appropriate one for the project. At Conduril Engenharia's suggestion, a grader was used to carry out the spreading task, which was then used throughout the project.

Compaction tests were carried out using a CAT CS 683E vibrating smooth drum roller (total weight: 18.8 t with 13.3 t on the 2.134 m wide vibrating drum) and a CAT PS 360C pneumatic-tyre compactor ballasted with water (1.93 t/wheel) (Refer also to Figure 12-8). The vibrations of the drum roller, unfortunately, caused transverse cracks after 4 passes. This phenomenon is common on sandy or slightly plastic materials. To avoid this, and to achieve dry densities greater than 95 % of the maximum Standard Proctor reference density, the following operating process was chosen: 4 passes of a vibrating cylinder followed by 10 passes of a pneumatic roller. Finally, on the cofferdam, it was decided to limit compaction to two passes of the drum roller without vibration to initially flatten the surface of the bulk layer and then to apply fourteen passes of the tyre roller.

The field test also made it possible to develop the techniques for treating the surface of the layers before covering, namely: sweeping, light water spraying, and spreading powdered cement at a rate of 500 g/m² [2].

Tests on the prototype confirmed the following procedures to be used in the construction of the coffer dam:

- Treatment on the coffer dam embankment was not allowed to avoid the risk of untreated interlayers.
- Cement dosage: 10 % in foundation, 7 % in current backfill.
- Water content during manufacturing: between OMC+1% and OMC+3%.
- Water content during placement and compaction: between OMC and OMC +2%, i.e. some drying during handling and transportation allowed.
- Thickness of uncompacted layers: 340 mm.
- Thickness of compacted layers: between 270 mm and 300 mm.
- Transverse slope of the surface: 1 % to upstream and downstream.
- Surface treatment: sweeping, wetting, spreading of 500g/m² of cement.
- At each interruption, e.g. at the end of the working day, vertical cutting of the end of the layers and spreading of cement on the cut face before resuming implementation the next day.
- Maximum duration between the start of mixing and the end of compaction: 2 hours
- No night work.

5.4. QUALITY CONTROL

As the distance between the mixing in the borrow pit and the placement at the coffer dam was approximately 500 m, Conduril Engenharia set up two separate quality control teams:

- **Manufacturing:** periodic control of cement and water content, mixing depth and proper loading in dumpers.
- **Placement:** control of density and water content with a nuclear densitometer, thickness of layers, surface treatment, sampling of cemented soil for making test samples in the laboratory and measurement of the UCS.

At the request of the KRCC Site Engineer, advice was also provided by the SVTP specialists to his representatives on site for the supervision and quality assurance of both the manufacturing and placement processes.

6. CONSTRUCTION OF THE CEMENTED SOILS COFFER DAM

6.1. OVERVIEW OF CONSTRUCTION

The construction sequence for the cemented soils coffer is depicted in Figure 12.

The various steps shown in the figure are referenced in the following text in square parenthesis.

As foundation preparation was delayed due to difficult conditions, construction of the cemented soils portion of the coffer dam took place from December 2022 to July 2023. In total, more than 100,000 m³ of cemented soil was produced and placed using the plant described above. The maximum daily production was between 800 and 1000 m³/day. Stoppages were caused by maintenance and weather reasons as well as cement and fuel supply constraints.

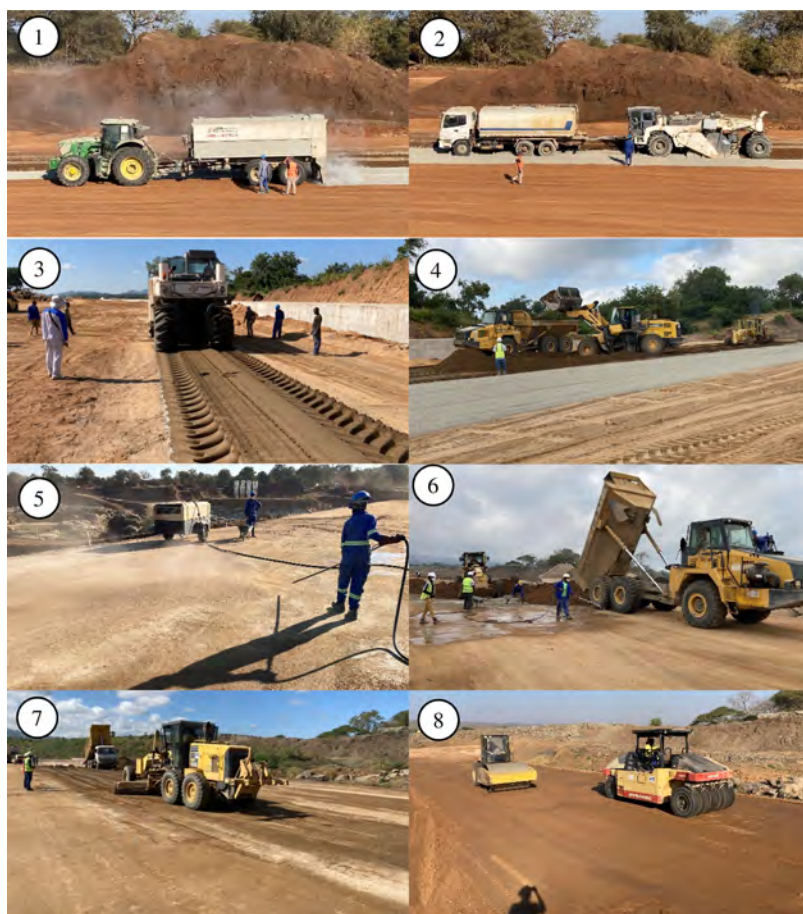


Fig. 12
CSD Construction Sequence
Séquences de construction du CSD

- | | |
|----------------------------------|----------------------------------|
| 1 Cement spreading | 1 Épandage de ciment |
| 2 Moisture conditioning & mixing | 2 Humidification et malaxage |
| 3 Mixed material | 3 Matériau malaxé |
| 4 Loading | 4 Chargement |
| 5 Surface cleaning | 5 Nettoyage de la surface |
| 6 Cement spreading and dumping | 6 Epandage et approvisionnement |
| 7 Dumping and spreading | 7 Approvisionnement et régalinge |
| 8 Compaction | 8 Compactage |

6.2. CEMENTED SOIL MANUFACTURE

The topsoil in the borrow area was stripped and stocked for later reinstatement of the area. Strips up to 100 m in length were then prepared by evening out the surface of the borrow area using a motor grader and lightly rolled using a 10 t smooth drum roller. The width of the strips was selected to match the volume of cemented soil required for the day's production as multiples of the width of the soil recycler as discussed below. It was not necessary to cut the borrow pit surface level as long as mild longitudinal slopes that the mixing equipment could traverse were maintained. The location of the strips nevertheless required appropriate planning to allow the mixing equipment to pass the prepared area and to turn around at each end of it.

Cement was spread using the tractor-pulled StreuMaster SW16 TC spreader based on a 300 mm milling depth [Figure 12-1]. Quality control of the mass of spread cement was provided on every mixing strip by placing 1/4 m² metal box on the prepared surface before spreading. The mass of spread cement was simply weighed on a balance scale on site to confirm that the correct dosage of cement was provided.

The cement and top 300 mm layer of soil were then mixed using the Wirtgen WR2000S recycler [Figure 12-2]. Prior to mixing, the in-situ moisture content was measured at various locations along the mixing strips. This initial moisture content was taken into account in setting the correct water to be dosed by the recycler. Verification tests were then undertaken after mixing, but visual confirmation of the moisture condition of the mixed cement and soils proved to be a reliable indicator of appropriate dosing.

The recycler traversed the width of the mixing strips in numerous lanes of 2 m width [Figure 12-3]. Once the second lane had been mixed, the first lane was uplifted by a front-end loader to be transported to the coffer dam [Figure 12-4]. While Articulated Dump Trucks (ADTs) were the preferred transport mechanism due to their low tyre pressures which limit damage to the cemented soils surfaces, transportation was supplemented by road trucks. These were found to be only slightly more damaging to the surfaces, except where significant turning movements were required, in which case extra care in surface preparation before dumping was required.

The borrow area was progressively exploited in the above manner, deepening the original landform by up to 10 m.

6.3. PLACEMENT AND COMPACTION

The surfaces of the coffer dam were prone to become loose as the cemented soil was compacted and the surface dried out. Continuous watering of the surface (curing) was required but this was not comprehensively implemented. As a result, immediately before the placement of new layers of mixed cemented soil, the surface was swept by manual labour and compressed air [Figure 12-5]. Cement was then spread manually over the surface as discussed in Section 5.3 above.

Ramps of excess cemented soils were constructed on both sides of the coffer dam structure to provide dedicated access locations for the dump trucks to access the placement surfaces (refer to Figure 13).



Fig. 13
Overview of Cemented Soil Placement
Aperçu de la mise en place du sol cimenté

Once on the surface of the coffer dam, the dump trucks generally travelled in reverse towards the placement front, where they discharged their load [Figure 12-6].

As per the trials, a motor grader, working primarily on the loose cemented material, spread the dumped material to the correct grade [Figure 12-7]. At various stages during the raising of the coffer dam, thin laminations were observed in the top surfaces of the layers. This was found to be caused by excessive final levelling with the motor grader, a practice which was stopped as soon as it was detected.

The two rollers were then applied to initially even out the surface and finally compact it [Figure 12-8]. Nuclear densitometer quality assurance testing was undertaken to ensure that the designated number of roller passes was adequate to achieve or exceed the 95 % Standard Proctor density requirement. Additional compaction was seldom required following this verification. Based on Conduril Engenharia's quality control records, all densities exceeded 95 % of the maximum Standard Proctor density, while water contents varied between 7.5 and 12.5 % relative to the target of between 10 and 12 %. The UCS values at 28 days of air curing on samples treated with 7 % cement taken on site and recompacted in the laboratory in CBR moulds ranged from 2.4 MPa to 6.5 MPa. The low values can be attributed to the low water contents of certain of the materials.

Adjustments, accompanied by training sessions, were made continuously during the execution of the work to correct deviations concerning, among other things, the correct use of the placement plant, access to the structure, attrition caused by the traffic of trucks and dumpers, surface treatment and the care taken with the quality of restarts after stoppages. Sensitive points were identified such as compaction at the abutments, compaction along curves and at the edges of the embankment despite a systematic safety over-width of at least 500 mm on each side. It should be noted that given the temporary nature of the cofferdam, it was not considered beneficial to remove these over-widths.

Although no specific transverse joints were included in the coffer dam structure, post-construction inspections confirmed that it remained free of major cracks. This demonstrates that the construction methods were effective in managing shrinkage, thereby ensuring the durability and integrity of the coffer dam.

7. CONCLUSIONS

The successful placement of cemented soils at the Kapichira Dam restoration site demonstrates the versatile use of cemented soils technology in hydraulic structures. Additionally, the following were concluded from the experience:

- While an abundance of sand may indicate that cemented soils technology is appropriate at a dam site, the experience at Kapichira shows that it is critical to first ensure that the physical properties of the sands are conducive to stabilisation.
- The correct construction plant which is appropriately operated with well-considered operational procedures is imperative for the successful construction of a cemented soils structure, especially when ambient temperatures restrict placement time.
- Additionally, training of site personnel in the correct procedures is essential to achieve the desired outcomes. It was found that educating site personnel on

the fundamental principles behind mixing, surface preparation, placing, spreading, and compaction procedures helped ensure these processes were correctly implemented.

- In-situ cement mixing in borrow areas provides an effective and efficient means to stabilise soils.
- In the case of the Kapichira cemented soil coffer dam, due to time limitations, accelerated testing regimes proved very useful in helping define mix proportions and confirming the hardened properties of the cemented soil. Generally, however, it is preferable to ensure that sufficient time is allocated to undertaking a comprehensive soil testing regime, including the investigations of the material sources. A minimum of four to five months is deemed appropriate for the whole process.

ACKNOWLEDGEMENTS

The authors are grateful to the Shire River Transformation Project for their support throughout design and construction, and permission to write this paper. The authors are grateful to the New Zealand Society on Large Dams for reviewing this paper.

REFERENCES

- [1] CEMENTED SOIL DAMS – ICOLD, BULLETIN 195 (2022)
- [2] SOIL-CEMENT FOR EMBANKMENT DAMS – ICOLD, BULLETIN 54 (1986)

COMMISSION INTERNATIONALE DES
GRANDS BARRAGES

VINGT-HUITIEME CONGRES DES
GRANDS BARRAGES
CHENGDU, MAI 2025

**FUTURE-PROOFING DAMS: STRATEGIES FOR SUSTAINABLE WATER
MANAGEMENT, TECHNOLOGICAL RETROFIT, AND CLIMATE RESILIENCE IN
THE CONTEXT OF DAM REFURBISHMENT (*)**

Cătălin POPESCU

Technical University of Civil Engineering Bucharest, PRES. OF ROCOLD

Petruța ISOFACHE

Aquaproiect S.A. Romania

Isabela BALAN

Prut Barlad Administration, Romanian Waters Authority

ROMANIA

SUMMARY

Dams and levees have long been central to water resource management, flood control, and hydroelectric power generation. However, the 21st century presents unprecedented challenges, including climate change, population growth, and evolving energy demands, necessitating, sometimes, the rethinking of how these infrastructures are designed, operated, and maintained. This article explores comprehensive strategies for future-proofing dams and levees to enhance their sustainability, resilience, and functionality.

As climate change drives more extreme weather patterns, including intense rainfall and prolonged droughts, it becomes crucial to design dams that can withstand these conditions while also contributing to ecological sustainability. Future

**Pérennité des barrages : stratégies de gestion durable de l'eau, modernisation technologique et résilience climatique dans le contexte de remise en état des barrages*

dams and levees must integrate durable and environmentally friendly materials, reducing their ecological footprint while enhancing their ability to protect ecosystems and biodiversity. This includes the integration of natural elements, such as vegetation, which can improve water quality and create habitats for local wildlife.

RÉSUMÉ

Les barrages et les digues jouent depuis longtemps un rôle central dans la gestion des ressources en eau, la lutte contre les inondations et la production d'énergie hydroélectrique. Cependant, le XXI^e siècle présente des défis sans précédent, notamment le changement climatique, la croissance démographique et l'évolution de la demande énergétique, qui nécessitent de repenser fondamentalement la conception, l'exploitation et l'entretien de ces infrastructures.

Ce rapport explore des stratégies complètes pour assurer la pérennité des barrages et des digues, visant à renforcer leur durabilité, leur résilience et leur fonctionnalité.

Alors que le changement climatique entraîne des conditions météorologiques extrêmes, telles que des précipitations intenses et des sécheresses prolongées, il devient essentiel de concevoir des barrages capables de résister à ces conditions tout en contribuant à la durabilité écologique. Les futurs barrages et digues doivent intégrer des matériaux durables et respectueux de l'environnement, réduisant leur empreinte écologique tout en améliorant leur capacité à protéger les écosystèmes et la biodiversité. Cela inclut l'intégration d'éléments naturels, tels que la végétation, qui peuvent améliorer la qualité de l'eau et créer des habitats pour la faune locale.

1. INTRODUCTION

The modernization of dam and levee infrastructure is essential for addressing contemporary demands in water management, flood control, and sustainable resource allocation. As climate change introduces more frequent and intense weather events, these infrastructures must adapt to ensure resilience, operational efficiency, and environmental stewardship. Advanced technologies, particularly in intelligent water management, play a pivotal role in optimizing water distribution across agricultural, industrial, and domestic sectors. By employing digitalization and automation, these systems utilize real-time monitoring through sensors and analytics, allowing for dynamic adjustments in water flow and minimizing resource losses.

Refurbishment efforts are equally critical for aging dams, especially those constructed in the last century, which may not meet current safety and environmental standards. Necessary upgrades include structural reinforcement, expanded discharge capacities, and modern hydromechanical and electrical systems. For instance, under Romania's National Recovery and Resilience Plan (PNRR), dams such as Cucuteni, Solești, and Căzănești are undergoing significant modernization. These upgrades aim to improve climate resilience, safeguard water resources, and promote sustainable use, incorporating advanced monitoring technologies and ecological enhancements.

Sustainability in dam design and refurbishment also addresses environmental impacts on river ecosystems. Essential measures include ensuring ecological flows, supporting sediment transport, and maintaining connectivity for aquatic species, thus minimizing disruptions to local biodiversity. This approach is aligned with global trends toward sustainable water management, focusing on not only securing water supplies but also preserving the health of aquatic ecosystems.

From an economic standpoint, effective implementation of these modernization strategies requires comprehensive cost-benefit analyses, sustainable funding sources, and robust regulatory frameworks that promote responsible development. Meaningful engagement with local communities and stakeholders is also essential, ensuring that project benefits are equitably distributed and that infrastructures meet the needs of diverse water users.

In summary, the future of dam and levee infrastructure lies in a holistic approach that integrates advanced technology, sustainable design, ecological considerations, and strong community involvement. By modernizing existing structures and designing new ones with these principles, we can establish resilient, long-lasting water management systems that benefit both human populations and natural ecosystems.

1.1. CLIMATE CHANGE AND ITS IMPACT ON DAMS AND LEVEES

The impacts of climate change on dam and levee infrastructure are becoming increasingly evident as extreme weather events grow in both frequency and severity. Climate patterns now exhibit intensified storms, prolonged droughts, and shifts in precipitation distribution, which challenge the stability and effectiveness of water management infrastructure worldwide. Tropical cyclones, hurricanes, and other storms bring high rainfall volumes, leading to flooding, soil saturation, and subsequent landslides. Simultaneously, areas with altered rainfall patterns may experience prolonged drought, exacerbating water scarcity and straining dam reservoirs.

1.1.1. *The effects of extreme weather patterns*

Extreme weather patterns, including intense rainfall, drought, and unusual temperature shifts, have significant and varied impacts on dam and levee performance. Heavy rainfall events can overwhelm dam spillways, potentially leading to flooding, structural strain, and downstream risks. The hazards associated with extreme rainfall are extensive:

- **Flooding and Structural Integrity:** Rapid water level increases can exceed a dam's design capacity, placing strain on its structural components and increasing the risk of overflow.
- **Soil Saturation and Landslides:** Excessive rainfall can saturate surrounding soils, destabilizing hillsides and causing landslides that threaten infrastructure, human safety, and transport corridors.
- **Erosion and Sediment Accumulation:** Increased erosion upstream leads to higher sediment loads in reservoirs, which can reduce storage capacity and hinder dam functionality.

Droughts, meanwhile, reduce inflows to reservoirs, impacting water availability for agriculture, industry, and municipal use. The effects of prolonged droughts include:

- **Water Supply Disruptions:** Limited water availability can disrupt supply chains, impacting agricultural output and leading to higher production costs.
- **Reduced Hydropower Generation:** Lower water levels directly reduce the operational capacity of hydropower facilities, impacting renewable energy output and grid stability.
- **Ecosystem and Agricultural Strain:** Droughts stress ecosystems and reduce soil moisture, leading to diminished agricultural yields and economic challenges for farming communities.

The economic impacts of these climate-induced conditions are substantial, from loss of agricultural productivity and increased food prices to costly infrastructure repairs following flood or drought-related damage.

1.1.2. *The need for climate-resilient infrastructure*

The unpredictability of future climate scenarios highlights the necessity for climate-resilient infrastructure. Designing dams and levees with adaptive, flexible approaches enables these structures to respond dynamically to climate variability. Moving forward, dam engineering must prioritize materials, construction methods, and monitoring systems that are resilient to a broader range of climatic extremes. These climate-resilient structures include components specifically adapted to withstand and function under heightened flood risk and prolonged drought conditions.

- **Adaptive Design and Flood Estimation:** Dams and levees need flood estimation methodologies that incorporate future climate variability. Flood models

should be equipped to handle a wider range of scenarios, ensuring that structural reinforcements align with evolving environmental conditions. Research in this area aims to develop robust design methods that consider uncertain flood risks, supporting decision-making in flood management and land use planning

- **Hybrid Infrastructure and Environmental Integration:** Projects focusing on climate resilience may combine traditional engineering with natural elements. For instance, vegetative cover along dam embankments can improve slope stability and reduce erosion under heavy rainfall conditions. In Romania, modernization efforts such as those applied to the Cucuteni Dam have integrated natural elements alongside traditional reinforcements to mitigate runoff, control erosion, and improve the environmental footprint of dam infrastructure

The shift toward resilient infrastructure underscores the importance of considering both present and future climate conditions in dam design and maintenance. As the climate continues to evolve, investments in flexible, adaptive infrastructure that supports robust and proactive flood and drought management strategies will be key to sustaining safe and effective water resource systems.

2. TECHNOLOGICAL ADVANCEMENTS IN WATER MANAGEMENT

2.1. INTELLIGENT WATER MANAGEMENT SYSTEMS

Adaptive management does not have to be specified a priori, but can emerge within a trusting relationship between stakeholders as long as they are willing and able to change their operational paradigm. [4]

2.2. REAL-TIME MONITORING AND AUTOMATION TECHNOLOGIES

Modern dam infrastructure relies on real-time monitoring systems to enhance operational safety and efficiency, with Fiber Bragg Grating (FBG) sensors playing a central role. Positioned at critical points such as the base of downstream slopes, FBG sensors detect deformations and seepage, providing both dynamic and static measurements across multiple channels. Each channel supports up to 20 interconnected sensors that monitor key variables, including strain, temperature, tilt, and pressure, crucial for assessing structural health under varying conditions.

FBG sensors' accuracy and resilience in temperature fluctuations make them ideal for long-term deployment, particularly in high-risk zones. Their application in Romanian dams (e.g., Cucuteni, Solești, and Căzănești) has demonstrated

effectiveness in early detection of structural shifts, seepage, and temperature changes, supporting timely maintenance interventions and reinforcing overall resilience.

The integration of FBG sensors with Supervisory Control and Data Acquisition (SCADA) systems further enables automated alerts and responses. SCADA systems aggregate sensor data, providing centralized oversight and triggering emergency protocols when thresholds are breached, such as adjusting spillway gates to reduce structural pressure. SCADA also facilitates predictive maintenance by analyzing trends from real-time data, allowing operators to schedule repairs before issues escalate. Future advancements, such as AI-driven analytics and enhanced remote monitoring capabilities, promise to expand these systems' predictive accuracy and ease of access, supporting even more robust infrastructure management.

3. REFURBISHMENT OF EXISTING INFRASTRUCTURE

Technical documentation for the rehabilitation of the existing infrastructure should include an assessment of the potential downstream environmental and social impacts.

In view of climate change, dams and reservoirs will and have to play an even more important role as mitigation and adaptation infrastructures in order to satisfy the vital needs in water, renewable energy and food in the different continents worldwide. [5]

3.1. CASE STUDY: CUCUTENI, SOLEȘTI, AND CĂZĂNEȘTI DAMS IN ROMANIA

The Cucuteni, Solești, and Căzănești dams, situated in the Prut-Bârlad hydrographic basin, serve critical roles in regional water management, flood control, and ecological support. As part of the Prut-Bârlad River Basin Risk Management Plan, these dams are undergoing extensive upgrades to meet modern safety, operational, and ecological standards. Common rehabilitation measures for these dams address structural integrity, hydromechanical systems, and ecological sustainability, aligning with Romania's Areas of Potentially Significant Flood Risk (APSFR) goals.

3.1.1. *Common interventions and upgrades*

- Structural Rehabilitation and Slope Stability:
 - The upstream slopes of each dam require restoration of concrete protection slabs and reinforcement of drainage systems to prevent erosion

- and stabilize slopes. Restoration includes vegetation regrowth on downstream slopes to improve soil stability and mitigate erosion, while ensuring a healthy vegetative cover to further protect structural integrity.
- Bottom outlets and spillways will undergo repairs to ensure optimal discharge capability, crucial for managing high inflows and preventing overflow risks.
 - Hydromechanical and Electrical System Upgrades:
 - All three dams will receive updated hydromechanical components, including replacement of bottom emptying sluices, medium water sluices, and cofferdams, ensuring efficient water discharge control. Mechanisms are being replaced with modern actuation systems to improve reliability under varying flow conditions.
 - Electrical systems powering these components, along with safety and control systems, will also be upgraded to align with current standards. Automation, powered by SCADA (Supervisory Control and Data Acquisition) systems, centralizes data collection and enables real-time monitoring for proactive response to environmental and operational fluctuations.
 - Advanced Monitoring with Fiber Bragg Grating (FBG) Sensors:
 - FBG sensors will be integrated across the dams to measure strain, stress, temperature, and other critical parameters, delivering high-resolution data for structural health monitoring. This data, processed through SCADA, facilitates predictive maintenance and early detection of potential structural issues, enhancing overall dam safety.
 - Ecological Flow and Connectivity:
 - **Fish Migration Support:** Each dam will incorporate a FishFlow siphon-type fish ladder, enabling upstream and downstream migration for aquatic species. These siphon ladders include vacuum-controlled air pumps to maintain flow consistency, allowing for a regulated ecological flow that supports biodiversity in the river basin.
 - **Sediment Management and Environmental Flow:** Bottom outlets in each dam are adjusted to support seasonal sediment flushing, which preserves channel depth and mitigates downstream sediment accumulation. The dams are also calibrated to release minimum environmental flows, ensuring that downstream habitats receive adequate water levels year-round.
 - Sustainable and Ecological Enhancements:
 - **Floating “Green” Islands:** Floating islands made of vegetation will be installed in each reservoir to improve water quality through natural filtration, reducing risks of eutrophication and providing habitat for local bird species. These islands promote a balanced ecosystem while enhancing the dams’ environmental impact profile.
 - **Forest Buffers and Waste Management:** Protective forest curtains around the reservoirs will be established to prevent wind and water erosion, reduce sediment inflow, and improve air quality. A floating waste capture system will also be implemented, consisting of recycled materials and floating arms to intercept debris and pollutants before they enter the waterbody.

3.1.2. *Site-specific details*

1. Cucuteni Dam (Voinești River, 1964)
 - **Structural Complexity:** Constructed from loessoid clays and divided into two main bodies, Cucuteni Dam spans 8,377 meters with a maximum height of 13.75 meters. It requires restoration of its drainage layer, support spur, and the road bridge over its spillway.



Fig. 1
Upstream view of Cucuteni dam
Vue amont du Barrage Cucuteni

- **Economic Impact:** Rehabilitation of Cucuteni Dam is expected to yield cost savings of approximately 40% over new construction and extend the dam's operational life by an estimated 30 years. The economic analysis further highlights benefits for regional agriculture and industry reliant on a steady water supply.

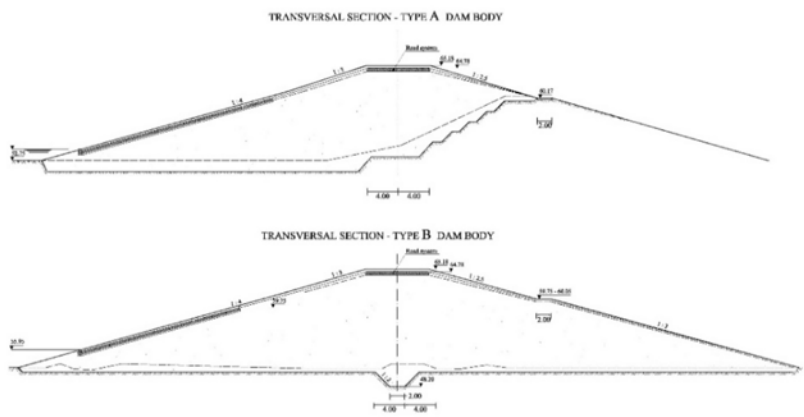


Fig. 2
Transversal cross section [7]
Coupe transversale du barrage Cucuteni

2. Căzănești Dam (Stavnic River, 1975)
- **Drainage and Channel Systems:** Căzănești features a two-stage drainage system (internal and downstream drains) critical for controlling seepage. The dam will receive unclogging works in discharge channels and restoration of the high-water spillway. A hydrometric station will be installed downstream, equipped with radar and video systems for monitoring water levels, temperature, and potential blockages.
 - **Cost-Benefit Analysis:** This rehabilitation offers a 35% cost reduction over building a new structure, with enhanced water retention and flood control yielding additional economic resilience for local communities.



yielding additional economic resilience for local communities.

Fig. 3
Aerial view of Cazanești Dam
Vue aérienne du Barrage Cazanești

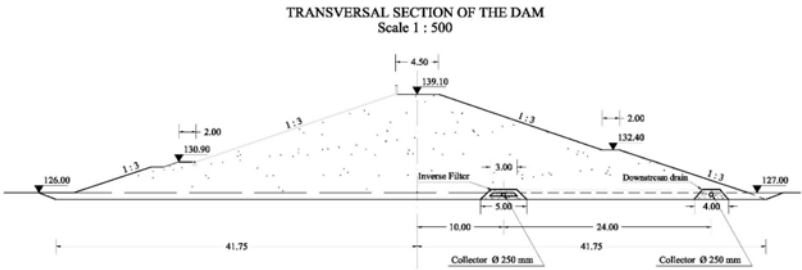


Fig. 4
Transversal cross section [8]
Coupe transversale du barrage Căzănești

3. Solești Dam (Vaslui River, 1974)
- **Drainage Mattress and Discharge Wells:** Solești is fitted with a 50-60 cm drainage mattress and multiple discharge wells that play a vital role in seepage control. Rehabilitation will include reinforcement of this drainage infrastructure to maintain stability.

- **Photovoltaic System for Energy Efficiency:** A new photovoltaic array (20 kW capacity) will be installed to power operational and monitoring equipment sustainably. This renewable energy solution aligns with national goals for reducing environmental footprints and operational costs.

3.1.3. *Environmental and economic considerations*

- Environmental Flow and Biodiversity Support:
 - The consistent ecological flow released through the bottom outlets ensures the sustainability of downstream habitats and supports biodiversity. Fish ladders provide critical connectivity, while sediment flushing at each dam prevents excessive sediment buildup, maintaining channel morphology and downstream habitat quality.
- Economic Viability and Lifecycle Extension:
 - The comprehensive upgrades planned for Cucuteni, Solești, and Căzănești dams are significantly cost-effective, with cost-benefit analyses projecting around 30-40% savings compared to new construction. Each dam's operational life is expected to extend by 25-30 years, benefiting water-dependent agricultural and industrial sectors.
- Comparative International Context:
 - These dam rehabilitations align with international projects emphasizing sustainability and structural resilience, such as Spain's Almendra Dam, where similar monitoring, ecological integration, and SCADA automation have been implemented. These cross-referenced practices underscore a holistic approach to dam modernization, balancing flood resilience, structural integrity, and ecological responsibility.

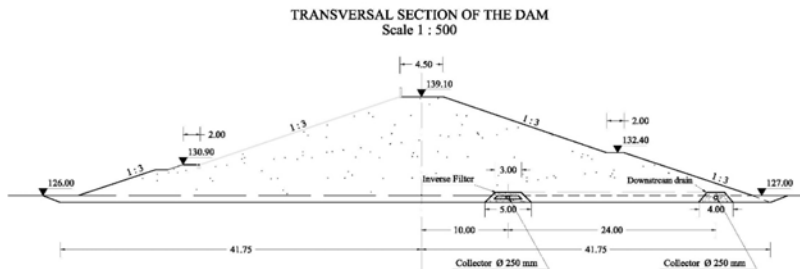


Fig. 5
Transversal cross section [9]
Coupe transversale du barrage Solești

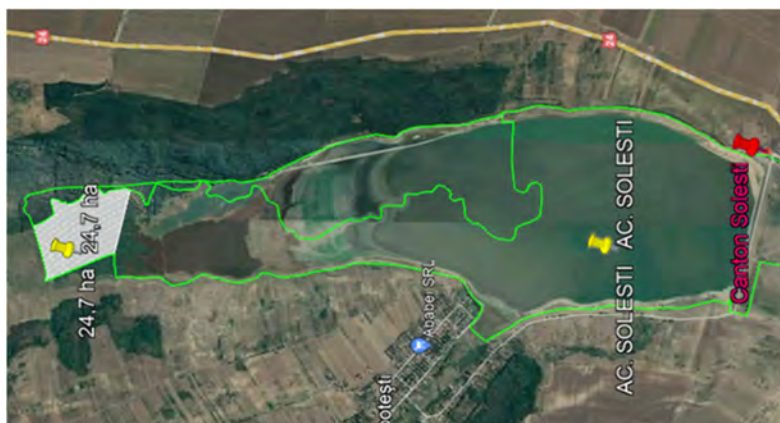


Fig. 6
Aerial view of Solesti Dam
Vue aeriennne du Barrage Solesti

3.2. ECOLOGICAL CONSIDERATIONS AND ENVIRONMENTAL IMPACT

It is mandatory that the measures adopted are not harmful to the good condition or the good ecological potential of water bodies, including surface and groundwater, and they will not lead to a significant increase in pollutant emissions to air, water or soil.

Significant increases in the generation, incineration or disposal of waste must be avoided, except for the incineration of non-recyclable hazardous waste.

- Risks of environmental degradation related to protecting water quality and avoiding water stress have been identified and addressed in accordance with the requirements set out in the Water Framework Directive and the river basin management plan.
- The potential impact of dam rehabilitation projects on the environment, including works located in the vicinity or in Natura 2000 sites, was assessed in accordance with the provisions of the EIA Directives, the Habitats Directive and the Birds Directive, with particular attention being paid to the project's potential impact on specific objectives / the minimum conservation measures established for the species and habitats for which the sites were designated, as well as the assessment of the cumulative impact (among proposed, existing or regulated investments) on environmental factors.

3.2.1. *Ensuring ecological flows and sediment transport*

The evacuation of the the ecological flow can be ensured by adjusting the opening of the bottom outlet gate (the classic solution used) or it can be ensured by the fish ladder proposed in the investment; the flow through the fish ladder is 10-50 l/s.

The minimum flow of sediments can be ensured by adjusting the opening of the bottom emptying valve (classic solution); the cleaning of the sediments in front of the culverts is usually done by fully opening them, the current and the speed driving the sediments deposited along the exploitation.

3.2.2. *Enhancing connectivity for aquatic species*

To ensure the longitudinal connectivity of the water course and to ensure the migration of fish downstream and upstream of the dam, a siphon-type tubular fish ladder called FishFlow will be installed.

This type of ladder is based on the principle of siphoning; that is, a siphon with an air bubble that defines the flow through the system. The siphon fish ladder shall be equipped with a vacuum pump that controls the volume of the air bubble to prevent the flow rate from changing due to the import or export of gas from the water.

A vent valve shall be provided as a safety measure to ensure that the siphon cannot start operating at full flow should the vacuum pump malfunction and pump continuously. The water to be siphoned will consequently flow over a conventional fish ladder in the downstream section of the river.

3.3. CONOMIC AND REGULATORY CONSIDERATIONS

The rehabilitation of the Cucuteni, Solești, and Căzănești dams must balance economic feasibility with stringent regulatory compliance to ensure sustainability and operational resilience. These interventions prioritize durability, with materials and construction methods intended to meet the minimum lifespan for hydrotechnical infrastructure, typically between 40 and 60 years. The extended operational lifespan provided by these upgrades reduces future maintenance needs, supports strategic water management, and enhances flood resilience.

3.3.1. *Cost-benefit analysis and funding strategies*

A detailed economic analysis was conducted in accordance with EU guidelines and the Methodology for Assessing Flood Damages and Losses, specifically tailored to meet the requirements of Cycle 2 of the EU Flood Directive. Developed by the HKV, DHI, and ESSENSYS consortium with support from the World Bank, this methodology offers an analytical framework to quantify both tangible and intangible impacts of flood events, facilitating comprehensive risk management. Key economic considerations include:

- **Monetary Damages and Loss Estimation:**
 - **Directly Tangible Damages:** Immediate repair costs for structural and mechanical components following flood events are factored into the analysis. These include repairs to spillways, embankments, and hydro-mechanical systems that directly affect operational safety.
 - **Indirectly Tangible Damages:** Economic impacts from disrupted water supply and irrigation are also considered, particularly relevant to agriculture-heavy regions. As these dams lack hydropower capabilities, the focus remains on preventing economic disruptions tied to water scarcity or flood damage.
 - **Intangible Damages:** Long-term ecological impacts, such as biodiversity loss and ecosystem disruption, are factored in as indirectly intangible damages. These are addressed through ecological enhancements to protect biodiversity and reduce adverse environmental impacts.
- **Cost-Benefit Assessment:**
 - The analysis indicates that rehabilitation yields approximately 30-40% cost savings over new construction, spreading the benefits over an extended operational lifespan of 25-30 years. Strategic water management, including consistent water supply and enhanced flood control, offers significant economic value by mitigating flood risks and ensuring agricultural productivity.
 - The cost-benefit analysis further highlights that preventive rehabilitation can avert costly emergency repairs and minimize the financial and environmental toll of flood damage, thus supporting stable economic conditions for the affected regions.
- **Funding Strategies:**
 - **EU Cohesion and Structural Funds:** EU support, through programs such as the Cohesion Fund, provides critical financing for these projects, given their alignment with EU objectives for environmental sustainability, flood resilience, and ecological restoration. This funding avenue is particularly relevant as these dams serve public goods rather than generating direct economic returns through hydropower.
 - **National and Regional Grants:** Romania's government, through its National Flood Risk Management Program, allocates grants specifically for strategic infrastructure improvements like these dams. Regional development funds also support projects that enhance water management and disaster resilience, addressing community needs without relying on private investment models.

- **Multilateral Development Bank Loans:** Loans from organizations like the World Bank provide another viable funding option. These institutions support projects with strategic importance in flood protection and water resource management, aligning with the dams' role in ensuring water security and reducing flood risk.
- **Eco-Services Valuation:**
 - The rehabilitation of the Cucuteni, Solești, and Căzănești dams offers substantial ecological services, which contribute to both environmental health and local economies. Key eco-services include water purification, carbon sequestration, biodiversity support, and flood mitigation. The financial valuation of these services is estimated at approximately €3,000–€5,000 per hectare annually, taking into account benefits such as habitat provision, water filtration, and floodplain management.
 - The floating “green” islands and forest curtains incorporated into each dam’s design offer water purification through natural filtration processes, which reduce treatment costs for downstream water use. Biodiversity support is enhanced by fish ladders and ecological flow management, which maintain species continuity and ecosystem health. By providing these eco-services, the dams contribute significant non-monetary value that sustains regional ecological stability and resilience against climate change impacts.

3.3.2. *The role of regulatory frameworks in sustainable development*

Romanian and EU regulatory frameworks guide the sustainable development of these hydrotechnical projects, ensuring economic and environmental stability alongside public safety. Compliance with these frameworks fosters resilience and safeguards ecological health while meeting operational and strategic objectives. Key regulatory influences include:

- **EU Flood Directive and Water Framework Directive:**
 - The EU Flood Directive mandates that member states develop flood risk management plans to reduce damage to human health, the environment, cultural heritage, and economic activities. Romania’s adaptation of this directive requires these dams to serve as key elements in a comprehensive flood risk reduction strategy.
 - The Water Framework Directive (WFD) stipulates that all water bodies must achieve a “good” ecological and chemical status. As part of compliance with WFD goals, these dam projects integrate measures such as ecological flow maintenance, fish ladders, and sediment management to sustain aquatic ecosystem health in the Prut-Bârlad basin.
- **Environmental Impact Assessment (EIA) and Strategic Environmental Assessment (SEA):**
 - The EIA Directive mandates that projects impacting the environment undergo a full assessment to identify and mitigate potential adverse

- effects. For the Cucuteni, Solești, and Căzănești dams, EIA studies focused on downstream impacts, including sediment flow adjustments, environmental flow requirements, and habitat preservation, ensuring that these interventions are sustainable.
- The SEA Directive complements the EIA by requiring strategic assessments of environmental implications for plans and programs that influence larger hydrological basins. For these dams, SEA assessments confirm the alignment of project objectives with broader environmental goals and validate their contribution to regional flood resilience.
 - Natura 2000 and Habitat Conservation Compliance:
 - These dam projects are located near environmentally sensitive areas, mandating adherence to the Natura 2000 conservation requirements under the Habitats and Birds Directives. Measures to maintain fish migration, ensure sediment transport, and sustain ecological flows protect the designated species and habitats within these areas.
 - Restoration activities include the installation of FishFlow siphon ladders to support migratory species, floating vegetated islands to aid in natural water purification, and forest buffers to mitigate erosion, all aligning with habitat preservation and biodiversity support.
 - National Building Standards for Hydrotechnical Infrastructure:
 - Romanian building standards set a minimum operational lifespan of 40-60 years for hydrotechnical structures, guiding material selection and construction techniques. For these dam rehabilitations, materials are selected for durability and resistance to hydrological pressures, accommodating potential climate-related stressors.
 - Design adaptations further ensure that these dams can handle increasing flood magnitudes and intensities, preserving both structural integrity and their ecological roles over the long term.
 - Community Engagement and Stakeholder Involvement:
 - Regulatory frameworks encourage public involvement in infrastructure projects, ensuring that the dams' rehabilitation addresses community needs for water availability, flood protection, and ecological integrity. Public consultations and informational sessions conducted during the planning phases have provided valuable local insights, facilitating alignment with stakeholder expectations.
 - Engaging with communities throughout the process has fostered support and cooperation for these upgrades, helping to ensure that the projects are not only regulatory compliant but also meet the practical needs of the populations they serve.

3.3.3. *Ensuring equitable benefits from dam projects*

To ensure that dam projects deliver benefits equitably across affected communities, it is essential to consider both direct and indirect social, economic, and

environmental impacts. Dams provide critical resources, such as water supply, flood control, and agricultural support, that are often lifelines for local communities. However, equitable benefit distribution requires engaging diverse stakeholders—local residents, industries, environmental organizations, and policymakers—early in the planning stages. By including these voices, project planners can ensure that the needs of different groups are considered, minimizing any potential adverse impacts and enhancing community support. This approach fosters transparency, building trust and collaboration, which are vital for the long-term success of dam projects.

While dam removal is sometimes pursued internationally to restore river ecosystems and support fish migration, this option is not universally applicable and is context-dependent. Rather than removal, the focus for many existing dams should be on adaptive measures that maintain ecological flow, install fish passage systems, and integrate advanced monitoring technologies to ensure both human and environmental needs are met. Systems like FishFlow's siphon fish ladders, widely used in Europe, are examples of such adaptations, promoting fish migration while preserving the dam's utility. Ensuring that dam projects balance ecological sustainability with human benefits is key to maximizing positive outcomes for all stakeholders and fostering resilient infrastructure that serves communities equitably.

3.4. COMMUNITY ENGAGEMENT AND STAKEHOLDER INVOLVEMENT

3.4.1. *The importance of local community participation*

Community involvement is crucial in the successful implementation and long-term sustainability of water infrastructure projects, especially for the dams at Cucuteni, Solești, and Căzănești in Romania. Both the project's provider and beneficiary are committed to engaging with local stakeholders to mitigate any potential risks and ensure smooth progress throughout the project lifecycle, from planning to post-implementation. Engaging the local community helps identify and address potential issues that might hinder project operations or environmental sustainability.

These dam projects align with the economic and social development agendas of Iași and Vaslui counties, as outlined in the regional plans for agriculture and sustainable rural development. Specific contributions include:

- **Enhanced Water Supply:** The projects aim to improve both the quantity and quality of the water supply for the local population, addressing a fundamental community need and fostering trust in regional water management efforts.
- **Economic and Agricultural Growth:** By ensuring reliable water availability for irrigation, these projects enable higher agricultural productivity and contribute to the local economy. The improved water storage capacity also supports local fishery potential, encouraging sustainable aquaculture that could provide additional revenue streams for the community.

- **Stakeholder Consultation and Feedback Mechanisms:** Early and consistent communication with community members helps to align the project's objectives with local needs, increasing project acceptance and fostering collaboration. Regular updates on project milestones, environmental impacts, and timelines build transparency and maintain public support.

By actively involving local stakeholders, the project not only gains valuable insights into regional needs but also builds a framework for long-term cooperation, enhancing the project's resilience, acceptance, and effectiveness in the local context.

3.4.2. *Direct and indirect benefits of the project*

The Cucuteni, Solești, and Căzănești dam rehabilitation projects deliver direct flood protection benefits and substantial indirect gains that strengthen infrastructure resilience, protect economic assets, and support ecosystem stability.

- **Direct Benefits**

The primary direct benefit is the enhanced flood control capacity, which mitigates the risk of catastrophic downstream flooding. By improving structural integrity and discharge systems, the project ensures the reliable containment and controlled release of floodwaters, thereby reducing potential damage to communities, infrastructure, and agriculture.
- **Indirect Benefits**
 - **Enhanced Safety and Reduced Social Costs:**
 1. **Risk Mitigation:** Strengthened infrastructure minimizes the danger to residents and the need for emergency response measures, which lowers social aid and sheltering costs during flood events.
 - **Economic Resilience and Property Value Protection:**
 1. **Infrastructure Stability:** By preventing damage to roads, utilities, and other networks, the project preserves vital infrastructure, minimizing repair costs and economic disruption.
 2. **Business Continuity:** By reducing flood-induced production interruptions, local industries experience fewer losses, fostering a more stable economic environment and encouraging future investments.
 - **Improved Quality of Life:**
 1. **Sustainable Water Supply and Ecosystem Health:** Enhanced water storage and flood control contribute to public health and quality of life, while supporting a favorable environment for economic growth and community development.
- **Environmental Benefits**

The project integrates environmental enhancements to maintain water quality, support biodiversity, and reduce ecological impacts:

 - **Floating "Green" Islands:** These islands act as natural water filters, prevent eutrophication, and provide habitat for wildlife, contributing to reservoir ecosystem stability.

- **Floating Waste Collection Systems:** Waste collection devices capture floating debris, improving water quality and reducing downstream pollution.
- **Ecological Flow and Fish Passage:** Ensuring ecological flow and installing fish ladders support aquatic habitat continuity, fish migration, and biodiversity.
- **Forest Curtains:** Protective tree lines reduce sedimentation, stabilize reservoir banks, and enhance carbon sequestration, supporting erosion control and air quality improvement.

3.5. COSTING AND PROJECT DEVELOPMENT

Given the requirements of Romania's **National Recovery and Resilience Plan (PNRR)**, which mandates a **green component** and a **digital component** for project eligibility, the cost allocation for the Cucuteni, Solești, and Căzănești dam rehabilitations includes designated budgets to fulfill these criteria. Compliance with these requirements ensures access to PNRR funding while enhancing environmental sustainability and digital modernization within the project.

- **Revised Cost Structure with PNRR Components**
 - In accordance with **HG 907/2016** and PNRR funding criteria, project costs are divided into **Base Investment Costs** and **Ancillary Costs**, with specific allocations for green and digital components. The following structure provides a balanced distribution to address these critical aspects.
- **Base Investment Costs (65-75%)**
 - These costs cover core construction, ecological, and digital components directly related to the dams' functionality and regulatory compliance.
- **Civil Engineering Works (50-55%):** This main category includes foundational construction elements like slope stabilization, spillway upgrades, and structural reinforcement. These works are fundamental to ensure dam safety, flood resilience, and operational longevity.
- **Green Component (10%):** In line with PNRR's green mandate, approximately 10% of the total budget is allocated to environmental sustainability measures, such as:
 - **Floating "Green" Islands** to enhance water quality through natural filtration and prevent eutrophication.
 - **Fish Ladders and Ecological Flow Management** to support aquatic biodiversity and maintain ecological connectivity.
 - **Forest Curtains** along the reservoir banks to reduce wind and water erosion, enhance biodiversity, and sequester carbon.
- **Digital Component (5-10%):** Dedicated to fulfilling PNRR's digitalization requirements, this portion funds digital technology integration, including:
 - **SCADA Systems** for real-time monitoring of water levels, structural stability, and flood control parameters.

- **Fiber Bragg Grating (FBG) Sensors** for monitoring strain, stress, and temperature across dam structures, supporting predictive maintenance and early warning systems.
- **Automated Data Transmission and Analysis Tools** for streamlined data collection, predictive analytics, and operational optimization.
- **Ancillary Costs (25-35%)**
 - Ancillary costs address regulatory compliance, detailed planning, management, and contingencies, ensuring project readiness and alignment with Romanian law and EU standards.
 - **Design and Engineering Studies (5-10%)**: Initial design and engineering analysis, mandated by HG 907/2016, account for 5-10% of the budget. These studies are critical for validating structural and environmental integrity and for integrating green and digital components effectively.
 - **Permitting, Environmental Impact Assessments (EIA), and Regulatory Compliance (5-8%)**: Around 5-8% is reserved for regulatory compliance, including EIAs, public consultations, and necessary permits to align the project with legal and environmental standards.
 - **Project Management, Monitoring, and Contingencies (10-15%)**: Up to **15%** of the budget is allocated for contingencies to manage unforeseen challenges, as stipulated by Chapter 7 of HG 907/2016. This category also covers project management, quality control, and post-implementation monitoring. The contingency fund, given PNRR's requirements, includes adaptive measures for green and digital components, ensuring flexibility for environmental or digital upgrades as needed.

This cost structure meets the dual demands of HG 907/2016 and PNRR requirements, supporting both **environmental sustainability** and **digital transformation**. The dedicated allocations for green and digital components not only ensure funding eligibility but also promote resilience, ecological integrity, and modernization in line with EU green and digital standards.

4. CONCLUSION

4.1. SUMMARY OF STRATEGIES FOR FUTURE-PROOFING DAMS

Recent flood events across Europe have underscored the critical need to enhance the resilience and sustainability of dam infrastructure. To future-proof dams effectively, the following strategies are essential:

1. **Structural Rehabilitation and Modernization**: Addressing aging infrastructure through comprehensive assessments and targeted repairs is vital. This includes reinforcing foundations, upgrading spillways, and ensuring the structural integrity of dams to withstand extreme weather events.

2. **Integration of Advanced Monitoring Systems:** Implementing Fiber Bragg Grating (FBG) sensors and Supervisory Control and Data Acquisition (SCADA) systems enables real-time monitoring of dam conditions. These technologies facilitate proactive maintenance and rapid response to potential issues, enhancing operational safety.
3. **Ecological and Environmental Enhancements:** Incorporating features such as fish ladders, floating islands to prevent eutrophication, and floating waste collection systems improves ecological connectivity and water quality. Ensuring adequate ecological flow supports aquatic ecosystems and aligns with environmental sustainability goals.
4. **Compliance with Regulatory Frameworks:** Adhering to national and European Union regulations, including the EU Floods Directive, ensures that dam operations meet safety and environmental standards. Regular audits and updates to operational protocols are necessary to maintain compliance.
5. **Community Engagement and Stakeholder Involvement:** Engaging local communities and stakeholders in the planning and implementation phases fosters transparency and addresses social concerns. This collaborative approach enhances public trust and ensures that projects meet the needs of affected populations.
6. **Financial Planning and Cost-Benefit Analysis:** Conducting thorough economic analyses, including cost-benefit assessments and funding strategies, ensures the financial viability of refurbishment projects. Allocating budgets for base investments and ancillary costs, such as design studies and environmental impact assessments, is crucial for comprehensive project planning.

4.2. THE PATH FORWARD FOR RESILIENT AND SUSTAINABLE WATER MANAGEMENT SYSTEMS

To develop resilient and sustainable water management systems, a multi-faceted approach is required:

- **Adoption of Integrated Water Resources Management (IWRM):** Implementing IWRM principles promotes the coordinated development and management of water, land, and related resources. This approach balances social, economic, and environmental objectives, ensuring sustainable water use.
- **Investment in Green and Digital Components:** Aligning with programs like the National Recovery and Resilience Plan (PNRR), incorporating green and digital components is essential. This includes investments in renewable energy sources, digital monitoring systems, and sustainable infrastructure practices.
- **Enhancement of Flood Mitigation Measures:** Developing comprehensive flood risk management plans that include both structural measures (e.g.,

levees, floodwalls) and non-structural measures (e.g., early warning systems, land-use planning) reduces vulnerability to flood events.

- **Promotion of Dam Removal Where Appropriate:** In cases where dams are obsolete or pose environmental risks, removal can restore river ecosystems and improve biodiversity. The European dam removal movement has seen significant progress, with a record number of barriers removed in recent years, this action as important as it might be seen has to be taken with great caution as the benefits have to be weighted before hand giving into the “green policy” with huge regrets later.
- **Strengthening of Policy and Regulatory Frameworks:** Updating and enforcing policies that promote sustainable water management practices, including the maintenance and refurbishment of existing infrastructure, is crucial. This ensures that water management systems are resilient to climate change and other emerging challenges.

By implementing these strategies, water management systems can be enhanced to meet current and future demands, ensuring the safety, sustainability, and resilience of water resources for communities across Europe.

REFERENCES

- [1] WASKO C., WESTRA S., NATHAN R., ORR H.G., VILLARINI G., HERRERA R.V., FOWLER H.J. Incorporating climate change in flood estimation guidance. *Philosophical Transactions A, The Royal Society Publishing*, 2021, 379: 20190548.
- [2] MARTEL J.L., BRISSETTE F.P., LUCAS-PICHER P., TROIN M., ARSENAULT R. Climate Change and Rainfall Intensity–Duration–Frequency Curves: Overview of Science and Guidelines for Adaptation. *Journal of Hydrologic Engineering*, 2021, Volume 26, Issue 10.
- [3] REYNARD N.S., KAY A.L., ANDERSON M., DONOVAN B., DUCKWORTH C. The evolution of climate change guidance for fluvial flood risk management in England. *Progress in Physical Geography: Earth and Environment*, 41(2), 2017, 222–237.
- [4] IRADUKUNDA P., MWANAUMO E.M., KABIKA J. A review of integrated multicriteria decision support analysis in climate-resilient infrastructure development. *Environmental and Sustainability Indicators*, Volume 20, 2023, 100312, ISSN 2665-9727.
- [5] SCHLEISS A.J. Sustainable and safe development of dams and reservoirs as vital water infrastructures in this century - the important role of ICOLD. International Dam Safety Conference, 2018, Kerala, India.

- [6] WATTS R., RYDER D.S., ALLAN C., COMMENS S. Using river-scale experiments to inform variable releases from large dams: a case study of emergent adaptive management. *Marine and Freshwater Research*, 61 (7):786–797, 2009.
- [7] AQUAPROIECT S.A. Documentation for approval of intervention works for improving safety operating conditions of permanent accumulation Cucuteni, on the Voinești river, Iași county. PRUT-BARLAD WATER BASIN ADMINISTRATION, 2023.
- [8] AQUAPROIECT S.A. Documentation for approval of intervention works for improving safety operating conditions of permanent accumulation Căzănești, on the Stăvnic river, Vaslui county. PRUT-BARLAD WATER BASIN ADMINISTRATION, 2023.
- [9] AQUAPROIECT S.A. Documentation for approval of intervention works for improving safety operating conditions of permanent accumulation Solești, on the Vaslui river, Vaslui county. PRUT-BARLAD WATER BASIN ADMINISTRATION, 2023.
- [10] ICOLD (International Commission on Large Dams). Dam Safety and Risk Management. International Commission on Large Dams, 2019. Guide for the safety and risk management associated with large dams.
- [11] UNESCO-IHP. Sustainable Management of Water Resources in Agriculture. Food and Agriculture Organization (FAO), 2017. Analysis of the role of dams in sustainably securing water resources for agriculture.
- [12] WORLD COMMISSION ON DAMS (WCD). Dams and Development: A New Framework for Decision-Making. Earthscan Publications Ltd., 2000. Comprehensive evaluation of the environmental and societal impacts of dams with recommendations for future sustainable management.
- [13] INTERNATIONAL COMMISSION ON LARGE DAMS (ICOLD). Dam Safety and Risk Management. ICOLD, 2019. Guide for managing risks and ensuring dam safety in the context of modern requirements.
- [14] IPCC (INTERGOVERNMENTAL PANEL ON CLIMATE CHANGE). Climate Change 2021: Impacts, Adaptation, and Vulnerability. Cambridge University Press, 2021. Detailed report examining the impact of climate change on hydrological infrastructure, including dams, and necessary adaptation strategies.
- [15] INTERNATIONAL COMMISSION ON LARGE DAMS (ICOLD). Flood Risk Management for Dams. ICOLD, 2019. Guide on flood risk management for dams, emphasizing the effects of extreme precipitation.

- [16] THOMAS, J. Sustainable Concrete for Infrastructure. *Journal of Sustainable Construction*, 2015.
- [17] NATIONAL RECOVERY AND RESILIENCE PLAN (PNRR), Romania. National Recovery and Resilience Plan Guidelines, 2021. Strategic plan guiding sustainable and digital infrastructure developments with green components mandatory for funding.
- [18] FISHFLOW INNOVATIONS. Fish siphon ladder systems for sustainable fish migration solutions. FishFlow Innovations, Netherlands. Available at: fishflowinnovations.nl.

COMMISSION INTERNATIONALE DES
GRANDS BARRAGES

VINGT-HUITIEME CONGRES DES
GRANDS BARRAGES
CHENGDU, MAI 2025

ROSSWIESE RESERVOIR – REFURBISHMENT OF A 65-YEAR-OLD DRAINAGE SYSTEM FOR THE NEXT 65 YEARS (*)

Florian LANDSTORFER
Dam Safety Engineer
VERBUND HYDRO POWER

AUSTRIA

SUMMARY

Rosswiese reservoir was built in the 1950s as a reservoir with an asphalt surface lining. A comprehensive drainage system was built for several purposes. After 65 years of operation, the asphalt lining had to be renewed and this opportunity for an inspection and modernization of the drainage system should be seized. Based on the works carried out, investigation as well as refurbishment, important and helpful lessons for future projects and the upgrading of existing drainage systems could be learned. The main challenge is to foresee future developments, that enable new methods of monitoring, investigation, or refurbishment. Although often seen as minor important, the ability to inspect and repair a drainage system can have a major impact on the safety assessment of a dam or a reservoir. Therefore, the design of a drainage system has to be done carefully.

RÉSUMÉ

Le réservoir de Rosswiese a été construit dans les années 1950 avec une membrane asphaltique. Un système de drainage en dessous de la membrane a été

*Rénovation d'un système de drainage vieux de 65 ans pour les 65 prochaines années

installée. Après 65 années d'utilisation, la membrane asphaltique a dû être changée. En même temps, les drainages ont été vérifiés. Après un contrôle vidéo, seulement des réparations locales ont été entreprises. Ces travaux ont permis d'acquérir une meilleure connaissance pour des travaux similaires de maintenance ou des nouveaux projets dans le futur. Lors de la planification et construction d'un barrage, il est nécessaire de planifier la possibilité de faire des inspections vidéo sans interruption majeure de l'exploitation de la centrale hydroélectrique.

1. INTRODUCTION

Rosswiese reservoir is an artificial reservoir with an asphalt surface lining and was commissioned in 1958. The reservoir is used as a daily reservoir for a hydro power plant. After 65 years of operation the asphalt lining had to be renewed. Important boundary conditions for the project were the limited space on site for the machinery and the short time slot due to the economic importance of the dam. The comprehensive refurbishment included the removal of the sediments in the reservoir, a new asphalt lining and an upgrade of the drainage system.

2. DESCRIPTION OF THE RESERVOIR

2.1. KEY DATA

- Dam crest 1.196 m asl
- Length of dam crest 535 m
- Max. operating level 1.194 m asl
- Min. operating level 1.180 m asl
- Max. dam height ~23,5 m
- Dam volume ~125.000 m³
- Reservoir volume 204.000 m³
- Slope waterside 1 : 1,75
- Slope airside 1 : 1,5
- Catchment area 114 km²
- Annual inflow 124.000.000 m³

2.2. GEOLOGY

The reservoir is situated on a roughly 100 m wide terrace that was formed by a rock hummock. A geological exploration showed that on the downhill rim of the

terrace the crystalline rock is only 0,2 to 2,0 m below ground surface. On the uphill side, the rock was about 10 m below ground surface, due to the hummock. The overlying strata consists of moraine material. The crystalline foundation mainly consists of mica schist and slate gneiss. The general slope inclination of the mountain is 25° to 35° .

2.3. DESIGN

Due to the topography, the uphill slope of the reservoir, about 25 % of the crest length, was excavated into the natural slope, as shown in figure 1.

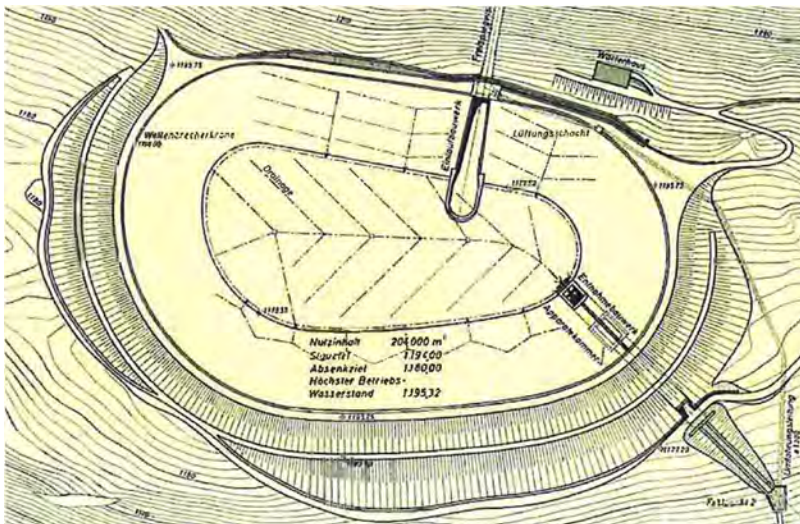


Fig. 1
Layout plan
Plan de situation

The lower part of the downhill side dam and the biggest part of the foundation are founded on rock. Figure 2 shows the typical cross section of the dam and the rock surface before the beginning of construction, marked by the red line. The dam was built as a zoned dam with the strictest requirements for the material on the water side and less strict requirements on the airside.

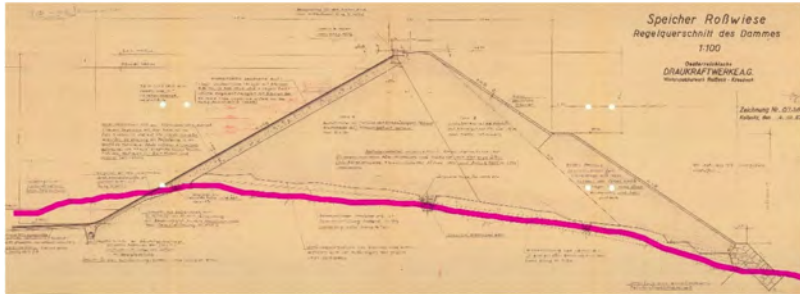


Fig. 2
Cross section of the dam
Profil en travers du barrage

2.3.1. Sealing

As the sealing element, a surface lining made of asphalt concrete was chosen. The lining consists of:

- Mastix
- 2 x 4,5 cm dense asphalt layer
- 6 cm binder asphalt layer

In order to level the roughness of the excavated rock at the uphill slope, a layer of lean-mixed concrete was placed. Furthermore, this concrete was designed as a drainage layer and therefore it was placed as a double-grain concrete. The same design was chosen, if the lower part of the dam had been excavated from the rock. In the upper parts of the dam, a 80 cm layer of frost blanket gravel was placed as a levelling course for the asphalt lining. At the bottom of the reservoir a 15 cm layer of non-angular gravel was placed as a levelling course.

2.3.2. Drainage system

The drainage system can be split in 3 sections, which have been designed for different purposes. The whole drainage system is made of concrete pipes with an inner diameter varying from 200 mm to 400 mm. The weep holes of the pipes have a diameter of about 20 mm. Hence, fine material could enter the pipe, because the minimum diameter of the surrounding material did not match the weep hole diameter and no filter material had been placed around the drainage pipes. An overview of the drainage system is given in figure 3. Drainage pipes are drawn as dashed lines, collector pipes are drawn as solid lines.

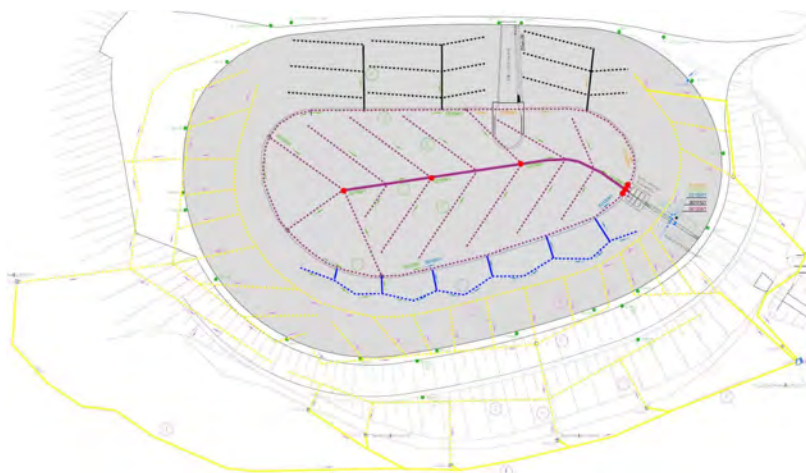


Fig. 3
Drainage system – overview
Système de drainage – vue d'ensemble

At the downhill slope of the reservoir, drainage pipes at the joint concrete – frost blanket gravel (blue lines in figure 3), have been installed in order to drain the frost blanket. These pipes drain to the circumferential drainage at the dam toe and some of them from there on to the collector pipe in the middle of the reservoir. In addition, there are drainage pipes at the joint bedrock – dam body (yellow lines in figure 3). These pipes drain to the downhill dam toe.

At the uphill slope of the reservoir, the drainage system (black lines in figure 3), was built for 2 purposes. The first one is to monitor leakage through the asphalt lining. The second purpose is to relief mountain water from the rock underneath the asphalt lining and thus reduce the risk of a damage of the asphalt lining due to mountain water. In case of a water flow in this part of the drainage system, leakage cannot be distinguished from mountain water as both of them flow through the same pipes.

At the bottom of the reservoir (purple lines in figure 3), a system of perforated drainage pipes, placed in a herringbone and as a circumferential drainage at the waterside dam toe was installed. In the middle of the reservoir, a non-perforated collector pipe drains the water from the herringbone pipes to the measuring weir. At each connecting point, except the connection to the collector pipes in the slopes, a concrete shaft was built. In total 14 shafts were built, 6 access shafts (red dots in figure 3 and 4) with a steel lid, that enabled an access to the drainage pipes, and 8 non-access shafts, which had been covered by the asphalt lining. So only a part of the drainage

system (green lines in figure 4) was accessible, as shown in figure 4. The accessibility of the collector pipes at the waterside dam toe depended on the curvature of the pipe and the ability of the camera to tow the cable along the curvature due to the friction. The predominant part of the drainage system was built at the joint bedrock – dam body, but only a very small part of it is accessible for camera inspection.

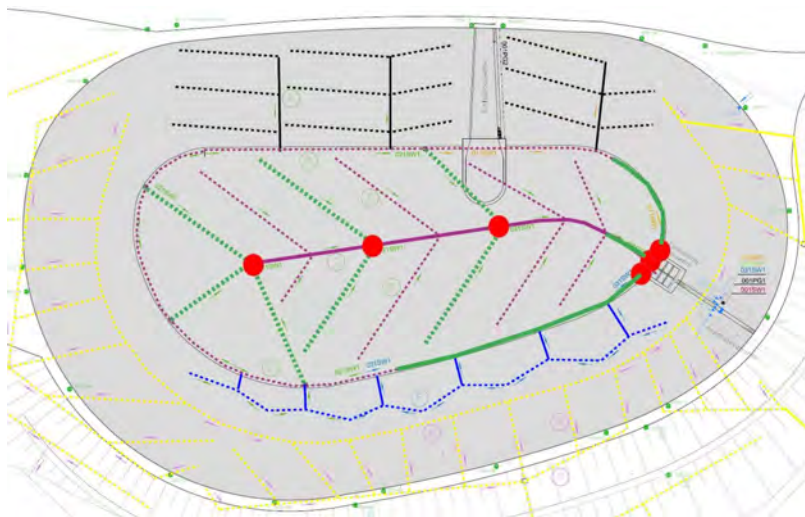


Fig. 4
Drainage system – accessible pipe runs
Système de drainage – gaine accessible

2.4. MEASUREMENTS

The drainage system at the bottom, the uphill slope and the downhill slope of the reservoir is split in three sections. Each can be measured manually and the sum of all three of them is monitored automatically. The drainage system at the dam foundation is split in 9 sections. At the beginning, each could be measured only manually. After more than 30 years of operation, a collector pipe was built at the downhill dam toe in order to enable an automated measurement of the seepage. Since then, the sum of all nine sections is monitored automatically.

The seepage measurements are complemented by geodetical measurements. These include a leveling of the wave breaker and deformation measurements of some specific points.

3. REFURBISHMENT PROJECT

After more than 60 years of operation, a complete renewal of the asphalt lining was necessary. The time needed for these works should be used to refurbish other components of the reservoir, that are under water during regular operation. One of these components is the drainage system.

3.1. BOUNDARY CONDITIONS

The project had 2 main boundary conditions that had an influence on the decision, whether and how to refurbish the drainage system. The most important boundary condition was the available construction time.

Due to the wintery conditions in this mountainous region the possible construction period from a technical point of view lasts from late April to first half of October. The biggest financial loss, if the reservoir is out of operation, would occur in May and June, as shown in figure 4, because of snowmelt. These 2 aspects shortened the allowed time for an empty reservoir from last week of June to end of October, with the need of having finished the asphalt works by end of September due to the decreasing temperatures in autumn. This means, the removal of the sediments, the removal of the old asphalt and the placing of the new asphalt had to be done within 3 months.

The second boundary condition was the limited space for site facilities around the reservoir and the limited space for simultaneous works in the reservoir. All possible refurbishments of the drainage system had to comply with these boundary conditions.

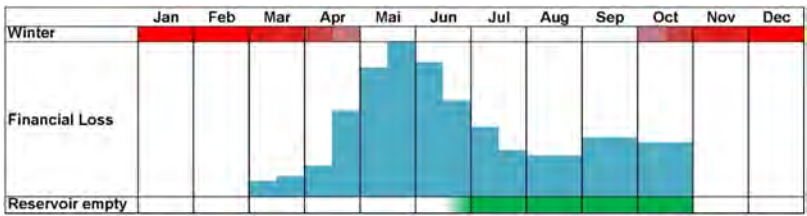


Fig. 5
Boundary conditions
Conditions aux limites

3.2. PREPARATORY WORKS & REHABILITATION CONCEPT

In order to get a better idea of the current condition of the drainage system at the bottom, the reservoir was emptied 2 years before the planned refurbishment for a partial camera inspection of the drainage system, the first inspection since the commissioning of the reservoir in 1958. For the inspection, one of the access shafts was opened and the condition of the corrosion protection of the steel lid was inspected visually. The steel lid and the concrete parts of the shaft were in a very good condition.

After the opening of the shaft, all accessible drainage pipes were inspected with a camera. As shown in figure 6, in some parts of the drainage pipes nearly 50 % of the cross section was filled with fine sediments.



Fig. 6
Drainage pipe, filled with sediments
tuyau de drainage, rempli de sédiments

Based on this finding and the boundary conditions the following concept for the refurbishment of the drainage system was defined:

- No complete replacement of the pipes due to limited time and space, although the diameter of the weepholes does not match the grain diameter of the surrounding material. The perforations of new pipes would have been too large as well for the fine material and therefore a material, complying with filter rules, had to be placed around new pipes. This would have meant too much time-consuming work.
- Opening of all access shafts and also the shafts that were covered by the asphalt sealing
- Cleaning of all pipes at the bottom with a pressure washer followed by a camera inspection
- Upgrading the existing non-access shafts at the connecting points to access shafts
- Building 2 new access shafts in order to reduce the length of the segments for camera inspection
- Necessary repair works only with systems for trenchless internal pipe rehabilitation
 - clamp sleeve made of steel
 - short liner made of glass-fiber hose and impregnated with resin

The fact that these systems may cover some of the weep holes is over-compensated by the improved stability of the repaired pipe compared to a broken pipe.
- Replacement of short sections of the pipes only if repair is not possible

As the general condition of the drainage system was unknown, the length of the sections that needed to be repaired could not be predicted, although these works had an influence on the critical path of the whole project. Hence, it was clear, that adjustments of the rehabilitation concept might be necessary.

3.3 CAMERA INSPECTION

After cleaning the pipes, the planned camera inspection was carried. Most of the segments could be inspected over the full length. In some cases, it was necessary to inspect a segment from both ends to be able to inspect the whole segment. In general, the condition of the pipes was quite good. Deviations from normal conditions could be classified, as follows:

- Step joint between two pipe segments
- Longitudinal cracks with no effect on the stability of the pipe
- Circumferential cracks with no effect on the stability of the pipe
- Crack system that resulted in a broken pipe, as shown in figure 7

Fortunately, no collapsed pipes were found that required a replacement of a complete section of a pipe. Repairing the first three classes of defects would have meant more or less a replacement of all drainage pipes at the bottom. Moreover, it

was assumed, that most of the cracks had already occurred during construction in the 1950s or in the very early phase of operation and that the cracks did not propagate since then, as the surcharge load caused by the operation of the reservoir had not changed since the commissioning. Based on this assumption and the findings of the camera inspection, it was decided to repair only the fourth class of defects.



Fig. 7
Broken drainage pipe
tuyau de drainage cassé

3.4. ADJUSTMENTS

After the decision was made, which defects, and how many of them should be repaired, some adjustments of the rehabilitation concept were necessary.

- The position of the shafts covered by asphalt deviated from the position in the as built drawings. This meant that the asphalt lining had to be opened on a wider area and the shafts had to be searched. The minimum deviation was about 2 m and the maximum deviation was about 8 m.
- The contractor recommended not to use clamp sleeves for several reasons. In case of a step joint of 2 pipe sections, a clamp sleeve could cause problems

for future camera inspections. But more important was the system of installation. To brace the clamp sleeve in the existing pipe, a packer has to be pumped with a pressure of 3 – 4 bar (= 0,3 – 0,4 MPa). This pressure might enlarge existing cracks and thus make the defect even worse. Therefore, the decision was made to use only short liners for repair works. Short liners require a pressure in the packer of ~2,5 bar (= 0,25 MPa).

- All shafts were too small to use to robots needed for trenchless internal pipe rehabilitation. The robots have a length of 1,0 – 1,2 m and the shafts were 0,5 x 0,5 m or 0,7 to 0,7 m. As a consequence, the decision was made, that pipes where a shortliner was necessary, should be opened with cuts on a length of 1,0 – 1,5 m to be able to place the robot in the pipe. After finishing the repair works the opening should be closed with a half-shell and covered with lean concrete or binder asphalt.

3.5. EXECUTED WORKS

3.5.1. Shafts

All planned new shafts and the upgrade of the existing shafts, both marked by the green dots in figure 8, could be built without any problem. Now, there are in total 16 access shafts so that the whole drainage system in the foundation, marked by the green lines in figure 8, can be inspected. All of the new and upgraded shafts have a steel lid. The corrosion protection of the steel lids and the mounting parts of the existing shafts could be renewed on site.

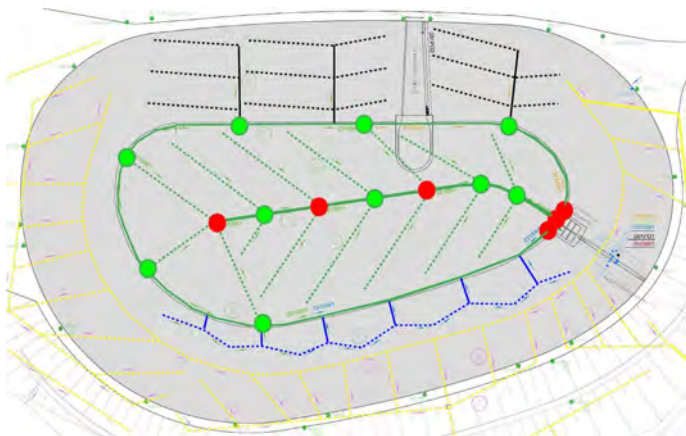


Fig. 8
Drainage system – after upgrade
Système de drainage – après modernisation

3.5.2. *Opening of pipes*

The openings of the herringbone pipes at the bottom were situated close to the shafts in the middle of the reservoir no matter where the defects of the pipe were. In the middle of the reservoir, the location of the pipe run was known while the ending point might have deviated from the drawings and therefore might have required an additional time-consuming search. The openings of the pipe along the waterside dam toe were also placed close to other shafts for the same reason.

3.5.3. *New findings*

After the cleaning and camera inspection, but before the repair works the reservoir was hit by a thunderstorm including heavy rainfall. A repeated camera inspection prior to the repair works showed newly sedimented material in pipes of the herringbone that are on the uphill side. The only explanation is mountain water, caused by the rainfall, as the whole pipe run is covered by asphalt and the reservoir is emptied. This means that parts of the herringbone pipes unexpectedly relief the mountain water in addition to the pipes under the uphill slope. The new sediments required an additional cleaning of the affected pipes.



Fig. 9
Installation of shortliner
Installation de chemisage partiel

3.5.4. *Installation of shortliners*

Instead of a robot, the contractor used a packer without wheels that had to be pushed into the pipe and slid on the floor of the pipe, as shown in figure 9. This method to place the packer at the right position has a limited length due to the axial stiffness of the push rod. Additional reinforcing rods, tied to the push rod, increased the stiffness, so that all planned reparations could be carried out.

In some of the pipes runs, the defects were concentrated on a short length, so that two defects could be repaired with one short liner. Altogether 6 pipes runs were opened and 12 shortliners were installed. In average 3 – 4 shortliners per day could be installed.

4. LESSONS LEARNED

- Repair works of an existing drainage system can be costly. Therefore, new drainage systems must be designed carefully by an experienced engineer. The main challenge is that future technical developments cannot be predicted over a period of several decades, like the past developments could not be foreseen during design in the 1950s.
- A drainage system design should enable a camera inspection as much as possible.
- A drainage system design should enable a camera inspection without the need to empty the reservoir, especially in case of a sediment deposit in the reservoir.
- If access shafts for a camera inspection are needed, think big. The additional costs of construction of a larger shaft are negligible compared to the costs afterwards, caused by a too small shaft.
- A drainage system design should enable a cleaning of the pipes with a pressure washer without the need to empty the reservoir, especially in case of a sediment deposit in the reservoir.
- Trenchless internal pipe rehabilitation methods are cost saving and time saving but have to be adapted to the situation on site.
- For trenchless internal pipe rehabilitation, a pipe run should have an access shaft at both ends.

REFERENCE

- [1] MUSSNIG R., GASSER G. Der Wochenspeicher Rosswiese *Österreichische Zeitschrift für Elektrizitätswirtschaft*, 1958, Nr. 6.

COMMISSION INTERNATIONALE DES
GRANDS BARRAGES

VINGT-HUITIEME CONGRES DES
GRANDS BARRAGES
CHENGDU, MAI 2025

EMPOWERING LARGE DAMS FOR THE FUTURE BY USING GENERATIVE ARTIFICIAL INTELLIGENCE (*)

Lakshmin BACHU
Principal Engineering Consultant, TETRA TECH CANADA INC.

CANADA

SUMMARY

Generative Artificial Intelligence (Gen AI) is a response to the challenge of maintaining large dams by enabling the integration and synthesis of large amounts of data during the life of dams. The report presents the techniques of Generative Artificial Intelligence and proposes applications of the assistance provided by these approaches in the field of safety reviews, optimisation of emergency plans and operation.

RÉSUMÉ

L'Intelligence Artificielle Générative est une réponse au défi de la maintenance des grands barrages en permettant d'intégrer et synthétiser de grandes quantités de données au cours de la vie des barrages. Le rapport présente les techniques de l'Intelligence Artificielle Générative et propose des applications de l'aide apportée par ces méthodes dans le champ des revues de sûreté, de l'optimisation des plans d'urgence et de l'exploitation.

*Assurer l'avenir des grands barrages en utilisant l'Intelligence Artificielle Générative

1. INTRODUCTION

Maintaining the safety of large dams is crucial for public safety, environmental preservation, and economic stability. In Canada and across the globe, large water and mining dams face unique challenges due to operational demands, socio-economic factors, and extreme climate variability. Water dams are vital for hydro-electric power, water supply, irrigation, and flood control, while mining dams manage tailings. Traditional/manual methods of dam safety management are labor-intensive and expensive, highlighting the need for advanced technologies to help manage the large dams' operations, streamline processes, enhance data analysis, and improve predictive capabilities.

Managing dam safety involves addressing several key challenges. Data management is a significant issue, as large dams generate vast amounts of data over their lifetimes, including dam safety reports, structural health, environmental monitoring, and operational records. This data is often siloed and difficult to integrate, leading to inefficiencies in monitoring and maintenance. Operational inefficiencies are another challenge; routine inspections, maintenance, and emergency preparedness activities are labor-intensive and time-consuming, requiring significant financial and human resources, which can strain dam management operations. Extreme climate variability is also impacting dam safety, with increasing frequency and intensity of extreme weather events such as heavy rainfall and droughts placing additional stress on dam structures and necessitating more robust and adaptive management strategies. Lastly, the complexity of dam safety management increases the risk of human errors during data interpretation, inspections, and maintenance activities, potentially leading to overlooked issues and failures.

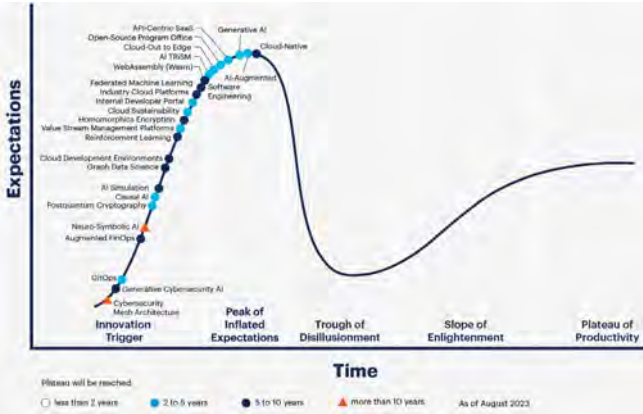


Fig. 1
Gartner Hype Cycle [1]Hype Cycle de Gartner

Dam safety has evolved significantly and mirrors technological advancements (Fig. 1), progressing from manual inspections to sensor networks and automated systems. Currently, Generative AI (GenAI) represents a transformative leap in this field. While traditional methods and earlier technologies improved efficiency, they often operated in isolation and required significant manual integration. GenAI, however, offers the ability to synthesize vast amounts of data from diverse sources in real-time, identifying patterns and predicting potential issues with impressive accuracy.

Gen AI can be used to enhance the precision and reliability of dam operations, improve emergency preparedness, and optimize maintenance schedules. As GenAI matures and integrates with established safety protocols, it has the potential to significantly enhance the safety, reliability, and sustainability of large dams. However, its implementation must be approached cautiously, considering the critical nature of dam infrastructure. The future of dam safety management lies in the thoughtful integration of AI-driven systems with human expertise, creating more resilient, adaptive, and efficient practices capable of addressing complex challenges posed by climate change, aging infrastructure, and evolving societal needs.

Hariri-Ardebili et al [2] highlight key technologies in dam engineering (Fig. 2), focusing on predictive modeling, real-time monitoring, and optimization. These technologies offer unique strengths for enhancing dam safety. By leveraging these unique strengths, GenAI can be used to elevate dam safety management to new levels of efficiency and reliability. This technology may help protect public safety, preserve environmental health, and support economic stability by providing a more comprehensive approach to monitoring and maintaining dam infrastructure. This paper aims to explore the potential applications of GenAI in transforming dam safety management. The objectives of this paper are to:

1. Provide an overview of GenAI.
2. Detail how GenAI can be applied to dam safety review (DRS) aspects.
3. Identify the challenges and future opportunities using GenAI.
4. Summarize the conclusions with best practices.

By examining these aspects, this paper aims to provide valuable insights and practical guidance for young professionals, practitioners, regulators, and researchers in integrating GenAI into dam safety management. The goal is to enhance the safety, reliability, and sustainability of large dams, ensuring dams continue to serve their critical functions effectively.



Fig. 2
An overview of dam technology
Un aperçu de la technologie des barrages

2. GENERATIVE ARTIFICIAL INTELLIGENCE

Generative AI (GenAI), a branch of artificial intelligence capable of creating content, encompasses several types of models, including Generative Adversarial Networks (GANs), transformers, and diffusion models. GANs use two neural networks—a generator creating new data and a discriminator evaluating it—in a competitive process to produce realistic outputs. Transformers, on the other hand, utilize attention mechanisms to process sequential data and have become particularly prominent in natural language processing tasks. More recently, diffusion models have gained significant traction in image generation tasks. These models work by gradually denoising random noise into coherent images, often guided by text prompts. This approach has shown remarkable results in generating high-quality, diverse images.

Furthermore, transformers are advanced AI models designed for understanding and generating human-like text. They are particularly useful for processing large amounts of text data and providing contextually accurate responses. Transformers such as Generative Pre-Trained Transformer (GPT)-3, GPT-4, and GPT-4o(Omni) developed by OpenAI [3] and Gemini developed by Google are becoming increasingly popular. GPT-3 generates detailed and context-aware text, and can be used for creating reports, answering queries, and automating text-based tasks. GPT-4 is an improved version of GPT-3 with better accuracy and understanding, making it even more effective for complex text generation and analysis tasks. GPT-4o is the latest version, optimized for faster and more efficient performance. It is designed to handle real-time interactions and provide quick, accurate responses. These models excel in processing extensive datasets, identifying patterns, and generating actionable insights, which are crucial for proactive dam management.

GenAI models are developed by training on large volumes of data, which can include both private datasets and publicly available information on the internet. The training process involves input data passing through multiple layers of neurons in a neural network. Each neuron's weight is adjusted using complex mathematical algorithms to minimize errors and improve accuracy. These models, known as large language models (LLMs), predict the next word in a sentence based on probabilistic estimates and other complex processes.

Integrating GANs and transformers may enhance dam safety management by generating high-quality images for inspection and detailed reports, offering robust solutions for monitoring, data analysis, predictive maintenance, and emergency preparedness. The field of GenAI is rapidly evolving, with new architectures and hybrid approaches continually being developed to address specific challenges and improve performance across various domains. Leveraging GenAI could allow dam safety management to transition from reactive to proactive strategies, potentially improving the resilience and reliability of dam infrastructure.

3. DAM SAFETY APPLICATIONS

GenAI distinguishes itself not only by its ability to synthesize, simulate, and predict, thereby surpassing the capabilities of traditional data analysis, but also by encompassing a wide range of features including text, vision, listening, voice recognition, programming, graphs, and numerical acumen. The multifaceted nature of GenAI allows it to interact and interpret various forms of data, enhancing its applicability and effectiveness across diverse data sources and scenarios. This technology may facilitate a paradigm shift from reactive to proactive strategies, which will be crucial for ensuring long-term safety and efficiency of dam infrastructures.

The power of GenAI lies in its exceptional ability to process vast datasets, collating information in a similar fashion to humans, and deriving insights that could elude conventional methods. In the context of dam safety, where numerous and intricate variables interact, this is particularly valuable. GenAI can analyze data from multiple sources, including previous reports, historical data, sophisticated sensor networks monitoring critical conditions and AI-augmented drone inspections, to offer predictive insights and decision-making support in uncertain scenarios. As we enter a new technological paradigm, the role of GenAI has the potential to be transformative in enhancing dam safety.

Development and finetuning of GenAI models as illustrated in Fig. 3 for the dam safety domain will enhance dam safety management. On a high level, the process begins with data documentation and governance, where historical performance data, inspection reports, and real-time monitoring data from Internet of Things (IoT) sensors and drones are collected and documented. The next step is data preparation, which includes cleaning, filtering, deduplication, and auditing to ensure the data's quality and relevance. This prepared data is then used in the model training phase, where pre-training and finetuning are conducted to develop models capable of developing dam safety reviews, predicting structural issues, optimizing maintenance schedules, and simulating various scenarios. By compartmentalizing these tasks into modules, each component can be developed, optimized, and maintained independently, enhancing the overall efficiency and flexibility of the model development process.

Following the training, the model evaluation phase assesses the model's capabilities, risks, and potential harms, ensuring it can effectively support proactive dam safety management. This evaluation includes testing the model's accuracy and identifying any potential issues. Finally, the model release phase involves thorough documentation, license selection, reproducibility checks, and usage monitoring to ensure the model's reliability in real-world applications. Additionally, the environmental impact and efficient use of resources are considered throughout the process. By implementing a modular approach, each step of the AI model development can be independently managed and improved, leading to more robust, scalable, and maintainable solutions for dam safety. This modular strategy not only enhances the precision and reliability of GenAI models but also facilitates continuous innovation and adaptation to new challenges in dam safety management.

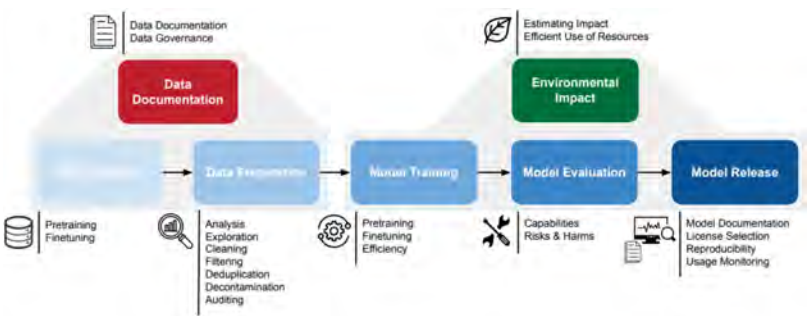


Fig. 3
An overview of GenAI model development [4]
Un aperçu du développement du modèle GenAI [4]

3.1. DAM SAFETY REVIEW APPLICATION

Integrating conventional approaches and advanced technology with GenAI offers transformative potential for enhancing completion of DSRs. This integration can make the process more efficient, accurate, and comprehensive with proper risk management in place. Below is a summary of how GenAI can be integrated into the DSR processes outlined in the CDA guidelines [5].

3.1.1. *Data and records review, and data book update*

Integrating GenAI with traditional procedures may significantly enhance the data and records review process. Traditionally, this task involves manually reviewing historical data, inspection reports, and maintenance logs, which can be time-consuming and prone to human error. GenAI can be used to streamline this process by summarizing large datasets, extracting key insights, and identifying patterns of concern. For instance, GPT-4 can quickly analyze and summarize documents containing historical data, while GenAI spatial tools like the ChatGPT plugin for Quantum Geographic Information System (QGIS) can visually present data, making it easier to identify patterns and areas of concern. Fine-tuning GenAI models with specific DSR reports and data can provide outputs tailored to each dam's unique characteristics, potentially significantly reducing review time and overall DSR completion time.

3.1.2. *Site inspection and staff interviews*

Site inspections and staff interviews traditionally require extensive manual effort and can result in delays and potential human errors. GenAI can be used to automate the creation of comprehensive inspection checklists based on historical data. During inspections, AI-enhanced drones and sensors could capture high-quality images and data, which are processed by GANs to detect structural defects. GenAI spatial tools could provide real-time geospatial visualization, enabling prompt assessment of issues. Additionally, GPT-4o models can be used to transcribe and analyze verbal interviews with staff, efficiently extracting key information. Images from site inspections can be automatically processed (Fig. 4) for potential dam safety concerns. Fine-tuning these models with data from previous inspections and interviews provides more accurate and relevant outputs. This integration may significantly reduce the time required for site inspections and staff interviews, enhancing the efficiency of dam safety engineers without replacing their expertise.

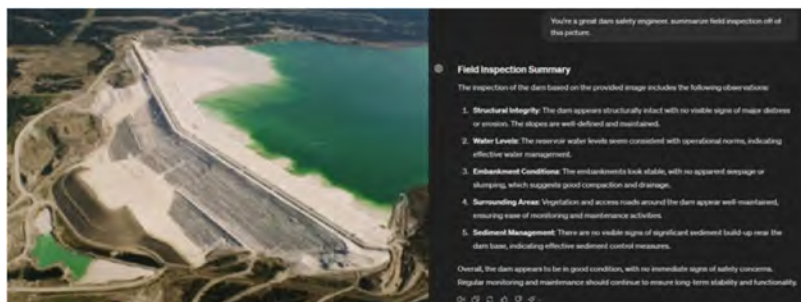


Fig. 4

Demonstration of ChatGPT interaction using dam pictures
Démonstration de l'interaction ChatGPT à l'aide d'images de barrage

3.1.3. *Consequence of dam failure and dam classification review*

Evaluating the potential impacts of a dam failure and reviewing its classification is traditionally a labor-intensive process, relying on manual assessment using historical data and expert judgment. GenAI can be used to automate this by analyzing historical data and possibly simulating various failure scenarios. It can be used to process parameters such as population at risk, environmental and cultural values, and infrastructure and economic impacts and provide the user with Microsoft (MS) WORD document (Fig. 5) for review. Tools like GPT-4o can be used to efficiently query and summarize documents, while GenAI GIS tools offer advanced geospatial visualizations to aid in the determination of potential failure scenarios. This allows for precise classifications and comprehensive risk assessments, reducing review time significantly.

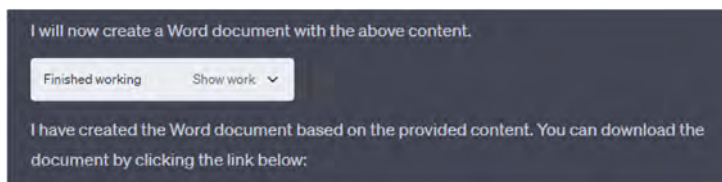


Fig. 5

An overview of GPT4o's ability to create MS Word file with DSR report template
Un aperçu de la capacité de GPT4o à créer un fichier MS Word avec le modèle de rapport DSR

3.1.4. Failure modes analysis

Failure Modes Analysis (FMA) involves evaluating potential failure modes and their impacts, a task that is thorough and time-consuming. GenAI can be used to streamline FMA by automating data analysis and facilitating real-time discussions during workshops. GPT-4o can be used to provide visual aids (Fig. 6) such as functional diagrams and geospatial visualizations, helping to identify and prioritize potential failure modes. It can also assist in developing presentation slides and documenting workshop findings, reducing the FMA process time significantly.

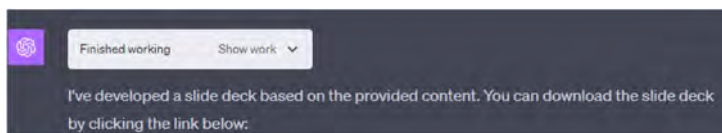


Fig. 6

An overview of GPT-4o's ability to create MS PowerPoint slides with DSR workshop template
Un aperçu de la capacité de GPT4o à créer des diapositives MS PowerPoint avec le modèle d'atelier DSR

3.1.5. Dam safety analysis and review

This involves comprehensive technical assessments of the dam's safety, covering hydrotechnical, geotechnical, structural, mechanical, and electrical aspects. GenAI can be used to analyze large datasets from historical data, inspection reports, and real-time sensor inputs to identify potential safety concerns. GPT-4 could enable engineers to query specific aspects of a dam's performance and summarize key findings efficiently. GenAI spatial tools provide advanced geospatial visualizations for a thorough assessment, helping an engineer simulate flood scenarios and predict geotechnical assessments. This integration could potentially enhance the accuracy and efficiency of dam safety analyses.

Fig. 7 shows a program developed by the author using GPT-4 for hydrometric flow data acquisition and analysis. The program, named Hydat-FlowGPT, reads the inputted hydrometric station names, acquires the corresponding flow data from HYDAT database in Canada [6], and performs flow-frequency analysis which is helpful to identify dam's inflow design flood (IDF). Similarly, for a geotechnical purpose, AI could analyze soil and other data and/or previous geotechnical assessments to help predict geotechnical assessments.

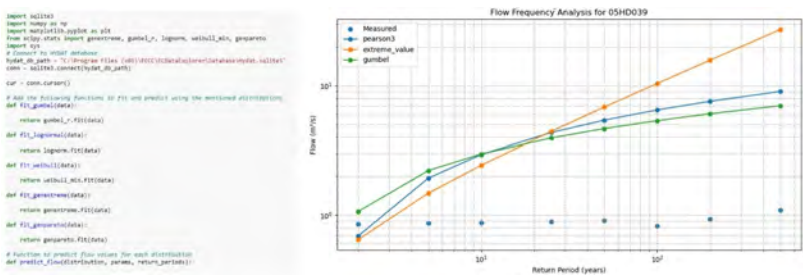


Fig. 7
A snapshot of the code developed using GPT-4 and design flow frequency plot
Un instantané du code développé à l'aide de GPT4 et du tracé de fréquence de flux de conception

3.1.6. *Operation, maintenance, and surveillance review*

Assessing a dam's operational procedures, maintenance practices, and surveillance activities traditionally requires detailed manual review. GenAI can be used to analyze large volumes of Operation, Maintenance, and Surveillance (OMS) data, identifying patterns and potential issues. GPT-4 could facilitate efficient querying and summarization of documents, while GenAI spatial tools can subsequently be used to visualize surveillance data, integrating real-time sensor inputs. This allows for prompt identification and response to maintenance needs, potentially significantly reducing the time required for OMS reviews.

3.1.7. *Emergency preparedness review*

This involves evaluating the dam's emergency response plans, traditionally requiring extensive manual effort and coordination. GenAI can be used to analyze large datasets of emergency plans and historical incident reports, identifying patterns and potential issues. GPT-4 could allow users to query specific documents and summarize key information, while GenAI spatial tools can subsequently be used to visualize emergency scenarios. This integration helps simulate various emergencies and optimize response strategies, likely reducing the review time for emergency preparedness significantly.

3.1.8. *Public safety and security review*

Assessing public safety measures and dam security involves manual inspections and reviews. GenAI can be used to analyze safety and security data, identifying patterns and vulnerabilities. GPT-4 could enable efficient querying and summarization of safety documents, while GenAI spatial tools subsequently visualize security data in real-time. This integration may help detect and mitigate potential security threats, reducing the review time for public safety and security.

3.1.9. *Dam safety management system review*

Evaluating the effectiveness of the dam safety management system traditionally involves a detailed manual review. GenAI can be used to analyze management system data, identifying patterns and issues. GPT-4 could facilitate efficient querying and summarization of management documents, while GenAI spatial tools subsequently visualize management system elements. This integration ensures a comprehensive overview of the system's effectiveness, potentially reducing the review time significantly.

3.2. *ADDITIONAL GENAI FEATURES FOR DAM SAFETY*

ChatGPT enables users to develop specialized GPTs by inputting various documents (i.e., knowledge base) and user instructions. This capability is particularly useful for reviewing DSR reports, data books, and historical DSR-related information. Users can ensure comprehensive and accurate evaluations by comparing the DSRs of interest with regulatory guidelines such as the CDA, the Mining Association of Canada (MAC), and the Global Industry Standard on Tailings Management (GISTM).

Multiple team members from various organizations such as dam owners, dam operators, and consultants can interact with the GPTs concurrently to be able to exchange and review information, and complete DSRs effectively with reduced laborious processes. The developed GPTs (Fig. 8) can provide potential deviations and/or compliance issues of the DSRs based on the given dam safety guidelines. Dam engineers/specialists can then evaluate the deviations with relatively less effort. The GPTs are also used for educational purposes of dam professionals. The CDA can deploy various GPTs for dam safety advisory purposes. Additionally, various AI agents can be developed to help complete DSRs.

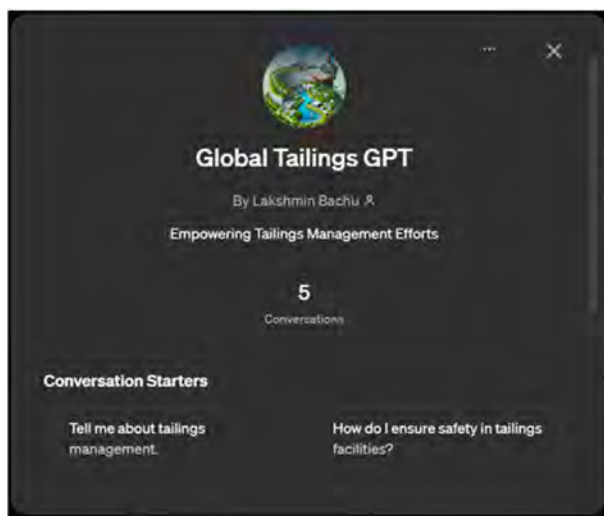


Fig. 8

Global Tailings GPT developed for public to interact with and learn about GISTM guidelines

Global Tailings GPT développ   pour que le public puisse interagir et en apprendre davantage sur les directives du GISTM

Another GenAI application for dam safety management is AI agents (Fig. 9) which are autonomous software entities designed to perform tasks, make decisions, and interact with their environment with minimal human intervention. Leveraging GenAI, these agents can potentially transform dam safety by automating data reviews, analysis, document preparations, continuously monitoring conditions, analyzing structural integrity, and predicting potential failures with unprecedented accuracy. For instance, AI-enhanced drones equipped with high-resolution cameras can capture detailed images of dam structures, while IoT devices provide real-time data on environmental and structural parameters.

GenAI models, fine-tuned with specific dam data, could be used to detect anomalies such as cracks or shifts in the structure and alert engineers immediately. Additionally, these agents could simulate stress scenarios caused by natural events like earthquakes or heavy rainfall, offering actionable insights for pre-emptive measures. By integrating data from weather forecasts, geological surveys, and maintenance records, AI agents may provide a holistic approach to dam safety. This seamless integration and predictive capability may not only enhance the reliability and safety of dam operations but also improve timely and cost-effective interventions, ultimately better safeguarding communities, and ecosystems.

Another GenAI application for dam safety management is AI agents which are autonomous software entities designed to perform tasks, make decisions, and interact with their environment without human intervention. Leveraging GenAI, these agents (Fig. 9) can transform dam safety by automating data reviews, analysis, document preparations, continuously monitoring conditions, analyzing structural integrity, and predicting potential failures with unprecedented accuracy. For instance, AI-enhanced drones equipped with high-resolution cameras can capture detailed images of dam structures, while IoT devices provide real-time data on environmental and structural parameters.

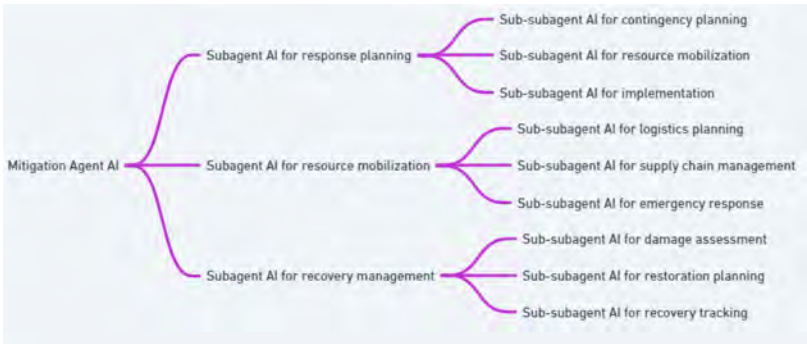


Fig. 9

An example of AI agents for dam safety management
Un exemple d'agents IA pour la gestion de la sécurité des barrages

Integrating GenAI and advanced technology into DSRs may reduce task completion time significantly, despite the initial high investment. Fine-tuning GenAI models with specific dam data improves accuracy and contextually relevant outputs. This comprehensive approach enhances the efficiency, accuracy, and quality of dam safety management. While substantial initial effort and technical expertise are required, proper risk mitigation ensures data privacy and addresses biases from limited data. By addressing these challenges, organizations may effectively and responsibly deploy GenAI in dam safety management, enhancing the reliability and safety of dam infrastructure. GenAI complements rather than replaces dam safety professionals, significantly enhancing their efforts in effective dam safety management.

4. CHALLENGES AND OPPORTUNITIES

The effectiveness of GenAI in dam safety management hinges on high-quality, comprehensive datasets. Poor data quality can lead to inaccurate predictions and ineffective safety measures. Biases in AI models, stemming from historical data, can

skew results. Mitigating these biases requires techniques such as bias detection algorithms, diverse training datasets, and continuous model evaluation. Handling sensitive infrastructure data necessitates robust cybersecurity measures. Encryption, access controls, and regular audits are vital to protect data integrity. AI systems must be designed to withstand cyber-attacks and prevent unauthorized access.

Compliance with data privacy regulations is crucial. Policies and technologies must safeguard personal and sensitive data to ensure legal compliance and stakeholder trust. Implementing GenAI systems demands specialized skills in AI, data science, and dam safety engineering. Effective deployment requires collaboration between AI specialists and dam safety engineers to ensure accurate application and interpretation of AI models. Continuous training and support for personnel are essential to stay updated with AI advancements. Regular training sessions and technical support help maintain a skilled workforce capable of leveraging GenAI for dam safety management. However, GenAI holds significant promise for transforming dam safety practices:

- **Enhanced Prediction and Analysis** - Improved predictive models can better forecast structural issues, maintenance needs, and environmental impacts. Real-time analysis of data from IoT sensors and drones enables rapid detection of anomalies and potential problems.
- **Customized AI Models** - Developing and fine-tuning AI models with dam-specific historical data and inspection reports can provide more accurate and relevant recommendations.
- **Advanced Monitoring and Maintenance** - Integration with IoT devices creates a more interconnected monitoring approach, feeding continuous real-time data to AI systems. AI-driven robotics can conduct detailed inspections and perform minor repairs in hard-to-reach or hazardous areas, enhancing safety and efficiency.
- **Proactive Management** - Continuous data streams enable AI to provide timely alerts and recommendations for maintenance and emergency response. AI can help optimize water usage, energy production, and environmental impact, supporting more sustainable dam management.
- **Climate Resilience** - AI can provide predictive insights into extreme weather events and long-term environmental changes, helping develop adaptive strategies for dam infrastructure.
- **Retrieval-Augmented Generation (RAG)** - RAG models combine retrieval-based and generation-based AI to enhance decision-making by integrating diverse data sources like structural health and environmental information, generating alerts, simulating emergency scenarios, and assessing risks, automating report generation for thorough documentation and compliance, by improving efficiency, accuracy, and proactive maintenance, these AI technologies can lead to better safety outcomes and decision-making, ultimately protecting public safety and the environment.

- Small Language Models (SLMs) are specialized AI systems trained on focused datasets, typically containing fewer than 1 billion parameters, in contrast to LLMs which often exceed 100 billion parameters. In the context of dam safety, SLMs offer several distinct advantages. Their targeted training allows them to develop specific expertise in dam engineering and safety protocols, potentially outperforming larger models in this niche domain. SLMs require significantly less computational power, making them suitable for on-site deployment at dam locations, even in remote areas with limited resources. They can process data and generate insights more rapidly than LLMs, enabling near real-time monitoring crucial for dam safety. SLMs can be effective with smaller datasets, which is beneficial in the dam safety field where comprehensive historical data may be limited. Their compact size enhances data security, as they can be deployed locally, reducing the need to transmit sensitive information to external servers. SLMs are also more easily updated with new safety regulations or emerging best practices, ensuring they remain current. Their efficiency makes them ideal for integration with IoT devices and sensor networks used in modern dam monitoring systems, such as piezometers and inclinometers. While specific studies on SLM performance in dam safety are limited, their potential to enhance risk assessment and management in this field is significant, offering a more tailored and responsive approach compared to larger, generalized models.

5. NEXT GENERATION GUIDELINES

Various organizations including CDA are developing its Next Generation Guidelines (NGG) to address evolving challenges in dam safety. These guidelines aim to incorporate advanced knowledge and practices into robust, adaptable standards. GenAI can significantly support this transformation, aligning with the dam community's vision for improved dam safety management.

GenAI may enhance dam safety by streamlining data integration and analysis, using models like GPT-4o to parse vast amounts of data in real-time. This could improve safety assessments and enable proactive maintenance. It may strengthen risk assessment and predictive modeling, better informing resilient designs and operational strategies to withstand extreme weather events. GenAI can be used to automate documentation by generating detailed reports and efficient review of safety plans, potentially reducing human error, and enhancing compliance. Through IoT integration and advanced analytics, GenAI could provide real-time monitoring, immediate alerts, and maintenance recommendations, boosting dam resilience. It may also support collaboration among AI specialists, dam safety engineers, and stakeholders with platforms for seamless communication and geospatial visualizations, improving effective safety strategies. Organizations/jurisdictions could potentially use GenAI tools such as GPTs to inform, educate, and engage dam

communities, thereby enhancing outreach efficiency and providing additional benefits.

Integrating GenAI into completing DSRs and other dam safety efforts requires addressing ethical considerations, biases, data security, and privacy. Employing various risk mitigation measures such as developing local GenAI models within organization/jurisdictions will help ensure data security and privacy. Using bias detection algorithms, diverse datasets, and continuous model evaluation ensures fair and accurate analyses. Prioritizing transparency, ethics, and robust security measures maintains public trust and safeguards sensitive information.

The NGG represents a forward-looking approach to dam safety management. Leveraging GenAI for data integration, predictive modelling, real-time monitoring, and collaboration enables dam communities to achieve safer, more resilient dam infrastructure, addressing current challenges and future uncertainties.

6. CONCLUSIONS

The integration of generative AI into dam safety management represents a transformative opportunity to enhance the safety, project management, reliability, and sustainability of critical dam infrastructure. By leveraging advanced AI models like GPT-4o and small language models, along with emerging technologies such as IoT sensors and drones, dam operators can transition from reactive to proactive safety strategies. This shift promises to streamline inspections, automate data analysis, enable predictive maintenance, and improve emergency preparedness.

However, the responsible implementation of GenAI in this domain requires careful consideration of data quality, bias mitigation, cybersecurity, and the need for specialized expertise. As the technology evolves, ongoing collaboration between AI specialists, dam safety engineers, and regulatory bodies will be crucial to realize its full potential while addressing ethical concerns.

Looking ahead, the future of dam safety management lies in customized AI models, advanced monitoring systems, and AI-driven robotics that can conduct detailed inspections in hazardous areas. These innovations, combined with GenAI's ability to process vast datasets and generate actionable insights, will empower dam operators to make more informed decisions, optimize resource allocation, and ultimately better protect communities and ecosystems.

As we enter a new technological paradigm, it is clear that GenAI will not replace human expertise but rather augment it. By embracing these advancements responsibly, the dam safety community can usher in a new era of infrastructure resilience, ready to face the challenges of extreme weather events and aging

infrastructure. The journey toward AI-enhanced dam safety has only just begun, and its potential to safeguard lives, property, and the environment is both exciting and profound.

REFERENCES

- [1] GARTNER. *Gartner Places Generative AI on the Peak of Inflated Expectations on the 2023 Hype Cycle for Emerging Technologies*. Gartner, 2023. Retrieved from <https://www.gartner.com/en/newsroom/press-releases/2023-08-16-gartner-places-generative-ai-on-the-peak-of-inflated-expectations-on-the-2023-hype-cycle-for-emerging-technologies>; accessed July, 2024.
- [2] HARIRI-ARDEBILI, M.A., MAHDAVI G., NUSS, L., LALL, U. The role of artificial intelligence and digital technologies in dam engineering: Narrative review and outlook. *Engineering Applications of Artificial Intelligence*, 2023. Volume 126, Part A, 106813, ISSN 0952-1976.
- [3] OPEN AI. Announcing GPT-40 in the API! OpenAI, 2024. Retrieved from <https://www.openai.com>, accessed July, 2024.
- [4] FMBCHEATSHEET. Foundation Model Training Overview. fmbcheatsheet, 2024. Retrieved from <https://fmcheatsheet.org/>; accessed July, 2024.
- [5] CDA. 2007 *Dam Safety guidelines*, 2013 Edition. Canadian Dam Association, 2023.
- [6] ECCC. National Water Data Archive : HYDAT. *Environment and Climate Change Canada*, 2018.

COMMISSION INTERNATIONALE DES
GRANDS BARRAGES

VINGT-HUITIEME CONGRES DES
GRANDS BARRAGES
CHENGDU, MAI 2025

CONSTRUCTION TECHNOLOGY OF 300M-LEVEL GRAVEL SOIL COREWALL ROCKFILL DAM FOR LIANGHEKOU HYDROPOWER STATION (*)

Dongming ZHANG, Chaofeng ZHANG & Aiguo WANG
Senior Engineer, Yalong River Hydropower Development Co., Ltd., Chengdu

CHINA

SUMMARY

The practice of the Lianghekou Hydropower Station project has filled the key technological gap in the intelligent filling of international 300m-level high corewall rockfill dams, comprehensively innovated the construction operation and management mode of earth and rock dams, provided the "Lianghekou Plan" for fundamentally solving the problem of construction quality control, and achieved a leap from digital construction to intelligent construction of high core rockfill dams, leading the development direction of construction technology in the field of water conservancy and hydropower engineering.

Lianghekou Hydropower Station is the first to create a complete set of winter construction technology for ultra-high earth rock dams in high altitude and cold regions at 300m level, innovate the prevention and control theory, technical standards and construction technology of anti-seepage soil materials in high altitude regions at home and abroad, and create a precedent for large-scale continuous construction of soil core walls in plateau permafrost regions in winter. It has developed a complete set of technical system for soil material mining, transportation, mixing, paving and rolling in winter, and invented a rapid retractor for thermal insulation materials, which has realized the rapid and continuous construction of the core wall under the conditions of large temperature difference and high cold and low temperature in winter, promoted technological progress and industrial upgrading, and helped innovate and develop.

**Technologie de construction d'un barrage zoné en enrochement de 300 mètres de haut en sol graveleux à la centrale hydroélectrique de Lianghekou*

RÉSUMÉ

Le projet de centrale hydroélectrique de Lianghekou a permis de combler les principales lacunes technologiques dans le remplissage des barrages en enrochement à noyau central de 300 m de hauteur, d'innover de manière exhaustive concernant le mode d'exploitation et de gestion des barrages zonés, de fournir le « plan Lianghekou » pour assurer le contrôle de la qualité de la construction, et passer de la construction numérique à la construction intelligente de barrages zonés en enrochement de grande hauteur, ouvrant ainsi la voie au développement de la technologie de construction dans le domaine du stockage de l'eau et de l'ingénierie hydroélectrique.

La centrale hydroélectrique de Lianghekou est la première à créer un ensemble complet de technologies de construction de barrages en terre-et enrochement de très haute altitude dans les régions froides, à innover dans le domaine de la prévention et du contrôle, les normes techniques et la technologie de construction des matériaux de sol anti-infiltration dans les régions de haute altitude en Chine et à l'étranger. Elle crée un précédent pour la construction continue à grande échelle de noyaux en terre dans les régions de pergélisol. Elle a permis de mettre au point un ensemble complet de systèmes techniques pour l'extraction, le transport, le mélange, la pose et le roulage des matériaux du sol en hiver, et d'inventer un rétracteur rapide pour les matériaux d'isolation thermique, ce qui a permis la construction rapide et continue du noyau dans des conditions de grande différence de température, de grand froid et de basse température en hiver. Sa construction a favorisé le progrès technologique et la modernisation industrielle, et a contribué à l'innovation et au développement.

1. ENGINEERING INTRODUCTION

Lianghekou Hydropower Station is located in the main stream of Yalong River in Yajiang County, Ganzi Prefecture, Sichuan Province, China. The development mission of the power station is mainly to generate electricity, taking flood control into account, and to promote local economic and social development.

The normal storage level of the reservoir is 2865.00m, with a total capacity of 10.767 billion m³ and a regulating capacity of 6.56 billion m³, which is the largest multi-year regulating reservoir in Sichuan Province, and is the backbone of the nationally planned Yangtze River flood control system, with a flood control task of not less than 2 billion m³ in the main flood season. The power station is installed with 6 sets of 500MW hydroelectric generator sets, with an installed capacity of 3,000MW and a multi-year average annual power output of 11 billion kW·h.

The engineering hub adopts the overall arrangement pattern of “river-blocking gravel soil corewall rockfill dam + right bank diversion power generation system + left bank flood discharge and release system + left and right bank diversion holes”, as shown in Fig.1 to 2. The dam is a gravel soil corewall rockfill dam with a crest elevation of 2875.00m and a maximum height of 303.00m, which is the highest earth and rock dam that has been built in the world. The total filling volume is about 44 million m³.

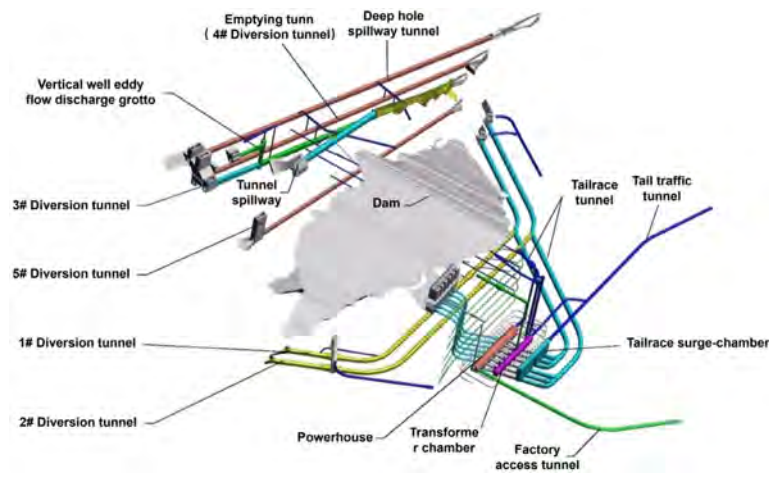


Fig. 1
Three-dimensional pivot arrangement of Lianghekou Hydropower Station

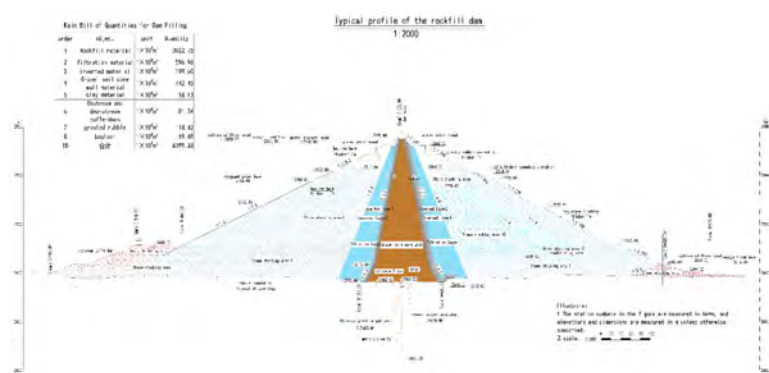


Fig. 2
Typical cross-section diagram of rockfill dam

2. YARD SELECTION AND CONSTRUCTION LAYOUT PLANNING

The project is located in the plateau and narrow valley and less arable land, then the dam construction materials mainly from the reservoir area yard, thus reducing the downstream temporary land acquisition of more than 500 immigrants, reducing temporary arable land expropriation and later replanting of more than 830 acres, as shown in Fig. 3. The construction site adopts mainly slag dumping to create land, solving more than 70% of the construction land.

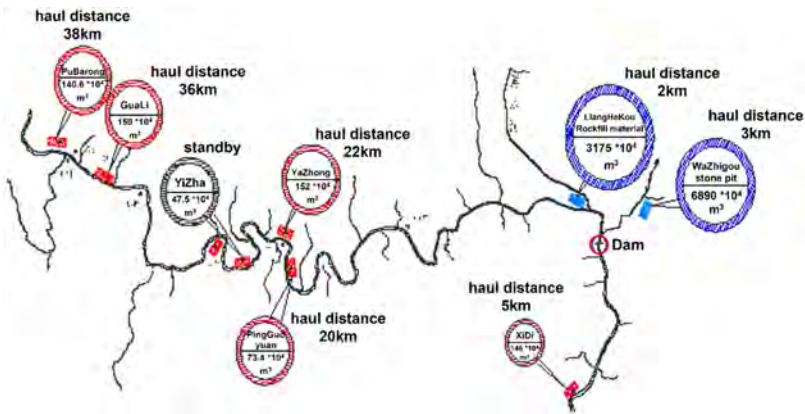


Fig. 3
Material yard planning

3. MINING OF COMPLEX SOIL QUARRIES

P5 is used as the main indicator for soil classification and zoning. The principle of using materials takes into account the economy and quality: close materials, low materials, unadulterated materials and type I soil is used first, so as to refine the construction, reduce the loss of soil materials, and take into account the water storage and economy, as shown in Table 1. Intelligent mining system is used to simulate mining with P5 fluctuation $\pm 10\%$ as the constraint boundary, and the analysis proposes “three-dimensional isoplasmic body” as the dynamic refinement of mining zoning. According to the existing survey and spatial information, the system adopts intelligent simulation to carry out the research on the layered and zoned mining plan of the material field, and takes the uniformity of the nature of the soil and material as the constraints, and recommends the refined zoned mining plan and gravel mixing ratio. At the same time, the use of continuous trough exploration, well exploration and other methods can better reflect the spatial distribution of material source traits.

Table 1
Physical properties of soil classification

SOIL CLASSIFICATION	<5MM CONTENT (%)	<0.075MM CONTENT (%)	<0.005MM CONTENT (%)	NATURAL MOISTURE CONTENT (%)	PLASTICITY INDEX	GRIT RATIO
Type I soil	86.1~92.0	63.2~80.0	16.6~31.3	11.6~15.1	11.8~16.4	6:4
Type II soil	75.2~78.4	49.9~63.2	14.9~21.0	8.7~11.7	11.0~15.6	7:3
Type III soil	49.8~58.7	29.9~34.7	8.9~12.0	6.5~8.3	11.6~14.1	none

4. COMPLETE SET OF WINTER CONSTRUCTION TECHNIQUES FOR COREWALL OF DAMS

The project belongs to a typical seasonal permafrost area. Meteorological data show that the annual average temperature in the dam site area is 10.9°C, the extreme maximum temperature is 35.9°C, the extreme minimum temperature is -15.9°C, and from mid-November to mid-February, the average temperature is lower than 5°C, and there will be nearly two months of freezing of winter construction of the corewall soil material of the dam.

The unfavorable meteorological conditions led to a significant reduction in the number of days for the construction of the dam's corewall fill, and the problem of freezing of the dam's corewall soil became one of the key constraints affecting the dam's progress. Facing the alpine and large temperature difference environment of 3000m above sea level, under the important influence of strong and high frequency freeze-thaw effect, structural damage of fill material and deterioration of engineering properties, the winter construction of the project is beyond the scope of application of the current specifications and existing experience, and there is no successful construction experience to be learned from both at home and abroad.

4.1. TECHNICAL ROUTE FOR WINTER CONSTRUCTION STUDY

Aiming at the key technical problems facing the winter construction of 300m-level gravel soil corewall rockfill dam, the project team has gone through seven years of scientific and technological research, and the technical route is shown in Fig. 4.

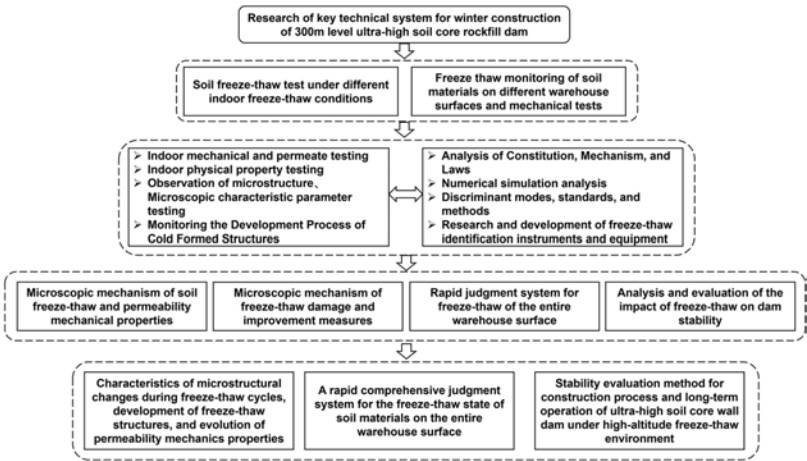


Fig. 4
Technology roadmap

4.2. RESEARCH FINDINGS

Table 2
Comparison of key technology system and application results of winter construction

COMPARISON ITEMS	RESULTS OF THE PROJECT	SIMILAR STUDIES AT HOME AND ABROAD
Characteristics and laws of changes in engineering properties of extra-high gravel soil corewall rockfill dams under high-frequency freezing and thawing in alpine cold	The characteristics and laws of the change of the engineering properties of the soil material of the corewall of extra-high gravel soil corewall rockfill dams under the action of high temperature difference, high frequency freezing and thawing in high cold, the breeding process and the change characteristics of the internal freezing and thawing structure of the soil material have been elucidated, the inner mechanism of the change of the engineering properties of the soil material has been revealed from the microscopic point of view, and the ontological relationship and the system of quantitative value have been constructed to conform to the actual situation[1].	<div>1. There is no research on the freeze-thaw engineering properties of soil materials for extra-high gravel soil corewall rockfill dams at high altitude;</div> <div>2. There is no study on the freeze-thaw mechanism of the impermeable soil material of the corewall of a dam from the micro and micro viewpoint.</div>

(Continued)

Table 2
Continued

COMPARISON ITEMS	RESULTS OF THE PROJECT	SIMILAR STUDIES AT HOME AND ABROAD
Temporal and spatial patterns of change and evolution of winter freezing and thawing of extra-high gravel soil corewall rockfill dams in high-altitude cold regions	The mechanism of ground-air coupling in plateau valley area and complex construction environment conditions was elucidated, the driving factors and main control elements of soil freezing and thawing were clarified, and the types of soil freezing and thawing in different freezing periods and the law of change in space and time were revealed, which provided theoretical guidance and basis for soil freezing and thawing prevention and control.	Most of the existing research on the nature of concrete freeze-thaw and the law of change, there is no systematic research on the space-time law of freezing and thawing of soil materials of alpine and extra-high gravel soil corewall rockfill dams.
Freezing and thawing monitoring prediction, identification technology and equipment for corewall freeze-thawing of extra-high gravel soil corewall rockfill dams in high-altitude cold regions	It has constructed a monitoring system for the prevention and control of winter freezing and thawing of extra-high gravel soil corewall rockfill dams, developed a system for predicting and forecasting the freezing and thawing of soil materials under complex construction environments, created technical methods for the prevention and control of freezing and thawing of large-area soil materials, and researched and developed key technological equipment for the identification of freezing and thawing of large-area soil materials and the prevention and control of soil materials.	<ol style="list-style-type: none"> Most of the existing researches adopt hand-work to carry out temperature monitoring for local soil bodies, and there is no large-area, multi-parameter, three-dimensional freezing and thawing monitoring in the air and space; There is no freeze-thaw identification system that combines point and surface, quantitative and qualitative, rapidity and accuracy.
Winter construction technology of extra-high gravel soil corewall rockfill dams in high altitude and cold area	A freeze-thaw prevention and control system for winter construction has been created, and a quality inspection and evaluation method for winter soil construction has been proposed; a technical quality standard for winter construction of soil materials for the corewall of extra-high gravel soil corewall rockfill dams has been established, and a complete set of technical methods for rapid construction of soil materials in winter has been formed, based on the core of the construction process, technology, and quality inspection and control.	<ol style="list-style-type: none"> There is no new type of heat preservation material and rapid put away equipment for corewall soil material; There is no complete set of corewall construction technology and large-scale continuous construction under low temperature conditions in winter.

4.3. PRACTICAL APPLICATIONS

4.3.1. *Constructing a new principle of freeze-thaw prevention and control for continuous winter construction of corewall of dams*

Based on the general principle of soil freezing and thawing prevention and control, the technical direction of freezing and thawing prevention and control was established, which is "energy replenishment for the mixing field and energy preservation for the corewall of the dam". Based on the change of winter climate environment, the change rule of freezing and thawing law of soil filling process, characteristics and intensity of prevention and control, the three stages of shallow freezing period, deep freezing period and shallow freezing period in the winter construction process are determined. Changing the previous construction principle of "not allowing freezing" of soil material, based on the new theory of "allowing freezing" of loose soil material under the condition of corewall control, it creatively puts forward the principle of "freezing soil is not dammed, freezing soil is not crushed, and the soil is not frozen after crushing", It creatively puts forward the general principle of freeze-thaw prevention and control of "not damming the frozen soil, not crushing the frozen soil, not freezing the soil after crushing, and preserving and enhancing the overall energy and temperature of the soil material"; establishes the general principle of construction of "fast construction and timely covering"; and specifies the "active and passive prevention and control techniques", "optimisation and control of the construction process" and other multi-means combination of prevention and control principles and ways. It has broken through the technical bottleneck of not being able to carry out construction when the temperature is lower than -10°C.

4.3.2. *Formation of three-dimensional soil freeze-thaw monitoring system*

Aiming at the difficulties in identifying and determining the freezing and thawing state and freezing strength of soil materials, a new type of freezing soil identification detector and soil surface freezing state assessment detector have been developed, which realizes the effective identification and precise distinction between soil surface frost, condensation ice and surface soil freezing[2]. It has established a revised mode of accurate measurement of remote infrared ground temperature, and a new mode of monitoring the freezing and thawing of the soil in the corewall of the dam with large-area infrared remote scanning, local proximity detection and observation of key parts, which realizes comprehensive mastery of freezing and thawing conditions of the soil in the whole surface of the silo and accurate identification, as shown in Fig. 5.

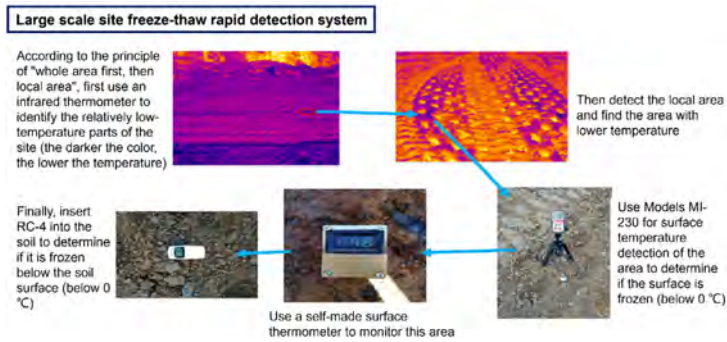


Fig. 5
Rapid test system for freeze-thaw soil on large filled surfaces

4.3.3. *Constructing new construction processes and methods to dramatically improve construction efficiency*

1. It puts forward the new construction technology of “multi-compartment surface graded prevention and control, rapid cross construction”, the method of short-term and long-term freezing and thawing prevention and control in the process of schedule control, and the method and way of flexible application of loose soil material and heat preservation material and joint freezing and thawing prevention and control. It realizes the change from “slow” to “fast” mode of soil filling, as shown in Fig. 6.



Fig. 6
Multi-compartment surface graded prevention and control and rapid cross construction

2. The construction of the soil quarry is carried out in strict accordance with the principle of “centralized mining of a small area at room temperature and covering transportation”. In the mixing of soil materials, the principle of mixing as it is used and covering with geomembrane to protect the finished materials is clearly defined. Contrary to the way of laying materials on top of each other during the flood season, gravel is used to cover the soil materials in winter to keep them warm, as shown in Fig.7.



Fig. 7

Interlayer paving with gravel on top and clay underneath

3. Active warming techniques and equipment for soil materials have been developed, comprehensively improving the ability and technical level of soil materials to prevent and control freezing and thawing[3,4]. The main ways include laying a shed-type heating power system on the filling surface of the corewall, laying sunshine boards in the mixing yard, and using the tail gas of modified dump trucks to heat up during transportation, and all of these researches have achieved very good results. Adopting passive heat preservation technology such as multi-layer composite fabric covering, independently researched and developed large area composite fabric fast retracting equipment (as shown in Fig. 8), which provides technical and equipment support for the prevention and control of freezing and thawing of the soil material in the whole continuous construction process of the corewall of the dam in the winter season, and effectively ensures the temperature of the milled soil material to reach the standard and prevents freezing, and greatly saves the investment of personnel and equipment.



Fig. 8

Fast take-up and take-down equipment for large-area composite fabrics

5. SET OF TECHNIQUES FOR RAINY SEASON CONSTRUCTION OF COREWALL OF DAMS

The rainy season lasts for a long time and the precipitation is concentrated, and the rainfall and the number of days from May to October account for 93.0% and 76% of the whole year respectively. The content of powder and viscous particles is high, and the standard of stopping work in rainy season is strict, the daily rainfall is 2mm or the rain intensity is 0.2mm/min, which is much stricter than the standard of 5mm. It is difficult to forecast rainfall, and the suddenness and randomness of rainfall in the dam area are obvious. Construction quality control in the rainy season is as follows [5–8].

5.1. MAIN MEASURES

5.1.1. *Daily rainfall <5mm*

Normal construction when rainfall is less than 5mm.

5.1.2. $5\text{mm} \leq \text{daily rainfall} < 10\text{mm}$

1. Continuous rainfall

Continuous rainfall of 5-10mm, with low rainfall per unit time, requires the use of flat rolling equipment to quickly smooth and level the gravel soil surface

before the rain; After the rain, based on the test results, a grader is used to scrape off about 5-10cm of the surface soil material of the filling warehouse. The cleaned soil material is directly removed from the core wall area and piled up in the sun drying area (near the upstream cofferdam); According to the test results, after scraping off the surface soil material in the filling area, a bulldozer is used to roughen the gravel soil surface. After passing the moisture content test, the filling warehouse surface immediately enters the normal construction procedure.

2. Sudden rainstorm

The sudden rainstorm with rainfall of 5~10mm has a large amount of rainfall per unit time and a short rainfall time. The rainfall in the construction area is mainly concentrated at night. According to the rainfall characteristics, the centralized leveling and rolling equipment will press the filling silo surface into a smooth surface before the rain; After the rain, based on the test results, a grader is used to cut off about 5-10cm of the surface soil material of the filling warehouse. The cleaned soil material can be spread in the testing area for sun drying or piled up in the sun drying area (near the upstream cofferdam); According to the test results, after scraping off the surface soil material in the filling area, a bulldozer is used to roughen the gravel soil surface. After passing the moisture content test, the filling warehouse surface immediately enters the normal construction procedure.

5.1.3. *Daily rainfall $\geq 10\text{mm}$*

1. Continuous rainfall

For continuous rainfall greater than 10mm, according to the weather forecast, before the rain, a flat rolling equipment is used to quickly roll the gravel soil surface flat and smooth, and plastic cloth is quickly covered (priority is given to covering the filling area and rolling area, if the rainfall is greater than 30mm, it must be fully covered). After the rain, a water pump is used to remove the rainwater manually, and the plastic cloth is removed after the cleaning is completed; Use a bulldozer to remove about 10-15 cm of the surface soil material from the filling warehouse, and then use a grader to finely level the gravel soil surface removed by the bulldozer. The removed soil material is directly removed from the core wall area and piled up in the sun drying area; Use a bulldozer to roughen the gravel soil surface, and after passing the moisture content test, immediately enter the normal construction procedure for filling the warehouse surface.

2. Sudden rainstorm

In case of sudden rainstorm greater than 10mm, according to the weather forecast, the unconstructed warehouse surface shall be polished by flat rolling equipment in advance, and the unconstructed warehouse surface shall be covered with plastic cloth 1~2 hours in advance. After the rain, the rainwater shall be removed by water pump assisted by manual means; For the area

covered with plastic sheeting, a bulldozer is used to remove about 10cm of the surface layer of the filling silo (the specific depth is determined according to the test results), and then a grader is used to finely level the cleared gravel soil surface. The cleared soil material is directly removed from the core wall area and piled up in the sun drying area; Use a bulldozer to roughen the gravel soil surface, and immediately enter the normal construction procedure after passing the moisture content test.

5.2. ADDITIONAL MEASURES

1. The dam surface adopts "turtle-back shape" or "one-way slope" construction, and after sealing the filling surface, for the local small-area water-logging, artificial scooping, sponge water absorption and other measures to exclude; for the soil with excessive water content, take the soil replacement method, and the replacement soil material takes the treatment measures such as turning sunshine and discarding. For soil material with water content exceeding the standard, soil material replacement will be adopted, and the replacement material will be subject to treatment measures such as turning sunshine and discarding.
2. Interceptor ditches are installed on the cover of the corewall and the side ditches on both sides, and PVC water pipes are used to divert the water to the transition material area, so as to avoid the rainwater from the cover area and the slopes on the left and right banks from flowing down the cover concrete to the corewall.
3. Before filling in the rainy season, the moisture content of the soil should be tested, and the soil with qualified moisture content can only be filled on the dam, and ensure that the moisture content of the soil is within the optimal moisture content control range.

5.3. COMPARISON OF CONSTRUCTION STRENGTH OF COREWALL DURING RAINY SEASON

The above measures resulted in a 130% increase in the rate of rise of the corewall during the rainy season and a 92% increase in the amount of corewall fill. As shown in Table 3.

Table 3
Comparison of construction strength of corewall during rainy season

PERIOD OF TIME		JUNE ~ SEPTEMBER 2017	JUNE ~ SEPTEMBER 2018	JUNE ~ SEPTEMBER 2019	JUNE ~ SEPTEMBER 2020	JUNE ~ SEPTEMBER 2021	TOTAL
Filling quantity in the tender document	Filling height (m)	5	5	5	5	5	25
	Filling volume (10 ⁴ m ³)	8.56	10.21	9.6	8.84	7.88	45.09
Actual filling volume	Filling height (m)	13.5	9.3	9.6	13.7	11.3	57.4
	Filling volume (10 ⁴ m ³)	16.59	18.19	17.92	22.96	10.86	86.52
Lifting rate	Filling height	170%	86%	92%	174%	126%	130%
	Filling volume	94%	78%	87%	160%	34%	92%

6. INTELLIGENT FILLING KEY TECHNOLOGY

In view of the project characteristics, corewall rockfill dam intelligent filling technology is utilized to effectively control the whole cycle of dam filling construction. In order to ensure the quality control of the rockfill dam under high-cold and high-altitude conditions, the project team independently researched and developed the intelligent monitoring technology for the whole process of rockfill dam with high corewall[9–11], as shown in Fig. 9.

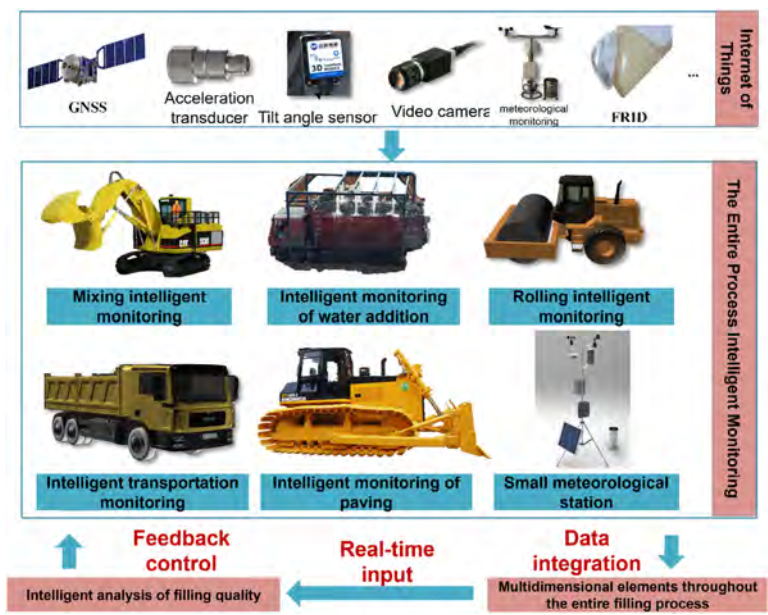


Fig. 9

Intelligent monitoring framework for the whole process of 300m-level high corewall rockfill dams

6.1. INTELLIGENT FILL TECHNOLOGY SITE CONSTRUCTION LAYOUT

The overall system of intelligent fill construction technology site construction includes mixing, transporting, adding water, paving, rolling, as well as the command center and unmanned rolling site mobile center. In the production stage of the dam material, the gravel soil material intelligent mixing process information automatic collection system is used to monitor the mixing situation, and the mixing quality evaluation model is established to comprehensively evaluate the mixing quality. In the dam material transportation stage, the intelligent monitoring system of transportation process is used to monitor the loading, transportation and unloading process of the dam material, and the path planning algorithm is used to optimize the transportation path and improve the transportation efficiency. For stacked rock materials, water needs to be added in the process of damming, and the intelligent water adding system for stacked rock dam materials is used to analyze the optimal amount of water to be added by taking into account multiple factors such as weather and moisture content, and to realize intelligent water adding through radio frequency sensing technology. The dam material needs to be leveled and compacted after it is loaded on the dam, and the intelligent monitoring system for leveling and compacting is adopted to

analyze the construction quality parameters and realize all-around quality evaluation by monitoring the mechanical equipments such as leveling machine and compacting machine. In addition, in view of the problems of high working intensity of roller compactor and great harm to human body, an unmanned roller compactor cluster cooperative operation system has been developed, which realizes the unmanned cooperative operation of roller compactor clusters through unmanned modification of mills and integration of various types of sensors and intelligent control technology, and greatly improves the degree of intelligence of the filling process.

6.2. INTELLIGENT MONITORING SYSTEM FOR THE ENTIRE FILLING PROCESS

6.2.1. *Intelligent monitoring technology for mixing gravel soil materials*

The blending quality of gravel soil material is an important link in the quality control of corewall rockfill dam. The traditional method is to take random samples on site after mixing is completed, which is difficult to reflect the uniformity of mixing. To address this issue, the project applies intelligent monitoring equipment for mixing construction, which realizes real-time collection, data transmission and processing of mechanical position information and operation status information, and real-time display through visualization interface, and alarm prompts if it does not meet the requirements of paving thickness control and mixing, thus realizing visualization and real-time monitoring of the mixing process. At the end of mixing, the corresponding graphical report can be generated to show the mixing situation and evaluate whether the mixing results are qualified or not by the number of mixing passes and other information. As shown in Fig. 10.

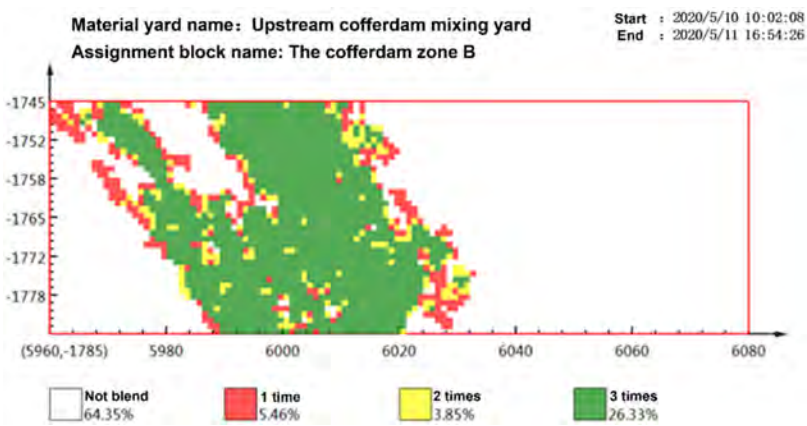


Fig. 10
Graphical report of mixing cycles

6.2.2. *Intelligent monitoring technology for dam material transportation*

This project has high filling intensity, large number of construction machinery and complicated links, if the transportation system on the dam is not reasonably organized, it is very easy to cause poor transportation, resulting in delayed schedule and other problems. This project applies the intelligent monitoring technology of transportation process with full line coverage to monitor the whole process from loading at the material yard to unloading at the dam surface by installing monitoring equipment on the transportation tipper. When it is found that the actual unloading place of the dump truck does not match with the unloading area, it will be alarmed through the monitoring PC terminal and PDA system, and alarm SMS will be sent to the relevant unit personnel in real time to guide and supervise the on-site rectification. At the same time, the system can realize the statistical analysis of the transportation intensity and the traffic flow on the road to the dam, providing data support for the decision-making of the relevant units.

6.2.3. *Intelligent monitoring technology for adding water to dam materials*

In general, the water content of rockfill dams is ensured by adding water to the dam material to improve the compaction quality, but it is not possible to accurately control the water content of the dam material. In order to maintain the design water content of the dam material during the rolling construction, the project applied a water dosing system for rockfill dam material considering the influence of meteorological factors, realizing the precise dosing amount during the transportation of the dam material. The developed dam material automatic water filling system consists of main parts such as automatic water filling station, data processing center and monitoring terminal. The center console automatically reads in the vehicle-related information, determines the amount of water, opens the solenoid valve to start adding water, and according to the real-time data sent by the flowmeter, determines in real time whether the amount of water added meets the design requirements. When the water is insufficient, it displays an alarm message for effective feedback control.

6.2.4. *Intelligent monitoring technology of compaction quality*

The project monitors the entire filling construction process of the dam, including the thickness of the material, the rolling parameters of the roller (including the speed of the roller, the number of rolling passes, the output state of the excitation force, the thickness of the compaction, etc.), through the installation of positional monitoring equipment on the bulldozer and the roller, as shown in Fig. 11. When the monitoring system discovers that the thickness of the paving material does not meet the standard, and there are construction irregularities such as overspeed and missed rolling of the roller, an alarm will be triggered through the monitoring PC terminal and PDA system, and real-time alarm messages will be sent to relevant personnel to guide and supervise on-site rectification, thereby ensuring the quality of the dam filling paving and rolling construction.

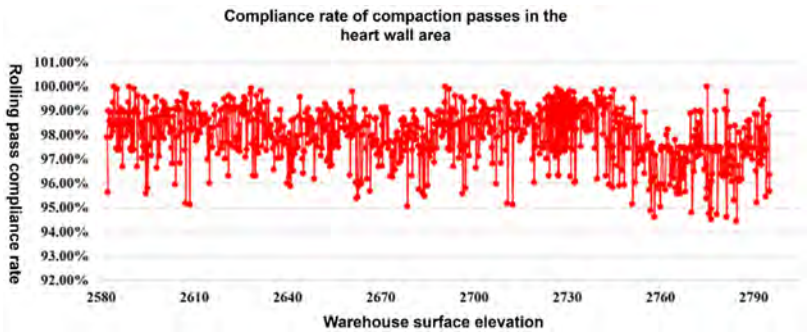


Fig. 11
Statistical chart of the compliance rate of the number of compaction passes in the corewall area

6.3. COLLABORATIVE OPERATION SYSTEM FOR UNMANNED CRUSHING MACHINE GROUP

The unmanned rolling machine group collaborative operation system (as shown in Fig. 12 to 13) is a new breakthrough in intelligent construction of water conservancy and hydropower engineering. The system adopts high-precision positioning and navigation, wireless communication, intelligent simulation, path tracking, intelligent obstacle avoidance, and machine group collaborative operation technologies to achieve real-time dynamic intelligent simulation of dam construction process and intelligent rolling operation of dam rolling machine group. It plays an important role in reducing manual labor intensity, improving construction efficiency, and ensuring project quality. At the same time, efficient collaborative operation management of unmanned crushing machine clusters has been achieved.

Data statistical analysis shows that during the construction process of the three types of material areas, the one-time compaction compliance rate of the unmanned rolling machine group has increased by an average of 5.67% compared to manual operations, the compaction efficiency has increased by an average of 17.29% compared to manual operations, and the construction cost (length of operation path) has decreased by an average of 12.63% compared to manual operations. Significant comprehensive benefits have been achieved, realizing large-scale and efficient collaborative construction of the unmanned rolling machine group under complex construction conditions.

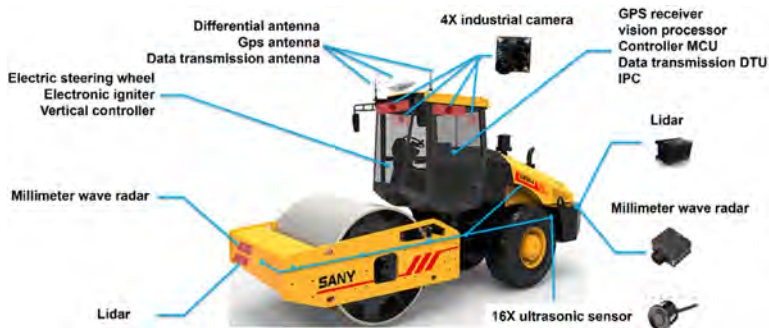


Fig. 12
Autonomous perception framework for modified unmanned rolling machine



Fig. 13
Integrated unmanned rolling machine

7. CONSTRUCTION QUALITY

In 2023, the reservoir will be filled to EL.2861.15m. The leakage rate of the grouting gallery at the bottom of the dam is only 0.17l/s. As of June 2024, the maximum settlement of the upstream rock filling area is 2609mm, accounting for 1.31% of the corresponding filling height. The maximum settlement of the core wall is 3342mm, accounting for 1.13% of the filling height of the core wall. The maximum settlement in the downstream rock filling area is 2893mm, accounting for 1.49% of the corresponding filling height. The construction quality is excellent, as shown in Table 4 to 9.

Table 4
Quality inspection results of gravel soil filling

TESTING ITEMS	PENETRATION INDICATORS			MOISTURE CONTENT INDEX		COMPACTION INDEX			GRADING INDEX			
	IN-SITU	INDOOR VERTICAL	INDOOR LEVEL	DIFFERENCE FROM WOP (%)		WET DENSITY (G/CM ³)	DRY DENSITY (G/CM ³)	COMPACTION DEGREE (%)	MAXIMUM PARTICLE SIZE (MM)	PS content (%)	<0.075MM CONTENT (%)	<0.005MM CONTENT (%)
				FULL MATERIAL	FINE MATERIAL							
Design value	< 1.×10 ⁻⁶			-1.5~+2.5		/	/	≥ 100	≤ 150	30~50	≥ 15	≥ 8
Number of detection groups	22	22	24	10320	8468	10321	10321	10321	3550	10321	3550	3550
Maximum value	8.49×10 ⁻⁶	7.65×10 ⁻⁶	6.18×10 ⁻⁶	2.6	2.0	2.46	2.28	109.8	114	48.2	55.0	20.9
Minimum value	2.05×10 ⁻⁶	3.07×10 ⁻⁶	1.43×10 ⁻⁶	-1.4	-1.8	2.26	2.07	100.0	61	31.2	37.6	8.8
Average value	4.24×10 ⁻⁶	4.59×10 ⁻⁶	4.58×10 ⁻⁶	0.7	-0.1	2.38	2.19	103.5	85	40.4	46.9	14.3
Qualification rate (%)	100	100	100	99.9	99.9	/	/	100	100	100	100	100

Table 5
Quality inspection results of contact clay filling (EL.2640m~2845m)

TESTING ITEMS	MOISTURE CONTENT INDEX		COMPACTION INDEX			GRADING INDEX		
	MOISTURE CONTENT	DIFFERENCE FROM WOP (%)	WET DENSITY (G/CM ³)	DRY DENSITY (G/CM ³)	COMPACTION DEGREE (%)	<5MM CONTENT (%)	<0.075MM CONTENT (%)	<0.005MM CONTENT (%)
Design value	/	+0.5~+3.5	/	/	94~100	> 90	> 75	> 24
Number of detection groups	3419	3419	3419	3419	3419	393	393	393
Maximum value	22.3	3.1	2.12	1.80	100.0	99.6	95.2	43.8
Minimum value	17.1	-0.5	2.02	1.67	94.0	91.1	77.1	24.1
Average value	19.2	1.6	2.07	1.74	97.3	96.6	84.8	29.5
Qualification rate (%)	/	98.1	/	/	100	100	100	100

Table 6
Penetration test results of contact clay material

TESTING ITEMS	DESIGN INDICATORS (CM/S)	NUMBER OF GROUPS	PERMEABILITY COEFFICIENT (CM/S)		
			MAXIMUM VALUE	MINIMUM VALUE	AVERAGE VALUE
In-situ	< 1×10 ⁻⁶	16	9.14×10 ⁻⁷	5.29×10 ⁻⁷	6.58×10 ⁻⁷
Indoor vertical		23	8.45×10 ⁻⁷	4.64×10 ⁻⁹	5.89×10 ⁻⁷
Indoor level		23	7.51×10 ⁻⁷	3.41×10 ⁻⁷	5.14×10 ⁻⁷

Table 7
Penetration test results of filter material I

TESTING ITEMS	DESIGN INDICATORS (CM/S)	NUMBER OF GROUPS	PERMEABILITY COEFFICIENT (CM/S)		
			MAXIMUM VALUE	MINIMUM VALUE	AVERAGE VALUE
In-situ	$\geq 1 \times 10^{-3}$	163	2.14×10^{-2}	1.79×10^{-3}	5.70×10^{-3}

Table 8
Penetration test results of filter material II

TESTING ITEMS	DESIGN INDICATORS (CM/S)	NUMBER OF GROUPS	PERMEABILITY COEFFICIENT (CM/S)		
			MAXIMUM VALUE	MINIMUM VALUE	AVERAGE VALUE
In-situ	$\geq 1 \times 10^{-2}$	164	6.60×10^{-1}	1.70×10^{-2}	6.00×10^{-2}

Table 9
Penetration test results of transition material

TESTING ITEMS	DESIGN INDICATORS (CM/S)	NUMBER OF GROUPS	PERMEABILITY COEFFICIENT (CM/S)		
			MAXIMUM VALUE	MINIMUM VALUE	AVERAGE VALUE
In-situ	$\geq 5 \times 10^{-2}$	43	9.30×10^{-2}	5.98×10^{-2}	7.31×10^{-2}

REFERENCES

[1] ZHANG M, LU J, PEI W, LAI Y, YAN Z, WAN X. Laboratory study on the frost-proof performance of a novel embankment dam in seasonally frozen regions. *Journal of Hydrology*. 2021, 602: 126769.

[2] LIANG J, LIU D. Temperature rising and anti-freezing performance of gravel-clay mixed with PCM applying infrared radiation during winter construction. *Case Studies in Construction Materials*. 2024, 21: e03483.

[3] CHEN B, HE M, HUANG Z, WU Z. Long-tern field test and numerical simulation of foamed polyurethane insulation on concrete dam in severely cold region. *Construction and Building Materials*. 2019, 212: 618–34.

- [4] ZHANG X-F, LI S-Y, LI Y-L, GE Y, LI H. Effect of superficial insulation on roller-compacted concrete dams in cold regions. *Advances in Engineering Software*. 2011, 42(11): 939–43.
- [5] HUANG Z, SHEN Z, XU L, SUN Y, LI H, LIU D. Seepage characteristics of core rockfill dam foundation with double cutoff walls in deep overburden: A case study. *Case Studies in Construction Materials*. 2024, 21: e03576.
- [6] CHEN Y, HU R, ZHOU C, LI D, RONG G, JIANG Q. A new classification of seepage control mechanisms in geotechnical engineering. *Journal of Rock Mechanics and Geotechnical Engineering*. 2010, 2(3): 209–22.
- [7] RICE JOHN D, DUNCAN JM. Findings of Case Histories on the Long-Term Performance of Seepage Barriers in Dams. *Journal of Geotechnical and Geoenvironmental Engineering*. 2010, 136(1): 2–15.
- [8] TORABI HAGHIGHI A, TUOMELA A, HEKMATZADEH AA. Assessing the Efficiency of Seepage Control Measures in Earthfill Dams. *Geotechnical and Geological Engineering*. 2020, 38(5): 5667–80.
- [9] LIN W, WANG J, REN B, YU J, WANG X, ZHANG T. Robust optimization of rolling parameters of coarse aggregates based on improved response surface method using satisfaction function method based on entropy and adaptive chaotic gray wolf optimization. *Construction and Building Materials*. 2022, 316: 125839.
- [10] ZHANG Q, AN Z, LIU T, ZHANG Z, HUANGFU Z, LI Q, YANG Q, LIU J. Intelligent rolling compaction system for earth-rock dams. *Automation in Construction*. 2020, 116: 103246.
- [11] SHI M, WANG J, LI Q, CUI B, GUAN S, ZENG T. Accelerated Earth-Rockfill Dam Compaction by Collaborative Operation of Unmanned Roller Fleet. *Journal of Construction Engineering and Management*. 2022, 148(7): 04022046.

COMMISSION INTERNATIONALE DES
GRANDS BARRAGES

VINGT-HUITIEME CONGRES DES
GRANDS BARRAGES
CHENGDU, MAI 2025

ON DESIGN AND CONSTRUCTION TECHNOLOGY OF LARGE SILO FOR SAND AND GRAVEL SYSTEM IN HIGH ALTITUDE AREA (*)

Peng CHAO, Liu CHAOJIAN, Luo JINGSONG, Liu MINGWAN & Xie SIXIANG
Hydropower Bureau Tibet Construction Engineering Co., Ltd, Tibet, Lhasa

CHINA

SUMMARY

In order to realize the safe and rapid construction of large silo of semi-finished materials for large-scale gravel system in high altitude area, by adjusting the traditional steel semi-finished product silo of sand processing system to large silo structure and adopting inverted chain method, the difficulty of silo construction is reduced, the installation efficiency of silo is improved, and dust emission is reduced in the process of stacking. At the same time, during the whole construction process, the laser calibrator is used to carry out the real-time observation of the level, verticality and ovality of the silo wall upper mouth, and the electric chain-down centralized control device is adopted to ensure the chain-down synchronous lifting, so that the silo in the lifting process always under uniform force. This provides valuable experience for the follow-up of similar projects.

RÉSUMÉ

Afin de réaliser la construction sûre et rapide d'un grand silo de matériaux semi-finis pour un système de gravier à grande échelle dans une zone de haute

**Conception et technologie de construction d'un grand silo pour sables et graviers en haute altitude*

altitude, on adapte le silo traditionnel de produits semi-finis en acier du système de traitement du sable à la structure du grand silo. On retient la méthode de la chaîne inversée. Ainsi, la difficulté de la construction du silo est réduite, l'efficacité de l'installation du silo est améliorée et l'émission de poussière est réduite lors du processus d'empilage. En même temps, pendant tout le processus de construction, le calibre laser est utilisé pour observer en temps réel le niveau, la verticalité et l'ovalisation de la partie supérieure de la paroi du silo. Un dispositif de contrôle centralisé de la chaîne électrique est adopté pour assurer le levage synchronisé de la chaîne, de sorte que le silo soit toujours soumis à une force uniforme pendant le processus de levage. Cela permet d'acquérir une expérience précieuse pour le suivi de projets similaires.

1. INTRODUCTION

In traditional sand and gravel processing systems, semi-finished material silos are often built using steel and are semi-enclosed. However, such steel silos have notable drawbacks, including long construction periods, compact footprint, extensive conveyor galleries, and considerable dead storage capacity. With advancements in technology, large steel silos have evolved, providing advantages such as compact footprint, full enclosure, shorter construction periods, and reduced dead storage capacity. The JX Hydropower Station, the first to incorporate silos into a high-altitude hydropower station's sand and gravel aggregate processing system, features a large and complex structure. The silo measures 30 meters in diameter, 24 meters in height, with a capacity of 11,800 m³ and a storage volume of 19,470 tons. The silo is installed using an inverted method with chain hoists, supported by a 25-ton truck crane, leading to a shortened construction period and improved efficiency.

2. PROJECT OVERVIEW

The JX Hydropower Station, situated on the border of Sangri County and Gyaca County in Shannan, Xizang Autonomous Region, is the third of eight planned hydropower stations along the middle reaches of the Yarlung Tsangpo River, spanning from the Woka River estuary to Lang County. The station has a total installed capacity of 600 MW, utilizing three 200 MW Francis-type turbine-generator units. Classified as a Category II project, it is considered a large-scale (Class 2) development. The key components of the station include water-retaining structures, flood discharge and energy dissipation structures, and a water diversion power generation system.

The sand and gravel processing system for the JX Hydropower Station is located 1.9 km downstream of the dam site in JX Village. The semi-finished material silo is designed as a cylindrical structure with a diameter of 30 meters and a height of 24 meters. The foundation height is 0.3 meters, the vertical section of the silo body is 13.2 meters high, and the multi-faceted steel structure roof reaches a height of 10.5 meters. The entire silo weighs approximately 250 tons. The structural design of the silo is shown in Figure 1, and a real-life photograph can be seen in Figure 2.

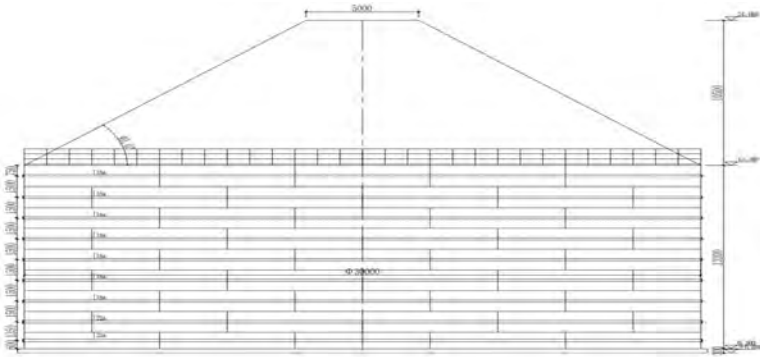


Fig. 1
Silo Elevation View



Fig. 2
Real-Life Photograph of the Silo

3. ANALYSIS OF KEY CHALLENGES AND SOLUTIONS

3.1. HIGH CONSTRUCTION DIFFICULTY AND PRECISION REQUIREMENTS.

1. The silo, weighing 250 tons, presents substantial challenges due to its large construction workload and tight project timeline, which impose significant demands on lifting operations and installation precision. To address these challenges, an inverted method is used, significantly reducing the amount of work performed at height, easing the lifting process, and expediting construction progress.
2. BIM technology is employed for modeling, facilitating pre-installation simulations and plan comparisons to ensure feasibility, enhance precision, and accelerate the installation process.
3. Throughout the silo installation, a laser calibration instrument monitors the levelness, verticality, and ellipticity of the silo wall's upper edge in real time, ensuring precise installation.
4. Given that the primary construction period is in winter, welding rods are kept warm in an insulated box and used as needed. After welding, asbestos blankets are applied to insulate the weld seams.

3.2. SIGNIFICANT SAFETY RISKS DURING CONSTRUCTION.

The project's short timeline, heavy lifting loads with electric chain hoists, and winter conditions pose significant safety risks during construction.

1. Increase personnel and equipment for the silo installation to ensure that on-site progress meets project milestones.
2. Conduct a safety briefing on lifting operations before construction begins, assign a dedicated supervisor to oversee lifting operations, thoroughly inspect all lifting equipment to meet required standards, and strictly adhere to the "Ten No-Lift" rule.
3. Utilize a centralized control device for the electric chain hoists to ensure synchronized lifting and prevent the silo from tilting or toppling during the process.
4. Schedule lifting operations during daylight hours to take advantage of better visibility and avoid nighttime work.
5. Assign personnel to remove snow and ice from the construction site daily to maintain safety.

4. CONSTRUCTION EQUIPMENT LAYOUT

The silo is installed using an inverted method with chain hoists[1], supported by a 25-ton truck crane. Electric chain hoists are uniformly arranged in a concentric circle inside the silo, positioned 400 mm from the silo walls. A total of 38 electric chain hoists, each with a 10-ton capacity, are used for the lifting operations. These hoists are mounted on inverted columns made of galvanized steel pipes with a diameter of $\phi 219 \times 10$ mm. The columns stand 3.5 meters high, with the lifting lugs, bases, and stiffeners made from 16 mm thick steel plates. The layout of the inverted columns is illustrated in Figure 3.

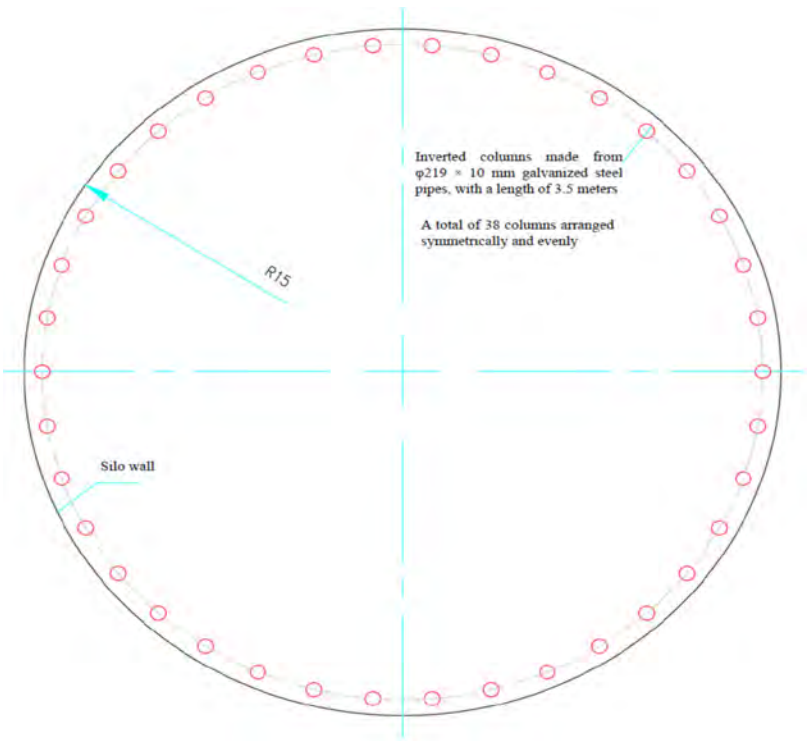


Fig. 3
Layout of Inverted Columns

The inverted columns should be symmetrically and evenly arranged with the center of the silo as the reference point. The distance between the columns and the silo wall must align with the vertical line of the electric chain hoists and the lifting lugs

fixed at the top of the columns. Each pair of symmetrical columns is secured with 19 steel wire ropes, each measuring $6 \times 37 - \phi 15$ mm, with a total length of 32 meters (including an additional 1 meter on each side). The columns must be vertically aligned during installation and fully welded to the embedded steel plates in the concrete foundation. Two reinforcing diagonal braces, made from $\angle 75 \times 7$ angle steel, are installed 2.5 meters above the base of each column to provide additional reinforcement. The horizontal angle between each brace and the ground, as well as the angle between the two braces, is set at 45° .

The silo is divided into 10 segments per layer, with each segment measuring 9.42 meters \times 1.5 meters (length \times width). The backing bars are fabricated in sections, similar to the silo segments, and are divided into 10 sections, each made from [25-channel steel arcs, with each section being 9.42 meters long. Backing bars are installed at the base of the four columns that divide the silo wall into four equal sections. Four 16-ton jacks are used to lift the backing bars, ensuring a snug fit against the silo wall, and the backing bars are secured to the wall using gantry clamps. To expedite the backing bar installation, the jacks are positioned between adjacent columns and must be arranged symmetrically. Additionally, to ensure a secure fit between the backing bars and the wall, the backing bars should be fabricated concurrently with the wall panels in a temporary metal processing factory, with the curvature of the backing bars matching that of the silo wall. Lifting lugs are welded to the backing bars and fully welded. Electric chain hoists, controlled by a centralized control system, are used to lift the lugs and achieve the lifting of the silo. Besides the centralized control system, a separate lifting device for the electric chain hoists is also required.

A schematic of the electric chain hoist lifting is shown in Figure 4.

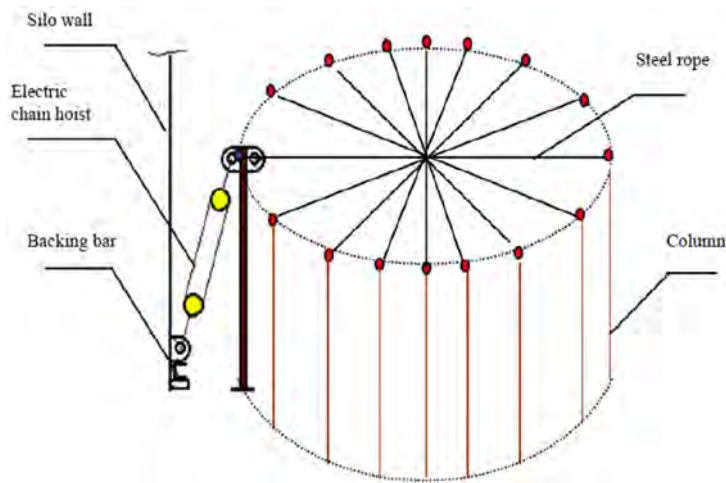


Fig. 4
Layout of Electric Chain Hoists

5. DESIGN PROPOSAL

5.1. DESIGN BASIS

- Code for Design of Steel Silo Structures (GB 50884-2013)

5.2. STEEL SILO CONFIGURATION

- Wall thickness: -8 mm—6 m
-10mm—3m
-12mm—3m
-14mm—1.2m
- Vertical stiffener: I-beam type 14—13.2 m—80 pieces
- Circumferential stiffening ribs: [16a—7 ribs
[20a—2 ribs

5.3. BASIC PARAMETERS

- Silo diameter (D) = 30 m
- Height of the vertical section of the silo (H) = 13.2 m
- Material bulk density (γ) = 16 kN/m³
- Angle of internal friction of the material (α) = 35°
- Friction coefficient between the material and steel plate (μ) = 0.35
- Lateral pressure coefficient (k) = $\tan^2 (45^\circ - \phi/2) = 0.271$
- Hydraulic radius (ρ) = $d_n/4 = 7.5$ m
- Wind load shape coefficient (μ_s) = 0.8
- Elastic modulus of steel (E) = 206×10^3 N/mm²
- Design tensile and compressive strength of Q235 steel = 215 N/mm²
- Design tensile strength of Q235 steel for secondary butt welds (f^w_t) = 215 N/mm²
- Design shear strength of Q235 steel for fillet welds (f^w_t) = 160 N/mm²

5.4. LOAD AND LOAD EFFECT COMBINATIONS

1. Silo wall height (H) = 13.2 m
Actual material depth (s) = 16.7 m

2. Standard value of horizontal pressure exerted by the stored material on the unit area of the silo wall[2]:

$$P_{hk} = C_h \gamma \rho \left(1 - e^{-\frac{\mu_k s}{\rho}} \right) / \mu = 2 * 16 * 7.5 * (1 - e^{-0.35 * 0.271 * \frac{16.7}{7.5}}) / 0.35$$

$$= 130.3 \text{ KN/m}^2$$

3. Wind load:

According to the specifications: Height variation coefficient (μ_z) = 1.29;

Shape coefficient (μ_s) = 0.8

Wind-induced vibration coefficient (β_z) = 1.64

Basic wind pressure (W_0) = 0.3 KN/m²

The standard value of the wind load is: $W_k = \beta_z \mu_s \mu_z W_0 = 1.64 * 0.8 * 1.29 * 0.3 = 0.51 \text{ KN/m}^2$

Standard value of vertical pressure on the unit perimeter of the silo wall due to wind load is:

$$q_{wk} = w_k * \frac{\pi d_n h_n}{2(\pi d_n + h_n)} = 0.51 * \frac{\pi * 30 * 24}{2 * (\pi * 30 + 24)} = 4.9 \text{ KN/m}$$

4. Standard value of vertical pressure on the unit perimeter of the silo wall due to permanent load:

Assuming the silo weight (W) = 2,500 KN

$$q_{gk} = \frac{W}{\pi d} = 2,500 / 30\pi = 26.5 \text{ KN/m}$$

5. Standard value of the vertical frictional force at depth S exerted by the stored material on the unit area of the silo wall:

$$P_{fk} = \mu P_{hk} = 0.35 * 130.3 = 45.6 \text{ KN/m}^2$$

6. Standard value of the total frictional force exerted by the stored material on the unit perimeter of the silo wall:

$$q_{fk} = C_f \rho \left[\gamma s - \frac{\gamma \rho l - e^{-\frac{\mu_k s}{\rho}}}{\mu_k} \right] = 1.1 * 7.5 * (16 * 16.7 - 240.4) = 221.3 \text{ KN/m}$$

7. According to relevant specifications, vertical seismic effects can be disregarded for ground-mounted steel silos

8. Standard value of the vertical pressure on the unit perimeter of the silo wall due to roof and rooftop building variable loads:

$$q_{Qik} = \frac{500}{30\pi} = 5.3 \text{ kN/m}$$

9. Basic combination for horizontal pressure on the unit area of the silo wall:

$$P_h = 1.3P_{hk} = 1.3 \cdot 130.3 = 169.4 \text{ kN/m}^2$$

10. Basic combination of vertical forces on the unit perimeter of the silo wall:

When wind load is considered:

$$\begin{aligned} q_v &= 1.2q_{gk} + 1.3q_{fk} + 1.4 \cdot 0.6 \sum (q_{wk} + q_{Qik}) \\ &= 1.2 \cdot 26.5 + 1.3 \cdot 221.3 + 1.4 \cdot 0.6 \cdot (4.9 + 5.3) = 328.1 \text{ kN/m} \end{aligned}$$

5.5. SILO STRUCTURAL CHECKING CALCULATION

1. Configuration of the silo at height (H) = 13.2 m
 Plate thickness: - 14 mm
 Stiffener: 80 pieces, I-beam type 14, cross-sectional area (A_s) = 21.5 cm²,
 moment of inertia (I_s) = 712 cm⁴
2. Silo wall
 - (1) The plate is treated as a tensile member under horizontal forces:
 At H = 13.2 m, the plate thickness is 14 mm

$$\sigma_t = P_h d_n / 2t \leq f$$

$$\sigma_t = 169.4 \cdot 30 / (2 \cdot 14) = 181.5 \text{ N/mm}^2 < 215 \text{ N/mm}^2$$

- (2) The plate is treated as a compressive member under vertical forces:

$$\sigma_c = q_v / t = 328.1 / 14 = 23.4 \text{ N/mm}^2 < 215 \text{ N/mm}^2$$

- (3) Equivalent stress under combined effect of circumferential tension and vertical pressure:

$$\sigma_{zs} = \sqrt{\sigma_t^2 + \sigma_c^2} - \sigma_t \sigma_c = 171 \text{ N/mm}^2$$

$$< 215 \text{ N/mm}^2 \text{ (Requirement satisfied)}$$

- (4) The stress on the butt welds on silo wall is calculated as:

$$\sigma_t = \frac{N}{L_w t} = 181.5 \text{ N/mm}^2 \leq f_t^w \text{ (215 N/mm}^2 \text{)}$$

3. Stiffener

The strength of the cross-section of the stiffening rib or the combination of stiffening rib and silo wall is calculated as:

$$N = q_v b$$

$$\sigma = \frac{N}{A} \pm \frac{M}{W_n} \leq f$$

Requirement satisfied

4. Strength of the stiffener and silo wall connection

Design vertical force transmitted to the stiffening rib per unit height of the silo wall:

$$V = \left[1.2 P_{gk} + 1.3 C_f P_{fk} + \left(1.2 q_{gk} + 1.4 \sum q_{Qik} \right) / h_s \right] b$$

$$V = [1.2 * 26.5 + 1.3 * 1.1 * 45.9 + (1.2 * 26.5 + 1.4 * 5.3) / 13.2] * 1.1781$$

$$= 118.3 \text{ KN/m}$$

When using fillet welds, calculate:

The connection between the stiffener and the silo wall is achieved by double-sided 3 mm fillet welds, each 200 mm long, spaced 500 mm apart;

$$\tau_f = \frac{VL}{h_e L_w} \leq f_f^w$$

$$\tau_f = 118.3 * 700 / 3 / 200 / 2 = 69 \text{ N/mm}^2 < 160 \text{ N/mm}^2 \text{ (Requirement satisfied)}$$

5. Silo stability under vertical loads

1. When vertical wind-resistant I-beams are present, the equivalent thickness of the silo wall is calculated as:

$$t_s = \sqrt[3]{12 \left(\frac{I_s}{b} + \frac{A_s e_s^2}{b} + t e_1^2 + t e_1^2 + \frac{t^3}{12} \right)}$$

$$t_s = \sqrt[3]{12 \left(\frac{7120000}{1178.1} + \frac{2150 * 70^2 + 14 * 7^2}{1178.1} + 14 * 7^2 + \frac{14^3}{12} \right)} = 57.6 \text{ mm}$$

2. Under vertical axial loads, the following calculation applies:

$$\sigma_c \leq \sigma_{cr} = k_p E t / R$$

$$k_p = \frac{1}{2} / \pi * (100 * t / R)^{\frac{3}{8}}$$

$$k_p = 0.111$$

$$\sigma_{cr} = 87.85 \text{ N/mm}^2 > \sigma_c \text{ (Requirement satisfied)}$$

3. When both vertical pressure and horizontal pressure from stored materials are combined, the following calculation applies:

$$\sigma_c \leq \sigma_{cr} = k_p' E t / R$$

$$k_p' = k_p + 0.265 \frac{R}{t} \sqrt{\frac{P_{hk}}{E}} = 0.166$$

$$\sigma_{cr} = 131.3 \text{ N/mm}^2 > \sigma_c \text{ (Requirement satisfied)}$$

6. Conclusion

Q.109 - R.30

The silo wall structure meets the strength and stability requirements for a height of 13.2 m.

5.6. CHECKING CALCULATION RESULTS FOR SILO STRUCTURE AT DIFFERENT CALCULATED HEIGHTS

The checking calculation results are detailed in Table 1.

Table 1
Checking Calculation Results for Silo Structure at Different Calculated Heights

CALCULATED HEIGHT (M)	MATERIAL DEPTH (M)	DESIGN HORIZONTAL PRESSURE PER UNIT AREA OF SILO WALL (KN/M ²)	DESIGN VERTICAL PRESSURE PER UNIT PERIMETER OF SILO WALL (KN/ M)	PLATE THICKNESS (MM)	HORIZONTAL STRESS IN SILO WALL (N/MM ²)	VERTICAL STRESS IN SILO WALL (N/ MM2)	STIFFENER	STRESS IN STIFFENER CROSS- SECTION (N/MM ²)	EQUIVALENT THICKNESS BASED ON STIFFNESS (TS) (MM)	CRITICAL STRESS IN SILO WALL (N/ MM ²)	CONCLUSION
6	9.5	100.9	131.6	8	189.2	16.5	I-beam type 14	49.8	56.7	119.5	Requirement satisfied
9	12.5	130.3	198.9	10	195.5	19.9	I-beam type 14	64.2	56.9	124.5	Requirement satisfied
12	15.5	158.7	283.0	12	198.3	23.6	I-beam type 14	77.3	57.2	129.1	Requirement satisfied
13.2	16.7	169.4	328.1	14	181.5	24.3	I-beam type 14	76	57.6	131.3	Requirement satisfied

6. SILO CONSTRUCTION

6.1. CONSTRUCTION PROCEDURE

The construction process flow for the silo is shown in Figure 5.

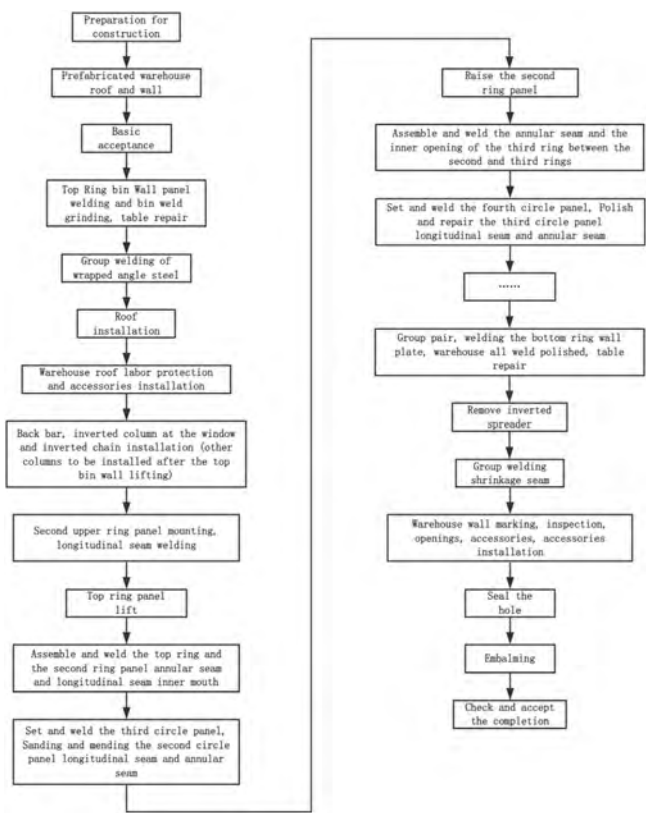


Fig. 5
Silo Construction Procedure

6.2. PREFABRICATION

The silo wall and roof steel plates are fabricated in the metalworking shop according to the dimensions specified in the drawings. After fabrication, these components are stored in the shop's storage area and transported to the construction site prior to installation. Effective measures must be implemented to prevent deformation of prefabricated components during temporary storage, transportation, and on-site storage.

6.2.1. Silo wall prefabrication

Upon arrival, the steel plates are beveled according to the dimensions specified in the drawings at the metalworking shop. All wall panels should be marked and stacked in order after cutting and forming. A designated person must recheck the geometric dimensions of the wall panels, complete a self-inspection record form, and archive it.

After the silo wall panels are cut and processed according to the dimensions specified in the drawings, they are inspected by a dedicated person for quality assurance and self-inspection record forms are completed. The panels are then

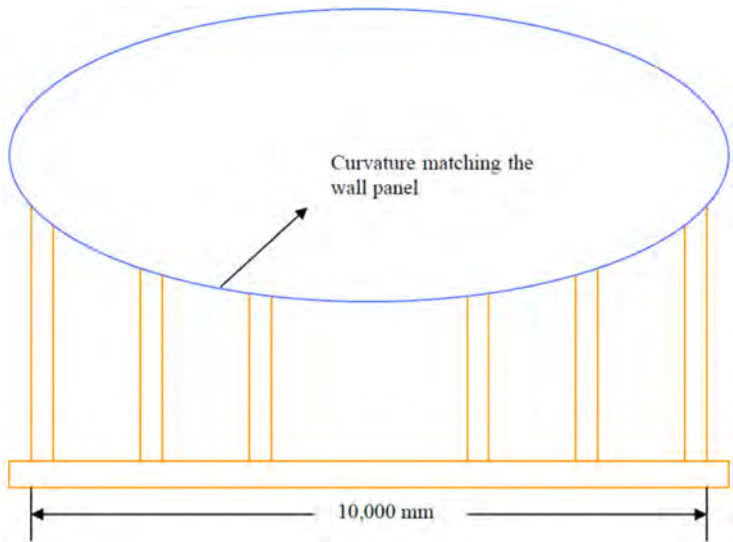


Fig. 6
Storage and Transport Molds for Rolled Wall Panels

lifted using a 16-ton truck crane and subjected to roll forming operations with a roll bending machine. This rolling operation should be carried out by experienced technicians. The curvature of each silo wall panel must comply with the allowable values defined in the specifications.

After rolling and verifying the curvature of the wall panels, they should be stored on molds with matching curvature. During transport from the metalworking shop to the construction site, wall panels should be placed on similar molds to prevent deformation and damage. The storage and transport molds used for the rolled wall panels are shown in Figure 6:

6.2.2. Silo roof prefabrication

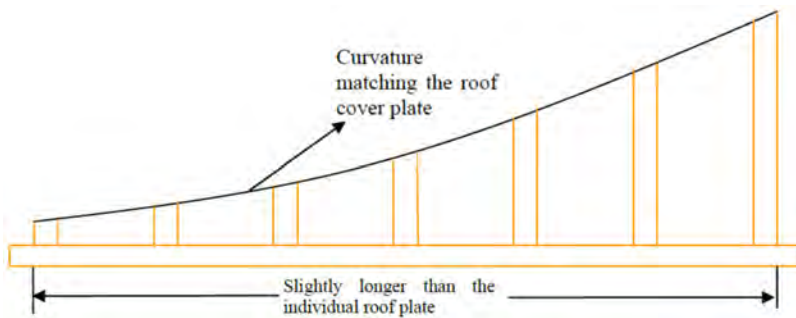


Fig. 7
Storage and Transport Molds for Individual Roof Plate

The silo roof components should be prefabricated precisely according to the dimensions specified in the drawings. For the roof cover plates, weld seams should be staggered during prefabrication to prevent stress concentrations that could compromise structural safety. Reinforcement should be fabricated and formed at the temporary metalworking shop, and their curvature checked using a template that matches the rib curvature. The silo roof cover plates should be joined using butt welding with full penetration. All 74 roof cover plates must be welded to the reinforcement using the designated molds. After fabrication, the curvature of each cover plate should be verified with a template matching the plate's curvature. The curvature deviation must not exceed the allowable limits defined in the specifications and design drawings.

The storage and transport molds for individual roof plates are shown in Figure 7:

6.2.3. *Prefabrication of accessories and fittings*

In accordance with site conditions, accessories and fittings for the silo are prefabricated at the metalworking shop. After prefabrication, these components are transported to the site for ground assembly. A 25-ton truck crane is utilized for lifting, which minimizes high-altitude work and speeds up the installation process on site. Once the accessories and fittings are formed and pass inspection, they should be properly labeled and stored at the designated location.

6.3. TRANSPORTATION

The silo walls and roof are loaded onto a 16-ton truck crane at the metalworking shop and transported to the site using a 15-ton flatbed truck.

6.4. INSTALLATION CONSTRUCTION

6.4.1. *Foundation acceptance*

Inspect the surface quality and structural dimensions of the silo concrete foundation according to the design drawings and relevant standards. Ensure that the elevation deviation of the foundation center point and the elevation differences around the connection between the silo wall and the foundation do not exceed the specified values in the design drawings and specifications, and the concrete foundation must be free of through cracks.

6.4.2. *Installation of top ring of wall panels and lower ring*

Install the top ring of wall panels in layers and sections according to the layout drawing, ensuring all panels are installed in the same direction (either clockwise or counterclockwise). Use a laser calibration instrument throughout the installation process to monitor the wall panels and ensure that the top ring of wall panels meet the required levelness, verticality, and ellipticity. Once the levelness, verticality, and ellipticity of the wall panels are adjusted, secure the panels with support brackets. To prevent deformation during welding and ensure welding quality, place three anti-deformation arc reinforcement plates at the longitudinal seam of the wall panels. Weld the longitudinal seams in the order of outer seam → root cleaning → inner seam. After completing all longitudinal seams, grind the seams to ensure they are flush with the silo wall.[3]

After the top ring of wall panels are installed as per the construction drawings and the seams pass the inspection, proceed with the installation of the lower ring. The lower ring should be made of $\angle 50 \times 5$ angle steel, with the longitudinal seams of the top ring of wall panels staggered from the lower ring's joints by at least 200 mm.

Leave one wall panel uninstalled on each layer before construction to serve as an access opening for personnel and equipment. After the remaining wall panels have been inspected and approved, install the closing wall panel. Check the quality of the closing panel before proceeding to install the next layer of wall panels, and repeat this process accordingly.

6.4.3. *Silo roof installation*

Once the top cycle of wall panels are installed and quality-checked, proceed with the installation of the roof cover plate and roof accessories. Install the roof installation scaffold inside the silo, ensuring its axis aligns with the silo axis. The scaffold height is 12 m (with the roof height at 10.5 m and the height of the top cycle of wall panels at 1.5 m), and the scaffold's upper surface should be parallel to the upper surface of the lower ring. Install two rings of steel ring beams between the central scaffold and the lower ring, ensuring the upper surface of the steel ring beams is parallel to the upper surface of the lower ring. Mark the positions for individual roof plates on the central scaffold, steel ring beams, and lower ring. Use a 25-ton truck crane to lift the roof plates according to the marked positions for assembly and welding. After installing and quality-checking the roof cover plates, create holes for the inverted columns. After the roof cover plates are welded, proceed with the installation of the roof guardrails and the creation of holes for connecting pipes.

6.4.4. *Installation of the second ring to the bottom ring of wall panels*

To ensure installation quality, place an adjustment plate on the top ring of wall panels, and install two adjustment plates symmetrically on each of the eight lower rings. All adjustment plates should have a 300 mm surplus length, which will be cut off during the installation of the closing wall panel.

Install backing bars for lifting on the inner side of each ring of wall panels, 100 mm from the bottom of the wall. Fix the backing bars with jacks and weld the gantry clamps to the backing bars and walls.

Place 38 inverted steel columns in a concentric circle at a distance of 400 mm from the silo wall, ensuring their positions align with the roof's hole positions. Weld the columns to the embedded steel plates in the concrete foundation using full penetration. Install two reinforcing diagonal braces (made of $\angle 75 \times 7$ angle steel) on the side of each column that is away from the silo wall. Weld lifting lugs onto the backing bar below each column. Install a 10-ton electric chain hoist on the side of

each column facing the silo wall. A total of 38 electric chain hoists should be installed, aligned within the same vertical plane as the lifting lugs.

After completing the installation of all inverted machinery, place the second ring of wall panels 300 mm from the outer side of the top ring of wall panels, and weld all longitudinal seams of the second ring in a counterclockwise or clockwise direction. Use two 3-ton manual chain hoists at the closing wall panel to tension both sides and prevent deformation during welding. Begin welding longitudinal seams from the outer seams inward. Only after the longitudinal seams have passed inspection should the lifting of the top ring of wall panels commence. To prevent difficulties in lifting the top ring of wall panels or accidentally lifting the lower ring of wall panels, which could lead to safety incidents, ensure that the two 3-ton hand hoists are properly loosened before lifting. Prepare and inspect the following before lifting:

1. Attach the lifting hook to the lifting lug and tighten the chain hoist;
2. Check the connection of the chain hoists;
3. Check the fixation between the backing bar and the silo wall;
4. Check the fixation of the gantry clamp onto the backing bar and the silo wall;
5. Check the condition of the diagonal braces.

After passing inspection, lifting can commence. During the silo lifting, experienced technicians should centrally control the electric chain hoists to ensure synchronized operation. Assign a dedicated person to monitor the smooth and proper

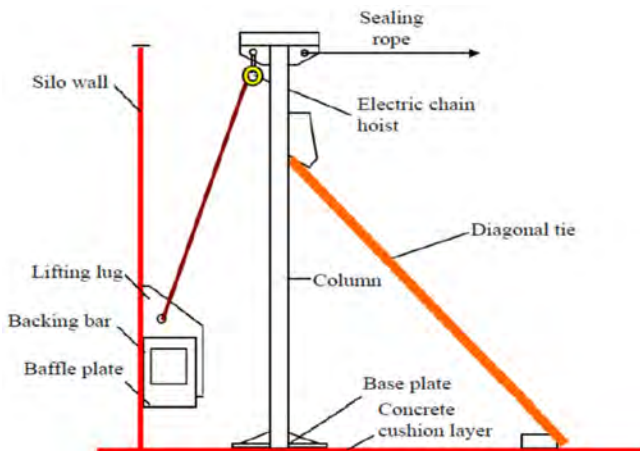


Fig. 8
Silo Wall Inverted Lifting

functioning of the lifting process. If any abnormalities are detected, halt the lifting immediately and troubleshoot the issues before resuming. When the wall reaches approximately 500 mm in height, stop the lifting to check the lifting performance, the height of the wall, the load on the hoists, and check for any abnormalities in the lifting lugs, backing bars, and inverted columns. If no abnormalities are detected, continue lifting. If any electric chain hoist is lifting unsynchronously, adjust it individually using the control device until it matches the height and load conditions of the properly functioning hoists. Once synchronization is achieved, continue with centralized control for synchronized lifting[4]. Repeat this process until the silo wall reaches a height of 1.5 meters.

The schematic diagram of the silo wall lifting is as follows:

After the silo wall is lifted to the specified height, retighten the manual chain hoists at the closing wall panel. Assign on-site personnel to measure the circumference of the wall, and have dedicated workers cut and adjust the reserved steel plate at the adjustment section. Install the closing wall panel and weld the longitudinal seams, then align the circumferential seams on the top ring of wall panels with the lower ring of wall panels. During this alignment, individually adjust the electric chain hoists' lifting height using the control device to ensure seamless alignment of the circumferential seams. The welding should follow this order: inner circumferential seam → outer longitudinal seam of the closing wall panel → outer circumferential seam. After all outer seams are tack welded, clean the root of the inner weld seam. Upon passing the weld quality inspection, proceed to weld the inner seam. Once both the inner and outer welds are tack welded, allow them to cool naturally to room temperature before removing the backing bars. The backing bars are then lowered using the electric chain hoists and positioned 100 mm below the second ring of wall panels, where they are secured with jacks. Next, install the remaining 28 columns at the embedded column foundation locations, ensuring each column is suspended from an electric chain hoist at the top. The installation method for these columns mirrors that of the previously installed 10 columns. Use 14 steel wire ropes (6*37 - ϕ 15 mm, 32 meters long) for diagonal bracing. Then, grind and smooth the longitudinal seams, circumferential seams, and temporary tack welds on the inside of the top ring of wall panels to make the welds flush with the wall surface.

Begin installing the third ring of wall panels outside the second ring, ensuring the direction of installation is consistent with that of the previous panels. Once aligned and tack welded, proceed to weld the longitudinal seams. The preparation and inspection work before lifting will follow the same procedures as for the top ring of wall panels. After passing inspections, start lifting the panels again, following this sequence: alignment and welding of longitudinal seams on the sealing wall panel → alignment, welding, and inspection of circumferential seams → removal of backing bars from the upper ring of wall panels → installation on the lower ring of wall panels. Repeat this process seven times until the bottom ring of wall panels are fully installed.

When aligning and welding the bottom ring of wall panels, select one of the 10 panels as the silo access adjustment panel, based on the actual site conditions. All construction equipment, materials, and debris inside the silo should be manually removed through this opening. According to the drawings, cut an entry hole in the bottom ring of wall panels near the construction road inside the site. Afterward, align and reposition the arch-shaped edge plate at the adjustment panel, and install the sealing adjustment panel, then weld the longitudinal and circumferential seams of this panel.

6.4.5. *Accessory installation*

Install vertical stiffeners, circumferential stiffening ribs, roof guardrails, and ladders on the silo walls. The guardrails on the silo roof should be installed concurrently with the roof structure. Meanwhile, the ladders, vertical stiffeners, and circumferential stiffening ribs should be installed during the inverted wall installation process to minimize high-altitude work.

Table 2
Investment Comparison Before and After Structural Adjustment of the Semi-Finished Material Silo

NO.	ITEM	BEFORE OPTIMIZATION	COST (RMB10,000)	AFTER OPTIMIZATION	COST (RMB10,000)
1	Structural form	Earth excavation	3	Earth excavation	2
2		C25 concrete	71	C25 concrete	/
3		C15 concrete	5	C15 concrete	4
4		C30 concrete	/	C30 concrete	24
5		Rebar	26	Rebar	23
6		Spiral steel pipe A325*8	1	Spiral steel pipe A325*8	/
7		Steel corrugated pipe A3500*7	/	Steel corrugated pipe A3500*7	27
8		M7.5 grouted stone retaining wall	4	M7.5 grouted stone retaining wall	/
9		M10 grouted stone retaining wall	9	M10 grouted stone retaining wall	4
10		Embedded parts	3	Embedded parts	5
11		Structural steel	101	Structural steel	222
12	Lifting equipment	25-ton truck crane	6	25-ton truck crane	9
13		10-ton electric hoist	/	10-ton electric hoist	4
14	Management costs	5-month construction period (RMB300,000 /month)	150	3-month construction period	90
15	Benefits from early commissioning	/	/	Added benefits from 2 months of early commissioning	80
16	Total		379	Total	334

7. TECHNICAL AND ECONOMIC ANALYSIS

The transition from a traditional semi-enclosed steel structure to a fully enclosed large silo for the sand and gravel processing system has accelerated the construction progress of the semi-finished material silo. A comparison of the technical and economic aspects before and after the structural adjustment is presented in Table 2.

As shown in Table 2, while the investment in structural optimization, design, and construction measures increased, the overall project completion time was significantly shortened. This resulted in savings on management costs and added revenue from the early commissioning of the sand mixing system. Overall, the adjusted plan saved RMB550,000 (3,790,000–3,240,000) compared to the original plan.

8. CONCLUSION

The large fully enclosed semi-finished material silo for the sand and gravel system in high altitude area offers numerous advantages, including a compact footprint, full enclosure, shorter construction period, and reduced dead storage capacity. By optimizing the structure and installation method of the semi-finished material silo, the project not only enables fast and safe construction, but also effectively protects arable land while significantly mitigating dust generation during material stacking. These improvements have a clear positive impact on environmental protection in the ecologically fragile regions of Xizang.

REFERENCES

- [1] ZHANG XIPENG. Application of "Inverted Method with Chain Hoist" in Stainless Steel Storage Tanks and Deformation Control. *Science and Technology Innovation Herald*, 2018,15(22): 42–43.
- [2] LIU CHAO, LI YUEXIAO, *et al.* Research on Silo Structure Design. *Jiangxi Building Materials*, 2023(01): 118–120.
- [3] ZHENG KAI. Discussion on Welding Deformation Control in Vertical Tank Installation. *Modern Industrial Economy and Informationization*, 2022,12(06): 320–322.
- [4] LING YAQING, CHEN HAIDONG. Construction Technology for Lifting Large Vertical Storage Tanks Using Electric Hoists. *Construction Technology*, 2018, 47(S1): 522–525.

COMMISSION INTERNATIONALE DES
GRANDS BARRAGES

VINGT-HUITIEME CONGRES DES
GRANDS BARRAGES
CHENGDU, MAI 2025

**RESEARCH ON HIGH-JOINT TECHNOLOGY OF COMPOSITE DAM IN
ZUNGERU HYDROELECTRIC POWER PROJECT (*)**

Xiaoming LI

Project Chief Engineer, SINOHYDRO Engineering Bureau 8 CO. LTD, Changsha

Shuiyang YU

Assistant Engineer, SINOHYDRO Engineering Bureau 8 CO. LTD, Changsha

Lingxue KONG

*Project Deputy Chief Designer, Powerchina Kunming Engineering CO. LTD,
Kunming*

CHINA

SUMMARY

The dam of Zungeru Hydroelectric Power Project in Nigeria is composed of a roller compacted concrete dam and two asphalt concrete core wall rockfill dams, with a joint height of 85 meters. However, there are few composite dam types in the world, and the joint height is also below 70 meters. For composite dams, the design and construction quality of joints are particularly important, which will directly affect the quality and safety of the whole dam. This project has made breakthrough progress through the design and construction technology research of high joint. After impounding, no abnormal deformation or seepage was found at the joint of the composite dam. The Zungeru dam provides a broader development prospect for the application of similar types of composite dams in the future.

**Recherche sur la technologie du joint de grande hauteur du barrage composite de l'aménagement hydroélectrique de Zungeru*

RÉSUMÉ

Le barrage de la centrale hydroélectrique de Zungeru au Nigeria est un barrage hybride composé d'un barrage en béton compacté au rouleau et d'un barrage en enrochement à noyau en béton bitumineux. La hauteur commune des deux barrages est de 85 mètres. La hauteur du joint entre les deux structures est inférieure à 70 m. Pour les barrages hybrides, la conception et la qualité de construction des joints sont particulièrement importantes, ce qui affecte directement la qualité et la sécurité de l'ensemble du barrage. Ce projet a permis de réaliser des progrès importants grâce à la recherche conjointe sur la conception et la technologie de construction. Après mise en eau, aucune déformation ou infiltration anormale n'a été constatée au niveau du joint du barrage composite, offrant ainsi des perspectives de développement plus larges pour des applications ultérieures de type similaire.

1. PROJECT INTRODUCTION

The Zungeru Hydroelectric Power Project (HPP) is located on Kaduna River, 17km northeast of Zungeru Town in Niger state, Federal Republic of Nigeria. The characteristic levels of the Zungeru HPP include the normal operation level at EL.230.00m, the design flood level at EL.230.10m, the maximum operation level at EL.231.00m, and the dead water level at EL.223.00m. The total reservoir storage capacity of the project is $10.01 \times 10^9 \text{m}^3$, with the normal operation level corresponding to a reservoir storage of $9.39 \times 10^9 \text{m}^3$ and a dead reservoir storage of $6.89 \times 10^9 \text{m}^3$. The dam has been designed to regulate water flow annually with a gross installed capacity of 700MW ($4 \times 175 \text{MW}$). The water retaining structure consists of a composite dam, comprising a roller compacted concrete (RCC) gravity dam and asphalt concrete core rockfill (ACR) dam on both sides, with a total length of 2360m. The RCC dam spans 1090m and reaches a maximum height of 101m. The maximum height of the joint between the RCC dam and the rockfill dam is 85 meters. Other significant structures in the project include the penstock, powerhouse, tailrace channel, plunge pool, switchyards, and two transmission lines, etc.

2. DESIGN OF COMPOSITE DAM

The asphalt concrete core wall rockfill dam and the roller compacted concrete gravity dam adopt an "insertion type" connection joint. The asphalt concrete core wall is only connected to the contact surface of the gravity dam side, and the core wall should have greater resistance to deformation at the joint and strong bonding ability at the joint surface [1]. Therefore, on the basis of chiseling the surface of the concrete dam at the

joint, asphalt mortar is set up. The gravity dam adopts an arc-shaped joint surface with a “Z” shaped copper waterstop, and the asphalt concrete core wall at the joint is locally expanded into a fan-shaped section to ensure the anti-seepage safety of the joint.

The joint of the composite dam is connected in a “ rockfill wraps RCC dam “ form. Due to the significant shear force at the joint of the wrapped area and the gravity dam after impounding, there may be significant shear displacement during earthquakes, which can easily lead to cracks. The joint between the wrapping area and the gravity dam cannot be filled and compacted using heavy machinery, making it difficult to compact. In order to reduce risks and improve the seismic resistance of the joint, the transition material at the joint is extended both upstream and downstream sides of the joint[2]. It is advisable to use manual cooperation with other construction machinery to fill the transition, and compact it with light rolling equipment.

The wrapping part is located in dam block 7 #~17 #, among which the block 7 #~9 # are variable cross-section dam blocks. The upstream slope varies from 1:0 to 1:0.3, and the downstream slope varies from 1:0.75 to 1:0.5 from block 7 # to 9#. The side and upstream and downstream surfaces of the 7 # dam section are casted in a stepped shape starting from EL.157.00m, as shown in Fig.1. The lowest elevation of the asphalt core wall is EL.157.00m, the top elevation is EL.234m, and the maximum height is 77m. The core wall thickness of the ACR dam is changed along the elevation: 1.0m thickness from EL.157.00m to EL.175.00m,; 0.8m thickness from EL.175.00m to EL.205.00m, 0.6m thickness from EL.205.00m to EL.234m. The joint varies from the typical thickness to 3m in a fan-shape within the scope of 3 meters away from the gravity dam. The contact area of the RCC dam is an arc with a radius of 3.9 meters. The specific joint style is shown in Fig. 2.

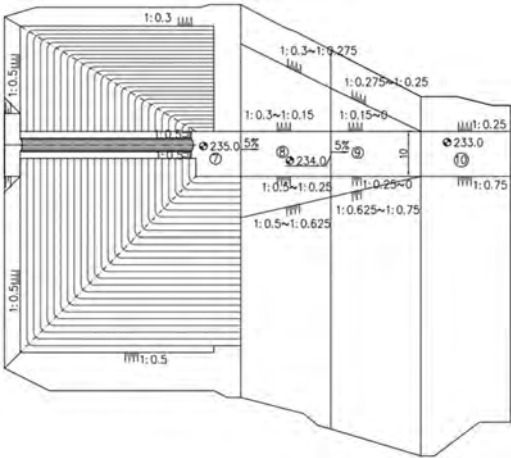


Fig. 1
RCC Dam Joint Plan

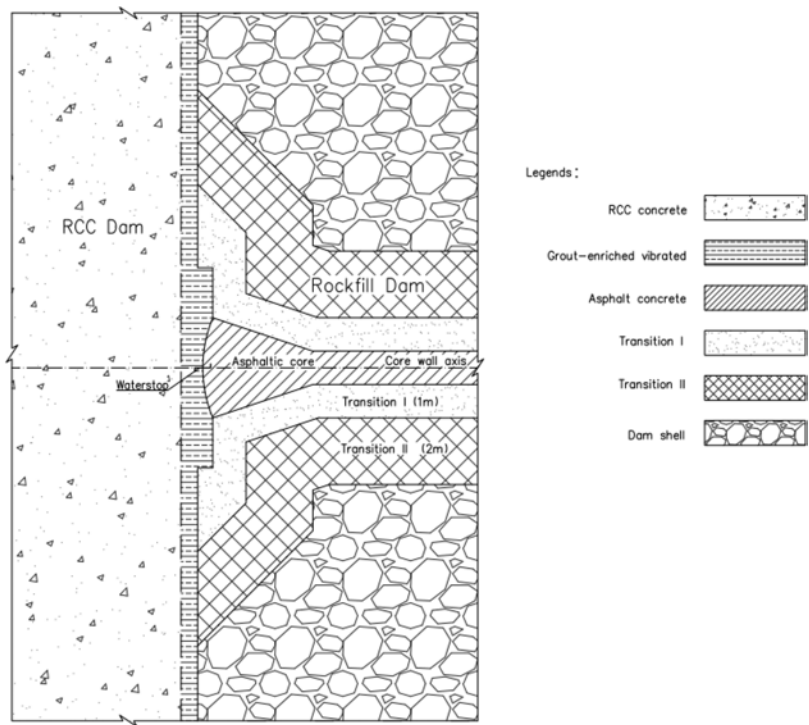


Fig. 2
Composite dam Joint Plan

3. CONSTRUCTION TECHNOLOGY FOR JOINT POSITIONS

3.1. JOINT CONSTRUCTION OF PROCESS FLOWCHART

Prior to construction of the joint at the dams, a trial placement of joint asphalt shall be carried out.

The construction process diagram of the joint between rockfill dam and RCC dam is shown in Fig. 3.

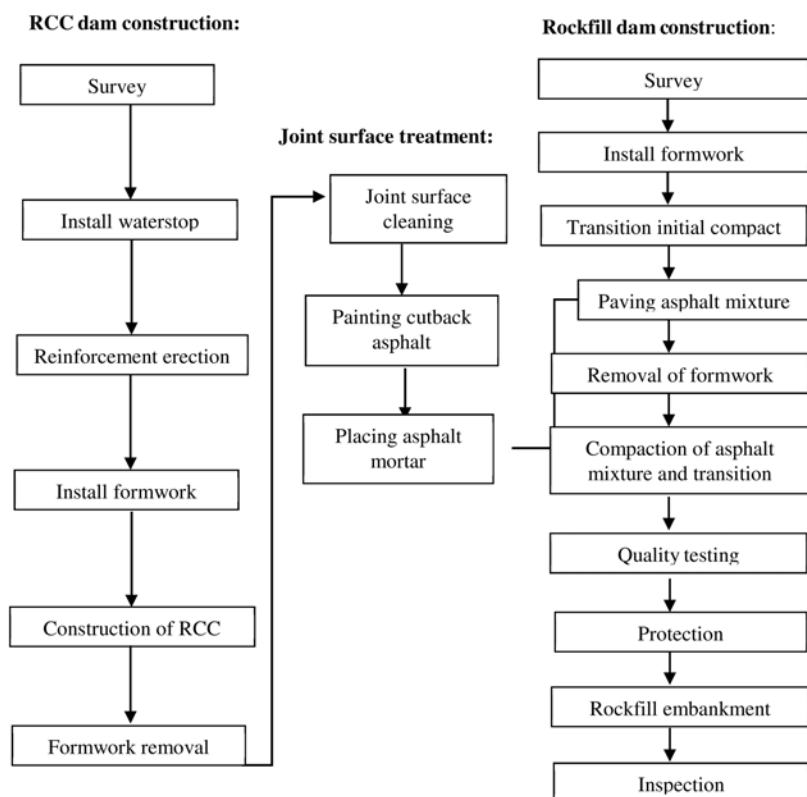


Fig. 3
Joint construction process flowchart

3.2. JOINT SURFACE TREATMENT PROCESS

The surface of cement concrete that is connected to asphalt concrete needs to be equipped with anti-crack reinforcement. Before starting the construction of asphalt concrete, the surface of cement concrete should be chiseled rough, and an axe or steel wire brush should be used to clean all the floating slurry, milk skin, waste residue, and adhesive dirt on the surface of cement. High pressure air should be used to blow dry, and locally humid areas should be dried with air blow to ensure that the concrete surface is clean and dry.

Before laying asphalt mixtures, the surface of the concrete and waterstop shall be dry and clean, and a layer of cutback asphalt (asphalt: petrol=3.5:6.5) shall be

applied to ensure there are no gaps. The dosage is about 0.2kg/m^2 . After the cut-back asphalt dries up, a layer of asphalt mortar shall be laid.

When placing asphalt mortar, the surface must be kept clean. The asphalt mortar thickness is about 1-2cm with ratio of asphalt: cement: sand=1:1:2. Asphalt mortar should not be too thick, otherwise a large amount of asphalt will backflow to the surface during concrete construction. After placing, the asphalt mortar should be uniform and flat, without flowing, bulging, and firmly adhered to the concrete.

When placing asphalt mortar or asphalt mixture, pay attention to protecting and correcting the copper waterstop sheet. No damage shall be caused to the waterstop.

3.3. CONSTRUCTION OF JOINT SECTION OF RCC DAM

When constructing RCC or GERCC in the joint section of RCC dam, turnover formwork is generally used. Special formwork should be used at the interface with the core wall to ensure that the waterstop copper sheet is firmly positioned and there is no leakage of grout from the formwork gap.

When placing RCC, it is prohibited to directly discharge concrete at the waterstop to prevent displacement and deformation of the waterstop. During the construction process, the quality of concrete vibration should be ensured. When vibrating near the waterstop, use an immersion vibrator or other small vibrator to compact the concrete to avoid honeycombs, over vibration and waterstop damage. During the vibration process, prevent the vibrator from directly touching the waterstop, which may cause the waterstop to shift. Reasonably arrange the pouring and vibration procedures, and pay attention to avoiding concentrated bleeding at the waterstop. The concrete construction of the joint section of RCC dam should be at least 2 lifts (6m) higher than the working surface of the core wall rockfill dam, to avoid turnover formwork that hinders the construction of the joint and affects the construction quality. If waterstop has to expose for a long time, proper methods such as wooden boards cover shall be carried out to protect waterstop.

3.4. CONSTRUCTION OF ASPHALT CONCRETE CORE WALL

The “fan-shaped” widened area at the core wall joint is paved manually and compacted with a small machine.

When paving the core wall manually, modified ZL50 loaders or excavators with a hopper is used to carry the asphalt mixture into the block after it is unloaded. Carefully spread and level the asphalt mixture to avoid separation of the mixture.

After the asphalt mixture is spread manually, it is first statically rolled after the formwork is removed, and then synchronously rolled with the transition. The asphalt mixture is rolled with a special vibrating roller which is less than 1.5t. The corners or slopes where the vibrating roller cannot reach are compacted with small flat vibrators. Vibration shall be stopped when "oil return" on the surface of the asphalt concrete, over vibration shall be avoided to prevent the aggregate sinking.

3.5. TRANSITION MATERIAL CONSTRUCTION

The joint of the composite dam is connected in a "rockfill wraps RCC dam" form. At the joint area, the rockfill material is not easy to compact, which can easily cause cracks during earthquakes. To reduce this risk, the transition material at the joint should be extended on both upstream and downstream sides. Before placing the transition, it is advisable to cover the surface of the core wall with rainproof cloth or other materials to prevent sand, stones, and debris from falling into the core wall. The covering width should exceed the formwork on both sides by more than 30cm.

The transition on both sides of the core wall should be paved and compacted simultaneously to prevent formwork deviation and displacement. The transition on both sides of the core wall should be compacted using a small vibrating roller with a capacity of less than 3.0t.

3.6. ROCKFILL MATERIAL CONSTRUCTION

Strictly control the blasting parameters when selecting rockfill from excavation materials, remove oversized stones, and ensure that the excavation materials meet the particle size grading requirements of the rockfill material.

The slope of the upstream of the rockfill dam is 1:2.2, while the slope of the downstream is 1:2.0. In order to avoid the concentration of big stones at the RCC dam surface, and to make it easier to compact, and to reduce settlement and deformation during operation, the joint surface should be backfilled with a transition 1.0m~2.0m wide.

The rockfill material is transported from the tailrace channel excavation area by a 25t dump truck, and then transported to the site after water is added. The rockfill is paved by the CAT D8R bulldozer with assistant by VOLVO EC300DL excavator. During the paving process, the normal burial and monitoring of observation instruments should be ensured, and effective measures should be taken to protect the embedded instruments and measurement marks intact.

Within a range of 2 meters from the joint surface, the rockfill is rolled parallel to the joint surface, and the rockfill is compacted two more passes within a range of 20 meters from the joint surface. The corners that are difficult to compact should have a thinner paving thickness and be compacted with a light vibrating roller or a flat vibrator or other compacting machinery.

When rockfill embankment, the main control is the compaction parameters. Samples are taken every 25,000 cubic meters to measure the dry density and gradation and keep records. After each layer is tested according to the requirement, the next layer embankment can be continued. The measured dry density and compaction parameters should be statistically analyzed to study improvement measures.

4. JOINT MONITORING

4.1. LAYOUT OF MONITORING INSTRUMENTS

Pressure stress gauges, displacement gauges, and seepage pressure gauges are installed on the side contact surface of the joint between the RCC dam and rockfill dam.

4.2. DATA STATISTICS AND ANALYSIS

4.2.1. *Contact surface pressure*

According to the statistical data of pressure gauge observation, the lateral pressure before impounding was between 0.15 and 0.60 MPa. After impoundment, the lateral pressure did not increase much. The maximum stress at the 1/2 dam height position of the side contact surface was 0.69 MPa. The monitoring results of the joint part pressure are closely related to the embankment height. The pressure increases with the increase of embankment height, but the increase of pressure lags behind the increase of embankment height and is closely related to seasonal changes, that is, it changes periodically, with obvious increase in rainy season. The pressure is relatively stable, and the pressure of the side contact surface is always in a pressure state during the completion period and impounding period, and there is no detachment phenomenon.

4.2.2. *Shear displacement*

The shear displacement meter readings before impounding varied between 13.9 and 94.0 mm, and after impounded, the shear displacement meter readings varied between 14.1 and 105.6 mm, with little change. The monitoring results of the shear displacement at the joint showed an obvious linear relationship with the embankment height, and the size of the displacement was closely related to the embankment height, that is, the higher the embankment height, the greater the displacement, and the shear displacement changes at the joints of the upstream and downstream were basically the same. After impounding, the upstream and downstream shear displacements did not undergo a sudden change or significant change.

4.2.3. *Osmotic pressure*

Before impounding, the osmometers installed upstream and downstream of the joint were in a pressure-free state. After impounding, the monitoring results of the upstream osmotic pressure of the joint showed an obvious linear relationship with the reservoir water level. The osmotic pressure changed with the upstream reservoir water level (increased or decreased), and the pressure size was basically consistent with the reservoir water level change. The osmotic pressure sensors arranged at different elevations downstream have a value of 0, that is, there was no pressure, which indirectly indicated that there was no leakage from the joint.

5. CONCLUSION

Due to the composite dam being a combination of two different dam types, the design and construction of the joint of two dams play a very important role in dam safety. The joint height of Zungeru dam reaches 85m which is higher than most dam joint. More than 3 years have passed since Zungeru HPP impounded, all the monitoring data shows that the dam is in a good operation condition. The design structure and construction technology of Zungeru HPP give an experience for the composite dam joint, and provided more references for the development of composite dams.

REFERENCES

- [1] WU CHANGSHENG. Experimental and research on asphalt concrete core wall of rockfill dams. *Haihe River Water Conservancy*, pp.21–22, 2001
- [2] XIE WEIDONG. Stress and strain analysis of rockfill body in rolled asphalt concrete core wall dam. *Inner Mongolia water conservancy*, pp.8–9, 2009

COMMISSION INTERNATIONALE DES
GRANDS BARRAGES

VINGT-HUITIEME CONGRES DES
GRANDS BARRAGES
CHENGDU, MAI 2025

INTELLIGENT MANAGEMENT AND CONTROL SYSTEM OF CONCRETE DAM CONSTRUCTION (*)

Guoyuan LAN & Qi SUN

*Research Institute of Green and Intelligent Construction, China Gezhouba Group
Co., Ltd, Wuhan*

CHINA

SUMMARY

To enhance the innovation of concrete dam construction, this study develops a comprehensive intelligent management and control system for concrete dam construction, consisting of (1) the control level: the smart command center for real-time data collection, analysis, and decision-making, (2) the theory level: the design and development of mathematical models for the smart command center, and (3) the function level: five function modules of system application, including BIM design, pouring area design, concrete production, transportation, and pouring. The proposed system has been successfully implemented in an ongoing concrete dam construction. Besides, the technical performance indicators for each of the function modules are summarized, showing the feasibility and reliability of the proposed system. This aim of this study is to manage and control concrete dam construction, support decision-making, shorten the waiting time during construction, and thus ultimately improve concrete construction efficiency.

*Système intelligent de gestion et de contrôle de la construction de barrage en béton

RÉSUMÉ

Afin d'améliorer l'innovation dans la construction de barrages en béton, cette étude développe un système de gestion et de contrôle intelligent complet pour la construction de barrages en béton, constitué de (1) le niveau de contrôle : le centre de commande intelligent pour la collecte, l'analyse et la prise de décision en temps réel, (2) le niveau théorique : la conception et le développement de modèles mathématiques pour le centre de commande intelligent, et (3) le niveau fonctionnel : cinq modules fonctionnels d'application du système, incluant la conception BIM, la conception des zones de bétonnage, la production de béton, le transport et le bétonnage. Le système proposé a été mis en œuvre avec succès dans une construction de barrage en béton en cours. Les indicateurs de performance technique pour chacun des modules fonctionnels sont résumés. Ils démontrent la faisabilité et la fiabilité du système proposé. L'objectif de cette étude est de gérer et contrôler la construction de barrages en béton, d'aider à la prise de décision, de réduire les temps d'attente pendant la construction, et ainsi améliorer ultimement l'efficacité de la construction en béton.

1. INTRODUCTION

Dams are normally located in mountainous gorges, where the concrete dam construction is numerous in the pouring area, large in scale, and heavy in workload with tight schedules and poor visibility [1]. The concrete dam construction consists of concrete production, transportation, and pouring. Particularly, in addition to construction safety, a smooth dam concrete pouring process depends on the pouring area design and the concrete production supply. In this case, the management and control system for concrete dam construction needs to be customized, enabling real-time data recording, data analysis, design optimization, and decision-making throughout the entire process.

To achieve this, a lot of studies have adopted advanced technologies in the field of concrete dam construction, such as the adoption of building information modeling (BIM), internet of things (IoT), artificial intelligence (AI), high-precision global navigation satellite system or inertial navigation system (GNSS/INS) positioning, sensors, etc [2–5]. However, few of them have been effectively implemented, and there is still room to investigate intelligent production and construction technology of dam concrete [6].

This study develops a comprehensive intelligent management and control system for concrete dam construction, consisting of (1) the control level: the smart command center for real-time data collection, analysis, and decision-making, (2) the theory level: the design and development of mathematical models for the smart

command center, and (3) the function level: different modules of system application, such as BIM design, pouring area design, concrete production, transportation, and pouring. This study aims to manage and control concrete dam construction, support decision-making, shorten the waiting time during construction, and thus ultimately improve concrete construction efficiency.

2. METHODOLOGY

This section introduces the methodology of this study, consisting of the smart command center (the control level), mathematical models (the theory level) and five function modules (the function level) (see Fig. 1). The smart command center is developed upon mathematical models, which collects and analyzes data collected from various sources of these modules, and finally provides real-time monitoring, timely feedback, and optimization suggestions for decision-making. The following subsections present each of the modules in detail.

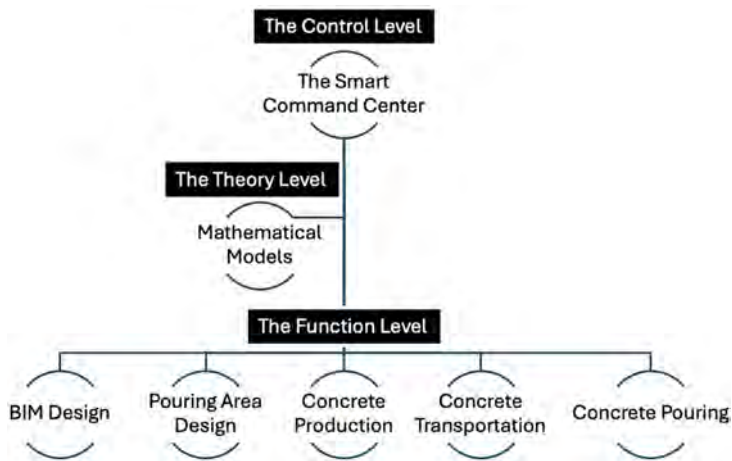


Fig. 1
The hierarchy model of a novel intelligent management and control system.

2.1. BIM DESIGN

This module is to develop BIM models with varying Levels of Detail (LOD) using A/B platform BIM software (i.e., Autodesk or Bentley software). The dam

architecture models are parameter-driven, using Revit software with a plug-in (e.g., Dynamo or Grasshopper), for rapid modeling and modification of BIM elements. Particularly, this study investigates the modeling and visualization solutions for large-scale columnar components of arch dams. To consider the factors affecting dam concrete pouring, the sequence logic of dam block placement is designed as a crucial variable while developing BIM models. These models are divided into section BIM or layered BIM to represent different sections and layers of the dam block. Besides, these models have mapped the virtual devices of embedded sensors for dam health monitoring and control, including thermometers, cooling water pipes, temperature measurement fibers, formwork locating devices, etc.

2.2. POURING AREA DESIGN

In addition to storing and collecting sensor data, the BIM models are used to calculate core parameters concerning the concrete dam construction, such as unit volume, layer areas, key control points of pouring coordinates, etc. Fig. 2 displays the system interface for pouring area design and 3D visualization of the BIM model. AI algorithms are designed to deal with these data for dam concrete pouring area design. The pouring area design would impact the scheduling of concrete production supply, particularly the arrangement of vehicle dispatch, cable crane control, and the pouring sequence. With the model geometry and attribute information provided by BIM models, the intelligent pouring area design can help optimize the utilization rate of pouring machines, shorten construction duration, and enhance monthly pouring intensity.



Fig. 2
System interface for pouring area design and 3D visualization of the BIM model.

2.3. CONCRETE PRODUCTION

The concrete production module adopts technologies of IoT and remote control to schedule, manage, and monitor the concrete production process, with the incorporation of enterprise resource planning (ERP) systems, manufacturing execution systems (MES), and supervisory control and data acquisition (SCADA) systems. While tracking and analyzing the operation status of these aforementioned systems, the concrete production can achieve the following functions: automatic control of pre-cooling and pre-heating temperatures at the concrete outlet, aggregate storage monitoring, hardware expansion of conveyor belts, pump control of powder material feeding, real-time synchronization of system data, dust and sewage treatment, air supply management and control in compressed air stations, etc.

2.4. CONCRETE TRANSPORTATION

The concrete transportation module is designed to integrate hardware and software with the technology of precise positioning and real-time radar detection. The positioning accuracy is controlled within 1 cm in horizontal and 2 cm in vertical. The cable crane paths are pre-defined based on the concrete loading and pouring coordinates. Besides, the automatic hook insertion technique is developed that enables automatic concrete loading and offloading. As a result, drivers can monitor the operation information and movement process in the cab, which helps to track and guide transport vehicles in real time to coordinate with mixing plants and cable cranes.

Fig. 3 shows the system interface for cable crane control. The following factors are considered for transportation control, including the pouring volume of dam blocks, the number of transport vehicles in operation, transport vehicle speed, transport vehicle loading capacity, and the distance between the mixing plant and the cable crane loading place. The purpose is to help cable cranes quickly, accurately, and safely arrive at the pouring location for concrete delivery and return, meanwhile, reducing the dock waiting time and increasing work efficiency.

such as thick slurry casting in drill pipes; and (5) information networking: wireless data transmits with a central server for remote control and monitoring.

Last, the study employs an intelligent temperature control system to monitor the temperature of air and concrete throughout the entire pouring process. While detecting the unusual temperature, this system can send alerts to the command center and leverage water cooling for different pouring areas of dam concrete. The design principle for cooling control is to achieve a slow and stable cooling process, ensuring that temperature control indicators (i.e., target temperature, cooling rate, temperature range, air temperature difference within the warehouse) are fully under control with less variance.

3. IMPLEMENTATION RESULTS

The methodology proposed in this study has been implemented in a dam project currently under construction. Due to security reasons, more details and data of this dam project cannot be presented in this paper. The following technical performance indicators of the proposed work are summarized in the following:

1. The smart command center for dam construction operated safely and reliably, reducing waiting and preparation time for each process during dam construction, thereby enhancing work efficiency.
2. The intelligent management and control system for arch dams is established, utilizing the BIM model (ranging from LOD 300 to LOD 500) created by the owner to optimize the pouring area design, concrete production, transportation, and pouring.
3. The sequence logic of dam block placement designed in this study saved over 30% of the time compared to the original pouring schedule.
4. The intelligent pouring area design met actual needs, with an increase of 20% in work efficiency compared to the original design.
5. The transportation control of cable cranes reached a positioning accuracy of less than 1cm in horizontal and 2 cm in vertical.
6. The automatic delivery of the cable crane has been safe and reliable, reducing the time for a single transport cycle by 5% compared to the original design.
7. The bucket of cable cranes was designed to reduce its weight by at least 1.5 tons, with a capacity increase of no less than 0.6m^3 , leading to a 6% improvement in material transport efficiency.
8. The transportation vehicle command and dispatching control was implemented, applying a multi-objective theoretical data model to achieve seamless coordination between vehicles, mixing plants, and cable cranes, shortening the docking time, and improving work efficiency. The new system saved more than 30% of the time and increased the average hourly working time of cable cranes by more than 2% compared to the traditional design.

9. The concrete pouring control, particularly the vibrating, grouting, and water cooling have been real-time monitored throughout the entire pouring process, enabling timely emergency detection and decision-making.

4. CONCLUSIONS

To achieve a smooth dam concrete pouring process and construction safety, the management and control system for concrete dam construction needs to be customized, enabling real-time data recording, data analysis, design optimization, and decision-making throughout the entire process. In this case, this paper presents an intelligent management and control system based on mathematical modeling, integrating with advanced technologies including BIM, IoT, AI, high-precision GNSS/INS systems, sensors, etc. The system consists of a smart command center and five function modules, including design, pouring area design, concrete production, transportation, and pouring.

The proposed system has been successfully implemented in an ongoing concrete dam construction. First, the section and layered BIM models of the arch dam were developed; these models also mapped the virtual devices of the actual sensors embedded in the dam. Second, with the use of AI algorithms, a BIM-based module for arch dam pouring area design was developed, achieving a shorter pouring period and higher work efficiency. Third, the concrete production module integrated with the ERP, MES, and SCADA systems to schedule, manage, and monitor the concrete production process. Fourth, the concrete transportation module was developed for tracking and guiding transport vehicles in real time to coordinate with mixing plants and cable cranes. The designed system integrated with GNSS/INS technology achieved stable and reliable positioning. Last, the concrete pouring module was designed for intelligent process control of concrete vibrating, grouting, and water cooling, enabling real-time monitoring and timely decision-making. To conclude, the performance of the function modules verifies the feasibility and reliability of the proposed system.

REFERENCES

- [1] AFZAL J., YIHONG Z., ASLAM M., & QAYUM M. (2022). A study on thermal analysis of under-construction concrete dam. *Case Studies in Construction Materials*, 17. <https://doi.org/10.1016/j.cscm.2022.e01206>

- [2] ZHOU Y., BAO T., SHU X., LI Y., & LI Y. (2023). Bim and ontology-based knowledge management for DAM Safety Monitoring. *Automation in Construction*, 145, 104649. <https://doi.org/10.1016/j.autcon.2022.104649>
- [3] MIN Q., ZHANG, M., LI M., HE Y., BORDAS S. P. A., & ZHANG H. (2024). Hydraulic fracturing simulation of concrete dam integrating intelligent crack detection and refined modeling methods. *Engineering Structures*, 305, 117760. <https://doi.org/10.1016/j.engstruct.2024.117760>
- [4] WANG R. (2016). Key technologies in the design and construction of 300 m ultra-high arch dams. *Engineering*, 2(3), 350–359. <https://doi.org/10.1016/j.eng.2016.03.012>
- [5] ZHAO S., KANG F., & LI J. (2024). Intelligent segmentation method for blurred cracks and 3D mapping of width nephograms in concrete dams using UAV photogrammetry. *Automation in Construction*, 157, 105145. <https://doi.org/10.1016/j.autcon.2023.105145>
- [6] HARIRI-ARDEBILI M. A., MAHDAVI G., NUSS L. K., & LALL U. (2023). The role of Artificial Intelligence and digital technologies in DAM Engineering: Narrative Review and outlook. *Engineering Applications of Artificial Intelligence*, 126, 106813. <https://doi.org/10.1016/j.engappai.2023.106813>

COMMISSION INTERNATIONALE DES
GRANDS BARRAGES

VINGT-HUITIEME CONGRES DES
GRANDS BARRAGES
CHENGDU, Mai 2025

DATA AUGMENTATION SCHEME FOR PREDICTIVE MAINTENANCE OF DAMS: A CASE STUDY OF AN ARCH DAM (*)

Dongming LI & Yang CHAO

*College of Water Conservancy and Hydropower Engineering, Hohai University,
Nanjing*

Shuying HUANG

School of Law, Hohai University, Nanjing

CHINA

SUMMARY

This study addresses the issues of outlier detection complexity and difficulty in operational state prediction in dam predictive maintenance by proposing an improved K-shape clustering method that incorporates spatial distance of measurements into the clustering factors. By combining the clustering method with the confidence interval method, an outlier detection method for dam monitoring data is achieved. Additionally, by integrating the clustering center line with the LSTM method, a prediction for the operational state of dams is realized. Using real monitoring data from an arch dam in Yunnan as a case study, a comparison between the proposed data augmentation scheme and traditional schemes demonstrated that the improved clustering method proposed in this study has higher accuracy in outlier detection and higher data accuracy in prediction. This indicates that the method proposed in this study holds significant value for predictive maintenance of large concrete structures.

**Augmentation des données de surveillance pour la maintenance prédictive des barrages – étude de cas d'un barrage-voûte*

RÉSUMÉ

Cette étude aborde les problèmes de complexité de détection des valeurs aberrantes et de difficulté de prédiction de l'état opérationnel dans la maintenance prédictive des barrages. Elle propose une méthode de traitement améliorée qui intègre la distance spatiale des mesures dans les facteurs de regroupement. En combinant la méthode de regroupement avec la méthode de l'intervalle de confiance, une méthode de détection des valeurs aberrantes pour les données de surveillance des barrages est obtenue. De plus, en intégrant la ligne centrale de regroupement avec la méthode LSTM, une prédiction pour l'état opérationnel des barrages est réalisée. En utilisant les données de surveillance réelles d'un barrage-voûte au Yunnan comme étude de cas, une comparaison entre le schéma d'augmentation de données proposé et les schémas traditionnels a démontré que la méthode de regroupement améliorée proposée dans cette étude présente une précision plus élevée dans la détection des valeurs aberrantes et une meilleure précision des données dans les prédictions. Cela indique que la méthode proposée dans cette étude a une valeur significative pour la maintenance prédictive des grandes structures en béton.

1. INTRODUCTION

The concept of Predictive Maintenance (PdM) originated in the 1970s. With the development and widespread application of computer technology [1], it has been extensively utilized in production and manufacturing industries, gradually becoming a crucial component of contemporary Structural Health Monitoring (SHM). PdM employs sensors and automated data acquisition techniques to predict and prevent the occurrence and escalation of accidents [2]. In contrast, there is Run-to-Failure (R2F) and preventive maintenance [3]. Undoubtedly, for large concrete structures such as dams, the cost of unplanned maintenance is unacceptable, while comprehensive preventive maintenance requires substantial labor resources and can easily fall into the contradiction between over-maintenance and untimely maintenance [4]. PdM, on the other hand, determines maintenance actions by regularly inspecting physical parameters of equipment, establishing material degradation relationships, and locating stress sources to implement corrective measures before accidents occur [5]. Furthermore, PdM, as a crucial tool, combined with relevant information, facilitates more informed decision-making and enhances project sustainability (e.g., reducing waste and improving energy/resource efficiency) [6,7]. When applied to concrete structures such as dams, it ensures long-term stable and safe operation of the project.

However, predictive maintenance is highly dependent on data [8]. For large concrete structures like dams, their operating environment is dynamic, with frequent

updates of multi-source dynamic data and poor coordination in data collection and storage. This implies that over different time periods, the datasets (including physical quantities such as settlement, deformation, and temperature) contain changes in risk factors from the external environment, degradation of the structure's own performance, as well as erroneous or missing information. Eliminating errors and discovering trends from monitoring data plays an irreplaceable role in predictive maintenance decision-making. This constitutes our primary motivation for exploring a data augmentation scheme for predictive maintenance applicable to the main structure of dams.

Our case study focuses on a concrete arch dam located in Yunnan Province, China. In this case, rapid fluctuations in environmental factors such as sunlight, temperature, and water level lead to significant variations in the collected data. In essence, the configuration and combination of risk factors differ at each inspection, and there is also some data loss. Although the monitoring system installed on this arch dam provides a wealth of data, using these data for dam behavior assessment is challenging due to their uneven spatial distribution within the dam and significant quality variations. Indiscriminate use of monitoring data may introduce low-quality and redundant information into the PdM process, reducing its efficiency. Consequently, data filtering becomes a crucial component of model updating to eliminate redundant information, enhance information utilization efficiency, and ensure high-quality information [9]. However, there exists a research gap in data filtering and effective utilization, necessitating more in-depth and comprehensive studies.

Methods for identifying anomalies in dam monitoring time series can be categorized into three main types [10–13]: statistical process control (primarily the process line method), statistical detection methods and mathematical model discrimination methods. Subsequently, some researchers introduced more complex statistical models, such as ARMA and ARIMA, to improve the accuracy of anomaly detection by modeling the trend and periodicity of time series [13,14]. Early anomaly detection methods were primarily based on statistical principles, determining whether data points were anomalous by setting upper and lower thresholds.

Despite the progress made in anomaly detection by the aforementioned methods, certain limitations persist. For instance, most of these methods assume a deterministic functional relationship between environmental and effect variables, whereas in practical applications, this relationship may exhibit uncertainty and time-variability. Moreover, these methods inadequately consider the types and distribution characteristics of anomalies, making it challenging to adapt to complex anomaly patterns. Consequently, developing a more robust and adaptive anomaly detection method remains an urgent issue to be addressed. Therefore, we propose a novel data filtering and imputation scheme for dam deformation analysis.

Considering the prevalent temporal periodicity and spatial dependence or correlation in the spatiotemporal series of dam monitoring data[15], this study proposes a data filtering and missing value imputation method based on an improved K-shape clustering approach, tailored to the characteristics of dam monitoring data. The main innovations are as follows: An enhanced K-shape clustering approximation evaluation method is proposed, which strengthens the spatiotemporal correlation of dam monitoring data clusters and is utilized for filtering multidimensional dam monitoring data; The improved clustering method is integrated with LSTM techniques to achieve imputation of missing values and enhance imputation accuracy; The information filtering method is applied to engineering practices, validating its effectiveness.

The second section introduces the improved K-shape clustering method, elucidating the distinctions between the enhanced clustering algorithm and traditional clustering methods, as well as its significance and rationality. It is then integrated with LSTM algorithms to achieve outlier detection, prediction of future dam conditions, and imputation of missing values. The third section of the article, based on practical engineering case studies, demonstrates the differences and advantages of the improved K-shape clustering method compared to traditional clustering methods, and designs experiments to verify its efficacy. Finally, the fourth section summarizes the primary application methods and future prospects of the improved clustering model in predicting the behavior and operational maintenance of large concrete structures.

2. METHODOLOGY

In the field of time series data analysis, the k-Shape algorithm is designed specifically for time series clustering. This algorithm was proposed by Paparrizos and Gravano (2015)[16].

The biggest advantage of the k-Shape algorithm is that it effectively captures the shape features of time series and shows high robustness to noise and outliers. Unlike traditional Euclidean distance, this algorithm measures shape similarity between time series using standardized cross-correlation distance, effectively addressing the shortcomings of Euclidean distance in time series clustering problems and providing more powerful tools for time series data analysis. The k-Shape algorithm proposes a clustering effectiveness evaluation scheme based on centroid calculation, using the Silhouette Coefficient and Distortion to comprehensively evaluate clustering effectiveness, thereby determining the optimal number of clusters.

In multi-dimensional information scenarios such as dam monitoring, multiple sensors are usually relied upon to comprehensively perceive the physical space.

The spatial correlation between sensor data is crucial for data interpretation. Therefore, this study, based on the k-Shape algorithm, introduces the spatial attributes of sensors to improve the shape similarity measurement method, achieving classification of measurement points based on both temporal and spatial factors.

For data sequences $X_s = \{X_{s,1}, X_{s,2}, \dots, X_{s,a}\}$ and time series $Y_s = \{Y_{s,1}, Y_{s,2}, \dots, Y_{s,b}\}$, to achieve shift invariance, sliding operations are performed and zeros are padded in the remaining positions:

$$X_{s(k)} = \begin{cases} \left(\overbrace{0, \dots, 0}^{|k|}, X_{s,1}, X_{s,2}, \dots, X_{s,m-k} \right), & k \geq 0 \\ \left(X_{s,1-k}, \dots, X_{s,m-1}, X_{s,m}, \underbrace{0, \dots, 0}_{|k|} \right) & k < 0 \end{cases} \quad [1]$$

Where $X_{s(k)}$ denotes the time series after a shift of k ; $X_{s(0)}$ is the original time series.

Based on the shifting sequence $X_{s(k)}$, the cross-correlation sequence $CC_\omega(X_s, Y_s) = (c_1, c_2, \dots, c_\omega)$ can be obtained, and the cross-correlation sequence is defined as follows:

$$C_\omega(X_s, Y_s) = R_{\omega-n}(X_s, Y_s) \quad [2]$$

$$R_k(X_s, Y_s) = \begin{cases} \sum_{l=1}^{n-k} x_{s,l+k} y_{s,l}, & k \geq 0 \\ R_{-k}(X_s, Y_s), & k < 0 \end{cases} \quad [3]$$

The cross-correlation series value $C_\omega(X_s, Y_s)$ in Equation (3) has a length equal to the number of shift sequences. The corresponding ω is obtained. Based on the value ω , $k = \omega - n$ can be obtained, and the corresponding shift sequence $X_{s(k)}$ is the optimal matching sequence.

Obviously, the monitoring data of large concrete structures is influenced by the spatial variability of the measurement points, material strength [17], the degree of deterioration [18], and structural operating principles [19]. The spatiotemporal series of the monitoring data often exhibit a certain degree of spatial autocorrelation. For example, according to the coefficient normalization method described in the literature and combining it with the spatial correlation characteristics of dam sensors, it is

defined as:

$$NCC_c(X_s, Y_s) = \frac{CC_w(X_s, Y_s)}{\sqrt{R_0(X_s, X_s)} \cdot \sqrt{R_0(Y_s, Y_s)}} - r_a \frac{d(v_X, v_Y)}{\max(d)} NCC_c \in (0, 2) \quad [4]$$

In the formula, r_a is the distance correlation coefficient, $r_a \in [0, 1]$ representing the importance of spatial distance on the shape of spatiotemporal series, which is related to the structural load form; $d(v_X, v_Y) = \sqrt{\sum_{i=1}^3 (v_{X,i} - v_{Y,i})^2}$ is the physical distance between points i and j , $\frac{d(v_X, v_Y)}{\max(d)}$ with a range between 0 and 1; $v_{X,i}$ are the spatial coordinates of measuring point i , and $\max(d)$ is the maximum distance between the spatial coordinates of all measuring points. $NCC_c(X_s, Y_s)$ is positively correlated with the degree of similarity between series; the larger the $NCC_c(X_s, Y_s)$, the stronger the correlation between the series, and vice versa.

To construct a shape-based distance measure, the following calculation formula is defined:

$$ISBD(X_s, Y_s) = 1 - \max NCC_c(X_s, Y_s) \quad ISBD \in (0, 3) \quad [5]$$

To improve the computational process of shape-based distance similarity measure, the discrete Fourier transform (DFT) inner product of X_s and Y_s is used, followed by an inverse discrete Fourier transform (IDFT). The specific calculation formulas are as follows:

$$CC(X_s, Y_s) = F^{-1} \{ (X_s)(Y_s) \} \quad [6]$$

$$F(x_k) = \sum_{r=0}^{|x|-1} x_r e^{-2jrk\pi/|x|} \quad [7]$$

$$F^{-1}(x_r) = \sum_{k=0}^{|x|-1} (x_k) e^{2jrk\pi/|x|} \quad [8]$$

In the formula, F represents the Fourier transform, and F^{-1} represents the inverse Fourier transform; $j = \sqrt{-1}$; $k = 0, 1, \dots, |x| - 1$; $r = 0, 1, \dots, |x| - 1$.

In the k-Shape algorithm, the centroid is used to represent the features or patterns of a class of data. Based on equation [2], after obtaining the set $c = \{c_1, c_2, \dots, c_m\}$ containing m clusters, the cluster centroids of all clusters can be calculated using equation [9].

$$\mu^{(d+1)} = \frac{1}{N} \sum_{i=1}^N X_i^{(d)} \cdot \frac{\mu_i^{(d)}}{X_i^{(d)}} \quad [9]$$

Here, $\mu_i^{(d)}$ represents the average value of the cluster centroid X_i in the d -th iteration, $X_i^{(d)}$ represents the shape of the time series X_i in the d -th iteration, N is the number of time series in the cluster, and $\| \cdot \|$ represents the Euclidean norm.

Equation (9) normalizes and weighted averages all time series in the current cluster to update the cluster centroid. Since the cluster centroid represents the trends and features of all time series in the cluster, reflecting the data trend of the cluster, it shows good robustness for non-smooth and abrupt sequences.

This paper uses the cluster centroid combined with the confidence interval method to identify outliers. The confidence interval method is based on mathematical statistics theory and is a method to determine discrete values from a mathematical perspective, with good outlier detection efficiency for data following specific distribution patterns.

To analyze the distribution pattern that the outlier samples follow, data is processed according to the following steps:

Firstly, select a cluster of data, then smooth and normalize the sample data to calculate its centroid. Solve the differences between each time series in the cluster and the centroid, arrange them in ascending order to form a difference distribution.

Subsequently, divide the sample range into n small intervals Δ/n and calculate the frequency of sample data in each interval Δ/n , result shown in Fig. 1.

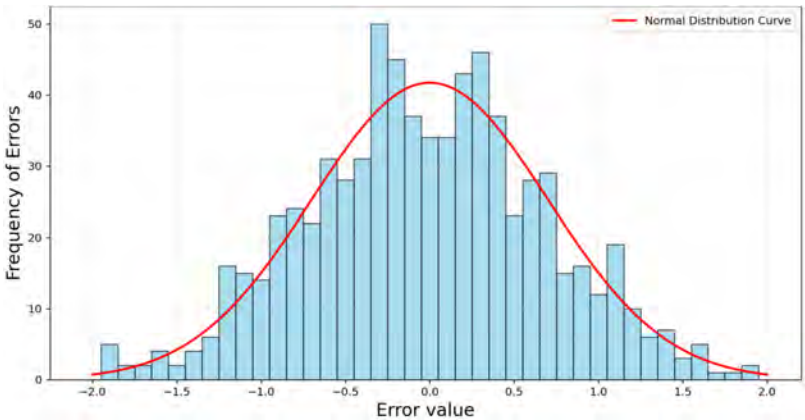


Fig. 1
The normal distribution curve and the error distribution frequency.

From Fig. 2, it can be observed that the differences show a tendency to follow a normal distribution. Therefore, the differences between the time series in the cluster and the centroid can approximately be regarded as following a normal distribution.

Assuming the central line $\mu_j = \{x_1, x_2, \dots, x_t\}$ is a stationary sequence that satisfies a certain probability distribution, the mean value $\bar{\mu}_j$ and standard deviation σ_{μ_j} of the sequence are respectively:

$$\bar{\mu}_j = \frac{1}{t} \sum_{i=1}^t x_i \quad [10]$$

$$\sigma_{\mu_j} = \sqrt{\sum_{i=1}^t (x_i - \bar{\mu}_j)^2 / (t - 1)} \quad [11]$$

We believe that after smoothing and normalization, the clustered central line can reduce distribution anomalies caused by systematic errors, therefore using the same threshold for upper and lower limits in anomaly detection within the same cluster. The threshold is derived from the 95% confidence interval of the central line's spatio-temporal sequence values, calculated as:

$$\mu_j^u | \mu_j^d = \{x_1 \pm 1.96SE, x_2 \pm 1.96SE, \dots, x_t \pm 1.96SE\} \quad [12]$$

$$SE = \sigma_{\mu_j} / \sqrt{t} \quad [13]$$

Where μ_j^u, μ_j^d are the upper and lower boundaries of the central line's confidence interval. If the time series sample values within the same cluster fall within these boundaries, they are considered normal; otherwise, they are anomalies.

Monitoring data reflects the displacement or deformation of the dam caused by loads acting on it [20]. For dam monitoring data, common influencing factors include static water load, dynamic water load, temperature load, seismic load, and time-dependent load. These loads are actually the effects of external natural conditions such as water level, temperature, and wind speed on the dam concrete. Apart from some special combination loads, such as encountering an earthquake at normal storage level, these natural conditions generally have a certain periodicity or regularity. This provides the basis for using the LSTM (Long Short-Term Memory) model to predict and analyze the operational state of the dam.

LSTM [21] is a type of recurrent neural network model, and its unit structure is shown in the figure. The updating of unit states is controlled by the forget gate, input gate, and output gate. The updating of unit states is controlled by the forget gate, input gate, and output gate. The data in the unit state is determined to be discarded or added by the forget gate and input gate, respectively, while the output gate determines the output of the unit state. The LSTM model is mature and widely used due to its effectiveness in processing and predicting time series data. Its application in dam deformation prediction is extensive and accurate, especially in predicting the

displacement peaks and troughs [22]. Therefore, this paper selects the LSTM method, combined with the characteristics of physical distance associated with the data measured by sensors.

Based on the improved spatiotemporal clustering of monitoring data, multi-point data within the same cluster are used as input variables, and the target point data are used as dependent variables to construct an effective information extraction and prediction method for concrete dams with multiple measurement points.

An LSTM unit, which consists of three parts: the forget gate, the input gate, and the output gate:

1. In the forget gate, h_{t-1} is the previous output value; x_t is the current input value; C_{t-1} is the previous cell state; F_t is the forget function that determines the retention of the previous time step information.

$$F_t = \sigma(W_{fh} \cdot h_{t-1} + W_{fx} \cdot x_t + b_f) \quad [14]$$

2. In the input gate, C_t is the current cell state; I_t is the input function that determines whether to update the current cell state to C_t ; \tilde{C}_t is the cell candidate vector at the current time step; \tanh is the hyperbolic tangent function responsible for compressing the cell state between -1 and 1. The input gate generates the input to the next hidden layer C_t through x_t , h_t , and \tilde{C}_t , as calculated by the following formula:

$$\begin{aligned} I_t &= \sigma(W_{ih} \cdot h_{t-1} + W_{ix} \cdot x_t + b_i) \\ \tilde{C}_t &= \tanh(W_{ch} \cdot h_{t-1} + W_{cx} \cdot x_t + b_c) \\ C_t &= F_t \odot C_{t-1} + \tilde{C}_t \odot I_t \end{aligned} \quad [15]$$

In the equation[15], W_{fx} , W_{ix} , W_{cx} , and W_{ox} are weight matrices applied to the current input sequence; W_{fh} , W_{ih} , W_{ch} , and W_{oh} are weight matrices applied to the output sequence; b_f , b_i , b_c , and b_o are the corresponding bias vectors; \odot denotes the Hadamard product.

3. The output gate is used to determine what information at the current time step needs to be transferred from the cell state to the output, combined with the activation function \tanh , to obtain the final output h_t .

$$\begin{aligned} O_t &= \sigma(W_{oh} \cdot h_{t-1} + W_{ox} \cdot x_t + b_o) \\ h_t &= O_t \odot \tanh(C_t) \end{aligned} \quad [16]$$

In the equation, σ is the sigmoid function; b_o is the bias term.

LSTM can effectively utilize time series data of different time periods to predict the next value in the time series during forward propagation, achieving supplementation of missing values and prediction of potential risks.

$$\{P\} = W_1\{X_1\} + W_2\{X_2\} + \cdots + W_k\{X_k\} \quad [17]$$

Where $\{P\}$ represents the computed sequence value for the target measuring point; W_k is the weight of measuring points; $\{X_k\}$ is the time series of measuring point. The following process is adopted to enhance data accuracy:

Step 1: Read the monitoring sequence from the database of the automated data collection system and preprocess the data sequence through normalization and physical logical elimination.

Step 2: Use the improved spatiotemporal clustering algorithm to perform spatial clustering on the monitoring sequence and solve the center line of each cluster's spatiotemporal sequence; calculate the 95% confidence interval of each cluster center line and set upper and lower threshold values for outlier verification.

Step 3: When the time series rolls forward, divide the previous spatiotemporal sequence into a training set and a test set; construct a multi-point sequence LSTM model to represent the target measuring point sequence, and through training obtain the weights of the multi-point sequence, and verify the reliability of these weights.

Step 4: During the forward rolling process, maintain the length of the test set, expand the training set, and compare the predicted values of the measuring points obtained from the training of multi-point data with actual data to determine if they are outliers and check if they meet the warning standard.

Step 5: Compared with the center line, if it is an outlier or the value is missing, use the predicted value as the imputation value for the missing measurement point to achieve data filling. If the time series trends in the cluster consistently increase or reach the warning value, execute the alarm procedure. It should be noted that when the amount of data for the independent variable measuring point is small, the accuracy of representing the target measuring point is poor.

3. ARCH DAM CASE

A hydropower station is located in the mountainous canyon area of western Yunnan Province, a region characterized by abundant hydropower resources, favorable topographical and geological conditions, and stable water availability. The hydropower station primarily generates electricity while also providing significant benefits in flood control, irrigation, silt retention, tourism, and reservoir shipping, as shown in Fig. 4. The dam site features a hot and dry climate, with an average annual rainfall of 987.2 mm and an average annual temperature ranging between 14.3°C and 19°C. The crest elevation of the dam is 1245.00 m, with the foundation excavation elevation at 950.50 m, the maximum dam height at 294.5 m, and the crest length along the centerline arc at 892.786 m. The normal water storage level of the dam is 1240 m, the multi-year average operating water level is 1181 m, the check

flood level is 1242.51 m, the dead water level is 1166 m, and the total storage capacity is 15.132 billion cubic meters. The project consists of a concrete double-curved arch dam, spillway openings on the dam body, an energy dissipation pool and secondary dam downstream, a left-bank spillway tunnel, a right-bank diversion and generation system, and the power transmission works, as shown in the Fig. 4. The arch dam is divided into 43 sections, with the spillway sections being 22 m to 26 m wide and the remaining sections being 20 m wide.



Fig. 4
Arch dam views: (a) Front view (b) Side view

The monitoring of horizontal deformation of the dam body uses surface deformation monitoring points, plumb lines, dam crest GPS, and a laser 3D measurement system, while the vertical displacement monitoring uses leveling points, hydraulic leveling instruments, dam crest GPS, and a laser 3D measurement system.

A total of 45 segments of plumb lines were arranged to monitor the horizontal deformation and deflection of the dam body, segmented in the corridors of various layers of 9 dam sections: 4#, 9#, 15#, 19#, 22#, 25#, 29#, 35#, and 41#, as shown in Fig. 5.

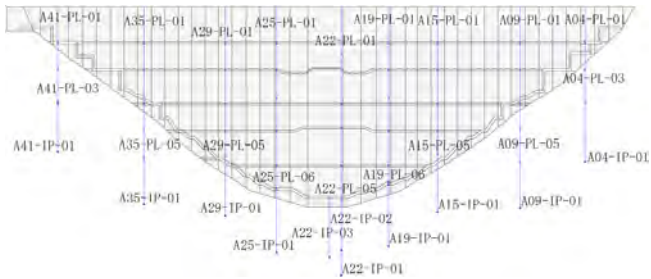


Fig. 5
Schematic Diagram of Monitoring Instrument Layout

To verify the effectiveness of the outlier detection and missing value imputation methods proposed in this paper, the displacement monitoring sequence of the arch dam is taken as the research object. The following figure shows the detected values from some of the displacement monitoring instruments:

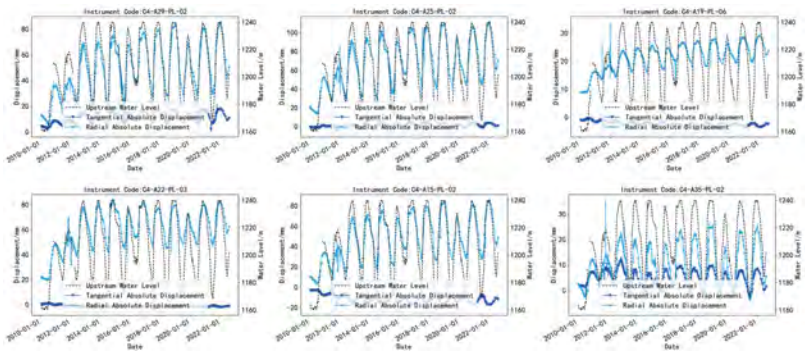


Fig. 6
Diagram of the Relationship Between Partial Monitoring Data and Water Level

It can be seen from Fig. 6 that, generally, the radial displacement values are positively correlated with the water level, and the radial displacement fluctuates periodically. The period from January 1, 2018, to January 1, 2022, was selected for analysis. The time series curves of monitoring values and water level relationships for a cluster of clustering results are shown in Fig. 7.

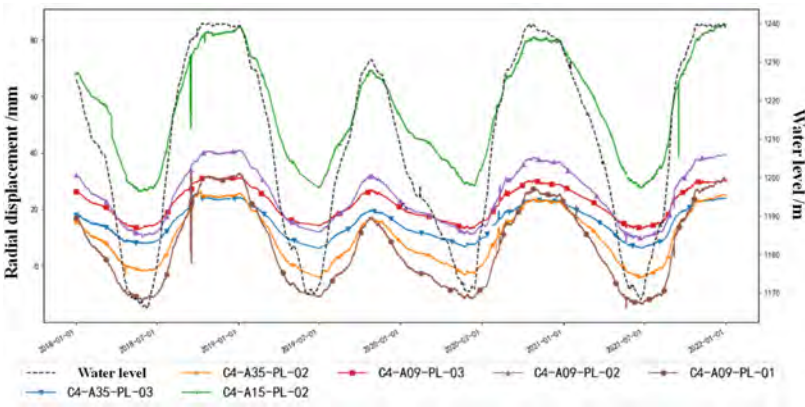


Fig. 7
Time Curves of Measurement Values with Water Level for Each Monitoring Point in a Cluster Result

The improved clustering method from Equation [4] in this paper was used to cluster the displacement monitoring data. To make the clustering differences significant, the distance correlation coefficient r_a was set to 1 and the obtained spatiotemporal sequence cluster is shown in the Fig. 8:

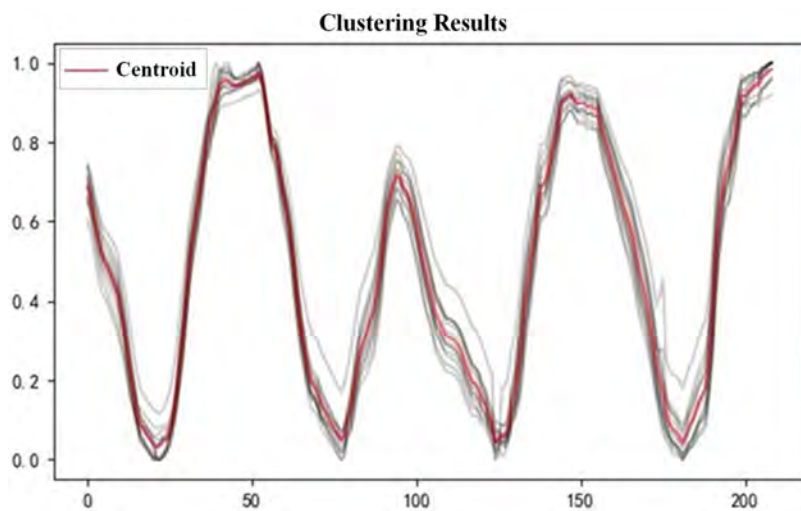


Fig. 8
Normalized Clusters and Cluster Centroids

The clustering results of different clusters are mapped onto the dam model. The clustering division results of displacement measurement points are as shown in the figure. It can be seen that the clustering results exhibit the following characteristics:

(1) The clustering results are influenced by the partitioning of dam construction materials.(2) Horizontally, the clustering results exhibit a symmetrical form along the river, which matches the radial displacement characteristics of the arch dam.(3) Vertically, it is divided into three zones, and it can be observed that the deformation monitoring points in each zone are basically symmetrically distributed along both sides of the arch crown beam. The monitoring sequence variation patterns within the same zone have high similarity, as shown in Fig. 8, reflecting the spatial distribution characteristics of the dam body deformation.

To validate the outlier detection performance of the proposed method, precision P, recall R, and weighted evaluation metric F were selected to compare and analyze the results from the aspects of detection accuracy, sensitivity to anomalous

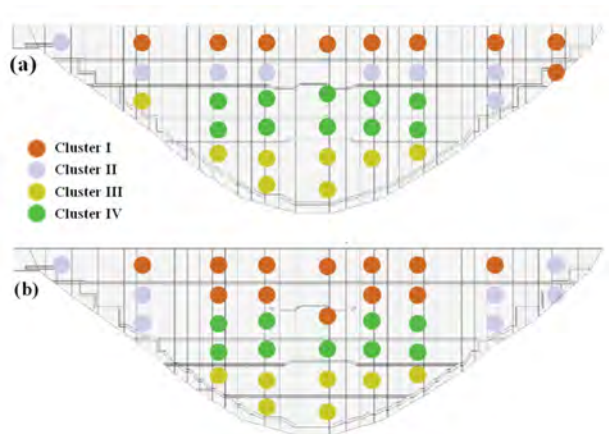


Fig. 9
Differences in Clustering Methods: (a) Dam Zones Obtained by the Original Clustering Algorithm; (b) Dam Zones Obtained by the Improved Clustering Algorithm

values, and comprehensive detection performance. Taking the two displacement measurement points C4-A09-PL-03 and C4-A35-PL-03 as examples, anomalous data were manually pre-checked and multiple gross errors were randomly set. Then, the algorithm was used to identify anomalies in the pre-checked original data sequence, and the algorithm recognition results were evaluated against manual identification using the above metrics.

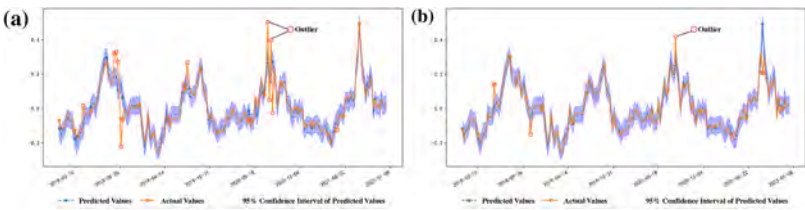


Fig. 10
Time History Curve of Measurement Values, Cluster Centroid Line, Confidence Interval, and Outliers: (a) C4-A09-PL-03; (b) C4-A35-PL-03

As shown in Fig. 10, it can be seen that the original difference sequence exceeds the confidence interval range of the centerline at gross error points. By comparing with the Isolation Forest (IForest) and K-Nearest Neighbors (KNN)

algorithms, the proposed algorithm shows higher metrics than other algorithms, improving detection accuracy. The evaluation metrics for measurement points are shown in Table 1.

Table 1
Evaluation Metrics for Identifying Anomalous Values at Monitoring Points

POINT ID		C4-A09-PL-03	C4-A35-PL-03
P	This Study	0.978	0.989
	IForest	0.911	0.862
	KNN	0.884	0.858
R	This Study	0.98	0.982
	IForest	0.906	0.869
	KNN	0.862	0.903
F	This Study	0.978	0.985
	IForest	0.908	0.865
	KNN	0.872	0.879

To validate the effectiveness of the proposed algorithm for missing value imputation, this paper artificially removes a segment of non-missing values from the sequence. The algorithm is then used to impute the missing values in the sequence. The root mean square error (RMSE), mean absolute error (MAE), maximum absolute error (MAXE), and coefficient of determination (R^2) between the imputed and actual values are used as control indicators. The calculation for

It is considered that the smaller the RMSE, MAE, and MAXE, and the larger the R^2 , the better the model performance. Using the time series of monitoring values from C4-A29-PL-04 as target measurements, training is conducted using LSTM. During the calculation, the model's activation function is the sigmoid function, and the Adam optimization algorithm is used to update the parameters of each layer during training. Comparing the multi-point model with the traditional hydrostatic-seasonal-temporal (HST) model, as shown in Table 2, the multi-point model yielded a maximum error of 0.578, an average maximum error of 0.079, and a maximum root mean square error of 0.101, all of which are smaller than the errors obtained by the HST model. While having lower errors, the determination coefficients are all greater than those obtained by the HST model.

As shown in Fig 11, the errors obtained by the multi-point model are significantly smaller than those obtained by the traditional HST model, effectively improving the accuracy of missing value imputation. The average error and maximum error of multiple sequences demonstrate the effectiveness of the missing value imputation method proposed in this paper.

Table 2
Imputation Error for Missing Values at Monitoring Points

POINT ID	C4-A29-PL-04	
	This study	HST model
MAXE	0.578 mm	0.826 mm
MAE	0.079 mm	0.151 mm
RMSE	0.101 mm	0.186 mm
R ²	0.978	0.950

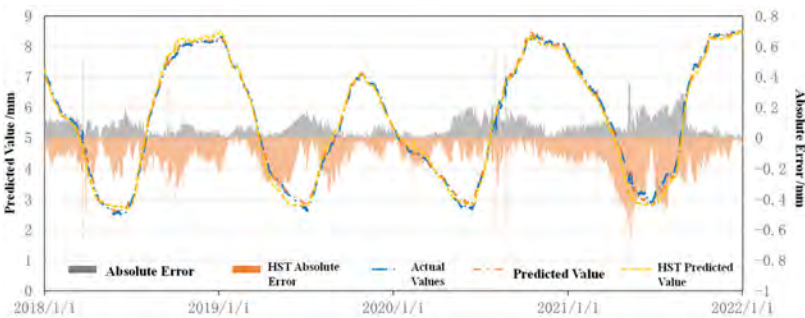


Fig. 11
Imputation Error of Missing Values at Monitoring Points: Predicted and Difference Values of the Measurement Time Series for C4-A29-PL-04 Using the Method Presented and the HST Method.

4. CONCLUSION

This study, based on an improved spatiotemporal clustering method of monitoring sequences, explores the methods for handling gross errors and missing values in monitoring sequences. The main work includes the following:

1. Introducing spatial coordinate data of sensors, the time series K-shape similarity measure method has been improved, and clustering analysis has been conducted on displacement sensors. By comparing with the zoning of dam construction materials and the physical quantity distribution patterns of the dam body, the rationality of the improved algorithm is demonstrated. This provides analytical tools for studying effective information extraction methods from the perspective of temporal and spatial similarity in monitoring sequences.
2. Based on the clustering results, combining the clustering method with the confidence interval method, an outlier detection method for monitoring

sequences is proposed. Compared with traditional outlier detection methods (isolation forest, nearest neighbor method), it is proven that the proposed method can effectively improve the accuracy of outlier detection.

3. Using multiple measured value sequences and a target measured value sequence within the same partition, a multi-point representation model for missing data imputation was constructed.

Combined with the predictive maintenance needs of a specific arch dam case in Yunnan Province, the proposed method was applied to the safety monitoring system of this project, and the proposed method was validated. The main conclusions are:

1. Comparing the outlier detection method proposed in this paper with traditional outlier detection methods (isolation forest, nearest neighbor method), it is proven that the proposed method can effectively improve the accuracy of outlier detection.
2. Training and comparing the multi-point model with the traditional hydrostatic-thermo-time model, results show that the multi-point model's training outcomes are closer to the measured values, providing higher accuracy in missing data imputation, thus offering a reliable data foundation for subsequent analysis.

REFERENCES

- [1] GIANNOULIDIS, A., GOUNARIS, A., NASKOS, A. *et al.* Engineering and evaluating an unsupervised predictive maintenance solution: a cold-forming press case-study. *J Intell Manuf* (2024).
- [2] W. ZHANG, D. YANG AND H. WANG, "Data-Driven Methods for Predictive Maintenance of Industrial Equipment: A Survey," in *IEEE Systems Journal*, vol. 13, no. 3, pp. 2213–2227, Sept. 2019,
- [3] CALABRESE, MATTEO, MARTIN CIMMINO, FRANCESCA FIUME, MARTINA MANFRIN, LUCA ROMEO, SILVIA CECCACCI, MARINA PAOLANTI, GIUSEPPE TOSCANO, GIOVANNI CIANDRINI, ALBERTO CARROTTA, and *et al.* 2020. "SOPHIA: An Event-Based IoT and Machine Learning Architecture for Predictive Maintenance in Industry 4.0" *Information* 11, no. 4: 202.
- [4] KYM FRASER; HANS-HENRIK HVOLBY; CHIHIRO WATANABE. *A review of the three most popular maintenance systems: how well is the energy sector represented?* *International Journal of Global Energy Issues (IJGEI)*, Vol. 35, No. 2/3/4, 2011.

- [5] KANG, H.S., LEE, J.Y., CHOI, S. *et al.* Smart manufacturing: Past research, present findings, and future directions. *Int. J. of Precis. Eng. and Manuf.-Green Tech.* 3, 111–128 (2016).
- [6] MOYNE, JAMES, AND JIMMY ISKANDAR. 2017. "Big Data Analytics for Smart Manufacturing: Case Studies in Semiconductor Manufacturing" *Processes* 5, no. 3: 39.
- [7] JAY LEE, BEHRAD BAGHERI, HUNG-AN KAO, A *Cyber-Physical Systems architecture for Industry 4.0-based manufacturing systems*, Manufacturing Letters, Volume 3,2015, Pages 18–23.
- [8] YAGUO LEI, NAIPENG LI, LIANG GUO, NINGBO LI, TAO YAN, JING LIN, Machinery health prognostics: A systematic review from data acquisition to RUL prediction, *Mechanical Systems and Signal Processing*, Volume 104,2018, Pages 799–834.
- [9] LI B, YANG J, HU D. Dam monitoring data analysis methods: A literature review. *Struct Control Health Monit.* 2020; 27:e2501.
- [10] BISGAARD, SØREN, AND MURAT KULAHCI. 2005. "Quality Quandaries: The Effect of Autocorrelation on Statistical Process Control Procedures." *Quality Engineering* 17 (3): 481–89.
- [11] J. FOX, Outliers in Time Series, *Journal of the Royal Statistical Society: Series B (Methodological)*, Volume 34, Issue 3, July 1972, Pages 350–363,
- [12] RAO, J. N. K. (1972). [Review of Time Series Analysis Forecasting and Control, by G. E. P. Box & G. M. Jenkins]. *Econometrica*, 40(5), 970–971.
- [13] CHANG, I., TIAO, G. C., & CHEN, C. (1988). Estimation of Time Series Parameters in the Presence of Outliers. *Technometrics*, 30(2), 193–204.
- [14] RAO, J. N. K. (1972). [Review of Time Series Analysis Forecasting and Control, by G. E. P. Box & G. M. Jenkins]. *Econometrica*, 40(5), 970–971
- [15] J. KUSUMA, L. DOHERTY and K. RAMCHANDRAN, "Distributed compression for sensor networks," *Proceedings 2001 International Conference on Image Processing (Cat. No.01CH37205)*, Thessaloniki, Greece, 2001, pp. 82–85 vol.1
- [16] JOHN PAPARRIZOS, LUIS GRAVANO Authors Info & Claims. k-Shape: Efficient and Accurate Clustering of Time Series. *ACM SIGMOD Record*, Volume 45, Issue 1Pages 69 – 76.
- [17] TAOZHI XU, JIE LI, *Assessing the spatial variability of the concrete by the rebound hammer test and compression test of drilled cores*, *Construction and Building Materials*, Volume 188,2018,Pages 820–832.

- [18] *Spatial variability of concrete electrical resistivity and corrosion rate in laboratory conditions*, *Construction and Building Materials*, Volume 306, 2021,124777.
- [19] SHAOWEI WANG, CONG XU, YI LIU, HAO GU, BO XU, KUN HU, *Spatial association-considered real-time risk rate assessment of high arch dams using observed displacement and combination prediction model*, *Structures*, Volume 53,2023,Pages 1108–1121.
- [20] MALTESE, ANTONINO, Claudia Pipitone, Gino Dardanelli, Fulvio Capodici, and Jan-Peter Muller. 2021. "Toward a Comprehensive Dam Monitoring: On-Site and Remote-Retrieved Forcing Factors and Resulting Displacements (GNSS and PS-InSAR)" *Remote Sensing* 13, no. 8: 1543.
- [21] SEPP HOCHREITER, JÜRGEN SCHMIDHUBER; Long Short-Term Memory. *Neural Comput* 1997; 9 (8): 1735–1780.
- [22] LIU C, PAN J, WANG J. An LSTM-based anomaly detection model for the deformation of concrete dams. *Structural Health Monitoring*. 2024;23 (3):1914–1925.

COMMISSION INTERNATIONALE DES
GRANDS BARRAGES

VINGT-HUITIEME CONGRES DES
GRANDS BARRAGES
CHENGDU, MAI 2025

**STUDY ON THE RAPID CONSTRUCTION TECHNOLOGY OF A LARGE SAND
AND GRAVEL PROCESSING AND CONCRETE PRODUCTION SYSTEM IN A
HIGH-ALTITUDE CANYON AREA (*)**

Liu CHAOJIAN & Deng BING
*Tibet Construction Engineering Co., Ltd., No.9 Hydropower Bureau,
Lhasa*

CHINA

SUMMARY

For the safe and rapid construction of large-scale sand and gravel processing and concrete production systems in high-altitude canyon areas, through the optimization of system layout and structural form, new steel structure silos and large inflatable air film silos are used to replace the traditional steel structure semi-enclosed silo. At the same time of adopting the above methods, BIM technology is used to optimize the structural design of the steel structure in the construction process, realize the "digital twin" of construction and design in the BIM technology scenario, and use the low-temperature season covering insulation process to realize the rapid construction of each civil structure of the system. Innovating the construction technology, optimizing the design structure, and optimizing the construction plan are the keys to the rapid construction of large-scale sand mixing systems in high-altitude canyon areas.

**Étude de la technologie de construction rapide d'un important système de traitement de sable et de gravier et de production de béton dans une vallée de haute altitude*

RÉSUMÉ

Le système de traitement du sable et du gravier à grande échelle et de production de béton dans la région de la vallée de haute altitude est sûr et rapide. Grâce à l'optimisation de la disposition du système et de la forme structurelle, un nouveau silo à structure en acier et un grand silo à film d'air gonflable sont utilisés pour remplacer le silo semi-fermé traditionnel à structure en acier. En même temps que l'adoption de la méthode ci-dessus, la technologie BIM est utilisée pour optimiser la conception de la structure en acier dans le processus de construction, réaliser le « jumeau numérique » de la construction et de la conception dans le scénario de technologie BIM, et utiliser le processus d'isolation de couverture de la saison à basse température pour réaliser la construction rapide de chaque structure du système. L'innovation dans la technologie de construction, l'optimisation de la structure de conception et l'optimisation du plan de construction sont les clés de la construction rapide de systèmes de mélange de sable à grande échelle dans les zones de haute altitude.

1. INTRODUCTION

The sand and gravel processing and concrete production system of a hydropower station plays an important role, i.e. the “grain silo” for the main construction of the hydropower station. With the acceleration of infrastructure and clean energy construction in the Xizang Autonomous Region in recent years, the number of hydropower projects built in high-altitude canyon areas has gradually increased. In this context, it should be noted that the commissioning time of the sand and gravel processing and concrete production system often restricts the commencement of the construction of the main project construction. JX Hydropower Station is one of China's key national projects to support the economic development of Xizang, and its sand and gravel processing and concrete production system is the largest of its kind in the middle reaches of the Yarlung Zangbo River at present. Due to the constraints of the canyon terrain in the area where the hydropower station is located, the arrangement of the entire sand and gravel processing and concrete production system is extremely compact; due to the commissioning schedule, the civil construction, installation of metal structures, and the mechanical and electrical installation are required at the same time period during the system construction, causing great interference with the construction. In addition, there are old walnut trees in the system area that need to be protected in situ, and adjacent sections will occupy the construction workspace for the system during construction, which places higher demands on the construction organization of the system. Finding a way to reasonably optimize the arrangement plan and accelerate the construction progress under the circumstances of restricted construction site layout, in-situ protection of the

walnut trees, and great interference with the construction of various working procedures is the key to ensuring the rapid construction of a large sand and gravel processing and concrete production system in a high-altitude canyon area. This is also the focus of this study. [2]

2. PROJECT OVERVIEW

Located above the Zangmu Canyon section of the mainstream of the Yarlung Zangbo River in Shannan Prefecture, JX Hydropower Station is the third stage of the eight-stage development program of the hydropower in the middle reaches of the Yarlung Zangbo River, and consists of water-retaining structures, flood discharge and energy dissipation structures, a water diversion & power generation system, a booster station, a fishway, etc. The sand and gravel processing and concrete production system for the JX Hydropower Station is arranged in JX Village located 1.9 km downstream of the dam site. It mainly undertakes the task of producing 2,264,400 m³ of concrete for the main works, including the diversion tunnel and dam, the powerhouse, etc. Specifically, the sand and gravel processing system is designed to meet the strength of 130,000 m³/month in the peak period of concrete in demand; the concrete production system is designed to meet the strength of 130,000 m³/month in the peak month of concrete in demand, 56,000 m³/month in the peak period of roller-compacted concrete in demand, and 85,000 m³/month in the peak period of normal concrete in demand. The materials for the hydropower station mainly come from the excavation works of the diversion tunnel, dam and powerhouse. The wastewater treatment system of the station meets the requirements for treating the wastewater from the sand, gravel and concrete systems, and the wastewater is recycled after treatment, instead of being discharged.

JX Hydropower Station is located in the climate zone of the Qinghai-Tibet Plateau, which is characterized basically by low temperatures, thin air, dry atmosphere, unusually strong solar radiation, high evaporation, large temperature differences between the day and night, and frozen slope surfaces. In this zone, the multi-year average temperature is 9.3°C, the extreme maximum and minimum temperatures are 32.5°C and -16.6°C, respectively, the multi-year average precipitation is 527.4 mm, the multi-year average evaporation is 2,084.1 mm, the multi-year average relative humidity is 51%, the multi-year average atmospheric pressure is 685.5 hpa, the multi-year average wind speed is 1.6 m/s, the maximum wind speed over the years is 19.0 m/s, the multi-year average sunshine duration is 2,605.7h, and the maximum frozen soil depth over the years is 19 cm. The arrangement of the sand and gravel processing and concrete production system of JX Hydropower Station is shown in Figure 1.



Fig. 1

Three-dimensional Arrangement Plan of the Sand and Gravel Processing and Concrete Production System for JX Hydropower Station

3. ANALYSIS AND SOLUTIONS OF PROJECT FOCUS AND DIFFICULTIES

The old walnut trees on the construction site are difficult to protect in situ, and the conditions for overall construction layout are unfavorable.

The system is arranged over an area of 51,000 m². According to the environmental assessment report for the project, there are 13 ancient walnut trees in the system area that need to be protected in situ and must not transplanted or cut down. This makes the construction of the system, already with a compact arrangement, even more difficult, so the original arrangement design scheme has to be optimized and adjusted.

Since the sand and gravel processing and concrete production system is in close proximity to the former S508 Provincial Highway, the S508 Provincial Highway rerouting line, the Dagu Scenic Area, and the construction camp in front of it, its construction is subject to great interference, as well as cross-interference during earth-rock excavations.

According to the contract documents, the S508 rerouting section shall have basic traffic conditions three months after the commencement of the sand and gravel processing and concrete production system, and the relocation of the local villagers' shops and the test room for the S508 rerouting section in the plant area shall be completed on time. During the project implementation, none of the above work was finished, and the former S508 Provincial Highway was under continuous

traffic control, leading to a serious delay in the earth-rock excavations. In addition, since the system is in close proximity to the Dagū Scenic Area and the construction in front of it, the 13 ancient walnut trees on the site need to be protected during the excavation and blasting operations. To this end, the mode of earth-rock excavations must be adjusted in the light of the tight schedule, heavy tasks and high protection requirements.

The civil construction of the system was delayed due to interference caused by the construction of adjacent sections, which resulted in the system construction period spanning the low-temperature and windy season. To this end, counter-measures should be developed to ensure the quality and safety during the construction.

Due to the interference caused by the construction of adjacent sections, the commencement of the project lagged behind the original bidding phase, which resulted in the civil construction of key construction parts of the system, such as the finished material silo, semi-finished material silo and air-cooled material silo, being postponed to the low-temperature season, overlapping with the peak period of the system's metal structure installation, which posed a quality risk. In addition, the delay in the installation of the metal structures caused by the delay in civil construction led to a potential safety hazard to the lifting operations during the windy season. To this end, corresponding special measures for the system construction during the low-temperature and windy season should be developed to ensure quality and safety during the system construction.

The sand and gravel processing and concrete production system has a large volume of work and short construction period in terms of steel structure construction and installation and equipment installation, and the installation precision of some steel structures and equipment is high according to requirements.

According to the design documents, the sand and gravel processing and concrete production system contains a total of 46 sets of large equipment, 52 sets of belt conveyors, and 3,200 t of metal structure trusses and columns; the installation period of the metal structures and equipment is only 6 months, the required precision of equipment installation in crushing workshop is high, and the spatial anisotropic structure of the discharging hopper in the screening workshop is complex; influenced by the narrow site and the distribution of the ancient walnut trees, there is spatial cross-interference among the metal structure trusses and columns. To this end, the drawings for the production and installation of the equipment and trusses in the above-mentioned sites should be refined, and a secondary optimization design should be done by using the BIM software, so as to realize the "digital twin" of the on-site construction and the BIM digital demonstration, to reduce the on-site reworking due to collision, to accelerate the construction progress, and to ensure that the construction quality meets the requirements.

4. OPTIMIZATION OF THE LAYOUT OF THE SAND MIXING SYSTEM

4.1. OPTIMIZATION OF THE LAYOUT OF THE SAND MIXING SYSTEM

According to the requirements of the project EIA report, the 13 walnut trees in the system must adopt the principle of in-situ protection, and the walnut trees shall not be transplanted. Combined with the topography, the centralized layout of each equipment workshop was adopted, the processing technology was optimized, and the original first screen, second screen, third screen, four screen workshop, sand making workshop and medium crushing, fine crushing and ultra-fine crushing workshop were merged and arranged into a screening workshop and a crushing workshop, and the positions of the remaining wastewater treatment systems, finished product silos, cementitious material tanks, mixing systems, refrigeration and heating and other auxiliary systems were all adjusted, and the layout of the belt conveyor in the system was adjusted immediately. At the same time, in order to reduce the impact on the walnut tree, the crown and DBH of each walnut 2 in the system were measured, and the impact of the belt conveyor and civil structure layout on the walnut tree in the design stage was reduced.

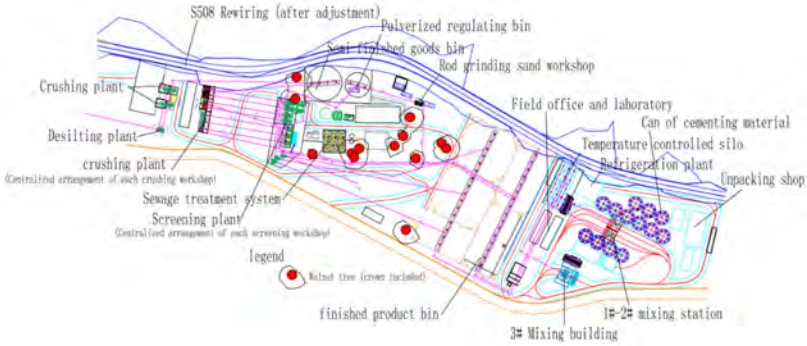


Fig. 2
Layout of the sand mixing system after entering the site

After adjusting the arrangement, the arrangement of the belt machine in the system is more concentrated than that in the bidding stage, especially the arrangement of the interchange belt machine in the crushing workshop and the screening workshop is intensive, the layout of the low-line belt machine at the bottom of the screening workshop is extremely dense, the number of hoppers in the screening workshop is large, the special-shaped structure is complex, and the operation space is small. The length of the high-line belt machine from the

screening workshop to the finished product silo has increased greatly compared with the original bidding plan, and the longest length of the belt machine has reached 165m. The rest of the tape machines take the angle of the belt to shorten the arrangement distance of the subsystem and reduce the interference to the walnut tree.

In addition, in order to speed up the progress of system construction, and at the same time combined with the requirements of environmental water protection in the plateau area, the semi-finished product silo and ultra-fine crushing adjustment silo in the system are adjusted from the traditional semi-enclosed form of steel structure roof to the fully enclosed silo of steel structure and the fully enclosed silo of steel structure hemispherical fully enclosed. According to the layout of the finished silo, combined with the terrain, the linear arrangement of the silo was adjusted to a centralized arrangement, and a new type of inflatable air film silo was used to replace the traditional semi-enclosed steel structure silo.

4.2. OPTIMIZATION OF MIXING SYSTEM LAYOUT

In the bidding stage, the mixing system is equipped with three HL240-2S3000L mixing buildings. After the project entered the site, considering that the construction period of the power station may increase the peak intensity during the construction period, the capacity of the mixing system was adjusted during the technical implementation stage. The two HL240-2S3000L mixing plants arranged in the original mixing system were adjusted to two HZ320-2S4500 mixing stations, and the mixing capacity of the mixing system was increased by 145,000 cubic meters per month after the mixing arrangement of the buildings and stations. After the mixing system is adjusted, the corresponding positions of the ash tank, unpacking workshop, heating workshop and so on are adjusted together. At the same time, in order to solve the problem that the mixing station cannot be air-cooled for the aggregate for the second time, the distance between the air-cooled silo and the mixing station is shortened to reduce the temperature loss, and the feeding belt of the mixing station is fully enclosed to form a constant temperature belt corridor to ensure the stability of the aggregate temperature of the upper station.

In order to solve the control interference of the mixing system after the mixing arrangement of the building station and reduce the later operation cost, the mixing system adopts the advanced concrete production intelligent system to realize the automatic control of the decentralized system, remote data collection, and the integration of the control unit, so as to realize the improvement from automation to intelligence, centralized monitoring and centralized decision-making.

5. RAPID CONSTRUCTION TECHNOLOGY OF SAND MIXING SYSTEM IN CANYON AREA

5.1. BIM DIGITAL TWIN TECHNOLOGY FOR THE SAND AND GRAVEL PROCESSING AND CONCRETE PRODUCTION SYSTEM

The sand and gravel processing and concrete production system was modeled, and the design drawings were checked. In particular, the trusses and columns of the belt conveyors in the middle of the crushing workshop and screening workshop were analyzed and checked for collision, and 3D modeling was performed for the discharging hoppers of the belt conveyors in the crushing workshop and screening workshop. The digital twin was realized in the construction process. For the BIM 3D model, see Figure 3; for the structural collision check, see Figure 4.

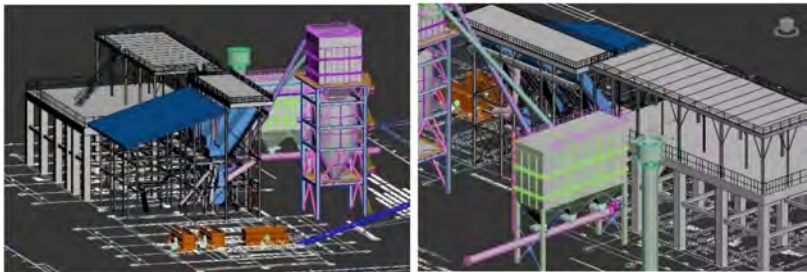


Fig. 3
BIM 3D Model (Partial)

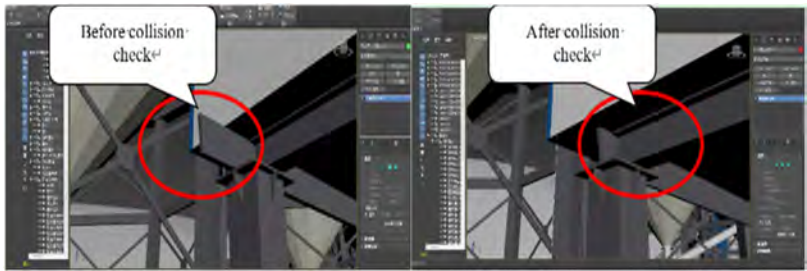


Fig. 4
Structural Collision Check of the BIM 3D Model

By applying the BIM modeling digital twin technology, the design of the steel trusses in the system was synchronized with the site construction, which was simulated in the BIM scenario, including the assembly of the steel structures, realizing the rapid site construction of the steel structures. During the civil construction of the system, based on the construction site and the results of the BIM construction design, all kinds of steel trusses in the system were pre-fabricated in batches and modules for installation one after another after completion of the civil construction. For large equipment in the system, the procurement plan was submitted in advance and preparations were made to access the construction site in advance, taking into account the special factors in Xizang.

5.2. RAPID CONSTRUCTION TECHNOLOGY OF A LARGE SILO

The semi-finished material silo in the sand and gravel processing and concrete production system has a diameter of 30 m, a straight height of 13.2 m, and a multi-faceted steel top with a height of 10.5 m. The vertical section of the silo is divided into nine layers, and from the top to the bottom are the first to the ninth layer in sequence. The first to fourth layers are all 1.5 m high and 8 mm thick; the fifth and sixth layers are both 1.5 m high and 10 mm thick; the seventh and eighth layers are both 1.5 m high and 12 mm thick; the ninth layer is 1.2 m high and 14 mm thick. The top of the silo consists of 74 installation units (3 mm thick), and the silo is approximately 200 t in total. Traditionally, the silo is built from the bottom up, with sections being hoisted and installed separately in stages. In order to expedite the construction progress, an inverted method is adopted, with the silo assembled from the top down and layer by layer.

Based on the silo's design, 38 10t electric chain hoists are evenly positioned on a concentric circle 400 mm from the silo wall. These hoists are affixed to inverted columns made of $\varphi 219 \times 10$ steel pipes at a height of 3.5 m. The hoisting lugs at the top of these columns, and base plates and rib plates are made of $\delta=16$ mm steel plates. The lower end of each silo wall is reinforced with backing bars made from [25 channel steel and the silo wall is secured with backing bars through gantry clamps. Hoisting lugs are welded onto the backing bars beneath the electric chain hoists. These hoists, through a control device, hoist the hoisting lugs, passing force to the backing bars and the silo wall, thereby hoisting the silo wall. These hoists can work either simultaneously or individually. The layout of the inverted columns is illustrated in Figure 5, and the sectional lifting process of the silo in Figure 6.

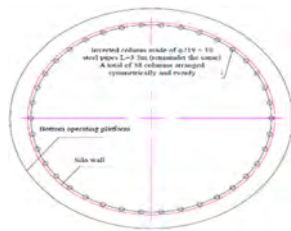


Fig. 5
Plan Layout Diagram of Inverted
Columns

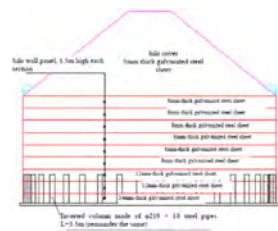


Fig. 6
Schematic Diagram of Sectional Silo
Hoisting

5.3. RAPID CONSTRUCTION TECHNOLOGY OF LARGE-SCALE AIR-DOME SILO

The finished material silo at the JX Hydropower Station, part of the sand and gravel processing system, represents the first use of an air-dome silo structure in high-altitude hydropower engineering. Given the unique features of materials to be stored in this project, a high-weather-resistant, high-strength UV-resistant, corrosion-resistant, hail-resistant, anti-mildew, self-cleaning, and aging-resistant PVDF membrane is adopted. This membrane is factory-made and meets Class B1 fire protection standards. The construction of the entire air-dome silo structure can be completed in 15 days.

5.3.1. *Rapid construction technology of the mixing system*

The mixing system comprises 13 1,500 t fly ash silos, two HZ320-2S4500 mixing stations, one HL240-2S3000L mixing plant, and auxiliary facilities including the unpacking workshop, power distribution room, weighbridge, and admixture workshop. Due to the relatively concentrated layout of the mixing system, the construction of the mixing stations, mixing plant, and fly ash silos extends a long period and occupies a large installation area. Influenced by the long construction period, and the position of the system, the construction site is extremely narrow during the installation, necessitating a well-organized sequence for the installation of the foregoing facilities.

Considering the small amount of civil engineering work, the foundations of the mixing stations and the mixing plant are poured first during the construction. Simultaneously, the foundation of the fly ash silos, which affects the commissioning of the first mixing station, is also poured. Different from the mixing plant, the mixing stations have a simpler structure. Therefore, the equipment installation for the mixing stations takes precedence during the construction process.

Concurrently with the installation of the mixing stations, the fly ash silos influencing the commissioning of the first mixing station are fabricated and installed. Subsequently, the mixing plant is installed and constructed, along with the fabrication and installation of the remaining fly ash silos. Due to the significant space requirements for fabricating the fly ash silos, the space-efficient and ground-level Lipp tank-making installation technique is implemented for the silos' tops, eliminating the need for scaffolding. This technique involves a construction process based on "spiral, double folding, and interlocking" methods. On this basis, the fly ash silo bodies are timely hoisted, and a streamlined production, hoisting, and reinforcement workflow is established, thereby promptly vacating the installation site.

The mixing stations and the mixing plant are installed in a coordinated manner from the bottom up, synchronized with the installation of mechanical components, in a segment-by-segment manner. The process commences with the installation of the mixer support frame, followed by the installation of the cement and fly ash silo support structures along with the gradual elevation of segments. Concurrently, the staircases are raised to facilitate access and streamline the installation process. The installation process follows the sequence of the mixer support frame, lower column base, discharge layer, mixing layer, storage layer, feed layer, and ends with commissioning and trial operation. Subsequently, electrical wiring, water supply systems, material conveyor belts, and external enclosure structures will be installed for each level. Upon completion of the installation of the fly ash silos, mixing stations, and mixing plant, additional facilities such as unpacking workshops, power distribution rooms, and weighbridges will be constructed. Finally, roadways, site hardening, drainage, and landscaping works will be carried out.

5.3.2. *Construction technology of large-scale air-cooled material silos in low-temperature seasons*

According to the schedule, the air-cooled material silo and the screening workshop of sand and gravel processing and concrete production system will be constructed in low-temperature seasons. This project is located in a high altitude, where the low-temperature season is characterized by strong winds, dry conditions, and low environmental temperatures. Therefore, strict insulation measures are essential during construction in low-temperature seasons.

Concrete pouring insulation is primarily achieved by the use of heat storage methods during low-temperature seasons. To address the large area and height of the air-cooled material silo and ensure good pouring quality, a large-area warm house is erected in the pouring silo. Specifically, the all-round scaffold is adopted within the silo inside, while external support frames of a warm house are separately erected outside. Warm air blowers are provided inside to

provide internal heating. Outside, a three-proof fabric or PVC-coated tarpaulin is used for wrapping. To insulate the floor structure, a 3 cm-thick rubber sponge is affixed to the exterior of the formwork. Concrete pouring is scheduled during daytime high-temperature periods through concrete pumping. Upon completion, plastic film and 3 cm-thick rubber sponge are used to cover and insulate the poured concrete.

5.3.3. *High-altitude hoisting and construction technology of complex metal structures*

The construction of the sand and gravel processing and concrete production system faces several safety challenges as a result of the layout of the engineering structures, including high-altitude operations, cross operations, overweight hoisting, hoisting in winter, and oxygen deficiency in high altitude. Throughout the system construction phase, a total of 3,200 t metal structures will be installed, 90% of which involves high-altitude hoisting, totalling 2,700 t. A total of 46 sets of large equipment will be installed, all of which will be hoisted. During the peak construction period when there is a large number of hoisting equipment and various interferences, technical management measures will be adopted during construction to ensure safe and efficient hoisting of metal structures in the sand and gravel processing and concrete production system.

1. Plan ahead to minimize cross operations, and rationally arrange civil and metal structure construction based on the construction intensity of each workspace to prevent cross operations. When cross operations are necessary, implement protective measures, and separate upper and lower workspaces using protective sheds erected with rack pipes, and wooden templates to ensure safe operations.
2. Conduct thorough safety briefings prior to construction considering the substantial hoisting workload and high hoisting safety risks; arrange a dedicated supervisor for each hoisting workspace to oversee and command the hoisting process; and implement strict inspections of hoisting equipment before hoisting to ensure compliance with hoisting requirements and strictly adhere to the “Ten Prohibitions for Hoisting” principle. Whenever possible, conduct hoisting operations during daytime and in warmer temperatures to avoid nighttime hoisting.
3. Arrange a dedicated safety officer for daily safety supervision and management; inspect hoisting machinery, wire ropes, and other hoisting gear before hoisting; operate cranes in strict adherence to its safety operation regulations to guarantee the compliance and legality of the hoisting equipment’s usage, and thus ensure its safe operation; and implement comprehensive monthly inspections of all hoisting equipment, and arrange dedicated personnel to oversee hoisting operations to achieve comprehensive hoisting safety management.

6. TECHNO-ECONOMIC ANALYSIS

On the basis of the research on rapid construction technologies for sand and gravel processing and concrete production systems in high-altitude canyon areas, the system layout and construction technology at the original bidding phase are optimized, resulting in cost savings. For a detailed comparative analysis of the technical and economic aspects, see Table 1.

Table 1
Comparison of Investments before and after the Optimization of the Rapid Construction Technologies for Sand and Gravel Processing and Concrete Production Systems in High-Altitude Canyon Areas

NO.	ITEM		ORIGINAL PLAN	AMOUNT (CNY 10,000)	PLAN AFTER ADJUSTMENTS	AMOUNT (CNY 10,000)
1	Optimized structure layout	Optimized system layout	Stepped and functionally zoned dispersed	1,252.7	Stepped, with optimized processing techniques and centralized layout of equipment workshops	1,092.7
2		Optimized layout of the mixing system	Single layout, including three HL240-2S3000L mixing plants	2,379	Mixed layout, including two HZ320-2S4500 mixing stations and one HL240-2S3000L mixing plant	1,122.8
3		Optimized finished material silo	Steel semi-enclosed material silo	521.5	New PVDF membrane in a fully enclosed inflatable structure	552.1
4	Rapid construction technology	BIM digital twin technology	N/A	/	BIM digital twin technology adopted to conduct collision checks on the system and achieve digital twin	18
5		Rapid construction technology of large silos	Traditionally, the silo is built from the bottom up, with sections being hoisted and installed separately in stages.	155.8	Innovatively, an inverted method is adopted, with the silo assembled from the top down and layer by layer.	64
6		Rapid construction technology of the mixing system	Traditionally, fly ash silos are hoisted and assembled in section.	35.9	The Lipp tank-making technology is adopted, including a construction process based on "spiral, double folding, and interlocking" methods to process fly ash tanks.	598.1

(Continued)

Table 1
Continued

NO.	ITEM		ORIGINAL PLAN	AMOUNT (CNY 10,000)	PLAN AFTER ADJUSTMENTS	AMOUNT (CNY 10,000)
7		Construction technology of large-scale air-cooled material silos in low-temperature seasons	N/A	/	Warm air blowers are provided inside to provide internal heating. Outside, a three-proof fabric or PVC-coated tarpaulin is used for wrapping. A 3cm-thick rubber sponge is affixed to the exterior of the formwork. Upon completion of concrete pouring, plastic film and 3 cm-thick rubber sponge are used to cover and insulate the poured concrete.	45
					Personnel are organized and equipment is constructed in low-temperature seasons.	660
8	Management costs	/	The construction period stipulated in the original contract is 14 months, with a project management cost of CNY 1.47 million per month.	2,058	The main contract construction period is shortened to 9 months after the implementation of the rapid construction technology.	1,323
9	Total			6,402.9		5,475.7

According to the table above, the rapid construction technologies of sand and gravel processing and concrete production systems in high-altitude canyon areas lead to a reduction in costs related to the layout of the mixed layout of stations and plant in spite of the slightly increased costs in BIM technology implementation, air-dome silo construction, and construction in low-temperature seasons. Additionally, with the early completion of the main construction phase and savings in project management costs, a total investment reduction of CNY 9.272 million (CNY 64.029 million - CNY 54.757 million) is achieved compared with the original bidding phase.

7. EPILOGUE

In high-altitude canyon areas, the installation of sand and gravel processing and concrete production systems is highly challenging for complicated layout, complex structural organization, and substantial construction interference. Particularly, there is no comparable construction experience for reference within the hydropower industry for the application of air-dome silos, mixed layout of plants and stations, and BIM digital twin in large-scale sand and gravel processing and concrete production systems in high-altitude regions. By optimizing design structures, adopting new construction processes, employing intelligent construction methods, and establishing various safety measures, construction interferences from civil and metal structures during the sand and gravel processing and concrete production system construction are reduced, accelerating the construction progress. On this basis, rapid and secure construction of sand and gravel processing and concrete production systems in high-altitude canyons is achieved, providing valuable reference experience for similar future projects.

REFERENCES

- [1] CHEN JINGSHOU. *Research and Application of Air-Supported Membrane Structure Enclosure Technology in Sand and Gravel Aggregate Stockyards. Yunnan Water Power*, 2023.
- [2] LI JIANFENG, LI QIYANG, ZHU XIAOMIN. *Design, Construction, and Operational Management of the Artificial Sand and Gravel System at Kongquegou, Xiaowan Hydropower Station. Construction Machinery Technology & Management*, 2007.

COMMISSION INTERNATIONALE DES
GRANDS BARRAGES

VINGT-HUITIEME CONGRES DES
GRANDS BARRAGES
CHENGDU, MAI 2025

**RESEARCH ON DYNAMIC MIX PROPORTION DESIGN METHOD OF
CEMENTED GRAVEL (*)**

Guangwen GUO
China Gezhouba Group Co., Ltd.

Kaiyan TAN
China Gezhouba Group Co., Ltd.

Shengmin ZHU
China Gezhouba Group Survey and Design Co., Ltd., Wuhan

Bo MINYUE
Gezhouba Group Testing Co., Ltd., Yichang

CHINA

SUMMARY

From the principle of strength generation of cemented gravel, this paper finds its key control indexes as sand rate and paste margin, and provides a dynamic proportion design method of cemented gravel under different graded sand rates. By establishing the relationship between different sand rates, different paste margins and binder strengths, combined with the design strength level, regression calculation of the proportion of the mix can be conducted, so as to derive curves of the mixing proportion of cementitious materials and water for different grades of binder under different sand rates, to realize dynamic control of the proportion parameters. This method is scientific and reasonable and reduces the input of materials and human resources to reduce the cost.

*Méthode de conception dynamique des proportions de mélange des sols cimentés

RÉSUMÉ

Selon le principe de génération de résistance des sols cimentés, ce rapport identifie le taux de sable et la marge de pâte comme les principaux indices de contrôle, et propose une méthode de conception de proportions dynamiques des classes de sable pour les sols cimentés. En établissant la relation entre les différents taux de sable, les différentes marges de pâte et les résistances des liants, et en combinant le niveau de résistance de conception, un calcul de régression des proportions du mélange peut être effectué afin d'en déduire des courbes des proportions de matériaux cimentaires et d'eau pour différents grades de liant selon différents taux de sable, afin de réaliser un contrôle dynamique des paramètres de proportion. Cette méthode est scientifique et raisonnable, et elle réduit les investissements en matériels et en ressources humaines pour diminuer les coûts.

1. INTRODUCTION

Cemented gravel refers to the use of cementitious materials and gravel, by mixing, paving, vibration crushing formed by a certain strength of the material, this dam building technology is different from conventional earth and gravel dams and gravity dams, the significant effect is to bring: a substantial reduction in costs, environmental protection, efficient and rapid construction of high security dams [1–3].

At present, the domestic projects have been built in the cemented gravel ratio design method is mainly with reference to the “cemented granular material dam construction technical guidelines” (SL 678-2014) ratio design method, ratio design principle is to determine the “ratio control range” [4]. According to the strength of cemented gravel preparation, select 2 to 3 cementing material dosage, in each cementing material dosage, respectively, according to the coarsest grading, the finest grading and average grading gravel proportion, in a wider range of different water consumption for the strength test, the establishment of the different grades of 28d age and design age compressive strength, modulus of elasticity and water consumption of the relationship between the determination of the appropriate to meet the requirements of the construction VC value. Determine the suitable range of water consumption to meet the requirements of construction VC value and the corresponding suitable range of strength, i.e. “proportion control range”. Finally, the amount of cementitious materials is selected according to the “proportion control range” under different amounts of cementitious materials. Under the dosage of cementitious materials, the minimum value of the design age strength of the average graded cementitious gravel in the “proportion control range” shall meet the requirement of formulated strength, while the minimum value of the design age

strength of the finest graded cementitious gravel in the “proportion control range” shall not be lower than the design strength [5,6].

In fact, the cemented gravel is a semi-rigid material, the internal voids often can not reach the state of complete package, thus causing the use of the ratio design method has the following aspects of the problem:

1. The full package theory design makes the paste dosage increase, can not give full play to the skeleton advantage of cemented gravel material.
2. In order to meet the finest, average, the coarsest grades within the package line of cemented gravel performance to meet the design requirements, so the different grades of the recommended ratio are used with the same cementing material, wet sieve molding makes three grades of cemented gravel strength and elasticity of the model difference is large, which leads to the overall deformation characteristics of the cemented gravel there is an imbalance in the phenomenon, but also not helpful to the quality control for future construction.

In order to solve this problem, a new proportion design method was approached, to ensure that the strength of different grades of cemented gravel is balanced. Research on a dynamic adjustment of cemented gravel ratio design method was conducted, which is more balanced than the existing method to design the different grades of strength. Indoor simulation of the field molding process was carried out, to ensure the design of the mix proportion is more scientific and reasonable, which is helpful to quality control of construction.

2. DESIGN CONCEPT

The internal structure of cemented gravel is composed of natural gravel + cementitious materials + water, when the paste composed of cementitious materials + water is enough, the gravel is suspended in the paste, this cemented gravel is actually a kind of natural graded gravel concrete, the strength of which is mainly dependent on the strength of the paste itself and the strength of the interface between the paste and the aggregate, at this time, through the reduction of the interface, reduce the water-cementitious material ratio, and increase the strength level of the binder itself. In this case, by reducing the interface, reducing the water-cementitious material ratio, increasing the strength grade of the cementitious material itself and so on, higher strength of cemented gravel can be obtained. However, cemented gravel is often not high strength requirements, you can use “lean” gravel, that is: cementitious materials + water paste is not enough to completely fill the gravel voids, this kind of cemented gravel is a kind of semi-rigid material, for the “binary strength” composition, mainly affected by the grading and cementitious materials, cementitious materials and aggregate interface strength,

and the cementitious materials and aggregate interface strength. Influenced by grading and cementing material cementation two factors, at this time should give priority to make full use of the contribution of grading to the strength, when the strength is insufficient to add cementing material will be fine particles into larger particles, play a supplement to the large particles, optimize grading, enhance the role of the skeleton, the use of the "paste margin method" according to the different grading (sand rate) to carry out Dynamic proportion design, can give full play to the skeleton effect of coarse aggregate in the binder system, when the skeleton effect is not enough to support the design strength requirements using the least amount of cementitious materials will be fine particles cemented together to form a thicker particles, fill the porosity, thus contributing to a larger skeleton support, in order to obtain the required strength. The so-called "binary strength" theory is that the strength consists of two dimensions: the skeleton effect of gravel and the cementing effect of cementitious materials.

3. EXPERIMENTAL STUDY

3.1. RAW MATERIAL REQUIREMENTS

Cemented gravel is composed of gravel, water, cement, fly ash, admixtures and other raw materials, using the actual raw materials used in the project, and its technical requirements are as follows:

1. Gravel should be hard texture; apparent density shall not be less than 2450kg/m³; gravel water content shall be relatively stable; the water content of the sand should not be greater than 6%.
2. The mud content in the gravel should not exceed 5%, and the content of clay lump should not exceed 0.5%, and the concentration of clay lumps should be avoided.
3. For the gravel the rate of the fine aggregate less than 5mm should be 18% ~ 35%, and that of coarse aggregate with particle size between 5mm and 40mm be 35% ~ 65%.
4. Cement shall conform to the silicate series cement of GB175-2007.
5. Fly ash shall comply with the relevant provisions of GB/T1596.

3.2. DESIGN APPROACH

As shown in the following equation below, the main principle is the paste filling margin method: select a fly ash admixture and water cementitious ratio according to experience, carry out different sand rates (the coarsest, average, the finest,

interpolation or extension of two to three), different paste margins and strength relationship, resulting in different sand rate under the relationship between the paste margin and the strength of the curve interpolated value from the selected proportion (paste margin, sand rate, water cement ratio), so that different gradations of cemented gravel material. The relationship between the sand rate and water consumption and cementitious materials of different grades of cemented gravel is thus obtained, so as to achieve the purpose of on-site dynamic control of the mixing ratio:

$$\alpha = (1 - m_s/\gamma_{gv} - m_r/\gamma_g) / (m_s/\gamma_{sv} - m_s/\gamma_s) \quad [1]$$

where α is the paste margin (the volume ratio of mortar to sand void), m_r is the mass of stone per square of material (kg/m^3), m_s is the mass of sand per square of material (kg/m^3), γ_g is the apparent density of coarse aggregate (kg/m^3), γ_s is the apparent density of sand (kg/m^3), γ_{gv} is the vibrated density of coarse aggregate (kg/m^3), γ_{sv} is the vibrational density of sand (kg/m^3).

3.3. DESIGN STEPS

The design steps are as follows:

1. Select different sand rates from 10% to 40% (including the coarsest, average, and finest graded sand rates) and different paste margins from 0.6 to 2.6 for compressive strength tests under different combinations. The water cement ratio and paste margin should be selected based on experience in the appropriate range, as far as possible to be able to encompass the gradation range of the recommended mix proportion. For the indoor test, gravel grading treatment is done by mixing method, scaling down to less than 40mm grain size, and molding is done by vibratory compaction method.
2. The relationship between different paste margins and the strength of cemented gravel at different sand rates were established.
3. According to the relationship graph between different paste margins and the strength of cemented gravel strength, find out the paste margin of the minimum cementitious material to meet the design strength requirements at all levels of sand ratio, and derive the proportion parameters (unit water consumption, cement dosage, fly ash dosage) through calculation.
4. Establish the relationship curves between different sand rates and the total amount of cementitious materials and water consumption under satisfying the design strength grade.
5. Through the above test, the relationships of mix proportion for the same design strength and different sand rate are established. On-site according to the sand rate to find fit ratio, fit ratio dynamic adjustment, so as to solve the problem of large strength dispersion, uneconomical.

Through the above test, the relationship between the same design strength, different sand rate of the fit ratio is derived. On-site according to the sand rate to find fit ratio, fit ratio dynamic adjustment, so as to solve the problem of large strength dispersion, uneconomical.

4. ENGINEERING EXAMPLES

Cemented gravel design index for the modulus enhancement area at the back side of the high toe pier in A hydraulic project: compressive strength of 10MPa at 90d, strength guarantee rate of 80%; cement: fly ash ratio (reference value of 4:6), the coarsest grading, the finest grading and average grading of the gravel ratio is shown in Table 1.

Table 1
Gradation of gravel used in the mix proportion test

TESTING RESULTS	GRADATION (%)						
	200- 100MM	100 TO 80MM	80 TO 60MM	60- 40MM	40- 20MM	20 TO 5MM	<5MM
Finest gradation	5.1	5.0	7.4	13.7	14.7	20.4	33.7
coarsest gradation	32.9	7.9	8.5	13.4	14.6	12.5	10.2
Average gradation	18.8	6.2	8.5	13.4	17.9	15.7	19.5

For the indoor tests, gravel grading treatment was done by mixing method and scaled down to less than 40mm particle size. Forming is done by vibratory compaction method with fixed water-cementitious material ratio of 0.50, and the relationship curves between different sand rates (10%, 20%, 25%, 30%, 35%, 40%) of cemented gravel and different paste margins (0.6, 1.0, 1.4, 1.8, 2.2, 2.6) and strength are carried out. The water-cementitious material ratio and paste margin should be selected empirically to encompass as much as possible the recommended mixes within the grading range. For the indoor tests, gravel grading treatment is done by mixing method and scaling down to less than 40mm grain size for molding. The relationship between paste margin and the strength of cemented gravel at design age was tested under different sand rates, and the specific test results are shown in Fig.1.

The above test results show that, in the case of sand rate is unchanged, with the increase of paste margin, the strength of the cementitious material also increases. Because, with the increase in the margin of the gray body, the cement paste fill

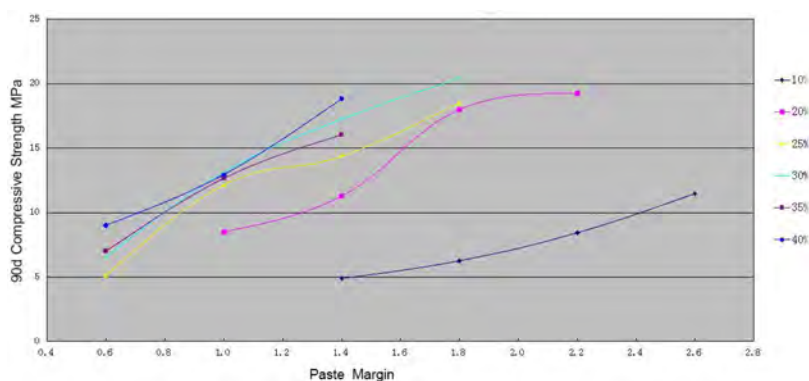


Fig. 1
Relationship between paste margin and 90-day compressive strength at different sand rates.

pore space of the fine aggregate to obtain a smaller porosity and thus contribute to a larger structural support role, and play a role in increasing the strength.

According to the results of 90d strength under different sand rate, the relationship between paste margin and cementitious material strength under different graded sand rate is shown in Fig. 1, so as to regress to the relationship between paste margin and strength under different sand rate, so as to preferably select the minimum cementitious material corresponding to the paste margin as the selected proportion parameter of cemented sand gravel is shown in Table 2, and finally, the relationship between different sand rate and cementitious material to satisfy the design strength grade is shown in Fig. 2. The relationship between different sand rate and water consumption is shown in Fig. 3.

Table 2
Recommended mix proportions for different sand rates for C₉₀ 10

SAND RATE, %	PASTE RMARGIN	MORTAR MARGIN	WATER-TO-BINDER RATIO	AMOUNT OF MATERIAL, KG/M ³			CEMENTITIOUS MATERIAL, KG/M ³
				WATER	CEMENT	FLY ASH	
10	2.42	0.55	0.50	60	48	72	120
20	1.16	0.88	0.50	57	46	69	115
25	0.91	1.07	0.50	56	45	68	113
30	0.80	1.33	0.50	59	47	71	118
35	0.79	1.67	0.50	67	54	80	134
40	0.73	2.02	0.50	70	56	84	140

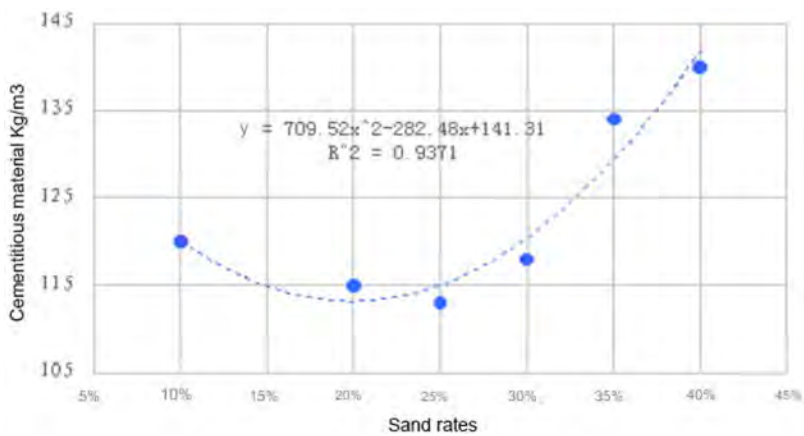


Fig. 2
Relationship between sand rate and cementitious material.

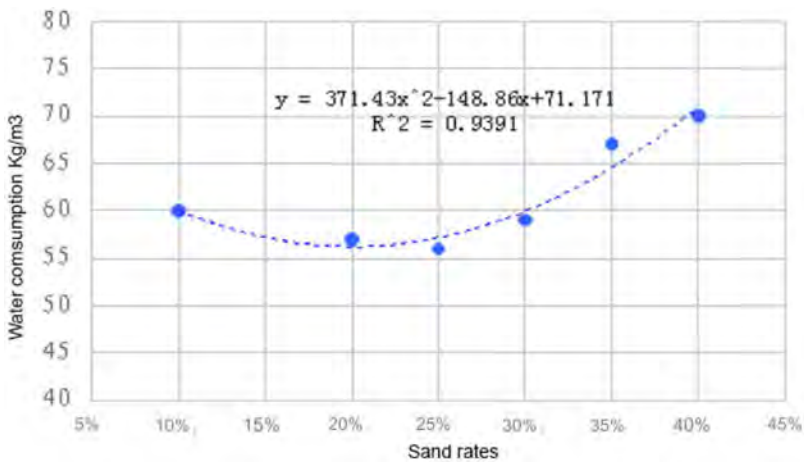


Fig. 3
Relationship between sand rate and unit water consumption.

From the test results in Fig. 2 and Fig. 3 above, it can be seen that the water consumption and amount of cementitious material of cemented gravel under different sand rates are different, in the case of sand rate less than 25% , with the increase of sand rate the cementitious material is smaller and the water

consumption is smaller; and in the case of 25% sand rate or more, with the increase of sand rate the cementitious material is larger and the water consumption is higher. Because the strength of cemented gravel is low, the contribution of the aggregate skeleton to the strength should be full used. According to the different gradation of the aggregate skeleton and paste contribution to the strength of the grading of the cemented material is classified, the thicker the gradation, the greater the contribution of the skeleton, and vice versa the greater the contribution of the paste, when the amount of fine aggregates are more than that of coarse aggregate to suspend the coarse aggregates, the role of the skeleton is not obvious, and the strength of the coarse aggregates is lowered, and the voids need to be filled by the cement paste agglomerates.

Therefore, in order to obtain a more homogeneous binder strength with the least amount of cementitious material, the paste margin method and the critical particle size control method (particles below 5 mm) were used for the proportion design. From Fig. 3 and Fig. 4, it can be seen that the water consumption and cementitious materials are minimized at 25% sand rate, when the gravel filling effect is the best, and the key particle size content in the skeleton can obtain smaller porosity thus contributing to a larger structural support.

5. APPLICATION EFFECTS

5.1. VALIDATION OF SAMPLING RESULTS FROM A BATCHING PLANT

Test results of 129 groups of samples of C₉₀ 10 (from September 20, 2022 to October 25, 2022) from a batching plant shows that for different gradation of cemented gravel, the 28d and 90d compressive strength are in accordance with the design requirements. And 28d compressive strength are between 8MPa and 14.7MPa, 90d compressive strength between 11.7MPa and 19.7MPa. The specific test results are shown in Table 3.

Table 3
Field Sampling Performance Test Results for Cemented Gravel

STRENGTH CLASS	AGE	NO. OF GROUPS	COMPRESSIVE STRENGTH, MPA			CONTENT BELOW 5MM, %		
			MAX.	MIN.	AVERAGE	MAX.	MIN.	AVERAGE
C90 10	28	85	14.7	8.0	9.3	30.1	20.5	23.2
	90	44	19.7	11.7	13.9	30.1	20.5	23.3
Remarks	Molding time period: 2022.09.20~2022.10.25							

5.2. FIELD CORING VERIFICATION

Two groups of core were taken from the drill holes in the cemented gravel area, and the compressive strengths were 14.3 MPa and 16.5 MPa respectively, which were greater than 10 MPa. The core sample acquisition rate reached more than 72.5%, which is shown in Fig. 4 and Fig. 5.



Fig. 4
Field coring.

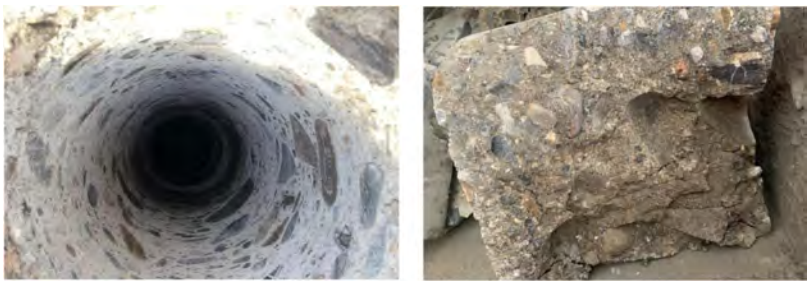


Fig. 5
Core sample compressive strength test.

6. CONCLUSIONS

The following conclusions are drawn from the application of cemented gravel of the modulus enhancement area of the high toe pier in a hydroelectric project. First, the grading simulation method (mixing method) is used to scale down the

maximum particle size of 200 mm gravel to 40 mm, the gravel skeleton structure remains unchanged from the original grading, and the filling rate (paste margin) is basically unchanged, so the results are more realistic. Second, through the calculation of paste margin, find out the relationship between paste margin and strength under different sand rate, and then according to the actual sand rate in the field through the regression to find out the proportion, and make dynamic adjustment of the proportion to ensure the balanced performance of different grades of cemented gravel. The grading gravel with small filling rate increases cementitious material, and the grading gravel with large filling rate reduces cementitious material, so as to solve the problem of large strength dispersion and uneconomical. The method is more reasonable and scientific, and can reduce the input of materials and human resources to reduce the cost when compared with various performance test methods currently used for the cemented gravel.

REFERENCES

- [1] SUN MINGQUAN. Research on Mechanical Properties, Durability and dam type for cemented gravel materials. Beijing:China Water Resources and Hydropower Press, 2016:2–5.
- [2] FEND WEI, JIA JINSHENG, MA FENGLING. Research on durability performance of cemented gravel dam construction materials and development of new protective materials. *Journal of Water Resources*, 2013,44(4):500–504.
- [3] SUN MINGQUAN, YANG SHIFENG, QINGQING. TIAN, etc. A review on mechanical properties, Durability and Dam Types of Cemented gravel Materials. *People's Yellow River*, 2016,38(7):83–85, 99.
- [4] JIA JINSHENG, ZHAO CHUN, MIAO LUN, etc. Development and application of construction quality monitoring system for cemented gravel dam. *Journal of China Institute of Water Resources and Hydropower Research*, 2018,16(1):1–8.
- [5] LIU ZHONGWEI, JIA JINSHENG, FENG WEI, etc. Latest application and practice of cemented gravel dam in small and medium-sized water conservancy projects. *Water conservancy and hydropower technology*, 2018,49(5):44–49.
- [6] YAN LIN, HE JIANXIN, YAND HAIHUA, etc. Research on design and engineering application of cemented gravel mix proportion. *People's Yellow River*, 2020,42(2):85–88.

COMMISSION INTERNATIONALE DES
GRANDS BARRAGES

VINGT-HUITIEME CONGRES DES
GRANDS BARRAGES
CHENGDU, MAI 2025

THREE DIMENSIONS OF BREAKTHROUGHS IN CHINA'S HYDRAULIC CONCRETE CONSTRUCTION (*)

Hougui ZHOU
China Energy Construction Group Corporation, Beijing

Kaiyan TAN
*Research Institute of Green and Intelligent Construction, China Gezhouba Group
Co., Ltd, Wuhan*

CHINA

SUMMARY

Along with the rapid development of China's water conservancy and hydro-power construction, the hydraulic concrete construction technology continues to make breakthroughs. This paper focuses on three dimensions to be described: using 80% ultra-high dosage fly ash for ultra-low heat composite cementitious materials to reduce the concrete adiabatic temperature rise by 9.6 °C, and with the establishment and implementation of intelligent temperature control system and model, the temperature of the mass concrete is under control, to achieve the dam concrete effective crack prevention and crack-free; with optimization of the combination of concrete mixing, transportation, pouring, formwork, curing and other equipment and technology, the dam height is 305m, and single lift is up to a height of 4.5 m.; by adopting precision measurement and control technology and developing high-strength special formwork and construction technology for hydraulic structures,

**Trois axes d'évolutions majeures dans la construction des aménagements hydrauliques en béton en Chine*

the shape control of concrete dam structures was of high precision of millimeter-level.

RÉSUMÉ

Parallèlement au développement rapide de la construction hydraulique et hydroélectrique en Chine, la technologie de construction en béton hydraulique continue de faire des percées. Cet article se concentre sur trois dimensions. L'utilisation de 80 % de cendres volantes à très haute dose pour matériaux cimentaires composites à très faible chaleur, permettant de réduire l'élévation de température adiabatique du béton de 9,6 °C, et avec la mise en place et la mise en œuvre d'un système et d'un modèle de contrôle de température intelligents, la température du béton de masse est maîtrisée afin d'assurer une prévention efficace des fissures et la construction sans fissures dans le béton du barrage. Avec l'optimisation de la combinaison d'équipements et technologies de mélange, transport, coulée, coffrage, durcissement et autres pour le béton, la hauteur du barrage atteint 305 m et une coulée de bétonnage peut atteindre une hauteur de 4,5 m. Grâce à l'adoption de la technologie de mesure et contrôle de précision et au développement de coffrages spéciaux et robustes ainsi que de technologies de construction pour les structures hydrauliques, le contrôle de la forme des structures de barrage en béton atteint une précision élevée au niveau du millimètre.

1. INTRODUCTION

China's concrete dams started in the early 1950s, since then, hydraulic concrete development is very fast, basically every 10 years to leap a step. Accordingly, hydraulic concrete construction technology has also made great progress, such as the priority use of bulk cement trucks, introducing chemical and mineral admixtures, automatic identification of concrete transportation, horizontal and vertical transportation integration, cantilever formwork, pouring mechanical support and concrete curing, etc. [1]. With a large number of concrete dam projects such as Three Gorges, Xiangjiaba, Xiluodu, Jinping, Ertan, Dagangshan, Guanyinyan, Longtan etc. Were completed and put into operation, hydraulic concrete construction technology continues to appear new breakthroughs in construction technology from mechanization, automation, digitalization, intellectualization to intelligent construction, and at the same time, a series of key problems of hydraulic concrete construction such as cracking of mass concrete, high dams, fast construction problems, high precision concrete construction. At the same time, a series of key problems for hydraulic concrete

construction, such as cracking of mass concrete, rapid construction of high dams, high-precision concrete construction, the contradiction between construction progress and cost, quality, etc., have all been overcome through in-depth scientific research and experimentation of the corresponding engineering carriers, the the research and innovation have been tested by the engineering applications, which has formed the world's high point in the construction of hydraulic concrete.

2. DIMENSION 1: DAM TEMPERATURE

Hydraulic concrete, as the most important construction materials for water conservancy and hydropower engineering, is characterized by frequent or periodic water action, large volume and long life. Because of often contacting with the environmental water, it generally require impermeability, freezing resistance, corrosion resistance, low heat and low shrinkage, and in the structures of high-speed water scouring, the requirements of the scour resistance, abrasion resistance and resistance to cavitation, etc. should also be met. In recent decades, the development of hydraulic concrete materials has made great achievements, from original four-component with cement, sand, stone and water developing to a variety of cement-based cementitious materials composite, a variety of mineral admixtures based on fly ash, a variety of chemical admixtures based on needs, and its performance has also undergone great changes. However, cement concrete is a brittle material, and prone to various cracks so as to affecting the bearing capacity, durability and waterproofing of concrete structures. Among them, temperature crack is one of the most common and difficult to prevent hazardous cracks in mass concrete, and it can be deemed an important problem that always accompanies the development of concrete construction technology, and it is also one of the topics of concrete construction technology with great professional depth. From the construction point of view, the essence is to control the temperature of the concrete, usually from two directions including materials and workmanship. Specific temperature control measures are: (1) optimize the concrete raw materials and proportion to reduce the total heat, (2) reduce the external heat source, (3) surface insulation to prevent cold damage caused by sudden drop in temperature, and (4) water forced cooling with the pipes embedded in concrete. However, until subversive breakthroughs in the concrete materials is achieved, temperature control comprehensive measures will be taken, because temperature rise from concrete hydration heat is high and shrinkage is large.

2.1. DEVELOP INTELLIGENT WATER COOLING TO REALIZE THE TEMPERATURE OF THE DAM BODY UNDER CONTROL

“Personalized water cooling” was used in Three Gorges Project Phase III dam concrete construction for the first time, that is, according to the different

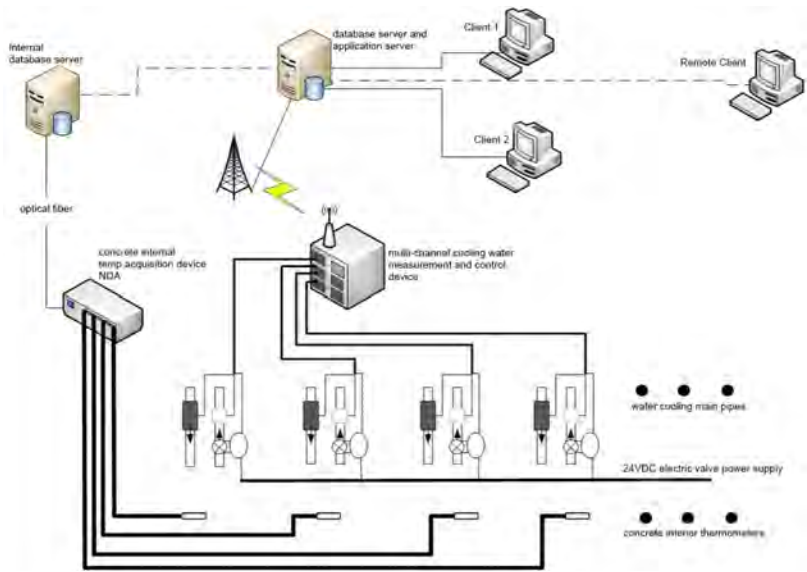


Fig. 1
Schematic diagram for structure and principle of intelligent control system of concrete water cooling.

requirements of different parts of the concrete adopting different flows and different temperatures of the water, creating a construction miracle with a “crack-free” dam [2]. Personalized water cooling is a fine control measures, because more timely and accurate control requirements for information acquisition, calculation and analysis, and water control. Intelligent control system for water cooling of mass concrete [3] can achieved precise temperature control of dam concrete. A typical intelligent control system structure and principles are shown in Fig.1 below. The system includes flow meters, thermometers and electric control valves installed in the cooling water pipeline, and thermometers installed in concrete, and it collects flow and temperature data through measurement and control equipment, and communicates with the server through wired communication or Wi-Fi, and then the master program installed on the server calculates

and analyzes the data and controls the electric control valve switches so as to realize the intelligent control of water cooling.

Different from the above cooling water control system, “an intermittent through-break mass concrete cooling water control system” [4,5] adopts the principle of “bang-bang Control”, establishes an adaptive equivalent flow control model, and controls the water cooling in accordance with the technical requirements of “crack-free concrete”. Adopting the principle of “bang-bang Control”, the system establishes an adaptive equivalent flow control model to control the water cooling according to the technical requirements of “crack-free concrete”, so that the concrete can be cooled down to achieve the efficacy of “eliminating harm”. Intelligent control system through the perception of the internal temperature of the concrete to control the water pipe valves, valves open water cooling, to be the center of the concrete temperature dropped to below the target temperature, close the valve to stop the water, the concrete temperature began to rise, when the center of the point temperature rises to above the target temperature, the valve reopened water. Due to the hysteresis effect of heat transfer and cooling water stored in the water pipe to continue heat exchange, open the valve again when the water, the surrounding concrete temperature is lower than the center part, the temperature gradient is much smaller than the initial water, the concrete “cold shock” is also much smaller, in addition, can be adjusted by the valve opening degree “duty cycle”, to realize the concrete temperature. In addition, by adjusting the valve opening “duty cycle”, to realize the small interval automatic on and off, further reducing the amplitude of the “cold shock”, so the control model of the water cooling will not bring additional damage to the concrete. Although the water passage is intermittent, but the cooling effect is the same, the total amount of cooling water is basically the same, can be said to be a new small temperature difference, adaptive equivalent flow cooling water passage method. Compared with other cooling water intelligent control system, this adaptive equivalent flow control model directly with the concrete temperature for decision-making control, completely free of the flow and inlet and outlet water temperature three parameters, its system compared to the system shown in Fig.1 eliminates the inlet and outlet water temperature and flow test mechanism, especially after the application of the wireless control valve of the whole system is more clean, significantly reduces the cost and failure rate, and the reliability has been greatly improved. Reliability has been greatly improved. In addition, this intermittent alternating water in the early concrete structure will produce a low-value, ultra-low-frequency dynamic stress, play the role of “vibration dissipation”, so that the internal unbalanced stress within the concrete structure tends to homogenize, to reduce the concentration of internal stress in the concrete, dissipate the harmful stress, improve the crack resistance of the concrete structure, thus effectively preventing and controlling the emergence of concrete cracks. Prevention and control of concrete cracks, undoubtedly this is a “strong body” type of “Xingli” measures [6]. It can be predicted that this kind of intelligent temperature control technology will bring new opportunities to the application of mass concrete.

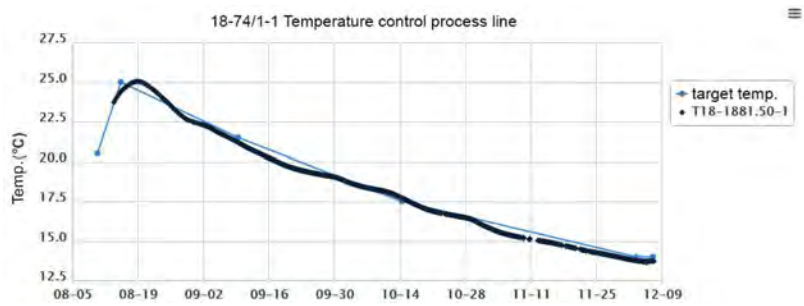


Fig. 2
Typical temperature control process line for adaptive equivalent flow (intermittent on-off method).

The dam of Jinping I Hydropower Station on the main stream of Yalong River in China is the world’s highest hyperbolic arch dam, with concrete volume of more than 5 million m³ and dam height of 305 m. Compared and tested several intelligent control systems for water cooling, the “Adaptive Equivalent flow Intelligent Control System” for the intelligent control of water cooling for the dam was finally adopted, which has been fully applied to the right bank dam of Jinping I dam project since April 2013, with a total of 280 sets of cooling water pipes installed in 104 blocks and the control effect is good. Its typical control line is shown in Fig. 2 below.

The thin solid line in Fig.2 is the pre-set target temperature process line, and the thick solid line is the measured temperature process line. It shows that the measured temperature process line is basically consistent with the preset target temperature process line. Adaptive equivalent flow (intermittent on-off method) control system can fully meet the design requirements to achieve the “early cooling, small temperature difference, slow cooling” temperature control goals.

2.2. DEVELOP ULTRA-LOW HEAT COMPOSITE CEMENTITIOUS MATERIALS TO REPLACE CEMENT, TO SOLVE THE PROBLEM OF THE ORIGIN OF THE CONCRETE TEMPERATURE CONTROL

In order to completely prevent and control the temperature cracks in concrete, after long term of research exploration and practice from ordinary construction concrete to hydraulic concrete, experts and scholars in the hydraulic industry found that taking the method of ultra-high dosage of composite cementitious materials in concrete will be an effective and reliable way [7–11]. It has been suggested that the physical role of fly ash in concrete, i.e., filling of pores, is more important than any

chemical reaction at an early stage [12]. The contribution of fly ash to strength is more sensitive to the water-cement ratio than to that of cement [13]. Therefore, concrete with fly ash should be formulated with the lowest possible W/C+F [13]. Any use of fly ash as a cement replacer to formulate fly ash concrete starting with pure cement concrete at a higher W/C (e.g., 0.55 or greater) is unlikely to work well, and the contribution of fly ash to strength is certainly not significant, even at 90d of age or a little longer [13]. The study also points out that using fly ash as a separate component, rather than as a replacement for cement, can break the current limitations on maximum fly ash mixes, so that the concrete on a wider scale can be designed to meet the specific requirements of hydraulic structures, so as to produce hydraulic ultra-high mix fly ash concrete [13].

In the design of ultra-high admixture of fly ash concrete, equal paste proportion design method [14] will be used, other than the traditional equal replacement method or super replacement method and other design methods. It is realized through the determination of the minimum paste volume of concrete V_p for the dense packing aggregates, and using the characteristics of fly ash that the density is only about 2/3 of cement, and when using equal mass of fly ash to replace the cement, the powder volume will increase. When keeping paste volume basically unchanged (taking into account the economy and durability). When keeping the paste volume basically unchanged (taking into account the economy and durability, take the minimum paste volume V_p), in the case of ultra-high dosage of fly ash water consumption can be significantly reduced, thereby reducing the water-cementitious ratio, so that strength and other properties of the concrete with ultra-high dosage of fly ash can be ensured while keeping the total amount of cementitious material not increase significantly. Quantitative relationship between fly ash dosage and water-cementitious ratio is shown in the following equation [1,2]. Because the paste volume is basically unchanged, the impact on properties of concrete from the change of paste volume is reduced, and the changes in the composition of the material changes can be actually reflected in the properties of concrete.

$$V_v(\text{paste}) = V_c(\text{cement}) + V_f(\text{flyash}) + V_w(\text{water}) \quad [1]$$

$$V_v = M[(1-a)/p_c + a/p_f + b/p_w] \quad [2]$$

where V_v is the volume of paste determined on the basis of the reference concrete, a is the fly ash admixture, b is the water-cementitious material ratio, and M is the total amount of cementitious material.

Ultra-high admixture fly ash concrete mixes have significant thixotropy, and the workability cannot be objectively reflected using the static slump method. To study the improved method of evaluating the workability of concrete, i.e., the Vibro consistency method was selected to determine the workability of freshly-mixed fly ash concrete mixes, starting from the acceptability and workability. Cubic specimens of 300 mm × 300 mm × 300 mm are used for direct vibration test of reference concrete and ultra-high-mixed fly ash concrete with vibrating rod, and the control

range of VB value of ultra-high-mixed fly ash concrete is determined by the time of flattening the concrete with vibrating rod as 16 s ~ 20 s.

C₁₈₀ 40 dam body concrete (medium heat 42.5 grade cement + 35% admixture of fly ash) in a hydropower project was used as the reference concrete, and the equal paste proportion design method as well as the improved concrete workability evaluation method were used. Class I, II, III ash fly were respectively used to design the hydraulic ultra-high fly ash concrete C₁₈₀ 40 with fly ash dosage as high as 80%, and all the properties meet the actual engineering design requirements. Compared with the reference concrete, the compressive strength of ultra-high-mixed fly ash concrete is lower than the reference concrete strength except for the early compressive strength of concrete with Class III fly ash, which is higher than the compressive strength of concrete with other grades of fly ash and other ages; the axial tensile strength and ultimate tensile value of concrete with ultra-high-mixed fly ash at 28d and 90d are relatively low, and are close to that at 180d, and the ultimate tensile value of concrete is around $1.2 \times 10^{-4} \sim 1.4 \times 10^{-4}$; the modulus of elasticity of ultra-high dosage fly ash concrete is lower than that of the reference concrete, in which the modulus of elasticity of Class I and Class II fly ash concrete at the age of 180d is about 25GPa, lower than that of Class III fly ash concrete by about 2.5 GPa, the freezing resistance of ultra-high dosage fly ash concrete is reduced compared with that of the reference concrete, and the 28d freezing resistance grades of the concrete using Class II and Class III fly ash are only F50 and F75, and the freezing resistance grade of late concrete only reaches F200. The freezing resistance of concrete with Class I fly ash is better than that of concrete with Class II and III fly ash, but it is still lower than that of the reference concrete, and the reason for the low freezing resistance of ultra-high dosage fly ash concrete should be related to the low air content of the concrete. Due to the high dosage of fly ash, fly ash particles in the less full combustion will absorb the particles in air-entraining agent to cause air-entraining agent poor dispersion effect in the concrete. In addition, water reducing agent dosage is high, the concrete water gel is relatively small, the concrete mix is more viscous, but also affects the effect of the air-entraining effect of the concrete, so despite the air-entraining agent dosage increased by 3 to 4 times, but concrete air content is still low, which leads to a reduction in the freezing resistance of concrete; ultra-high dosage fly ash concrete impermeability grade have reached W14, to meet the requirements of the project concrete; ultra-high dosage fly ash concrete dry shrinkage value are less than the dry shrinkage value of the reference concrete, and with the age growth, the gap between the dry shrinkage value is getting bigger and bigger, 180d age of the dry shrinkage of the ultra-high dosage fly ash concrete is smaller than the reference concrete by about 30%; ultra-high dosage fly ash concrete absolute shrinkage value is less than the reference concrete; ultra-high dosage fly ash concrete absolute shrinkage value is less than the reference concrete, the dry shrinkage value is less than the reference concrete. The adiabatic temperature rise of ultra-high fly ash concrete is much lower than that of the reference concrete, and its maximum temperature rise is 9.6°C lower than that. It shows that in the case of ultra-high admixture of fly ash, even if ordinary silicate cement is used, concrete with very low hydration temperature rise can be formulated, which

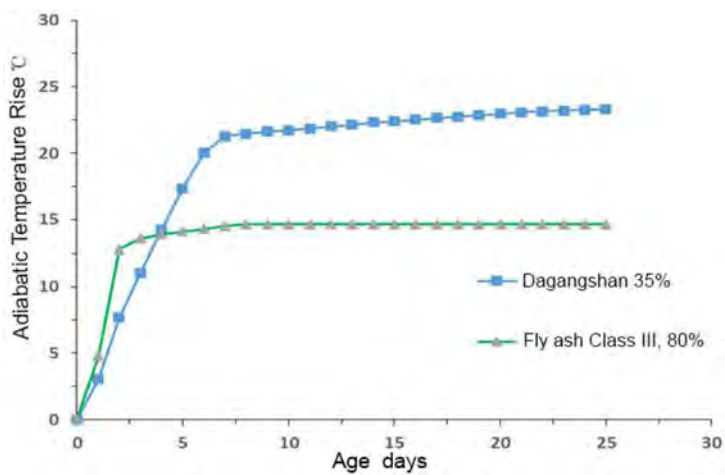


Fig. 3
Measured adiabatic temperature rise curve.

Table 1
Cracking temperature/°C for two types of concrete

NOS.	FLY ASH MIXING AMOUNT/%	TEMPERATURE MATCHING MODE	ADIABATIC MODE
GF-0	35	−0.42	−9.18
GF-1	80	−15.27	−11.78

can replace the existing conventional practice of formulating mass concrete with medium- and low-heat cements, and expand the space for the application of ordinary silicate cement in mass concrete. The test comparison diagram are shown in Fig. 3 below. The temperature stress test method [15–21] was used to conduct the concrete cracking resistance test and the test results are shown in Table 1 below.

The results from Table 1 show that, the cracking temperature of ultra-high fly ash-mixed concrete is lower than that of the reference concrete, both in the temperature matching mode and the adiabatic mode. The cracking temperature can be used as an index to comprehensively evaluate the cracking sensitivity of concrete and the overall cracking resistance of concrete, and the lower the cracking temperature, the better the cracking resistance. Therefore, according to the cracking temperature, which is the core evaluation index of concrete cracking susceptibility in the temperature-stress test, the cracking susceptibility of ultra-high fly ash concrete is better than that of the reference concrete, and the performance index of ultra-high fly ash concrete is better under the temperature matching mode.

The research results show that: only the material selection and proportioning design methods have substantial breakthroughs, does hydraulic concrete realize the deserved characteristics, so as to solve the problem of temperature control of the concrete from the source, and to change fundamentally the status quo of the “no dam, no crack”, and to improve significantly the essential quality of the dam concrete, and thus improving the durability and safety of dam operation.

3. DIMENSION 2: CONSTRUCTION HEIGHT

Table 2
List of super-high concrete dams built and under construction in China

NOS.	NAME	DAM HEIGHT (M)	RIVER	LOCATION	CONSTRUCTION STATUS	DAM TYPE
1	Jinping I	305	Yalongjiang	Sichuan	constructed	hyperbolic arch dam
2	Xiaowan	294.5	Lancangjiang	Yunnan	constructed	hyperbolic arch dam
3	Baihetan	289	Jinshajiang	Yunnan	under construction	hyperbolic arch dam
4	Xiluodu	285.5	Chang Jiang	Sichuan	constructed	hyperbolic arch dam
5	Udongde	265	Jinshajiang	Yunnan	under construction	hyperbolic arch dam
6	Laxiwa	250	Yellow River	Qinghai	constructed	hyperbolic arch dam
7	Ertan	240	Yalongjiang	Sichuan	constructed	hyperbolic arch dam
8	Goupitan	230.5	Wujiang	Guizhou	constructed	hyperbolic arch dam
9	Dagangshan	210	Daduhe	Sichuan	constructed	hyperbolic arch dam
10	Guangzhao	200.5	Beipanjiangr	Guizhou	constructed	crushed concrete gravity dam
11	Huangdeng	203	Lancangjiang	Yunnan	under construction	crushed concrete gravity dam

3.1. DAM HEIGHT

There are about 20 super-high dams over 200m in China, including about 11 concrete dams (Table 2). According to China’s water resources development plan, a number of high dams and reservoirs need to be constructed on the Jinsha, Lancang, Nu, Yalong, Dadu and upper reaches of the Yellow River in the western part of the country, with a planned dam height of up to 315 m. These dams are facing great challenges due to the high reliability requirements under complex conditions, limited

construction experience, lack of technical standards, etc., and the key technological issues that need to be researched and tackled include the following: stability of dam foundation and shoulder, seismic protection in strong seismic zones, mass concrete dams, and the construction of concrete dams. The key technical issues to be studied and overcome include: dam foundation and shoulder stabilization, seismic protection in strong earthquake zones, temperature control and crack prevention of mass concrete, flood dissipation and anti-abrasion, stability of high and steep slopes, and high quality and efficient construction technology.

In the construction of hydraulic concrete dams under the terrain conditions of high mountain valleys, a highly efficient, fast, process-oriented and remote-controlled operation mode with cable cranes as the main means of pouring is adopted; while the concrete pouring by tower belt machine under the slightly open terrain conditions combines the functions of horizontal concrete transportation, vertical transportation and silo fabrication into a single one, which has the significant advantages of continuity, high efficiency and multi-purpose use of a single machine. On the basis of the above two modes of operation, supporting the development of the arm belt machine, pouring multifunctional machine, negative pressure chute, high-pressure water hosing machine, the overall flip formwork and other pouring equipment, to improve the installation efficiency by more than 10 times, and successfully solved the problem of combination of quality and efficiency for the high concrete dam construction. High-quality, safe and rapid construction technology in combination with the new concept of high efficiency, energy saving and the whole process without blind spot for a high-concrete dam has been finalized, which has been applied to projects such as Three Gorges of Changjiang river and Xiangjiaba Dam of Jinshajiang river, and have created the excellent achievement of "crack-free dam" in terms of quality, and a series of new world records in terms of efficiency, such as 5,480,000 m³/year, 553,500 m³/month, 22,000 m³/day, and 1,278 m³/shift, etc., and fully realize safe, high-quality and high-efficiency construction of high concrete dam.

3.2. HEIGHT OF DAM RISE

Due to the structural design needs and construction capacity constraints, as well as temperature control and other reasons, the dam bulk concrete is generally divided into blocks of layered pouring construction, layered pouring layer height is generally 1.5 m ~ 2.0 m, the Three Gorges project breakthroughs 3.0 m. layer height is too large for the template, as well as the temperature control is challenging, and the actual project for the safety of floods and to speed up the progress of the need for a greater pouring layer height, this This requires innovative breakthroughs. Jinping Class I through the test demonstration and the whole dam to promote the 4.5 m layer pouring, topped the new height of the dam body layer.

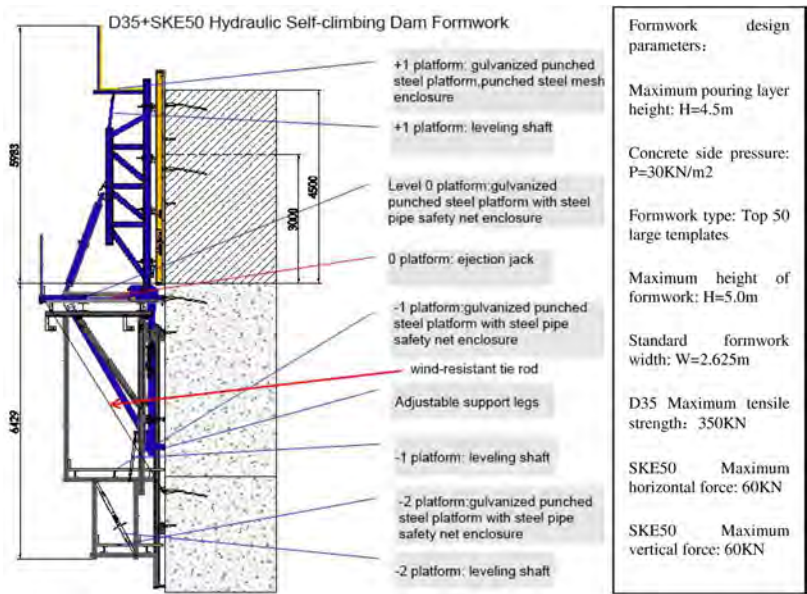


Fig. 4
Schematic structure of hydraulic self-climbing formwork type D35+SKE50.

4.5 m rising layer pouring concrete will produce more lateral pressure on the formwork, resulting in a great increase in the difficulty of formwork deformation control; at the same time, the maximum temperature and maximum stress of the dam body have increased, and the temperature control pressure has increased. In order to solve the template deformation problem and ensure that the dam body shape meets the design requirements, double brace cantilever large template and 4.5 m straight shaped hydraulic self-climbing template (Fig.4) were developed.

In order to solve the temperature control problem, first of all, through the simulation calculation to analyze the temperature field of 3 m layer pouring and 4.5 m layer pouring under the same conditions, and came to the following conclusions: 4.5 m layer pouring concrete temperature change rule is similar to 3 m layer pouring; 4.5 m layer pouring maximum temperature to meet the design standard requirements, than 3 m layer pouring maximum temperature is about 0.3 °C higher. In order to ensure that the dam concrete temperature control requirements can be met, according to the results of calculations, take a series of targeted measures:

1. Conduct concrete pouring and resource allocation planning; 4.5 m layer pouring using the paving method of pouring to improve the intensity of the

warehouse to 180 m³/h or more, in the warehouse configuration, “four flat, four vibration” warehouse vibration equipment, and outside the warehouse The “four flat, four vibration” vibrating equipment was installed in the silo, and 10 sprayers were set up around the silo to cool down the silo;

2. Accelerate concrete conveying and pouring;
3. Shorten laying time of cooling water pipes;
4. Strengthen deformation control of the formwork;
5. Strengthen temperature control of the concrete, including:
 - pre-cooling of concrete aggregates using primary and secondary air-cooling measures;
 - Using cold water and ice to reduce the temperature of the concrete at a batching plant;
 - Accelerating vibration compaction and coverage of the concrete layer during pouring process (covering time within 4 h);
 - Conduct site spraying during high-temperature seasons (period) , so as to reduce the ambient temperature;
 - Lay three layers of HDPE pipes in each 4.5 m layer lift according to the 1.5m × 1.5m for water cooling.

It shows that, after taking the above innovative measures, the concrete form deviation of 4.5 m layer pouring is realized in accordance with the design requirements, but it is slightly larger than that of 1.5 m and 3 m layer thickness; the temperature change process of 4.5 m layer thickness concrete is similar to that of 3 m layer thickness, and the maximum temperature is slightly higher than that of 3 m layer thickness pouring silo, with an average of about 0.05 °C higher.

4.5 m layer lift thickness pouring key technology breaks through the limitations of the normal concrete arch dam layer thickness, provides an effective technical means for flexible organization of construction and accelerate the construction progress, and has a wide range of application prospects and promotion value [22,23].

4. DIMENSION 3: PROCESS ACCURACY

All along, hydraulic concrete construction has been regarded as a “clumsy” process in people’s mind, and the quality of construction depends on the individual level of the operator, and the error is measured in centimeters, etc. Starting from the 1960s, fair-faced concrete has been increasingly used in various fields of construction engineering, and after entering the 21st century, fair-faced concrete began to be applied to hydraulic buildings. Concrete began to be applied to hydraulic buildings, and DL/T 5306 was compiled and released in 2013 on the basis of summarizing the experience of the projects of Three Gorges Power Station, Sichuan Qingju, Luding, Tongzitou, Tingzikou, and Guangzhao Power Station Plant, etc.

Though the quality defects of fair-faced concrete are still prevalent at present, with the wide application of mirror fair-faced concrete, the Concrete this “clumsy” building materials will be more “fine” image rewrite people’s ideas for the “high-precision concrete” development has laid the ideological foundation. Certain concrete structure and metal structure joint work, such as the Three Gorges Ship Lifter Project, the concrete construction precision requirements are very high, up to the mm level, and reinforcing steel, gold knot, electromechanical embedded parts construction interference, gold knot embedded parts, equipment between the gap grouting difficulty, narrow space, complex environment, the difficulty of measuring the precision of the towering buildings, towering compartments of the tower room structural deformation of the columns of the complexity of the factors affecting the deformation of the construction control difficulty, which requires the concrete construction and the installation of the gold knot every This requires strict control of every aspect of concrete construction and installation of gold knots, and technological innovation of key control points (such as templates, installation of embedded parts, equipment installation, etc.).

For hydraulic concrete, “high-precision concrete” is a brand-new concept and standard. It refers to the implementation of hydraulic concrete construction as a carrier, in each step of concrete production, transportation, pouring, care, etc., in order to meet the requirements of high precision, the application of highly sophisticated technology and highly refined technology, to produce high-grade and exquisite finished concrete products. Since the most crucial element for realizing the above requirements and goals is human beings, the major premise for implementation is that high-precision concrete must be sublimated into a concept. The essence of high-precision concrete is far from being as simple as pouring concrete carefully, it is the synergistic integration and overall enhancement of the whole concrete construction “one-stop” system, and the high-precision needs and requirements for all the results generated by all the links and processes constitute the code of conduct, forming the concept of high-precision concrete of the Water Works [24].

Hydraulic high-precision concrete is, first of all, highly precise. It is a significant increase in the requirements for the level of precision, at least one order of magnitude higher, which forms a strict control from the surface or external structure. This precision requirement has reached the precision level of ordinary metal structural parts machining in hydraulic structure. Secondly, it is highly fine (exquisite). As a result of the substantial increase in precision requirements, inevitably triggered by the construction method and process of transformative improvement, which is formed from the process of the whole process control of the high degree of refinement. It is, on the one hand, in the process of process nodes, in order to improve the degree of refinement and add the necessary operating procedures, such as work-piece or part of the handover after the implementation of appropriate reprocessing, concrete leveling and vibration process strictly separate operations; on the other hand, in the course of a single process operation, in strict accordance with the process operating procedures, to fully ensure that the duration of the operation of

the “degree of saturation”. On the other hand, in the process of single process operation, strictly follow the process operation procedure, fully guarantee the operation duration “saturation degree”, so that the process to achieve the degree of “full maturity”. The third is high-grade and exquisite. High-precision concrete for waterworks from the external appearance, high-precision concrete spreading, smooth, accurate contour size, color and luster uniformity, no surface imperfections, giving people a delicate appearance. From the inner characteristics, high precision concrete physical and mechanical indicators to meet the design requirements, solidity, permeability, durability and other good performance, structural function to play excellent.

Taking the high-precision concrete construction of the tower of the Three Gorges Project as an example, in the process of construction, guided by the concept of “high-precision concrete”, we have carried out technological innovations in various aspects, including structural design, formwork technology, reinforcement bar production and installation, construction measurement technology, construction deformation monitoring, concrete pouring, second-phase concrete construction, gap grouting, and metal structure installation and matching construction. Process innovations are carried out in various aspects, including:

1. Applying high-precision rebar installation technology and high-precision measurement and control technology, and installing full-height accurate positioning for each rebar in the dense parts of embedded parts. Innovative measures include: configuration of advanced CNC bending machine, cutting machine, straightening machine and other processing equipment to improve the processing accuracy of steel bars; arrangement of testing steel platform, the platform set up a variety of angles of the standard piles and standard ruler, inspection of steel bars and the shape of the accuracy of the angle of steel bars, control the processing accuracy of the steel bars from the factory; vertical reinforcement bars to straight threaded socket connection is the main horizontal bars to lap welding is the main, when the vertical reinforcement bars lap welding, the offset head welding, to ensure that the affected steel bars will be welded. The vertical reinforcement is mainly connected by straight-threaded socket, and the horizontal reinforcement is mainly connected by lap welding, and when the vertical reinforcement is welded by lap welding, the off-set welding is used to ensure that the main reinforcement is connected in the same axis; the main reinforcement is located by the reinforcement locating frame, and the protective layer of the vertical reinforcement is controlled according to the positive deviation; the head of the tie wire is bent to the inner side of the wall to avoid the formation of rust stains due to the exposure of the exposed, which affects the quality of the fair-faced concrete.
2. Construction technology of the hydraulic self-elevating formwork and the construction technology of the formwork continuous rise are adopted, and the bidirectional limitation of the overhanging formwork is designed and manufactured. The upper opening is adjustable and has a two-way limit function,

Table 3
Statistics of tower concrete shape test results

ITEM	AXIS	VERTICALITY	CROSS-SECTION	FLATNESS
Points measured	2255	2680	2798	2683
Points of pass	2255	2672	2785	2682
Maximum deviation	5mm	12mm	-10m~+15mm	6mm
Percentage of pass	100%	99.7%	99.5%	99.9%

which can prevent both outward mold running and inward shrinkage, thus ensuring the precision requirements of pouring concrete.

3. Applying various advanced measuring equipment such as laser tracking instrument, measuring robot, etc., designing and making various kinds of precise tooling, carrying out deformation monitoring and implementing deformation compensation measures.
4. Simulate the precise installation of metal structure under operating conditions to overcome the influence of deformation of tower columns on the installation accuracy of equipment under working conditions. Through the implementation of a full set of hydraulic high-precision concrete construction technology, it has realized that the deviation of the concrete structure of the 146 m-high tower column of the Three Gorges shiplifter, and the verticality and parallelism of the rack and nut columns installed at a height of more than 120 m meet the pre-determined requirements and reach the precision of millimeter level. The statistics of the results of high-precision concrete shape tracking inspection of the tower column of the Three Gorges Project shiplifter are shown in Table 3.

The results from Table 3 shows that the average percentage of pass of tower concrete shape deviation is above 99.5%, indicating that the structure precision control is excellent, and all deformations of the tower are in a highly controlled state.

In order to judge the quality of concrete pouring for the tower column structure of the shiplifter, ultrasonic testing was carried out on the concrete pouring quality of the key parts of the shiplifter structure subject to force, including the rack, nut column, longitudinal guiding guide rail, balancing weight rail and longitudinal contact beams, etc. The testing method is ultrasonic diagonal penetration CT. A total of 307 parts of the ultrasonic testing was carried out, and the results show that the concrete compactness pass rate was 100%, and the good rate reached 95.3%.

It can be foreseen that through the application of "high-precision" concrete construction technology, and "high toughness fiber concrete (UHTCC)" [25], a high degree of precision, high-grade detailed, high-strength and high toughness of concrete structures can be constructed, which provides new options for the designer of hydraulic structures, and even partially replace metal structures.

5. CONCLUSIONS

China's hydraulic concrete construction technology has been continuously innovated along with the development of China's hydropower and has made breakthrough technological progress in many dimensions, which is of great and far-reaching significance.

Adopting the design method of equal paste proportion and the improved concrete workability evaluation method, developing 80% ultra-high-mixed fly ash hydraulic concrete, solving the problem of the origin of concrete temperature control, and implementing the intelligent temperature control system to realize the new breakthroughs in the technology of dam body temperature and crack control.

Developed large-scale high-strength hydraulic self-climbing formwork, optimized the pouring process, strengthened temperature control and other measures, creating a new height of 4.5 m for a single-layer pouring of hydraulic concrete, and laying a foundation for the fast, high-quality and safe construction of 300m-class extra-high concrete dams.

Based on the concept of "high-precision concrete", we have established the concept of "high-precision concrete" on the basis of hydraulic clear-water and mirror concrete, and have achieved a new record of mm-level deviation for 150m-level concrete structures. It is expected that the use of hydraulic high-precision concrete construction technology, together with high-performance concrete materials, such as UHTCC, will completely refresh the application field and application prospects of hydraulic concrete.

REFERENCES

- [1] ZHOU HOUGUI. Progress and problems of hydraulic concrete construction technology. *China Three Gorges Construction*, 2003(3), 11–13
- [2] ZHOU HOUGUI. Construction technology and practice of crack-free concrete dam. *Hydropower Generation*, 2010, 36(2): 1–4+16.
- [3] ZHOU HOUGUI, TAN KAIYAN, etc. Intelligent cooling ventilation system for concrete [P]. China Patent, 201010228838.8, 2010-07-16.
- [4] CHEN C.Y., ZHOU H.G., etc. An intermittent pass-through mass concrete cooling ventilation control system [P]. China Patent, 201210333844.9, 2015-2-18.

- [5] JIANG XIAOBING, YU YING. Research and application of crack control technology for mass concrete. *China Energy Construction*.
- [6] TAN KAIYAN, ZHOU HOUGUI, etc. *A method of mass concrete abatement to control cracks [P]*. China Patent, 201410365667.1, 2016-04-06.
- [7] AMERICAN CONCRETE INSTITUTE. *Report on high-volume fly ash concrete for structural applications*. aci 232.3r-14, 2014.
- [8] DAVIS R E, CALSON R, KELLY J W, etc. Properties of cements and concretes containing fly ash. *ACI Journal Proceedings*, 1937, 33(5): 577-612.
- [9] DUNSTAN M R H. Development of high fly ash content concrete. *Proceedings-Institution of Civil Engineers*, 1983, 74(3): 495-513.
- [10] DUNSTAN M R H, THOMAS M D A, CRIPWELL J B, etc. Investigation into the long-term in-situ performance of high fly ash content concrete used for structural applications. *Proceedings of the Fourth CANMET/ACI International Conference on Fly Ash, Silica Fume, Slag and Natural Pozzolans in Concrete*, SP-132, V. M. Malhotra, ed. American Concrete Institute, Farmington Hills, MI, 1992: 1-20.
- [11] MALHOTRA V M, MEHTA P K. *High-performance high-fly ash concrete for building sustainable and durable structures*. Fourth edition. Supplementary Cementing Materials for Sustainable Development Inc., Ottawa, ON, Canada, 2012.
- [12] QIN WEI-ZU. Integral theory of durability of concrete structures. *Construction Technology*, 2003, 34(1): 19-22.
- [13] ZHOU HOUGUI, ZHANG ZHENYU. Design and experimental research on hydraulic ultra-high dosage fly ash concrete. *Journal of Hydropower Generation*, 2017, 36(5): 1-9.
- [14] CHENG WEIJIA. *Research on durability evaluation based on modern concrete design concept*. Beijing: Tsinghua University Master Thesis, 2005.
- [15] ZHANG GUOZHI, TU LIUQING, XIA WEIHUA, etc. Research on evaluation index of early cracking of concrete. *Concrete*, 2005(5): 13-17.
- [16] CAI YUEBO, DING JIANTONG, CHEN BO, etc. Comprehensive evaluation of crack resistance of dam concrete based on temperature-stress testing machine. *Journal of Southeast University (Natural Science Edition)*, 2010, 40(1): 171-175.
- [17] CHEN BO, SUN WEI, DING JIANTONG. Progress of research on crack resistance of concrete based on temperature-stress test. *Journal of Silicate*, 2013, 41(8): 1124-1133.

- [18] LIN ZHI-HAI, Qin Wei-Zu, Zhang Shi-Hai, etc. Evaluation of early temperature stress development and crack resistance of concrete. *Construction Technology*, 2003, 34(1): 34–35.
- [19] ZHANG T. *Research on the influencing factors of early cracking susceptibility of concrete*. Beijing: Tsinghua University, 2006.
- [20] LI FEI. *Research on the development and relaxation process of early confining stress in concrete*. Beijing: Tsinghua University, 2009.
- [21] SHEN D, JIANG J, SHEN J, etc. *Influence of curing temperature on autogenous shrinkage and cracking resistance of high-performance concrete at an early age*. *Construction and Building Materials*, 2016, 103: 67–76.
- [22] HUANG DANYONG, YANG WEISEN. Promotion and application of concrete construction technology for 4.5m ascending layer. *Sichuan hydropower generation*, 2016, 35(4):71–73(93)
- [23] MA JINGANG, WEI NING, YANG YOUSHAN, JIANG Rong. Construction technology of 4.5 m ascending concrete for high arch dam of Jinping hydropower station. *Hydropower and New Energy*, 2011, 96(4):4–6
- [24] ZHOU HOUGUI. Technological innovation and practice of hydraulic high-precision concrete construction. *China Engineering Science*, 2013, 15(9):4–8
- [25] LIU J.T. RESEARCH on active powder concrete based on nanomaterials and its basic mechanical properties. *Zhejiang University*, 2016

COMMISSION INTERNATIONALE DES
GRANDS BARRAGES

VINGT-HUITIEME CONGRES DES
GRANDS BARRAGES
CHENGDU, MAI 2025

ANALYSIS AND EVALUATION OF 3K SAFETY FACTORS OF EXTRA HIGH ARCH DAMS UNDER VALLEY DEFORMATION EFFECTS (*)

Chenfang JIANG, Heng CHENG & Qiuqing ZHOU
China Institute of Water Resources and Hydropower Research, Beijing

Guoxin ZHANG
China Institute of Water Resources and Hydropower Research, Beijing
State Key Laboratory of Simulation and Regulation of Water Cycle in River Basin,
Beijing

Bo YANG
China Institute of Water Resources and Hydropower Research, Beijing

CHINA

SUMMARY

Valley deformation exerts compression on arch dams, leading to irreversible deformation and affecting the working condition and long-term safety of the dam. In order to ensure the long-term safe operation of arch dams under valley deformation effects, taking a certain arch dam in Southwest China as an example, a finite element mesh model of the arch dam-foundation system is constructed. The current valley deformation load is inverted, and the actual pouring processes of the dam body are simulated. The water pressure overload method is adopted to calculate and analyze the ultimate bearing capacity of the arch dam under the current valley deformation effects, and evaluate its 3K safety factors. The results show that through the engineering analogy of 3K safety factors, it can be seen that under the

**Analyse et évaluation de la sûreté de très grands barrages-voûtes sous l'effet de la déformation des appuis*

current valley deformation effects, the safety level of this arch dam meets the regulatory requirements. This can provide reference for the subsequent evaluation of the overall safety degree of extra high arch dams under valley deformation effects.

RÉSUMÉ

La déformation de la vallée peut comprimer un barrage-voûte, entraînant une déformation irréversible qui affecte le fonctionnement et la sûreté à long terme du barrage. Afin de garantir le fonctionnement à long terme des barrages-voûtes sous l'effet de la déformation de la vallée, un modèle aux éléments finis a été établi en prenant l'exemple d'un barrage-voûte du sud-ouest de la Chine. L'inversion de la charge de déformation actuelle de la vallée simule le processus de déformation réelle du corps du barrage. La capacité portante limite du barrage sous l'effet de la déformation réelle de la vallée a été analysée à l'aide de calculs de surcharge hydrostatique et son coefficient de sécurité a été évalué. Les résultats montrent que le niveau de sûreté de ce barrage-voûte est conforme aux exigences du Code sous l'effet de la déformation de la vallée. Cela peut servir de référence pour une évaluation ultérieure de la sécurité globale des grands barrages-voûtes sous l'influence de la déformation des appuis.

1. INTRODUCTION

Some typical 300m-level extra high arch dams, such as Jinping I, Xiaowan, and Xi Luodu, have been in operation for many years in China. During their operation, significant valley contraction deformations have been observed in Jinping I and Xi Luodu arch dams. Among them, Xi Luodu has experienced a larger magnitude of valley contraction deformation that has not yet converged, surpassing general engineering experience and understanding. Arch dams are statically indeterminate structures and are highly sensitive to foundation deformations. Valley contraction exerts compression on arch dams, which can potentially have a significant adverse impact on the working condition and long-term safety of the dam [1,2]. Therefore, valley deformation has become a focal point and challenge for both the dam engineering community and academia. Few serious dam accidents in history have been primarily caused by valley deformation, such as the Beauregard arch dam in Italy [3] and the Zeuzier arch dam in Switzerland [4]. Existing engineering cases have demonstrated the irreversibility of valley contraction deformations. Arch dams will operate for a long time under the compression of the surrounding mountains. Analyzing and evaluating the safety margin of arch dams under valley deformation effects during long-term operation is crucial to ensure their long-term safe operation.

The overall safety assessment of arch dams has been studied by domestic and foreign scholars. Zhou Weiyuan et al. [5,6], Qiang Tianchi et al. [7], Huang Yansong et al. [8], Ning Yu et al. [9] and Dong Jianhua et al. [10] have all used nonlinear finite element overload methods to analyze the failure processes, overall stability, and ultimate bearing capacity of Jinping I arch dam, Xiaowan arch dam, Laxiwa arch dam, and Baihetan arch dam, Yebatan arch dam respectively. Wang Renkun et al. [11] conducted an analysis of the cracking and failure process and overall safety degree of Xi Luodu arch dam without considering the effects of valley contraction. Yang Xuechao [12] conducted a safety evaluation of the Xiluodu arch dam under the limit state of valley contraction by progressively overloading the deformation of valley contraction. Zhou Weiyuan [13] proposed a 3K safety factor evaluation method for break-away overload safety factor K1, nonlinear deformation overload safety factor K2, and the ultimate overload safety factor K3. Cheng Li [14] explained the significance and control of the 3K safety factors based on the overload failure process of ultra-high arch dams. Currently, in arch dam design and numerical analysis, considerations mainly include water pressure, temperature, self-weight, uplift pressure, sediment pressure, wave pressure, ice pressure, and seismic loads, while the effects of valley contraction are not taken into account, resulting in a lack of safety evaluation criteria for arch dams under valley contraction deformations.

Based on the latest geological data and structural design achievements of an arch dam in Southwest China, this paper establishes a three-dimensional numerical model of the entire arch dam. The self-developed SAPTIS finite element simulation analysis software [15–17] is used to comprehensively simulate the geological boundary conditions and the effects of valley deformation loads in the dam body and foundation. The water pressure overload method is employed to analyse the deformation of the arch dam body and foundation rock mass, as well as the development process of yielding state. The 3K safety factors of the arch dam-foundation system under valley deformation effects is determined, and the overall safety of the arch dam is evaluated through engineering analogy. This study provides a basis for the safe operation of arch dams.

2. ENGINEERING GEOLOGICAL OVERVIEW

The dam of this hydropower station adopts a concrete double-curvature arch dam, making it an extra high arch dam. The dam site is located in a section of the river with a straight channel and steep valley slopes. The cross-section of the river valley exhibits a relatively symmetrical “U” shape, with a wide and gentle valley floor. The mountains on both sides of the valley are steep and robust, with the terrain

converging towards the riverbed below the I-line. Above the I-line and below the III-line, the slope terrain gradually opens up.

The riverbed bedrock and the slopes on both sides of the valley are mainly composed of basalt ($P_2\beta$), with limestone (P_1m) only exposed at the bottom of the riverbed in the entrance section of the gorge, dipping below the basalt downstream. There is a residual layer of sand shale (P_2x) with a thickness of about 2~15m on the valley shoulders of both sides. At the bottom of the basalt, there is a layer of lacustrine mud shale ($P_2\beta_n$), which is pseudo-conformable to the limestone. The Quaternary loose deposits of different origins are unconformable to the aforementioned bedrock. Limestone (P_1m) is exposed at the bottom of the bedrock valley near the mouth of the Dousha Creek in the dam area, dipping below the basalt downstream. Drilling reveals a thickness of 260-280m. Between the limestone and basalt, there is a layer of lacustrine mud shale ($P_2\beta_n$), which is pseudo-conformable to the limestone. The thickness of this layer varies greatly, generally ranging from 2~3m, with a maximum thickness of 5.1m revealed by drilling. The basalt is a continental basaltic volcanic rock that erupted intermittently in multiple stages. The total thickness in the dam area is 490~520m, which can be divided into 14 lava flow layers, with each lava flow layer generally being 25~40m thick.

In the vicinity of the dam, no major faults or fractures are observed. The interlayer displacement zones in the basalt layers are mainly developed along the primary bedding planes, with two main forms: planar and fractured. The planar type is characterized by straight segments along the bedding planes, or the development of layer joints at 1-2m above the bedding plane when there is significant undulation along the plane. Overall, the planar type is relatively straight, stable, and has a small variation in the thickness of the fractured zone. The internal displacement zones are mainly developed in the lower part of the basaltic lava in the lava flow layers, while the upper conglomerate lava does not show significant development.

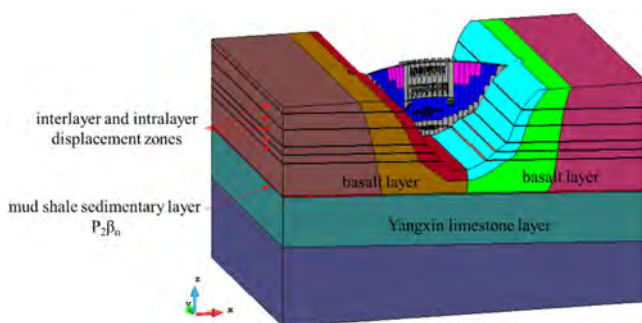


Fig. 1
Engineering geological numerical model diagram

3. CALCULATION MODEL AND CALCULATION METHODS

3.1. ESTABLISHMENT OF THE CALCULATION MODEL

The dam of the hydropower station is a hyperbolic arch dam. In the 12# to 19# dam sections, 7 surface holes, 8 deep holes, and 10 diversion bottom holes are arranged (6 low-level bottom holes at an elevation of 410m, and 4 high-level bottom holes at an elevation of 450m). Considering the real geological structure of the dam site and the real structural materials of the dam, a finite element grid model of the arch dam foundation during the reservoir operation period is constructed. The model consists of a total of 292,790 elements and 338,841 nodes, including the foundation (including interlayer and intralayer displacement zones, basalt layer, Yangxin limestone layer, mud shale sedimentary layer $P2\beta n$, etc.), the dam body (including orifice, gate pier, supporting hinged beam, buttress, fillet, etc.), transverse joints, and construction joints (construction joints for surface hole beams are set in the middle of the surface hole gate pier, and construction joints are also set when the upstream gate pier is detached from the surface hole beam during pouring, and they have been backfilled during the reservoir operation period). The coordinate system of the model is as follows: x direction points to the left bank of the arch dam, y direction points to the upstream side of the arch dam, and z direction points vertically upward.

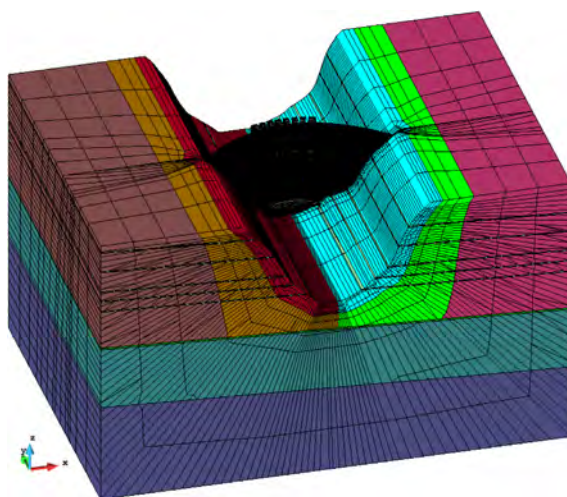


Fig. 2

Integrated finite element model of the arch dam-foundation system

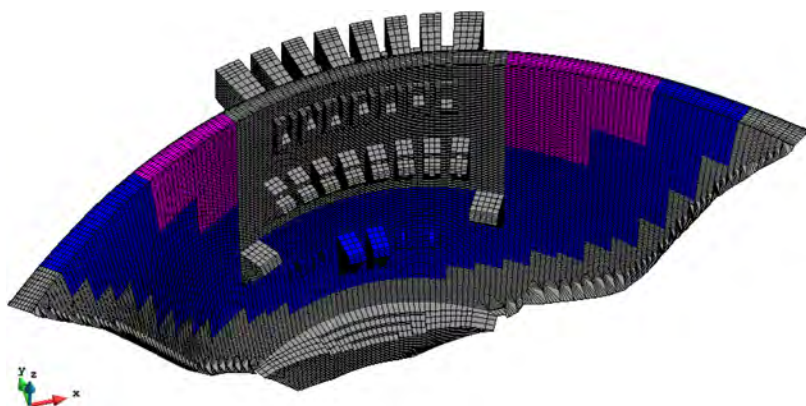


Fig. 3
Finite element model of the arch dam

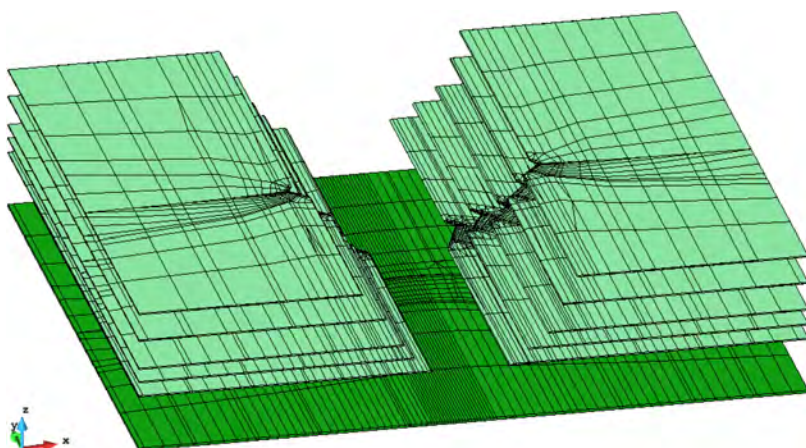


Fig. 4
The typical interlayer and intralayer shear zones on the left and right banks & the finite element mesh model of $P_2\beta_n$ in the foundation

3.2. CALCULATION LOAD AND CALCULATION METHODS

The calculation load includes self-weight, static water pressure from upstream and downstream, and deformation load caused by valley amplitude. By referring to

the deformation evolution process and yield failure of the dam-foundation system, the hydraulic overload method is used to analyze the overall safety of the dam-foundation system under the effect of valley amplitude deformation.

In the nonlinear calculation, the open-closed iteration method from the DDA method [18–20] is introduced, and the DP yield criterion is used for materials. The interlayer and interlayer shear zones and the $P_2\beta_n$ in the foundation are simulated using joint elements that satisfy the Mohr-Coulomb yield criterion, effectively reflecting the tensile and compressive failure and shear failure of weak structural surfaces.

In the local coordinate system, the stress-displacement relationship of the joint element is given by:

$$\{\sigma\} = \begin{Bmatrix} \tau_s \\ \sigma_n \end{Bmatrix} = \frac{1}{h} [\mathbf{K}] \begin{Bmatrix} \Delta u \\ \Delta v \end{Bmatrix} = \frac{1}{h} [\mathbf{K}] [\mathbf{N}] \{\delta\}^e \quad (1)$$

where τ_s is the shear stress, σ_n is the normal stress, h is the thickness of the joint element, Δu is the shear relative displacement of the joint element, Δv is the normal relative displacement of the joint element, $\{\delta\}^e$ is the nodal displacement of the element, $[\mathbf{N}]$ is the shape function matrix, $[\mathbf{K}]$ is the stiffness matrix of the element, determined by:

$$[\mathbf{K}] = \begin{bmatrix} k_{ss} & k_{sn} \\ k_{ns} & k_{nn} \end{bmatrix} \quad (2)$$

where k_{ss} is the shear stiffness, k_{nn} is the normal stiffness, k_{sn} is the stiffness considering shear coupling effect, k_{ns} is the stiffness considering normal coupling effect.

Due to the difficulty in determining the numerical values of the coupling stiffness terms, it is generally assumed that k_{sn} and k_{ns} are both equal to 0.

Based on the principle of virtual work, the above equation is transformed into the finite element equation:

$$[\mathbf{F}]^e = \frac{t}{h} \int_{-l/2}^{l/2} [\mathbf{N}]^T [\mathbf{K}] [\mathbf{N}] dx' \{\delta\}^e = [\mathbf{K}]^e \{\delta\}^e \quad (3)$$

where $[\mathbf{K}]^e$ is the stiffness matrix of the joint element in the local coordinate system, and the stiffness matrix in the global coordinate system is given by:

$$[\mathbf{K}]^G = [\mathbf{T}]^{-1} [\mathbf{K}]^e [\mathbf{T}] \quad (4)$$

where $[K]^G$ is the stiffness matrix in the global coordinate system, and is the coordinate transformation matrix related to the inclination angle θ of the structural surface.

When the normal stress on the joint element reaches its tensile stress threshold, denoted as $\sigma_n \geq f_{t0}$, the element undergoes tensile opening. When the shear stress on the joint element reaches the Mohr-Coulomb strength failure criterion, denoted as $F = |\tau_s| - (C_0 + f_0 \sigma_n) \geq 0$, the element undergoes shear sliding.

In numerical analysis, the overall safety of the dam-foundation system is typically evaluated using the strength reduction method or the hydraulic overload method [5–11,21]. When using the hydraulic overload method, only the upstream water pressure load is increased by a certain factor during the calculation, while other loads remain unchanged. The safety is evaluated based on the overload factor, denoted as K , which is the ratio of the calculated weight of water to the actual weight of water, i.e., $K = \gamma/\gamma_w$. The overload factor under characteristic conditions is used as a safety factor to measure the ultimate bearing capacity of the dam. The main calculation process is as follows:

1. Improve the method of applying the deformation load caused by valley amplitude, and provide the calculation basis for special loads.
2. The dam body is constructed in layers according to the actual pouring progress (27 layers), and the stress distribution of the dam body matches the actual stress state of the dam body during the construction period.
3. Apply upstream water level (based on normal storage level), downstream water level, deformation caused by valley amplitude, and other loads to evaluate the overall safety of the dam-foundation system through hydraulic overload analysis.

4. INVERSE ANALYSIS OF MATERIAL PARAMETERS AND MODEL BOUNDARY DEFORMATION DISTRIBUTION FOR THE DAM-FOUNDATION SYSTEM

Based on the research by Chai Dong et al. [22] on the influence of valley deformation, considering the lithological changes near $P_2\beta_n$, the displacement load is applied at the truncated boundary of the model to simulate the contraction deformation of the valley, as shown in Fig. 5. Based on the monitoring data of valley deformation, dam deformation, and material parameters, displacement is applied at the model boundary, considering self-weight load, water load, and temperature load. The entire process of arch dam construction, impoundment, and operation is simulated. By performing forward analysis, the relationship between dam deformation and load variation is obtained. The objective function is set to minimize the differences between the calculated values and the monitoring values of

temperature, valley deformation, and dam deformation. The optimal displacement at the truncated boundary of the model and the thermodynamic parameters of the dam body and foundation rock mass are inversely obtained. The inverted elastic modulus of the dam body is $E = 47.8 \text{ GPa}$, Poisson's ratio $\nu = 0.167$, linear expansion coefficient $= 7.01 \times 10^{-6}/^{\circ}\text{C}$, unit weight $= 24 \text{ kN/m}^3$, cohesion $c = 3.0 \text{ MPa}$, and friction angle $f = 58.3^{\circ}$. The physical and mechanical parameters of the rock mass at the dam site and the main structural surfaces are listed in Table 1.

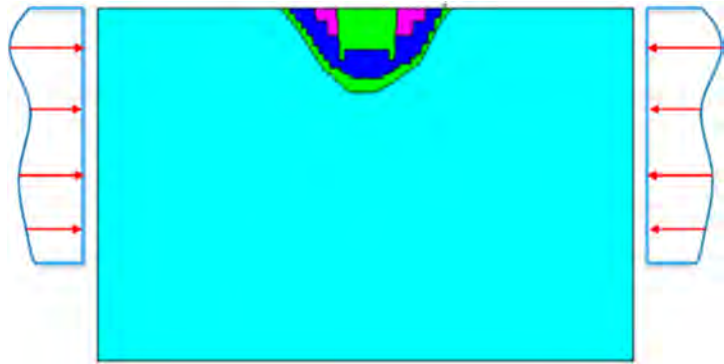


Fig. 5
Schematic diagram of the loading method for valley deformation

Table 1
Physical and mechanical parameters of the rock mass at the dam site and major structural surfaces

MATERIALS	ELASTIC MODULUS /GPA		POISSON'S RATIO	COHESION/ MPA	FRICTION ANGLE/°
	HORIZONTAL	VERTICAL			
Class II rock mass	22~30	16~22	0.20	2.5	53.47
Class III1 bedrock	14~20	13~16	0.20	2.2	50.66
Class III2 bedrock	7~9	5~8	0.20	1.4	50.19
Class IV 1 bedrock	4~5	3.5~4.5	0.20	1.0	45.57
Class V 2 bedrock	1.0~2.6	0.7~1.2	0.20	0.5	35.00
Fault zone (P ₂ β _n)	0.7~1.1	0.4~0.5	0.32	0.155	17.50

The comparison between the calculated and measured values of valley deformation for the survey lines and the comparison between the calculated and measured values of radial deformation for the vertical measurement points of the

dam show that the calculated evolution of valley deformation and radial deformation of the dam body closely matches the measured values. This indicates that the obtained displacement magnitude and distribution at the boundaries are reasonable, further confirming the rationality of the inverted parameters for the dam body and foundation materials.

5. OVERALL SAFETY ASSESSMENT OF DAM FOUNDATION

The ultimate bearing capacity of the dam-foundation system under the influence of valley deformation was calculated using the hydraulic overload method. The calculation was performed with a step size of $0.1\gamma_w$ times for overload, and the results were extracted every $0.5\gamma_w$ times until convergence was not achieved. Fig. 6 to 8 show the relationship curves between deformation and overload multiplier at different parts of the arch dam along the river axis. It can be observed that the deformation in the river direction at different parts of the dam gradually increases with the increase in the overload multiplier. The development process of deformation on the left and right abutments of the dam is generally symmetrical, with slightly larger deformation on the right abutment than on the left abutment. During the overload process, before 4.0 times the load, the deformation in the river direction of the dam develops almost linearly. Afterwards, the rate of increase in deformation gradually accelerates. Starting from 6.0 times, the calculated deformation of the dam continues to increase, and the rate of deformation significantly accelerates, and the calculation does not converge, reaching the ultimate bearing capacity.

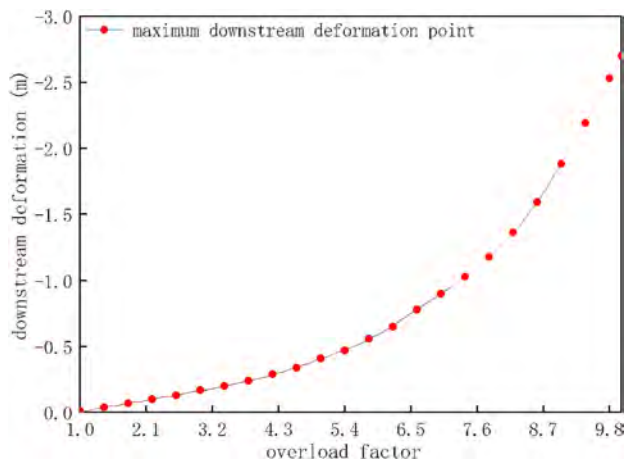


Fig. 6
Relationship between maximum downstream deformation point and overload factor in the downstream direction

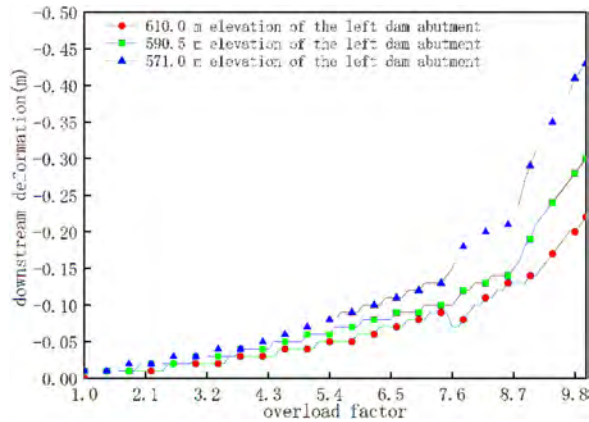


Fig. 7
Relationship between left bank abutment deformation in the downstream direction and overload factor

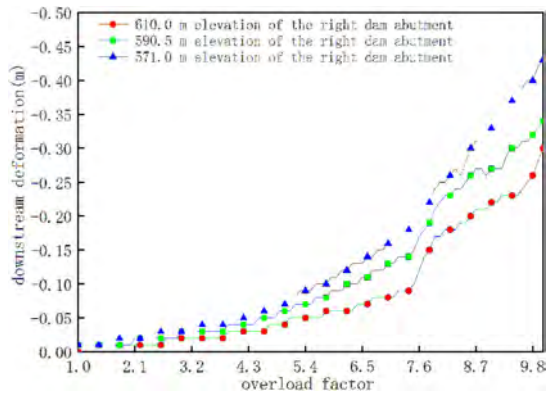


Fig. 8
Relationship between right bank abutment deformation in the downstream direction and overload factor

Meanwhile, in Fig. 9, the yield behavior of the dam-foundation system is presented for overload factors of 1.0, 1.5 and 6.0. Specifically, when $X\text{-kindfail}=1$, it represents tensile yielding, while $X\text{-kindfail}=2$ represents shear yielding. The results indicate that during the overload process, when the overload factor is less than 1.0,

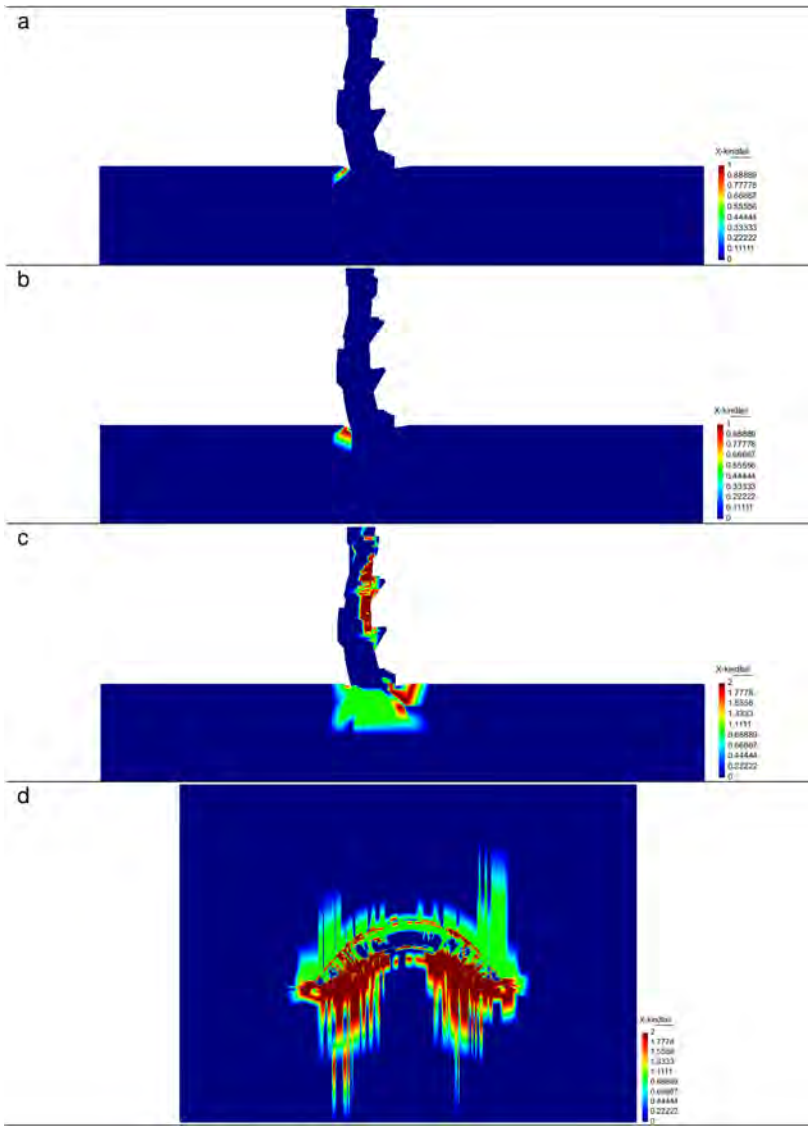


Fig. 9

Distribution of yielding zones of the dam-foundation system under typical overload factors. (a) Arch crown beam profile, 1.0 time. (b) Arch crown beam profile, 1.5 times. (c) Arch crown beam profile, 6.0 times. (d) Dam foundation (plan view), 6.0 times

only the upstream foundation experiences tensile yielding. At an overload factor of 1.5, significant yielding occurs at the dam heel, gradually extending to the seepage curtain. At around 6.0 times the overload factor, a continuous yielding zone forms between the dam body and the bedrock, indicating the possibility of instability and failure of the arch dam. Additionally, based on the cross-section at an elevation of 610m, it is evident that the extent and rate of yielding in the right bank abutment are significantly greater than those in the left bank abutment.

In summary, it can be observed that using the nonlinear finite element method, the breakaway overload safety factor K_1 is 1.0~1.5, which means that before the overload reaches 1.5 times, the arch dam is basically in an elastic working state. The nonlinear deformation overload safety factor K_2 is 4.0, which means that as the load factor increases, local yielding and failure continue to accumulate, and displacement non-linearity gradually becomes prominent. When the load further increases, the arch dam is in a nonlinear failure process, and when the ultimate overload safety factor K_3 reached 6.0, the overall calculation becomes unstable. Compared with other engineering projects, it can be seen that under the influence of current valley deformation, the safety levels of the dam of this hydropower station meet the regulatory requirements.

6. CONCLUSIONS

This paper adopts the nonlinear finite element analysis method to comprehensively simulate the controlling geological boundary conditions of dam and foundation and the evolution of valley deformation loads. By comparing and analyzing the deformation and yielding zones of the dam foundation rock mass and structural surfaces under valley width effects, the safety of a specific high arch dam under valley width effects is evaluated. The deformation and yielding process of the dam body and foundation rock mass are analysed using the water pressure overload method, and the overall safety of the dam-foundation system under valley width deformation is assessed. The following conclusions are drawn:

1. By analysing the evolution pattern of valley width deformation load and inverting the boundary conditions, it is verified that the simulated radial deformation results of the dam in the finite element analysis are in good agreement with the measured results, improving the application of valley width deformation load in finite element simulations of high arch dams.
2. Under the feedback of the current valley width deformation load, the breakaway overload safety factor K_1 is 1.0~1.5, the nonlinear deformation overload safety factor K_2 is 4.0, and the ultimate overload safety factor K_3 is 6.0.
3. Considering 3K safety factors, each safety factor meets the regulatory requirements under the current valley deformation. It is recommended to continuously monitor and analyse the overall safety of the arch dam based on the latest feedback of valley width deformation load in the future.

ACKNOWLEDGMENTS

The authors are grateful for the financial support from the National Key R&D Program of China (No. 2021YFC3090102); State Key Laboratory of Watershed Water Cycle Simulation and Regulation funded project (No. SKL2022ZDO5).

REFERENCES

- [1] LONDE P. The Malpasset dam failure. *Engineering Geology*, vol. 24(1/2/3/4), pp. 295–329, 1987.
- [2] LOMBARDI G. Kolnbrein dam: an unusual solution for an unusual problem. *International Water Power & Dam Construction*, vol. 43(6), pp. 31–34, 1991.
- [3] FRIGERIO A., MAZZA .The rehabilitation of Beauregard dam: the contribution of the numerical modeling. *12th International Benchmark Workshop on Numerical Analysis of Dams*. Vienna, pp. 343–352, 2013.
- [4] ZANGERL C., EVANS K F., EBERHARDT E., ET AL.Consolidation settlements above deep tunnels in fractured crystalline rock: Part 1—Investigations above the Gotthard highway tunnel. *International Journal of Rock Mechanics and Mining Sciences*, vol. 45(8), pp. 1195–1210, 2008.
- [5] ZHOU W., CHEN X. Overall stability analysis of Jinping double-curved arch dam. *Journal of North China Institute of Water Conservancy and Hydroelectric Power*, vol. 2001(03), pp. 31–34, 2001.
- [6] YU T., REN Q. Overall safety assessment of Jinping high arch dam. *Chinese Journal of Rock Mechanics and Engineering*, vol. 2007(04), 787–794, 2007.
- [7] QIANG T., YANG R., SHEN D., ET AL. Three-dimensional nonlinear finite element analysis of stability of Xiaowan double-curved arch dam. *Yunnan Hydropower*, vol. 2000(01), pp. 68–70+76, 2000.
- [8] HUANG Y., ZHOU W., CHEN X., ET AL. Overall stability analysis of Laxiwa double-curved arch dam. *Rock and Soil Mechanics*, vol. 2003(S2), pp. 235–238, 2003.
- [9] NING Y., XU W., ZHENG W., ET AL. Analysis of reinforcement effect and overall safety evaluation of Baihetan arch dam and dam shoulder. *Chinese Journal of Rock Mechanics and Engineering*, vol. 2008(09), pp. 1890–1898, 2008.
- [10] DONG J., LIU C., CHEN J., ET AL. Deformation characteristics and stability analysis of arch dam abutment with deep unloading rock mass. *Engineering Science and Technology*, vol. 51 (03), pp. 43–51, 2019.

- [11] WANG R., LIN P., ZHOU W. Study on cracking and stability of high arch dam on complex foundation. *Chinese Journal of Rock Mechanics and Engineering*, vol. 2007(10), pp. 1951–1958, 2007.
- [12] YANG X., GAO K., ZHAO W., ET AL. (2018). Analysis of the Safety Impact of Valley Shrinkage Deformation on Xiluodu Arch Dam. *Journal of Water Resources and Architectural Engineering*, vol. 16 (01), pp. 72–78, 2018.
- [13] ZHOU W. Structure stability of rock mass engineering. *Chinese Journal of Rock Mechanics and Engineering*, vol. 29(9), pp. 1729–1753, 2010.
- [14] CHENG L. Study on the mechanism and control of the deformation and failure of super high arch dams. *Tsinghua University*, 2017.
- [15] ZHANG G. SPTIS: Development and application of software for structural multi-field simulation and nonlinear analysis (Part 1). *Water Resources and Hydropower Engineering*, vol. 44(1), pp. 31–44, 2013.
- [16] ZHOU Q., & ZHANG G. SPTIS: Development and application of software for structural multi-field simulation and nonlinear analysis (Part 2). *Water Resources and Hydropower Engineering*, vol. 44(9), pp. 39–43, 2013.
- [17] ZHANG L., & ZHANG G. SPTIS: Development and application of software for structural multi-field simulation and nonlinear analysis (Part 3). *Water Resources and Hydropower Engineering*, vol. 45(1), pp. 52–55, 2014.
- [18] SHI G. H. *Block System Modeling by Discontinuous Deformation Analysis* Southampton, UK and Boston, USA: Computational Mechanics Publications, 1993.
- [19] ZHANG G., LI H., & HUANG T. Three-dimensional discontinuous deformation analysis theory and its application in rock slope engineering. *Chinese Journal of Rock Mechanics and Engineering*, vol. 29(10), pp. 2116–2125, 2010.
- [20] ZHOU S., & YANG J. Research on DDA numerical method and its engineering application. *Rock and Soil Mechanics*, vol. 21(2), pp. 123–125, 2000.
- [21] LI T., WANG R., YOU Q., ET AL. Research on safety evaluation methods for high arch dams. *Journal of Hydraulic Engineering*, vol. 38(Supplement), pp. 78–83 (105), 2007.
- [22] CHAI D., CHENG H., MAO Y., ET AL. Analysis of real deformation characteristics and influencing factors of ultra-high arch dams under valley width contraction effects. *Water Resources and Hydropower Science*, vol. 40(11), pp. 107–110, 2022.

COMMISSION INTERNATIONALE DES
GRANDS BARRAGES

VINGT-HUITIEME CONGRES DES
GRANDS BARRAGES
CHENGDU, MAI 2025

**EXPERIENCES IN DETERMINING THE PHYSICAL AND MECHANICAL
PARAMETERS OF SOFT SOIL DAM FOUNDATION (*)**

Xingxing ZHANG

*Professor, Geotechnical Engineering Department,
China Institute of Water Resources and Hydropower Research, Beijing*

Jianzheng SONG

*Senior Engineer, Geotechnical Engineering Department,
China Institute of Water Resources and Hydropower Research, Beijing*

Xuedong ZHANG

*Professor, Geotechnical Engineering Department,
China Institute of Water Resources and Hydropower Research, Beijing*

Rui WANG

*Ph.D Candidate, Geotechnical Engineering Department,
China Institute of Water Resources and Hydropower Research, Beijing*

CHINA

SUMMARY

This paper delves into the experiences gained in determining the physical and mechanical parameters of soft soil foundations for dam construction. When constructing dams on soft soil bases, meticulous calculations and analyses are imperative to evaluate dam stability and predict deformations, which heavily rely on parameters such as shear strength, compression coefficient, and permeability

**Expériences de détermination des paramètres physiques et mécaniques des sols meubles de fondation de barrages*

coefficient of soft soil. The primary methods to obtain these parameters encompass laboratory tests and field tests. However, test data are often scattered and indirect, necessitating expertise for proper evaluation. Drawing from the author's experience, despite the varying sedimentary environments in China, soft soils exhibit certain common patterns in their physical and mechanical properties. Notably, a strong correlation exists between the shear strength, compression coefficient, and permeability coefficient of soft soil and its cohesive particle content and void ratio. These parameters can be roughly estimated based on the cohesive particle content and void ratio, further refined through specific laboratory or field tests. Among the field tests, the Cone Penetration Test (CPT) and the Vane Shear Test (VST) are effective methods for obtaining the in-situ shear strength of soft soil foundations. The cone tip resistance (q_c) of the CPT test demonstrates a close relationship with the in-situ undrained shear strength of soft soil. Regarding the permeability coefficient of soft soil, significant variations are observed depending on the measurement method employed. Consequently, it is recommended to adopt the upper limit of the permeability coefficient obtained from laboratory tests or pumping tests when assessing dam foundation leakage. Conversely, for slope stability analyses and calculations of excess pore water pressure, it is advisable to utilize the lower limit of the permeability coefficient from laboratory tests or results from lateral pressure tests, CPTU (CPT with Piezocone) tests, and consolidation tests.

RÉSUMÉ

Ce rapport examine en profondeur l'expérience de la détermination des paramètres physico-mécaniques des fondations sur sol meuble pour la construction de barrages. Lors de la construction d'un barrage sur une fondation en sol, des calculs et des analyses méticuleux doivent être effectués pour évaluer la stabilité du barrage et prédire la déformation. Celle-ci repose en grande partie sur des paramètres tels que la résistance au cisaillement, le coefficient de compression et le coefficient de pénétration du sol meuble. Les principales méthodes d'obtention de ces paramètres comprennent des tests en laboratoire et des tests in situ. Cependant, les données de test sont souvent décentralisées et indirectes et nécessitent une expertise pour effectuer une évaluation appropriée. Selon l'expérience des auteurs, bien que les environnements sédimentaires varient en Chine, les sols présentent certains modèles communs dans leurs propriétés physiques et mécaniques. Il est à noter qu'il existe une forte corrélation entre la résistance au cisaillement, le coefficient de compression, le coefficient de pénétration de ces matériaux et leur teneur en particules visqueuses et leur rapport poreux. Ces paramètres peuvent être estimés grossièrement en fonction de la teneur en particules visqueuses et du rapport poreux et affinés par des essais spécifiques en laboratoire ou sur le terrain. Dans les essais in situ, le test de pénétration statique (CPT) et le test de cisaillement (VST) sont des méthodes efficaces pour obtenir la résistance au cisaillement in situ des sols. La résistance à la

pointe du cône (QC) du test CPT est étroitement liée à la résistance au cisaillement non drainé in situ. En ce qui concerne le coefficient de perméabilité, des variations significatives sont observées selon la méthode de mesure utilisée. Par conséquent, il est recommandé d'appliquer la limite supérieure du coefficient de perméabilité obtenue par des essais en laboratoire ou des essais de pompage lors de l'évaluation de l'infiltration de la base du barrage. En revanche, pour l'analyse de la stabilité de la pente et le calcul de la pression interstitielle, il est recommandé d'utiliser la limite inférieure du coefficient de perméabilité dérivée des résultats d'essais en laboratoire ou d'essais de pression latérale, d'essais CPTU (CPT avec cône piézoélectrique) et d'essais de consolidation.

1. INTRODUCTION

Soft soil typically encompasses saturated clays characterized by a porosity ratio exceeding unity and a natural moisture content surpassing the liquid limit. This type of soil exhibits distinct properties including low permeability, high compressibility, diminished shear strength, and heightened sensitivity. When constructing embankment dams atop soft foundations, pronounced challenges related to stability and deformation inevitably arise.

During embankment construction on soft soil, the low permeability hinders the effective drainage of pore water, leading to the accumulation of excessive pore water pressure. This excessive pressure can precipitate landslides, posing significant hazards[1]. Furthermore, the inherent low deformation modulus of soft soil contributes to substantial deformation of the dam foundation post-construction, jeopardizing the integrity and safety of structures like impermeable walls. The challenges are comparable when attempting to raise higher embankments on deep clay or silt deposits, where similar issues of stability, deformation, and the management of pore water pressures must be meticulously addressed to ensure the long-term stability and safety of the structures.

As such, when embarking on the design of embankment dams grounded on soft soil, meticulous and comprehensive calculations and analyses becomes imperative, aimed at rigorously assessing the dam's stability and projecting its deformation behavior. The precision of these calculations is intimately linked to the intricate physical and mechanical parameters inherent in the soft soil.

Currently, the acquisition of these parameters primarily involves laboratory and field tests, albeit with test data often scattered and indirect. Accurate evaluation of soft soil's physical and mechanical properties based on these results necessitates substantial experience and expertise. Chinese soft soils, though formed in diverse sedimentary environments, share common patterns in their properties, allowing for rough estimates of mechanical properties based on particle composition

and porosity. This paper provides a comprehensive overview of these experiences and insights.

2. TYPICAL EMBANKMENT DAMS ON SOFT FOUNDATIONS IN CHINA

China boasts a considerable number of embankment dams constructed on soft soil foundations, several exceeding 50 meters in height. While most of these dams' foundations have undergone successful treatment, a few have relied on slower construction rates or the use of loading berms for stabilization. Table 1 showcases some representative cases, highlighting foundation descriptions, treatment methods, and performance outcomes.

Table 1
Typical embankment dams on soft foundations in China

Name/ Description	Year of completion	Province	Dam height (m)	Description of foundation	Foundation treatment	Performance
Siming lake	1963	Zhejiang	16.82	Muddy clay, 7m thick	No treatment	Three slides during construction. After completion, operate normally
Yingxiong	1972	Zhejiang	12	Muddy clay, about 10m thick, locally mixed with peat, thickest 1.5m	No treatment	Sliding occur when filling to a height of 8m. After completion, operate normally.
Du lake	1972	Zhejiang	17.5	Layer 1: Silty clay, 16m thick; Layer 2: gravel, 2-5m thick; Layer 3: clay and heavy silty clay, 10m thick	Sand well, depth of 12-14m, diameter of 0.42m, spacing of 3m.	Cracks appeared at the left dam during construction. After completion, operate normally.
Wuping[2]	2001	Yunnan	52	Soft clay,	Vibrating stone piles, replacement rate is 32%~40%	Normally during construction and operation
Chushandian	2020	Henan	27.4	Silty clay, locally extremely soft soil , 9~11m thick	Replace some extremely soft soil. 72% of the foundation treated by compacted sand piles, diameter of 0.5m, spacing of 1.5m~2.5m.	Normally during construction and operation
A plain reservoir	2021	Xinjiang	23	silty clay, over 80m thick	No treatment, slowing construction to 3 years.	Normally during construction and operation
Lawa upstream cofferdam	2021	Sichuan	59	Silt and silty clay, about 50m thick.	Vibrating stone piles, with a pile diameter of 1.2m, spacing of 2.5m~3.0m.	Normally during construction and operation

3. CORRELATION BETWEEN PARTICLE COMPOSITION, POROSITY, AND OTHER PARAMETERS

The shear strength, compression coefficient, and permeability coefficient of soft soil are intricately linked to its particle composition and porosity. An increase in cohesive particle content (particles smaller than 0.005mm) tends to lower shear strength, compression coefficient, and permeability coefficient, when porosity or dry density remains constant. Conversely, a similar particle composition with increased porosity results in lower shear strength and compression coefficient but higher permeability coefficient. These correlations are supported by extensive research and illustrated in Table 2, which summarizes typical physical and mechanical parameters of Chinese soft soils.

Table 2
Parameters of some typical soft soils in China

Name of project	Soil name	Dry density (g/cm ³)	Void ratio	Content of cohesive particles
Wuping	Silty clay, silty sand	0.9~1.1	1.5~2.1	20%
Chushandian	Low liquid limit clay	1.55	0.7	27.4%
lawa	Silty sand	1.45	0.86	7%
lawa	Sandy silt	1.39	0.94	10%
lawa	Silt	1.38	0.96	18.9%
lawa	Sandy clay	1.35	1.0	34.9%
Siming lake	Gravel silty clay	1.31~1.65	—	11.6%~38.1%
Siming lake	Muddy silty clay	1.19~1.28	—	—
Zhuyin	Muddy clay	1.18	—	—
Zhuyin	Silt	0.98	—	—
Huao lake	Muddy clay	1.19	1.27	43.2%

Name of project	Soim name	av_{1-2} (MPa-1)	φ_u (°)	c_u (kPa)	Permeability coefficient (cm/s)
Wuping	Silty clay, silty sand	1.5~2.5	15.3	15.5	$6.9 \times 10^{-8} \sim 2.2 \times 10^{-3}$
Chushandian	Low liquid limit clay	0.195~0.370	3.9~11.5	3.2~69	$1.1 \times 10^{-8} \sim 1.6 \times 10^{-4}$
lawa	Silty sand	0.20	14.2	128	5.0×10^{-4}
lawa	Sandy silt	0.26	7.9	38	$6.2 \times 10^{-5} \sim 3.9 \times 10^{-4}$
lawa	Silt	0.36	19.1	57	$1.8 \times 10^{-6} \sim 5.4 \times 10^{-5}$
lawa	Sandy clay	0.44	15.4	58	$1.5 \times 10^{-6} \sim 7.1 \times 10^{-6}$
Siming lake	Gravel silty clay	$E_s=2.5-7$	7.6~25.4	8.3~52.6	$6.7 \times 10^{-7} \sim 6.9 \times 10^{-5}$
Siming lake	Muddy silty clay	$E_s=2.32-4.38$	5.4~10.6	8.1~14.1	—
Zhuyin	Muddy clay	1.10	7.1	4.7	2.57×10^{-6}
Zhuyin	Silt	1.94	4.7	2.7	3.92×10^{-7}
Huao lake	Muddy clay	1.806	5	15	5.4×10^{-8}

4. IN-SITU UNDRAINED SHEAR STRENGTH

The in-situ undrained shear strength of soft soil foundation is crucial for assessing dam stability during construction. Traditional laboratory tests, such as triaxial and direct shear tests, may yield unreliable results due to sample disturbance. In-situ testing methods, notably vane shear test (VST) and static cone penetration test (CPT), effectively overcome this limitation. The VST directly measures in-situ undrained shear strength but offers fewer and more scattered data points. In contrast, CPT provides continuous, accurate, and reproducible results, albeit requiring conversion from cone tip resistance (q_c) and lateral resistance (f_s) to shear strength using region-specific methods or empirical formulas.

Fig. 1 shows VST results and CPT results of clay in the plain reservoir in Xinjiang province listed in Table 2. Its cone q_c is about 2~10MPa, and the peak shear stress tested by VST varies from 59kPa~274kPa. Fig. 2 shows VST results and CPT results of clay in the Huao Lake. Its q_c is about 0.3~0.5MPa, and the peak shear stress tested by VST varies from 14.5kPa~18kPa. It can be seen that the q_c of CPT test is roughly proportional to the in-situ undrained shear strength measured by VST test.

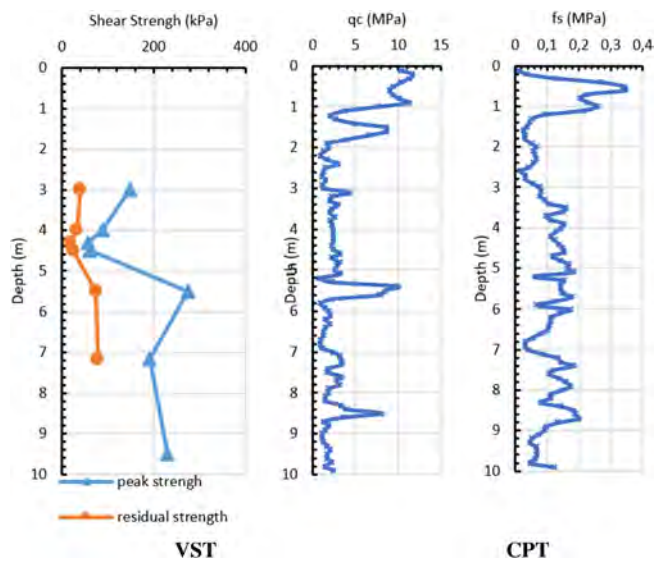


Fig. 1
Results of VST and CPT of a plain reservoir in Xinjiang.(Left:CPTS, Right: CPT)

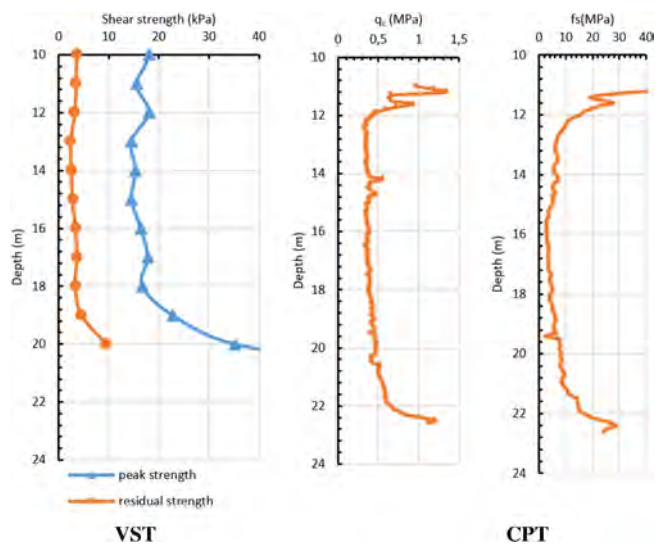


Fig. 2
Results of VST and CPT of Muddy clay in Huao Lake.

5. PERMEABILITY AND CONSOLIDATION COEFFICIENTS

When undisturbed soil samples are procured from a foundation for laboratory seepage tests, a notable range of variation in the permeability coefficient frequently emerges. This coefficient, measured within the confines of the laboratory, displays a sensitivity to the dimensions of the sampled specimen, thereby posing a dilemma in selecting an appropriate permeability coefficient for numerical analysis of the foundation [3–5]. Various methods for assessing the in-situ permeability coefficient include borehole pumping tests, lateral pressure tests, pore pressure static cone penetration tests (CPTU), among others. Notably, permeability coefficients obtained through borehole pumping tend to align with the upper bounds of laboratory measurements, whereas those derived from lateral pressure tests or CPTU tests often converge towards the lower limits observed in laboratory settings. Fig. 3 illustrates this variation in permeability coefficients, as measured by various laboratory and field methods, for a foundation beneath a plain reservoir in Xinjiang. Notably, land subsidence was observed during the pumping test, and the permeability coefficient estimated through back-analysis of this subsidence is also depicted in Fig 3. Given the potential for orders of magnitude variation in soil permeability, consolidation analysis necessitates the adoption of a geometric mean, as indicated by the thick solid line in Fig. 3.

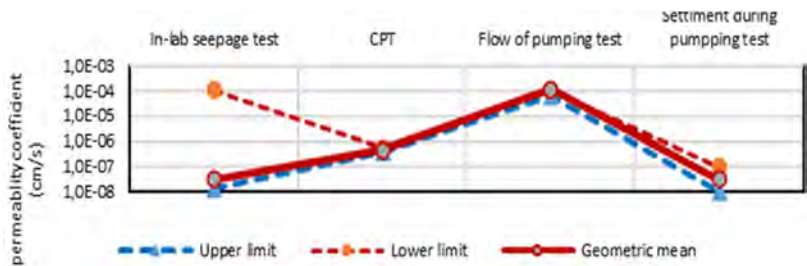


Fig. 3
Permeability coefficient obtained by different tests of a foundation beneath a plain reservoir in Xinjiang.

The choice of permeability coefficient testing method is crucial, as it is tailored to specific seepage problems. For assessing dam foundation leakage, it is advisable to adopt the upper limit of laboratory-measured permeability coefficients or the results from borehole pumping tests. Conversely, for slope stability analysis and evaluating the potential generation of excess pore water pressure during construction, the lower limit of laboratory-measured permeability coefficients, or results from

lateral pressure tests, CPTU tests, and consolidation tests, is recommended. Furthermore, in the analysis of excess pore water pressure, the utilization of consolidation coefficients offers a more convenient alternative to permeability coefficients, as it is less influenced by fluctuations in soil density.

6. CONCLUSIONS

From a comprehensive review of dam construction experiences on soft soil foundations in China, it becomes evident that the shear strength, compression coefficient, and permeability coefficient of soft soils exhibit a robust correlation with the content of cohesive particles and void ratio. This correlation underscores the fundamental significance of utilizing these two properties as a basis for approximating the mechanical characteristics of soft soils. Furthermore, the application of field tests, particularly the Cone Penetration Test (CPT) and the Vane Shear Test (VST), emerges as a highly effective approach to accurately obtain the in-situ undrained shear strength of soft soil foundations. Notably, the cone tip resistance (q_c) recorded during CPT tests displays a strong correlation with the in-situ undrained shear strength, thereby enhancing the reliability of the obtained data.

In addressing the issue of variability in permeability coefficients, it is crucial to acknowledge that different methods yield diverse results. When assessing the potential for dam foundation leakage, it is prudent to adopt the upper limit of permeability coefficients derived from laboratory tests or borehole pumping tests. Conversely, for slope stability analyses and evaluations of excess pore water pressure during construction, employing the lower limit of permeability coefficients obtained through laboratory tests or results from lateral pressure tests, CPTU tests, and consolidation tests is advisable. Moreover, in scenarios involving the analysis of excess pore water pressure, the utilization of consolidation coefficients offers a more convenient and less density-dependent alternative to permeability coefficients.

Overall, the integration of comprehensive laboratory and field test data, along with an in-depth understanding of the fundamental properties and correlations within soft soils, provides a solid foundation for ensuring the stability and longevity of dam structures constructed on these challenging foundations.

ACKNOWLEDGMENTS

The authors are grateful for the National Natural Science Foundation of China (No.52078212).

REFERENCES

- [1] CHEN Z.Y., SUN P., ZHANG X.X. Discussion on total stress method for stability analysis on slope of embankment and dam on saturated soft soil foundation. *Water Resources and Hydropower Engineering*, 2020, 51(12): 1–8.
- [2] CHEN Z.Y., ZHANG T.M. *Dam construction technology on soft foundation of Wuping Reservoir in Yunnan*. Beijing: China WaterPower Press, 2004.
- [3] TAYLOR D.W. *Fundamentals of soil mechanics*. John Wiley and Sons Inc, New York, 1984.
- [4] HUANG D., ZENG B., WANG Q.L. *Correlation study on the probability of void ratio, grading parameters, and permeability coefficient of coarse-grained soil*. *Journal of Hydraulic Engineering*, 2015, 46(08): 900–907.
- [5] LIU Y.F., ZHENG D.S., YANG B. Microscopic simulation of influence of particle size and gradation on permeability coefficient of soil. *Rock and Soil Mechanics*, 2019, 40(01): 403–412.

COMMISSION INTERNATIONALE DES
GRANDS BARRAGES

VINGT-HUITIEME CONGRES DES
GRANDS BARRAGES
CHENGDU, MAI 2025

**EFFECT RESEARCH OF ANTI-STRIPPING ADDITIVES TO WATER
SUSCEPTIBILITY OF HYDRAULIC ASPHALT CONCRETE (*)**

Zhengxing WANG

*State Key Laboratory of Simulation and Regulation of Water Cycle in River Basin,
Beijing*

China Institute of Water Resources and Hydropower Research (IWHR), Beijing

Lintao MA

*State Key Laboratory of Simulation and Regulation of Water Cycle in River Basin,
Beijing*

China Institute of Water Resources and Hydropower Research (IWHR), Beijing

Ziqiang YANG

POWERCHINA BEIJING ENGINEERING CORPORATION LIMITED, Beijing

Jutao HAO, Shifa XIA & Xiaogang WANG

*State Key Laboratory of Simulation and Regulation of Water Cycle in River Basin,
Beijing*

China Institute of Water Resources and Hydropower Research (IWHR), Beijing

CHINA

SUMMARY

In order to apply the acid aggregate to the merely 10cm thick impervious facing of asphalt concrete in the hydraulic engineering, the inadequacies of the

**Recherche sur l'effet des additifs améliorant l'adhésivité sur la susceptibilité de l'eau dans le béton bitumineux*

present standard must be studied and revised, such as the adhesion of coarse aggregate to bitumen be no less than grade 4, which is evaluated through the boiling water test, and discrete and inaccurate in practice. In this paper, tests to the surface free energy and the adhesion grade were conducted and compared. The test of sessile drop (SD) device was used to measure the contact angles of the bitumen and aggregate, and a reasonable or good contact angle value can be obtained by the low-rate dynamic measuring of the XG-CAMB1 standard goniometer. It is found out through test that the ambient temperature will affect the contact angle measuring of bitumen, and the impact can be eliminated by lowering the temperature to 2°C; The debonding work W_{BWA} of aggregate and bitumen in the presence of water is a good parameter to distinguish the acidic aggregate and the basic aggregate. From the debonding work W_{BWA} results, the most effective amounts of SK are predicted around 0.8 percent of bitumen to impede the water damage of asphalt concrete. Meanwhile, the prolonged boiling water test is also verified to appraise the adhesion properties of aggregate and bitumen, and the similar queues from acidic aggregate to basic aggregate can be established by the stripping-start time (SST) of the prolonged boiling

RÉSUMÉ

Afin d'utiliser des granulats acides pour un revêtement imperméable de 10 cm d'épaisseur de béton bitumineux, les insuffisances de la norme actuelle doivent être étudiées et révisées. L'adhérence du granulat au bitume est évaluée par l'essai à l'eau bouillante, essai qui se révèle discret et imprécis dans la pratique. Dans cet article, des tests sur l'énergie libre de surface et le degré d'adhérence ont été menés et comparés. Le test de la goutte libre (SD) a été utilisé pour mesurer les angles de contact du bitume et du granulat, et une valeur raisonnable de l'angle de contact peut être obtenue par la mesure dynamique à faible vitesse du goniomètre standard XG-CAMB1. Les tests ont montré que la température ambiante affecte la mesure de l'angle de contact du bitume et que l'impact peut être éliminé en abaissant la température à 2°C. Le travail de décollement du granulat et du bitume en présence d'eau est un bon paramètre pour distinguer le granulat acide du granulat basique. D'après les résultats, les quantités les plus efficaces de SK sont de l'ordre de 0,8 pour cent de bitume pour empêcher les dommages causés par l'eau au béton bitumineux. Parallèlement, l'essai d'ébullition prolongée (WBWA) est également vérifié pour évaluer les propriétés d'adhérence des granulats et du bitume.

1. INTRODUCTION

The impervious asphalt concrete has been more and more applied in the reservoir engineering of China, while the site availability of qualified alkaline aggregate has now and then formed a restriction to its economic feasibility. There have been indeed some applications of acid aggregate modified by anti-strip additives (such as amine, hydrated lime, etc.) in the project of asphalt concrete core dams, with its impervious core being more than 50 centimeters thick (Hao et al., 2018)[1]. The air void of hydraulic asphalt concrete is standardly regulated to be less than 3% in volume according to its imperviousness demand, which is helpful to reduce the stripping susceptibility of acid aggregate to the impervious component of asphalt concrete, especially with such a big thickness. Some test has even shown no detrimental effects of using strip-prone aggregates to the dense-grade hydraulic asphalt (air void 2-3%), even for specimens conditioned by the exposure to 100 freeze-thaw cycles at +25°C to -25°C (Wang et al. 2010)[2]. Nevertheless, doubt still exists to the application of acid aggregate to the impervious facing of asphalt concrete, which is only about 10 centimeters thick, even though with its air void less than 3%.

There are two requirements for the selection of coarse aggregate in the design code of China [3]. Firstly the alkaline aggregate is preferably applied, and the argument to the use of acid aggregate should be experimentally demonstrated. Secondly, the adhesion grade of coarse aggregate to bitumen is required to be no smaller than four by the boiling water test (relevant to the ASTM D3625/3625M-2012), and the index of hydraulic stability of asphalt concrete is required to be no less than 0.90 by the hydraulic stability test (relevant to the index of reduced compressive strength of ASTM D1075-2011).

In the present design code (SL 501-2010)[3] and test code (DL/T 5362-2006) [4] of China, there is no difference to the requirements of core wall and facing slab, and both require, and In the practice of hydraulic project, the above demand of index of hydraulic stability could be easily met by the present test code (9.10 of DL/T 5362-2006)[4] to the impervious asphalt concrete, even the stability index larger than 1.0 could illogically appear at times, which raises doubt to the feasibility of these standards to the stripping susceptibility of asphalt concrete facing. In some research, the boiling time has been extended to be more than three minutes in the boiling water test, the soak time and the water temperature have also been extended and raised in the hydraulic stability test (Wang et al., 2010)[2].

In order to apply a local acid aggregate to the asphalt concrete of a reservoir project with impervious facing, two problems have to be solved at present, (1) the selection of anti-strip additive to the project, some anti-strip agent have already been available in market for the highway asphalt concrete, which could be referenced by the hydraulic asphalt concrete; (2) the feasibility study of the above test code and the design code, such as, is the grade four of adhesion of coarse aggregate to

bitumen proper and sufficient? Due to the interpretation of human eyes, the results of boiling water test are always discrete and inaccurate in practice.

A new method has been developed since 1990s to evaluate the stripping susceptibility of aggregate from bitumen, and its theoretical basis of surface free energy (SFE) has been founded in 1980s (van Oss, 2002; Hefer et al., 2006) [5,6]. Even though some imperfections still exist in this method at present, such as the temporary assumption of unity (one) for the Lewis component ratio of the acid to the base, γ_w^+/γ_w^- , for water at 20°C (van Oss, 2002) [5], the distinct difference of SFE component of aggregate between the universal sorption device (USD) method and the sessile drop (SD) device method (Koc & Bulut, 2014) [7], the selection puzzle of the appropriate probe liquids during the test (Hefer et al., 2006) [6], etc.

In practice, two testing devices have been adopted for the SFE measurements of aggregates, the universal sorption device (USD) and the sessile drop (SD) device. Koc and Bulut (2014)[7] have used the SD device to measure the contact angles directly on aggregates (including limestone, granite and rhyolite), and the solved SFE components are in agreement with the results in the literature of the similar geological materials, while they are not in agreement with the results from the USD (Koc & Bulut, 2014)[7]. To the anti-stripping additives, the SFE method has been applied to study the effect of coating the surfaces of aggregates on the amount of moisture sensitivity of asphalt mixture, the USD method and the Wilhelmy plate method were used for the aggregates and the bitumen respectively, and the anti-stripping additives of both nonpolar and polar hydrophobic have been tested (Nejad et al., 2018)[8].

In regard to bitumen, Wei et al. (2014)[9] have made experiment with the SD device to investigate the correlative relationships between the chemical composition and the surface free energy (SFE) of bitumens, and found that the saturates, aromatics, wax and asphaltenes have negative effects to the SFE of bitumen, and a good positive logarithmic relationship exists between the ratio of resins/asphaltenes and the SFE of bitumen (Wei et al., 2014) [9]. The moisture susceptibility of foamed warm asphalt mixes has also been evaluated through the SFE approach by some researchers, the SD method was found after a check to be a suitable method to characterize the contact angles of the foamed and unfoamed bitumen (Liu et al., 2017) [10], and the warm mix additive can improve the spreadability of bitumen over the aggregate (Kadar, 2015) [11].

With respect to the mechanical properties of asphalt concrete, a correlative relation has been found between the SFE properties of bitumen-aggregate and the mechanical properties by Moraes et al. (2017) [12]. They have investigated the bonding strength between aggregate and bitumen before and after conditioned in water as measured by the Asphalt Bond Strength (ABS) test, and the results were compared to estimates of work of cohesion and work of debonding calculated from the SFE components. The experimental results have showed that the ABS and the

SFE properties of different bitumens are generally in agreement, the higher work of cohesion results in higher pull-off strength (Moraes et al., 2017) [12].

The authors of this paper have compared the tests to the SFE properties and the adhesion grade to evaluate the adhesion of bitumen-aggregate interfaces. The test of sessile drop (SD) device other than USD was used to measure the contact angles of the bitumen and aggregate, in the light of the work of Koc and Bulut (2014) [7], and the adhesion grades are evaluated by the boiling water test. The main objective is to investigate the feasibility of the present standards, and evaluate the effects of some anti-stripping additives to the stripping susceptibility of hydraulic asphalt concrete.

2. MATERIALS

Four bitumens of normal grade were prepared, including LYS-70, ZHY-50, ZHY-70 and ZHY-90, with their properties listed in Table 1.

Table 1
Properties of bitumens (Test method: DL/T 5362-2006)[4]

Items	LYS-70	ZHY-50	ZHY-70	ZHY-90
Penetration (0.1mm, 25 °C)	63	37	71	88
Softening point (°C)	53.8	53.0	52.2	45.0
Ductility, cm (5cm/min, 15°C)	>150	53	>150	>150
Ductility, cm (1cm/min, 4°C)	45.4	-	50.1	42.0
Flashing point, °C	272	>230	>260	289
Solubility, %	99.9	99.8	99.9	99.9
Wax content, %	1.8	1.2	1.2	1.8
Mass loss after RTFOT, %	0.11	0.20	0.09	0.02
Penetration ratio after RTFOT, %	71.3	74.3	70.3	71.0
Ductility after RTFOT, cm (15 °C)	83.2	18.0	>100	>100
Ductility after RTFOT, (4°C)	8.1	-	8.1	12.0
Softening point rise after RTFOT, (°C)	3.8	3.2	3.3	2.0

The tested aggregates included those of acidic, basic and neutral, which were BHT Limestone, BHT Basalt, QBT Granite, LY Limestone and LY Granite. The chemical compositions of these aggregates are listed in table 2. Others included the

loss on ignition and other compositions. According to the “Code for chemical analysis tests of rock and soil for hydropower and water conservancy engineering (DL/T 5357-2006)”, aggregate with SiO₂ content being lower than 52% be classified as basic, and higher than 65% be classified as acidic. The adhesion grades of these aggregates are given in Table 3, in which, the results of the two granites do not meet the demand of standard, except the result of LY granite to the bitumen of LYS-70.

Table 2
Chemical composition test results of aggregates (Test method: DL/T 5357-2006)

Aggregate	SiO ₂ (%)	Fe ₂ O ₃ (%)	Al ₂ O ₃ (%)	CaO (%)	MgO (%)	Others (%)	Acid-base
BHT Limestone	47.30	10.47	14.86	13.32	6.78	7.27	Basic
BHT Basalt	50.62	10.75	16.35	2.06	0.49	19.73	Basic
QBT Granite	65.38	8.55	13.31	2.52	0.66	9.58	Acidic
LY Limestone	50.42	13.03	5.32	16.01	6.58	8.64	Basic
LY Granite	75.74	2.74	3.83	5.03	1.64	11.02	Acidic

Table 3
Adhesion grade of aggregates to the bitumens of Table 1 (DL/T 5362-2006)[4]

Three anti-stripping additives, SK-AS, XT-2 and TR-500s, have been collected from market to do the present test. Among them, only XT-2 is an amine additive.

3. TEST TO SURFACE FREE ENERGY PROPERTIES

3.1. REVIEW OF SURFACE FREE ENERGY THEORY

The scientific investigation of contact angles with Young’s statement in 1805 can be written in the following form

$$\gamma_s = \gamma_{sl} + \gamma_l \cos \theta \tag{1}$$

Where γ is the surface tension (or surface free energy per unit area) and the subscripts s, sl, and l refer to the solid-vapor, solid-liquid, and liquid-vapor interfaces respectively (Good, 1992)[13].

The γ has been further written into a summation of two terms as follows, where γ^{LW} is the apolar component, with “LW” standing for “Lifshitz-van der Waals”, and γ^{AB} is the polar Lewis acid-base (AB) component (van Oss et al. 1987) [14].

$$\gamma = \gamma^{\text{LW}} + \gamma^{\text{AB}} \quad (2)$$

According to the Good and Girifalco's combining rule together with Fowkes' hypothesis, the “LW” interface free energy of different substances, i and j, can be written as (van Oss et al. 1987)

$$\gamma_{ij}^{\text{LW}} = \left(\gamma_i^{\text{LW}} - \gamma_j^{\text{LW}} \right)^2 \quad (3)$$

The acid-base component γ^{AB} of a pure substance can be expressed in terms of the product of its electron-acceptor (γ^+) and electron-donor (γ^-) parameters, and the acid-base component γ_{ij}^{AB} across an interface between substance i and j can be calculated by a combining rule suggested by Small (van Oss et al. 1987) [14].

$$\gamma^{\text{AB}} = 2\sqrt{\gamma^+ \gamma^-} \quad (4)$$

$$\gamma_{ij}^{\text{AB}} = 2\left(\sqrt{\gamma_i^+} - \sqrt{\gamma_j^+}\right)\left(\sqrt{\gamma_i^-} - \sqrt{\gamma_j^-}\right) \quad (5)$$

Substituting (2) ~ (5) into (1), we can obtain the following basic SFE equation (6) of a sessile liquid drop on a solid.

$$\gamma_l(1 + \cos \theta) = 2\left(\sqrt{\gamma_i^{\text{LW}} \gamma_j^{\text{LW}}} + \sqrt{\gamma_i^+ \gamma_j^-} + \sqrt{\gamma_j^+ \gamma_i^-}\right) \quad (6)$$

In order to determine three unknown SFE components, γ_s^{LW} , γ_s^+ and γ_s^- , of a substance “s”, at least three probe liquids of known SFE characteristics (γ_1^{LW} , γ_1^+ and γ_1^-) are needed to measure their contact angles (θ_1 , θ_2 and θ_3) on the substrates “s”, and the three SFE unknown quantities can be solved from the set of equations constructed from equation (6) in terms of γ_s^{LW} , γ_s^+ and γ_s^- (Good 1992) [13].

From the result of the SFE components above, the work of adhesion W of the interface between the bitumen and aggregate can be calculated. The concepts of work of adhesion, W, was introduced by Dupré in 1869, which can also be expressed by the thermodynamic free energy G. In a process of bring together reversibly the bitumen (B) and the aggregate (A) in the presence of water (W), the free energy change per unit area is the free energy of adhesion, ΔG_{BWA} , which is the negative of

the work of adhesion, W_{BWA} (van Oss et al. 1987; Good 1992) [13,14].

$$\Delta G_{BWA} = -W_{BWA} = \gamma_{BA} - \gamma_{BW} - \gamma_{AW} \quad (7)$$

Substituting (2) ~ (5) into (7), the following formula (8) can be arrived at and used to evaluate the adhesion works of aggregate and bitumen in the presence of water W_{BWA} (i.e., work of debonding). For an asphalt mix to be durable and resistant to water damage, it is desirable that the magnitude of W_{BWA} be as small as possible to reduce moisture sensitivity.

$$\begin{aligned} W_{ABW} &= \gamma_{AW} + \gamma_{BW} - \gamma_{AB} \\ &= 2\gamma_W^{LW} + 4\sqrt{\gamma_W^+ \gamma_W^-} + 2\left(\sqrt{\gamma_A^{LW} \gamma_B^{LW}} + \sqrt{\gamma_A^+ \gamma_B^-} + \sqrt{\gamma_B^+ \gamma_A^-}\right) \\ &\quad - 2\left(\sqrt{\gamma_A^{LW} \gamma_W^{LW}} + \sqrt{\gamma_A^+ \gamma_W^-} + \sqrt{\gamma_W^+ \gamma_A^-}\right) \\ &\quad - 2\left(\sqrt{\gamma_W^{LW} \gamma_B^{LW}} + \sqrt{\gamma_W^+ \gamma_B^-} + \sqrt{\gamma_B^+ \gamma_W^-}\right) \end{aligned} \quad (8)$$

3.2. SELECTION OF PROBE LIQUIDS

An important factor in determining SFE components is the proper selection of probe liquids, which must not chemically react or dissolve the tested bitumen or aggregate. According to the work of van Oss 2002[5] and Hefer 2006[6], etc., five probe liquids were used to the measurement. These are distilled water, glycerol, ethylene glycol, formamide, and diiodomethane, and thereafter abbreviate to W, G, EG, F, and D respectively. The SFE components of these liquids are listed in Table 4 (van Oss 2002, Hefer 2006, etc.) [5,6].

Table 4
SFE components of probe liquids at 20 °C (mJ/m²) (data from: van Oss 2002) [5]

Liquid	γ	γ^{LW}	γ^{AB}	γ^+	γ^-	Polarity
Distilled water (W)	72.8	21.8	51.0	25.5	25.5	Bipolar
Glycerol (G)	64	34	30	3.92	57.4	Monopolar
Ethylene glycol (EG)	48	29	19	1.92	47.0	Monopolar
Formamide (F)	58	39	19	2.28	39.6	Monopolar
Diiodomethane (D)	50.8	50.8	0	0	0	Non-polar

If the contact angles θ_i ($i=1, \dots, n$) of the selected n probe liquids are obtained on solid s , then we can use equation (6) to construct a set of n equations in terms of the three unknowns of γ_s^{LW} , γ_s^+ and γ_s^- :

$$\gamma_{li}(1 + \cos \theta) = 2 \left(\sqrt{\gamma_s^{LW} \gamma_{li}^{LW}} + \sqrt{\gamma_s^+ \gamma_{li}^-} + \sqrt{\gamma_s^- \gamma_{li}^+} \right) \quad i=1, 2, \dots, n \quad (9)$$

From equations (9), only three probe liquids ($n=3$) are needed to solve the three unknowns of the tested solid s . In spite of this theoretical correctness, combinations of no less than three probe liquids should be selected and needed to reduce the unduly sensitiveness of the solution of the equation set to small measurement errors of contact angles. The condition number of the matrix of surface energy components of the selected liquids is the mathematical measure of this sensitiveness. The smaller the condition number, the less the sensitiveness will be (Hefer et al. 2006) [6]. The condition numbers of some proper combinations of probe liquids were calculated based on the linear algebra theory and given in Table 5, and the meanings of the abbreviated letters to the probe liquid are the same to those listed in Table 4. In the case of n being more than three, the minimization algorithm of least square of error was used to solve the redundant equations (10) for the surface energy components of solids.

Table 5
Probe liquid combinations with small condition numbers

n	Combination	Condition number	n	Combination	Condition number
3	W-G-D	4.895	4	W-G-EG-D	4.971
	W-EG-D	4.468		W-EG-F-D	4.933
	W-F-D	5.174		W-G-F-D	5.276
5	W-G-EG-F-D	5.499	-	-	-

Furthermore, if probe liquids are properly chosen for a given solid surface, a plot of $\gamma_l \cos \theta$ vs. γ_l exists for a large number of pure liquids with different molecular properties, in which the values of $\gamma_l \cos \theta$ change smoothly with γ_l and depend only on γ_l and γ_s , independent of any specific intermolecular forces of the probe liquids and solids (Kwok et al. 1999)[16]. This plot of $\gamma_l \cos \theta$ vs. γ_l was also used to check the contact angle results of this paper. Because the conventional goniometer sessile drop technique may produce contact angles violating the basic assumptions of constancy of γ_l for a given probe liquid and the constancy of γ_s from going liquid to liquid, the low-rate dynamic contact angle technique was adopted, which allows one to distinguish good contact angles from bad ones on noninert surfaces, as studied by Kwok et al. (1997) [15].

3.3. SAMPLE PREPARATION

Due to the complication of the contact angle phenomena, the experimentally observed apparent contact angle may not be equal to its ideal counterpart described in the Young equation (1), the chemical heterogeneity and the roughness of the sample surface could deviate the test and make the result of measurement meaningless (Kwok, 1997) [15]. Care must be taken to the sample preparation, as demonstrated by Koc et al. (2014) [7]. The sample surfaces should be relatively flat, smooth, and clean, in order to obtain the reasonable contact angles.

For the bitumen sample, the microscopic glass slides were firstly rinsed with solutions of toluene and acetone, then conditioned in the boiling solution of sodium hydroxide for 20 minutes, and rinsed with the deionized distilled water. After cleaned and dried in an ultrasonic bath, the slides were dipped into the melting bitumen of about 130-150°C, and hanged in an oven till no excess bitumen dropping off. Take the glass slides out of oven, and cool them to ambient temperature in a desiccator with anhydrous calcium sulfate crystals overnight.

For the aggregate sample, aggregate blocks ranging from 15cm to 20cm in size are more easily processed on cutting machine, and were firstly cut with a diamond saw into sample plates of about 8mm~10mm thick and 50mm in size, surface polished to remove cutting traces using different grades of specific powders of silicon carbide and alumina oxide grit mixed with water, wiped with soft cloth to remove fine particles, and finally washed with soap, water and alcohol, and wiped and rubbed with paper towels saturated with hexane. The aggregate surfaces must be relatively flat, smooth, and clean, so that representative contact angles can be obtained. After dried in an oven at 105°C for 12 hours, cool the samples to room temperature in a desiccator.

3.4. MEASUREMENT OF CONTACT ANGLE

Just as what was said by Kwok, et al. (1997, 1999) [15,16], the experimentally observed apparent contact angle may or may not be equal to the Young contact angle, θ_y , in equation (1) due to various complexities. Nevertheless, the experimental advancing contact angle, θ_a , can be expected to be a good approximation of θ_y . Low-rate dynamic contact angle measurement from ADSA-P (Axisymmetric Drop Shape Analysis-Profile) allows one to distinguish good contact angles from bad ones on noninert surfaces [15, 16]. Taking these cognitions as reference, dynamic contact angles were measured by the XG-CAMB1 standard goniometer, the liquid drop was added dynamically from above up to approximately 5mm radius by a motor-driven syringe at the speed of

0.5 microliters per second for bitumen and 1.0 microliters per second for aggregate, at the same time, a sequence of pictures of the drop was taken at a rate of one image every two seconds. The apparent contact angle was obtained by averaging the right angle and left angle of the image through the tangent at the three-phase contact point of the drop.

Firstly, the contact angles of the probe liquids on bitumens were measured, and the skip-stick phenomena were found out to the contact angles of all the probe liquids on the bitumen of LYS-70#. As described by Kwok, et al. (1997) [15], this type of results should be discarded due to the lack of understanding of its mechanism. By that time, it was guessed that this skip-stick of contact angle could be related to the sticking character of bitumen surface, and reduced by lowering the temperature, which was verified by the measurements at lower temperatures, as shown in Figure 1. It can be seen from Figure 1 that the range of the sudden decreasing of contact angles reduces at 10°C comparing to that at 20°C, and disappears at 2°C. The averaged contact angles of the flat straight section of each figure are 107.26° at 10°C, and 103.68° at 2°C respectively. Similar phenomena on bitumen were also found to other probe liquids excepting glycerol and diiodomethane. At lower temperatures, glycerol is too thick to measure the contact angle, and diiodomethane will congeal at 2°C. Therefore, only water, ethylene glycol and formamide shown in Table 4 can be used to the measurement at 2°C, and the results are given in Table 6. The results of bitumen LYS-70# modified with different amounts of SK antistipping additives are given in Table 7.

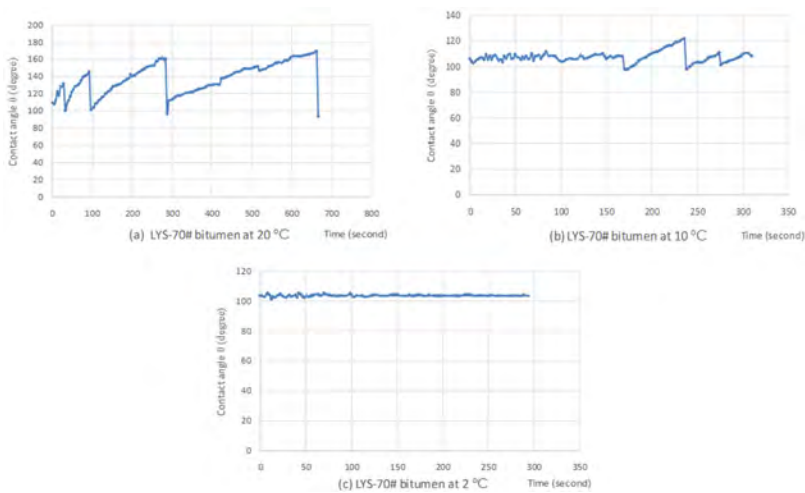


Fig. 1
Contact angles of water on bitumen LYS-70# at different temperatures

Table 6
Contact angles on bitumens at 2°C

Probe liquid	ZHY-50#	ZHY-70#	LYS-70#	ZHY-90#
Water	118.49	103.79	104.06	108.43
Ethylene glycol	75.63	75.65	74.55	82.85
Formamide	89.32	83.46	93.73	88.62

Table 7
Contact angles on LYS-70# bitumen with SK additive at 2°C

SK amount (%)	0.0	0.2	0.4	0.6	0.8	1.0	1.2
Water	104.06	108.31	108.35	109.06	113.10	107.25	104.23
Ethylene glycol	74.55	77.40	70.02	78.16	78.04	76.96	91.38
Formamide	93.73	92.73	92.66	94.73	86.18	92.21	77.55

As for the tests of aggregates, even though the skip-stick behavior above was not found, the contact angles were still measured at 2°C for the adhesion evaluation of aggregate to bitumen, and the results are given in Table 8 with some shown in Figure 2 as demonstration.

Table 8
Contact angles on aggregates at 2°C

	LY Granite	QBT Granite	BHT Basalt	BHT Limestone	LY Limestone
Water	41.01(40.19)	45.02(49.18)	46.99(40.02)	63.44(61.44)	82.20
Ethylene glycol	15.72	20.42	21.48	36.20	54.88
Formamide	13.08	53.82	14.96	25.36	51.41

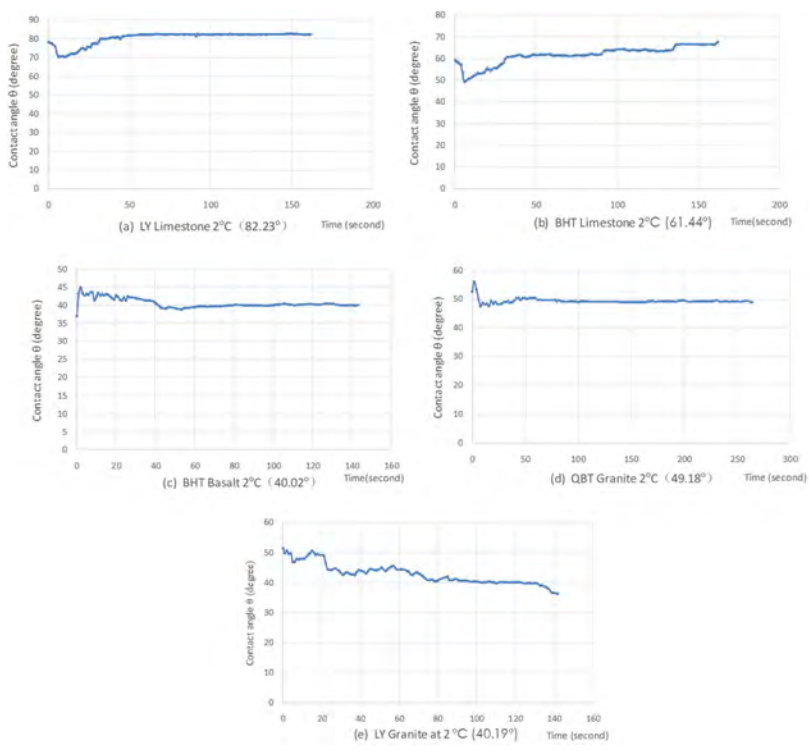


Fig. 2
Contact angles of water on aggregates at 2°C

3.5. DETERMINATION OF SFE COMPONENTS

The plot of $\gamma_i \cos \theta$ vs. γ_i from the above results of contact angles are shown in Figure 3, including those of aggregates, bitumens and LYS-70# bitumen with different amounts of SK anshripping additives. Except some solitary points, such as the angle of formamide on QBT granite, good correlativities can be seen from the apparent curves of $\gamma_i \cos \theta$ vs. γ_i shown in these plots.

Solving the unknowns $\sqrt{\gamma_s^{LW}}$, $\sqrt{\gamma_s^+}$ or $\sqrt{\gamma_s^-}$ of the equation set (10) from the measured contact angles θ_i , the SFE components $\sqrt{\gamma_{li}^{LW}}$, $\sqrt{\gamma_{li}^+}$ or $\sqrt{\gamma_{li}^-}$ of the probe liquid i have to be used, and these SFE components at low temperature should be known because of the contact angle measuring above under 2°C. From a handbook it is known that the surface free energy of water under 2°C is 75.31mJ/m², larger than its relevant value of 72.88mJ/m² under 20°C. Because the more details

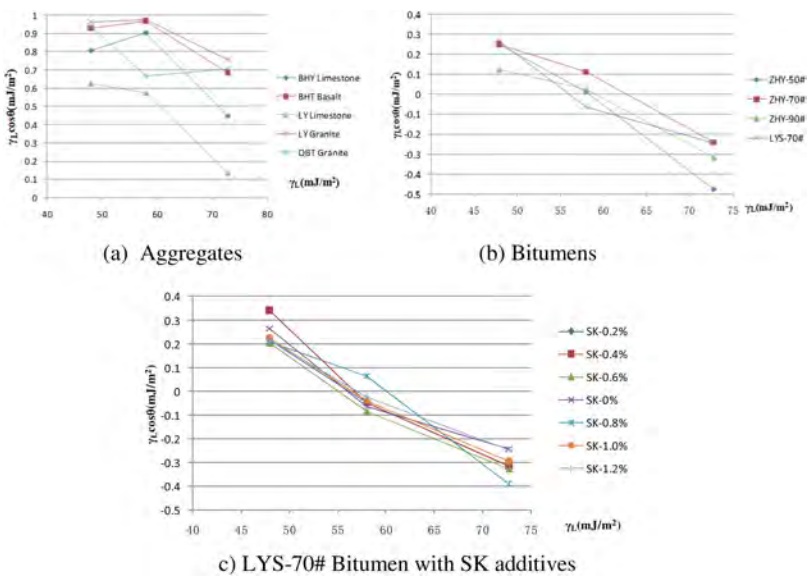


Fig.3
Values of $\gamma_1\cos\theta$ vs γ_1 from the results of contact angles

of the SFE components under 2°C of the corresponding probe liquids above are not available from reference at present, the SFE values of liquid under 20°C shown in Table 4 had to be used to solve the above unknowns as below.

Using the above contact angles θ , the surface free energy (SFE) components of bitumens and aggregates can be solved from the equation set (10) as shown in Table 9, in which if an irrational negative value of $\sqrt{\gamma_s^{LW}}$, $\sqrt{\gamma_s^+}$ or $\sqrt{\gamma_s^-}$ appeared, the relevant $\sqrt{\gamma_s^{LW}}$, $\sqrt{\gamma_s^+}$ or $\sqrt{\gamma_s^-}$ would be set zero, with other components being solved by the least square errors.

Table 9
SFE components of bitumens and aggregates

	γ^{LW}	γ^+	γ^-	γ^{AB}	γ
ZHY-50#	0.47	13.86	0.00	0.00	0.47
ZHY-70#	12.62	2.01	0.62	2.23	14.85
ZHY-90#	13.50	0.86	0.36	1.12	14.62
LYS-70#	0.00	16.62	1.88	11.19	11.19
LYS-70	0.21	14.04	0.59	5.78	5.99
(continued)					

Table 9 Continued

	γ^{LW}	γ^+	γ^-	γ^{AB}	γ
+0.2%SK					
LYS-70 +0.4%SK	0.00	19.90	0.22	4.15	4.15
LYS-70 +0.6%SK	0.00	16.37	0.65	6.53	6.53
LYS-70 +0.8%SK	9.31	3.20	0.00	0.00	9.31
LYS-70 +1.0%SK	0.27	13.73	0.79	6.57	6.84
LYS-70 +1.2%SK	0.86	10.62	1.74	8.59	9.45
BHT Lime- stone	59.06	0.00	10.99	0.00	59.06
BHT Basalt	58.63	0.00	25.37	0.00	58.63
LY Lime- stone	57.93	0.00	16.62	0.00	57.93
LY Granite	57.67	0.00	31.57	0.00	57.67
QBT Granite	57.17	0.00	28.16	0.00	57.17

From the SFE components shown in Table 9, the debonding works of aggregate and bitumen in the presence of water W_{BWA} can be calculated from the formula (8), and given in Table 10, which shows the queues of aggregates from acidic to basic according to their values of W_{BWA} . All the values of W_{BWA} are negative, similar to the results of Alvarez (2012) [17].

Table 10
Debonding works of aggregate and bitumen in the presence of water W_{BWA} (mJ/m²)

	BHT Limestone	LY Limestone	BHT Basalt	QBT Granite	LY Granite
ZHY-50#	-31.60	-30.17	-27.25	-27.31	-26.21
ZHY-70#	-48.93	-43.56	-36.48	-34.75	-32.40
ZHY-90#	-53.21	-47.08	-39.07	-37.04	-34.39
LYS-70#	-12.35	-11.56	-9.26	-9.64	-8.72
LYS-70+0.2%SK	-22.35	-20.99	-18.10	-18.20	-17.11
LYS-70+0.4%SK	-20.19	-19.98	-18.42	-19.00	-18.32
LYS-70+0.6%SK	-18.18	-17.34	-14.98	-15.34	-14.40
LYS-70+0.8%SK	-52.56	-47.83	-41.42	-39.97	-37.83
LYS-70+1.0%SK	-21.67	-20.23	-17.27	-17.34	-16.22
LYS-70+1.2%SK	-21.35	-19.17	-15.39	-15.14	-13.78

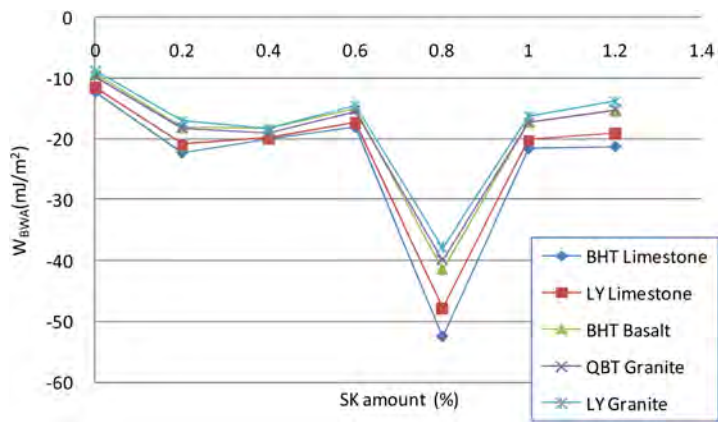


Fig.4
Relations between debonding works W_{BWA} and SK amounts

From Table 10, the effect plot of SK amount on the debonding work W_{BWA} can be drawn in Figure 4, and the most effective amounts of SK are predicted around 0.8 percent of bitumen to impede the water damage of asphalt concrete, which need to be confirmed by the water stability test.

From Table 10, the clue of the threshold value W_{TBWA} of W_{BWA} could be conjectured existing between the acidic aggregate and the basic aggregate, which can be estimated by averaging the closest two values of W_{BWA} of BHT Basalt and QBT Granite, and given in Table 11 and Figure 5, together with the SFE values of γ_A of the corresponding bitumens. From Picture 5, the threshold value W_{TBWA} may be correlated to the sort and the surface free energy γ_A of the bitumen, only if the three solitary points could be explained properly.

Table 11 Threshold value W_{TBWA} (mJ/m^2) between acidic aggregate and basic aggregate										
Bitumen	ZHY50	ZHY70	ZHY90	LYS70	0.2% SK	0.4% SK	0.6% SK	0.8% SK	1.0% SK	1.2% SK
$\gamma_A(\text{mJ}/\text{m}^2)$	0.47	14.85	14.62	11.19	5.99	4.15	6.53	9.31	6.84	9.45
W_{TBWA} (mJ/m^2)	Clue	-27.28		-9.45	-18.15	-18.71	-15.16		-17.30	-15.27
	Solitary		-35.61	-38.05				-40.69		

4. TEST TO ADHESION GRADE BY BOILING WATER

According the test code of DL/T 5362-2006[4], for each aggregate, five stone particles from 13.2mm to 19.0mm in size are washed clean by water, dried and heated in oven for one hour at a temperature of 105°C, and then cooled to ambient temperature. Dip the particles one by one into the melting bitumen of about 140°C for 45 seconds, and hang them in air with wire to drop off the surplus bitumen for

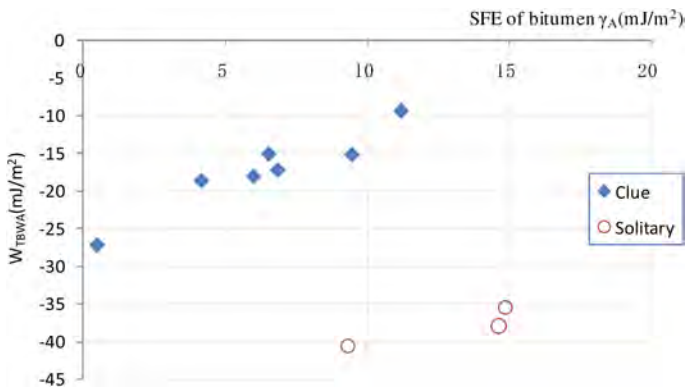


Fig. 5

The probable relation between the threshold value W_{TBWA} and SFE value of bitumens

15 minutes. Immerse the particles in a beaker full of boiling water, and keep the water slightly boiling without foam for 3 minutes. Take out the boiled particles, and examine by skilled observer the stripping extent of bituminous coating from the particles. The adhesion grades are evaluated according to the stipulations given in Table 12.

Table 12
Adhesion grades stipulated in DL/T 5362-2006[4]

Segregation of bitumen coat from aggregate grain surface after boiling	Adhesion grade
Bitumen coat entirely preserved, and stripping area percentage is close to zero.	5
Small portion of bitumen coat stripped off, thickness of remaining bitumen coat is not uniform and stripping area percentage is less than 10%.	4
Bitumen coat is locally stripped off, stripping area percentage is less than 30%.	3
Bitumen coat is mostly stripped off, stripping area percentage is more than 30%.	2
Bitumen coat is entirely stripped off and floating on the water surface, stone particles are basically uncovered or exposed.	1

The adhesion grade results of the tested aggregates by the stipulating process above have been already given in the foregoing Table 3, and those of all the three alkaline aggregates are five in adhesion grade, and can not be further separated from each other by the process. Even to the bitumen LYS-70, the adhesion grade of the acid aggregate of LY granite is four and very close to those of alkaline aggregates. Obviously the above standard process of boiling water can not be resorted to distinguish the modified effects of anti-stripping additives. Therefore in the test below, the boiling time to stone particles with bitumen coat will be prolonged, and a parameter of stripping-start time (SST) will be introduced to quantitatively evaluate the adhesion behavior, which means the moment of bitumen coat starting stripping from the stone particle. Furthermore in a test below, the bitumens of Table 1 with anti-stripping additives were used to test the distinguishment result of the new method, and the amounts of additives were all fixed at 0.4 percent of the bitumen mass. The test results are given in Table 13, which shows an obvious better modifying effect of SK-AS than the other two additives.

Table 13
Stripping-start time (SST, min) of bitumen with different additives

Aggregate	SK-AS (0.4%)				XT-2 (0.4%)	TR-500s (0.4%)
	LYS-70	ZHY-50	ZHY-90	ZHY-70	ZHY-70	ZHY-70
BHT Limestone	51	>60	42	48	9	6
BHT Basalt	36	>60	30	39	4	6
QBT Granite	12	30	5	24	0.33	1.5
LY Limestone	39	>60	36	39	0.5	6
LY Granite	15	42	9	15	15	2
SST Range/min	39	>30	37	33	~15	4

From Table 6, the aggregates can be sorted into a decreasing queue of SST as BHT limestone, LY limestone, BHT basalt, LY granite and QBT granite. Meanwhile, the higher the bitumen grade, the weaker the adhesion will be. Further SST tests with different amount of SK-AS were also conducted as shown in Table 14, from which the prolonged boiling water test can be referred to as an effective way to relatively evaluate the adhesion property of aggregate and bitumen.

Table 14
Stripping-start times of LYS-70 bitumen with different amount of SK additive

Amount of SK-AS (%)	0	0.2	0.4	0.6	0.8	1.0	1.2
LY limestone	15	18	39	54	>60	>60	>60
LY granite	2.5	9	15	30	36	51	>60

5. CONCLUSIONS

1. A reasonable or good contact angle value of aggregate and bitumen can be given by the low-rate dynamic method of this paper.
2. The ambient temperature can affect the contact angle measuring of bitumen, and the impact can be eliminated by lowering the temperature to 2°C.
3. The debonding work of aggregate and bitumen in the presence of water W_{BWA} is a good parameter to distinguish the acidic aggregate and the basic aggregate, and the relevant threshold values W_{TBWA} may be correlated to the type and the surface free energy γ_A of the bitumen.
4. From the debonding work W_{BWA} results, the most effective amounts of SK are predicted around 0.8 percent of bitumen to impede the water damage of asphalt concrete, which need to be confirmed by the water stability test.
5. The prolonged boiling water test can be used to appraise the adhesion properties of aggregate and bitumen, and the similar queues from acidic aggregate to basic aggregate can be established by the stripping-start time (SST) of the prolonged boiling water test and the debonding work W_{BWA} of the SFE test, except a local inconformity of two aggregates of QBT granite and LY granite.

ACKNOWLEDGMENTS

The authors are grateful for the financial support from State Key Laboratory of Simulation and Regulation of Water Cycle in River Basin [grant number SM0112B242018]

REFERENCES

- [1] HAO, J.T., LIU, Z.H., WANG, Z.X. (2018). Development and prospect of hydropower project with asphalt concrete impervious elements in China [J], *Journal of Hydraulic Engineering*, 2018, 49(9), 1137–1147. (in Chinese)
- [2] WANG, W.B., ZHANG, Y.B., HÖEG, K., ZHU, Y. (2010). Investigation of the use of strip-prone aggregates in hydraulic asphalt concrete, *Construction and Building Materials*, 2010, 24(11), 2157–2163.
- [3] Design Code of Asphalt concrete Facings and Cores for Embankment Dams [S]. SL 501-2010, Standard of Ministry of Water Resources of the People's Republic of China, 2010 (in Chinese).

- [4] Test Code for Hydraulic Bitumen Concrete[S]. DL/T 5362-2006, Electric Power Industry Standard of the People's Republic of China, 2006.
- [5] VAN OSS, C.J. (2002). Use of the combined Lifshitz–van der Waals and Lewis acid–base approaches in determining the apolar and polar contributions to surface and interfacial tensions and free energies, *Journal of Adhesion Science and Technology*, 2002, 16(6), 669–677.
- [6] HEFER, A. W., BHASIN, A., LITTLE, D. N. (2006). Bitumen Surface Energy Characterization Using a Contact Angle Approach. *Journal of Materials in Civil Engineering*, ASCE, 2006, 18(6), 759–767.
- [7] KOC, M., BULUT, R. (2014). Assessment of a Sessile Drop Device and a New Testing Approach Measuring Contact Angles on Aggregates and Asphalt Binders, *Journal of Materials in Civil Engineering*, ASCE, 2014, 26(3): 391–398.
- [8] NEJAD, F. M., ASADI, M., HAMED, G. H., ESMAEELI, M. R. (2018). Using Hydrophobic Coating on Aggregate Surfaces to Reduce Moisture Damage in Asphalt Mixture, *Journal of Materials in Civil Engineering*, ASCE, 2018, 30(10): 04018238.
- [9] WEI, J.M., DONG, F.Q., LI, Y.A., ZHANG, Y.Z. (2014). Relationship analysis between surface free energy and chemical composition of asphalt binder, *Construction and Building Materials*, 71 (2014), 116–123.
- [10] LIU, S.J., YU, X., DONG, F.Q. (2017). Evaluation of moisture susceptibility of foamed warm asphalt produced by water injection using surface free energy method, *Construction and Building Materials*, 131 (2017), 138–145.
- [11] KAKAR, M.R., HAMZAH, M.O., AKHTAR, M.N., WOODWARD, D. (2015). Surface free energy and moisture susceptibility evaluation of asphalt binders modified with surfactant-based chemical additive, *Journal of Cleaner Production*, 2016, 112(4), 2342–2353.
- [12] MORAES, R., VELASQUEZ, R., BAHIA, H. (2017). Using bond strength and surface energy to estimate moisture resistance of asphalt-aggregate systems, *Construction and Building Materials*, 130 (2017), 156–170.
- [13] GOOD, R. J. Contact angle, wetting, and adhesion: a critical review[J], *Journal of Adhesion Science and Technology*, 1992, 6(12), 1269–1302.
- [14] VAN OSS, C.J., CHAUDHURY, M.K., GOOD, R.J. (1987). Monopolar Surfaces, *Advances in Colloid and Interface Science*, 28 (1987) 35–64, Elsevier Science Publishers B.V., Amsterdam - Printed in the Netherlands.
- [15] KWOK, D.Y., GIETZELT, T., GRUNDKE, K., JACOBASCH, H.-J., NEUMANN, A. W. (1997). Contact Angle Measurements and Contact Angle Interpretation. 1. Contact Angle Measurements by Axisymmetric Drop Shape

Analysis and a Goniometer Sessile Drop Technique, *Langmuir*, 1997, 13(10), 2880–2894.

- [16] KWOK, D.Y., NEUMANN, A. W. (1999). Contact angle measurement and Contact Angle Interpretation, *Advances in Colloid and Interface Science*, 81 (1999), 167–249.
- [17] ALVAREZ, A.E., OVALLES, E., MARTIN, A.E. (2012). Comparison of asphalt rubber-aggregate and polymer modified asphalt-aggregate systems in terms of surface free energy and energy indices, *Construction and Building Materials*, 2012, 35(10), 385–392.

COMMISSION INTERNATIONALE DES
GRANDS BARRAGES

VINGT-HUITIEME CONGRES DES
GRANDS BARRAGES
CHENGDU, MAI 2025

**COUPLED HYDRATION AND CALCIUM LEACHING DETERIORATION
MODELS FOR MEDIUM\LOW HEAT CEMENT CONCRETE IN DAM
STRUCTURES (*)**

Wenwei LI

*Professorate Senior Engineer, Hydraulic Concrete Institute,
China Three Gorges Corporation, Beijing*

Huamei YANG

*Associate Professor, Hydraulic Concrete Institute,
China Three Gorges Corporation, Beijing*

Shuguang LI

*Professorate Senior Engineer, Hydraulic Concrete Institute,
China Three Gorges Corporation, Beijing*

Huite WU

*PhD, Hydraulic Concrete Institute,
China Three Gorges Corporation*

CHINA

SUMMARY

Dam concrete serves as a critical foundation for dam integrity, with medium/ low heat cement being widely adopted in China due to its superior crack resistance. The hydration process plays a pivotal role in the development of dam concrete properties. Additionally, submerged sections of dam concrete are particularly

**Modèles couplés d'hydratation et de détérioration par lixiviation du calcium du béton de ciment à chaleur moyenne/basse dans les barrages*

vulnerable to calcium leaching. In this study, a coupled model is developed to simulate both the hydration process and calcium leaching deterioration in medium/low heat cement concrete. The model first predicts the hydration dynamics and the evolution of hydration products based on key parameters. It then assesses the distribution of calcium ions within the concrete and simulates the calcium leaching-induced degradation of mechanical properties. These results offer critical insights into the interaction between hydration and leaching processes, providing essential theoretical and technical support for the safety assessment and longevity prediction of dam concrete, thereby contributing to the enhancement of dam durability and reliability.

RÉSUMÉ

Le béton de barrage est un élément fondamental pour l'intégrité d'un barrage. Du ciment moyen/faible chaleur est généralement adopté en Chine en raison de sa résistance supérieure à la fissuration. Le processus d'hydratation joue un rôle central dans le développement des propriétés du béton du barrage. De plus, les sections submergées de béton de barrage sont particulièrement vulnérables à la lixiviation du calcium. Dans cette étude, un modèle couplé est développé pour simuler à la fois le processus d'hydratation et la détérioration par lixiviation du calcium dans le béton de ciment à moyenne et basse chaleur. Le modèle prédit d'abord la dynamique d'hydratation et l'évolution des produits d'hydratation en fonction de paramètres clés. Il évalue ensuite la distribution des ions calcium dans le béton et simule la dégradation des propriétés mécaniques induite par la lixiviation du calcium. Ces résultats offrent un aperçu critique de l'interaction entre les processus d'hydratation et de lixiviation, fournissant un soutien théorique et technique essentiel pour l'évaluation de la sûreté et la prévision de la longévité du béton, contribuant ainsi à l'amélioration de la durabilité et de la fiabilité des barrages.

1. INTRODUCTION

To reduce the heat of hydration and improve the crack resistance of concrete, medium/low heat cement is commonly used as the primary binder system in dam concrete. This binder system has been widely applied in mega hydraulic projects such as the Three Gorges Dam, Baihetan Dam, and Wudongde Dam. Most regions of dam concrete are submerged underwater for extended periods. When in long-term contact with fresh water, significant dissolution occurs. The dissolution process first leads to the leaching of calcium hydroxide from the hydration products, resulting in a reduction of the internal alkalinity of the concrete. This, in turn, causes the dissolution of other hydration products within the concrete, leading to a decline in

mechanical properties and threatening the service life of the structure. The dissolution process in dam concrete is extremely slow and is typically studied using accelerated laboratory tests or simulation methods. However, laboratory accelerated tests often have long test cycles and face challenges in determining the acceleration rate. Current simulations also have limitations, particularly in their insufficient consideration of hydration products.

The most commonly used dissolution simulation based on the mass conservation of cement-based materials[1] typically requires manual input of material parameters such as calcium hydroxide content, C-S-H content, and porosity. These parameters are usually obtained through experiments and are often used to validate accelerated tests. However, such models consider only a limited number of hydration products, usually focusing on the dissolution of calcium hydroxide and C-S-H, despite the fact that cement hydration produces various hydration products. Additionally, during the dissolution process, the pore structure of the concrete changes over time, but traditional dissolution models seldom account for the time-varying characteristics of the pore structure. Therefore, this study conducted a coupled hydration-dissolution simulation for dam concrete, utilizing thermodynamic and kinetic models of cement hydration. GEMS software was used to calculate the long-term hydration of dam concrete. Based on the hydration simulation results, the reaction-transport simulation for long-term dissolution of dam concrete was carried out using the partial differential equation module of Comsol.

2. HYDRATION SIMULATION

The main difference between Ordinary Portland Cement (OPC), Medium-Heat Cement (MHC), and Low-Heat Cement (LHC) lies in their mineral composition. Table 1 shows the mineral composition of these three typical types of cement. Cement hydration is primarily a dissolution and precipitation process, governed by equations (1)-(4) [2–4]. These equations are used to calculate the degree of hydration of individual minerals (α_t), with the slowest rate controlling the overall hydration rate. The values for K1, K2, K3, N1, N2, and N3 are selected according to the literature[2]. Additionally, the water-cement ratio effect is considered based on equation (5). The hydration of the three types of cement was calculated using the GEMS software in combination with the CEMDATA18 cement hydration thermodynamic database [4]. The water-cement ratio was uniformly set at 0.5, the hydration temperature at 25°C, and the hydration time at 1000 days. The calculation results are shown in Figure 1. The mass development of clinker and hydration products over 1000 days of hydration for the three types of cement is shown in Figure 1. Taking the most typical hydration products, C-S-H and calcium hydroxide, as examples, the C-S-H content increases and the calcium hydroxide content decreases after 1000 days of hydration in OPC, MHC, and LHC, consistent with trends reported in the existing literature [5,6], thereby validating the reliability of the

model. Additionally, it can be observed that the residual C2S content after 1000 days of hydration increases from OPC to MHC to LHC, indicating that LHC and MHC have greater hydration potential after 1000 days, with considerable room for further growth in hydration product content.

Table 1
Typical Mineral Composition of Three Types of Cement

Mineral composition (wt. %)	OPC	MHC	LHC
C ₃ S	60.5	47.5	30.1
C ₂ S	14.2	28.3	48.2
C ₃ A	4.6	1.6	1.2
C ₄ AF	14.5	15.8	15.1
Gypsum	4.0	3.8	3.7

$$R_j=\min(R_1,R_2,R_3) \tag{1}$$

$$R_1=\frac{K_1}{N_1}(1-\alpha_t)(-\ln(1-\alpha_t))^{(1-N_1)} \tag{2}$$

$$R_2=\frac{K_2(1-\alpha_t)^{2/3}}{1-(1-\alpha_t)^{1/3}} \tag{3}$$

$$R_3=K_3(1-\alpha_t)^{N_3} \tag{4}$$

$$f_{w/c}=\left(1+4.444*\left(\frac{w}{c}\right)-3.333*\alpha_t\right)^4 \tag{5}$$

where, R_j represents the hydration rate of different clinkers, α_t represents the hydration rate of different clinkers, K_1 , K_2 , K_3 , N_1 , N_2 and N_3 represent the hydration parameters, and $f_{w/c}$ is the water-cement ratio factor.

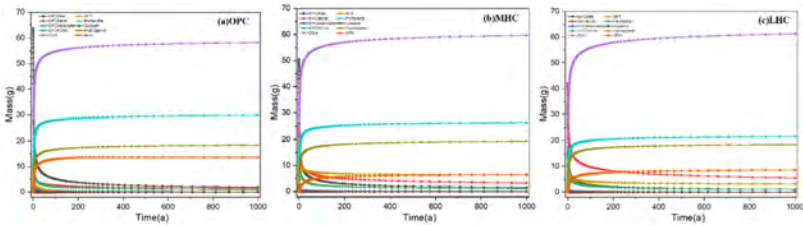


Fig. 1
Development of Hydration Products over 1000 Days of Hydration for Three Types of Cement with a Water-Cement Ratio of 0.5: (a) OPC Hydration, (b) MHC Hydration, (c) LHC Hydration.

3. LEACHING SIMULATION

The leaching simulation is based on the principle of mass conservation and uses thermodynamic simulation as the initial condition. The calculation is based on the mass conservation of calcium ions, with the primary governing equation given by Equation (6) [6]. The flux of calcium ions is determined by Equation (7) [7]. The diffusion coefficient of calcium ions, which varies with changes in the pore structure, can be determined by Equation (8) [8]. During the leaching process, as hydration products dissolve, the porosity of calcium ions also changes. Therefore, Equation (10) is used to calculate the development of calcium ion porosity as material dissolution progresses. Throughout the leaching process, the calcium ions in the concrete pore solution and the solid phase calcium follow solid-liquid conservation, which can be divided into three stages: the leaching of calcium hydroxide, the decalcification of C-S-H gel, and the transformation of C-S-H gel into silica gel. The overall process is governed by Equation (11) [9].

$$\frac{\partial \theta C_{al}}{\partial t} + \frac{\partial \theta C_{as}}{\partial t} = \text{div} F_{ca} \quad (6)$$

In the equation, θ represents the porosity of the concrete, C_{a1} represents the calcium ion concentration in the pore solution, C_{as} represents the calcium ion concentration in the solid phase, and F_{ca} represents the diffusion flux of calcium ions.

$$F_{ca} = - \left(\frac{\theta \delta D_{Ca}}{\tau} \right) \nabla C_{aliquid} \quad (7)$$

In the equation, δ represents the pore blockage factor, τ represents the tortuosity of the pores, and L_{Ca} represents the calcium ion diffusion coefficient.

$$L_{Ca} = [0.001 + 0.07\theta_c^2 + 1.8H(\theta_c - \theta_0)(\theta_c - \theta_0^2)]d_0 \quad (8)$$

In the equation, θ_c represents the initial porosity, θ_0 is set as 18%, d_0 is the initial calcium ion diffusion coefficient, and H is determined according to Equation (9).

$$H(x) = \begin{cases} 1, & x > 0 \\ 0, & x \leq 0 \end{cases} \quad (9)$$

$$\theta(x, t) = \theta(x, 0) + \frac{M_{CH}}{\rho_{CH}} [Q_{CH}(x, 0) - Q_{CH}(x, t)]$$

In the equation, $\theta(x, 0)$ represents the initial porosity, M_{CH} is the relative molecular mass of calcium hydroxide, ρ_{CH} is the density of calcium hydroxide, $Q_{CH}(x, 0)$ is the initial concentration of calcium hydroxide, and $Q_{CH}(x, t)$ is the

concentration of calcium hydroxide in the solid.

$$Ca_{solid} = \begin{cases} C_{CSH} \left(\frac{Ca_{liquid}}{Ca_{satu}} \right)^{\frac{1}{3}} \left(-\frac{2}{\partial^3} Ca_{liquid}^3 + \frac{3}{\partial^2} Ca_{liquid}^2 \right) & 0 \leq Ca_{liquid} \leq x_1 \\ C_{CSH} \left(\frac{Ca_{liquid}}{Ca_{satu}} \right)^{\frac{1}{3}} & x_1 \leq Ca_{liquid} \leq x_2 \\ C_{CSH} \left(\frac{Ca_{liquid}}{Ca_{satu}} \right)^{\frac{1}{3}} + \frac{C_{CH}}{(Ca_{satu} - \beta)^3} (Ca_{liquid} - \beta) & x_2 < Ca_{liquid} \end{cases} \quad (10)$$

Based on the above equations and the material parameters after 1000 days of cement hydration, the finite difference method was used to calculate the product distribution for 100 years of leaching for the three types of cement. Taking the distribution of C-S-H, calcium hydroxide, and ettringite as examples, the predicted results are shown in Figure 2. The leaching fronts of the three hydration products decrease in the order of OPC, MHC, and LHC, indicating that LHC has the best leaching resistance, followed by MHC, and OPC is the least resistant. Defining the leaching front of calcium hydroxide as the leaching depth, it is found that after 100 years, OPC has leached to a depth of 2.4 cm, MHC to 2.2 cm, and LHC to 2.0 cm. The leaching depth development of medium/low heat cement is significantly lower than that of ordinary Portland cement.

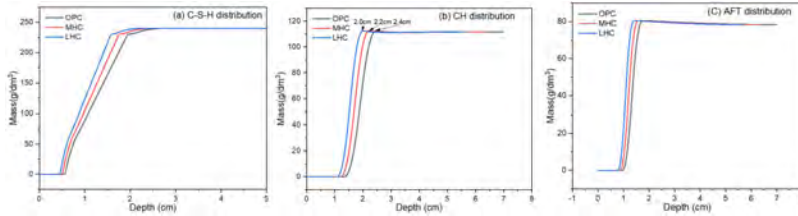


Fig. 2

Distribution of Products After 100 Years of Leaching for Three Types of Cement as a Function of Depth: (a) Depth Distribution of C-S-H, (b) Depth Distribution of CH, (c) Depth Distribution of Ettringite.

4. CONCLUSION

This study utilized the thermodynamics and kinetics of cement hydration, using GEMS software to calculate the long-term hydration of medium/low heat cement, with comparisons made to ordinary Portland cement (OPC). Based on the hydration simulation results, coupled hydration-leaching calculations were

performed. The partial differential equation module of Comsol was used for the leaching simulation to assess the long-term leaching of dam concrete. The results indicate that after 1000 days of hydration, the C-S-H content increased and the calcium hydroxide content decreased in OPC, MHC, and LHC, with LHC showing the greatest hydration potential. After 100 years of leaching, OPC leached to a depth of 2.4 cm, MHC to 2.2 cm, and LHC to 2.0 cm. The leaching fronts of C-S-H, calcium hydroxide, and ettringite decreased across OPC, MHC, and LHC, indicating that LHC has the best leaching resistance.

REFERENCES

- [1] GÉRARD, B., C. LE BELLEGO, AND O. BERNARD, Simplified modelling of calcium leaching of concrete in various environments. *Materials and Structures*, 2002. 35(10): p. 632–640.
- [2] LOTHENBACH, B. AND F. WINNEFELD, Thermodynamic modelling of the hydration of Portland cement. *Cement and Concrete Research*, 2006. 36(2): p. 209–226.
- [3] PARROT, L. Prediction of cement hydration. in *Proceedings of the British Ceramic Society*. 1984.
- [4] LOTHENBACH, B., ET AL., Cemdata18: A chemical thermodynamic database for hydrated Portland cements and alkali-activated materials. *Cement and Concrete Research*, 2019. 115: p. 472–506.
- [5] WANG, L., ET AL., Environmental evaluation, hydration, pore structure, volume deformation and abrasion resistance of low heat Portland (LHP) cement-based materials. *Journal of Cleaner Production*, 2018. 203: p. 540–558.
- [6] ZENG, H., ET AL., Performance evolution of low heat cement under thermal cycling fatigue: A comparative study with moderate heat cement and ordinary Portland cement. *Construction and Building Materials*, 2024. 412.
- [7] ISHIDA, T. AND K. MAEKAWA, AN INTEGRATED COMPUTATIONAL SYSTEM OF MASS/ENERGY GENERATION, TRANSPORT AND MECHANICS OF MATERIALS AND STRUCTURES. *Doboku Gakkai Ronbunshu*, 1999.
- [8] GARBOCZI, E.J. AND D.P. BENTZ, Computer simulation of the diffusivity of cement-based materials. *Journal of Materials Science*, 1992. 27(8): p. 2083–2092.
- [9] WAN, K., L. LI, AND W. SUN, Solid–liquid equilibrium curve of calcium in 6mol/L ammonium nitrate solution. *Cement and Concrete Research*, 2013. 53: p. 44–50.

COMMISSION INTERNATIONALE DES
GRANDS BARRAGES

VINGT-HUITIEME CONGRES DES
GRANDS BARRAGES
CHENGDU, MAI 2025

EXPERIENCES AND LESSONS FROM GROUTING OF DEEP OVERBURDEN DAM FOUNDATION UNDER HIGH WATER HEAD (*)

Bifeng WANG

Deputy Chief Engineer, Sinohydro Foundation Engineering Co., LTD

Fangcai XU

Deputy Manager, Sinohydro Foundation Engineering Co., LTD,

Minghua ZHAO

Deputy Chief Engineer Sinohydro Foundation Engineering Co., LTD

Yushu TANG

Deputy Chief Engineer, Sinohydro Foundation Engineering Co., LTD

CHINA

SUMMARY

A clay core rockfill dam with a overburden foundation depth of 148m, as seepage control system, a suspended concrete cutoff wall with a depth of 110m is installed in the riverbed section, overburden grouting and rock grouting are performed under the cutoff wall; while in the slope section of both banks, rock grouting or rock grouting under the cutoff wall are performed. 4 rows of overburden grouting was designed at the beginning, but unfortunately, 2 rows of overburden grouting was performed finally due to various reasons. After impoundment, water seepage pressure at partial section is higher than normal, and water seepage discharge, water and sand gushing, subsidence in the river course are observed in the

**Expériences et leçons tirées de l'injection de coulis dans les fondations de barrages sous forte charge et avec des hauteurs d'eau importantes*

downstream area. It takes 10 years for the seepage defects repair, not only drainage works for pressure relief are performed for the area where water seepage is abnormal, but also five stages of reinforcement grouting works are performed totally. The first four stages are not comprehensive and weak targeting, and the drilling and grouting technology, grouting slurry etc. are not entirely suitable for the complicated geological condition. Although grouting result is not satisfactory, but a lot of experience has accumulated and the main leakage passage is targeted accurately. Based on the experience from the first four stages of reinforcement grouting, the drilling and grouting technology, grouting slurry are comprehensively improved for the fifth stage, including newly designed orifice-closed device, Barite Powder Weighted Mud, Silica sol (HSS), HSC and HPSC paste grouting slurry etc. The water seepage control of deep overburden is finally achieved successfully under 60 high water head. This example shows that the quality of seepage control works is critical for dam foundation before impoundment, not only for design but also for construction. The cost is too much if remedial measures are taken after impoundment.

RÉSUMÉ

Pour un barrage en enrochement à noyau d'argile avec une profondeur de fondation de 148 m, un voile d'injection d'une profondeur de 110 m est construit dans le lit de la rivière afin de contrôler les infiltrations. L'injection des morts-terrains et l'injection des roches sont effectuées sous le voile d'étanchéité tandis que sur les deux rives, l'injection des roches ou l'injection des roches sous le mur de séparation sont effectuées. L'injection de 4 rangs de morts-terrains a été conçue au départ, mais malheureusement, 2 rangs de morts-terrains ont finalement été réalisés pour diverses raisons. Après la mise en eau, la pression d'infiltration d'eau dans la section partielle est supérieure à la normale, et l'on observe dans la zone en aval une décharge d'infiltration d'eau, des jaillissements d'eau et de sable, et un affaissement du cours de la rivière. Il faut 10 ans pour réparer les défauts d'infiltration. Non seulement des travaux de drainage pour soulager la pression sont effectués dans la zone où l'infiltration d'eau est anormale, mais aussi cinq étapes de travaux d'injection de renfort sont effectuées. Les quatre premières étapes ne sont pas complètes et ne ciblent pas les problèmes, et la technologie de forage et d'injection, la boue d'injection, etc. ne sont pas entièrement adaptées aux conditions géologiques compliquées. Bien que le résultat de l'injection ne soit pas satisfaisant, de nombreuses expériences ont été accumulées et la principale zone de passage des fuites est ciblée avec précision. Sur la base de l'expérience des quatre premières étapes d'injection de renforcement, la technologie de forage et d'injection et la boue d'injection sont améliorées de manière exhaustive pour la cinquième étape, y compris un dispositif de fermeture d'orifice nouvellement conçu, de la boue pondérée à la poudre de barytine, de la solubilité de silice HSS, de la boue de pâte HSC et HPSC, etc. Le contrôle d'écoulement d'eau de la surcharge profonde est finalement réussi sous 60 m de hauteur d'eau élevée. Cet exemple

montre que la qualité des travaux de contrôle des écoulements est critique pour la fondation du barrage avant la mise en eau, non seulement pour la conception mais aussi pour la construction. Le coût est trop élevé si des mesures correctives sont prises après la mise en eau.

1. GENERAL DESCRIPTION

A hydro-power station with a capacity of 920MW is located in Dadu River in South-west of China. The main function of this station is for electric power generation, and the storage capacity of reservoir is 240 million cubic meter. The multi-purpose structure consists of clay core rockfill dam, spillway tunnel, diversion tunnel and power house. The maximum height of the dam is 79.5m.

Cutoff wall was started in Dec. 2008, and completed in Apr. 2010. Curtain grouting of dam foundation was completed in Jun. 2011. Impoundment in stages was started after flood in 2011. Abnormal water seepage at dam foundation emerged in 2013, and reinforcement grouting was performed from 2013 until significant results was achieved in 2022, the safety hazards of dam foundation was eliminated finally.

2. GEOLOGICAL CONDITIONS

The average depth of the overburden is 120~130m with a maximum depth of 148.6m. It is composed of:

- ④ boulders and gravel (high water permeability, $k=5.08 \times 10^{-2}$ cm/s $\sim 4.09 \times 10^{-1}$ cm/s)
- ③-2 gravel and sand
- ③-1 boulders and gravel, gravelly soil (medium to high water permeability, $k=3.96 \times 10^{-4}$ cm/s $\sim 9.07 \times 10^{-2}$ cm/s)
- ②-3 silty sand and silt
- ②-2 gravel and gravelly soil (medium to high water permeability $k=3.06 \times 10^{-4}$ cm/s $\sim 1.92 \times 10^{-2}$ cm/s)
- ②-1 boulders and gravel (medium to high water permeability $k=3.06 \times 10^{-4}$ cm/s $\sim 1.92 \times 10^{-2}$ cm/s)
- ① boulders and gravel (medium to high water permeability $k=3.06 \times 10^{-4}$ cm/s $\sim 1.92 \times 10^{-2}$ cm/s)

In right dam abutment, there are collapse and slope accumulation block gravel soil with a depth of several meters, ③-1 boulders and gravel, gravelly soil and ②-2 gravel and gravelly soil, all with medium to high water permeability.

Generally, there are possibility of concentrated seepage, piping failure, and seepage control stability of the overburden is poor as a whole. See Figure 1.

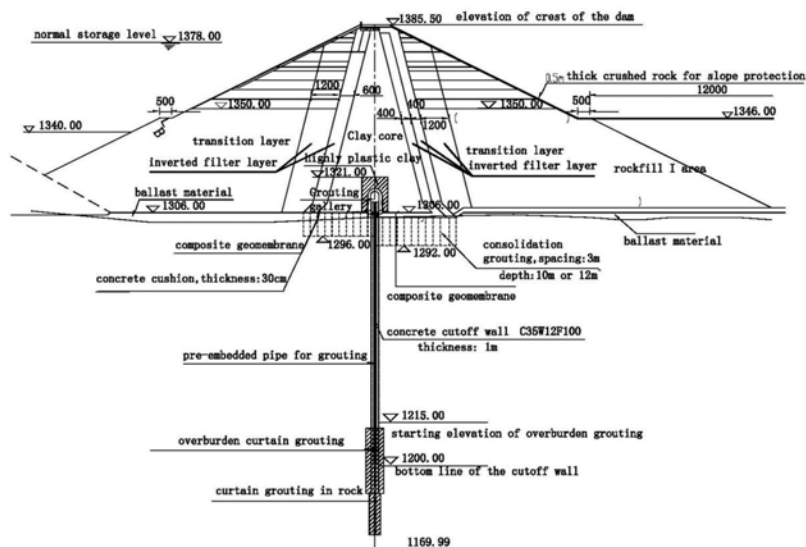


Fig. 1
Typical longitudinal section of the dam foundation

The bedrock at river valley is diorite. The water permeability of the surface bedrock at dam abutments on both banks is medium to high ($q \geq 10 \sim 100\text{Lu}$), while weak permeable at river valley with a permeability of $q=1 \sim 10\text{Lu}$. There are seepage paths from the abutment to the valley.

3. DESIGN OF SEEPAGE CONTROL OF DAM FOUNDATION

The system consists of concrete cutoff wall with curtain grouting under cutoff wall, and a grouting gallery with a dimension of $3.5\text{m} \times 4.5\text{m}$ is installed between the top of cutoff wall and the bottom of the clay core. The elevation of the base slab of grouting gallery is 1310.5m. 4 rows of PVC pipe with a diameter of 110mm are embedded along the axis of dam for further curtain grouting works under cutoff wall. See Figure 2.

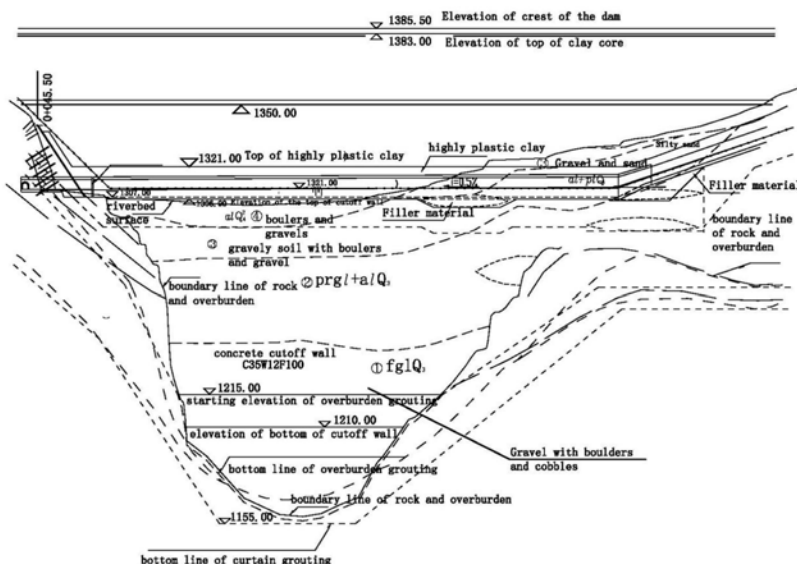


Fig. 2
Typical cross section of the dam foundation

The length of seepage control system is 751.5m with a chainage of 0+096.50m~0+655.00m from the left bank to right bank, including curtain grouting of grouting gallery in left bank (chainage No. 0+096.00m~0+077.00m), curtain grouting under cutoff wall (chainage No. 0+077.00m~0+526.33m), and curtain grouting of grouting gallery in right bank (chainage No. 0+526.00m~0+655.00m).

The length of axis of the cutoff wall is 449.33m, the cutoff wall with a thickness of 1.0m is embedded into the bedrock 1.0m at both banks, while in the river course section, the cutoff wall is suspended in the overburden with a depth of 110m, the elevation of the top and bottom of the cutoff wall is 1310.00m and 1200.00m. Reinforcement cage with a height of 8m is installed at the top area of the cutoff wall.

Four rows of curtain grouting is designed in riverbed section, in which 2 rows of curtain grouting in cutoff wall with a row spacing of 0.6m, and a hole spacing of 1.5m or 2.0m. The depth of grouting holes depends on the boundary line between the overburden and the bedrock, normally, 10m into the bedrock (water permeability less than 3Lu).

1 row of curtain grouting with a hole spacing of 1.5m or 2.0m are designed in the upstream and downstream of the cutoff wall respectively, the row distance to the grouting holes in the cutoff wall is 0.8m. The depth of grouting holes depends on the

boundary line between the overburden and the bedrock, normally, 5m into the bedrock (water permeability less than 5Lu). The first grouting stage started from 15m higher than the bottom line of the cutoff wall.

1 row of curtain grouting is arranged from the chainage No.0-096.00m~0-065.00m and 0+605.00m~0+655.00m, with a hole spacing of 2m, the grouting holes will be drilled into the rock with a water permeability of less than 3Lu. 2 rows of grouting holes with a row spacing of 1.2m and a hole spacing of 2m are designed for the remaining chainages.

The extent of curtain grouting from dam abutment to rock mass is determined by seepage calculation results, that is 90.5m from left abutment, and 123.05m from right abutment, but they all doesn't reach relatively impermeable rock layers or ground water.

Only two rows of curtain grouting in the cutoff wall were performed before impoundment due to various reasons, the grouting holes in the upstream and downstream of cutoff wall was canceled.

The quality requirements for cutoff wall: the compressive strength $R_{28} \geq 25\text{MPa}$; $R_{90} \geq 25\text{MPa}$; $R_{180} \geq 25\text{MPa}$; and the elastic modulus $E_{28} \leq 30\text{GPa}$; $E_{180} \leq 35\text{GPa}$. The water permeability should be less than 0.1Lu by water pressure test of check holes in the cutoff wall.

The quality requirements for curtain grouting works: the water permeability of check holes for grouting holes (in the rock section) in the cutoff wall should be less than 3Lu; for grouting holes (in the rock section) outside of the cutoff wall should be less than 5Lu; the water permeability of check holes in the overburden section should be less than 10Lu. Acceptance rate should be more than 90% and the unqualified value should be less than 150% of the criteria above.

4. CONSTRUCTION OF SEEPAGE CONTROL WORKS

4.1. EXECUTION OF CUTOFF WALL

The construction duration is from Dem. 2008 to Apr. 2010, the total area of cutoff wall is 37,889m².

4.1.1. *Trench excavation*

For trenches with a depth more than 100m, "percussion and grab" method and "percussion and chopping" method are combined for trench excavation. The

percussion rigs CZ-A、CZ-9 was used for the drilling of main hole (the first bite), the upper part of second bite between main holes was grabbed by HS843HD and HS855HD grab (depth less than 90m), the remaining was chopped by percussion rig or chisels.

4.1.2. *Supporting slurry and trench cleaning*

Clay slurry was used for excavation of main hole, bentonite mixed with clay slurry was chosen for excavation of the second bite between main holes, MMH mud for poor geological sections. The performance of slurry meets the specification requirements. "Air lifting " method was used for trenching cleaning.

4.1.3. *Installation of reinforcement cage and grouting pipe*

The fabrication and dimension of reinforcement cage meets the specification requirements, and be installed into the trench according to design. Spacers are fixed on the reinforcement cage to ensure the thickness of concrete cover. Grouting pipes are positioned in place by steel frame.

4.1.4. *Concreting and connection of panels*

Concrete with a slump of 18cm~22cm and a diffusivity of 34cm~40cm was placed into the excavated trench by tremie method. The primary panels and the secondary panels are connected by stop end (Steel joint pipe).

4.1.5. *Quality inspection*

1. Concrete quality

During concreting, concrete samples were taken for standard curing in curing room. These samples will be tested after different ages. The test results of compressive strength, elastic modulus, impermeability and frost resistance etc. are shown as Table 1.

In addition, coring in the cutoff wall and water pressure test were conducted after completion of the cutoff wall. 9 check holes with a total length of 502.21m were drilled, the core recovery rate is 100% with a maximum core length of 6m, the surface of the core is smooth without voids and pits. 90 water pressure tests were performed with a maximum permeability of 0.09 Lu (within the specification 0.1Lu) . The average compressive strength of the core sample is 45.2MPa, with a maximum value of 55.6MPa and a minimum value of 38.9MPa.

Table 1
Results of concrete performance

Items	Compressive strength (MPa)			Elastic modulus (GPa)		Impermeability level	Frost resistance level
	28d	90d	180d	28d	180d	28d	180d
Specification	≥ 25	≥ 30	≥ 35	≤ 30	≤ 35	≥ W12	≥ F100
Max. value	41.3	39.6	47.5	36.1	38.2	≥ W12	≥ F100
Min. value	24.7	30.6	36.1	26.3	34.3		
Average value	41.3	34.6	41.0	29.9	35.7		
Standard deviation (σ)	5.41	6.20	5.52	/	/	/	/
Strength assurance rate (%)	99.0	100	100	/	/	/	/
Pass rate (%)	99.0	100	100	100	100	100	100

4.2. CONSTRUCTION OF CURTAIN GROUTING

4.2.1. Drilling and grouting method

The grouting holes were drilled by geological drill rig XY-2、XY-2PC for rock , and drill rig with casingYD-90A for overburden, after the hole was drilled to the stage to be grouted, Φ91mm PVC pipe was installed into the hole, and the cement grout was injected into the space between the hole and the PVC pipe.

The orifice-closed grouting method (a grouting method without packer only used in China) was adopted for all grouting works. The orifice closing device is installed at the top of the hole, drilling the hole with downstage method, after completion of the grouting of first stage, drill the hole again to the next stage, and grouting continuously until the completion of the grouting holes.

The hole inclination is higher than the requirements in the Specification.

The drilling and grouting works were conducted by three rows, from downstream row to upstream row; and grouting holes in the same row were drilled and grouted by three sequences, firstly primary holes, then secondary holes and tertiary holes. The grouting equipment were 3SNS type grouting pump, ZJ400 high-speed mixer and grouting recorder GMS 2007L.

The grouting cement is OPC with a strength of 42.5MPa. Cement clay grout with water-solid ratios of 4:1、 3:1、 2:1 and 1:1 was used for overburden grouting, the mix ratio of the cement clay grout in the centralized mixing plant was water:

cement:clay=1.6:1:0.6. As for rock grouting, cement grout with six ratios i.e. 5:1、3:1、2:1、1:1、0.8:1、0.5:1 was adopted.

The maximum grouting pressure is 3.5MPa for rock, as for overburden grouting, the maximum grouting pressure is 2.5MPa for primary holes, while 2.9MPa for secondary holes. The criterion for termination of grouting is as follows:

After the grout take has become no more than 1L/min at the maximum design grouting pressure, the grouting injection will be continued for 60min.

4.2.2. *Grouting results*

The total grouting quantities are 34,935m, and with average grout take 132.87kg/m (including cement and clay). the grout take is relatively low at the chainage of 0+105m~0+250m for overburden grouting works.

4.2.3. *Quality inspection of grouting works*

69 check holes with 679 water pressure tests were performed for the curtain grouting of dam foundation and dam abutments. The permeability are satisfied with the specified standards, which is no more than 3Lu, 5Lu and 10Lu respectively for different chainages.

5. WATER SEEPAGE AND TREATMENT MEASURES AFTER IMPOUNDMENT

5.1. BRIEF INTRODUCTION OF WATER SEEPAGE AND TREATMENT MEASURES

Initial impoundment was conducted in Aug. 2011, the water seepage is measured as 500L/s at flow-measuring weir behind the cutoff wall, and the values of 3 piezometers were unusually high.

The first stage reinforcement grouting (first half) was conducted from Mar. 2012 to Oct.2012, the working scopes include the downstream curtain of the cutoff wall, and the connection of primary panel and the secondary panel at steep rock section. the water seepage is measured as 400L/s at flow-measuring weir behind the dam in Dec. 2012.

The water inrush occurred in Mar. 31, 2013 at the slope toe of right bank, downstream of the dam. The elevation is 1306m, the distance is 448m to the axis of the dam and 200m to dam toe. The initial water seepage is 5L/s. The water seepage

area collapsed in Apr. 15, 2013, and the water seepage with dark gray fine particles increased to 200L/s. Emergency reverse pressure filtration was conducted on the water inrush area in Apr. 18, 2013.

The first stage reinforcement grouting (second half) with a chainage No. of 0+250m~0+288m was conducted from Apr. 2013 to Jun. 2013. Pressure relief works (including drainage hole) at the water inrush area were performed at the end of Aug. 2013.

The second stage reinforcement grouting with a chainage No. of 0+235m~0+285m was conducted from Jul. 2014 to Feb. 2015, the grouting holes are located at the cutoff wall and downstream of the cutoff wall.

The third stage reinforcement grouting with a chainage No. of 0+250m~0+256m was conducted from Aug. 2015 to May. 2016, the grouting holes are located at the strong permeable zone.

The fourth stage reinforcement grouting with a chainage No. of 0+220m~0+280m was conducted from Jul. 2017 to Jul. 2018. The water seepage is measured as 267.96 L/s at flow-measuring weir behind the dam in Sep. 2018, while 49.76 L/s at water inrush area.

The fifth stage reinforcement grouting with a chainage No. of 0-95.6m~0+64m and 0+100.0m~0+220.0m was conducted from Sep. 2020 to Dec. 2021.

5.2. THE REINFORCEMENT GROUTING WORKS

The five stage reinforcement grouting works and water seepage results are shown as Table 2. There are total drilling length 83,002.11m, grouting length 58,479m.

Due to complicated geological conditions, lack of newly improved grout technologies (such as HSC, HPSC, HSS etc.), drilling and grouting under 60m high water head and unclear positioning of water leakage, after the completion of 4 stages reinforcement grouting, the overall seepage control effect is not significant and the water seepage and pressure are not satisfied with the anticipated design value.

But after the completion of the fifth stage reinforcement grouting, significant achievement has been made and the water seepage is finally controlled.

Table 2
The reinforcement grouting quantities and water seepage

Stages	Period	Chainage No.	Hole arrangements	Grouting method and grouting pressure	Quantities (m)	Water seepage(L/s)	
						Before grouting	After grouting
First stage (first half)	2012.3~2012.10	0+80.0~0+250.3, 0+288.0~0+310.0	Single row, hole spacing:1.5~2m, hole depth: 95.81~160.2m	orifice-closed grouting method Maximum grouting pressure: 3MPa	Drilling: 14095 Grouting: 13542	450 (behind the dam)	365 (behind the dam)
First stage (second half)	2013.4~2013.6	0+250.0~0+288.0	Same as above	Same as above	Drilling and grouting 1508	360 (behind the dam)	349 (behind the dam)
Second stage	2014.7~2015.2	0+235.0~0+285.0	Double row Row spacing:1.2m Hole spacing:1.2m hole depth: 66.2m~121.2m	orifice-closed grouting method Maximum grouting pressure: 3.5MPa	Drilling: 7604 Grouting: 4927	292 (behind the dam) 209 (downstream)	273 (behind the dam) 104 (downstream)
		0+38.0~0+77.0	Single row, hole spacing: 1.2m, hole depth: 41.2~44.5m	Same as above	Drilling: 1474 Grouting: 1385		
Third stage	2015.8~2016.5	0+250.0~0+256.0	Double row Row spacing:1.2m Hole spacing:1.2m Hole depth: 110m~120m	Same as above	Drilling: 1744 Grouting: 1097	285 (behind the dam) 121 (downstream)	273 (behind the dam) 108 (downstream)
Fourth stage	2017.7~2018.8	0+220.0~0+280.0	Double row Row spacing: 0.6m Hole spacing: 1.2~2m hole depth: 60m~153m	Sleeve grouting method for over-burden Maximum grouting pressure: 5MPa	Drilling: 12652 Grouting: 6428	268 (behind the dam) 80 (downstream)	273 (behind the dam) 61 (downstream)
Fifth stage	2020.9~2021.12	0+95.6~0+64.0 0+100.0~0+220.0	Double row Row spacing: 0.6~1.5m Hole spacing: 1.5~2m hole depth: 40m~172m	Sleeve grouting method for over-burden Maximum grouting pressure: 4.5MPa	Drilling: 43924 Grouting: 29592	154 (behind the dam) 47 (downstream)	13 (behind the dam) 0 (downstream)

5.3. THE FIFTH STAGE REINFORCEMENT GROUTING WORKS

Based on the information provided by monitoring results from the beginning of the impoundment, and the experience from the first four stages reinforcement grouting works, the main seepage path is targeted at the alluvium stratum under the

cutoff wall. To ensure the success of seepage control, a serial of new technologies are developed, including drilling and grouting technology, grout slurry etc.

5.3.1. *Working scope and layout of the drilling hole*

The working scope for the fifth reinforcement grouting included overburden grouting with a chainage No. of 0+100m~0+220m and bedrock grouting at left bank with a chainage No. of 0-95.60m~0+64.00m. Three rows of grouting holes for chainage No. of 0+100m~0+220m, in which 2 rows in the embedded pipes in the cutoff wall and 1 row in the downstream of the cutoff wall.

1 row of grouting holes with hole spacing of 2m for bedrock grouting with a chainage no. of 0-96.50m~0+0.00m, while 2 rows of grouting holes with row distance of 1.5m, and hole spacing of 2m for chainage no. of 0+0.00m~0+64.00m.

5.3.2. *Drilling technology*

1. To solve the problem of water and sand influx during the drilling process, special orifice-closed device is designed and manufactured for the drilling works, which is shown as Figure 3 (Chinese Patent No.: ZL2020 1 0365373.4).
2. To solve the problem of collapse during the drilling process, special Barite Powder Weighted Mud is developed for the drilling works. The main components is as follows: Barite Powder, Plant gum and Surfactant etc. The performance of the mud is shown as Table 3.

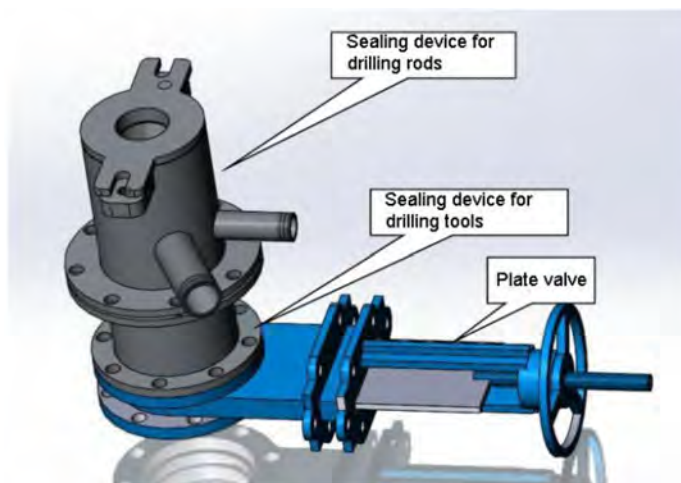


Fig. 3
special orifice-closed device

In general, although some holes are drilled by down-stage method with grouting in case of collapse, but the application of orifice-closed device and Barite Powder Weighted Mud makes the drilling works through the alluvium stratum and installation of casing under 60m water head very successful, and makes the installation of sleeve pipe very smooth for further grouting.

Table 3
Performance of Barite Powder Weighted Mud

Description	Density (g/mL)	Diffusance (mm)	Viscosity (mPa.s)	Yield point/plastic viscosity
Barite Powder Weighted Mud	1.8~2.0	165~180	20.0~35.0	0.3~0.5

5.3.3. Grout slurry

Different grout slurries are selected for different geological conditions, which is as following:

1. Cement grout

The Portland cement grout is used for rock grouting, the water cement ratio is 5:1、3:1、2:1、1:1、0.8:1、0.5:1.

2. HSC Anti-Washout and rapid hardening grout paste

The main components of HSC are sulphotoaluminate cement and accelerating admixture, which is mixed with two kinds of water cement ratio of 0.8:1 and 0.6:1. HSC grout slurry with characteristic of rapid hardening and adjustable setting time, is used for general leakage passage.

3. HSPC non-dispersible underwater, Anti-Washout and rapid hardening grout paste

HSPC, the key material for successful seepage control, is mixed by HSC (water cement ratio of 0.6:1) with special flocculants. It has characteristic of rapid hardening, non-dispersible underwater and Anti-Washout, mainly used for comparatively larger leakage passage. The properties of the HPSC grout paste are shown as Table 4 and Figure 4.

4. Cement-Sodium Silicate Slurry

Cement-sodium silicate slurry is made by cement grout with a water cement ratio of 0.5:1 and sodium silicate (volume ratio of 15% cement grout), the cement grout and sodium silicate are separately injected and mixed in the hole. It is mainly used for large leakage passage with high speed of flowing water, such as the front line of grouting holes at the upstream of cutoff wall. In view of poor durability of cement-sodium silicate, the total amount of cement-sodium silicate used account for 6.1% only of total grouting works for alluvium stratum at the river section.

Table 4
The properties of the HPSC grout paste

Performance	Density (g/L)	Diffusivity (mm)	Time of loss of fluidity (min)	Setting time (min)		Rheological parameters	
				Initial setting	Final setting	Yield strength (kpa)	Plastic viscosity (mPa·s)
Rapid hardening and erosion control	1.6~1.7	120~140	40~50	60~70	70~80	20~25	300~350



Fig. 4
HSPC non-dispersible underwater, Anti-Washout and rapid hardening grout paste

5. HSS new type of nano solution (colloidal silica sol)
- HSS new type of nano solution is developed specially for the grouting of sand stratum (Chinese Patent No.: ZL2020 1 0365373.4). HSS is a kind of chemical grout with low viscosity, adjustable setting time, low permeability, non-toxic and good durability. It is used for the grouting of multilayer sand lens with a depth of 90~130m. HSS is composed of solution A and solution B, and mixed together on site.

Solution A: Silica solution+Silane crosslinker+accelerator promoter

Solution B: Hydroxyl curing agent

The properties of the HSS new type of nano solution are shown as Table 5 and Figure 5.

Table 5
The properties of HSS new type of nano solution

Items	Properties	Test conditions
Viscosity(mPa·s)	1.00~10.00	20°C
pH value	3.0~14.0	Slurry
Density (g/cm ³)	1.000~1.300	Depending on the mount of hardener
Appearance	Colorless, uniform, transparent liquid	Slurry
Flavor	No flavor	Slurry
Gelation time	3min~180min	Depending on the mount of hardener
Compressive strength (MPa)	0.3~1.5	Cubic sand sample
Permeability(cm/s)	$10^{-10} \sim 10^{-7}$	Cubic sand sample
Anti-extrusion gradient	≥ 300	/

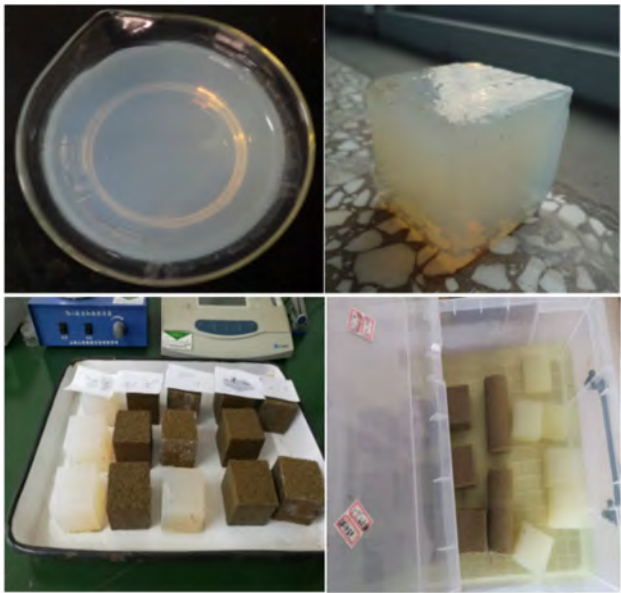


Fig. 5
HSS new type of nano slurry (Gel and cubic sand sample)

5.3.4. *Grouting technology*

1. grouting equipment

High pressure screw pump with maximum grouting pressure of 6MPa, and maximum displacement of 60L/min, is selected for grout paste with high yield strength and high viscosity.

2. grouting technologies

Sleeve grouting method is adopted to replace the orifice-closed grouting method (traditional down-stage grouting method in China) for overburden grouting works.

As mentioned above, based on the experience from the first four stages of reinforcement grouting, the drilling and grouting technology, grouting slurry are comprehensively improved for the fifth stage, The water seepage control of deep overburden under 60 high water head is finally achieved successfully.

5.3.5. *Quality inspection*

8 check holes are drilled along the axis of grouting line, and cement stones are found in the samples from different depths. Core recovery is 75% for sand stratum, while 80% for alluvium stratum below 130m.

The Lugeon test results: less than 10Lu for alluvium stratum; less than 5Lu for curtain grouting of shallow rock and 3Lu for curtain grouting of deep rock, which are satisfied with design requirements.

The grout take for 4 check holes for overburden area at river section is 22.3kg/m~72.2kg/m, while 21.86kg/m for check holes for rock grouting at left bank.

6. WATER SEEPAGE OF DAM FOUNDATION AFTER THE FIFTH STAGE REINFORCEMENT GROUTING

After the fifth stage reinforcement grouting, the water seepage at measuring weir behind the dam and water inrush area at downstream of the dam decreases from 154.21L/s, 46.97L/s to 13.32L/s, 0L/s separately. The detail is shown as Table 6.

Table 6

Water seepage results of dam foundation after the fifth stage reinforcement grouting

Date	Reservoir level (m)	Water seepage (L/s)	
		Measuring weir behind the dam	Water inrush area at downstream of the dam
2020-9-16	1377.52	154.21	46.97
2020-12-4	1375.65	148.37	40.23
2021-6-24	1376.59	115.10	20.14
2021-11-24	1376.10	23.12	3.22
2022-2-9	1374.82	13.32	0

7. EXPERIENCES AND LESSONS

1. For seepage control of deep overburden dam foundation, there are successful cases in China, such as Xiabandi multi-purpose water control project in Xinjiang Uygur Autonomous Region. The overburden depth of dam foundation is 149m, a cutoff wall with a depth of 85m combined with 4 rows of overburden grouting works of 60m under the cutoff wall were designed and performed, which proved to be successful until now. So it is feasible for the design of combination of upper cutoff wall with curtain grouting under the cutoff wall. As for this project, it is necessary and proper to design 4 rows of overburden grouting hole, but unfortunately, only 2 rows of grouting holes in the cutoff wall were carried out due to various reasons. The total drilling and grouting quantities for five stages reinforcement grouting works is 83002.11m and 58479m, which is 1.7 times of that before impoundment. To this mistake resulted in a intensive cost.
2. The orifice-closed grouting method (traditional down-stage grouting method in China) was used for overburden and bedrock grouting works before impoundment, with cement grout and cement-clay grout, the completed grouting quantities is 34,935m with a average grout take of 132.87kg/m (including cement and clay). but as mentioned above, the grouting quantities are "optimized" from 4 rows to 2 rows, which proved to be the main reason of abnormal water seepage.

This also raises another question, the "optimized" curtain grouting is imperfect, why are the results of the check holes satisfied with the design requirements? Is there an issue with inspection techniques and methods, or Inspection mechanism, or both?

3. From the experiences of previous 4 stages reinforcement grouting, Significant results have been achieved after the completion of the fifth stage reinforcement grouting. The Main reasons of the success are:
 - water leakage way and work scope were targeted accurately.
 - b) newly improved construction equipment and technologies, newly developed many kinds of targeted grout, such as HSC, HPSC, HSS etc. for overburden drilling and grouting under high water head, Which is relatively insufficient for previous 4 stages reinforcement grouting.
4. It takes 10 years and intensive cost for the reinforcement grouting works. This case gives profound lessons as follows: the seepage control of the dam foundation is the lifeline of the dam, it should attach much importance to the design and construction with careful and discreet attitude. Try to do the best on the line with clear cost for seepage control works before impoundment, and you may yield twice the result with half the effort; otherwise, it will be very difficult to mend the fold after a sheep is lost after impoundment, and you will just get half the results with double the effort.

REFERENCES

- [1] ZHANG JINGXIU, *Seepage control for dam foundation and grouting technology*. Beijing: China Water&Power Press, 2002 (in Chinese)
- [2] XIE WU, Research and study of new type of Silica solution. Innovation and Development of Foundation Engineering Technology of water conservancy and hydro-power engineering, 2023 (in Chinese)
- [3] Construction Report of reinforcement grouting for deep overburden dam foundation of A hydro-power station in China, 2022 (in Chinese)

COMMISSION INTERNATIONALE DES
GRANDS BARRAGES

VINGT-HUITIEME CONGRES DES
GRANDS BARRAGES
CHENGDU, MAI 2025

**A REFINED ANALYSIS METHOD FOR THE OPERATIONAL BEHAVIOR OF
NYABARONGO II DAM ON A VIBRO-REPLACEMENT STONE COLUMN
COMPOSITE FOUNDATION (*)**

Li YUAN

Doctoral Candidate, Hohai University

Qiankun LIU

*Senior Engineer, Project Manager of Nyabarongo II Project, STECOL Corporation
Ltd, Tianjin*

Fei WANG

Doctoral Candidate, Hohai University

Tongchun LI

Professor, Hohai University

Jianguo LI

Professor Level Senior Engineer, STECOL Corporation Ltd, Tianjin

CHINA

SUMMARY

Nyabarongo II Dam in Rwanda is a clay core rockfill dam on soft soil foundation. The vibro-replacement stone columns are used to form composite foundations, which enhance bearing capacity and accelerate drainage. When analyzing the operational behavior of a dam on the composite foundation, the large scale of

**Méthode d'analyse du comportement du barrage de Nyabarongo II sur un sol composite renforcé par des colonnes ballastées*

the stone column group cannot be ignored. Moreover, clay core rockfill dams often arrange geomembranes upstream of the core wall to enhance their impermeability. In such cases, the vibro-replacement stone columns and geomembranes, as small-scale detailed structures, bring challenges in refined analysis of the operational behavior of the clay core rockfill dam on the composite foundation. This article proposes a simplified interpolation method that inserts stone column elements into the foundation elements according to their position, and the relationship between the two sets of meshes is established through interpolation coefficients. This method can easily and quickly build the composite foundation model, which not only solves the problem of simulating a large number of stone columns in actual engineering, but also considers the influence of stone columns on the dam. Furthermore, this article uses a coupled model that includes membrane elements and isoparametric elements to establish a coordinated relationship between the geomembrane and the clay core, which effectively addresses the stress and deformation analysis of the geomembrane applied on the surface of the clay core. By combining the two methods described above, a refined analysis approach is developed for studying the operational behavior of the clay core rockfill dam on a vibro-replacement stone column composite foundation. This approach provides theoretical and technical support for the safety evaluation and design optimization of clay core rockfill dams on similar composite foundations.

RÉSUMÉ

Le barrage de Nyabarongo II au Rwanda est un barrage en enrochement à noyau d'argile sur une fondation en sol meuble. Les colonnes ballastées sont utilisées pour former des fondations composites, qui améliorent la capacité portante et accélèrent le drainage. Lors de l'analyse du comportement opérationnel d'un barrage sur une fondation composite, la grande échelle du groupe de colonnes ne peut être ignorée. De plus, les barrages de remblai d'argile disposent souvent de géomembranes en amont de la paroi du noyau pour améliorer leur imperméabilité. Dans de tels cas, les colonnes ballastées et les géomembranes, en tant que structures détaillées à petite échelle, posent des défis dans l'analyse détaillée du comportement opérationnel du barrage sur sa fondation. Ce rapport propose une méthode d'interpolation simplifiée qui insère des éléments de colonne dans les éléments de fondation en fonction de leur position, et la relation entre les deux ensembles de mailles est établie par des coefficients d'interpolation. Cette méthode permet de construire facilement et rapidement le modèle de fondation composite. Ce modèle résout le problème de la simulation d'un grand nombre de colonnes et tient également compte de l'influence des colonnes sur le barrage. De plus, ce rapport utilise un modèle couplé comprenant des éléments de membrane et des éléments isoparamétriques pour établir une relation coordonnée entre la géomembrane et le noyau d'argile, ce qui permet de traiter efficacement l'analyse des contraintes et des déformations de la géomembrane appliquée sur la surface du

noyau d'argile. En combinant les deux méthodes décrites ci-dessus, une analyse détaillée est développée pour étudier le comportement opérationnel du barrage en enrochement à noyau argileux sur une fondation composite en colonnes ballastées. Cette approche fournit un soutien théorique et technique pour l'évaluation de la sûreté et l'optimisation de la conception de barrages similaires.

1. INTRODUCTION

The dam of Rwanda Nyabarongo II hydropower project faces practical challenges in its design and implementation. This is because the foundation of the dam site has a relatively thick layer of soft soil cover. The maximum excavation depth of the weak foundation in this project exceeds 40m, and there are significant engineering quantities and difficulties in excavation and support, high risks of stability and flood during the construction period, and difficulties in foundation pit drainage and maintenance. Other methods are not suitable in terms of investment, safety, construction period and economy, so the vibro-replacement stone column method is proposed for foundation reinforcement at this stage. In addition, the use of geomembrane at the bottom of the clay core wall of the dam to extend the seepage diameter and improve the anti-seepage performance. Therefore, in order to assist the Nyabarongo II dam design and construction, it is necessary to analyze the operation behavior of clay core dam on composite foundation with detailed structures such as stone columns and geomembrane.

Stone columns can effectively improve the bearing capacity of the foundation, reduce the total settlement and uneven settlement of the foundation, improve the consolidation rate and improve the liquefaction resistance. There are many methods for modeling gravel piles, and the applicability of different methods depends on what is being studied and the type of analysis [1]. The mechanical properties of a single stone column are often considered from elastic or elastic-plastic models. In view of the seepage capacity of the single stone column, the model is often established from aspects of vertical drainage well [2], seepage stress coupling [3]. and so on.

In practical engineering, because of the large site and the large number of stone columns, it is very difficult to simulate the foundation with stone columns. Considering that plane strain conditions are often met in geotechnical engineering, a simplified method is to convert stone columns into equivalent walls by plane strain conversion method, so as to solve the two-dimensional plane strain problem of foundation containing stone columns. The conversion methods include that the diameter of the axisymmetric model of the stone column is equivalent to the width of the wall of the plane strain model, the drainage capacity of the axisymmetric model of the stone column is equivalent to the drainage capacity of the wall of the plane strain model, and so on [4]. In addition, the homogenization method is often considered in engineering, which does not need to model every stone column,

simplifying the modeling and calculation process. For example, the equivalent stiffness and equivalent permeability coefficients of homogenized foundations are calculated by modifying factors [5], and so on.

Geomembrane has been widely used in water conservancy projects as a part of anti-seepage system because of its good anti-seepage effect. Considering that the geomembrane cracking or breaking may bring hidden dangers to the seepage prevention of the whole project, the seepage prevention of geomembrane usually needs to be calculated and demonstrated. The study of geomembrane properties usually focuses on seepage and strength. For example, the empirical formula for calculating leakage is obtained by combining theory [6], laboratory test and field data [7]. Study on tensile properties of unidirectional geomembranes and multidirectional geomembranes and shear properties of composite geomembranes [8]. However, it is difficult to simulate geomembrane on dam scale because of its thin thickness and great difference in mechanical properties from dam materials. The finite element method is often used to calculate the stress and deformation of earth and rockfill dams, but the finite element numerical simulation of geomembrane is rarely studied. Therefore, how to reasonably consider the role of geomembrane in three-dimensional finite element calculation remains to be solved.

In this paper, a simplified interpolation algorithm is proposed to simulate the behavior of composite foundation with stone columns, and a coupling model of thin film element and isoparametric element is used to simulate geomembrane. Combining the two methods and the actual situation of the dam, this paper presents a refined analysis approach for studying the operational behavior of the clay core rockfill dam on a vibro-replacement stone column composite foundation.

2. METHODOLOGY

2.1. STONE COLUMN GROUP SIMULATION METHOD

2.1.1. *Biot consolidation theory*

In this paper, a simplified u-p model is used, assuming that the foundation is completely saturated soil and the foundation solid particles are incompressible. The acceleration term of the u-p model is also ignored, and the finite element equation after spatial discretization is:

$$\begin{cases} Ku - Qp_w = F_u \\ Q^T \dot{u} + Hp_w + Sp_w = F_p \end{cases} \quad (1)$$

Where, K is the stiffness matrix; Q is the coupling matrix; H is the permeability matrix; S is the compressibility matrix. F_u and F_p represent the load vector at the solid phase nodes and liquid phase nodes respectively.

Eq.[1] is discretized in the time domain by the generalized Newmark method as follows (the pore pressure p_w subscript w is omitted):

$$\begin{bmatrix} \beta\Delta t K & -\theta\Delta t Q \\ -\theta\Delta t Q^T & -\theta\Delta t(S + \theta\Delta t H) \end{bmatrix} \begin{Bmatrix} \Delta \dot{u}_n \\ \Delta \dot{p}_n \end{Bmatrix} = \begin{Bmatrix} F_{n+1}^u \\ -\theta\Delta t F_{n+1}^p \end{Bmatrix} \quad (2)$$

Eq.[2] is the basic equation for the finite element method to solve the consolidation of saturated soil, where, $n + 1$ and n represent the time step; Δt represents the time difference between time steps; β and θ are the Newmark parameters and the parameters generally are 0.5 when using the implicit solution method. The second equation of Eq.[2] is multiplied by $-\theta\Delta t$ for the symmetry of the whole coefficient matrix.

2.1.2. Simplified interpolation algorithm

In engineering projects, because of the large number and range of stone columns, when the foundation elements are divided by finite element method, the difficulty of subdivision of the whole model will be greatly increased if the coordinated mesh is used. From the perspective of multi-scale modeling, the whole foundation can be established without considering the stone columns, and then the stone column elements can be automatically generated within the foundation elements based on the location and size of the stone columns. In this way, the modeling difficulty of the two-step modeling is less and the element shape is better.

At this time, it is assumed that the influence of the construction process on the calculation, the change of the permeability coefficient in the construction disturbance area, and the nonlinear contact relationship on the interface between the stone column and the soil are not considered. The foundation elements and the stone column elements are taken as a complete calculation domain. The position with the same geometric coordinates in the overlapping area of the column elements and the foundation element should have the same displacement and pore pressure, then the node displacement and pore pressure of the column elements can also be obtained by interpolation of the nodes of the foundation elements. The linear relationship between two sets of displacement and pore pressure variables is established as follows, and the formula is valid at each time step.

$$\begin{Bmatrix} u_n^c \\ p_n^c \end{Bmatrix} = \begin{bmatrix} R_u & 0 \\ 0 & R_p \end{bmatrix} \begin{Bmatrix} u_n^s \\ p_n^s \end{Bmatrix} \quad (3)$$

Where, superscript s is the foundation element, superscript c is the stone column element, R_u and R_p , respectively, are the interpolation coefficient matrix of

displacement and pore pressure, which is assembled by the foundation element shape function corresponding to the node position of each stone column, and the relationship of variables between stone column and foundation expressed by shape function as shown in Fig. 1.

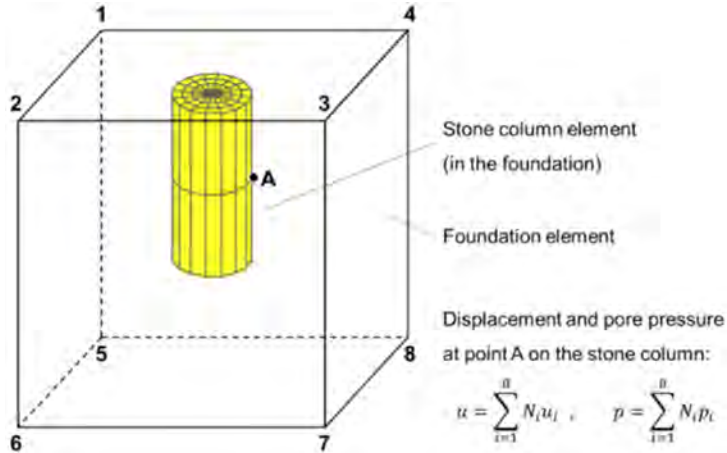


Fig. 1

The relationship of variables between stone column and foundation expressed by shape function

Relation entre la colonne et la fondation exprimée par fonction de forme

When $n = 0$, the derivative of displacement and pore pressure of stone column and foundation with respect to time is 0, then the basic variables of displacement and pore pressure in Eq.[2] should also satisfy the interpolation relation of Eq.[3].

The degrees of freedom of the variables is divided into two groups of foundation elements and stone column elements, and their relationship is written as follows:

$$\begin{Bmatrix} u_n \\ p_n \end{Bmatrix} = [u_n^c \quad u_n^s \quad p_n^c \quad p_n^s]^T = \begin{bmatrix} T_u & 0 \\ 0 & T_p \end{bmatrix} \begin{Bmatrix} u_n^s \\ p_n^s \end{Bmatrix} \quad (4)$$

$$[T_u] = [R_u \quad I]^T \quad (5)$$

$$[T_p] = [R_p \quad I]^T \quad (6)$$

Where, T_u and T_p represents the transformation matrix of the degrees of freedom of displacement and pore pressure respectively.

Similarly, the basic unknown variables of displacement and pore pressure, along with their derivatives with respect to time can be expressed using the above transformation relationship. By substituting the transformation relation into Eq.[2] and simultaneously multiplying the transpose of a transformation matrix, the finite element consolidation governing equation based on the simplified interpolation algorithm is obtained as follows:

$$\begin{bmatrix} \beta\Delta t\tilde{\mathbf{K}} & -\theta\Delta t\tilde{\mathbf{Q}} \\ -\theta\Delta t\tilde{\mathbf{Q}}^T & -\theta\Delta t(\tilde{\mathbf{S}} + \theta\Delta t\tilde{\mathbf{H}}) \end{bmatrix} \begin{Bmatrix} \Delta\dot{\mathbf{u}}_n^u \\ \Delta\dot{\mathbf{p}}_n^p \end{Bmatrix} = \begin{Bmatrix} \tilde{\mathbf{F}}_{n+1}^u \\ -\theta\Delta t\tilde{\mathbf{F}}_{n+1}^p \end{Bmatrix} \quad (7)$$

Where, $\tilde{\mathbf{K}} = \mathbf{T}_u^T \mathbf{K} \mathbf{T}_u$, $\tilde{\mathbf{Q}} = \mathbf{T}_u^T \mathbf{Q} \mathbf{T}_p$, $\tilde{\mathbf{S}} = \mathbf{T}_p^T \mathbf{S} \mathbf{T}_p$, $\tilde{\mathbf{H}} = \mathbf{T}_p^T \mathbf{H} \mathbf{T}_p$, $\tilde{\mathbf{F}}_{n+1}^u = \mathbf{T}_u^T \mathbf{F}_{n+1}^u$, $\tilde{\mathbf{F}}_{n+1}^p = \mathbf{T}_p^T \mathbf{F}_{n+1}^p$.

The displacement and pore pressure of foundation can be obtained by solving Eq.[7]. Then, the displacement and pore pressure of stone columns can be further calculated by interpolating coefficient matrix according to Eq.[3]. Other results such as stress can be processed on the basis of displacement.

2.2. GEOMEMBRANE COUPLING SIMULATION METHOD

2.2.1. Properties of geomembrane elements

The geomembrane element used in this paper is a spatial quadrilateral four-node element. First, rotate the coordinates of the four nodes of the planar quadrilateral element on the three-dimensional global coordinate system xyz to the planar local coordinate system $\bar{x}\bar{y}\bar{z}$, as shown in Fig. 2. The rotation matrix is $[\mathbf{C}]$ as follow:

$$[\mathbf{C}] = \begin{bmatrix} \cos(\bar{x}, x) & \cos(\bar{x}, y) & \cos(\bar{x}, z) \\ \cos(\bar{y}, x) & \cos(\bar{y}, y) & \cos(\bar{y}, z) \\ \cos(\bar{z}, x) & \cos(\bar{z}, y) & \cos(\bar{z}, z) \end{bmatrix} \quad (8)$$

The local coordinates and displacements of a point i in the local coordinate system calculated based on the coordinates and displacements of the point in the global coordinate system are as follows:

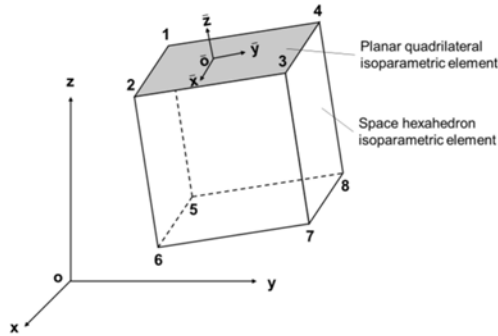


Fig. 2

Coupling diagram of space hexahedron isoparametric element and planar quadrilateral isoparametric element

Diagramme de couplage de l'élément isoparamétrique de l'hexaèdre spatial et de l'élément isoparamétrique du quadrilatère

$$\begin{bmatrix} \bar{x} \\ \bar{y} \\ \bar{z} \end{bmatrix} = [C] \begin{bmatrix} x \\ y \\ z \end{bmatrix} \quad (9)$$

$$\{\bar{\delta}_i\} = \begin{bmatrix} \bar{u} \\ \bar{v} \\ \bar{w} \end{bmatrix} = [C] \begin{bmatrix} u \\ v \\ w \end{bmatrix} = [C] \{\delta_i\} \quad (10)$$

In the local coordinate system, the relation between the nodal force and the nodal displacement of a planar quadrilateral element in Fig. 2 is as follows:

$$[\bar{k}] \{\bar{\delta}\}^e = \{\bar{F}\}^e, \quad \{\bar{\delta}\}^e = \begin{Bmatrix} \bar{\delta}_1 \\ \bar{\delta}_2 \\ \bar{\delta}_3 \\ \bar{\delta}_4 \end{Bmatrix}, \quad \{\bar{F}\}^e = \begin{Bmatrix} \bar{F}_1 \\ \bar{F}_2 \\ \bar{F}_3 \\ \bar{F}_4 \end{Bmatrix} \quad (11)$$

Because the z axis of the local coordinate system of Eq.[11] is perpendicular to the planar quadrilateral element, the degree of freedom of the z axis is eliminated when the stiffness matrix of the planar quadrilateral element is established. Where, $\{\bar{\delta}_i\} = [\bar{u} \ \bar{v}]^T$ and $[\bar{k}] = \int [\bar{B}]^T [\bar{D}] [\bar{B}] dV$

In order to establish the global stiffness matrix of multiple planar quadrilateral elements with different normal directions and coupled hexahedral elements, a unified global coordinate system must be determined and the stiffness matrix of each planar quadrilateral element in the local coordinate system must be converted to the global coordinate system.

The nodal displacement and nodal force of the whole element in the global coordinate are represented by $\{\delta\}^e$ and $\{F\}^e$ respectively, and the conversion process is similar to Eq.[10], as follows:

$$\{\bar{\delta}\}^e = [L]\{\delta\}^e, \quad \{\bar{F}\}^e = [L]\{F\}^e \quad (12)$$

$$[L] = \begin{bmatrix} C & 0 & 0 & 0 \\ 0 & C & 0 & 0 \\ 0 & 0 & C & 0 \\ 0 & 0 & 0 & C \end{bmatrix} \quad (13)$$

According to Eq.[11] and the latter equation of Eq.[12]:

$$\{F\}^e = [L]^{-1}\{\bar{F}\}^e = [L]^{-1}[\bar{k}]\{\bar{\delta}\}^e = [L]^{-1}[\bar{k}][L]\{\delta\}^e \quad (14)$$

Since $[L]$ is an orthogonal matrix, $[L]^{-1} = [L]^T$. According to Eq.[14], the element stiffness matrix $[k]$ in the global coordinate is as follows:

$$[k] = [L]^{-1}[\bar{k}][L] \quad (15)$$

After the element stiffness matrix in the global coordinate system is calculated and assembled, the global stiffness matrix $[K]$ of the model can be obtained.

2.2.2. Coupling calculation of geomembrane element and hexahedron element

The geomembrane element and a surface of the hexahedron element are geometrically consistent, as shown in Fig. 2. Therefore, on the basis of dividing the mesh of hexahedral elements, the nodes of the mesh at the surface of the structure are taken as the nodes of the geomembrane elements, so as to form the mesh of geomembrane elements. The element stiffness matrixes of geomembrane elements and hexahedron elements are formed respectively, and the global stiffness matrix is assembled according to a unified node system.

According to all the nodal displacements, the stresses of Gaussian points or nodes inside the structure are calculated by the corresponding equation of the hexahedron elements. And according to the nodal displacements of surface nodes, the stresses of Gaussian points or nodes are calculated by the equation of geomembrane elements.

3. ENGINEERING EXAMPLE CALCULATION AND ANALYSIS

3.1. PROJECT SUMMARY

The dam of Rwanda Nyabarongo II hydropower project is a clay core rockfill dam, which with the foundation reinforcement using vibro-replacement stone column recommended scheme. The dam has a crest elevation of 1414.00m, a crest width of 8.00m, a crest length of 363.00m and a maximum height of 59.00m. The upstream dam slope ratio is 1:2.0, the downstream dam slope ratio is 1:1.8. In order to enhance the stability of the upstream and downstream dam slopes, a backfilling platform is set between the cofferdam and the dam body in the upstream of the dam body, the elevation of the platform is 1,372.00m; a rockfill slope is set at the platform near the dam slope, with a slope top height of 1,380.00m; and a graded slope is set at the downstream of the dam body, with a slope top height of 1,382.50m.

Filling materials are zoned into clay core (including contact clay), filter, transition, main rockfill material of dam shell, filter cushion material of core foundation, gravel cushion material of the upstream dam shell foundation, gravel drainage material of the downstream shell and backfill zone foundation, as well as upstream and downstream backfill material. The typical section of Nyabarongo II dam as shown in Fig. 3.

At the detailed design stage, the geological survey revealed that the river bed overburden thickness ranges from 7.5 to 45.45m, consisting of alluvial (Q4^{pal}) and lacustrine soft soil (Q4^l). Among them, the alluvium layer is composed of ① Silty sand with sludgy soil, ② medium and fine sand, and ④ gravel with sand. The lacustrine deposits are distributed throughout the whole area, with a thickness of 16.3m~28.5m, which is composed of ③-1 sludgy soil and ③-2 peaty soil, and are deposited alternately in spatial distribution. The bedrock of the dam site is the sandstone and shale, sandstone mainly includes argillaceous sandstone, quartz sandstone and calcareous sandstone.

The vibro-replacement stone column with a diameter of 1.2m is set to strengthen the soft soil of dam foundation. The stone column is extended to ④ gravel with sand layer, and the maximum depth of stone column is about 36m. The layout of stone column is determined according to the section of the dam along the river bed. The replacement rate of 0.35 is adopted within the foundation where upper dam body height is more than 40m and soft soil is more than 20m depth; the replacement rate of 0.30 is adopted where upper dam body height is more than 40m and soft soil is less than 20m depth. The replacement rates of 0.30, 0.25 and 0.20 are adopted within the foundation where upper dam body height ranges from 25m to 40m, 17m to 25m, and is less than 17m.

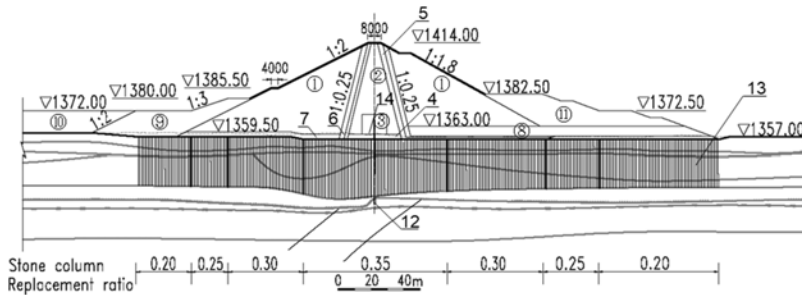


Fig. 3
The typical section of Nyabarongo II dam
Coupe type du barrage de Nyabarongo II

1	Mixed rockfill	1	Mélange de roche
2	Clay core	2	Noyau d'argile
3	Contact clay	3	Argile de contact
4	Filter cushion	4	Filtre
5	Filter layer (width 3m)	5	Filtre (largeur 3m)
6	Transition layer (width 3m)	6	Couche de transition (largeur 3m)
7	Gravel cushion	7	Couche de gravier
8	Gravel drainage layer	8	Couche de drainage de gravier (thickness 6m) (épaisseur 6m)
9	Upstream backfill zone	9	Zone de remblai en amont
10	Upstream disposal	10	Dépôt amont
11	Downstream backfill zone	11	Zone de remblayage aval
12	Concrete cutoff wall	12	Mur de coupure en béton (thickness 0.8m) (épaisseur 0.8m)
13	Vibro-replacement stone column replacement (diamètre 1.2m)	13	Colonne (diamètre 1.2m)
14	Composite geomembrane	14	Géomembrane Composite

Considering the short seepage diameter of the contact part between the cutoff wall and the clay core, in order to improve the reliability of the seepage control system, a composite geomembrane is arranged upstream and downstream of the contact part between the top of the cutoff wall and the clay core. The inner side of the geomembrane is anchored to the cutoff wall, and the outer side is flat on the bottom edge of the contact clay.

3.2. MODEL AND PARAMETER

3.2.1. *Finite element model*

The typical section of the dam was selected for three-dimensional finite element analysis, and the width of the dam section was set at 20m. The material partition was referred to Fig. 3 and a small amount of simplification was made on this basis. The finite element model takes the dam axis direction as x direction, along the river direction as y direction and vertical direction as z direction which is shown in Fig. 4. Among it, the stone columns were automatically generated in the foundation using the simplified interpolation algorithm. There were 1712 stone columns with different replacement ratios in the range of mode, and the final finite element model had a total of 336,804 nodes and 166,804 elements.

Fixed constraints were applied to the bottom of the model, normal constraints were applied to the side of the model, and the upstream water level was set as the normal water level of 1410.00m and the downstream water level was set as the corresponding 1358.05m. In the seepage calculation, the water head boundary is also set according to the water level.

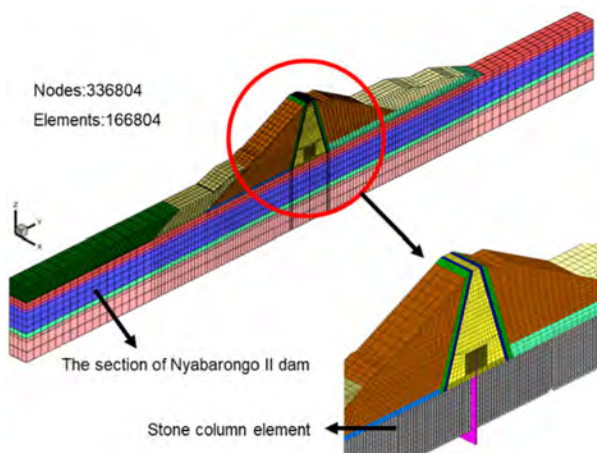


Fig. 4

The finite element model of Nyabarongo II dam typical section
Le modèle par éléments finis de la section typique du barrage de Nyabarongo II

3.2.2. *Material seepage and mechanical parameters*

Duncan-Chang model was used for static analysis which is a widely used nonlinear elastic model. The seepage and Duncan-Chang parameters are shown in Table 1 and Table 2 respectively.

Table 1
Permeability coefficient for dam zoned and foundation materials

Name of Material	Permeability coefficient (cm/s)
Mixed rockfill	1×10^{-2}
Clay core	1×10^{-5}
Contact clay	5×10^{-6}
Filter material	5×10^{-3}
Transition material	5×10^{-2}
Gravel cushion and drainage materials	5×10^{-1}
Backfill zone	1×10^{-3}
Concrete cutoff wall	1×10^{-7}
Stone column	5×10^{-3}
Geomembrane	1×10^{-11}
①- Silty sand with sludgy soil	1×10^{-5}
②- Medium and fine sand	1×10^{-4}
③-1 Sludgy soil	1×10^{-7}
③-2 Peaty soil	1×10^{-7}
④ Gravel with sand	1×10^{-7}
Sandstone and shale	1×10^{-7}

Table 2
The parameters of Duncan-Chang model

Material	ρ_{sat} (g/cm ³)	c (kPa)	φ_0 (°)	$\Delta\varphi$ (°)	K	n	R_f	K_b	m
Mixed rockfill	2.05	/	43.3	3.9	500	0.38	0.63	200	0.32
Clay core	1.95	30	25.0	/	180	0.50	0.80	90	0.60
Contact clay	1.80	5	16.0	/	108	0.35	0.60	45	0.45
Filter material	2.05	/	50.1	8.4	630	0.33	0.74	250	0.31
Transition material	2.20	/	52.5	8.0	750	0.25	0.71	300	0.30
Gravel cushion and drainage materials	2.10	/	45.0	6.0	600	0.36	0.65	240	0.31
Backfill zone	1.92	67.9	28.3	/	220	0.46	0.67	90	0.40

(Continued)

Table 2
Continued

Material	ρ_{sat} (g/ cm ³)	c (kPa)	φ_0 (°)	$\Delta\varphi$ (°)	K	n	R_f	K_b	m
Stone column	2.21	/	46.0	7.5	1100	0.32	0.72	530	0.28
①- Silty sand with sludgy soil	1.75	3	13.0	/	40	0.75	0.70	16	0.70
②- Medium and fine sand	2.00	/	27.0	/	300	0.40	0.70	120	0.50
③-1 Sludgy soil	1.53	28.8	22.8	/	52	0.50	0.60	15	0.45
③-2 Peaty soil	1.57	30.3	23.0	/	53	0.50	0.60	15	0.60
④ Gravel with sand	2.05	/	38	/	510	0.45	0.68	230	0.28

Linear elastic model is adopted for the bedrock of the dam, geomembrane and concrete. The density of bedrock, geomembrane and concrete are 2.4g/cm³, 1.0g/cm³ and 2.4g/cm³, the elastic modulus of which are 3GPa, 100MPa and 30GPa and the Poisson's ratio of which are 0.25, 0.49 and 0.167.

3.3. CALCULATION AND ANALYSIS

3.3.1. Seepage analysis

Based on the permeability coefficient in Table 1, the calculated seepage field of the dam under normal water level is shown in Fig. 5 (for the convenience of analysis, the results of the middle section of the dam section are taken).

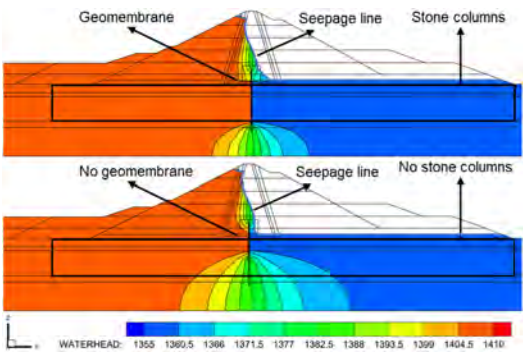


Fig. 5

Seepage analysis results of stone columns and geomembrane with or without setting (Unit: m)
Résultats des analyses d'infiltration des colonnes de Pierre et de la géomembrane avec ou sans prise (Unité: m)

As can be seen from Fig. 5, since the permeability coefficient of stone columns is larger than that of ③ sludgy soil and peaty soil, the comprehensive permeability coefficient of composite foundation increases after stone columns are installed. The dense area of hydraulic gradient is transferred from the positions of ③ sludgy soil and peaty soil, ④ gravel with sand and bedrock (sandstone and shale) in front and back of the concrete cutoff wall to the bottom of the concrete cutoff wall. The hydraulic gradient of ③ sludgy soil and peaty soil was reduced, and its permeability stability was improved.

Geomembrane installed at the bottom of clay core wall has relatively little influence on the seepage field in clay core wall, and the main influence area is the bottom of clay core wall. Due to the water insulation effect of geomembrane, the hydraulic gradient at the bottom of clay core wall is slightly increased. Contact clay is combined with clay core wall and concrete cutoff wall for seepage prevention and the hydraulic gradient of contact clay is large without geomembrane. After geomembrane is set to extend the seepage diameter, the hydraulic gradient of contact clay is slightly reduced.

3.3.2. Static analysis

The static calculation includes the construction period and the impoundment period of the dam. In the process of water level change, the displacement field coupled with the seepage field is calculated according to the Biot theory. In addition, the process of stone column construction is not considered in the analysis, and the ground stress of the composite foundation is balanced before calculation. The main analysis include the calculation steps after dam filling and after impoundment (normal water level).

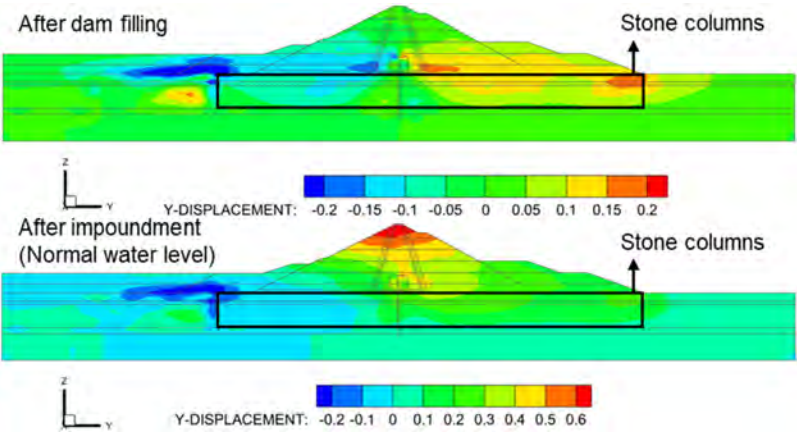


Fig. 6

The horizontal displacement along river displacement of composite foundation and dam (Unit: m)

Déplacement horizontal le long de la rivière déplacement de la fondation composite et du barrage (Unité: m)

Fig. 6 shows the result of horizontal displacement along river after dam filling and after impoundment. After dam filling, the maximum horizontal displacement to upstream is 0.37m, located in the upstream backfill zone. The maximum horizontal displacement to downstream is 0.20m, located at the foot of the downstream slope. After impoundment, the maximum horizontal displacements to upstream and downstream are 0.33m and 0.74m respectively. The horizontal deformation to upstream changes little, and the horizontal deformation to downstream increases, especially from the middle to the top of the dam. The horizontal deformation to downstream increases significantly under the action of upstream water load and seepage field in the dam body.

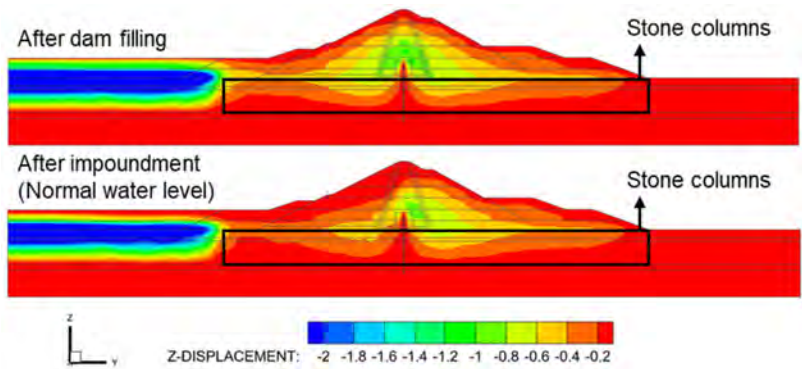


Fig. 7

The vertical displacement of composite foundation and dam (Unit: m)
Le déplacement vertical de la fondation composite et du barrage (Unité: m)

Fig. 7 shows the result of vertical displacement after dam filling and after impoundment. Due to the low mechanical properties of ① silty sand with sludgy soil and ③ sludgy and peaty soil, there is a great settlement by upstream disposal pressure outside the range of foundation reinforced by stone columns. The maximum settlement is 3.43m and 2.96m after dam filling and impoundment, respectively. The maximum settlement of the dam is 1.04m after filling and 0.93m after impoundment, and the maximum settlement position changes from the middle of the dam to the downstream under the action of upstream water load.

It can be clearly seen from Fig. 7 that within the reinforcement range of stone columns, the settlement of ① silty sand with sludgy soil and ③ sludgy and peaty soil is small, indicating that stone columns have played a good role in strengthening the foundation, and the composite foundation can bear the construction of the dam

above. Therefore, it can be shown that the refined simulation method proposed in this paper can well simulate the deformation of deep soft soil foundation reinforced by stone columns.

Fig. 8 shows the major principal (compressive) stress distribution (the stress is positive with tension) of the stone column group after dam filling and after impoundment. It can be seen that the major principal stress of the stone column on the upstream side generally decreases from dam filling to impoundment, while the major principal stress on the downstream side does not change significantly. This is because after the impoundment of upstream, the seepage field in the foundation and dam changes, and the upstream pore pressure increases, which plays a floating role on the dam and reduces the pressure of the dam on the foundation stone column. It can be noted that after dam filling, the distribution of major principal stress on the upstream and downstream sides of the concrete cutoff wall is basically symmetrical, which reflects that the stone column is mainly affected by the dam's weight when there is no water level difference between the upper and lower sides. The method proposed in this paper can analyze the stress of a single stone column in the foundation, which is also an advantage over the homogenization method.

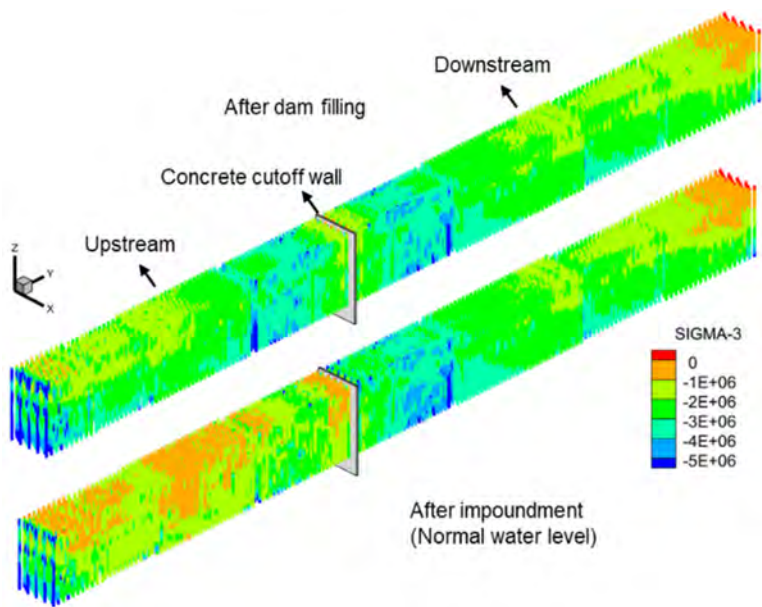


Fig. 8

Major principal stress of stone column group (Unit: Pa, compressive stress is negative)

Contrainte principale majeure du groupe de la colonne de Pierre (Unité: Pa, contrainte de compression est négative)

4. CONCLUSIONS

Based on the engineering characteristics of Nyabarongo II dam, which uses stone columns to strengthen deep silty soft soil foundation and geomembrane to extend the seepage diameter at the bottom of core wall, a refined analysis method is proposed in this paper, which can simulate small scale detailed structures such as stone columns and geomembrane while simulating seepage and mechanical behavior of dam and foundation. The application of the refined analysis method in the calculation of seepage field and displacement field is verified by the engineering example of a typical dam section. According to the analysis results, the stone column simulated by this method can significantly reflect the drainage and supporting effects in the foundation, avoiding the large amount of modeling time cost and calculation cost required for the coordinated modeling of the foundation and stone column. In addition, the simulated geomembrane can also well reflect the effect of extending the seepage diameter at the bottom of the core wall and the influence of the corresponding seepage field on the displacement and stress. Therefore, the refined analysis method of composite foundation clay core dam proposed in this paper can provide support for the design and safety evaluation of similar projects.

REFERENCES

- [1] CASTRO J. Modeling stone columns. *Materials*, 2017, 10(7): 782.
- [2] BARRON R. A. Consolidation of fine-grained soils by drain wells by drain wells. *Transactions of the American Society of Civil Engineers*, 1948, 113(1): 718–742.
- [3] BORGES J. L., DOMINGUES T. S., CARDOSO A. S. Embankments on soft soil reinforced with stone columns: numerical analysis and proposal of a new design method. *Geotechnical and Geological Engineering*, 2009, 27: 667–679.
- [4] TAN S. A., TJAHYONO S., OO K. K. Simplified plane-strain modeling of stone-column reinforced ground. *Journal of geotechnical and geoenvironmental engineering*, 2008, 134(2): 185–194.
- [5] NG K. S., TAN S. A. Simplified homogenization method in stone column designs. *Soils and Foundations*, 2015, 55(1): 154–165.

- [6] GROSS B A. Evaluation of flow from landfill leakage detention layers. *Proc. of the 4th International Conference on Geotextiles Geomembranes and Related Products*, 1990, 2: 481–486.
- [7] ELOY-GIORNI C., PELTE T., PIERSON P., *ET AL.* Water diffusion through geomembranes under hydraulic pressure. *Geosynthetics International*, 1996, 3(6): 741–769.
- [8] INGOLD T. S. A laboratory investigation of soil-geotextile friction. *Ground Engineering*, 1984, 17(8).

COMMISSION INTERNATIONALE DES
GRANDS BARRAGES

VINGT-HUITIEME CONGRES DES
GRANDS BARRAGES
CHENGDU, MAI 2025

**STUDY AND DESIGN ON VIBRO-REPLACEMENT STONE COLUMN
TREATMENT FOR DEEP ULTRA-SOFT DAM FOUNDATION (*)**

Huifeng ZHENG

*PhD, Professor Level Senior Engineer, Huadong Engineering Corporation Ltd,
Hangzhou*

Qiankun LIU

*Senior Engineer, Project Manager of Nyabarongo II Project, STECOL Corporation
Ltd, Tianjin*

Jianguo LI

Professor Level Senior Engineer, STECOL Corporation Ltd, Tianjin

Shuo ZHENG

PhD, Huadong Engineering Corporation Ltd, Hangzhou

CHINA

SUMMARY

The riverbed foundation of the clay core rockfill dam of Nyabarongo-II Multipurpose Development Project in Rwanda of East Africa is covered by a deep overburden with maximum depth exceeding 45m, where the lacustrine peaty and silty ultra-soft soil in a flow to soft plastic state is about 40m. The foundation treatment scheme of dam is the vital technical issue of this project. The full excavation scheme for such a deep and ultra-soft soil foundation has significant difficulties and huge risks in terms of technical feasibility and safety, and it is un-implementable.

**Étude et conception du renforcement par colonnes ballastées d'un sol de fondation très meuble*

Therefore, the vibro-replacement stone column scheme is proposed for reinforcement the ultra-soft soil foundation. The trial test of vibroflotation stone column carried out on site shows applicability of forming stone column in peaty and silty soil with depth more than 40m. And the detections and testing conducted on stone columns indicates good performance and meets the design requirements. Analysis and calculation show that, after the dam foundation is treated with stone column, the anti-sliding stability and seepage stability of the dam meet the requirements, and the settlement dam is in a normal state. The vibro-replacement stone column implemented in dam foundation in this project is the deepest in deep and ultra-soft soil of the current engineering practice around the world, which can provide useful reference for similar projects with complicated dam foundations.

RÉSUMÉ

La fondation du lit de la rivière du barrage en enrochement à noyau argileux du projet de développement polyvalent de Nyabarongo-II au Rwanda, en Afrique de l'Est, est recouverte par une couche de terrain profond dont la profondeur maximale dépasse 45 mètres, où le sol ultra-meuble, dans un état plastique, atteint environ 40 mètres. Le schéma de traitement de la fondation du barrage est un enjeu technique vital pour ce projet. L'excavation complète présente des difficultés significatives et d'énormes risques en termes de faisabilité technique et de sécurité. Elle n'est donc pas réalisable. Par conséquent, un schéma de colonnes ballastées est proposé pour renforcer la fondation en sol ultra-meuble. L'essai des colonnes réalisé sur site montre la faisabilité de la formation de colonnes ballastées dans un sol limoneux d'une profondeur supérieure à 40 mètres. Les mesures et les tests effectués sur les colonnes indiquent de bonnes performances et répondent aux exigences de conception. L'analyse et le calcul montrent qu'après traitement de la fondation du barrage, la stabilité au glissement et les infiltrations répondent aux exigences, et le barrage est en état normal. Les colonnes mises en œuvre dans la fondation du barrage dans ce projet sont les plus profondes dans le monde, ce qui peut fournir une référence utile pour des projets similaires avec des fondations de barrage compliquées.

1. INTRODUCTION

In water conservancy or hydropower project, limited by poor geological conditions, dams have to be constructed on deep and Soft, even ultra-soft soil characterized by high compressibility, sensitivity, and rheology, as well as low strength and permeability, which presents significant challenges for foundation treatment and dam construction, such as excessively high pore pressure, low bearing capacity and large deformation [1].

During dam filling and loading on the natural soft soil foundation without treatment, a drainage and consolidation process must be accompanied. If the filling rate is too fast, the pore water within the soft soil cannot be drained in time, leading to an increase in pore pressure and a decrease in effective stress, maybe suffering potential dam failures such as or foundation instability or landslides [2]. So the low dams are generally supported on the soft soil due to the poor engineering characteristics, which does not exceed 25 meters in China according to similar project case data.

Excavating out the soft soil overburden to locate the foundation on bedrock will have more stability and safety of the dam. However, open excavation will result in a deep soft soil foundation pit, posing significant challenges in excavation and support, with prominent safety risks during construction and huge quantities of pit support work [3].

With the development of foundation treatment methods and improvements in technological levels, the height of dams built on soft soil foundations is also increasing. The main purpose of treatment for soft soil foundation is to improve the strength, reduce compressibility, minimize and uneven settlement of the foundation, and prevent sliding failure and settlement cracks in the dam. Common treatment methods include excavation and replacement, preloading with surcharge, installing drainage wells, vibro-replacement stone columns [4], laying geosynthetics, and etc.

Currently, under the condition of foundation treatment, the height of embankment dams constructed on soft soil foundations have increased to nearly 50.0 meters [5–7]. For instance, the Wuping clay core rockfill dam in China has a height of 49.0 meters, and the Lomex tailings dam in Canada has a height of 43.0 meters. The foundation treatment for these dams primarily relies on vibro-replacement stone columns [8–12]. Although there are successful cases of dam construction on soft soil foundations, the height of dams built on soft soil foundations has not yet exceeded 50 meters, challenges such as selecting the appropriate reinforcement measurement and effectiveness evaluation arise [13].

The riverbed foundation of a clay core rockfill dam in Nyabarongo-II Multipurpose Development Project in Rwanda of East Africa is covered by a deep overburden with maximum depth exceeding 45m, where the lacustrine peaty and silty ultra-soft soil in a flow to soft plastic state is about 40m. In the case of dam height of 59m, the ultra-soft soil foundation treatment scheme of embankment dam is the vital technical issue of this project. The full excavation scheme for the dam foundation has significant difficulties and huge risks in terms of technical feasibility and safety, such as difficult excavation, support and stability maintenance for poor foundation pit, which results in that the open excavation scheme is un-implementable. Therefore, the vibro-replacement stone column scheme is proposed for reinforcement the ultra-soft soil foundation. The trial test of vibroflotation stone column carried out on site shows applicability of forming stone column in deep peaty and silty soil. And the detections and testing conducted on stone columns indicate that the length, diameter, strength,

compactness and deformation modulus, as well as bearing capacity of stone column meet the design requirements. Analysis and calculation show that after the dam foundation is treated with stone column, the anti-sliding stability and seepage stability of the dam meet the requirements, and the settlement dam is in a normal state. The study and design on vibro-replacement stone column treatment of embankment dam foundation in deep and ultra-soft soil in this project can provide useful reference for similar projects with complicated dam foundations.

2. GENERAL LAYOUT

The Nyabarongo-II Multipurpose Development Project under construction is located on the Nyabarongo River, the longest river in Rwanda, 20.5 km from the capital Kigali. The total reservoir capacity is 803 million m^3 , and the installed capacity of the power station is 43.50 MW. The general layout consists of a clay core rockfill dam, and an open spillway, a water diversion power generation system, as well as a flushing and empty tunnel on the left bank (See Figure 1).



Fig. 1

General layout of the Nyabarongo-II Multipurpose Development Project

3. GEOLOGICAL CONDITIONS OF ALLUVIUM OF RIVERBED

According to the geological survey in the detailed design stage, the thickness of the alluvium of river bed is 7.5m~45.45m, which is composed of alluvial (Q^{4pal}) and lacustrine (Q^{4l}) soft soil. Among them, the alluvium layer is composed of ① Silty sand with sludgy soil, ② medium and fine sand, and ④ gravel with sand. The

lacustrine deposits are distributed throughout the whole area, with a thickness of 16.3m~28.5m, which is composed of ③₋₁ Sludgy soil and ③₋₂ peaty soil, and are deposited alternately in spatial distribution. As revealed by the boreholes, there is confined artesian water in ④ gravel with sand layer, where the water head is about 1 m above ground, with the elevation of about 1359.94m~1360.5 m.

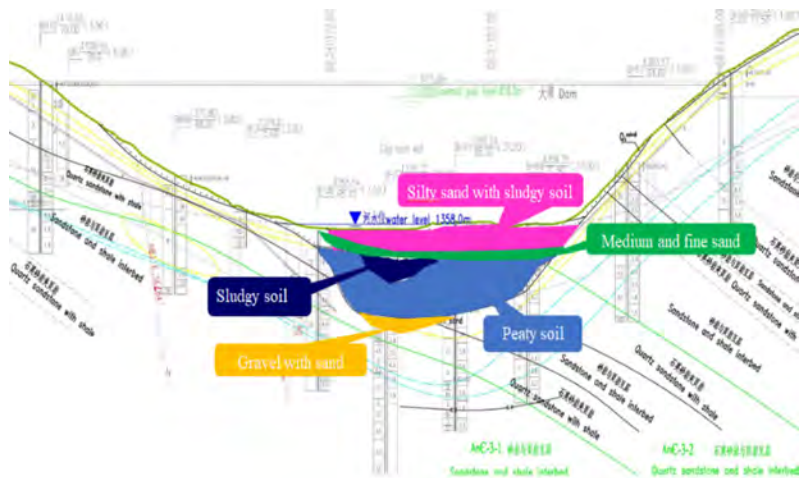


Fig. 2
Geological profile of soft soil at dam in the riverbed overburden

A total of 16 cone penetration holes have been completed on site, and the details of statistical results are shown in Table 1 for the range value and average value of cone probe tip resistance q_c and side frictional resistance f_s of each soil layer.

Table 1
Double-bridge Cone Penetration Test (CPTU) Results

SOIL LAYER	SOIL	PROBE TIP RESISTANCE Q_c (MPa)		FRICTIONAL RESISTANCE F_s (kPa)	
		RANGE VALUE	AVERAGE VALUE	RANGE VALUE	RANGE VALUE
①	Silty sand with sludgy soil	0.17~1.2	0.49	0.02~23.3	8.65
②	Medium and fine sand	1.62~5.80	3.02	0.14~48.75	18.22
③ ₋₁	Sludgy soil	0.15~0.62	0.41	0.36~8.45	5.28
③ ₋₂	Peaty soil	0.54~2.11	1.16	0.06~22.5	10.43



Fig. 3
Photograph of core samples of each soft soil layer drilling in riverbed

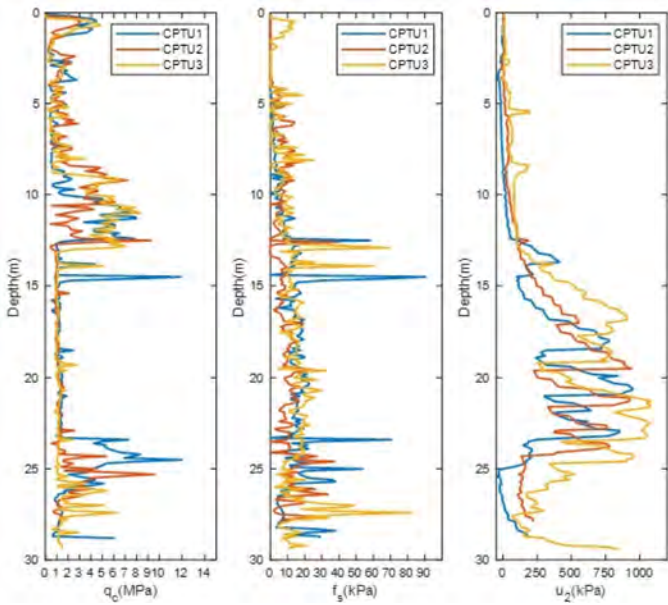


Fig. 4
CPTU test results on soil layers of riverbed

4. SELECTION OF DAM FOUNDATION TREATMENT SCHEME

4.1. SCHEME COMPARISON OF FOR FOUNDATION TREATMENT

Nyabarongo-II Dam has the characteristics of low strength, high water content, fluidity and thixotropy. The foundation treatment scheme is the critical technical issue, and the technical comparison between the open excavation scheme and the treatment scheme of dam foundation is carried out. The core foundation of the open excavation scheme is located on the bedrock, and the stability of the dam is relatively safe, but there are prominent difficulties and risks in the technical feasibility and safety of the scheme.

On the contrary, the stone column treatment scheme at the dam foundation only removes 1 to 3 meters of humus soil from the top of the overburden of the river bed, and the degree of mechanized construction of stone column scheme avoids the insurmountable difficulties and huge risks brought by the deep foundation pit excavated in deep ultra-soft soil, such as difficult excavation, support and stability maintenance for poor foundation pit, which results in that the open excavation scheme is un-implementable. At the same time, the construction period can meet the contract requirements, and the impact on land acquisition and environmental protection is relatively low. From the comprehensive comparison of the technical feasibility and construction safety, construction period, land acquisition and environmental protection of the dam foundation treatment schemes, the vibro-replacement stone column is adopted as the dam foundation treatment scheme.

4.2. TRAIL TEST OF VIBRO-REPLACEMENT STONE COLUMN

In order to verify the applicability, design and construction parameters of vibro-replacement stone column of Nyabarongo-II Multipurpose Development Project, the trial test has been carried out on site. The test area is located in the riverbed beach of downstream dam foundation (See Figure 5), and a total of 29 stone columns are arranged for construction and test.



Fig. 5
Schematic diagram of the in-situ test area of stone column in dam foundation

The top of the stone column was excavated out after construction, and the detected density was 1.875g/cm^3 , considering the raw crushed stone deposit density is 1.43 g/cm^3 , the conversion compactness coefficient was 0.76.

The N63.5 dynamic penetration test (DPT) was carried out in the stone column, and the average blow counts after correction was 40, indicating that the stone columns was in a very dense state as a whole, and according to the relationship between DPT and deformation modulus and bearing capacity, the deformation modulus of the test stone column was more than 30MPa, and the characteristic value of bearing capacity was more than 500kPa, which met the design requirements; the CPTU and SPT tests of soil surrounding stone column showed that the compaction effect of soil layers containing sand between columns is obvious, especially in the ② medium and fine sand layers. While, there is no significant change in the cone tip resistance in the ③ -2 peaty soil layer, indicating that neither significant compaction effect nor significant disturbance is caused to ③ -2 peaty soil layer by the vibroflotation construction (See Figure 6 and Figure 7).

The load test shows that the bearing capacity of both the Single Stone Column and the Single Stone Column Composite Foundation meet the requirements.

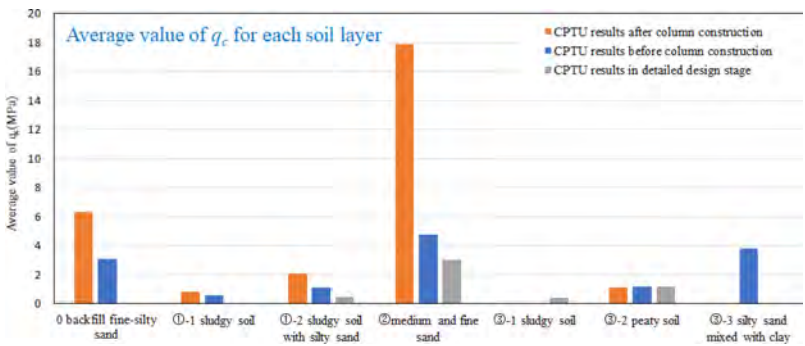


Fig. 6
Comparison of average value of q_c of CPTU for each soil layer before and after stone column construction

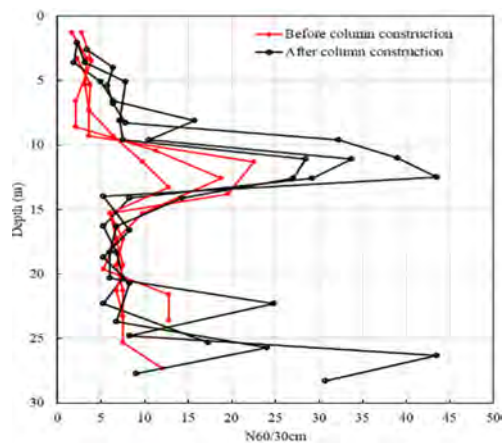


Fig. 7

Comparison of blow counts of SPT before and after stone column construction

5. CLAY CORE ROCKFILL DAM STABILITY CALCULATION

5.1. ARRANGEMENT OF STONE COLUMN AT THE FOUNDATION OF THE NYABARONGO DAM

The crest elevation of the clay core rockfill dam is 1414.00m, the maximum dam height is 59.0m, and the crest length is 363.0m. The slope ratio of the upstream dam is 1:2.0, and the slope ratio of the downstream dam is 1:1.8. Dam filling materials are divided into clay core wall (including contact clay), filter material, transition material, upstream dam shell material, upstream gravel cushion material, foundation filter cushion material, downstream dam shell material and foundation filter material, downstream dam foundation transition material, downstream gravel drainage material, and upstream and downstream slope protection (See Figure 8).

The vibro-replacement stone column with a diameter of 1.2m is adopted to improve the dam foundation, which is located on the bottom of ④ gravel with sand layer in the river bed and on the weathered bedrock on both sides of the bank. The layout of stone column is determined according to the section of the dam along the river bed, the details are as follows:

- The replacement rate of 0.35 is adopted within the foundation where upper dam body height is more than 40m and soft soil is more than 20m in depth.
- The replacement rate of 0.30 is adopted within the foundation where upper dam body height is more than 40m and soft soil is less than 20m in depth; The

replacement rate of 0.30 is also adopted within the foundation where upper dam body height is 25m~40m.

- The replacement rate of 0.25 is adopted at the foundation where upper dam body height is 17m~25m.
- The replacement rate of 0.20 is adopted at the foundation where upper dam body height is less than 17m.

Two 0.8m thick plastic concrete cut-offs are employed to the anti-seepage of dam foundation, which extends 3m into the clay core at the top end and into moderately weathered rock for 1.0m at the bottom end respectively. Meanwhile, high plastic contact clay of 20m wide and 4m height is arranged in the area around the top of cut-offs.

As a safety margin measure to assist the clay core, a PVC geomembrane with thickness of 3mm is arranged at upstream surface and bottom of the clay core.

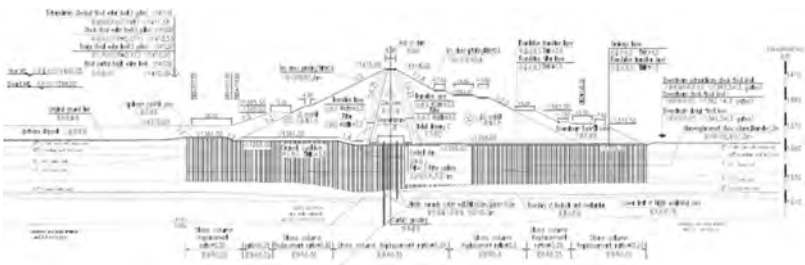


Fig. 8
Profile of design for vibro-replacement stone column treatment

5.2. CALCULATION AND ANALYSIS

5.2.1. Anti-sliding stability calculation

Geoslope software was adopted to calculate the anti-sliding stability of the dam, and the results are shown in Table 2, Figure 9 and Figure 10. The calculation results show that the safety factor of stability for the dam slope and foundation are from 1.424 to 2.019 after treatment of stone column, which are higher than the allowable values (1.3~1.5) according to the stipulations of EM 1110-2-1982. The stability of the dam meets the requirements.

Table 2
Anti-sliding Stability Calculation Results of Dam Slope

NO.	CONDITION DESCRIPTION		CALCULATED VALUE (SLIDE OUT OF THE DAM SLOPE)	CALCULATED VALUE (SLIDE OUT OF THE DAM FOUNDATION)	ALLOWABLE VALUE
1	Condition 1	Time of completion upstream dam slope	1.593 / 1.585	1.844 / 1.768	1.3
2		Time of completion,down- stream dam slope	1.533 / 1.518	2.019 / 1.988	
3	Condition 2	Stable seepage period at normal water level, upstream dam slope	1.537 / 1.513	1.917 / 1.838	1.5
4		Stable seepage period at normal water level,down- stream dam slope	1.533 / 1.518	1.894 / 1.871	
5	Condition 3	Rapid drawdown of water level, upstream dam slope	1.593 / 1.585	1.429 / 1.424	1.3

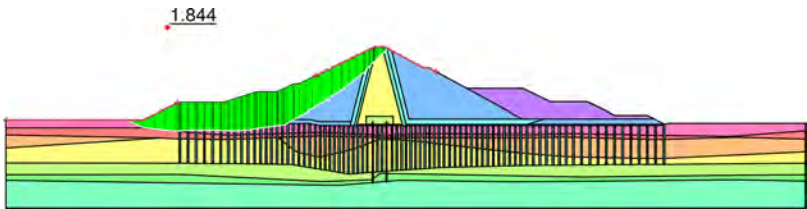


Fig. 9
Calculation Results of Upstream Dam Slope Stability under Condition 1

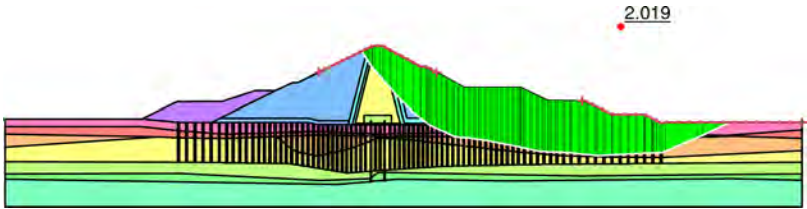


Fig. 10
Calculation Results of Downstream Dam Slope Stability under Condition 1

5.2.2. *Seepage calculation*

Seep/W seepage analysis module in GeoStudio software is used for dam and dam foundation seepage calculation. The seepage analysis results indicate that the seepage stability of the dam body and the dam foundation meets the requirements, and the impervious system of the dam and foundation is safe.

Table 3
Seepage Calculation Results

Calculation conditions	seepage volume m ³ /d/m		Maximum seepage gradient of clay core	Maximum seepage gradient of contact clay	Cut-off wall Maximum seepage gradient J _r		Maximum seepage gradient of downstream foundation J _r
	dam body	dam foundation			upstream	downstream	
normal water level	0.451	0.312	3.51	10.98	29.50	35.21	<0.01
highest water level	0.490	0.293	3.11	10.08	27.83	32.78	<0.01

5.2.3. *Finite element static analysis*

The static calculation results based on the Duncan-Chang model using Geodyna software show that the major and minor principal stresses are 1.56MPa and 0.70MPa, respectively when the dam filling is completed. The use of stone columns for foundation treatment effectively improves the drainage performance of the foundation. The excess pore water pressure in the foundation underneath the dam is basically dissipated. During the completion period, the maximum upstream displacement along the river is 0.36m, which is located at the upstream slope toe; the maximum downstream displacement is 0.22m, which is located at the downstream slope toe (Figure 11). The maximum settlement of the dam body is located in the middle of the dam body, which is 0.95m (Figure 12). During the full storage period, the maximum upstream displacement along the river is 0.32m; the maximum downstream displacement is 0.60m (Figure 13), and the maximum settlement of the dam body is 0.88m. The stress and deformation of the dam during the construction period and impoundment period are in a normal state.

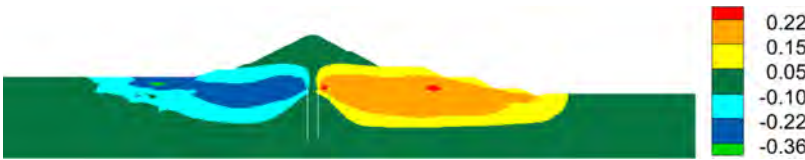


Fig. 11
The horizontal displacement after dam filling (Unit: m)



Fig. 12
The vertical displacement after dam filling (Unit: m)



Fig. 13
The horizontal displacement after impoundment (Unit: m)

6. CONCLUSION

The riverbed foundation of a clay core rockfill dam in Nyabarongo-II Multipurpose Development Project in Rwanda is covered by a deep overburden with maximum depth exceeding 45m, where the lacustrine peaty and silty ultra-soft soil in a flow to soft plastic state is about 40m. In the case of dam height of 59m, the ultra-soft soil foundation treatment scheme of embankment dam is the vital technical issue of this project. The full excavation scheme for the dam foundation has significant difficulties and huge risks in terms of technical feasibility and safety, such as difficult excavation, support and stability maintenance for poor foundation pit, which results in that the open excavation scheme is un-implementable. Therefore, the vibro-replacement stone column scheme is proposed for reinforcement the ultra-soft soil foundation. The trial test of vibroflotation stone column carried out on site shows applicability of forming stone column in deep peaty and silty soil. And the detections and testing conducted on stone columns indicate that the length, diameter, strength, compactness and deformation modulus, as well as bearing capacity of stone column meet the design requirements. Analysis and calculation show that after the dam foundation is treated with stone column, the anti-sliding stability and seepage stability of the dam meet the requirements, and the settlement dam is in a normal state. The study and design on vibro-replacement stone column treatment of embankment dam foundation in deep and ultra-soft soil in this project can provide useful reference for similar projects with complicated dam foundations.

REFERENCES

- [1] SHEN ZHUJIANG. *Theoretical soil mechanics*[M]. Beijing: China Water Resources and Hydropower Press, 2000.
- [2] SHEN ZHUJIANG, YI JINDONG. Comparison of models in deformation analysis of beach soft ground under embankment[J], *Chinese Journal of Geotechnical Engineering*, 1987, 9(6): 39–45.
- [3] SHEN ZHUJIANG. SHEN Zhujiang, *Selected Papers on Soil Mechanics*[M]. Beijing: Tsinghua University Press, 2005.
- [4] LI YANG. Study on Multiscale Mechanical Analysis Method of Stone-column Composite Foundations[D]. *Tsinghua University*, 2018.
- [5] CHEN ZUYU, ZHOU XIAO GUANG, CHEN LIHONG, *et al.* Treatment Technology of Soft Foundation Dam Construction of Wuping Reservoir[J]. *Journal of China Institute of Water Resources and Hydropower Research*, 2004, (03): 9–13.
- [6] HE LIN, ZHANG BANGQUAN. Construction technology of dam foundation vibration and flotation reinforcement treatment of Renzong seawater reservoir power station in Tianwan River Basin[J]. *Sichuan Hydroelectric Engineering*, 2006, (04): 78–81.
- [7] LI JINYUAN. Application of foundation treatment with vibro-replacement stone piles to YINPING hydropower station [J]. *Chinese Journal of Rock Mechanics and Engineering*, 2013, 32(S1): 2968–2976.
- [8] HARALAMBOS SAROGLU, ANTONIOU ANDREAS-A, PATERAS SPYROS-K. Ground improvement of clayey soil formations using stone columns: A case study from Greece[J]. *International Journal of Geotechnical Engineering*, 2009, 3(4): 493–498.
- [9] S-CALEB DOUGLAS, SCHAEFER VERNON-R. Stone Columns: Lessons Learned, Settlements, and Future Project Considerations[J]. *Geotechnical Special Publication*, 2015, 612–626.
- [10] W-A EYRE, WOLSTENHOLME D-R, MCKENNA J-M. Performance of an embankment supported by stone columns in soft ground[J]. *Géotechnique*, 1975, 25(1): 51–59.
- [11] G-A MUNFAKH, SARKAR S-K, CASTELLI R-J. PAPER 20 Performance of a test embankment foundation stone columns [J]. *Thomas Telford*, 1984.

- [12] S BASARKAR. Ground Strengthening by Vibro-Stone Columns—A Case Study GROUND STRENGTHENING BY VIBRO-STONE COLUMNS—A CASE STUDY[J]. 2020.
- [13] SUN CHAO. *Finite element analysis of soft foundation dam based on reservoir engineering[D]*. North China University of Water Resources and Electric power, 2018.

COMMISSION INTERNATIONALE DES
GRANDS BARRAGES

VINGT-HUITIEME CONGRES DES
GRANDS BARRAGES
CHENGDU, MAI 2025

SAFETY CHALLENGES AND OPERATIONAL CONSIDERATIONS FOR CASCADE RESERVOIR DAMS (*)

Jianfan ZHOU

Northwest Engineering Corporation Limited, Xi'an

Kunming LU

Northwest Engineering Corporation Limited, Xi'an

Gaofeng ZHANG

Northwest Engineering Corporation Limited, Xi'an

CHINA

SUMMARY

The cascade reservoir dams have become a major livelihood project with strategic and overall impact on social and economic development in China, which play an important role in flood protection, water supply, and power support. Under the new situation, the cascade reservoir dams in China are facing new challenges. These include climate change, low informatization and intelligence level, inadequate technologies, insufficient emergency ability, outdated management concept. The further implementation suggestions are given for cascade reservoir dams from five aspects in this paper, including strengthen the flood control system, enhance automation and information level, improve technology and the level emergency management, renovate concepts. The research aims to provide useful ideas for improving the safety level of cascade reservoir dams.

**Enjeux de sûreté et gestion opérationnelle de barrages en cascade*

RÉSUMÉ

L'aménagement de barrages en cascade est devenu un enjeu majeur avec un impact stratégique et global sur le développement socio-économique de la Chine. Ces aménagements jouent un rôle important dans la protection contre les inondations, l'approvisionnement en eau et l'hydroélectricité. Dans la nouvelle situation, les projets de réservoirs en cascades font face à de nouveaux défis. Ces défis comprennent le changement climatique, le faible niveau d'informatisation, l'insuffisance de la technologie, l'insuffisance des capacités d'urgence et l'obsolescence des concepts de gestion. Ce rapport présente des recommandations pour la poursuite de la mise en œuvre d'aménagements en cascade à partir de plusieurs aspects: renforcer le système de protection contre les inondations, augmenter le niveau d'automatisation et d'informatisation, améliorer le niveau technique et le niveau de gestion des urgences, faire émerger de nouveaux concepts. Il vise à fournir des idées utiles pour améliorer le niveau de sécurité des barrages de réservoir en cascade.

1. INTRODUCTION

The cascade reservoir group refers to a complex system comprising multiple reservoirs in the same basin, which has obvious advantages, such as full utilization of water flow, rolling project development and coordinated power dispatching [1]. Despite generating enormous economic benefits, dams may break and cause destructive floods, resulting in giant threats to the downstream residents and the socio-economic [2–4]. Compared with ordinary reservoirs, the dam risk in cascade reservoirs has transmission and superposition effects. One of the cascade dam breaks can easily lead to successive dam breaks in downstream reservoirs, resulting in serious losses [5]. In July 2021, the Yongan-Xinfa cascade reservoirs in the Nenjiang River Basin in China collapsed, causing 16,660 residents to be affected and 217 kilometers of farmland to be flooded [6]. With the continuous promotion of cascade hydropower development in the basin, the safety issue of cascade reservoir dam groups has become a public safety problem. It is critical to carry out safety management and prevention throughout the entire basin and lifecycle of cascade reservoir dam groups to improve the safety of the basin.

With the transformation of dam management mode from traditional safety management to risk management in China, risk analysis and assessment has been widely recognized by researchers as an important way for reservoir dam's management [7,8]. The theory and technology of a single reservoir dam is becoming increasingly abundant, which has been conducted on risk analysis studies involving multiple levels. Professor Bowles from Utah State University first

proposed and defined the concept of reservoir group risk analysis. In China, Yang et al [9]. proposed a framework to access the risk of cascade reservoirs based on systems engineering theory; Wang et al [10,11]. analyzed the transmission and superposition effects of risks in cascade reservoirs, and proposed relevant concepts and methods for risk probability calculation, dam failure risk consequence assessment, and engineering grade classification. Scholars [12,13] have conducted research on the safety management and risk assessment of cascade reservoir dam groups in China, such as the Dadu River, Lancang River. The above research provides ideas for the risk elimination and safety management of multiple series of cascade reservoirs.

In order to improve the safety level of dams, ensure the safety of people's lives and property, the authors summarized the safety management issues and challenges faced by China's cascade reservoir dams, and proposed management measures for safe operation of dams in this research.

2. OVERVIEW OF CASCADE RESERVOIR DAMS IN CHINA

At present, hydropower construction in China is at the peak concerning the development of cascade reservoirs in river basins. The cascade reservoirs account for 48% of China's built reservoir projects and 50% of the reservoir projects under construction [14]. Currently, A series of cascade reservoirs have been planned and constructed in China [15]. such as the upper reaches of the Yellow River, the middle and lower reaches of the Jinsha River, the upper reaches of the Yangtze River, the Yalong River, the Dadu River, the middle and lower reaches of the Lancang River, the Hongshui River of the Nanpan River, and the Wujiang River have initially formed a continuous distribution, end-to-end connection, and stepped distribution of cascade reservoirs. there are currently 13 major control reservoir projects built in the upper reaches of the Yangtze River Basin, located on the main stream of the Yangtze River, the lower reaches of the Jinsha River, the Yalong River, the Minjiang River, the Wujiang River, and the Jialing River. which have played an important role in flood prevention and disaster reduction in the middle and upper reaches of the Yangtze River. The upper reaches of the Yellow River have been utilizing the benefits of cascade joint operation since the 1980s and 1990s. 24 cascade reservoirs, including Chengyangxia, Liujiaxia, and Haibowan, have been built in the upper reaches of the Yellow River. The development of cascade reservoirs has brought comprehensive benefits such as power generation, flood control, and water supply. In the next 20 years, the main rivers in China, such as Jinsha River, Yalong River, Dadu River and Lancang River, will continue to carry out cascade development and construction of river basins, forming more than 100 cascade reservoirs (including tributaries), that are successive [16].

3. REQUIREMENTS OF CASCADE RESERVIOR DAMS IN THE NEW ERA

In the new era, China's strategic goals, such as dual carbon goals, high-quality economic and social development, and national water security have put forward higher requirements for dam safety. The cascade reservoir dams should ensure the safety of all factors, the safety of the entire basin, and the safety of the entire life cycle, and improve the level of dam safety.

3.1. ALL FACTOR SAFETY

China's water conservancy construction has entered a new era, and the connotation of dam safety has gradually shifted from traditional single project safety to comprehensive safety that includes the integration and coordination of engineering safety, ecological safety, and environmental safety. Among them, engineering safety is the most fundamental and important part of reservoir dam safety. Ecological security and environmental security are the practice of China's ecological civilization concept. Building eco-friendly reservoirs and promoting harmonious coexistence between reservoir dams and the ecological environment are the new connotations of reservoir dam safety in the new era.

3.2. RIVER BASIN SAFETY

With the development and construction of the cascade reservoir group, the safety of the leading reservoir, as the main controlling reservoir in the basin, is crucial. At the same time, the planning, design, management and scheduling of the cascade reservoir group cannot be ignored. Therefore, with the safety of leading reservoirs as the core, focusing on the planning, design, and operation management of cascade reservoir groups has important strategic significance for China's water resource security.

3.3 WHOLE LIFE SAFETY

As an important infrastructure related to national economy and people's livelihood, reservoir dams must implement the requirements of high-quality development. This requires adhering to high-quality standards and strict control at all stages of dam planning, design, construction, operation, and decommissioning, in order to ensure the safety and reliability of reservoir dams throughout their entire life cycle.

4. CHALLENGES FACED BY CASCADE RESERVOIR DAMS

While China's reservoir dams have achieved remarkable results, they also face risks and challenges.

4.1. THE IMPACT OF EXTREME WEATHER

Affected by global climate change, extreme events such as heavy rainfall in China have increased and intensified, and the level of climate risk is tending to rise. Flood, as the driving force of dam overtopping, is the main cause of dam failure. Earthquakes are the main factors inducing landslides. The strong action of earthquakes and the repeated vibration of aftershocks destroy the internal structure of the slope earth rock, resulting in the overall landslide and instability. In addition to the above factors, dam leakage, improper dispatching and some other factors, are added uncertain risks, that may occur in engineering practice.

According to the statistics of dam failures in China, earth rock dams account for more than 95% of the total number of dam failures, becoming the main dam failure type [17]. More than 95% of the dams in China's reservoirs are earth and rock dams, and most of them are old dams built before the 1980s. Due to their low design standards and long service life, structural aging is inevitable. If they encounter complex and changing climate environments or extreme geological disasters, these earth and rock dams are likely to become weak parts in cascade reservoirs, with systematic risks of first collapsing and then evolving into watershed scale reservoirs [18].

In addition, Under the extreme weather conditions, the complex engineering characteristics of high dam projects increase the potential risks to the safe operation of dams. At present, high dams with a height of over 200m in China are mainly concentrated in high mountains and valleys of western region, with engineering characteristics such as high altitude, high seismic intensity, high slopes, and extremely complex geological conditions [19].

4.2. SLOW DEVELOPMENT OF INFORMATIZATION AND INTELLIGENCE

The monitoring and perception ability of small and medium-sized reservoirs is still insufficient, which is one of the main weak links in the safety of cascade reservoir groups. Due to funding constraints and other reasons, there are problems such as incomplete monitoring projects, low automation level of

monitoring and collection, low integrity rate of monitoring and perception facilities, and a general lack of application of new intelligent inspection and aerial sensing methods. The intelligent analysis and early warning capability of dams also needs to be improved. At present, most reservoirs have not yet established intelligent safety analysis and warning systems, and their risk control capabilities are relatively weak, making it difficult to timely assess the operational status of dams.

4.3. WEAK EMERGENCY MANAGEMENT AND SECURITY TECHNOLOGY

The current level and ability of reservoirs to respond to emergencies are still insufficient. There are multiple issues present. Some reservoirs lack the ability to identify and early warn ultra standard floods caused by extreme weather. The effectiveness and operability of emergency plans are insufficient. Public risk awareness also needs to be strengthened. The construction of emergency shelter facilities is insufficient, and some of the high dams and large reservoirs that have been put into operation lack emergency venting facilities or have insufficient emergency venting capabilities. In the event of extreme events such as earthquakes and floods exceeding standards, the potential risks are high.

There are weak links in dam safety assurance technology. Now the safety monitoring and hazard investigation capabilities are weak for dam seepage environment. Conventional monitoring methods such as electricity and magnetism are difficult to accurately detect underwater damage. The development of equipment and integrated control technology for deep water environment, complex processes, and fine operations of dams need to be improved.

4.4. IMPERFECT MANAGEMENT CONCEPTS AND SYSTEMS

The safety concept of the reservoir dam system, which needs to coordinate all factor safety, whole basin safety, and whole life cycle safety under the new situation, has not yet been fully formed. Among the 13 cascade hydropower bases in China, the safety standards for both built and under construction reservoir dams are designed based on a single reservoir, lacking a systematic concept of considering the overall safety of the basin and the risk sharing of urban floods along the river embankments. A systematic safety management and risk prevention mechanism for cascade reservoir groups in the basin has not yet been formed.

5. SAFETY OPERATION AND MAINTENANCE MEASURES FOR CASCADE RESERVIOR DAMS

5.1. STRENGTHEN THE FLOOD CONTROL SYSTEM OF CASCADE RESERVOIR DAMS

The first important thing is to continuously focus on Risk mitigation and reinforcement of small and medium-sized reservoir dams and earth-rock dams, which are the weaker part of cascade reservoir dams. Strengthen rainfall monitoring and forecasting capability is also important. In the context of global climate change, extreme weather events occur frequently. It is necessary to further strengthen network of rainwater monitoring stations in the reservoir area, expand the application of modern technologies such as remote sensing, enhance the monitoring ability of rainwater, improve the prediction period and accuracy of river floods, realize the prediction of flood impact range and flood risk warning, and ensure the safe operation of the reservoir group.

Furthermore, Implement joint flood control operation among Cascade Reservoirs. The joint flood-prevention control in reservoir group can play the remarkable role in weakening flood peak, protecting the defending target in downstream. The cascade reservoirs in the basin have formed a complex dam system, where cascade affects each other, increasing the risk of the basin system and making prevention and control more difficult. We need to consider security issues comprehensively from the perspective of watershed system security, strengthen joint prevention and control, integrate resources from all parties, share data with each other, and jointly do a good job in watershed flood control scheduling. It is suggested to assign different risk prevention and control objectives and safety standards to each cascade dam based on its risk characteristics, and to comprehensively consider the design flood standards of the cascade reservoir group, formulate corresponding flood control scheduling plans, and ensure the safety of the dam under extreme combination conditions.

5.2. BUILD A SMART DAM SAFETY MANAGEMENT SYSTEM FOR CASCADE RESERVOIR DAMS

Combined with digital technologies such as the internet of things, remote sensing technology to enhance the monitoring ability of dams. Implement the intelligent transformation of dam safety monitoring facilities, including add automated devices and strengthen the intelligent analysis of reservoir monitoring data to achieve real-time analysis and future trend prediction. For small reservoirs, new technologies, equipment, and products that are automated, intelligent, and inclusive

should be adopted to achieve full coverage and ensure timely maintenance and normal operation of monitoring facilities.

Accelerate the promotion of digital twin projects is an effective method to enhance the safety management level of cascade reservoir. With the help of digital twin technology, data governance is accumulated and gradually carried out, so that while the physical entity construction of the dam project is carried out, digital twins are synchronously constructed in the information space, which can achieve the informatization, visualization, and intelligence of dam safety management throughout the entire process.

5.3. INCREASE THE DEVELOPMENT OF TECHNOLOGIES FOR CASCADE RESERVOIR DAMS SAFETY

In the future, we need to gradually overcome the difficulties of precise detection technology and equipment for complex hidden dangers such as deep burial, deep water, and long-distance of reservoir dams. The research and development of emergency response technologies, materials, equipment, and construction processes for complex hazards such as buried culverts under dams, contact leakage, dam foundation piping, and deep-water defects will further enhance the ability to handle complex hazards in reservoir dams. Overcome core technical challenges such as the mechanism and process of dam failure in high dams and large reservoirs, simulation methods for the evolution of dam failure floods in cascade reservoirs, and prediction and forecasting theories, accelerate the research and development of safe and efficient emptying technologies and facilities for high dams and large reservoirs, formulate relevant design specifications and operating standards, and enhance the safety guarantee capabilities of high dams and large reservoirs.

5.4. IMPROVE THE SAFETY AND EMERGENCY MANAGEMENT LEVEL OF CASCADE RESERVOIR DAMS

Develop a standardized professional model system for disaster prediction, dam failure analysis, risk assessment, emergency response, and other related areas, and establish a reservoir dam safety emergency platform. The platform is oriented towards multiple management levels, covering various functions and businesses such as reservoir risk management and early warning, emergency information release, emergency response and disposal. It supports multi-user and multi device management business applications such as personal computers and mobile terminals, forming a decision-making mode of multi department, multi field, and multi-regional linkage, realizing timely release, rapid acquisition, and rapid

response of emergency information, and improving the emergency management capability and disposal efficiency of reservoirs. Update the emergency plan in a timely manner according to the changes in the operating environment of the reservoir dam, ensuring that the emergency plan can truly play a scientific guiding role. At the same time, strengthen emergency safety publicity, training, and emergency drills for reservoirs, enhance public awareness of reservoir dam risks and emergency risk avoidance capabilities.

5.5. INNOVATE THE SAFETY MANAGEMENT CONCEPT AND MODEL OF CASCADE RESERVOIR DAMS

Establish an operational management system that is compatible with the concept of system safety, transform the current one-sided emphasis on the safety of the project itself in reservoir dam safety management, and form a reservoir dam system safety concept that comprehensively considers engineering safety, public safety, and ecological safety.

Strengthen the safety management of the entire basin. We need to establish a watershed operation management organization to unify and coordinate the construction, operation, and scheduling management of reservoir groups within the watershed, especially flood control scheduling, in order to ensure the safety of reservoir dams throughout the watershed. Through the unified management and scheduling of water resources in the basin, the comprehensive utilization of cascade reservoirs can be achieved, and the safety of reservoir groups and dam projects can be improved.

Strengthen dynamic security management throughout the entire lifecycle. It is necessary to strengthen the safety management of reservoir dam operation and retirement stages, and consider it in the planning and design stage. Establish a long-term mechanism for the operation, maintenance, and reinforcement of reservoir dams, evaluate the operating environment and functions of reservoir dams in a timely manner, adjust their scheduling and application methods, management modes, and safety management standards in a timely manner based on changes in their operating environment and functions, and comprehensively improve the institutionalization, standardization, and standardization level of reservoir dams.

6. CONCLUSIONS

After years of construction, the development pattern of cascade reservoirs in China has basically taken shape. Cascade reservoirs have brought benefits in flood

control and resource utilization of the basin. In the new era, the safety concept and requirements for reservoir dams have changed. Cascade reservoir dam groups are more complex than single reservoirs. This paper analyzes the current development status and challenges faced by cascade reservoir dams. In view of the problems, safety operation management measures are put forward for cascade reservoir dams, strengthen the construction of flood control safety system, establish a smart dam safety management system, increase the research and development of core technologies, improve the engineering safety and emergency management level of dam groups, innovate safety concepts and models. The study can provide reference for the further development of cascade reservoirs, and contribute to China's water resource and energy security.

REFERENCES

- [1] ARDESHIRTANHA K., SHARAFATI A. Assessment of Water Supply Dam Failure Risk: Development of New Stochastic Failure Modes and Effects Analysis. *Water Resource Management*, vol. 34, pp. 1827–1841, 2020.
- [2] FAN H., HE D., WANG H. Environmental consequences of damming the mainstream LancangMekong River: a review. *Earth-Science Reviews*, vol. 146, pp. 77–91, 2015.
- [3] LATRUBESSE E., ARIMA E., DUNNE T., *et al.* Damming the rivers of the Amazon basin. *Nature*, vol. 546, no. 7658, pp. 363–369, 2017,
- [4] ZHANG W., LI J., LEI X., *et al.* When to start an adaptation strategy in response to climate change in reservoir system management. *Journal of Hydrology*, vol. 603, 2021a.
- [5] CAO Z., HUANG W., PENDER G., *et al.* Even more destructive: Cascade dam break floods. *Flood Risk Management*, vol. 7, pp. 357–373, 2014.
- [6] WANG T., LI Z., GE W., *et al.* Calculation of dam risk probability of cascade reservoirs considering risk transmission and superposition. *Journal of Hydrology*, vol. 609, 2022.
- [7] GE W., LI Z., LI W., *et al.* Risk evaluation of dam-break environmental impacts based on the set pair analysis and cloud model. *Nature Hazards*, vol. 104, pp. 1641–1653, 2020a.
- [8] GE W., QIN Y., LI Z., *et al.* An innovative methodology for establishing societal life risk criteria for dams: a case study to reservoir dam failure events in China. *International Journal of Disaster Risk Reduction*, vol. 49, no. 2, 2020b.

- [9] YANG Y., REN Q. W., TIAN Y., *et al.* Risk analysis for a cascade reservoir system using the brittle risk entropy method. *Science China Technological Sciences*, vol. 59, pp. 882–887, 2016.
- [10] WANG T., LI Z.K., GE W., *et al.* Risk Consequence Assessment of Dam Breach in Cascade Reservoirs Considering Risk Transmission and Superposition. *Energy*, vol. 265, 2023.
- [11] WANG T., LI Z.K., GE W., *et al.* Risk Assessment Methods of Cascade Reservoir Dams: A Review and Reflection. *Natural Hazards*, vol. 115, no. 2, pp. 1601–1622, 2022.
- [12] WANG T., LI Z.K., GE W., *et al.* Calculation of dam risk probability of cascade reservoirs considering risk transmission and superposition. *Journal of Hydrology*, vol. 609, 2022.
- [13] LIANG Z.M., HUANG H.P., CHENG L., *et al.* Safety assessment for dams of the cascade reservoirs system of Lancang River in extreme situations. *Stoch Environ Res Risk Assess*, vol. 31, pp. 2459–2469, 2017.
- [14] HU L.M., YANG X., LI Q., *et al.* Numerical Simulation and Risk Assessment of Cascade Reservoir Dam-Break. *Water*, vol. 12, 2020.
- [15] WANG T., LI Z.K., GE W., *et al.* Risk assessment methods of cascade reservoir dams: a review and reflection. *Natural Hazards*, vol. 115, pp. 1601–1622, 2023.
- [16] LIU B., WANG C., LIU Z., *et al.* Cascade surface and borehole geophysical investigation for water leakage: A case study of the Dehou reservoir China. *Engineering Geology*, vol. 294, 2021.
- [17] LI Z., WANG T., GE W., *et al.* Risk Analysis of Earth-Rock Dam Breach Based on Dynamic Bayesian Network. *Water*, vol. 11, 2019.
- [18] HU W., LL Y., FAN Y., *et al.* Flow amplification from cascading landslide dam failures: Insights from flume experiments. *Engineering Geology*, vol. 297, 2022.
- [19] ZHOU J., ZHOU X., DU X., *et al.* Research on design of dam-break risks control for cascade reservoirs. *Journal of Hydroelectric Engineering*, vol. 1, pp. 1–10, 2018.

COMMISSION INTERNATIONALE DES
GRANDS BARRAGES

VINGT-HUITIEME CONGRES DES
GRANDS BARRAGES
CHENGDU, MAI 2025

DESIGN OF FOUNDATION TREATMENT FOR BATANG TORU HEPP (*)

Hangning ZHANG, Li YUANKE, Feiya HUANG & Yishu LIN
POWERCHINA Beijing Engineering Corporation Limited, Beijing

CHINA

SUMMARY

This article proposes the use of curtain grouting, consolidation grouting, and contact grouting to improve the stability and anti-seepage effect of the dam foundation of the Batang Toru HEPP, which is located in a high seismic zone and has weak rock mass and low bearing capacity. Optimize the layout of consolidation and contact grouting based on the actual geological conditions on site. Through on-site inspection data, it can be concluded that optimized foundation treatment measures can not only ensure the stability of the dam foundation, but also facilitate construction, shorten the construction period, and improve project economic benefits, this provides a theoretical basis and engineering experience for the foundation treatment of other projects.

RÉSUMÉ

La centrale hydraulique de Batang Toru en Indonésie est située en zone de sismicité significative ; la fondation du barrage présente des problèmes de fragilité de la roche et une faible capacité portante. Ce rapport propose d'utiliser l'injection d'étanchéité, l'injection de consolidation et l'injection de collage pour améliorer la

**Conception du traitement des fondations de l'aménagement hydroélectrique de Batang Toru*

stabilité et l'imperméabilité de la fondation du barrage. Selon des données d'essai des conditions géologiques actuelles et l'optimisation des opérations d'injection de consolidation et d'injection de collage, les mesures de traitement de fondation optimisées peuvent non seulement assurer la stabilité de la fondation du barrage, mais également faciliter les travaux, raccourcir la durée de construction, et améliorer les avantages économiques du projet, fournir aussi une base théorique et une expérience d'ingénierie pour d'autres traitements de fondations d'ingénierie.

1. INTRODUCTION

The Batang Toru HEPP in Indonesia is located in a high seismic zone with weak rock mass, high density of crack development, and insufficient bearing capacity. The blasting during the excavation of the dam body caused disturbance to the bedrock on the bank slope. In response to this complex geological condition, many problems occurred during the design and construction processes, which also led to the inability to use conventional methods for foundation treatment in this project. In order to address the various problems that occurred in this project, the design team needs to study the design scheme based on the actual situation.

At present, many domestic and foreign engineering projects have developed mature design schemes for foundation treatment under different geological conditions. [1][2] The permeability rate based on water pressure test is currently widely used for permeability and grouting quality evaluation [3]. Gao Yu et al [4]. evaluated and analyzed the construction quality of dam foundation curtain grouting using the Lu value obtained from water pressure test and the decreasing cement slurry injection rate during grouting process. J.S. Lee et al. combined numerical methods and grouting tests to analyze the grouting effect of joints and rock fractures [5]. More and more hydropower projects are constantly exploring process measures suitable for un-covered consolidation grouting [6]. Zhou Weiyuan et al. [7][8] studied the grouting reinforcement effect of weakly weathered rock mass in the foundation of Ertan Arch Dam. Curtain grouting, consolidation grouting [9][10], and contact grouting have been widely used in dam foundation treatment.

The load of blasting excavation causes damage to the rock mass, changes in the rock environment, and deformation of the rock mass under impact lead to changes in the physical and mechanical properties of the rock mass, weakening its physical and mechanical properties [11][12]. At the same time, for special projects in high seismic areas with poor geological conditions, there are still insufficient reference cases and successful experiences. Therefore, the aim is to provide necessary engineering experience for other similar projects at home and abroad by focusing on the design experience of foundation treatment and grouting effect testing for this project [13][14][15][16].

2. PROJECT OVERVIEW

The Batang Toru HEEP hydropower station in Indonesia is located on the Batang Toru River in the southern of North Sumatra Province, with a total installed capacity of 510 MW. The dam adopts an arc-shaped gravity dam and is situated on tuff. It consists of left and right bank retaining dam sections and a discharge dam section located in the middle of the river channel, with a dam crest elevation of EL.436.0 meters, a maximum dam height of 74.0 meters, and a dam crest length of 137.44 meters.

According to the geological survey and dam foundation acceptance, there are unloading rock masses on both sides of the bank with strong permeability. After water storage, there are leakage problems in the dam foundation and bank slope. The surface of the proposed dam location is mainly weakly weathered rock mass, with a crack spacing of 0.3-0.6m, mostly open and some wider than 1cm. The rock mass is loose, with low bearing capacity and poor deformation resistance. The crack spacing of the slightly weathered rock mass is 0.5-1m, and the opening degree is generally less than 5mm. The rock mass is relatively tight, with high bearing capacity and shear strength, but low deformation parameters. To improve the mechanical properties of the rock mass and enhance the anti-seepage capacity, the foundation treatment design of curtain grouting, consolidation grouting, and contact grouting has been carried out for this project.

3. CURTAIN GROUTING

3.1. LAYOUT OF CURTAIN GROUTING

3.1.1. *Initial design*

In the initial layout of the curtain grouting, a single row of curtain grouting holes is set up upstream of the grouting gallery at elevations 367.00, 395.50, and 436.00 of the dam. At the same time, another row of curtain grouting holes is arranged upstream of the service gate shaft on the left bank at elevation 436.00 of the dam crest. Three sequence holes are constructed with a spacing of 1.5m between the holes. This double row curtain arrangement provides better anti-seepage effect. The specific layout is shown in Figure 1.

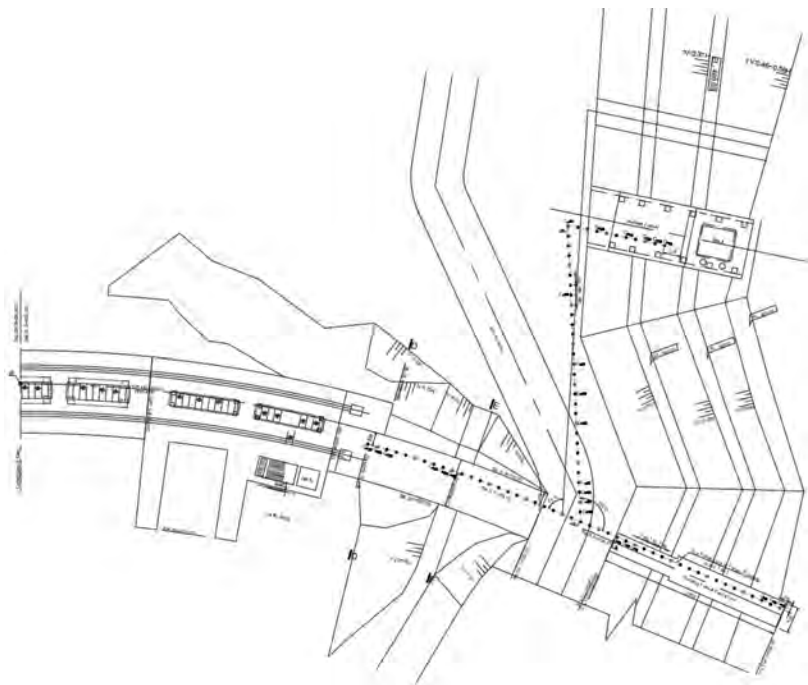


Fig. 1
Layout of curtain grouting of left bank

3.1.2. *Optimize design*

After the completion of the initial design, the design team found that drilling and grouting directly near the service gate shaft under high grouting pressure may have a certain impact on the lining of the service gate shaft. In addition, the construction operation of the double row layout will be more complex during construction. Taking into account the above factors, we have optimized the initial design plan.

Move the position of the left bank grouting hole to the upstream of the service gate shaft and lead the grouting hole along the 436.00 platform into the grouting hole. Due to the fact that the service gate shaft has pressure in the front and no pressure in the back, the curtain upstream of the gate shaft will undergo overlapping curtain grouting to form a closed area, which can effectively reduce the leakage of pressurized water into the gate shaft. The specific layout is shown in Figure 2.

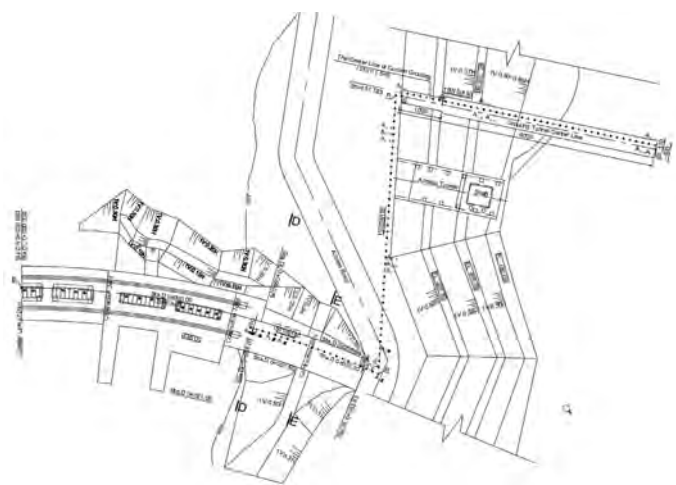


Fig. 2
Optimize layout of curtain grouting of left bank

3.2. PRODUCTIVE TESTING

3.2.1. Selection of testing area

The grouting gallery at elevation 436.00 on the left bank is located on tuff with a joint width of 1-5 mm, mainly composed of three types of surrounding rock. Considering that it will not interfere with the construction of other projects during the construction process, a test area is selected in the grouting gallery 436.00 on the left bank for dam curtain grouting experiments. The spacing between the holes is 1.5m, the depth of the holes into the rock is 45m (55m for the pilot hole), and the length of the testing area is 24m. The construction is carried out in three sequences.

17 holes are arranged in the experimental area, and 2 inspection holes are arranged according to the principle of 10% of the inspection holes. The hole positions are shown in the following Figure 3.

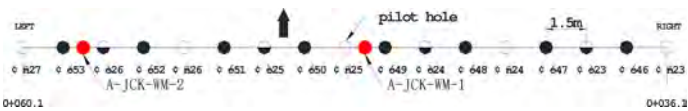


Fig. 3
Layout of grouting hole

3.2.2. *Experimental parameters*

According to the water pressure situation of the pilot hole, the Lu values of sections 1–3 are 96.67Lu, 30.69Lu, and 15.61Lu respectively. During the water pressure process, water leaks out from the contact position between the heavy concrete cover and the grouted side wall, resulting in a relatively high permeability rate. The permeability rate of sections 4–12 is less than 2Lu. During the 1–3 stages of grouting, there is leakage of grout from the contact position between the heavy concrete cover and the grouting hole, as well as from the side walls and arch positions, making it difficult to seal. Therefore, measures such as plugging, depressurization, flow restriction, and repeated grouting are adopted before the grouting is completed, and the grout is basically lost from the leakage position. The subsequent production holes in sequence I will be constructed from bottom to top. When the last section (41–45.3m into the rock) is pressurized, the pressure is 1MPa and the maximum permeability is 1.71Lu. However, when the grouting pressure exceeds 1.5MPa and 2.5MPa, there will be a rapid increase in flow rate and a decrease in pressure. Therefore, pressure and flow limiting grouting will be adopted, but it still cannot reach the designed grouting pressure of 3.5MPa.

According to the construction situation of the pilot hole, in order to improve the grouting effect and adjust the grouting pressure, the water permeability rate of the A-I-23 hole and the bottom section (tenth section, 41–45.7m) before grouting was 1.5Lu. During grouting, it was left to set three times, but four times still did not meet the end standard. The maximum pressure of 2.5MPa was temporarily used to end the grouting, and the ninth, eighth, and seventh sections were continued to be grouted until they reached 2.5MPa. Therefore, based on the actual situation, it is considered to adjust the maximum pressure to 2.5 MPa. The pressure change is divided into three levels, namely 0.5 MPa (first section, rock penetration 0–2m), 1.5 MPa (first section, rock penetration 2–5m), and 2.5 MPa (third section, rock penetration 5–10m and below). Subsequent construction will be controlled according to the pressure per step.

The water cement ratio of the grout is divided into six levels: 5:1, 3:1, 2:1, 1:1, 0.8:1, and 0.5:1. Based on the permeability of each section, the water cement ratio of the grout is 5:1. The grouting slurry changes step by step from thin to thick.

3.3. WATER PRESSURE TEST

During the construction process, all holes are pressurized with water before grouting, curtain grouting is pressurized with water before grouting, each section of the pilot hole is pressurized with water, and the contact section, bottom section, and entire hole of the remaining I and II sequence holes are pressurized with water. The entire hole and bottom section of the III sequence holes are pressurized with water.

Excluding the whole hole pressure water, according to existing data, there are a total of 36 sections of pressure water. There are 6 sections with a permeability rate greater than 30Lu, with a minimum permeability rate of 30.69Lu and a maximum permeability rate of 93.57Lu. Among them, 5 sections are the first sequence contact section and the second section of the pilot hole, accounting for 16.7%; 30Lu \geq permeability rate \geq 3Lu, only one section, is the third section of the pilot hole, with a permeability rate of 15.61Lu, accounting for 2.8%; The permeability of the remaining 25 sections is less than 3Lu, accounting for 80.5%. The specific data is shown in the following figure.

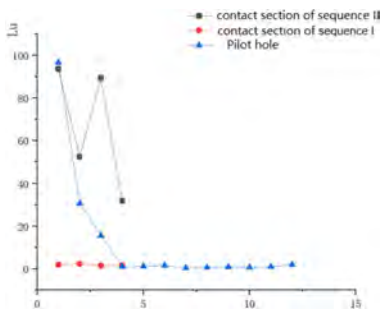


Fig. 4
Contact section and pilot hole pressure
water data

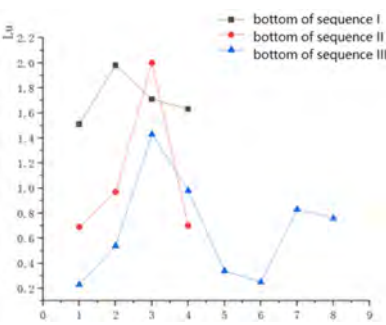


Fig. 5
Water pressure data of the bottom
section of the hole

Before pouring, the contact section of sequence I was pressurized with water for 5 sections, and the permeability rate was all greater than 30Lu, with an average value of 72.76Lu; The pre irrigation water pressure of the second sequence contact section is 4 sections, with an average permeability of 1.88Lu, all of which are less than 3Lu. During the construction of Phase III, no separate pre injection water pressure was applied to the contact section. Bottom section of the hole: 5 sections of pressurized water before injection in sequence I, with an average value of 1.76Lu and a maximum value of 1.98Lu. Stage II pressure water 4, with an average value of 1.09Lu and a maximum value of 2Lu; Stage III pressurized water 8, with an average value of 0.67Lu and a maximum value of 1.43Lu. The permeability rate of pressurized water before pouring in the bottom section of the hole is less than 3Lu, indicating that the bottom line of the curtain meets the construction requirements; After being grouted in stages I and II, the average permeability rate before grouting gradually decreased within the same depth range, indicating that the permeability rate of the bedrock gradually decreased after being grouted in stages.

4. CONSOLIDATION GROUTING AND BANK SLOPE CONTACT GROUTING

4.1. INITIAL DESIGN

In the zoning design of the dam, CVC is used within a range of 3m at the bottom of the dam and 1m on both sides of the bank slope, while RCC is mainly used for the rest. Moreover, the slopes on both sides are steep. If conventional covered heavy consolidation grouting is used, the concrete cannot continuously rise, greatly delaying the construction progress. Therefore, based on the actual characteristics of the project, an initial consolidation grouting plan has been formulated:

In the preliminary design of foundation treatment, we considered the method of uncovered heavy consolidation grouting. These methods have been proven effective in many similar projects, not only providing necessary foundation stability and anti-seepage capabilities, but also accelerating the construction progress of this project and improving the quality of concrete pouring.

After the normal concrete pouring of 3m on the foundation surface is completed and the concrete strength reaches 50% of the design strength, boreholes are drilled and covered heavy consolidation grouting is carried out, while uncovered heavy consolidation grouting is used in other areas.

4.2. OPTIMIZATION DESIGN PROPOSAL

After conducting a detailed investigation of the geological conditions on site, we found that there are some unfavorable factors, such as rock relaxation, low bearing capacity, and the presence of dense fracture zones. These factors can affect the grouting effect and long-term stability of the foundation. Therefore, it is necessary to optimize the preliminary design plan. In order to ensure the required grouting pressure under adverse geological conditions, a method of adding covered weight was added on the basis of no cover weight. After optimizing the design, the second version of the design plan was obtained:

After the normal concrete pouring of 3m on the foundation surface is completed, boreholes are drilled and covered heavy consolidation grouting is carried out. Then, a combination of covered heavy and uncovered heavy grouting is carried out on each level of slope: first, uncovered heavy consolidation grouting is carried out on the lower half of the slope (with a spacing of $3 \times 3\text{m}$ between grouting holes), and then covered heavy consolidation grouting is carried out on the remaining slope through a guide pipe.

Based on the above consolidation grouting scheme and the characteristics of the project, in order to reduce the interference of consolidation grouting on contact grouting, we choose to use the grouting system of consolidation grouting for the arrangement of contact grouting. Pre use consolidation grouting holes as contact grouting holes, and embed contact grouting main pipes on the bedrock surface in advance. During consolidation grouting construction, the range of consolidation grouting 3m away from the contact surface is considered as the contact section, that is, consolidation grouting below 3m is carried out first. After the consolidation grouting is completed and the gap between the dam concrete and the bedrock surface is opened, the pre embedded contact grouting system is used for contact grouting, which also serves as a supplementary consolidation grouting.

4.3. PRODUCTIVE TESTING

4.3.1. *Selection of experimental area*

According to the pouring sequence of the dam foundation concrete, the earliest pouring warehouse was selected as the test area. After the heavy concrete pouring was completed and the concrete strength reached 50%, the drilling and grouting experiment began.

4.3.2. *Experimental parameters*

Grouting pressure: The grouting pressure of the first sequence hole with a depth of 5m shall not exceed 0.3mpa, and the grouting pressure of the second sequence hole shall be 0.3~0.5mpa; For a first sequence hole with a depth of 8m, the grouting pressure for section 0-2m shall not exceed 0.3mpa, and the grouting pressure for section 2-8m shall be 0.6mpa; The second sequence hole with a depth of 8m has a grouting pressure of 0.3-0.5mpa for section 0-2m and 0.8mpa for section 2-8m; The grouting pressure for the first sequence hole with a depth of 15m shall not exceed 0.3mpa for the 0-2m section, 0.6mpa for the 2-7m section, and 1mpa for the 7-15m section; The second sequence hole with a depth of 15m has a grouting pressure of 0.3-0.5mpa for section 0-2m, 0.8mpa for section 2-7m, and 1mpa for section 7-15m.

Slurry water cement ratio and variable slurry standard: The slurry water cement ratio is divided into four levels: 2:1, 1:1, 0.8:1, and 0.5:1. The grouting slurry changes step by step from thin to thick.

4.3.3. *Experimental results*

After the completion of grouting in the experimental area for 3 days, the construction of inspection holes will be carried out, and post grouting water pressure inspection will be conducted. Two inspection holes are arranged in the experimental area. The first section of inspection hole JCK-GJ8-1 has a permeability of 1.59Lu, the second section has a permeability of 0.61Lu, and the third section has a permeability of 0.07Lu; The first section of JCK-GJ8-2 has a permeability rate of 0.34Lu, the second section has a permeability rate of 0.45Lu, and the third section has a permeability rate of 0.29Lu, which meets the design requirements. The quality inspection of consolidation grouting in the test area has been qualified.

The results of the water pressure test are shown in the table 1 below

Table 1
Results of the water pressure test at consolidation grouting test area

No.	Initial depth of test (m)	End depth of test (m)	Length of test (m)	Time (min)	Permeability rate(Lu)	Notes
GJ8-1-8	1.73	6.78	5.05	21	5.15	I sequence
GJ8-1-15	1.75	3.75	2.00	21	28.20	I sequence
	3.75	8.75	5.00	21	3.52	I sequence
	8.75	16.87	8.12	21	5.26	I sequence
GJ8-2-7	1.75	6.78	5.03	21	4.44	II sequence
GJ8-2-19	1.75	3.75	2.00	21	14.42	II sequence
	3.75	8.75	5.00	21	1.67	II sequence
	8.75	16.80	8.05	21	1.45	II sequence
JCK-GJ8-1	1.75	3.75	2.00	21	1.59	Test hole
	3.75	8.75	5.00	21	0.61	Test hole
	8.75	16.75	8.00	21	0.07	Test hole
JCK-GJ8-2	1.74	3.74	2.00	21	0.34	Test hole
	3.74	8.74	5.00	21	0.45	Test hole
	8.74	16.74	8.00	21	0.29	Test hole

After comparing the pre grouting water pressure of each section with the water pressure of the inspection hole, the permeability of each section gradually decreased after grouting, and the effect of surface loosening circle was extremely obvious. The average permeability of the inspection hole was 0.07Lu, with a maximum of 1.59Lu, which meets the design requirements, and the quality of consolidation grouting is qualified.

4.4. FINAL PLAN

According to the experimental results and design plan, the consolidation grouting of the dam foundation was completed. However, during the grouting of the two bank slopes, when the pressure rose to 0.1 MPa (design pressure 0.6 MPa), a large number of cracks were observed on the slope surface and grouting hole wall (about 7 meters away from the injection point), causing grouting leakage. Although attempts were made to solve this problem by sealing surface cracks, increasing slurry concentration, limiting flow rate, intermittent grouting, and waiting for solidification, the leakage problem still exists. Even after waiting for solidification and subsequent re drilling and grouting, there is still leakage that cannot meet the design standards.

To ensure the quality of consolidation grouting, the grouting scheme was adjusted as follows: the consolidation grouting at the positions of both bank slopes was changed to covered heavy consolidation grouting. After each completion of the 1.8m thick concrete pouring, boreholes were drilled on the concrete surface at a 45° angle to the bedrock surface (this angle can indirectly increase the thickness of the concrete cover weight, so that the 1.8m concrete can achieve a 2.5m cover weight effect), and covered heavy consolidation grouting was carried out. Due to the change in consolidation grouting method to covered heavy consolidation grouting, if the contact grouting system is still buried in advance, it will cause damage to the buried contact grouting system during consolidation grouting drilling. After research by the design team, it was decided to drill a contact grouting system near the consolidation grouting hole. Grouting hole, with a depth of 3m below the bedrock surface, and buried with a contact grouting branch pipe, And bury the main pipe on the warehouse surface and lead it downstream of the dam body. This method not only ensures the quality of consolidation grouting, but also minimizes the delay in construction progress caused by traditional methods.

4.5. TEST RESULTS

4.5.1. Water pressure test

Table 2
Results of consolidation grouting test

No.	Initial depth of test (m)	End depth of test (m)	Length of test (m)	Time (min)	Permeability rate(Lu)	Notes
GJ2-1-1 Right	3.25	6.25	3.00	21	74.72	I sequence
	6.25	11.25	5.00	21	18.16	I sequence
	11.25	20.50	9.25	21	4.13	I sequence
GJ2-1-1 Left	3.32	6.32	3.00	21	85.69	I sequence
	6.32	11.32	5.00	21	22.21	I sequence
	11.32	19.77	8.45	21	5.60	I sequence
GJ2-2-5 Right	1.62	4.62	3.00	21	27.70	II sequence
	4.62	9.62	5.00	21	11.85	II sequence
	9.62	18.87	9.25	21	4.16	II sequence
GJ2-2-4 Left	1.85	4.85	3.00	21	25.30	II sequence
	4.85	9.85	5.00	21	11.27	II sequence
	9.85	18.35	8.50	21	4.37	II sequence
JCK-GJ2-1	5.73	8.73	3.00	22	1.19	Test hole
	8.73	14.92	6.19	23	2.11	Test hole
	3.34	6.34	3.00	22	1.78	Test hole
JCK-GJ2-2	6.34	11.34	5.00	22	2.26	Test hole
	11.34	20.58	9.24	23	1.03	Test hole
	5.73	8.73	3.00	22	1.19	Test hole

4.5.2. *Sonic wave test*

The sonic wave test result can be seen below

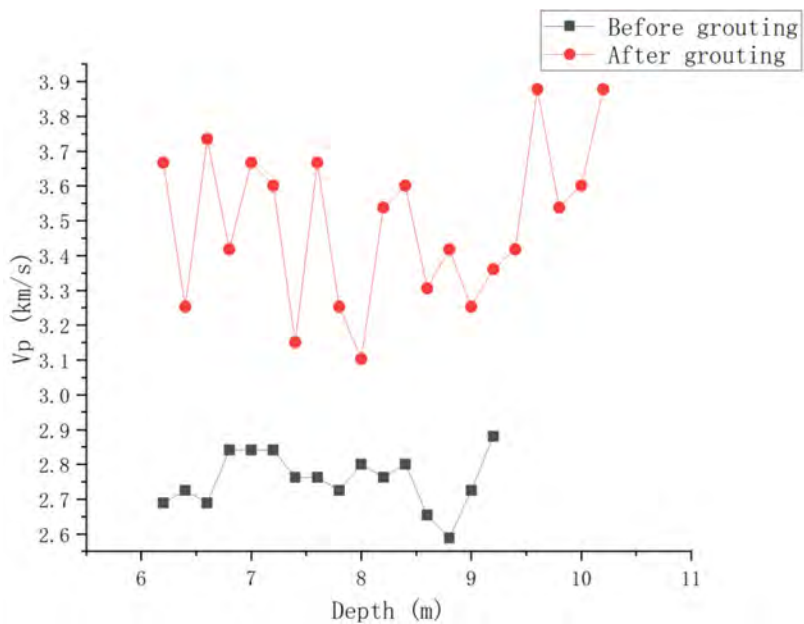


Fig. 6
Sonic wave test result

The average permeability rate of the inspection hole is 1.59Lu, with a maximum of 2.26Lu. According to the results of the sonic wave test, there is a significant increase in wave velocity before and after irrigation. Therefore, it can be proven that the effect of consolidation grouting is effective, and the quality of the consolidation grouting is qualified.

5. CONCLUSION

The following conclusions were drawn through experiments:

1. Through the water pressure test of the curtain grouting inspection hole, the grouting pressure of the dam foundation curtain grouting is divided into three

levels, namely 0.5MPa (first section, 0-2m into the rock), 1.5MPa (first section, 2-5m into the rock), and 2.5MPa (third section, 5-10m and below into the rock). The design water cement ratio is reasonable in six levels: 5:1, 3:1, 2:1, 1:1, 0.8:1, and 0.5:1. The permeability rate of two inspection holes is qualified and meets the design requirements, indicating that the grouting pressure and water cement ratio are reasonable. The permeability rate of the bottom section of all holes before grouting is less than 3Lu, indicating that the bottom line of the curtain meets the technical requirements.

2. The dam foundation is designed with four water cement ratios of 2:1, 1:1, 0.8:1, and 0.5:1 for the cover weight consolidation grouting, and the permeability of two inspection holes is qualified, meeting the design requirements. The grouting pressure of the shallow layer (first section) in the irrigation area is lower than that of the lower second and third sections, but the amount of grout consumed is significantly greater than that of the lower bedrock, indicating that the shallow bedrock is affected by excavation disturbance, with more developed cracks and fractured rock layers. The second and third sections have a small amount of slurry consumption, low pre irrigation water permeability, relatively intact rock layers, and fewer cracks. The average wave velocity before grouting in the sonic wave test was 2.75km/s, and after grouting, it increased to 3.49km/s, with a significant increase, which can reflect that the optimized design scheme still achieved good results while meeting the actual engineering requirements to the greatest extent possible.
3. Through data analysis of curtain and consolidation grouting tests, the optimized design scheme meets the requirements of impermeability and stability. Despite multiple adjustments to the scheme due to the complex rock structure caused by high seismic zones, it still effectively improves the integrity of the dam foundation and enhances the bearing capacity of the foundation.

ACKNOWLEDGMENTS

The authors are grateful for the financial support from the National Key R&D Program of China (No. 2017YFC1501100), the National Natural Science Foundation of China (Nos. 51809221 and 51679158).

REFERENCES

- [1] JING H, LIS. P. Experimental study on volume Tractarian of rocks in full stress-strain process. *Journal of China university of innig and technology*, 1999, 9(1): 33-37

- [2] SHUNSUKE SAKURAI. Development of a new tunneling method to fill the gap between shield tunneling method and rock bolt and shot Crete method.1993.
- [3] MIGUEL A. SÁNCHEZ; ALBERTO FOYO; CARMEN TOMILLO. Application of the Lugeon Test in Landfill Hydrologic Studies[J]. *Environmental and Engineering Geoscience*, 2006.
- [4] GAO YU, FENG CHANGZHEN, XING YULIANG. Quality Management and Evaluation of High Pressure Curtain Grouting for the Foundation of Guanyinge Reservoir [J]. *Water Resources and Hydropower Engineering*, 1995, 1995 (09): 51–54.
- [5] LEE J S, BANG C S, MOK Y J, ET AL. Numerical and experimental analysis of penetration grouting in jointed rock masses[J]. *International Journal of Rock Mechanics and Mining Sciences*, 2000, 37(7):1 027–1 037.
- [6] Application of Consolidation Grouting with out Cover Weight in Goupitan Hydropower Station Project, 2009, 23(03):47-50.
- [7] MA S.C. Feasibility of consolidation grouting without concrete cover in Three Gorges Project. *China Three Gorges Construction*, 1999,3:10–12.
- [8] ZHOU WEIYUAN, YANG RUOQIONG, YAN GONGRUI. Study on the efficacy of grouting reinforcement of slightly weathered rock masses at the Erta arch dam abutments[J]. *Chinese Journal of Rock Mechanics and Engineering*, 1993, 12(2):138–150.(in Chinese))
- [9] JIA F.M, YANG H. Construction of non-cover-weight consolidation grouting on its back-slope of left-bank dam of Longtan Hydropower Station. *Water Power*, 2005,31(4):60–61.
- [10] LIU R.Y., LIU F., YU X.J. Major technical issues in consolidation grouting design of Stage II works of TGP. *Yangtze River*, 2004,35(1):15–16.
- [11] ZHANG W.J., LU W.B., CHEN M., ET AL. Analysis of Consolidation Grouting Effect of Rock Mass Based on Comparison of Wave Velocity Before and After Grouting. *Chinese Journal of Rock Mechanics and Engineering*, 2012,31 (3):469–478.
- [12] PING Y., JIANG Z.J. Analysis of permeability characteristics of fractured rock mass based on pressure water test. *China Rural Water and Hydropower*, 2014,9:166–188.
- [13] CHENG X., ZHANG F.X. *Construction and Effect Testing of Civil Grouting*. Tongji University Press, 1998.
- [14] MU X.R., HUANG X.G. Ultrasonic Detection of Grouting Effect. *Journal of China Coal Society*, 1995,20(3):298–303.

- [15] GUO G.L., DENG K.Z., HE G.Q. Grouting Consolidation and Detection of Fractured Rockmass Foundation over Abandoned Mine Goaf. *Journal of China University of Mining & Technology*, 2000,29(3):293–296.
- [16] WANG G.G., DU M.F., MIAO X.C. Mechanism of Copmaction Grouting and Effect Examination. *Chinese Journal of Rock Mechanics and Engineering*, 2000,19(6):670–673.

COMMISSION INTERNATIONALE DES
GRANDS BARRAGES

VINGT-HUITIEME CONGRES DES
GRANDS BARRAGES
CHENGDU, MAI 2025

**RESEARCH ON THE SAFETY MONITORING INDICATORS OF THE NAM NGUM
5 HYDROPOWER STATION DAM IN LAOS (*)**

Yang GUANG
Deputy Director of Hydro
POWERCHINA International Group Limited

Zhang SHUAI
Deputy Director, Planning and Design Department
Information Technology Research Institute
POWERCHINA Kunming Engineering Corporation Limited

Luo MINGQING
Deputy Director, Technical Management Department
POWERCHINA Resources Limited

CHINA

SUMMARY

When calculating safety monitoring indicators for dams, current methods such as mathematical statistics, the limit state method, and structural calculation tend to be used in isolation, failing to accurately reflect the true operational state of the dam. To address this issue, safety monitoring indicators should be established based on a combination of monitoring data, design results, and various calculation methods like confidence interval estimation, typical small probability analysis, and structural calculations. By integrating these approaches with regulatory guidelines, this study

**Recherche d'indicateurs de surveillance de la sûreté du barrage hydroélectrique de Nam Ngum 5 au Laos*

aims to determine acceptable thresholds for monitoring effects under different operational conditions at the Nam Ngum 5 Hydropower Station dam. The research focuses on principles for selecting monitoring points and evaluating the data quality of initial monitoring sites to identify suitable monitoring indicators. Through the application of mathematical and structural calculation methods, the safety monitoring data of the Nam Ngum 5 Hydropower Station dam is analyzed. The findings from these analyses are used to comprehensively establish monitoring indicators for key monitoring points at the Nam Ngum 5 Hydropower Station, accompanied by application guidelines to meet the operational management and safety evaluation requirements.

RÉSUMÉ

Lors du calcul des indicateurs pour la surveillance de la sécurité des barrages, les méthodes actuelles telles que les statistiques mathématiques, l'état limite et le calcul structural ont tendance à être utilisées de manière isolée, ce qui ne permet pas de refléter avec précision l'état opérationnel réel du barrage. Pour remédier ce problème, des indicateurs de surveillance de la sécurité devraient être établis en se basant sur une combinaison de données de surveillance, de résultats de conception et de diverses méthodes de calcul telles que l'estimation par intervalle de confiance, l'analyse de petites probabilités typiques et les calculs structuraux. En intégrant ces approches aux normes, cette étude vise à déterminer des seuils acceptables pour les effets de surveillance sous différentes conditions opérationnelles au barrage de la centrale hydroélectrique de Nam Ngum 5 au Laos. La recherche se concentre sur les principes de sélection des points de surveillance et sur l'évaluation de la qualité des données des sites de surveillance initiaux pour définir les indicateurs de surveillance appropriés. À travers l'application des méthodes de calcul mathématique et structural, les données de surveillance de sécurité du barrage de la centrale hydroélectrique de Nam Ngum 5 sont analysées. Les résultats de ces analyses sont utilisés pour établir de manière exhaustive des indicateurs de surveillance pour les points de surveillance clés de la centrale hydroélectrique de Nam Ngum 5, accompagnés des principes d'application pour répondre aux exigences de gestion opérationnelle et d'évaluation de la sécurité de l'ouvrage.

1. RESEARCH BACKGROUND

The safety monitoring of dams is a critical aspect of dam safety management. This involves deploying monitoring instruments at various locations to swiftly and

accurately ascertain the operational status of dams and related structures. The data gathered through this process provides essential support for the safety evaluation of these structures. For the entities responsible for the secure operation of dams, it is imperative to continuously collect safety monitoring data and promptly comprehend the operational status of dams through specific safety monitoring indicators, ensuring the safe operation of hydropower stations. Consequently, two primary requirements arise: the establishment of a real-time online monitoring system and the development of quantitative evaluation standards, namely, safety monitoring indicators.

The development of monitoring indicators for dam safety is predicated on the dam and foundation's historical capacity to endure loads. This estimation aids in forecasting the ability to withstand future loads, thereby determining the extreme values of monitoring effects under specific load combinations and significance levels. However, since the load-bearing capacity of dams and foundations fluctuates with changes in materials and environmental factors, estimating safety indicators is a complex issue. Relying on a single method to establish these indicators, without considering the specific circumstances of the dam, often fails to provide scientific guidance for dam safety management during their operational period.

Standards such as the "Code for Dam Safety Monitoring Information Analysis" (DL/T 2340-2021) and the "Technical Specification for Online Safety Monitoring System of Hydropower Dam in Operation" (DL/T 2096-2020) specify that key monitoring locations or sections should be selected based on engineering characteristics and monitoring data analysis. These standards suggest choosing monitoring points that most sensitively reflect the dam's safety state, visually indicate significant project conditions, and exhibit significant amplitude or trend changes requiring focused attention. They provide fundamental principles for selecting monitoring points for water-retaining structures, spillways, slopes, etc. They also recommend that safety monitoring indicators during the dam's operational period should be determined based on monitoring data analysis and methods such as comprehensive comparison, confidence interval, etc.

Building on the existing industry work, this paper uses the Nam Ngum 5 Hydropower Station as a case study to explore comprehensive techniques for formulating monitoring indicators based on multiple criteria. It addresses aspects such as deformation, seepage, and stress-strain. By integrating methods like comprehensive comparison, confidence interval, typical small probability, structural calculation, and engineering experience, and combining these with practical engineering insights, it proposes comprehensive application criteria for monitoring indicators. This approach mitigates the limitations of using a single method to establish monitoring indicators, thereby providing more robust guidance for reservoir and dam operation management.

2. PROJECT OVERVIEW

2.1. PROJECT DESCRIPTION

The Nam Ngum 5 Hydropower Station is situated on the Nam Ting River, a tributary on the right bank of the upper reaches of the Nam Ngum River in Laos. The dam site is approximately 300 kilometers north of the capital, Vientiane, nestled in the mountainous region of northern Laos. The main dam is located in Vientiane Province, while the powerhouse is in the neighboring Xiangkhuang Province. Highways 7 and 13 traverse the northern and western parts of the basin, respectively. The dam site controls a drainage area of 483 square kilometers, which accounts for 2.9% of the total basin area, with an average annual flow of 22.8 cubic meters per second and an annual runoff of 719 million cubic meters.

The power station employs a mixed development approach solely aimed at power generation. The project principally consists of four parts: the headworks, water conveyance system, powerhouse hub, and tailwater structures. The headworks feature a 100.5-meter high roller-compacted concrete single-curve gravity arch dam and a 55-meter high power station intake structure; the water conveyance system includes an 8.73-kilometer water conveyance tunnel, a 174-meter high surge chamber, and a 1.19-kilometer pressure pipeline; the powerhouse hub comprises a 53-meter deep semi-underground main and auxiliary powerhouse, switchyard, and operation village; the tailwater structures include a tailwater gate shaft and a 475-meter long tailwater tunnel.

The design flood level is EL1100.27 meters, and the check flood level is EL1101.84 meters; the normal reservoir level is EL1100.00 meters, the dam crest elevation is EL1103.00 meters, the dam base elevation is EL1004.00 meters, the maximum dam height is 100.50 meters, and the dam crest width is 6.0 meters.

The dam design flood standard is a 1000-year flood, with the check flood standard being a 10,000-year flood. The powerhouse design flood standard is a 100-year flood, with the check flood standard being a 200-year flood. Temporary construction structures (such as cofferdams and diversion tunnels) are designed for a 10-year low-water flood.

The reservoir began impounding on February 29, 2012, and has been operating normally for 12 years.

2.2. OVERVIEW OF THE MONITORING SYSTEM

The safety monitoring system of the Nam Ngum 5 project includes monitoring of deformation in the hub area, environmental variables, the arch dam, dam foundation and abutments, water conveyance and power generation system structures, hub area slopes, and the safety monitoring of the diversion tunnel plug.

1. Inspection: Including routine inspections, annual inspections, and special inspections.
2. External Deformation Monitoring Network: Including plane displacement monitoring network and vertical displacement monitoring network.
3. Deformation Monitoring: Including surface deformation and deflection monitoring, vertical displacement, deep rock mass deformation, and surrounding rock convergence.
4. Seepage Monitoring: Including seepage pressure monitoring, uplift pressure monitoring, dam seepage monitoring, and groundwater level monitoring.
5. Stress-Strain and Temperature Monitoring: Including concrete and structural stress-strain, rebar stress, temperature of the dam foundation and concrete, and dam body joints and cracks monitoring.
6. Support Effect Monitoring: Including ordinary mortar anchor stress monitoring.
7. Environmental Variables Monitoring: Including upstream and downstream water levels, reservoir water temperature, and meteorological monitoring.

3. COMPREHENSIVE CALCULATION TECHNIQUE FOR MONITORING INDICATORS

To address the prevalent issues of inadequate representativeness in selecting monitoring indicator points, the multiplicity yet uniformity of calculation methods, and the absence of practical application guidance, a comprehensive calculation technique for monitoring indicators has been developed. This technique encompasses the exhaustive selection of indicator points, multi-criteria comprehensive calculation, and holistic application principles.

1. Based on existing design outcomes and data analysis, in conjunction with regulations, analogous engineering experience, and selection principles such as the most representative dam sections, the most critical monitoring locations, and the most sensitive projects for detecting anomalies, preliminary monitoring points needing calculation into monitoring indicators are identified.
2. Utilizing the standard deviation calculation formula and considering the allowable error per standards and the required instrument accuracy, the initially selected monitoring points for formulating monitoring indicators are

evaluated. Points passing this error evaluation are chosen as the monitoring indicator calculation points.

3. For the selected monitoring indicator points, the confidence interval estimation method and the typical small probability method are employed to calculate the monitoring indicators, deriving preliminary results of monitoring indicators calculated through these mathematical methods. Additionally, structural calculation results are compiled based on engineering archives, such as reservoir safety evaluation design self-inspection reports and project completion safety evaluation reports.
4. Considering the strengths and weaknesses of the confidence interval estimation method and the typical small probability method, and integrating design calculation results, standard allowable values, and historical extreme values, comprehensive calculation principles for monitoring indicators are established. Monitoring indicators for each monitoring point are then calculated based on these principles.

For the seepage monitoring project, when the results obtained using the confidence interval estimation method, the typical small probability method, and the period extreme value (from the time of impoundment to the normal water level to the present) do not exceed the standard permissible values, the maximum value among the aforementioned methods is generally adopted. However, if these values exceed the standard permissible values, the standard permissible value becomes the primary reference. Given the nature of the monitoring objects, including the dam foundation pressure pipes and dam foundation seepage volume, no minimum monitoring index is established.

5. The calculated monitoring indicators are utilized to guide the safety monitoring of the reservoir dam. The relationship between subsequent measured values and the monitoring indicators is employed to assess the operational state of the monitoring points.

4. COMPREHENSIVE CALCULATION OF MONITORING INDICATORS

4.1. SELECTION OF MONITORING INDICATOR MEASUREMENT POINTS

According to the data quality evaluation method of the measurement points, based on design results, experience from similar projects, qualitative and quantitative analysis of data, a comprehensive selection of 11 seepage monitoring measurement points for formulating monitoring indicators was made. The comprehensive selection of monitoring indicator measurement points and the analysis period are shown in Table 1.

Table 1
Comprehensive Selection of Seepage Monitoring Indicators for the Dam

MEASUREMENT POINT ID	MONITORING INDICATOR ITEM	INSTALLATION LOCATION	ANALYSIS PERIOD
UP1-1	Uplift Pressure at 3# Dam Section	Below dam 0+012.000 Right of dam 0+008.310	2016-2022
UP1-2	Uplift Pressure at 3# Dam Section	Below dam 0+025.800 Right of dam 0+008.310	2016-2022
UP2-1	Uplift Pressure at 2# Dam Section	Below dam 0+009.300 Right of dam 0+050.830	2016-2022
UP3-1	Uplift Pressure at 5# Dam Section	Below dam 0+009.300 Left of dam 0+050.762	2016-2022
P1-2	Seepage Pressure at 3# Dam Section	Below dam 0+014.000 Right of dam 0+008.310	2016-2022
P1-3	Seepage Pressure at 3# Dam Section	Below dam 0+026.000 Right of dam 0+008.310	2016-2022
P2-3	Seepage Pressure at 2# Dam Section	Below dam 0+026.000 Right of dam 0+050.839	2016-2022
P3-2	Seepage Pressure at 5# Dam Section	Below dam 0+014.000 Left of dam 0+050.762	2016-2022
P3-3	Seepage Pressure at 3# Dam Section	Below dam 0+026.000 Left of dam 0+050.762	2016-2022
LY3-1	Seepage Flow in EL1010m Corridor	Below dam 0+027.500 Right of dam 0+009.560	2016-2022
LY3-2	Seepage Flow in EL1010m Corridor	Below dam 0+027.500 Right of dam 0+007.060	2016-2022

4.2. RESULTS OF MATHEMATICAL MODEL CALCULATIONS

4.2.1. Calculation Results of Confidence Interval Method

The basic principle of the confidence interval method is: first, based on the monitoring data of the Nam Ngum 5 Hydropower Station, a statistical model is established between the monitoring effect and the influencing factors by analyzing the influencing factors and factor model. Then, the difference ($\hat{E}-E$) between the monitored effect value (\hat{E}) under various loads and the measured value (E) is calculated using the model. This value has a $1-\alpha$ probability of falling within the confidence band ($\Delta=\pm t^*S$).

When the multiple correlation coefficient R of the statistical model is less than 0.8, and the ratio of the confidence interval to the extreme value interval of the

measuring point is greater than 50%, the monitoring index result determined by the confidence interval estimation method is not used as the main basis for the comprehensive determination of the monitoring index. Its results are for reference only and should be used as the comprehensive determination result only when other judgment methods or results are lacking.

Using the stepwise regression analysis method, a regression analysis of the monitoring index measurement points is conducted to obtain the regression coefficients of the measurement points, multiple correlation coefficient R , standard deviation S , etc. The monitoring index determined by the confidence interval method is obtained, and the results of the dam monitoring index determined by the confidence interval method are shown in Table 2.

Table 2
Dam Monitoring Indicators calculated by Confidence Interval Method

MEASUREMENT POINT ID	LOWER LIMIT OF MONITORING INDICATOR	UPPER LIMIT OF MONITORING INDICATOR	RATIO OF CONFIDENCE INTERVAL TO MAXIMUM VALUE INTERVAL	R	REMARKS
P1-2	/	159.66	40.18%	0.95	Water Head (m)
P1-3	/	92.22	75.27%	0.81	Water Head (m)
P2-3	/	105.26	35.57%	0.92	Water Head (m)
P3-2	/	73.25	57.68%	0.87	Water Head (m)
P3-2	/	156.96	36.24%	0.91	Water Head (m)
UP1-1	/	155.29	54.76%	0.87	Water Head (m)
UP1-2		60.62	75.58%	0.83	Water Head (m)
UP2-1		330.55	40.97%	0.89	Water Head (m)
UP3-1	/	180.46	41.11%	0.92	Water Head (m)
LY3-1	/	0.75	41.91%	0.90	Seepage Flow (L/s)
LY3-2	/	1.23	33.53%	0.94	Seepage Flow (L/s)

4.2.2. Calculation Results of the Typical Small Probability Method

From the measured data, according to the different types of dams and specific conditions of each dam, the monitoring effect X_{mi} is selected during the unfavorable

load combinations. Then, X_{mi} is a random variable. From the series of observational data, a sample space with a sample size of n can be obtained, and its statistical characteristics can be estimated using the following two formulas:

$$\bar{X} = \frac{1}{n} \sum_{i=1}^n X_{mi} \quad [1]$$

$$\sigma_x = \sqrt{\frac{1}{n-1} \left(\sum_{i=1}^n X_{mi}^2 - n\bar{X}^2 \right)} \quad [2]$$

Next, statistical test methods (such as A-D test, K-S test) are used to conduct distribution tests to determine the distribution function $f(x)$ of its probability density $F(x)$ (such as normal distribution, log-normal distribution, and extreme value type I distribution).

Let X_m be the extreme value of the monitoring effect. If the dam will exhibit abnormal behavior or danger when $X > X_m$, the probability is P :

$$P(X > X_m) = P_\alpha = \int_{\alpha_m}^{+\infty} f(x) dx \quad [3]$$

After determining the distribution of X_m , the main issue in estimating X_m is to determine the failure probability P_α (hereinafter referred to as α), the value of which depends on the importance of the dam. For concrete dams, α is generally taken as 1% or 5%. After determining α , X_m can be directly obtained from the distribution function:

$$X_m = F^{-1}(\bar{x}, \sigma_x, \alpha) \quad [4]$$

For the typical small probability method, monitoring indicators are calculated. When the sample time series is less than four years, the monitoring indicator results calculated by the typical small probability method are only for reference. Only when other evaluation methods or results are lacking, the monitoring indicator results calculated by the typical small probability method are taken as comprehensive calculation results.

The monitoring indicators calculated using the typical small probability method, which are the results of dam monitoring indicators under the typical small probability method, are shown in Table 3.

Table 3
Dam Monitoring Indicators calculated by Typical Small Probability Method

MEASUREMENT POINT ID	INDICATOR TYPE	STATISTICAL DISTRIBUTION	DISTRIBUTION PARAMETERS	MONITORING INDICATOR
P1-2	Maximum Value	Normal Distribution	$E=108.1795, \sigma_2=10.1468$	131.79
P1-3	Maximum Value	Extreme Value Type I Distribution	$P_a=0.015, P_u=46.2295$	244.30
P2-3	Maximum Value	Normal Distribution	$E=89.7021, \sigma_2=18.8632$	120.73
P3-2	Maximum Value	Extreme Value Type I Distribution	$P_a=0.0408, P_u=16.2742$	89.07
P3-3	Maximum Value	Log-Normal Distribution	$E=4.9368, \sigma_2=0.0071$	141.65
UP1-1	Maximum Value	Log-Normal Distribution	$E=4.8707, \sigma_2=0.1083$	155.85
UP1-2	Maximum Value	Log-Normal Distribution	$E=3.817, \sigma_2=0.209$	64.12
UP2-1	Maximum Value	Normal Distribution	$E=197.7667, \sigma_2=106.5404$	373.03
UP3-1	Maximum Value	Extreme Value Type I Distribution	$P_a=0.0194, P_u=26.5383$	179.71
LY3-1	Maximum Value	Extreme Value Type I Distribution	$P_a=4.0033, P_u=0.1176$	0.86
LY3-2	Maximum Value	Extreme Value Type I Distribution	$P_a=2.5736, P_u=0.1387$	1.29

4.2.3. Comprehensive Calculation of Monitoring Indicators

According to the comprehensive calculation technology for monitoring indicators mentioned above, the comprehensive monitoring indicators for the seepage of the Nam Ngum 5 Hydropower Station dam are as follows:

Table 4
Comprehensive Calculation Table of Dam Monitoring Indicators

MEASUREMENT POINT ID	INDICATOR TYPE	CONFIDENCE INTERVAL METHOD	TYPICAL LOW PROBABILITY	PERIOD EXTREMUM	LIMIT VALUE ACCORDING TO THE RELATED STANDARD	COMPREHENSIVE CALCULATION
P1-2	Maximum Value	159.66	131.79	178.06	300.50	178.06
P1-3	Maximum Value	92.22	244.30	121.68	166.70	121.68
P2-3	Maximum Value	105.26	120.73	111.30	58.00	58.00
P3-2	Maximum Value	73.25	89.07	98.67	140.00	98.67
P3-3	Maximum Value	156.96	141.65	150.43	47.70	47.7
UP1-1	Maximum Value	155.29	155.85	150.09	330.51	155.29
UP1-2	Maximum Value	60.62	64.12	68.61	332.19	68.61
UP2-1	Maximum Value	330.55	373.03	324.94	185.50	373.03
UP3-1	Maximum Value	180.46	179.71	174.25	176.18	176.18
LY3-1	Maximum Value	0.75	0.86	0.67	/	0.86
LY3-2	Maximum Value	1.23	1.29	1.06	/	1.29

4.2.4. *Recommendations for Application of Monitoring Indicators*

The recommendations for the application of seepage monitoring indicators are as follows:

Table 5
Seepage Monitoring Indicators Application Table

MONITORING ITEM	MEASURED POINT VALUE	MEASUREMENT EVALUATION	CORRESPONDING MEASURES
Dam Foundation Uplift Pressure B	$B \leq$ Monitoring Indicator	Normal	/
	Monitoring Indicator $< B \leq$ Specification Allowable Value	Basically Normal	Monitor value changes.
	Specification Allowable Value $< B \leq$ Historical Maximum Value (greater than specification allowable value measurement point)	Basically Normal	Monitor value changes, increase observation frequency and manual comparison if necessary.
	$B >$ Historical Maximum Value (greater than specification allowable value measurement point)	Warning	<ul style="list-style-type: none"> Retake measurements and monitor value changes; If the value shows a trend change, conduct on-site inspection and patrol, and carry out analysis and evaluation of monitoring data; Prepare a special analysis report and hold a special meeting if necessary.
Dam Seepage Flow C	$C \leq$ Monitoring Indicator	Normal	/
	$C >$ Monitoring Indicator	Warning	<ul style="list-style-type: none"> Retake measurements and monitor value changes; If the value shows a trend change, conduct on-site inspection and patrol, and carry out analysis and evaluation of monitoring data; Prepare a special analysis report and hold a special meeting if necessary.

5. CONCLUSION

Given that the load-bearing capacity of dams and their foundations fluctuates with changes in materials and environmental factors, estimating safety indicators is an inherently complex task. Relying solely on a single method to determine these indicators fails to provide adequate scientific guidance for the safety management of dams during their operational lifespan.

This paper develops a comprehensive monitoring indicator calculation technique based on the integrated selection of indicator measurement points, multi-

criteria comprehensive calculation, and the holistic application of criteria. By initially screening and meticulously selecting the seepage monitoring indicator measurement points for the Nam Ngum 5 Hydropower Station dam, a total of 11 safety monitoring indicator measurement points were determined. Utilizing actual measurement data, confidence interval estimation methods, and typical small probability methods, mathematical models of the monitoring indicators at the proposed measurement points were calculated. The comprehensive calculation of monitoring indicators was performed based on these calculation results, along with the characteristics of different monitoring projects, historical extreme values (interval extremes), design calculation values, and standard permissible values.

According to the calculated monitoring indicators, application recommendations and response measures for different monitoring projects were provided, thus facilitating the daily monitoring management of the power plant. This approach aims to swiftly assess the safety status of the hydropower station dam and offer scientific guidance for its operation, while also serving as a reference for similar projects.

REFERENCES

- [1] WU ZHONGRU, ET AL. Theory and Application of Dam Safety Synthetical Analysis and Assessment [J]. *Advances in Science and Technology of Water Resources*, 1998, (03): 5–9+68.
- [2] YANG JIE, WU ZHONGRU. Present Conditions and Development of Dam Safety Monitoring and Control Researches Home and Abroad [J]. *Journal of Xi'an University of Technology*, 2002, (01): 26–30.
- [3] WEI DERONG. On Working out Dam Safety Monitoring Index [J]. *Dam and Safety*, 2003, (06): 24–28.
- [4] LI BING. Research on Intelligent Analysis Method for Deformation Monitoring of Gravity Dam [D]. *Xi'an University of Technology*, 2021.
- [5] LI ZHANCHAO, HOU HUIJING. Theory and Methods on Dam Safety Monitoring Indexes [J]. *Water Power*, 2010, 36 (05): 64–67.
- [6] ZHANG LIBING, ZHANG SHUAI, XU HOULEI. Comprehensive Formulation and Application of Safety Monitoring Indexes of Jinghong Dam[J]. *Water Power*, 2018, 44 (06): 103–106.

COMMISSION INTERNATIONALE DES
GRANDS BARRAGES

VINGT-HUITIEME CONGRES DES
GRANDS BARRAGES
CHENGDU, MAI 2025

THE RESEARCH AND APPLICATION OF KEY TECHNOLOGIES FOR THE CONSTRUCTION OF SMART SITES IN LARGE HYDROPOWER STATIONS (*)

He ZHANGUO

Power China Huadong Engineering Corporation Limited, Zhejiang Hangzhou

Yan JIANGPING

Yalong River Hydropower Development Corporation Limited, Sichuan

Jiao KAI

Yalong River Hydropower Development Corporation Limited, Sichuan

Huang CHENGJIA

Power China Huadong Engineering Corporation Limited, Zhejiang Hangzhou

Zhai HAIFENG

Yalong River Hydropower Development Corporation Limited, Sichuan

Pan HAIJING

Power China Huadong Engineering Corporation Limited, Zhejiang Hangzhou

CHINA

SUMMARY

To address the current challenges in the construction of large hydropower stations, such as high safety risks, difficulty in safety management, and challenges in construction quality control, digital, automated, and intelligent methods have been adopted. By leveraging advanced technologies like the Internet of Things (IoT),

**Recherche et application de technologies clés pour la construction de systèmes intelligents dans les grandes centrales hydroélectriques*

cloud computing, and big data, a comprehensive smart construction site system has been developed, covering all aspects, elements, and processes. This system enables intelligent management throughout the entire lifecycle of the hydropower station, from design and construction to operation management, offering broad market potential and significant application value.

RÉSUMÉ

Pour relever les défis actuels dans la construction de grandes centrales hydroélectriques, tels que les risques élevés de sécurité, la difficulté de gestion de la sécurité et les défis dans le contrôle de la qualité de la construction, des méthodes numériques, automatisées et intelligentes ont été adoptées. En tirant parti de technologies avancées comme l'Internet des objets (IoT), le cloud computing et le big data, un système complet de chantier intelligent a été développé, couvrant tous les aspects, éléments et processus. Ce système permet une gestion intelligente tout au long du cycle de vie de la centrale hydroélectrique, depuis la conception et la construction jusqu'à la gestion de l'exploitation, offrant un large potentiel de marché et une valeur d'application significative.

1. PROJECT OVERVIEW

The Kala Hydropower Station is located in Muli County, Liangshan Prefecture, Sichuan Province, China, and is the seventh hydropower station on the middle reaches of the Yalong River. The primary purpose of the station is power generation, with an installed capacity of 1,020 MW. The reservoir's normal water level is 1,987.0 meters, with a dead water level of 1,982.0 meters. The normal storage capacity is 237.8 million cubic meters, and the regulation storage capacity is 36.5 million cubic meters. The key infrastructure includes a roller-compacted concrete gravity dam, flood discharge structures on the dam, an energy dissipation pool downstream of the dam, and a power generation facility on the right bank. The station is situated in a deep mountain gorge, where the geological conditions are complex, the scale of the project is substantial, and the technical challenges are significant.

2. BACKGROUND AND SIGNIFICANCE

With the rapid economic development, the field of large-scale engineering construction is undergoing dramatic changes. The application of technologies such as BIM (Building Information Modeling), the Internet of Things (IoT), and Artificial Intelligence (AI) has provided a visualized and quantifiable collaborative management platform for

engineering projects. This has significantly enhanced the level of digitalization and intelligence, bringing about fundamental transformations to the entire industry.

In complex large-scale hydraulic and hydropower engineering projects, there are high safety risks, significant challenges in safety management, and difficulties in construction quality control. Traditional management and monitoring technologies no longer fully meet the demands of project construction.

Leveraging the Kala Hydropower Station, digitalization, automation, and intelligent methods have been adopted, integrating advanced technologies such as IoT, cloud computing, and big data to develop a smart construction site system that covers all business aspects, elements, and processes. The research and application of intelligent safety monitoring technology, intelligent construction technology, and an intelligent construction platform for hydropower stations have been realized. This system enables intelligent management throughout the entire lifecycle of the hydropower station, from design and construction to operation management, offering broad market prospects and significant application value. It also provides valuable insights for innovative management approaches in similar domestic engineering projects.

3. SMART CONSTRUCTION SITE DEVELOPMENT APPROACH AND SYSTEM ARCHITECTURE

3.1. DEVELOPMENT APPROACH

To address the high safety risks and challenges in safety management during hydropower station construction, intelligent safety monitoring technologies have been developed and applied. These include intelligent management of the work environment's safety (such as control of hazardous areas and detection of small forest fire sources), intelligent vehicle and traffic management, risk control, and hazard mitigation.

To enhance the efficiency of hydropower station construction management, reduce manual labor, and precisely control construction quality, an intelligent construction platform for hydropower stations has been developed and implemented. This includes technologies such as drone-based geological surveys, quality inspection and evaluation via PAD applications, and intelligent laboratories.

3.2. SYSTEM ARCHITECTURE

The smart construction site application architecture is shown in the diagram below. By developing and establishing an integrated, efficient management platform

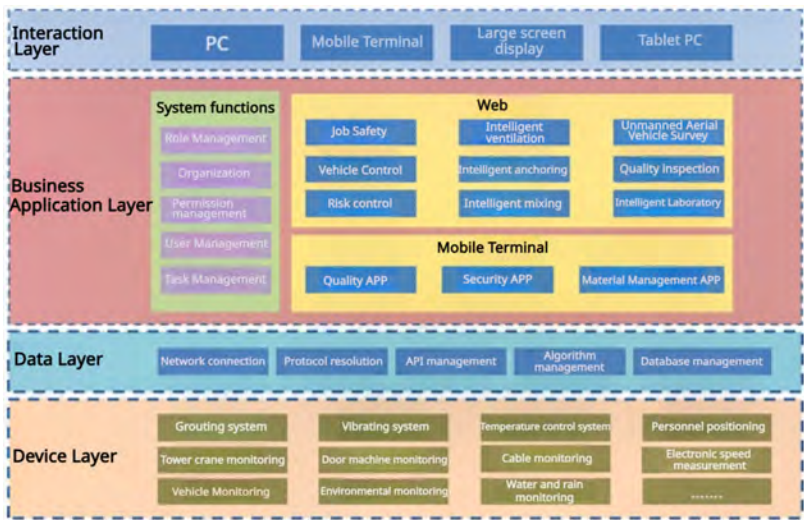


Fig. 1
Smart Construction Site System Architecture

that combines on-site and remote operations, information aggregation, and rapid response, the system covers the entire project, all elements, all processes, and all participating parties across multiple levels. This platform meets real-time, online, interactive, and streamlined technical requirements. Ultimately, it caters to the needs of users at different levels through a multi-terminal integration approach.

4. APPLICATION OF INTELLIGENT SAFETY MONITORING IN CONSTRUCTION

4.1. INTELLIGENT MANAGEMENT OF WORK ENVIRONMENT SAFETY**

By conducting real-time monitoring of hazardous areas, potential dangers can be promptly identified, allowing for early warning and appropriate measures to be taken (such as landslide warnings) to ensure the safety of personnel and effectively prevent safety incidents. The precise detection of small forest fire sources can effectively prevent forest fires and enhance fire prevention and control capabilities.

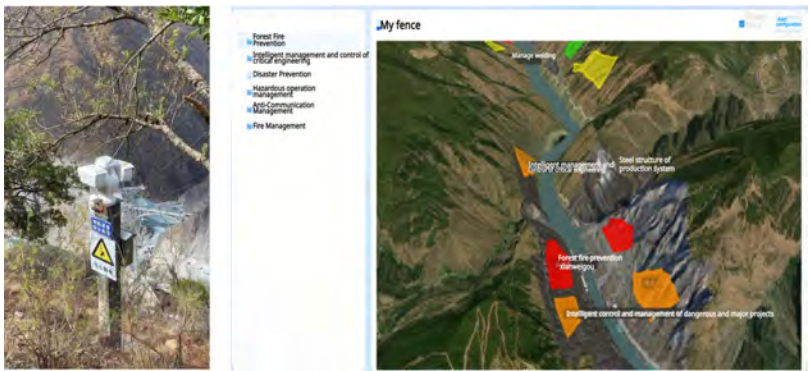


Fig. 2
Intelligent Management System for Work Environment Safety

4.2. RISK MANAGEMENT AND HAZARD MITIGATION

Establish a dynamic risk management database for the Kala Hydropower Station, integrating the control and management of safety hazards to achieve dynamic risk control, early warning analysis, and mitigation of risks.

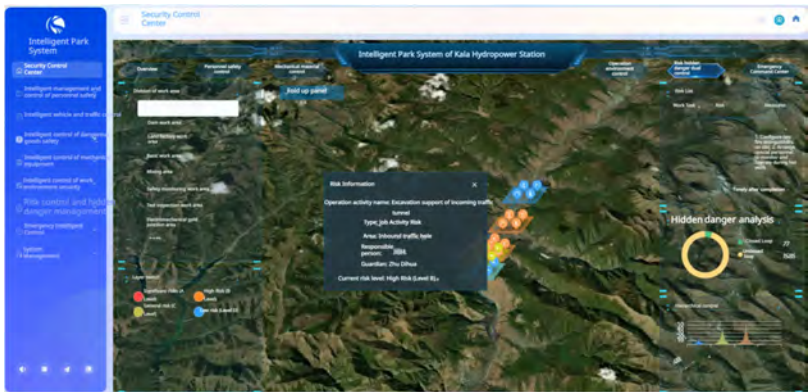


Fig. 3
Risk Management and Hazard Mitigation System

4.3. INTELLIGENT IDENTIFICATION OF HAZARDOUS CONSTRUCTION BEHAVIORS

The intelligent identification system for hazardous construction behaviors at the hydropower station uses computer vision and deep learning technologies to monitor operational behaviors at the construction site in real time, automatically detecting and issuing warnings for dangerous behaviors.



Fig. 4
Intelligent Identification of Hazardous Construction Behaviors

4.4. INTELLIGENT MANAGEMENT OF SPECIAL EQUIPMENT

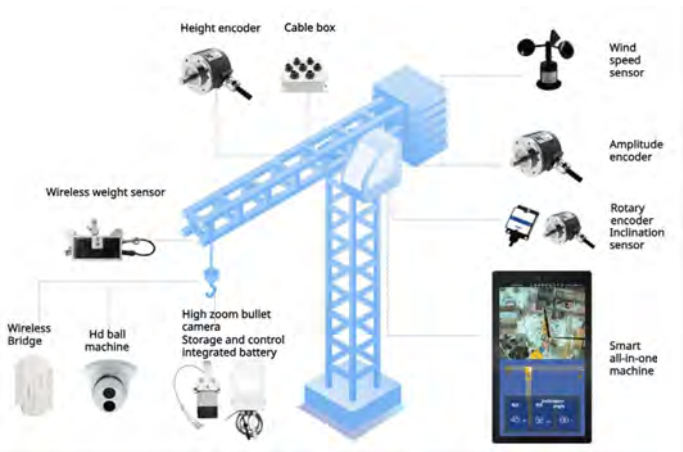


Fig. 5
Intelligent Management System for Special Equipment

By utilizing technologies such as the Internet of Things (IoT), big data, and artificial intelligence (AI), the system real-time monitors the operating status, location, and operator behavior of special equipment. It automatically identifies potential hazards and rule violations, providing early warnings and taking appropriate actions.

5. INTELLIGENT CONSTRUCTION PLATFORM APPLICATIONS

5.1. DRONE-BASED GEOLOGICAL SURVEY

Utilizing drones equipped with high-precision sensors, geological data for site selection and construction areas of the hydropower station can be obtained, providing a basis for design and ensuring construction safety. Additionally, drone-based geological survey technology can monitor the impact of the hydropower station's operation on the surrounding environment.

5.2. QUALITY INSPECTION PAD APPLICATION

By incorporating specialized inspection software into a PAD, the system enables rapid collection, processing, analysis, and quality assessment of engineering data. This improves inspection efficiency and quality, reduces manual labor, minimizes error rates, and ensures the quality of the project.

5.3. INTELLIGENT LABORATORY

Leveraging technologies such as the Internet of Things (IoT), big data, and artificial intelligence (AI), the intelligent laboratory utilizes automated testing equipment and smart algorithms to automatically generate test reports and provide real-time alerts for non-conformities. This enhances testing efficiency and quality while reducing error rates.

6. KEY INNOVATIONS

1. Development of an Intelligent Safety Monitoring System for Large Hydropower Station Construction: This system comprehensively ensures the safety of both

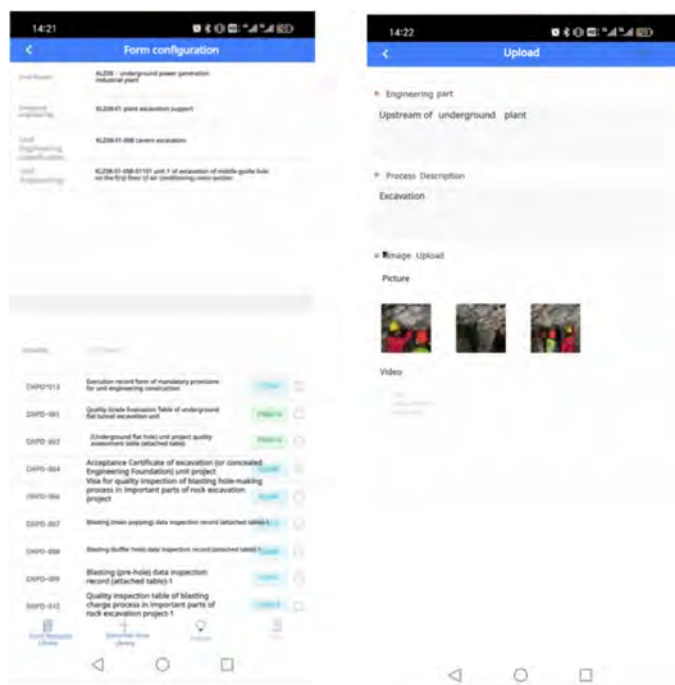


Fig. 6
Quality Inspection PAD Application.

- the construction and operation of the hydropower station. By utilizing video surveillance and artificial intelligence algorithms, it provides real-time monitoring and early warning for unsafe behaviors and scenarios at the construction site, significantly enhancing construction safety.
2. Creation of a Comprehensive Smart Construction Platform for Large Hydropower Stations: This platform covers all business aspects, elements, and processes, incorporating eight intelligent business management functions and five intelligent construction applications. Through digitalization, automation, and intelligence, it achieves smart management throughout the entire lifecycle of the hydropower station—from design and construction to operational management. It facilitates information sharing and collaborative work, employing advanced smart technologies such as the Internet of Things (IoT), cloud computing, and big data to automate and optimize equipment monitoring, operational management, and maintenance tasks.

7. CONCLUSIONS

The research and application of smart construction site technologies at the Kala Hydropower Station have gained significant influence within the industry. Various organizations, including the China Electric Power Construction Enterprise Association, the Hydropower Engineering Society, the China Institute of Water Resources and Hydropower Research, State Power Investment Corporation (SPIC), and State Grid New Energy, have visited the Kala Hydropower Station for research and learning on intelligent management and control. Leading domestic universities such as Tsinghua University and Tianjin University have conducted specialized research projects at the station, cultivating a group of highly skilled professionals in the comprehensive management of large hydropower projects.

All units and experts agree that the smart construction site system at the Kala Hydropower Station is highly operational and has strong promotional value. This technology meets a significant demand in the construction of large hydropower stations, offering broad market prospects and substantial application value, with considerable social benefits.

REFERENCES

- [1] XIE LINGFEI, LI DE. "3D Collaborative Design of Hydraulic and Hydropower Engineering Based on BIM Technology." **China Rural Water and Hydropower**, 2020 (03): 105–111.
- [2] LIU JING, ZHANG XU, JIN LEI, *ET AL.* "Standards for BIM Model Construction and Digital Handover in Hydraulic Engineering." **People's Yellow River**, 2021, 43 (S2): 268–271.
- [3] CHEN WENLIANG, WANG LIANG, WANG CHENG, *ET AL.* "Application of BIM Technology in Hydraulic Engineering Construction." **Hydraulic Technology Supervision**, 2021 (06): 43–44, 70.
- [4] FEI YIXIN, YE XUEFEN, LIU ZIXI. "Research on Whole-process Quality Control of Hydraulic Engineering Construction Based on BIM." **Hydraulic Technology Supervision**, 2023 (01): 17–20, 97.
- [5] GUO GUANGZHI, WANG JIA, LI LUOGANG. "Application and Development Prospects of BIM Technology in Hydraulic Construction." **Hydraulic Planning and Design**, 2021 (10): 7–10.

- [6] WANG LIJUAN. "Organization and Preservation of Electronic Archives in Hydropower Survey and Design Units." **Hydraulic Technology Supervision**, 2008 (02): 39–41.
- [7] LI JUNLIAN. "A Brief Analysis of the Differences Between Electronic and Paper Archives in Hydraulic Engineering." **Henan Water Resources and South-to-North Water Diversion**, 2014 (18): 82–83.
- [8] QI BING, ZHU XIAOKAI, XU XIAOHUA. "Application of Electronic Archives in Hydraulic Engineering Construction Management." **Hydraulic Construction and Management**, 2007 (10): 57–58.

COMMISSION INTERNATIONALE DES
GRANDS BARRAGES

VINGT-HUITIEME CONGRES DES
GRANDS BARRAGES
CHENGDU, MAI 2025

CONDITION OF DAMS AND LEVEES IN POLAND - ISSUES, STATISTICS, AND CHALLENGES (*)

dr inż. KRZYSZTOF RADZICKI

Department of Geoengineering and Water Management, Faculty of Environmental Engineering and Energy, Cracow University of Technology

mgr inż. MACIEJ SIEIŃSKI

Director, Centre for Technical Control of Dams, IMGW-PIB

dr inż. hab. TOMISŁAW GOŁĘBIEWSKI PROF. PK

Head, Department of Geoengineering and Water Management, Faculty of Environmental Engineering and Energy, Cracow University of Technology

mgr Dagmara ZELAYA-WZIĄTEK

Centre for Technical Control of Dams, IMGW-PIB

mgr Zbigniew DMITRUK

Centre for Technical Control of Dams, IMGW-PIB

POLAND

SUMMARY

Climate change poses significant challenges to the maintenance and safety of Poland's damming structures. Research indicates that catastrophic floods, such as the one in September 2024, may statistically occur twice as frequently and with greater intensity than previously recorded. At the same time, a critical issue is already the inadequate technical condition of a large proportion of damming structures, especially dams, as well as the extensive total length of levees, which

**État des barrages et des digues en Pologne – questions, statistiques et enjeux*

presents challenges in terms of inspection and the costs associated with potential repairs and upgrades. This article provides comprehensive and up-to-date data on the condition of damming structures in Poland and briefly describes the dam failure in Stronie Śląskie, which occurred on September 15, 2024. The most significant risks and challenges faced by relevant authorities and engineers in Poland, both in the current situation and in the future, are identified. Key systemic and technical solutions are proposed that should be considered to mitigate the increasing risks of damming structures failures due to climate change and the ongoing aging of these structures.

RÉSUMÉ

Le changement climatique pose d'importants défis à l'entretien et à la sécurité des barrages polonais. Les recherches indiquent que les inondations catastrophiques, telles que celle de septembre 2024, pourraient statistiquement se produire deux fois plus fréquemment et avec une plus grande intensité qu'auparavant. Dans le même temps, l'état technique inadéquat d'une grande partie des structures d'endiguement, en particulier les barrages, ainsi que la grande longueur totale des digues, constituent déjà un problème critique, qui pose des défis en termes d'inspection et de coûts associés à d'éventuelles réparations et mises à niveau. Cet article fournit des données complètes et actualisées sur l'état des structures de barrage en Pologne et décrit brièvement la rupture du barrage de Stronie Śląskie, qui s'est produite le 15 septembre 2024. Les risques et les défis les plus importants auxquels sont confrontés les autorités compétentes et les ingénieurs en Pologne, à la fois dans la situation actuelle et dans le futur, sont identifiés. Des solutions systémiques et techniques clés sont proposées pour atténuer les risques croissants de défaillance des structures d'endiguement dus au changement climatique et au vieillissement de ces structures.

1. INTRODUCTION

Maintaining the adequate condition of numerous damming structures, particularly given the significant, often cumulative costs of necessary and concurrent repairs for many of them, currently represents a global challenge faced even by highly developed countries (Duminda et al., 2021; ASCE, 2021). In the new millennium, and particularly over the last decade, there has been a marked deterioration in the condition of damming structures in Poland (Dmitruk et al., 2022; NIK, 2015; Świdorska & Lebiecki, 2011). This decline results, first, from longstanding neglect in the funding of water management and, second, from the global challenge of aging hydrotechnical infrastructure. One of the key tools with the potential to

mitigate this issue is the development and implementation of advanced methods for the assessment and monitoring of hydrotechnical structures.

Structures such as dams, weirs, levees, and canal's dikes play a crucial role in ensuring stable and sustainable socio-economic development and functionality in most countries, including Poland. Depending on their specific functions, they are essential at various levels, particularly on regional and nationwide scales, for flood protection, providing immediate reserves of dispatchable power to meet peak load demands through the potential energy stored in water. They also contribute to stabilizing grid overloads, especially from wind and solar power plants, generating green energy from hydropower, and supplying water to agriculture, industry, and the population. In this context, the availability of large quantities of water is also essential for the intensively developing energy production sectors worldwide and in Poland. This includes cooling nuclear power plants, producing biomass for energy purposes, and generating hydrogen. The crucial role of water retention structures in the development and functioning of regions and nations has led to the construction of a substantial number of these facilities, including in Poland. Many of them are now over 50 years old. As technological and economic development continues and population levels rise, there remains an ongoing need for the construction of new facilities. For example, the Goczałkowice and Kozłowa Góra reservoirs, created through the construction of large earth dams, are essential for supporting water intake facilities that supply drinking water to over 3 million people in the Upper Silesia region. Additionally, these reservoirs play a crucial role in flood protection of areas along the Upper and Middle Vistula River, including the cities of Cracow and Sandomierz. The Dobczyce Dam provides a vital water intake for the city of Cracow, supplying water to approximately 350,000 residents, and also offers significant flood protection for the floodplain areas of the Raba River, especially in the cities of Dobczyce and Gdów. The Racibórz dry reservoir dam is a key flood protection measure not only for Wrocław but also on a larger, regional scale, protecting flood-prone areas in the Silesian, Opole, and Lower Silesian provinces, safeguarding nearly 1.3 million residents. One of many other examples of essential damming structures are the levees in Cracow city. With a total length of nearly 80 kilometers, they protect a significant portion of the city from the threats posed by surges of the Vistula River and its backflow into its tributary channels.

In the following sections of the article, we will present statistics on the technical condition and state of structural safety of dams and levees. We will briefly describe the collapse of the earth dam in Stronie Śląskie. Subsequently, we will discuss significant current challenges and offer preliminary proposals for improving the present condition of hydraulic structures in Poland.

2. TECHNICAL CONDITION AND STATE OF STRUCTURAL SAFETY OF THE DAM STRUCTURE

In Poland, damming structures are assessed based on their technical condition and safety status. The technical condition of a structure is classified as good, sufficient or insufficient, while the safety status is categorized as safe, safe with attention or unsafe. All hydraulic structures, including damming structures, are classified into classes from I to IV. Class I structures are considered the most critical in terms of their functional importance and/or pose a significant risk to human safety and property in the event of failure. For example, the Goczałkowice, Solina, Tresna, and Jeziorsko dams are classified as Class I, while the Chańcza and Kozłowa Góra dams are classified as Class II.

The database of the technical condition and safety of hydraulic structures in the System for the Registration and Control of Damming Structures in Poland is maintained by the National Service for Safety of Damming Structures, as mandated by law. This service is carried out by the Institute of Meteorology and Water Management – National Research Institute, which includes the Center for Technical Control of Dams (CTKZ – Centrum Technicznej Kontroli Zapór). The CTKZ is statutorily responsible for the assessment of Class I and II hydraulic structures owned by the State Treasury.

The technical condition of a structure impacts its usability. Poor technical condition can limit its functionality or even lead to its decommissioning. The technical condition of a structure is not the same as its safety status, though they are closely related. There could be situations where the overall condition of a dam, for example, is insufficient due to numerous but moderately advanced destructive processes that currently do not pose a significant risk for safety. On the other hand, the safety status of this structure may be classified as safe with attention, accompanied by specific repair recommendations. Conversely, for another structure previously in good condition, an incident such as a drive failure of spillway gates would immediately reclassify its technical condition as unsatisfactory and its safety status as endangered safety.

In the case of damming structures, a flood wave resulting from their failure can pose a significant threat to a large number of people and/or cause substantial material losses, particularly for large dams. In recent years, there has been a notable increase in dam failures worldwide, underscoring the critical importance of good technical condition and safety of these hydraulic structures. Unfortunately, in September 2024, one such incident occurred in Poland. It will be briefly described later in this article. A year prior, the second most catastrophic dam failure in history took place. Extreme rainfall, likely linked to climate change, led to the filling and rupture of a dam situated above the city of Derna in Libya. A large part of the city was destroyed, with over 10,000 people losing their lives. The dam was in a severely deteriorated technical condition.

3. STATE OF DAMS IN POLAND

The issue of the overall deterioration of the condition of damming structures is most evident in dams, particularly earthen dams. A significant number of them, due to poor technical conditions, are subject to orders from the Regional Construction Supervision Inspectorates to maintain lowered water levels. Consequently, these structures are unable to perform their functions effectively. Importantly, this problem concerns not only individual structures but also entire groups of significant dams, located within the same regions. In the extreme weather phenomena such as floods or droughts, this significantly increases the risk of:

- extended extremely low flows in river that will not be replenished by water from reservoir retention,
- catastrophic flood risks when entire groups of dams fail to function properly as reservoirs within a given region.
- limitations on local and even regional water supply for the population, agriculture, and industry.
- dam failure if it is not in a good technical state if; in cases of high flood, decision-makers (e.g., the provincial governor) have to take the risky decision to fill the reservoir in order to protect the region from flooding, or, during severe flood events, the reservoir may fill spontaneously.

The statistics regarding the current technical condition and safety status of Class I and II dams in Poland are indirectly presented in Tables 1 and 2. They present the status of so-called Complexes of Hydrotechnical Structures (CHS) of Class I and II for the year 2023. Such a complex consists of at least one or more dams, such as a main dam and side dams, along with accompanying hydrotechnical structures, e.g., a hydropower plant. The tables present statistics categorized by the areas under the jurisdiction of the Regional Water Management Boards (RZGW - Regionalne Zarządy Gospodarki Wodnej) which are responsible in Poland for water management in the water regions.

The largest number of CHSs is located within the jurisdiction of the Wrocław Regional Water Management Authority (RZGW Wrocław), as well as in the mountainous and foothill areas overseen by the Kraków and Gliwice RZGWs, with respective counts of 25, 22, and 18 CHSs. Simultaneously, as indicated in Tables 3 and 4, over 30% of the CHSs identified in these regions (specifically 32%, 36%, and 33%) are in insufficient technical condition. Moreover, a significant percentage, specifically 20%, 36%, and 22%, are in unsafe condition. In this context, we reiterate a question that has already been posed, to which no attempt to find an answer has yet been made: by how much do the risks in a given region increase with regard to a reduction in the capacity to provide protection against floods and droughts if a significant number of damming structures are in an inadequate and/or unsafe condition in the region?



Fig. 1
Map of the boundaries of the Regional Water Management Authorities (RZGW) and location of Stronie Śląskie dam.

Table 1
The technical condition of Complexes of Hydrotechnical Structures (CHS), Classes I and II in Poland in 2023, based on annual CTKZ report.

	AMOUNT OF CHS ON THE AREA	TECHNICAL CONDITION OF CHS CLASSES I AND II		
		INSUFFICIENT	SUFFICIENT	GOOD
Poland	108	21%	53%	26%
RZGW regions				
Białystok	1	0%	100%	0%
Bydgoszcz	3	0%	67%	33%
Gdańsk	12	0%	67%	33%
Gliwice	18	33%	44%	22%
Kraków	22	36%	55%	9%
Lublin	1	0%	100%	0%
Poznań	12	8%	75%	17%
Rzeszów	5	0%	40%	60%
Szczecin	1	0%	100%	0%
Warszawa	8	0%	38%	63%
Wrocław	25	32%	40%	28%

Table 2
The safety state of Complexes of Hydrotechnical Structures (CHS), Classes I and II in Poland in 2023, based on annual CTKZ report.

	AMOUNT OF CHS ON THE AREA	SAFETY STATE OF CHS CLASSES I AND II		
		UNSAFETY CONDITION	SAFE WITH ATTENTIONS	SAFE
Poland	108	17%	39%	44%
RZGW regions				
Białystok	1	0%	100%	0%
Bydgoszcz	3	0%	33%	67%
Gdańsk	12	8%	25%	67%
Gliwice	18	22%	50%	28%
Kraków	22	36%	45%	18%
Lublin	1	0%	100%	0%
Poznań	12	0%	17%	83%
Rzeszów	5	0%	0%	100%
Szczecin	1	0%	0%	100%
Warszawa	8	0%	25%	75%
Wrocław	25	20%	52%	28%

4. STATE OF LEVEES IN POLAND

The total length of all levees in Poland is approximately 8,500 km. This includes about 520 km of Class I, 2,600 km of Class II, and 2,070 km and 3,020 km of Class III and Class IV levees, respectively. The System for the Registration and Control of Damming Structures contains data on levees with a cumulative length of 5,983 km. Additional sections of the levees are systematically examined, and their condition is recorded in the database. Tables 3 and 4 present the percentage distribution of assessments regarding the technical condition and safety status of the levees. A significant correlation is observed between the technical condition and the safety status of the levees. Only 3% of the total length of the levees is in an unsafe condition; however, nearly all of these are located within the jurisdiction of a single RZGW Rzeszów. A substantial 65% of the levees listed in the database are in sufficient technical condition, and 68% are deemed safe with attentions. Nonetheless, considering that a significant portion of these will require repairs in the near future, coupled with the total length of levees in Poland amounting to 8,500 km, this situation creates a considerable potential burden on the State Treasury's budget over the long term. Consequently, the issue of minimizing repair costs and optimizing their implementation over time is of paramount importance.

Table 3
The technical condition of levees, Classes I and II in Poland in 2023, based on annual CTKZ report.

	TECHNICAL CONDITION OF LEVEES		
	INSUFFICIENT	INSUFFICIENT	INSUFFICIENT
Poland	3%	65%	32%
RZGW regions			
Białystok	0%	66%	34%
Bydgoszcz	0%	100%	0%
Gdańsk	0%	50%	50%
Gliwice	0%	51%	49%
Kraków	0%	77%	23%
Lublin	0%	41%	59%
Poznań	1%	84%	14%
Rzeszów	25%	54%	21%
Szczecin	0%	24%	76%
Warszawa	0%	65%	35%
Wrocław	1%	62%	37%

Table 4
The safety state of levees, Classes I and II in Poland in 2023, based on annual
CTKZ report.

	SAFETY STATE OF CHS CLASSES I AND II		
	UNSAFETY CONDITION	SAFE WITH ATTENTIONS	SAFE
Poland	3%	68%	29%
RZGW regions			
Białystok	0%	66%	34%
Bydgoszcz	0%	100%	0%
Gdańsk	0%	62%	38%
Gliwice	0%	54%	46%
Kraków	0%	78%	22%
Lublin	0%	42%	58%
Poznań	1%	82%	17%
Rzeszów	25%	52%	23%
Szczecin	0%	24%	76%
Warszawa	0%	77%	23%
Wrocław	0%	60%	40%

5. STRONIE ŚLĄSKIE DAM COLLAPSE

Between September 13 and 16, catastrophic rainfall occurred over south-western Poland, induced by the depression named Boris, which affected a significant portion of Central Europe. In the Kłodzko Valley (Figure 1), which includes the mountainous catchment area of the Morawka stream, where an earthen dam of the dry reservoir is located in Stronie Śląskie (Figure 1), extreme cumulative precipitation was recorded, exceeding 400mm of H2O during this period. Notably, within a 24h from September 14 to 15, the total precipitation amounted to over 200 mm of H2O. The Stronie Śląskie dam was constructed in 1907 and has a height of 16 meters. The reservoir's capacity was 1.38 million cubic meters.

On Friday, September 13, at approximately 11:00 PM, the reservoir began to accumulate water. The following day, around 9:13 PM, the maximum impoundment level was exceeded. Water started to overflow over the top spillway. During the night, the water level rose to the crest of the dam. A low wall made of sandbags was placed along the crest of the dam. On Sunday, September 15, in certain areas, water began to seep locally through the sandbag wall onto the airside slope near the masonry structure of the spillway. At around 10:35 AM, very dynamic erosion (see Fig. 2) of the embankment began in this area, leading to the formation of a breach

extending over thirty meters in length. The deepening of the breach halted only upon reaching a protruding rocky ridge, on which this section of the dam is situated. According to periodic condition assessment reports, the dam was in good technical condition.



Fig. 2
The initial phase of the dam failure in Stronie Śląskie (source: user @aborowicz, platform X)



Fig. 3
The dam in Stronie Śląskie after the failure, viewed from the airside.



Fig. 4
View of the cross-section of the dam breach in Stronie Śląskie.



Fig. 5
The dam in Stronie Śląskie after the failure, viewed from the waterside.

The wave created by the breached dam reached several meters in height as it struck the buildings located a few hundred meters away in the town of Stronie Śląskie. Several buildings were completely destroyed during the wave's passage, while numerous others sustained significant damage. As a result of the flooding in Stronie Śląskie and the downstream town of Łądek Zdrój, a total of 10 lives were lost. After the disaster, it became evident that there had been no communication in the region

both prior to and during the event, which relied solely on the GSM network. The information regarding the threat of a wave from the breached dam reached the lower-lying areas only several dozen minutes after the catastrophe occurred.

The Morawka stream is a tributary of the Biała Łądecka River, both of which are located in the Kłodzko Valley. The Biała Łądecka River flows into the Oder River, one of the two largest rivers in Poland. It is estimated that the flood in September 2024 on the Oder River had an occurrence probability of approximately 1 in 100 years and was significantly less severe than the flood of 1997, which had an occurrence probability of about 1 in 300 years. In contrast, in the Kłodzko Valley, the water level rise was greater than that observed in 1997. The event resulted in the complete filling of all existing dry reservoirs in the Kłodzko Valley. In the case of the dam in Stronie Śląskie, constructed over 100 years ago, the capacity of the unmodernized spillways and outlets proved to be inadequate, leading to overflow. Conversely, the newly constructed dry reservoirs, designed with outlet and spillway capacities in accordance with current regulations, safely managed the flood waves.

In the Kłodzko Valley, the construction of several additional dry reservoirs was planned according to a concept proposed in 2018. One of these reservoirs, with a capacity of 1.9 million cubic meters, was to be located just above the dam in Stronie Śląskie. Had it been completed in time, it would likely have prevented a disaster. The local population of the Kłodzko Valley opposed the construction of the reservoirs, followed by local and subsequently national politicians. The program for the construction of these reservoirs was canceled. The total losses in the Kłodzko Valley, estimated at 3.5 billion PLN as a result of the September floods, exceeded the value of the most extensive version of the proposed additional dry reservoirs.

6. DISCUSSION ON THE ISSUE AND POSSIBILITIES FOR ITS MITIGATION

If the functions and safety of damming structures are so essential, it may be worth asking what the consequences would be of a systemic collapse in the maintenance of these structures in Poland, resulting in significant limitations or the complete exclusion of a considerable portion from use. Furthermore, what if this issue were to affect not only individual structures but entire groups of structures within a single region? An important action would be the identification of key threats in this problematic area for specific regions and the country as a whole, as well as the risk analysis of their occurrence and consequences. Subsequently, it would be essential to determine potential preventive actions. Such threats could include, for instance, the simultaneous dysfunction of several large retention structures in a given region designed to mitigate drought or flood risks, or the overtopping of a dam that is in insufficient condition. Additionally, the occurrence of dam failures in a domino effect—where more than one subsequent dam downstream is affected—or the combination of a dam failure with levee breaches poses significant risks. For

example, Grela (2023) analyzed the last two scenarios for Kraków. The findings indicate that the failure of the Goczałkowice Dam or the Tresna Dam, and consequently the Porąbka Dam, would lead to the flooding of over 20% of Kraków and losses exceeding 30 billion PLN.

Currently, we are in a period where decisions regarding the implementation or omission of actions that ensure the proper functioning and safety of damming structures, as well as their improvement, will be crucial for the development of agriculture, industry, and the overall economy of individual countries, including Poland. These decisions are also significant for safety concerning droughts and floods, thereby affecting levels of prosperity and social tensions. Consequently, these challenges are not only technical in nature but also political. Generally, for new damming structures, it is essential to design and execute them in a manner that minimizes the risks of catastrophic failures and significant malfunctions. For existing structures, effective management and maintenance are crucial, not only to mitigate these risks but also to extend their operational lifespan while simultaneously optimizing operational costs (Duminda et al., 2021). In light of the flooding experiences of 2024, it is crucial to assess the maximum capacity of spillways and outlet structures of dams in the context of climate change and the increasing risk of the frequency and magnitude of catastrophic floods. This is particularly relevant for older constructions.

In Poland, every dam is required to have an official document titled "Water Management Instruction," which defines, among other things, the principles for managing floodwaters for that specific dam. It is essential to verify and update these instructions. Many of them are outdated in light of changing precipitation patterns; however, they must be strictly followed by dam managers under the threat of criminal liability. A significant issue is that this document is linked to the entire procedure for obtaining a permit to manage water resources at the dam, a process that can take several years. There are current proposals to legally separate the amendment of such Instructions from the necessity of updating the entire permit for water management at the dam.

In addition to increasing investment in water management, addressing the identified issues also necessitates lateral thinking and actions that, above all, facilitate a significant reduction in repair costs and the optimization of the time required for their implementation.

Consequently, there is currently a global trend towards the intensive development of detection methods and research into destructive processes, alongside an increased emphasis on structures monitoring. This approach aims to obtain reliable and early information regarding the progression of these processes, including their parameters, locations, geometries, and dynamics of development.

This is a crucial issue because, firstly, early detection of destructive processes allows for more time to undertake and better plan subsequent actions, and/or

reduces the extent of necessary repair interventions, as damages and resultant harms are often still minimal at that stage. Secondly, accurate and reliable information regarding the parameters of the destructive process enables the execution of a precise, optimized, and often significantly limited renovation or deferral of such work. In the case of major renovations, this aspect is crucial for the financial burden on the budget of the managing entity, particularly for a group of interconnected structures. It determines whether the inevitable renovations, anticipated over the long lifespan of the structure, will need to be conducted more frequently or less frequently— e.g., two times rather than three within a century—and whether they can be executed to a limited extent. Thirdly, the monitoring of structures based on reliable and accurate methods for detecting destructive processes, implemented in key elements and/or zones of the structure and/or its surroundings, including the substrate, in conjunction with appropriate data analysis tools and user notification systems regarding potential problems and threats, enables the real-time detection of early stages of destructive processes. This significantly enhances the safety of the structure and reduces the risks of significant failures.

In the case of entities such as the Regional Water Management Authorities (RZGW) or groups/energy companies managing multiple structures or entire systems of hydraulic engineering facilities, such precise and reliable information would significantly optimize global maintenance costs while simultaneously ensuring the required level of safety.

It is currently important to enhance the effectiveness of investigations and monitoring of destructive processes in earth damming structures, particularly intensive seepage processes, including leakages and the resulting erosion processes. Additionally, expanding the capabilities for investigating the foundations of these structures is equally important.

Currently, with the advancement of sophisticated measurement tools, three groups of methods are being particularly developed and increasingly applied in Poland due to their fundamental advantages in practical use.

Currently, with the advancement of sophisticated measurement tools, three groups of methods are being particularly developed and increasingly applied in Poland, due to their essential application advantages. Firstly, these include remote sensing methods, especially laser scanning (Lidar), photogrammetry, and the use of data from orthophotomaps, which enable the identification of zones of surface degradation of structures and/or destructive processes (e.g., external erosion) or external signs of internal destructive processes (e.g., cavities, zones of surface internal erosion, leaks) (Zelaya Wziątek et al., 2018). An important advantage of conducting measurements from an aerial perspective is the rapid and non-invasive acquisition of spatial data over extensive areas (Bakula et al., 2018). Thanks to these features, remote sensing methods are also very useful in conducting reconnaissance for the purpose of selecting sites for more detailed subsurface investigations.

Secondly, high-resolution, non-invasive, and comprehensive geophysical methods are being developed, particularly through the introduction of advanced computational techniques at the stages of processing, visualization, and interpretation. These techniques aim to extract useful information from digital data and reduce interpretative ambiguity while shifting from qualitative to quantitative interpretation (Gołębiowski et al., 2021; Gołębiowski et al., 2022; Gołębiowski and Małysa, 2018). Geophysical methods enable relatively rapid examination of large structural areas, allowing for the identification of potential zones of uncertainty and the likelihood of destructive processes within the structure and its foundation. This, in turn, guides the targeted application of more precise investigative methods, including geotechnical assessments and/or sensor-based monitoring.

Thirdly, thermo-active linear sensors are being developed and systematically implemented to enable continuous monitoring along the damming structure through temperature measurements, allowing for early and precise detection of leakages and erosion processes within its body and foundation (Radzicki, 2017; Radzicki et al., 2021; Radzicki & Stoliński, 2023; ICOLD 2017). Furthermore, the use of these sensors in innovative quasi-two- or quasi-three-dimensional monitoring significantly enhances the detail of the analysis of individual processes, their parameters, and the precise geometry and dynamics of their development within the structure and/or its foundation (Radzicki 2015).

The implementation of an optimized methodology for investigating dam structures is of fundamental importance, particularly one that incorporates the specified methods, maximizing effectiveness while minimizing research costs and time. For instance, a proposal for such a methodology in flood embankment studies and its implementation was presented by Radzicki et al. (2021). Research and development efforts, especially those related to study methods and methodologies for their application, should progress intensively in the coming years. This is crucial for achieving significant outcomes in reducing the extent of repairs, minimizing their costs, optimizing the time required for their execution, and enhancing the safety of water-retaining structures.

7. CONCLUSIONS

Years of neglect in the ongoing funding of water management in Poland, combined with the aging of numerous hydraulic structures, have led to inadequate technical conditions, particularly concerning the safety of many of these structures. This situation necessitates urgent repairs in the short term. Such maintenance poses a significant financial challenge for many entities managing these structures, including energy companies, individual Regional Water Management Authorities (RZGW), and, more broadly, the state budget. Furthermore, a crucial issue—especially in light of the recent dam failure in Stronie Śląskie—is the need to reassess the

capacity of spillways and discharge outlets of older dams and to update their Water Management Instructions.

The continued lack of decisive actions aimed at improving the condition of dam structures may adversely affect the stability and hinder the sustainable functioning and socio-economic development of Poland. In addition to increasing funding in this area, optimizing and significantly reducing the costs of individual repairs is also of paramount importance. This could facilitate the development, implementation, and broader application of modern methods for the examination and monitoring of dam structures, particularly earth dams, which allow for earlier, more accurate, and reliable detection of destructive processes.

ACKNOWLEDGMENTS

This article is significantly based on a publication that appeared in Polish in the journal *Inżynier Budownictwa* (Civil Engineering) issue 6/2024, titled "Stan budowli piętrzących w Polsce – cz. I. Zagadnienia problemowe i wyzwania" (Radzicki et al, 2024). This manuscript has been expanded to include conclusions drawn from the flood that occurred in September 2024 and the dam disaster in Stronie Śląskie. The authors express their gratitude to the publisher for granting permission to use the article.

REFERENCES

- [1] ASCE (2021), Report card for America's infrastructure, https://infrastructure-reportcard.org/wp-content/uploads/2020/12/National_IRC_2021-report.pdf, accessed 2024-04-15 14h58
- [2] BAKUŁA K., ZELAYA WZIĄTEK D., WEINTRI B., JĘDRYKA D., RYFA T., PILARSKA M., KURCZYŃSKI Z. (2019) Multi-Sourced, Remote Sensing Data In Levees Monitoring: Case Study Of Safedam Project. The International Archives of the Photogrammetry, Remote Sensing and Spatial Information Sciences – ISPRS Archives Volume XLII-3/W, pp 101 - 108, Istanbul
- [3] CTKZ (2020), Wytyczne wykonywania badań, pomiarów, ocen stanu technicznego oraz ocen stanu bezpieczeństwa budowli piętrzących wodę centrum technicznej kontroli zapór, pod red. E. Sieiński, P. Śliwiński, IMGW-PIB, Warszawa, 97 s.

- [4] DMITRUK Z., SIEINSKI E., SIEINSKI M., WIATKOWSKI M. (2023), Raport o stanie bezpieczeństwa budowli piętrzących wodę w Polsce według stanu na dzień 31.12.2023 r., Centrum Technicznej kontroli Zapór IMGW-PIB
- [5] DMITRUK Z., SIEINSKI M., WIATKOWSKI M. (2022), Zbiorniki zaporowe – aktualne zagadnienia ich funkcjonowania i oceny stanu bezpieczeństwa, *Gospodarka Wodna* 10/2022, s.1-10, doi: 10.15.199/22.2022.10.1
- [6] DUMINDA P., SMAKHTIN V., WILLIAMS S., NORTH T., CURRY A., (2021), Ageing Water Storage Infrastructure: An Emerging Global Risk, United Nations University – Institute for Water Environment and Health, Report, 29 s., https://inweh.unu.edu/wp-content/uploads/2021/01/Ageing-Water-Storage-Infrastructure-An-Emerging-Global-Risk_web-version.pdf
- [7] FRY J.-J., 2012. How to prevent embankments from internal erosion failure?, International Symposium on Dams for a changing world, Kyoto, Japan, 5 June, p. 6
- [8] GOŁĘBIEWSKI T., PIWAKOWSKI B., ĆWIKLIK M., 2022. Application of complex geophysical methods for the detection of unconsolidated zones in flood dikes. *Remote Sensing, MDPI*, vol. 14, no. 3, pp. 1–24.
- [9] GOŁĘBIEWSKI T., PIWAKOWSKI B., ĆWIKLIK M., BOJARSKI A., 2021. Application of combined geophysical methods for the examination of a water dam subsoil. *Water, MDPI AG*, vol. 13, no. 21, art. no. 2981, pp. 1–25.
- [10] GOŁĘBIEWSKI T., MAŁYSA T., 2018. The application of non-standard GPR techniques for the examination of river dikes. *Czasopismo Techniczne, Politechnika Krakowska*, vol. 115, nr 7, s. 121–138.
- [11] GRELA, J. Assessment of the Potential Flood Hazard and Risk in the Event of Disasters of Hydrotechnical Facilities—The Exemplary Case of Cracow (Poland). *Water* 2023, 15, 403. doi: 10.3390/w15030403
- [12] ICOLD (2017) *Internal Erosion Of Existing Dams, Levees and Dikes, and their Foundation*. Bulletin no. 164, CRC Press, Paris
- [13] KLEDYŃSKI Z. (2006). Remonty budowli wodnych. Oficyna Wydawnicza Politechniki Warszawskiej. Warszawa. 212 s.
- [14] NIK, (2015) Nadzór nad stanem technicznym i stanem bezpieczeństwa wodnych budowli piętrzących – informacja o wynikach kontroli, KSI.410.002.00.2015, Nr ewid. 174/2015/P/15/051/KSI, s.78
- [15] RADZICKI K., (2015) The concept of quasi-3d monitoring of seepage and erosion processes and deformations in dams and dikes, considering in particular linear measurement sensors, *Czasopismo Techniczne - Środowisko*, 2-Ś/2015, s. 129-139

- [16] RADZICKI K., (2017) Termomonitoring procesów filtracyjno-erozyjnych w zaporach i wałach przeciwpowodziowych– dotychczasowy rozwój oraz kluczowe zagadnienia aplikacyjne, *Gospodarka Wodna*, 6/2017, s. 168-174
- [17] RADZICKI, K, GOŁĘBIEWSKI T, ĆWIKLIK, M, STOLIŃSKI, M. (2021), A new levee control system based on geotechnical and geophysical surveys including Thermal-active sensing: a case study from Poland. *Engineering Geology J.* doi: 10.1016/j.enggeo.2021.106316
- [18] RADZICKI, K, M, STOLIŃSKI, M (2023), Pilotażowe w Polsce zastosowanie metody termicznej analizy procesów filtracyjnych w tym monitoringu przecieków na zaporze ziemnej Kozłowa Góra, Bezpieczeństwo obiektów hydrotechnicznych, IMGW–PIB, Warszawa, s. 121-133
- [19] RADZICKI K., SIEŃSKI M., GOŁĘBIEWSKI T., ZELAYA-WZIĄTEK D., DMITRUK Z. (2026), Stan budowli piętrzących w Polsce. Cz. 1, Zagadnienia problemowe i wyzwania, *Inżynier Budownictwa*, 6/2024, s. 66-72
- [20] ŚWIDERSKA J., LEBIECKI P. (2011), Stan bezpieczeństwa budowli piętrzących wodę w Polsce na koniec 2009 roku, Awarie budowlane, *Proc.: Międzyzdroje 24-27 maja 2011*, s.8
- [21] ZELAYA WZIĄTEK D, SIEŃSKI E., BAKUŁA B, SALACH A., KURCZYŃSKI Z., WEINTRIT B. (2018), Identification of the levees failure vulnerability based on multi-sources monitoring, 27-my Kongres Wielkich Zapor, *Wiedeń*, s.736-749

COMMISSION INTERNATIONALE DES
GRANDS BARRAGES

VINGT-HUITIEME CONGRES DES
GRANDS BARRAGES
CHENGDU, MAI 2025

IDENTIFYING POTENTIAL FRACTURED ROCK MASSES INDRILLING DATA USING DBSCAN METHOD (*)

Siyang CHEN

*School of Civil and Transportation Engineering, Beijing University of Civil
Engineering and Architecture, Beijing
Key Laboratory of Simulation and Regulation of Water Cycle in River Basin, China
Institute of Water Resources and Hydropower Research*

Haohan XIAO & Long JIANG

*Key Laboratory of Simulation and Regulation of Water Cycle in River Basin, China
Institute of Water Resources and Hydropower Research, Beijing*

CHINA

SUMMARY

The goal of this study is to improve the precision and efficiency of detecting fractured rock masses using the DBSCAN clustering algorithm, crucial for stability analyses in geology and engineering. By equipping drilling rigs with sensors, a large dataset was gathered and analyzed with DBSCAN to locate fractured areas. The study determined the best EPS value by analyzing k-nearest neighbor distances and assessed how different EPS and minPts settings affect the identification process. Results show DBSCAN effectively separates noise and clusters data for detailed fracture mapping. At minPts=8, the clustering index peaks, ensuring accurate identification. The study also confirms DBSCAN's reliability and adaptability at various data collection rates, providing an automated, unbiased method for fractured rock mass detection in geotechnical engineering.

**Utilisation de la méthode DBSCAN pour identifier les masses rocheuses fracturées dans les données de forage*

RÉSUMÉ

L'objectif de cette étude est d'améliorer la précision et l'efficacité de la détection des masses rocheuses fracturées à l'aide de l'algorithme DBSCAN, qui est essentiel pour l'analyse de la stabilité en géologie et en ingénierie. En équipant la plateforme de forage de capteurs, un grand ensemble de données a été collecté et analysé avec DBSCAN pour localiser les zones fracturées. L'étude a déterminé les valeurs optimales d'EPS en analysant la distance K du voisinage immédiat et a évalué comment différents paramètres affectaient le processus d'identification. Les résultats montrent que DBSCAN sépare efficacement les données de bruit et de clustering pour une cartographie détaillée des fissures. À $\text{minpts} = 8$, l'indice de clustering atteint un pic, assurant une identification précise. L'étude a également confirmé la fiabilité et l'adaptabilité de DBSCAN à divers taux de collecte de données, offrant une approche automatisée et non biaisée pour la détection de masses rocheuses fissurées en géotechnique.

1. INTRODUCTION

Understanding the structural integrity of rock masses is vital for applications in geology and engineering such as mining and construction [1]. Fractured rock masses, with their variable stability and permeability, pose significant challenges [2,3]. Real-time drilling data, integrated with sensors, offers a robust basis for analyzing these complexities, aiding in rig optimization and formation interpretation [5,6]. However, the challenge lies in efficiently identifying fractured masses from vast datasets.

Recent advances in big data mining and machine learning, particularly unsupervised clustering algorithms like DBSCAN, show promise for enhancing fractured rock mass identification [7,8]. DBSCAN excels in revealing patterns in complex, unlabeled data by clustering based on density [9,10]. Its structural parameters, 'eps' and 'minPts', critically affect fracture identification, necessitating further research on their optimal values [11].

This study applies the DBSCAN method to drilling data to identify potential fractured rock masses, aiming to improve the precision of fracture detection. The method could automate and objectify fracture identification, advancing insights in rock mechanics and geotechnical engineering.

2. DATA SOURCE

2.1. DRILLING DATA ACQUISITION

This study employed a Digital Drilling System (DDS) for in-situ drilling tests to assess fractured rock masses. The DDS monitors displacement, speed, and pressure with sensors on the drilling rig, adaptable to various drilling modes by adjusting speed (N) and force (F), and records parameters in real time at different frequencies as needed.

Data collection occurred at the Dongzhuang Water Conservancy Project in Shaanxi, China, yielding over a billion records. The project, part of the Weihe River defense system, aims to control floods, reduce sediment, and improve environmental conditions. This study focused on a subset of this data, specifically targeting typical examples of interlaced fractured rock masses and intact rock masses within the engineering test area. The dataset included 3,392 records with fractured rock mass lengths of 5 mm, 10 mm, and 20 mm, as illustrated in Fig 1. After excluding outliers from the beginning and end of the data collection period, 3,310 valid records were retained, providing a robust foundation for the analysis.

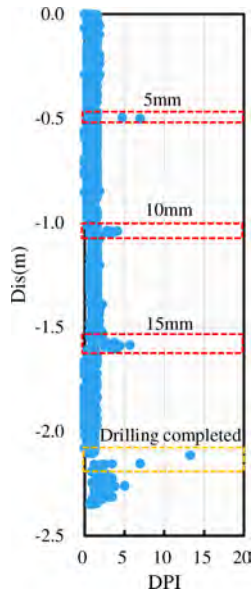


Fig. 1
Relationship between drilling depth and DPI in fractured rock mass during drilling.

2.2. DRILLING PROCESS INDEX

During the drilling process, variations in drilling pressure and speed can result in significant fluctuations in drilling speed. Consequently, using drilling speed alone as a criterion for evaluating rock mass parameters may not be reliable. To address this issue, Cao et al [13] proposed a new normalized parameter called the Drilling Process Index (DPI), which accounts for the influences of drilling pressure (F), speed (N), and torque (M) on drilling speed (V). This index is specifically designed for homogeneous materials and is defined as follows:

$$DPI = \alpha \cdot V \cdot F^{-0.5} \cdot N^{-0.5} \quad (1)$$

where α is a parameter related to rock strength. In this study, the α is set at 15.01 based on test data.

The DPI index, once established, helps estimate the distribution of fractured rock masses by setting thresholds. Cao et al. [13] found that DPI values between 0 and 2 indicate intact rock, while values above 2 suggest fracturing. However, reliance on a single DPI threshold is limited due to the influence of acquisition frequency.

This study introduces an unsupervised clustering method using the DPI index to automatically and accurately delineate fractured rock masses in real time, improving the reliability of rock mass classification.

3. METHOD DESCRIPTION

3.1. DBSCAN ALGORITHM

DBSCAN (Density-Based Spatial Clustering of Applications with Noise) is a clustering algorithm that identifies clusters of varying shapes based on point density [14]. It categorizes points as Core, Border, or Noise Points. Core Points have at least minPts neighbors within an eps-radius; Border Points are within the neighborhood of Core Points but do not meet the minPts criterion; Noise Points are outliers. DBSCAN does not need the number of clusters specified beforehand and excels at handling noise and large datasets. In this study, DBSCAN is used to detect fractured rock masses, leveraging its ability to find regions of similar density and potential anomalies.

3.2. KNN DISTANCE PLOT

Choosing the right structural parameters for DBSCAN is challenging due to data distribution, noise, high-dimensional space, and limited prior knowledge. Traditional methods like domain expertise and grid search offer only approximate parameter estimates and require substantial computational effort. This study uses the KNN distance plot to determine the optimal eps value and a data traversal to find the suitable minPts.

The fundamental concept of the KNN distance plot is to aid in the selection of an appropriate eps value by examining the distribution of distances to the nearest neighbors for each data point. Initially, for each data point in the dataset, the distances to its k nearest neighbors (k -th Nearest Distance) are computed. In this study, the Euclidean distance metric is utilized for distance calculation, which is determined using the following formula:

$$d(P, Q) = \sqrt{(x_1 - x_2)^2 + (y_1 - y_2)^2} \quad (2)$$

In the formula, P and Q represent two points in space, which can be of any dimension. The expressions $(x_1 - x_2)^2$ and $(y_1 - y_2)^2$ denote the squared differences in the x and y coordinate axes between points P and Q , respectively. After calculating the distances, each data point in the dataset is associated with a k -th Nearest Distance value.

The sorted k -th Nearest Distance values are plotted to identify an “elbow point” in the K -distance graph, indicating a transition from stable to rapidly increasing distances. This elbow point’s value determines the optimal eps. The KNN distance plot is computationally efficient, quickly identifies the elbow point, and is robust to noise and outliers. It offers a systematic, data-driven method for selecting eps, surpassing the accuracy and reliability of empirical rules or random choices.

3.3. IDENTIFICATION METHOD FOR FRACTURED ROCK MASS

The process for identifying fractured rock masses using borehole data involves applying the DBSCAN algorithm, with a focus on optimizing the eps and minPts parameters via KNN distance plots and iterative refinement. Clustering is followed by evaluation using the silhouette coefficient (S) and Calinski-Harabasz index (CH) to assess the quality of the unsupervised clusters, tailored to the dataset’s specifics. The formulas for calculating these evaluation indices are provided

below:

$$S = 1 - \frac{a}{b} \quad (3)$$

$$CH = \frac{3n(n-1)}{\sum_{i=1}^n d^2(x_i, c_i)} \quad (4)$$

In this context, 'a' measures the average intra-cluster distance of a sample point, and 'b' the average distance to the nearest non-own cluster. $d(x_i, c_i)$ is the distance from sample point x_i to its cluster centroid, while $d(x_i, C)$ is the average distance to all cluster centroids. The silhouette coefficient, S ($1 \leq S \leq 1$), close to 1 indicates high similarity within the cluster and low similarity with others. The Calinski-Harabasz index, CH ($0 < CH$), increases with stronger intra-cluster similarity and weaker inter-cluster similarity.

The workflow culminates in a visual representation of the fractured rock mass, analyzing abnormal distributions to gauge fracturing extent. Parameter optimization and clustering efficacy are critical, forming the core of this paper's discussion.

4. RESULTS AND DISCUSSION

The accurate determination of DBSCAN's ϵ ps and minPts parameters is essential for identifying fractured rock masses. ϵ ps dictates the neighborhood size, affecting cluster count and structure; too small, and clusters fragment, increasing noise, while too large, and diverse densities merge. MinPts sets the cluster density threshold; too low, and noise is misclassified, too high, and legitimate clusters may not form. This section explores the impact of ϵ ps and minPts on the clustering outcomes for fractured rock masses.

4.1. INFLUENCE OF EPS PARAMETERS ON FRACTURED ROCK MASSES IDENTIFICATION

With other structural parameters of the DBSCAN algorithm held constant, the k-th Nearest Distance plot for various data points is presented in Fig 2(a). It displays the k-th Nearest Distance plot, revealing an elbow at position 1614, indicating a optimal ϵ ps range (0.394, 0.402, 0.697). Unsupervised clustering with these ϵ ps values, shown in Fig 2(b)~(d), reveals that ϵ ps selection critically impacts outlier detection.

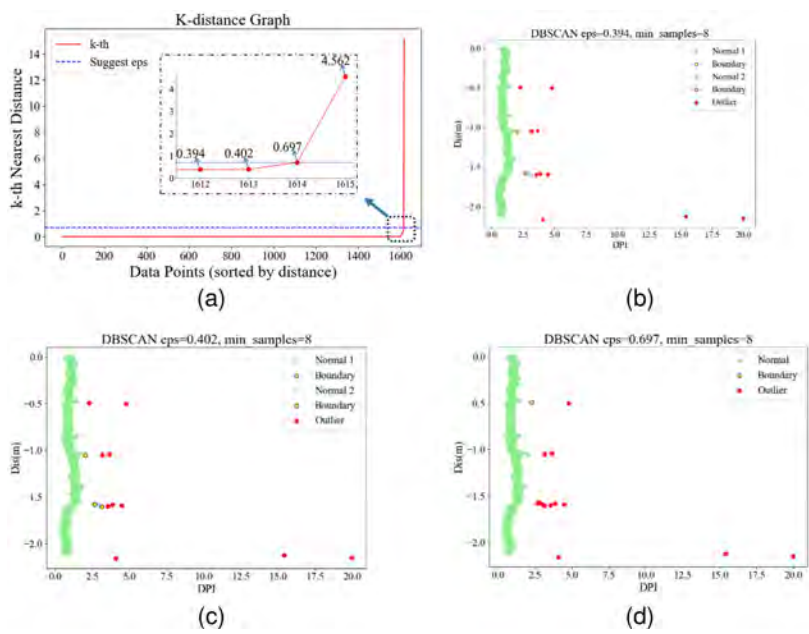


Fig. 2

(a) k-th Nearest Distance plot and Identification results of fractured rock mass under different eps: (b) eps = 0.394; (c) eps = 0.402; (d) eps = 0.697

An eps of 0.697, derived from the elbow, provides the best fracture detection results. A low eps value leads to over-segmentation, misclassifying some anomalies, as seen in Fig 2(b) and 2 (c). Conversely, a high eps value results in under-segmentation, missing less extreme fractures. The k-th Nearest Distance plot's elbow position is key to selecting an appropriate eps, improving fracture detection accuracy.

4.2. INFLUENCE OF minPts PARAMETERS ON FRACTURED ROCK MASSES IDENTIFICATION

Fig 3(a) shows the effect of varying minPts (3-15) on evaluation metrics at an eps of 0.697. Metrics S and CH stabilize at minPts=8, suggesting no added precision beyond this threshold. Fig 3(b) ~ 3 (d) illustrate fractured rock mass identification for minPts values of 5, 8, and 12. The optimal clustering, with S=0.810 and

CH=357.398, is achieved at minPts=8, confirming the proposed method's efficacy in precise identification.

In conclusion, proper eps and minPts selection is vital for accurate fractured rock mass identification. The KNN distance plot and data iteration methods provide a robust means for parameter determination. The application of DBSCAN in this study offers a valuable reference for rock mass fracture identification in research and practice.

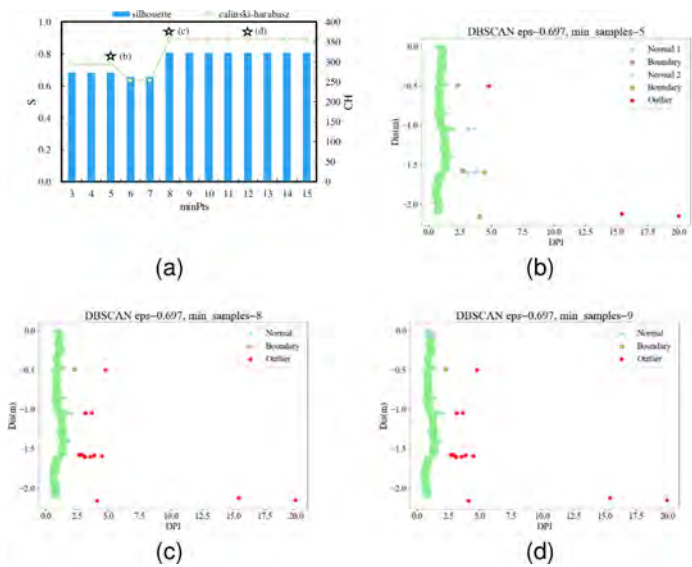


Fig. 3

Identification results of fractured rock mass under different minPts: (a) S and CH values; (b) minPts = 5; (c) minPts = 8; (d) minPts = 9

4.3. FRACTURED ROCK MASS IDENTIFICATION RESULTS

To assess the efficacy of the DBSCAN algorithm proposed for identifying fractured rock masses, DPI data at varying frequencies were analyzed (Fig 4). The data show consistent trends in DPI values with depth, though numerical discrepancies exist. This highlights the inadequacy of threshold-based DPI methods for fracture identification in intact rock. The DBSCAN algorithm consistently identified fractured rock masses across different data frequencies with consistent structural parameters, demonstrating its robustness and versatility for rock mass fracture detection.

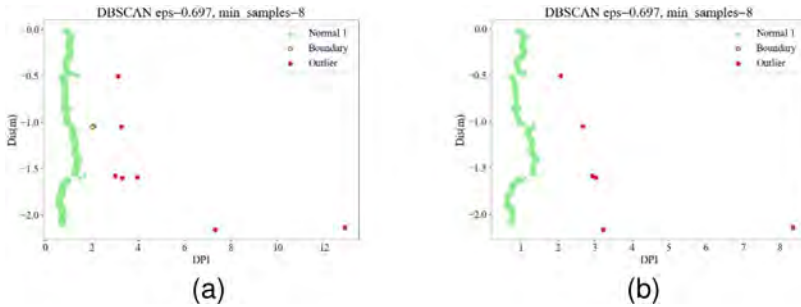


Fig. 4

Fractured rock mass identification results under different collection frequencies (a) 0.5Hz; (b) 0.25Hz

5. CONCLUSION

This study examines the use of the DBSCAN algorithm for detecting fractured rock masses, emphasizing the importance of choosing suitable EPS and minPts parameters for precise fracture identification. The k-th Nearest Distance plot is validated as an effective tool for optimizing EPS, crucial for clustering accuracy and avoiding over- and under-segmentation. The research determines that an optimal minPts value is 8. The DBSCAN algorithm's robust performance across various data frequencies is demonstrated, highlighting its utility in rock fracture detection. The proposed unsupervised clustering method provides an efficient and reliable strategy for identifying fractured rock masses, with significant implications for rock mass stability assessment in geological engineering.

REFERENCES

- [1] WANG, J., XU, H., CHEN, W., WANG, C., & HAN, Z. Evaluation method for rock mass structure integrity based on borehole multivariate data. *International Journal of Geomechanics*. 2022.
- [2] GUO, H. S., FENG, X. T., LI, S. J., YANG, C. X., & YAO, Z. B. Evaluation of the integrity of deep rock masses using results of digital borehole viewers. *Rock Mechanics and Rock Engineering*. 2017.
- [3] YI, W., WANG, M., ZHAO, S., TONG, J., & LIU, C. The effect of rock hardness and integrity on the failure mechanism of mortar bolt composite structure in a jointed rock mass. *Engineering Failure Analysis*. 2023.

- [4] WANG, Y., CAO, R., SHE, L., ZHAO, Y., & PI, J. Evaluation of Rock Abrasiveness Based on a Digital Drilling Test. *Geotechnical Testing Journal*. 2021.
- [5] SHANG F., YU W., GUO Z., YU Z., SHAN W., CAO R, & EN X. Estimation of optimal drilling efficiency and rock strength by using controllable drilling parameters in rotary non-percussive drilling. *Journal of Petroleum Science and Engineering*. 2020.
- [6] WANG, G., LV, Z., ZHONG, L., LI, Z., FU, Q., LI, Y., ... & ZHANG, Z. Double-layer pipe dual-gradient drilling wellbore pressure calculation model and parameters optimization. *Geoenergy Science and Engineering*. 2023.
- [7] XIAO H, CHEN Z, CAO R. Prediction of shield machine posture using the GRU algorithm with adaptive boosting: A case study of Chengdu Subway project. *Transportation Geotechnics*. 2022.
- [8] XIAO H, ZHENG L, ZHANG D. Noise Reduction of TBM Big Tunneling Data by Butterworth Filter. *Journal of Physics: Conference Series*. 2023.
- [9] XIAO H, CAO R, FENG S. Intelligent Attitude Control Method for Shield Tunneling Machines Considering a Rectifying Mechanism: A Case Study of the Chengdu Subway. *International Journal of Geomechanics*. 2024.
- [10] CELEBI, M. E., & AYDIN, K. (EDS.). *Unsupervised learning algorithms*. Cham: Springer. 2016.
- [11] SCHUBERT E, SANDER J, ESTER M. DBSCAN revisited, revisited: why and how you should (still) use DBSCAN. *ACM Transactions on Database Systems (TODS)*. 2017.
- [12] ZHOU, A., ZHOU, S., CAO, J., FAN, Y., & HU, Y. Approaches for scaling DBSCAN algorithm to large spatial databases. *Journal of computer science and technology*. 2000.
- [13] CAO R, WANG Y, ZHAO Y, WANG X, HE S, PENG L. In-situ tests on quantitative evaluation of rock mass integrity based on drilling process index. *Chinese Journal of Geotechnical Engineering*. 2021.
- [14] SCHUBERT, ERICH. "DBSCAN revisited, revisited: why and how you should (still) use DBSCAN." *ACM Transactions on Database Systems (TODS)*. 2017.

COMMISSION INTERNATIONALE DES
GRANDS BARRAGES

VINGT-HUITIEME CONGRES DES
GRANDS BARRAGES
CHENGDU, MAI 2025

HARCOV DAM - EXPERIENCE OF THE OPERATOR AND TECHNICAL SAFETY SUPERVISORS FROM THE ONGOING RECONSTRUCTION (*)

Pavel SVATOŠ & Jiří KREMSA, Ph.D.
Povodí Labe, State Enterprise

Tomáš KLEMŠA
VODNÍ DÍLA – TBD, JSCo

CZECH REPUBLIC

SUMMARY

The Harcov Dam in the city of Liberec in the Czech Republic was built between 1902 and 1904 primarily to reduce flood flows and flood mitigation in the area downstream of the dam. After more than a century of operation, it was necessary to implement an overall reconstruction of this dam to fulfil the current requirements for hydraulic capacities of the outlet structures (bottom outlets and spillway), especially for the control of flood flows. An unfavourable fact is also the long-term increased uplift on the foundation joint of the dam body even during normal water level in the reservoir. Currently, complex reconstruction works on the Harcov dam are ongoing. During this reconstruction, significant changes were made in the structures and parameters of this historical dam. The technical solution includes increasing the capacity of the outlet structures, as well as the modification of the stepped chute. The uplift on the foundation joint of the dam body is going to be reduced by sealing the subsoil with the grout curtain made from the new grouting gallery built along the upstream toe of the dam. The contribution describes the technical solution and experience gained from ongoing reconstruction works.

**Le barrage Harcov – Expériences de l'exploitant et des employés en charge du contrôle technique et de la sécurité tirées des travaux de rénovation en cours*

RÉSUMÉ

Le barrage Harcov à Liberec (République tchèque) a été édifié dans les années 1902-1904 dans le principal but de réduire les débits des crues et d'assurer une protection partielle du territoire en aval du réservoir contre les effets des inondations. Après plus d'un siècle d'exploitation, il a été nécessaire de procéder à une rénovation globale de l'ouvrage hydraulique afin de satisfaire les exigences en vigueur concernant les capacités des ouvrages de transférer de l'eau, et notamment de transférer la vague de contrôle d'inondation. Les poussées s'accroissant depuis longtemps sur l'assise de fondation du barrage et les infiltrations apparaissant sur le parement aval constituaient également un élément négatif. Les travaux de rénovation du barrage et des installations de l'ouvrage hydraulique Harcov, entraînant une modification fondamentale des paramètres de cet ouvrage hydraulique historique, sont en cours. La conception technico-structurale consiste avant tout en une augmentation de la capacité des vidanges de fond et du déversoir d'évacuation des crues sur le couronnement, y compris l'aménagement de la cascade sous le déversoir. La mesure essentielle pour une limitation des effets de la poussée sur le corps du barrage est une étanchéification de la couche sous-jacente à l'aide d'un rideau d'injection réalisé à partir de la nouvelle galerie d'injection près du pied amont du barrage. Le rapport porte sur la conception technique et les expériences tirées de la réalisation des travaux de rénovation.

1. INTRODUCTION

For the Harcov dam in Liberec (Czech Republic, Europe), which is a more than 100-year-old masonry dam made of blocks of stone, a flood safety assessment was prepared in 2006 [1]. The basis for the assessment was the hydrographs of theoretical flood waves with a recurrence period of 10,000 years derived from one- or two-days' rainfall determined in the hydrological study of the Czech Hydrometeorological Institute [2]. The results of the flood wave transformation show that the theoretical flood waves cannot be transformed in the reservoir flood retention storage and in both cases the crest of the dam will overflow by 70 cm, and 20 cm, respectively. The main reason for this is the insufficient capacity of the bottom outlets and spillway, which will not be able to convey even less extreme flows below the 100-year theoretical flood wave. The stability of the dam is also adversely affected by the long-term increased uplift in the area of the dam foundation joint and by seepage through the dam masonry reaching the downstream face of the dam.

In order to ensure the safety of this historic dam during extreme flood situations, as well as to ensure its safety and long-term durability in its normal operating condition, it was necessary to design measures that would increase the stability of the dam body and the capacity of the structures to safely pass flood flows. The

technical design, its impact and expected financial costs were elaborated in the Study of the measures from 2008 by VODNÍ DÍLA-TBD, JSCo [3]. The results of the performed stability calculations showed that the degree of safety against sliding and overturning of the dam body does not reach the values required by the standard at the level of the dam crest. Based on the findings, the study recommended, among other things, increasing the capacity of the spillway by lowering the spillway crest and reducing the uplift by sealing the subsoil with a grout curtain implemented from a grouting gallery designed at the toe of the dam. In 2010, the above-mentioned measure to enhance the spillway capacity was verified by a physical hydraulic model built by the Faculty of Civil Engineering of the Czech Technical University in Prague [4,5]. Subsequently, an engineering-geological survey was conducted in 2012 by AZ CONSULT [6]. The assessment and selection of a suitable option for the reconstruction of the dam and the rehabilitation of the dam subsoil was conducted by the preparation of the Proposal of Measures from 2015 by VODNÍ DÍLA-TBD, JSCo [7], taking into account the above-described surveys. As part of the preparation of the project documentation for the construction permit by VALBEK [8], an additional geological survey was carried out in 2017 by AZ-GEO [9]. The detailed design documentation was prepared in 2020 by VALBEK [10], which was used as the tender documentation for the selection of the contractor. The construction work started in 2022, after more than 15 years of preparation. The general contractor is GARDENLINE in association with YUCON CZ. Completion is expected in April 2025.

After the tank was drained and the soil berm protecting the upstream face was removed, it turned out that the historical documentation, which served as one of the main bases for the design of the technical solution of the reconstruction, did not fully correspond to reality. It was necessary to take into account the actual conditions of some of the structures in the detailed design documentation. Only the structures with the most significant changes are mentioned below.



Fig. 1

Aerial view of the dam during reconstruction.
Vue aérienne du barrage lors de sa reconstruction

2. CONSTRUCTION OBJECTS

2.1. UPSTREAM SOIL BERM AND THE COFFERDAM

The cofferdam, which is designed to protect the site from a 2-year flood wave, is created from the excavated soil berm. The water transfer is provided by a pipe with a diameter $D = 1.6$ m with an inlet structure at the toe of the cofferdam made of reinforced concrete, which passes through a homogeneous cofferdam with an upstream face geomembrane and a stone cover. In the protected area, the pipeline is connected to a distribution object behind the upstream toe of the dam. From the manifold, two concrete-lined pipes $D = 1.0$ m lead to the inlet of the intake galleries to the bottom outlets. The inlets to these two pipes can be gated by a sluice gate with electro-mechanical actuators. The manifold is equipped with a rectangular opening gated by a sluice gate also with an electromechanical actuator. This will be opened in the event of the need for controlled flooding of the protected area due to the risk of flooding by overtopping of the cofferdam.

2.2. SEDIMENT REMOVAL FROM THE RESERVOIR

The design of sediment removal was based on the measurement of sediments by divers during full filling of the reservoir by mechanical probing of the sediment thickness in about 20 transverse profiles. After draining the reservoir and subsequent removal of part of the sediment in the temporary cofferdam area, it was found that it was not a fine sediment deposit in a single layer. The sediment was separated by an intermediate layer of weathered granite, which has significantly greater strength and resistance to probe penetration. This fact could not be detected by probing with divers. The thickness of the deposits, and hence their volume, was significantly greater than assumed in the project documentation. Based on the observations, the amount of sediment was determined to be 26,180 cubic metres. As no further draining of the reservoir is currently planned and it was deemed unrealistic to extract the sediment at the operational level in the middle of the town, it was decided to remove all of the sediments. Upon completion of the work, the actual volume of sediment extracted was quantified at 51,180 cubic metres.

2.3. DOWNSTREAM FACE

The construction works on the upstream face consisted mainly of repairing the ashlar from scaffolding erected to the full height of the dam. Once the work had commenced, it was necessary to reduce the anticipated extent of the repointing, particularly in terms of the depth of removal of the original mortar. This was due to the considerable strength of the mortar combined with the highly variable joint widths and the requirement to preserve the stones without edge damage. Another specificity was the applied water pressure to clean the stones and joints so that no major damage would occur, and the cleaned area would be visually uniform, even taking into account the varying degree of weathering of the individual stones after more than 100 years of operation of the dam.

2.4. UPSTREAM FACE

The project's technical solution was based on the assumption of the need to restore the non-functional original sealing element, which consists of a layer of cement plaster on the stone masonry of the upstream face with a double coating of varnish made of paraffin, rubber, tar pitches and oils with sulphur additives. The project foresaw the necessity to remove the coating including this layer due to its degradation after more than 100 years of dam operation, which was anticipated due to the long-observed seepage on the downstream face, especially in the left part of the dam. After the removal of this layer, the restoration of the sealing function is to

be ensured by sprayed insulation based on ethylene vinyl acetate polymers applied on a levelling layer of fine-grained sprayed concrete and protected against mechanical damage by a 10 cm thick layer of concrete reinforced by an anchored rebar mesh. After removal of the upstream berm, the cement plaster was found to have not only the satisfactory flatness required for spraying the insulation but also cohesion with the facing ashlar, verified by tear-off tests. However, in order to apply the sprayed insulation, it was necessary to remove the original coating, which is unsuitable as a substrate for sprayed insulation, with a high-pressure water jet. Based on practical tests, it was found that the application of a water pressure of 2 500 bar was efficient.

2.5. RUBBLE MASONRY — CENTRAL PART OF THE DAM

After evaluation of the results of seepage tests carried out during the geological survey, it was shown that the rubble masonry of the dam has very high permeability and can be evaluated as poor quality mainly due to the assumed high degradation of the mortar. As a measure to improve mainly the mechanical and physical properties of the rubble masonry, the project proposed to grout the dam body.

After evaluation of the grouting in the test field, it was found that it was possible to change the projected quantity of grouting mixture per metre of a borehole from 157 litres to approximately 50 litres and to increase the maximum grouting pressure from 0.2 MPa to 1.3 MPa. Furthermore, it has been shown that the use of the originally designed chemical materials is pointless, and the grouting can be completely implemented with a significantly cheaper clay-cement mixture.

The boreholes used for grouting tests were extended compared to the design [8] so that they extend at least 0.5 m into the subsoil of the dam. In the lower part of some boreholes, completely weathered granite was found in the subsoil of the dam, which had to be regrouted. The average consumption of clay-cement grouting mixture was 52.26 litres per metre of a borehole. According to the results of the water pressure tests, the permeability of the rubble masonry dropped 4 times after the grouting. On the basis of the favourable results of the test grouting, the detailed design documentation for this part of the project was completed.

2.6. GROUTING GALLERY

The grouting gallery with a total length of approximately 130 m is located in front of the upstream face slightly below the level of the foundation joint of the dam body. The entrance shaft is located on the right abutment near the new operational

facility from where the grouting gallery continues to the left abutment - where it terminates at the interface between the dam body and the spillway. It is a reinforced concrete structure divided by sealed expansion joints into individual blocks approximately 6 m long. The gallery was implemented on the underlying levelling concrete. Only at the intersection of the gallery with the intake tunnels to the towers of the bottom outlets has undermining been carried out under the protection of an "umbrella" of horizontal micropiles above the profile of the tunnel. After partial open excavation in the vicinity of the bottom outlet structures, it was found that the base of the towers did not extend to the level of the foundation joint of the dam body. It was necessary to stabilise the area close to the excavation, which is very complicated in terms of material composition and consists of poor-quality concrete, individual stones and weathered granite. During the excavation of the new gallery, which was carried out mainly in a rock environment, springs of water at the foundation joint, which were not foreseen by the project, were detected. In the vicinity of the left bottom outlet, laboratory analysis revealed the carbonate aggressiveness of the water on the concrete, and it was necessary to use the corresponding concrete quality.

2.7. GROUT CURTAIN

The grout curtain is to be an impermeable element that will eliminate the seepage under the foundation joint of the dam and thus significantly reduce the uplift forces acting on the dam body. Based on the results of the test grouting, the technological procedure was modified, which envisaged only upward grouting using cement and polyurethane-based grouts. It was now possible to use materials based on clay-cement or micro-cement, which means significant savings in material costs. Another change made as part of the detailed design documentation was the re-routing of the grout curtain on the left side at the first and second spillway sections. This change represents a significant cost reduction in ensuring stability to the local road, which is routed near the left abutment. The actual observed parameters in the route of the grout curtain, based on the implementation of the test grouting field, led to significant changes in the project design documentation. The grouting boreholes are drilled through the underlying concrete of the grout gallery.

The following findings from the surveys conducted and their evaluation are fundamental to the subsoil:

- In all boreholes, granite was encountered below the level of the foundation joint in various stages of weathering.
- For the whole borehole length, even non-weathered, otherwise solid granite is cracked (the most frequent cracks are almost vertical 70° – 90°), and the disintegration is piecewise to block-like. The bedrock is highly permeable and fractured in various ways, and seepage from the reservoir through the bedrock is therefore significant.

- The bedrock is disturbed by distinctive fissure systems. The depth of the open section of the fissure system is at least 15 m below the level of the dam foundation joint.
- The foundation rock downstream of the dam is less permeable than the rock directly beneath the dam body, which causes an increase in the uplift pressure on the foundation joint.

The results of the field tests carried out so far show that the right part of the dam contains the largest number of rock types, including weathered coarse-grained granite. A test grouting field has been designed in these areas. The average consumption of the clay-cement grouting mixture was 50.62 litres per linear meter and that of the micro-cement grouting mixture was 65.29 l/bm. The permeability of the subgrade was shown to be reduced 8 times. The fundamental finding is that the foundation rock can be grouted reasonably well using clay-cement grouts and micro cement grouts.

2.8. DRAINAGE BOREHOLES

The stability assessment of the dam body carried out by VODNÍ DÍLA-TBD, JSCo as part of the "Design of measures to ensure the safety of the dam during floods" [7] showed that the factor of safety against sliding under extreme loading conditions is unsatisfactory. A significant negative effect entering into the calculation is the uplift at the foundation joint of the dam body. To monitor it and to reduce it, if necessary, in the short term, 5 relief boreholes will be used, which will be routed from the grouting gallery at a slightly downward angle under the foundation joint of the dam body. Given the presence of heavily weathered parts of the "Liberec granite", the implemented drilling works have shown significant instability of the borehole lining and the presence of pressurised water, it was necessary to modify the design and equipment of the borehole.

3. DAM SURVEILLANCE AND MEASUREMENTS

3.1. DAM SURVEILLANCE DURING RECONSTRUCTION

Compared to the dam surveillance carried out during the normal operation of the dam, the frequency of selected measurements is increased, the operability of the transmission of measurement results is improved and new measurements and observations aimed at evaluating the construction progress are also introduced. The specialised geodetic measurements and evaluation of results are carried out by the staff of the authorised organisation VODNÍ DÍLA-TBD, JSCo. The construction

works (construction of the grouting gallery, manhole, grout curtain, banana works, etc.) require an extensive and organised system of surveying, monitoring the effects of blasting, excavation, embedding and grouting and, last but not least, a quality control. To ensure these specialised activities, the contractor or investor has contracted the assistance of several professional organisations (drilling and grouting supervision, blasting, construction laboratories, etc.).

3.2. DEFORMATION OF THE DAM BODY DETERMINED BY GEODETIC MEASUREMENTS

This involves measuring and monitoring the horizontal and vertical displacements of the dam. Since the construction, the horizontal displacements of the “Inze type” masonry dams in the Jizera Mountains, built in 1904–1909, have been monitored using the method of the intentional straight line. This consists of a direct reading of the displacement using a gauge placed on two control pillars of the dam crest. The equipment was at the limit of its useful life during the preliminary design of the rehabilitation project. In addition, construction work on the dam crest would damage the equipment and the continuity of measurement would be lost anyway. Therefore, it was proposed to reinstall the equipment for horizontal displacement measurements in the Measurement Design for Construction. The original control points were replaced with stainless steel Leica prism mandrels with installation under the top ledge of the dam crest on the downstream face. To monitor the vertical profile in the centre of the dam, twin fixed mini prisms were installed on the downstream face. The existing reference grid consisting of the original piers on both river banks was extended with two new geodetic piers with lateral centring in the dam abutments. The stabilised points of the reference grid were further supplemented by four control points installed outside the zone of expected deformation of the dam (rock outcrops, substructure, etc.). The coordinates of the control points are determined by geodetic measurement and evaluation and then the horizontal displacement vectors are calculated. These vectors represent the movements of the dam in the horizontal direction during the construction period and are measured monthly.

Over the past 24 years, horizontal displacements at the dam crest have ranged from 2 mm (upstream) to 3 mm (downstream) throughout the year. Thus, the total horizontal displacement of the embankment was no more than 5 mm, and no increasing trend was observed. During construction, during the first year, the differences in the magnitude of the determined horizontal displacements were minimal. There were no significant effects of reservoir drawdown, water pressure reduction, or uplift reduction from the fall of 2022 to the end of 2023. These results were attributed to the arching effect of the masonry dam and the upstream soil berm surcharge. Completely different results for the horizontal displacement measurements were found in 2024. Since June, the upstream tilt of the embankment has been occurring and has not yet stopped. Currently, the maximum upstream tilt is 9.3 mm. Mining work is underway at the toe of the dam to establish the grouting

gallery and grout curtain. The cause of the horizontal displacements is so far primarily attributed to thermal loading of the dam. This has been supported by the removal of the upstream soil berm. Sustained and prolonged pumping of seeping water near the upstream toe from the construction pit can also influence the displacement. For the time being, it is anticipated that the development of horizontal displacements will be stopped or significantly reduced by the end of October and that the dam safety will not be compromised.

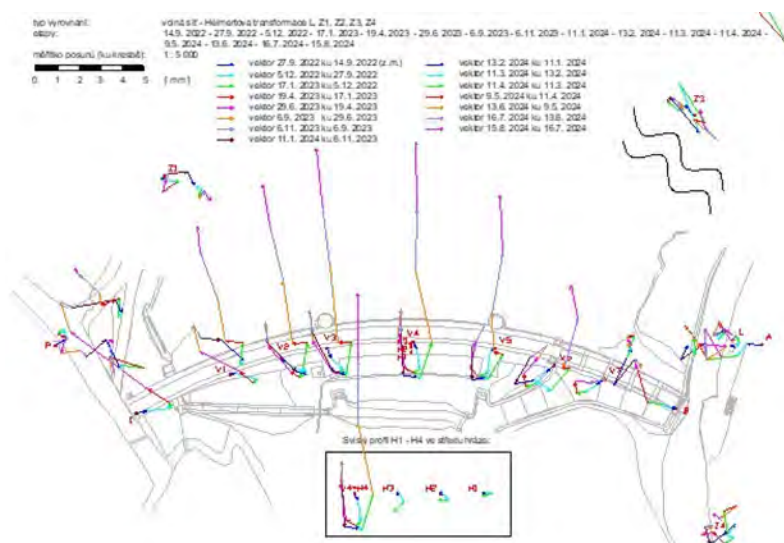


Fig. 2

Horizontal shifts during the reconstruction of the dam.

Déplacements horizontaux lors de la reconstruction du barrage.

The results of the horizontal displacements are matched by geodetic measurements of the vertical displacements using a high-precision levelling method. A measured displacement is considered to be 2,5 times the mean measurement error. In this case, it is a value higher than 1.0 mm. In this case, too, control points were added before the start of construction, namely at the downstream toe of the dam, in the crest area on the downstream side, at the towers and at the inlets to the bottom outlets. The vertical displacements of the dam have ranged from 0 to +2.8 mm over the last 24 years prior to the start of the works. More significant movements (subsidence of approximately 5.0 mm) have been monitored since June 2024. Therefore, the frequency of measurements has now been increased to twice a month. The causes of vertical dam deformation are similar to those for horizontal displacements and have been described above.

3.3. INCLINATIONS OF THE TOWERS OF THE BOTTOM OUTLETS

Before the reservoir was drained, inclinometers were installed inside the towers of the bottom outlets at the level of the dam crest. The results of the measurements show agreement with the geodetic measurements made at the dam crest. Both towers show a downstream tilt during the winter months due to the cooling of the dam. The displacements in the direction perpendicular to the upstream/downstream direction are approximately half of the measured maxima in the direction of the flow and do not show a cyclical regime of temperature loading. This type of measurement is more flexible than the geodetic measurement mentioned above and presents a suitable complement to it and can also be used for control.

3.4. DEFORMATION OF INFLOW GALLERIES

Due to the lack of knowledge of the foundation of the object and the design of the grouting gallery under the structure of the inflow galleries, a VR3D deformation base was installed on the joint in the ceiling. Later, this base was fitted in the same location in the right inlet after the water was transferred to the left outlet. In the horizontal direction, a joint closing of approximately 1.0 mm was found (a sudden increase since August 2023). It is likely to open after the dam cools down in autumn 2024.

4. CONCLUSION

The main part of the Harcov masonry dam will be mostly preserved in its original state. Grouting from a new gallery under the dam, reconstruction of the dam crest and partial changes to the shape of the river channel downstream of the dam will take place. Drainage and observation boreholes will be drilled in the dam body and its immediate surroundings, and waterproofing will be applied to the upstream face of the dam. New technological equipment will be installed at the bottom outlets with a higher but safe discharge capacity that the Harcovský Brook channel downstream of the reservoir can accommodate. As part of the reconstruction, modern equipment for operation will be installed, e.g. new dam lighting, elements of automatic monitoring of water management and dam surveillance, and the electrical installations including the control system will be completely rehabilitated.

The dam is a cultural-historical heritage; therefore, the existing character of the dam must be preserved, and the entire reconstruction was continuously consulted with the National Heritage Office in the city of Liberec.

During the reconstruction, the reservoir is drained to allow for a comprehensive modification of the upstream face of the dam and upstream soil berm and the removal of more than 51 thousand cubic meters of sediment from the reservoir.

After the reconstruction, the dam will be able to safely pass floods with the required return period. The Harcov Dam has been serving as flood protection for the downstream area since 1904 and has so far been without any major repairs. In the event of extreme floods, it will be possible to discharge much more water from the Harcov dam in a controlled manner than at present and thus prevent overtopping. These measures will also ensure that the 10,000-years-flood wave can be safely passed over the dam's crest without endangering the stability of the dam, which is necessary in terms of today's legislation in the Czech Republic.

REFERENCES

- [1] VODNÍ DÍLA-TBD, JSCo, J. Chroumal (2006).
- [2] CZECH Hydrometeorological Institute, R. Tyl, M. Boháč (2005).
- [3] VODNÍ DÍLA-TBD, JSCo, D. Richtr, T. Klemša (2008).
- [4] CTU in Prague, Faculty of Civil Engineering, Department of Hydraulic Structures, L. Satrapa, Hydraulic research of the Harcov dam, Prague.
- [5] M. ZUKAL, M. KRÁLÍK. Hydraulic model of Harcov historical dam. In: CESB 13 Central Europe towards Sustainable Building 2013. Prague: GRADA PUBLISHING, 2013. p. 935-938. ISBN 978-80-247-5015-6.
- [6] AZ CONSULT, spol. s.r.o., K. Alföldi et al. (2012).
- [7] VODNÍ DÍLA-TBD, JSCo., D. Richtr, T. Klemša (2015) Design of measures to ensure the safety of water works during floods, Prague.
- [8] VALBEK spol. s.r.o. (2017): Documentation for the building permit "Harcov hydroelectric power station, ensuring the safety of the waterworks during floods", Ústí nad Labem.
- [9] AZ GEO, s.r.o., R. Králík (2017): supplementary engineering-geological survey "Harcov dam, ensuring the safety of the dam during floods", Ostrava.
- [10] VALBEK spol. s.r.o. (2020): Documentation for the execution of the construction "Harcov dam, ensuring the safety of the dam during floods", Ústí nad Labem.

COMMISSION INTERNATIONALE DES
GRANDS BARRAGES

VINGT-HUITIEME CONGRES DES
GRANDS BARRAGES
CHENGDU, MAI 2025

CHALLENGES IN THE SAFETY MANAGEMENT OF LARGE PORTFOLIO OF AGING DAMS IN THE INDIAN CONTEXT (*)

J. CHANDRASHEKHAR IYER

Former Chairman, Central Water Commission, New Delhi

INDIA

SUMMARY

Dam building across rivers in India had been a tradition over centuries. The Grand Anicut (dam) across the River Cauvery in the southern peninsula is a monumental structure that was built around 1st century AD, and is still in use for over two millennium. Dams play a key role for the agricultural and industrial development, drinking water supply, power generation, flood moderation and other social needs, aiding a rapid growth of India's economy and self-sufficiency.

As per the National Register of Large (Specified) Dams published by Central Water Commission (CWC) and National Dam Safety Authority (NDSA) in the year 2023, the country has built 6138 operational large dams spread across several states, with a live storage capacity of the order of 250 billion cubic metre, while many more dams are under construction. Significant percentage of these dams are more than 25 years of age. The safety management of the large portfolio of aging dams in terms of operation, maintenance and rehabilitation, and the associated risks is a challenging inter-disciplinary task.

The hydrological safety review of older dams, designed and constructed as per the earlier prevailing codal provisions, have indicated in certain cases, inadequate spillway capacity to pass the revised flood discharge, calling for implementation of suitable non-structural and/or structural measures for the dam. The

**Défis de la gestion de la sûreté d'un grand parc de barrages vieillissants en Inde*

hydraulic, structural and seismic design of older dams need to align with the latest codal provisions. Operational shortcomings have been experienced in many dams, like the lack of provision of stop log gates for lowering and maintaining the spillway crest gates, no walkway or access for inspection of the gates, lack of low-level outlets to manage the reservoir, and lack of required dam instruments.

The walk-through visual inspections of the upstream and downstream dam faces and other inaccessible locations are rather difficult and time-consuming. The routine inspections need to be supplemented with innovative technology-driven solutions for condition assessment and repairs. The deterioration of the reservoir face elements of the dam body is often seen to manifest itself into leaching and seepage in the drainage gallery of dams, a phenomenon commonly seen but not so commonly studied and remedied by the dam owners.

Deferred maintenance due to either budgetary constraint or possibly due to lack of quality manpower is affecting the condition of the dam assets. The gates, hoists and related appurtenant structures in aging dams need comprehensive health check-up periodically, for deciding on their timely repairs, replacement or modernization.

While the dams themselves may not have significantly changed, risk factors could have. Settlements typically tend to grow around and in the downstream of the dams along the river course, because of the expectation of regular water supply, making more and more people and property vulnerable to flood hazard, even under normal dam water release situation, not to mention of the uncontrolled release during a failure. Risk-informed decision making therefore provides a defensible basis for making decisions and helps to identify the greatest risks and prioritize efforts to minimize or eliminate them.

The sustained policy initiatives and the dam rehabilitation & improvement projects steered by the Central Government in the last over four decades have shown the dam owners in the country, the right direction towards operation, maintenance and rehabilitation measures to be undertaken in the dams and ensure their operational safety.

The enactment of the Dam Safety Act of 2021 has brought a paradigm shift in the way dam owner should manage, operate and maintain its dams. The Act calls for exhaustive documentation, periodic comprehensive dam safety evaluation, inspection schedules, risk assessment studies, emergency action plan and many other protocols that would significantly aid in the efficient management of the large dams. This paper discusses few of the challenges in the safety management of large portfolio of aging dams in the Indian context.

RÉSUMÉ

En Inde, la construction de barrages sur les rivières est une tradition qui remonte à plusieurs siècles. Le barrage de Grand Anicut sur le fleuve Cauvery, est une structure monumentale qui a été construite vers le 1^{er} siècle de notre ère et qui est toujours utilisée depuis plus de deux millénaires. Les barrages jouent un rôle clé dans le développement agricole et industriel, l'approvisionnement en eau potable, la production d'électricité, la modération des crues et d'autres besoins sociaux, contribuant ainsi à la croissance rapide de l'économie indienne et à son autosuffisance.

Selon le registre national des grands barrages (spécifiés) publié par la Commission centrale de l'eau (CWC) et l'Autorité nationale de sécurité des barrages (NDSA) en 2023, le pays a construit 6138 grands barrages opérationnels répartis dans plusieurs États, avec une capacité de stockage de l'ordre de 250 milliards de mètres cubes, tandis que de nombreux autres barrages sont en cours de construction. Un pourcentage important de ces barrages a plus de 25 ans. La gestion de la sécurité de ce vaste portefeuille de barrages vieillissants en termes d'exploitation, d'entretien et de réhabilitation, ainsi que des risques associés, est une tâche interdisciplinaire difficile.

L'examen de la sécurité hydrologique des barrages plus anciens, conçus et construits conformément aux réglementations antérieures, a montré, dans certains cas, que la capacité du déversoir était insuffisante pour laisser passer le débit de crue révisé, ce qui nécessite la mise en œuvre de mesures appropriées pour le barrage. La conception hydraulique, structurelle et sismique des barrages plus anciens doit être alignée sur les pratiques les plus récentes. De nombreux barrages présentent des lacunes opérationnelles, telles que l'absence de vannes d'arrêt pour l'abaissement et le maintien des vannes de crête du déversoir, l'absence de passerelle ou d'accès pour l'inspection des vannes, l'absence d'exutoires de faible niveau pour gérer le réservoir et l'absence des instruments de barrage requis.

Les inspections visuelles des parements amont et aval des barrages et d'autres endroits inaccessibles sont assez difficiles et prennent beaucoup de temps. Les inspections de routine doivent être complétées par des solutions technologiques innovantes pour l'évaluation de l'état et les réparations. La détérioration des éléments de la face du réservoir du corps du barrage se manifeste souvent par des lixiviations et des infiltrations dans la galerie de drainage des barrages, un phénomène couramment observé mais pas aussi couramment étudié et réparé par les propriétaires de barrages.

La maintenance différée, due à des contraintes budgétaires ou peut-être à un manque de main-d'œuvre qualifiée, affecte l'état des actifs des barrages. Les vannes, les treuils et les structures annexes des barrages vieillissants doivent faire l'objet d'un bilan de santé complet à intervalles réguliers, afin de décider de leur réparation, de leur remplacement ou de leur modernisation en temps opportun.

Si les barrages eux-mêmes n'ont pas changé de manière significative, les facteurs de risque, eux, ont pu changer. Les habitations ont généralement tendance à se développer autour et en aval des barrages le long du cours d'eau, en raison de l'attente d'un approvisionnement régulier en eau, ce qui rend de plus en plus de personnes et de biens vulnérables aux risques d'inondation, même dans une situation normale de libération de l'eau du barrage, sans parler de la libération incontrôlée lors d'une défaillance. La prise de décision en fonction du risque fournit donc une base défendable pour la prise de décision et aide à identifier les risques les plus importants et à prioriser les efforts pour les minimiser ou les éliminer.

Les initiatives politiques soutenues et les projets de réhabilitation et d'amélioration des barrages pilotés par le gouvernement central au cours des quatre dernières décennies ont montré aux propriétaires de barrages du pays la bonne direction à suivre en ce qui concerne les mesures d'exploitation, d'entretien et de réhabilitation à prendre dans les barrages et à assurer leur sécurité opérationnelle.

La promulgation de la loi sur la sécurité des barrages de 2021 a entraîné un changement de paradigme dans la manière dont les propriétaires de barrages doivent gérer, exploiter et entretenir leurs barrages. La loi prévoit une documentation exhaustive, une évaluation périodique complète de la sécurité des barrages, des calendriers d'inspection, des études d'évaluation des risques, un plan d'action d'urgence et bien d'autres protocoles qui contribueraient de manière significative à la gestion efficace des grands barrages. Ce document examine quelques-uns des défis posés par la gestion de la sécurité d'un vaste portefeuille de barrages vieillissants dans le contexte indien.

1. INTRODUCTION

Dam building across rivers in India had been a tradition over centuries. The Grand Anicut (dam) across the River Cauvery in the southern peninsula is a monumental structure that was built around 1st century AD, and is still in use for over two millennium. Dams have traditionally played a key role in agricultural and industrial development, providing drinking water, power generation, flood moderation and other social needs. As per the National Register of Large (Specified) Dams published by Central Water Commission (CWC) and National Dam Safety Authority (NDSA) in the year 2023, the country has built 6138 operational large dams spread across several states, with a live storage capacity of the order of 250 billion cubic metre, while many more dams are under construction. The country ranks third in the world in terms of the number of large dams after China and USA. The country has seventy-seven important dams with height above 100 m or gross storage above one billion cubic metre. The decade-wise distribution of construction of large dams in India is shown in Fig. 1.

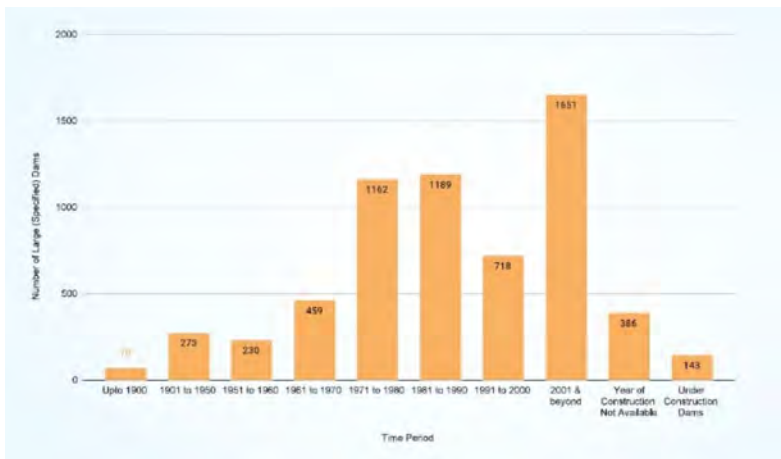


Fig. 1

Decade-wise distribution of construction of large dams in India (Source: CWC and NDSA National Register of Large (Specified) Dams (2023))

While the country ranks third in the world in terms of large number of dams, the per capita water storage is rather low. The temporal and spatial disparity in the rainfall and runoff pattern in the country is significantly large, with around 80% of annual rainfall occurring during monsoon season from June to September. While some areas in Brahmaputra, Ganga and other major rivers are suffering from floods, some other areas in the country reel under severe drought.

It is therefore evident that the country needs to create more storages across the rivers, to meet the water needs round the year, mitigate the effects of recurring droughts and floods, to build resilience against the impacts of climate change and to ensure water and food security for the growing population. It is equally important that the large inventory of dam assets already created over the last many decades infusing huge upfront investments, including associated social and environmental costs, are well operated, maintained and rehabilitated by the dam owners ensuring their safety and longevity for future generations to reap the benefits.

The country had fewer than 300 large dams at the time of independence in the year 1947. A significant percentage of these dams are more than 25 years of age. As the country needed more storages for the growing population, thrust over all these years has been on building more and more dams. The budgetary allocations for operation and maintenance of existing dam assets have rather been low. Safety management of the dam assets is vital for the country as a compromised or unsafe dam constitutes a major hazard and public safety concern.

The failure of a dam and/or its foundation or of the appurtenant structures could normally be attributed to inadequacy in stability, or durability, or function, or to any unforeseeable events. As per the records maintained by the CWC, there are reported failures of 42 large dams in the last around 100 years. India's worst dam disaster was the failure of 26 m high masonry and earth fill Machu-II dam on Machu River, in the state of Gujarat in the year 1979, killing nearly 2000 people.

2. SUSTAINED INITIATIVES

Sustained policy initiatives were taken by the Central Government in the last over four decades towards promoting unified procedures and best practices of dam safety in the country. The initial steps in this direction include establishment of a Dam Safety Organization within the CWC in the year 1979, and constitution of a National Committee on Dam Safety (NCDS) in the year 1987. NCDS was mandated to evolve and suggest changes in the planning, specifications, construction, operation & maintenance practices and analyze the causes of major historical dam incidents and dam failures.

The Dam Safety Assurance and Rehabilitation Project (DSARP) was implemented during 1991 to 1999 by the Government with the support of World Bank, wherein safety of 33 dams were evaluated and effectively rehabilitated. This project brought about heightened awareness about dam rehabilitation across the various dam owning States.

Subsequently, the Government implemented Phase-I of the Dam Rehabilitation and Improvement Project (DRIP) during the years 2012 to 2021, with the support of World Bank, wherein safety of 223 dams were evaluated and effectively rehabilitated. The objective of DRIP was primarily to improve the safety and operational performance of the selected dams, along with institutional strengthening with a system-wide management approach.

Under DRIP phase-I, design flood reviews of the selected dams were carried out for evaluating the hydrological safety. Increase in design flood was addressed through structural and/or non-structural measures. The operational safety improvement included overhauling of existing gates and hoists, replacing outlived gates, and implementing automated gate operation through SCADA system. The seepage issues were generally addressed through measures like pointing, grouting of dam body and foundations, joint treatment and upstream face treatment.

The structural stability requirements included interventions like repair of deformed slopes, slope protection works, re-sectioning of dam body, reaming of porous/foundation drains, backing concrete etc. The basic facilities at dam site viz. approach roads, bridges, lighting in the dam area and in drainage galleries, stand-by

generators during emergency operations etc. were restored and improved. Images of a dam spillway prior to and after renovation and modification under DRIP – I are shown in Fig. 2.



Fig. 2
Renovation and modification of a dam spillway

A web-based asset management tool viz. Dam Health and Rehabilitation Monitoring Application (DHARMA) was developed to support the effective collection and management of dam data. Manuals for Operation and Maintenance as well as Emergency Action Plan for the selected dams, as well as thirteen guidelines on a range of related topics were published and disseminated for the benefit of the dam owners in the country. Riding on the success of DRIP phase-I, DRIP phase-II and III have commenced in the year 2021, with the support of World Bank and AIB, which envisages rehabilitation, improvement and related protocols for 736 large dams in the country, in a time frame of 10 years.

3. CHALLENGES

In India, around 98% of the large dams are owned by the State Governments, while the public sector utilities, private companies and other local bodies own the remaining around 2%. Besides the large dams, there are thousands of medium and small dams in the country, not falling under the definition of large dams. The institutions at the national and state levels are incessantly working to promote unified dam safety culture. However, managing such a large portfolio of aging dams in terms of operation, maintenance, rehabilitation and dealing with the associated risks has its share of challenges. The author intends to discuss few of these challenges in this paper.

3.1. PLANNING FOR SAFETY EVALUATION AND REHABILITATION

Any dam safety evaluation and rehabilitation design would require the information and documents pertaining to all dimensions and processes that have gone into the dam building. This normally would include planning aspects, site selection, geology, geotechnics, hydrology, foundation design, hydraulic and structural design, hydro-mechanical design, construction materials and construction techniques adopted, instrumentation, operation and maintenance protocols, history of distress incidents including 'as-constructed' drawings and photographs. In case of older dams, availability of all the requisite and reliable information is often a challenge. Further, with frequent change of working personnel, missing of baseline information/documents cannot be ruled out.

Safety evaluation and proposing rehabilitation measures in such dams with scanty baseline information, would rather turn out to be a cumbersome re-engineering exercise. Fresh laboratory tests and geological/geotechnical or geophysical investigations may have to be carried out and if not feasible, rehabilitation solutions may have to rely on reasonable assumptions.

A digital asset and document management system therefore needs to be implemented at all the large dams in the country, to systematically record the assets and maintain all the dam documents, which could enable easy online retrieval for the dam owners and others concerned.

3.2. TECHNOLOGY-DRIVEN DAM HEALTH MONITORING

Perpetual monitoring of the health of the dam and appurtenant structures is the primary responsibility of the dam owner. Instruments installed in and around the dam aid in understanding the behaviour and response of the dam elements to the various loadings. Instrumentation further serves the purposes of quality control, design validation, construction control and legal protection in sharing risk with third parties.

Reportedly, very few older dams have been instrumented in the country. Further, the dams being monitored have only a few instruments. Instruments like open standpipe piezometers in earthen dams and uplift pressure gauges in concrete gravity dams were commonly provided in older dams. Limited instrumentation limits our complete understanding of the dam behaviour. The damaged or non-functional instruments further restrict our understanding. In such dams, wherever required and feasible, suitable instruments may have to be installed afresh for studying the dam behaviour for better understanding and evolving suitable remedial solutions.

The geophysical techniques could help in estimation of anomalous zones leading to seepage, piping, internal erosion and other distress issues in dams. Dam health monitoring system could consider potential failure mode-based instrumentation, and integrating instrumentation and telemetry with data collection and dissemination software.

The walk-through visual inspections of the upstream and downstream dam faces and other inaccessible locations normally performed are rather difficult and time-consuming. These routine inspections need to be supplemented with innovative technology-driven solutions for condition assessment and repairs. Automated and data-driven assessment for cracks and distress could use unmanned aerial vehicles equipped with sensors for rapid and comprehensive dam health monitoring, delivering better coverage and accuracy. The analysis of the results could facilitate in considering focused maintenance solutions.

Water being a scarce resource, rather than fully emptying the reservoir for inspection and repair, sensors and robotic machines loaded on remotely operated underwater vehicles could work in deeper waters, without limitation of communication and endurance. The deterioration of the reservoir face elements of the dam body is often seen to manifest itself into leaching and seepage in the drainage gallery of several dams in the country, a phenomenon commonly seen but not so commonly studied and remedied.



Fig. 3
Effect of acidic reservoir water and condition of drainage galleries

A typical case of the effect of acidic reservoir water on the dam body and the condition of drainage galleries in one of the projects in the country is shown in Fig. 3. All the components of the dam in contact with water as well as the underwater components of the intake, water conductor system and hydropower power plant were adversely affected, calling for close and detailed component-wise inspections and rehabilitation/replacement, including addressing the root cause of acidity in the reservoir water.

3.3. ADAPTATION TO NEW APPROACHES AND ADVANCEMENTS

One of the greatest challenges in dam safety management is to align the older dams with the evolving standards, particularly with respect to the hydrological, hydraulic, structural and seismic safety considerations. The dam owners need to rapidly adapt to the new approaches and advancements in management of the dams. The hydraulic and structural design approach of dam and appurtenant structures undergoes continuous refinement and calls for compliances to the revised codal provisions. Seismic zones in the country have undergone changes in the revised Indian standards, due to which the stability of dam and spillway in such cases need to be re-assessed, and wherever needed, suitable rehabilitation works must be undertaken. The effects of climate change are also subjecting to changes in the loading conditions on the dam.

The hydrologic design criteria for fixing the spillway capacity is stipulated in the Bureau of Indian Standard issued in the year 1985. According to this, the criteria for classification of dams into small, intermediate and large is based on gross storage behind the dam and the hydraulic head. The classification for the dam is greater of the two indicated parameters. The inflow design flood for safety of dam is 100-year flood, Standard Probable Flood (SPF) and Probable Maximum Flood (PMF) for small, intermediate and large dams respectively.

Hydrological safety reviews have revealed that the inflow design flood adopted in certain dams built prior to 1985 do not satisfy the revised Indian Standard. As a result, spillway capacity has been assessed to be insufficient to pass the revised flood discharge, calling for implementation of suitable structural and/or non-structural remedial measures. The recent inclusion of Glacial Lake Outburst Flood (GLOF) in the mountainous glacial fed rivers in computing the design flood would require reassessment of the adequacy of the existing dam spillways in such rivers for the new design flood values. Construction of an additional spillway or exploring the possibility of retrofitting the plugged diversions tunnels used during construction could help to alleviate such a problem. A suitable site for additional spillway may not be available adjacent to all the dam locations, particularly in the mountain gorges.

The heavily sediment-laden rivers in the Indian Himalayas are a serious cause of concern for the operation of the dams and run-of-river hydropower projects. Precious storage is being lost on account of sedimentation. Abrasion of the dam spillways & water conductor system, hydro-mechanical and electro-mechanical underwater components of power plant, blocking of the outlets, loss of power generation are some of the other concerns. In projects wherein no provision of low-level outlets was earlier made, reservoir capacity has drastically reduced due to sedimentation.

The provision of low crest orifice spillways has enabled achieving complete drawdown during flushing and re-create river flow like conditions in the reservoir. Reservoir drawdown sediment flushing in combination with sluicing through low level spillways have significantly helped in preserving the gross/live storage capacity of the reservoirs and smooth running of the power plant in the hydropower projects in the Indian Himalayas owned by NHPC Ltd, a Government of India enterprise.

Operational shortcomings have been experienced in certain dams, like the lack of provision of stop log gates for lowering and maintaining the spillway crest gates, no walkway or access for inspection of the gates and lack of low-level outlet gates. The gates in the older dams are by and large operated manually or electrically operated. The automation of dam gate operation using the Supervisory Control and Data Acquisition System (SCADA) wherever feasible needs to be implemented as this would additionally provide valuable hydraulic data that could be beneficially used for various hydraulic and related optimization studies.

The gates, hoists and related appurtenant structures in dams need comprehensive health check-up periodically, for deciding on their timely repairs, replacement or modernization. The dam gates and hoists that have outlived their life need to be replaced in a phased manner.

One such recent example under DRIP is the replacement and extension of the useful lives of all the 136 sluice gates and their hoisting equipment, located at three different levels, in the 100-year-old Krishna Raja Sagara (KRS) dam in southern India. As observed in many older dams, there was no provision of stoplogs in this project as well, and the gate erection works were therefore to be carried out when the reservoir water level was below the sill level of the gate. Images of the leakages in the sluice gate at 114 feet level before rehabilitation, and leakage arrested after gate replacement is shown in Fig. 4.

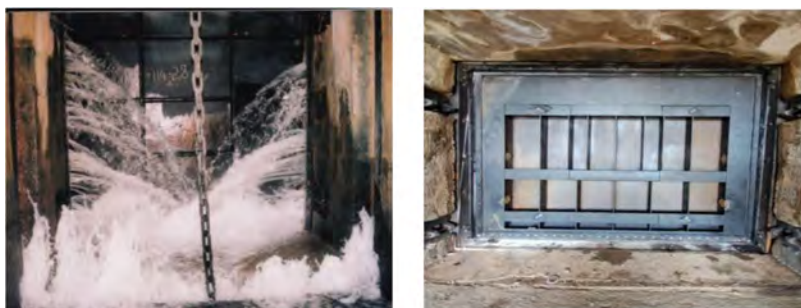


Fig. 4

(a) Leakages in the sluice gate at 114 feet level before rehabilitation. (b) Leakage arrested after gate replacement (from KRS dam site erection)

It is equally important that the proposed rehabilitation solutions sync well with as-constructed parent structure. The existing track base in KRS dam is made up of cast iron material and in new gate replacement work it was proposed to weld track plate in the existing track base embedded into the masonry by welding. Due to higher carbon content, welding of the cast iron would develop cracks. Therefore, in order to minimise cracking phenomenon, the localised heating, combined with slow cooling and preheating was advised to decrease the heat effected zone. It was also advised to use nickel-based electrode but even after many alternatives of trial run of welding with special electrodes, either hair cracks were developed or bonding of deposited metal with base metal was not properly achieved due to lack of proper fusion of base metal. Hence, an alternative proposal of screwing embedded parts in lieu of welding was recommended. This is demonstration of one of the many technical challenges encountered and successfully implemented, and pointer to the many such that lie ahead as more of the aging dams are taken up for rehabilitation.

3.4. INSTITUTIONAL STRENGTHENING AND CAPACITY BUILDING

The Dam Safety Act of 2021 has stipulated four-tier institutional mechanism, two at the National level and two at the State level. The National Committee on Dam Safety (NCDS) and the National Dam Safety Authority (NDSA) at the national level, and the State Committee on Dam Safety (SCDS) and the State Dam Safety Organisation (SDSO) at the State level. Further, each dam is managed by a Dam Safety Unit (DSU).

The dam safety management is primarily an inter-disciplinary task that would encompass engineering, science and technology, environment, project

management, disaster management, information technology and other related disciplines besides, administration and finance. The dam owners need to provide a technically robust dam safety unit comprising of professionals and staff capable of handling high-end technical activities related to implementation of major rehabilitation works, survey and investigations, laboratory testing, hydrological, meteorological, geological and geotechnical issues, instrumentation, gates and hoists, construction, repair and retrofitting, and related domain areas.

The key stakeholders in dam safety evaluation and management process could include dam owners, Central & State Governments, academic and research institutions, public and private companies, rehabilitation and repair agencies, manufacturing and construction industries, information technology services, multilateral banking and non-banking financial institutions, besides other allied services and industries.

Managing a large portfolio of over 6000 large dams and thousands of medium and small dams in the country require quality and experienced manpower in sufficient number to man the positions at various levels, capable of handling specialized activities like dam break modelling, hydraulic and numerical modelling, inundation mapping, preparation of emergency action plans, operation and maintenance manuals and risk assessment studies. The continuing education, knowledge sharing and capacity building of water resources and dam professionals through domestic and international experts is being scaled up by all the dam owning organizations and institutions, under the mentorship of CWC. Under DRIP, two premier institutions viz. Indian Institute of Technology, Roorkee and Indian Institute of Science, Bengaluru have established International Centres of Excellence in dams. Many other institutions spread across the country are gearing up for imparting related training modules and organizing courses.

Adequate long-term operational budgets are key to manage the dam assets responsibly. Investment in dams is more an investment in green economy. The dam owners are addressing the critical maintenance works through their budgetary allocations. Deferred maintenance due to either budgetary constraint or due to lack of quality manpower is one of the reasons adversely affecting the condition of the dam assets. Ensuring operational safety of the large dams, and timely compliances to the provisions stipulated in the Act and subsequent notifications, significant financial resources would be required by the dam owners in the short-term perspective.

3.5. RISK-INFORMED DECISION MAKING

Risk-informed decision-making process is adopted widely for portfolio management of dams. Such an analyses is essential for categorising the risks and

rationalising the resources and funds required for rehabilitating the existing dams. Risk-informed decision making provides a defensible basis for making decisions and helps to identify the greatest risks and prioritize efforts to minimize or eliminate them. Dams need to be thoroughly assessed for risk using a periodic review mechanism process including a site inspection, review of original design/ construction/performance and analysis of potential failure modes and consequences of failure. This assessment also needs to highlight the requirement of new studies, investigations, and instrumentations for reducing uncertainty.

While the dams themselves may not have significantly changed, risk factors may have. Settlements typically tend to grow around dams and in the downstream along the river course, because of the expectation of regular water supply, making more and more people and property vulnerable to flood hazard. This vulnerability is even under normal dam water release situation, not to mention of the uncontrolled release during a failure. Downstream consequences determination should be an integral part of the reservoir operation schedule and emergency action plan. The Dam Safety Act mandates every dam owner to periodically carry out the risk assessment studies, and first such study within five years from the date of commencement of the Act.

3.6. ENVIRONMENTAL AND SOCIAL SAFEGUARDS

Some of the rehabilitation activities may induce environmental and social impacts to a varying extent. The rehabilitation works could require forest, environmental or wildlife clearance, permission for tree felling, permission for access through forest, permission for reservoir desilting work, rehabilitation and resettlement of affected people etc. It is important that the rehabilitation work specifications are consistent with applicable regulations, and project documents indicate any specific environmental and social safeguards, or specific health and safety requirements. Integrated environmental and social assessment need to be carried out for every rehabilitation activity through inspection of the dam, stakeholder consultation at dam and basin levels, for ascertaining the likely impacts. Based on the nature and magnitude, the impacts are to be categorized, and commensurate mitigation measures planned.

4. ENACTMENT OF THE DAM SAFETY ACT, 2021

The enactment of the Dam Safety Act in the year 2021 has brought a paradigm shift in the way dam owners should manage, operate and maintain its dams in India. The Act calls for exhaustive documentation, national level data base,

surveillance and inspection, periodic comprehensive dam safety evaluation, risk assessment, emergency action plan and many other protocols that would significantly aid in efficient management and ensuring safety of the large dams. The dam rehabilitation projects driven by the Central Government viz. DSARP, DRIP phase-I and ongoing DRIP phases II & III have proved a catalyst in strengthening the capabilities of the dam owners in a big way and to rapidly align with the enabling provisions of Dam Safety Act of 2021, thereby moving towards creating a robust dam safety ecosystem in the country.

5. SUMMARY

The paper discusses few of the challenges in the safety management of large portfolio of aging dams in the Indian context. The main takeaways from the paper are summarised as under:

1. A digital asset and document management system needs to be implemented at all the large dams in the country, to systematically record the assets and maintain all the dam documents, which could enable easy online retrieval for the dam owners and others concerned.
2. The routine inspections need to be supplemented with innovative technology-driven solutions for condition assessment and repairs. Automated and data-driven assessment for cracks and distress could use unmanned aerial vehicles equipped with sensors for rapid and comprehensive dam health monitoring, delivering better coverage and accuracy. The analysis of the results could facilitate in considering focused maintenance solutions.
3. One of the greatest challenges in dam safety management is to align the older dams with the evolving standards, particularly with respect to the hydrological, hydraulic, structural and seismic safety considerations. The dam owners need to rapidly adapt to the new approaches and advancements in management of the dams.
4. Managing a large portfolio of over 6000 large dams and thousands of medium and small dams in the country require quality and experienced manpower in sufficient number to man the positions at various levels, capable of handling specialized activities like dam break modelling, hydraulic and numerical modelling, inundation mapping, preparation of emergency action plans, operation and maintenance manuals and risk assessment studies. The scaling up of knowledge sharing and capacity building of water resources and dam professionals through domestic and international experts need to continue.
5. Deferred maintenance due to either budgetary constraint or due to lack of quality manpower is one of the reasons adversely affecting the condition of the dam assets. Adequate long-term operational budgets are key to manage the dam assets responsibly. Investment in dams is more an investment in green economy.

6. Risk-informed decision making provides a defensible basis for making decisions and helps to identify the greatest risks and prioritize efforts to minimize or eliminate them.
7. It is important that the rehabilitation work specifications are consistent with applicable regulations, and project documents indicate any specific environmental and social safeguards, or specific health and safety requirements.
8. The enactment of the Dam Safety Act in the year 2021 has brought a paradigm shift in the way dam owners should manage, operate and maintain its dams in India. The Act calls for exhaustive documentation, national level data base, surveillance and inspection, periodic comprehensive dam safety evaluation, risk assessment, emergency action plan and many other protocols that would significantly aid in efficient management and ensuring safety of the large dams.

REFERENCES

- [1] CENTRAL WATER COMMISSION, Dam Safety Organisation “*Report on Dam Safety Procedures*”, Ministry of Jal Shakti, New Delhi, 1986.
- [2] CENTRAL WATER COMMISSION and National Dam Safety Authority, “*National Register of Large (Specified) Dams*”, Ministry of Jal Shakti, New Delhi, 2023.
- [3] CENTRAL WATER COMMISSION website, Ministry of Jal Shakti, Government of India <https://www.cwc.gov.in>
- [4] DAM REHABILITATION and Improvement Project website, Central Water Commission, Ministry of Jal Shakti, Government of India, <https://damsafety.cwc.gov.in>
- [5] HARI DEV, MAHABIR DIXIT, SEHRA R.S. (2022) “Instrumentation for safety of dams – Issues, challenges and lessons learnt in Indian context” *Proceedings of the International Dam Safety Conference*, Jaipur, India.
- [6] MINISTRY OF LAW AND JUSTICE (Legislative Department), The Gazette of India Notification (2021), “*The Dam Safety Act 2021, No. 41 of 2021*”, 14th December 2021, New Delhi.
- [7] MISHRA A., SINGH RAHUL K., TRIPATHI V. (2022), “Rehabilitation and replacement of 136 numbers of sluice gates & their hoisting equipment of Krishna Raja Sagara dam- A case study” *Proceedings of the International Dam Safety Conference*, Jaipur, India.
- [8] SAINI V.K., MANJUSHA MISHRA, SHUKLA S.D. (2022) “Sediment management in run-of-the-river hydropower plants in Himalayan region” *Proceedings of the International Dam Safety Conference*, Jaipur, India.

GENERAL REPORT ON QUESTION 109

RAPPORT GÉNÉRAL SUR LA QUESTION 109



Taylor & Francis

Taylor & Francis Group

<http://taylorandfrancis.com>

COMMISSION INTERNATIONALE DES
GRANDS BARRAGES

VINGT-HUITIEME CONGRES DES
GRANDS BARRAGES
CHENGDU, MAI 2025

QUESTION 109

**DAMS AND LEVEES
FIT FOR THE FUTURE**

**DES BARRAGES ET DES DIGUES
PRÊTS POUR L'AVENIR**



Shuguang LI

*PhD, Professor-level senior engineer, China Three Gorges Corporation
Member, ICOLD technical committee on operation, maintenance and rehabilitation
of dams
Member, CHINCOLD technical committee on inspection, repair and enhancement
of hydraulic structures*

CHINA/CHINE

GENERAL REPORTER

TABLE OF CONTENTS

1. INTRODUCTION864

2. SUMMARY OF RECEIVED REPORTS864

3. MANAGEMENT OF AN AGING PORTFOLIO OF DAMS IN TERMS
OF OPERATION, MAINTENANCE AND REHABILITATION869

 3.1. Features of fit-for-the-future dams and levees869

 3.2. Manage strategies for the aging dams and levees.....870

4. SAFETY DURING CONSTRUCTION AND REHABILITATION.....872

 4.1. Innovative dam building techniques873

 4.1.1. New foundation-sustaining techniques873

 4.1.2. New types of dams874

 4.1.3. Innovations in dam-building materials877

 4.1.4. Intelligent dam-building techniques880

 4.1.5. Dam safety, hydraulics related880

 4.2. Safety monitoring and analyses of aging dams883

 4.3. Rehabilitation and safety enhancement of aging dams886

5. SPECIAL CASE FOR SMALL DAMS AND LEVEES888

6. INCREASINGLY DIFFICULT SITES - DAMS AND THEIR NEW
CHALLENGES.....890

7. NEED FOR GLOBAL CAPACITY BUILDING.....891

8. CONCLUSIONS.....892

ACKNOWLEDGEMENTS.....893

REFERENCES.....893

1. INTRODUCTION

This General Report for Question 109, “Dams and levees fit for the future”, was approached as a review of the state of the art concerning the themes considered, referring to the reports received where appropriate.

Dams and levees are important infrastructures for the society. Their benefits include flood control, energy production, water supply, river flow regulation, navigation and so on. As we are stepping into the second quarter of the 21st century, global climate change, urbanization and sustainable development pose higher demands to dams and levees. We have to respond and make dams and levees fit for the future and that’s the reason that we set this question in ICOLD Congress 2025. Scientists and engineers in the ICOLD community should make best efforts to ensure the safety of the dams and levees, whether under construction or ageing, so that we could enjoy their long-term benefits in the future.

Reports during the latest two congresses have already focused on similar themes, such as Q103, “Small dams and levees” and the sub-Question, “impacts of climatic change on needs and designs of dams, reservoirs and levees” in Q107, “Dams and climate change”.

2. SUMMARY OF RECEIVED REPORTS

As contributions for Q.109, a total of 51 reports have been received, from 20 countries belonging to five continents. China and France submitted 20 and 6 reports, respectively, which represents 50% of the total.

Table 1
Reports from different countries

COUNTRIES	NUMBER OF REPORTS	REPORTS
France	6	R10,R16,R17,R20,R21,R25*
Portugal	1	R1
Sweden	3	R2,R3,R4
Switzerland	3	R5,R6*,R7
Norway	1	R11*
Austria	2	R11*,R27
Italy	1	R15

(Continued)

Table 1
Continued

COUNTRIES	NUMBER OF REPORTS	REPORTS
Netherlands	2	R18,R19
United Kingdom	1	R22
Romania	1	R26
Poland	1	R48
Czech Republic	1	R50
Canada	3	R8,R9,R28
Ghana	1	R23*
South Africa	2	R23*,R24
Malawi	1	R25*
New Zealand	1	R25*
Japan	3	R12,R13,R14
India	1	R51
Thailand	1	R6*
China	20	R29~R47,R49

*Reports having authors from more than one country.

Table 2 below summarizes the distribution of reports by continent, showing that Asia and Europe contributed for 90% of the total.

Table 2
Reports from different continents

CONTINENT	NUMBER OF REPORTS	COUNTRIES
Asia	25	4
Europe	22	12
Africa	3	3
America	3	1
Oceania	1	1
Total	51**	

** Some reports have authors from different continents.

The themes for Q109, Dams and levees fit for the future, are listed below:

1. Management of an aging portfolio of dams in terms of operation, maintenance and rehabilitation, including risk-based approaches,
2. Safety during construction and rehabilitation,

3. Special case for small dams and levees,
4. Impact of new contracting practices on dam safety (e.g. private sector involvement, EPC contracts),
5. Increasingly difficult sites - dams and their new challenges,
6. Need for global capacity building.

Table 3 Summaries the reports submitted to Q109 themes, including the number of reports.

Table 3
Number of reports contributed to each theme in Question 109

SECTION	THEME	NUMBER OF RE-PORTS	REPORT NUMBERS
3. Management of an aging portfolio of dams in terms of operation, maintenance and rehabilitation	1	10	R2,R9,R13,R20,R22,R26, R28,R44, R48,R51
4. Safety during construction and rehabilitation	2	35	R1,R3,R4,R7,R8,R10~R16,R18, R23~R25,R27,R29, R31~R33, R35~R43, R45~R47,R49,R50
5. Special case for small dams and levees	3	3	R17,R19,R21
6. Increasingly difficult sites - dams and their new challenges	5	5	R1,R5,R6, R30, R34
7. Need for global capacity building	6	1	R8

From Table 3 we can see that the majority of the reports focuses on Theme 1 and Theme 2 while only a few reports contribute to Theme 3, Theme 5 and Theme 6. No report contributes specifically to Theme 4.

3. MANAGEMENT OF AN AGING PORTFOLIO OF DAMS IN TERMS OF OPERATION, MAINTENANCE AND REHABILITATION

3.1. FEATURES OF FIT-FOR-THE-FUTURE DAMS AND LEVEES

Although no clear definition has been given by ICOLD community on dams and levees fit for the future so far, after reviewing all the submitted reports for Q109, fit-for-the-future dams and levees can be characterized by “**P-I-E-R-C-E-S**”, which is a combination of the initials of seven words, namely, **S**afety, **R**esilience, **I**ntelligence, **E**co-friendliness, **E**conomy, **C**ompliance, and **P**articipation.

- (1) **Safety.** Dams and levees fit for the future must be safe, which is a top priority. The dams and levees should be safe in their whole life cycles, including the design, construction, operation, maintenance, rehabilitation and decommission stages, involving efficient, robust and reliable technical and non-technical solutions.
- (2) **Resilience.** Dams and levees fit for the future must be climate-resilient infrastructures. Dams and levees should be designed with adaptive, flexible approaches enabling these structures to respond dynamically to climate variability, and should prioritize materials, construction methods, and monitoring systems that are resilient to a broader range of climatic extremes, such as extreme heavy rainfall and prolonged droughts.
- (3) **Intelligence.** Dams and levees fit for the future must be intelligent, which means they could integrate edge, smart technologies and systems to enhance their safety, resilience and operational efficiency. In the future, the dams and levees could be exposed to facilities that sense, think, make decisions and respond like humans equipped with intelligent techniques, such as different IoT based sensors, machine-learning algorithms, AI-based decision-making system, drones and robotics.
- (4) **Eco-friendliness.** Dams and levees fit for the future must be ecologically and environmentally friendly and have to meet long term environmental requirements. They would incorporate features such as fish ladders, floating islands to prevent eutrophication, and floating waste collection systems improving ecological connectivity and water quality. Adequate ecological flow should be ensured to support aquatic ecosystems and aligns with environmental sustainability goals.
- (5) **Economy.** Dams and levees fit for the future must be economic. Financial planning and cost-benefit analysis should be conducted in their whole life cycle. Balance between costs, safety and function should be made not only in the design stage or maintenance stage, but in the whole lifetime.
- (6) **Compliance.** Dams and levees fit for the future must comply with regulatory frameworks. In addition, they need to meet stringent safety standards not only for present conditions but also for anticipated future challenges brought by for example climate change, extreme weather events.
- (7) **Participation.** Dams and levees fit for the future must involve all the stakeholders, including the government agencies, banks and investors, owners, operators, experts, researchers, local communities, media and public. Effective stakeholder engagement is crucial for the success of dams and levees, ensuring that most perspectives are considered and already implemented. Potential domestic or international conflicts are also to be addressed.

3.2. MANAGE STRATEGIES FOR AGING DAMS AND LEVEES

Ten reports contributed to this theme and authors from European, American and Asian countries presented their thoughts and suggestions in managing aging dams in terms of operation, maintenance and rehabilitation.

Based on recent flood events across Europe and several case studies of upgrading 50-year-old earth dams, Report **R26** from Romania provided a framework to make future-proofing dams, including strategies for sustainable water management, technological retrofit, and climate resilience in the context of dam refurbishment. Report **R48** from Poland proposed key systemic and technical solutions to mitigate the increasing failure risks of aging dams and levees due to climate change. Report **R2** introduced a government assignment completed in 2023 on the impact of climate change on dam safety in Sweden and explained applications in six aspects of the national strategy for climate adaptation for dam safety. Report **R22** from UK provided an overview of the historical development of puddle clay dams which comprise over 60% of the British reservoirs and introduces the challenges faced in risk assessment and significant improvement in design and maintenance. Report **R51** discussed the challenges faced by India in managing 6,138 large dams, many of which are more than 25 years old. It provided several suggestions to improve the aging dam safety including technology-driven health monitoring, adaptation to new standards and technological developments, strengthening institutional capabilities, and risk assessment.

Although the numbers, types, ages, technical features and safety status of dams and levees, presented in the above-mentioned reports are significantly different in various countries, some governments realize the importance of ensuring safety for the future and are making efforts in realizing the goal. Management of aging dams and levees requires a multidisciplinary approach combining engineering, environmental science, economics, and social policy, but also requires participation from all the dam/levee shareholders. Case studies related with dam failures shows that embankment dams are more vulnerable to climate change. Safety monitoring of low or small-scale embankment dams and levees should be enhanced and regarded as key concerns for the owners or operators.

As dams age, their structural integrity may deteriorate, increasing the risk of failure. Therefore, it's essential to adopt risk-based approaches to ensure safety and efficiency in operation, maintenance, and rehabilitation. **R20** introduced the Safety Review Risk Assessment (SaRRA) for large dams in France, which was implemented in 2007 and so far, approximately 650 SaRRA projects have been completed, making them a core component of risk management and prevention systems. The results or database are quite instructive for all the dam stakeholders not only in France but also in the world. **R9** showed the results of a Quantitative risk assessment (QRA) completed for a Potential Failure Mode (PFM) of concern at Waterton Dam located in southern Alberta, Canada. It demonstrated QRA can bring in more in-depth understanding of key potential failure modes allowing for the proactive intervention measures, informing instrumentation design and monitoring measures to enhance the safety of the dam. However, nowadays the QRA process can be expensive, time consuming and costly and a tradeoff is the use of engineering judgment.

In the past years, researchers focus not only on the safety of the dam, but also the safety of the cascading reservoirs and the influences of the dam to its ecology and environment. Report **R44** discusses the safety challenges and operational considerations faced by China's cascading reservoir dams. It proposes five suggestions to improve overall safety level of cascading reservoir dams such as establishing a smart dam safety management system, improving the engineering safety and emergency management level of dam groups. **R13** from Japan introduced a series of measures to mitigate long-term turbidity in the downstream of Hitotsuse Dam, which was built over 60 years ago. A series of turbidity-mitigation measures were taken and verified effective, reducing the adverse effects of the dams to the environment and ecology.

With the development of intelligent techniques, Artificial Intelligence (AI) has been applied more and more. Report **R28** from Canada provides an overview of Generative AI (GenAI) development and introduces details how GenAI can be applied to the field of dam safety review (DRS), including data and records review, site inspection, dam classification, failure modes analysis, dam safety analysis, dam operation, maintenance and surveillance.

To summarize the above reports in this theme, although it remains a great challenge to build or upgrade aging dams and levees into fit-for-the-future ones characterized by "P-I-E-R-C-E-S", several countries are already taking multifaceted managing strategies, intelligent and state-of-the-art measures and making important progress in making dams and levees safe during their whole lifetime, resilient to climate change, friendly and harmonious to the ecology and economically viable in the life cycles.

4. SAFETY DURING CONSTRUCTION AND REHABILITATION

As stated in Section 3, safety is the top priority for dams during the whole lifecycle. Nearly 40 of all the 51 reports provide latest progress regarding dam safety, contributing to theme 2, Safety during construction and rehabilitation. They are summarized in three sub-themes, 1) Innovative dam building techniques, 2) Progress in safety monitoring and analyses of existing dams and, 3) Progress in rehabilitation and safety enhancement of aging dams.

4.1. INNOVATIVE DAM BUILDING TECHNIQUES

Twenty-two reports contribute to this theme. They provide a panorama of the latest innovations worldwide in dam engineering, including new foundation-sustaining techniques, application of new types of dams, new dam building materials, and intelligent construction technologies. It is worth mentioning that sixteen of the reports are from China. This agrees with the fact that China holds the most dams and reservoirs in the world and has recent world-class 300m-high dam construction in process.

4.1.1. *New foundation-sustaining techniques*

To build a fit-for-the-future dam, a sustainable foundation that can support the dam throughout its lifecycle is needed and crucial. The sustainable dam foundation here refers to a foundation that features structural stability, durability, environmental compatibility, and economic viability. Despite of dam types, the key requirements for a sustainable foundation include, adequate load-bearing capacity, settlement resistance, earthquake resistance, geological compatibility, drainage, impermeability, and durability.

Seven reports contribute to this sub-theme and four are about foundation sustaining techniques for embankment dams on soft soil foundations and deep overburden layers (**R38**, **R41**, **R42** and **R43**), while the other three are for hard-fill dams or concrete dams on rock foundation with severe faults (**R24**, **R45** and **R49**).

Report **R38** includes comprehensive reviews in dam construction experiences on soft soil foundations in China. Assessing the dam's stability and projecting its deformation behaviour rely heavily on physical and mechanical parameters inherent in the soft soil. It suggested that for assessing dam foundation leakage the upper limit of the permeability coefficient obtained from laboratory tests or pumping tests could be adopted. For slope stability analyses and calculations of excess pore water pressure, we can utilize the lower limit of the permeability coefficient from laboratory tests or results from lateral pressure tests, CPTU tests, and consolidation tests.

Reports **R42** and **R43** introduce study and design of the foundation treatment for a clay core rock-fill dam in Rwanda, with a maximum height of 59 m. The deep ultra-soft dam foundation is 40m thick of lacustrine peaty and silty ultra-soft soil in a liquid to plastic state. After a fine analysis, vibro-replacement stone columns are used to strengthen the soft soil foundation and geomembrane to extend the seepage diameter at the bottom of core wall. The detections and testing conducted on the stone columns indicates they performance well and meets the design requirements.

Report **R41** introduces an experience and lesson learned from a foundation grouting project under deep cover layer in a clay core rock-fill dam in southwest China, which is 110 m high. The overburden depth of dam foundation is 149m, a cutoff wall with a depth of 85m combined with 4 rows of overburden grouting works

of 60m under the cutoff wall were designed and performed, which proved to be successful until now. However, it takes 10 years and intensive cost for the reinforcement grouting works, demonstrating that seepage control of the dam foundation is the lifeline of the dam, and it should be given as much attention as possible in the design and construction stages.

Report **R24** discusses geological challenges faced during the construction of two hard-fill dams about 40m in height and their solutions. The two dams in South Africa are both on rock foundation with many faults affecting the dams' safety. Consolidation grouting and shear keys were used, and the overall dam stability was improved. Report **R45** discusses the design of foundation treatment for the Batang Toru HEPP in high seismic area in Indonesia, aimed at enhancing its stability and anti-seepage capability. The dam is an arc-shaped gravity dam with a maximum height of 74m situated on tuff. The challenges faced include weak rock foundation, high density of fractures, and low bearing capacity. The optimization of drilling patterns and the application of curtain grouting, consolidation grouting, and contact grouting techniques were used to address these issues.

Report **R49** discusses the use of the DBSCAN (Density-Based Spatial Clustering of Applications with Noise) algorithm for identifying fractured rock masses using drilling data. It could provide an automated, unbiased method for fractured rock mass detection and thus has a good potential application in geotechnical engineering for all kinds of dams.

To sum up, the above seven reports shared their challenge-overcoming experiences in ensuring sustainable foundations with various geological conditions. Cutoff walls and extensive grouting to control seepage for a 110m high clay-core rock-fill dam with a 149m deep cover layer, vibro-replacement stone columns and geomembrane to strength thick ultra-soft soil foundation and control seepage, grouting techniques to enhance the seismic resistance, shear keys to improve stability in faulted rock foundation, are introduced. Principles to select physical and mechanical parameters for the soft soil foundation, as well as DBSCAN algorithms to unbiasedly identifying fractured rock masses are also addressed. All the case studies or experiences mentioned above provide useful and valuable reference for dam projects with similar geological conditions.

4.1.2. *New types of dams*

Traditional types of dams, while effective in many cases, may not always address the challenge in building fit-for-the-future dams. New types of dams, which offer innovative, better solutions in at least one aspect in the "P-I-E-R-C-E-S" features, are necessary and essential for dams fit for the future. Three reports contribute to applications of Cemented Soil Dam (**R25**), Cemented Sand and Gravel Dam (**R35**) and composite dam (**R31**).

A. Cemented Soil Dam and Cemented Sand and Gravel Dam

According to Bulletin 195 ^[1], Cemented Material Dam (CMD) is defined as a series of new dam types utilizing cementitious binder together with various natural or manufactured materials in the construction of dam. CMD has technical advantages including building dam safe, quickly and sometimes economically in an environment-friendly way, and decreasing the risk of overtopping failure. CMD includes Cemented Soil Dams (CSD), Cemented Sand and Gravel Dams (CSGD), Rock-Filled Concrete Dams (RFCD) and Faced Symmetrical Hard-fill Dams (FSHD). Reports **R25** and **R35** have applications of CSD and CSGD, respectively.

CSD uses soil mixed with cement and other cementitious materials as dam building materials. Report **R25** describes the process of building a coffer dam using cemented soil technology at Kapichira Dam in Malawi. The maximum dam height is 14m and the crest width is 6 m with a symmetrical upstream and downstream slope ratio of 1:1.5. The report introduces in detail the design, preparation of the sand, cement, soil, on site laboratory testing, full-scale tests, and the construction process (see Fig. 1, Fig. 2). Cemented soil technology quickly and effectively response to the emergency and lay the foundation for subsequent comprehensive restoration work and has a great application potential in hydraulic structures.

Report **R35** discusses a new dynamic proportion design method for CSGD, aiming to address issues such as large strength differences and poor economic efficiency in traditional CSG mixture design. Through indoor simulation experiments, the relationship between the strength of cemented sand and gravel and the combination of sand ratio and paste margin was determined, and a new dynamic proportion design method was proposed based on optimizing the combination of these two factors. Ultimately, this method has been successfully applied in a hydropower project's high toe pier modulus enhancement area, and its effectiveness and feasibility were verified by the practical engineering results.

B. Composite Dam

A composite dam is a type of dam that combines two or more different materials or structural types to leverage the advantages of each, optimizing the dam's performance, stability, and cost-effectiveness. Composite dams are often used in situations where a single type of dam construction may not be suitable due to geological, environmental, or economic constraints. Appropriate design, construction, and maintenance are essential to ensure its long-term performance.

Report **R31** discusses the construction of a composite dam at the Zungeru Hydroelectric Power Project in Nigeria, which is composed of a roller compacted concrete (RCC) dam and two asphalt concrete core rock-fill dams. The joint height of the dam is 85 meters, which is bigger than most dam joints. The design and construction of the joint of these two dams (Fig. 3) plays a crucial role in ensuring the

safety of the dam. It describes the construction technology and monitoring of the joint, including surface treatment of the cement concrete, installation of water stops, construction of the joint section of the RCC dam, construction of the asphalt concrete core, construction of the transition material, and monitoring of the joint pressure, displacement, and osmotic pressure. The report concludes that the design and construction quality of the joints directly affect the quality and safety of the entire dam, and Zungeru dam provides a broader development prospect for the application of similar types of composite dams in the future.



Fig. 1

CSD Construction Sequence at Kapichira dam in Malawi

Séquence de Construction CSD au barrage de Kapichira au Malawi

1. Cement spreading
2. Moisture conditioning & mixing
3. Mixed material
4. Loading
5. Surface cleaning
6. Cement spreading and dumping
7. Dumping and spreading
8. Compaction



Fig. 2
Overview of Cemented Soil Placement at Kapichira dam in Malawi
Aperçu de la mise en place du sol cimenté

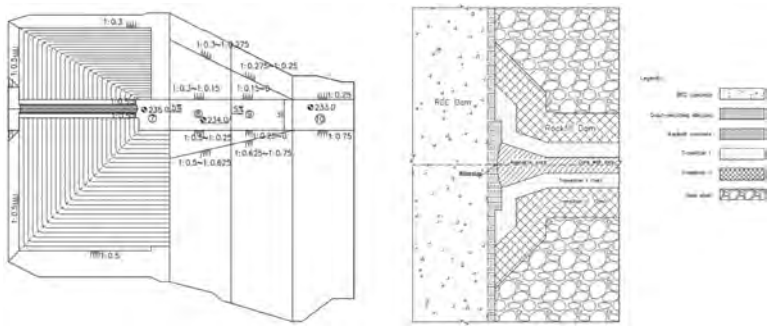


Fig. 3
Joint plan for RCC dam and the composite dam at Zungeru Dam in Nigeria
Plan conjoint pour le barrage RCC et le barrage composite du barrage de Zungeru au Nigeria

4.1.3. Innovations in dam-building materials

Innovative dam-buildings materials that have the abilities to address the limitations of traditional materials, improve the performance and sustainability of dams are essential for dams fit for the future. Report **R36** summarized three breakthroughs in China's concrete dam construction in the past few years, which are breakthroughs in dam height, breakthrough in dam temperature controlling and breakthrough in concrete process accuracy. Among them the most innovative breakthrough is expansive low-heat Portland cement and the high crack-resistance dam concrete.

A. Expansive low-heat Portland cement

For high concrete dams, the dam concrete must be highly cracking resistant. Low heat cement as well as expansive agent are two essential pathways to improve the crack-resistance of dam concrete. The first-generation of low-heat Portland cement (LHC) which was manufactured and firstly used at a large scale in the construction of Hoover Dam in 1930s ^[2]. However, because of its shortcomings such as low early strength, large autogenous volume shrinkage and high manufacturing cost, the applications in dam engineering were quite limited after final application in Detroit Dam in 1953.

Ettringite-based or calcium oxide-based shrinkage compensation concrete, made with either an expansive cement (Type K, M, S) or expansive components (Type K, M, G), is used to minimize cracking caused by drying shrinkage ^[3]. Since the expansion occurs at early age and doesn't match the cooling and shrinking process of dam concrete, this type of concrete cannot be used in dams. Magnesium oxide-based shrinkage compensation concrete (MgO concrete), made with lightly burnt MgO powder (as an additive), has been applied in about 30 small concrete dams in China ^[4] and the results in minimizing thermal cracks and simplifying temperature-control measures are significant. The reason is that the expansion of MgO after hydration closely matches the shrinking process of dam concrete as it cools. However, due to the difficulties in uniformly distributing MgO powder in dam concrete and concerns that uneven distribution of MgO might cause uneven expansion leading to cracks, MgO concrete hasn't been applied in high dams with heights over 100 m so far.

Accordingly, a new type of low-heat Portland cement which is MgO-based and expansive in autogenous volume deformation was invented in China to improve the cracking resistance of dam concrete by concurrently adjusting both its thermal property and deformation property ^[5]. Expansive low-heat Portland cement (ELHC) has advantages of autogenous expansion, lower hydration heat, higher early strength, lower energy consumption and carbon emission. The autogenous volume deformation change is expansive and the 28d expansion is no less than 0.08%. ELHC concrete is characterized by its high resistance to cracking, allowing for a simplified yet efficient and cost-effective temperature controlling scheme. For the first time, ELHC concrete was extensively used in the construction of the Baihetan and Wudongde hydropower plants, including the 300m high arch dams, powerhouses, tunnels, etc. No cracks have been observed in dams since the construction began 8 years ago. ELHC and ELHC concrete have since been applied to CFRDs, railways and bridges, demonstrating significant potential for further application and delivering substantial technical, economic and social benefits.

Most engineers are concerned about the durability of ELHC concrete. Report **R40** explains the differences in durability between OPC (ordinary Portland cement), MHC (mediate heat Portland cement) and expansive LHC using coupled hydration and calcium leaching deterioration models. The results indicate that after 1000 days of

hydration, the C-S-H content increased and the calcium hydroxide content decreased in the three cements while LHC shows the greatest hydration potential. After 100 years of leaching, the leaching-affected depths of OPC, MHC and LHC are 2.4 cm, 2.2 cm, and 2.0 cm, respectively. The leaching fronts of C-S-H, calcium hydroxide, and ettringite all decreased across OPC, MHC and LHC, indicating that LHC has the best leaching resistance. It concludes that LHC is the best in durability against leaching (Fig. 4).

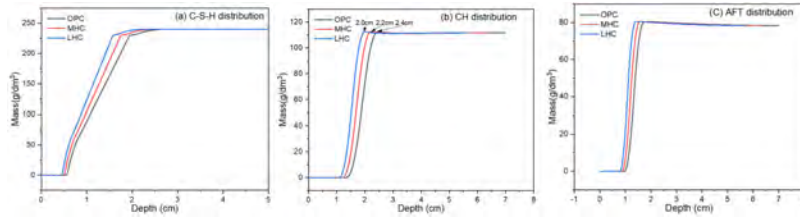


Fig. 4

Distribution of hydration products after 100 years of leaching for OPC, MHC and LHC as a function of depth: (a) C-S-H, (b) CH, (c) Ettringite.

Distribution des produits d'hydratation après 100 ans de lixiviation pour OPC, MHC et LHC en fonction de la profondeur: (a) C-S-H, (b) CH, (c) Ettringite.

B. Application of acidic aggregates in asphalt concrete

In general, for embankment dams with impervious structure made of asphalt concrete, acidic aggregates are not commonly used in asphalt concrete because of their poor compatibility or adhesion with the asphalt binder, which would result in an inadequate water stability. However, for asphalt concrete lining projects where only acidic aggregates can be found, report **R39** proposed a new way of using them by anti-stripping additives, which can significantly improve the adhesion between acidic aggregates and asphalt. The report also proposed an effective parameter for distinguishing between acidic and basic aggregates and predicting the optimal dosage of anti-stripping additives to prevent water damage to asphalt concrete. Acidic aggregates and anti-stripping additive were used in the upper reservoir of Yimeng pumped storage power plant (PSPP) in Shandong, China in 2021^[6]. So far, the anti-seepage properties of the asphalt concrete lining are excellent.

To sum up, a new type of cement called expansive low-heat Portland cement (ELHC) was developed in China and ELHC-based high cracking-resistance dam concrete was produced. No thermal cracks have been observed so far after applications in Wudongde and Baihetan ultra-high arch dams indicating that this is probably a fundamental new material for fit-for-the-future dams. Asphalt concrete made with acidic aggregates and anti-stripping additives to improve the adhesion between the aggregates and asphalt were produced and applied in the upper

reservoir of a PSPP, providing a feasible way to apply local acidic aggregates in asphalt concrete.

4.1.4. Intelligent dam-building techniques

Fig. 5 is an overview of new technologies that can be applied in dam engineering [7] as well as in warning systems and monitoring which are so important for fit for purpose dam safety during the life of dams'. Reports **R29**, **R32** and **R47** introduced innovative intelligent techniques in dam construction in China.



Fig. 5
An overview of new technologies in dam engineering [7]
Un aperçu des nouvelles technologies dans l'ingénierie des barrages

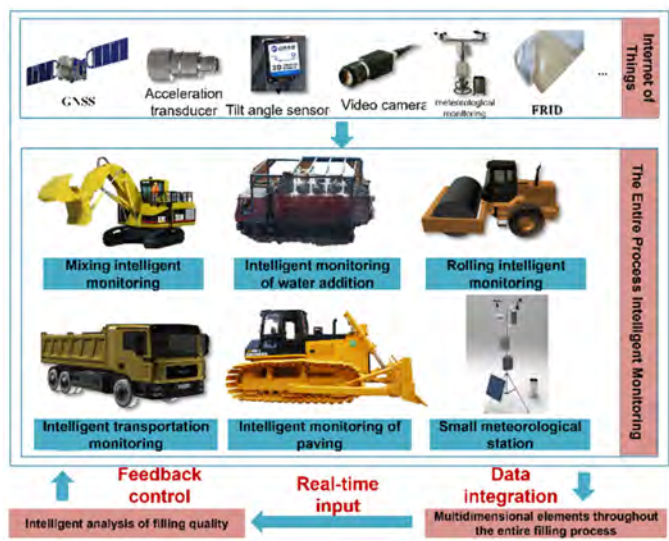


Fig. 6
The intelligent monitoring framework for the whole construction process of
Lianghekou Hydropower Station
*Le cadre de surveillance intelligente pour l'ensemble du processus de construction
de la centrale hydroélectrique de Lianghekou*

Reports **R29** introduced the intelligent construction techniques applied in construction of Lianghekou gravel soil core rockfill dam with a maximum height of 303.00m, the highest earth and rock dam in the world. The dam was built in alpine region with the crest elevation at 2875.00m. In this project, the engineers created a complete set of winter construction technology for ultra-high earth rock dams in high altitude and cold regions, and create a precedent large-scale continuous construction of soil core walls in plateau permafrost regions in winter using intelligent filling technology, which effectively controlled the whole cycle of dam filling construction. The overall system of intelligent fill construction technology includes mixing, transporting, adding water, paving, rolling, as well as the command center and unmanned rolling site mobile center (Fig. 6).

Report **R32** discusses the development of an intelligent management and control system for concrete dam construction, which consists of a smart command center for real-time data collection, analysis, and decision-making, the design and development of mathematical models for the smart command center, and five function modules of system application, including BIM design, pouring area design, concrete production, transportation, and pouring. The proposed system aims to

manage and control concrete dam construction, support decision-making, shorten the waiting time during construction, and ultimately improve concrete construction efficiency. The methodology was applied in a dam project currently under construction. The technical performance indicators of the proposed work are summarized, demonstrating the feasibility and reliability of the proposed system.

Report **R47** introduced the development of an intelligent construction site which was applied in Kala hydropower plant with an installed capacity of 1,020 MW. The main dam is a RCC dam with a maximum high of 123m. The intelligent site includes intelligent safety monitoring technologies, and an intelligent construction platform for hydropower stations. The layout is shown in Fig. 7. The intelligent safety monitoring system provides real-time monitoring and early warning for unsafe behaviours and scenarios at the construction site, significantly enhancing construction safety. The platform covers all business aspects, elements, and processes, incorporating eight intelligent business management functions and five intelligent construction applications. The intelligent site at Kala hydropower plant is a model for construction and management from dams or levees for the future. It meets a significant demand in the construction of large hydropower stations, offering broad market prospects and substantial application value, with considerable social benefits.

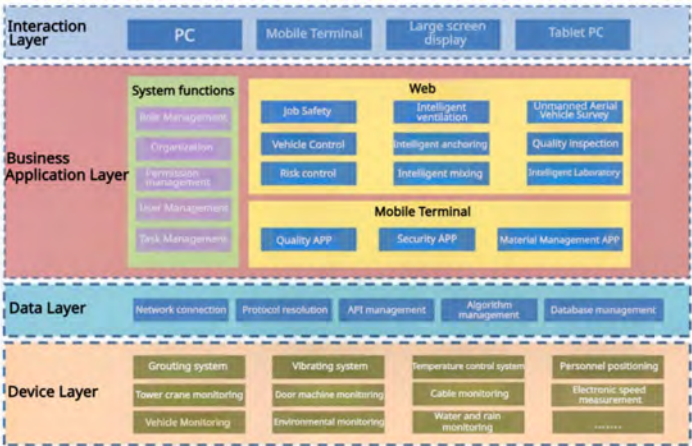


Fig. 7
Intelligent Construction Site System Layout.
Disposition intelligente du système de chantier

As can be seen from the above reports, more and more intelligent technologies or systems are being developed and applied in dams built recently. Intelligent dams would gradually be more and more realized in the near future.

4.1.5. *Dam safety, hydraulics related*

Damages in the stilling basin in Sweden were found in several low head facilities after several decades of normal operation without being exposed to design flood or extreme flooding events. Report **R3** tried to reveal the mechanism by physical scale model tests with numerical modelling. They found that cracks in prototype, in the concrete along the upstream slope of the stilling basin, could be a possible explanation to the initiation of damages in the real structure. After initiation of concrete damages, pressure fluctuations in general, potentially together with cavitation could make damages progress by causing vibrations on the rebars. This indicates that high cracking resistance concrete is not only need for concrete dams but also for abrasion resistant concrete in the stilling basin with low water head, or abrasion resistant concrete in the tunnel lining with low head or low velocities.

To summarize Section 4.1, major technical progress regarding foundation-sustainability, dam types, dam building materials, and intelligent technologies were introduced. For foundation sustainability, various techniques to control the seepage, enhance the bearing capacity and improve resistance to settlement and seismicity for dams on ultra-soft soil foundation, faulted rock foundation were addressed. Applications of cemented soil dam, cemented sand and gravel dam, and a composite dam combining a RCC dam and two asphalt concrete core rock-fill dams were introduced. A new type of cement, called expansive low heat Portland cement was developed in China and the dam concrete is highly cracking resistant, showing a great potential in thermal control for high concrete dams. Asphalt concrete based on acidic aggregates with anti-stripping additives was developed and applied in PSPP. Intelligent techniques or systems to improve dam safety in the construction and monitoring stages were developed, playing a significant role in ensuring the 303m high Lianghekou gravel soil core rock-fill dam, the highest earth and rock dam in the world.

4.2. SAFETY MONITORING AND ANALYSIS OF AGING DAMS

Eight reports contribute to the latest technical progress in safety monitoring and analysis of existing dams, including a 60 years old embankment (**R10**), 100m high concrete arch dams (**R46, R14**), 300m high arch dams (**R37, R33**) and erosion-affected ones (**R4, R11, R21**).

Report **R10** discusses the importance of detecting abnormal behavior in dams through advanced analysis methods and introduces two advanced monitoring data analysis methods: machine learning-based anomaly detection and numerical modeling using distributed fiber sensing technology. Both methods, performed on the displacement data of a French concrete gravity dam with a height of 31m, and on a canal embankment nearly 60 years old with a length of 5.250 km, respectively, have shown their interest and technical advantages to improve capabilities of interpretation of monitoring data.

Report **R46** develops a comprehensive dam monitoring indicator calculation technique based on the integrated selection of indicator measurement points, multi-criteria comprehensive calculation, and the holistic application of criteria. The method was applied in Nam Ngum 5 RCC arch dam in Laos, with a maximum height of 100.5m, providing quick assessment of the safety status of the dam and offering scientific guidance and support for its operation.

Report **R37** aims to assess the safety performance of an ultra-high arch dam in southwestern China under the influence of valley contraction deformation by conducting comprehensive nonlinear finite element analysis, considering the controlling geological boundary conditions of the dam and foundation, as well as the evolution of valley deformation loads. The results show that under the current valley deformation effects, the safety level of this arch dam expressed by 3K safety factors meets the regulatory requirements. However, continuous monitoring of valley deformation is necessary to ensure long-term dam safety operation.

Report **R33** proposed a data augmentation scheme for predictive maintenance (PdM) of dams and application in an ultra-high arch dam (maximum height 294.5m) in China. The improved K-means clustering method proposed combines spatial distance information of sensor measurement points to improve the classification accuracy and efficiency of time series data. Additionally, the combination of the improved clustering centroid line and Long Short-Term Memory (LSTM) models enables effective prediction of dam operation status. By comparison the improved K-means clustering method is demonstrated significantly improves the accuracy of abnormal detection and enhances the precision of data prediction, providing valuable references for predictive maintenance of large concrete structures.

Report **R14** introduced 60-year-long in-situ monitoring results on a concrete arch dam (87m high) in cold region in Japan. Dynamic modulus of elasticity of dam concrete estimated from ultrasonic velocity showed that Otori dam is maintained perfectly even after 60 years (Fig. 8), suggesting that the soundness of the dam is secured. The specimens also maintained high dynamic modulus percentage, but differences were observed depending on mix proportion. The study demonstrates that reasonable design and construction measures are crucial for ensuring the long-term performance of concrete structures in freeze-thaw environments.

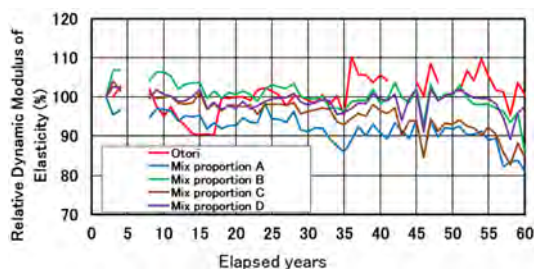


Fig. 8

Changes over Time in the Relative Dynamic Modulus of Elasticity
Évolution dans le temps du module d'élasticité dynamique relatif

In report **R11**, an innovative approach is used to assess the stability of a dam structure measuring 100m in length, 65m in width, and 57m in height, situated on a soil foundation characterized by excessive pore water pressure and reduced effective stresses resulting from static liquefaction during construction and subsequent internal erosion. The focus is on calculating deep-seated bearing failure mechanisms. Safety factors are calculated by the Shear Strength Reduction (SSR) method with the innovative two stages calibration process. Finally, the importance of actual measurement data such as CPTs, drainage rates, and pore water pressures is emphasized.

The main cause of dam and embankment failure is erosion, internal and external erosion, which was not covered by the European standards (Eurocodes). Report **R21** introduced a set of recommended guidelines for assessing erosion risk issued in 2024 by the French Committee for Large Dams (CFBR) after 7 years' work. The recommendations, for the first time encompasses internal and external erosion in a common 7-step methodology based on the concept of erosion paths and can be applied in dams, canals and levees. They propose three levels of analysis for internal erosion and three types of justification for external erosion.

Report **R4** introduced the optimization of riverbank protection design by combining hydraulic modelling with turbulence-based design methods. The two-dimensional hydraulic model was developed using high resolution bathymetry from multibeam echo-soundings and LiDAR topography. The turbulence was modelled using the two-equation, depth-averaged k-epsilon model. The combined method is applied in the tailwater channel of a hydroelectric power station in northern Sweden, over 60 years old. Results showed that the existing bank protection measures are insufficient to withstand the impact of flood events, especially in areas with high flow velocity and strong turbulence. Repair solutions were proposed, including increasing the thickness of the rock layer and changing the rock size to improve the effectiveness of the bank protection. The new method can contribute to a better understanding of erosion phenomena and to optimal bank protection design.

To summarize this section, dam safety monitoring, analysis, and maintenance integrating advanced technologies, data-driven approaches, and robust design principles to enhance dam safety and longevity were addressed. The advanced technologies include machine learning-based anomaly detection, numerical modeling using distributed fiber sensing, data augmentation scheme for predictive maintenance (PdM), and long-term monitoring of dams by NDT such as ultrasonic velocity. Guidelines for assessing erosion risk with a 7-step methodology based on the concept of erosion path, shear strength reduction (SSR) method, and hydraulic modelling combined with turbulence-based design method, were also addressed, respectively.

4.3. REHABILITATION AND SAFETY ENHANCEMENT OF AGING DAMS

As dams age, they would experience deterioration that may compromise their safety, efficiency, and functionality. Thus, rehabilitation activities of dams include strengthening dam's structure, improving spillway capacity, controlling leakage, upgrading monitoring systems, stabilizing foundation, and dam lifting are needed. Seven reports contributed to this theme, and they covered a wide range of rehabilitation activities for aging dams. The oldest rehabilitated dam is a masonry dam 120 years old (**R50**), the oldest concrete dams are 100 years old (**R7**, **R15**), and the oldest asphalt lining dam is 65 years old (**R27**).

Report **R50** introduced an ongoing reconstruction project of the Harcov masonry dam in Czech Republic, which was built between 1902 and 1904 primarily to control flood flows and is now a cultural-historical heritage. After a century of operation, the dam faces the need to upgrade its spillway capacity to meet modern standards, ensuring the 10,000-years-flood wave safely passing over. The reconstruction work includes increasing the spillway capacity, modifying the stepped overflow channel, and reinforcing the foundation of the dam to address long-term ground uplift issues. The main part of the Harcov masonry dam will be mostly preserved in its original state. New technological equipment will be installed including automatic monitoring of water management and dam surveillance. This reconstruction project will be a good demonstration of balancing preservation of historical heritage with modern demands.

Report **R23** provides a detailed plan for the refurbishment of the spillway of the Kpong Dam, which was running for 40 years old and located on the Volta River in Ghana. In addition to common aging factors such as aging equipment, corrosion, the presence of alkali aggregate reaction (AAR) in concrete is the leading factor that adversely affected the operation of the spillway. A multi-faceted approach involved a site condition assessment of the gates and infrastructure is taken. To deal with AAR, the so-called cancer of concrete structures, a convergence meter system comprising six 12 m long convergence meters were installed in the Kpong powerhouse to enable the monitoring of concrete swelling. Spillway concrete assessment including, 1) pier crack mapping, 2) analysis of the levels of the 21 survey monuments, and 3) concrete core sampling and laboratory analysis were carried out. Extensive additional repairs such as sealing all the cracks in the spillway concrete and associated equipment are required to ensure future reliable gate operations. Although a thorough and systematic approach are going to be carried out, the longevity of gated spillways still remains uncertain because of the complexity in controlling the AAR residual expansion.

Report **R7** provides a comprehensive condition assessment for concrete cores from 100-year-old Mühleberg Hydropower Plant (HPP) in Switzerland. The main structure of the HPP, including a 20m high gravity dam and the powerhouse, was built with high slump "poured concrete". However, the exact mixing proportion

could not be revealed because of the missing technical documents. Two condition assessments on drilled concrete core samples were carried out in 1980 and 2015, respectively, and the compression strength and elastic modulus remain at a good level with no obvious signs of degradation. However, microscopic examinations of thin sections revealed indications of two ageing phenomena, AAR and leaching. Even though a historical AAR could clearly be detected across the entire concrete water retaining structure, no significant structural damage due to an AAR was found. The reason that AAR subsided after a certain time is due to the relatively low cement content in the concrete and possibly a lower alkali content in the cement. It was therefore concluded that the potential for this reaction must be taken into account in any future refurbishment and retrofit measures.

From reports **R23** and **R7** it is clear that AAR is still the dominant factor affecting the structural integrity and the service life of concrete dams. For those dams built with alkali-active aggregates, extensive measures have to be taken to reduce the adverse effects. Also, we can conclude that methods to determine water-cement ratio by concrete cores for those very old concrete dam without any technical data are needed for the condition assessment and service life prediction.

Report **R15** provides a detailed re-evaluation of the effects of rehabilitation works carried out 30 years ago to control the upstream leakage in Ceresole Reale Dam in Italy, a concrete gravity dam built in 1927-1930. The rehabilitation project performed in 1990s involved installing a flexible exposed geomembrane system, new reinforced concrete blocks, and adding new drainage systems and grouting curtains. After more than thirty years of operation, monitoring data shows that despite of some expected partial decay of the exposed geomembrane, the overall watertightness and structural performance of the Ceresole Reale Dam remained excellent, ensuring its operation in completely safe conditions.

Report **R27** describes the refurbishment project of Rosswiese reservoir in Austria, which was built in 1958 with an asphalt surface lining. After 65 years of operation, the asphalt lining had to be renewed together with the removal of the sediments in the reservoir and an upgrade of the drainage system. Challenges come from the limited space on site for the machinery and the short time slot due to the economic importance of the dam.

Due to the increase in extreme weather events caused by climate change, existing dams face the need to enhance their flood control capability. Dam-lifting is an effective means of increasing the capability. Report **R12** investigated the feasibility of lifting 70-year-old Shin-Katsurazawa Dam in Niigata City, Japan. The dam will be raised from a height of 63.6m to 75.5m, and the water storage capacity will increase from 92 million m³ to 147 million m³. Firstly, the mechanical properties of the old dam's concrete were determined through core sample testing, providing data support for further design. Secondly, based on the changes in reservoir water levels throughout the year, an optimized construction plan was proposed to minimize stress during high-elevation concrete pouring when the water level is low. Finally,

through actual construction records and simulation analysis, the effectiveness of the proposed construction plan was verified, concluding that maintaining minimum water levels during dam-lifting work can effectively reduce stress generated by water level changes and ensure structural safety.

Report **R16** explored and recommended methods for reinforcing existing concrete dams using passive anchors. After a state-of-the-art literature review of the passive anchor, the authors proposed an innovative method that accounts for the dilatancy and confinement effects. After several benchmarks the main elements concerning French draft guidelines relating to the use of passive anchors to reinforce existing concrete dams are described, namely: corrosion protection of the anchors, monitoring and surveillance of dams reinforced by passive anchors. Although there is still much work to do, the results of this study may be adopted by other interested committees or international committees to further advance relevant regulations and technical development in the field.

To conclude this section, global case studies of rehabilitation activities for aging dams, including upgrading dams while preserving historical and environmental values, spillway refurbishment considering the presence of AAR, leakage control by geomembrane, dam lifting to adapt to climate change, long term monitoring by NDT such as ultrasonic velocity, dam reinforcing using passive anchors are addressed. The dams, whose ages are from 40 to 120 years old, are representative and the experiences are of great significance for references for the other dams in the world.

5. SPECIAL CASE FOR SMALL DAMS AND LEVEES

In recent years, ICOLD and many national committees, including the CFBR (French Committee on Dams and Reservoirs) have paid more and more attention to small dams and levees, because of their equal importance with large dams and levees in terms of the social utility and the risks they pose. An in-depth discuss was done at the Vienna Congress in 2018 under Q103 "Small Dams and Levees".

Three reports contributed to this theme, addressing the design, maintenance and safety analysis for small dams and levees.

Report **R17** discusses the design, construction, operation, and governance of small dams and flood control levees in France, highlighting their similarities and differences as well as the challenges they face. While both types of water management infrastructure share basic hydraulic functions such as holding and managing water levels, there are significant differences in their approach due to the varying emphasis placed on environmental impact. For instance, flood control levees prioritize protecting specific areas from flooding, while small dams may focus more on agricultural

irrigation or hydroelectricity generation. The report delves into the design principles, common issues, and solutions for small dams, as well as the construction standards, risk management, and engineering details for flood control levees.

Report **R19** introduced a levee renovation project in the village of Well near the province of Limburg, the Netherlands, to meet future climate challenges. An adaptive, fit for future design approach is proposed and applied in Project Well. In the new design procedure, it is no longer a pre-decided levee geometry which dictates the required fill properties, but rather the available fill properties which determine the levee geometry (Fig. 9). Project Well became one of the most sustainable levee improvement projects in the Netherlands, demonstrating how to ensure safety while balancing the eco-environmental values, economy, the historical context of the area and the water management.



Fig. 9
Main steps of traditional and alternative design approach
Principales étapes de l'approche traditionnelle et alternative de la conception

Report **R18** from the Netherlands proposed a safety assessment method for small levees with beaver burrowing during high-water events. An improved agent-based model (ABM) to simulate the behavior of beavers was developed, considering multiple factors such as wind speed, temperature, precipitation, flood duration, age, experience, and individual effects of beavers. By comparing the model's predictions with field observations, it was found that the model effectively predicts the location of beaver burrows but is currently insensitive to hydro-meteorological conditions. To further validate the model, more comprehensive data, especially on beaver behavior and levee's locations should be collected to improve its accuracy. After all it provides a new methodological tool for understanding and managing risks caused by beaver activity on levees.

To conclude this section, similarities and differences are addressed in the design, construction and operation stages between small dams and levees. Adequate attention should be paid to small dams and levees to make them fit for the future so that we can continuously enjoy their benefits.

6. INCREASINGLY DIFFICULT SITES - DAMS AND THEIR NEW CHALLENGES

Dams are still in great need for water management, power generation, and so on. However, many of the most suitable sites for dam construction, where a good balance between engineering feasibility, economic benefits, and environmental impact could be found, have already been developed. So, dams are likely to be built in increasingly difficult sites such as remote mountainous regions with complex geological conditions, high slope, high elevation, severe coldness, and earthquake, resulting of new challenges in dam building. Five reports introduced their experiences in overcoming challenges in ensuring dam safety during construction against landslides (**R1**), heavy local rainfall (**R6**), complex geological conditions (**R5**), and high environmental demands (**R30**, **R34**).

Report **R1** provides a successful experience in dealing with slope failure event during the construction of the Alto Tâmega dam, located on the Tâmega River, a right-bank tributary of the Douro River in the North of Portugal. The dam has a maximum height of 104.50 m and a concrete volume of about 223,000 m³, founded on a metamorphic rock mass mainly composed of mica schists, with a powerhouse located at the downstream toe. During rainy periods, a major landslide occurred on the right bank slope, immediately downstream of the dam's insertion surface, involving a rock volume of about 23,000 m³. The engineering measures include, 1) resurfacing of the insertion surface of four blocks of the dam; 2) construction of a new concrete structure to partially restore the geometry and the loading conditions of the rock mass existing before the landslide; 3) extension of the rock gallery under the affected zone, to survey the rock mass foundation in depth and promote waterproofing and drainage of the rock mass; 4) updating of the monitoring plan, including the definition of additional instrumentation to install in the new concrete structure, as well as adjustments to monitor the foundation area on the right bank. The construction works took place normally, following well-defined planning and strict safety control. The first filling of the reservoir occurred as planned. The dam has been in operation since February 2023, with very good performance.

Report **R5** provides an introduction of the design, construction, and monitoring of dam grouting gallery under complex geological conditions. Moglice Dam, located in southeastern Albania, is one of the highest rock-filled dams in the world, with an asphalt core and a height of 170m. During construction, because of the new geological revelations along the central and lower left abutment, and unfavourable geology with a rocky roof plunging up to 65 meters below the planned gallery, the gallery had to be revised. The design team succeeded in adapting the initially validated design while continually making the necessary improvements. Optimizations to the technical design were conditioned by discoveries made during the construction excavation process. The refined design and its implementation were recently verified by three and a half years of performance monitoring data in collaboration with the dam operator.

Report **R6** introduces the successful flood management during the construction of the Nam Theun 1 RCC dam in Laos, which is 187m high. The report provides detailed descriptions of the diversion channel schemes, and implementation steps for flood management plans. In the 2018, 2019, 2020 and 2021 rainy seasons the diversion tunnel reached its capacity and the cofferdams, and the main dam were overtopped and the floods passed safely through the construction site without causing unexpected damage to the dam and other structures.

Reports **R30** and **R34** focus on JX Hydropower Station built-in high-altitude region in China, where the elevation is over 3000 m, facing harsh terrain, tight schedule, and ancient walnut tree preservation. **R34** discusses the rapid construction techniques for a large-scale sand and gravel processing and concrete production system. Through optimization of the system layout and adoption of new technologies, the project was successfully constructed, including local protection measures for ancient walnut trees, interference management in the construction site, and construction techniques during low-temperature seasons. It also introduces innovative solutions like utilizing BIM technology for digital twin simulation, applying novel air dome structure materials for building large storage tanks, and developing intelligent systems suitable for high-altitude regions for concrete production. **R30** focuses on the design and construction techniques of a large semi-finished steel material storage tank for JX Hydropower Station. It was installed using the inverted method and effectively shortened the construction period and improved the efficiency.

To conclude, as high dams are going to be built in increasingly difficult sites, more and more experiences are being gathered in overcoming the new challenges such as complex geological challenges, extreme natural disasters, and severe environmental conditions and high environmental protection demands.

7. NEED FOR GLOBAL CAPACITY BUILDING

Only report **R8** contributed to this theme. It focused on the factors impacting transboundary projects and the solutions. After recalling the brief history of water related conflicts between countries, analyzing factors leading to conflict or cooperation, it advised to mitigate the conflicts by treaties and agreements. Collaborative resolution of disputes through treaties and agreements is essential to minimize the potential for conflicts over transboundary projects. In developing new ways to reduce the potential for conflict best practices must cover items such as dam safety and emergency management, regionally integrated risk, hazard, and vulnerability assessments that factor into the impacts on communities, infrastructure, and property. The assessment of environmental and cultural heritage assets, joint emergency management coordination, stakeholder engagement, and emergency

exercise practices should be integral to these best practices. Finally, the report calls for strengthening dam safety, enhancing emergency management measures and improving cooperation between neighboring countries to address conflicts linked to transboundary dams, where different legal, socioeconomic, cultural and institutional framework for dam safety need to coexist.

Accordingly, organizations such as the International Commission on Large Dams (ICOLD) and the World Bank Group as well as National Dam Safety Committees and regulatory authorities (local and national) need to play a role in the development and implementation of best practice guidance specifically tailored to the unique needs of transboundary dams including due recognition of the importance of dam safety and emergency management as well as clear and transparent communication with the public.

8. CONCLUSIONS

Fifty one reports from all over the world contributed to Question 109, "Dams and levees fit for the future". Although no clear definition has been given by ICOLD community on dams and levees fit for the future so far, we think their features can be characterized by "P-I-E-R-C-E-S", namely, Safety, Resilience, Intelligence, Eco-friendliness, Economy, Compliance, and Participation.

Safety is a top priority for dams and levees fit for the future. Dams and levees should be safe in their whole lifetime, including the design, construction, operation, maintenance, rehabilitation and decommission stages, involving efficient, robust and reliable technical and non-technical solutions. A great majority of the 51 reports are about safety of dams and levees, including foundation-sustainability, safety design for new dams and levees, safety ensuring techniques during construction, safety monitoring, safety status evaluation and safety enhancement by rehabilitation for aging ones.

For foundation sustainability, various techniques to control the seepage, enhance the bearing capacity and improve resistance to settlement and seismicity for dams on ultra-soft soil foundation, faulted rock foundation were addressed. Applications of cemented soil dam, cemented sand and gravel dam, and a composite dam combining a RCC dam and two asphalt concrete core rock-fill dams were introduced. A new type of cement, called expansive low heat Portland cement was developed in China and the dam concrete is highly cracking resistant, showing a great potential in thermal control for high concrete dams. Asphalt concrete based on acidic aggregates with anti-stripping additives was developed and applied in PSPP. Intelligent techniques or systems to improve dam safety and efficiency in the construction and monitoring stages were developed, playing a significant role in ensuring the safety of 300m high dams in China, including Lianghekou, Wudongde

and Baihetan dams. Intelligent technologies are going to be applied more widely in the near future.

Climate-resilience is also a distinctive feature for dams and levees fit for the future. They must be designed with adaptive, flexible approaches to respond to variability, unpredictability, extremity and uncertainty caused by climate change. Dams and levees need to be eco-friendly so that they can coexist harmoniously with the ecosystem and the nature during the whole lifetime. For dams to be built in increasingly difficult sites such as remote mountainous regions with complex geological conditions, heavy rainfall, high environmental demands, severe coldness, we already gathered successful experience in fighting against those challenges and they can be good reference for dams to be built in similar difficult sites.

Management of aging dams and levees requires a multidisciplinary approach combining engineering, environmental science, economics, and social policy. It also requires participation and collaboration with all the dam/levee shareholders. Although the numbers, types, ages, technical features and safety status of dams and levees are significantly different in various countries, some countries have already realized the importance of ensuring safety for the future and are taking integrated measures and making great progress.

ACKNOWLEDGEMENTS

I would like to sincerely thank Dr. Jean-Pierre Tournier and Mr. Danie Badenhorst for their valuable suggestions and great help in the analysis and summary of the reports.

REFERENCES

- [1] Cemented Soil Dams – ICOLD, Bulletin 195 (2022).
- [2] ACI PRC-207.1-21. Mass Concrete-Guide. ACI 2022.
- [3] ACI PRC223-21. Shrinkage-Compensating Concrete. ACI 2021.
- [4] DU, C. A review of Magnesium Oxide in concrete. *Concrete International*. 2005, 27: 45–50.

- [5] LI, W., FAN, Q., LI, X., *ET AL*. Development and application of specific low heat Portland cement for building ultra-high arch dams. *Journal of hydro-electric engineering*, 2017, 36(3): 113–120.
- [6] WANG, Z, YANG, B, XIA, S. Key technologies for the application of acidic aggregates in asphalt concrete anti-seepage facing. Proceedings of the annual meeting of the CFRD technical committee at China Hydraulic Society, 2023.
- [7] HARIRI-ARDEBILI, M.A., MAHDAVI G., NUSS, L., LALL, U. The role of artificial intelligence and digital technologies in dam engineering: Narrative review and outlook. *Engineering Applications of Artificial Intelligence*, 2023. Volume 126, Part A, 106813, ISSN 0952-1976.

COMMISSION INTERNATIONALE DES
GRANDS BARRAGES

VINGT-HUITIEME CONGRES DES
GRANDS BARRAGES
CHENGDU, Mai 2025

QUESTION 109

**DAMS AND LEVEES
FIT FOR THE FUTURE**

**DES BARRAGES ET DES DIGUES
PRÊTS POUR L'AVENIR**



Shuguang LI

*PhD, Ptofesseur-Ingénieur principal, China Three Gorges Corporation
Membre du comité technique de la CIGB sur l'exploitation, l'entretien et la
réhabilitation des barrages
Membre du comité technique CHINCOLD sur l'inspection, la réparation et
l'amélioration des structures hydrauliques*

CHINA/CHINE

RAPPORTEUR GÉNÉRAL

TABLE DES MATIERES

1.	INTRODUCTION	897
2.	RÉSUMÉ DES RAPPORTS REÇUS	897
3.	GESTION D'UN PORTEFEUILLE VIEILLISSANT DE BARRAGES EN TERMES D'EXPLOITATION, D'ENTRETIEN ET DE RÉHABILITATION	900
3.1.	CARACTÉRISTIQUES DES BARRAGES ET DES DIGUES ADAPTÉS À L'AVENIR	900
3.2.	STRATÉGIES DE GESTION DES BARRAGES ET DES DIGUES VIEILLISSANTS	901
4.	SÉCURITÉ PENDANT LA CONSTRUCTION ET LA RÉHABILITATION	903
4.1.	TECHNIQUES INNOVANTES DE CONSTRUCTION DE BARRAGES	903
4.1.1.	Nouvelles techniques de maintien des fondations	904
4.1.2.	Nouveaux types de barrages	906
4.1.3.	Innovations dans les matériaux de construction des barrages.	909
4.1.4.	Techniques intelligentes de construction de barrages	911
4.1.5.	Sécurité des barrages et hydraulique.	915
4.2.	SURVEILLANCE ET ANALYSE DE LA SÉCURITÉ DES BARRAGES VIEILLISSANTS	915
4.3.	RÉHABILITATION ET AMÉLIORATION DE LA SÉCURITÉ DES BARRAGES VIEILLISSANTS	918
5.	CAS PARTICULIER DES PETITS BARRAGES ET DES DIGUES	921
6.	DES SITES DE PLUS EN PLUS DIFFICILES - LES BARRAGES ET LEURS NOUVEAUX DÉFIS	923
7.	NÉCESSITÉ D'UN RENFORCEMENT DES CAPACITÉS AU NIVEAU MONDIAL	925
8.	CONCLUSIONS	926
	REMERCIEMENTS	927
	RÉFÉRENCES	927

1. INTRODUCTION

Ce rapport général pour la question 109, “Des barrages et des digues adaptés à l’avenir”, a été abordé comme une revue de l’état de l’art concernant les thèmes considérés, en se référant aux rapports reçus lorsque cela s’avérait nécessaire

Les barrages et les digues sont des infrastructures importantes pour la société. Ils permettent notamment de lutter contre les inondations, de produire de l’énergie, de fournir de l’eau, de réguler le débit des cours d’eau et d’assurer la navigation. Alors que nous entrons dans le deuxième quart du 21^e siècle, le changement climatique mondial, l’urbanisation et le développement durable imposent des exigences plus élevées aux barrages et aux digues. Nous devons réagir et faire en sorte que les barrages et les levées soient adaptés à l’avenir, et c’est la raison pour laquelle nous avons posé cette question lors du Congrès 2025 de la CIGB. Les scientifiques et les ingénieurs de la communauté de la CIGB doivent faire de leur mieux pour assurer la sécurité des barrages et des digues, qu’ils soient en cours de construction ou vieillissants, afin que nous puissions profiter de leurs avantages à long terme

Les rapports des deux derniers congrès se sont déjà concentrés sur des thèmes similaires, tels que la Q103, “Petits barrages et digues” et la sous-question “impacts du changement climatique sur les besoins et la conception des barrages, réservoirs et digues” de la Q107, “Barrages et changement climatique”.

2. RÉSUMÉ DES RAPPORTS REÇUS

En ce qui concerne les contributions pour Q.109, un total de 51 rapports a été reçu, provenant de 20 pays appartenant aux cinq continents. La Chine et la France ont soumis respectivement 20 et 6 rapports, ce qui représente 50% du total.

Tableau 1
Rapports de différents pays

PAYS	NOMBRE DE RAPPORTS	RAPPORTS
France	6	R10,R16,R17,R20,R21,R25*
Portugal	1	R1
Suède	3	R2,R3,R4
Suisse	3	R5,R6*,R7

(Continued)

Tableau 1
Continued

PAYS	NOMBRE DE RAPPORTS	RAPPORTS
Norvège	1	R11*
Autriche	2	R11*,R27
Italie	1	R15
Pays-Bas	2	R18,R19
Royaume-Uni	1	R22
Roumanie	1	R26
Pologne	1	R48
République tchèque	1	R50
Canada	3	R8, R9, R28
Ghana	1	R23*
Afrique du Sud	2	R23*,R24
Malawi	1	R25*
Nouvelle-Zélande	1	R25*
Japon	3	R12, R13, R14
Inde	1	R51
Thaïlande	1	R6*
Chine	20	R29~R47,R49

* Rapports dont les auteurs proviennent de plus d'un pays.

Tableau 2
Rapports de différents continents

CONTINENT	NOMBRE DE RAPPORTS	PAYS
Asie	25	4
L'Europe	22	12
Afrique	3	3
Amérique	3	1
Océanie	1	1
Total	51**	

** Certains rapports sont rédigés par des auteurs de différents continents.

Le tableau 2 ci-dessous résume la répartition des rapports par continent, montrant que l'Asie et l'Europe ont contribué à 90 % du total.

Les thèmes de la Q109, Barrages et digues adaptés à l'avenir, sont énumérés ci-dessous :

1. Gestion d'un portefeuille vieillissant de barrages en termes d'exploitation, d'entretien et de réhabilitation, y compris des approches fondées sur les risques,
2. Sécurité pendant la construction et la réhabilitation,
3. Cas particulier des petits barrages et des digues,
4. Impact de nouvelles pratiques contractuelles sur la sécurité des barrages (par exemple, participation du secteur privé, contrats EPC),
5. Des sites de plus en plus difficiles - les barrages et leurs nouveaux défis,
6. Nécessité d'un renforcement des capacités au niveau mondial.

Le tableau 3 résume les rapports soumis aux thèmes de la Q109, y compris le nombre de rapports.

Tableau 3
Nombre de rapports contribuant à chaque thème de la question 109

SECTION	THÈME	NOMBRE DE RAP-PORTS	CHIFFRES DU RAPPORT
3. Gestion d'un portefeuille vieillissant de barrages en termes d'exploitation, d'entretien et de réhabilitation	1	10	R2,R9,R13,R20,R22,R26, R28,R44, R48,R51
4. Sécurité pendant la construction et la réhabilitation	2	35	R1,R3,R4,R7,R8,R10~ R16,R18, R23~ R25,R27,R29, R31~ R33, R35~ R43, R45~ R47,R49,R50
5. Cas particulier des petits barrages et des digues	3	3	R17, R19, R21
6. Des sites de plus en plus difficiles - les barrages et leurs nouveaux défis	5	5	R1,R5,R6, R30, R34
7. Nécessité d'un renforcement mondial des moyens propres	6	1	R8

Le tableau 3 montre que la majorité des rapports se concentrent sur les thèmes 1 et 2, tandis que seuls quelques rapports contribuent aux thèmes 3, 5 et 6. Aucun rapport ne contribue spécifiquement au thème 4.

3. GESTION D'UN PORTEFEUILLE DE BARRAGES VIEILLISSANTS EN TERMES D'EXPLOITATION, D'ENTRETIEN ET DE RÉHABILITATION

3.1. CARACTÉRISTIQUES DES BARRAGES ET DES DIGUES ADAPTÉS À L'AVENIR

Bien qu'aucune définition claire n'ait été donnée par la communauté de la CIGB sur les barrages et les digues adaptés à l'avenir jusqu'à présent, après avoir examiné tous les rapports soumis pour la Q109, les barrages et les digues adaptés à l'avenir peuvent être caractérisés par "P-I-E-R-C-E-S", qui est une combinaison des initiales de sept mots, à savoir, Sécurité, Résilience, Intelligence, Convivialité écologique, Economie, Conformité et Participation.

- (1) **Sécurité.** Les barrages et les digues adaptés à l'avenir doivent être sûrs, ce qui est une priorité absolue. Les barrages et les digues doivent être sûrs tout au long de leur cycle de vie, y compris aux stades de la conception, de la construction, de l'exploitation, de l'entretien, de la réhabilitation et du démantèlement, en faisant appel à des solutions techniques et non techniques efficaces, robustes et fiables.
- (2) **Résilience.** Les barrages et les digues adaptés à l'avenir doivent être des infrastructures résistantes au climat. Les barrages et les digues doivent être conçus selon des approches adaptatives et flexibles permettant à ces structures de répondre de manière dynamique à la variabilité du climat, et doivent donner la priorité aux matériaux, aux méthodes de construction et aux systèmes de surveillance qui résistent à une gamme plus large d'extrêmes climatiques, tels que les fortes pluies extrêmes et les sécheresses prolongées
- (3) **Intelligence.** Les barrages et les digues adaptés à l'avenir doivent être intelligents, ce qui signifie qu'ils pourraient intégrer des technologies et des systèmes de pointe et intelligents pour améliorer leur sécurité, leur résilience et leur efficacité opérationnelle. À l'avenir, les barrages et les digues pourraient être exposés à des installations qui détectent, pensent, prennent des décisions et réagissent comme des humains équipés de techniques intelligentes, telles que différents capteurs basés sur l'IdO, des algorithmes d'apprentissage automatique, un système de prise de décision basé sur l'IA, des drones et la robotique.
- (4) **Respect de l'environnement.** Les barrages et les digues adaptés à l'avenir doivent être écologiques et respectueux de l'environnement et répondre aux exigences environnementales à long terme. Ils devraient comporter des éléments tels que des échelles à poissons, des îles flottantes pour prévenir l'eutrophisation, et des systèmes flottants de collecte des déchets améliorant la connectivité écologique et la qualité de l'eau. Un débit écologique adéquat devrait être assuré pour soutenir les écosystèmes aquatiques et s'aligner sur les objectifs de durabilité environnementale.
- (5) **Économie.** Les barrages et les digues adaptés à l'avenir doivent être économiques. La planification financière et l'analyse coûts-avantages

- doivent être menées tout au long de leur cycle de vie. L'équilibre entre les coûts, la sécurité et la fonction doit être établi non seulement au stade de la conception ou de l'entretien, mais pendant toute la durée de vie de l'ouvrage.
- (6) **Conformité.** Les barrages et les digues adaptés à l'avenir doivent être conformes aux cadres réglementaires. En outre, ils doivent répondre à des normes de sécurité strictes, non seulement pour les conditions actuelles, mais aussi pour les défis futurs anticipés, tels que le changement climatique et les événements météorologiques extrêmes.
 - (7) **Participation.** Les barrages et les digues adaptés à l'avenir doivent impliquer toutes les parties prenantes, y compris les agences gouvernementales, les banques et les investisseurs, les propriétaires, les exploitants, les experts, les chercheurs, les communautés locales, les médias et le public. L'engagement efficace des parties prenantes est crucial pour la réussite des barrages et des digues, car il garantit que la plupart des points de vue sont pris en compte et déjà mis en œuvre. Les conflits nationaux ou internationaux potentiels doivent également être pris en compte.

3.2. GÉRER LES STRATÉGIES DE VIEILLISSEMENT DES BARRAGES ET DES DIGUES

Dix rapports ont contribué à ce thème et les auteurs des pays européens, américains et asiatiques ont présenté leurs réflexions et suggestions sur la gestion des barrages vieillissants en termes d'exploitation, d'entretien et de réhabilitation.

Sur la base d'inondations récentes en Europe et de plusieurs études de cas portant sur la modernisation de barrages en terre vieux de 50 ans, le rapport **R26** de la Roumanie a fourni un cadre pour assurer l'avenir des barrages, y compris des stratégies de gestion durable de l'eau, de modernisation technologique et de résilience climatique dans le contexte de la remise en état des barrages. Le rapport R48 de la Pologne a proposé des solutions systémiques et techniques clés pour atténuer les risques croissants de défaillance des barrages et des digues vieillissants en raison du changement climatique. Le rapport **R2** présente une mission gouvernementale achevée en 2023 sur l'impact du changement climatique sur la sécurité des barrages en Suède et explique les applications dans six aspects de la stratégie nationale d'adaptation au climat pour la sécurité des barrages. Le rapport **R22** du Royaume-Uni donne un aperçu de l'évolution historique des barrages en puddle clay, qui représentent plus de 60 % des réservoirs britanniques, et présente les défis à relever en matière d'évaluation des risques et d'amélioration significative de la conception et de l'entretien. Le rapport **R51** a examiné les défis auxquels l'Inde est confrontée dans la gestion de 6 138 grands barrages, dont beaucoup ont plus de 25 ans. Il présente plusieurs suggestions pour améliorer la sécurité des barrages vieillissants, notamment la surveillance de l'état de santé par la technologie, l'adaptation aux nouvelles normes et aux développements technologiques, le renforcement des capacités institutionnelles et l'évaluation des risques.

Bien que le nombre, le type, l'âge, les caractéristiques techniques et l'état de sécurité des barrages et des digues, présentés dans les rapports susmentionnés, diffèrent considérablement d'un pays à l'autre, certains gouvernements sont conscients de l'importance d'assurer la sécurité pour l'avenir et s'efforcent d'atteindre cet objectif. La gestion des barrages et des digues vieillissants nécessite une approche multidisciplinaire combinant l'ingénierie, la science de l'environnement, l'économie et la politique sociale, mais aussi la participation de tous les actionnaires des barrages et des digues. Les études de cas relatives aux ruptures de barrages montrent que les barrages en remblai sont plus vulnérables au changement climatique. La surveillance de la sécurité des barrages en remblai et des digues à petite échelle doit être renforcée et considérée comme une préoccupation majeure pour les propriétaires ou les exploitants.

Au fur et à mesure que les barrages vieillissent, leur intégrité structurelle peut se détériorer, augmentant ainsi le risque de défaillance. Il est donc essentiel d'adopter des approches basées sur le risque pour garantir la sécurité et l'efficacité de l'exploitation, de la maintenance et de la réhabilitation. Le rapport **R20** a introduit l'évaluation du risque de révision de la sécurité (SaRRA) pour les grands barrages en France, qui a été mise en œuvre en 2007. À ce jour, environ 650 projets SaRRA ont été menés à bien, ce qui en fait une composante essentielle des systèmes de gestion et de prévention des risques. Les résultats ou la base de données sont très instructifs pour tous les acteurs du secteur des barrages, non seulement en France mais aussi dans le monde entier. **R9** a montré les résultats d'une évaluation quantitative des risques (EQR) réalisée pour un mode de défaillance potentiel (MDP) préoccupant au barrage de Waterton, situé dans le sud de l'Alberta, au Canada. Elle a démontré que l'évaluation quantitative des risques peut apporter une compréhension plus approfondie des principaux modes de défaillance potentiels, permettant des mesures d'intervention proactives, informant la conception des instruments et les mesures de surveillance pour améliorer la sécurité du barrage. Cependant, de nos jours, le processus d'évaluation quantitative des risques peut être coûteux, long et onéreux, et le compromis consiste à faire appel au jugement des ingénieurs.

Ces dernières années, les chercheurs se sont concentrés non seulement sur la sécurité du barrage, mais aussi sur celle des réservoirs en cascade et sur l'influence du barrage sur l'écologie et l'environnement. Le rapport **R44** examine les défis en matière de sécurité et les considérations opérationnelles auxquels sont confrontés les barrages-réservoirs en cascade en Chine. Il propose cinq suggestions pour améliorer le niveau général de sécurité des barrages à réservoirs en cascade, telles que l'établissement d'un système intelligent de gestion de la sécurité des barrages, l'amélioration de la sécurité technique et le niveau de gestion des urgences des groupes de barrages. **R13**, du Japon, a présenté une série de mesures visant à atténuer la turbidité à long terme en aval du barrage de Hitotsuse, construit il y a plus de 60 ans. Une série de mesures d'atténuation de la turbidité ont

été prises et leur efficacité a été vérifiée, ce qui a permis de réduire les effets néfastes des barrages sur l'environnement et l'écologie.

Avec le développement des techniques intelligentes, l'intelligence artificielle (IA) est de plus en plus utilisée. Le rapport **R28** du Canada donne un aperçu du développement de l'IA générative (GenAI) et présente en détail comment la GenAI peut être appliquée au domaine de l'examen de la sécurité des barrages (DRS), y compris l'examen des données et des dossiers, l'inspection des sites, la classification des barrages, l'analyse des modes de défaillance, l'analyse de la sécurité des barrages, l'exploitation des barrages, l'entretien et la surveillance

Pour résumer les rapports susmentionnés sur ce thème, bien que la construction ou la modernisation de barrages et de digues vieillissants en barrages et digues adaptés à l'avenir et caractérisés par le "P-I-E-R-C-E-S" reste un grand défi, plusieurs pays adoptent déjà des stratégies de gestion à multiples facettes, des mesures intelligentes et de pointe et réalisent des progrès importants pour rendre les barrages et les digues sûrs pendant toute leur durée de vie, résistants au changement climatique, conviviaux et harmonieux pour l'écologie et économiquement viables au cours de leur cycle de vie.

4. SÉCURITÉ PENDANT LA CONSTRUCTION ET LA RÉHABILITATION

Comme indiqué dans la section 3, la sécurité est la priorité absolue pour les barrages tout au long de leur cycle de vie. Près de 40 des 51 rapports présentent les derniers progrès réalisés en matière de sécurité des barrages, contribuant ainsi au thème 2, Sécurité pendant la construction et la réhabilitation. Ils sont résumés en trois sous-thèmes : 1) Techniques innovantes de construction des barrages, 2) Progrès dans la surveillance et l'analyse de la sécurité des barrages existants et 3) Progrès dans la réhabilitation et l'amélioration de la sécurité des barrages vieillissants.

4.1. TECHNIQUES INNOVANTES DE CONSTRUCTION DE BARRAGES

Vingt-deux rapports contribuent à ce thème. Ils offrent un panorama des dernières innovations mondiales en matière d'ingénierie des barrages, y compris les nouvelles techniques de soutien des fondations, l'application de nouveaux types de barrages, les nouveaux matériaux de construction des barrages et les technologies de construction intelligentes. Il convient de noter que seize des rapports proviennent de Chine. Cela s'explique par le fait que la Chine possède le plus grand nombre de

barrages et de réservoirs au monde et qu'elle a récemment entrepris la construction d'un barrage de 300 mètres de haut de classe mondiale.

4.1.1. *Nouvelles techniques de maintien des fondations*

Pour construire un barrage adapté à l'avenir, il est nécessaire et crucial de disposer d'une fondation durable capable de soutenir le barrage tout au long de son cycle de vie. La fondation durable d'un barrage se réfère ici à une fondation qui présente une stabilité structurelle, une durabilité, une compatibilité environnementale et une viabilité économique. Quels que soient les types de barrages, les principales exigences d'une fondation durable sont les suivantes : capacité portante adéquate, résistance au tassement, résistance aux tremblements de terre, compatibilité géologique, drainage, imperméabilité et durabilité

Sept rapports contribuent à ce sous-thème et quatre d'entre eux portent sur les techniques de maintien des fondations pour les barrages en remblai sur des fondations en sol meuble et des couches de mort-terrain profondes (**R38**, **R41**, **R42** et **R43**), tandis que les trois autres concernent les barrages en remblai dur ou les barrages en béton sur des fondations rocheuses présentant des failles importantes (**R24**, **R45** et **R49**).

Le rapport **R38** comprend des études complètes sur les expériences de construction de barrages sur des fondations en sol meuble en Chine. L'évaluation de la stabilité du barrage et la projection de son comportement de déformation dépendent fortement des paramètres physiques et mécaniques inhérents au sol meuble. Il est suggéré que pour évaluer l'étanchéité des fondations du barrage, la limite supérieure du coefficient de perméabilité obtenue à partir d'essais en laboratoire ou d'essais de pompage pourrait être adoptée. Pour les analyses de stabilité des pentes et les calculs de l'excès de pression de l'eau interstitielle, nous pouvons utiliser la limite inférieure du coefficient de perméabilité obtenu à partir d'essais en laboratoire ou de résultats d'essais de pression latérale, d'essais CPTU et d'essais de consolidation.

Les rapports **R42** et **R43** présentent l'étude et la conception du traitement des fondations d'un barrage en enrochement à noyau d'argile au Rwanda, d'une hauteur maximale de 59 m. Les fondations profondes du barrage sont constituées d'une épaisseur de 40 m de sol lacustre tourbeux et limoneux ultra-doux à l'état liquide à plastique. Après une analyse fine, des colonnes de pierre de vibro-remplacement sont utilisées pour renforcer la fondation du sol mou et la géomembrane pour étendre le diamètre d'infiltration au bas de la paroi du noyau. Les détectations et les tests effectués sur les colonnes de pierre indiquent qu'elles fonctionnent bien et qu'elles répondent aux exigences de conception.

Le rapport **R41** présente l'expérience et les leçons tirées d'un projet d'injection dans les fondations sous une couche de couverture profonde dans un barrage en

enrochement à noyau d'argile dans le sud-ouest de la Chine, d'une hauteur de 110 mètres. La profondeur des morts-terrains de la fondation du barrage est de 149 m, un mur de séparation d'une profondeur de 85 m combiné à 4 rangées de travaux d'injection dans les morts-terrains de 60 m sous le mur de séparation ont été conçus et réalisés, ce qui s'est avéré être un succès jusqu'à présent. Cependant, les travaux d'injection de renforcement ont pris 10 ans et ont coûté cher, ce qui démontre que le contrôle des infiltrations dans les fondations du barrage est la ligne de vie du barrage et qu'il faut lui accorder autant d'attention que possible lors des phases de conception et de construction.

Le rapport **R24** traite des défis géologiques rencontrés lors de la construction de deux barrages en remblai dur d'une hauteur d'environ 40 m et de leurs solutions. Les deux barrages d'Afrique du Sud reposent tous deux sur des fondations rocheuses présentant de nombreuses failles affectant la sécurité des barrages. Des coulis de consolidation et des clés de cisaillement ont été utilisés et la stabilité globale du barrage a été améliorée. Le rapport **R45** traite de la conception du traitement des fondations de la centrale hydroélectrique de Batang Toru, située dans une zone sismique élevée en Indonésie, dans le but d'améliorer sa stabilité et sa capacité à lutter contre les infiltrations. Le barrage est un barrage-poids en forme d'arc d'une hauteur maximale de 74 m situé sur du tuf. Les défis à relever sont la faiblesse de la fondation rocheuse, la densité élevée des fractures et la faible capacité portante. L'optimisation des schémas de forage et l'application de techniques d'injection en rideau, d'injection de consolidation et d'injection de contact ont été utilisées pour résoudre ces problèmes.

Le rapport **R49** traite de l'utilisation de l'algorithme DBSCAN (Density-Based Spatial Clustering of Applications with Noise) pour identifier les masses rocheuses fracturées à l'aide de données de forage. Il pourrait fournir une méthode automatisée et impartiale pour la détection des masses rocheuses fracturées et a donc un bon potentiel d'application dans l'ingénierie géotechnique pour tous les types de barrages.

En résumé, les sept rapports susmentionnés ont partagé leurs expériences de défis à relever pour assurer des fondations durables dans des conditions géologiques variées. Des murs de séparation et une injection extensive pour contrôler l'infiltration pour un barrage en enrochement à noyau d'argile de 110 m de haut avec une couche de couverture de 149 m de profondeur, des colonnes de pierre de vibro-remplacement et une géomembrane pour renforcer les fondations en sol ultra-doux épais et contrôler l'infiltration, des techniques d'injection pour améliorer la résistance sismique, des clés de cisaillement pour améliorer la stabilité des fondations en roche fissurée, sont présentés. Les principes de sélection des paramètres physiques et mécaniques pour les fondations en sol mou, ainsi que les algorithmes DBSCAN pour identifier de manière impartiale les masses rocheuses fracturées sont également abordés. Toutes les études de cas ou expériences mentionnées ci-dessus constituent une référence utile et précieuse pour les projets de barrage présentant des conditions géologiques similaires.

4.1.2. *Nouveaux types de barrages*

Les types de barrages traditionnels, bien qu'efficaces dans de nombreux cas, ne permettent pas toujours de relever le défi de la construction de barrages adaptés à l'avenir. De nouveaux types de barrages, qui offrent des solutions innovantes et meilleures dans au moins un aspect des caractéristiques "P-I-E-R-C-E-S", sont nécessaires et essentiels pour construire des barrages adaptés à l'avenir. Trois rapports traitent des applications des barrages en terre cimentée (**R25**), des barrages en sable et gravier cimentés (**R35**) et des barrages composites (**R31**).

A. Barrage en terre cimentée et barrage en sable et gravier cimenté

Selon le Bulletin 195 ^[1], les barrages en matériaux cimentés (CMD) sont définis comme une série de nouveaux types de barrages utilisant un liant cimentaire avec divers matériaux naturels ou manufacturés dans la construction du barrage. Les barrages en matériaux cimentés présentent des avantages techniques, notamment la construction de barrages sûrs, rapides et parfois économiques, dans le respect de l'environnement, et la réduction du risque de rupture par débordement. Les barrages en béton armé comprennent les barrages en terre cimentée (CSD), les barrages en sable et gravier cimentés (CSGD), les barrages en béton armé (RFCD) et les barrages symétriques en remblai dur (FSHD). Les rapports **R25** et **R35** présentent des applications des barrages en sable cimenté et en gravier cimenté, respectivement.

Un barrage CSD utilise de la terre mélangée à du ciment et d'autres matériaux cimentaires comme matériaux de construction de barrages. Le rapport **R25** décrit le processus de construction d'un batardeau utilisant la technologie du sol cimenté au barrage de Kapichira au Malawi. La hauteur maximale du barrage est de 14 m et la largeur de la crête est de 6 m avec un rapport de pente symétrique en amont et en aval de 1:1,5. Le rapport présente en détail la conception, la préparation du sable, du ciment et du sol, les essais en laboratoire sur le site, les essais en grandeur réelle et le processus de construction (voir Fig. 1, Fig. 2). La technologie du sol cimenté permet de répondre rapidement et efficacement à l'urgence et de jeter les bases d'un travail de restauration complet ultérieur ; elle a un grand potentiel d'application dans les structures hydrauliques.

Le rapport **R35** traite d'une nouvelle méthode de conception dynamique des proportions pour le CSGD, visant à résoudre des problèmes tels que les grandes différences de résistance et la faible rentabilité de la conception traditionnelle des mélanges de CSG. Grâce à des expériences de simulation en salle, la relation entre la résistance du sable et du gravier cimentés et la combinaison du ratio de sable et de la marge de pâte a été déterminée, et une nouvelle méthode de conception dynamique des proportions a été proposée sur la base de l'optimisation de la combinaison de ces deux facteurs. Enfin, cette méthode a été appliquée avec succès dans la zone d'amélioration du module de la pile de la pointe d'un projet hydroélectrique, et son efficacité et sa faisabilité ont été vérifiées par les résultats de l'ingénierie pratique.



Fig. 1

Séquence de construction de CSD au barrage de Kapichira au Malawi

1. Épandage de ciment
2. Humidification et malaxage
3. Matériau malaxé
4. Chargement
5. Nettoyage de la surface
6. Epandage et approvisionnement
7. Approvisionnement et régalage
8. Compactage



Fig. 2

Vue d'ensemble de la mise en place d'un sol cimenté au barrage de Kapichira au Malawi

B. Barrage composite

Un barrage composite est un type de barrage qui combine deux ou plusieurs matériaux ou types de structure différents afin de tirer parti des avantages de chacun, optimisant ainsi les performances, la stabilité et la rentabilité du barrage. Les barrages composites sont souvent utilisés dans des situations où un seul type de construction de barrage ne convient pas en raison de contraintes géologiques, environnementales ou économiques. Une conception, une construction et un entretien appropriés sont essentiels pour garantir leur performance à long terme.

Le rapport **R31** traite de la construction d'un barrage composite dans le cadre du projet de centrale hydroélectrique de Zungeru au Nigeria, qui se compose d'un barrage en béton compacté au rouleau (RCC) et de deux barrages en enrochement à noyau de béton bitumineux. La hauteur du joint du barrage est de 85 mètres, ce qui est plus important que la plupart des joints de barrage. La conception et la construction du joint de ces deux barrages (Fig. 3) jouent un rôle crucial pour assurer la sécurité du barrage. Le rapport décrit la technologie de construction et la surveillance du joint, y compris le traitement de surface du béton de ciment, l'installation d'arrêts d'eau, la construction de la section du joint du barrage en béton armé, la construction du noyau en béton bitumineux, la construction du matériau de transition et la surveillance de la pression du joint, du déplacement et de la pression osmotique. Le rapport conclut que la qualité de la conception et de la construction des joints affecte directement la qualité et la sécurité de l'ensemble du barrage, et que le barrage de Zungeru offre une perspective de développement plus large pour l'application de types similaires de barrages composites à l'avenir.

de refroidissement et de rétrécissement du béton des barrages, ce type de béton ne peut pas être utilisé dans les barrages. Le béton de compensation du retrait à base d'oxyde de magnésium (béton MgO), fabriqué avec de la poudre de MgO légèrement brûlée (comme additif), a été appliqué dans environ 30 petits barrages en béton en Chine ^[4] et les résultats en matière de minimisation des fissures thermiques et de simplification des mesures de contrôle de la température sont significatifs. La raison en est que l'expansion du MgO après l'hydratation correspond étroitement au processus de rétrécissement du béton du barrage lorsqu'il se refroidit. Cependant, en raison des difficultés à distribuer uniformément la poudre de MgO dans le béton du barrage et des craintes qu'une distribution inégale de MgO ne provoque une expansion inégale entraînant des fissures, le béton de MgO n'a pas été appliqué jusqu'à présent dans les barrages de plus de 100 m de haut.

Par conséquent, un nouveau type de ciment Portland à basse température, à base de MgO et expansif dans la déformation volumique autogène, a été inventé en Chine pour améliorer la résistance à la fissuration du béton des barrages en ajustant simultanément ses propriétés thermiques et ses propriétés de déformation ^[5]. Le ciment Portland expansif à basse température (ELHC) présente les avantages d'une expansion autogène, d'une chaleur d'hydratation plus faible, d'une résistance initiale plus élevée, d'une consommation d'énergie et d'une émission de carbone plus faibles. Le changement de déformation volumique autogène est expansif et l'expansion à 28 jours n'est pas inférieure à 0,08 %. Le béton ELHC se caractérise par sa grande résistance à la fissuration, ce qui permet de mettre en place un système de contrôle de la température simplifié, mais efficace et rentable. Pour la première fois, le béton ELHC a été largement utilisé dans la construction des centrales hydroélectriques de Baihetan et de Wudongde, y compris les barrages en arc de 300 m de haut, les centrales électriques, les tunnels, etc. Aucune fissure n'a été observée dans les barrages depuis le début de la construction il y a 8 ans. L'ELHC et le béton ELHC ont depuis été appliqués aux CFRD, aux chemins de fer et aux ponts, démontrant un potentiel significatif pour d'autres applications et apportant des avantages techniques, économiques et sociaux substantiels.

La plupart des ingénieurs sont préoccupés par la durabilité du béton ELHC. Le rapport **R40** explique les différences de durabilité entre OPC (ciment Portland ordinaire), MHC (ciment Portland à chaleur médiate) et LHC expansif en utilisant des modèles couplés d'hydratation et de détérioration par lixiviation du calcium. Les résultats indiquent qu'après 1000 jours d'hydratation, la teneur en C-S-H augmente et la teneur en hydroxyde de calcium diminue dans les trois ciments, tandis que le LHC présente le plus grand potentiel d'hydratation. Après 100 ans de lixiviation, les profondeurs affectées par la lixiviation de l'OPC, du MHC et du LHC sont respectivement de 2,4 cm, 2,2 cm et 2,0 cm. Les fronts de lixiviation du C-S-H, de l'hydroxyde de calcium et de l'ettringite ont tous diminué dans l'OPC, le CMH et le LHC, ce qui indique que le LHC présente la meilleure résistance à la lixiviation. On en conclut que le LHC est le meilleur en termes de durabilité contre la lixiviation (Fig. 4).

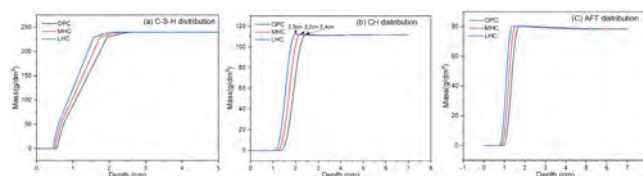


Fig. 4

Distribution des produits d'hydratation après 100 ans de lixiviation pour OPC, MHC et LHC en fonction de la profondeur : (a) C-S-H, (b) CH, (c) Ettringite.

B. Application de granulats acides dans le béton bitumineux

En général, pour les barrages en remblai avec une structure imperméable en béton bitumineux, les agrégats acides ne sont pas couramment utilisés dans le béton bitumineux en raison de leur faible compatibilité ou adhésion avec le liant bitumineux, ce qui entraînerait une stabilité à l'eau inadéquate. Toutefois, pour les projets de revêtement en béton bitumineux où seuls des granulats acides peuvent être trouvés, le rapport **R39** propose une nouvelle façon de les utiliser grâce à des additifs anti-décapage, qui peuvent améliorer de manière significative l'adhérence entre les granulats acides et l'asphalte. Le rapport propose également un paramètre efficace pour distinguer les agrégats acides des agrégats basiques et prédire le dosage optimal des additifs anti-décapage afin de prévenir les dommages causés par l'eau au béton bitumineux. Des granulats acides et un additif anti-affoulement ont été utilisés dans le réservoir supérieur de la centrale à accumulation par pompage de Yimeng (PSPP) à Shandong, en Chine, en 2021 ^[6]. Jusqu'à présent, les propriétés anti-infiltration du revêtement en béton bitumineux sont excellentes.

En résumé, un nouveau type de ciment appelé ciment Portland expansif à basse température (ELHC) a été développé en Chine et un béton de barrage à haute résistance à la fissuration à base d'ELHC a été produit. Aucune fissure thermique n'a été observée jusqu'à présent après des applications dans les barrages à voûte ultra-haute de Wudongde et Baihetan, ce qui indique qu'il s'agit probablement d'un nouveau matériau fondamental pour les barrages de l'avenir. Un béton bitumineux composé de granulats acides et d'additifs anti-décapage pour améliorer l'adhérence entre les granulats et l'asphalte a été produit et appliqué dans le réservoir supérieur d'une PSPP, offrant ainsi un moyen réalisable d'appliquer des granulats acides locaux dans le béton bitumineux.

4.1.4. Techniques intelligentes de construction de barrages

La figure 5 donne un aperçu des nouvelles technologies qui peuvent être appliquées à l'ingénierie des barrages ^[7] ainsi qu'aux systèmes d'alerte et de

surveillance qui sont si importants pour assurer la sécurité des barrages pendant leur durée de vie. Les rapports **R29**, **R32** et **R47** ont présenté des techniques intelligentes innovantes dans la construction de barrages en Chine.

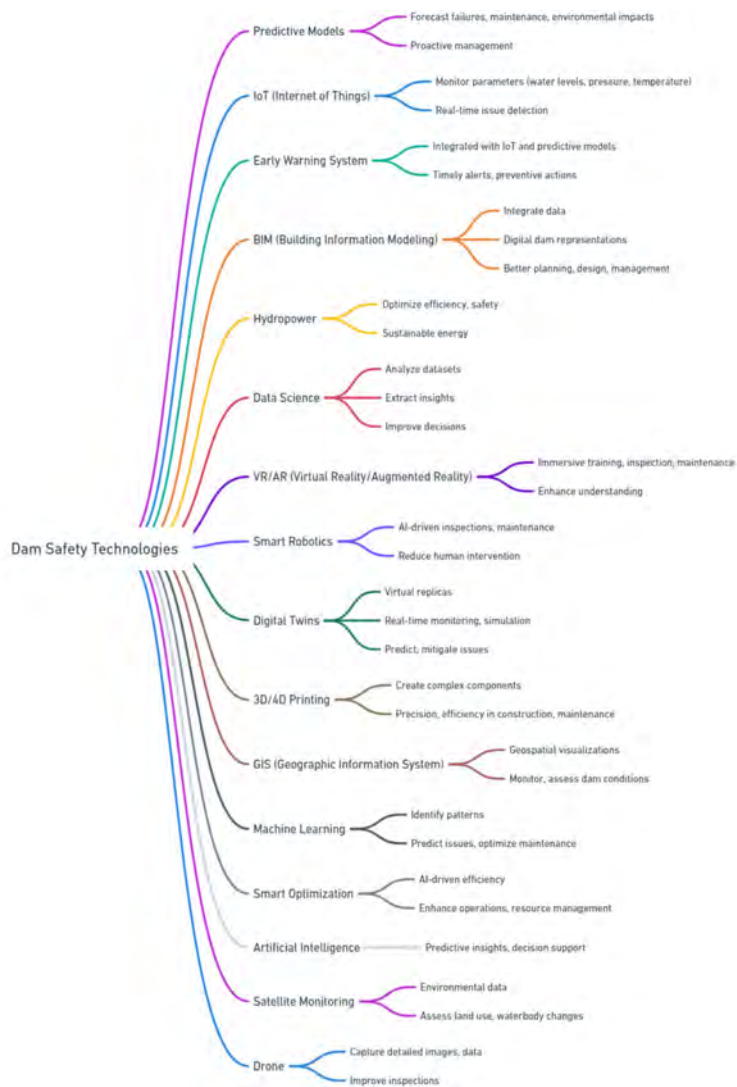


Fig. 5
Un aperçu des nouvelles technologies dans l'ingénierie des barrages

Le rapport **R29** présente les techniques de construction intelligentes appliquées à la construction du barrage en enrochement à noyau de gravier de Lianghekou, d'une hauteur maximale de 303,00 m, le plus haut barrage en terre et en roches du monde. Le barrage a été construit dans une région alpine avec une altitude de crête de 2875,00m. Dans le cadre de ce projet, les ingénieurs ont créé un ensemble complet de technologies de construction hivernale pour les barrages en terre et en roche de très grande hauteur dans les régions froides et de haute altitude, et ont créé un précédent de construction continue à grande échelle de murs en terre dans les régions de plateau pergélisolé en hiver en utilisant la technologie de remplissage intelligent, qui a contrôlé efficacement l'ensemble du cycle de construction de remplissage du barrage. Le système global de la technologie de construction de remblai intelligent comprend le mélange, le transport, l'ajout d'eau, la pose, le roulage, ainsi que le centre de commande et le centre mobile du site de roulage sans personnel (Fig. 6).

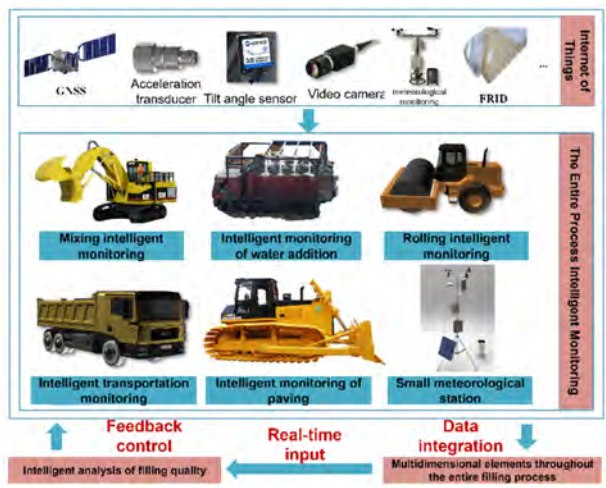


Fig. 6
Cadre de surveillance intelligent pour l'ensemble du processus de construction de la centrale hydroélectrique de Lianghekou

Le rapport **R32** traite du développement d'un système intelligent de gestion et de contrôle pour la construction de barrages en béton, qui consiste en un centre de commande intelligent pour la collecte de données en temps réel, l'analyse et la prise de décision, la conception et le développement de modèles mathématiques pour le centre de commande intelligent, et cinq modules fonctionnels d'application du système, y compris la conception BIM, la conception de la zone de coulée, la

production de béton, le transport et la coulée. Le système proposé vise à gérer et à contrôler la construction de barrages en béton, à soutenir la prise de décision, à réduire le temps d'attente pendant la construction et, en fin de compte, à améliorer l'efficacité de la construction en béton. La méthodologie a été appliquée à un projet de barrage en cours de construction. Les indicateurs de performance technique du travail proposé sont résumés, démontrant la faisabilité et la fiabilité du système proposé.

Le rapport **R47** présente le développement d'un chantier intelligent qui a été appliqué à la centrale hydroélectrique de Kala, d'une capacité installée de 1 020 MW. Le barrage principal est un barrage en béton armé d'une hauteur maximale de 123 mètres. Le site intelligent comprend des technologies intelligentes de surveillance de la sécurité et une plate-forme de construction intelligente pour les centrales hydroélectriques. L'agencement est présenté à la figure 7. Le système intelligent de surveillance de la sécurité permet de surveiller en temps réel et d'alerter rapidement les comportements et scénarios dangereux sur le site de construction, ce qui améliore considérablement la sécurité de la construction. La plateforme couvre tous les aspects, éléments et processus commerciaux, en incorporant huit fonctions de gestion commerciale intelligente et cinq applications de construction intelligentes. Le site intelligent de la centrale hydroélectrique de Kala est un modèle de construction et de gestion de barrages ou de digues pour l'avenir. Il répond à une demande importante dans la construction de grandes centrales hydroélectriques, offrant de vastes perspectives de marché et une valeur d'application substantielle, avec des avantages sociaux considérables.

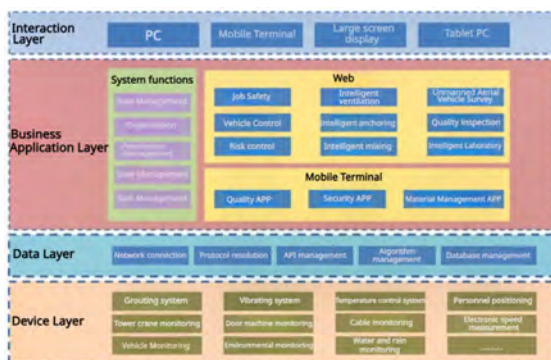


Fig. 7

Mise en place d'un système de chantier intelligent.

Comme le montrent les rapports ci-dessus, de plus en plus de technologies ou de systèmes intelligents sont développés et appliqués aux barrages construits récemment. Les barrages intelligents seront de plus en plus réalisés dans un avenir proche.

4.1.5. *Sécurité des barrages et hydraulique*

Des dommages dans le bassin de tranquillisation en Suède ont été constatés dans plusieurs installations de faible hauteur après plusieurs décennies de fonctionnement normal sans avoir été exposées à des crues de conception ou à des inondations extrêmes. Le rapport **R3** a tenté de mettre en évidence le mécanisme par des essais sur des modèles physiques à l'échelle et par la modélisation numérique. Ils ont constaté que des fissures dans le prototype, dans le béton le long de la pente en amont du bassin de tranquillisation, pourraient être une explication possible de l'initiation des dommages dans la structure réelle. Après l'apparition des dommages au béton, les fluctuations de pression en général, potentiellement associées à la cavitation, pourraient faire progresser les dommages en provoquant des vibrations sur les barres d'armature. Cela indique que le béton à haute résistance à la fissuration n'est pas seulement nécessaire pour les barrages en béton, mais aussi pour le béton résistant à l'abrasion dans le bassin de tranquillisation avec une faible hauteur d'eau, ou le béton résistant à l'abrasion dans le revêtement du tunnel avec une faible hauteur d'eau ou de faibles vitesses.

Pour résumer la section 4.1, les principaux progrès techniques concernant la durabilité des fondations, les types de barrages, les matériaux de construction des barrages et les technologies intelligentes ont été présentés. En ce qui concerne la durabilité des fondations, diverses techniques de contrôle des infiltrations, d'amélioration de la capacité portante et de la résistance au tassement et à la sismicité pour les barrages sur des fondations en sol ultra-tendre et en roches faillées ont été abordées. Les applications des barrages en sol cimenté, des barrages en sable et gravier cimentés et d'un barrage composite combinant un barrage en béton armé et deux barrages en enrochement à noyau de béton bitumineux ont été présentées. Un nouveau type de ciment, appelé ciment Portland expansif à basse température, a été développé en Chine et le béton du barrage est très résistant à la fissuration, montrant un grand potentiel dans le contrôle thermique des barrages en béton de grande hauteur. Un béton bitumineux à base de granulats acides et d'additifs anti-décapage a été mis au point et appliqué dans le cadre de la PSPP. Des techniques ou des systèmes intelligents ont été mis au point pour améliorer la sécurité des barrages aux stades de la construction et de la surveillance. Ils ont joué un rôle important dans la construction du barrage de 303 mètres de haut de Lianghekou, le plus haut barrage en terre et en roches du monde.

4.2. SURVEILLANCE ET ANALYSE DE LA SÉCURITÉ DES BARRAGES VIEILLISSANTS

Huit rapports contribuent aux derniers progrès techniques en matière de surveillance et d'analyse de la sécurité des barrages existants, y compris un remblai vieux de 60 ans (**R10**), des barrages-voûtes en béton de 100 m de haut (**R46**, **R14**),

des barrages-voûtes de 300 m de haut (**R37**, **R33**) et des barrages affectés par l'érosion (**R4**, **R11**, **R21**).

Le rapport **R10** traite de l'importance de la détection des comportements anormaux dans les barrages grâce à des méthodes d'analyse avancées et présente deux méthodes avancées d'analyse des données de surveillance : la détection d'anomalies basée sur l'apprentissage automatique et la modélisation numérique utilisant la technologie de détection par fibre optique distribuée. Les deux méthodes, appliquées aux données de déplacement d'un barrage-poids français en béton d'une hauteur de 31 m et d'un canal en remblai de près de 60 ans d'une longueur de 5,250 km, respectivement, ont montré leur intérêt et leurs avantages techniques pour améliorer les capacités d'interprétation des données de surveillance.

Le rapport **R46** développe une technique de calcul des indicateurs de surveillance des barrages basée sur la sélection intégrée des points de mesure des indicateurs, le calcul multicritères et l'application holistique des critères. La méthode a été appliquée au barrage-voûte en béton armé de Nam Ngum 5 au Laos, d'une hauteur maximale de 100,5 m. Elle a permis d'évaluer rapidement l'état de sécurité du barrage et d'offrir des conseils et un soutien scientifique pour son exploitation.

Le rapport **R37** vise à évaluer la performance de sécurité d'un barrage à voûte ultra-haute dans le sud-ouest de la Chine sous l'influence de la déformation de la contraction de la vallée en effectuant une analyse non linéaire complète par éléments finis, en tenant compte des conditions limites géologiques de contrôle du barrage et de la fondation, ainsi que de l'évolution des charges de déformation de la vallée. Les résultats montrent que sous les effets actuels de la déformation de la vallée, le niveau de sécurité de ce barrage voûte exprimé par les facteurs de sécurité 3K répond aux exigences réglementaires. Cependant, une surveillance continue de la déformation de la vallée est nécessaire pour assurer la sécurité à long terme du barrage.

Le rapport **R33** propose un schéma d'augmentation des données pour la maintenance prédictive (PdM) des barrages et l'applique à un barrage à ultra-haute voûte (hauteur maximale de 294,5 m) en Chine. La méthode améliorée de regroupement K-means proposée combine les informations de distance spatiale des points de mesure des capteurs pour améliorer la précision et l'efficacité de la classification des données de séries temporelles. En outre, la combinaison de la ligne de centroïde de regroupement améliorée et des modèles de mémoire à long terme (LSTM) permet de prédire efficacement l'état de fonctionnement du barrage. En comparaison, la méthode améliorée de regroupement des K-moyennes améliore de manière significative la précision de la détection des anomalies et la précision de la prédiction des données, fournissant ainsi des références précieuses pour la maintenance prédictive des grandes structures en béton.

Le rapport **R14** présente les résultats de la surveillance in situ sur 60 ans d'un barrage-voûte en béton (87 m de haut) dans une région froide du Japon. Le module

d'élasticité dynamique du béton du barrage, estimé à partir de la vitesse des ultrasons, a montré que le barrage d'Otori est parfaitement maintenu même après 60 ans (Fig. 8), ce qui suggère que la solidité du barrage est assurée. Les échantillons ont également conservé un pourcentage élevé de module dynamique, mais des différences ont été observées en fonction de la proportion du mélange. L'étude démontre que des mesures raisonnables de conception et de construction sont cruciales pour assurer la performance à long terme des structures en béton dans des environnements de gel-dégel.

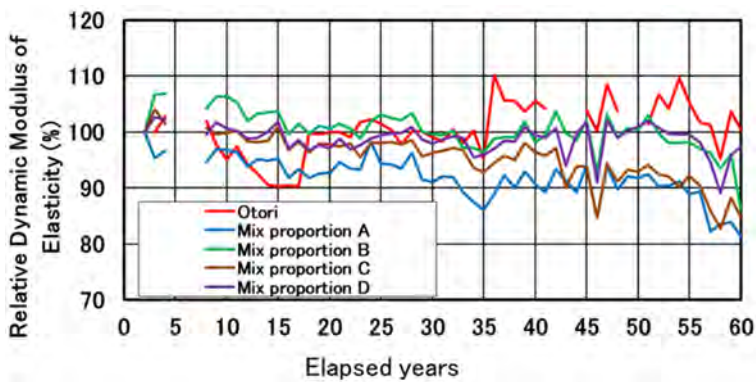


Fig. 8
Évolution dans le temps du module d'élasticité dynamique relatif

Dans le rapport **R11**, une approche innovante est utilisée pour évaluer la stabilité d'une structure de barrage mesurant 100 m de long, 65 m de large et 57 m de haut, située sur une fondation de sol caractérisée par une pression d'eau interstitielle excessive et des contraintes effectives réduites résultant d'une liquéfaction statique pendant la construction et d'une érosion interne subséquente. L'accent est mis sur le calcul des mécanismes de défaillance des appuis en profondeur. Les facteurs de sécurité sont calculés par la méthode de réduction de la résistance au cisaillement (SSR) avec le processus innovant de calibrage en deux étapes. Enfin, l'importance des données de mesure réelles telles que les CPT, les taux de drainage et les pressions d'eau interstitielle est soulignée sur le site.

La principale cause de rupture des barrages et des remblais est l'érosion, interne et externe, qui n'était pas couverte par les normes européennes (Eurocodes). Le rapport **R21** a introduit un ensemble de lignes directrices recommandées pour l'évaluation du risque d'érosion, publiées en 2024 par le Comité français des grands barrages (CFBR) après 7 ans de travail. Les recommandations, pour la première fois, englobent l'érosion interne et externe dans une méthodologie commune en 7 étapes basée sur le concept de trajectoires d'érosion

et peuvent être appliquées aux barrages, canaux et levées. Elles proposent trois niveaux d'analyse pour l'érosion interne et trois types de justification pour l'érosion externe.

Le rapport **R4** a présenté l'optimisation de la conception de la protection des berges en combinant la modélisation hydraulique avec des méthodes de conception basées sur la turbulence. Le modèle hydraulique bidimensionnel a été développé en utilisant la bathymétrie à haute résolution des échosondages multifaisceaux et la topographie LiDAR. La turbulence a été modélisée à l'aide du modèle k-epsilon à deux équations et à moyenne de profondeur. La méthode combinée est appliquée au canal de fuite d'une centrale hydroélectrique du nord de la Suède, vieille de plus de 60 ans. Les résultats ont montré que les mesures de protection des berges existantes sont insuffisantes pour résister à l'impact des inondations, en particulier dans les zones où la vitesse d'écoulement est élevée et où il y a de fortes turbulences. Des solutions de réparation ont été proposées, notamment l'augmentation de l'épaisseur de la couche rocheuse et la modification de la taille des roches afin d'améliorer l'efficacité de la protection des berges. La nouvelle méthode peut contribuer à une meilleure compréhension des phénomènes d'érosion et à une conception optimale de la protection des berges.

Pour résumer cette section, la surveillance, l'analyse et la maintenance de la sécurité des barrages intégrant des technologies avancées, des approches basées sur les données et des principes de conception robustes pour améliorer la sécurité et la longévité des barrages ont été abordés. Les technologies avancées comprennent la détection d'anomalies basée sur l'apprentissage automatique, la modélisation numérique utilisant la détection par fibre distribuée, le schéma d'augmentation des données pour la maintenance prédictive (PdM), et la surveillance à long terme des barrages par CND, comme la vitesse ultrasonique. Les lignes directrices pour l'évaluation du risque d'érosion avec une méthodologie en 7 étapes basée sur le concept de trajectoire d'érosion, la méthode de réduction de la résistance au cisaillement (SSR), et la modélisation hydraulique combinée à la méthode de conception basée sur la turbulence, ont également été abordées.

4.3. RÉHABILITATION ET AMÉLIORATION DE LA SÉCURITÉ DES BARRAGES VIEILLISSANTS

Au fur et à mesure que les barrages vieillissent, ils subissent une détérioration qui peut compromettre leur sécurité, leur efficacité et leur fonctionnalité. Par conséquent, les activités de réhabilitation des barrages comprennent le renforcement de la structure du barrage, l'amélioration de la capacité de l'évacuateur de crues, le contrôle des fuites, l'amélioration des systèmes de surveillance, la stabilisation des fondations et le levage du barrage. Sept rapports ont contribué à ce thème et ont couvert un large éventail d'activités de réhabilitation des barrages

vieillissants. Le plus ancien barrage réhabilité est un barrage en maçonnerie âgé de 120 ans (**R50**), les plus anciens barrages en béton ont 100 ans (**R7**, **R15**) et le plus ancien barrage avec revêtement en asphalte a 65 ans (**R27**).

Le rapport **R50** présente un projet de reconstruction en cours du barrage en maçonnerie de Harcov, en République tchèque, qui a été construit entre 1902 et 1904 principalement pour contrôler les flux d'inondation et qui constitue désormais un patrimoine culturel et historique. Après un siècle d'exploitation, le barrage doit améliorer la capacité de son déversoir pour répondre aux normes modernes et garantir que l'onde de crue de 10 000 ans passe en toute sécurité. Les travaux de reconstruction comprennent l'augmentation de la capacité du déversoir, la modification du canal de débordement en gradins et le renforcement des fondations du barrage pour résoudre les problèmes de soulèvement du sol à long terme. La partie principale du barrage en maçonnerie de Harcov sera en grande partie conservée dans son état d'origine. De nouveaux équipements technologiques seront installés, notamment pour le contrôle automatique de la gestion de l'eau et la surveillance du barrage. Ce projet de reconstruction sera une bonne démonstration de l'équilibre entre la préservation du patrimoine historique et les exigences modernes.

Le rapport **R23** fournit un plan détaillé pour la remise en état de l'évacuateur de crues du barrage de Kpong, situé sur la rivière Volta au Ghana, qui fonctionne depuis 40 ans. Outre les facteurs de vieillissement habituels tels que le vieillissement des équipements et la corrosion, la présence d'une réaction alcaline des agrégats (RAA) dans le béton est le principal facteur qui a nui au fonctionnement de l'évacuateur de crues. Une approche à multiples facettes impliquant une évaluation de l'état du site des vannes et de l'infrastructure est adoptée. Pour faire face à l'AAR, ce qu'on appelle le cancer des structures en béton, un système de mesure de convergence comprenant six mètres de convergence de 12 m de long a été installé dans la centrale électrique de Kpong pour permettre la surveillance du gonflement du béton. L'évaluation du béton de l'évacuateur de crues, y compris 1) la cartographie des fissures des piliers, 2) l'analyse des niveaux des 21 bornes de mesure, et 3) l'échantillonnage de carottes de béton et l'analyse en laboratoire, ont été effectués. Des réparations supplémentaires importantes telles que le scellement de toutes les fissures dans le béton du déversoir et l'équipement associé sont nécessaires pour assurer un fonctionnement fiable des vannes à l'avenir. Bien qu'une approche complète et systématique soit en cours, la longévité des déversoirs à vannes reste incertaine en raison de la complexité du contrôle de l'expansion résiduelle de l'AAR.

Le rapport **R7** fournit une évaluation complète de l'état des carottes de béton provenant de la centrale hydroélectrique de Mühleberg (HPP), vieille de 100 ans, en Suisse. La structure principale de la centrale, qui comprend un barrage-poids de 20 m de haut et la centrale électrique, a été construite avec du "béton coulé" à fort affaissement. Cependant, la proportion exacte du mélange n'a pas pu être révélée en raison de l'absence de documents techniques. Deux évaluations de l'état des carottes de béton foré ont été effectuées en 1980 et 2015, respectivement, et la

résistance à la compression et le module d'élasticité restent à un bon niveau, sans signes évidents de dégradation. Cependant, les examens microscopiques de sections minces ont révélé des indications de deux phénomènes de vieillissement, l'AAR et la lixiviation. Bien qu'un AAR historique ait pu être clairement détecté sur l'ensemble de la structure de retenue d'eau en béton, aucun dommage structurel significatif dû à un AAR n'a été constaté. La raison pour laquelle l'AAR s'est atténué après un certain temps est due à la teneur relativement faible en ciment dans le béton et peut-être à une teneur plus faible en alcali dans le ciment. Il a donc été conclu que le potentiel de cette réaction doit être pris en compte dans toutes les mesures de rénovation et de modernisation futures.

Les rapports **R23** et **R7** montrent clairement que le RAA reste le principal facteur affectant l'intégrité structurelle et la durée de vie des barrages en béton. Pour les barrages construits avec des granulats alcali-actifs, des mesures importantes doivent être prises pour réduire les effets négatifs. Nous pouvons également conclure que des méthodes permettant de déterminer le rapport eau-ciment à l'aide de carottes de béton pour les barrages en béton très anciens ne disposant d'aucune donnée technique sont nécessaires pour l'évaluation de l'état et la prédiction de la durée de vie.

Le rapport **R15** fournit une réévaluation détaillée des effets des travaux de réhabilitation effectués il y a 30 ans pour contrôler les fuites en amont du barrage de Ceresole Reale en Italie, un barrage-poids en béton construit en 1927-1930. Le projet de réhabilitation réalisé dans les années 1990 comprenait l'installation d'un système de géomembrane souple exposée, de nouveaux blocs de béton armé et l'ajout de nouveaux systèmes de drainage et de rideaux d'injection. Après plus de trente ans d'exploitation, les données de surveillance montrent qu'en dépit d'une dégradation partielle attendue de géomembrane exposée, l'étanchéité globale et les performances structurelles du barrage de Ceresole Reale sont restées excellentes, garantissant son exploitation dans des conditions totalement sûres.

Le rapport **R27** décrit le projet de rénovation du réservoir de Rosswiese en Autriche, qui a été construit en 1958 avec un revêtement de surface en asphalte. Après 65 ans d'exploitation, le revêtement en asphalte devait être rénové, tout en éliminant les sédiments dans le réservoir et en améliorant le système de drainage. Les défis sont liés à l'espace limité sur le site pour les machines et au court laps de temps en raison de l'importance économique du barrage.

En raison de l'augmentation des phénomènes météorologiques extrêmes provoquée par le changement climatique, les barrages existants doivent renforcer leur capacité de contrôle des inondations. Le rehaussement des barrages est un moyen efficace d'accroître cette capacité. Le rapport **R12** a étudié la faisabilité du rehaussement du barrage de Shin-Katsurazawa, vieux de 70 ans, dans la ville de Niigata, au Japon. Le barrage passera d'une hauteur de 63,6 m à 75,5 m, et la capacité de stockage de l'eau augmentera de 92 millions de m³ à 147 millions de m³. Tout d'abord, les propriétés mécaniques du béton de l'ancien barrage ont été

déterminées grâce à des essais sur des échantillons de carottes, ce qui a permis d'obtenir des données pour la suite de la conception. Ensuite, en se basant sur les variations des niveaux d'eau du réservoir tout au long de l'année, un plan de construction optimisé a été proposé afin de minimiser les contraintes lors du coulage du béton en altitude lorsque le niveau d'eau est bas. Enfin, l'efficacité du plan de construction proposé a été vérifiée à l'aide de dossiers de construction réels et d'une analyse de simulation, ce qui a permis de conclure que le maintien de niveaux d'eau minimums pendant les travaux de levage du barrage peut réduire efficacement les contraintes générées par les variations du niveau d'eau et garantir la sécurité de la structure.

Le rapport **R16** a étudié et recommandé des méthodes de renforcement des barrages en béton existants à l'aide d'ancrages passifs. Après une revue de la littérature sur l'ancrage passif, les auteurs ont proposé une méthode innovante qui tient compte des effets de dilatation et de confinement. Après plusieurs repères, les principaux éléments du projet de lignes directrices françaises relatives à l'utilisation d'ancrages passifs pour renforcer les barrages en béton existants sont décrits, à savoir : la protection contre la corrosion des ancrages, le contrôle et la surveillance des barrages renforcés par des ancrages passifs. Bien qu'il reste encore beaucoup à faire, les résultats de cette étude peuvent être adoptés par d'autres comités intéressés ou par des comités internationaux afin de faire progresser les réglementations pertinentes et le développement technique dans ce domaine.

Pour conclure cette section, des études de cas globales sur les activités de réhabilitation des barrages vieillissants, y compris la modernisation des barrages tout en préservant les valeurs historiques et environnementales, la rénovation des déversoirs en tenant compte de la présence d'AAR, le contrôle des fuites par géomembrane, le levage des barrages pour s'adapter au changement climatique, la surveillance à long terme par CND comme la vitesse ultrasonique, le renforcement des barrages à l'aide d'ancrages passifs, sont abordées. Les barrages, dont l'âge varie entre 40 et 120 ans, sont représentatifs et les expériences sont d'une grande importance en tant que références pour les autres barrages dans le monde.

5. CAS PARTICULIER DES PETITS BARRAGES ET DES DIGUES

Ces dernières années, la CIGB et de nombreux comités nationaux, dont le CFBR (Comité français des barrages et réservoirs), ont accordé de plus en plus d'attention aux petits barrages et aux levées, en raison de leur importance égale à celle des grands barrages et des levées en termes d'utilité sociale et de risques qu'ils présentent. Une discussion approfondie a été menée lors du Congrès de Vienne en 2018 sous la Q103 "Petits barrages et levées"

Trois rapports ont contribué à ce thème, traitant de la conception, de l'entretien et de l'analyse de la sécurité des petits barrages et des digues.

Le rapport **R17** traite de la conception, de la construction, de l'exploitation et de la gouvernance des petits barrages et des digues de protection contre les inondations en France, en soulignant leurs similitudes et leurs différences, ainsi que les défis auxquels ils sont confrontés. Si les deux types d'infrastructures de gestion de l'eau partagent des fonctions hydrauliques de base telles que le maintien et la gestion des niveaux d'eau, il existe des différences significatives dans leur approche en raison de l'importance variable accordée à l'impact sur l'environnement. Par exemple, les digues de protection contre les inondations ont pour priorité de protéger des zones spécifiques contre les inondations, tandis que les petits barrages peuvent se concentrer davantage sur l'irrigation agricole ou la production d'hydroélectricité. Le rapport examine les principes de conception, les problèmes courants et les solutions pour les petits barrages, ainsi que les normes de construction, la gestion des risques et les détails techniques pour les digues de protection contre les inondations.

Le rapport **R19** présente un projet de rénovation des digues dans le village de Well, près de la province de Limburg, aux Pays-Bas, afin de répondre aux défis climatiques futurs. Une approche de conception adaptative et adaptée à l'avenir est proposée et appliquée au projet Well. Dans la nouvelle procédure de conception, ce n'est plus une géométrie de digue prédéfinie qui dicte les propriétés de remblai requises, mais plutôt les propriétés de remblai disponibles qui déterminent la géométrie de la digue (Fig. 9). Le projet Well est devenu l'un des projets d'amélioration des digues les plus durables des Pays-Bas (), démontrant comment assurer la sécurité tout en conciliant les valeurs éco-environnementales, l'économie, le contexte historique de la région et la gestion de l'eau.

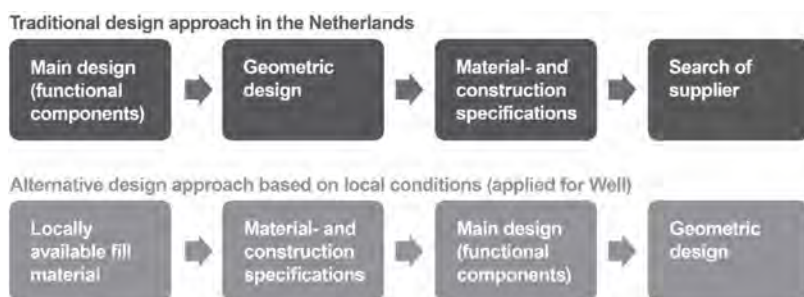


Fig. 9

Principales étapes des approches traditionnelles et alternatives de conception

Le rapport **R18** des Pays-Bas propose une méthode d'évaluation de la sécurité des petites digues où les castors creusent des terriers pendant les crues. Un modèle amélioré basé sur des agents (ABM) pour simuler le comportement des castors a été développé, prenant en compte de multiples facteurs tels que la vitesse du vent, la température, les précipitations, la durée de l'inondation, l'âge, l'expérience et les effets individuels des castors. En comparant les prédictions du modèle avec les observations sur le terrain, il a été constaté que le modèle prédit efficacement l'emplacement des terriers de castors mais qu'il est actuellement insensible aux conditions hydrométéorologiques. Pour valider davantage le modèle, des données plus complètes, en particulier sur le comportement des castors et l'emplacement des digues, devraient être collectées afin d'améliorer sa précision. Après tout, ce modèle fournit un nouvel outil méthodologique pour comprendre et gérer les risques causés par l'activité des castors sur les digues.

En conclusion de cette section, les similitudes et les différences entre les petits barrages et les digues aux stades de la conception, de la construction et de l'exploitation sont abordées. Les petits barrages et les digues doivent faire l'objet d'une attention particulière afin d'être adaptés à l'avenir et de nous permettre de continuer à profiter de leurs avantages.

6. DES SITES DE PLUS EN PLUS DIFFICILES - LES BARRAGES ET LEURS NOUVEAUX DÉFIS

Les barrages sont toujours nécessaires pour la gestion de l'eau, la production d'électricité, etc. Cependant, bon nombre des sites les plus appropriés pour la construction de barrages, où un bon équilibre entre la faisabilité technique, les avantages économiques et l'impact sur l'environnement pourrait être trouvé, ont déjà été aménagés. Il est donc probable que les barrages soient construits dans des sites de plus en plus difficiles, tels que des régions montagneuses éloignées présentant des conditions géologiques complexes, une forte pente, une altitude élevée, un froid intense, et des tremblements de terre, ce qui pose de nouveaux défis en matière de construction de barrages. Cinq rapports ont présenté leurs expériences en matière de sécurité des barrages pendant leur construction face aux glissements de terrain (**R1**), aux fortes pluies locales (**R6**), aux conditions géologiques complexes (**R5**) et aux exigences environnementales élevées (**R30**, **R34**)

Le rapport **R1** présente une expérience réussie de gestion d'un événement de rupture de pente pendant la construction du barrage Alto Tâmega, situé sur la rivière Tâmega, un affluent de la rive droite de la rivière Douro dans le nord du Portugal. Le barrage a une hauteur maximale de 104,50 m et un volume de béton d'environ 223 000 m³. Il est fondé sur une masse rocheuse métamorphique principalement

composée de micaschistes, avec une centrale électrique située à la pointe aval. Pendant les périodes de pluie, un important glissement de terrain s'est produit sur la pente de la rive droite, immédiatement en aval de la surface d'insertion du barrage, impliquant un volume de roches d'environ 23 000 m³. Les mesures d'ingénierie comprennent : 1) le resurfaçage de la surface d'insertion de quatre blocs du barrage ; 2) la construction d'une nouvelle structure en béton pour restaurer partiellement la géométrie et les conditions de chargement du massif rocheux existant avant l'éboulement ; 3) l'extension de la galerie rocheuse sous la zone affectée, pour étudier la fondation du massif rocheux en profondeur et promouvoir l'imperméabilisation et le drainage du massif rocheux ; 4) la mise à jour du plan de surveillance, y compris la définition d'instruments supplémentaires à installer dans la nouvelle structure en béton, ainsi que des ajustements pour surveiller la zone de la fondation sur la rive droite. Les travaux de construction se sont déroulés normalement, suivant un planning bien défini et un contrôle de sécurité strict. Le premier remplissage du réservoir a eu lieu comme prévu. Le barrage est en service depuis février 2023, avec de très bonnes performances.

Le rapport **R5** présente une introduction à la conception, à la construction et à la surveillance des galeries d'injection de barrages dans des conditions géologiques complexes. Le barrage de Moglice, situé dans le sud-est de l'Albanie, est l'un des plus hauts barrages en enrochement du monde, avec noyau en asphalte et une hauteur de 170 mètres. Pendant la construction, en raison de nouvelles révélations géologiques le long de la culée centrale et de la culée inférieure gauche, et d'une géologie défavorable avec un toit rocheux plongeant jusqu'à 65 mètres en dessous de la galerie prévue, la galerie a dû être révisée. L'équipe de conception a réussi à adapter la conception initialement validée tout en apportant continuellement les améliorations nécessaires. Les optimisations de la conception technique ont été conditionnées par les découvertes faites au cours du processus d'excavation de la construction. La conception affinée et sa mise en œuvre ont été récemment vérifiées par trois ans et demi de données de surveillance des performances en collaboration avec l'exploitant du barrage.

Le rapport **R6** présente la gestion réussie des inondations lors de la construction du barrage RCC de Nam Theun 1 au Laos, d'une hauteur de 187 mètres. Le rapport fournit des descriptions détaillées des schémas de canaux de dérivation et des étapes de mise en œuvre des plans de gestion des inondations. Lors des saisons des pluies 2018, 2019, 2020 et 2021, le tunnel de dérivation a atteint sa capacité, les batardeaux et le barrage principal ont été débordés et les inondations ont traversé le chantier en toute sécurité sans causer de dommages inattendus au barrage et à d'autres structures.

Les rapports **R30** et **R34** se concentrent sur la centrale hydroélectrique JX intégrée dans une région de haute altitude en Chine, où l'altitude est supérieure à 3 000 m, et qui est confrontée à un terrain difficile, à un calendrier serré et à la préservation des noyers anciens. L'article **R34** traite des techniques de construction rapide d'un système de traitement du sable et du gravier et de production de béton à

grande échelle. Grâce à l'optimisation de la disposition du système et à l'adoption de nouvelles technologies, le projet a été construit avec succès, y compris les mesures de protection locales pour les noyers anciens, la gestion des interférences sur le site de construction et les techniques de construction pendant les saisons de basse température. Il présente également des solutions innovantes telles que l'utilisation de la technologie BIM pour la simulation de jumeaux numériques, l'application de nouveaux matériaux de structure de dôme d'air pour la construction de grands réservoirs de stockage, et le développement de systèmes intelligents adaptés aux régions de haute altitude pour la production de béton. Le projet **R30** se concentre sur la conception et les techniques de construction d'un grand réservoir de stockage de matériaux semi-finis en acier pour la centrale hydroélectrique JX. Il a été installé en utilisant la méthode inversée, ce qui a permis de raccourcir la période de construction et d'améliorer l'efficacité.

En conclusion, comme les barrages de grande hauteur vont être construits dans des sites de plus en plus difficiles, de plus en plus d'expériences sont accumulées pour surmonter les nouveaux défis tels que les défis géologiques complexes, les catastrophes naturelles extrêmes, les conditions environnementales sévères et les exigences élevées en matière de protection de l'environnement.

7. NECESSITE D'UN RENFORCEMENT MONDIAL DES MOYENS PROPRES

Seul le rapport **R8** a contribué à ce thème. Il s'est concentré sur les facteurs ayant un impact sur les projets transfrontaliers et sur les solutions. Après avoir rappelé la brève histoire des conflits liés à l'eau entre les pays, analysé les facteurs conduisant au conflit ou à la coopération, il conseille d'atténuer les conflits par des traités et des accords. La résolution collaborative des différends par le biais de traités et d'accords est essentielle pour minimiser les risques de conflits liés aux projets transfrontaliers. En développant de nouvelles méthodes pour réduire le potentiel de conflit, les meilleures pratiques doivent couvrir des éléments tels que la sécurité des barrages et la gestion des urgences, les évaluations régionales intégrées des risques, des dangers et de la vulnérabilité qui prennent en compte les impacts sur les communautés, les infrastructures et les biens. L'évaluation du patrimoine environnemental et culturel, la coordination conjointe de la gestion des urgences, l'engagement des parties prenantes et les exercices d'urgence doivent faire partie intégrante de ces meilleures pratiques. Enfin, le rapport appelle au renforcement de la sécurité des barrages, à l'amélioration des mesures de gestion des urgences et à l'amélioration de la coopération entre les pays voisins pour résoudre les conflits liés aux barrages transfrontaliers, où différents cadres juridiques, socio-économiques, culturels et institutionnels pour la sécurité des barrages doivent coexister.

En conséquence, des organisations telles que la Commission internationale des grands barrages (CIGB) et le Groupe de la Banque mondiale, ainsi que les comités nationaux de sécurité des barrages et les autorités réglementaires (locales et nationales) doivent jouer un rôle en dans l'élaboration et la mise en œuvre d'orientations sur les meilleures pratiques spécifiquement adaptées aux besoins uniques des barrages transfrontaliers, y compris la reconnaissance de l'importance de la sécurité des barrages et de la gestion des situations d'urgence, ainsi que d'une communication claire et transparente avec le public.

8. CONCLUSIONS

Cinquante et un rapports du monde entier ont contribué à la question 109, “ Des barrages et des digues adaptés à l'avenir ”. Bien qu'aucune définition claire n'ait été donnée par la communauté de la CIGB sur les barrages et les digues adaptés à l'avenir jusqu'à présent, nous pensons que leurs caractéristiques peuvent être caractérisées par la sécurité, la résilience, l'intelligence, la convivialité écologique, l'économie, la conformité et la participation.

La sécurité est une priorité absolue pour des barrages et des digues adaptés à l'avenir. Les barrages et les levées doivent être sûrs tout au long de leur durée de vie, y compris aux stades de la conception, de la construction, de l'exploitation, de l'entretien, de la réhabilitation et de la mise hors service, en faisant appel à des solutions techniques et non techniques efficaces, robustes et fiables. La grande majorité des 51 rapports portent sur la sécurité des barrages et des levées, notamment la durabilité des fondations, la conception de la sécurité pour les nouveaux barrages et levées, les techniques de garantie de la sécurité pendant la construction, la surveillance de la sécurité, l'évaluation de l'état de la sécurité et l'amélioration de la sécurité par la réhabilitation des barrages et levées vieillissants.

En ce qui concerne la durabilité des fondations, diverses techniques de contrôle des infiltrations, d'amélioration de la capacité portante et de la résistance au tassement et à la sismicité pour les barrages sur des fondations en sol ultra-tendre et en roches faillées ont été abordées. Les applications des barrages en sol cimenté, des barrages en sable et gravier cimentés et d'un barrage composite combinant un barrage en béton armé et deux barrages en enrochement à noyau de béton bitumineux ont été présentées. Un nouveau type de ciment, appelé ciment Portland expansif à basse température, a été développé en Chine et le béton du barrage est très résistant à la fissuration, montrant un grand potentiel dans le contrôle thermique des barrages en béton de grande hauteur. Un béton bitumineux à base de granulats acides et d'additifs anti-décapage a été mis au point et appliqué dans le cadre de la PSPP. Des techniques ou des systèmes intelligents ont été mis au point pour améliorer la sécurité et l'efficacité des barrages aux stades de la

construction et de la surveillance, jouant un rôle important dans la sécurité des barrages de 300 m de haut en Chine, notamment les barrages de Lianghekou, de Wudongde et de Baihetan. Les technologies intelligentes vont être appliquées plus largement dans un avenir proche

La résilience climatique est également une caractéristique distinctive des barrages et des digues adaptés à l'avenir. Ils doivent être conçus selon des approches adaptatives et flexibles pour répondre à la variabilité, à l'imprévisibilité, à l'extrémité et à l'incertitude causées par le changement climatique. Les barrages et les digues doivent être respectueux de l'environnement afin de pouvoir coexister harmonieusement avec l'écosystème et la nature pendant toute leur durée de vie. Pour les barrages à construire dans des sites de plus en plus difficiles tels que les régions montagneuses éloignées avec des conditions géologiques complexes, de fortes précipitations, des exigences environnementales élevées, un froid sévère, nous avons déjà acquis une expérience réussie dans la lutte contre ces défis et ils peuvent être une bonne référence pour les barrages à construire dans des sites difficiles similaires.

La gestion des barrages et des digues vieillissants nécessite une approche multidisciplinaire combinant l'ingénierie, la science de l'environnement, l'économie et la politique sociale. Elle nécessite également la participation et la collaboration de tous les actionnaires des barrages et des digues. Bien que le nombre, le type, l'âge, les caractéristiques techniques et l'état de sécurité des barrages et des digues varient considérablement d'un pays à l'autre, certains pays ont déjà pris conscience de l'importance d'assurer la sécurité pour l'avenir et prennent des mesures intégrées qui leur permettent de réaliser des progrès considérables.

REMERCIEMENTS

Je tiens à remercier sincèrement le Dr Jean-Pierre Tournier et M. Danie Badenhorst pour leurs précieuses suggestions et leur aide précieuse dans l'analyse et la synthèse des rapports.

RÉFÉRENCES

- [1] Barrages en terre cimentée - CIGB, Bulletin 195 (2022).
- [2] ACI PRC-207.1-21. Guide du béton de masse. ACI 2022.
- [3] ACI PRC223-21. Béton compensant le retrait. ACI 2021.

- [4] DU, C. Une revue de l'oxyde de magnésium dans le béton. *Concrete International*. 2005, 27: 45–50.
- [5] LI, W., FAN, Q., LI, X., ET AL. Development and application of specific low heat Portland cement for building ultra-high arch dams. *Journal of hydro-electric engineering*, 2017, 36(3): 113–120.
- [6] WANG, Z, YANG, B, XIA, S. Key technologies for the application of acidic aggregates in asphalt concrete anti-seepage facing. Actes de la réunion annuelle du comité technique du CFRD à la China Hydraulic Society, 2023.
- [7] HARIRI-ARDEBILI, M.A., MAHDAVI G., NUSS, L., LALL, U. Le rôle de l'intelligence artificielle et des technologies numériques dans l'ingénierie des barrages : Narrative review and outlook. *Engineering Applications of Artificial Intelligence*, 2023. Volume 126, Part A, 106813, ISSN 0952-1976.